General Disclaimer

One or more of the Following Statements may affect this Document

- This document has been reproduced from the best copy furnished by the organizational source. It is being released in the interest of making available as much information as possible.

- This document may contain data, which exceeds the sheet parameters. It was furnished in this condition by the organizational source and is the best copy available.

- This document may contain tone-on-tone or color graphs, charts and/or pictures, which have been reproduced in black and white.

- This document is paginated as submitted by the original source.

- Portions of this document are not fully legible due to the historical nature of some of the material. However, it is the best reproduction available from the original submission.

Produced by the NASA Center for Aerospace Information (CASI)

4 JUNE 1971

LMSC-A989142
ACS-124B

CR-124417

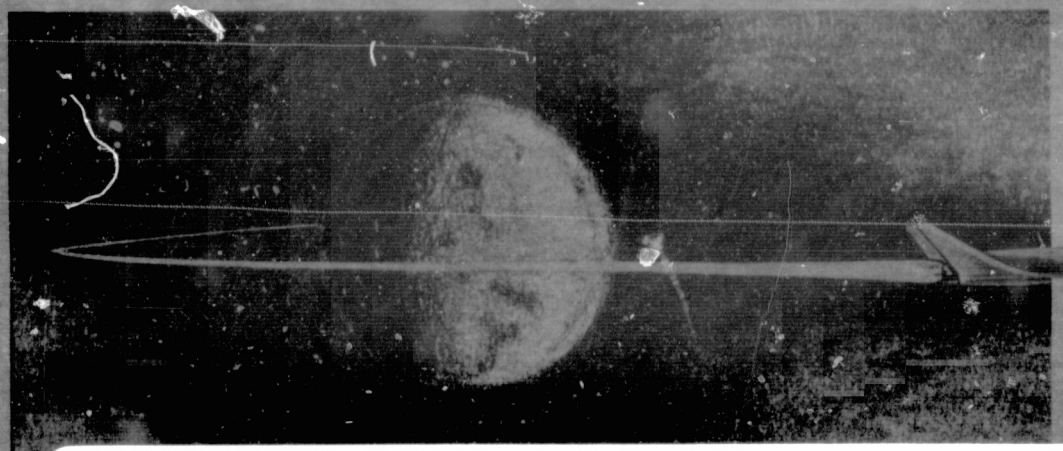

(NASA-CR-124417) STUDY OF ALTERNATE SPACE SHUTTLE CONCEPTS. VOLUME 2. PART 1: CONCEPT ANALYSIS AND DEFINITION (Lockheed Missiles and Space Co.) 671 p HC $35.75

N73-32772

Unclas
CSCL 22B G3/31 18185

FINAL REPORT

STUDY OF ALTERNATE SPACE SHUTTLE CONCEPTS

VOLUME II — PART I
CONCEPT ANALYSIS AND DEFINITION



Contract NAS 8-26362

Prepared for George C. Marshall Space Flight Center by
Manned Space Programs, Space Systems Division

LOCKHEED MISSILES & SPACE COMPANY
A GROUP DIVISION OF LOCKHEED AIRCRAFT CORPORATION
SUNNYVALE, CALIFORNIA

MSFC-DRL No. 216
Line Item No. 4

LMSC-A989142
ACS-124
2 June 1971

FINAL REPORT

STUDY OF ALTERNATE SPACE SHUTTLE CONCEPTS

VOLUME II - PART I

CONCEPT ANALYSIS AND DEFINITION

Contract NAS 8-26362

Prepared for George C. Marshall Space Flight Center
by Manned Space Programs, Space Systems Division

LOCKHEED MISSILES & SPACE COMPANY
SUNNYVALE CALIFORNIA

PRECEDING PAGE BLANK NOT FILMED

FOREWORD

This is the final report of a Phase A Study of Alternate Space Shuttle Concepts by the Lockheed Missiles & Space Company (LMSC) for the National Aeronautics and Space Administration George C. Marshall Space Flight Center (MSFC). The eleven-month study, which began on 30 June 1970, is to examine the stage-and-one-half and other Space Shuttle configurations and to establish feasibility, performance, cost, and schedules for the selected concepts. This final report consists of four volumes as follows:

Volume I	–	Executive Summary
Volume II	–	Concept Analysis and Definition
Volume III	–	Program Planning Data
Volume IV	–	Cost Data

PRECEDING PAGE BLANK NOT FILMED

CONTENTS

PART I

Section		Page
	CONDENSED CONTENTS OF REPORT	xi
1	INTRODUCTION AND SUMMARY	1-1
	1.1 Background	1-1
	1.2 Study Results	1-2
	1.3 Study Conclusions and Recommendations	1-23
2	STAGE-AND-ONE-HALF SYSTEM	2-1
	2.1 Requirements, Groundrules, and Assumptions	2.1-1
	2.2 Summary of LS 200-10 System Characteristics	2.2-1
	2.2.1 General Design Considerations, Operations and Performance	2.2-1
	2.2.2 Droptank System and Droptank - Orbiter Interface Characteristics	2.2-36
	2.2.3 Orbiter Design Characteristics	2.2-39
	2.2.4 System Design and Performance Characteristics Summary Tables	2.2-57
	2.3 Summary of LS 200-5 System Characteristics	2.3-1
	2.4 Performance and Sizing	2.4.1-1
	2.4.1 System Sizing	2.4.1-1
	2.4.2 Ascent Trajectory	2.4.2-1
	2.4.3 Payload Performance	2.4.3-1
	2.4.4 Airbreather Performance	2.4.4-1
	2.4.5 Re-entry Trajectory	2.4.5-1
	2.4.6 System Sensitivities	2.4.6-1
	2.4.7 Ferry Capability	2.4.7-1
	2.4.8 Performance Dispersions	2.4.8-1
	2.5 System Design	2.5-1
	2.5.1 LS 200-5 System	2.5-1
	2.5.2 LS 200-10 System	2.5.2-1
	2.5.3 Droptank System	2.5.3-1

Section

		Page
2.6	Aerodynamics	2.6-1
2.6.1	Introduction	2.6-1
2.6.2	Aerodynamic Requirements	2.6-1
2.6.3	Configuration Description (Orbiter)	2.6-1
2.6.4	Flight Characteristics	2.6-3
2.6.5	Aerodynamic Requirements (Launch Vehicle)	2.6-7
2.6.6	Configuration Description (LV)	2.6-7
2.6.7	Flight Characteristics (LV)	2.6-7
2.7	Aerothermodynamics	2.7-1
2.7.1	Aerothermodynamic Prediction Methods	2.7-1
2.7.2	Entry Heating Boundaries	2.7-3
2.7.3	Entry Thermal Environment	2.7-5
2.7.4	Thermal Protection System	2.7-12
2.8	Structures	2.8-1
2.8.1	Introduction	2.8-1
2.8.2	Materials	2.8-2
2.8.3	Structural Criteria	2.8-10
2.8.4	Structural Loads	2.8-17
2.8.5	Structural Arrangement	2.8-28
2.9	Propulsion	2.9-1
2.9.1	Main Propulsion System	2.9-1
2.9.2	Orbit Maneuvering Propulsion System	2.9-14
2.9.3	Attitude Control Propulsion System	2.9-19
2.9.4	Airbreathing Propulsion System	2.9-26
2.10	Power Systems	2.10-1
2.10.1	Electrical Power System	2.10-1
2.10.2	Hydraulic Power System	2.10-6
2.11	Environmental Control/Life Support System	2.11-1
2.11.1	Atmosphere Supply and Control	2.11-11
2.11.2	Thermal and Humidity Control	2.11-12

Page intentionally left blank

Section		Page
2.11.3	Carbon Dioxide and Trace Contaminant Control	2.11-13
2.11.4	Food and Water	2.11-13
2.11.5	Waste Management, Personal Hygiene, First Aid	2.11-14
2.12	Avionics Systems	2.12-1
2.12.1	Data Management System	2.12-2
2.12.2	Guidance Navigation	2.12-4
2.12.3	Communications	2.12-7
2.12.4	Control Display	2.12-10
2.12.5	Software	2.12-14
2.13	Flight Control System	2.13-1
2.13.1	Vehicle Control During Ascent	2.13-1
2.13.2	Vehicle Control During Approach and Landing	2.13-10
2.13.3	Actuation Requirements	2.13-14

PRECEDING PAGE BLANK NOT FILMED

CONDENSED CONTENTS OF REPORT

VOL. I

Section			Page
1	INTRODUCTION		1-1
2	STUDY OBJECTIVES		2-1
3	RELATIONSHIP TO OTHER NASA EFFORTS		3-1
4	METHOD OF APPROACH AND PRINCIPAL ASSUMPTIONS		4.1-1
	4.1	Stage-and-One-Half System	4.1-1
	4.2	Two-Stage System	4.2-1
	4.3	Incremental Two-Stage Development	4.3-1
	4.4	Mission Requirements and Main Rocket Performance	4.4-1
5	BASIC DATA GENERATED AND SIGNIFICANT RESULTS		5.1-1
	5.1	Stage-and-One-Half System	5.1-1
	5.2	Two-Stage	5.2-1
	5.3	Incremental Two-Stage Development	5.3-1
	5.4	Concept Cost and Schedule Comparisons	5.4-1
6	STUDY CONCLUSIONS		6.1-1
	6.1	Stage-and-One-Half System	6.1-1
	6.2	Delta-Body Orbiter	6.2-1
7	STUDY LIMITATIONS		7-1
8	IMPLICATIONS FOR RESEARCH		8-1
9	SUGGESTED ADDITIONAL EFFORTS		9-1

VOL. II

PART I

Section		Page
1	INTRODUCTION AND SUMMARY	1.1-1
	1.1 Background	1.1-1
	1.2 Study Results	1.1-2
	1.3 Study Conclusions and Recommendations	1.1-23
2	STAGE-AND-ONE-HALF SYSTEM	2-1
	2.1 Requirements, Groundrules, and Assumptions	2.1-1
	2.2 Summary of LS 200-10 System Characteristics	2.2-1
	2.3 Summary of LS 200-5 System Characteristics	2.3-1
	2.4 Performance and Sizing	2.4-1
	2.5 System Design	2.5-1
	2.6 Aerodynamics	2.6-1
	2.7 Aerothermodynamics	2.7-1
	2.8 Structures	2.8-1
	2.9 Propulsion	2.9-1
	2.10 Power Systems	2.10-1
	2.11 Environmental Control/Life Support System	2.11-1
	2.12 Avionics Systems	2.12-1
	2.13 Flight Control System	2.13-1

VOL. II

PART II

2	STAGE-AND-ONE-HALF SYSTEM (Cont)	
	2.14 Mass Properties	2.14-1
	2.15 Droptank System	2.15-1
	2.16 Safety and Abort	2.16-1
	2.17 Operations	2.17-1

VOL. II

PART II

Section		Page
2	STAGE-AND-ONE-HALF SYSTEM (Cont)	
	2.18 Development Test	2.18-1
	2.19 System Costs	2.19-1
	2.20 Separation Analysis	2.20-1
3	TWO-STAGE SYSTEM	3-1
	3.1 Requirements, Groundrules, Assumptions	3.1-1
	3.2 Summary of LS 400-7A System	3.2-1
	3.3 Performance and Sizing	3.3.1-1
	3.4 System Design	3.4-1
	3.5 Aerodynamics	3.5-1
	3.6 Aerothermodynamics	3.6-1
	3.7 Structures	3.7-1
	3.8 Propulsion	3.8-1
	3.9 Power and Avionics	3.9-1
	3.10 Mass Properties	3.10-1
	3.11 Operations	3.11-1
	3.12 System Costs	3.12-1
4	CONVERSION SYSTEM	4-1
	4.1 Requirements, Groundrules, and Assumptions	4.1-1
	4.2 General Considerations	4.2-1
	4.3 Alternative Vehicle System Characteristics	4.3-1
	4.4 Technical Conversion Feasibility	4.4-1
	4.5 System Design	4.5-1
	4.6 Structures	4.6-1
	4.7 Propulsion	4.7-1
	4.8 Subsystems	4.8-1
	4.9 Mass Properties	4.9-1
	4.10 Operations	4.10-1
	4.11 System Cost Analysis	4.11-1

VOL. II

APPENDIX A

Reference No.	Engineering Memorandum No.	
2.15.3-1	L2-02-05-M1-5	Summary Droptank Impact Location and Dispersions Analysis
2.15.3-3	L2-02-05-M1-4	Six-Degree-of-Freedom Analysis of Body Motion and Trajectory Dynamics of a Single LS 200-5 Droptank
2.15.3-4	L2-02-01-M1-4	LS 200-5 Single Droptank Aerodynamic Characteristics
2.15.3-5	L2-02-05-M1-2	Stage-and-One-Half Droptank Impact Envelopes for NASA Design Mission Launch Trajectory
2.15.3-7	L2-02-05-M1-3	Droptank Impact Variation - High Altitude Staging Conditions
2.15.3-8	L2-02-01-M1-5	Droptank Dispersion Study - Thermostructural Analysis
2.15.3-9	L2-05-05-M3-2	Determination of Droptank Impact Hazards
2.15.3-11	L2-05-03-M3-3	Determination of Costs Required to Reduce Droptank Impact Hazards
2.15.3-13	L2-05-02-M1-2	Effects of Droptank Polyurethane Foam Insulation Decomposition

VOL. II

APPENDIX B

	L2-01-06-M1-1B	Electrical Power System Preliminary Baseline For Stage-and-One-Half Including Redundancy
	L2-01-03-M1-1B	Data Management System Preliminary Baseline For Stage-and-One-Half Including Redundancy
	L2-01-03-M1-5	Incremental Two-Stage Avionics Development Analysis

APPENDIX B (CONT'D)

Reference No.	Engineering Memorandum No.	
	L-1-02-10-M1	Establishment of Orbiter Structural Design Criteria
	L2-11-01-M1-1	Finite Element Modeling and Structural Sizing for the LS 400-7 Two-Stage Orbiter Fuselage Structure
	L2-11-04-M5-1	Two-Stage Delta-Body Orbiter Tanks Structural Analysis Model LS 400-7

VOL. III

Section		Page
1	INTRODUCTION	1-1
2	PROGRAM PLANNING REQUIREMENTS	2-1
	2.1 Program Integration	2.1-1
	2.2 Management	2.2-1
	2.3 Engineering	2.3-1
	2.4 Manufacturing	2.4-1
	2.5 Test	2.5-1
	2.6 Operations	2.6-1
	2.7 Facilities	2.7-1
	2.8 Support Services	2.8-1
	2.9 Personnel Systems	2.8-1
	2.10 Quality Assurance	2.9-1
	REFERENCES	2.9-2
3	SUPPORTING RESEARCH AND TECHNOLOGY	3-1

VOL. IV

1	INTRODUCTION	1-1
2	GENERAL COSTING ASSUMPTIONS	2-1
3	STAGE-AND-ONE-HALF ($1\frac{1}{2}$-B System) COST	3-1
	3.1 Costing Assumptions	3-1
	3.2 Cost Summary	3-2
	3.3 Detailed Cost Estimates (Form A)	3-2
	3.4 Funding Schedules (Form D)	3-27
	3.5 Stage-and-One-Half Technical Characteristics Data	3-33

VOL. IV

Section			Page
4	TWO-STAGE (2-B System) COST ANALYSIS		4-1
	4.1	Costing Assumptions	4-1
	4.2	Cost Summary	4-3
	4.3	Detailed Cost Estimates (Form A)	4-4
	4.4	Funding Schedules (Form D)	4-31
	4.5	Two-Stage Technical Characteristics Data	4-37
5	CONVERSION SYSTEM ($1\frac{1}{2}$-C/2-C) COST ANALYSIS		5-1
	5.1	Costing Approach	5-1
	5.2	Costing Assumptions	5-2
	5.3	Cost Summaries	5-3
	5.4	Detailed Cost Estimates (Form A)	5-22
	5.5	Funding Schedules (Form D)	5-22
	5.6	Conversion System Technical Characteristics Data	5-27
6	PROGRAM COST COMPARISON		6-1
7	CONCLUSIONS		7-1

Section 1

INTRODUCTION AND SUMMARY

1.1 BACKGROUND

This is Volume II of the final report on Lockheed's Phase A Study of Alternate Space Shuttle Concepts. The eleven-month study, which began on 30 June 1970, was initially to study stage-and-one-half concepts and arrive at one or more preferred configurations for the low and high crossrange requirements (200 and 1500 nautical miles).

At the fourth month of the study, a preferred, lifting-body configuration for both crossrange requirements was selected by LMSC and approved by NASA for further design and analysis. Then, at the end of the sixth month of the study, NASA directed that the remaining effort be applied to three specific tasks: (1) Droptank Impact and Dispersion, (2) Growth to Two-Stage, and (3) Continuation of Stage-and-One-Half System Analysis. The second of these tasks, Conversion to Two-Stage, involved the study of a stage-and-one-half system which could subsequently be converted to a two-stage, fully reusable system.

Three different space shuttle systems have been defined and analyzed as a result of this study. The first is a stage-and-one-half system optimized to meet program requirements. The second is a two-stage, fully reusable system also designed to meet program requirements. The third is a convertible system which operates initially as a stage-and-one-half system and is subsequently converted to a two-stage, fully reusable system by reconfiguration of the orbiter vehicle and development of a booster vehicle. The design and performance of this third system must necessarily be compromised somewhat to facilitate the conversion. The body of this report treats each of these three systems in order. For each system, the applicable requirements, groundrules and assumptions

are defined. Then the characteristics of that system are listed and a detailed description and analysis of the system is presented. Finally, a cost analysis for the system is shown. At the back of this volume and in each of the other volumes of this report is a foldout Design Evolution Diagram which depicts the various configurations evolved during the study and their differences and relationships to the study. It is suggested that the reader unfold this chart for easy reference while studying the report.

During the seventh month of the study, NASA made significant changes in some of the Level 1 Space Shuttle requirements which forced a redesign of the systems. The most important of these changes include: (1) the change from the 415K lb to the 550K lb thrust main engine, (2) the change from the high and low cross-range requirement to a single, 1100 nm crossrange requirement, (3) the addition of a due east launch, 65K payload mission and a south polar launch, 40K payload mission, and (4) the use of JP-4 instead of LH_2 fuel for the air-breathing engines. Each of the three systems presented in this report meets the new Level 1 requirements. In the stage-and-one-half system section, an additional configuration, the LS 200-5, is presented which meets the Space Shuttle requirements as defined at the beginning of the study.

Late in the ninth month of the study, another task was added which extended the contract period for one more month to the end of June 1971. This additional task is for the study of external liquid hydrogen tanks for a two-stage space shuttle orbiter. Since this new task is quite independent of the other portions of the study, it will be covered in a separate, addendum report to be delivered at the end of the study and will not be treated in this report.

1.2 STUDY RESULTS

A comprehensive summary of the results of the study is included in Volume I, Executive Summary, of the report. That document also presents the Lockheed conclusions and recommendations resulting from the study. A brief summary of the study results, showing the system configurations and comparing their performance and costs is presented here.

During the first three months of the study, a comprehensive analysis and trade-off study was performed to derive the best stage-and-one-half system in terms of performance and cost. This study examined straight wing, delta wing, and delta body configurations for both the low and high crossrange application. The study showed that the delta body configuration was superior to all others examined from the standpoint of weight, aerodynamic performance, and cost. It was shown to be superior for both the low and the high crossrange application.

The lifting body configuration was further refined during the ensuing two months and a recommended configuration, the LS 200-5, was presented at the midterm review on 1 Dec. This configuration is shown in Fig. 1.2-1. Figure 1.2-2 is an inboard profile of the LS 200-5 orbiter vehicle. A summary weight statement for this configuration (as of 1 Dec 1970) is shown in Table 1.2-1. Table 1.2-1 shows a 27,115 lb payload capability to the reference high crossrange mission (against a 25,000 lb requirement) for a gross liftoff weight of 3.52 million lb. The same vehicle to the low crossrange mission has a payload capability of 40,648 lb.

In support of the vehicle system design during the first five months of the study, a number of trade studies and analyses were performed: These included the following:

1. A comparison of droptank configurations showed the V-shaped tank configuration to be lowest in weight.
2. A comparison of upward rotation vs downward rotation of the droptanks for separation showed upward rotation to be lower in system weight.
3. A detailed study of expendable vs recoverable droptanks showed the expendable tanks to be more cost effective.
4. A comparison of internal vs external LO_2 lines from the droptanks to the vehicle showed the internal lines to be more cost effective.
5. A comparison of active vs passive TPS and metallic vs nonmetallic TPS showed the passive, nonmetallic system to be lower risk and lower cost.

Fig. 1.2-1

BASELINE VEHICLE SYSTEM (LS 200-5)

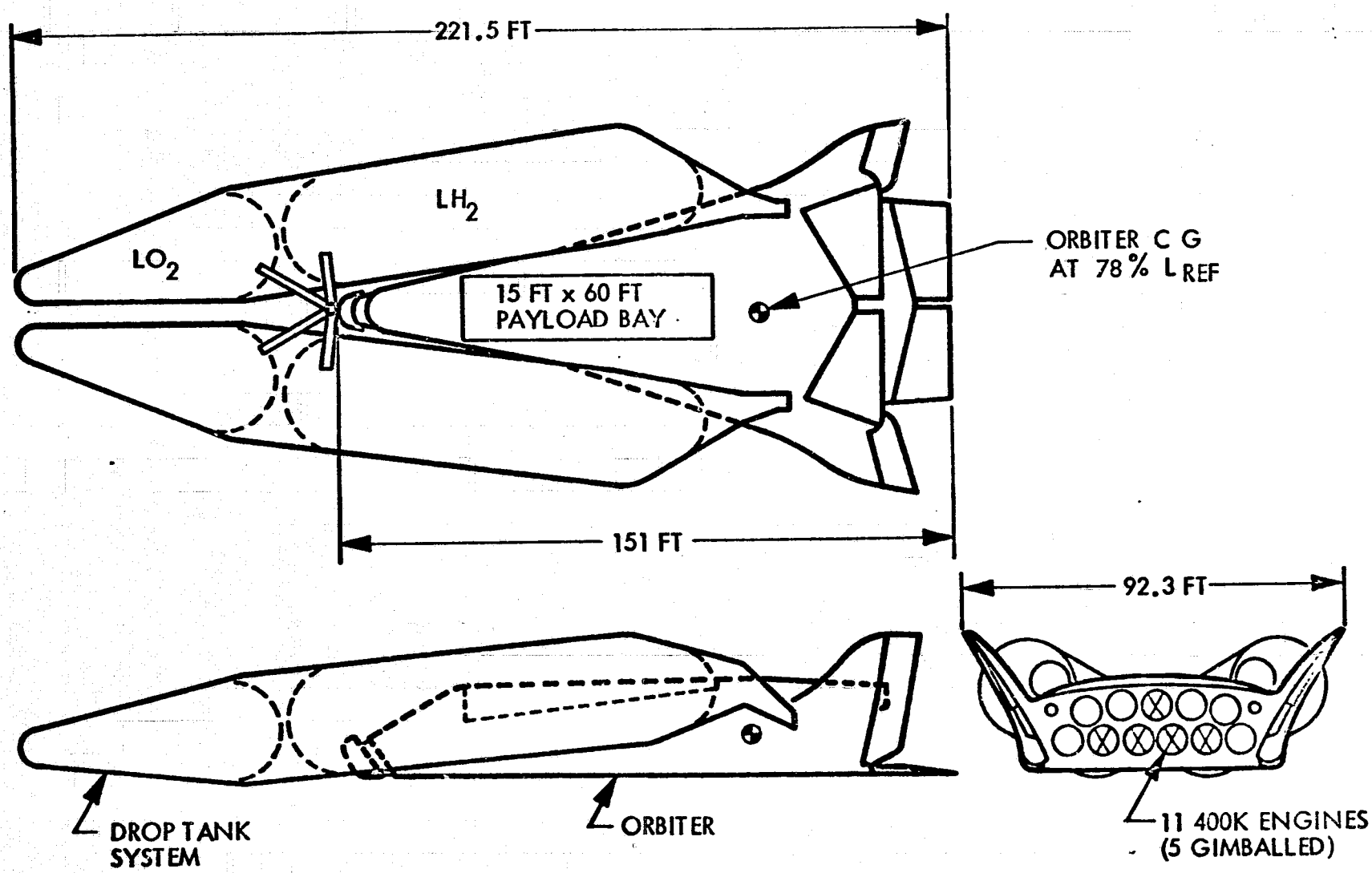

Fig. 1.2-2

LOCKHEED

LS 200-5 ORBITER INBOARD PROFILE

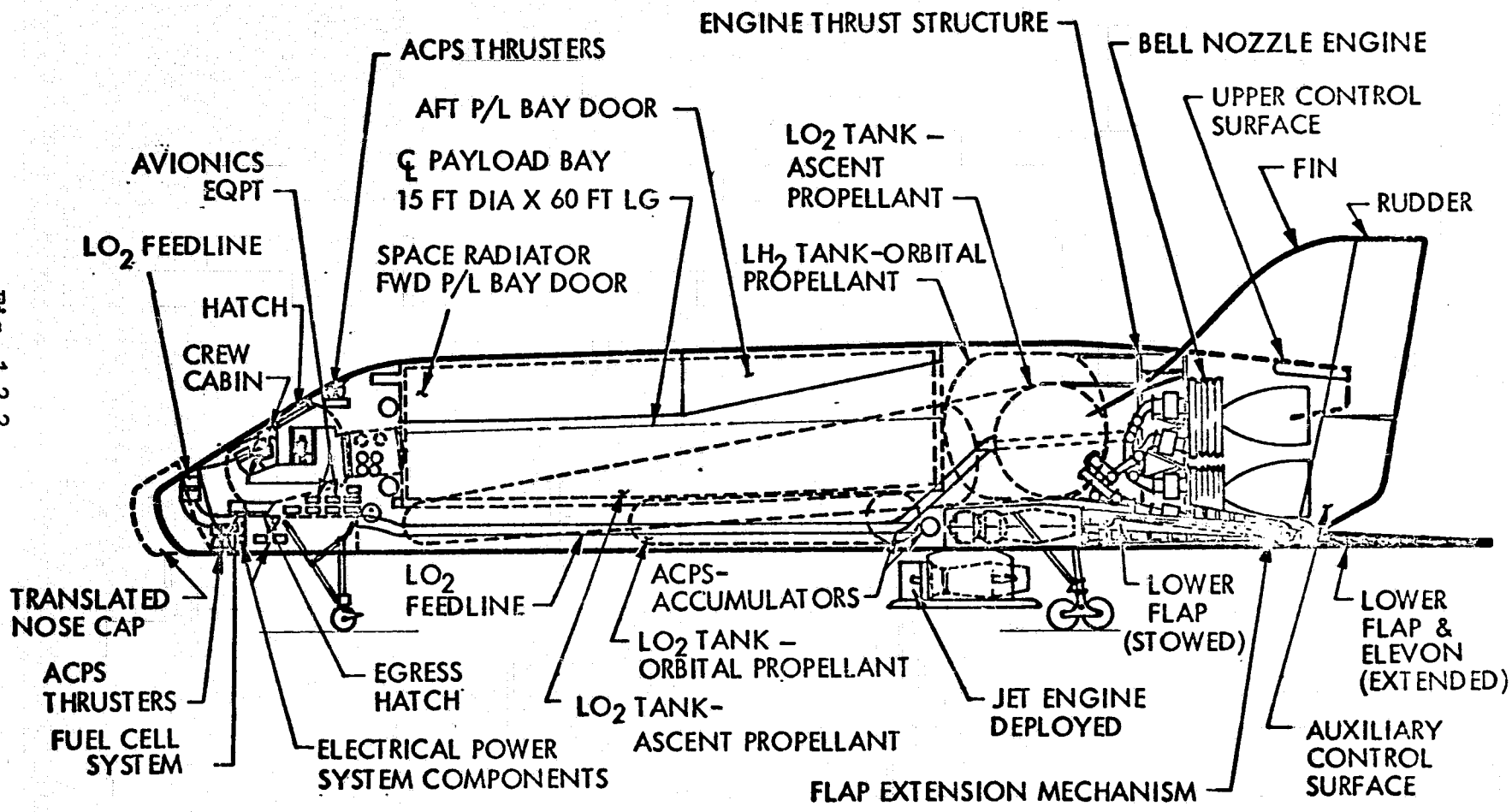

D02229

Table 1.2-1

LOCKHEED

HIGH CROSS RANGE WEIGHT SUMMARY (LS 200-5)

SUBSYSTEM	ORBITER WEIGHT (LB)	DROP TANK WEIGHT (LB)	TOTAL (LB)
AEROSURFACES STRUCTURE	17,897		
*BODY STRUCTURE	52,745	83,198	
THERMAL PROTECTION	40,860	4,058	
LANDING GEAR	11,154		
PROPULSION – MAIN ASCENT	87,223	5,729	
PROPULSION – AIRBREATHING	16,550		
PROPULSION – MANEUVER/ACPS	7,292		
PRIME POWER SOURCES	1,620		
ELECTRICAL SYSTEM	3,704		
HYDRAULICS	2,073		
SURFACE CONTROLS	3,810		
AVIONICS	3,762	301	
ENVIRONMENTAL CONTROL	1,274		
PERSONNEL PROVISIONS	210		
CONTINGENCY (10 PERCENT LESS ICD ENG)	19,253	9,329	
DRY WEIGHT	269,427	102,615	
PERSONNEL AND EFFECTS	725		
PAYLOAD	27,115		
RESERVES, RESIDUALS, AND LOSSES	20,517	8,612	
PROPELLANT – ASCENT	191,700	2,859,637	
PROPELLANT – AIRBREATING	3,477		
PROPELLANT – MANEUVER/ACPS	36,175		
LAUNCH WEIGHT	549,136	2,970,864	3,520,000

*INCLUDES 1200 LB PENALTY FOR 70K PAYLOAD CAPABILITY

6. A comparison of aluminum vs all-titanium fuselage structure showed that most of the fuselage should be of aluminum for lowest system weight.

7. A comparison of helium vs autogenous propellant tank pressurization systems showed the autogenous system to be more cost effective.

8. A comparison of cascade vs parallel (or manifolded) propellant feed systems showed that cascade feed of the LO_2 and manifolded feed of the LH_2 was lowest in weight.

9. A comparison of JP vs LH_2 fuel for the airbreathing propulsion system showed LH_2 to provide a lower program cost.

10. A comparison of steel, aluminum, titanium, and beryllium for the thrust structure showed titanium to be best from a weight and risk standpoint.

11. A comparison of ACPS thrusters use vs RL-10 engines for orbit maneuvers showed the RL-10's to be lower in system weight.

12. Attitude control propulsion system (ACPS) studies examined thruster size, number, and locations; valve types; propellant pressure; propellant storage and feed systems; and redundancy analyses. The study showed that a high-pressure gas system was lower in system weight than a low-pressure system.

13. Electrical power system (EPS) studies examined fuel cell, APU, and airbreather engine-driven power sources; power conversion and power inversion systems; aluminum vs copper power distribution busses; and redundancy analyses.

14. Primary engine gimballing studies showed that only five of the eleven main engines needed to be gimballed ($\pm$ 7 deg) and the remaining six could be fixed.

15. Preliminary engine expansion ratio studies showed that the engines could utilize a 53:1 expansion ratio fixed nozzle for best performance and for preventing plume impingement on aft surfaces. The ICD engine at 35:1 expansion ratio had been optimized for booster performance.

16. Hydraulic power system studies showed that the use of vehicle-supplied hydraulic power for engine gimballing and for aerodynamic control surface actuation was lower in weight than having hydraulic pumps on the main engines for gimbal actuation.

17. Avionics system studies showed that a combination of centralized and dedicated data processing equipment provided the most viable vehicle data management system.

18. A ground operation analysis was performed to derive facility and operations costs associated with operation from KSC, WTR, and from a new, inland site. For the 445 flight mission model, modification of KSC facilities provided the lowest program cost.

19. A comparison of costs associated with manufacturing the droptanks at the Michoud facilities and shipping them by barge to KSC vs building a facility to manufacture them at KSC, showed that using the Michoud facility provided a lower program cost.

Most of these trade studies as well as many others conducted under the study, are documented in detail in the monthly progress reports furnished under the contract and will not be detailed in this report. A total of 2862 pages of documentation are included in the nine monthly progress reports delivered to date. In addition, approximately 1800 presentation charts used in the nine monthly program reviews have been delivered to NASA MSFC.

Work on the study since the redirection in January, 1971, has resulted in the derivation of three space shuttle systems, all meeting the 20 January, Level 1 system requirements. These systems are a conventional stage-and-one-half system derived from the LS 200-5, a conventional two-stage system, and a stage-and-one-half system which can be converted to a two-stage system.

The stage-and-one-half system, designated LS 200-10, is shown in Fig. 1.2-3. A more detailed three-view drawing of the orbiter is shown in Fig. 1.2-4. Table 1.2-2 summarizes the major weight and performance values for the LS 200-10

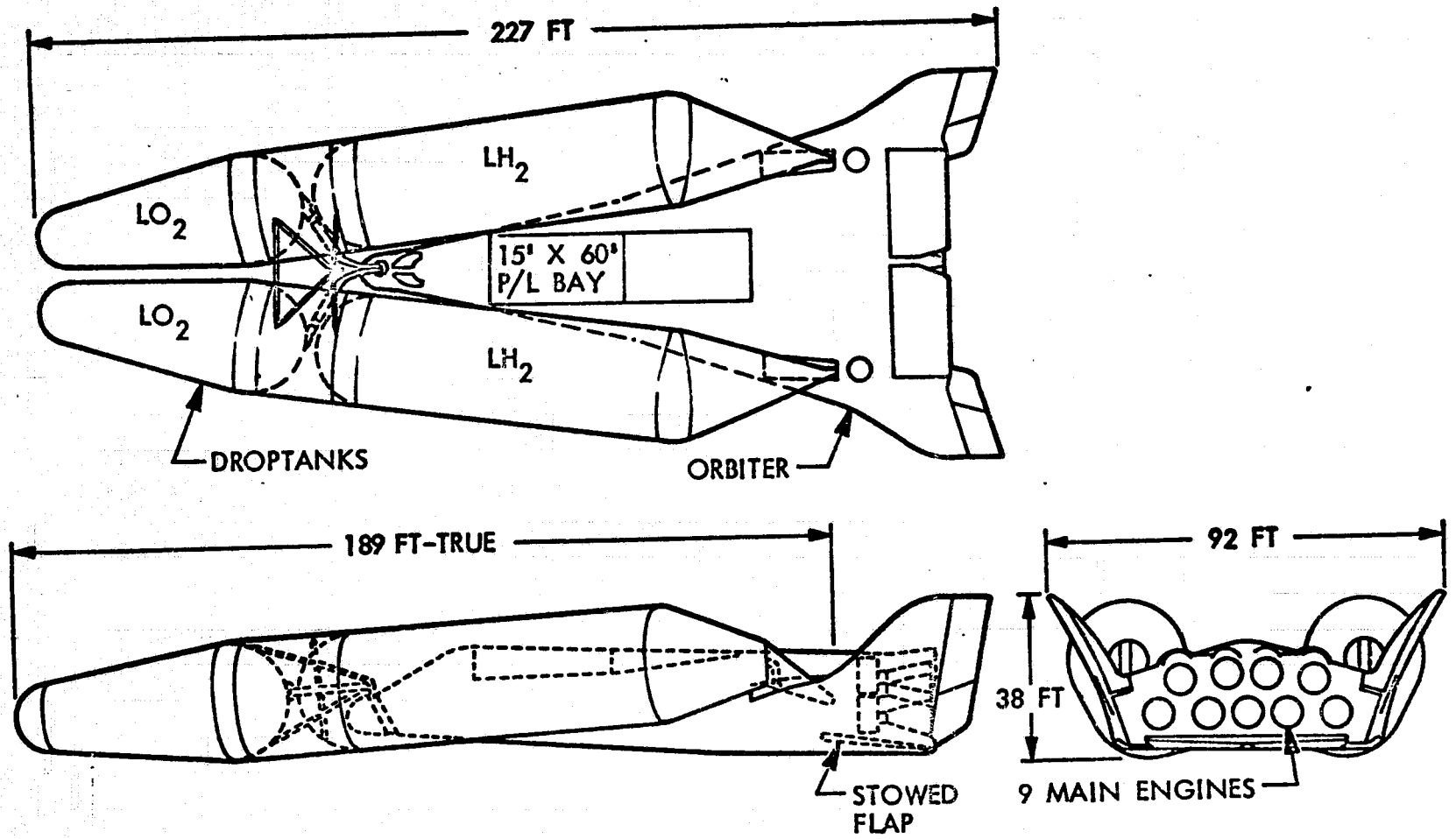

Fig. 1.2-3

Figure 1.2-3

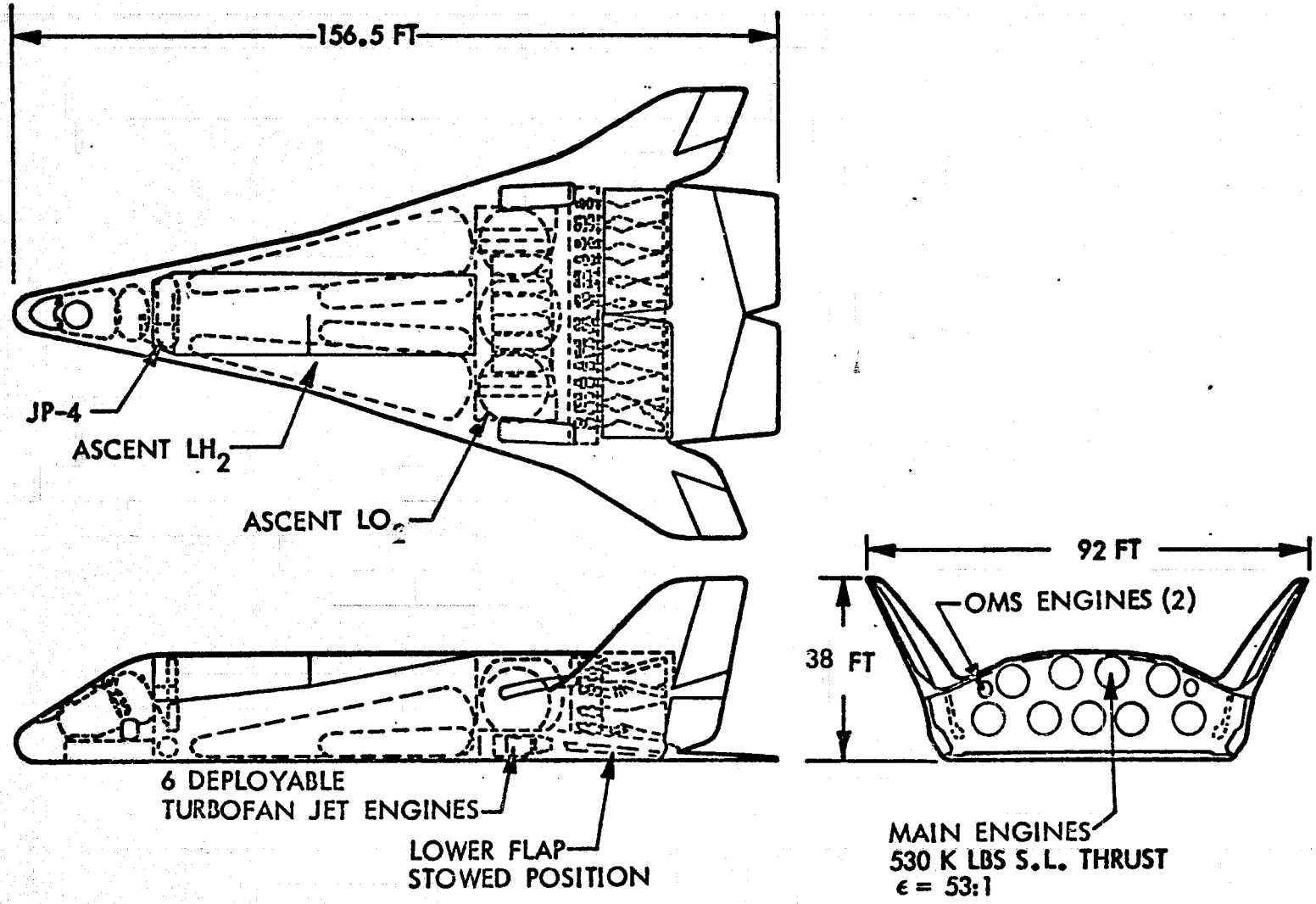

Fig. 1.2-4

Figure 1.2-4

Table 1.2-2

LS 200-10 PERFORMANCE SUMMARY

MISSION PARAMETER	DUE EAST LAUNCH 100 NM	SOUTH POLAR LAUNCH 100 NM	55 DEG INCL. 270 NM ORBIT
PAYLOAD - (10^3 LB)	65	40	25
GLOW - (10^6 LB)	3.45	3.59	3.81
ORBITER DRY WEIGHT (10^3 LB)	270	270	294
DROPTANKS DRY WEIGHT (10^3 LB)	112	112	112
ORBITER LAUNCH WEIGHT (10^3 LB)	614	588	630
ON-ORBIT ΔV (FT/SEC)	650	650	1500
STAGING VELOCITY (IDEAL) (FT/SEC)	22034	23107	23107
AIRBREATHING SYSTEM WT (10^3 LB)	0	0	30.1
LANDING WEIGHT W/O PAYLOAD, (10^3 LB)	274.4	274.4	300.4

Table 1.2-2

for the new design mission and for the two reference missions. As shown in the table, the 55° inclined orbit mission, with the 25,000 lb payload and go-around capability, sizes the system. It has excess capability for the other two missions, hence the droptanks are offloaded and the GLOW is correspondingly reduced as shown in the Table.

The two-stage system, designated LS 400-7A is shown in Fig. 1.2-5. It comprises a delta body orbiter and a booster design based on the McDonnell Douglas booster as reported in March 1971 documents. No booster design effort has been applied to the study. The McDonnell Douglas booster was simply scaled to the required size. Figure 1.2-6 is a three-view of the LS 400-7A orbiter. Table 1.2-3 summarizes the performance and weights for the two-stage, LS 400-7A system. Here the system is sized by the south polar launch, 40K payload mission; particularly by the requirement to abort to orbit with one engine out. It should be noted that the system shown here is not fully optimized. A true optimization would involve scaling both the orbiter and the booster down in size to produce the lowest weight or lowest cost system.

The convertible stage-and-one-half orbiter is shown in Fig. 1.2-7. As a stage-and-one-half system, it employs nine primary engines and for the two-stage system the engines, propellant tanks, and thrust structure are replaced as shown in the figure. Table 1.2-4 shows the performance of the system in both the stage-and-one-half and two-stage configurations. The performance of these convertible system configurations is not directly comparable with the baseline systems shown above because there was an additional design iteration in the baseline systems, reflecting more refined requirements, structures, and weights analyses. However, the conclusions drawn from the study regarding the convertible system are still valid.

Cost models for the stage-and-one-half system, the two-stage system, and the convertible system were developed in the study and applied to the derived systems. The cost analyses are based on the costing assumptions shown in Table 1.2-5. A comparison of costs for development plus the 445 flight, ten-year operational program for the stage-and-one-half system and the two-stage system is shown in Table 1.2-6. The stage-and-one-half system totals $8 billion and the two-stage

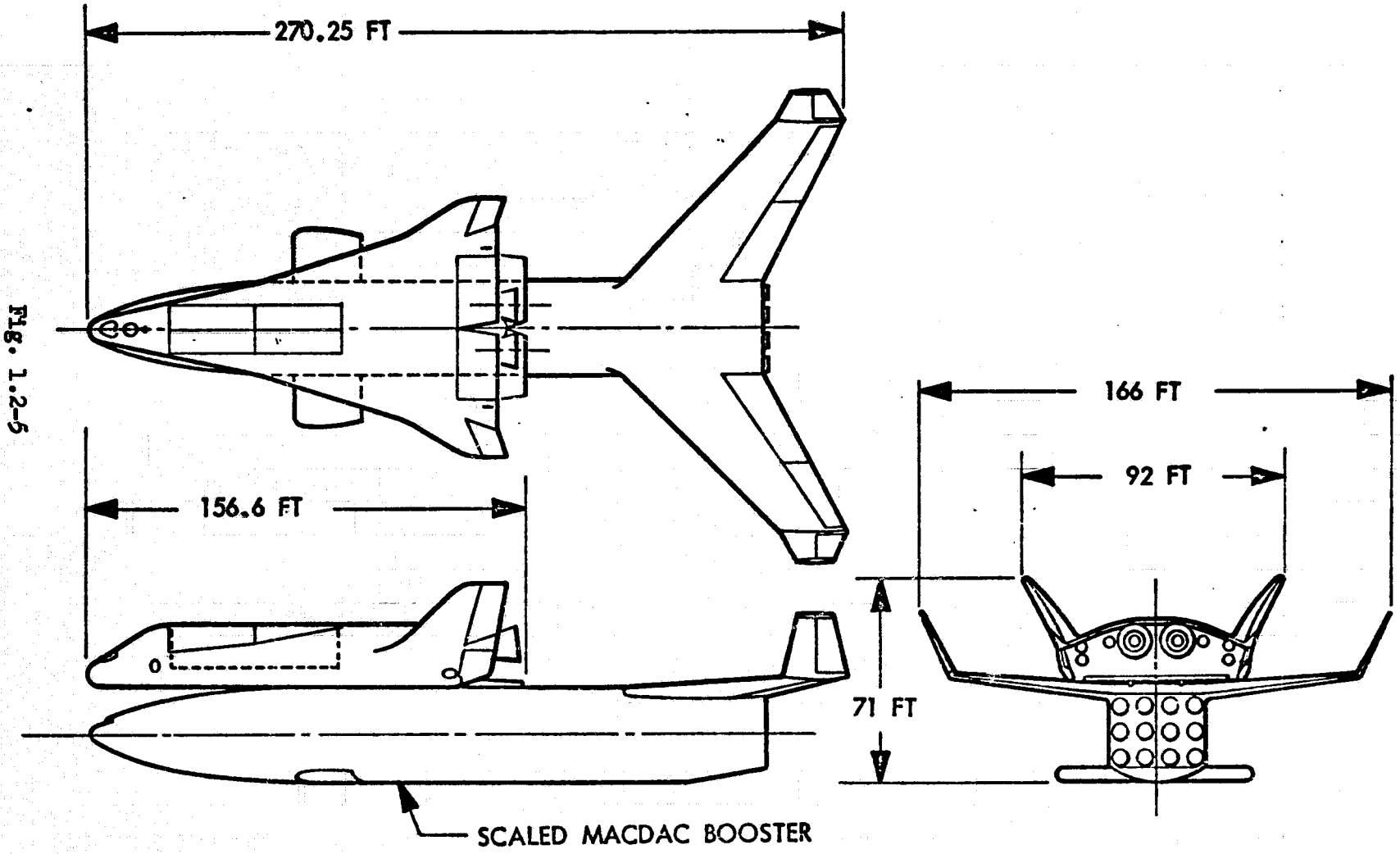

Figure 1.2-5

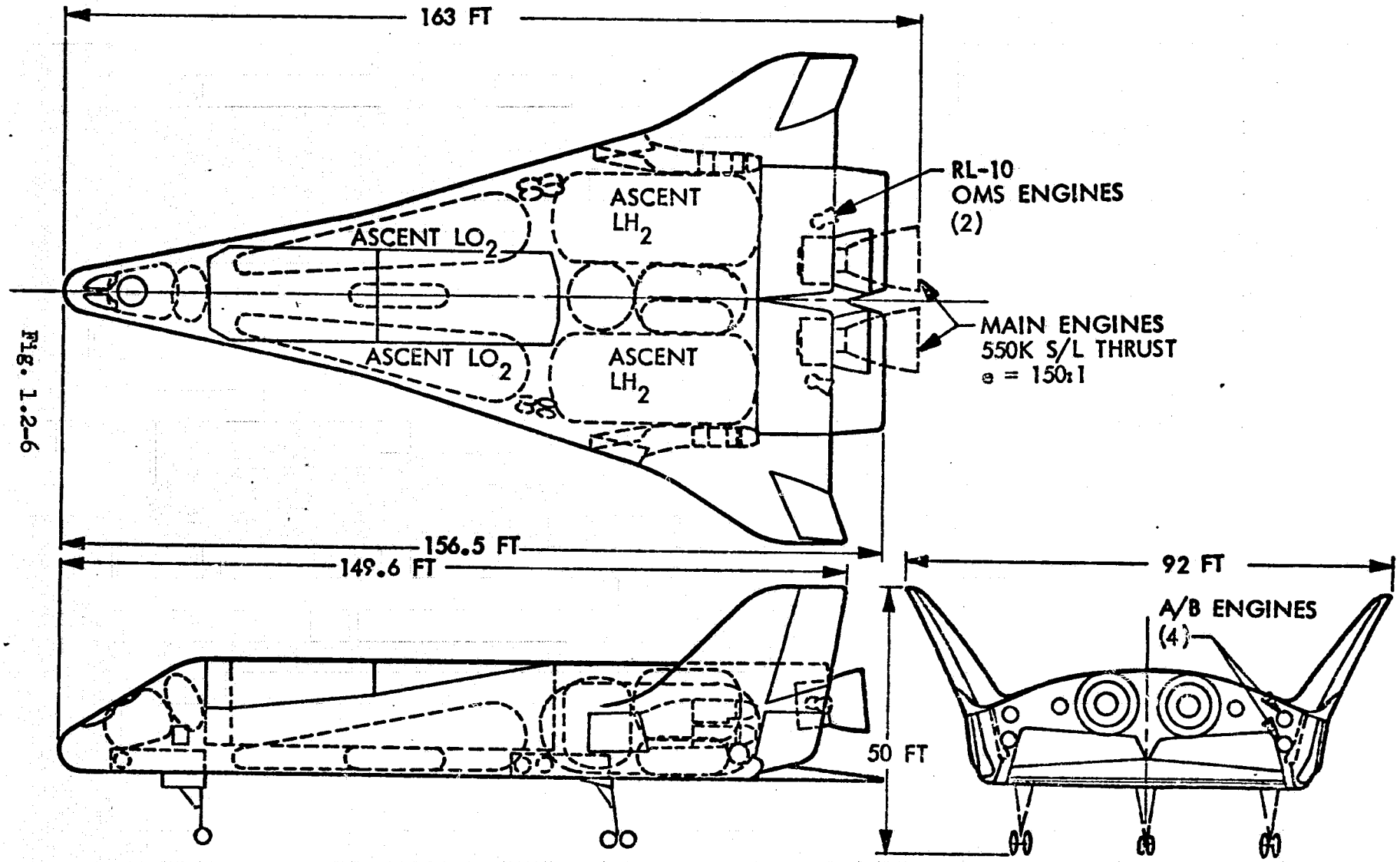

Fig. 1.2-6

1-14

IMSC-A980472
Vol II

D03021

Figure 1.2-6

Table 1.2-3

LS 400-7A PERFORMANCE SUMMARY

Mission Parameter	Due East Launch 100 NM	South Polar Launch 100NM	55 Deg. Incl. 270 NM ORBIT
*PAYLOAD (10^3 LB)	79.6 (65)	40 (40)	36 (25)
** GLOW - (10^6 LB)	4.14	4.12	4.13
ORBITER DRY WEIGHT (10^3 LB)	188	188	206
BOOSTER LAUNCH WEIGHT (10^3 LB)	3287	3292	3289
ORBITER LAUNCH WEIGHT (10^3 LB)	857	831	832
ON-ORBIT ΔV (FT/SEC)	1859	2114	1500
STAGING VELOCITY REL. (FT/SEC)	14649	15689	15644
AIRBREATHING SYSTEM WT. (10^3 LB)	0	0	24.6
LANDING WEIGHT W/O PAYLOAD (10^3 LB)	194	193	212

* Performance capability; the mission requirement is shown in parentheses.

** This GLOW could be reduced by off loading the booster propellant tanks for those missions where the capability exceeds the requirement.

Table 1.2-3

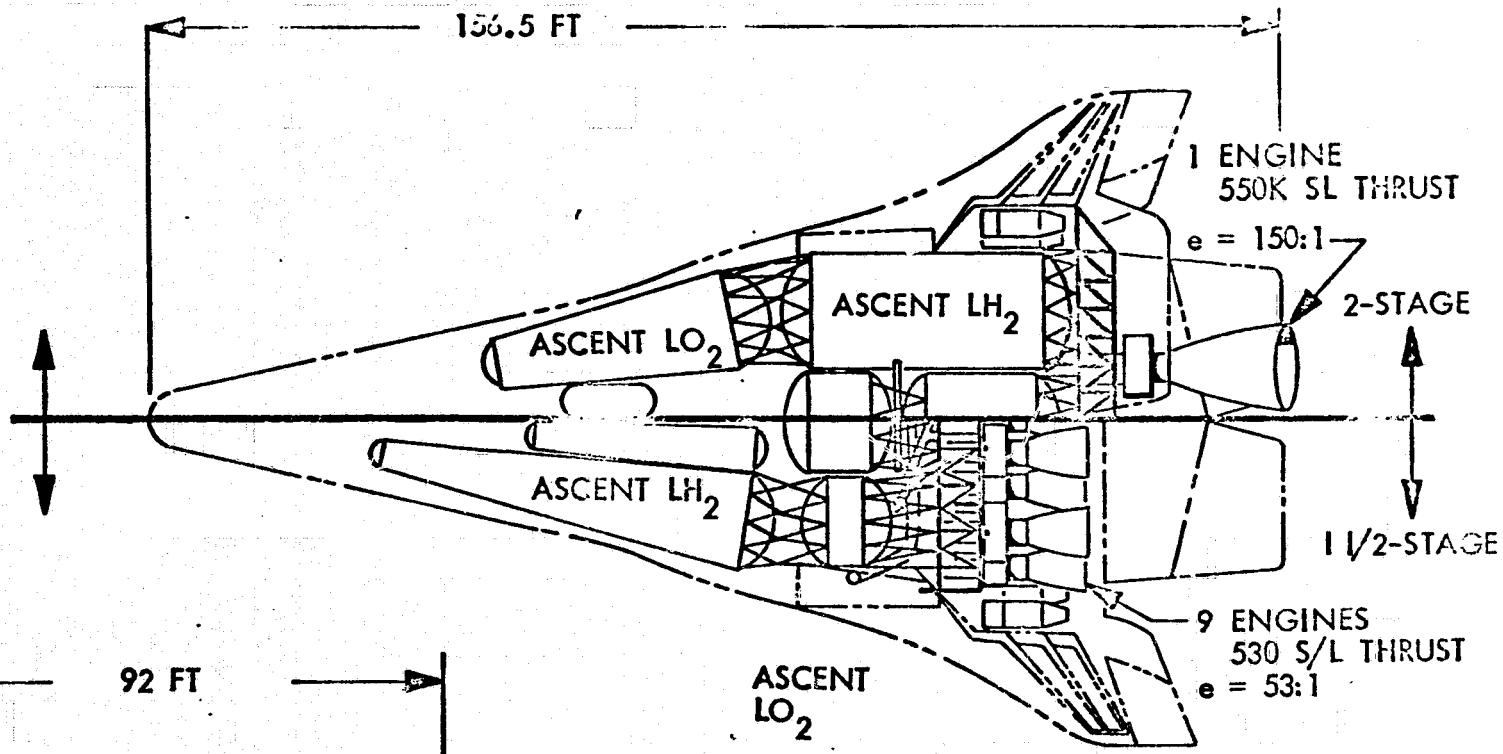

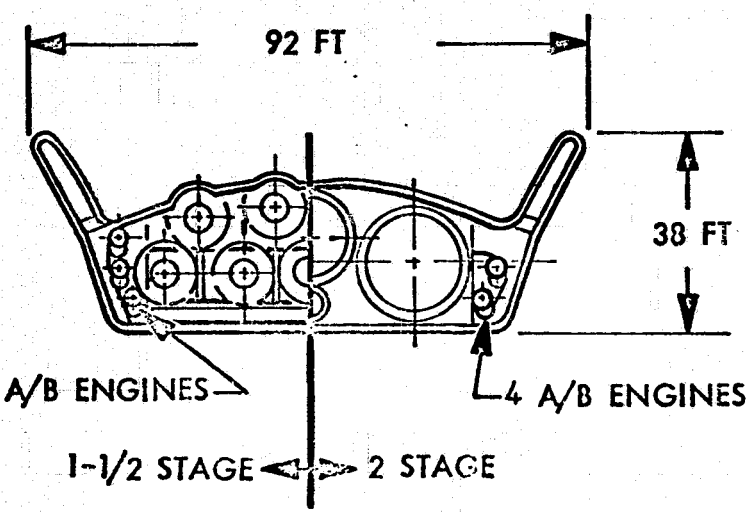

D02041

Figure 1.2-7

Table 1.2-4

CONVERTIBLE SYSTEM PERFORMANCE SUMMARY

Mission	Due East Launch 100 NM		South Polar Launch 100 NM		55 Deg Incl. 270 NM ORBIT	
Configuration	1½-Stage	2-Stage	1½-Stage	2-Stage	1½-Stage	2-Stage
Payload (10^3 LB)	84.6	74.5	39.0	42.8	13.5	25
GLOW (10^6 LB)	3.82	4.21	3.82	4.21	3.82	4.21
Orbiter Dry Wt (10^3 LB)	280	200	280	200	300	212
Droptank/Booster Dry Wt (10^3LB)	122.8	493.5	122.8	493.5	122.8	493.5
Orbiter Launch Wt (10^3 LB)	655	870	620	838	628	844
On-Orbit ΔV (FT/SEC)	650	1000	650	1000	1500	1500
Staging Velocity Rel (FT/SEC)	17500	9000	18000	9400	17900	9380
Airbreathing System Wt (10^3 LB)	0	0	0	0	33	24
Landing Weight W/O Payload (10^3 LB)	286	206	286	206	306.5	218

Table 1.2-4

Table 1.2-5

LOCKHEED

KEY COSTING ASSUMPTIONS

	1-1/2-B	2-B	1-1/2-C	2-C
DDT&E				
NUMBER OF EQUIVALENT GROUND TEST ORBITERS	2	2	2	1
NUMBER OF EQUIVALENT GROUND TEST BOOSTERS	-	2	-	2
NUMBER OF FLIGHT TEST ORBITERS	3	3	2	3
NUMBER OF FLIGHT TEST BOOSTERS	-	3	-	3
NUMBER OF SETS OF TEST DROPTANKS	3	-	3	-
SPARES FACTOR FOR TEST HARDWARE	15%	15%	15%	15%
NUMBER OF OPERATIONAL FACILITIES	1	1	← 1 →	
RECURRING				
FLIGHT TEST ORBITERS USED FOR OPERATIONS	3	3	2	3
FLIGHT TEST BOOSTERS USED FOR OPERATIONS	-	3	-	3
NUMBER OF OPERATIONAL FLIGHTS	445	445	← 445 →	
NUMBER OF PRODUCTION ORBITERS	3	3	0-4	0-3
NUMBER OF PRODUCTION BOOSTERS	-	1	-	1
NUMBER OF ORBITERS CONVERTED	-	-	-	0-3
LEARNING ON TURNAROUND OPERATIONS	90%	90%	90%	90%
GENERAL				
COSTS EXCLUDE NASA IN-HOUSE SUPPORT				
COSTS EXCLUDE CONTRACTOR FEE				
COSTS IN 1970 DOLLARS				

☐ DEPENDENT UPON BOOSTER PHASING

D02L16. (1)

jad

Table 1.2-6

SPACE SHUTTLE TOTAL PROGRAM COST COMPARISON

	STAGE-AND-ONE-HALF SYSTEM	TWO-STAGE SYSTEM
DDT&E	$4.38B	$6.73B
PRODUCTION	0.49	0.56
OPERATIONS	1.27	1.73
DROPTANKS	1.89	-
TOTAL	$8.03B	$9.02B
PEAK ANNUAL FUNDING	$1.16B	$1.82B
FIRST MANNED ORBITAL FLIGHT	4/78	4/78

Table 1.2-6

system, $9 billion. The peak annual funding for the stage-and-one-half system is $1.16 billion and for the two-stage system it is $1.82 billion. The lower cost of the stage-and-one-half system results principally from the lower RDT&E cost associated with the development of only one complex vehicle rather than two. If the traffic model is less than 445 flights, the saving afforded by the stage-and-one-half system is even greater.

Total program costs for the convertible system depend upon the date of the conversion. An analysis was made to define a program which gave a first manned orbital flight (FMOF) date for the stage-and-one-half system of April 1978, and which reduced the peak annual funding to levels more acceptable than those of the pure two-stage. The analysis showed that a delay of four years between FMOF of the stage-and-one-half system and FMOF of the two-stage conversion came closest to meeting the requirements. The total program cost for this conversion system was shown to be $11.0 B and the peak annual funding is $1.29 B. The cumulative costs vs time for all three systems are shown in Fig. 1.2-8 and the annual funding by year for all three systems is shown in Fig. 1.2-9.

Under Task 1, Droptank Impact and Dispersion, a detailed analysis of droptank reentry dynamics, heating, and dispersions was performed. The analysis showed that the addition of about 2,500 lb of insulation to the stage-and-one-half system droptanks would assure their intact reentry. An analysis of ship and aircraft traffic in the 1980 time period showed that the probability of the droptanks impacting a ship or aircraft on a single launch varied between one chance in ten-million and one in one-hundred-thousand, depending upon the launch site and launch azimuth. The system can assure open ocean impact of the droptanks for essentially all launch azimuths and for all orbit inclinations for launches from KSC, WTR, or from the inland site.

The results of the wind tunnel tests on the delta body orbiter configuration showed that the vehicle exhibits neutral or better longitudinal and directional stability subsonically and hypersonically for all required flight attitudes.

OVERALL CUMULATIVE COST COMPARISON

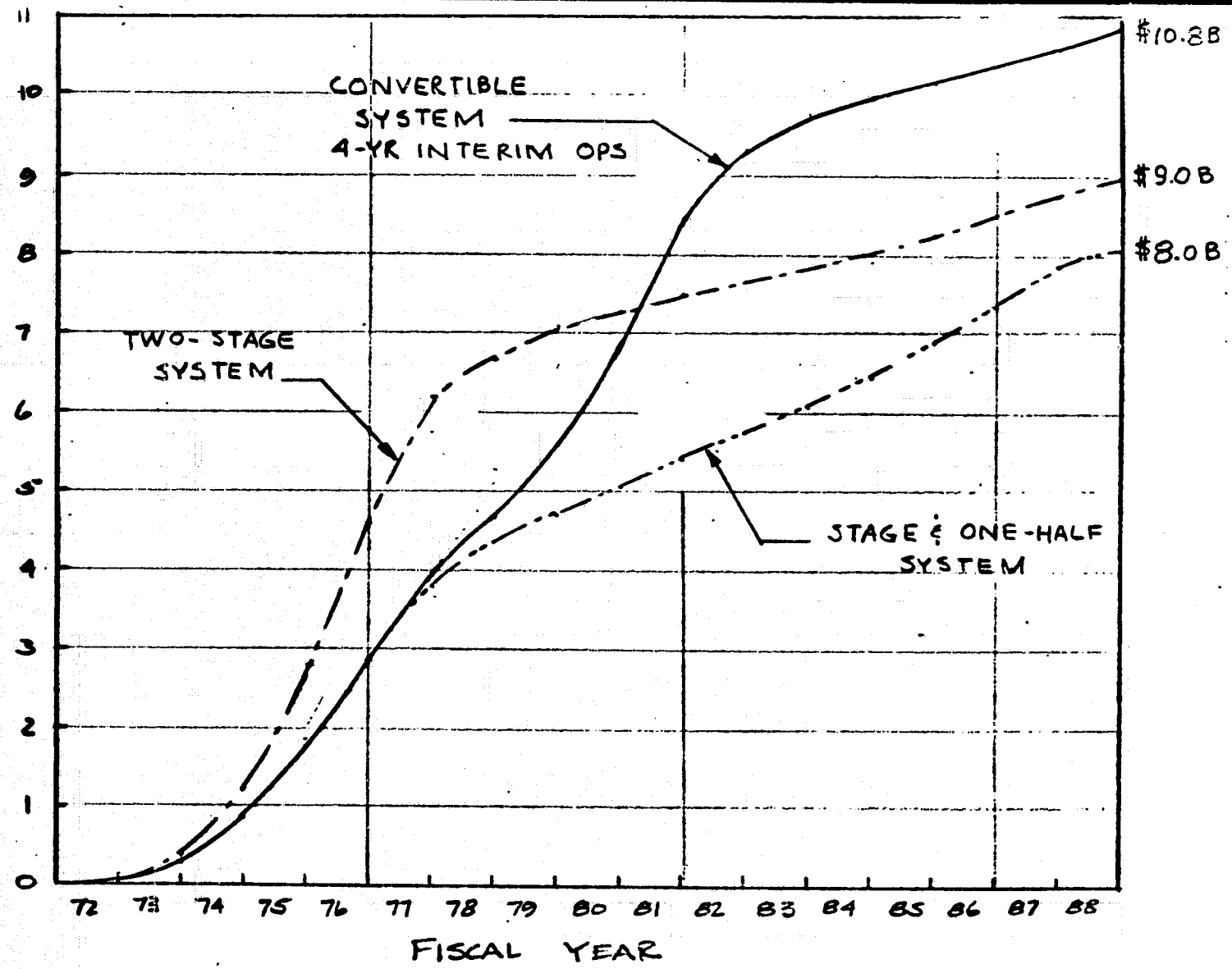

Fig. 1.2-8

D02856 (1)
jad

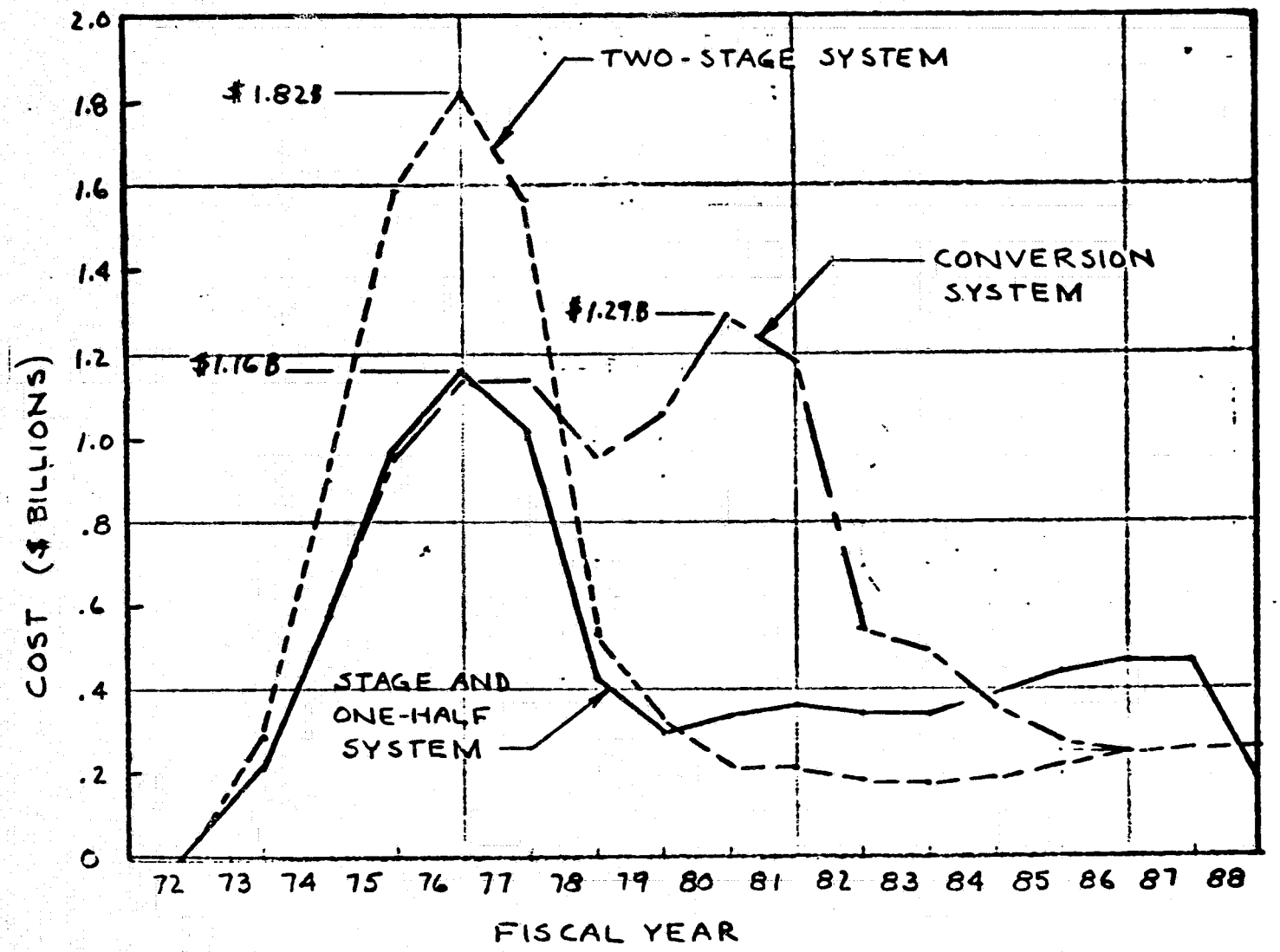

Fig. 1.2-9 Overall Annual Cost Comparison

Also, the subsonic and hypersonic maximum lift-to-drag ratios are 5.8 and 1.7, respectively; equaling or bettering the predicted values. The wind tunnel data were obtained on the LS 200-5 stage-and-one-half orbiter configuration. The data are essentially applicable to the LS 200-10 stage-and-one-half configuration and the performance could be improved somewhat for the LS 400-7A, two-stage orbiter.

1.3 STUDY CONCLUSIONS AND RECOMMENDATIONS

The principal conclusions derived from the study are as follows:

1. The best stage-and-one-half Space Shuttle configuration comprises a lifting body orbiter with expendable, V-shaped droptanks.
2. The stage-and-one-half system is feasible and, with a gross system liftoff weight of 3.82 million lb, can meet all of the space shuttle system requirements for a total program cost of $8 billion and within an annual funding limitation of $1.16 billion. It provides a cost savings of $1 billion over the two-stage system and saves even more if the traffic model is less than 445 flights.
3. The risk of impacting land, ships, or aircraft with the stage-and-one-half system droptanks is acceptably low, the safety being better than that for commercial airlines on a per-flight basis.
4. A two-stage Space Shuttle based on the Lockheed lifting body orbiter configuration can meet all system requirements for a gross liftoff weight of 4.13 million lb. The total program cost for this two-stage system is $9 billion and the peak annual funding is $1.82 billion for a FMOF date of April 1978.
5. A convertible system which flies as a stage-and-one-half system starting in April 1978 and as a two-stage system in July 1982 is feasible at a total program cost of $11.0 billion. The peak annual funding for the convertible system is $1.29 billion.

The principal Lockheed recommendations derived from the study are:

1. The orbiter for either the two-stage or the stage-and-one-half system should be a delta (lifting) body configuration.

2. Development of the stage-and-one-half system is recommended on the basis of lower development cost, lower total cost, lower peak funding, and better performance.

3. If the two-stage system is pursued, the primary engine thrust level should be reduced to the 400 to 450K range so that three engines can be used on the orbiter to ease the engine-out, abort-to-abort requirement. The resulting added complexity of a few more engines on the booster is more than offset by the lower total system size.

4. For either a two-stage or a stage-and-one-half system, the airbreathing engines should use LH_2 fuel because of the resulting lower total system size and lower cost. In the rare cases of alternate site landings by either the booster or the orbiter, LH_2 can easily be trucked to the vehicle for refueling along with other GSE which is needed in any case. In addition, the use of LH_2 fuel permits abort from staging by either system, for the orbiter LH_2 can be used by the airbreathing engines to fly to a landing site.

Section 2
THE STAGE-AND-ONE-HALF SYSTEM

A stage-and-one-half system consists of a reusable orbiter vehicle and expendable droptanks. The orbiter vehicle includes all of the engines and subsystems. The droptanks carry only a portion of the ascent propellant and are staged during ascent. If the droptanks are designed to be simple and efficient as propellant carriers, the system can exhibit a lower gross liftoff weight than a two-stage system and a considerably lower total dry weight, since only one vehicle is required. Therefore, the development cost of the stage-and-one-half system is considerably lower than that of the two-stage system. Operational costs for the stage-and-one-half system are higher than those for the two-stage system because of the expendable droptanks. Consequently, the answer to which of the systems provides the lowest total program cost depends upon the total number of launches in the program.

Lockheed has been studying space shuttle systems continuously under company funding for more than five years and under government contracts for more than three years. Most of this work has been on the stage-and-one-half system.

At the outset of the ACS study, a design analysis of various orbiter configurations was made to derive the best configuration for the stage-and-one-half systems. Configurations studied included high and low straight wings, delta wings, swept wings, canards, and lifting body configurations. The analysis, documented in the first three monthly reports of the study, showed that the lifting body orbiter configuration was best for both the high and low cross-range applications. It provides a lower system weight, better overall aerodynamic performance, more predictable aerothermodynamic characteristics, and a lower total program cost than any of the other configurations studied. The principal reasons for the superiority of the lifting body orbiter are: (1) the lifting body provides a large base area for mounting the large complement

of primary engines required by the stage-and-one-half orbiter, (2) the lifting body has the best volumetric efficiency in terms of usable volume per square foot of total wetted area, and (3) the lifting body provides a clean, proven aerothermodynamic shape for lifting reentry and for hypersonic flight.

2.1 REQUIREMENTS, GROUNDRULES, AND ASSUMPTIONS

At the outset of the study, the applicable space shuttle requirements were defined in the Statement of Work and comprised three parts: (1) Appendix A, containing 14 baseline system requirements, (2) Appendix B, containing 5 mission requirements, and (3) Appendix C, containing 49 desired systems characteristics. These requirements plus five additional requirements added to the study at the first monthly review are documented in the first monthly report and will not be repeated here. These requirements were essentially the same as those applied to the Phase B studies and were complied with by Lockheed in this Phase A study during the first six months.

On 20 January 1971, new Level 1 requirements were generated by NASA applicable to all Phase A and Phase B studies. These requirements are listed below and are followed by comments regarding their impact or applicability on the study and on the stage-and-one-half system.

Level 1 - Space Shuttle Program Requirements

(1) The shuttle shall be a reusable two (2)-stage vehicle.

(2) The cargo bay shall be sized to have clear volume of 15 ft diameter by 60 ft length. Payloads shall be equal to or less than 15 ft in diameter and 60 ft in length including handling rings, attachment fittings for the deployment mechanism and docking, and cargo bay storage fittings. The standardized deployment mechanism(s) and tie points shall be chargeable to the orbiter and shall not occupy the clear volume. Deployment clearance shall be provided by the orbiter.

(3) IOC baseline is the second half of 1977.

(4) Deleted

(5) The design mission shall be a 100 NM due east circular orbit. The design mission insertion orbit shall be 50 x 100 NM and for purposes of performance comparison calculations, the vehicle shall be considered to be launched from a latitude of 28.5 degrees North; the

reference mission(s) of major interest are: (1) 100 NM South Polar circular orbit; (2) 270 NM at 55 degrees inclination.

(6) The orbiter shall have a nominal hypersonic aerodynamic crossrange capability of 1100 NM.

(7) Deleted

(8) Mission duration (from liftoff to landing) of 7 days of self-sustaining lifetime shall be provided. For missions in excess of 7 days, the weight of the expendables shall be charged against the payload.

(9) The space shuttle shall be capable of operating within the cargo range from zero to maximum capability.

(10) The orbiter shall have sufficient propellant to provide 1,500 fps on-orbit ΔV capability (in excess of amount required to attain the design insertion orbit with a maximum payload for the 270 at 55 degrees inclination reference mission). The tanks shall be sized to provide 2000 fps ΔV capability.

(11) The booster and orbiter shall be baselined to have goaround capability.

(12) The booster and orbiter crew and the orbiter passengers environment shall be shirtsleeve.

(13) The booster shall be capable of returning to the launch site.

(14) All vehicle stages shall be capable of ferry flights between airports.

(15) Integrated vehicle vertical takeoff and individual vehicle horizontal landing shall be the vehicle mode of operation.

(16) A communication satellite system is assumed to be available.

(17) Launch rates will vary from a minimum of 25 to a maximum of 75 per year.

(18) The space shuttle shall have an all-azimuth launch capability.

(19) The shuttle shall provide safe mission termination capability. This includes rapid crew and passenger egress prior to liftoff and intact abort after liftoff. Intact abort implies the capability of the

booster and orbiter to separate and continue flight to a safe landing; the orbiter to land with a full payload.

(20) 550,000 lb sea level thrust bell-type engines will be baselined in both the orbiter and booster stages.

(21) The intended combined storage and operational service life of this system is 10 years after IOC. A booster/orbiter life of 100 missions will be provided with a cost effective level of refurbishment and maintenance.

(22) For the design reference mission, rescue operations (including personnel transfer) must be completed within 48 hours after notification.

(23) JP will be baselined as fuel for all airbreathing engines. The airbreathing engines shall be capable of being removed from the orbiter with minimum scar weight. The orbiter shall be capable of flight with or without the airbreathing engines installed.

(24) All subsystems except primary structure and pressure vessels shall be designed to fail operational after the failure of the most critical component and to fail safe for crew survival after the second failure. Electronic systems shall be designed to fail operational after failure of the two most critical components and to fail safe for crew survival after the third failure. The space shuttle main engine shall be designed to fail safe for crew survival after the failure of the most critical component. The main engine electronic system shall be designed to fail operational after failure of the most critical component and to fail safe for crew survival after the second failure. Individual subsystems may be revised by Level II decision where improvements in cost and effectiveness would result.

(25) Survivability against hazards from radiation as specified in Joint DOD/NASA Survivability Characteristics document(s) dated 16 June 1969.

(26) Total space shuttle turnaround time from landing to launch readiness should be less than two weeks. The removal and replacement time shall be minimized with on-board checkout and module accessibility.

(27) Launch trajectory load factors shall not exceed 3g and entry trajectories shall not exceed 3g for the orbiter.

(28) The space shuttle crew/passengers compartment atmosphere and total pressure shall be compatible with the space station and space base.

(29) Vehicle payload is baselined to be 65,000 lb into the due east 100 NM circular orbit with the airbreathing engines removed from the orbiter. The weight of passengers and removable provisions for passengers shall be charged to the payload. The orbiter shall have the capability to land 40,000 lb of payload with nominal wind and load factors (airbreathing engines removed) and larger payloads with reduced structural safety factors.

(30) The orbiter shall be capable of a once-around trajectory with a one-engine-out condition at and/or after booster orbiter separation for the design and reference missions.

(31) Booster and orbiter shall be designed for maximum interchangeability (common components and spares to be interchangeable).

Requirement No. 1 is not applicable to the stage-and-one-half system.

Regarding requirement No. 3, the IOC date, Lockheed has complied with NASA planning documents in using a first manned orbital flight (FMOF) date of April 1978.

Regarding requirement No. 5, the design mission, later NASA direction specified that the required payload is 65,000 lb to the due east launch mission, 40,000 lb to the south polar launch mission, and 25,000 lb to the 55 deg, 270 NM orbit mission; the first two are without the orbiter airbreathing propulsion system installed and the last one with the airbreathers installed.

Regarding requirement No. 18, all-azimuth launch, the stage-and-one-half system suffers a payload degradation for some launch azimuths if open ocean impact of the droptanks is obtained. However, for all known or planned NASA and DoD missions, there is no launch azimuth problem with the stage-and-one-half system.

Requirement No. 20 changed the primary engine from a 415,000 lb thrust level to 550,000 lb thrust level. This change in itself does not appreciably impact the stage-and-one-half system; however, the resulting engine ICD showed a degradation in the installed-thrust-to-weight ratio of the engine which does penalize all systems. **A minor deviation to the ICD engine is taken wherein an expansion ratio of 53:1 is used rather than the ICD value of 35:1.**

Requirement No. 25 changed the airbreathing propulsion system fuel from liquid hydrogen to JP. This increases the GLOW for the stage-and-one-half system by about 160,000 lb and results in a higher total program cost even after allowing $75 million for conversion of the A/B engine to LH_2 fuel.

Costing groundrules applicable to the study are defined in detail in Volume IV of this report. The principal costing groundrules used here are:

(1) Costs are divided into:

  (a) Design, Development, Test and Engineering Costs

  (b) Recurring Production Costs

  (c) Operations Costs

  (d) Droptank Production Costs

(2) Costs are based on constant 1970 dollars

(3) Operations costs are based on the NASA, 445-flight, 10-year mission model having a peak launch rate of 75 launches per year.

(4) A single KSC launch site is assumed.

(5) Cost reporting is to be in accordance with the Phase A portion of MF-030.

(6) Costs include engine costs and facilities but exclude fees.

For purposes of program planning and costing, it is assumed that the Phase C/D Contract would start in 1 April 1972; first manned orbital flight would be April 1978; and the program would be completed at the end of 1988.

2.2 SUMMARY OF LS 200-10 SYSTEM CHARACTERISTICS

2.2.1 General Design Considerations, Operation, and Performance

2.2.1.1 Sizing Considerations. The stage-and-one-half system differs from the two-stage system inasmuch as the installation of a large portion of the ascent propulsion system weight becomes a major factor determining system performance, vehicle sizing, and design. The chief effect on sizing is that the booster stage is characterized by a very high λ' (exceeding 0.96) and the injection stage by a relatively low λ', which may drop to below 0.48. This compares with corresponding typical λ' values of 0.81 for the booster and of 0.70 for the orbiter with the two-stage system. Consequently, the two-stage systems are characterized by staging velocities of about 10,000 ft/sec, while the stage-and-one-half designs are bound to optimize at much higher staging velocities; under certain conditions these may approach the orbit injection velocity. However, the optimal condition is attained with a portion of the ascent propellant still in the orbiter. Keeping the droptanks to orbit injection would result in a single-stage system with uncompetitive low λ' value. However, system performance is relatively insensitive to the quantity of orbiter ascent propellant. As a result, the stage-and-one-half system orbiter is sized primarily by the requirements to provide space for the payload bay and the required base area for installation of the rocket engines.

Inclusion of the major portion of the propulsion system weight in the orbiter affects performance and vehicle design by the resulting increase in inert weight and shift of the center-of-gravity to the rear. Both effects are highly critical to performance and flight characteristics. Inert weight in the orbiter trades directly with payload capability, and balancing the vehicle cg with the aerodynamic force center, especially for the no-payload flight condition, becomes a determining design consideration.

Consequently, the stage-and-one-half system is more sensitive than the two-stage system to rocket engine weight characteristics, since engine thrust-to-

weight ratio directly affects payload capability and the critical cg location.

A liftoff thrust-to-weight ratio of 1.25 was selected as best representing considerations of control authority, payload delivery capability, and propulsion system integration. Consequently, nine 530,000 lb sea level thrust, main rocket engines are installed in the orbiter. Their characteristics correspond to the specification documented in the Space Shuttle Main Engine ICD 13M15000B, except that the expansion ratio was increased from 35:1 to 53:1. The primary reason for this deviation was to avoid exhaust plume impingement on the aft surfaces without moving the engines so far back as to impair the cg balance of the vehicle. In addition, a moderate performance increase was obtained, since this change brings the nozzle expansion ratio close to optimum value for the stage-and-one-half system. Costs for this modification were determined to be relatively insignificant. With this arrangement, a nominal gross liftoff weight (GLOW) of 3.816 Mlb is obtained.

The 1½-Stage Baseline system is sized and designed to satisfy the Space Shuttle Level I mission requirements in conjunction with the other requirement for providing for abort-through orbit capability under the one main engine-out condition at staging. These requirements are summarized in Table 2.2-1.

Table 2.2-1

MISSIONS	NASA DESIGN	NASA REF.	NASA REF.
Insertion Orbit, nm	50 x 100	50 x 100	50 x 100
Mission Orbit, circular, nm	100	100	270
Orbit Inclination, deg	28.5	90	55
Payload, 1000 lb	65	40	25
Airbreather System	Removed	Removed	In
Abort (Engine-Out From Staging)	NA	NA	NA
On-Orbit Velocity, ft/sec	650	650	1500
With design payload	650	650	1500
For sizing OMP tanks	NA	NA	2000

Of these requirements, the airbreather in/out and the abort requirements have significantly different design effects on the stage-and-one-half and two-stage reusable systems. The airbreather system weight in the stage-and-one-half orbiter is approximately 40 percent greater than for the two-stage orbiter. Removal of the airbreather system for due east and polar missions, therefore, is to the advantage of the stage-and-one-half concept. Engine-out from staging is a consideration not applicable to the stage-and-one-half system, since in nominal operation, two of three available engines are used. The on-orbit velocity is NASA-supplied for the 55 deg mission and is LMSC-established for the other two. Evaluating these data with regard to specific 1½-stage system characteristics, it appears that the critical design condition is established by the 55 deg inclination mission due to the large airbreather system weight and the 1500 ft/sec post-injection orbit velocity increment requirement. The ascent tanks are sized for injection into the insertion orbit and FPR, and the OMP tanks for satisfying the orbit velocity requirements of that mission. For the other missions, the tank capacities and their assigned functions determine payload capability. Orbiter ascent tanks are always full regardless of mission requirements, and either the droptank or OMP tank capacities determine maximum payload capacities. Since the 270 nm 55 deg mission is the critical, excess payload capacity is obtained for the due east and south polar missions with fully loaded droptanks, and the droptanks are offloaded, resulting in reduced GLOW and increase in liftoff thrust-to-weight ratio, for obtaining the design payloads with these two missions.

2.2.1.2 Configuration. The stage-and-one-half Baseline vehicle configuration selected by Lockheed, Model LS 200-10, is shown in Fig. 2.2-1. It consists of a fully reusable orbiter using a modified delta planform configuration in combination with an expendable, single, V-type droptank module composed of two identical tank assemblies straddling the orbiter in the yaw plane. The droptank module is connected to the orbiter at three attach points, one forward at the orbiter nose and two aft, symmetrically arranged forward of the main engines. All three are located at the upper orbiter surface, avoiding the necessity of penetrating the heat shield in the areas of very high surface temperatures. All rocket and airbreathing engines and attitude control

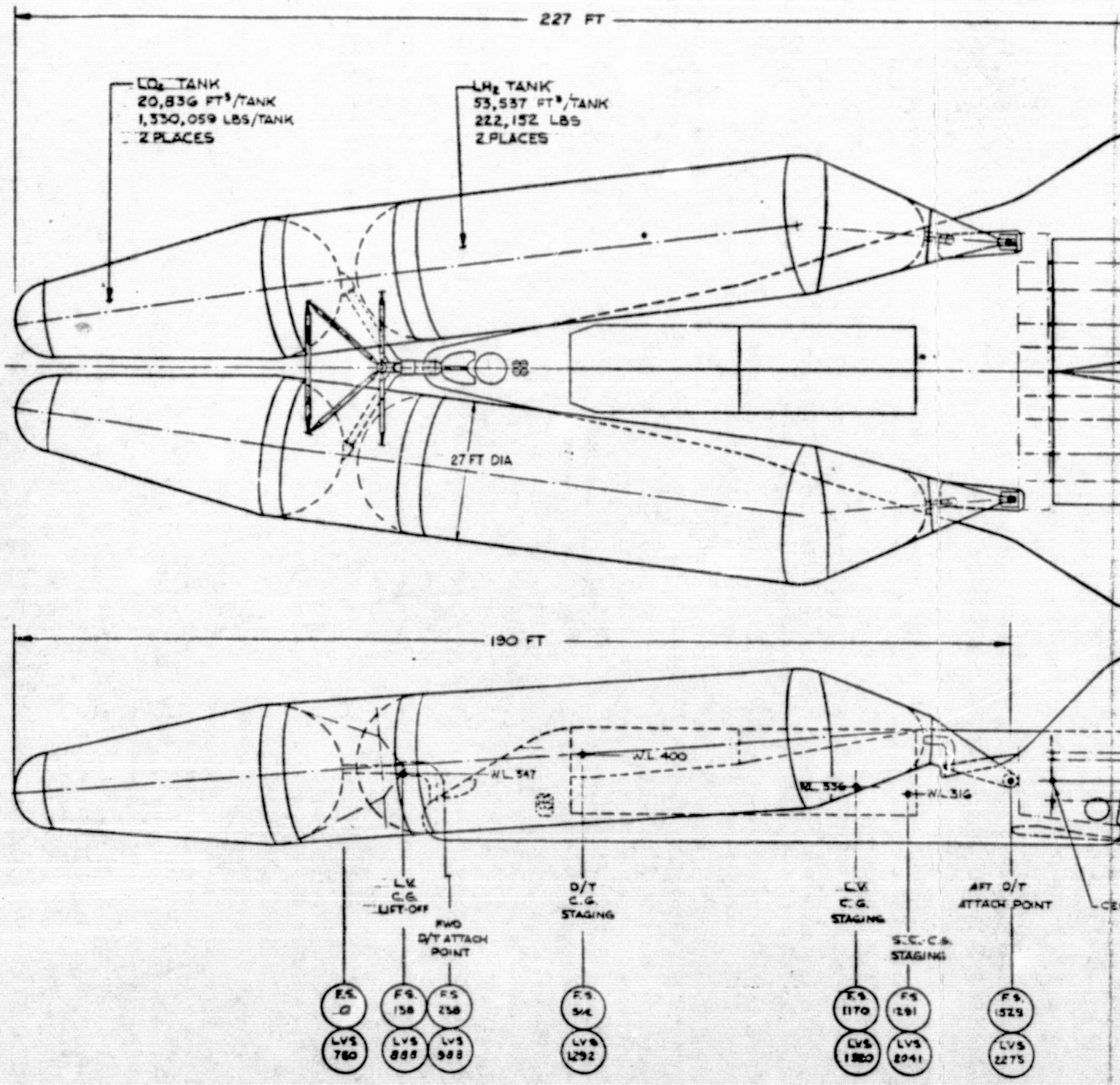

FOLDOUT FRAME

REPRODUCIBILITY OF THE ORIGINAL PAGE IS POOR

LIMITED CALIBRAS LIFE | LIMITED OPERATING LIFE

REVISIONS			
ZONE	DESCRIPTION	DATE	APP

PRECEDING PAGE BLANK NOT FILMED

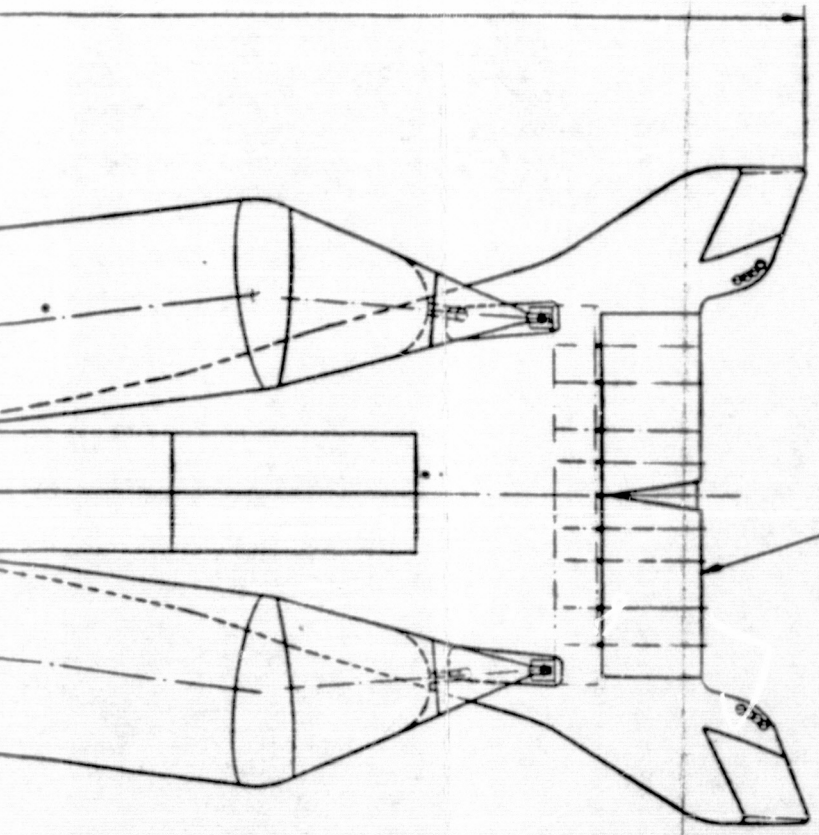

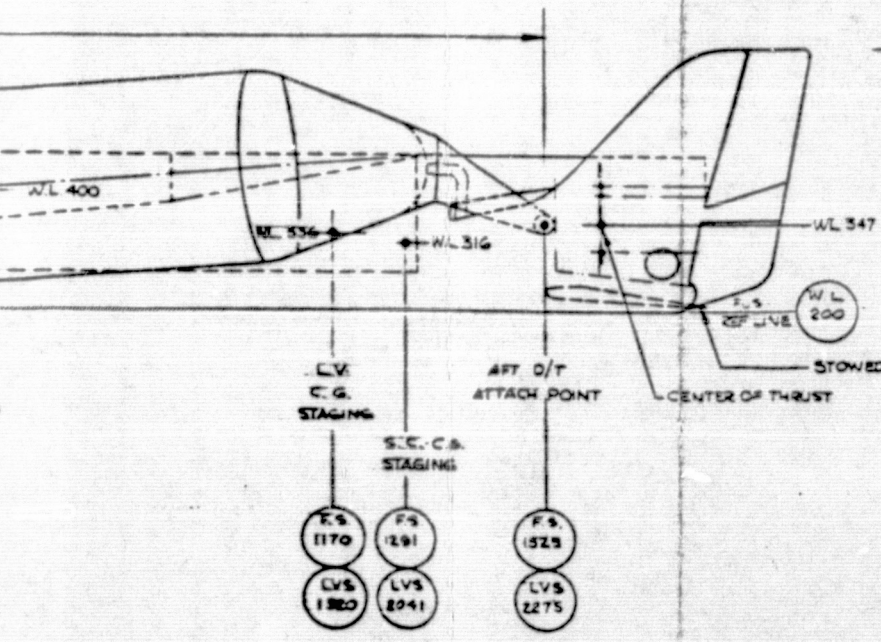

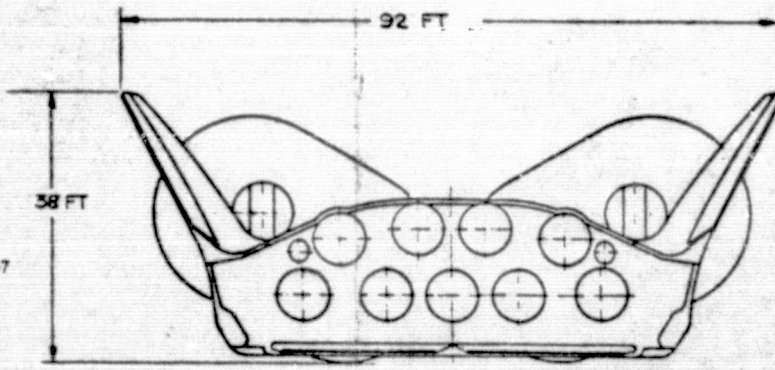

Fig. 2.2-1

QTY REQD	CODE IDENT	PART OR IDENTIFYING NO	NOMENCLATURE OR DESCRIPTION	MATERIAL DESCRIPTION OR NOTE	MATERIAL SPECIFICATION	ZONE

PARTS LIST

INTERPRET DWG PER	UNLESS OTHERWISE SPECIFIED DIM ARE IN INCHES. TOLERANCES ON: FRACTIONS ± 1/16, DECIMALS .X ± .1, .XX ± .03, .XXX ± .010, ANGLES ± 2 DEG	DATE 5-12-71	LOCKHEED MISSILES & SPACE COMPANY, A GROUP BY SUBS OF LOCKHEED AIRCRAFT CORP, SUNNYVALE, CALIFORNIA
		DWN	LAUNCH VEHICLE DELTA BOOST - STAGE 1 1/2 MODEL LS 200-10
		APVD	
		APVD	
		ENGRG	
		CHKR	
		APVD	SIZE E, CODE IDENT 07987, DRAWING NO SKS 100061
NEXT ASSY	USED ON	CONTR	
APPLICATION		APVD	SCALE, SHEET

thrusters are assembled in the orbiter. The droptank module contains only the necessary elements for storing the propellants during ascent, and the plumbing and instrumentation required for propellant transfer and pressurization, and pressure, temperature, and fluid level control. Thus, by reducing the function of the droptanks to that of a tank proper, and by selecting a configuration permitting a highly weight-effective design, a very high propellant fraction is obtained. Consequently, staging is achieved at a high velocity, exceeding 18,000 ft/sec, resulting in negligible aerodynamic loads during separation and large droptank impact ranges compatible with multi-azimuth launch requirements.

2.2.1.3 Ascent and Droptank Separation. The basic stage-and-one-half mission profile is shown in Fig. 2.2-2, assuming operations at KSC. Launch is accomplished vertically from either a LUT or a fixed launch pad. All engines are ignited on the ground and operated at NPL during a hold-down period of approximately 0.5 sec until the vehicle is released. The resulting design ascent trajectory characteristics are shown in Figs. 2.2-3 and 2.2-4. During the prestaging ascent phase, the acceleration is maintained at 3g level by throttling and shutting down the engines in a sequence minimizing specific impulse losses. Propellant losses associated with the sequential engine shutdown are greatly reduced by recirculation into the tanks of the LO_2 residuals in the individual engine feed lines. This is done by the application of pressurant gas without the addition of any moving components to the system. Full attitude control, including for the most adverse one-engine-out failure mode is attained by providing the 5 center engines with $\pm$ 7 degree gimbal capability.

Separation of the droptank module from the orbiter, shown in Fig. 2.2-5, is effected in a near zero-q environment, without requiring assistance from additional impulses by the moment produced by main engine thrust and the offset empty droptank center of gravity. It is initiated by releasing the forward joint, which permits the intact droptank assembly to rotate "over the shoulder" about the aft pivot attachments. At the appropriate time, when the droptanks have swung back approximately 60 deg, the latter are released to complete separation. Stability and control during the staging maneuver are continuously maintained by the orbiter control system.

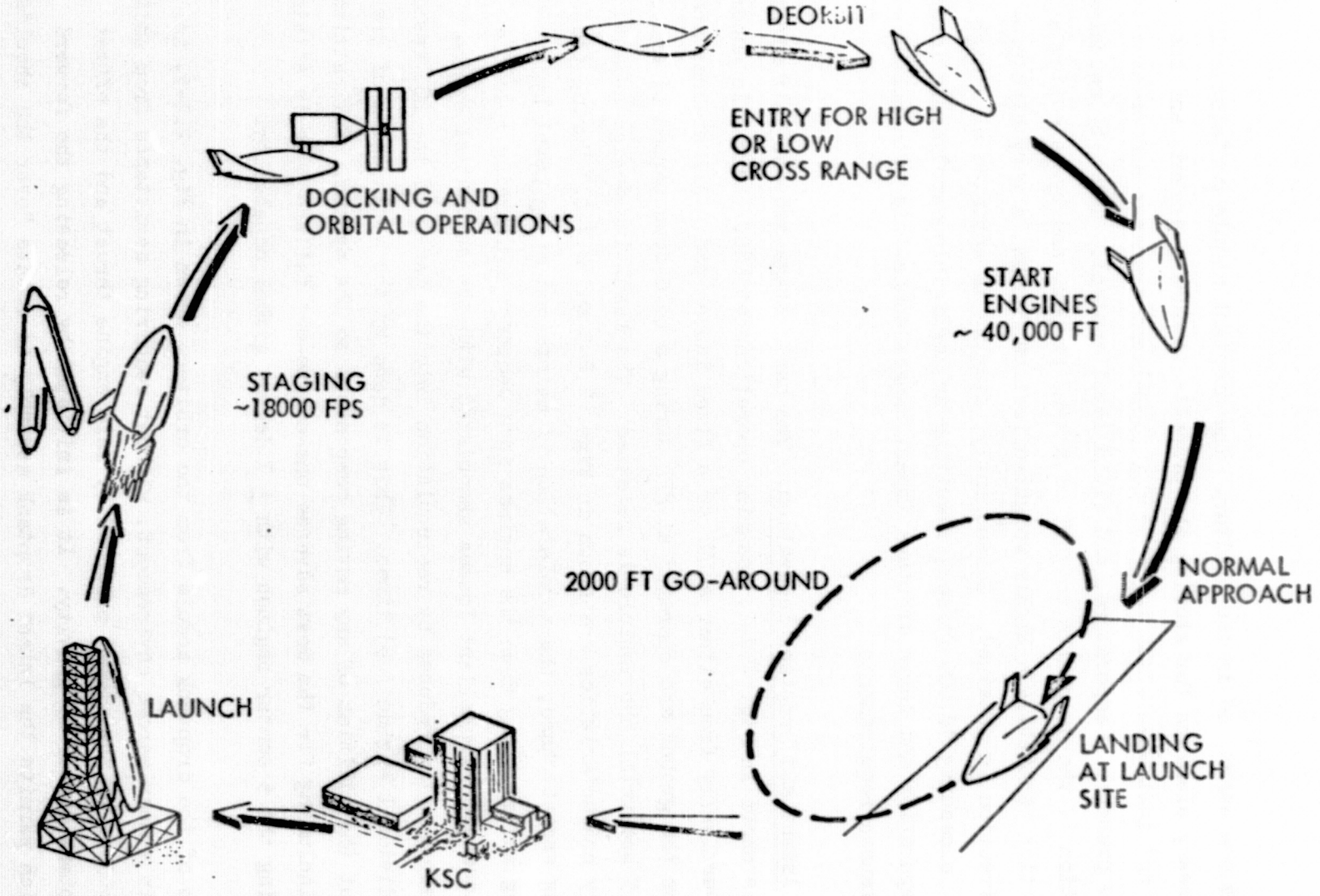

D02195

Fig. 2.2-2 Stage-and-One-Half Baseline Mission Profile

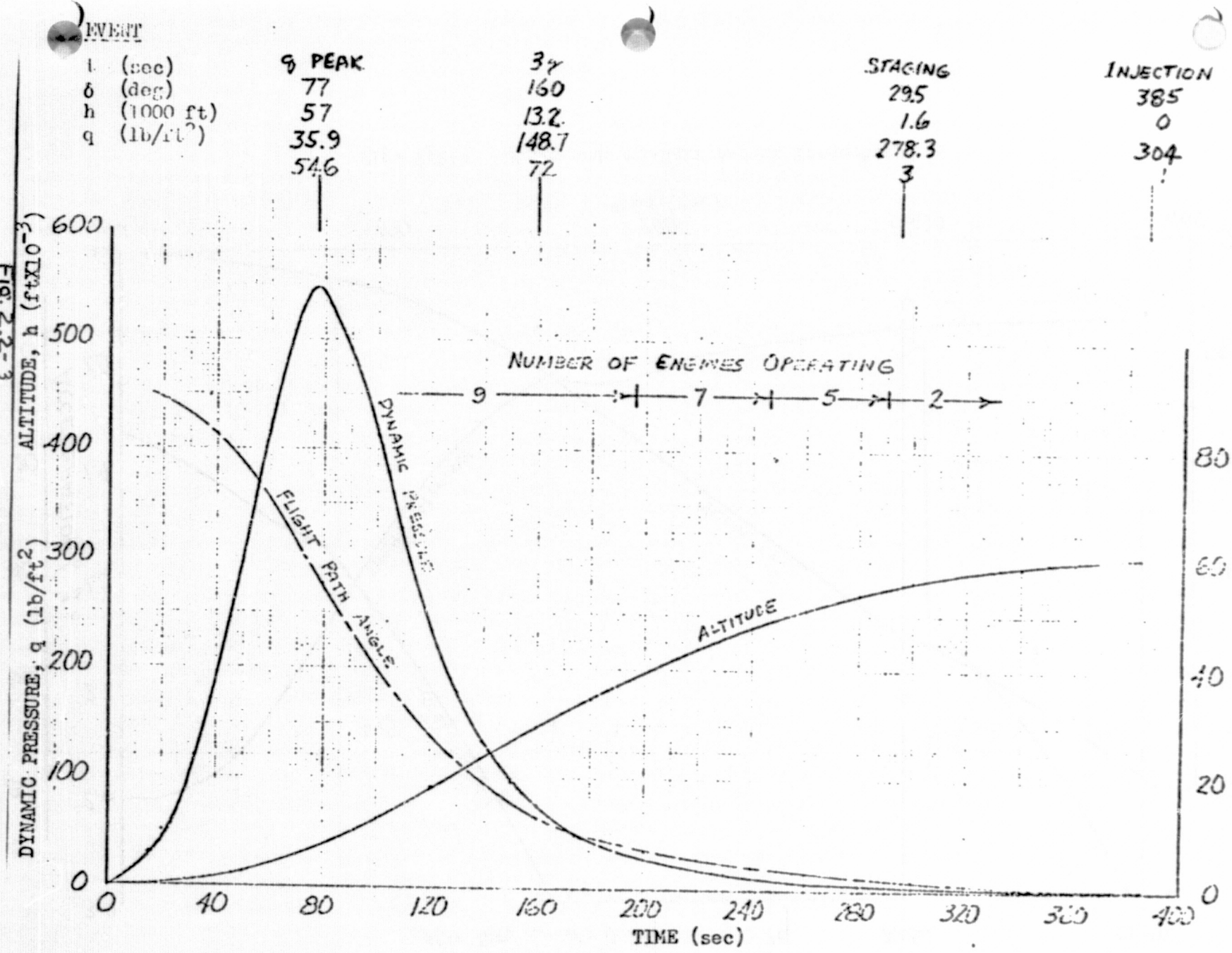

Fig. 2.2-3 Stage-and-One-Half Ascent Trajectory

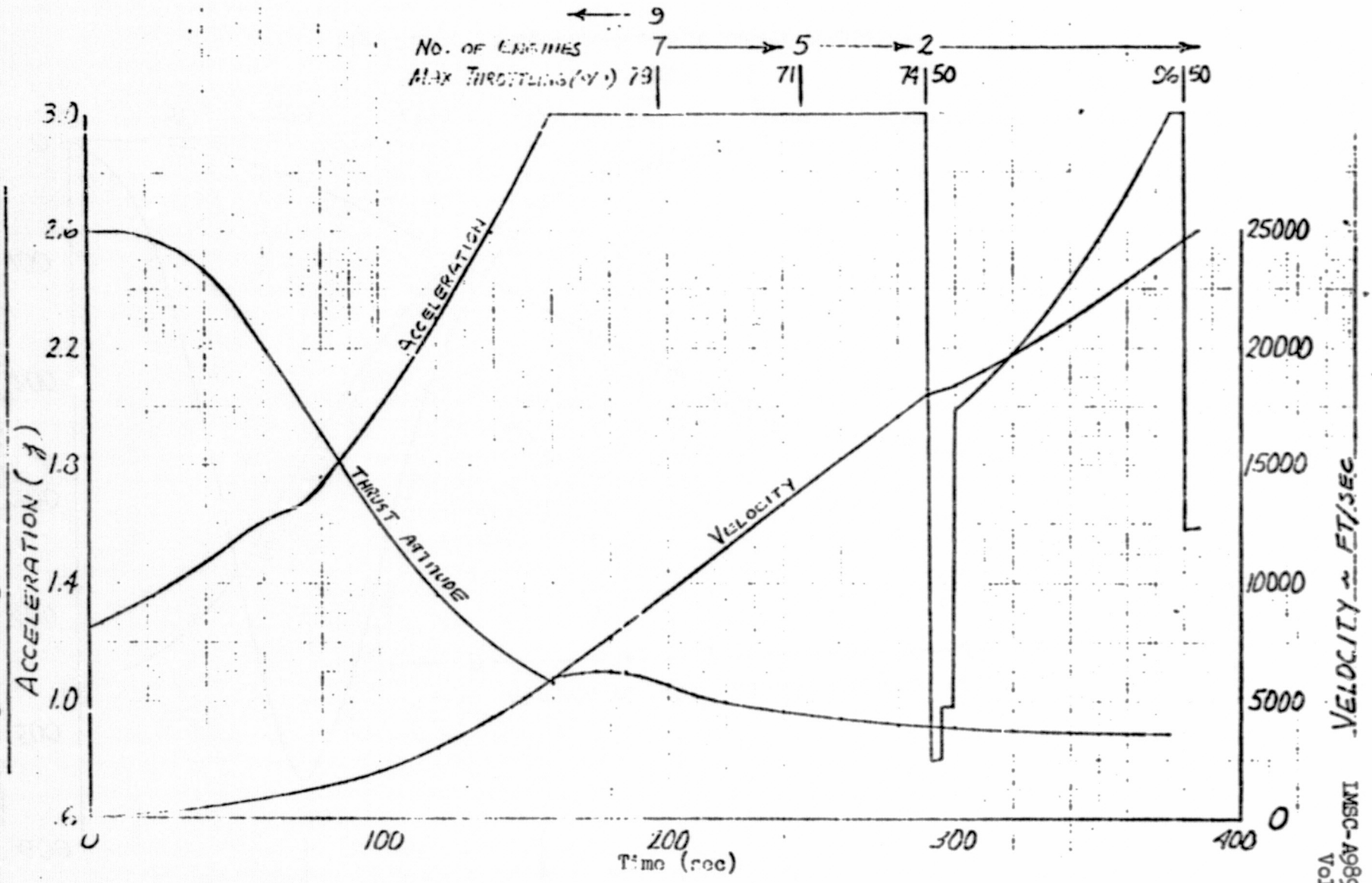

Fig. 2.2-4

Fig. 2.2-4 Stage-and-One-Half Ascent Trajectory

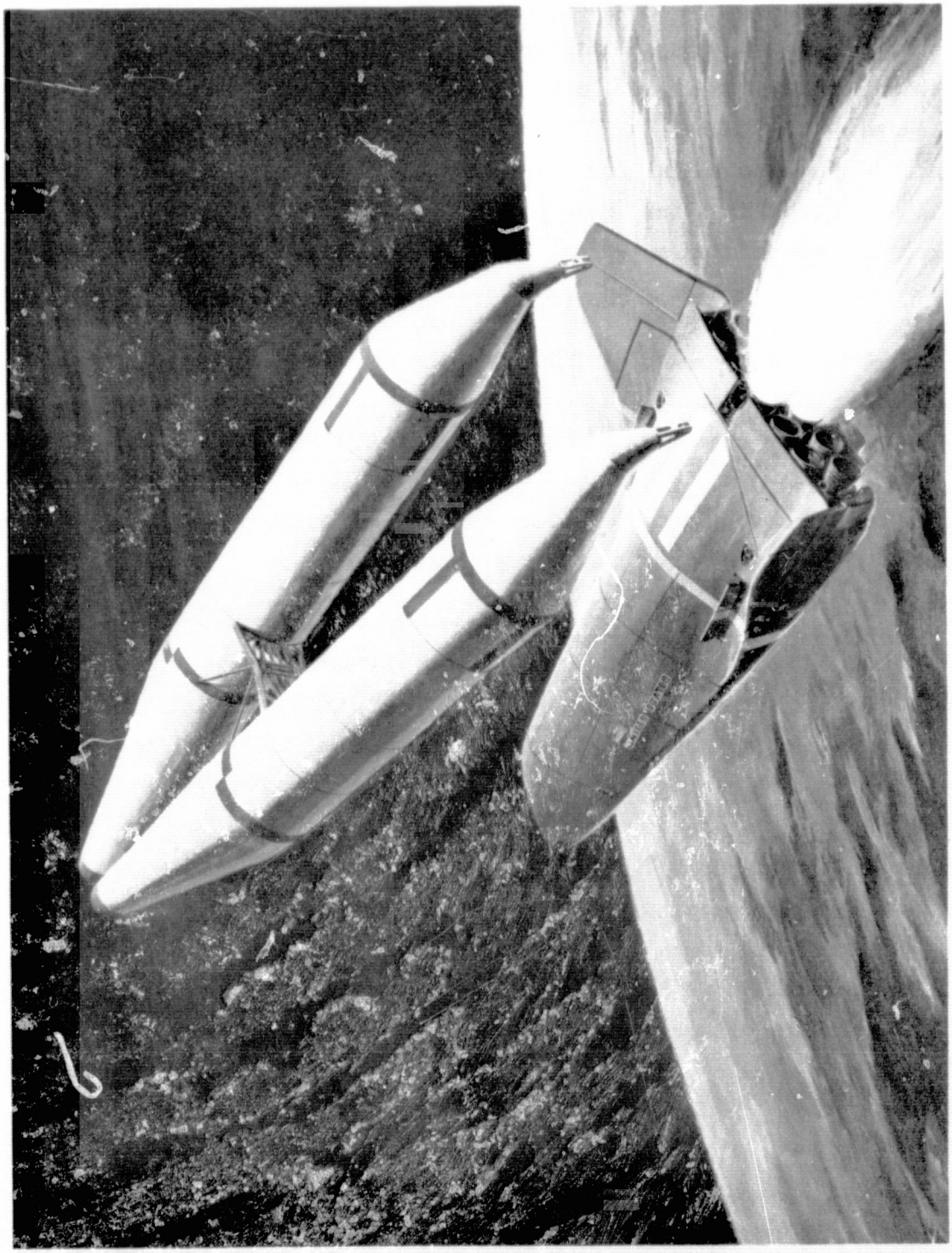

Fig. 2.2-5 Droptank Separation

Fig. 2.2-5

After sufficient clearance from the orbiter is attained, the tank module is disjoined into the two tank assemblies by breaking the intertank tie structure with an explosive charge. Controlled venting of the tank gases then gently separates the tanks. This controlled separation of the tank assemblies is considered essential for assuring intact tank reentry, a prerequisite for minimum fragmentation and, hence, low accident probability. Nominal drop-tank impact is 900 nm downrange from the launch site into the open ocean.

After separation, one of the three post-separation main engines is shutdown and the other two are operated at NPL until the point is reached at which they are simultaneously throttled down for maintaining the acceleration at the 3g limit. The nonoperating engine remains fully operative during this period. Since failure to ignite is the most probable engine failure mode, with this approach an optimum compromise between reliability and minimum performance loss from engine throttling is achieved.

2.2.1.4 Orbit Maneuvers and Flight Control. Orbital maneuvering capability, except for low velocity increment maneuvers, and deorbit capability, is provided by an orbital maneuvering propulsion system (OMPS) consisting of two RL10 engines in combination with a separate propellant tank and feed system designed for the long storage time requirement. Under normal operation, only one engine is used, the second remaining operative as a standby, providing full fail-operational capability for the one-engine-out failure mode. Both engines have gimbal capability providing pitch and yaw control during single-engine operation. This arrangement trades a high degree of reliability and safety for a moderate loss in performance. Fail-safe operation capability could be provided by either adding a third RL10 engine or by using ACPS thrusters. Trade studies resulting in the selection of either approach have not been completed.

An attitude control propulsion system (ACPS) adds roll control capability for single RL10 engine operation and provides on-orbit full attitude control capability and the small three-axis translatory impulses for docking, station keeping, and similar maneuvers. It also supplies attitude control capability

for the initial reentry phase prior to the onset of sufficient aerodynamic pressure to assure full aerodynamic control authority. There is no dependency of the delta-body configuration on the ACP system beyond this time.

2.2.1.5 Entry After Deorbiting. Entry maneuvers can be performed for either high or low crossrange requirements. Angle-of-attack and bank angle histories are controlled automatically or manually for landing sites lying within a 2200 nm wide by 2000 nm long footprint. Inherent with delta-body orbiter design is the capability to increase the footprint size, (up to 3600 nm wide and 4000 nm long) through increased TPS insulation thickness. Minimum time and insulation weight maneuvers were assumed for the design of the thermal protection system with the maximal temperature at the orbiter nose constrained to 2800°F and at the remaining lower surface, including leading edges, to 2300°F.

2.2.1.6 Subsonic Flight. An airbreathing system can be installed for controlling the glide slope to a value compatible with instrument landing requirements and for providing go-around capability within FAA engine-out climb gradient requirements. The engines use JP-4 fuel stored in a forward tank and are installed inside the orbiter close to the center-of-gravity to permit their removal with minimum scar weight. Prior to landing, they are deployed into the airstream from the lower surface of the orbiter.

The landing approach begins at approximately 100,000 ft and is designed to permit landing without engines or with airbreathing engine failures. If airbreathing engines are onboard, the engines are started and idled at approximately 40,000 ft and are available to flatten and extend the glide path or perform a go-around. The performance of the system with airbreathing engines permits maintenance of a go-around climb gradient of 2.7 percent in the approach configuration with engine-out to 5,000 ft altitude or 3.7 percent in the landing configuration to 8,000 ft altitude. Landing speeds as low as 146 knots (excluding ground effect) can be achieved. Landing speed at L/D_{Max} would be 182 knots at 14 deg angle-of-attack. With payload-in, the landing speed is increased by 13 knots. Ground effect is estimated to reduce these landing speeds by 14 knots.

2.2.1.7 Ferry Capability. A ferry kit consisting of a JP propellant tank in the payload bay, and possibly some aerodynamic fairings for the main rocket engines will provide approximately 280 nm range with 65,000 lb of fuel. Larger ranges can be obtained by in-flight refueling. Cruise altitude is over 12,000 ft or 9,000 ft with engine-out. This performance is related to a standard day and take-off from a sea-level airport. For more stringent requirements, an additional jet engine would be required. Installation on a pylon attached by an adapter to payload support fixtures in the payload bay is considered a possible solution.

2.2.1.8 Ground Operations. A baseline operations concept to support a stage-and-one-half shuttle is conceived to utilize, to the largest extent feasible, existing Saturn/Apollo equipment and facilities. The Main Launch Base is at KSC and includes use of the Vertical Assembly Building (VAB), Launch Pad 39, some existing support areas, and a new airfield, Droptank Manufacturing Building, and Maintenance Annex. This concept is shown pictorially in Fig. 2.2-6.

After landing at the new airfield, the heat stored in the insulation is removed by coolant air-flow provided by ground equipment to prevent overheating of aluminum structures. The orbiter then is transported on its own landing gear to the new Purge and Safing Area for offloading, purging, and safing. Scheduled and unscheduled maintenance as well as payload installation are performed at the new Maintenance Annex to the VAB. The vehicle is delivered on its own landing gear to the VAB, where erection (by transportable aisle crane and high bay crane), lift and installation onto a LUT-type launcher (same base dimensions as existing LUT) and vertical mating with droptank (manufactured in Tank Manufacture Building) are accomplished in an existing VAB high-bay cell. For transfer to the pad, an existing Crawler/Transporter, and for the installation at the pad, existing pedestal supports are used. After installation of a new flame deflector in the existing flame trench, the operations are completed by hookup of propellant and other ground support lines, loading of propellants, crew and passengers, countdown, and launch.

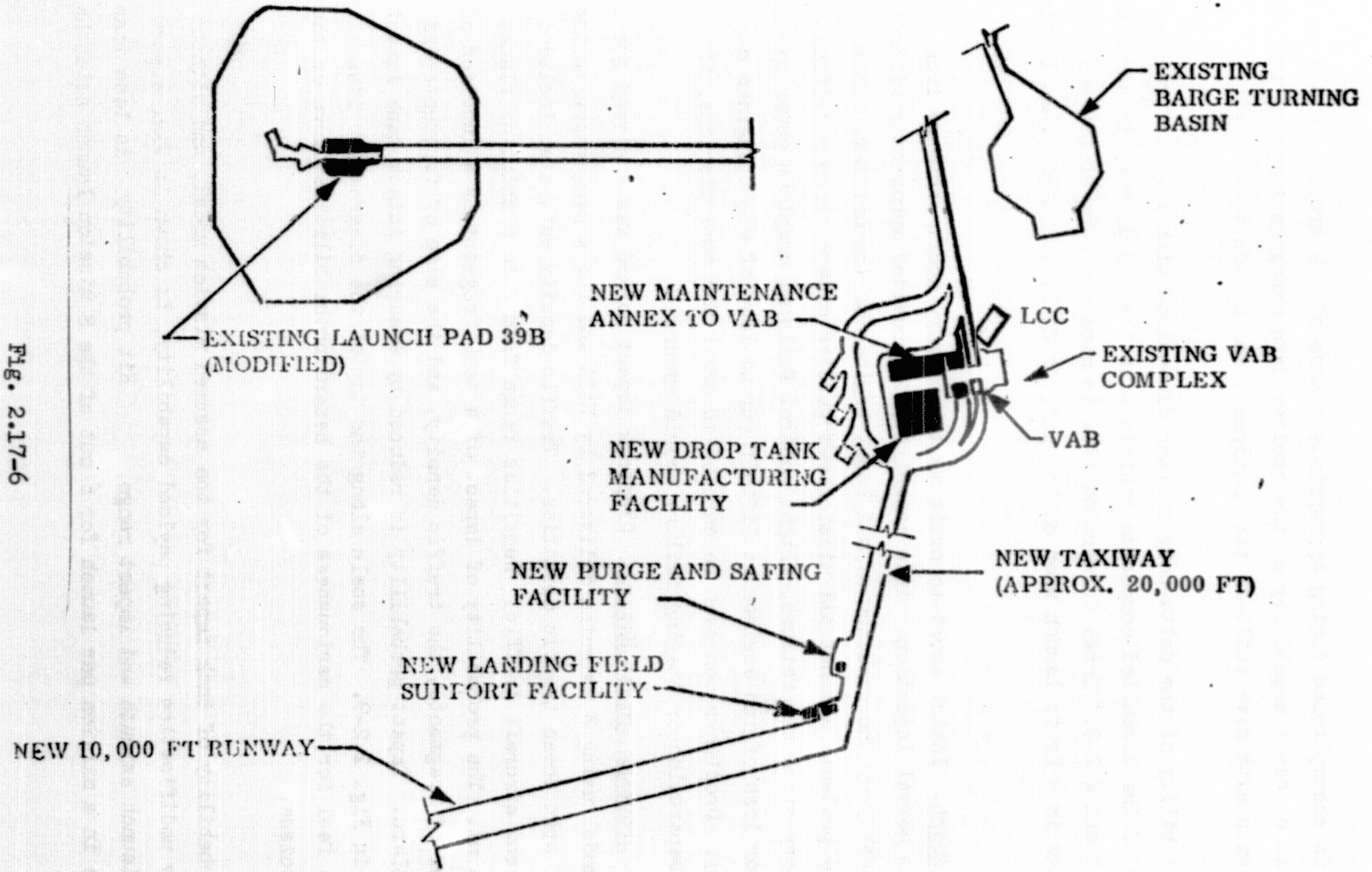

Fig. 2.2-6 1½ Stage Space Shuttle Facility Conceptual Layout

Checkout is accomplished during appropriate phases of the ground operations by the onboard checkout capability of the orbiter data management system in conjunction with extensive built-in test equipment and an AGE data complex.

The compatibility of the delta-body orbiter dimensions with the VAB transfer aisle and of the assembled composite vehicle with the VAB doorway is shown by Fig. 2.2-7 and 2.2-8. Total turnaround time is nineteen 8-hr shifts and response time is 2 hr to launch when on the pad, or 24 hr to launch when in the VAB.

2.2.1.9 Abort. Intact abort-to-orbit is the primary abort sequence from liftoff to normal injection. This capability is provided inherently without design penalty by the presence of all boost engines on the orbiter. This abort mode protects against all mission emergencies except those resulting from primary structure failure, flight control failure, complete power system failure, or loss of two engines at liftoff (up to loss of eight engines at injection). Droptanks can even be carried to orbit for some missions, if droptank separation or staging failure should occur.

2.2.1.10 Droptank Impact Hazard. Droptank impact hazard was analyzed for a mission model using 8 azimuths delivered by NASA and for a projection to the 1980's of open ocean traffic densities. Traffic density estimates included shipping and aircraft traffic. Densities range from 2 to 6 ships or planes per 10,000 sq mi. The probability of impact of a tank fragment is a function of the number of fragments, the traffic density, and the size of fragments and ship or plane. Impact probability is reduced by assuring intact tank impact as shown in Fig. 2.2-9. The scale along the top of the diagram provides intuitive feel for the seriousness of the hazard probaibilities shown on the lower abscissa.

Actual probability of tank impact for the assumed mission model, and without trajectory modification reducing payload capability, is shown in Fig. 2.2-10 for each launch azimuth and impact range. Hit probability is less than one chance in a million per launch for 6 out of the 8 mission launch azimuths

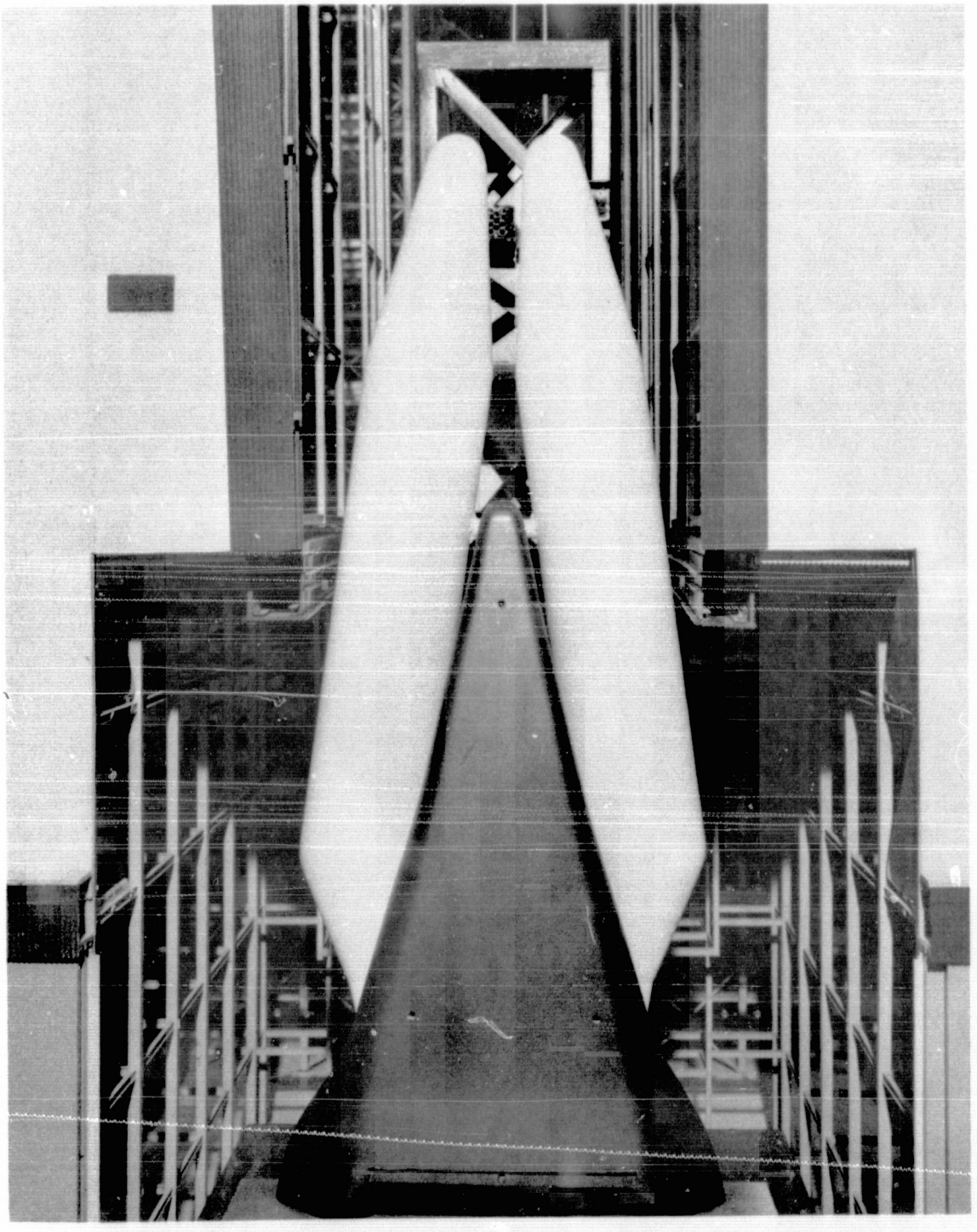

Fig. 2.2-7 Stage-and-One-Half in VAB Doorway

Fig. 2.2-7

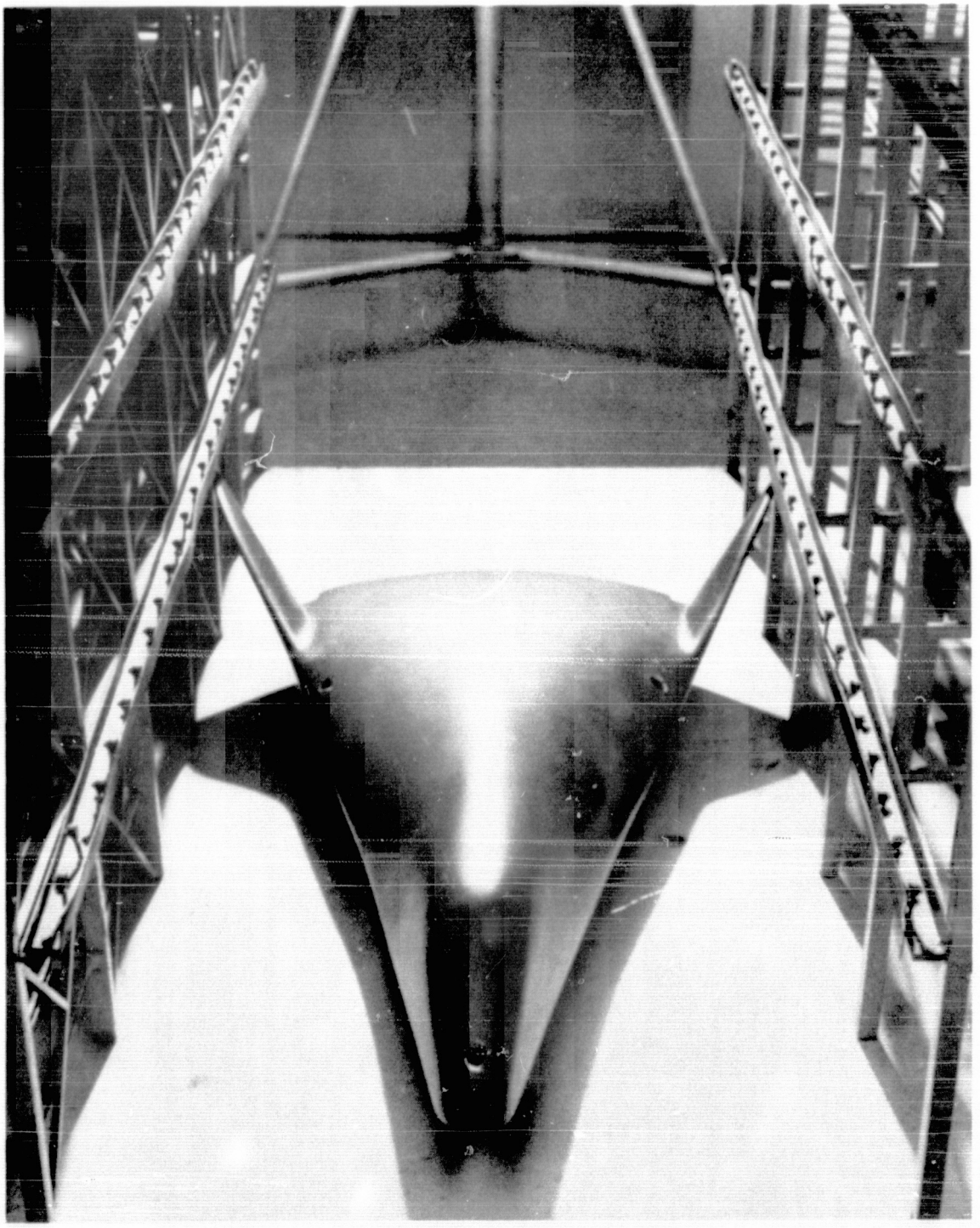

Fig. 2.2-8 Stage-and-One-Half in Transfer Aisle

Fig. 2.2-8

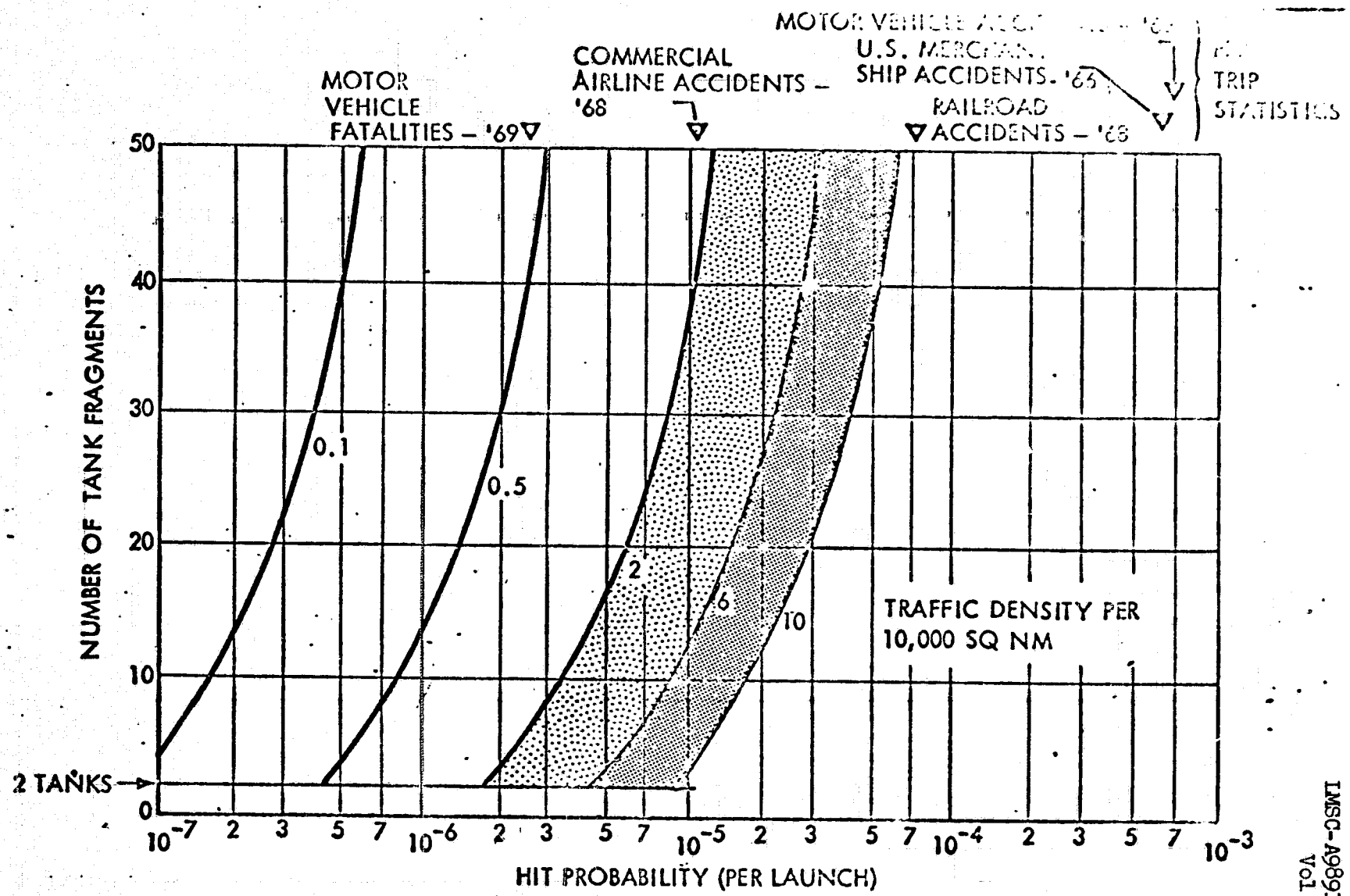

Fig. 2.2-9 Droptank Hit Probability

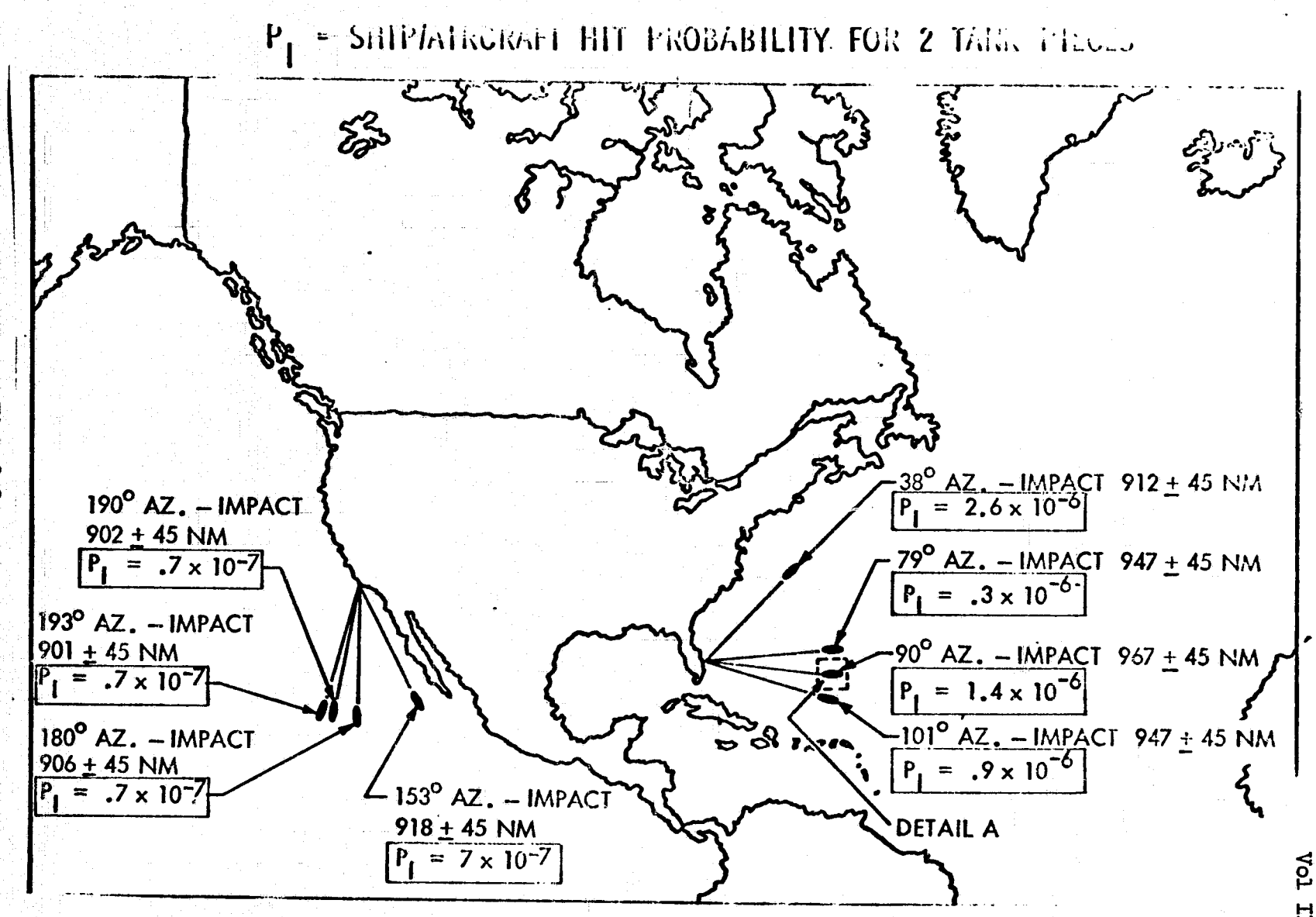

Fig. 2.2-10 Mission Droptank Impact Probabilities

which is considerably less than currently considered acceptable by NASA and also considerably less than one in one-hundred-thousand that is currently DOD for the impact of expendable stages at ETR. No impact area surveillance or control is required or recommended.

2.2.1.11 Aerodynamics and Stability. The alignment of the center-of-gravity of the orbiter and droptanks is shown in Fig. 2.2-11. The center-of-gravity travels along the thrust axis during fill and boost. This results in a highly aerodynamically stable configuration during boost and a stable configuration when mounted on the pad in either empty or loaded condition. The offset droptank-empty center-of-gravity provides the rotation moment to cause droptank separation as was discussed earlier.

Diagrams showing the stability and performance characteristics for the two extreme center-of-gravity locations and for appropriate trim conditions over the entire speed regime are presented in Figs. 2.2-12, 13, and 14. They demonstrate that the orbiter is aerodynamically stable and controllable under all conditions of operationally possible combinations of speed, center-of-gravity location, and flight attitude. The data shown are based on the results of extensive wind tunnel tests performed at Lockheed, Langley, and Ames on the LS200-5 configuration.

2.2.1.12 Aerothermodynamics. The thermal protection system is designed on the basis of temperature distributions obtained with entry trajectories constrained by heating boundaries consistent with temperature limits of 2300°F for the lower orbiter surface and fin leading edge, and 2800°F for the nose cap. Temperatures are relatively uniform on the lower surface and there is no evidence of shock impingement or flow interaction effects on fins or other parts of the vehicle. Heat shield materials are selected to provide a 200°F margin over the calculated temperatures assumed as the design limits, and insulation thickness is determined to limit the temperature of aluminum structures to 300°F and of titanium structures to 600°F.

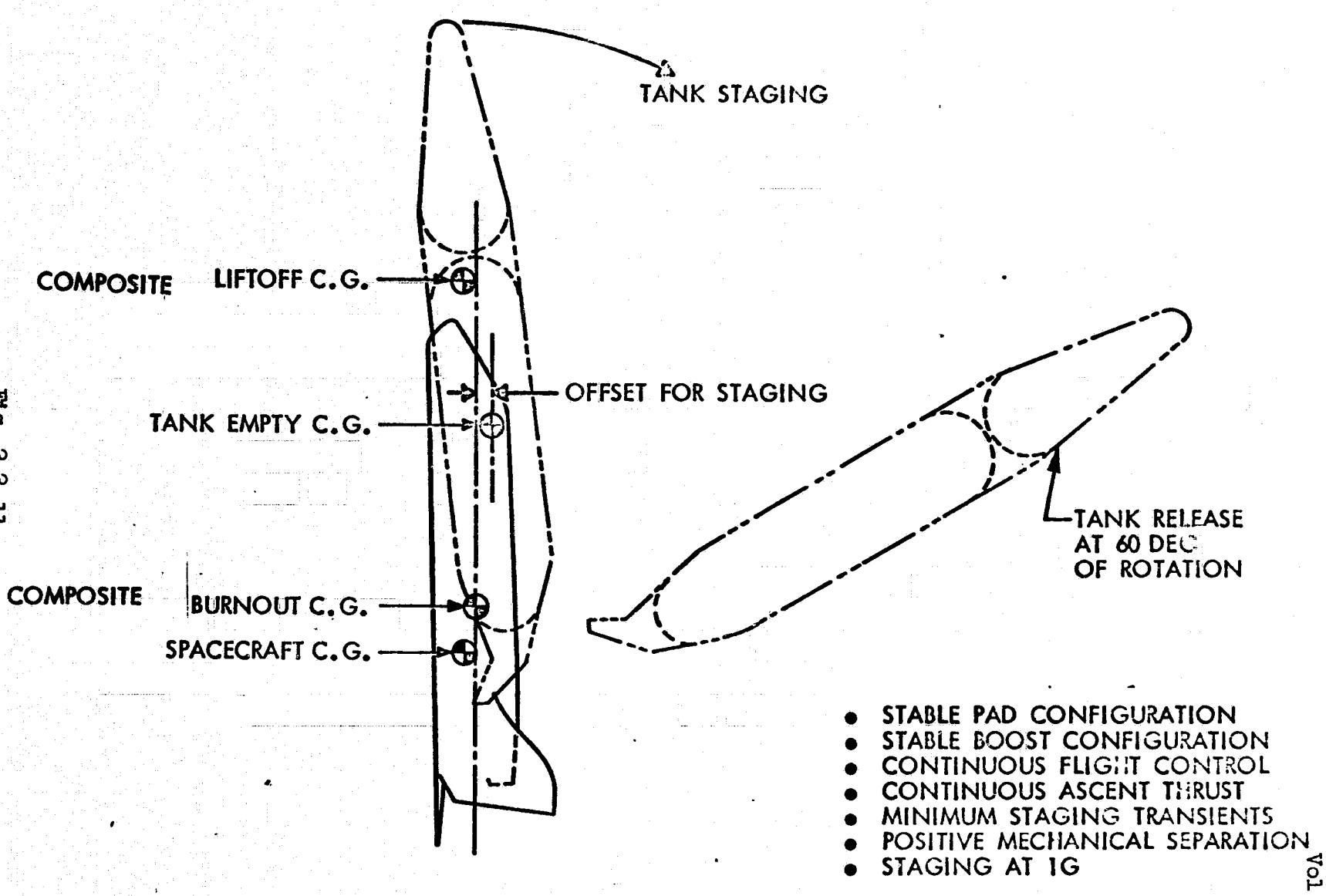

D03074 **Fig. 2.2-11 Stage-and-One-Half Launch Configuration Balance and Alignment**

(RE 222 TRAJECTORY)

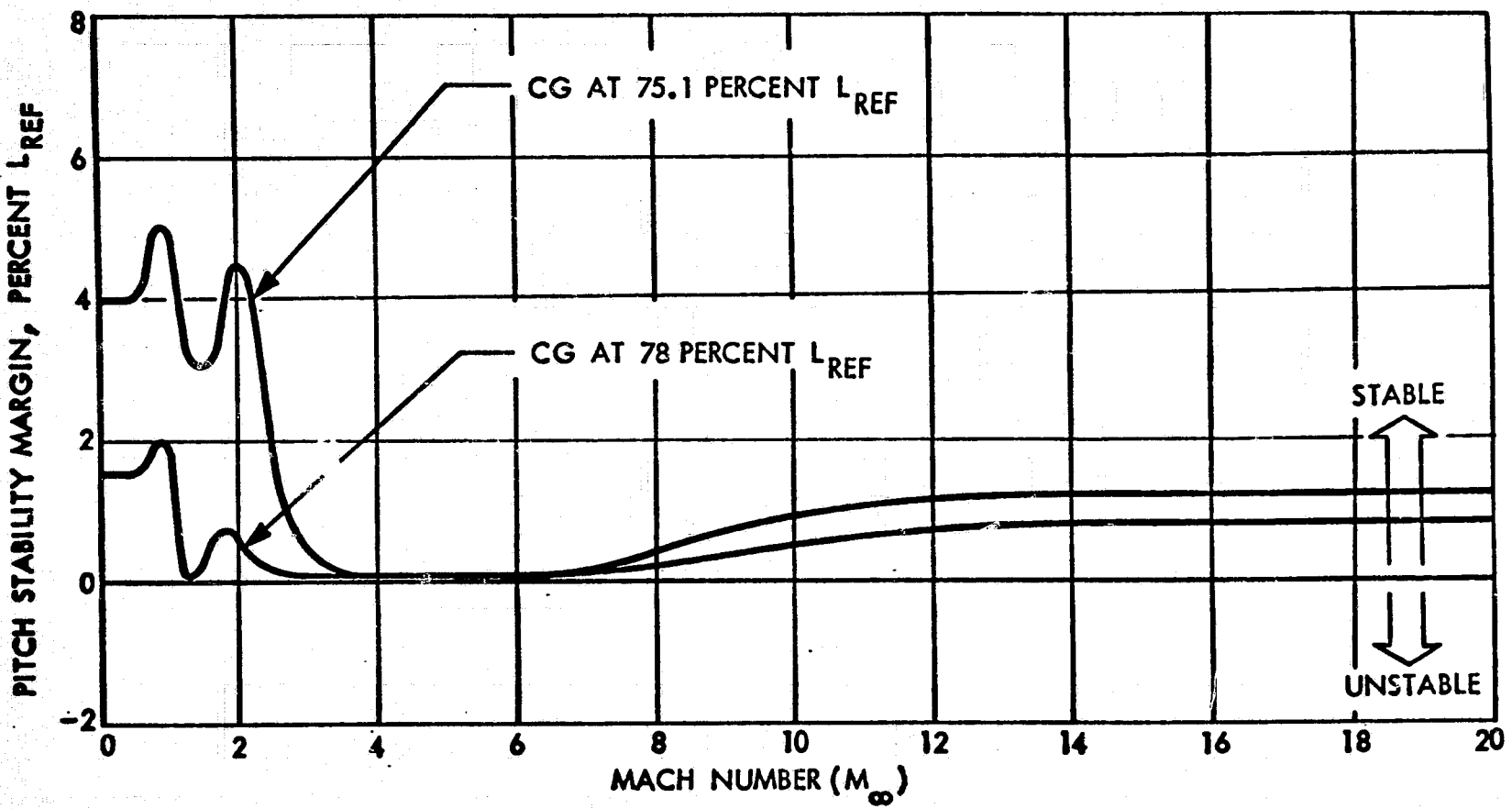

REFERENCE:

- LOCKHEED 6 FT X 12 FT TEST L-324
- AMES 6 FT X 6 FT TEST 542
- LANGLEY UPWT TEST 955

D03259

Fig. 2.2-12 1-1/2 Stage Delta Body Orbiter Longitudinal Stability Summary

(RE 222 TRAJECTORY)

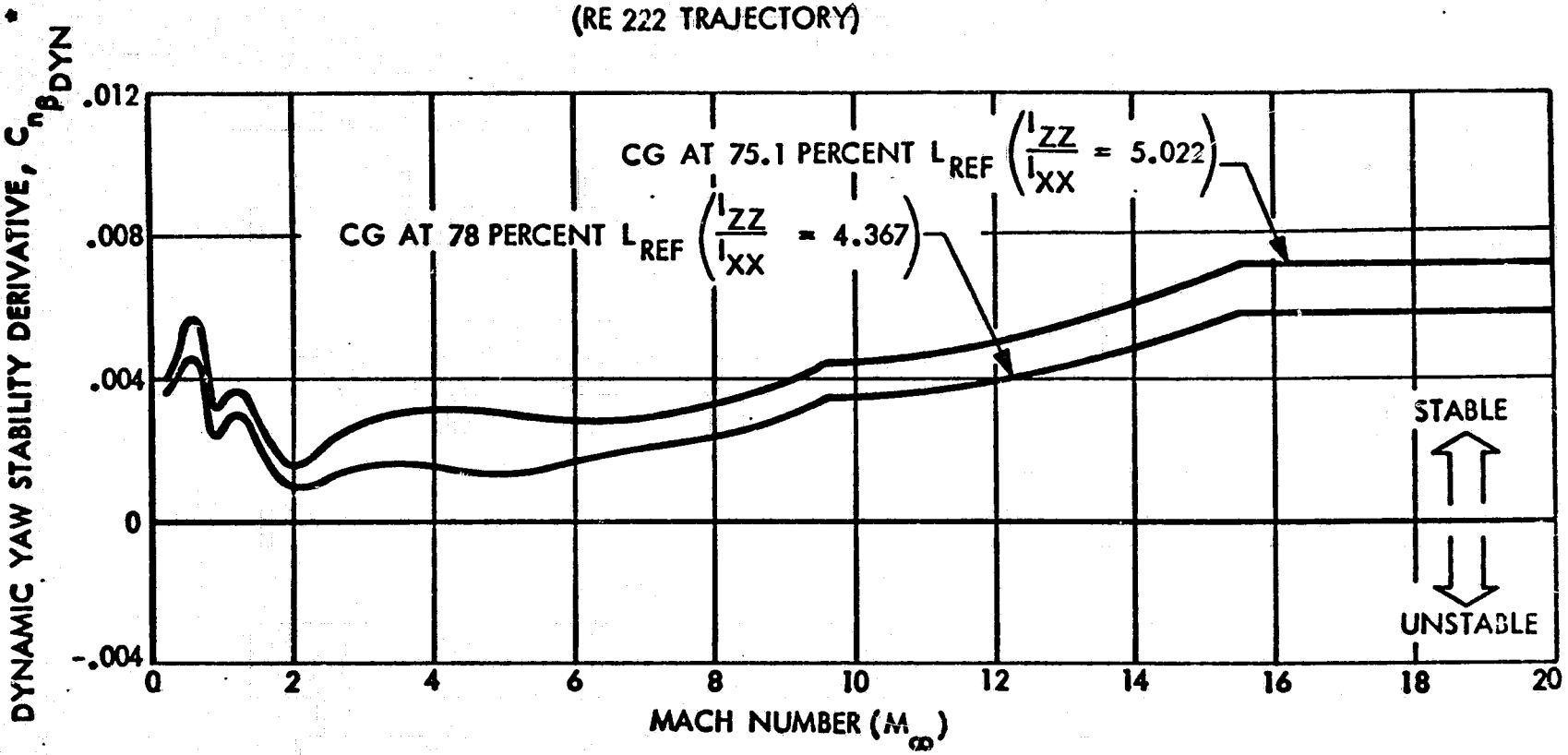

REFERENCE:

- LOCKHEED 8 FT X 12 FT TEST L-324
- AMES 6 FT X 6 FT TEST 542
- LANGLEY UPWT TEST 955

*BASED ON L_{REF}

Fig. 2.2-13 1-1/2 Stage Delta Body Orbiter Directional Stability Summary

AERODYNAMIC LIFT-TO-DRAG SUMMARY

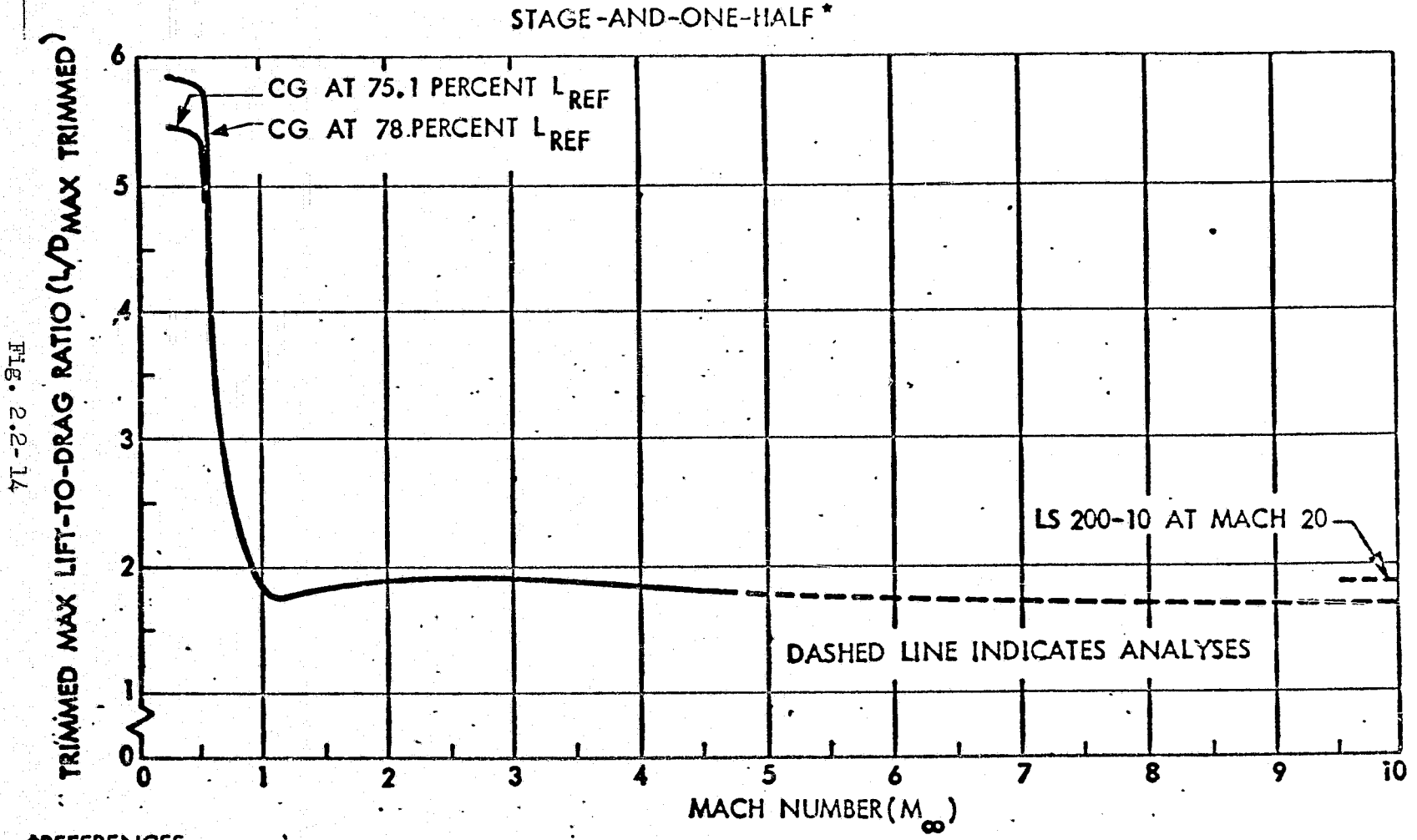

*REFERENCES:

- LOCKHEED 8 FT X 12 FT TEST NO. L-324
- AMES 6 FT X 6 FT TEST NO. 542
- LANGLEY UPWT TEST NO. 955

D03065

Fig. 2.2-14 1-1/2 Stage Delta Body L/D Summary

2.2.1.13 Payload Performance. The payload performance capability, including related values of GLOW and thrust-to-weight ratio is shown in Table 2.2-2 for the two conditions of either off-loaded droptanks, providing the design payload for all missions, or for fully loaded droptanks, indicating the inherent growth potential of the $1\frac{1}{2}$-stage system for the two 100 nm missions. The payload performance quoted is nominal, except that for the main propulsion and orbit maneuver propulsion systems, -3 sigma specif impulse values are used. The propellant reserves considered in the determination of the system inert weights are listed in Table 2.2-4. A growth/uncertainty factor of 10 percent is applied to all dry weights with the exception of the main rocket engines. Structural verification and nominal flight characteristics are based on the assumption of maximum payload of 40K for entry and landing.

The corresponding allocation of the OMP propellant for the orbital velocity increments is shown for the three missions and the system providing the design payloads in section 2.2-4 in Table 2.2-7.

Table 2.2-2

PAYLOAD PERFORMANCE CHARACTERISTICS

Mission	Design Mission Due East	Reference Mission South Polar	Reference Mission 270 nm, 55 deg Inc.
Payload Specified, klb	65	40	25
Airbreather Engine System	Out	Out	In
Droptank Fully Loaded			
Payload, klb	95.1	54.6	25.0
Liftoff T/W	1.245	1.260	1.250
GLOW, Mlb	3.832	3.789	3.816
Droptank Offloaded			
Payload, klb	65.0	40.0	25.0
Liftoff T/W	1.38	1.33	1.25
GLOW, Mlb	3.450	3.588	3.816

2.2.1.14 All Azimuth Launch Capability. All-azimuth launch capability for the stage-and-one-half can be obtained by adjusting the tank staging conditions to cause the tanks to impact in open ocean areas. This is accomplished at the expense of payload, if the tank impact range is increased much beyond the normal impact distance of 900 nm. This is illustrated in Fig. 2.2-15, for the case of the airbreather engine system (including cruise propellant) installed. With that system removed, the indicated payload capability would be increased by about 30,000 lb.

2.2.1.15 Sensitivities and Growth. Performance sensitivity and growth of the stage-and-one-half are illustrated in Table 2.2-3 and in Fig. 2.2-16. Zero payload sensitivity to orbiter and droptank weight growth during the first 18 months of development can be obtained by permitting the tank size to change, with the resulting reduction in thrust-to-weight ratio as shown in Fig. 2.2-16.

2.2.1.16 System Payload and Operational Growth Potential. After the system is developed and operational, the performance can be increased further by deleting airbreathers (+34,000 lb payload), reducing droptank insulation (+1300 lb payload), retrofitting advanced materials (+18,000 lb payload), upgrading main engine performance (+35,000 lb payload), reducing TPS for low crossrange (+12,000 lb payload), or reducing the thrust-to-weight ratio by using excess droptank volumes designed into the system initially (+11,000 lb payload). The total potential performance growth, if all these actions were taken, is up to 81 klb payload added to the polar and east missions and 107 klb added to the 55 deg inclined mission.

Addition of drop engines, kick stages, or strap-on concepts can further increase the payload to as much as 300,000 lb and can include capability for large-diameter payloads. Reductions in recurring cost after the system is operational (a form of growth) can be accomplished by (1) introducing advanced low-cost tank manufacturing methods into the tank production schedule or (2) eventually developing a booster and converting the stage-and-one-half orbiter to a two-stage orbiter.

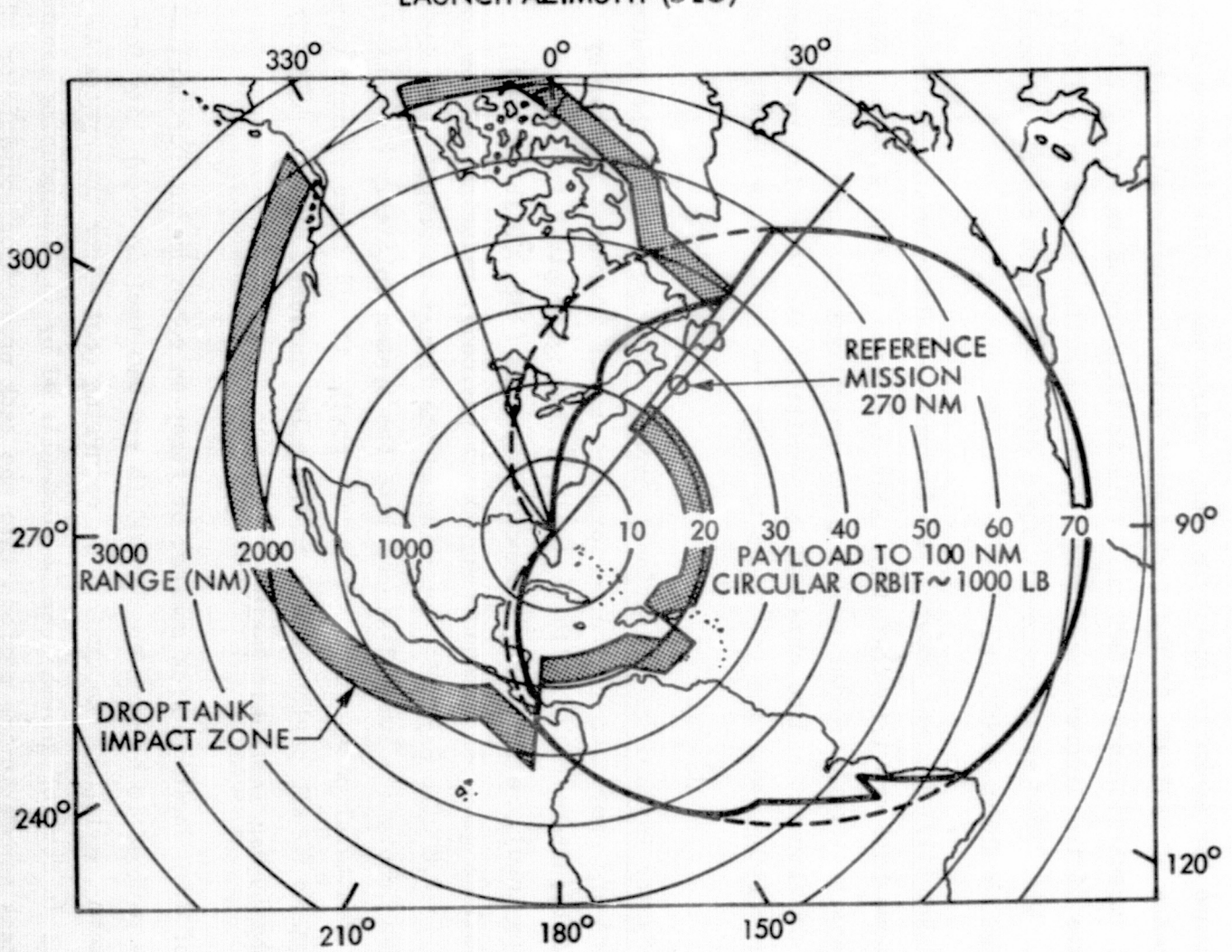

D02186

Fig. 2.2-15 $1\frac{1}{2}$ Stage All Azimuth Launch Performance

Table 2.2-3

STAGE-AND-ONE-HALF SENSITIVITY PARTIALS

VARIABLE DESIGN DROPTANKS, CONSTANT PAYLOAD

$$\frac{\partial(\text{GLOW})}{\partial(\text{Inert Weight, Orbiter}} = 25.6^*$$

$$\frac{\partial(\text{GLOW})}{\partial(\text{Inert Weight Droptank}} = 10.7$$

$$\frac{\partial(\text{GLOW})}{\partial(I_{sp}} = -39{,}900 \ \text{lbm}^2/\text{lbf-sec}$$

PAYLOAD SENSITIVITY

$$\frac{\partial PL}{\partial(\text{Inert Weight Orbiter})} = \text{Zero, and -1 or -3265 lb/percent}$$

$$\frac{\partial PL}{\partial(\text{Inert Weight Droptank})} = \text{Zero, and -0.457 or -561 lb/percent}$$

$$\frac{\partial PL}{\partial(I_{sp})} = 1890 \ \text{lbm}^2/\text{lbf-sec}$$

*With secondary effects

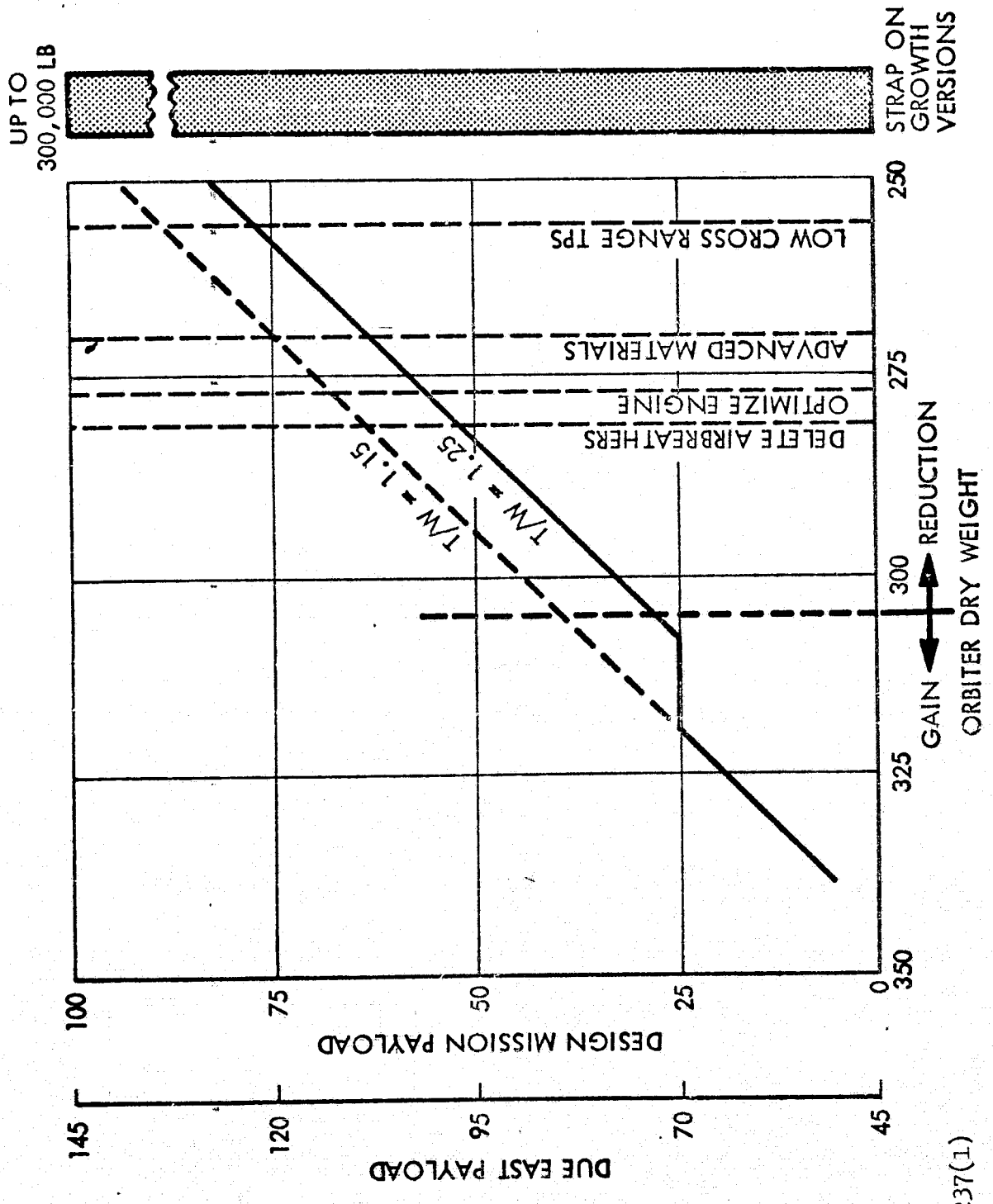

Fig. 2.2-16 1½ Stage Low Risk Performance Growth

Fig. 2.2-16

2.2.1.17 Modular Development, Production, Maintenance, and Growth Capability. The general arrangement and design of the 1½-stage vehicle system was guided by considerations for arriving at a system amenable to simple and efficient development, production and maintenance procedures and operations. This is achieved, as shown in Fig. 2.2-17, by separating the vehicle system into the three major modules of (1) droptank; (2) orbiter rocket propulsion, and (3) orbiter vehicle.

This modular concept is adopted at a lower level in the orbiter vehicle where major subsystems and assemblies are concentrated into distinct functional and spatial submodules, the principal of which are (1) electronics, service and crew systems, located in the vehicle nose; (2) major mechanisms for stowage and deployment of main landing gear and airbreather engines at the lower fuselage surface aft of the payload bay, and (3) aerodynamic surfaces including control and deployment mechanisms at the aft end of the airframe.

With this arrangement, the individual modules and submodules can to a large extent be designed, subintegrated, developed and tested independently, and finally assembled into the vehicle system with a major reduction in development and production effort and cost. Later removal for major maintenance operations or for growth by exchange with advanced equipment is possible with minimum interference with the remaining systems.

The propulsion module consists of the thrust structure, rocket engines, and orbiter propellant tanks. This module can be developed and cold-flow and hot-flow tested without the vehicle airframe system. Eventually, the droptanks can be added to the propulsion module and the entire launch system can be tested. The staging operation for the tanks can be duplicated on the ground using only the propulsion and droptank modules. The vehicle module, including the airframe, aerodynamic surfaces and controls crew compartment, payload bay and accommodations, and subsystems, could be flown with only a dummy propulsion system installed for interface control.

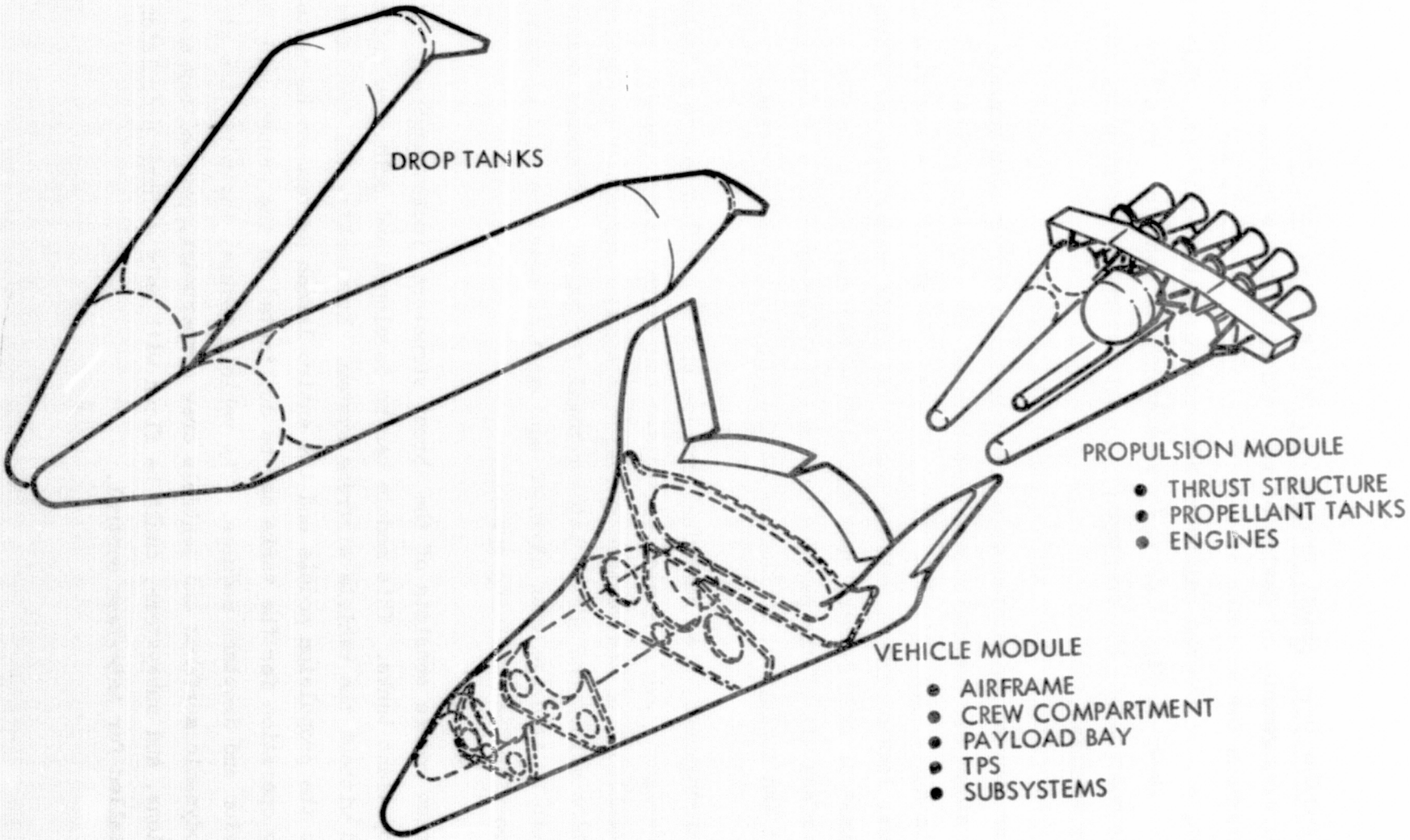

D02070 (1)

Fig. 2.2-17 Delta Body Modular Design Approach

Individual module assembly and removal are made possible by providing three major assembly joints in the vehicle structure which permit the separation of the airframe into four major assemblies. Low-cost production and ease and efficiency of maintenance and refurbishment operations are further enhanced by the large cross-sections which are provided by the delta-body concept throughout the entire airframe. These allow the installation of the required propellant quantities in tanks of simple geometric configurations with ample clearance space between the tanks, structures, and other subsystem equipment. This arrangement also permits, to a certain extent, modifications of the geometry of individual systems and subsystems without redesign of other major components.

2.2.1.18 Low Risk Potential. The 1½-stage systems concepts inherently provides a low risk potential primarily due to the following factors:

1. Only a single complex, and manned vehicle is required per flight, as against two with the two-stage system, which basically reduces the failure probability by a factor of two.
2. The separation maneuver is fully mechanically controlled and accomplished by the inertias of the modules involved under the action of the thrust forces of the operating main engines without requiring the addition of any active system.
3. Since staging occurs at 1g acceleration and near zero-q, no advanced aerodynamic parallel staging technology is required. The staging maneuver can be simulated closely on the ground for testing all involved structures and mechanisms, including propellant line disconnects under near operational conditions.
4. The possibility of flight testing the orbiter vehicle alone, without the assistance of a booster, permits evaluation of the operation of all systems involved under most critical flight conditions with minimum risk.

5. With all engines ignited and operating at NPL prior to launch, main engine in-flight starts are not required for normal operation. All engines are checked out by ground operations. In the event of engine failure to ignite, the mission can be scrubbed without abort.

6. The large number of engines installed permits assigning three engines for the post-separation phase, providing full fail-operational capability under the one-engine-out condition without the necessity for adding weight or reserve propellant for abort maneuvers.

7. The use of fixed position nozzles with the main rocket engines reduces system complexity and failure probability.

8. The possibility of adjusting system performance within a large margin by changing droptank propellant weight permits accommodating changes in orbiter characteristics or requirements during the development period without design changes on a highly complex second vehicle module.

2.2.1.19 System Design Characteristics Summary. The system design characteristics are discussed briefly in Sections 2.2-2 and 2.2-3 for the droptank module and the orbiter. The most important quantitative system design, dimensional, performance, and mass property characteristics are summarized in tabular form in Section 2.2-4.

Resolution of the 1½-stage technical issues was accomplished in a vehicle design which, without resorting to use of advanced materials for the primary structures, combines the required envelope for the installation of the payload, engines, and propellants with a configuration giving trimmable and stable flight and adequate performance characteristics over the entire mission profile. The extreme center of gravity locations listed in Table 2.2-4 indicate that they are within the permissible limits for stable flight established in Section 2.6, except for the condition with removed payload and airbreather engine system. However, since as shown by the data in Table 2.2-2, for this condition the ascent

payload potential highly exceeds the design requirement, this situation can easily be remedied by replacing the removed airbreather engine by approximately 2000 lb of ballast installed in the orbiter equipment compartment.

In conclusion, it can be stated that all established space shuttle performance, design, and operational requirements – with minor modifications from the latter for adjustment to specific $1\frac{1}{2}$-stage design conditions – can be satisfied, or exceeded with a vehicle system displaying a lower gross liftoff weight and an inherently higher reliability potential than a comparable two-stage system.

2.2.2 Droptank System and Droptank-Orbiter Interface Characteristics

The droptank module, shown in Fig. 2.2-18, consists of two symmetrical tank assemblies connected at the front by an intertank tie that resists only shear and torsional loads, and rigidly at the rear by the attach points through the orbiter thrust structure. Each tank assembly comprises a forward primarily conical LO_2 tank, an aft primarily cylindrical LH_2 tank, an intertank structure, and forward and aft support structures. All are manufactured of aluminum, except the aft support structures, which are made of titanium considering the highly concentrated load condition in this area.

The module is connected with the orbiter by a forward and two aft attach points which are arranged on the orbiter upper surface to avoid heat shield penetrations in the area of extreme surface temperatures. The forward attach mechanism uses a link tie mechanism, integrated with the intertank tie structure, which is connected to the orbiter nose by a fitting designed to resist loads only in the pitch direction. The two aft ties -- one at the end of each tank assembly -- are connected by ball-joints to the orbiter close to the thrust structure so that loads are reacted in all directions, but moments are not introduced into the orbiter. Consequently, free longitudinal movement between tanks and orbiter is possible for thermal expansions and contractions. The aft joints also permit upward rotation of the entire droptank module during the initial separation phase and include the mechanism required for ultimate release, completing the separation maneuver.

All propellant and gas line connections are arranged close to the attach points, permitting use of common and relatively small doors for reducing the number and size of the necessary heat shield penetrations. Two LO_2 transfer lines enter the orbiter at the location of the forward attach point, and the LH_2 transfer lines enter at the location of the aft attach points. Use of straight pull-apart line disconnects is made possible by the radial separation motion.

The droptank system includes propellant loading instrumentation and external insulation. Cork insulation is used in the forward cone section for protection

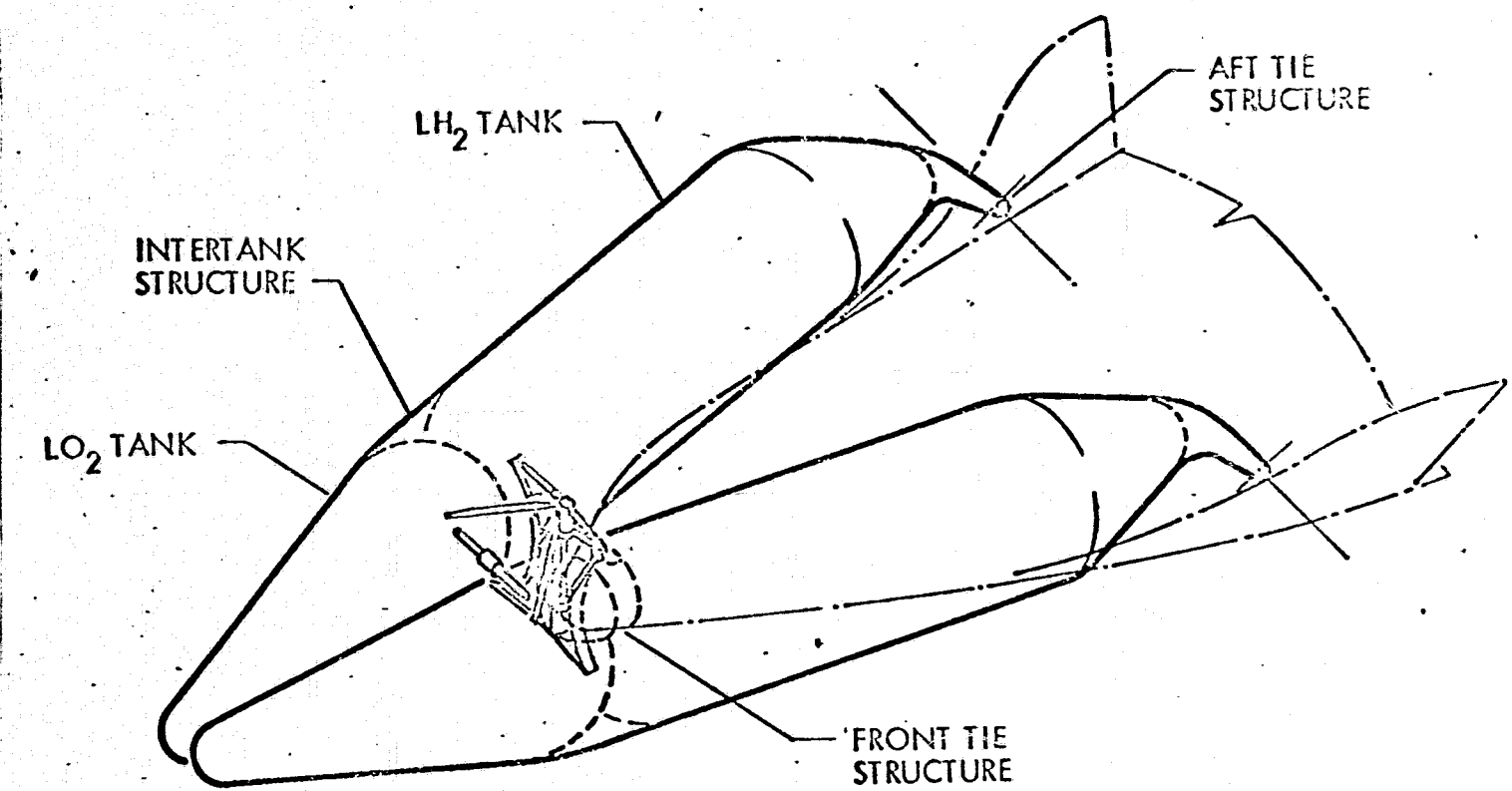

Fig. 2.2-18 Droptank Module

from ascent aerodynamic heating. Two lb per cu ft of spray polyurethane foam is used on the hydrogen tank and is sized to prevent cryopumping during ground hold. An additional 2400 lb of cork insulation is required over the entire surface of the tank **assemblies to protect the tank structure for intact entry.**

The droptank system was designed, loaded, and stressed in considerable detail to provide a basis for justifying tank weight and cost. Tank external loads were used in an LMSC buckling criteria computer program to establish tank skin gages, stringer dimensions, and ring requirements. The tanks operate at from 18 to 21 psia for the oxygen tanks and 26 to 27 psia for the hydrogen tanks. Liftoff loads are design critical. The resulting propellant fraction for the tank is 0.961, including structure insulation and instrumentation.

The tank design was conservatively based on use of expensive machine and chem-milled integral skins joined by fusion welding. This process does not reflect good mass production practice, but was chosen to obtain a conservative high tank cost. Alternate methods of manufacturing the tanks could be used to reduce cost with very little reduction in the propellant fraction. Lockheed, for example, has successfully manufactured a 17 ft long by 10 ft diameter cryogenic tank using a weld-bond process to join as-received sheet aluminum stock. Coupon tensile tests at room and cryogenic temperatures under load and vibration have verified the structural advantage of the spot-bond process.

2.2.3 Orbiter Design Characteristics

2.2.3.1 Configuration and Aeroshape. The general arrangement of the orbiter is shown in Fig. 2.2-19. The orbiter geometry is basically a modified delta body, characterized by large leading edge radii and a steeply sloped upper forward body to provide satisfactory pilot visibility and to improve volumetric efficiency. Multipurpose side fins provide directional and longitudinal stability and increase primarily subsonic lift. Aerodynamic stability and control are also provided by 9 additional aerodynamic surfaces. Two upper elevons are used primarily for longitudinal trim and roll control; a lower trim flap is used for longitudinal trim, and two elevons installed at this flap are used for pitch control and primarily high-speed roll control; and rudders and drag brakes located at the fins are employed for yaw control and are biased through the speed regime to provide satisfactory combination of pitch, roll, and yaw characteristics.

This configuration combines adequate flight performance, entry temperature control capability, and satisfactory flight control and stability characteristics with a high volumetric and structural design efficiency. It allows minimization of reentry time (through low-crossrange maneuver requirements) at flight attitudes not requiring transition maneuvers in the post-stall regime at transonic and subsonic speeds. The basically triangular planform provides the large base area required for the installation of the engines and aft location of the aerodynamic force center adequate to balance the resulting aft location of the center-of-gravity during reentry and landing. The location of the cg was further controlled by using a 53:1 nozzle expansion ratio for the main rocket engines, which permits moving the aerodynamic surfaces about 2 ft aft without undue plume impingement.

In order to further improve packaging efficiency of the delta-body configuration, the forward body sections are modified from ideal design conditions where roll-in would be determined solely by requirements for minimal reentry heating and minimal loss of directional stability and of lift-to-drag ratio at the hypersonic design angle-of-attack. The increased heating and instability

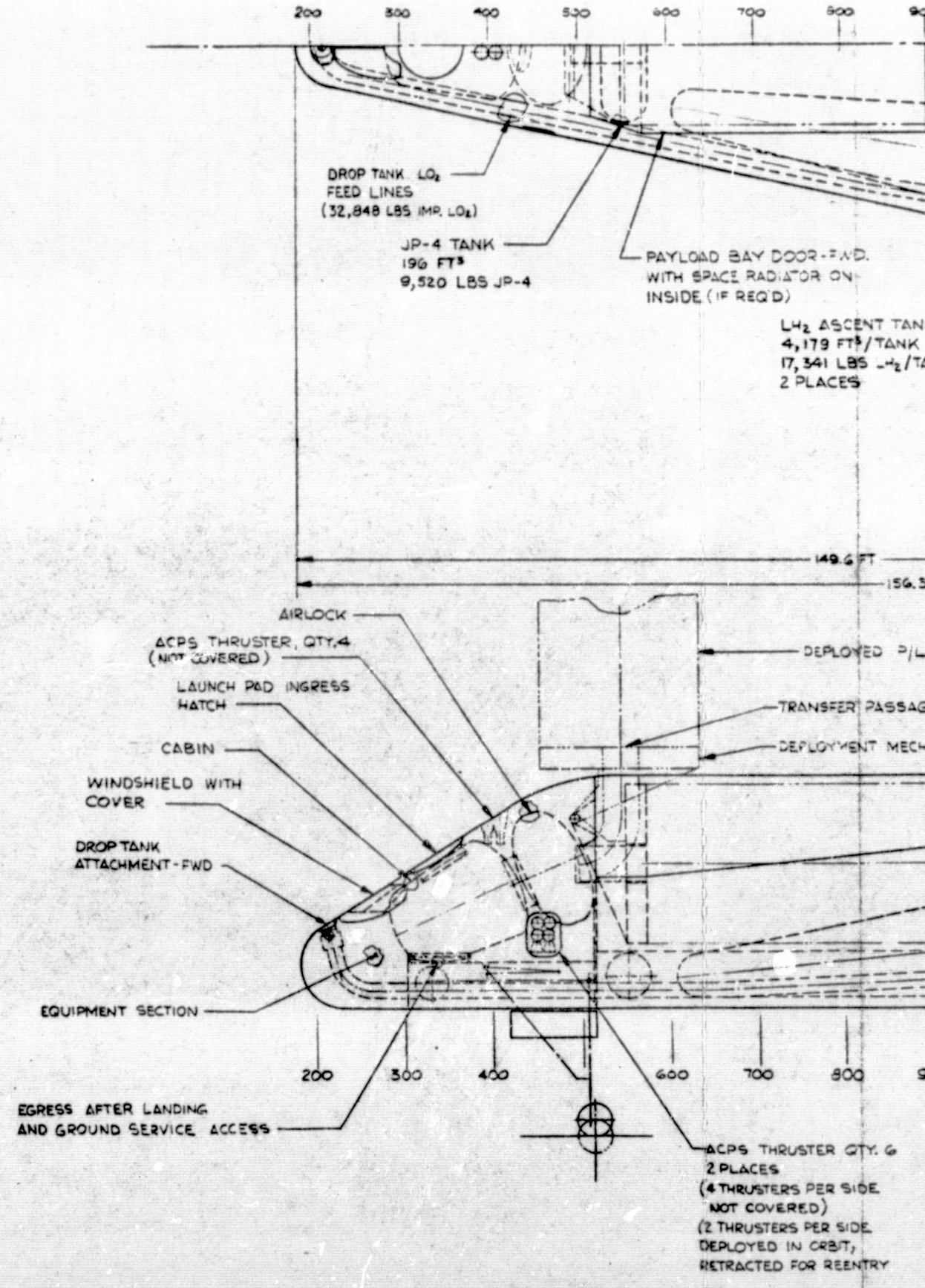

FOLDOUT FRAME

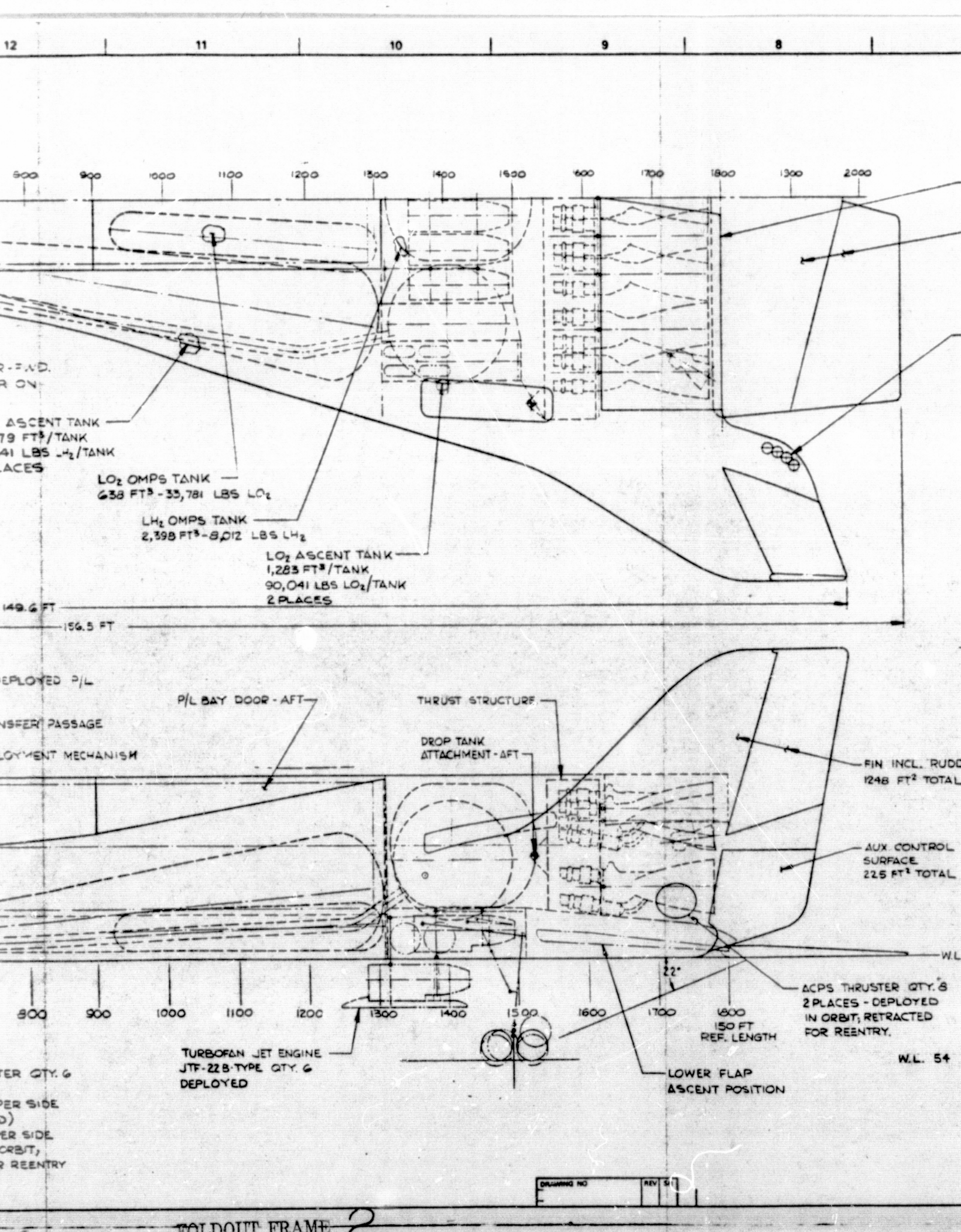

FOLDOUT FRAME 2

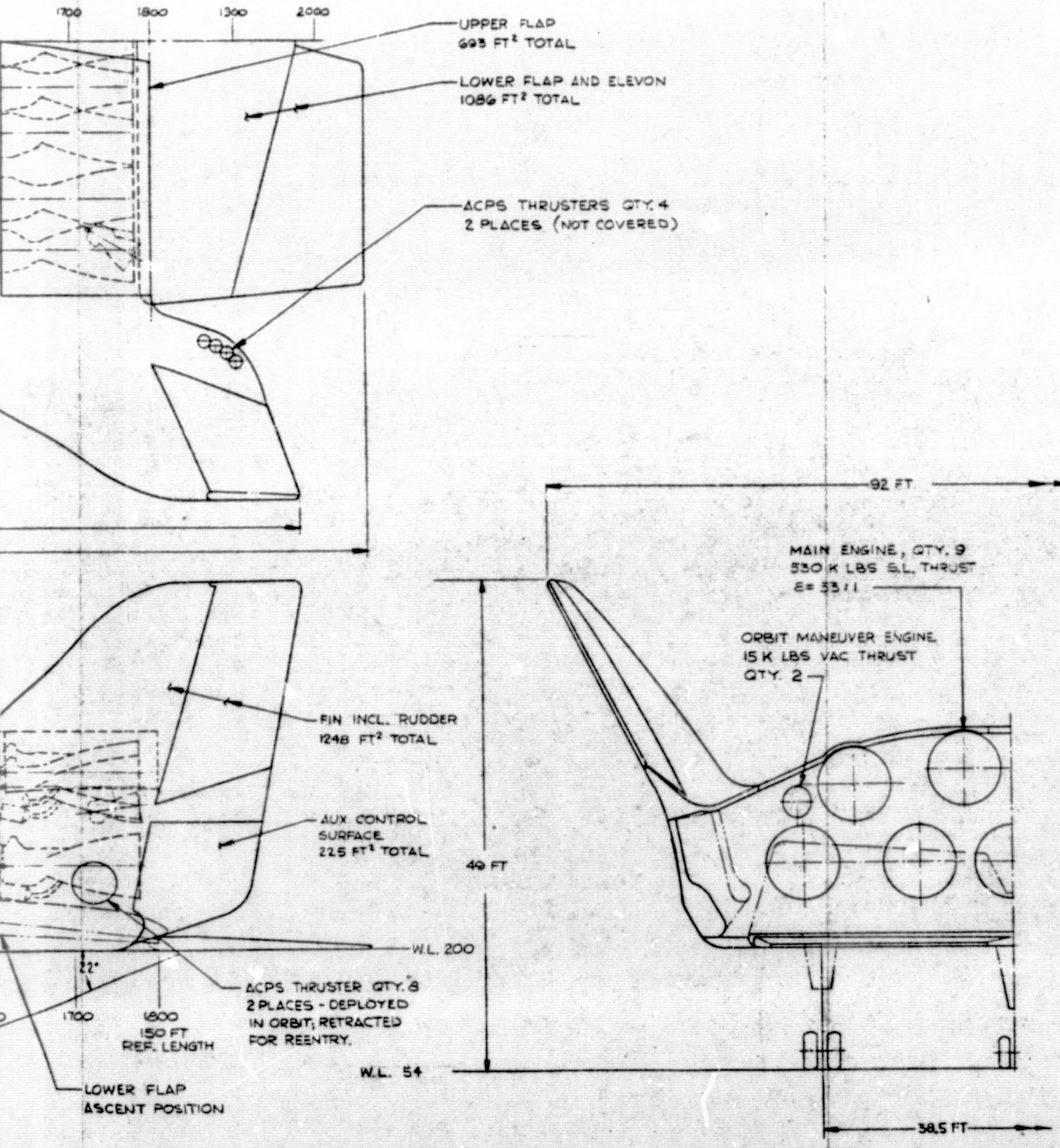

REV SH

FOLDOUT FRAME 3

REPRODUCIBILITY OF THE

LIMITED CALENDAR LIFE	LIMITED OPERATING LIFE

REVISIONS			
ZONE	LTR	DESCRIPTION	DATE	APVD
	A	LO_2 OMPS TANK WAS 631 FT³. 33,250 LBS; LH_2 OMPS TANK WAS 2,358 FT³. 7,859 LBS.; JP-4 TANK WAS 193 FT³ - 9,498 LBS. ADDED D/T LO_2 FEED LINE	4-23-71	

PRECEDING PAGE BLANK NOT FILMED

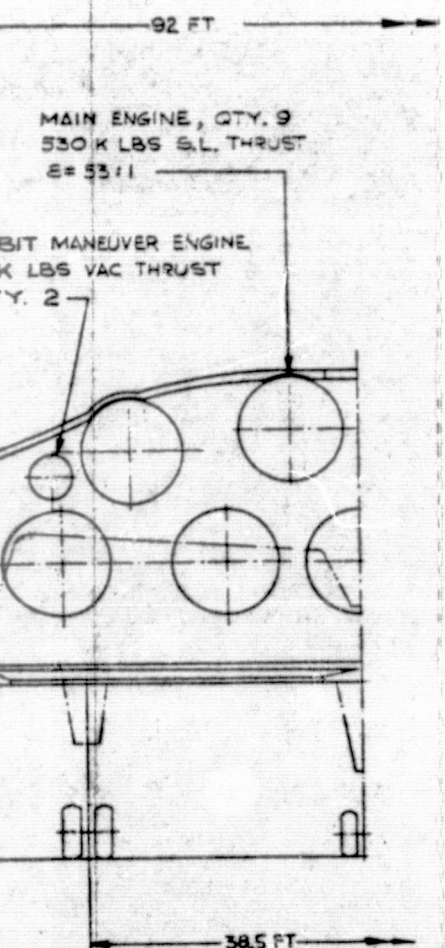

AREA:

REF. PLANFORM	4,878 FT²
TOTAL PLANFORM	6,846 FT²
BASE	1229 FT²

Fig. 2.2-19

QTY REQD	CODE IDENT	PART OR IDENTIFYING NO	NOMENCLATURE OR DESCRIPTION	MATERIAL DESCRIPTION OR NOTE	MATERIAL SPECIFICATION	ZONE

PARTS LIST

INTERPRINT DWG PER	UNLESS OTHERWISE SPECIFIED DIM ARE IN INCHES. TOLERANCES ON: FRACTIONS = ± 1/16 DECIMALS: .X = ± .1, .XX = ± .03, .XXX = ± .010 ANGLES = ± 2 DEG	DATE 4-6-71 DWN Hg Schmidt APVD APVD ENGRG CHKD APVD APVD	LOCKHEED MISSILES & SPACE COMPANY A GROUP DIVISION OF LOCKHEED AIRCRAFT CORPORATION SUNNYVALE, CALIFORNIA
NEXT ASSY USED ON APPLICATION	CONTR CCA/CI/FD		GENERAL ARRANGEMENT DELTA BODY - STAGE 1 1/2 MODEL LS-200-10
			SIZE J CODE IDENT 04851 DRAWING NO SKS 100053 SCALE SHEET

introduced by this front body bulging are compensated for by extending the area covered by the high-temperature resistant heat shield and by adjustment of rollout and toe-in of the side fins.

The resulting high volumetric efficiency provides for the installation of all vehicle subsystems without resorting to design solutions which are either expensive or contrary to efficienct maintenance and checkout operations. Easy access for maintenance, inspection, and modular component exchange from the vehicle interior, as well as ample additional space for changing or augmenting equipment, installations, or propellant loads, is provided throughout the vehicle.

2.2.3.2 Crew Accommodations. The crew cabin, installed in the orbiter nose section and on top of the front landing gear bay, is sized for the accommodation of two pilots and two additional crew members. Adequate pilot visibility during landing is easily obtained with the blunt-nose configuration. Ingress and egress during prelaunch operations is through a top hatch. An additional hatch in the cabin bottom permits egress after landing through the nose landing gear well. Ample additional space is available for later expansion of crew or passenger accommodations.

Aft of the cabin, an airlock, adequately sized for the installation of payload control and docking stations, is installed, permitting access to the payload bay through a short 60-in. diameter tunnel.

2.2.3.3 Payload Accommodations. The central vehicle section houses primarily the 15 ft diameter x 60 ft length payload bay and the two ascent LH_2 tanks. The bay is sufficiently aft to provide the space for the installation of the payload deployment mechanism between its forward bulkhead and the airlock. It is covered with hinged split doors, providing a clear opening over its entire projected area and also the surface required for the installation of space radiators.

2.2.3.4 Equipment Installation. Most support equipment is concentrated in the orbiter nose section adjacent to the crew accommodations. The heavy avionics equipment, fuel cells, and batteries occupy the space within approximately the first third of the length of the nose section. The tankage systems for the cryogenic ECS and power system reactants and most of the additional ECS equipment are located in the space left between the vehicle surface and the pressurized compartments, payload deployment mechanism, and forward landing gear bay.

2.2.3.5 Structural Arrangement. The overall structural concept is of a closed-V geometry, consisting of the thrust structure and the droptanks as shown in Fig. 2.2-20. The thrust structure serves the multiple functions of (1) distributing engine loads to the droptanks and to the orbiter propellant tanks and fuselage, (2) providing the orbiter strongback for the distribution of the loads from the aerodynamic surfaces into the fuselage, and (3) providing for the assembly of the pad hold-down attachments. The ascent tank assemblies are designed as two continuous beams which are aft rigidly attached to the thrust structure,and forward connected to bulkheads (coincident with the cargo bay bulkheads) by supports resisting only transverse loads. Thus, longitudinal displacements between tanks and fuselage for the accommodation of thermal expansion and contraction become possible. This arrangement results in short and direct paths for the major acceleration loads from engines to droptanks and orbiter tanks; and the orbiter tank assemblies, without being integrated with the primary structure, can be used for sharing the bending loads with the fuselage. Combining this arrangement with the deep body sections of the delta-body geometry, a system is obtained in which the entire forward section of the fuselage is only lightly loaded.

The resulting general orbiter structure concept is a conventional stringer and bulkhead airframe attached to the thrust structure. It supports the crew compartment, payload, landing gear, and vehicle equipment and is attached to the droptanks at the forward end for relatively small stabilizing shear loads of about only 50,000 lb.

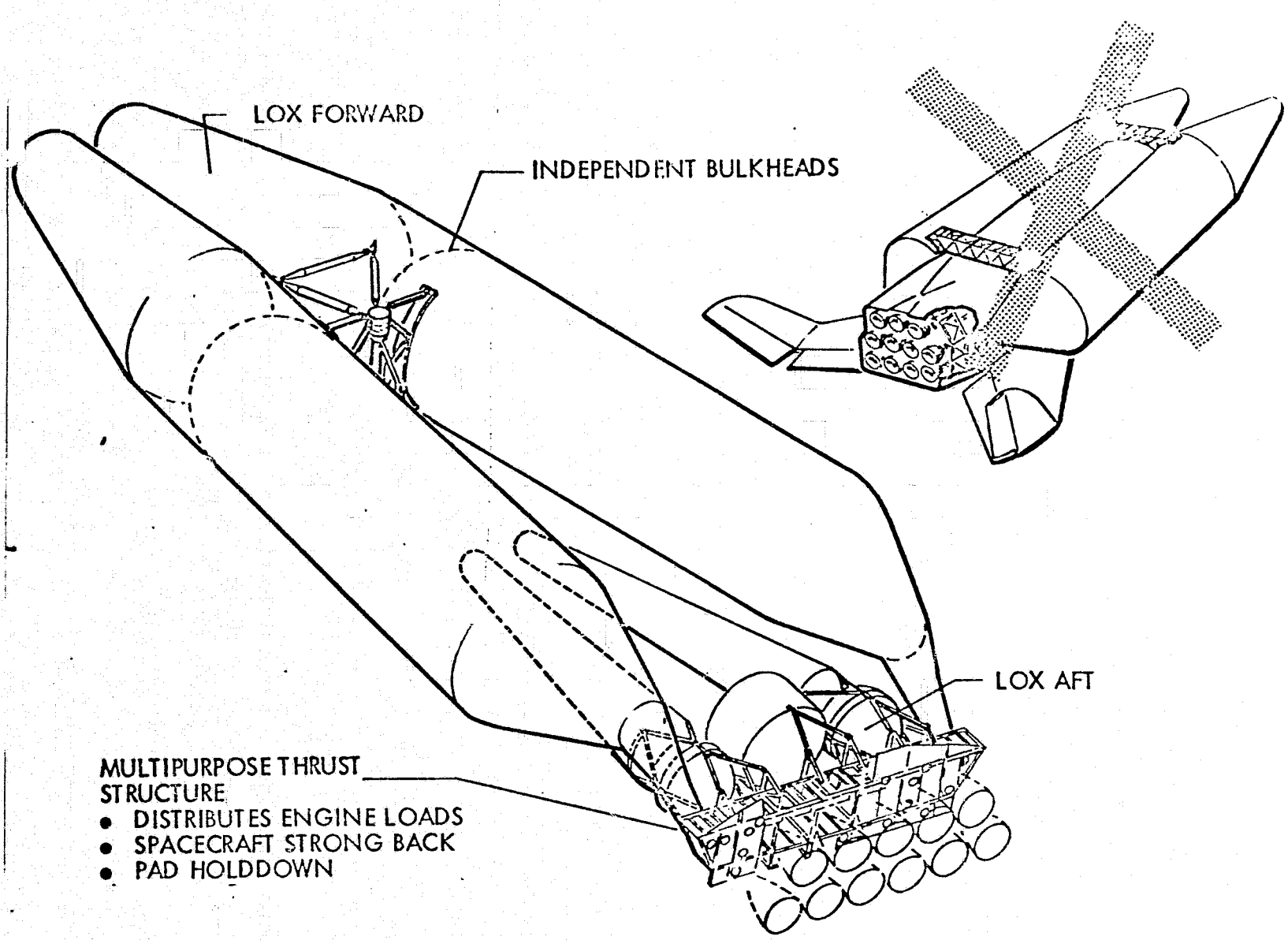

Fig. 2.2-20 Stage-and-One-Half Orbiter Structure Concept

2.2.3.6 Structural Materials: This design concept results in a highly efficient structure which provides the required low weight without resorting to the use of advanced materials or uncommon manufacturing methods. The entire fuselage with the exception of the thrust structure, is made of aluminum. Titanium alloy is used for the trim, flaps, and elevons, and for the payload doors and the thrust structure.

2.2.3.7 Thermal Protection System. The thermal protection system is fully reusable with the exception of flexible flame curtains used at the vehicle base. Heat shield materials were selected to provide a 200°F margin over the calculated temperatures assumed as the design limit, and insulation thickness was determined to limit the temperature of aluminum structures to 300°F and of titanium structures to 600°F. The materials used are titanium for temperatures up to 1000°F, LI-1500 for temperatures ranging from 1000°F to 2300°F, and coated tantalum for higher temperatures up to 2800°F.

Figure 2.2-21 illustrates distribution of TPS materials, design concepts and insulation thickness over the orbiter surface. Approximately 60 percent of the orbiter surface (including leading edges) is protected by LI-1500, which is a 15 lb/ft^3, all silica, rigid, external insulator being developed for NASA by Lockheed. On the orbiter fuselage, the LI-1500 is bonded to titanium subpanels which are attached, through rigid insulators, to aluminum primary frames. This concept was selected to provide for simple refurbishment. For the leeward surfaces experiencing temperatures below 1000°F, a titanium heat shield with internal fibrous insulation is used. On the outer fin and lower flap and elevon surfaces, as well as on the orbiter base, the LI-1500 insulator is directly bonded to the titanium structure. On the leeward fin surfaces, titanium skin is used without internal insulation. Flexible frame curtains are used at the base to protect the gimballed engines and the flap actuators. After touchdown, the heat stored in the insulation is removed during the safing phase by coolant air-flow provided by ground equipment to prevent overheating of aluminum structures.

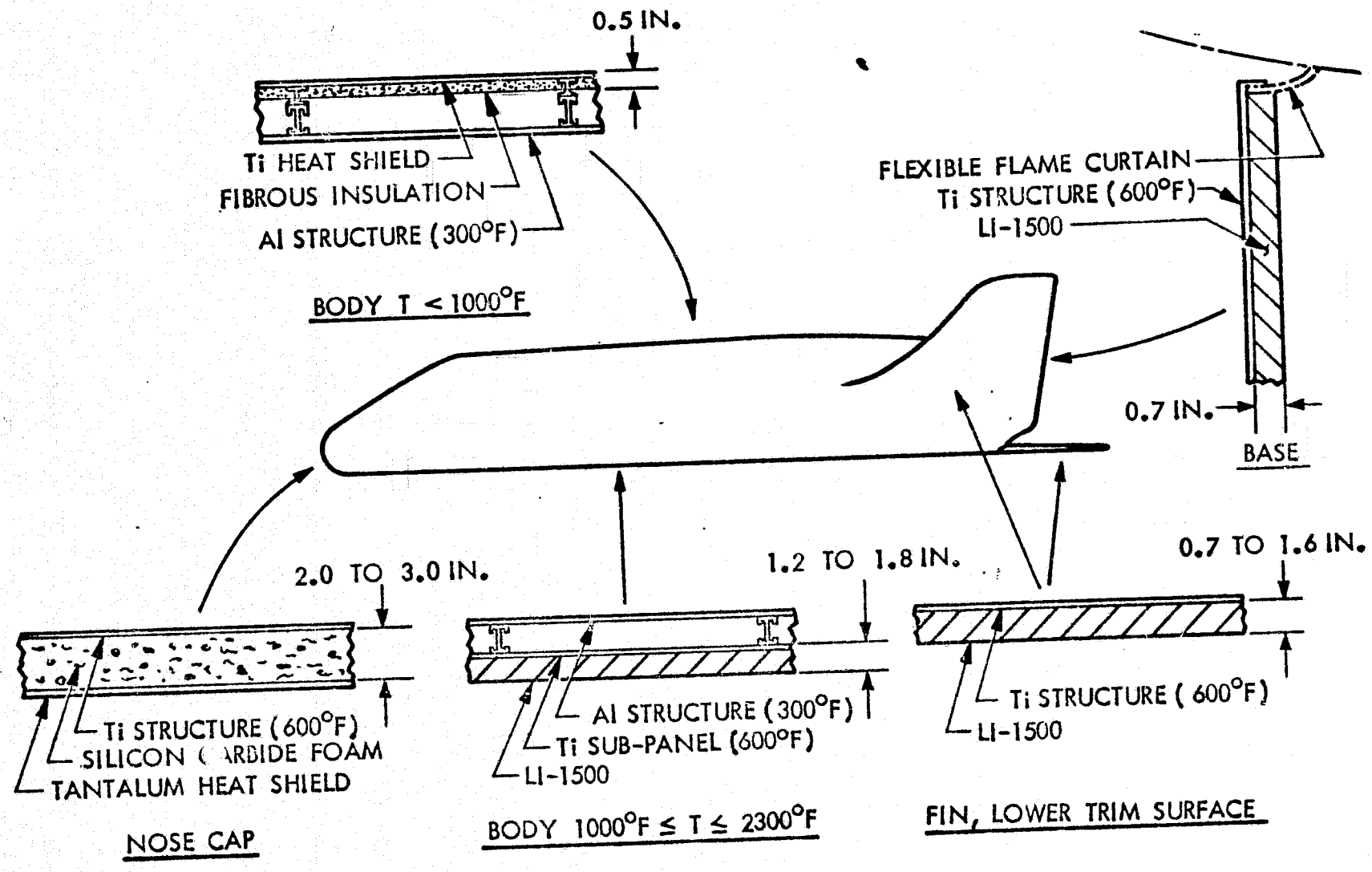

Fig. 2.2-21
2.2-47

D03076 (1)

Fig. 2.2-21 Delta-Body Thermal Protection System

In establishing the orbiter vehicle system, careful attention was given to keeping to a minimum the number of penetrations of the heat shield in general, and particularly on the surfaces exposed to high temperatures. All the openings required for the connection of the droptanks with the orbiter are located at the upper surface of the orbiter. Only three openings are required for this purpose, since the propellant and gas lines are routed so that their couplings share the openings with the structural attachments. On the lower surfaces, besides the inevitable disruptions caused by the hinges of aerodynamic surfaces, eight major penetrations are required: three for the landing gear, one for the deployment of the jet engines, and four for ACS thruster clusters. However, the first four of these penetrations are considered not critical, since their protecting doors need not to be opened prior to reentry. Consequently, seals can be applied and checked by ground operations.

2.2.38 Tankage and Propellant Systems. The propellants for the ascent and orbital operations are stored in separate tankage systems with only the orbital system designed for long-time storage. All the tanks are nonintegral with the basic vehicle structure and have a simple geometric shape, consisting only of spherical, cylindrical, and conical sections with circular cross-sections. All insulation is external. These characteristics are essential for low-cost development, manufacture, and maintenance and for efficient quality control and checkout. For the large ascent tank system, two spherical LO_2 tanks and two conical LH_2 tanks are used. The hydrogen tanks are forward-installed, along and partially underneath the cargo bay, and the LO_2 tanks behind and in line with the LH_2 tanks. The orbital tank system, consisting of single tanks, uses for the LH_2 a short cylindrical tank installed between the cargo bay and the thrust structure, and for the LO_2 a long cylindrical tank positioned under the cargo bay between the two ascent hydrogen tanks.

Crossfeeding capability between ascent and orbital tank systems is not provided, but could be installed if required. The ascent oxygen propellant flow is cascaded from the forward-located droptanks through the orbiter oxygen propellant tanks. The chosen design precludes any possibility for the engines to ingest a gas bubble. The two 19-in. diameter lines between the forward-located orbiter

droptank disconnects and the orbiter tanks are installed inside the orbiter. The ascent LH_2 is fed from the droptanks directly into the engine manifold system through connectors located near the aft droptank attach points.

Sizing and loading of the droptanks is biased so that oxygen depletion occurs prior to hydrogen depletion. Staging is signaled by propellant level sensors in the oxygen line inside the orbiter. At nominal staging conditions, there is no liquid oxygen remaining in the oxygen droptank and approximately 600 lb of liquid hydrogen will remain in the hydrogen tank.

Main propellant feed valves are closed on the orbiter side of both oxygen and hydrogen lines prior to staging. The cascade liquid oxygen design precludes any opportunity for the engines to ingest gaseous oxygen. The hydrogen cross-ship manifold, orbiter propellant tank, hydrogen valves, and a hydrogen circulation system are arranged so that the engines cannot ingest gaseous hydrogen. Circulation of oxygen through the feed system and vent system is provided by circulation pumps during ground hold to prevent oxygen geysering. Propellant losses associated with the sequential shutdown of the main rocket engines are greatly reduced by recirculation into the tanks of the LO_2 residuals in the individual engine feed lines. This is done by the application of pressurant gas without the addition of any moving components to the system.

The main propulsion propellant system is pressurized by gaseous oxygen and gaseous hydrogen bled from the main engines. Prepressurization for engine start is provided through the ventlines from ground supply. Mechanical relief valves are provided for overpressurization safety and backup. Control of pressure for venting and propellant feed is accomplished with redundant pressure switches in a fail operational, fail operational, fail safe redundancy arrangement.

For the Orbit Maneuver Propulsion system, the propulsion storage, thermal conditioning, acquisition and pressurization sub-systems are designed for 30-day storage capability in orbit. It is shared by the propellants for the ACPS and APU units. Helium is selected as pressurant on the basis of an appreciable weight saving in comparison to use of gaseous propellant bled from the RL10 engine.

2.2.3.9 Main Propulsion and Orbit Propulsion Rocket Engines. The nine 530,000 lb sea-level thrust main rocket engines are installed on a transverse thrust structure. Their characteristics and interface requirements are as defined by Space Shuttle Main Rocket Engine ICD 13 M 15000 B with the exception that the expansion ratio is increased to 53:1. Among the 9 engines, the central 5 are gimballed ± 7 deg in a square pattern, and the central 3 are manifolded to permit continued operation through and after separation. Of these central 3, only 2 are used, the third providing fail operational capability for the abort-through-orbit Level I requirement.

The two RL10A-3-3A engines used for the orbit maneuver propulsion system are also installed on the thrust structure. They are arranged outboard of the main engines on additional mounts, placing their nozzle exit planes in line with those of the main engines for avoiding exhaust plume impingement during operation of either engine system. Each engine is gimballed ± 4 deg and appropriately precanted in the null position to allow single engine operation as the normal mode.

2.2.3.10 Attitude Control Propulsion System. The attitude control propulsion system is a high-pressure GH_2/GO_2 system using 40 identical 1500-lb thrusters. Low thrust for limit cycle operation is obtained by pulsing the igniters of the thrusters. The liquid propellants are transformed into high-pressure gases by three independent conversion units consisting of gas generator, turbine, gear train, pumps, heat exchangers, and control equipment, which are designed under conservative assumptions not requiring development beyond current state-of-the-art. The gases are stored under 2000 psia pressure in three accumulator units for feeding the thrusters and the APU units. The conditioning, storage and feed subsystems are designed and sized so that full fail-operational and fail-safe capability is maintained throughout the entire system, and to permit continuous simultaneous operation of four thrusters.

The thrusters operate at a nominal chamber pressure of 250 psia which is associated with a relatively low system specific impulse of 362 sec. Use of a more advanced system operating at higher pressures and also using turbine

exhaust for impulse generation was not considered to provide a significant improvement. With the selected vehicle system, in which more than 90 percent of the maneuvering capability is provided by a separate, high-performance engine system, the gain in ACPS specific impulse would be nearly offset by the associated increase in system weight.

The thrusters are arranged on the orbiter in a pattern, shown in Fig. 2.2-22, satisfying all control and translatory impulse requirements under operational, fail-operational, and fail-safe modes of operation and for no cross coupling in all orbital modes of motion with the exception of yaw translation. During reentry, only the thrusters installed on the leeward orbiter surface and four side-oriented thruster pairs are used, the others (including all downward-directed) being retracted and covered by doors. The remaining active thrusters are adequate, since generation of pure couples is not required during reentry.

2.2.3.11 Airbreathing Propulsion System. The airbreathing propulsion system uses six PWA-JTF-22-A4 type JP-fueled engines. The JP propellant is stored in insulated tanks located forward of the payload bay. They are insulated and equipped with heater elements for extended storage in orbit. Redundant boost pumps backed by capability to pressurize the tanks provide for fuel feed to the engines. The engines are stowed prior to use inside the orbiter close to its cg in the space below the ascent oxygen and orbit maneuver hydrogen tanks between the two main landing gear wells, and mounted on a single door. After reentry, this door is deployed by a parallelogram linkage, placing the engines below the fuselage into the airstream. The remaining clearance of jet engine intakes from the ground is comparable with that of jet engine installations in present-day commercial aircraft.

2.2.3.12 Landing Gear. The tricycle landing gear is of conventional design and provides ample base, tread, and nose gear steering capability. The main gear is installed outboard of the jet engines in the space below the ascent oxygen and the orbit maneuver hydrogen tanks. The forward gear is installed below the crew cabin and airlock. The geometry and space allocations permit

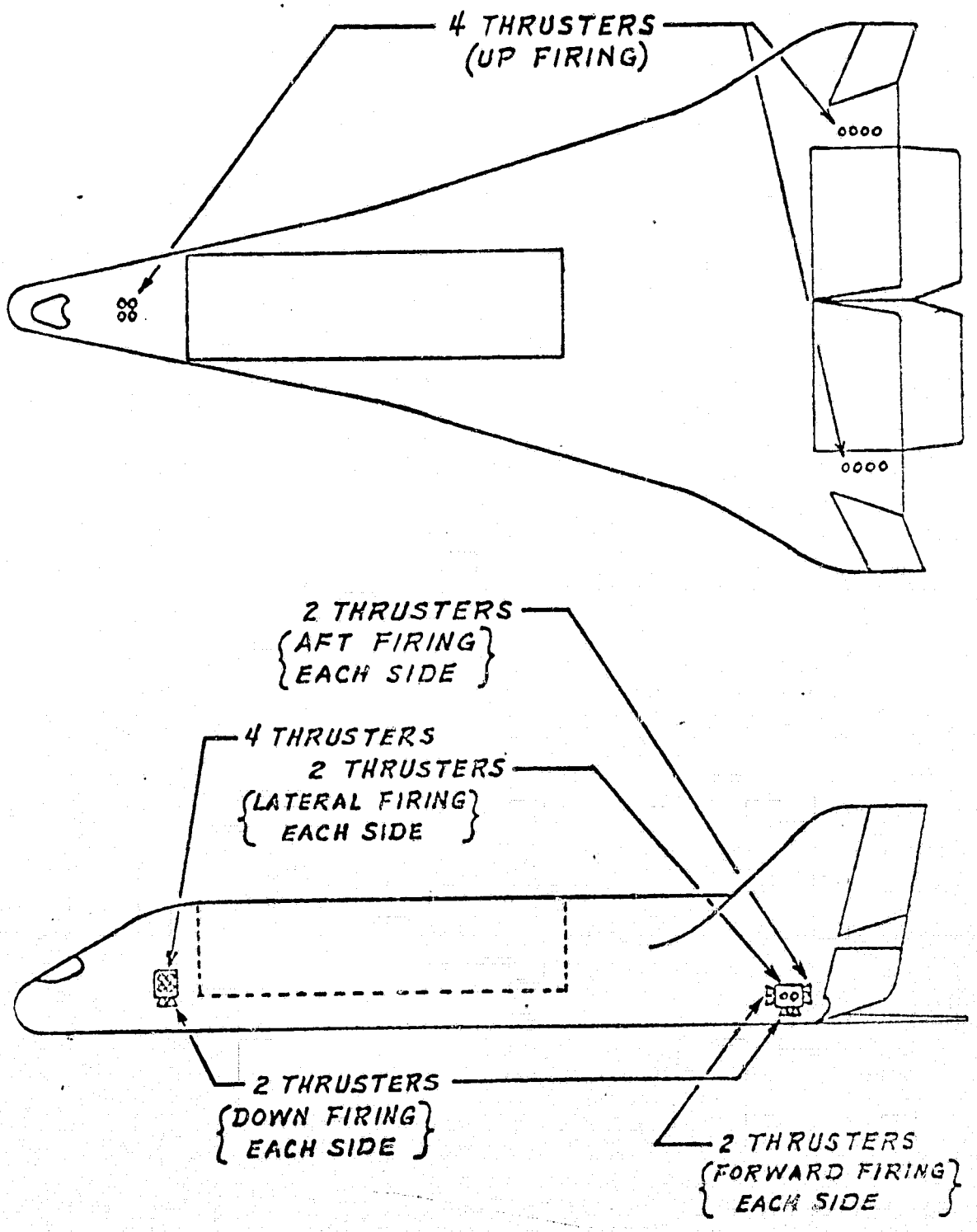

Fig. 2.2-22 ACPS Thruster Locations on Delta Body Orbiter

Fig. 2.2-22

stowage by forward retraction, providing free-fall capbility. Since the doors open only after reentry, they can be closed and sealed by ground operations. The gear is sized so that smaller footprint pressures are obtained on either flexible or rigid pavements than with the DC-8-55 model jet transport in its take-off condition.

2.2.3.13 Lower Flap - Elevon Assembly. The lower flap-elevon system is designed to be retracted during engine operation to avoid plume impingement effects. The assumed stowage conceptual design is similar to aircraft systems and was chosen to permit extension into operating position with least disturbance to the vehicle in a potential abort condition.

2.2.3.14 Environmental and Life Support System. The environmental control and life support system is designed to support a 2-man crew for 7 days. It provides for atmospheric supply, pressure control, carbon dioxide removal, humidity control, thermal control, food and water, waste management, personal hygiene, and first-aid.

The atmosphere supply and control is a two-gas system of oxygen and nitrogen with a partial pressure of oxygen of 3.1 psia and a total cabin pressure of 14.7 psia. Both gases are stored supercritically and heated prior to admittance to the cabin. The oxygen partial pressure is controlled by a polargraphic sensor and the total pressure is controlled by a total pressure regulator with the nitrogen. The oxygen source is shared with the fuel cells.

There are two coolant loops for thermal and humidity control: a water loop in the cabin and a Freon-21 loop external to the cabin. Heat is rejected by a space radiator located in the payload door and peak thermal loads are rejected with a water boiler. Humidity is controlled by a condenser heat exchanger with a coolant inlet temperature of 45° to 50°F. Cabin cooling requirements are relatively low because the cabin is shielded by the vehicle thermal protection system from the space environment. Carbon dioxide and odor are removed by lithium hydroxide and activated charcoal. Urine is vented or dumped

into space; feces and debris are dried and stored. Trace contaminants are eliminated by overboard leakage.

Food is a combination of frozen and freeze-dried products. Excess water is generated by the fuel cells and made available for drinking.

2.2.3.15 Power Systems. The power supply subsystem uses three main energy sources. Batteries are used for emergency supply of essential electrical loads for reentry to touchdown. Three 5-KW capillary matrix fuel cells support orbit electrical loads. Four oxygen/hydrogen APUs drive three 40 KVA AC generators and 12 hydraulic pumps to support heavy loads during prelaunch, ascent, and atmospheric flight. The gaseous propellants are supplied from the high-pressure storage spheres of the ACPS system.

Redundancy for the power sources is adequate. One fuel cell is sufficient to support the basic mission requirements except for short-term power peaks in ascent, rendezvous/docking, and separation. Triple redundancy is also provided in the APU-generator-hydraulic pump combinations to provide fail-operational, fail-operational, fail-safe capability.

Power distribution is accomplished through remotely located circuit breaker/control units and is configured by the data management system. Separate AC and DC bus systems and dual redundancy for all loads and quad redundancy for critical loads are provided. The DC bus can be supplied by the AC bus for backup. Aluminum wire is assumed for large gages.

2.2.3.16 Avionics Systems. The reduction in number of autonomous vehicles from two in the two-stage concept to one in the stage-and-one-half concept leads to a considerable simplification of the avionics system requirement for the overall space shuttle system.

Guidance and Navigation System. The guidance and navigation system provides independent position, velocity, and attitude information. It interfaces with navigation aids (military and civilian) for enroute and terminal entry, ferry, and landing phases. It accepts external position update information as available. It contains a dedicated computer which interfaces with the data management system. The baseline IMU is assumed to be a dodecahedron gyro/accelerometer arrangement currently under development.

Communications System. The communications system is sized for voice plus low data rate. It provides for satellite link communications (voice and data) and is compatible with existing ground-based communications links. UHF is used for EVA, other vehicle communications, and enroute communications.

Multiple Displays & Controls. Multipurpose displays employing electronic and film projection data are provided for the crew. Format and context of display data are under program control with manual override. Dedicated controls and displays are provided for limited function only. Support data for independent analyses of unanticipated events are stored off-line and are accessible to the crew on demand.

Data Management System. The data management system includes distributed redundant computers under central computer control. Computer hardware is identical; only software is peculiar. Standard peripheral interface units with limited special-purpose computational capability are provided.

The data management system is triply redundant with quad redundant executive control. It supplies integrated configuration control with all interfacing systems. It also supplies dedicated algorithm implementation for the flight control dedicated hardware and other interfaced systems.

Onboard Checkout System. Orbiter turnaround is expedited by use of the onboard checkout capability of the data management system working with extensive built-in test equipment (BITE) in the hardware elements of the vehicle.

Inflight status and data from the previous flight are used to adapt repetitive maintenance schedules to the present status of the vehicle, making more efficient use of personnel and facilities. The onboard data management system evaluates the repaired and refurbished systems to a limited extent and accesses data for use by technicians and a companion AGE data complex to perform a high level of systems readiness checks prior to release for erection.

The onboard capability of the data management system is employed during erection, transportation to the pad, launch, and flight to continually reverify the system capability validated during the maintenance cycle.

2.2.4 System Design and Performance Characteristics Summary Tables

Tables summarizing the design and performance characteristics of the Lockheed stage-and-one-half Baseline Model LS 200-10 vehicle system are presented in this section.

A summary of system design, performance, aerodynamic, and major subsystem characteristics is given in Table 2.2-4.

The data demonstrating and defining the capability of the system to satisfy the performance requirements of the three Level I missions are presented in Table 2.2-5 for the baseline system with offloaded droptanks providing the specified payloads, and in Table 2.2-6 for the system with fully loaded droptanks indicating the inherent growth potential for the two 100 nm missions.

The breakdown of propellant contained in the orbit maneuver tank system and the related incremental velocity requirements for maneuvers under nominal and abort flight conditions are presented for the baseline system and for the three missions in Table 2.2-7.

The major dimensional data of the vehicle system are summarized in Table 2.2-8.

A weight summary is presented in Table 2.2-9.

Table 2.2-4

PRINCIPAL VEHICLE SYSTEM CHARACTERISTICS OF STAGE-AND-ONE-HALF BASELINE SYSTEM LS 200-10

SYSTEM SUMMARY	
Concept	Stage-and-One-Half Single Expendable Droptank Module Reusable Orbiter
Configuration	Orbiter Modified Delta Planform Lifting Body
	Droptank Module V-Shaped Droptank Module, consisting of two identical tank assemblies (single LO_2 tank forward and single LH_2 tank aft) straddling orbiter in X-Y plane
	All engines and ACPS thrusters installed on orbiter.
	All engines ignited at liftoff.
Separation Mode	Intact Droptank Assembly rotates "over the top" of orbiter around aft attach point pivots. Motion effected by inertial forces generated by main engine operation without assistance from additional impulses
Crossrange	1100 nm hypersonic crossrange capability
Performance	Satisfies with Gross Liftoff Weight 3.45 ≤ GLOW ≤ 3.82 Mlb all Level 1 Mission Requirements
	Go-around capability with airbreathing propulsion system installed
	Orbiter trimmable and stable under all flight conditions
	Ferry capability with addition of fuel tanks and possibly aerodynamic fairings in kit form
Droptank Impact	For current mission model, all azimuths achievable with ocean impact.
	For extended requirements, omni-azimuth ocean impact capability achievable with minor loss in performance
Materials	Primary structures: Fuselage aluminum; Aerodynamic surfaces, thrust structure and cargo bay door titanium

Table 2.2-4 (Continued)

DIMENSIONS	Orbiter	Droptank (a) Module (b) Single Tank Assy	Composite
Total Length, ft	156.5	192	229
Span, ft	92.0		92
Height, ft			
- gear up	36.75		38
-gear down	49.0		49
Diameter, ft		27(b)	
Planform Area, ft^2	6846		
WEIGHTS, lb			
For 270 nm 55 deg inc. ref. mission Airbreathing propulsion system installed			
Dry	294,399	112,162	406,561
Ascent Propellant			
Impulse	239,209	3,063,218	3,302,427
Loaded	255,198	3,104,894(1)	3,360,093 (1)
Orbit Maneuver Propellant (2)			
Impulse	38,613		
Loaded	40,020		
Attitude Control Propellant (3)			
Impulse	1,211		
Loaded	1,773		
Cruise Propellant			
Impulse	8,430		
Loaded	9,921		
Cargo	25,000		

(1) Including 31,122 lb holddown propellant

(2) Including ACP propellant for generation of 142 ft/sec orbit ΔV

(3) Excluding ACP propellant for generation of 142 ft/sec orbit ΔV

Table 2.2-4 (continued)

WEIGHTS. (Cont'd)	Orbiter	Droptank (a) Module (b) Single Tank Assy	Composite
Landing	325,447		
Entry	334,808		
Staging, before/aft separation	630156/ 625642	122716/NA	752874/NA
Liftoff	630486	3,185,934	3,816,420
Propellant Fraction λ' Dry/Wet(4)	.488/.463	.9651/.9615	
Thrust/Weight Ratio			
Liftoff			1.2499
Maximum Ascent			3.000
At Staging			.500
After Staging			
Initial	1.956		
Final	3.00		

(4) Propellant Fractions are defined:

For the Orbiter

$$\lambda' \text{ Dry} = \frac{\text{Total loaded (ascent + OMP) propellant weight}}{\text{Liftoff less payload weight}}$$

$$\lambda' \text{ Wet} = \frac{\text{Total impulse (ascent + OMP) propellant weight}}{\text{Post separation less payload weight}}$$

For the Droptanks

$$\lambda' \text{ Dry} = \frac{\text{Total loaded (incl. holddown) propellant weight}}{\text{Liftoff + holddown propellant weight}}$$

$$\lambda' \text{ Wet} = \frac{\text{Total impulse propellant (without holddown) weight}}{\text{Liftoff weight}}$$

Table 2.2-4 (Cont'd)

	Orbiter	Droptank (a) Module (b) Single Tank Assy	Composite
CG LOCATION			
Orbiter Fuselage Sta., in.			
Ascent 65 Klb Payload IN/OUT, at			
Liftoff			145/132
Prestaging			1158/1181
Orbit Injection	1265/1333		
Reentry			
40 Klb Payload IN, ABES OUT	1314		
Payload OUT, ABES Eng. and Fuel IN	1348		
Payload OUT, ABES OUT	1374(1)		
Landing			
40 Klb Payload IN, ABES OUT	1317		
Payload OUT, ABES Eng. IN ABES Fuel OUT	1368		

(1) Can be reduced without changing payload capability, by 2000 lb ballast for compensating removal of airbreathing engines.

PLANFORM LOADING			
Maximum Loading Condition, lb/ft^2			
Reentry	48.9	NA	NA
Landing	47.5	NA	NA

RESERVES

Main Propulsion	FPR for 1 percent of ideal velocity capability to injection into reference insertion orbit
Orbit Maneuver Propulsion	Included in 1500 ft/sec ΔV requirement

Table 2.2-4 (Cont'd)

RESERVES (Cont'd)

Attitude Control Propulsion	10 percent
Airbreathing Propulsion	15 percent
Electric Power Reactants	20 percent
Environmental Control Atmosphere	1 day supply
APU Reactants	10 percent
Growth/Uncertainty Factor	Ten (10) percent of dry weight except main rocket engines

FLIGHT PERFORMANCE CHARACTERISTICS

270 nm 55 deg incl. Reference Mission

Ascent

Liftoff Thrust/Weight Ratio	1.25
q_{max}, lb/ft^2/at time, sec	546/77
αq_{max}, deg-lb/ft^2/at time, sec	2000 (assumed for load analysis)
βq_{max}, deg-lb/ft^2	Less critical for load analysis

Separation

Time, sec	295
Velocity ideal/relative, ft/sec	23,151/18,200
Thrust/Weight Ratio	1.0
q, lb/ft^2	3

Injection

Time, sec	385

Table 2.2-4 (Cont'd)

FLIGHT PERFORMANCE CHARACTERISTICS (Cont'd)

Entry	
Crossrange, nm	1100 by hypersonic maneuver
Footprint, nm	2200 wide, 2000 long
Angle-of-Attack, deg	34
Duration from 400 kft altitude to Mach = 1, min	29.2
Maximum Load Factor, g	1.3
Max q, lb/ft^2	310
Landing	
Capability	With or without ABES installed
Speed, kts	
At $\alpha_{L/D_{max}}$ /22 deg (tail scrape)	
40 klb cargo IN ABE OUT	195/164
Cargo OUT, ABE IN	182/146
Ground Effects	Not included, will reduce by about 14 kts
Powered Subsonic Flight	
Climb Gradient	2.7 percent to 5000 ft in approach configuration (gear-up, engine out)
	3.7 percent to 8000 ft in landing configuration (gear down)
Cruise Altitude, ft	
All engines	Over 12,000
Engine out	9,000
Go-Around Capability	Standard day climb from 200 ft altitude to 2000 ft altitude for return cruise to outer marker
Ferry Capability	Addition of kit providing JP-4 tank for approximately 55,000 lf fuel in cargo bay and possibly some aerodynamic fairings for a min rocket engines provides 280 nm range. Larger ranges by in-flight refueling.

Table 2.2-4 (Cont'd)

FLIGHT PERFORMANCE CHARACTERISTICS (Cont'd)	
Abort Capability	Intact abort to orbit from lift-off to normal injection. No hardware or propellant penalty.
AERODYNAMICS	
$\alpha_{L/D_{max}}$, nominal deg Entry/Landing	20/15
L/D_{max}, Hypersonic/ Subsonic	1.87(1)/5.45 to 5.85
Static Stability	
Longitudinal, directional, lateral	Neutral or better at all operating conditions
Trim and Control Authority	Adequate for all operation conditions
CG Location Capability	Adequate for all combinations of cargo IN/OUT and ABES IN/OUT
Transition Maneuver	Not required for high crossrange Stable, controllable transition at low hypersonic speeds if required for low crossranges
Handling Qualities	MIL SPEC 8795-B, Class 3 Level 1 from M2.5 to Landing. All conditions acceptable unaugmented except lateral/directional dutch roll mode (augmentation required)

NOTE:

(1) Based on hypersonic arbitrary body computer program, validity of which confirmed by wind tunnel data on LS 200-5 orbiter model.

Table 2.2-4 (Continued)

THERMAL PROTECTION SYSTEM

Orbiter

Type — Passive, fully reusable except for flame curtains used at vehicle base. Insulation designed to limit temperature to 300 deg on aluminum and to 600 deg on titanium substructures

Location	Temperature Range (^{o}F)	Concept and Material
Body	≤1000	Titanium Heat Shield Fibrous insulation
Body	1000-2300	LI-1500 Titanium subpanel
Fins, Control Surfaces	1000-2300	LI-1500 Titanium structure
Nose Cap	≤2800	Coated Tantalum Heat Shield Silicon Carbide Foam
Base	2300	LI-1500 on Titanium structure or support - Flexible flame curtains on gimballed engines

Droptanks

Forebody — Ablator (Insulcork)

Main Structure — Polyurethane Foam

PROPULSION

Location — Orbiter

Main Propulsion System

Propellant - Type — LO_2 - LH_2

O/F Ratio — 6:1

Table 2.2-4 (continued)

PROPULSION (Cont'd)

Engine	
Type	ICD 13M15000B
No. – Installed	9
– Operating Liftoff	9
– Operating At Staging	3
– Operating After Staging	2 out of 3
Expansion Ratio	53:1
Thrust, Klb Sea Level/Vac	530/612
Throttling Capability	50 percent
I_{sp} Minimum Guaranteed, SL/VAC, sec	383/442
Gimbal Capability, deg	± 7 in. square pattern

Attitude Control Propulsion System

Propellant – Type	High pressure GO_2 and GH_2
O/F Ratio (System)	3.3:1
I_{sp}, sec	
– System	352 to 362
– Thruster	420
Thrusters	
Number	40
Chamber Pressure, ps	250
Thrust, lb	1500
Thrust Modulation	
– Orbit Maneuvers	Thruster pulsing
– Deadband Control	Igniter pulsing
Minimum Impulse Bit, lb-sec	
– Thruster	50
– Igniter	5

Table 2.2-4 (continued)

Liquid – Gas Conversion Units	
– Number	3
– Gas Pressure, psia	500 to 2000
Sustained Operation Capability With Two Conversion Units Operating	4 thrusters at 100 percent thrust
Total Impulse From Stored Gas, lb-sec	87,500

Orbit Maneuvering Propulsion System

Propellant – Type	LO_2 and LH_2
O/F Ratio	5:1
Engine	
Type	RL10A-3-3A
Number	
– Installed	2
– Operating	1
– Reserve	1
Thrust (VAC), lb	15,000
Gimbal Capability, deg	± 4
I_{sp}, Minimum Guaranteed (VAC), sec	439
Flight Reserve	allowance included in Δ V capability

Airbreathing Propulsion System

Fuel – Type	JP-4
Engine – Type	Low bypass ratio turbofan JTF 22 A-4
– Number	6
– Installation	Deployable, internally stored near vehicle, c.g.
– Thrust rating (Sea Level, lb)	Classified

Table 2.2-4 (continued)

Ferry Propulsion System	
Fuel – Type	JP-4
– Weight, lb	Approximately 55,000
Type	Additional tanks in cargo bay and possibly aerodynamic fairings on main rocket engines installed in kit-form
Tankage	
– Installation	In cargo bay
– Capacity, lb	Approximately 55,000
Propellant Feed System	Orbiter ascent propellant system separated from orbital propellant system. Droptank LO_2 cascades through orbiter ascent tanks. Transfer lines installed in orbiter approximately 30,000 lb usable LO_2 contained in transfer lines. ACPS, OMPS, and APU propellants contained in orbital tankage. Propellant Utilization System active during entire main engine operation
PRIMARY STRUCTURAL MATERIALS	
Orbiter Fuselage and Tanks and Droptanks and Intertank Structure	Aluminum
Orbiter Thrust Structure, Aerodynamic Surfaces and Cargo Bay Door and Droptank Aft Support Structure	Titanium

Table 2.2-4 (continued

SYSTEM SENSITIVITIES

270 nm 55 deg inclination mission

Gross Liftoff Weight

System sizing unchanged except for droptank size.

$\frac{\partial (GLOW)}{\partial (Payload)}$ = 26.4 (payload delivered and returned)

$\frac{\partial (GLOW)}{\partial (\Delta V_{orbital})}$ = 536 lb/ft/sec

$\frac{\partial (GLOW)}{\partial (Inert_{Orbiter})}$ = 25.6 (with secondary effects)

$\frac{\partial (GLOW)}{\partial (Inert_{Droptank})}$ = 10.7

$\frac{\partial (GLOW)}{\partial (I_{sp})}$ = -39,900 lbm^2/lbf-sec

$\frac{\partial (GLOW)}{\partial (Thrust)}$ = -0.610 lbm/lbf (without engine penalty)
-0.046 lbm/lbf (with engine penalty)

Payload

$\frac{\partial (Payload)}{\partial (Inert_{orbiter})}$ = -1 or = -3265 lb/percent

$\frac{\partial (Payload)}{\partial (Inert_{Droptank})}$ = -0.457 or -561 lb/percent

$\frac{\partial (Payload)}{\partial (I_{sp})}$ = 1890 lbm^2/lbf-sec

NOTE:

$\frac{\partial (Payload)}{\partial (Parameter)}$ = 0 if droptank size is increased within feasible limits of liftoff thrust-to-weight ratio

Table 2.2-5

STAGE-AND-ONE-HALF BASELINE MISSION PERFORMANCE CHARACTERISTICS
CONFIGURATION: ORBITER 1-1/2-STAGE BASELINE MODEL LS 200-10
MODE: DROPTANKS OFFLOADED FOR SPECIFIED PAYLOAD PERFORMANCE

Mission	Design Mission Due East	Reference Mission South Polar	Reference Mission 270 nm, 55 deg Inc.
Airbreather Engine System	Out	Out	In
ORBITER			
Impulse Propellant, K lb			
Ascent	239.7	239.9	239.2
Orbit Maneuver(1)	17.0	15.8	38.6
Cruise	0	0	8.43
Flight Reserve Prop't Ascent, K lb	7.6	7.4	8.1
Dry Weight, K lb	270	270	294
Ignition Weight, K lb	609.2	582.9	625.1
DROPTANK			
Impulse Propellant, K lb	2,714	2,877	3,063
Liftoff Weight, K lb	2,836	3,000	3,186
% Propellant Offload	10.97	5.84	0.0
LAUNCH VEHICLE			
Staging Velocity, ft/sec ideal/relative approx.	22,034/17,900	23,107/18,000	23,151/18,000
Liftoff Thrust/Wt	1.38	1.33	1.25
GLOW, K lb	3,450	3,588	3,816
PAYLOAD, K LB			
Design	65	40	25
Calculated	65	40	25
ON-ORBIT ΔV, FT/SEC(1)	650	650	1,500
LANDING WEIGHT W/O PAYLOAD, K LB	274	274	300

Note: (1) Related to propellant contained in OMP tank system, detail breakdown in Table 2.2-7

Table 2.2-6

STAGE-AND-ONE-HALF BASELINE MISSION PERFORMANCE CHARACTERISTICS
CONFIGURATION: ORBITER 1-1/2-STAGE BASELINE MODEL LS 200-10
MODE: DROPTANKS FULLY LOADED

Mission	Design Mission Due East	Reference Mission South Polar	Reference Mission 270 nm, 55 deg Inc.
Airbreather Engine System	Out	Out	In
ORBITER			
Impulse Propellant, K lb			
Ascent	239.0	239.6	239.2
Orbit Maneuver(1)	18.6	16.6	38.78
Cruise	0	0	8.43
Flight Reserve Prop't Ascent, K lb	8.3	7.7	8.1
Dry Weight, K lb			
Ignition Weight, K lb	640.9	598.3	625.1
DROPTANK			
Impulse Propellant, K lb	3,063	3,063	3,063
Liftoff Weight, K lb	3,186	3,186	3,186
LAUNCH VEHICLE			
Staging Velocity ft/sec ideal/relative approx.	22,930/18,800	23,580/18,500	23,164/18,000
Liftoff Thrust/Wt	1,245	1.26	1.25
GLOW, K lb	3,832	3,789	3,816
PAYLOAD, K LB			
Design	65	40	25
Calculated	95.1	54.6	25
ON-ORBIT ΔV, FT/SEC(1)	650	650	1500
LANDING WEIGHT W/O PAYLOAD, K LB	274	274	300

Note: (1) Related to propellant contained in OMP tank system.

ORBITAL ΔV CAPABILITY AND PROPELLANT ALLOCATION FROM OMP TANK SYSTEM

1½-Stage Baseline Configuration Model LS 200-10

Mission	Design Due East(1)				Reference South Polar(1)			
Flight Condition	Normal		Abort		Normal		Abort	
Propellant and ΔV Increment, lb and ft/sec	ΔW_p	ΔV	ΔW_p	ΔV	ΔW_p	ΔV	ΔW_p	ΔV
FUNCTION								
Orbit Maneuvers	2,544	100 (0)	0	0	2,358	100 (0)	0	0
Plane Changes, Dispersions, Orbital FPR	2,727	108 (0)(2)	0	0	2,527	108 (0)(2)	0	0
Transfer and Rendezvous	4,426	142 (A)	0	0	4,103	142 (A)	0	0
Retro	7,319	300 (0)	4,147	170 (0)	6,781	300 (0)	3,842	170 (0)
Abort Maneuvers	NA	NA	0	0	NA	NA	0	0
Abort Roll Control	NA	NA	0	0	NA	NA	0	0
Reserve for Abort	0	0	NA	NA	0	0	NA	NA
Unused With Abort	NA	NA	12,869	480	NA	NA	11,927	480
TOTAL	17,016	650	17,016	650	15,769	650	15,769	650

LEGEND: (M) Used in main engine
(O) Used in orbit maneuver engine(s)
(A) Used in AC system thrusters

NOTES: (1) Droptanks offloaded for specified payload.
(2) All FPR.

Table 2.2-7

Table 2.2-7 (continued)

ORBITAL ΔV CAPABILITY AND PROPELLANT ALLOCATION FROM OMP TANK SYSTEM

$1\frac{1}{2}$-Stage Baseline Configuration Model LS 200-10

Mission	Reference 270 nm 55 deg Inclination			
Flight Condition	Normal		Abort	
Propellant and ΔV Increment, lb and ft/sec	ΔW_p	ΔV	ΔW_p	ΔV
FUNCTION				
Orbit Maneuvers	17,032	659 (O)	0	0
Plane Changes, Dispersions, Orbital FPR	5,118	199 (O)	0	0
Transfer and Rendezvous	4,406	142 (A)	0	0
Retro	12,058	500 (O)	410	170
Abort Maneuvers	NA	NA	0	0
Abort Roll Control	NA	NA	0	0
Reserve for Abort	0	0	0	0
Unused With Abort	NA	NA	38,204	1,330
TOTAL	38,614	1,500	38,614	1,500

LEGEND: (M) Used in main engine
(O) Used in orbit maneuver engine(s)
(A) Used in AC system thrusters

LOCKHEED MISSILES & SPACE COMPANY

Table 2.2-8

Summary of Dimensional Characteristics of Baseline

1 1/2-Stage Orbiter LS 200-10

VEHICLE GEOMETRY	
Linear Dimensions, Ft	
Length -	
- actual	156.5
Span	92
Height - gear up	36.75
- gear down	49
Areas, Ft^2	
Planform -	
- actual	6,846
Base	1,229
Wetted Area, Including Base	18,944
Volume, Ft^3	
Mold Line Volume	97,600
Angular Dimensions, Deg	
Sweep Angle	78
FIN GEOMETRY	
Number of Fins	2
Linear Dimensions, Ft	
Height	24.4
True Span	92
Root Chord	33.3
Tip Chord	16.75
Areas, Ft^2	
Projected (True) Area Per Fin (including rudder)	624
Wetted Area Per Fin	998

Table 2.2-8 (Cont'd)

Angular Dimensions, Deg	
Leading Edge Sweep	45
Roll Out,	30
Toe-In	4
Tip Wash Out	0
Volumes, Ft^3	
Mold Line Volume, Per Fin (Including rudder and auxiliary surface)	2,165
Aspect Ratio	2
Airfoil Section (Root)	Modified Clark Y

CONTROL SURFACES GEOMETRY

Upper Elevon	
MAC, ft	14.6
Span, ft/side	24
Area, ft^2	693
Hinge Line Sweep, Deg	0
Deflection Range, Deg	
- trailing edge down	0
- trailing edge up	30
- rate, deg/sec	15
Trim Flap	
MAC, ft	23
Span, ft	48
Area (including elevon), Ft^2	1,086
Hinge Line Sweep, Deg	0
Deflection Range, Deg	
- trailing edge down	+10
- trailing edge up	-25
- rate, de/sec	1
Lower Elevon	
MAC, ft	10
Span, ft/side	24
Area, ft^2	543
Hinge Line Sweep, Deg	15
Deflection Range, Deg	
- trailing edge down	+20
- trailing edge up	-15

Table 2.2-8 (Cont'd)

Rudder	
Number	2
MAC, Ft	10
Planform Area, Per Rudder, Ft^2	237
Hinge Line Sweep, Deg	15
Auxiliary Control Surfaces	
Number	2
MAC, Ft	11.25
Planform Area, Per Surface, Ft^2	112.5
Hinge Line Sweep, Deg	10

LEADING EDGES

Radius, Ft	
Fin	1
Body - Front	4
- Aft	3
Nose Cap (hemispherical)	4

Table 2.2-9

WEIGHT SUMMARY
1 1/2 - STAGE BASELINE VEHICLE SYSTEM LS 200-10

270 nm 55 deg Inclination Ref. Mission

Subsystem	Orbiter Weight (lb)	Droptank Weight (lb)	Total (lb)
Aerosurface Structure	18,050		
Body Structure	58,386	88,394	
Thermal Protection	35,716	7,144	
Landing Gear	11,988		
Propulsion – Main Ascent	105,858	6,102	
Propulsion – Airbreathing	20,603		
Propulsion – Maneuver/ACPS	6,901		
Prime Power Sources	1,620		
Electrical System	3,704		
Hydraulics	2,073		
Surface Controls	4,246		
Avionics	3,762	326	
Environmental Control	1,274		
Personnel Provisions	210		
Contingency (10 Percent Less ICD Eng)	20,008	10,196	
DRY WEIGHT	294,399	112,162	
Personnel and Effects	725		
PAYLOAD	25,000		
Reserves, Residuals and Losses	22,899	10,554	
Propellant – Ascent	239,209	3,063,218	
Propellant – Airbreathing	8,430		
Propellant – Maneuver/ACPS	39,824		
LAUNCH WEIGHT	630,486	3,185,934	3,816,420

2.3 SUMMARY OF LS 200-5 SYSTEM CHARACTERISTICS

During the first three months of the Alternate Concepts Study, a comprehensive analysis and trade-off study was performed to derive the best stage-and-one-half system in terms of performance and cost. This study examined straight wing, delta wing, and delta body orbiter configurations for both the low and high crossrange application. The study showed that the delta body configuration was for both applications superior to all others examined from the standpoint of weight, aerodynamic performance, and cost.

The delta body orbiter was further refined during the ensuing two months resulting in a recommended configuration, the LS 200-5, which was presented at the midterm review on 1 December 1970.

This configuration was used extensively as a point design, presenting a common baseline for detailed supporting studies in the areas of various vehicle technologies (primarily aerodynamics, thermodynamics, structures, propulsion, controls, other subsystems, and weights) which were conducted in substantial depth for the validation of the derived system characteristics.

Changes in requirements by NASA in late 1970 and January 1971 made it necessary to modify this configuration, resulting in the current stage-and-one-half baseline configuration LS 200-10 which is presented in Section 2.2 of this report. However, the differences between these two versions are small enough so that most of the results and conclusions derived from the supporting studies are still valid. Of particular importance is that the results of recently concluded aerodynamic test programs are directly applicable to the new configuration.

Because of this role of the LS 200-5 configuration, it appears advisable to present its design and performance characteristics. Abbreviated reporting in summary form, however, is adequate, since the LS 200-5 vehicle system and configuration were documented in detail in Revision A of the Design Data Book which was submitted to NASA on 1 December 1970.

The primary differences between the current and the older stage-and-one-half Baseline configurations are listed in Table 2.3-1.

Table 2.3-1

	LS 200-10	LS 200-5
Main Rocket Engine		
Type (Booster Engine ICD No.)	13M15000B	13M15000A
Thrust with 53:1 exp. ratio, lb		
sea level/vac	530/612	400/462
Weight Installed, lb (1)	7650	4720
Thrust/Weight ratio installed	69.2	84.8
Cruise Fuel, Type	JP-4	LH_2
Weight, lb	9700	4060
Droptanks	Additional insulation for assuring intact reentry (2400 lb)	
Design Crossrange, nm	1100	1500
TPS Weight, lb	35,700	40,860

Note (1) Including associated vehicle system installation weight

The combined effects of these changes amount to a reduction in inert weight for the LS 200-5 of about 19,000 lb. In addition, the weight reduction in the main engines also alleviated the cg balance for the vehicle. Finally, the reduced droptank inert weight increased the performance potential of the system. Consequently, the LS 200-5 system optimized at a somewhat smaller size and propellant weight than the current LS 200-10 Baseline configuration.

The resulting configuration is compared in Fig. 2.3-1 with the LS 200-10 system, and differences in the major design parameters[1] are listed in Table 2.3-2 :

Table 2.3-2

	LS 200-10	LS 200-5
Number of Main Rocket Engines	9	11
Number of Cruise Engines	6	5
Orbiter Dry Weight, klb	294.4	269.4
Orbiter Liftoff Weight, klb	630.5	549.1
GLOW, Mlb	3.816	3.520
Orbiter Impulse Propellant Load, klb		
Ascent	239.2	191.7
Orbit Maneuver	39.8	36.2
Cruise	8.4	3.5
Orbiter Length, ft	156.5	151.75
Orbiter Planform area, ft^2	6,846	6,660

Most of the basic system design characteristics, however, are basically identical, such as:

Aerodynamic configuration and relative cg location
Rocket engine specific impulse
Liftoff Thrust/Weight ratio (1.25)
Subsystem function, concept and design
Droptank arrangement and design, and separation method

(1) Quoted for the 270 nm 55 deg inclination Reference Mission

Figure 2.3-1

STAGE-AND-ONE-HALF CONCEPTS

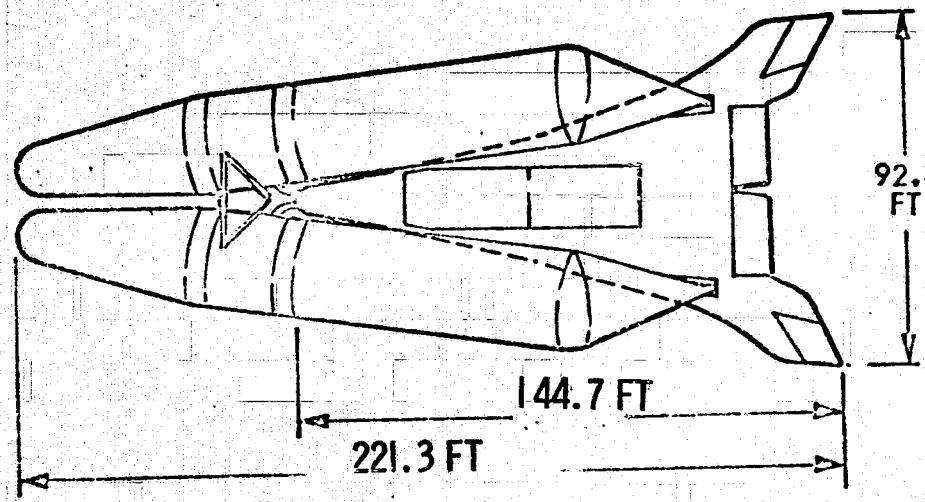

LS 200-5

MAIN ENGINES: 11-400K
GLOW: 3.52 MLB
PAYLOAD: 27.4 KLB TO 270 NM BY 55 DEG ORBIT
CROSSRANGE: 1500 NM

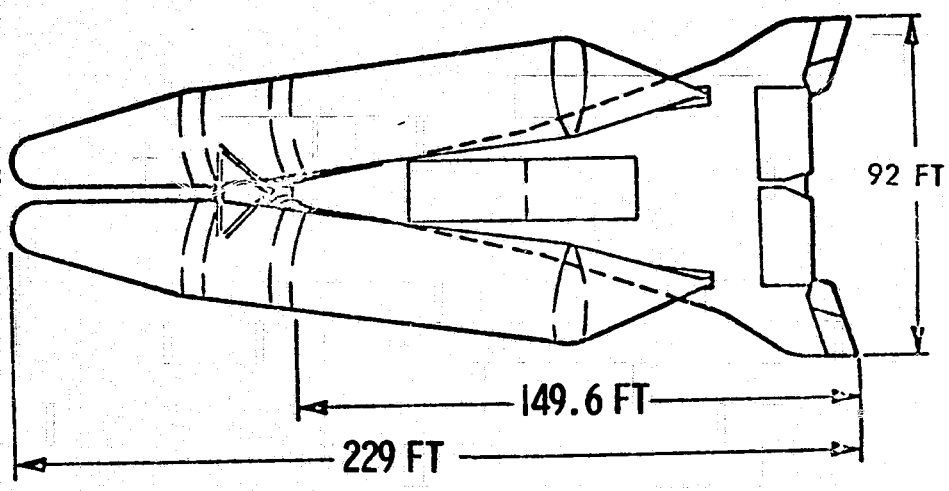

LS 200-10

MAIN ENGINES: 9-530K
GLOW: 3.82 MLB
PAYLOAD: 25.0 KLB TO 270 NM BY 55 DEG
CROSSRANGE: 1100 NM

Fig. 2.3-1

Also basically unchaged are the general arrangement of the orbiter and the structural concepts. However, some features reflecting a more mature design status of the current baseline configuration were not yet incorporated in the earlier design, such as

Deletion of movable nose cap (resulting in the necessity to increase the number of ACPS thrusters from 39 to 40 in the LS 200-10 design)

Design of Landing Gear

Addition of payload deployment mechanism

In addition, secondary differences exist resulting from the accomodation of the above changes, such as in: tank sizes, deletion of separate JP-4 tank system, and structural design details reflecting the differences in engine number, vehicle size and associated loads.

The LS 200-5 vehicle configuration is shown in Fig. 2.3-2 in the launch configuration and the orbiter general arrangement in Fig. 2.3-3. A detailed discussion of the design is presented in Section 2.5.1 of this report.

Summary information is presented in the following tables:

Table 2.3-3	Vehicle System and Subsystem Performance and Design Characteristics
Table 2.3-4	Weight Summary
Table 2.3-5	Mission Weight Summary
Table 2.3-6	System Mass Properties
Table 2.3-7	Sequence Mass Properties Statement

Comprehensive System Design and performance information is assembled in Volume II of the Design Data Book, Revision A, which was submitted to NASA on 1 December 1970.

REPRODUCIBILITY OF THE ORIGINAL PAGE IS POOR

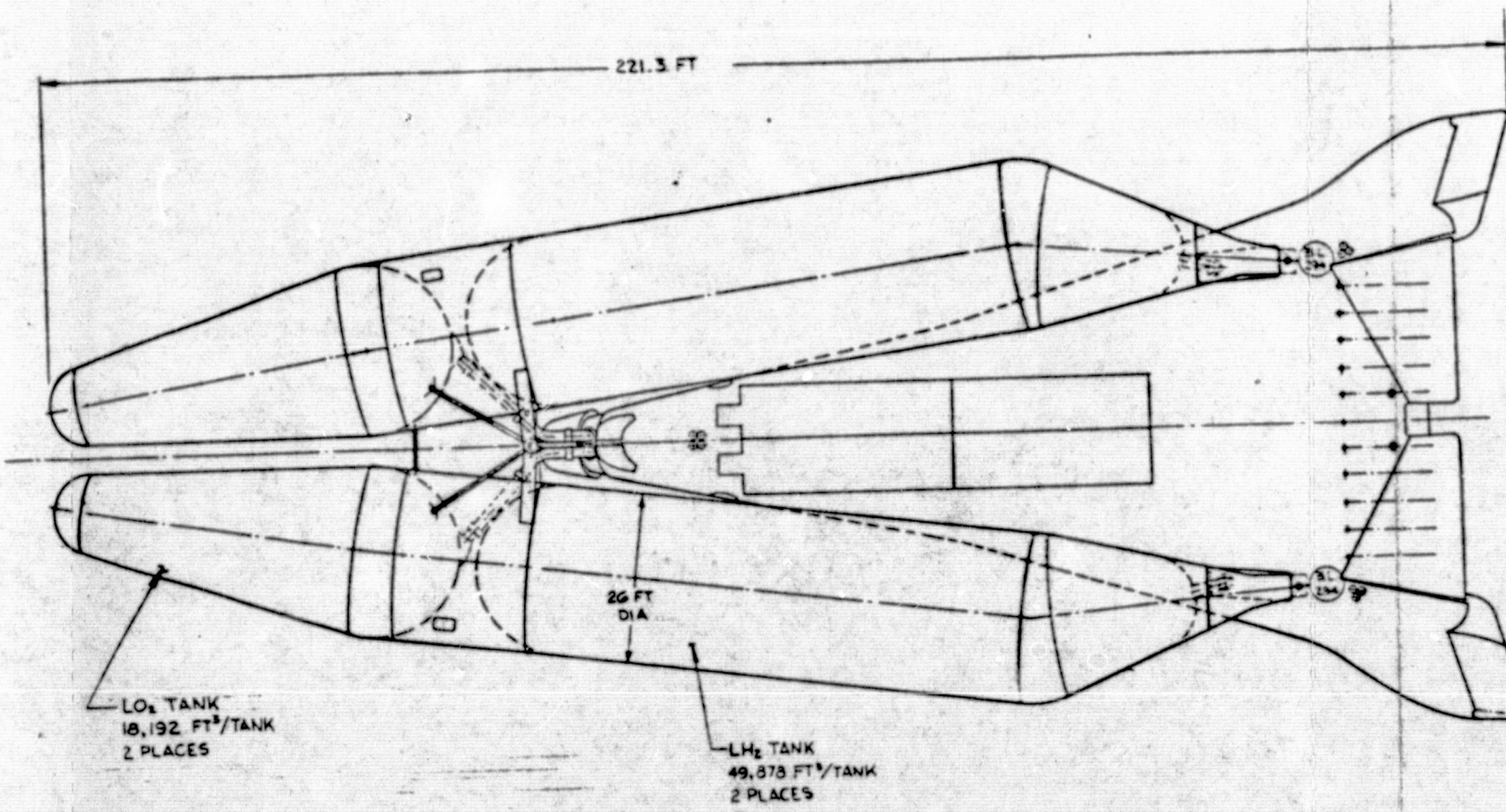

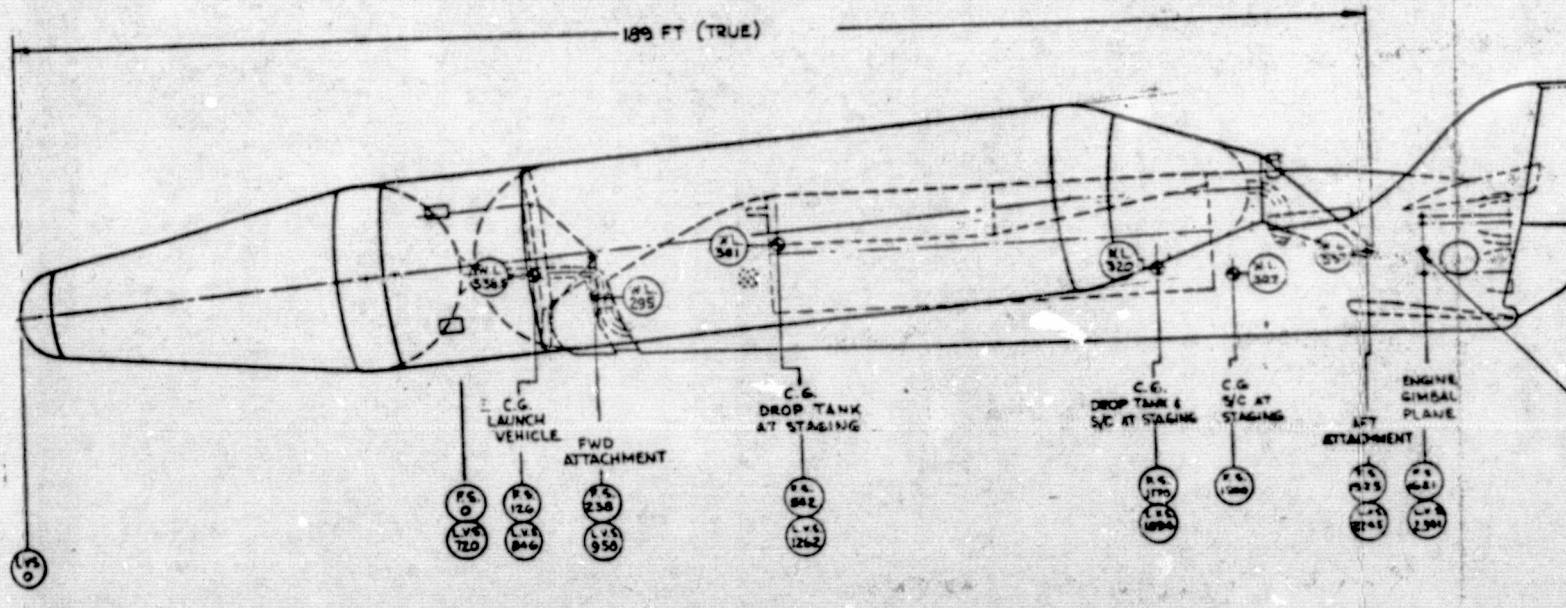

NOTES:
1. C.G. LOCATIONS ARE PRELIMINARY ESTIMATES.

FOLDOUT FRAME

REPRODUCIBILITY OF THE ORIGINAL PAGE IS POOR

LIMITED CALENDAR LIFE	LIMITED OPERATING LIFE

ZONE	LTR	REVISIONS DESCRIPTION	DATE	APVD
	A	C.G. LOCATIONS UPDATED		

PRECEDING PAGE BLANK NOT FILMED

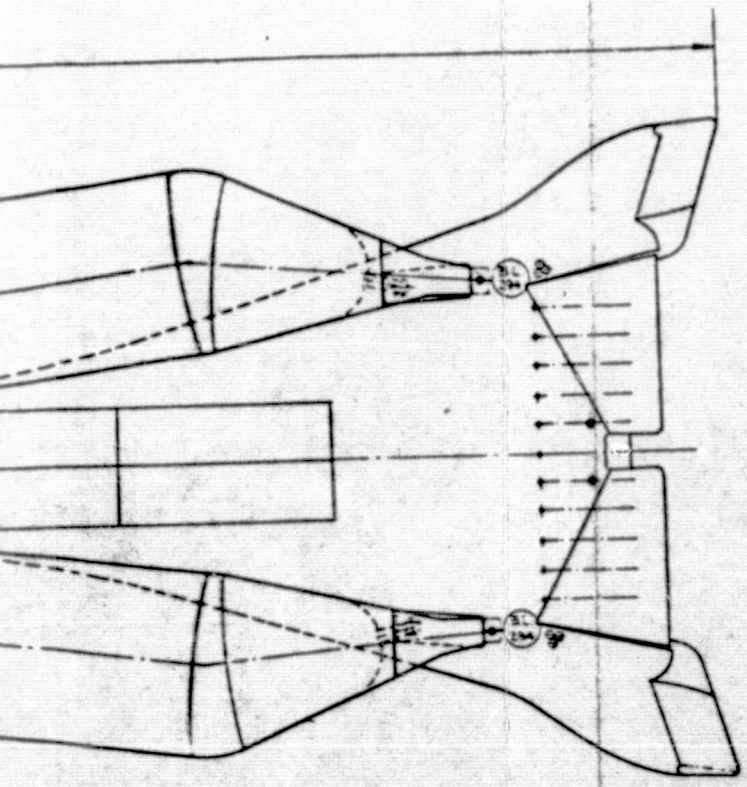

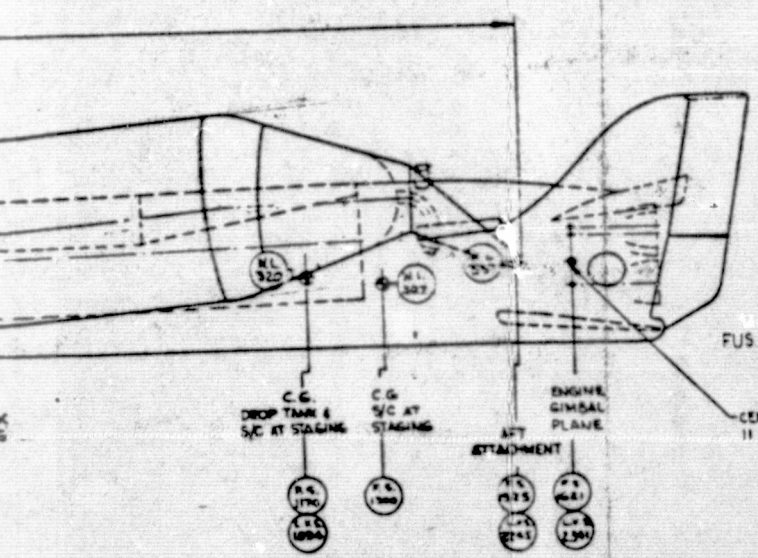

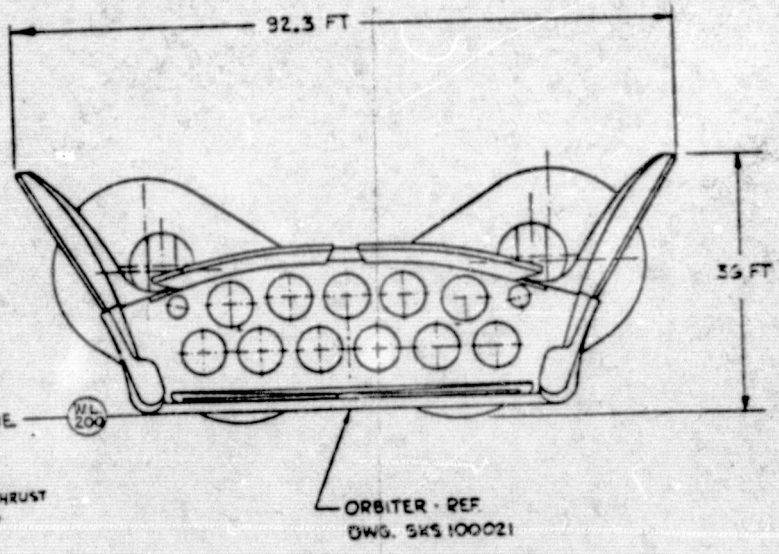

Fig. 2.3-2

QTY REQD	CODE IDENT	PART OR IDENTIFYING NO	NOMENCLATURE OR DESCRIPTION	MATERIAL DESCRIPTION OR NOTE	MATERIAL SPECIFICATION	ZONE	ITEM NO

PARTS LIST

NOTES:
1. C.G. LOCATIONS ARE PRELIMINARY ESTIMATES.

INTERPRET DWG PER	UNLESS OTHERWISE SPECIFIED DIM ARE IN INCHES. TOLERANCES ON FRACTIONS ± 1/16, DECIMALS: .X ± .1, .XX ± .03, .XXX ± .010, ANGLES ± 2 DEG	DATE Nov 17 '72	LOCKHEED MISSILES & SPACE COMPANY, A GROUP DIVISION OF LOCKHEED AIRCRAFT CORPORATION, SUNNYVALE, CALIFORNIA
		DWN Schm 12	
		APVD	LAUNCH VEHICLE DELTA BODY - STAGE 4 1/2 MODEL LS-200-5
		APVD	
		ENGRG	
		CHKR	
		APVD	SIZE E, CODE IDENT 06387, DRAWING NO SKS 100022, REV A
NEXT ASSY USED ON APPLICATION	CONTR CCA. CI/FD	APVD	SCALE 1/200, SHEET 1 OF 1

REPRODUCIBILITY OF THE ORIGINAL PAGE IS POOR

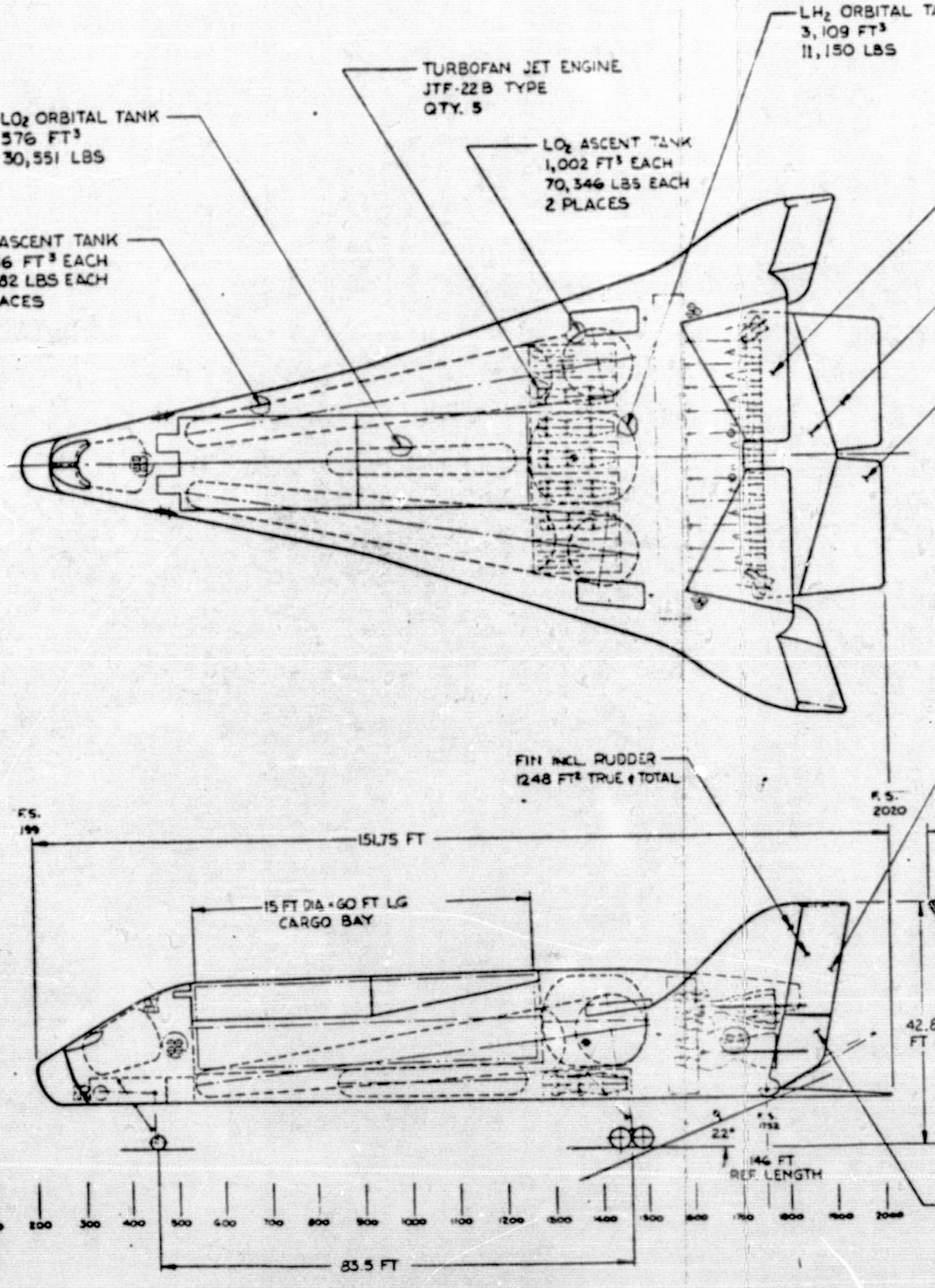

NOTES:

1. BASED ON TRIANGULAR AREA WITH APEX AT F
   BASE AT F.S. 1752 AND ALTITUDE OF 146 FT (REF
2. BASED ON AREA OF TOTAL ORBITER AS
   SHOWN IN PLAN VIEW.

FOLDOUT FRAME

REPRODUCIBILITY OF THE ORIGINAL PAGE IS POOR

PRECEDING PAGE BLANK NOT FILMED

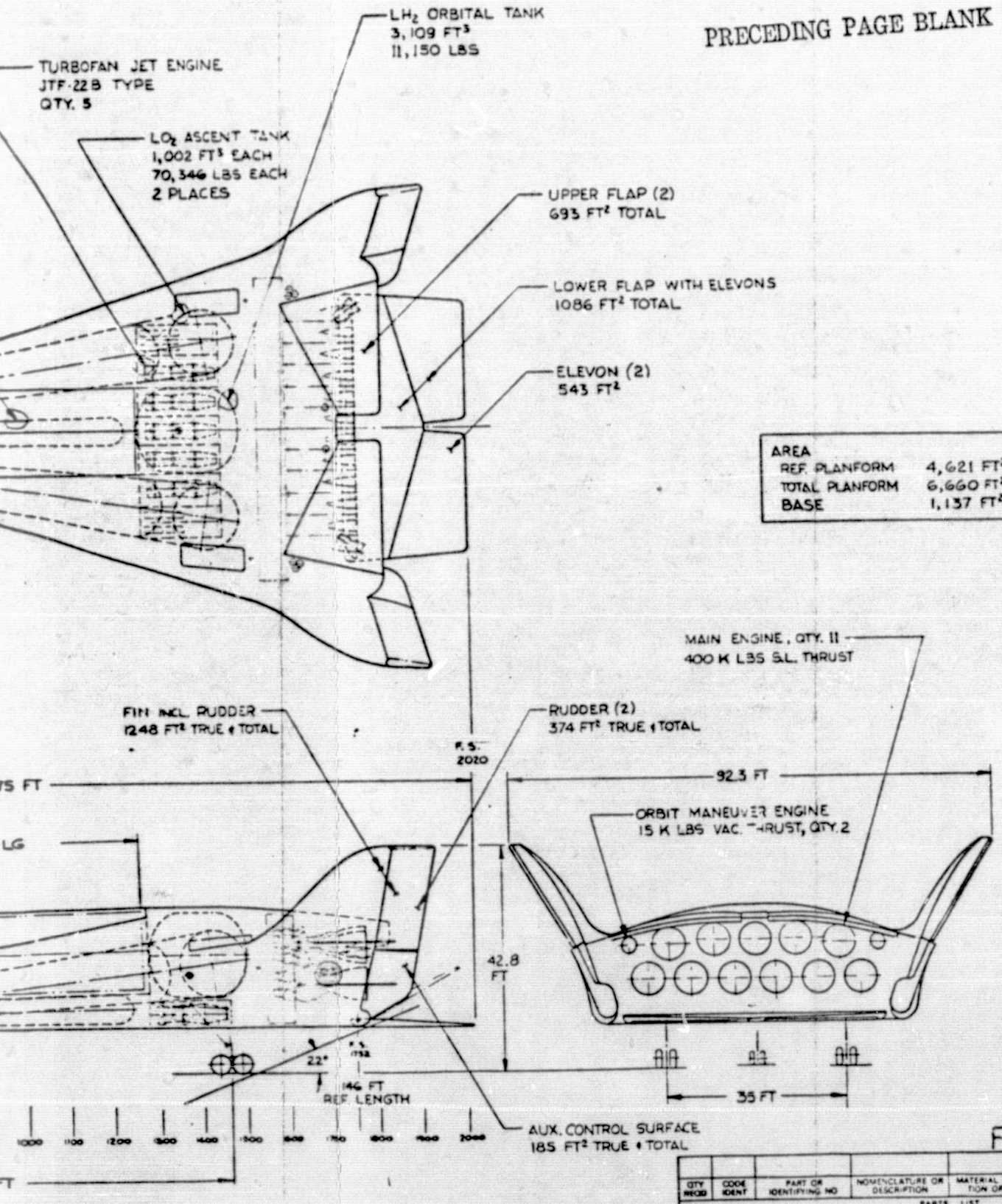

Fig. 2.3-3

NOTES:
[1] BASED ON TRIANGULAR AREA WITH APEX AT F.S. 0 BASE AT F.S 1732 AND ALTITUDE OF 146 FT (REF LENGTH)
[2] BASED ON AREA OF TOTAL ORBITER AS SHOWN IN PLAN VIEW.

LOCKHEED MISSILES & SPACE COMPANY
A GROUP DIVISION OF LOCKHEED AIRCRAFT CORPORATION
SUNNYVALE, CALIFORNIA

GENERAL ARRANGEMENT
DELTA BODY STAGE ϕ 1/2
MODEL LS-200-5

SIZE E | CODE IDENT 04887 | DRAWING NO SKS 100021 | REV -

PRECEDING PAGE BLANK NOT FILMED

Table 2.3-3

Vehicle System and Subsystem Performance and Design Characteristics

CONFIGURATION	
Concept	One-And-A-Half Stage. Single expendable drop-tank module Reusable Orbiter
Configuration	Modified lifting delta planform, lifting body orbiter V-shaped drop tank module, consisting of two identical tank assemblies (single LO_2 tank forward and single LH_2 tank aft) straddling orbiter in X-Y plane. All engines and ACPS thrusters installed on orbiter. All engines ignited at liftoff.
Separation Mode	Intact drop tank assembly rotates "over the top" of orbiter around aft attach point pivots. Motion effected by inertial forces generated by main engine operation without assistance from additional impulses.
High/Low CrossRange	Identical, except for adjustment of distribution/local thickness of TPS heat shield and insulation.

	Orbiter	Drop Tank (a)Module (b)Single Tank Assy.	Composite Vehicle
PHYSICAL CHARACTERISTICS			
Length, ft - reference	146	NA	206
- actual	151.75	(a) 189 (b) 190.5	221.3
Span, Ft	92.3	NA	92.3
Height, ft - gear up	34.5	NA	36.0
- gear down	42.8	NA	42.8
Diameter, ft	NA	(b) 26	NA
Planform Area, ft^2			
- reference	4,621	NA	12,463
- actual	6,660	NA	14,302
Sweep Angle, deg	78	85	NA
Droptank/Orbiter Incidence			-5° 2.5^1

Table 2.3-3 (Cont.)

	Orbiter	Drop Tank (a) Module (b) Single Tank Assembly	Composite Vehicle
WEIGHTS, lb High Cross Range Configuration			
Dry weight (including 10 percent contingency except on main engines)	269,427	102,615	NA
Inert weight (including all expendables except impulse propellant)	290,645	111,227	NA
Main propellant			
Impulse	191,700	2,859,637(2)	3,051,337(2)
Loaded	206,455	2,868,249(2)	3,074,704(2)
Orbital propellant (OMPS/ACPS)(1)			
Impulse	35,004	NA	35,004
Loaded	35,679	NA	35,679
Airbreathing Fuel (LH_2, including reserve)	3,999		3,999
Cargo	27,115	NA	NA
Reentry (with cargo)	305,760	NA	NA
Landing (with cargo)	301,350		
Gross Launch Weight	549,136	2,970,864	3,520,000
Propellant Fraction λ'			
Dry	NA	.9658	NA
Wet	.4163	.9628	NA
MASS CHARACTERISTICS, High Cross Range Config.			
CG Location, % L_{Ref}, Cargo in/out			
- ascent, prestaging			67.0/67.6 (3)
- ascent, burnout			74.5/75.6 (3)
- reentry	75.4/77.8		
- landing	76.6/78.0		
Planform Loading, Actual , lb/ft^2			
- reentry (cargo in)	46.3	NA	NA
- landing (cargo in)	45.7	NA	NA

(1) For 1500 ft/sec ΔV capability
(2) Without 28,843 lb propellant used during ground hold
(3) % of orbiter L_{Ref}

Table 2.3-3 (Cont.)

PERFORMANCE

Reference Mission:

Reference injection orbit is 50 x 100 nm, launch azimuth 28.5 deg-North. The design reference orbit is 270 nm circular with a 55 deg inclination.

Orbital Capability. 1500 ft/sec of usable capability in excess of the amount required to attain the reference insertion orbit. Tankage designed to hold propellant for additional 500 ft/sec capability at unchanged injection weight.

Payload Performance Characteristics:

Cross Range, nm	1,500	200
Alternatives		
(A) Cargo, lb	27,115	40,648
GLOW, lb	3,520,000	
Liftoff F/W	1.25	
(B) Cargo, lb	25,000	25,000
GLOW, lb	3,460,000	3,170,000
Liftoff F/W	1.27	1.39

(A) Point design LS 200-5

(b) Unchanged orbiter, droptanks resized for correct design payload.

Table 2.3-3 (Cont.)

	High Cross Range	Low Cross Range
Thrust/Weight Ratio		
Liftoff, Composite Configuration	1.25	
Separation, Orbiter	2.55	
Relative separation velocity (A), ft/sec	18,640	
Time of separation, sec (A)	299	
Time of injection, sec (A)	371	
q max, lb/ft^2 at time, sec (A)	524 @79	
q separation, lb/ft^2 at time, sec (A)	2 @ 299	
αq, max deg-lb/ft^2 @ sec (A)	< 1200 @ TBD	
βq, max deg-lb/ft^2 @ sec (A)	< 1800 @ TBD	
Drop tank impact range, nm (A)	1100 ± 50	
Entry		
Maximum load factor, g	1.2	1.9
Duration 400K to M = 1, min	33	15
Go-around (fuel equivalent) minutes (without 15 percent reserve)	9	
Landing speed, kts (cargo in/out)(A)	200/175	
FAR landing field, length, ft	12,000	
Ferry capability		
Range, nm	400	TBD
AERODYNAMICS		
Entry attitude, deg	$\alpha_{L/D_{max}} \approx 20$	$\alpha\ C_{\ell_{max}} \approx 55$
Transition maneuver	Not required	Hypersonic, stable and trimmable
L/D_{max} - hypersonic	1.7	.67
- subsonic	4.54	4.54
Allowable c.g. travel	Payload in/out Jet engines in/out	

Table 2.3-3 (Cont.)

	High Cross Range	Low Cross Range
Trim	Adequate for required flight attitudes	
Handling qualities	MIL SPEC 8785B Class 3, Level 1	
RESERVES		
Main Propulsion	FPR for 1 percent of ideal velocity capability to injection into reference injection orbit	
Orbit Maneuver Propulsion	Included in 1500 ft/sec ΔV requirement	
Attitude Control Propulsion	10 percent	
Airbreathing Propulsion	15 percent	
Electric Power Reactants	20 percent	
Environmental Control Atmosphere		
APU Reactants	10 percent	

THERMAL PROTECTION SYSTEM

Type: Passive, fully reusable

Orbiter

Location	Temperature Range (^{o}F)	Concept and Material
Body	≤ 1000	Corrugated Ti Heat Shield Dyna-Flex insulation
Body	1000-2300	LI-1500, Ti sub-panel

Table 2.3-3 (Cont.)

Location	Temperature Range (°F)	Concept and Material
Fins, Control Surfaces	1000-2300	LI-1500, Ti structure
Nose Cap	≤2750	Tantalum heat shield Dyna-Flex insulation
Base	≤2300	LI-1500 on Ti structure or support Flexible flame curtains on gimballed engines

Drop Tanks

Forebody	Ablator (Insulcork)
Main Structure	Polyurethane foam

PROPULSION

Location	Orbiter
Main Propulsion System	
Propellant - Type	LO_2-LH_2
- Weight, orbiter/drop tanks, lb	
loaded	206,455/2,897,092
impulse	191,700/2,859,637
reserve	7,346/ --
losses, residuals	7,409/8,612
ground hold	-- /28,843
O/F ratio	6:1
Engine	ICD 13 M 15000A
Type	
No. - installed	11
- operating liftoff	11
- operating at staging	3
- operating after staging	3
Expansion ratio	53:1
Thrust SL, /VAC, lb	400,000/ 462,000
Throttling capability	50%
I_{sp} minimum guaranteed, SL/VAC, sec	383/442

Table 2.3-3 (Cont.)

Attitude Control Propulsion System

Propellant - Type		High pressure GO_2 and GH_2
- Weight, lb		
loaded		5,077
impulse - translation	3,404	
- control	1,211	
reserve	462	
losses, residuals	0(1)	

(1) Included in residuals/losses allocated to Orbit Maneuvering Propsulion System

O/F ratio (system)	3:3:1
I_{sp}, System, Sec	352 to 362
Thrusters	
Number	39
Chamber pressure, psia	250
Thrust, lb	1500
Thrust modulation	
- Orbit maneuvers	Thruster pulsing
- Deadband control	Igniter pulsing

Orbit Maneuvering Propulsion System

Propellant - Type	LO_2 and LH_2
- Weight, lb.	
loaded	32,275
impulse	31,560
reserve	0(1)
losses, residuals	715
O/F ratio	5:1
Engine	
Type	RL10A-3-3A
Number	
- Installed	2
- Operating	1
- Reserve	1
Thrust (VAC), lb	15,000

(1) Flight reserve allowance included in ΔV capability requirement.

Table 2.3-3 (Cont.)

I_{sp}, minimum guaranteed, (VAC), sec	439
Airbreathing Propulsion System	
Fuel – Type	LH_2
– Weight, lb	3,990
– Impulse	3,475
– Reserve (15%)	525
Engine – Type	Low bypass ratio turbofan
– Number	5
– Installation	Deployable, internally stored near vehicle c.g.
– Thrust rating (sea level, lb)	≈ 19,000
Ferry Propulsion System	
Fuel – Type	LH_2
– Weight	TBD
Type	Additional engines and tanks installed in kit-form
Engine – Type	TBD
– Number	TBD
– Installation	On pylons mounted in cargo bay
Tankage – Installation	In cargo bay
– Capacity, lb	TBD

Table 2.3-3 (Cont.)

Propellant Feed System	Orbiter ascent propellant system separated from orbital propellant system. Drop tank LO_2 cascades through orbiter ascent tanks. ACPS, OMPS, ABPS, and APU propellants contained in orbital tankage Propellant Utilization System active during entire main engine operation
POWER	
Electric Power System	
Primary Power	O_2 - H_2 fuel cell 3 modules 3 kw each Reactants stored in separate cryogenic modular tankage system
Additional Power Source for Ascent and Atmospheric Flight	LO_2 - LH_2 APU
Emergency Power	Batteries
Energy, kwh	
Standard Mission	805 DC (fuel cell)
Emergency	12 DC

SUBSYSTEM	ORBITER WEIGHT (LB)	DROP TANK WEIGHT (LB)	TOTAL (LB)
AEROSURFACES STRUCTURE	17,897		
*BODY STRUCTURE	52,745	83,178	
THERMAL PROTECTION	40,860	4,053	
LANDING GEAR	11,154		
PROPULSION -- MAIN ASCENT	87,223	5,729	
PROPULSION -- AIRBREATHING	16,550		
PROPULSION -- MANEUVER/ACPS	7,292		
PRIME POWER SOURCES	1,620		
ELECTRICAL SYSTEM	3,704		
HYDRAULICS	2,073		
SURFACE CONTROLS	3,810		
AVIONICS	3,762	301	
ENVIRONMENTAL CONTROL	1,274		
PERSONNEL PROVISIONS	210		
CONTINGENCY (10 PERCENT LESS ICD ENG)	19,253	9,329	
DRY WEIGHT	269,427	102,615	
PERSONNEL AND EFFECTS	725		
PAYLOAD	27,115		
RESERVES, RESIDUALS, AND LOSSES	20,517	8,612	
PROPELLANT -- ASCENT	191,700	2,859,637	
PROPELLANT -- AIRBREATING	3,477		
PROPELLANT -- MANEUVER/ACPS	36,175		
LAUNCH WEIGHT	549,136	2,970,864	3,520,000

*INCLUDES 1200 LB PENALTY FOR 70K PAYLOAD CAPABILITY

Table 2.3-4 LS 200-5 Vehicle Weight Summary

Table 2.3-5

MISSION WEIGHT SUMMARY

CONFIGURATION: LS-200-5 | BY: | DATE: 12-1-70

SYSTEM	ITEM OR MODULE A	B	C	D	E	F	G	H
WING GROUP	N/A							
TAIL GROUP	17897							
BODY GROUP	52745							
INDUCED ENVIR PROTECTION	40860							
LANDING, RECOVERY, DOCKING	11154							
PROPULSION - ASCENT	87223							
PROPULSION - CRUISE	16550							
PROPULSION - AUXILIARY	7292							
PRIME POWER	1620							
ELECT CONVER & DISTR	3704							
HYDRA CONVER & DISTR	2073							
SURFACE CONTROLS	3810							
AVIONICS	3762							
ENVIRONMENTAL CONTROL	1274							
PERSONNEL PROVISIONS	210							
RANGE SAFETY & ABORT	0							
BALLAST	0							
GROWTH/UNCERTAINTY	19253							
SUBTOTAL (DRY WEIGHT)	269427							
PERSONNEL	725							
CARGO	27115							
ORDNANCE	0							
PROPELLANT - RESIDUAL	2821							
SUBTOTAL (INERT WT)	300088	300088	300088	300088	300088	300088	300088	300088
RESERVE PROPEL SERVICE	8609	8609	8609	8609	1263	1263	1263	1263
IN FLIGHT LOSSES	9087	8677	3965	3965	2121	492	467	0
PROPELLANT - ASCENT	191700	191700	191700	0	0	0	0	0
PROPELLANT - CRUISE w/o Res.	3477	3477	3477	3477	3477	3477	3477	0
PROPEL - MANEUV/ACS	36175	36175	36175	36175	15939	11789	465	0
TOTAL (GROSS WT) - LB	549136	548726	544014	352314	322888	317109	305760	301351
DROP TANKS - DRY	102615							
DROP TANK PROP - RESIDUAL	8612							
SUBTOTAL (DROP TANK INERT)	111227							
DROP TANK PROP - ASCENT	2859637							
SUBTOTAL (DROP TANK GROSS)	2970864							
TOTAL (COMPOSITE VEHICLE)	3520000							

DESIGNATIONS:

ITEM OR MODULE

A LAUNCH
B PRIOR SEPARATION
C AFTER SEPARATION
D INJECTION 50 NM x 100 NM
E ON ORBIT - 260 NM x 260 NM
F PRIOR RETRO
G AFTER RETRO
H LANDING

NOTES & SKETCHES:

DROP TANK = .9625

C.G. in % of 1752 in. (Ref. L)

CONDITION	C.G.
C - After Separation	74.1
G - After Retro	75.4
H - Landing	75.5

Table 2.3-6 SYSTEM MASS PROPERTIES

PAGE OF

CONFIGURATION LS-200-5

BY

DATE

NO.	MISSION EVENT	WEIGHT LB	CENTER OF GRAVITY INCHES			MOMENT OF INERTIA MILLION SLUG FT^2			PRODUCT OF INERTIA THOUSAND SLUG FT^2		
			X	Y	Z	ROLL	PITCH	YAW	ROLL-PITCH	PITCH-YAW	YAW-ROLL
2	Aero Surfaces	17897	1692	0	374						
3	Body	52745	1253	0	329						
4	TPS	40860	1256	0	275						
5	Landing Gear	11154	1220	0	238						
6	Main Propulsion	87223	1533	0	337						
7	Cruise System	16550	1371	0	231						
8	Aux. Propulsion	7292	1299	0	320						
9	Prime Power	1620	707	0	254						
10	Electrical	3704	791	0	263						
11	Hydraulic	2073	1379	0	245						
12	Surface Controls	3810	1720	0	296						
13	Avionics	3762	412	0	298						
14	Environmental Control	1274	623	0	376						
15	Personnel Prov.	210	387	0	340						
18	Contingency	19253	1284	0	305						
20	Personnel	725	365	0	330						
21	Cargo	27115	905	0	367						
23	Residuals	2821	1276	0	293						
24	Reserves	8609	1435	0	320						
25	In-Flight Losses	9087	1413	0	342						
26	Ascent Propellant	191700	1284	0	297						
27	Cruise Propellant	3477	1435	0	365						
28	Maneuver Propellant	36175	1144	0	264						

NOTES:

X = ROLL AXIS
Y = PITCH AXIS
Z = YAW AXIS

SEE "DIAGRAMS" FOR COORDINATE AXES DESCRIPTION.

SEQUENCE MASS PROPERTIES STATEMENT

PAGE OF

CONFIGURATION LS-200-5

BY

DATE 12/1/70

NO.	MISSION EVENT	WEIGHT LB	CENTER OF GRAVITY INCHES			MOMENT OF INERTIA MILLION SLUG FT^2			PRODUCT OF INERTIA THOUSAND SLUG FT^2		
			X	Y	Z	ROLL	PITCH	YAW	ROLL-PITCH	PITCH-YAW	YAW-ROLL
	After Staging	544,014	1298	0	307	4.79	16.2	19.2	0	1118	0
	Injection	352,314	1306	0	312	2.91	13.9	15.6	0	468	0
	Prior to Retro	317,109	1318	0	315	2.80	13.4	15.0	0	370	0
	Entry	305,760	1322	0	317	2.79	13.3	15.0	0	348	0
	Landing (Cargo In)	301,351	1325	0	309	2.90	13.6	15.2	0	284	0
	Landing (Cargo Out)	274,236	1366	0	303	2.90	12.8	14.3	0	441	0

NOTES:

X = ROLL AXIS
Y = PITCH AXIS
Z = YAW AXIS

SEE "DIAGRAMS" FOR COORDINATE AXES DESCRIPTION.

Table 2.3-7
Sequence Mass Properties Statement

LMSC-A989142
Vol II

LOCKHEED MISSILES & SPACE COMPANY

2.4 PERFORMANCE AND SIZING

2.4.1 System Sizing

A comprehensive review of the stage-and-one-half launch concept was accomplished early in the ACS contract. The purpose of the study was to review the system characteristics and to determine the significant parameters to the stage-and-one-half liftoff weight. Since the sizing study was conducted early in the contract, the data do not reflect the impact of the new Level 1 requirements which in January 1971 introduced new propulsion characteristics and the requirement of satisfying, in addition to the initial 55 deg-270 nm mission, two additional missions (polar and due east). While the absolute values derived are subject to change, the trends or variations of the system to input parameter variations remain the same. Since trend data are of particular importance in sizing, the information presented and the conclusions derived from the study remain valid.

2.4.1.1 Basic Sizing. A parametric analysis of the stage-and-one-half system is presented in Figs. 2.4-1 through 2.4-2. For the stage-and-one-half system, the ideal velocity is essentially independent of launch weight and staging velocity, for a constant initial thrust-to-weight ratio. The principal parameters affecting the analysis are the weights of the orbiter and the droptanks. The orbiter inert weight, for a given type of design, depends primarily on the propellant load and the number of engines.

Studies have demonstrated that the orbiter inert weight is linear with propellant loading. The sensitivity of orbiter inert weight to impulse propellant added is about 0.135 lb/lb (effective $\lambda' = 0.88$). Since the number of engines, and thus the engine weight, is proportional to launch weight (for constant thrust/weight), the orbiter inert weight can be approximated by the form

$$(1)\quad \text{Inert Wt} = K_1 + K_2 \times \text{Impulse Propellant} + K_3 \times \text{Launch Weight}$$

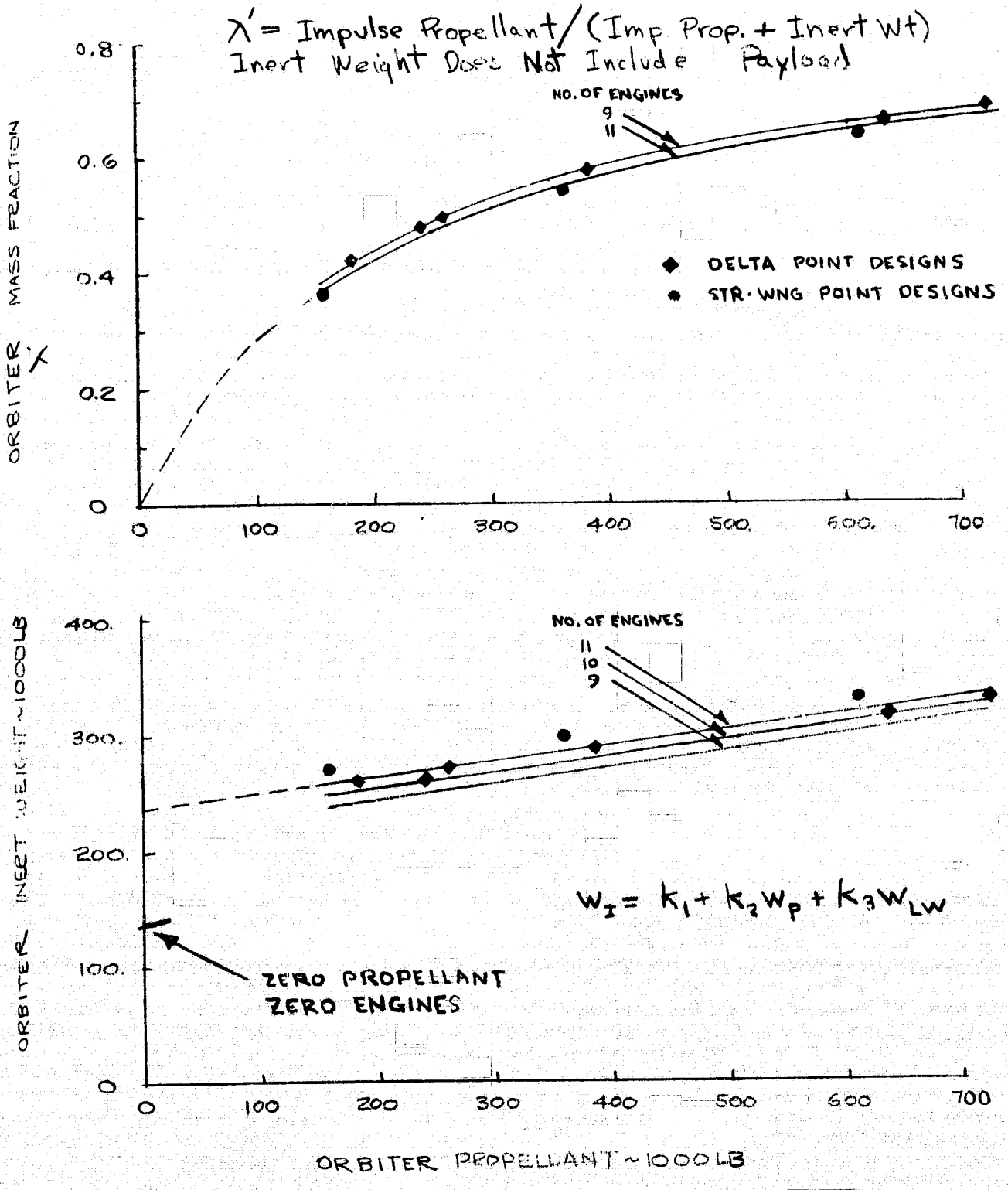

Fig. 2.4-1 Orbiter Weight Scaling

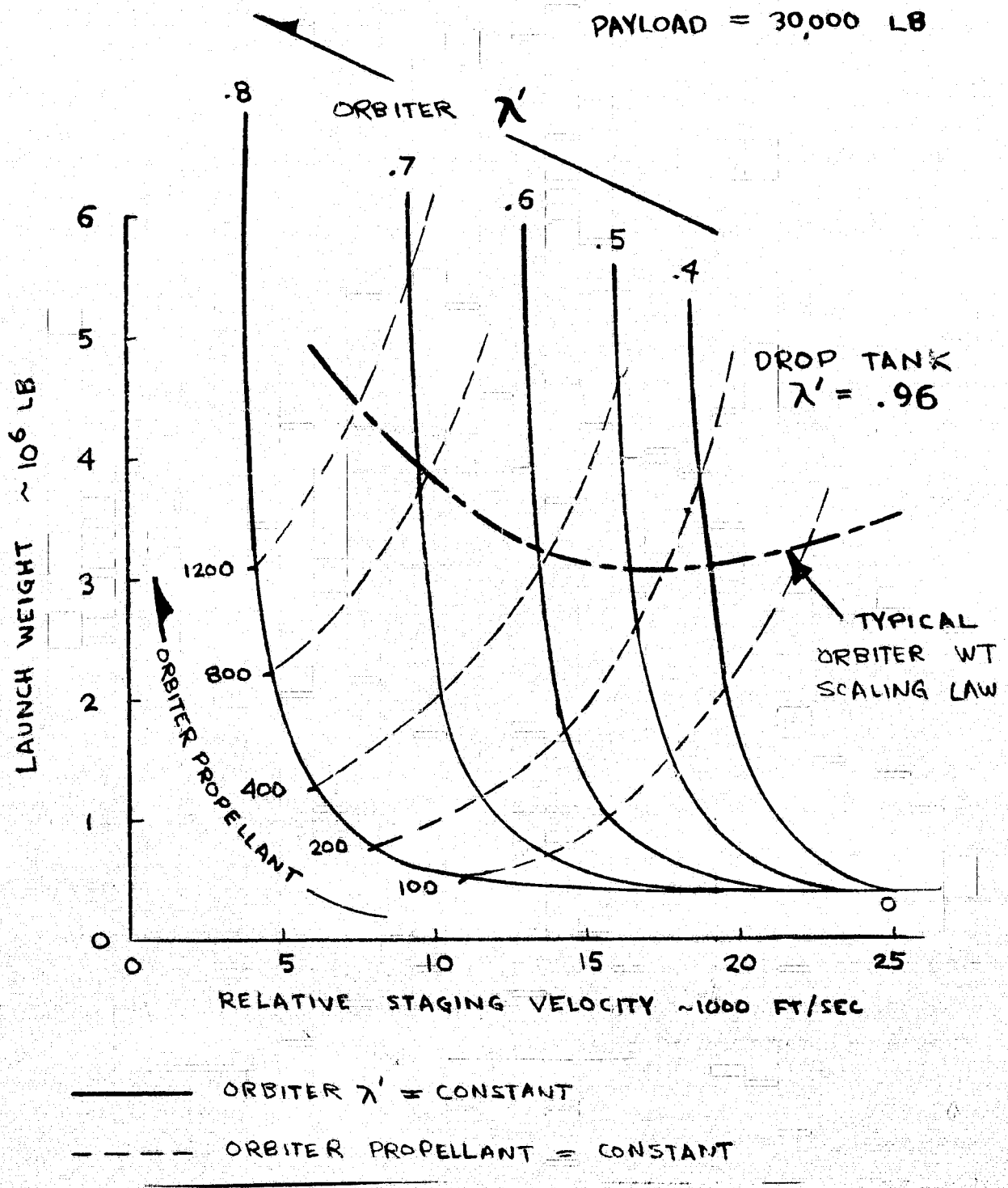

Fig. 2.4-2 Stage-and-One-Half Basic Performance

In Fig. 2.4-1, orbiter inert weight, propellant weight and mass fraction (λ') are shown. Values for several delta-body and straight-wing point designs are included.

The procedure for determining launch weight as a function of staging velocity is illustrated by Fig. 2.4-2. Launch weight and staging velocity for orbiters of constant mass fraction (λ') are shown by the solid lines. Superimposed is a grid of constant orbiter propellant curves (with orbiter inert weight varying). The orbiter mass fraction resulting from the inert weight law can be plotted on these two sets of curves knowing the propellant load. The results of this type of analysis are demonstrated in Fig. 2.4-3. The droptank λ' is assumed to be constant over the range of the droptank propellants examined. Orbiter weight growth (+20%, 0%, -20%) is assumed to occur to all three factors in the scaling equation, i.e., K_1, K_2, and K_3 in Equation (1) above are all changed proportionally. Note that for a droptank λ' of .96, a propellant load of 200,000 lb minimizes the system launch weight, regardless of orbiter inert weight growth.

These results are summarized in Fig. 2.4-4. The principal parameter affecting the optimum staging velocity (and optimum orbiter propellant loading) is the droptank λ'. Orbiter inert weight growth has little effect. The sensitivity of launch weight to orbiter inert weight and droptank inert weight is given in Fig. 2.4-5.

2.4.1.2 Propulsion Trades. Various propulsion trades involving ascent performance are presented in Figs. 2.4-6 to 2.4-8. The effect of number of engines, launch thrust-to-weight-ratio, engine expansion ratio, and number of engines on after droptank separation are examined.

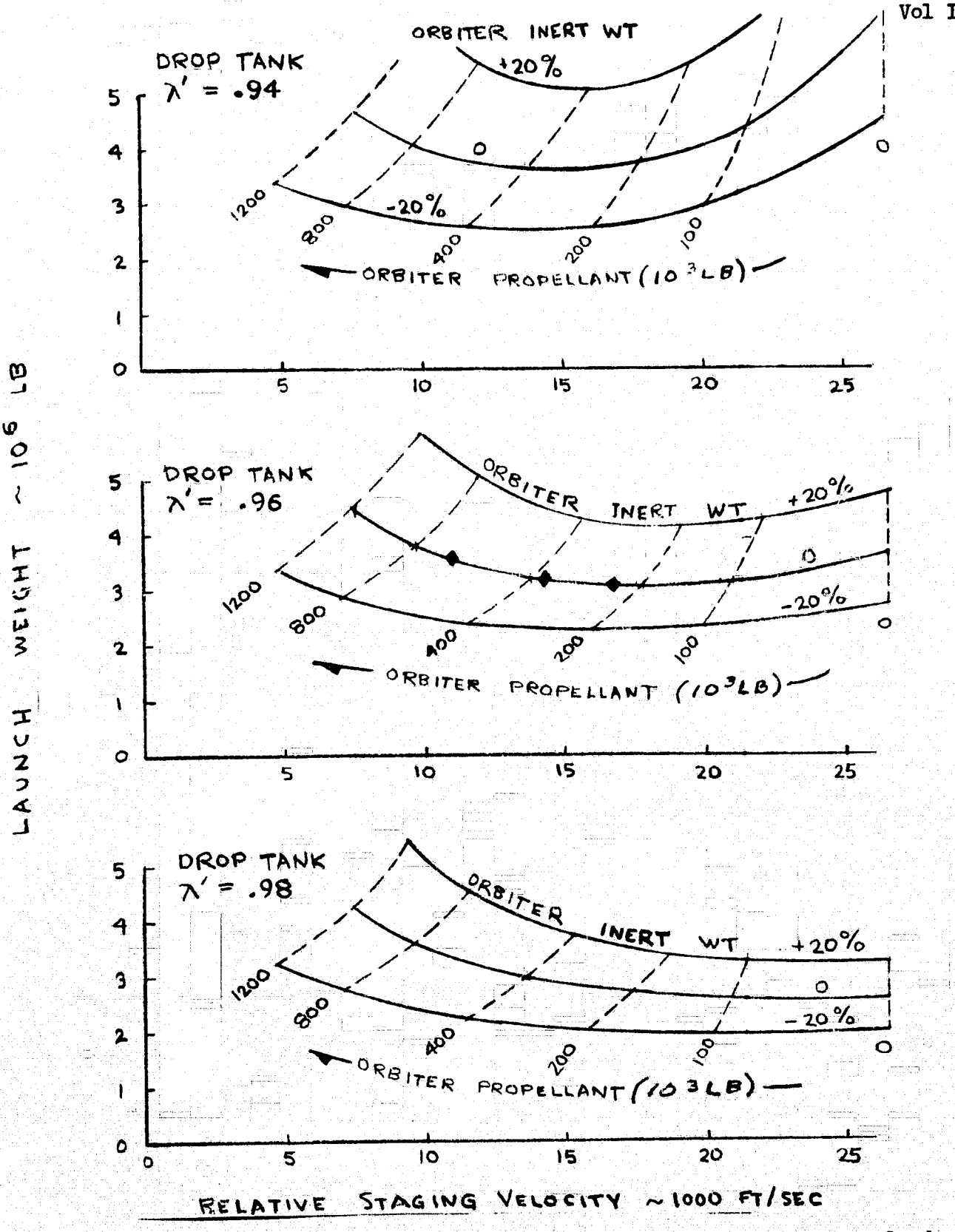

Fig. 2.4-3 Stage-and-One-Half Basic Performance For 30,000 LB Payload

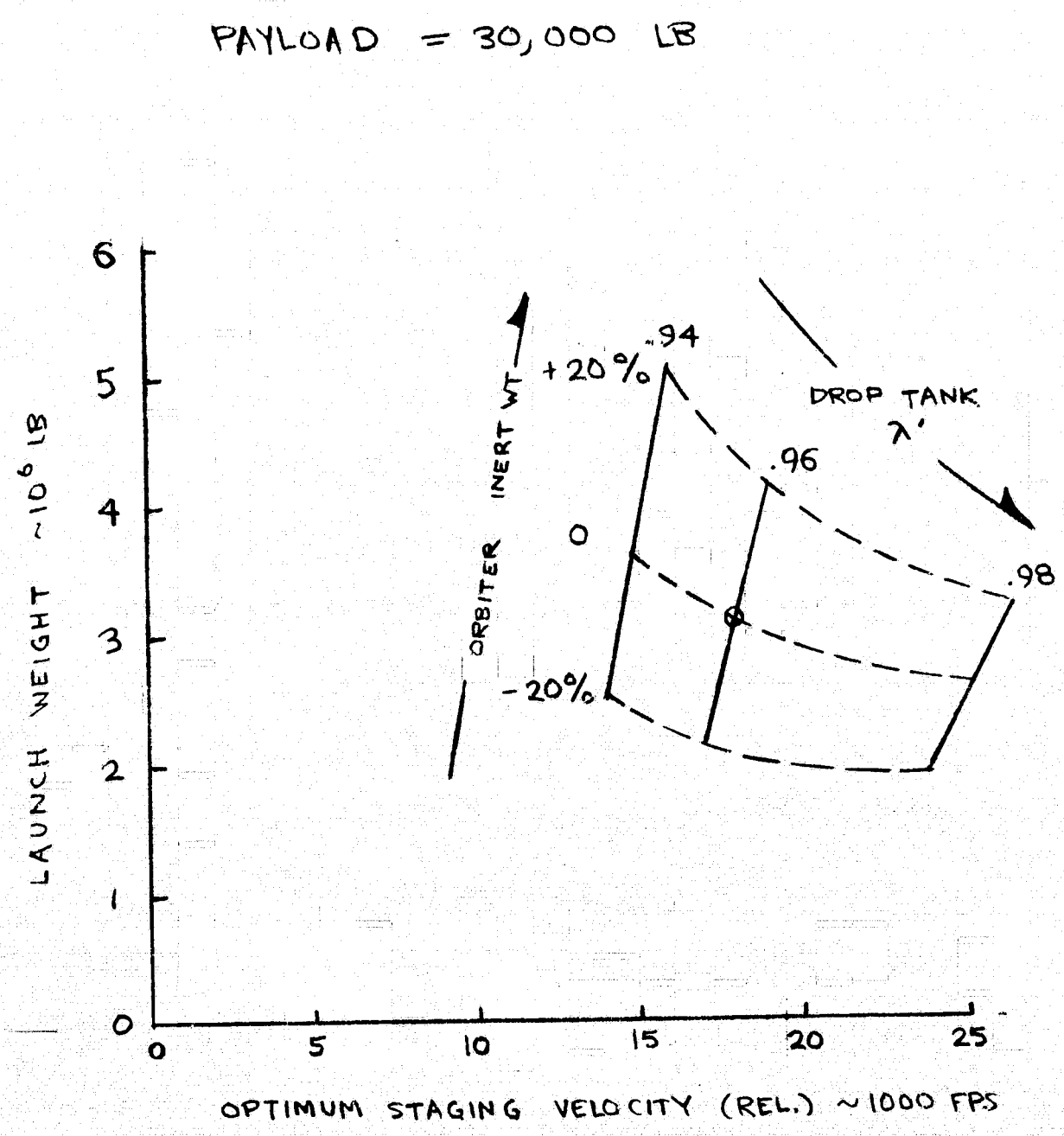

Fig. 2.4-4 Staging Velocity Optimization

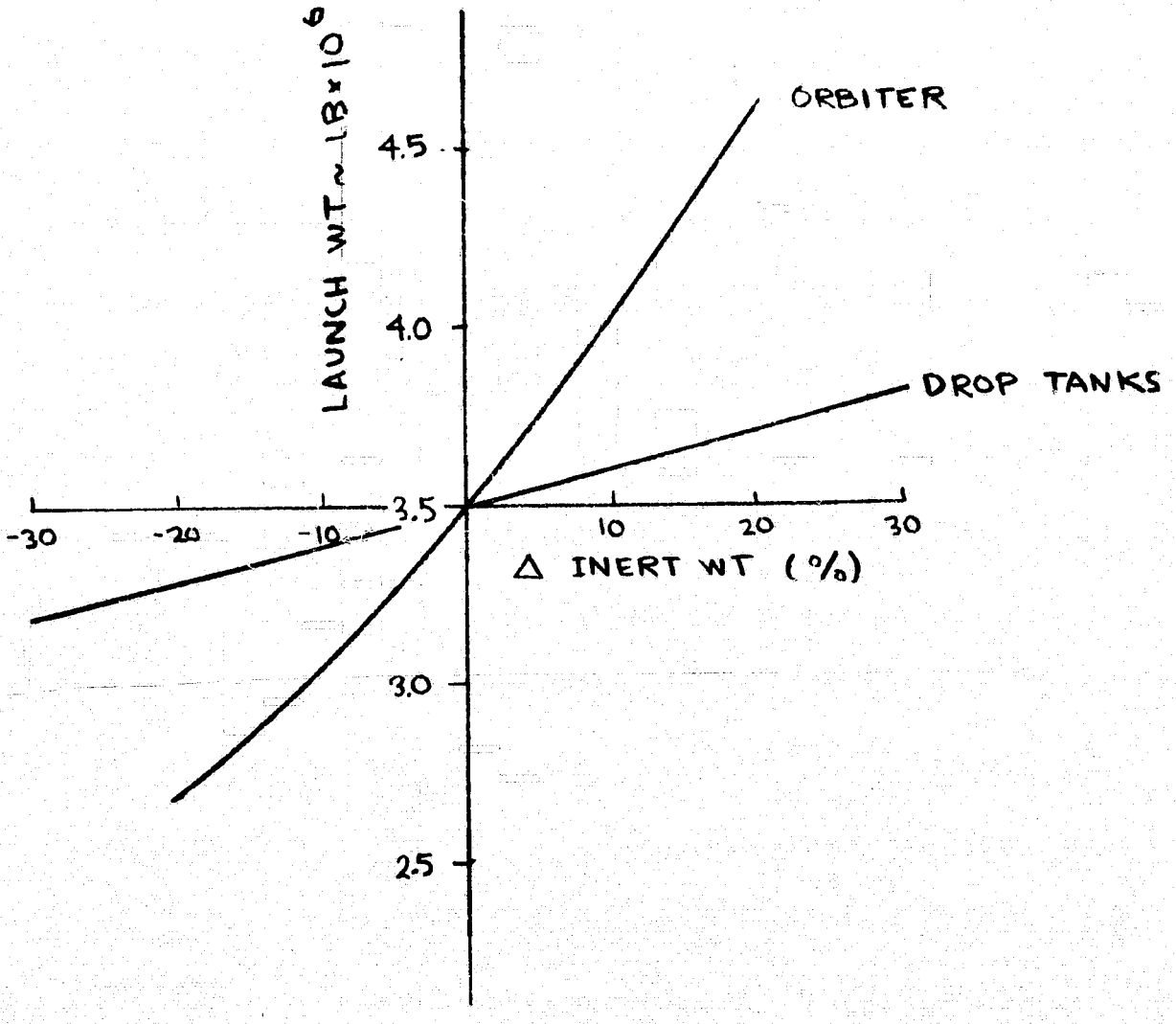

$$\frac{\partial\,(\text{Launch Weight})}{\partial\,(\text{Orbiter Inert Wt})} = 17 \text{ lb/lb}$$

$$\frac{\partial\,(\text{Launch Weight})}{\partial\,(\text{Drop Tank Inert Wt})} = 9.5 \text{ lb/lb}$$

Fig. 2.4-5 Sensitivity of Stage-and-One-Half To Inert Weight

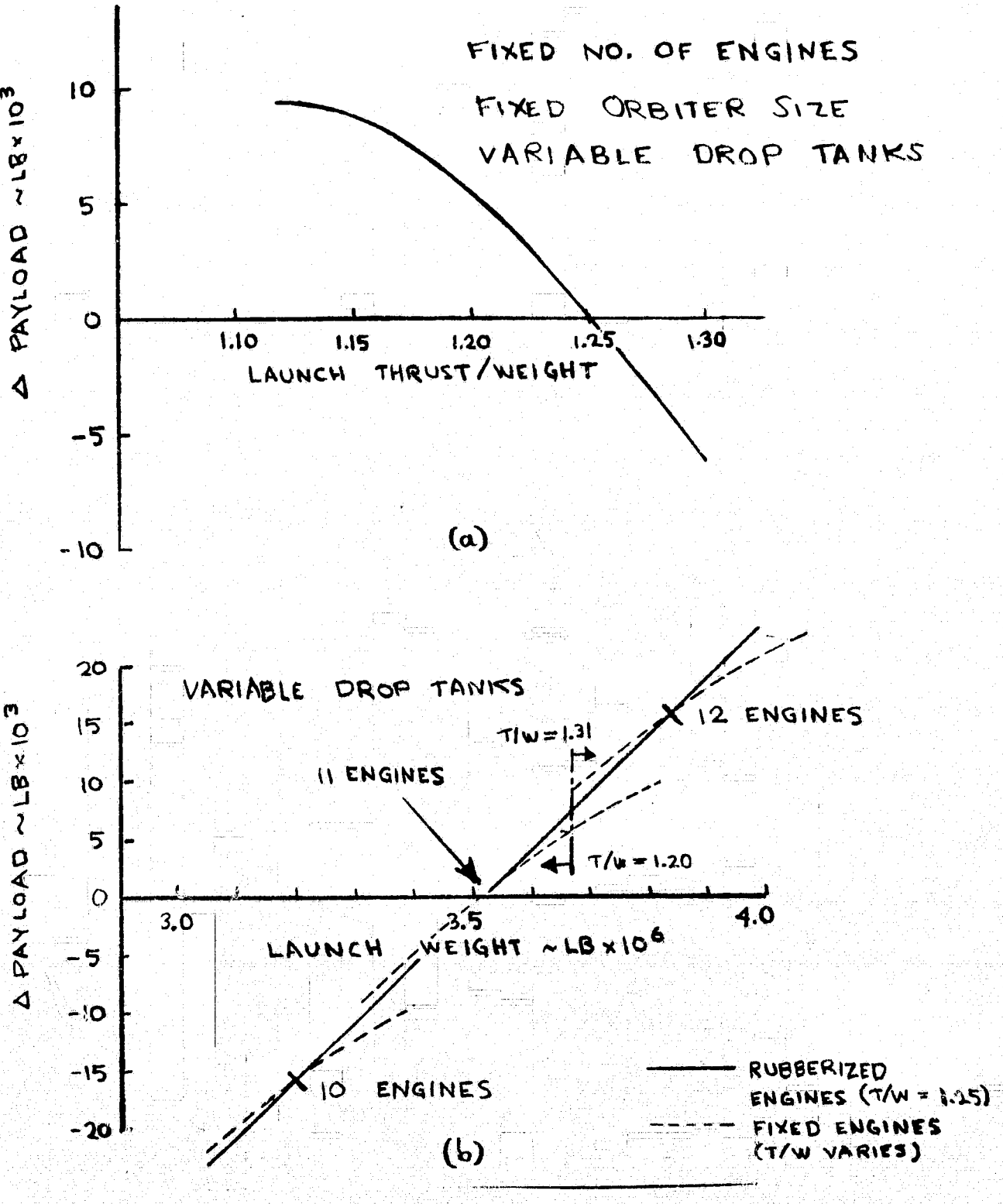

Fig. 2.4-6 Thrust/Weight and Engine No. Selection

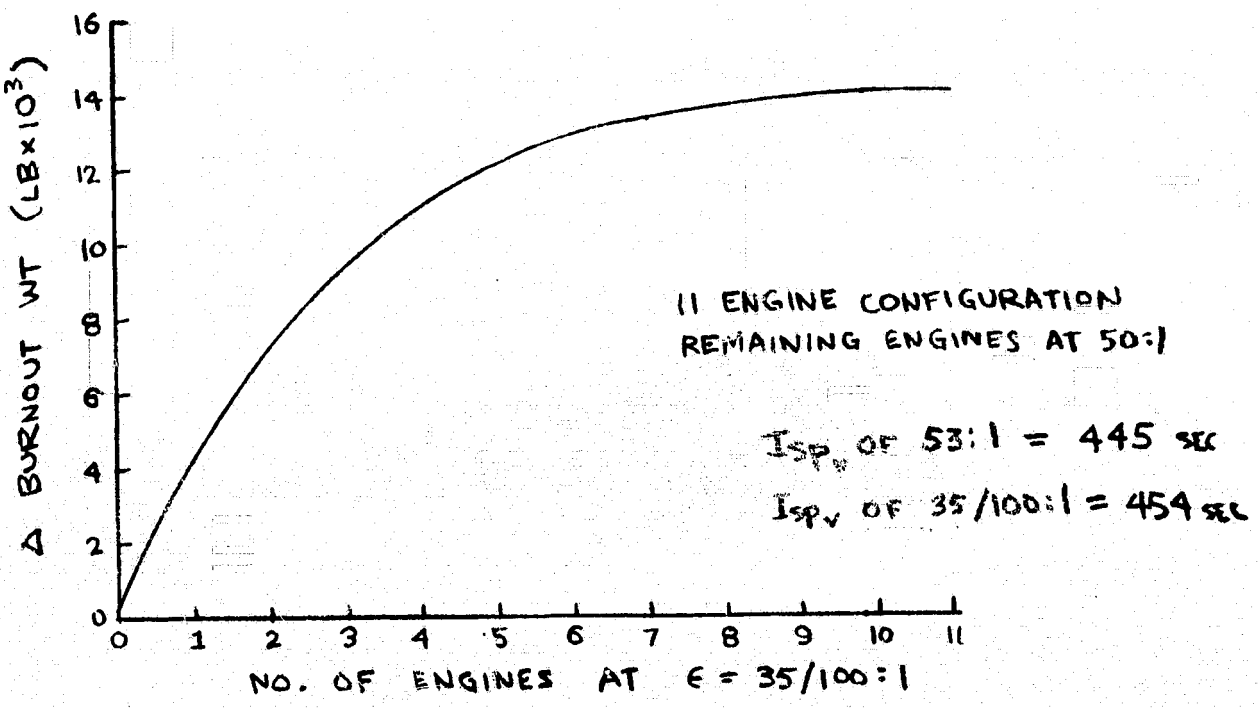

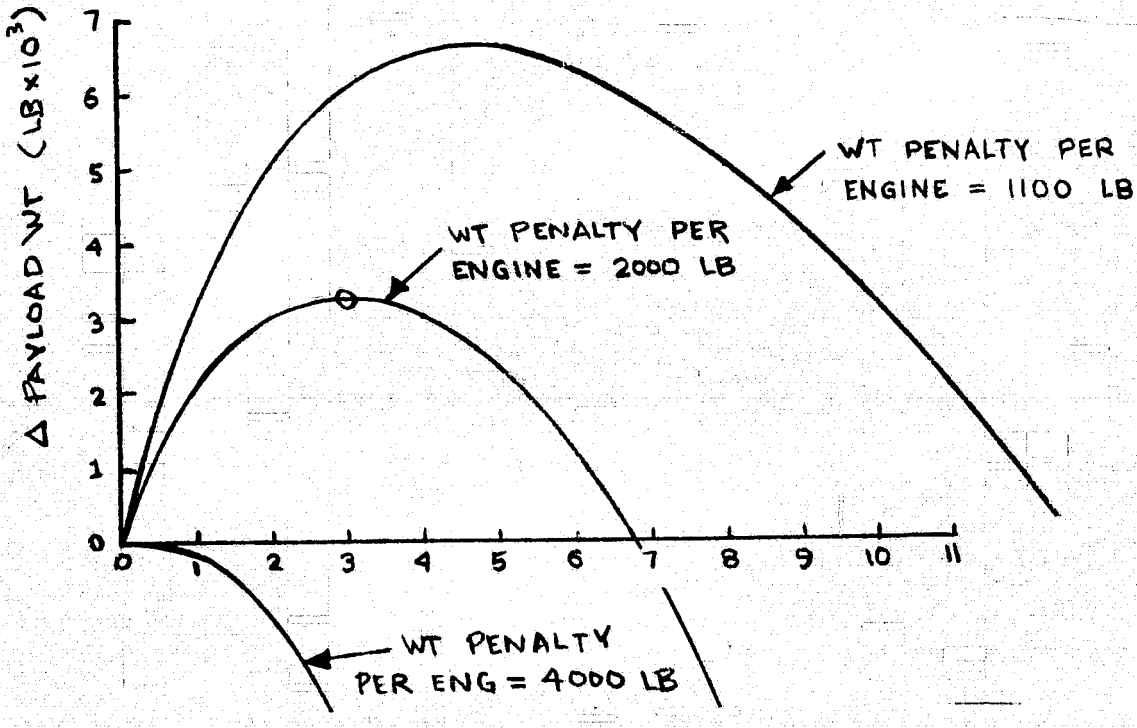

Fig. 2.4-7 Stage-and-One-Half Performance For Various Engine Nozzle Mixes

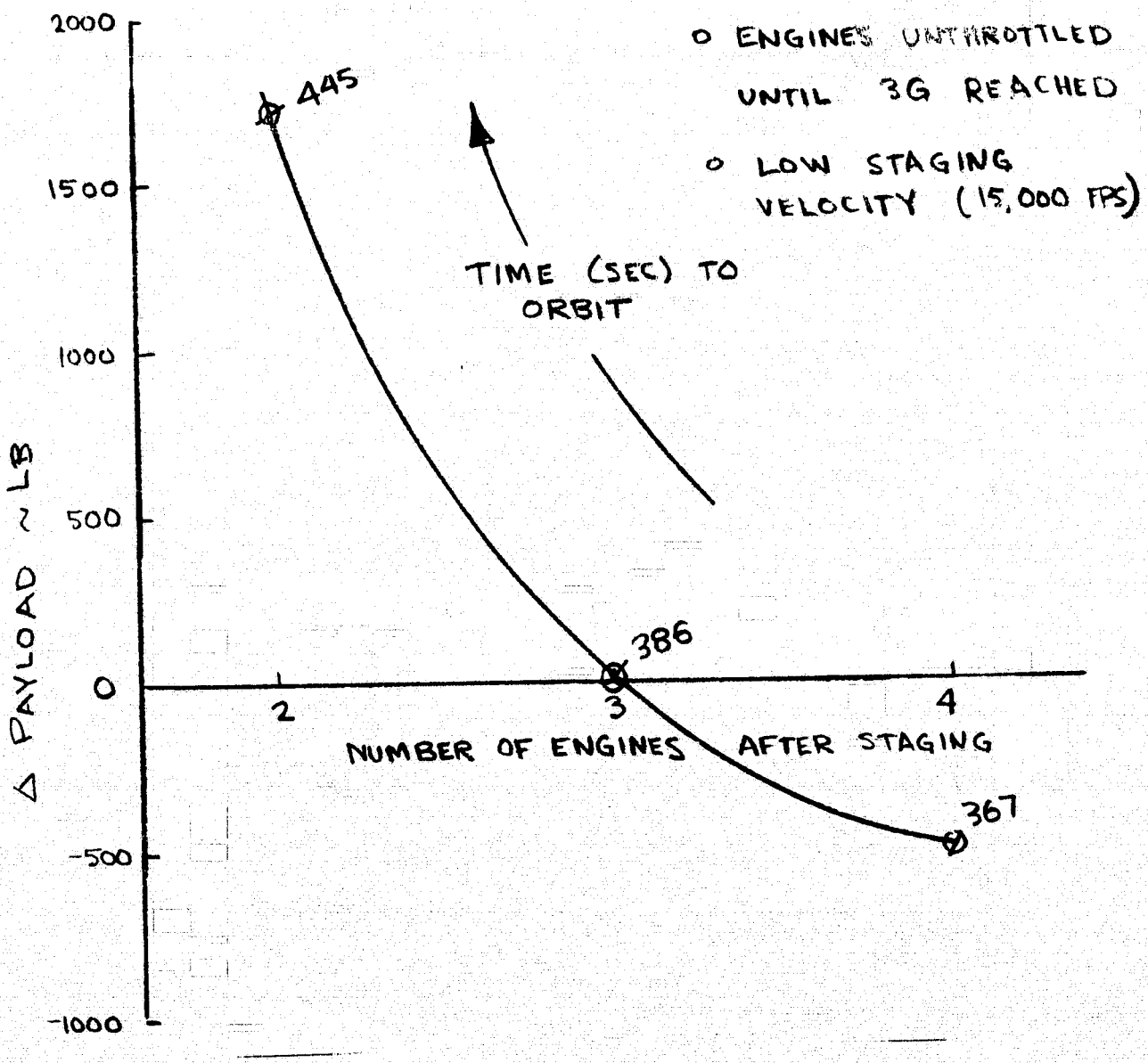

Fig. 2.4-8 Effect of No. Engines On After Staging On Performance

Launch thrust-to-weight effects are presented in Fig. 2.4-6. For a fixed number of engines (nominally 11), the launch thrust-to-weight can be varied by altering the size of the droptanks. As the T/W decreases, velocity losses increase (about 480 ft/sec per 0.10 unit T/W). However, since the launch weight increases, the net effect is to increase payload as T/W decreases. That is, for a fixed number of engines, maximum payload occurs for T/W lower than 1.25. However, for a fixed launch weight, maximum payload is delivered at a thrust-to-weight greater than 1.25. Going from an 11 to a 12 engine configuration, for the same launch weight (increasing T/W from 1.25 to 1.36) gives an additional 2000 lb payload, but because of base area problems and higher dynamic pressures, is not advisable. As the launch weight increases for a fixed number of engines, the T/W decreases. At same launch weight, it becomes advisable to add an additional engine. For example, at 3.67 Mlb, 4000 lb of payload are gained by going from 11 to 12 engines (increasing T/W from 1.20 to 1.31). Payload for various launch weights for the rubberized engine case is also shown. In this case, the number of engines (and thus engine weight) is assumed to be linear with launch weight, and not constrained to integral values. This results in constant T/W.

The effect of nozzle expansion ratio on performance is shown in Fig. 2.4-7. Only two types of nozzles are shown, a single-position 53:1 nozzle and a two-position 35:1/100:1 nozzle. For an 11 engine configuration, various numbers of the 53:1 nozzles are replaced by 35/100 nozzles. Because the vacuum characteristics of the 35/100 nozzle are superior to the 53:1, and the atmospheric characteristics about the same, burnout weight increases as more 35/100 nozzles are used. However, when the additional weight penalty of the 35/100 nozzle is accounted (heavier nozzle, increased base area, lower lift/drag, etc.), the payload vs. no. of 35/100 engines shows a maximum, depending on the size of the weight penalty. At present, the weight penalty appears to be about 2000 lb/engine, implying that three 35/100 engines should be used out of 11. However, the payload gain is only 3000 lb, and due to the increased complexity of design and operation, it is recommended that only 53:1 nozzles be employed. In this analysis, it is assumed that the 53:1 engines are shutdown first.

Payload as a function of number of engines burning after staging is presented in Fig. 2.4-8 for a 75 nm injection altitude. Because maximum payload is delivered for long burn times, 2 engines give more payload than 3 or 4. For the 50 nm injection altitude, 3 engines would be the optimum number. These trends will be discussed in the next section.

The throttling profiles used for the ascent trajectories are shown in Fig. 2.4-9. A combination of engine throttling and engine shutdown is assumed.

2.4.1.3 Trajectories Support. Ascent trajectories used for performance information were computed using PRESTO (Preliminary Rapid Earth-to-Space Optimization Program). This program generates point mass trajectories with optimized attitude control histories, useful for preliminary design work.

Table 2.4-1 summarizes the key performance/design parameters developed in this initial trajectory analysis which has been used to support the energy requirements attendant to the stage-and-one-half sizing.

Payload as a function of time to orbit for both 50 nm and 75 nm injection altitudes is presented in Fig. 2.4-10. The time to orbit was varied by altering the throttling profile after droptank separation. Maximum payload occurs at about 360-370 sec for the 50 nm case; and at about 475 sec for the 75 nm case. The effect of ascent drag on payload is shown on Fig. 2.4-11. Of these last three considerations, only the influence of injection orbit appears to be of significance.

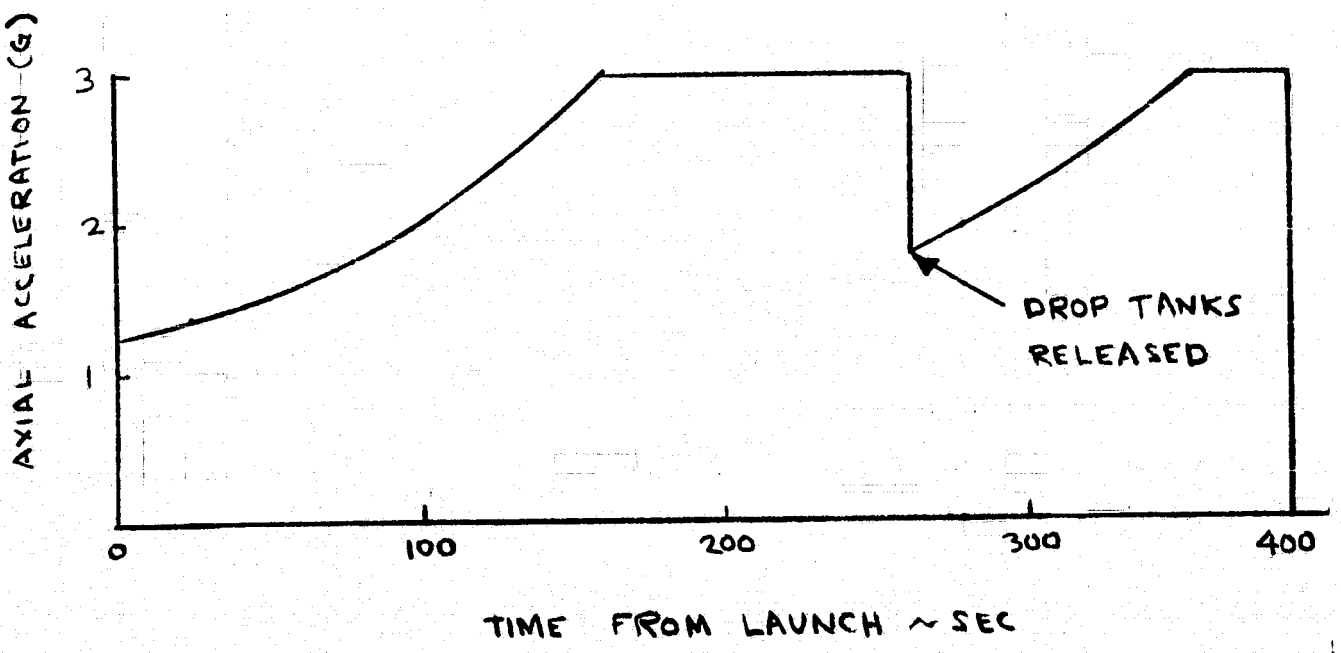

LAUNCH WEIGHT = 3.5 M

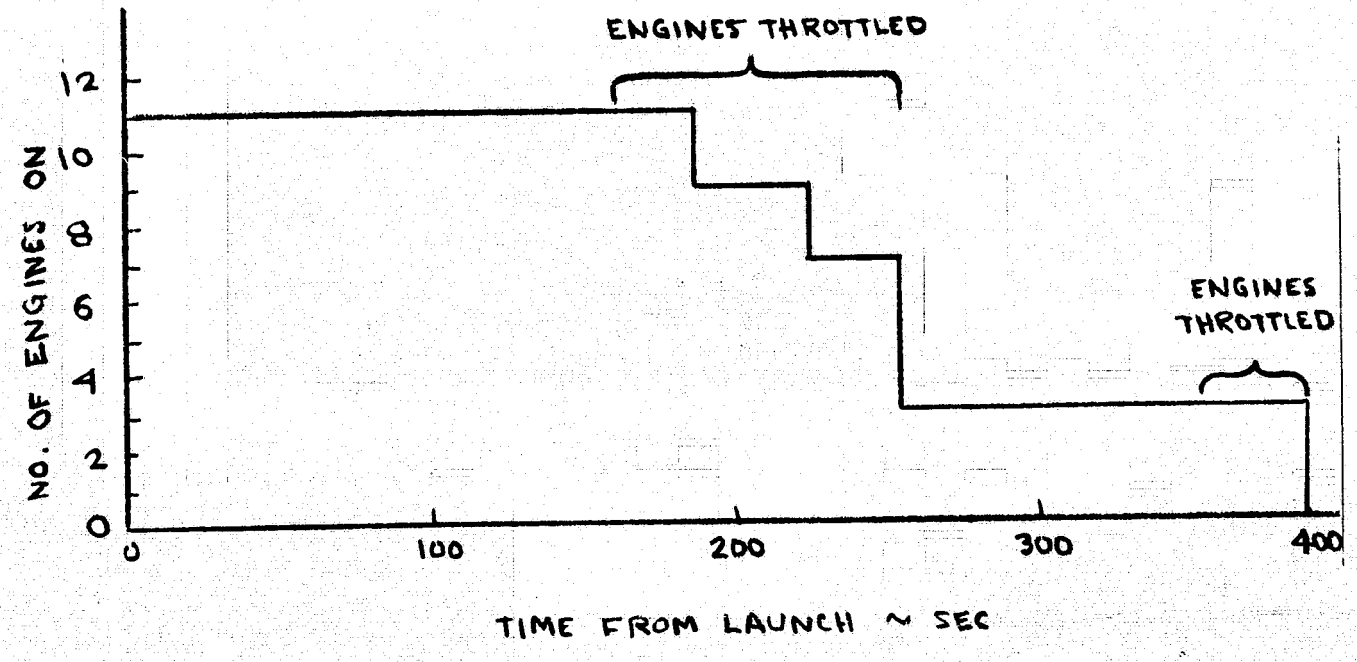

Fig. 2.4-9 Throttling Profiles

Table 2.4-1

TRAJECTORY DATA

- Peak Q 525 - 550 psf
- Time to Orbit 375 - 425 sec
- Staging Altitude > 260K ft
- Staging Q ~ 0
- Injection Altitude 50 nm

Table 2.4-1

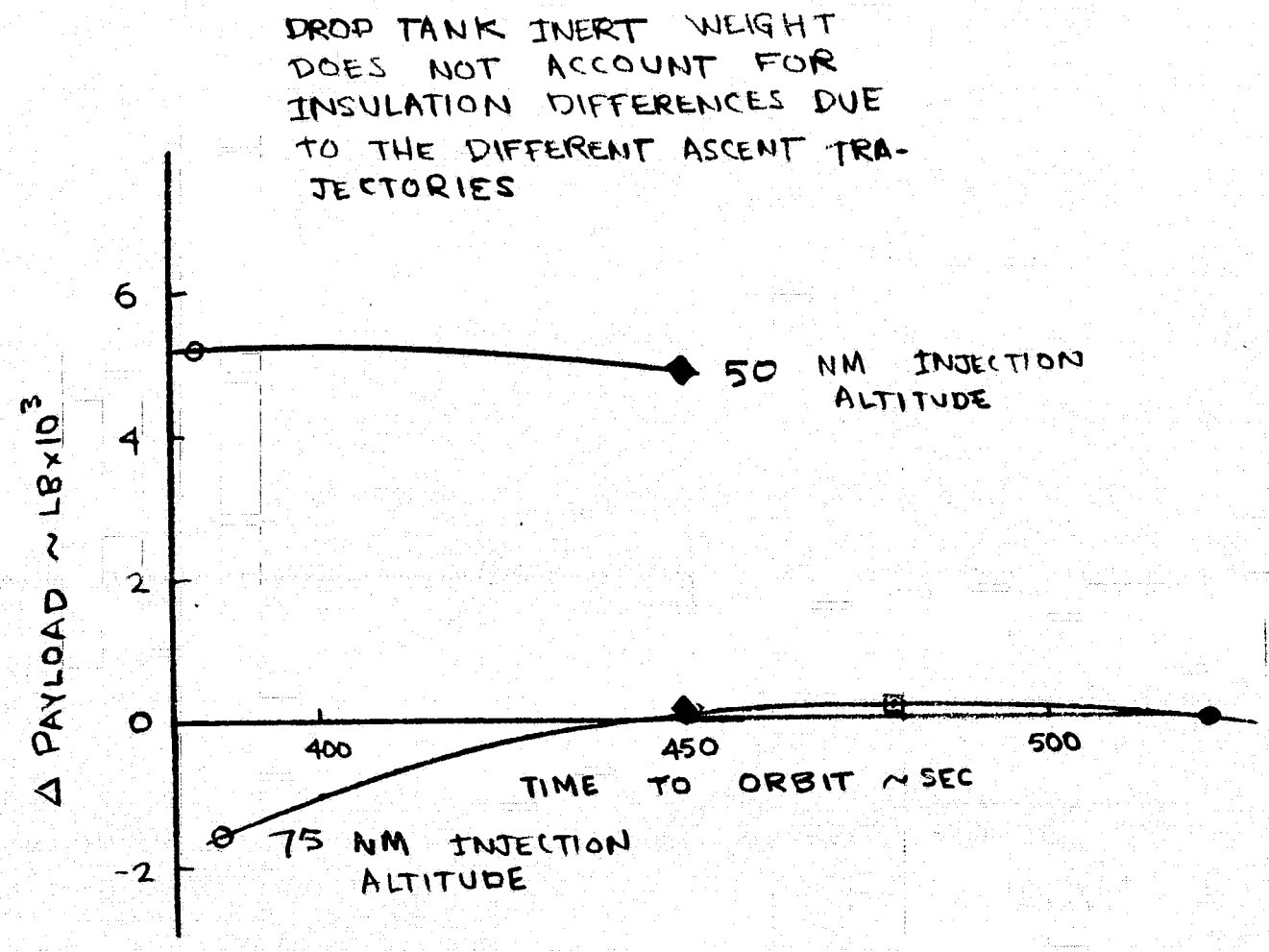

	T/W IMMEDIATELY AFTER STAGING (G)	MAX. AXIAL ACCELERATION AFTER STAGING (G)
o	1.8	3.0
◆	1.2	3.0
□	1.2	1.5
●	1.2	1.2

Fig. 2.4-10 Payload vs Time To Orbit

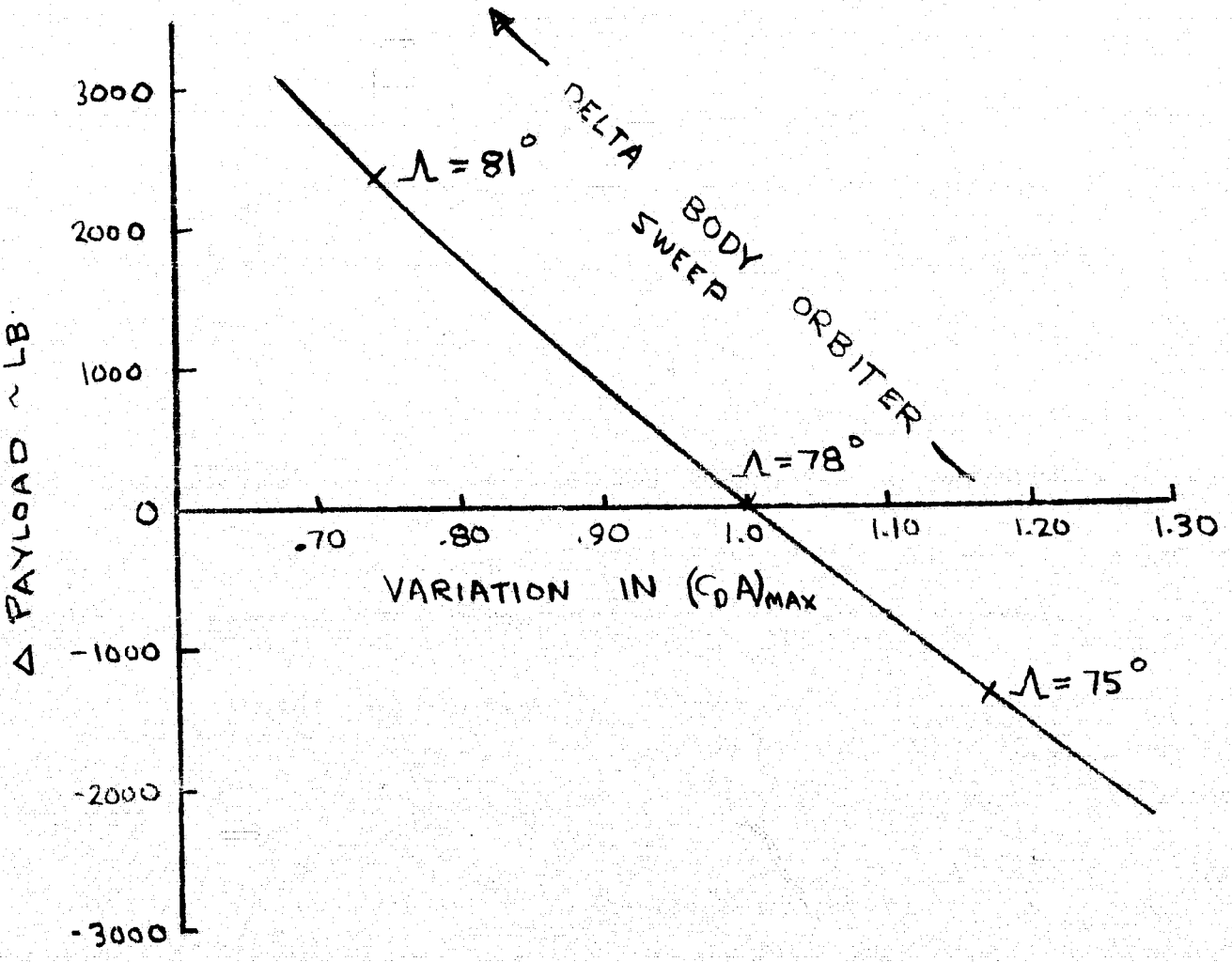

o ASCENT DRAG OF STRAIGHT WING TWICE THAT OF DELTA BODY, REDUCING PAYLOAD BY 6000 LB

Fig. 2.4-11 Effect of Ascent Drag On Payload

2.4.1.4 Sizing Conclusions - Primary Factors. The orbiter should be sized to contain 200,000 lb of propellant. Combining this requirement with the structurally efficient droptanks results in staging velocities in the order of 18,000 ft/sec (relative). It should be noted that this conclusion is based on a specific variation of orbiter size to propellant load, as determined in early design studies. For a given orbiter size, if some technique should be developed which maintains the simple tank arrangement but accomplishes additional propellant capacity, a benefit to payload would be accrued. To place improved propellant packaging in a high order of priority to the stage-and-one-half design is not required. Payload sensitivity to orbiter propellant is nonlinear, reducing from 0.12 lb/lb to 0.07 lb/lb for nominal propellant loads of 200,000 and 250,000 lb, respectively.

Injection into the 50 x 100 nm orbit is desirable from the standpoint of payload delivery. A 5000 lb payload loss results when the injection altitude is increased to the 75 x 100 nm condition.

The incorporation of all propulsion into the orbiter of the stage-and-one-half system, makes it necessary to regard the design issues, such as vehicle center of gravity, entry wing loading, and engine integration as first priority in developing the design launch thrust-to-weight ratio. In this regard, the stage-and-one-half system should be sized from the standpoint of maximum payload-to-launch thrust (not weight). Studies have shown that when attempting to maximize the payload to thrust, launch thrust-to-weight ratios of 1.11 appear best. Concern for control authority at liftoff presently requires the selection of a higher value. The recommended launch thrust-to-weight ratio for the stage-and-one-half system is 1.25, selected as an allowable and realistic value from Saturn launch system studies.

2.4.2 Ascent Trajectory

This section summarizes the considerations applied in the development of the representative stage-and-one-half ascent trajectory and involves the selection of launch thrust and main propulsion operating mode. Some of the ascent trade studies which entered into the decisions required for the ascent trajectory development are included.

Recently supplied power-on base drag corrections are investigated in the last section of the ascent studies. When reviewed, it will be seen that significant performance improvement to the stage-and-one-half system is promised. These new data have not been applied to the stage-and-one-half system in the studies, since it was felt that the information should be reviewed jointly by NASA and LMSC before any design changes to the stage-and-one-half system are undertaken.

2.4.2.1 Thrust-to-Weight Ratio. The unique characteristic of the stage-and-one-half system is the incorporation of all propulsion systems into one vehicle (orbiter). As described in Section 2.4.1, primary consideration is given to payload-to-thrust level rather than payload-to-launch weight. A launch thrust-to-weight ratio of 1.25 is selected as best representing the considerations of control authority, payload delivery capability, and propulsion system integration. Given a selected launch thrust-to-weight ratio, the performance investigation is directed toward the selection of a thrust-time history from liftoff to injection.

From early studies which investigated the effect of thrust profile upon performance prior to the introduction of acceleration constraints, it was learned that the best profile resulted from high thrust early in the trajectory to permit early reduction of the flight path angle, hence minimizing gravity losses during ascent. Once a low flight path angle was achieved, a much lower thrust level was initiated at an appropriate time to produce small thrust vector losses.

By introducing low acceleration constraints (2 or 3 g), it was found to be more optimum to again use high thrust early in the ascent trajectory and upon reaching the acceleration limit to maintain that acceleration level by throttling and engine shutdown.

Once droptank staging occurs, thrust level is of lesser importance due to the high staging velocities associated with the stage-and-one-half concept. For example, by operating at full thrust or the 3g boundary as compared to fully throttled (50 percent) operation from staging to injection, a payload benefit of 700 lb is realized. The first method is selected as the nominal operating mode for payload reporting but the final post-staging to injection mode remains flexible to either design or operational considerations. The capability of the stage-and-one-half system to operate along the 3g acceleration boundary over the major portion of the ascent profile where acceleration is critical results in the most efficient (low velocity loss) profile for any given initial thrust-to-weight ratio.

2.4.2.2 Acceleration Profile - Throttling/Shutdown Mode. The stage-and-one half launch vehicle has high thrust capability because all engines remain on board the vehicle from launch to orbit. Because of the excess of thrust, the ascent contraints of 3g maximum acceleration and 50 percent maximum throttling cannot always be satisfied to droptank separation. The method which was used to reduce thrust was the sequential shutdown of pairs of engines during the period that acceleration was constrained to 3g prior to droptank separation. The selection of engine pairs for shutdown was determined to minimize thrust moments or gimbaling requirements due to lack of symmetry in operating engine patterns which would result if only one engine were shutdown in sequence. Thus both engines of a pair occupied as near a location of symmetry as possible with respect to the center of mass.

The time sequencing for engine-pair shutdown was determined by the criterion that shutdown would occur when the remaining engines, operating at full power, would just provide 3g acceleration. Using this throttling technique, the 50

percent maximum throttling constraint was never reached during 3g acceleration. Aside from satisfying constraints, this method had the additional advantage of reducing the specific impulse degradation due to throttling. Figures 2.4-12a and -12b show the I_{sp} degradation as a function of the thrust ratio for an 11-engine and a 9-engine configuration. For the 11-engine configuration, maintaining 3g while using all engines would require throttling to 39 percent and result in an average loss in I_{sp} of about 2 sec. However, by using the throttling technique, of the original 11 operating engines, 5 remained in operation and required only 87 percent throttling to achieve the 0.39 thrust ratio prior to tank drop. With this method, the average I_{sp} loss amounted to 0.3 sec.

For the 9-engine configuration, 3-sigma I_{sp} degradation was used in addition to the I_{sp} loss due to throttling. The 3-sigma I_{sp} was dependent upon the number of engines (N) in operations by the following relationship

$$(I_{sp})_{3\text{-sigma}} = (I_{sp})_{\text{nominal}} - \frac{3}{\sqrt{N}}$$

This degradation is reflected in Fig. 2.4-12a by the fact that the I_{sp} ratio never reached unity after engine-pair shutdown commences. In addition, because of the greater thrust engines, the quantizing effect of throttling by engine elimination was reduced. Both influences had the effect of reducing the effectiveness of the method to lower I_{sp} loss. Whereas the 11-engine configuration lost an average 0.3 sec of I_{sp}, the 9-engine simulation loss was 1.1 sec.

2.4.2.3 Typical Stage-and-One-Half Ascent Trajectory. The definition of the stage-and-one-half ascent trajectory which satisfied all the constraints and achieved maximum payload to orbit was accomplished by the PRESTO computer program. This program was used for the nominal trajectory and for conducting the various trade studies used to determine the optimum thrust time characteristics, liftoff acceleration, and droptank staging velocity. The program was modified to simulate the stage-and-one-half characteristics, such as constant acceleration thrust profiles, I_{sp} degradation due to throttling, throttling by engine-pair elimination, engine half-thrust prior and after tank drop, and power-on base force.

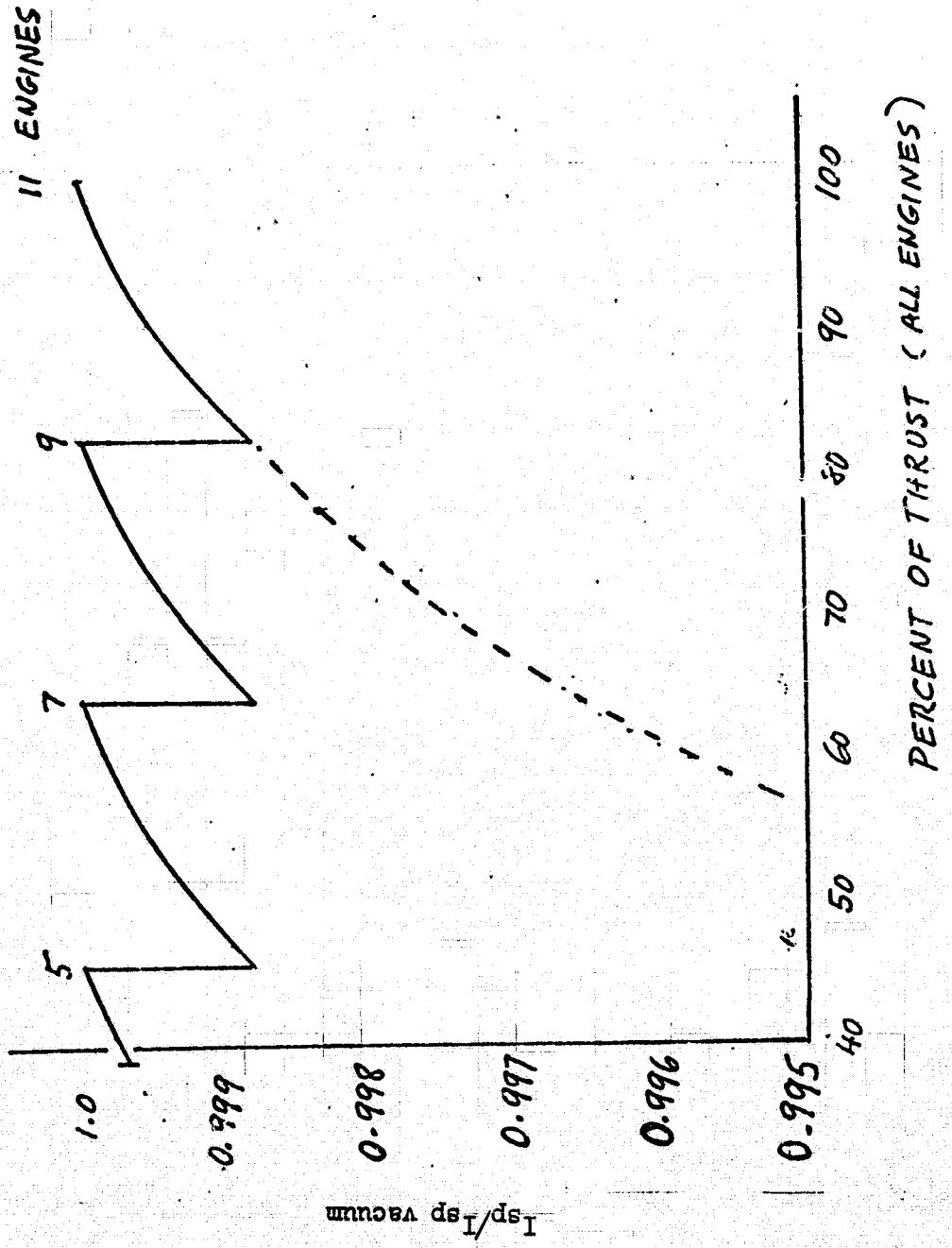

Fig. 2.4.2-12a Specific Impulse Degradation For Throttling (Eleven-Engine Configuration)

Fig. 2.4.2-12a

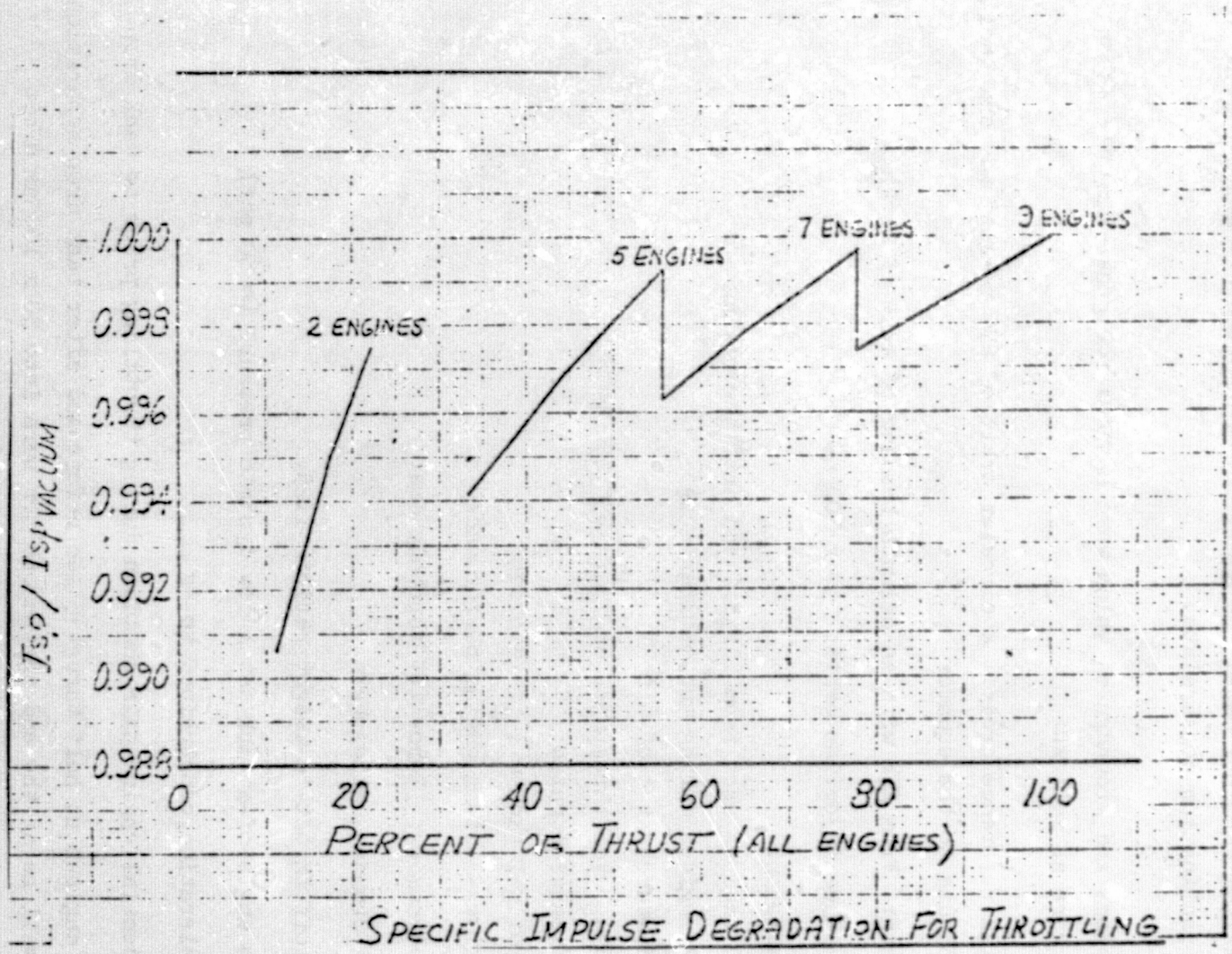

Fig. 2.4.2-12b Specific Impulse Degradation For Throttling
(Nine-Engine Configuration)

LOCKHEED MISSILES & SPACE COMPANY

PRESTO employs a steepest ascent gradient optimization technique to arrive at the optimum steering program satisfying the specified terminal conditions and yielding maximum terminal mass. In addition, the launch azimuth is optimized to satisfy inclination constraints.

The assumptions and groundrules which were assumed for generating the ascent trajectory were as follows:

- Design reference orbit: A circular orbit of 270 nm altitude and inclined at 55-deg to the equator
- Launch: From ETR with an azimuth heading of east of north
- Reference injection orbit: 50 x 100 nm
- Propulsion:
  - 9 engines used from liftoff and into throttling
  - 2 engines during the orbiter stage
  - Mixture ratio of 6 to 1
  - Sea level thrust per engine: 530,000 lb
  - Expansion ratio: 53 to 1
  - Nominal vacuum I_{sp}: 445 sec
  - Minus-3-sigma engine performance
- Aerodynamics: Zero-lift forebody drag
- 1962 Standard atmosphere
- Liftoff thrust-to-weight ratio: 1.25.
- Zero angle-of-attack until low dynamic pressure ($\approx$ 60 psf)
- Acceleration constrained to 3g
- Sequential engine-pair shutdown during throttling prior to tank drop
- Two engines at half thrust 5 sec before and after tank drop separation, as well as at the end of the orbiter burn into 50 x 100 nm orbit

These guidelines were used in simulating the optimum ascent trajectory with the sole exception of the half-thrust requirement 5 sec prior to orbit insertion.

This slight effect amounted to 44 lb less in burnout weight and an increase in time to injection of 2.4 sec.

Three-sigma engine performance for one engine would mean reducing the I_{sp} by 3 sec. However, for multiple engines, 3-sigma performance for the group meant less of a reduction and was dependent upon the number of engines operating (N). The I_{sp} for any number of engines was obtained by the formula,

$$(I_{sp})_{3\text{-sigma}} = (I_{sp})_{\text{nominal}} - \frac{3}{\sqrt{N}}$$

Table 2.4-2 represents a sequence of events and simplified weight breakdown for the reference ascent trajectory. This table includes some pertinent events to 50 x 100 nm injection. The 17 fps drag correction represents the velocity required to overcome drag in coasting from 50 x 100 nm.

Table 2.4-3 summarizes the velocity losses during ascent for both phases up to and after droptank separation. As can be seen, little velocity loss is incurred during the orbiter phase. This is attributed to the high staging velocity.

Some relevant trajectory parameters are presented in Fig. 2.4-13; namely, the relative flight path angle, dynamic pressure, and altitude as function of time from liftoff. Figure 2.4-14 presents the thrust attitude, acceleration and velocity histories from liftoff. Nine engines remain in operation until 196.8 sec after liftoff, at which time sequential engine-pair shutdown begins. Near the time the droptanks stage, the operating engines have been reduced to 5 until 5 sec prior to tank drop, when 2 engines are operating and remain so until injection.

2.4.2.4 Trade Studies for Ascent. Of major importance in arriving at the maximum payload to orbit is the impact of the various propulsion parameters on this payload. To insure that payload degradation was not the result of incorrect choices of these parameters, trade studies were conducted to seek the best

Table 2.4-1

Sequence of Events and Simplified Weight Breakdown —
Ascent Trajectory

EVENT	TIME (sec)	WEIGHT (lb)	REMARKS
Liftoff	0	3,816,000	T/W = 1.25
Impulse		-1,980,000	
Initiate Throttling	159.6	1,836,000	T/W = 3.0
7-Engine Operation	196.8		
5-Engine Operation	246.5		
2-Engine Operation	289.7		50 Percent Throttle
Impulse Propellant for Throttling Mode		-1,084,958	Droptank Impulse Propellant = 3,064,958
Droptank and Residuals	294.7	127,718	
Orbiter Weight at Staging	294.7	633,324	2-Engine at 50 Percent Throttle
2-Engine Operation	299.7		100-Percent Thrust
Impulse Propellant		-215,324	
Initiate Throttling	374.9	408,000	T/W = 3.0
Impulse Propellant		-14,800	
2-Engines at Half Power	380.3	393,192	5 sec
Injection in 50X100 Orbit	385.3	386,235	
Drag Correction (17 ft/sec)		-469	
Weight at 50X100 Orbit		385,776	

Table 2.4-1

Table 2.4-2

Velocity Losses During Ascent

	Droptank Phase (ft/sec)		Orbiter Phase (ft/sec)
Earth Rotation	-1		3
Gravity	4,140		40
Drag	338		5
Thrust Atmospheric Pressure	420		0
Thrust Attitude	44		20
Total	4,941		68
	TOTAL BOTH STAGES	5,009	

Table 2.4-2

Fig. 2.4-13 Stage-and-One-Half Ascent Trajectory

REPRODUCIBILITY OF THE ORIGINAL PAGE IS POOR

REPRODUCIBILITY OF THE ORIGINAL PAGE IS POOR.

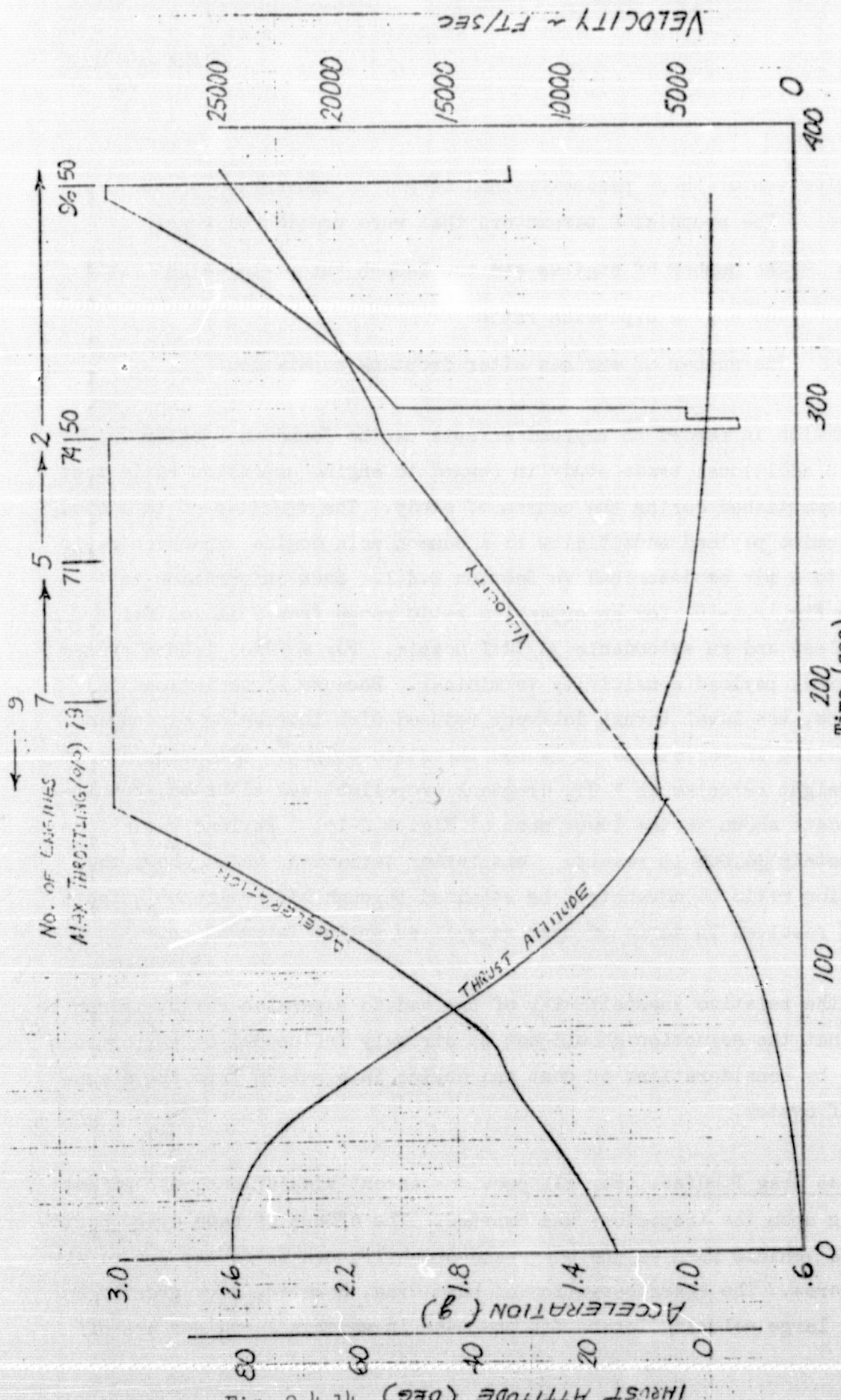

Fig. 2.4-14 Stage-and-One-Half Ascent Trajectory

Fig. 2.4-14

possible selection of these parameters and to get an indication of their sensitivities. The propulsion parameters that were considered were:

- The number of engines and the launch thrust-to-weight ratio
- The engine expansion ratio
- The number of engines after droptank separation

Such information in regard to payload effects can be found in Section 2.4.1. There was an additional trade study in regard to engine expansion ratio that has been accomplished during the course of study. The objective of this study was to determine payload sensitivity to a common main engine expansion ratio as opposed to a mix as described in Section 2.4.1. Such information is supplied in Fig. 2.4-15 for an expansion ratio range from 35:1 to 70:1 (fixed nozzles) and an extendable 35/70:1 nozzle. For a fixed launch system (upper figure), payload sensitivity is mininal. Because of variations in back pressure, sea level thrust delivery reduced with increasing expansion ratio, resulting in variations in launch thrust-to-weight. Since the design thrust-to-weight selected is 1.25, droptank propellant was adjusted, resulting in the data shown in the lower part of Fig. 2.4-15. Payload variations of approximately $\pm$4,000 lb result. This latter variation, which shows the 35:1 expansion ratio to advanatge, is attained through higher launch weights and must be resolved in terms of cost as well as engine integration.

Because of the relative insensitivity of payload to expansion ratio, it can be concluded that the selection should not be strongly influenced by performance issues, but by considerations of cost and engine integration into the stage-and-one-half system.

2.4.2.5 Base Drag Studies. For all previous ascent simulations, the effect of base drag upon the trajectory was omitted. The effect of base drag, particularly on a vehicle such as the stage-and-one-half, can be severe due to the large base area. The characteristics of base drag, however, vary greatly from rather large velocity losses for the case in which all engines are off

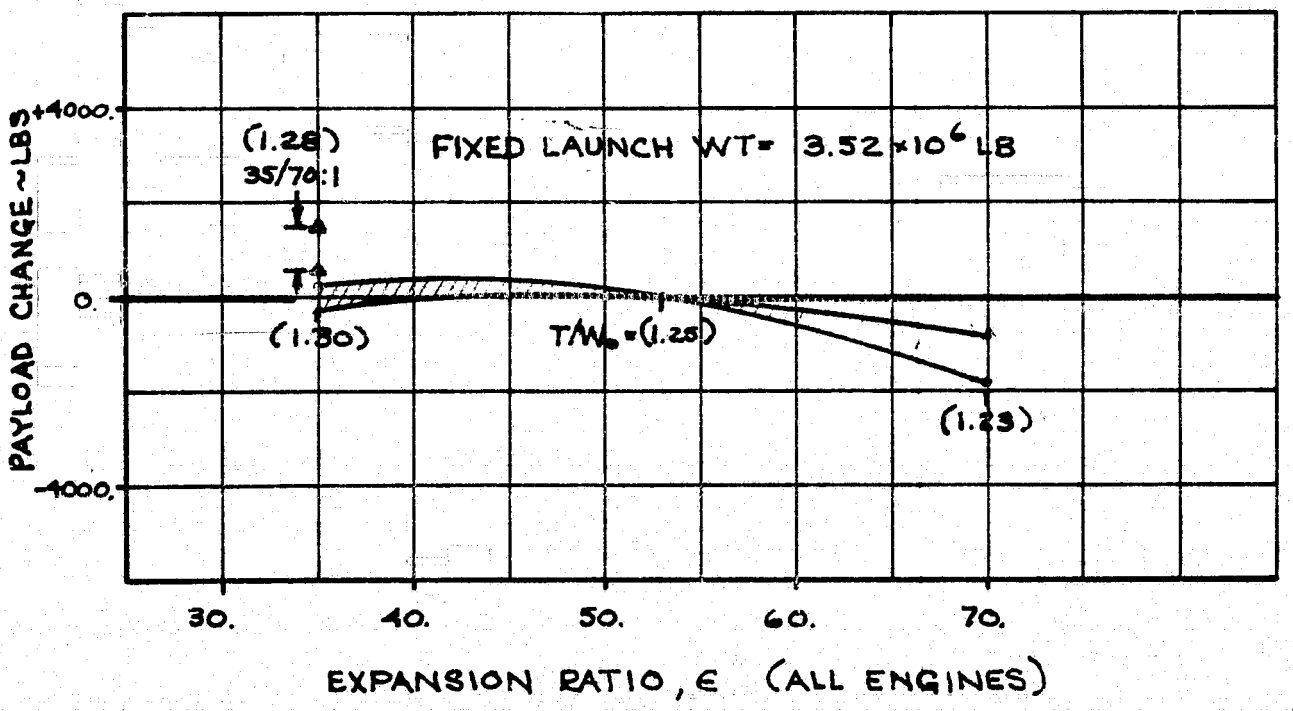

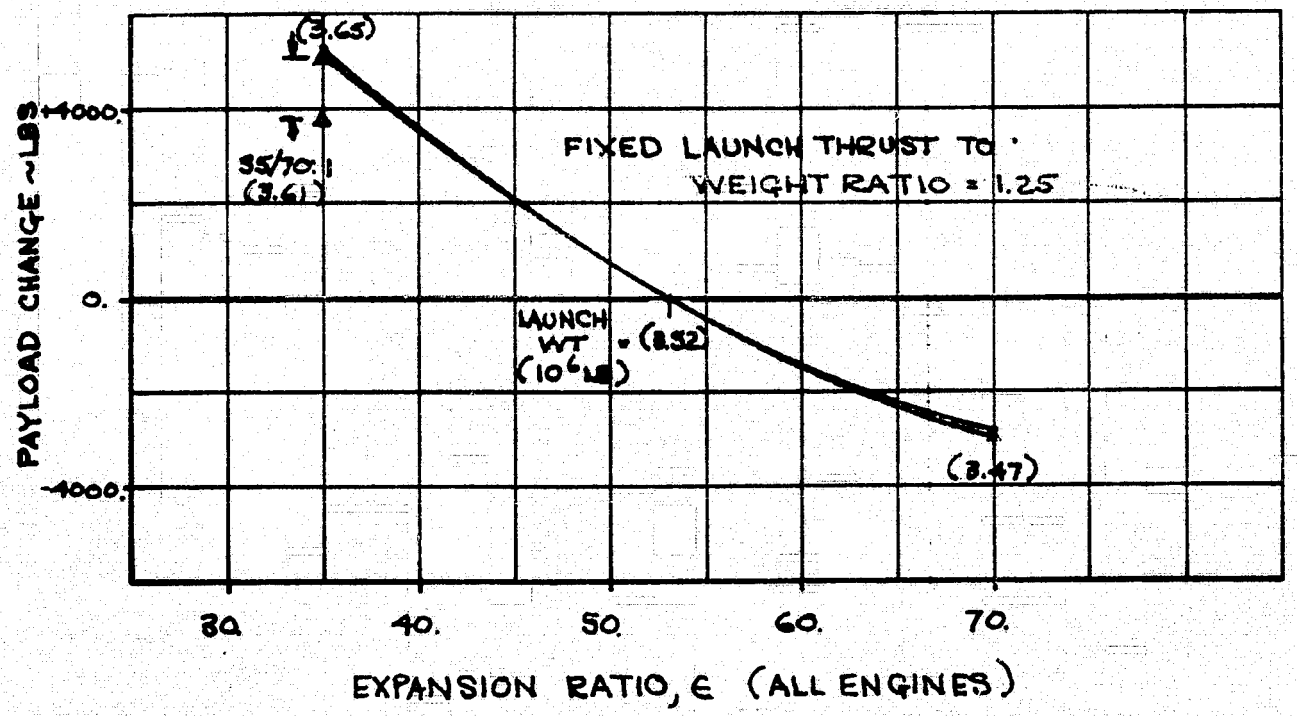

EXPANSION RATIO SUMMARY-FIXED FLOW RATE CASE

Fig. 2.4 -15 Stage-and-One-Half

to large velocity gains for the case in which they are all on.

Fig. 2.4-16 shows the drag coefficient for the stage-and-one-half. The upper curve was obtained from wind tunnel measurements of a scaled model and represents the power-off total drag. This power-off total drag is defined as the sum of forebody and power-off base drags. The lower curve represents the forebody drag only and was obtained from the power-off total drag by subtracting the power-off base drag. Beyond Mach 5, the effect of power-off base drag was assumed negligible. Previous trajectory simulations used drag characteristics similar to those given in Fig. 2.4-16 to represent the total aerodynamic effect for ascent to orbit.

The base drag with engines operating, however, is much different than with power off. In fact, base drag with power-on becomes beneficial at high altitudes by providing negative drag. Power-on base drag is represented by the product of reference base area and the difference between base and ambient pressures. This pressure difference is a function of altitude and is shown in Fig. 2.4-17. As can be seen, at low altitudes, base drag is unfavorable and quite significant. At maximum positive drag occurring at 10,000 ft, the base drag is more than three times the forebody drag. At altitudes above 37,000 ft, the base drag becomes negative and remains so for all higher altitudes.

The method used to simulate the base drag consisted of separating the total drag into three components. These consisted of (1) the power-off total drag, (2) the power-off base drag, and (3) the power-on base drag. With all engines operating, the total drag equaled the first component less the second plus the third. As engines were shutdown during the throttling phase, only a fraction of the second and third components was subtracted and added to the first. This fraction consisted of the ratio of operating engines to total engines. The fraction was used for the complete simulation even prior to throttling, when of course it was equal to unity. To add a certain amount of conservatism to the simulation, only 80 percent of the fraction was used in the simulation.

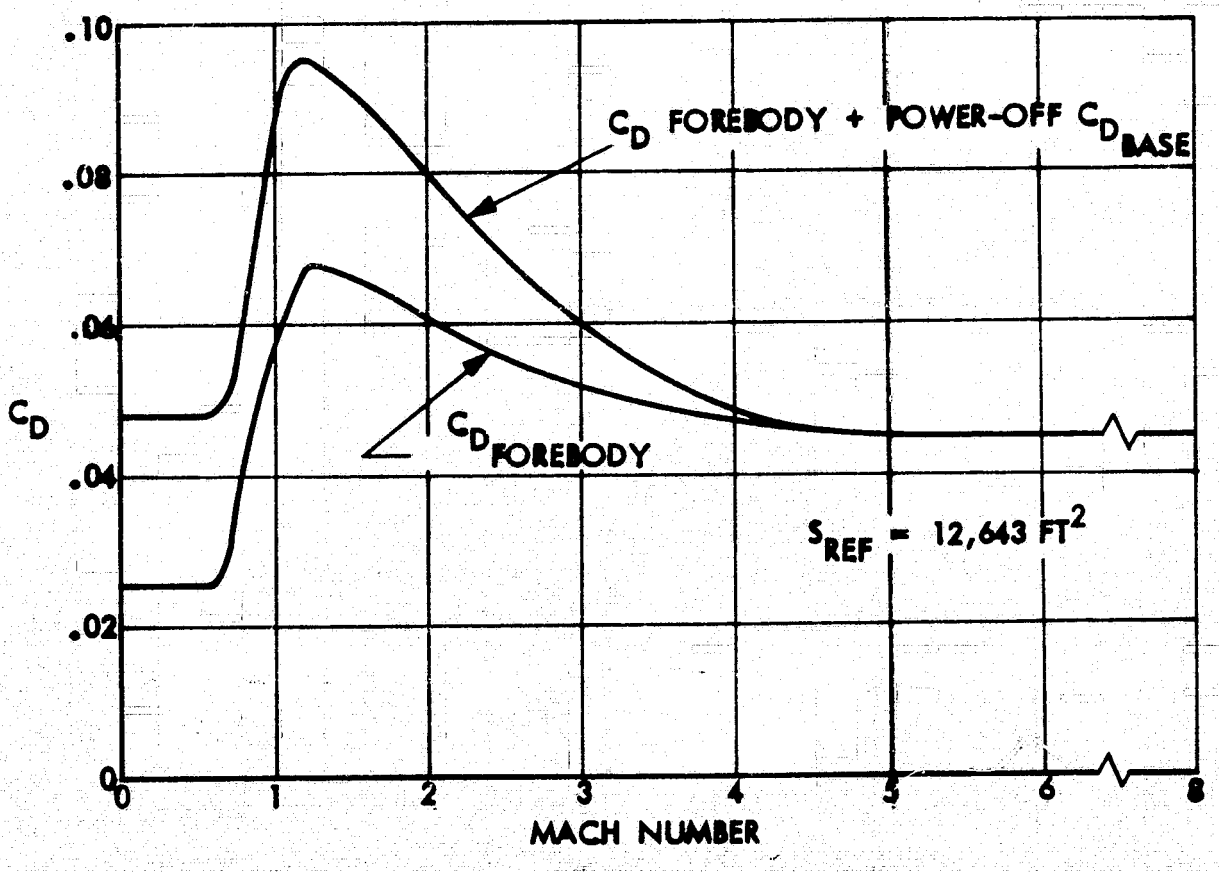

Fig. 2.4 -16 Launch System Drag Characteristics

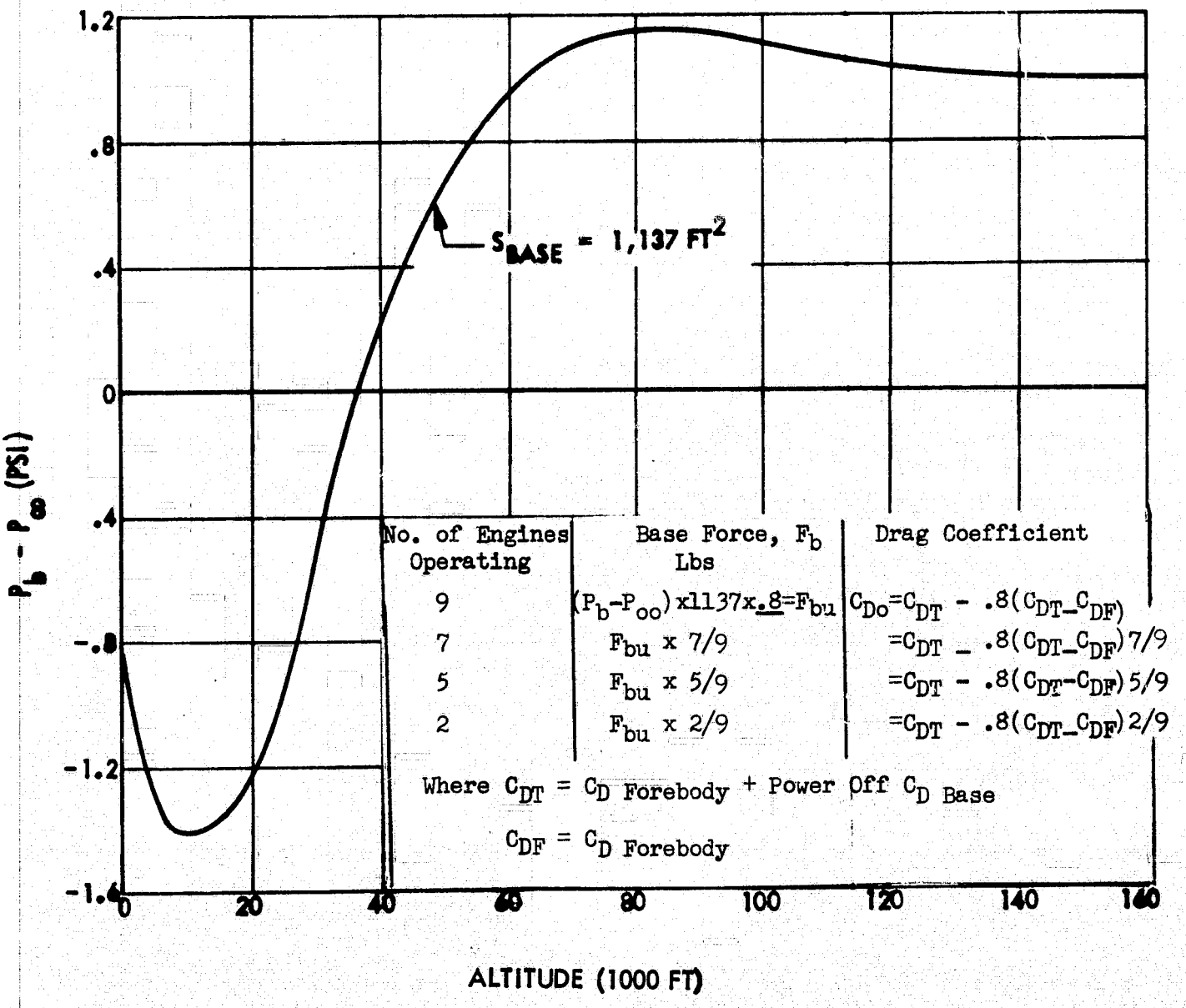

No. of Engines Operating	Base Force, F_b Lbs	Drag Coefficient
9	(P_b-P_{oo}) x1137x.8=F_{bu}	$C_{Do}=C_{DT}$ - .8(C_{DT}-C_{DF})
7	F_{bu} x 7/9	=C_{DT} - .8(C_{DT}-C_{DF})7/9
5	F_{bu} x 5/9	=C_{DT} - .8(C_{DT}-C_{DF})5/9
2	F_{bu} x 2/9	=C_{DT} - .8(C_{DT}-C_{DF})2/9

Where C_{DT} = C_D Forebody + Power Off C_D Base

C_{DF} = C_D Forebody

Fig. 2.4-17 Launch System Drag Characteristics

Simulation of the total drag rather than only the forebody drag produced a slightly different optimum ascent profile. To benefit from the base drag, the optimum trajectory was more lofted or flew higher to take advantage of the negative base drag sooner, even though this meant accepting slightly greater (17 fps) gravity losses. Because of the lofting, maximum dynamic pressure was reduced 23 psia to 523 psia, while droptank separation occurred 4,000 ft higher and 236 fps faster.

A more startling result of the simulation, however, was that the cumulative effect of the total drag resulted in a velocity gain rather than a velocity loss. The velocity gain amounted to 183 fps compared to 343 fps velocity loss associated with forebody drag only. In addition, the burnout weight to 50 x 100 nm orbit was 14,250 lb greater than the burnout weight using only forebody drag.

Because the performance gain is rather appreciable, the validity of the power-on base drag as presented should be verified for further study.

2.4.3 Payload Performance

The development of a multimission launch system involves the complex combination of nominal energy requirements, mission weights, and abort considerations. The influence on payload of these combined effects are both launch-weight and launch-concept dependent. It is therefore necessary to review these considerations and in particular to reflect those characteristics peculiar to the stage-and-one-half system.

2.4.3.1 Mission Requirements and Assumptions. Table 2.4-3 reviews the basic issues leading to launch system performance capability. The first four requirements are NASA supplied. Of these four, the airbreather in/out and the abort requirements have significantly different design effects on the stage-and-one-half and two-stage reusable systems. The airbreather system weight in the stage-and-one-half orbiter is approximately 40 percent greater than for the two-stage orbiter. Removal of the airbreather system for due east and polar missions, therefore, it is to the advantage of the stage-and-one-half concept. Engine-out from staging is a consideration not applicable to the stage-and-one-half system, since in nominal operation two of three engines available are used. Continuing in Table 2.4 -3, it is evident that 3σ engine performance serves as the basis of fixed vehicle performance as well as launch system sizing. The last item, on-orbit velocity, is NASA supplied for the 55 deg mission and is LMSC selected for the other two. The selection of 650 ft/sec is based on the considerations detailed in Table 2.4 -4.

Table 2.4 -3
BASIC MISSION REQUIREMENTS

Missions	NASA Design	NASA Ref.	NASA Ref.
Insertion Orbit (nm)	50 x 100	50 x 100	50 x 100
Mission Orbit (nm-circ)	100	100	270
Orbit Inclination (deg)	28.5	90	55
Payload (1000 lb)	65	40	25
Airbreather System	Removed	Removed	In
Abort (Engine-Out From Staging)	NA	NA	NA
Propulsion Specific Impulse	3σ	3σ	3σ
On-Orbit Velocity	650	650	1500

Table 2.4-4

FROM 50 x 100 NM INJECTION

	MINIMUM	USE
CIRCULARIZE @ 100 NM	92	100
CONTINGENCY	8	8
ACS MANEUVERING	142	142
CONTINGENCY	0	100
RETRO	262	300
TOTAL (FPS)	504	650

Table 2.4-4 Orbital Velocity Considerations

Impulsive velocity to circularize at 100 nm is 92 ft/sec; however, some time is involved and dependent on the thrust-to-weight ratio during the operation, some velocity loss will be encountered; 100 ft/sec is therefore selected. Injection weight will vary from one mission to the next; further influencing burn time. To account for this, an 8 ft/sec contingency has been selected. ACS maneuvering of 142 ft/sec was assumed as a requirement for the 55 deg-270 nm trajectory and is maintained for the polar and due east missions as well. To allow for orbital dispersion effects, an orbital contingency of 100 ft/sec is selected. Retro velocity is dependent on the entry flight path angle desired to initiate the entry mode. Typically the entry flight path angle is -1 deg from 100 nm orbits and requires a retro velocity of 262 ft/sec. Since entry flight path angles will vary with changes in mission return weight, an allowance of 300 fps is felt necessary. The minimum orbital velocity requirement is 504 ft/sec. For payload performance a value of 650 ft/sec is used to reflect operational variations that can be expected for multimission launch systems.

Orbiter tank capacities (ascent and on-orbit) are determined from the 55 deg, 270 nm mission. In this case, the orbiter ascent tanks are sized for both injection into the 50 x 100 nm orbit and flight propellant reserve. On-orbit tanks are sized for 2000 fps, although the mission requires 1500 fps. For other missions, it is the tank capacities and their assigned functions that determine payload capability. Orbiter ascent tanks are always full regardless of the mission requirement; therefore, either the droptank or on-orbit tank capacities determine maximum payload capability.

2.4.3.2 Payload Capabilities. For the considerations described, the multimission capability of the stage-and-one-half system (LS 200-10) is presented in Tables 2.4-5 and 2.4-6.

Maximum payload potential shown in Table 2.4-5 is determined for full droptank and orbiter ascent tanks. Although the orbiter FPR and ascent propellants are reported separately, it is the total of the two terms that is contained in the

in the orbiter ascent tanks. Ascent propellant therefore varies between missions, but the sum of ascent and FPR propellants is the fixed quantity as determined by the orbiter tank impulse capacity. On-orbit propellants as determined by the vehicle weights and on-orbit velocity requirements vary from 16,000 to 39,000 lb between missions and are always less than the 50,300 lb impulse propellant capacity required for 2000 ft/sec on-orbit velocity. Launch thrust-to-weight variations are minimal between missions and, while accounted for in velocity losses, the significant parameter influencing the ascent velocity is launch azimuth. As shown in Table 2.4.3-4, design payloads are achieved by offloading droptank propellant for the due east and polar missions. Launch thrust-to-weight ratio is seen to vary from 1.25 to 1.38 and the ascent velocities are adjusted to reflect these variations.

2.4.3.3 Conclusions. The 55 deg, 270 nm mission is the critical design mission for the stage-and-one-half launch concept, due to the large airbreather system weight, the 1500 fps on orbit requirement, and the engine out abort capability inherent in the system design. In designing for the critical mission, the stage-and-one-half promises greater payload growth potential to the due east and polar mission than any other launch concept under present consideration.

Table 2.4-5

STAGE-AND-ONE-HALF

MAXIMUM PAYLOAD POTENTIAL - FIXED LAUNCH VEHICLE

Mission	Due East	Polar	55 deg
Orbit Altitude (Circ nm)	100	100	270
GLOW (10^6 lb)	3.832	3.789	3.816
Droptank Propellant (10^6 lb)	3.063	3.063	3.063
Spacecraft Ignition Weight (1000 lb)	640.9	598.3	625.1
Spacecraft Ascent Propellant (1000 lb)	239.0	239.6	239.2
Spacecraft FPR Propellant (1000 lb)	8.3	7.7	8.1
Spacecraft On-Orbit Propellant (1000 lb)	18.6	16.6	38.78
Launch Thrust-to-Weight Ratio	1.245	1.26	1.25
Ideal Velocity			
– Ascent (fps)	29,580	30,870	30,035
– Staging (fps)	22,930	23,580	23,164
Payload	95.1	54.6	25

Table 2.4-6

STAGE-AND-ONE-HALF

DESIGN PAYLOAD - FIXED LAUNCH VEHICLE-OFFLOADED DROPTANKS

Mission	Due East	Polar	55 deg
Orbit Altitude (Circ - nm)	100	100	270
GLOW (10^6 lb)	3.451	3.587	3.816
Droptank Propellant (10^6 lb)	2.714	2.877	3.063
Spacecraft Ignition Wt (1000 lb)	609.2	582.9	625.1
Spacecraft Ascent Propellant (1000 lb)	239.7	239.9	239.2
Spacecraft FPR Propellant (1000 lb)	7.6	7.4	8.1
Spacecraft On-Orbit Propellant (1000 lb)	17.1	15.9	38.78
Launch Thrust-to-Weight Ratio	1.38	1.33	1.25
Ideal Velocity			
- Ascent	29,150	30,660	30,035
- Staging	22,030	23,107	23,164
Payload	65	40	25

2.4.4 Airbreather Performance

Any number of operational considerations can dictate the returning orbiter's attitude time-history and resulting environment. The study can be simplified by considering that the terminal envelope will be bounded on one side by maximum allowable dynamic pressure limitations and on the other side by maximum L/D flight. For present study purposes, maximum L/D flight has been analyzed, since it involves the longest airbreathing operating time of the possible terminal profiles that could be studied. In the development of nominal airbreather fuel requirements, a sea level airport and standard day conditions were assumed.

Considerations attendant to the development of the airbreather profile are shown in Fig. 2.4-18. Engine startup is attempted at an altitude of approximately 45,000 ft. At 35,000 ft, all airbreathers are assumed operating. To allow for fuel used in the airbreather startup process, a 5-sec full thrust operation is assumed to have taken place. Altitude reduction is accomplished through a spiral flight mode until 20,000 ft is attained where unbanked flight to the airport outer marker is achieved. During this operation, the airbreathers are set for flight idle mode operation.

It must be considered that there are presently no study requirements which define the outer marker reference altitude. It is therefore necessary to select a typical airport to develop the altitude at which the 3-deg glide slope is initiated. Such information is provided in "Basic Flight Manual and ATC Procedures," Part I AIM FAB, 1968; the outer marker is located 4 to 7 mi from the airport. The 7-mi distance and 3-deg glide slope place the landing vehicle at approximately a 2000 ft height, the altitude selected for study.

From 2000 to 200 ft, the returning orbiter's glide slope is maintained at 3 deg and is accomplished through airbreather thrust setting. Below 500 ft in the approach, thrust setting is increased to accommodate the additional gear drag.

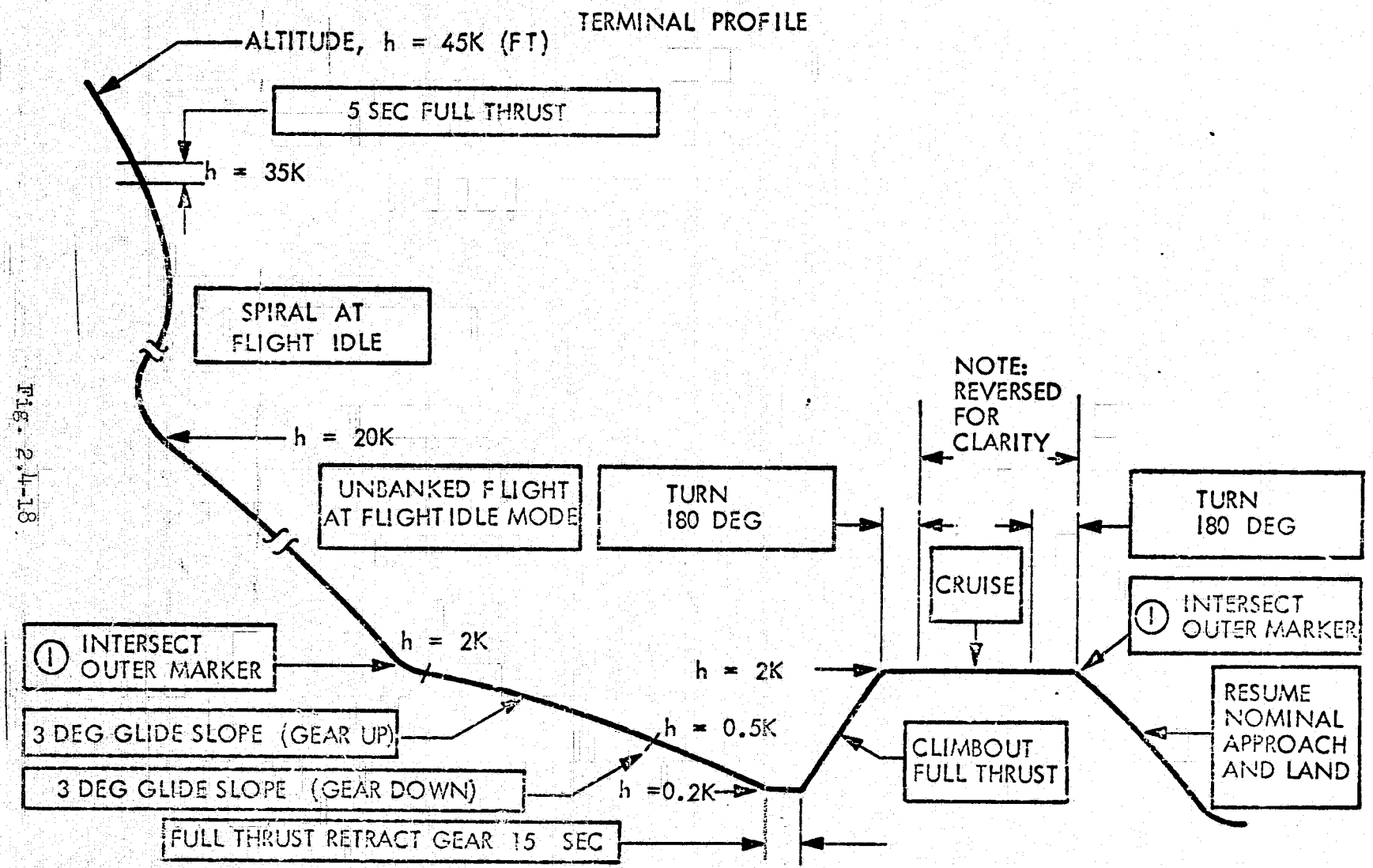

Fig. 2.4-18 Airbreather Performance

At 200 ft, the go-around procedure is initiated. The procedure is one of increasing the airbreather thrust setting to maximum and retracting the gear for climbout. The fuel requirement for this transient mode is developed by assuming a 15-sec full thrust operation in which no climbout altitude is accredited.

Climbout fuel requirements are complicated by the lack of go-around altitude criteria. A 2000-ft altitude is selected, placing the returning vehicle at the initial outer marker when the go-around maneuver is terminated. Nominal approach and landing are then resumed.

The selection of the 2000-ft altitude for go-around is the most significant profile parameter to airbreather fuel requirements, dictating both the climbout and the cruiseback fuel allotments. Had the middle marker altitude been selected as the target point for go-around termination, go-around could have been accomplished at an altitude as low as 275 ft. It is felt, however, that at the present time some conservatism is necessary to allow for fuel requirements consistent with higher airport altitudes and hot day conditions.

The additional factors in fuel determination are the return vehicle weights, aerodynamics, and airbreather characteristics. The 55-deg, 270-nm return weight of 333,000 lb is selected, since it is the only reference mission for which airbreather requirements are stated. With its 25,000-lb payload the vehicle c.g. is located at 75 percent of the reference length, resulting in a trimmed lift-to-drag ratio and lift coefficient of 5.55 and 0.54, respectively. Airbreather characteristics are representative of two types of engines: the P&W JTF-22A-4 and the GE F12B3. In both cases, the engine specification data are reduced 3 percent to account for duct losses. Engine specific fuel consumption is further increased by 2 percent to account for performance degradation between overhaul periods. Finally, a 15-percent fuel reserve is allowed in the determination of total fuel and tank volume requirements.

Study results as presented in Fig. 2.4 -19 are developed for a range of design startup weights of ±30,000 lb around nominal, and in addition considers the influence of n number of airbreathers. As can be developed from reviewing the data, the implication of variation in design startup weight and number of engines is an insensitive parameter to airbreather fuel requirements with the exception of the four engine configurations. Variations in airbreather fuel of approximately ±1,000 lb result for relatively large excursions in design weights when engine clusters of five or more are considered.

For any given weight, the fuel requirement dependency on the number of engines is primarily due to the influence of excess thrust during climbout. The effect is twofold in that reduction in excess thrust (number of engines) is seen in terms of increased climb time from 200 to 2,000 ft and, in addition, increased climb range. The orbiter therefore requires more fuel for climb as well as increased fuel to cruiseback to the initial outer marker point.

It should be considered also that the term "design" airbreather weight reflects the recommended approach to airbreather fuel requirements. Only when a change in either the orbiter inert weight (payload fixed) or the airbreather design mission requirement occurs should the data in Fig. 2.4-19 be used. In the normal operation of the space shuttle, the orbiter return payloads, and, therefore return weights, as well as the operating conditions (altitudes and ambient temperatures), can be expected to vary. In these latter circumstances, the proposed method would simply be to maintain the selected airbreather fuel and vary the climb and cruiseback altitude commensurate with the onboard fuel.

A significant study result is the indication that over the range of conditions explored, go-around can be achieved. As excess thrust goes to zero during climbout, the fuel requirement increases to infinity. The four airbreather configuration indicates that such a situation is beginning to occur. Such is not the case for the five and six engine arrangements, nor from the somewhat gentle variations in fuel requirements in Fig. 2.4-19 is there any indication that zero excess thrust is being approached. Therefore, it is felt that the

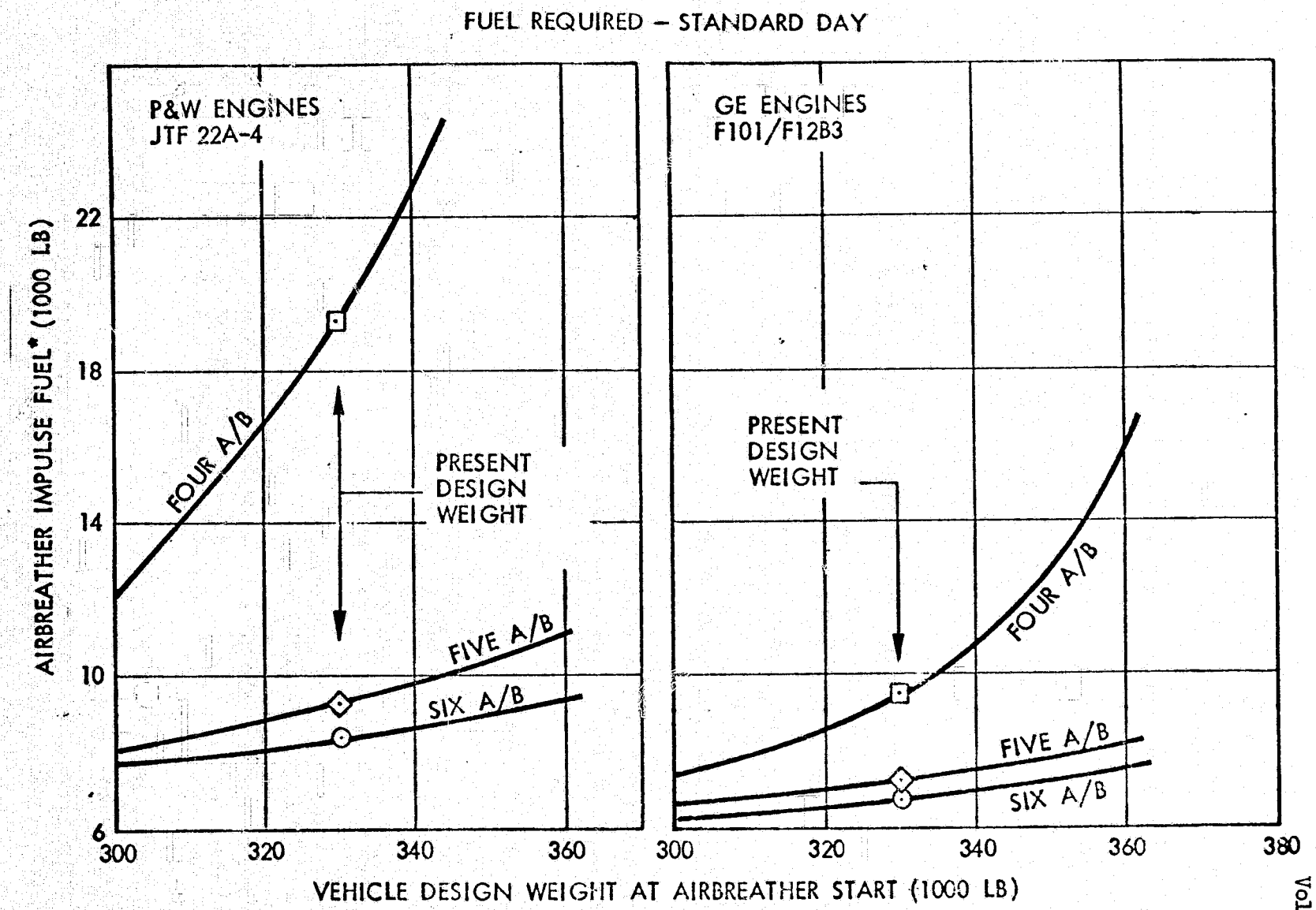

Fig. 2.4-19 Stage-and-One-Half Airbreather Performance

determining logic for airbreather fuel requirement is rational and sufficient for satisfactory orbiter operations, when five or more airbreathers are used.

Of particular concern to any reusable system is the airbreather system weight. Such data are reviewed in Fig. 2.4 -20 in which estimated engine weight (installed) is summed with the total JP fuel required for the terminal airbreather profile. For the P&W system, the four-engine system can be discarded from further consideration due to the excessive fuel requirement. This is not the case for the four-engine GE system, where due to the higher thrust per engine, the fuel required remains a reasonable quantity. In terms of comparison between the P&W and GE engines, with the exception of the four-engine configurations, the weights are within 1,000 lb of each other. Due consideration, however, must be given to the larger size of the GE system and its integration into the stage-and-one-half orbiter, an unmeasurable performance quantity.

The last performance considerations given to the selection of the airbreather system are the airport requirements directed primarily toward climb capability. Such is the case for the FAA transport-category airplanes which serve in this study not so much as design requirements for reusable systems but as reference points for performance comparison. In FAR Part 25, specific climb gradients must be achievable and demonstrated over the range of weights, altitudes, and ambient temperatures within the operational limits established for the airplane. With this in mind, a study has been accomplished which explores the considerations related to climb gradient capability. For a demonstration weight commensurate with the selected 55-deg mission (333,000 lb), demonstration altitude capability is shown for the FAA requirements specified in landing configuration (gear down, all engines operating) and approach (gear up, one engine out) in Figs. 2.4 -21 and 2.4 -22, respectively. Superimposed on the figures are the altitudes and maximum excursions in temperature corresponding to Anderson, Bergstrom, Hickham, and KSC locations. Since maximum excursions are used, five-engine arrangements appear adequate for nominal operations when the orbiter is in the landing configuration (all engines operating). The engine-out approach requirement (Fig. 2.4 -22) indicates too marginal a capability for the five-engine (one out) cluster. As an additional factor for consideration,

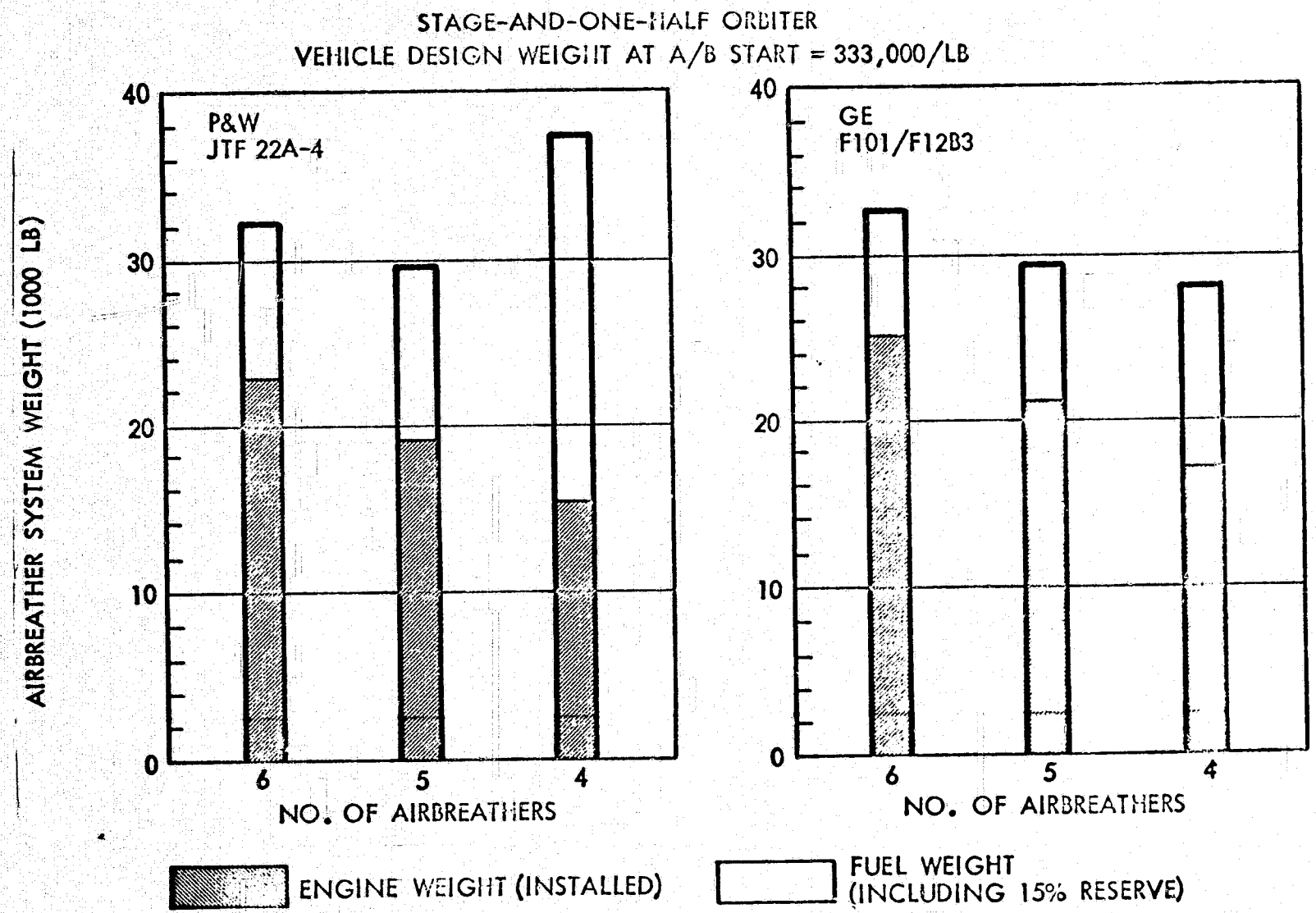

Fig. 2.4-20 Stage-and-One-Half Orbiter
Vehicle Design Weight at A/B Start = 333,000/lb

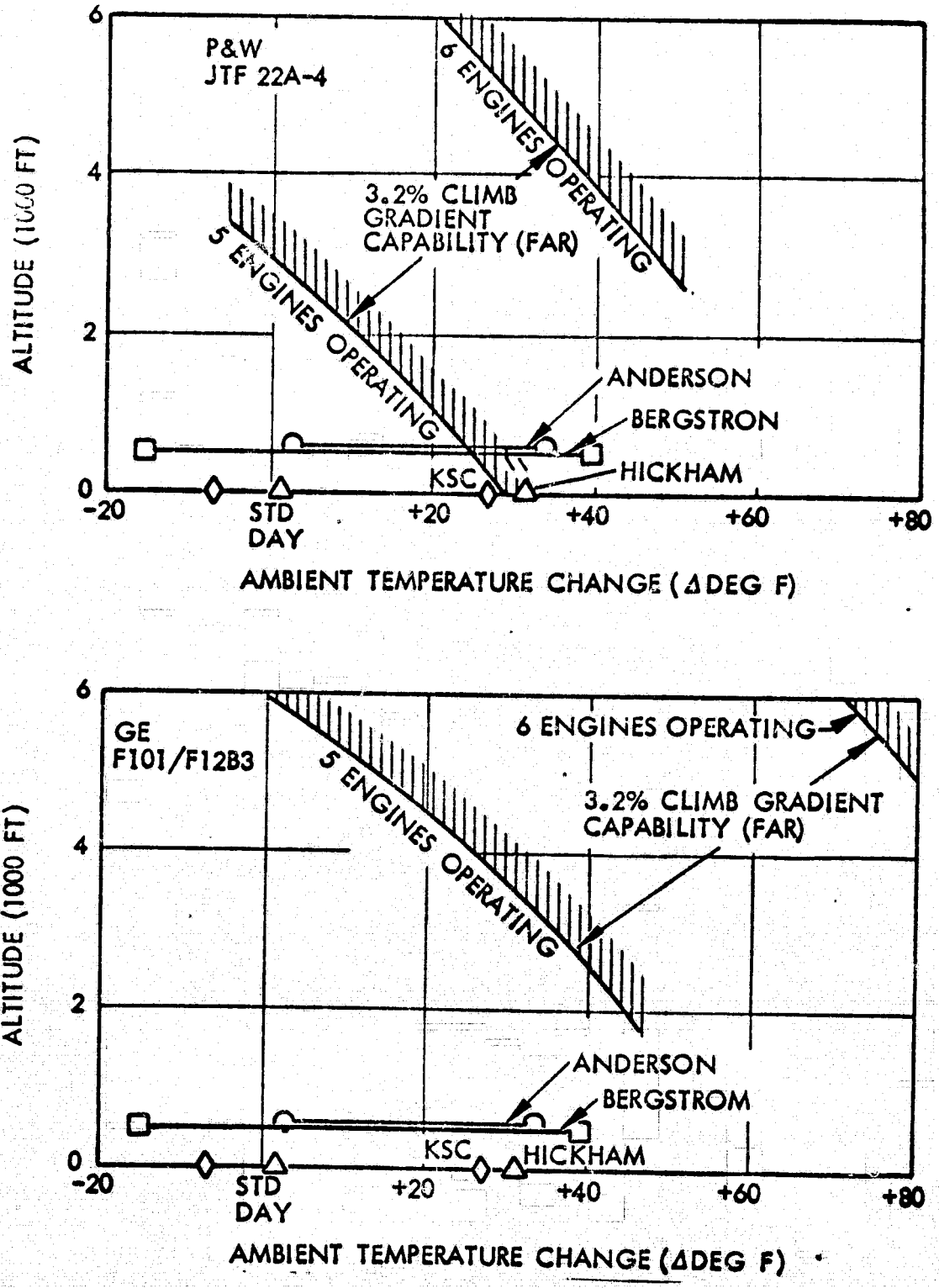

Fig. 2.4-21 Stage-and-One-Half Climb Summary - Landing Configuration

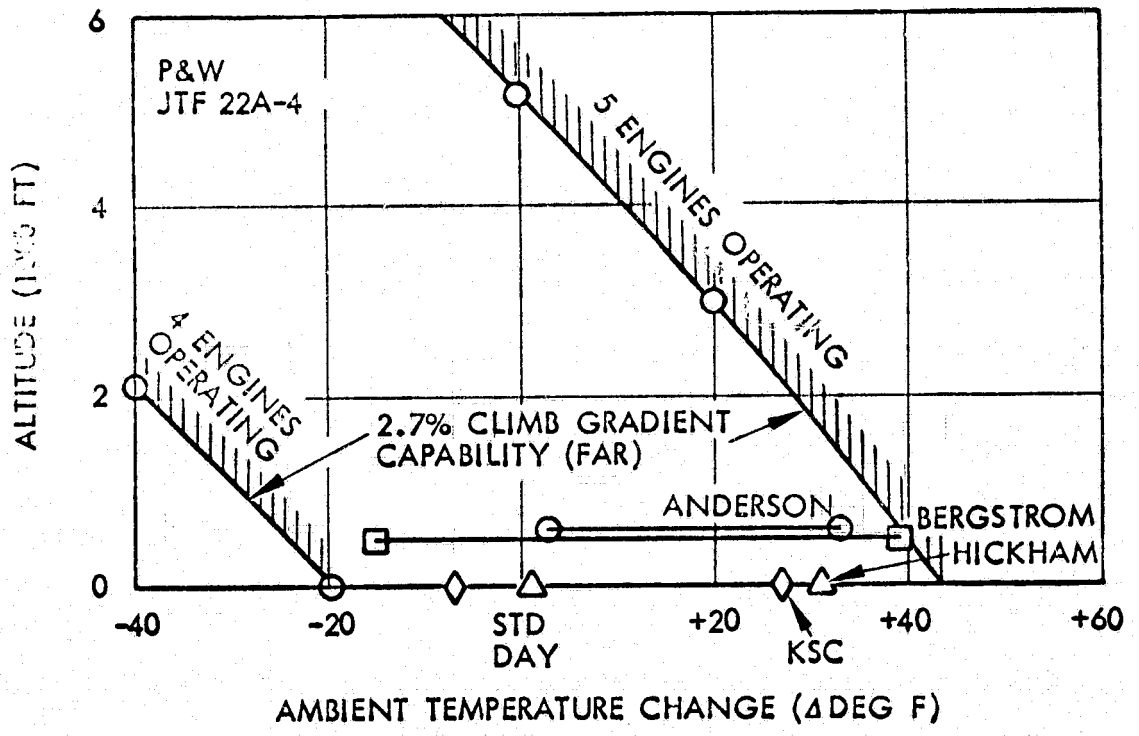

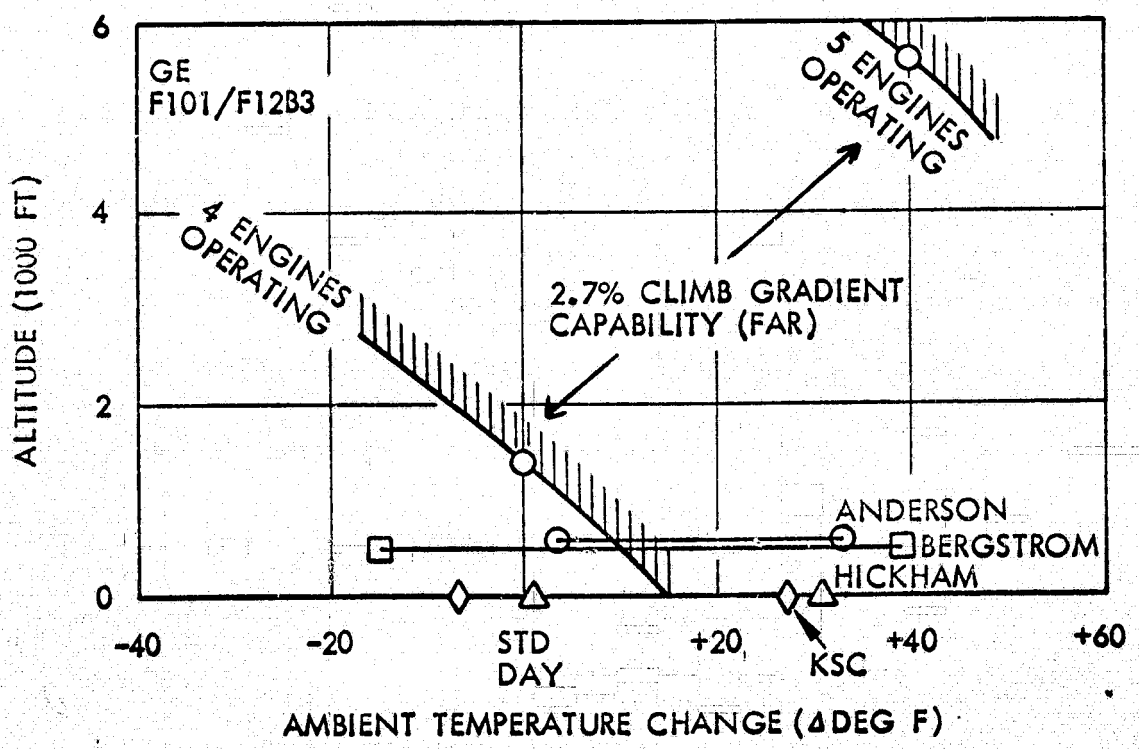

Fig. 2.4-22 Stage-and-One-Half Climb Summary - Approach Configuration

level-flight capability for engine-out operations is shown in Fig. 2.4-23. Included, in addition to the airport condition, is the NASA 10,000-ft engine-out condition. Whether this particular reference point is intended as a requirement for nominal mission operations or for ferry only, it is clear that for the stage-and-on-half orbiter a six-engine arrangement is required.

From the considerations reviewed, it appears that both the P&W and the GE engines can be accommodated in the stage-and-one-half orbiter. At present, six airbreathers of either system meet go-around FAA, gradient requirements, and engine-out level-flight requirements. Since the weight penalty for a six-engine configuration is only 1800 lb more than for a five-engine cluster, it is felt that adherence to the FAA climb gradient requirements is an acceptable feature to incorporate into the stage-and-one-half design. The P&W system has to its advantage 800 lbs less weight and a smaller envelope volume. The GE system shows superior performance both in thrust and specific fuel consumption and could be acceptable in a five engine cluster depending on the importance NASA places on engine-out performance of an orbit returning vehicle.

The representative airbreather terminal profile using six P&W JTF22A-4 engines is reviewed in Fig. 2.4-24. Total airbreather time from 40,000 ft through go-around and touchdown is 1052 sec. It should be noted that this airbreather time is added to the orbiter time from 400,000 ft to 40,000 ft for the purposes of determining thermal protection system (TPS) weight.

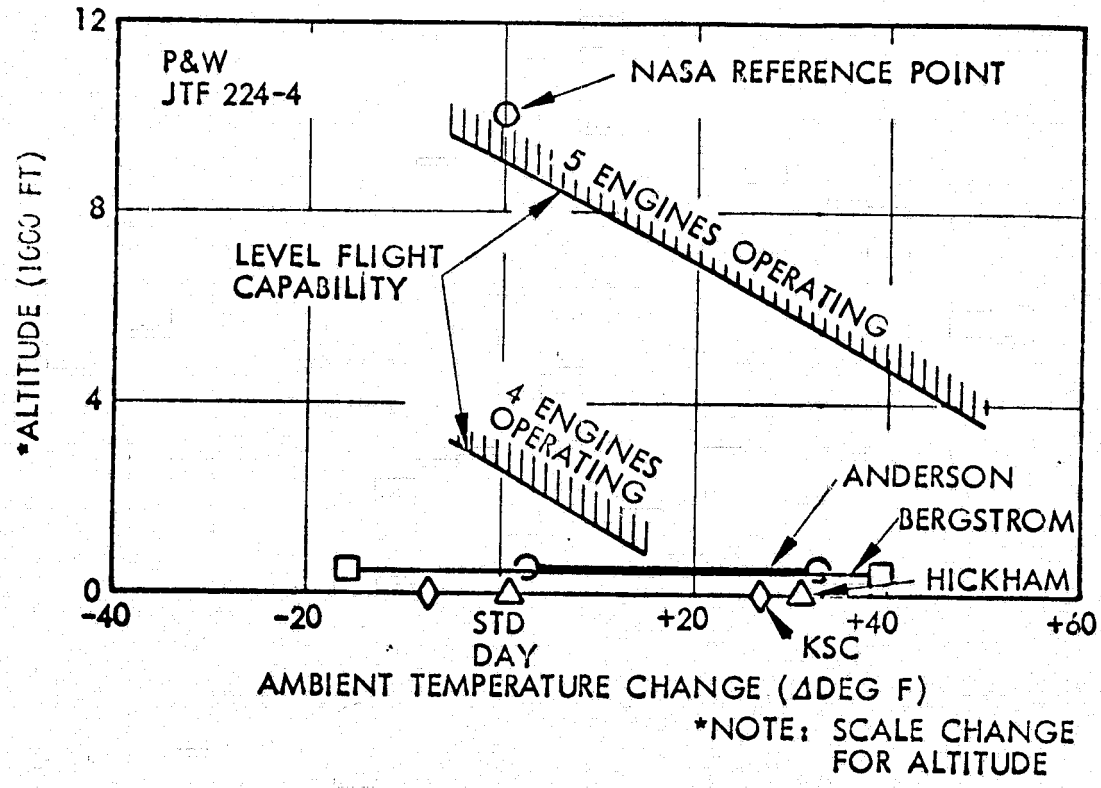

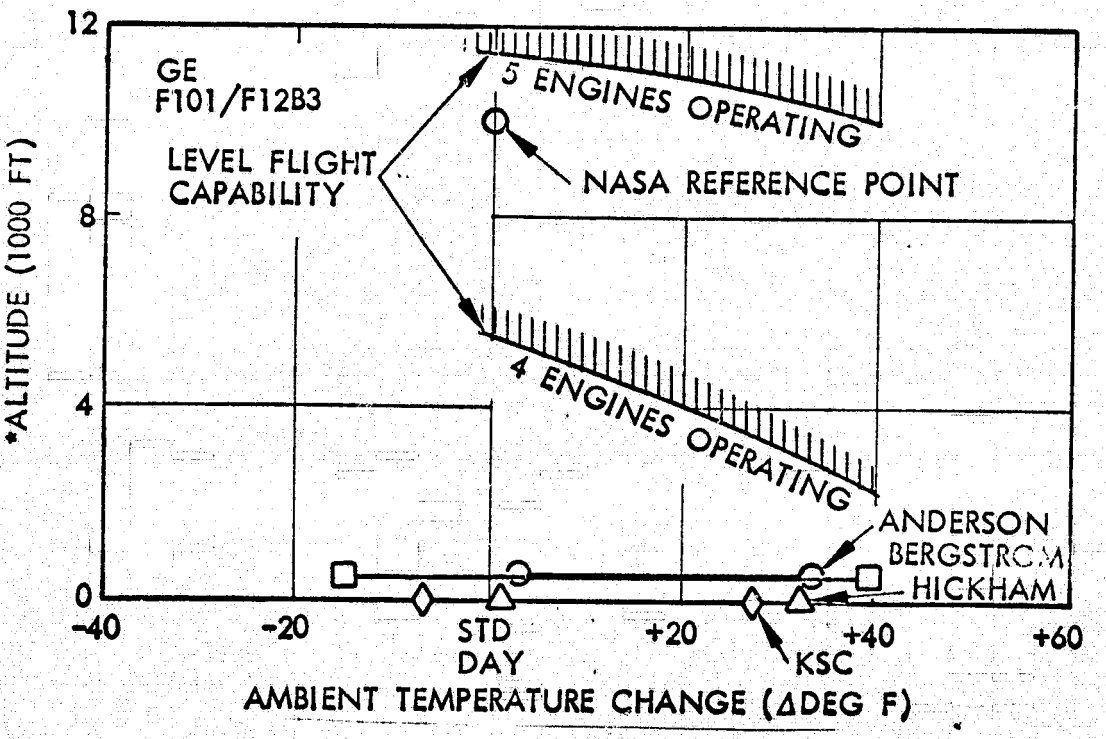

Fig. 2.4-23 Stage-and-One-Half Level Flight Ceiling - Cruise Configuration

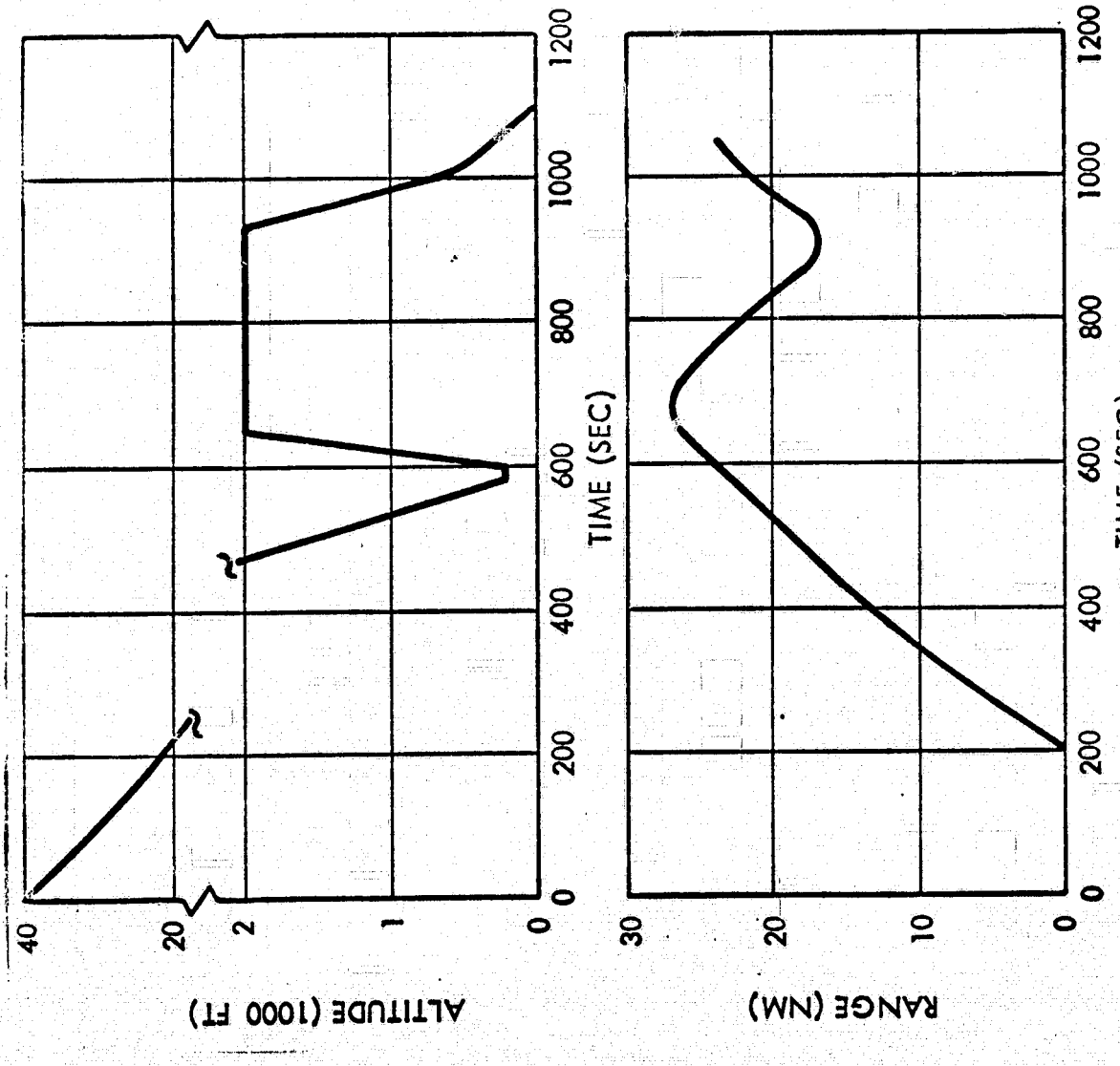

Fig. 2.4-24 (a) Stage-and-One-Half Orbiter - Terminal Airbreather Profile

Fig. 2.4-24 (a)

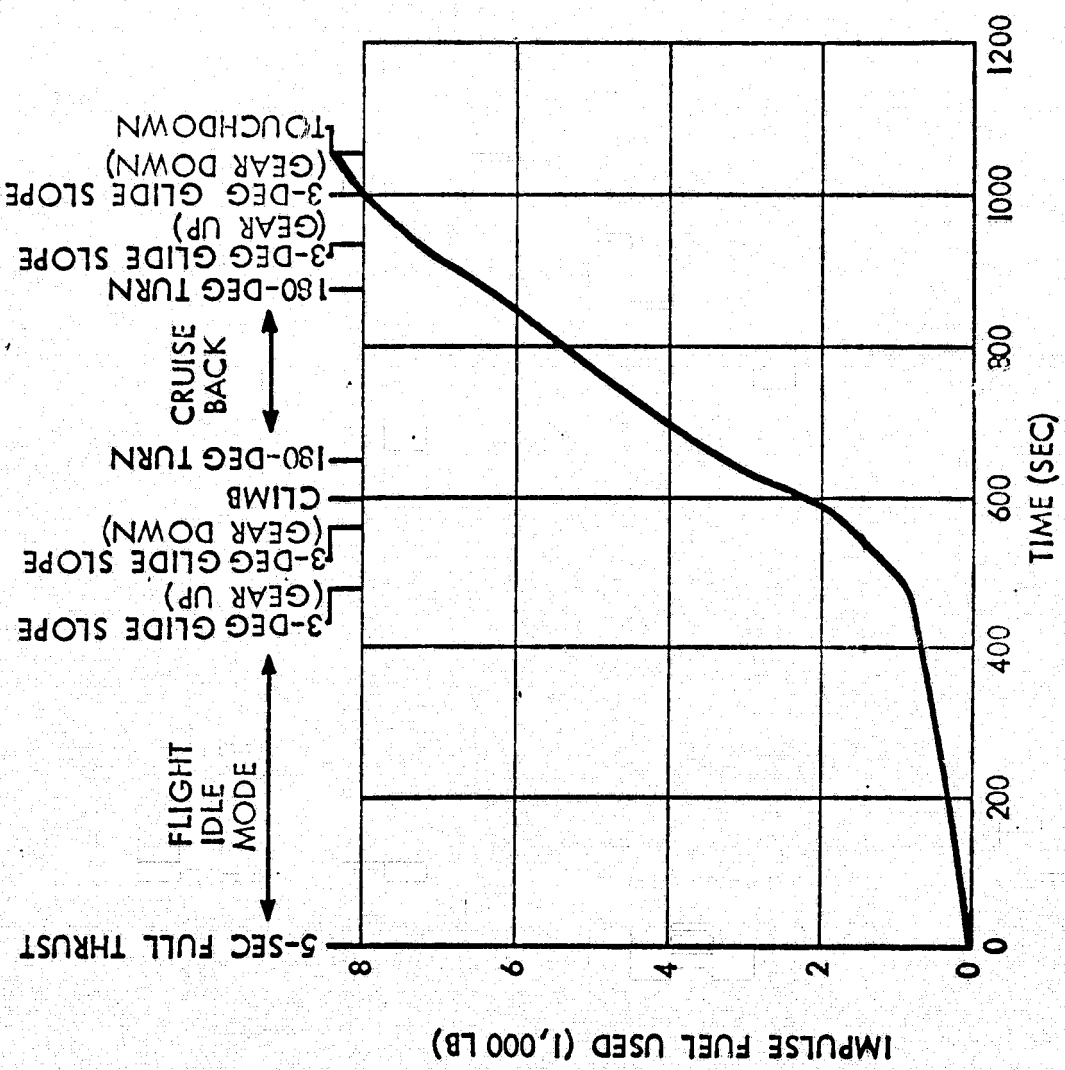

Fig. 2.4-24 (b) Stage-and-One-Half Orbiter - Terminal Airbreather Profile (Cont'd)

Fig. 2.4-24 (b)

2.4.5 Reentry Trajectory

A nominal reentry trajectory was determined for use in establishing the thermal protection system (TPS) for the stage-and-one-half vehicle. Variations from this nominal were then used to develop a representative footprint. The principal criterion in the trajectory design was to obtain a crossrange capability of approximately 1100 nm, while satisfying surface temperature constraints and achieving conditions for minimal TPS weight. The primary trajectory variable affecting TPS weight is reentry time, so the design objective, in a broad sense, is to obtain a minimum-time trajectory that does not exceed temperature limits and results in a reasonable environment of dynamic pressure and deceleration. Additional conditions and assumptions in the trajectory selection were as follows:

- Return from 270 nm orbit inclined at 55 deg
- Deboost from orbit by in-plane, horizontal retro thrust
- Control downrange by location of deboost point
- Have terminal point near 28 deg latitude

The initial entry flight path angle γ, which is a function of the retro ΔV, is directed by the values of angle-of-attack, α, and bank angle, χ selected and maintained during pullup. A larger deboost ΔV gives rise to a steeper (larger negative) γ and a smaller entry velocity. A steep entry angle can result in penetration of a given temperature boundary while too shallow an entry can result in a longer reentry time and greater total heating. Following pullup, trajectory control is maintained by the α, χ history selected. It is assumed that these can be controlled to desired values with sideslip angle maintained zero. The following subsections describe in greater detail the factors affecting selection of the reentry control parameters γ, α, and χ and present the characteristics of the reentry trajectory and the associated footprint that were obtained.

2.4.5.1 Control Parameter History. Reentry trajectory variables which are of greatest significance to minimization of TPS weight (i.e., minimum insulation thickness) are total surface heat and reentry time. Experience gained on lifting reentry analyses has indicated that for minimal TPS weight, the entry vehicle must be flown on or near the temperature constraint boundary over a major portion of the time. The temperature constraint boundary is specified in terms of altitude, velocity, and angle-of-attack. It represents the minimum altitude envelope of maximum temperature on the lower surface (2300°F), fin leading edge (2300°F), and nose cap (2800°F). The temperature boundary, therefore, is used to prescribe pullup conditions to be satisfied by the initial values of entry flight path angle, angle-of-attack, and bank angle.

To obtain maximum vertical lift until pullup at the temperature boundary, the bank angle initially is held at zero, wings level. The pullup point is defined here by a flight path angle of about -0.07 deg and values of altitude and velocity which lie on the temperature boundary curve corresponding to the angle-of-attack selected. Since previous analyses have also shown that it is effective to maintain α constant from entry to pullup and during the period on the temperature boundary, it follows that specification of an initial α and the pullup conditions then determine, uniquely, an entry value for γ. Thus, the critical factor in the trajectory design becomes the selection of the initial α .

A high angle-of-attack results in high drag; hence, shorter entry times, lower total heating and consequently lower TPS weights. However, a high angle-of-attack is adverse to achievement of high crossrange (downrange control is maintained by choice of retro point, which does not affect total heat or reentry time). Crossrange is maximized by requiring lower angles-of-attack, approaching the maximum L/D condition, and longer reentry times. Thus, the α chosen is a compromise between a high value (near maximum lift) for shorter flight time and a lower value (near maximum L/D) for greater crossrange. For the stage-and-one-half vehicle, an α of 35 deg and a corresponding entry of -1.7 deg were determined as best satisfying the needed compromise for crossrange and time.

Flight along the temperature boundary is maintained by modulating bank angle, starting from a value of approximately 90 deg. At some point, the crossrange effectiveness of this guidance mode deteriorates, and it becomes more effective to reduce to near the maximum L/D condition and fly above the temperature boundary. Thus, at a cutoff point corresponding to a velocity of 16,000 ft/sec, α is gradually lowered while following a constant flight path angle mode, with again a modulated χ. This mode provides a smooth flight path while also reducing χ, and it is followed until χ reaches a value of the order of 30 deg and α is reduced to about 25 deg. The next mode entered is one of constant α while reducing χ further to 20 deg. This mode is terminated when a heading change (relative azimuth) of about 118 deg is obtained. At this point, the major turning of the trajectory has been achieved and the remaining guidance modes are toward additional reductions in χ and α. Thus, a constant flight path angle mode is followed next, with α reduced to 10 deg and terminating when χ is also 10 deg. The final mode is with α and χ constant at 10 deg. This mode continues until an altitude of 20,000 ft is reached, at which point the trajectory computation is terminated.

The low α during the final portion of the trajectory is introduced mainly to insure avoidance of aerodynamic stability problems. Thus, the reentry trajectory may be characterized as consisting of essentially three α modes: (1) a relatively high α to avoid long flight times (α = 35 deg), (2) a value near maximum L/D (α = 25 deg) for maximizing crossrange, and (3) a low value for stability considerations (α = 10 deg). It is noted that the last mode is mainly a conservative maneuver and it is entirely possible to fly α = 15 deg to the terminal point without crossrange degradation.

2.4.5.2 Nominal Reentry Trajectory Characteristics. Trajectory data are presented in Figs. 2.4 -25 to 2.4 -30. Fig. 2.4 -25 shows the altitude-velocity history and also the histories of α and χ. Superimposed on the plot are the temperature boundary curve and also, for comparison, curves depicting a 300 psf dynamic pressure reference and a 3 g load factor referenced at α = 25 deg. The remaining figures are time histories of the various trajectory variables. Fig. 2.4 -26 presents altitude, velocity, dynamic pressure, crossrange, and downrange. In Fig. 2.4 -27 are shown angle parameters: flight path angle, bank angle, angle-of-attack, and heading change (change in azimuth relative to initial value). Axial, normal, and total load factors (deceleration levels in g's) is shown in Fig. 2.4 -28. Lift coefficient, L/D, and energy ratio (square of ratio of velocity to initial velocity) are given in Fig. 2.4 -29. Fig. 2.4 -30 presents various heating parameters: liminar stagnation point heat rate, $\dot{Q}_{LAM}$, and its integral, Q_{LAM}, on a 1 ft radius sphere, and heat rate $\dot{Q}_{SC}$ and its integral Q_{SC} on a 1 ft radius cylinder, assuming a sweep angle of 78 deg and a local angle of attack α.

It is seen that the trajectory developed a crossrange of 1,233 nm, with a flight time from entry of 1,847 sec. The time from retro to entry is 1,900 sec, making the total entry time 3,747 sec. While the resultant crossrange is 133 nm greater than required, it is felt that the slight reduction in time that can be accomplished in deriving the 1,100 nm trajectory will have little significance to the TPS weight. The entry environment can be described as mild, since during the total profile 310 lb/ft^2 of dynamic pressure and total load factors of 1.3 are not exceeded.

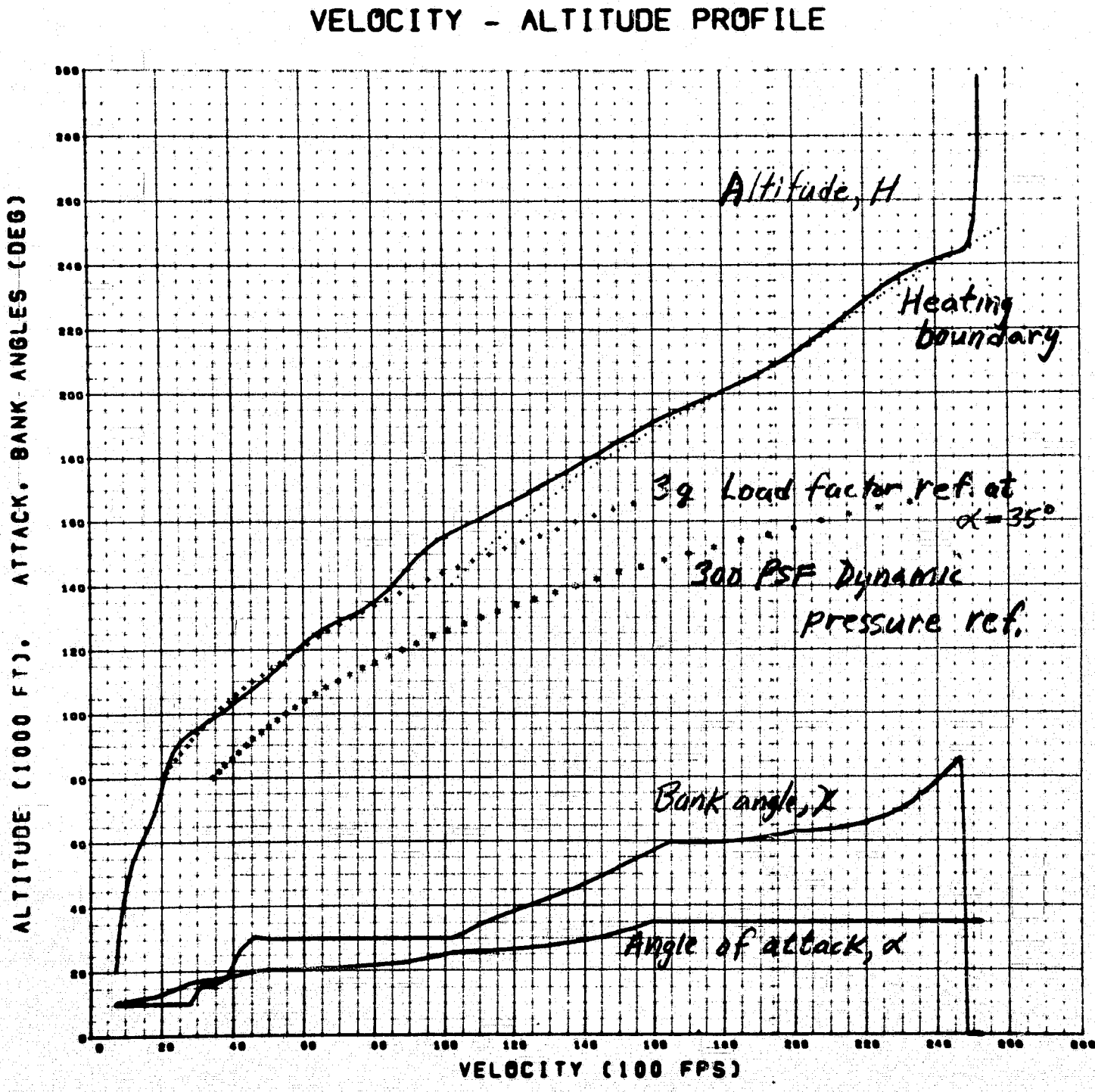

Fig. 2.4-25 Stage-and-One-Half Orbiter H-V Profile

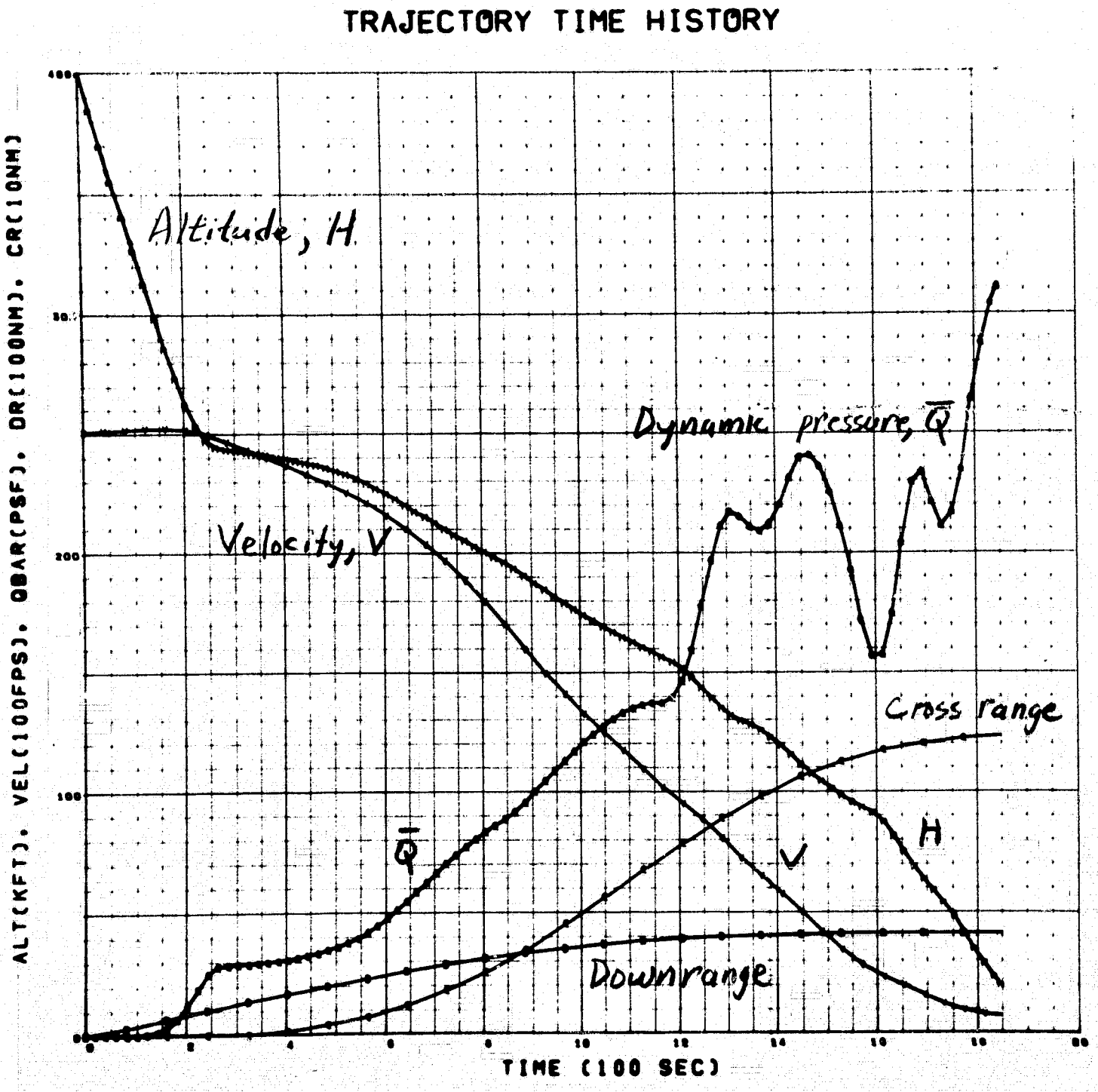

Fig. 2.4-26 Stage-and-One-Half Orbiter H, V, $\bar{Q}$ History

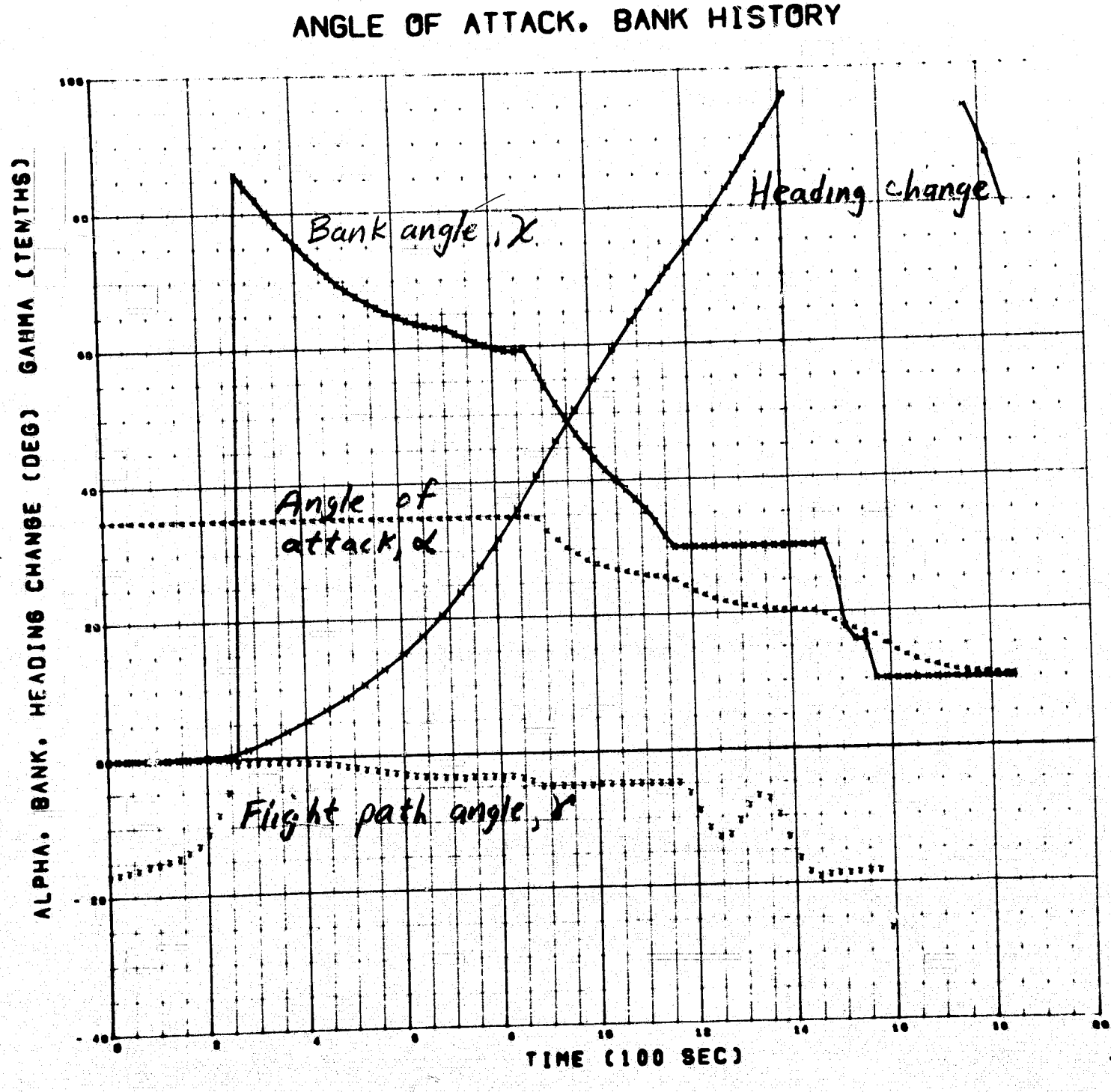

Fig. 2.4-27 Stage-and-One-Half Orbiter α, χ, γ History

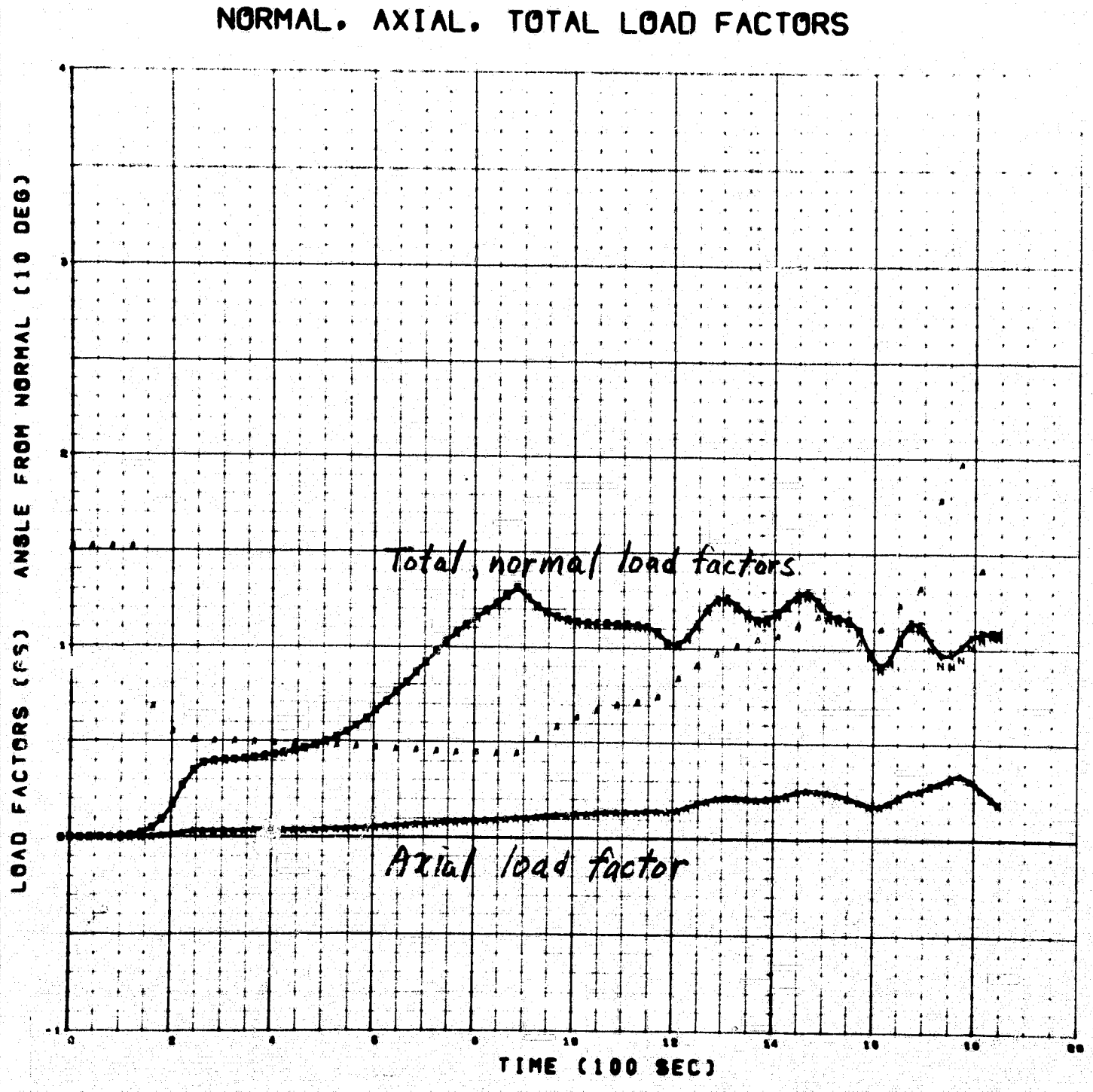

Fig. 2.4-28 Stage-and-One-Half Orbiter Load Factors

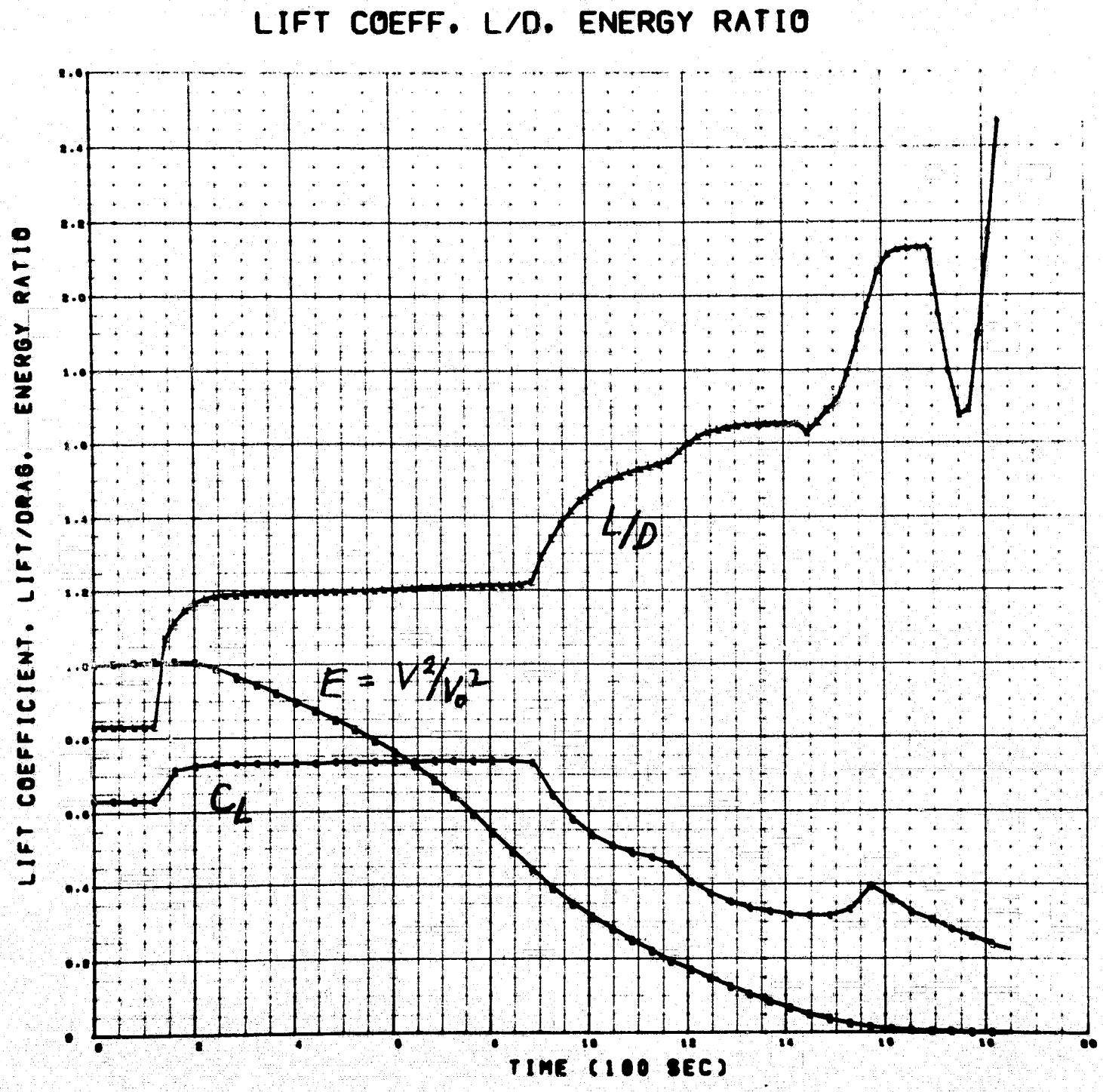

Fig. 2.4-29 Stage-and-One-Half Orbiter Lift Coefficient

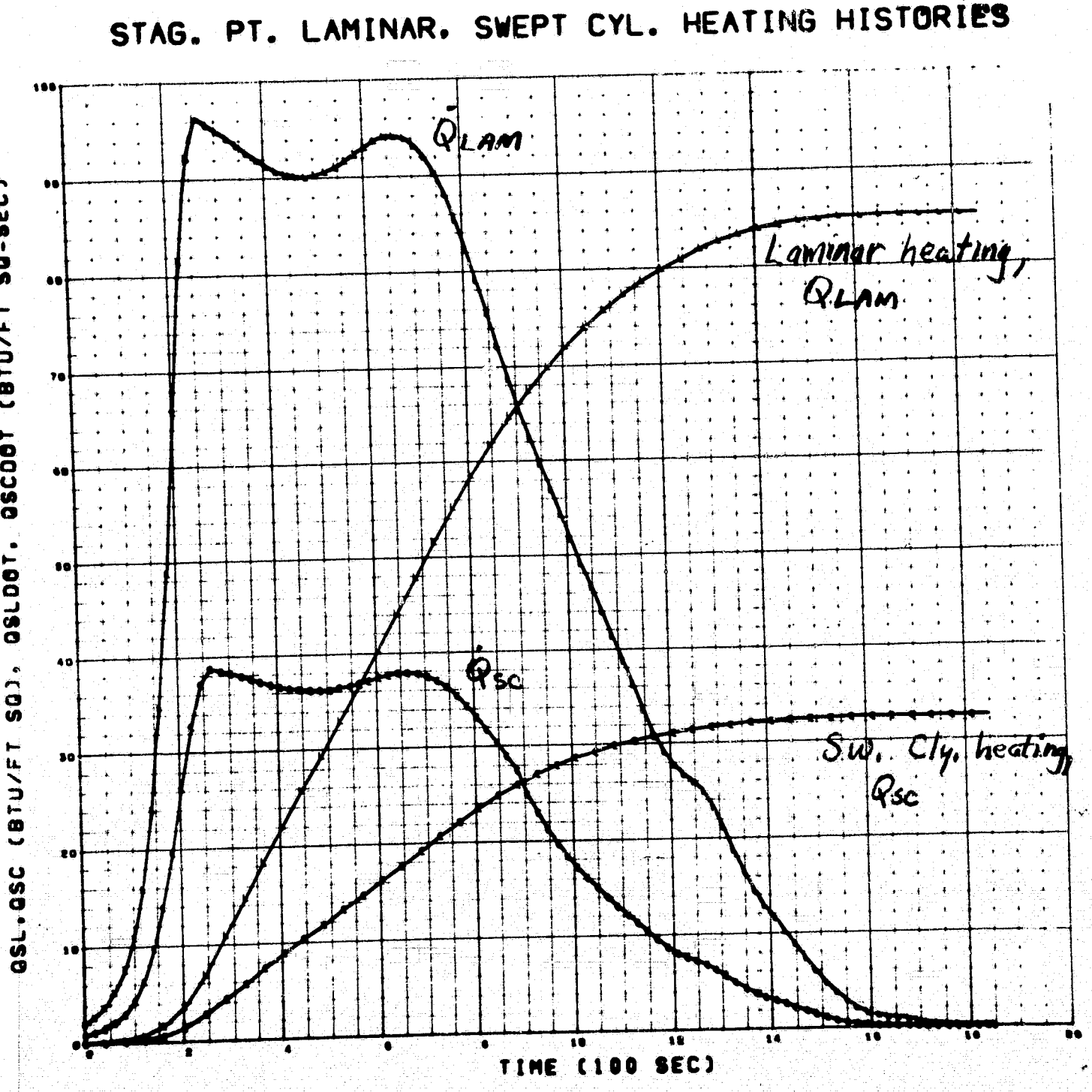

Fig. 2.4-30 Stage-and-One-Half Orbiter Heating History

2.4.5.3 Reentry Footprints. Reentry footprints were computed for the stage-and-one-half vehicle for the nominal case of return from a 270 nm orbit at 55 deg inclination, and for returns from 100 nm polar and 28.5 deg inclined orbits. All three cases utilized an identical series of control histories to obtain the discrete landing points which defined the footprint boundary. These control histories were systematic modifications of the nominal one described in the previous section. Two groups or types of control histories were developed, one associated with landing uprange from the reference landing point of the trajectory having the nominal control history, and one associated with landing downrange of the reference point. Each of these groups had subcases corresponding to banking left or banking right, after pullup, corresponding to landing approximately northwest or southeast, respectively, of the orbit track.

For each footprint, the geographic coordinates of the entry point were the same for all members of the family of trajectories defining the footprint. The entry point longitude was such that a landing at the longitude of KSC was achieved with the nominal control history. Likewise, the entry point latitude, for the polar and 55 deg orbits, obtained landing latitudes near 28 deg for the nominal cases. The entry point locations are shown below:

Orbit		Entry Location	
Altitude (nm)	Inclination (deg)	Latitude (deg)	Location (deg)
270	55	- 4.9	- 137.
100	90	-42.5	- 98.
100	28.5	0	- 140.2

The control histories for the three types of entry trajectories (nominal, uprange family, and downrange family) are summarized in Table 2.4-7. Each history is divided into a series of control phases, and for each phase the required values of angle-of-attack, α, and bank angle, χ, are shown. The χ values are specified either directly, or indirectly, as the value required to achieve a given condition; e.g., flight along the temperature boundary or maintaining a constant flight path angle. The third parameter shown is the

end condition which terminates the particular phase. In the case of the uprange family of trajectories, the only parameter varied between trajectories was the value of entry α: increasing α decreased range. For the downrange family, the only parameter varied was the bank angle value χ, which was used for terminating the second control phase, and as the value for the constant bank angle held during the third and fourth phases: decreasing χ increased range.

The initial phases of the nominal and uprange types were similar in that both required pullup at the temperature boundary at a γ of about -0.07°, followed by flight along the temperature boundary until the velocity was reduced to 16,000 fps. The third phases for these types were also similar, with α modulated to 25 deg and χ controlling a constant γ. The downrange type also required initial pullup at the temperature boundary, but with $\gamma = 0$. The next downrange phase then consisted of level flight, above the temperature boundary, until χ was reduced to a specified value (the parameter for this family). Both the uprange and downrange families had final α's of 25 deg, whereas the nominal had α reduced to 10 deg at the end.

For all three types, the initial control phase had α maintained at a constant value, α_e, from entry until pullup, with bank angle held zero. In the case of the uprange trajectories, varying α_e to decrease range required corresponding changes in the entry flight path angle, γ, in order that the pullup conditions would be satisfied. This is illustrated in Fig. 2.4-31 which shows curves of altitude versus velocity for various α's which satisfy the temperature boundary. Superimposed on these curves is a carpet plot of altitude versus velocity at pullup for various α_e and γ_e for the 270 nm, 55 deg inclination orbit. It is seen that increasing α_e requires generally greater negative γ_e, with pullup occurring at lower altitudes and velocities.

Latitude-longitude plots of the reentry footprints, based on the above control histories, are shown in Fig. 2.4-32 to 2.4-33, for the three orbit cases. The footprints are defined by a boundary curve encircling the computed landing

points. Note that the landing point as here defined corresponds to the terminal point in the trajectory computation, which is 20,000 ft altitude. Superimposed on the footprints are their respective orbit traces; these are referenced to the retro time of the nominal control history trajectory. The footprint boundary curves, as shown, can be considered as approximations to the limit curves defining the maximum downrange-crossrange control of the stage-and-one-half vehicle. Further variations in the control histories probably could produce small increases in the footprint size or shorter entry times.

The landing points for the uprange and downrange type trajectories are indicated on the figure by their respective values of α_e and χ_i. Also shown are interpolated contours of constant flight time from entry to landing. These illustrate the correlation of entry time with range; however, these contours are probably conservative with respect to that obtainable with a fully optimized descent. For example, the nominal control history cases developed generally shorter entry times for the downrange than the contours indicate: the entry times for the 100 nm orbit returns were 1750 and 2020 sec, respectively, for the polar and 28.5 deg inclinations, and 1847 sec for the 270 nm, 55 deg inclination case. The latter case was the basis of the TPS analysis, so the trajectories having flight times shorter than it will, in general, be compatible with the TPS design. Thus, the downrange trajectories, which have larger than nominal flight times, imply a greater heat load than the nominal design and hence the requirement for a thicker insulation and therefore greater TPS weight than the nominal.

Table 2.4-7

FOOTPRINT CONTROL HISTORIES FOR STAGE-AND-ONE-HALF ORBITER

Type	Phase	Angle-of-attack, α (deg)	Bank angle, χ Value/condition	End Condition
Nominal Case	1	35	0	T.B. pullup, $\gamma = -0.07^{\circ}$
	2	35	On T.B.	V = 16,000 fps
	3	35 → 25	Constant γ	$\chi = 30^{\circ}$
	4	25 → 20	30°	$H \cong 100^{\circ}$
	5	20 → 15	Constant γ	$\chi = 10^{\circ}$
	6	15 → 10	10°	V = subsonic
Uprange family	1	α_e (Varied from 35° to 55° to decrease range)	0	T.B. pullup, $\gamma = 0.-07^{\circ}$
	2	α_e	On T.B.	V = 16,000 fps
	3	α_e → 25	Constant γ	χ = subsonic
Downrange family	1	35	0	T.B. pullup, $\gamma = 0$
	2	35	Constant γ	$\chi = \chi_i$ (varied from 50° to 0° to increase range)
	3	35	χ_i	V = 16,000 fps
	4	35 → 25	χ_i	$H \cong 100^{\circ}$
	5	25	Constant γ	$\chi = 0$
	6	25	0	V = subsonic

Definitions:

α_e	entry angle-of-attack
γ	flight path angle
V	velocity
H	heading change relative to orbit plane
T.B.	temperature boundary
→	modulated to

Temperature Boundary and Pullup Constraints on Selection of Entry Angle-of-Attack and Flight Path Angle for Stage-and-One-Half Orbiter 270 NM, 55 DEG

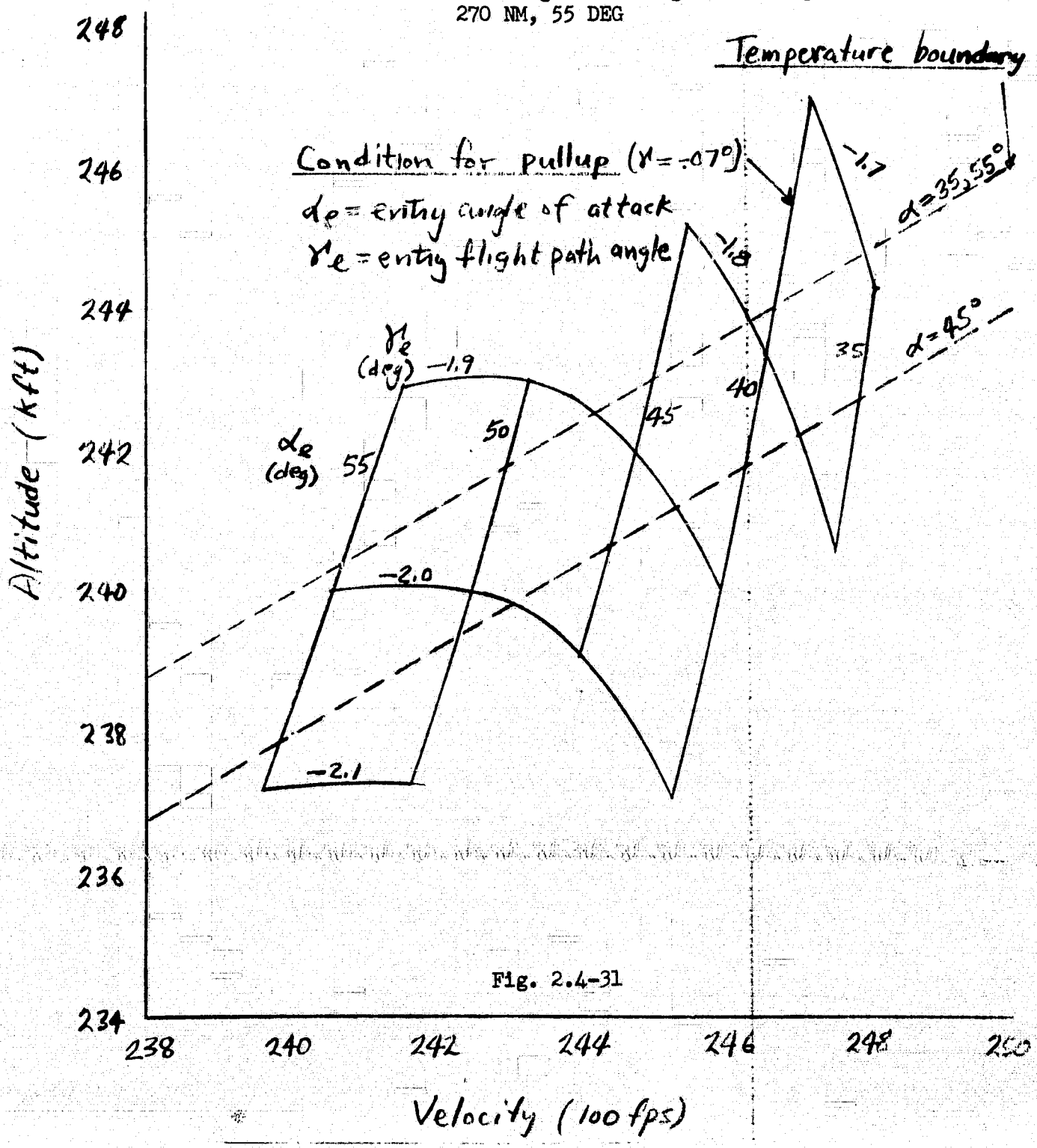

Fig. 2.4-31

LOCKHEED

STAGE-AND-ONE-HALF ORBITER

55-DEG 270-NM FOOTPRINT

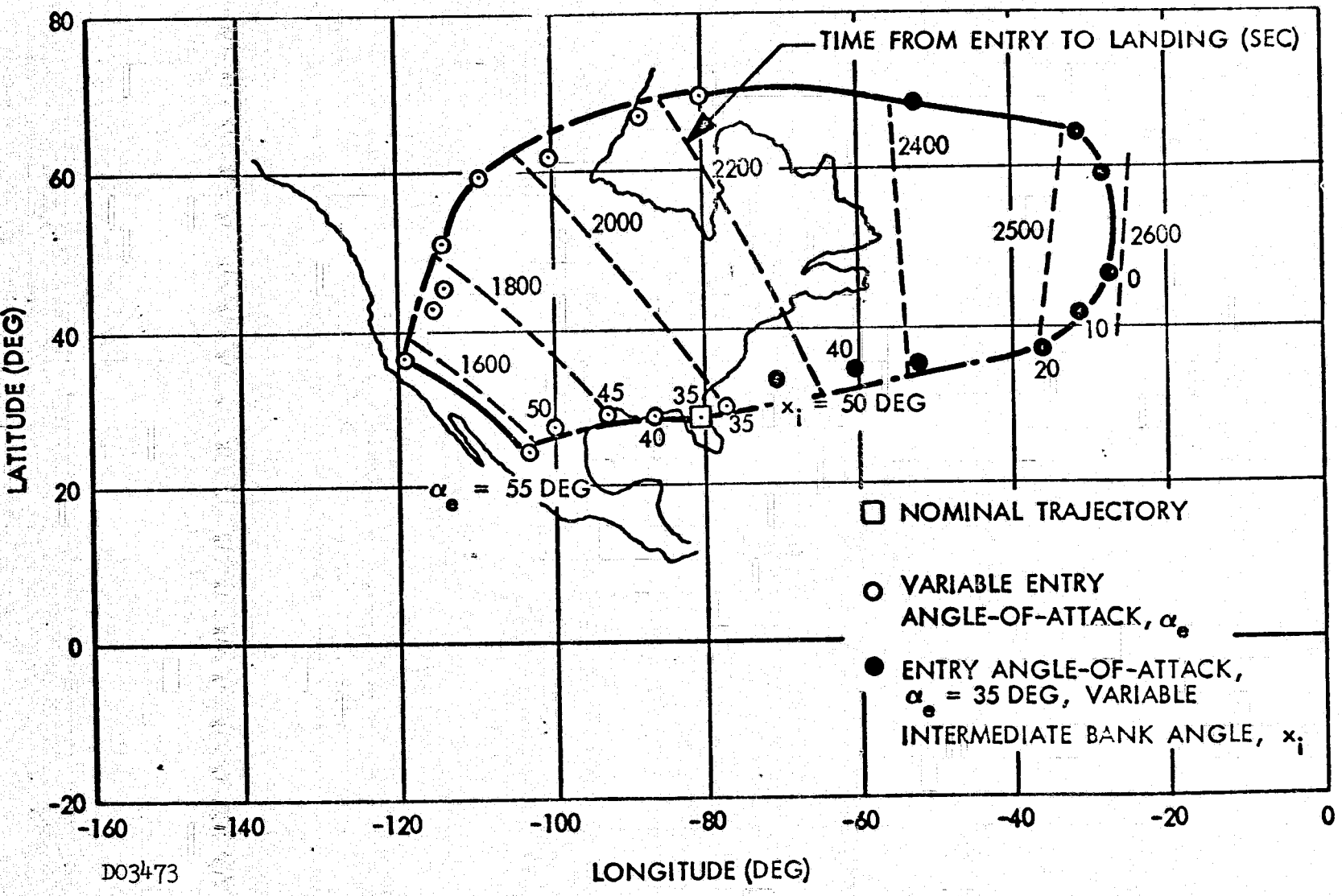

D03473

LOCKHEED

STAGE-AND-ONE-HALF ORBITER

28.5 DEG INCLINATION, 100 NM ENTRY FOOTPRINT

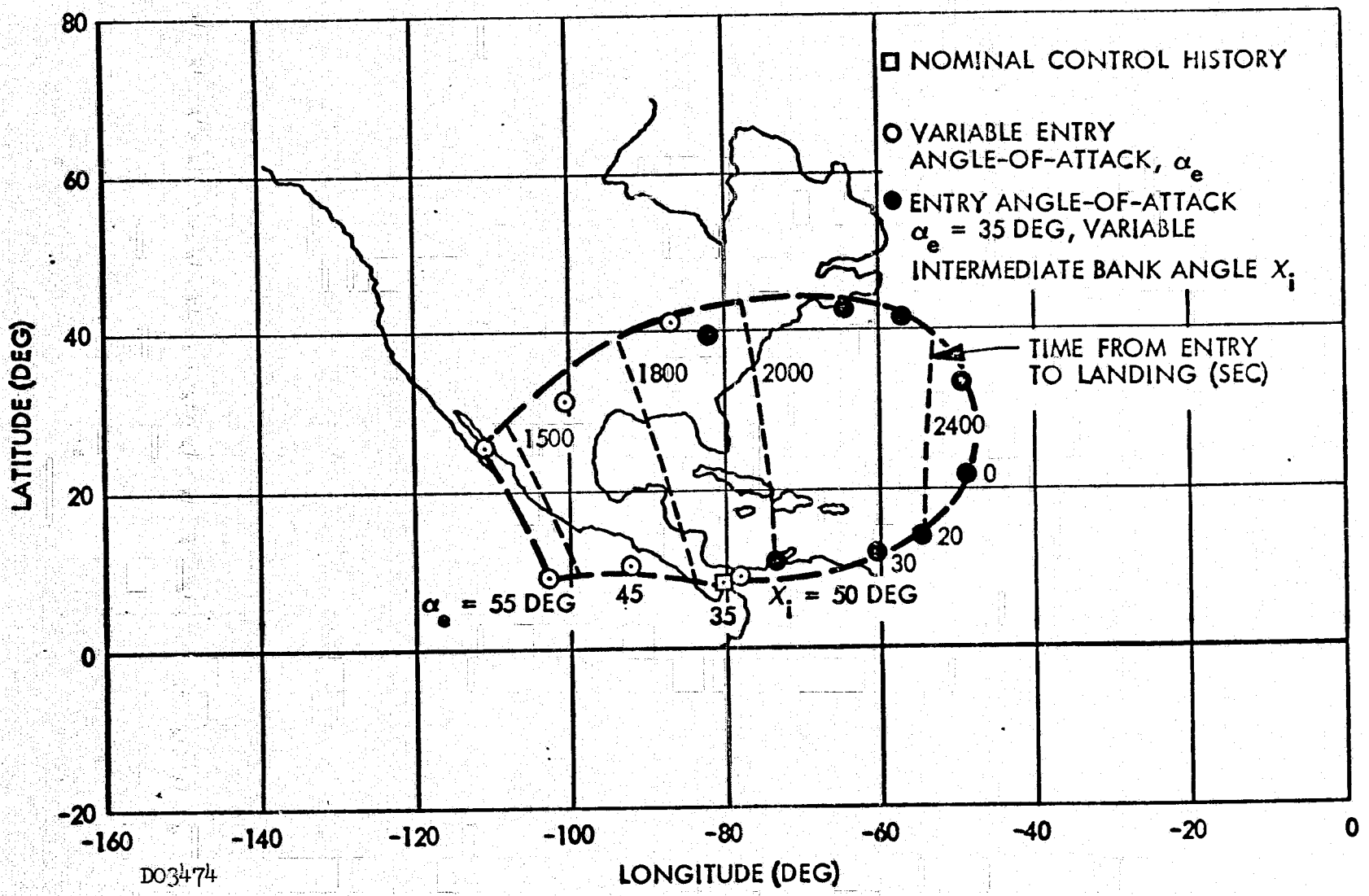

D03474

LOCKHEED

STAGE-AND-ONE-HALF ORBITER

POLAR, 100 NM ENTRY FOOTPRINT

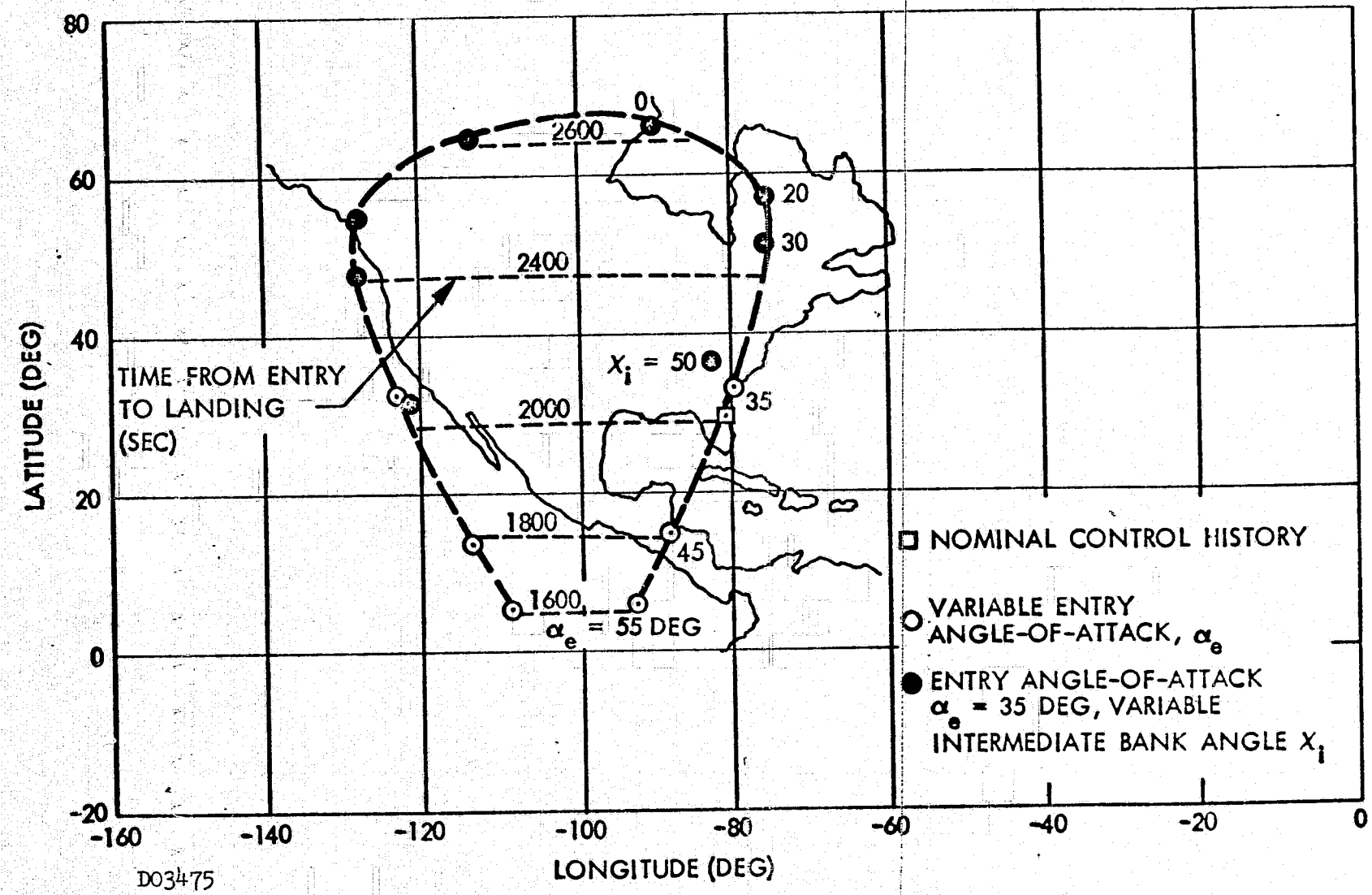

D03475

2.4.6 System Sensitivities

Performance and design sensitivities for the stage-and-one-half system are useful for design/cost tradeoffs, for evaluation of risk in program development due to design uncertainties, and for establishing flight performance requirements and guarantees. Two types of sensitivities are presented herein: variable gross liftoff weight (GLOW) and variable payload. The variable GLOW sensitivities assume rubberized (variable size) droptanks and fixed payload and orbiter size. This type of sensitivity is useful for tradeoffs early in the design process when the principal features of the orbiter design are already established and only relatively minor modifications are made. The droptank design is allowed to change, however. For the second type of sensitivity, variable payload, the entire vehicle design is assumed to be fixed, and any performance or weight change affects the payload capability of the vehicle. This type of sensitivity may be used to compute flight performance reserves or changes in payload capability because of different mission requirements.

The variable GLOW sensitivity assumes that only the droptanks are rubberized, and that the payload, the orbiter airframe size and propellant loading, and the main engine number and thrust level are all fixed. Rubberizing the droptanks is accomplished by changing the diameter of the tanks, rather than their length, so that the orbiter-droptank attach points remain fixed. Rubberizing the droptanks changes the launch weight, and thus the liftoff thrust-to-weight ratio $(T/W)_o$, since the thrust is fixed at 530,000 lb per engine.

As $(T/W)_o$ is reduced, the velocity losses to achieve orbit injection increase, so that the ideal velocity required from the droptanks must also increase. The ascent trajectories simulating variations in $(T/W)_o$ were all constrained to the same maximum αq (angle-of-attack x dynamic pressure) value, so that there will be no change in structural weight of the orbiter due to αq changes. Also, since the weight of the loaded droptanks decreases in the same proportion

as $(T/W)_o$ increases, the load carried by the thrust structure remains constant. Therefore, there will be no appreciable change in the orbiter structure due to changes in droptank size, when the number and thrust level of the main engines are held constant.

Table 2.4-8 shows the effect of weight and performance changes in GLOW and droptank and orbiter dry weight for the resupply mission with ABES in (55 deg inclination orbit, 50 x 100 nm plus 1500 ft/sec). Both ascent and return cargo are fixed at 25,000 lb. This mission is the critical mission for the Stage-and-One-Half System.

One sensitivity that requires additional clarification is that of weight of cargo landed. For this parameter, it is assumed that the jet engine size and thrust are fixed, but that jet engine propellant increases with landing weight to maintain go-around requirements. It is also assumed that the thermal protection system weight, landing gear and associated frames, and entry ACPS propellant are changed as the weight of cargo returned changes. However, the return cargo is not carried through any impulsive ΔV burn. Note that the sensitivity of orbiter inert to return cargo is used in the calculation of a variety of other partials, since any direct inert weight added to the orbiter requires a secondary increase in orbiter inert weight. For example, if one additional pound of weight is required for the crew cabin, an additional 0.136 lb of weight is required in landing gear, heat shield, etc. For a more detailed discussion of these sensitivities and how to use them, see Section 3.3.7.

The variable payload sensitivities for a fixed stage-and-one-half system are presented for the resupply mission and due east mission in Table 2.4 -9. These sensitivities assume all propellant and inert weights are fixed, as well as the thrust of the engines. The only weight which varies is the ascent payload. The effect of returning this payload on the orbiter dry weight is not accounted for, but its effect on ACPS reentry propellant and jet engine fuel (for the resupply mission only) is considered. This would be the case for a fixed vehicle, where no design changes in the vehicle are permitted, but propellant loadings may vary from mission to mission.

Table 2.4-8

STAGE-AND-ONE-HALF VARIABLE LIFTOFF

Parameter	$\frac{\partial (GLOW)}{\partial (Parameter)}$	$\frac{\partial (Droptank\ Inert)}{\partial (Parameter)}$*	$\frac{\partial (Orbiter\ Inert)}{\partial (Parameter)}$
Payload (lb)			
(1) Delivered and returned	26.4	3.10	0.175
(2) Returned only, not carried through any ΔV burn	3.1	0.31	0.136
On-Orbit ΔV (fps)	536	19.2	0
Ascent ΔV (fps)	591	21.1	0
Orbiter Inert Weight (lb)			
(1) No secondary effect	22.5	2.24	1.00
(2) With secondary effect	25.6	2.61	1.136
Droptank Inert Weight (lb)	10.7	1.37	0
Orbiter Propellant (lb)			
(1) No orbiter tankage penalty	-2.57	-.27	0
(2) Internal tank penalty only	-1.22	-.136	0.060
(3) Airframe enlarged and internal tank penalty	+0.35	+0.02	0.130
Specific Impulse, Thrust Constant (sec)	- 39,900	- 1430	0
Total Thrust, Specific Impulse Constant, (lb)			
(1) No engine weight penalty	- 0.610	- 0.022	0
(2) Engine weight penalty	- 0.046	- 0.0017	0.025

* To obtain sensitivity for droptank dry weight, multiply entries in this column by 0.923.

Table 2.4 -9

VARIABLE PAYLOAD SENSITIVITIES – STAGE-AND-ONE-HALF

Parameter	$\frac{(\text{Payload})}{(\text{Parameter})}$ Resupply (ABES In)	East (ABES Out)
On-orbit ΔV (fps)	- 23.1	- 26.3
Ascent ΔV (fps)	- 28.0	- 31.9
Orbiter Inert Weight (lb)	-1	-1
Droptank Inert Weight (lb)	- 0.457	- 0.511
Orbiter Propellant (lb)	0.170	0.187
Droptank Propellant (lb)	0.0464	0.0757
Specific Impulse, Thrust Constant (sec)	1890	2125
Total Thrust, Specific Impulse Constant (lb)	0.0282	0.0326
Thrust-to-Weight Ratio (.1 unit T/W)	10,700	12,440

2.4.7 Ferry Capability

2.4.7.1 Introduction. Orbiter ferry capability was explored parametrically to determine the feasibility of intracontinental (U.S.) ferry flight and any possible restrictions or conditions limiting that capability. Figure 2.4-35 shows a schematic ferry flight profile consisting of three major segments: takeoff, ferry, and landing. Each segment was further subdivided into segments amenable to simple analysis. These were:

(1) Takeoff
   (a) Acceleration at takeoff power
   (b) Rotation at takeoff power
   (c) Liftoff at takeoff power
   (d) Takeoff climb at takeoff power

(2) Ferry
   (a) Climb at takeoff power
   (b) Constant-altitude cruise
   (c) Descent at flight idle power

(3) Landing
   (a) Flare
   (b) Touchdown
   (c) Derotation
   (d) Free roll
   (e) Braking to full stop

2.4.7.2 Method of Calculation. All segments of the flight profile were computed by numerical integration of the appropriate differential equations of motion for each segment.

2.4.7.3 Environment. The severest conditions occur on takeoff and climb, when the orbiter is at maximum weight. The highest airport elevation to

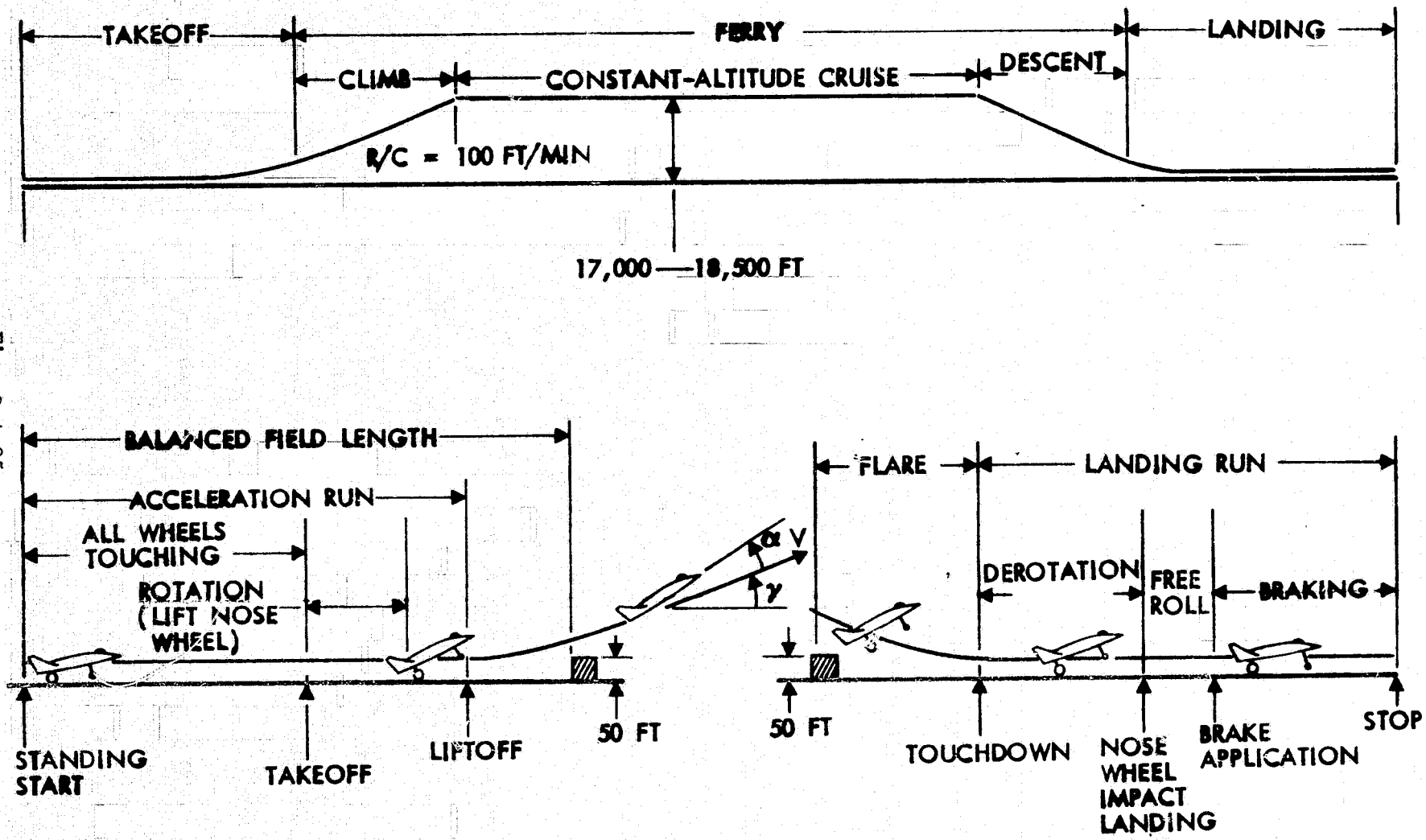

Fig. 2.4-35 Orbiter Ferry Flight Profile

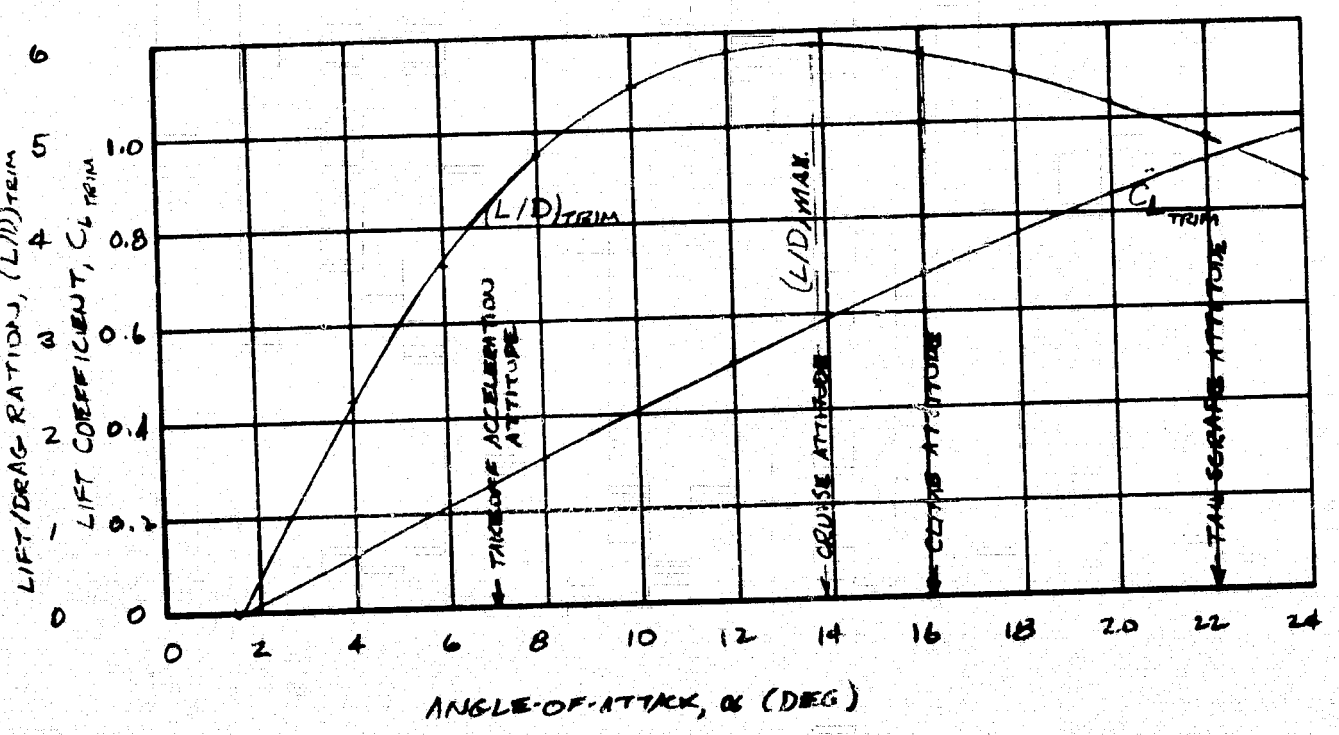

Fig. 2.4-36 Subsonic Trimmed Aerodynamic Characteristics

be encountered is assumed to be Holloman AFB and the most adverse takeoff conditions would occur on a hot day. Three atmosphere models were used in the takeoff and climb portions: the "standard day*," "tropical day**," and "hot day**."

2.4.7.4 Vehicle Characteristics: Powerplant and Aerodynamics. Turbofan engines were assumed for the ferry mission, using manufacturer's data for thrust levels and specific fuel consumption. Thrust lapse rates due to altitude and temperature were incorporated along with a 3 percent reduction in net thrust due to expected duct losses in the engine installations. Specific fuel consumption was increased by 3 percent due to ductlosses and by a further 2 percent for decreased engine performance between overhauls.

Orbiter aerodynamic characteristics are shown in Fig. 4.2-36 and are assumed to be independent of Mach number.

2.4.7.5 Takeoff. Balanced field length were determined for Holloman AFB (4094 ft above sea level and with a runway length of 12,228 ft) for a range of takeoff weights, number of airbreather (turbofan) engines, and ambient temperatures. Power levels were assumed to be set at takeoff levels and one engine was assumed to become inoperative at a speed where the distance between the point of engine loss and a point 50 ft above the end of the runway equaled the braking distance to bring the vehicle to a halt at the end of the runway. Figures 2.4-37 through 2.4-41 show the effect of weight, number of engines, and ambient temperatures on balanced field length for an altitude 4094 ft above sea level.

A six-engine configuration (five operative after the critical engine-loss point) with a 360,000 lb takeoff weight requires 12,000 ft of balanced field length (Fig. 2.4-37) even on a "standard day" with an ambient temperature of

*ICAO Standard Atmosphere (NACA TN3182)
**MIL-STD-210A, "Military Standard Climatic Extremes for Military Equipment" 30 Nov 1958.

44.4°F, and on a 94°F day (the upper limit of the maximum temperature range at Holloman) the takoff weight is decreased to 293,000 lb.

Seven engines (six operative at takeoff) improve takeoff weight on "standard" and "tropical" days with balanced field lengths of 9,100 and 11,500 ft, respectively, for a 360,000 lb configuration, but are not sufficient for "hot day" takeoff. Figure 2.4-43 shows the limitation of takeoff weight due to ambient temperature for a 7-engine 360,000 lb vehicle, with an upper limit of 82°F for a balanced field length of 12,200 ft. At ambient temperatures above 82°F, the maximum takeoff weight decreases to 348,800 lb at 94°F and 342,000 lb at 100°F.

Eight engines (seven operative at takeoff) on a 360,000 lb vehicle give enough thrust to provide a balanced field length of 10,900 ft even at an ambient temperature of 100°F (Fig. 2.4-44).

2.4.7.6 Climb Gradients. Steady-state (zero acceleration), engine-out climb gradients were calculated for 6 and 7 engines operative (corresponding to 7- and 8-engine vehicles) for a range of takeoff weights, takeoff conditions, ambient temperatures, and altitudes (i.e., airport elevations).

Takeoff and climb speeds were based on FAR* requirements for turbojet airplanes and the computed climb gradients compared to the minimum allowable for each condition of takeoff: takeoff with landing gear down at 1.15 V_S; takeoff with landing gear up at 1.15 V_S and final takeoff in the enroute configuration at 1.25 V_S where V_S is the stall speed. Plots of climb gradient vs air temperature are presented in Figs. 2.4-45 through 2.4-62. At the heaviest takeoff weight considered, there is no difficulty in meeting climb-gradient requirements on a "standard day" for either 6 or 7 engines operative at any airfield altitude on the list of selected potential airports. However, on "tropical" or "hot days" at the higher airfield elevations, it is not possible to satisfy

*Federal Aviation Regulations, Federal Aviation Agency, Part 25

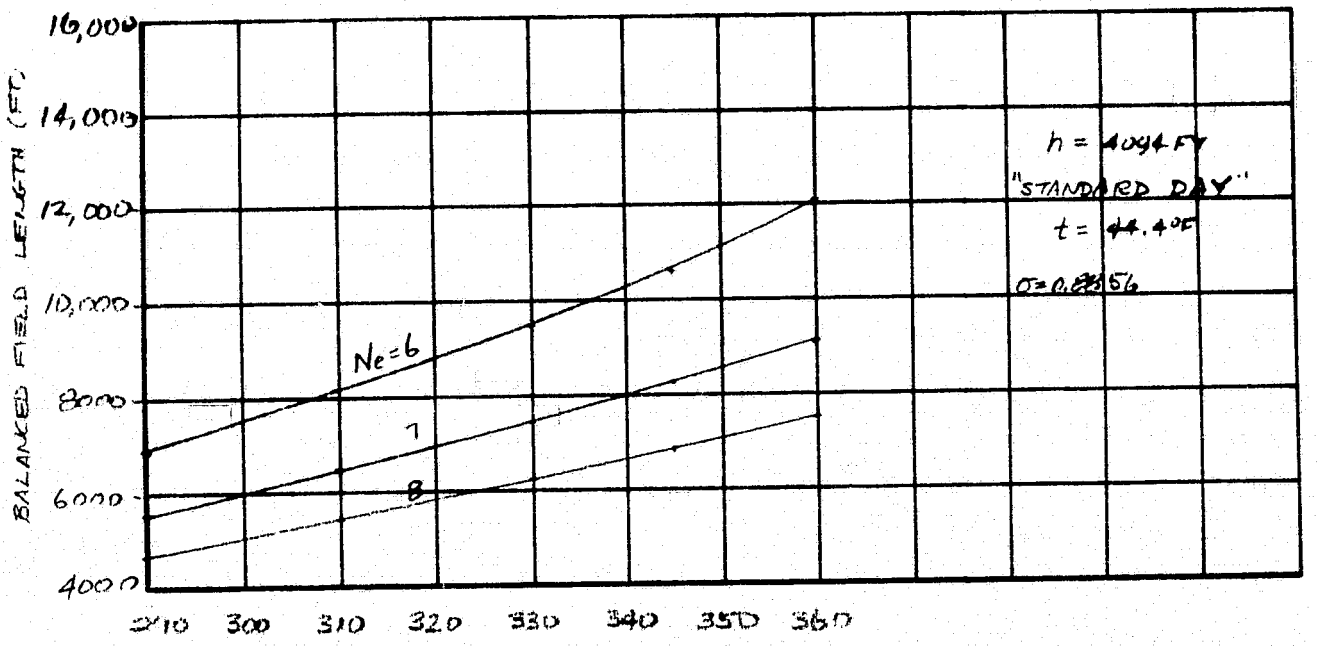

FIG. 2.4-37 BALANCED FIELD LENGTHS

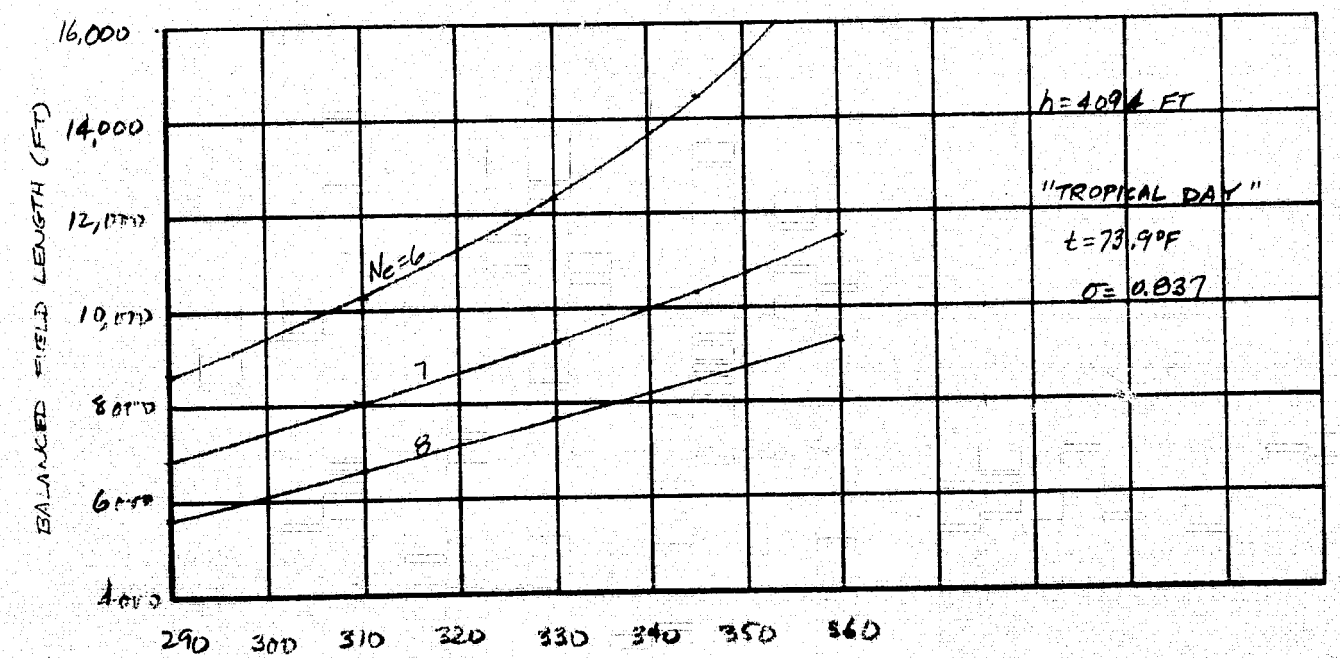

FIG. 2.4-38 BALANCED FIELD LENGTHS

LOCKHEED
CALIFORNIA COMPANY

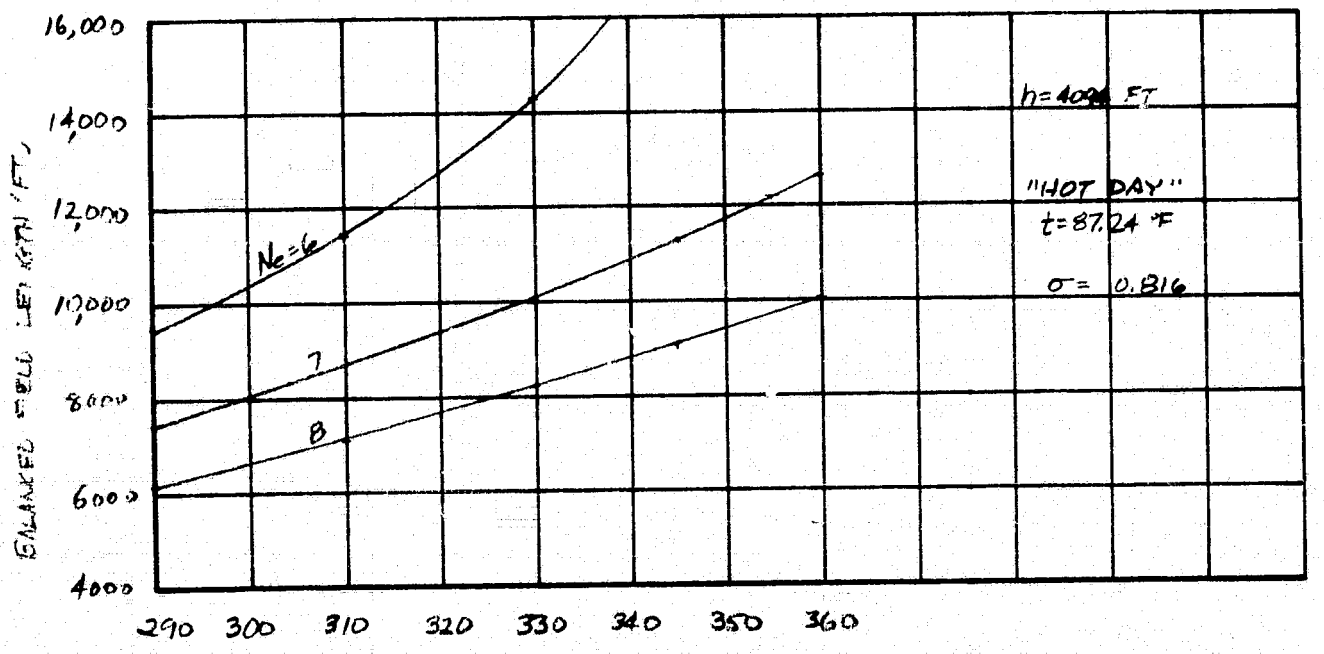

FIG. 2.4-39 BALANCED FIELD LENGTHS

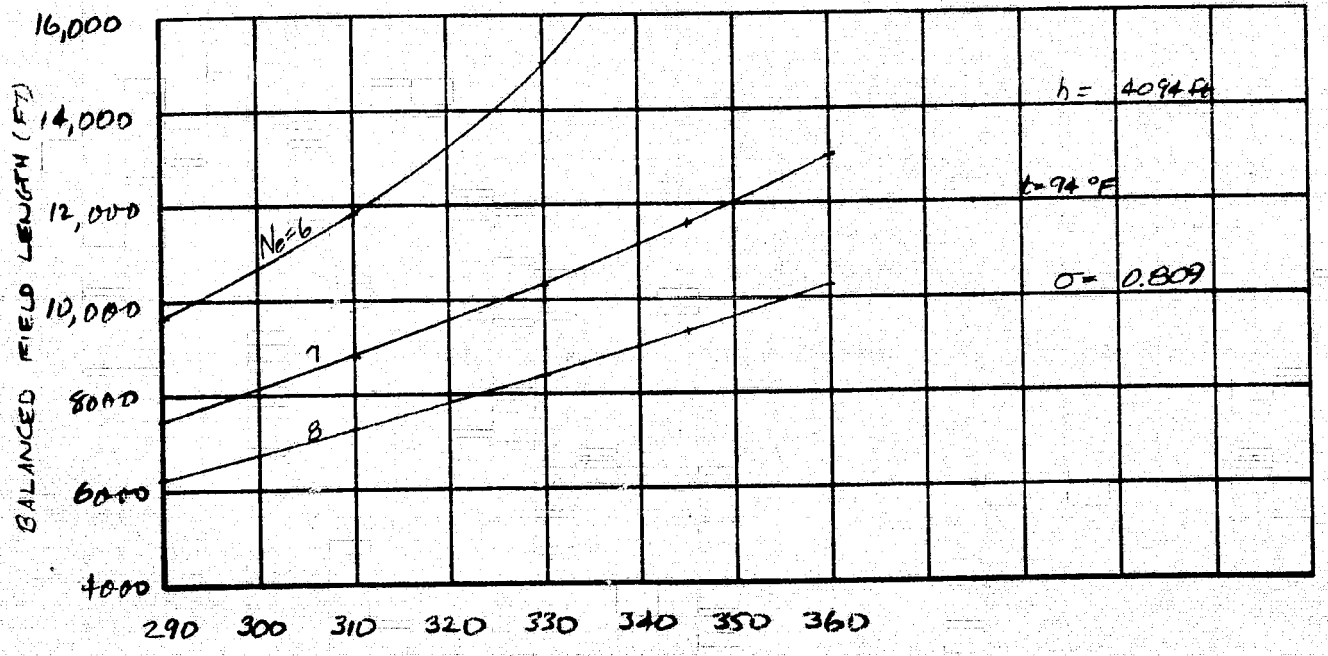

FIG. 2.4-40 BALANCED FIELD LENGTHS

LOCKHEED CALIFORNIA COMPANY

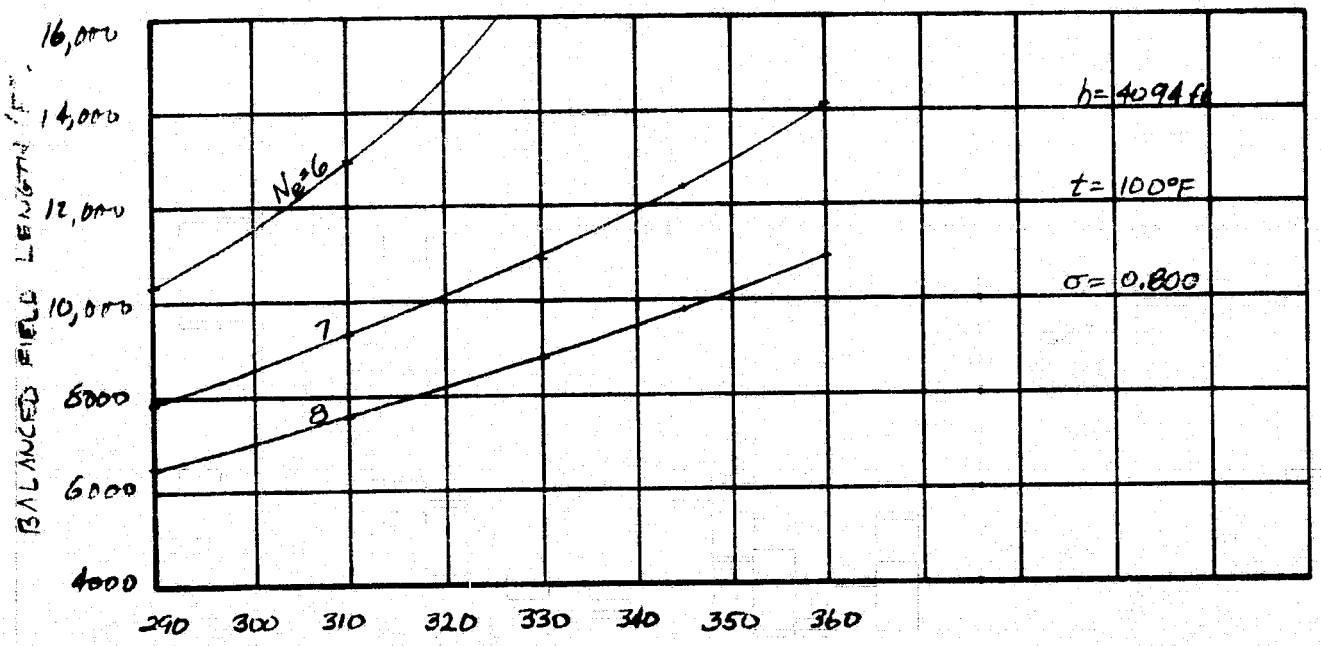

FIG. 2.4-41 BALANCED FIELD LENGTHS

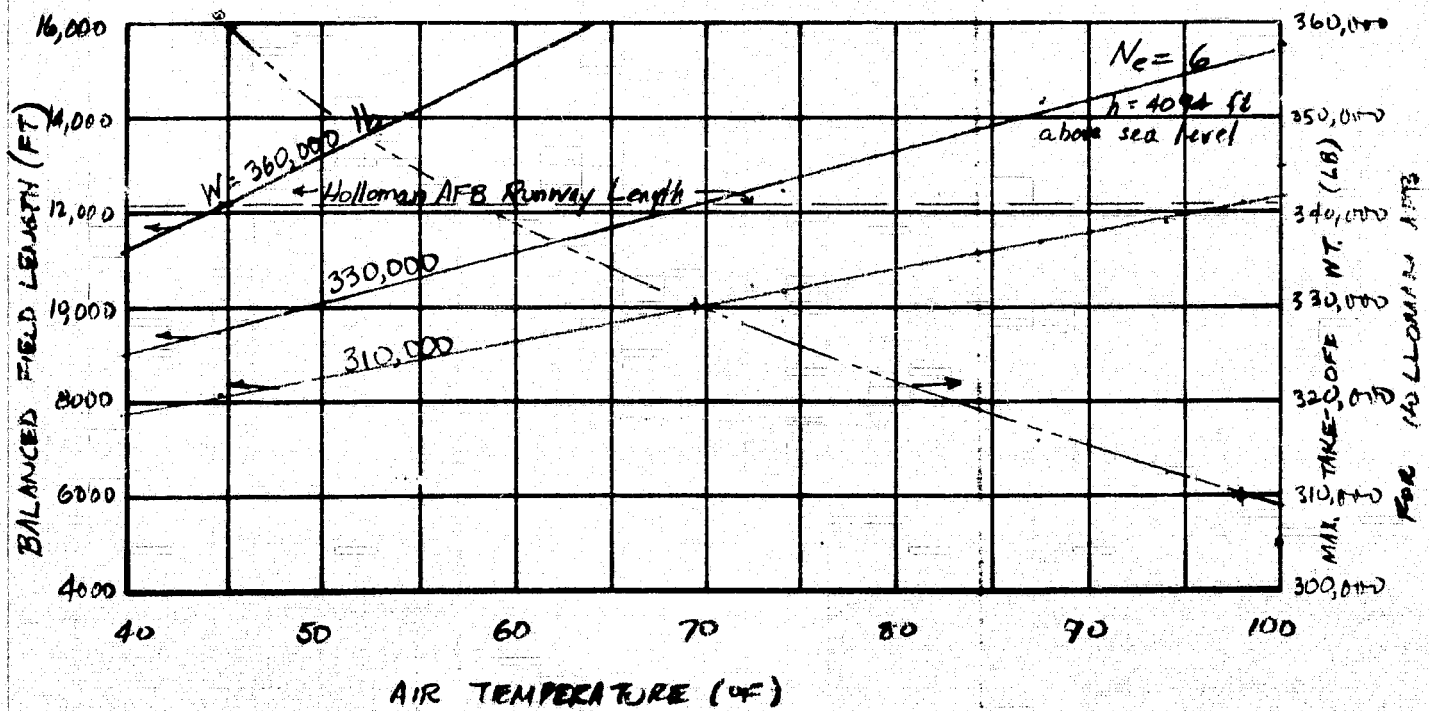

FIG. 2.4-42 BALANCED FIELD LENGTH SUMMARY

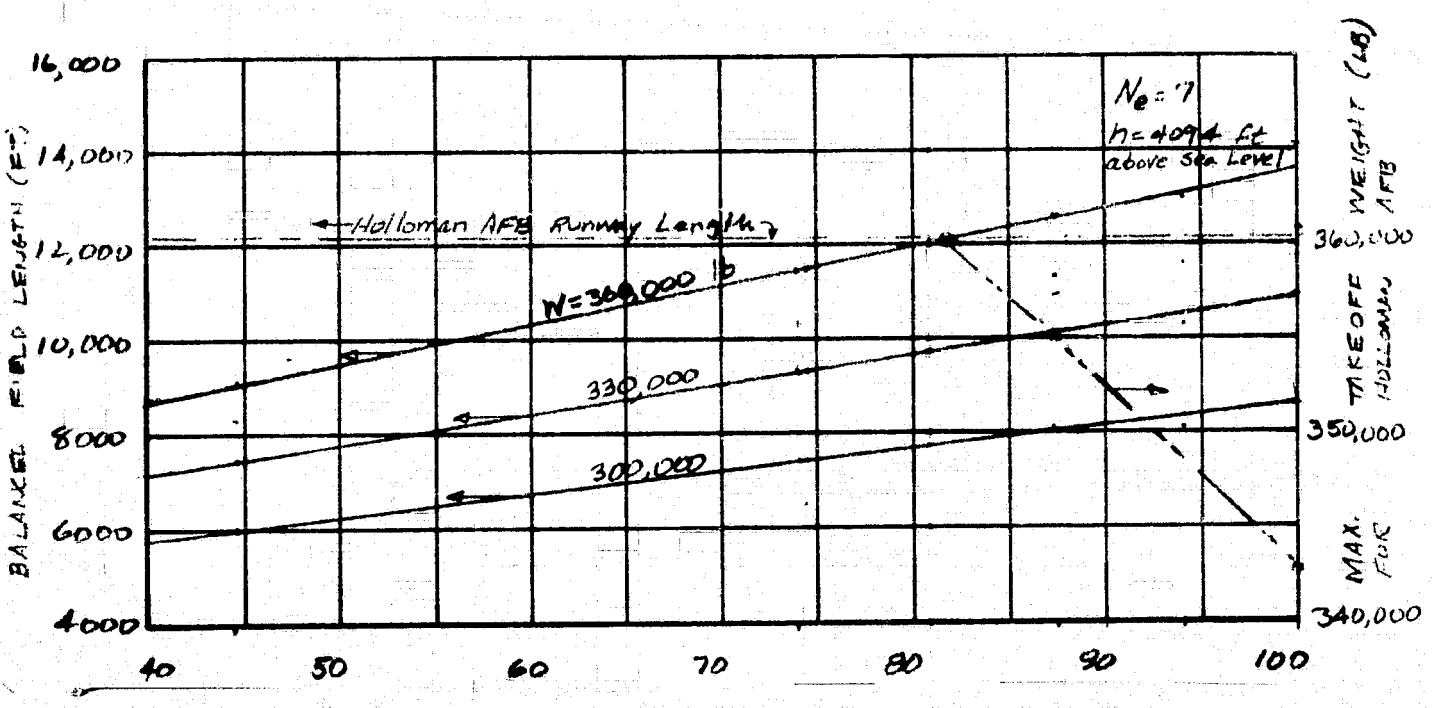

FIG. 2.4-43 BALANCED FIELD LENGTH SUMMARY

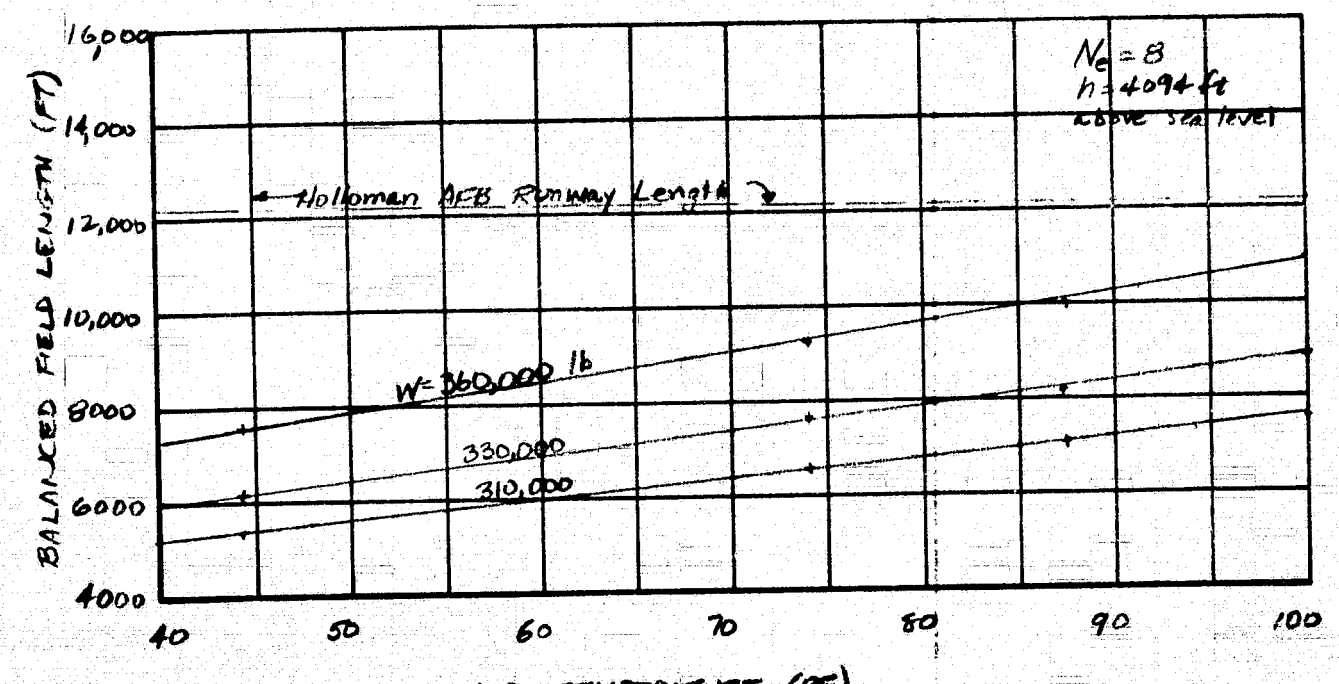

FIG. 2.4-44 BALANCED FIELD LENGTH SUMMARY

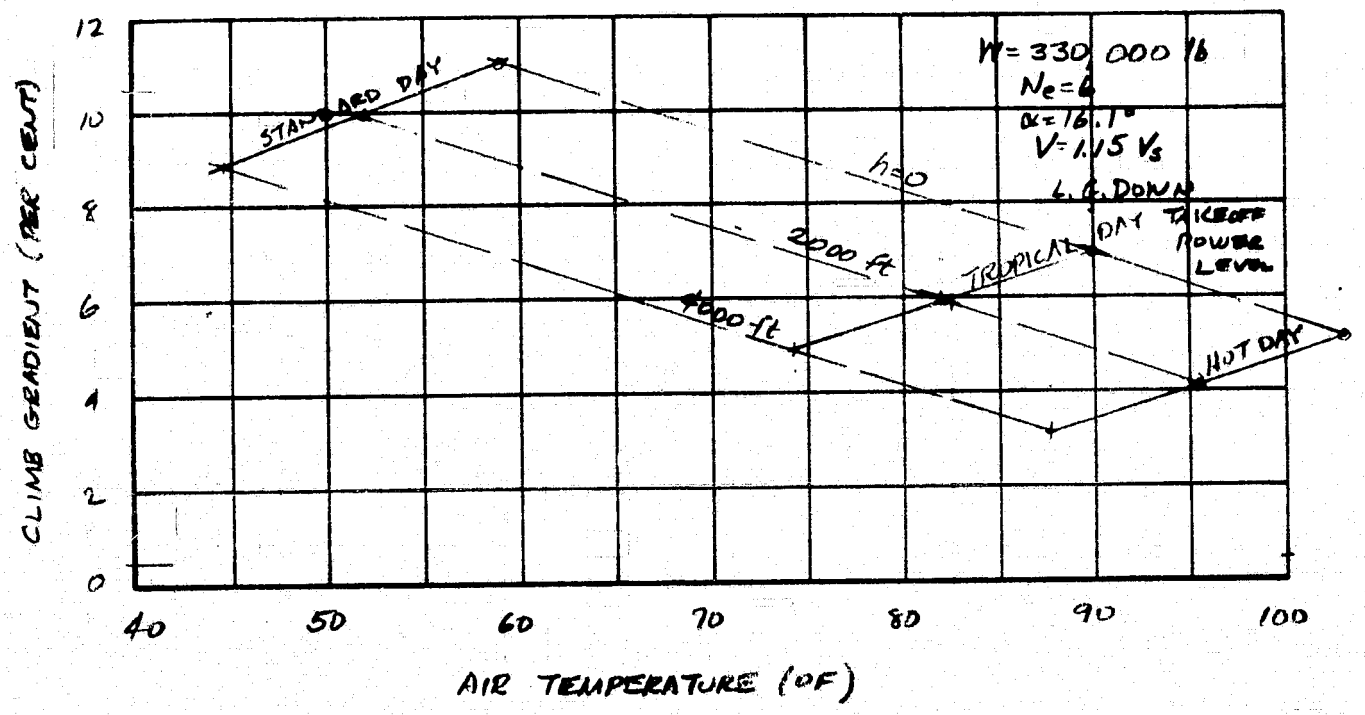

FIG. 2.4-45 CLIMB GRADIENTS

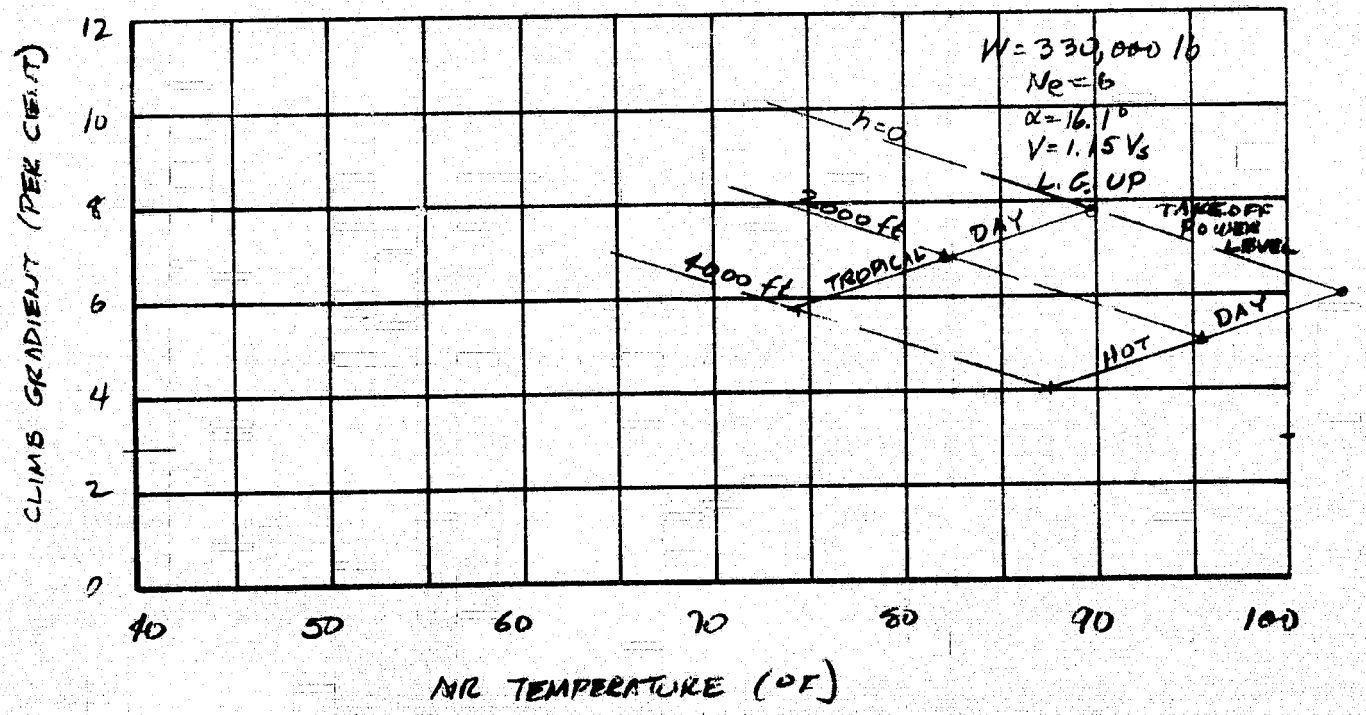

FIG. 2.4-46 CLIMB GRADIENTS

LOCKHEED CALIFORNIA COMPANY

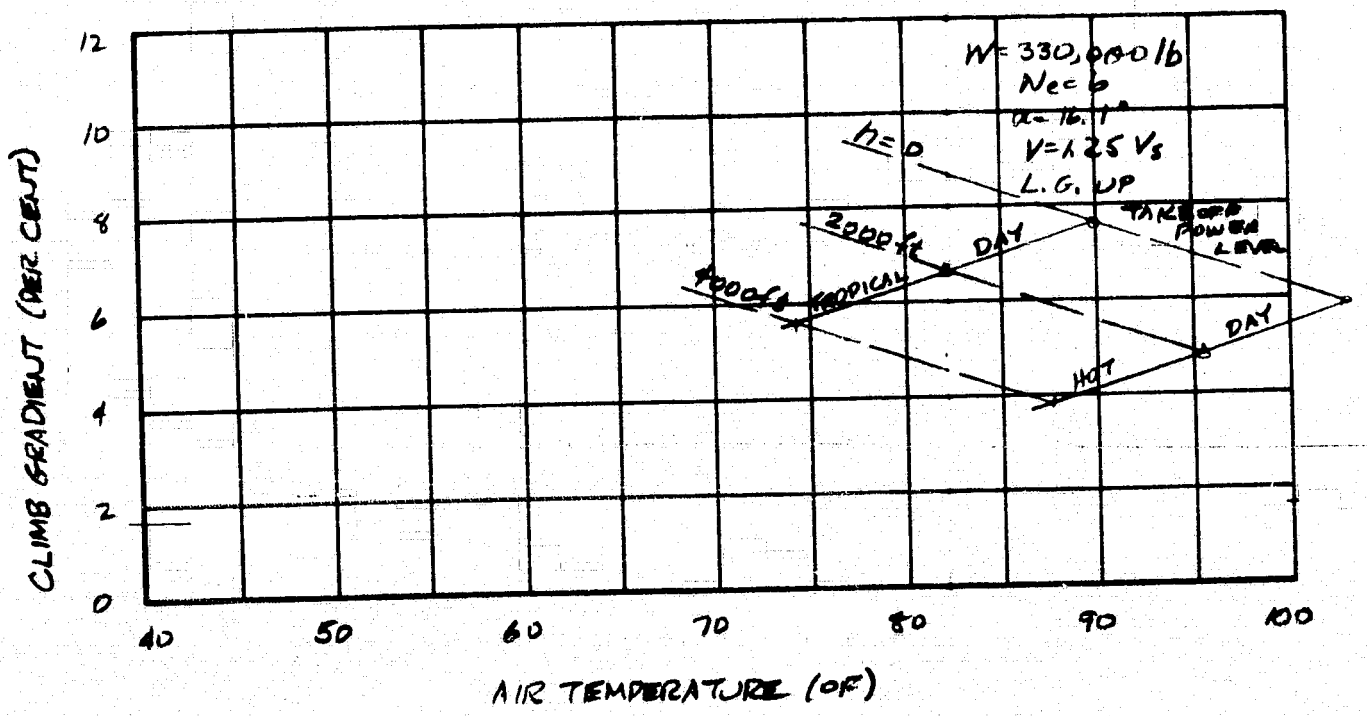

Fig. 2.4-47 Climb Gradients

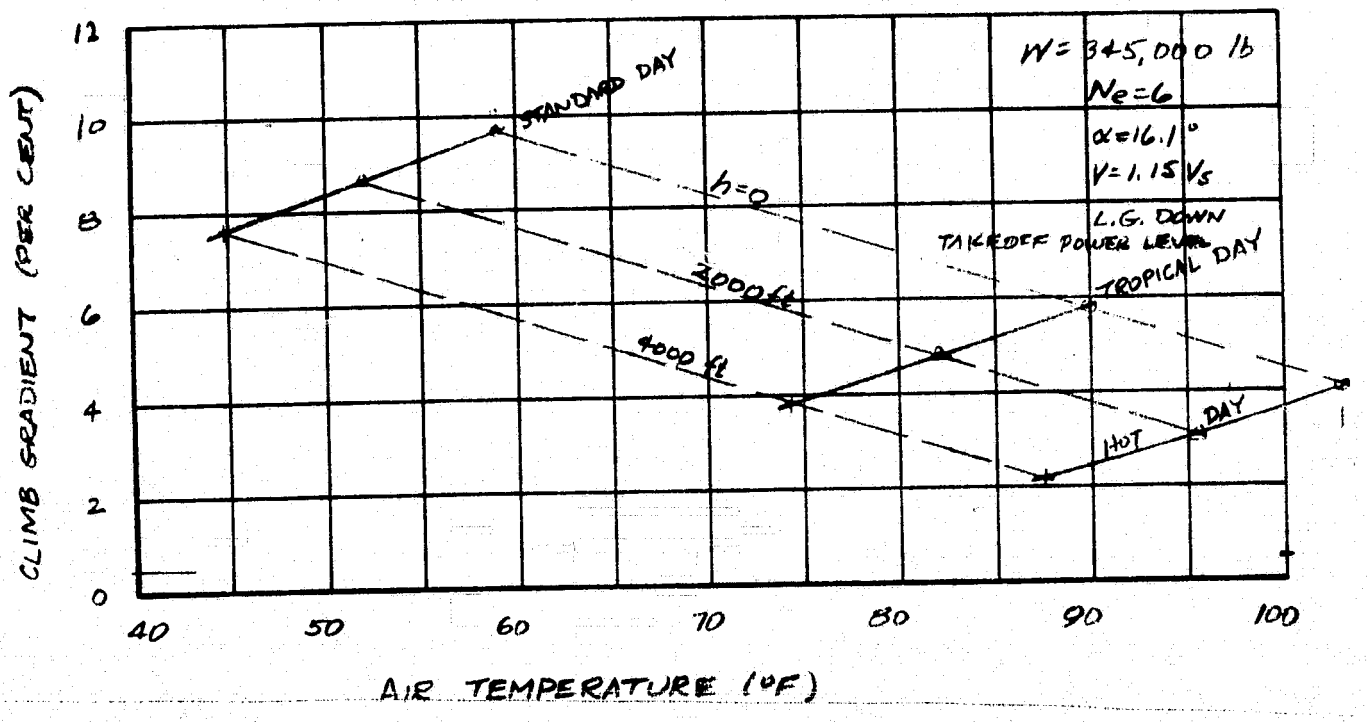

FIG. 2.4-48 CLIMB GRADIENTS

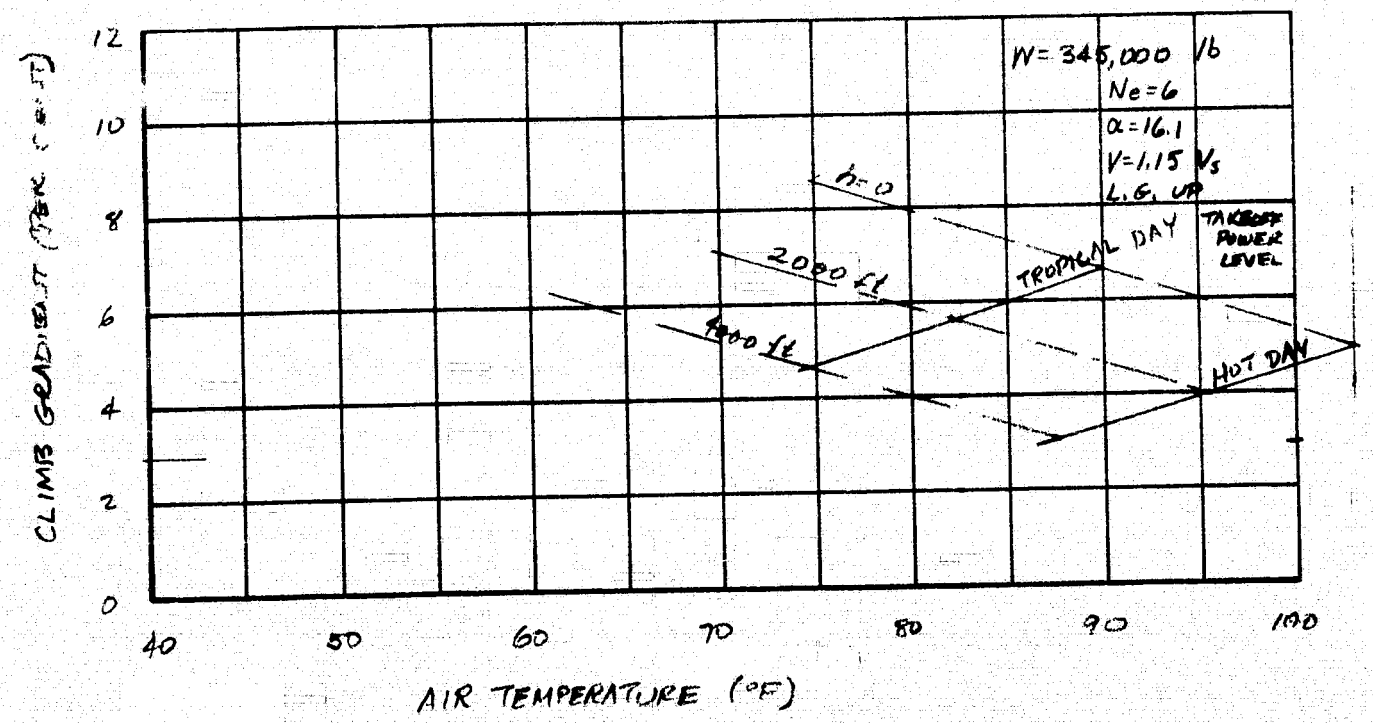

FIG. 2.4-49 CLIMB GRADIENTS

LOCKHEED CALIFORNIA COMPANY

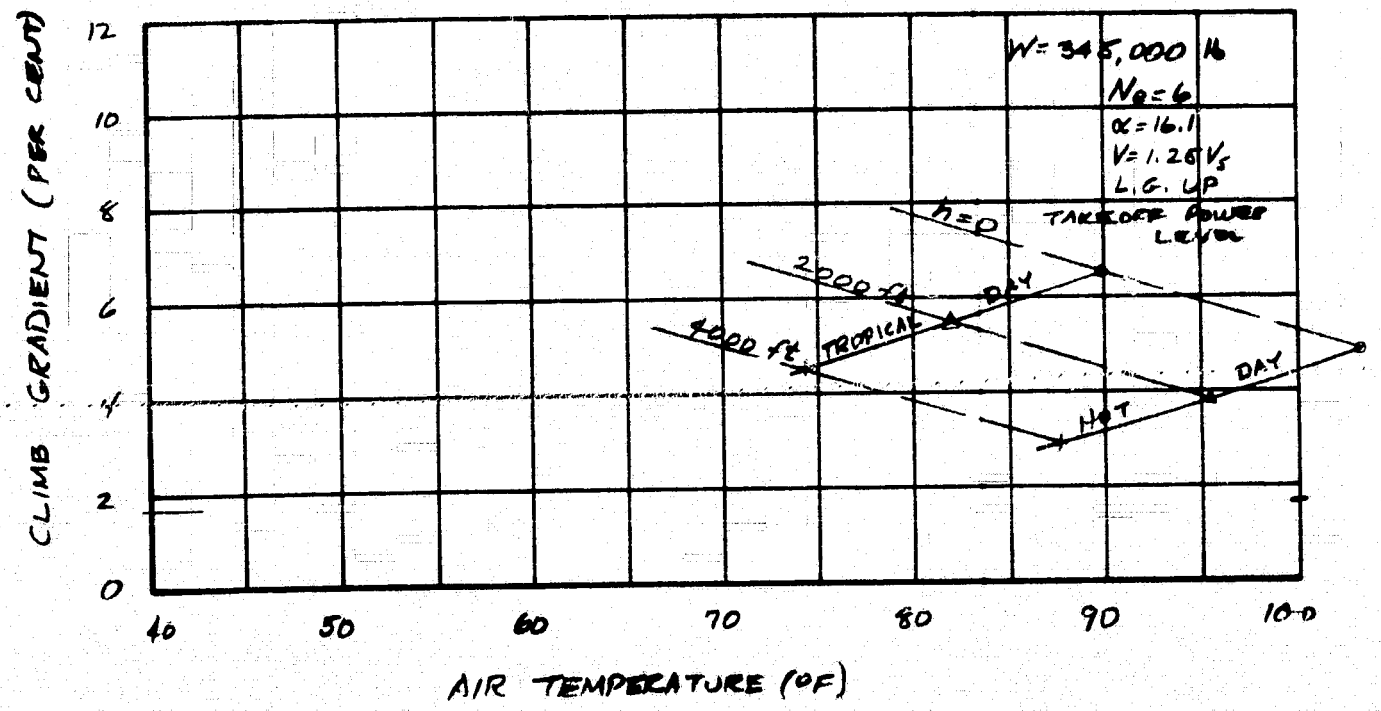

Fig. 2.4-50 Climb Gradients

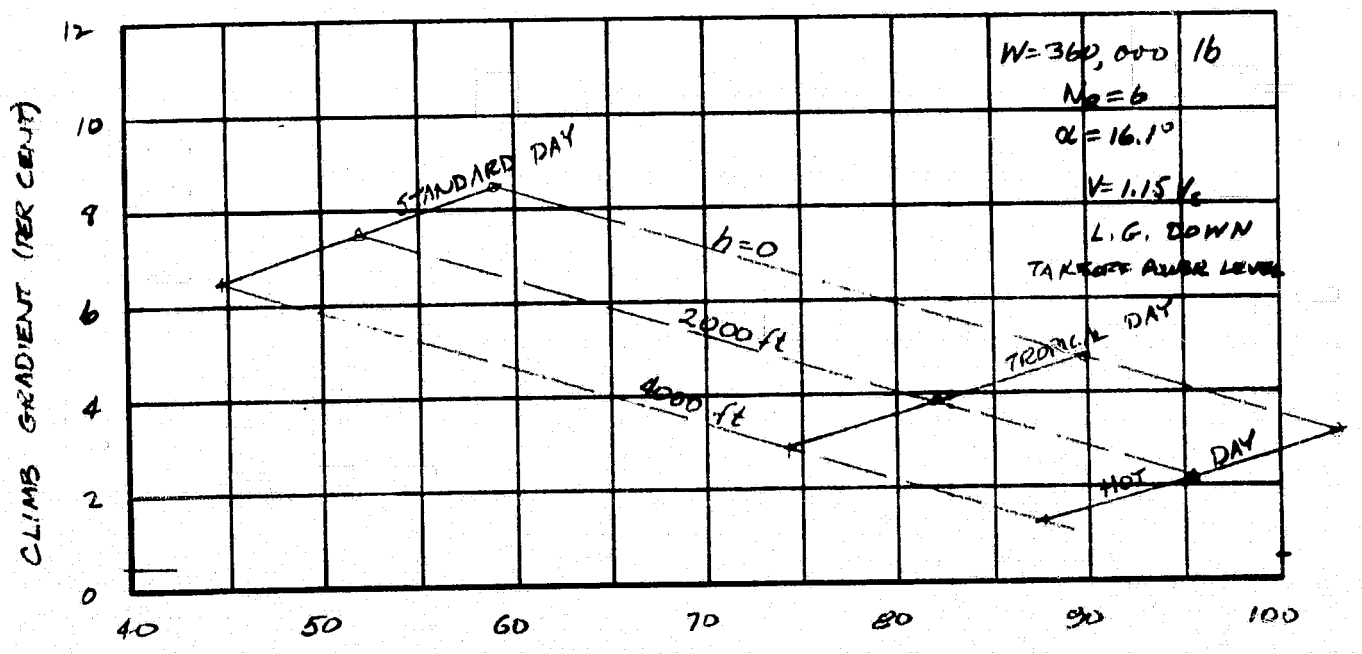

FIG. 2.4-51 CLIMB GRADIENTS

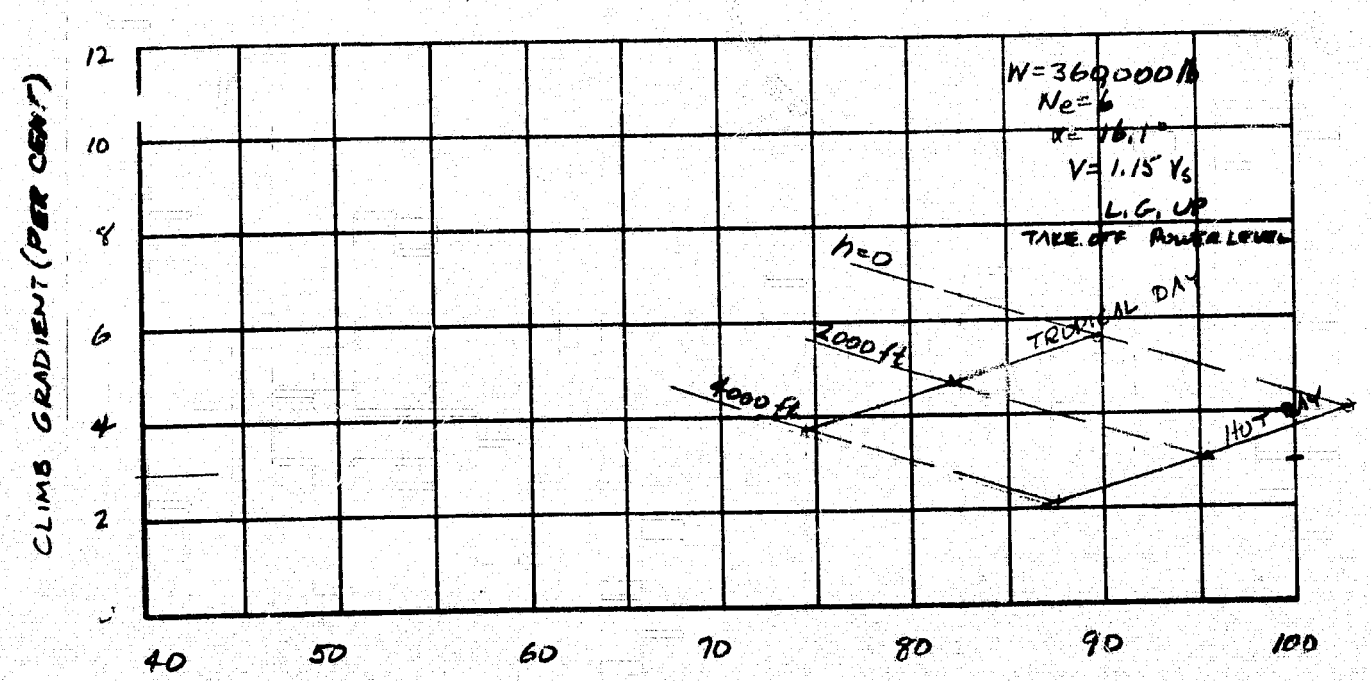

FIG. 2.4-52 CLIMB GRADIENTS

LOCKHEED CALIFORNIA COMPANY

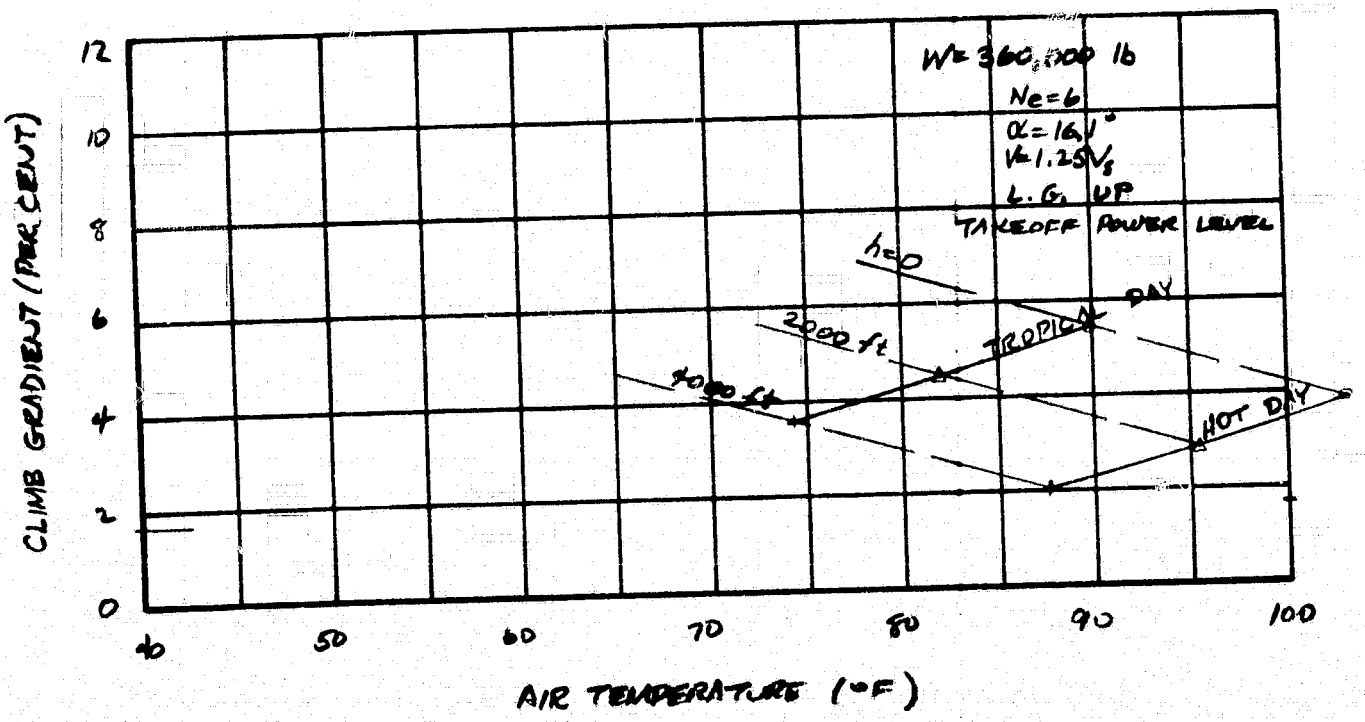

Fig. 2.4-53 Climb Gradients

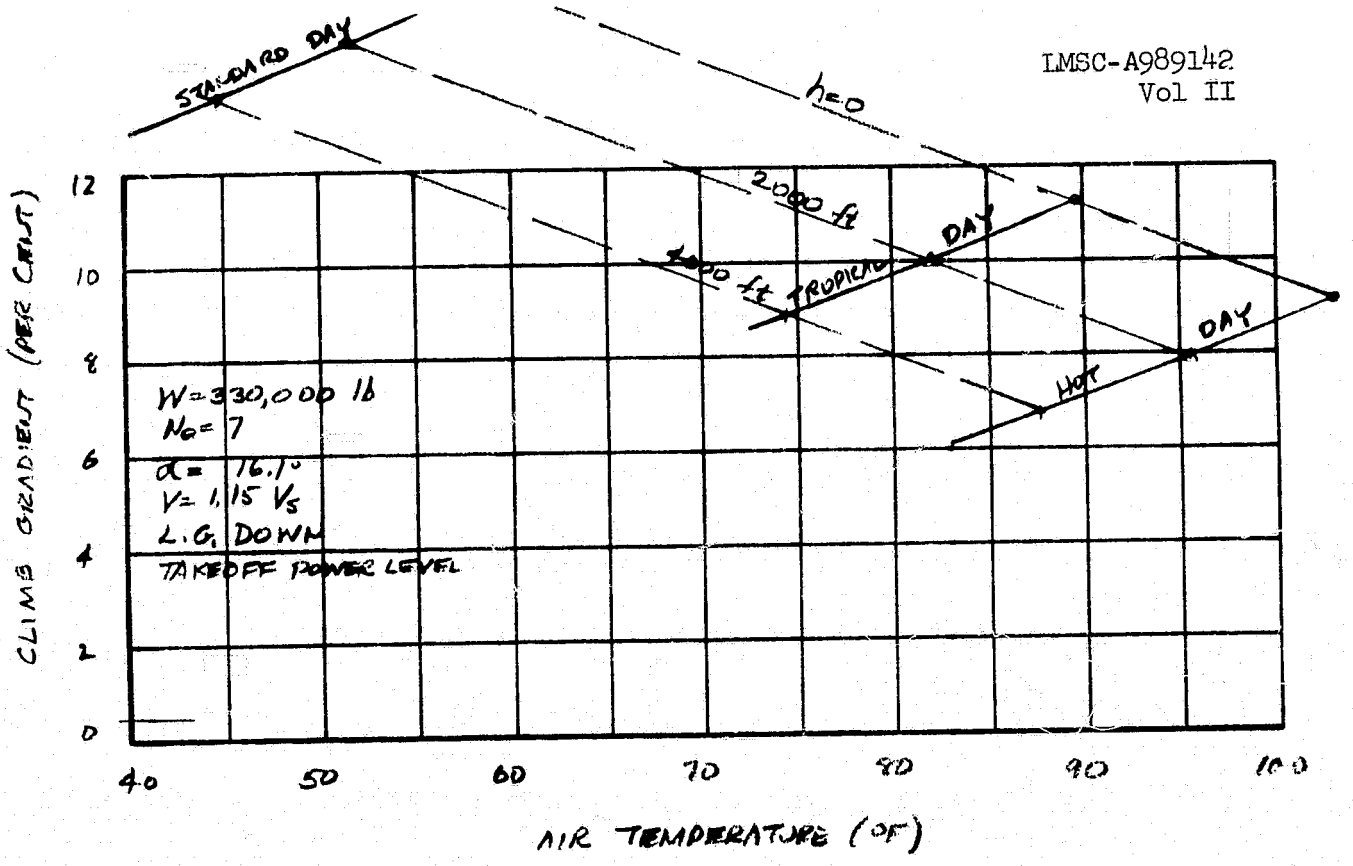

FIG. 2.4-54 CLIMB GRADIENTS

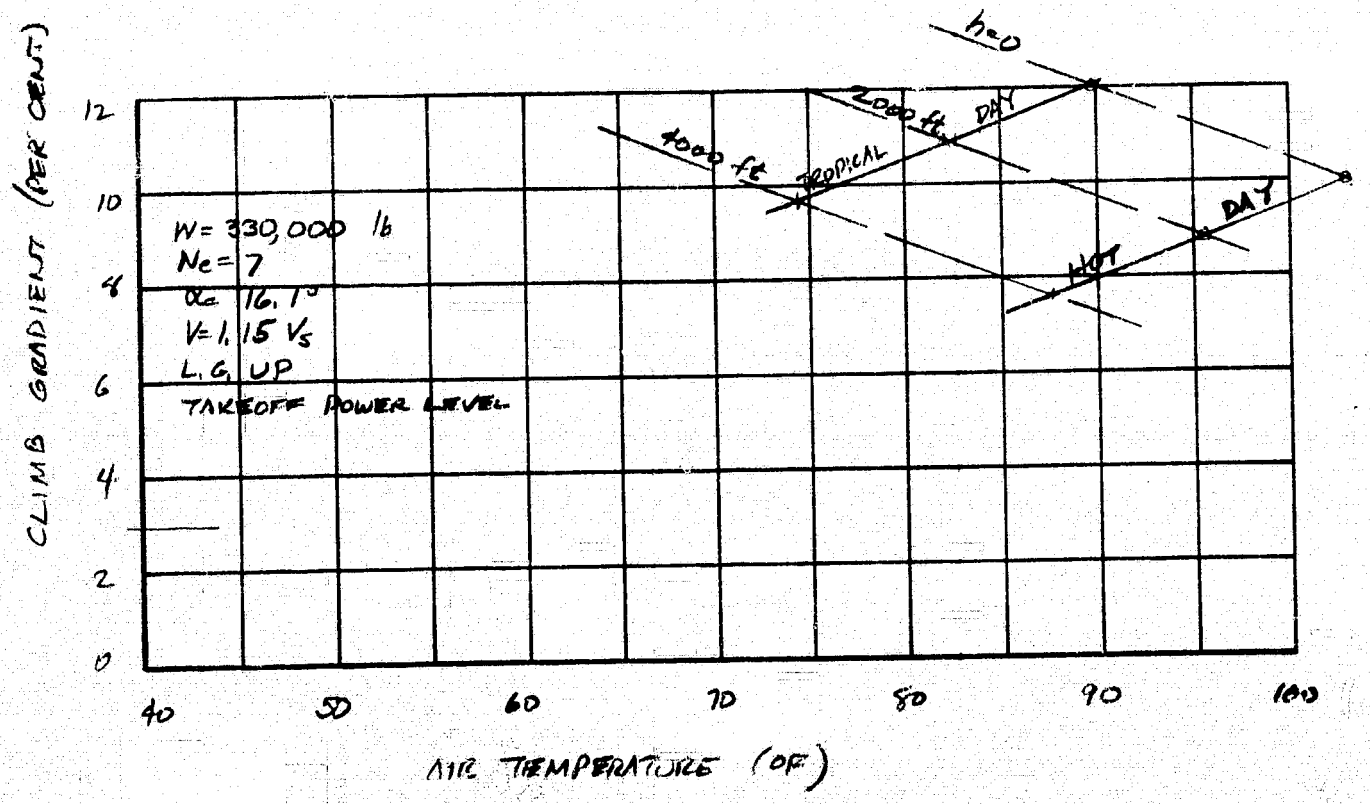

FIG. 2.4-55 CLIMB GRADIENTS

LOCKHEED
CALIFORNIA COMPANY

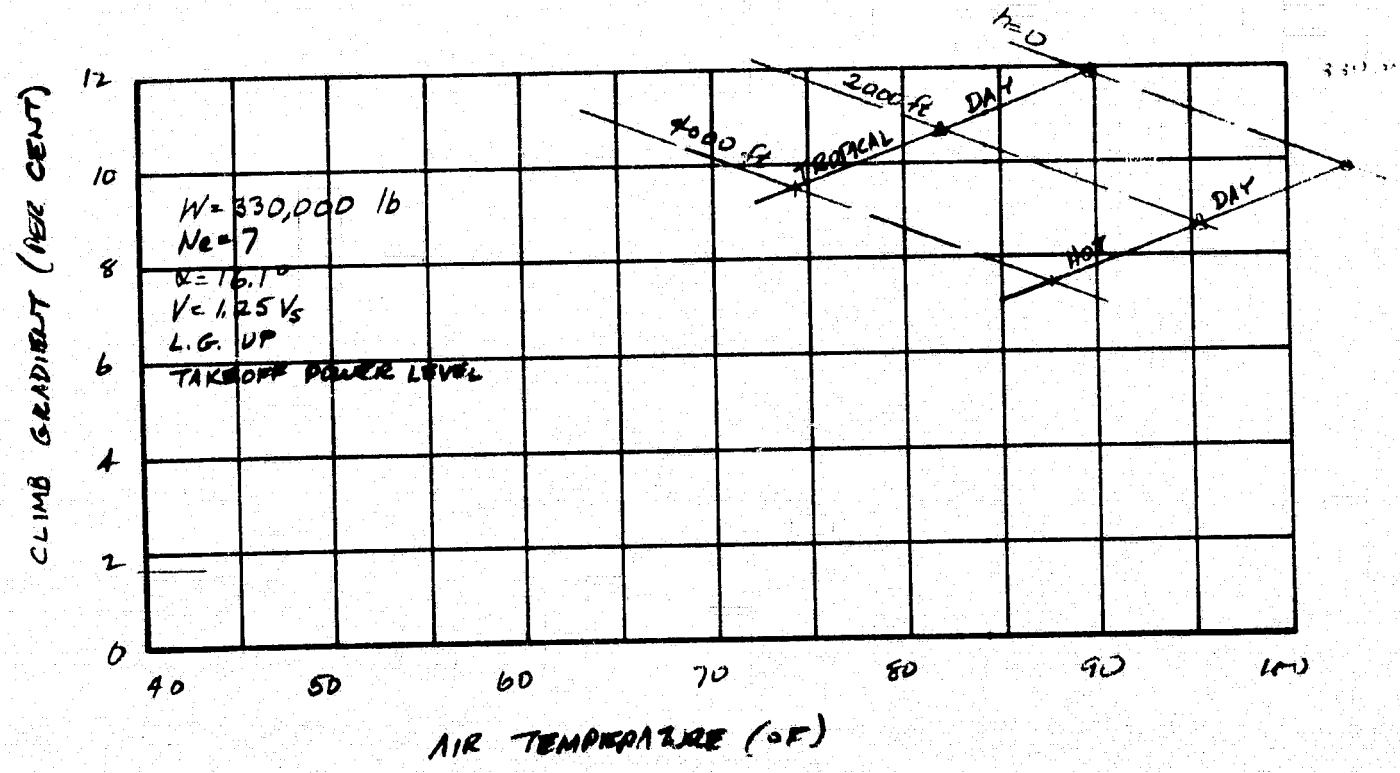

Fig. 2.4-56 Climb Gradients

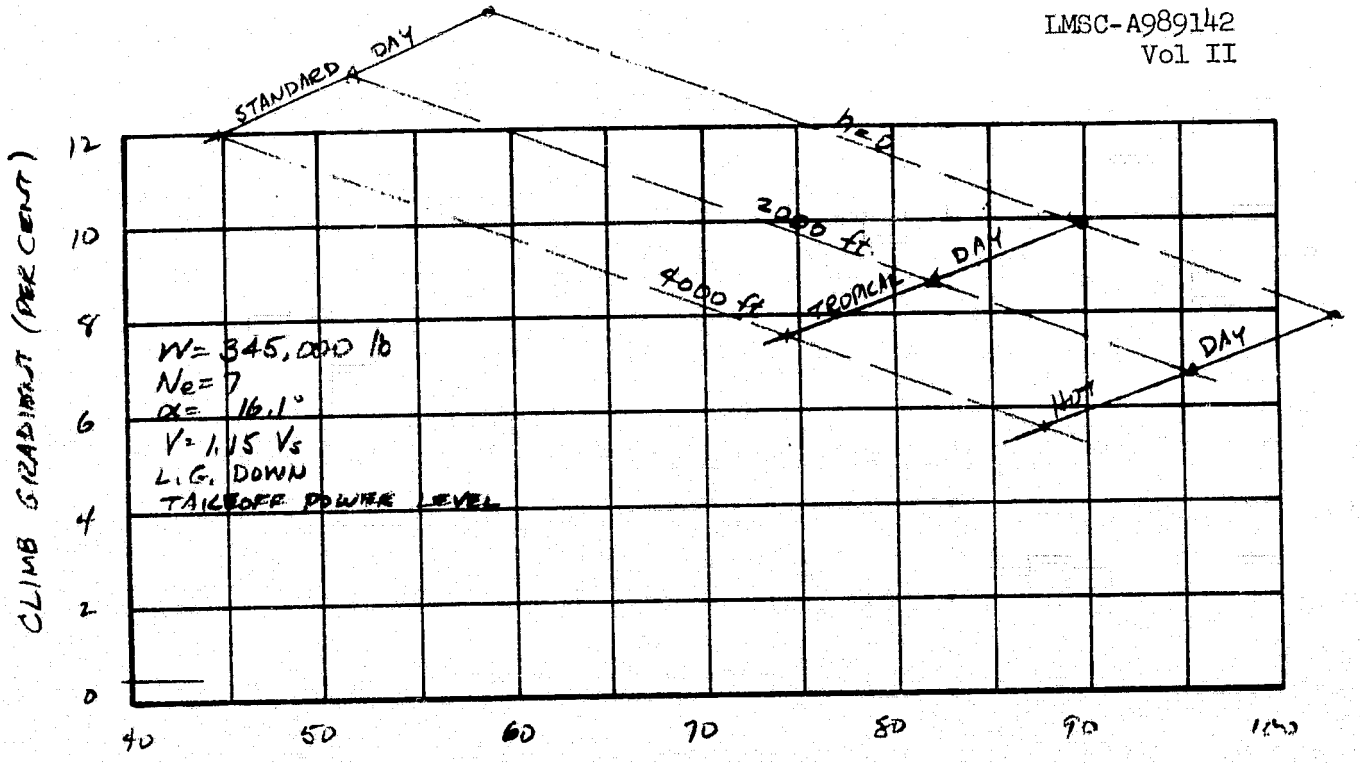

FIG. 2.4-57 CLIMB GRADIENTS

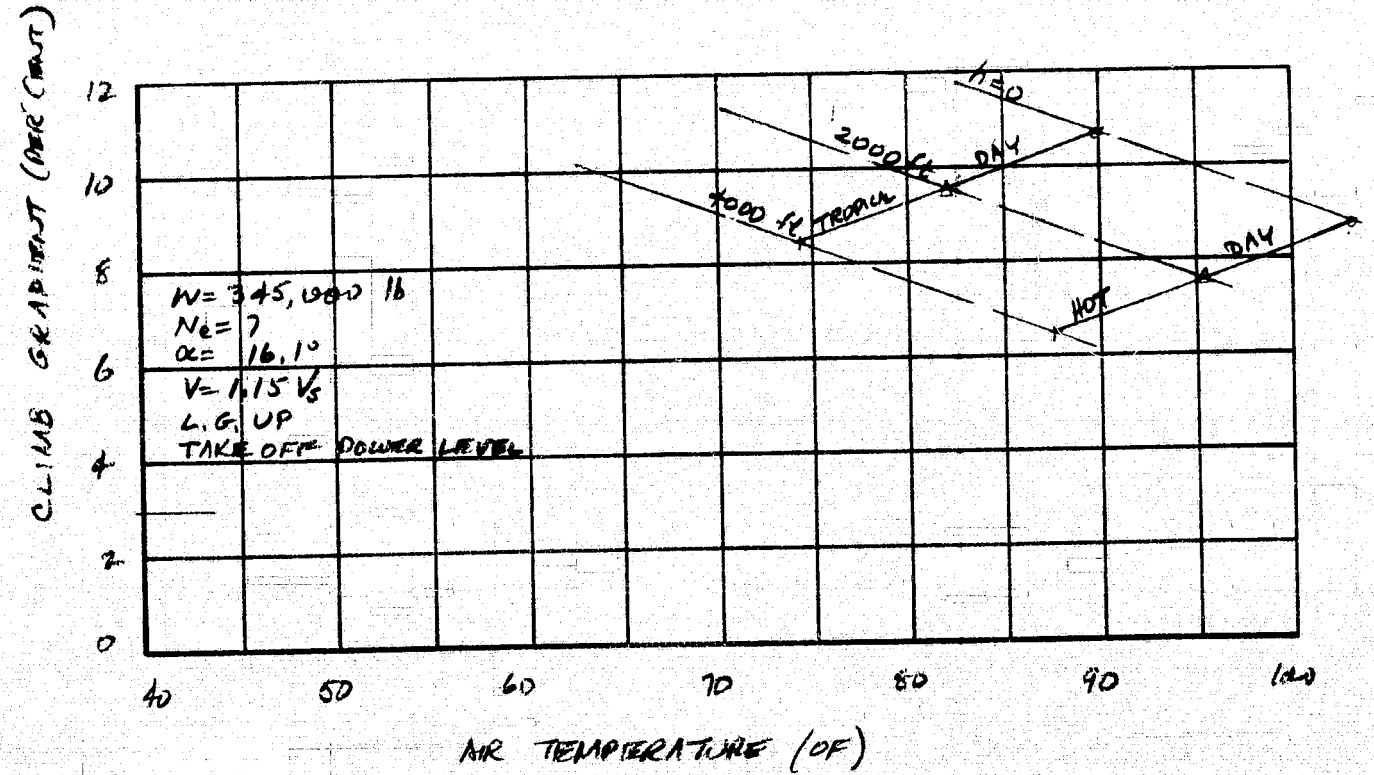

FIG. 2.4-58 CLIMB GRADIENTS

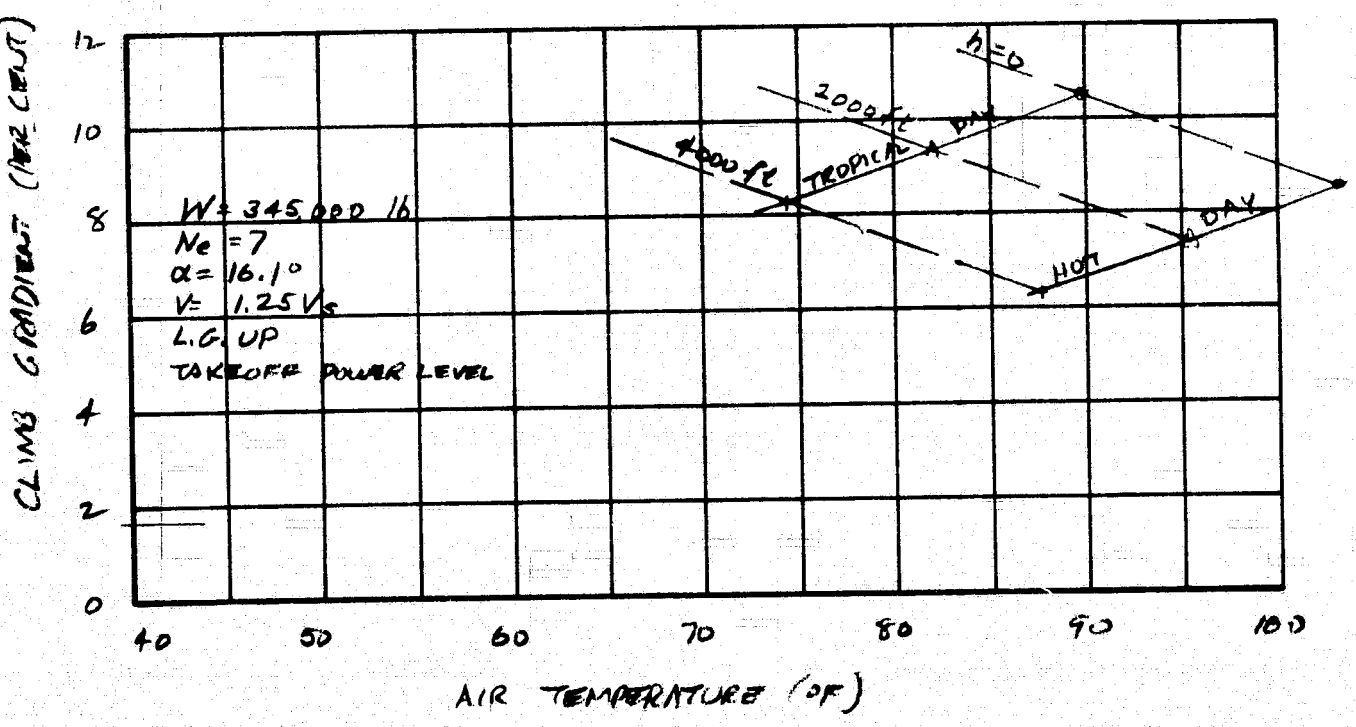

Fig. 2.4-59 Climb Gradients

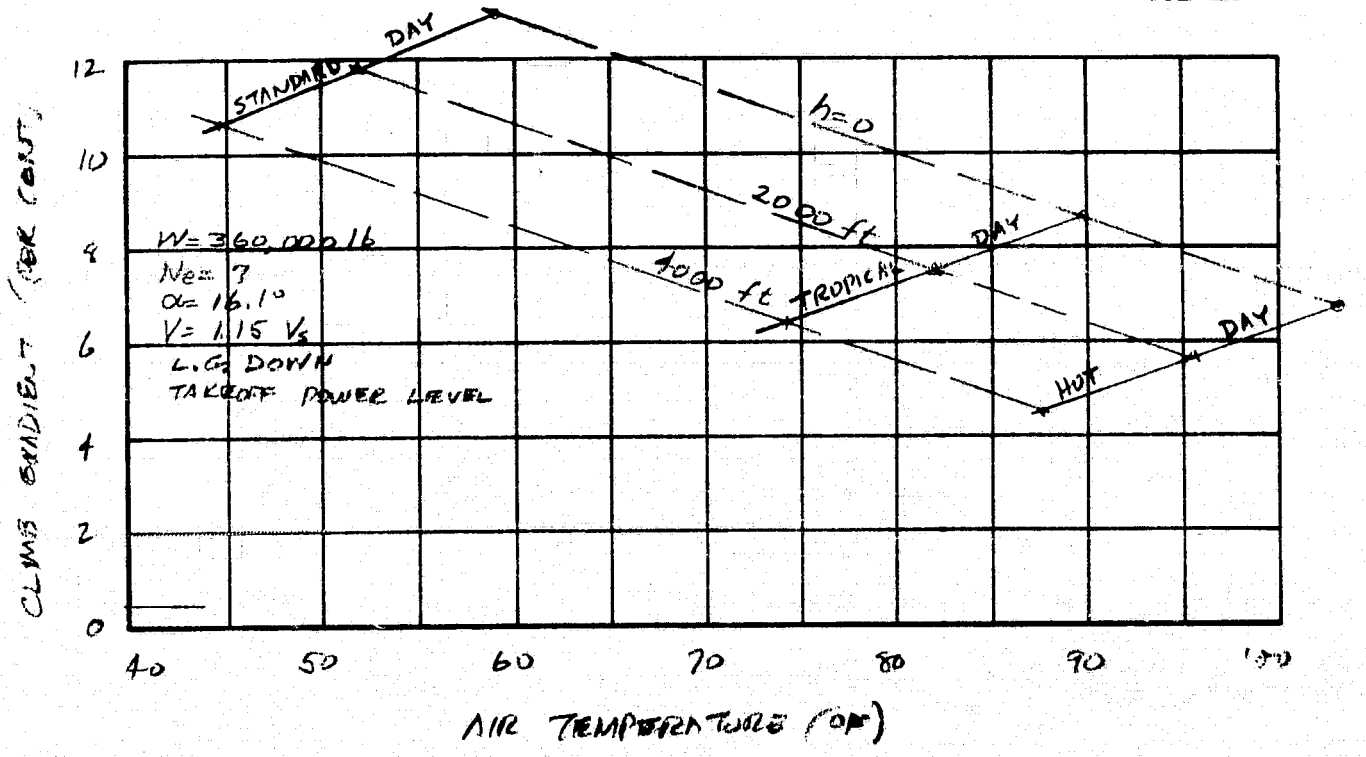

FIG. 2.4-60 CLIMB GRADIENTS

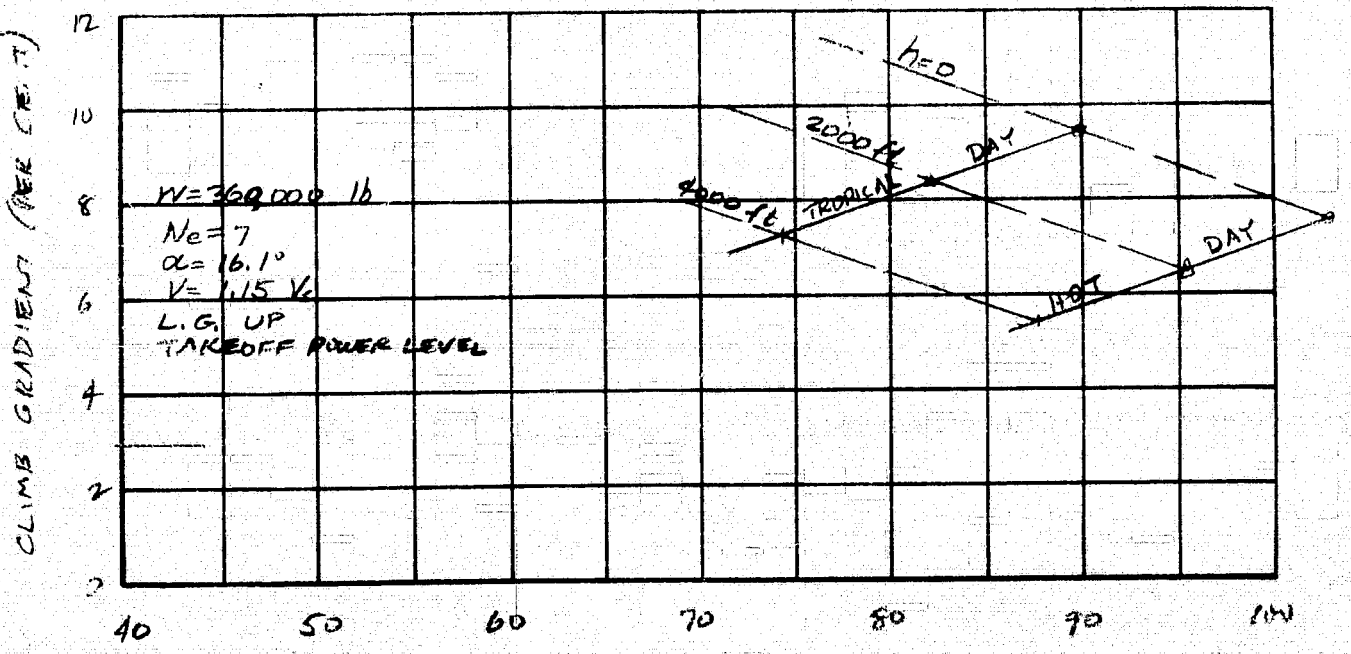

FIG. 2.4-61 CLIMB GRADIENTS

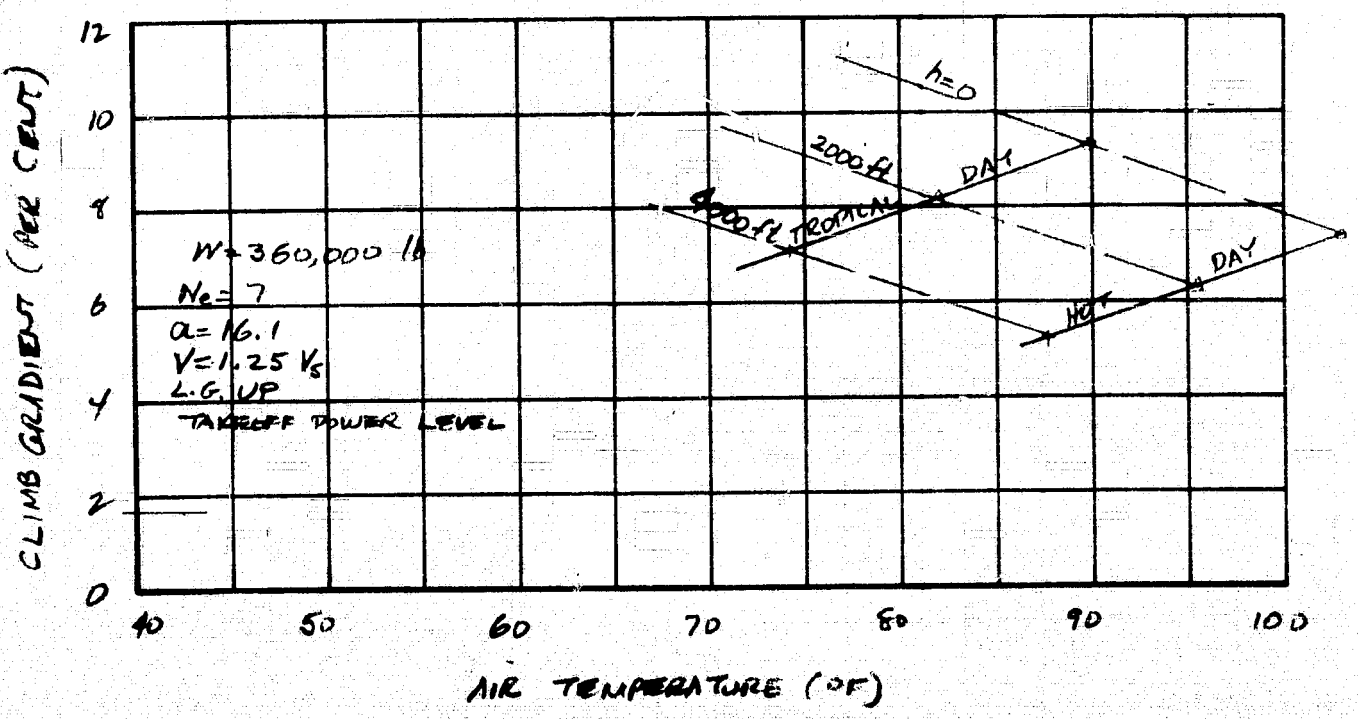

FIG. 2.4-62 CLIMB GRADIENTS

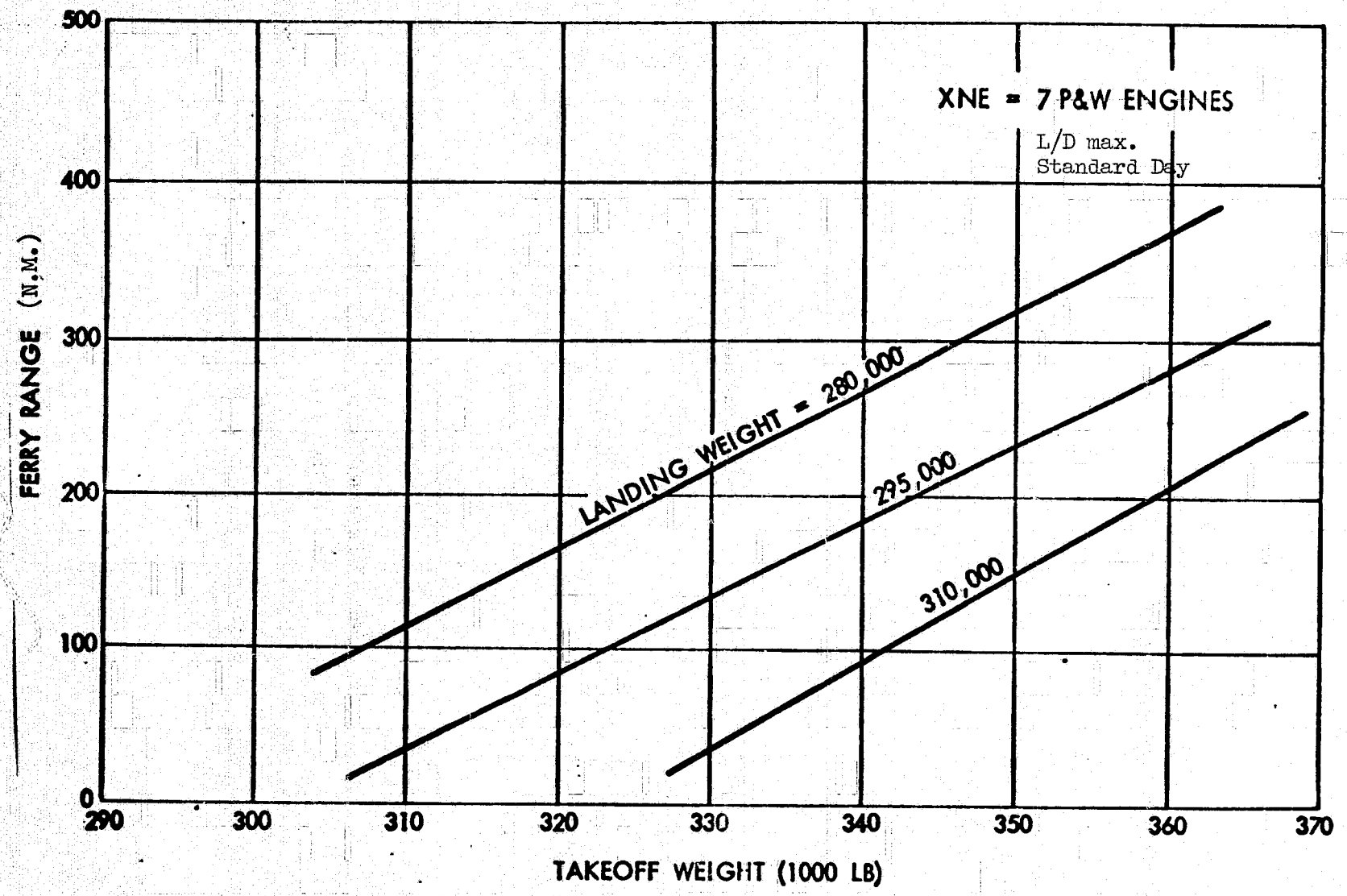

FIG. 2.4-63 **Stage-and-One-Half Ferry Capability**

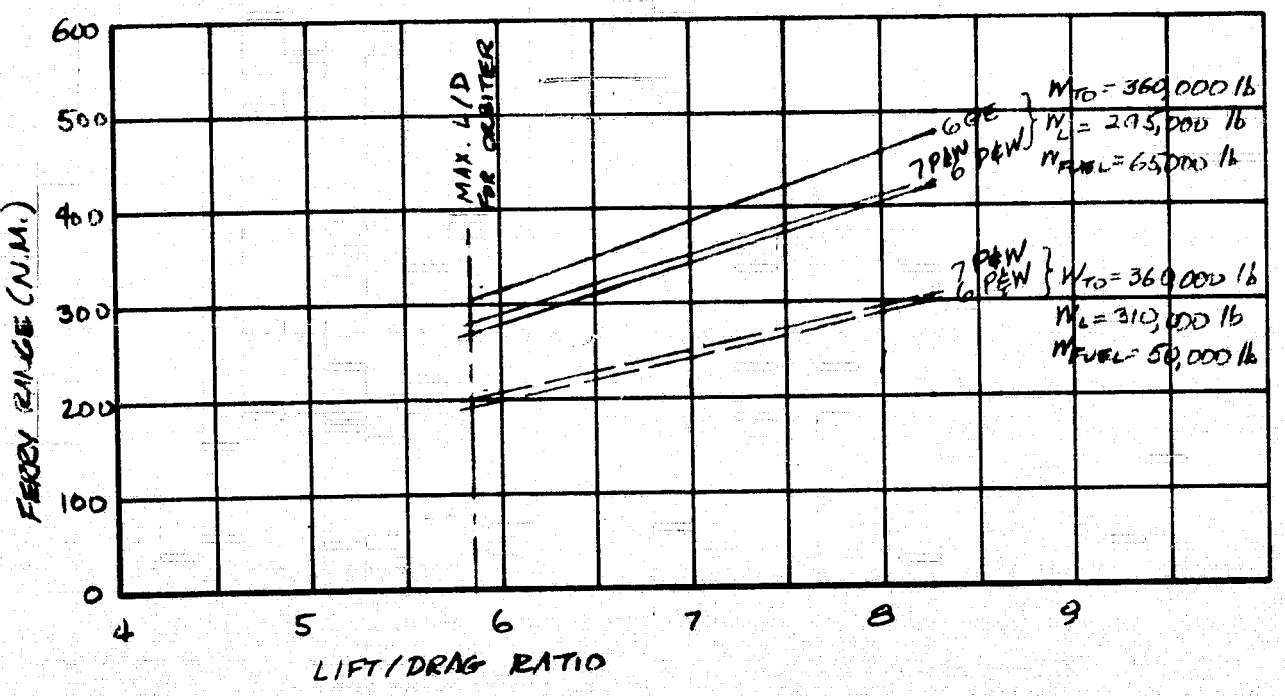

Fig. 2.4-64 Effect of L/D on Ferry Range

the climb-gradient requirements for the heavier takeoff weights, although all climb-gradients computed were positive.

FAR climb-gradient requirements for one engine inoperative are:

- Takeoff; landing gear attended: 0.5% (minimum)
- Takeoff; landing gear retracted: 3.0% (minimum)
- Final takeoff; enroute configuration: 1.7% (minimum)

2.4.7.7 Ferry Range. The ferry portion of the flight profile consists of a climb to cruise altitude, constant-altitude cruise between 17,000 and 18,500 ft, and a descent at flight idle power. Figure 2.4-63 shows ferry range for takeoff weights between 290,000 lb and 360,000 lb, and landing weights between 280,000 lb and 310,000 lb; the orbiter is assumed to be flying at maximum L/D for the particular aerodynamic characteristics selected.

Total ferry fuel is the difference between takeoff and landing weight with 7,000 lb allotted for descent and landing reserve and further reduction by the fuel consumed in 20 minutes of flight idle on the ground and one minute of full thrust for takeoff.

Figure 2.4-64 shows the effect of increased L/D on range for two engine types and two fuel loads. Increasing the number of engines from 6 to 7 results in a range increase of only about 10 nautical miles, but an increase in L/D provides nearly proportional increases in ferry range.

2.4.7.8 Landing. The landing segment consists of a flare, touchdown, derotation, nose-wheel touchdown, free roll, and braking to a stop, computed from groundrules and criteria commensurate with commercial airframe practice. Figure 2.4-65 shows the total landing distance from a 50 ft altitude to a full stop for landing weights between 280,000 lb and 330,000 lb. On the right-hand ordinate are two additional scales: the FAR field lengths for primary and alternate airports, computed by dividing the computed landing distance by 0.6 for primary and 0.7 for alternate airports.

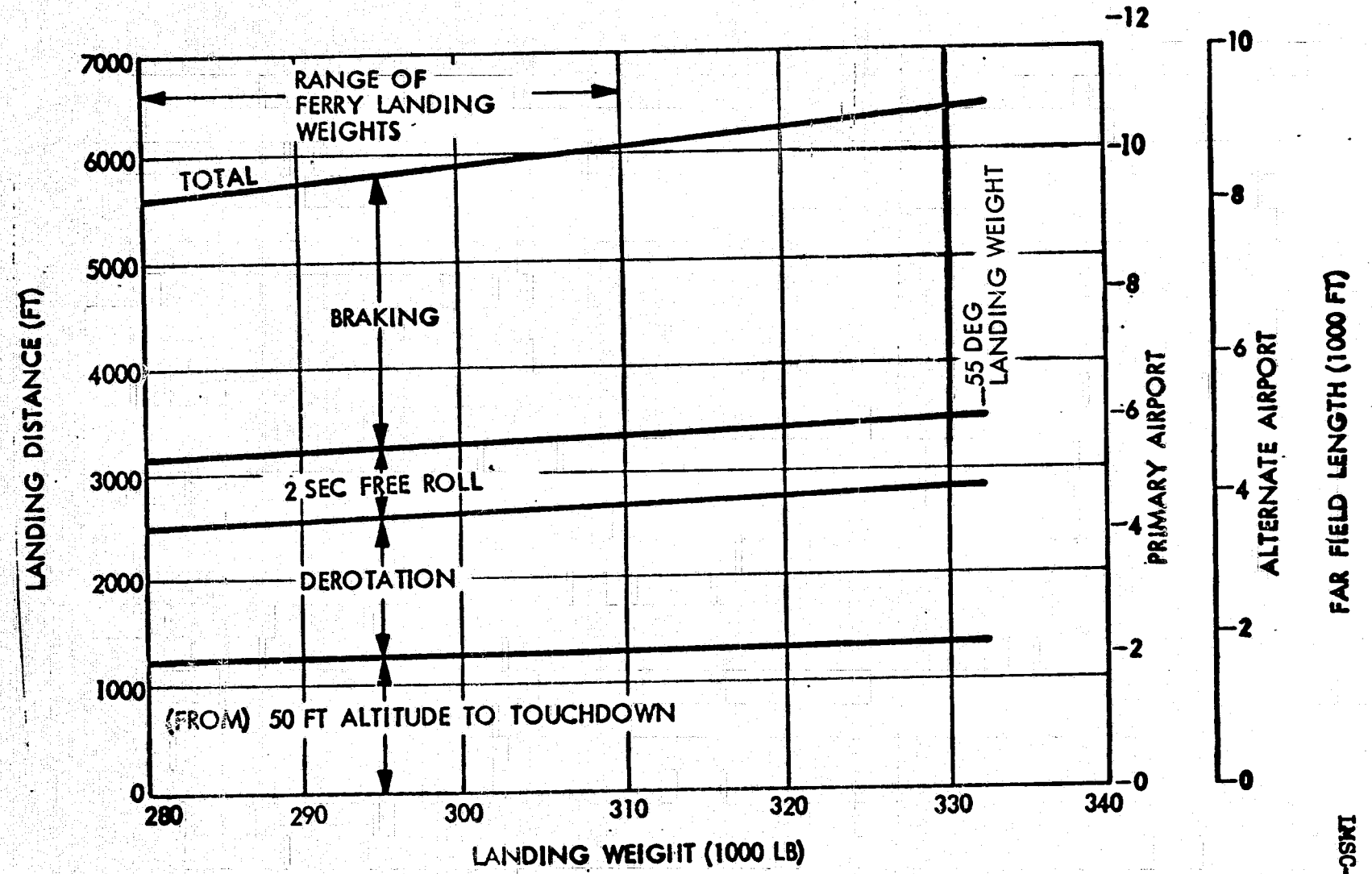

FIG. 2.4-65 **Ferry Performance Landing Distance**

2.4.7.9 Conclusions. The data show that a six-engine, 360,000 lb takeoff-weight orbiter can take off on a standard day from any anticipated airfield and can maintain satisfactory positive climb gradients for the same conditions. As ambient temperatures increase above "standard day" values, takeoff weights at high elevations become critical as shown in Fig. 2.4-42 where a reduction in takeoff weight must be made to satisfy balanced field length requirements.

The ferry range for a six-engine, 360,000 lb takeoff-weight orbiter is 270 nm for a "standard day." It may be concluded that no strap-on engines are required for standard day operations.

2.4.8 Performance Dispersions

All performance for the stage-and-one-half vehicle reflects the use of a 1-percent velocity reserve. This 300 ft/sec velocity reserve was included in the ascent velocity requirements to provide 3-sigma dispersion correctional capability.

To validate this velocity reserve, a preliminary performance dispersion study was conducted around the nominal ascent to 55 deg, 50 x 100 nm orbit. The dispersed trajectories were simulated with the PRESTO computer program. Consequently, these trajectories did not account for any magnification of the effects of the errors due to imperfect guidance. All perturbed ascent trajectories represented the optimum ascent trajectory corresponding to the particular error source which would not necessarily be true in reality. The degree of achiement in attaining the optimum trajectory would be a characteristic of the particular guidance system used and would depend on the guidance algorithms incorporated and the hardware tolerances and sensitivities used to implement the scheme. The same would be true of the navigation system on which guidance depends for state estimation.

While the guidance contribution to the individual velocity penalties associated with all errors was not included, its individual velocity penalty was considered. This estimate was taken from a previous study* in which the guidance and control equations were taken from those used successfully in the Poseidon and Agena inertial guidance systems. For the study, wind was used as the perturbing element to demonstrate the guidance system capability to reestablish nominal injection conditions. The resulting additional velocity required for nominal injection consisted of the effect of the wind and the response of the guidance system to this dispersion.

---

*LMSC-A955317A, "Space Shuttle Data, Volume VI, Performance and Flight Mechanics", 12 Sept 1969.

The optimum ascent trajectory with wind but without guidance simulation was generated to find the wind effect only. This additional velocity was subtracted from the additional velocity requirement with wind and guidance to yield the effect of guidance alone.

For this dispersion study, the guidance and control requirements was treated as an error in that the velocity contribution was root-sum-squared with the other error sources. Thus any coupling of the guidance and an actual error was disregarded. Actually some coupling should exist; however, it would differ depending on the error source. The ability of the guidance to correct for winds while keeping velocity losses low should be very demanding due to the randomness of this error source. Consequently, the velocity requirement due to guidance response found using winds should be about the largest requirement associated with any dispersion. For this preliminary study, treatment of the guidance response as an error acts as a good first approximation to a detailed closed-loop guidance simulation dispersion analysis.

The tolerances which were used for the various error sources were based upon engineering judgement. Exceptions to this were the propulsion tolerances of 10,000 lb thrust and 3 sec specific impulse per engine, which were design specifications.

Tolerances associated with error sources involving hardware items can be classified into three categories: (1) Batch, (2) Maiden Tag, and (3) Service Tag tolerances.

Batch tolerances are used to represent variations associated with the whole class of Space Shuttle vehicles. These tolerances define a 3-sigma performance reserve which has the ability to correct errors affecting performance 9,974 times out of 10,000. Using the performance reserve allows the performance to be defined for the whole shuttle class and represents the performance of

the worst shuttle in the class and in the worst environment. Because Batch tolerances apply to the whole group, they consequently possess the greatest magnitudes of the three categories.

Maident Tag tolerances apply to a specific shuttle vehicle prior to and shortly after its placement into service. Some of these tolerances are significantly smaller than the corresponding batch tolerances and are generally associated with the hardware items. One further subdivision may be made, that of reusable and expendable tolerances.

For the reusable components, tolerances will apply to the specific item and will reflect essentially the uncertainty in the measurements and the time variance which is different from the ensemble variance used for the batch tolerances. For example, thrust for a given engine will be known within the noise level of the measurement instruments. Deviations occurring from one sample firing to the next, however, will be uncertain due to the scarcity of this data.

Tolerances for expendable items contained in the Maiden Tag values may themselves be Batch or Tag (representing the specific item) values depending upon the degree of effort afforded to determine and incorporate tag values prior to each flight. For example, determining the propellant capacity of a droptank within measurement accuracy and incorporating this into a new reserve might not be worth the benefit.

Service Tag tolerances are a refinement of the Maiden Tag Reusable tolerances discussed earlier. As a shuttle is used, tag data may be reduced due to improved knowledge of the operating characteristics of a particular shuttle furnished from post-flight data. Maiden Tag Expendable tolerances would however be carried over to Service Tag and remain unchanged.

Table 2.4-61 presents the results of the dispersion study conducted on the stage-and-one-half. Error sources which are presented are grouped into six classes characterized by some commonality. The tolerances, where indicated, represent Batch values, while the algebraic sign represents which of the two possibilities produces a performance loss. The tolerance values shown would be reduced in the transition from Batch to Service Tag. Not all of the error sources would be changed from Batch to Tag; however, those contained within the vehicle and propulsion characteristics group as a rule would be changed.

The error sources given in Table 2.4-10 are generally self-descriptive; however, some items might require mention. Pre-liftoff propellant pertains to the variations in propellant (or time) between ignition of the motors and liftoff. The PU error reflects burning propellant at off-nominal mixture ratio and/or allowing a residual of fuel or oxidizer to occur. Launch azimuth accuracy applies to misalignment of the initial flight plane to the nominal plane. Finally, droptank separation time reflects carrying the droptanks after they are empty for the given time tolerance and includes two engines at half power for 10 sec plus the time tolerance.

The individual values of ΔV corresponding to each error source were obtained by (1) finding the additional (above nominal) amount of propellant required to obtain final orbit, and (2) multiplying this by the negative partial of velocity to burnout weight, which was 0.041 ft/sec/lb. The thirteen error contributions were then root-sum-squared (RSS) to obtain the performance reserve.

It is interesting to note that if the guidance were not treated as a separate error and if the same ratio of ΔV-without to ΔV-with guidance simulated found for winds (0.75) were applicable to all errors, then the RSS value would approximately equal the 1 percent nominal velocity used for performance. This however, would represent a conservative estimate, since the ratio would not be constant, and some of the twelve error contributions are unaffected by guidance, as for example, the propulsion utilization (PU) error.

Table 2.4-10 Dispersion Studies - Ascent Stage-And-One-Half

VEHICLE CHARACTERISTICS	ΔV (FPS)
Tank Weight (+3%)	50
Tank Propellant (-.5%)	60
Orbiter Weight (+.5%)	52
Orbiter Propellant (-.5%)	9
Drag (+10%)	41

PROPULSION CHARACTERISTICS	ΔV (FPS)
Thrust (10000#/Engine)	96
Isp (-3 Sec/Engine)	114
PU Error (0.5% Error)	17

PRE-LIFTOFF TOLERANCE	ΔV (FPS)
Drop Tank Propellant (-.1%)	12

ATMOSPHERE CHARACTERISTICS	ΔV (FPS)
Winds (Tail	112

GUIDANCE AND CONTROL	ΔV (FPS)
	38

MISCELLANEOUS

$$\Delta V_{FPR} = \sqrt{\Sigma (\Delta V)^2} = 217 = 0.72\% \text{ Nominal Ascent Velocity}$$

LOCKHEED MISSILES & SPACE COMPANY

2.5 SYSTEM DESIGN

2.5.1 LS 200-5 System

The recommended stage-and-one-half configuration system, presented at the mid-term review on 1 Dec 1970, was designated as Model LS 200-5. The design layout work documenting the physical definition of this arrangement is shown in the following drawings:

1. Launch Vehicle
   Delta-Body Stage-And-One-Half
   Model LS 200-5
   SKS 100022(A) - Fig. 2.5-1

2. General Arrangement
   Delta-Body Stage-And-One-Half
   Model LS 200-5
   SKS 100021 - Fig. 2.5-2

3. Structural and Plumbing Arrangement, Aft Section
   LS 200-5 Stage-And-One-Half
   SKG 100110 (A) (3 sheets) - Fig. 2.5-3

4. Alternate Nose Section
   Delta-Body Stage-And-One-Half
   Model LS 200-5
   SKS 100026 - Fig. 2.5-4

5. Plumbing System, Main Propulsion
   Delta-Body Stage-And-One-Half
   Model LS 200-5
   SKT 100218 - Fig. 2.5-5

6. Drop Tank Assembly
   Delta-Body Stage-And-One-Half
   Model LS 200-5
   SKT 100219 - Fig. 2.5-6

7. Separation System - Droptanks
   Delta-Body Stage-And-One-Half
   Model LS 200-5
   SKN 100303 - Fig. 2.5-7

8. Inboard Profile
   Delta-Body Stage-And-One-Half
   Model LS 200-5
   SKS 100023 (3 sheets) - Fig. 2.5-8

9. Passenger Space Allocation 12-Men Arrangement
   Delta-Body (Typical)
   Model LS 200-5
   SKT 100035 - Fig. 2.5-9

The launch vehicle concept shown in drawing SKS 100022-Rev. A (Fig. 2.5-1) indicates an arrangement with an overall length of approximately 222 ft, a span of approximately 92 ft, and a width (launch attitude) of approximately 36 ft. The locations of the three-point droptank-to-orbiter attachments are shown, as well as the locations of the principal system center-of-gravity conditions of interest with respect to the rocket engine and droptank aft hinge point positions. The droptank size is based on a 26 ft diameter cylinder, which results in a set of tanks approximately 190 ft long.

The model LS 200-5 Delta-Body Orbiter with a 146 ft reference length (approx. 152 ft overall) is shown in the general arrangement drawing SKS 100021 (Fig. 2.5-2). The orbiter has an approximate 92 ft span and stands some 43 ft

high, while in the static landing attitude. Principal propellant volumes and aerodynamic control surface areas are shown, along with their relative locations.

Integration of the principal systems located in the aft section of the orbiter is shown in drawing SKG 100110 (Fig. 2.5-3). The relative positions of the thrust structure, the ascent and orbit rocket engine systems, the droptank-to-orbiter aft attachment fittings, the main rocket engine plumbing lines, the ascent and orbit propellant tankage and support structure, the jet engine, main landing gear, and lower flap/elevon control surface stowage bays, fin spar attachment structure, and typical heat shield/airframe arrangement are shown with respect to each other.

Drawing SKS 100026 (Fig. 2.5-4) shows a possible alternate concept to the drop tank-to-orbiter LOX line arrangement. A single oxygen line is indicated, requiring a single disconnect.

The candidate concept for the main rocket engine system plumbing arrangement is shown in drawing SKT 100218 (Fig. 2.5-5) and indicates the dual droptank-to-orbiter oxygen lines entering the spacecraft at the nose section. The fluid, vent, and pressurization disconnects located in the aft end are shown in their relative locations with respect to the droptank attach fitting and the orbiter tankage and manifolding.

A droptank assembly drawing SKT 100219 (Fig. 2.5-6) shows the dropable tank arrangement concept for the Model LS 200-5 stage-and-one-half system. It consists of two tank assemblies interconnected to form a single system arranged in a V-type configuration. The design details are similar to those described for the droptanks reported in the fourth letter progress and status report (1 Oct to 1 Nov 1970) except as follows:

- The droptank geometry is compatible with the Model LS 200-5 orbiter.
- The droptank-to-orbiter oxygen lines enter the orbiter at the nose.
- The aft attachment fittings reflect the separation concept of tanks rotating up and aft with respect to the orbiter.
- The valve disconnect planes are perpendicular to the separation motion.
- The polyurethane insulation is essentially removed from the intertank structure, while the foam insulation thickness around the hydrogen tank has been increased.

Drawing SKN 100303 (Fig. 2.5-7) illustrates the aft separation system concept associated with the droptank arrangement for the Model LS 200-5. Two concepts of plumbing line separation are shown: the mechanical separating valve is the baseline approach and an ordinance-type system, using a pyrotechnic device, is an alternate concept.

An inboard profile of the Model LS 200-5 orbiter system is shown in drawing SKS 100023 (Fig. 2.5-8).

Space allocation for a possible 12-man arrangement, in which all the passengers are located in the nose section of a typical stage-and-one-half or two-stage orbiter, is shown in Design Drawing SKT 100035 (Fig. 2.5-9).

Design descriptions of major systems of the stage-and-one-half concept are illustrated by layout work performed on the earlier Model LS 200-3 arrangement. From a design standpoint, this arrangement is essentially the same as the LS 200-5. The following drawings portray these typical arrangements similar to both systems:

1. Launch Vehicle
   Delta-Body Stage-And-One-Half
   Model LS 200-3
   SKS 100014 - Fig. 2.5-10

2. General Arrangement
   Delta-Body Stage-And-One-Half
   Model LS 200-3
   SKS 100013 - Fig. 2.5-11

3. Droptank
   General Arrangement Stage-And-One-Half
   Model LS 200-3
   SKT 100206 - Fig. 2.5-12

4. Engine Gimbal Pattern
   Delta-Body Stage-And-One-Half
   Model LS 200-3
   SKS 100205 - Fig. 2.5-13

5. Contour Lines
   Delta-Body Stage-And-One-Half
   Model LS 200-3
   SKS-100011 - Fig. 2.5-14

6. Structural Arrangement (Basic)
   Delta-Body Stage-And-One-Half
   Model LS 200-3
   SKG 100106 - Fig. 2.5-15

7. Thrust Structure Concept
   Delta-Body Stage-And-One-Half
   Model LS 200-3
   SKG 100109 - Fig. 2.5-16

8. Major Structural Breakdown
   Delta-Body Stage-And-One-Half
   Model LS 200-3
   SKG 100107 - Fig. 2.5-17

9. Basic Load Paths
   Delta-Body Stage-And-One-Half
   Model LS 200-3
   SKG 100108 - Fig. 2.5-18

10. Visibility Study
    Delta-Body Stage-And-One-Half
    Model LS 200-3
    SKS 100010 - Fig. 2.5-19

11. Plumbing System - Main Propulsion
    Delta-Body Stage-And-One-Half
    Model LS 200-2, Baseline
    SKT 100211 - Fig. 2.5-20

12. Propellant Tank Space Allocation
    Delta-Body Stage-And-One-Half
    Model LS 200-3
    SKG 100210 - Fig. 2.5-21

13. Rocket Engine Arrangement
    Delta-Body Stage-And-One-Half
    Model LS 200-3
    SKT 100212 - Fig. 2.5-22

14. ACPS Aft Thruster Cluster
    Delta-Body Stage-And-One-Half
    Model LS 200-3
    SKS 100209 - Fig. 2.5-23

15. Flap Stowage Concept
    Delta-Body Stage-And-One-Half
    Model LS 200-3
    SKS 100015 - Fig. 2.5-24

16. Jet Engine Deployment Concept
    Delta-Body Stage-And-One-Half
    Model LS 200-3
    SKS 100302 - Fig. 2.5-25

17. Landing Gear Concept
    Delta-Body Stage-And-One-Half
    Model LS 200-3
    SKH 100301 - Fig. 2.5-26

An advanced launch vehicle general arrangement was configured and is shown in drawing SKS 100014 (Fig. 2.5-10). This arrangement constitues the Model LS 200-3 version of the candidate high-crossrange stage-and-one-half vehicle system. The vehicle has an overall length of 223 ft and width of approximately 88 ft. Indicated on the drawing are the nominal line of thrust of the multiple rocket engine system and its relationship to the various estimated system center of gravity locations and the general location of the droptank-to-spacecraft forward and aft attachment points. An overall height of 35 ft (end view) is also indicated.

The launch vehicle arrangement has the following design features:

- Over-the-top separation

- Aft D/T to S/C pivot tie connection is mounted directly to the rocket thrust structure
- System centers of gravity are approximately in-line with the nominal engine thrust line and the D/T aft pivot ties
- D/T empty center of gravity is well above the D/T aft pivot ties
- The propellant system plumbing disconnects are installed so that the disconnecting motion is in the same plane as the separation motion

The orbiter general arrangement is illustrated in drawing SKS 100013 (Fig. 2.5-11) for the Model LS 200-3 system. This drawing also serves as a cursory inboard profile, as the major internal components are indicated through the use of hidden lines. This drawing gives an overall view of the lifting body approach to the high-crossrange concept and differs from the baseline arrangement (SKS 100007 - Model LS 200-2) described in an earlier monthly report with regard to the following basic areas:

- The aft fuselage lower ramp is removed resulting in a straight bottom surface as shown. This change in body contour lines required the relocating of the rocket engine system and the upper surface boat-tailing
- Provisions are made for the stowage of the lower flap and elevon system during the launch and ascent modes of operation
- The nose gear is located further forward to enhance the integration of the fuselage structural frames needed to support both the nose gear and the crew compartment.
- The general location of the attitude control propulsion system thrusters is indicated in both the nose and aft sections of the fuselage

Drawing SKT 100206 (Fig. 2.5-12) describes the general arrangement of the droptank system for the Model LS 200-3. The changes over the baseline approach (SKT 100204) include:

- Relocation of the tank system with respect to the orbiter to enhance the natural separation geometry and to permit separation over-the-top and aft
- Aft and forward droptank attach points were relocated
- Tank diameter was reduced to reduce manufacturing requirements and to reduce the frontal drag of the total launch vehicle configuration

The general locations of the droptank attachment points are shown. The drawing indicates the three-point attachment system and the geometry associated with the droptank/orbiter separation scheme. This scheme is the same as described in the second monthly report except that the separation motion is to rotate the tank system up and aft with respect to the orbiter.

The intertank tie and the droptank-to-spacecraft forward attachment have been integrated and are shown on this drawing. The intertank tie resists shear and torsional loads but permits tank contraction due to the cryogenic propellant environment. The pivot pin consists of a triangular hangar-type arrangement to which a pin-ended link is attached. This link is connected to a fitting installed in the nose of the spacecraft and resists loads only in the pitch direction. The total integrated structural tie arrangement has been configured to be installed in the intertank structural area only.

The rocket engine gimbal pattern is shown in drawing SKS 100205 (Fig. 2.5-13). The five center engines are presently gimballed and a ± 7 deg square gimbal pattern is available as shown for each of these engines along with the requirement that any engine-out condition within these five would result in that engine being centered and stowed in its neutral position. No gang gimballing is required with this arrangement (ϵ = 53:1). The baseline location of the orbital maneuvering (RL-10) rocket engine system is indicated with ± 4 deg gimballing available. An alternate installation of this system

is shown along with the estimated locations of the various centers of gravity of interest. This alternate location implies a fixed installation of the RL-10 engines with any center of gravity excursions compensated for by the use of the attitude control propulsion system.

The Model LS 200-3 orbiter contour lines are shown in Drawing SKS 100011 (Fig. 2.4-14). The dash 3 system differs primarily from the baseline (SKS 10000 6) Model LS 200-2 with respect to the aft fuselage section in that the lower aft ramp has been eliminated.

A basic structural arrangement for the Model 200-3 orbiter configuration is shown in drawing SKG 100106 (Fig. 2.5-15). This drawing indicates the location of the main structural bulkheads, frames, rings, longerons and spars. The rocket engine thrust structure is omitted as it is shown in relatively more detail in drawing SKG 100109 (Fig. 2.5-16).

The airframe construction is similar to conventional aircraft except for the fuselage frames which are arranged external to the primary load-carrying skin. This is done to provide a base to which the aerodynamically shaped thermal protection heat shield panels can be conveniently attached. For descriptive purposes, the airframe structure is conveniently divided into four basic aerodynamically shaped sections. These sections are individually depicted in drawing SKG 100107 (Fig. 2.5-17). This drawing is similar to SKG 100101, described in the second monthly progress report, and reflects principally a change in the location of the droptank attachment points. Drawing SKG 100108 (Fig. 2.5-18) is an update of the Model LS 200-3 general arrangement changes.

Drawing SKG 100109 (Fig. 2.5-16) is the initial layout of the thrust structure concept required on the Model LS 200-3 spacecraft. The thrust structure geometry is determined chiefly by the rocket engine locations and the shape

of the delta-body aft section. The major structural elements for the thrust structure consist of two span wise beams and six vertical trusses. To accommodate the engine gimbal fitting attachments, the lower beam is straight and the upper spanwise beam is bent. Both beams are I-beams of conventional riveted construction which consist of T-section caps, Z-section web stiffeners spaced approximately on 24 in. centers with additional stiffeners added where concentrated loads are introduced, and a thin sheet material web. The vertical trusses are located to accommodate the engine gimbal fittings associated with the lower bank of rocket engines (the upper bank of rocket engines is attached on the upper spanwise beam at points midway between the vertical trusses). All the trusses are built up of elements consisting of I-beam weldments for the front and rear chords, circular tubes for most of the horizontal and diagonal members, shear-connected angles to the intersecting spanwise I-beam webs, and end fittings integral with the end members of the truss assembly. Support attachment lugs are provided for the gimbal actuators, engine stabilizer struts and spacecraft propellant tankage support struts on the appropriate beam or truss. For the upper bank of engines, the pitch gimbal actuators or stabilizer struts are attached to the base heat shield mounted lug system which is stiffened and reinforced locally with diagonal braces (not shown) to the beams. The base heat shield is essentially mounted to the smooth backfaces provided by the T-section aft caps of the spanwise beams and the I-beam aft chords of the vertical trusses. The base heat shield also serves as the shear material, preventing any translation of the beam system in a sideways direction.

A preliminary manufacturing sequence consists of the following:

- TIG machine weld the trusses in fixtures
- Set-up trusses in a jig to assure mating with the spacecraft airframe
- Assemble the spanwise beam webs to the trusses with mechanical fasteners/rivets

- Rivet the beam caps to the webs and fasten to the trusses with splice plates
- Install spacecraft tank support struts

The thrust structure is attached to the body shell in this concept at twenty (20) places: One (1) at each forward end of each truss (12); and one (1) at each end corner (cap) of each spanwise beam (8). Material implied here is titanium 6AL-4V.

Drawing SKS 100010 (Fig. 2.5-19) illustrates the potential pilot visibility associated with this configuration. A landing approach vision plot is shown for the side-by-side pilots' arrangement and windshield opening assumed. The vision evaluation includes the view of a 300 x 10,000 ft runway on a 3-deg glide slope at distances from runway end of 1 mile, 1/2 mile, and 1/4 mile. The specific pilot stations, fuselage angle with relation to the horizon, and the approximate rate of closure in feet per second are indicated. The angle of incidence throughout the assumed windshield panels is approximately 45 deg directly in front of the pilots and increases to approximately 60 deg at angles left and right of the pilot's design eye position. The actual windshield area will be determined after a consideration of pilot and structural weight analysis trade studies.

The baseline concept to the main rocket engine system plumbing arrangement is shown in drawing SKT 100211 (Fig. 2.5-20). The baseline launch vehicle configuration (Model LS 200-2) was used as this layout was initiated before the dash three model was started. The only basic change in the plumbing would be the relocation of the disconnects between the droptanks and the spacecraft to a more favorable position; namely, on top of the spacecraft.

The plumbing concept illustrated in this drawing is one in which the oxidizer is cascaded from the droptank system, through the spacecraft tankage, and then fed to the engines. The fuel system is a manifolded concept in which the fuel during droptank operation is routed directly to the spacecraft hydrogen manifold system and out to the individual engines, while after drop tank separation, the fuel is fed from the spacecraft tankage to the manifold and out to the operating engines. To accommodate this system approach the following design considerations were necessary:

- The hydrogen manifold system incorporates the necessary isolation valves to shut off all the lines except those associated with the three remaining engines and the spacecraft fuel tanks after the drop tank is separated and the eight outboard rocket engines are shutdown.
- The spacecraft oxygen ascent tanks are interconnected to permit the feeding of oxidizer to the eleventh rocket engine as well as to form the lower half of the oxidizer circulation system line to prevent gysering associated with the long slender oxidizer lines shown on the droptanks. The droptank oxidizer tanks are plumbed together as shown at the bottom of the tanks to form the other half of the oxidizer circulation system.
- The system fill lines are layed-out with the fill valves located as close as possible to their respective engine feedline assemblies with the remaining line arranged to allow for draining after the fill operation.
- The oxidizer vent is located at the base of the spacecraft as a result of striving to install all expensive valves (LOX pressurization quad valve) on the spacecraft, and to minimize heat shield penetrations.
- The fuel vent line is routed out the base and is provided with a coupling to permit connection with the ground facility vent stack system.

- Sloping lines are used to provide a gravity drain between tanks, manifolds, and engines.
- Single point filling of the total launch vehicle is provided for both fuel and oxidizer systems. The oxidizer tanks are filled in a reverse cascade manner, while the fuel tanks are filled in parallel with liquid sensors controlling the necessary tank shutoff valves when the tanks are full.
- The pressurization systems for the oxidizer and fuel are similar, as liquid oxidizer, and fuel is changed to gas at each rocket engine and then plumbed through the appropriate system of tie rod bellows into individual manifolds and then routed by a single line system to the tops of the required tankage. For the gimballed engines (5) a set of three tie-rod bellows is used on the outlet pressurization lines to allow for contraction and for gimballing. On the fixed engines, only one tie-rod bellows is necessary for the contraction motion.

Drawing SKG 100210 (Fig. 2.5-21) is an indication of the location, size, and shape of the spacecraft propellant tankage necessary for the Model LS 200-3 concept.

Drawing SKT 100212 (Fig. 2.5-22) is a rocket engine arrangement for the Model LS 200-3 orbiter. The engines have been relocated as a result of the change in orbiter contour lines and the engines are installed on a common fuselage station as a result of the more favorable center of gravity history reflected by the new droptank to spacecraft arrangement.

To provide a three-axis translation system and a three-axis attitude control system for the spacecraft, it appears necessary to deploy certain thrusters for operation. In the Model LS 200-3 arrangement, a concept for doing this is shown in drawing SKS 100209 (Fig. 2.5-23) for the aft thruster cluster

located on the side of the spacecraft. During the reentry mode of operation, this set of thrusters is not needed and is retracted within the spacecraft.

The concept for retracting the lower flap/elevon system into the spacecraft base area is shown in drawing SKS 100015 (Fig. 2.5-24). The control surfaces assembly is stowed so that no portion is aft of the rocket engine nozzle exit planes during ascent operation. The stowage geometry is similar to aircraft flap systems and was chosen to permit extension into the operating position with the least disturbance to the vehicle during a possible abort condition.

The conceptual method of deploying the spacecraft jet engine system is illustrated in drawing SKS 100302 (Fig. 2.5-25). The five (5) jet engines are door-mounted and the single door is deployed using a parallelogram linkage system. The engine intakes are approximately the same height above the ground as those installed on present-day commercial jet aircraft.

Drawing SKH 100301 (Fig. 2.5-26) illustrates the landing gear concept applicable to the stage-and-one-half orbiter system and specifically to the Model LS 200-3 spacecraft.

Shown is a conventional tricycle landing gear arrangement with approximately 90 percent of the weight of the spacecraft supported by the main gear system. Ample load during dynamic conditions is available on the nose gear to permit nose wheel steering. The basic gear geometry is shown with respect to the estimated center of gravity position and a stable gear is provided for ground operation.

The nose gear system consists of a shock strut (air-oil system), drag brace, side braces, jury strut, torque scissors, retraction/extension actuator, and dual wheels kinematically arranged to permit a fore-and-aft retraction and

extension motion which provides free-fall capability to the system. A rack-and-pinion steering system is indicated to permit a steering angle of approximately ± 60 deg. A jacking point and toe lug is shown to accommodate ground operations. Tire sizes chosen and listed are capable of 275 mph ground speeds and are currently used on modern jet aircraft.

The main landing gear system is similar kinematically to that of the nose gear. A 4-wheel bogie truck is employed with wheels arranged in a dual-tandem pattern. To prevent porpoising during brake applications, a set of brake equalizing rods is installed. To position the bogie truck for the stowage condition, a positioning spring would be employed (not shown) and mounted between the pivotable truck and the shock strut. An antiskid system would also be installed to prevent incipient skidding and therefore provide for more efficient system braking. Ground operation handling points such as towing and tie-down lugs are provided. The tires selected are capable of operating at maximum ground speed of 250 mph, and are currently used on a commercial supersonic transport.

A preliminary set of basic loads is shown for the typical landing and ground conditions of interest.

To indicate the compatibility of this landing gear system to modern jet aircraft airfields, a set of examples for a rigid and flexible pavement system is shown for this dual-tandem arrangement. The pavement design procedure is the current approach used by the FAA.

REPRODUCIBILITY OF THE ORIGINAL PAGE IS POOR.

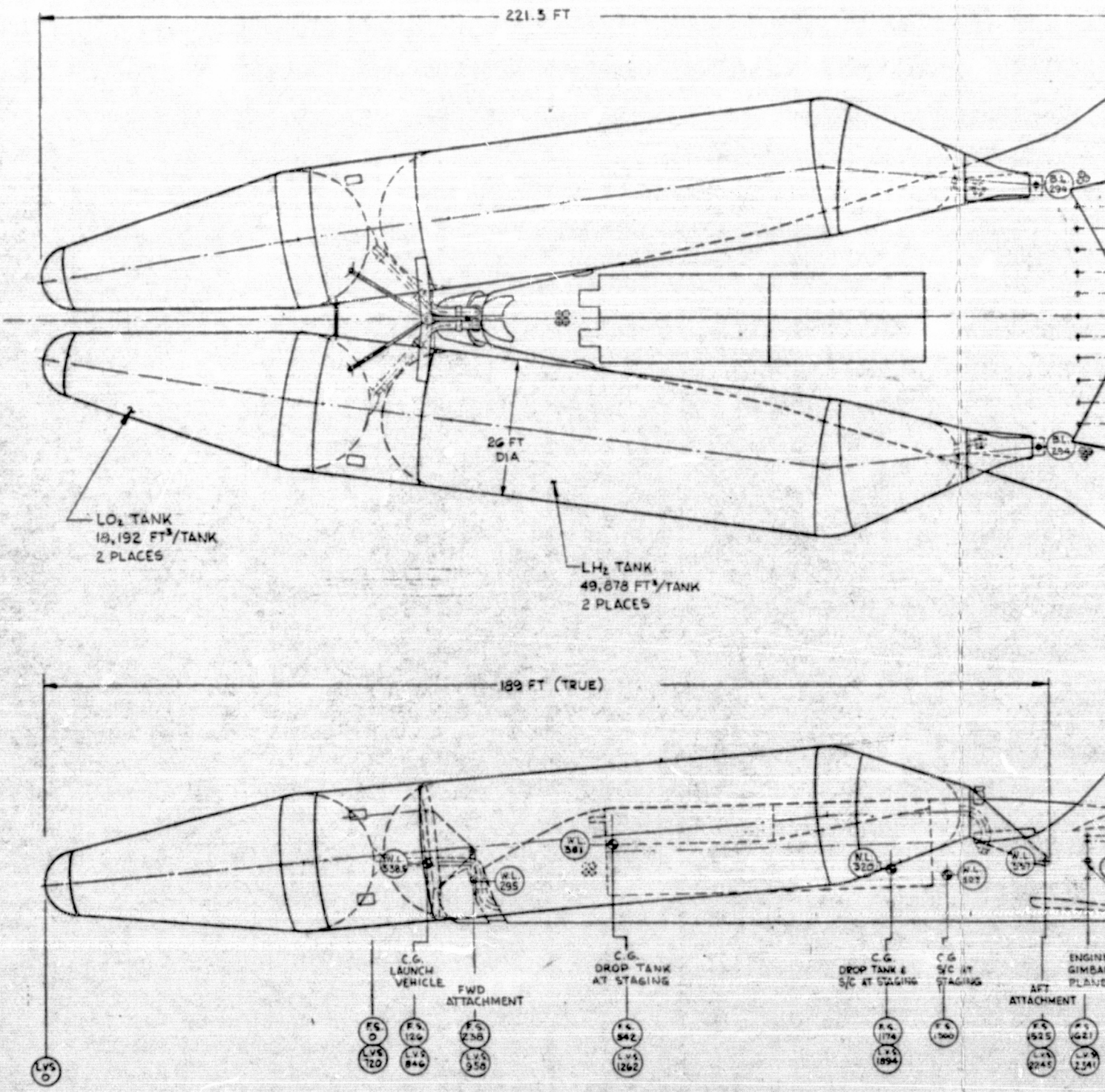

NOTES:
1. C.G. LOCATIONS ARE PRELIMINARY ESTIMATES.

FOLDOUT FRAME

REPRODUCIBILITY OF THE ORIGINAL PAGE IS POOR.

LIMITED CALENDAR LIFE	LIMITED OPERATING LIFE

REVISIONS				
ZONES	TR	DESCRIPTION	DATE	APVD
	A	C.G. LOCATIONS UPDATED		

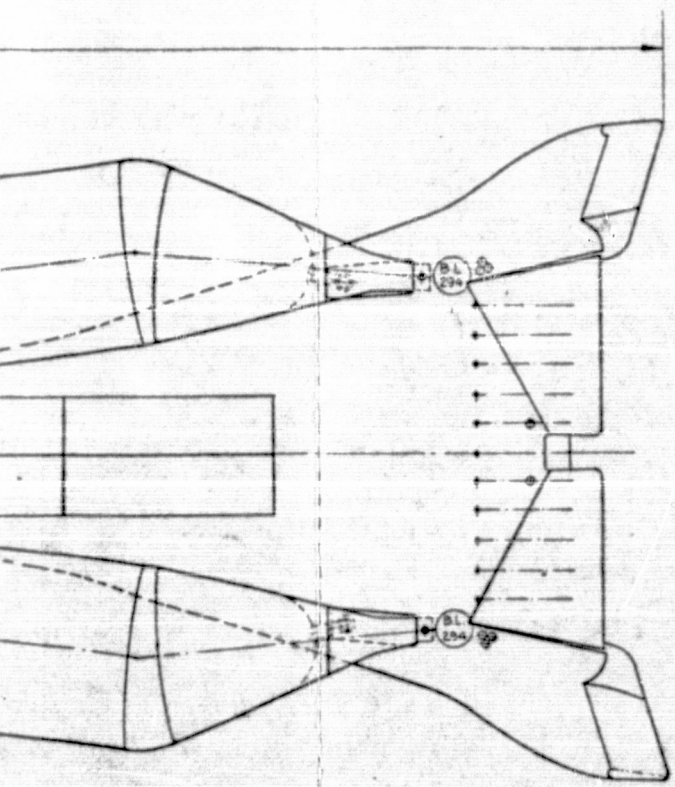

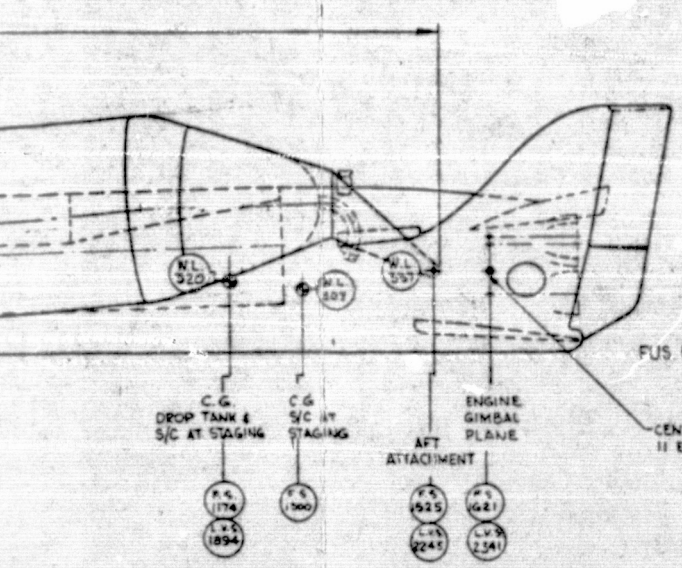

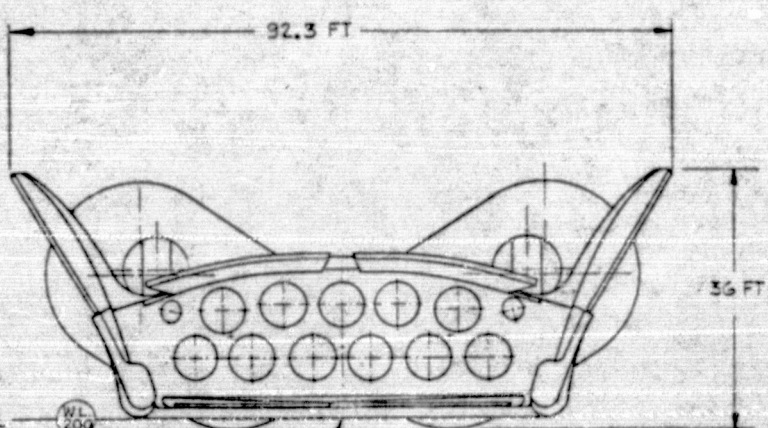

Fig. 2.5-1

QTY REQD	CODE IDENT	PART OR IDENTIFYING NO	NOMENCLATURE OR DESCRIPTION	MATERIAL DESCRIPTION OR NOTE	MATERIAL SPECIFICATION	ZONE	ITEM NO
PARTS LIST							

NOTES:
1. C.G. LOCATIONS ARE PRELIMINARY ESTIMATES.

INTERPRET DWG PER	UNLESS OTHERWISE SPECIFIED DIM ARE IN INCHES. TOLERANCES ON: FRACTIONS = ± 1/16; DECIMALS: .X = ± .1, .XX = ± .03, .XXX = ± .010; ANGLES = ± 2 DEG	DATE Nov 17, '70	LOCKHEED MISSILES & SPACE COMPANY, A GROUP DIVISION OF LOCKHEED AIRCRAFT CORPORATION, SUNNYVALE, CALIFORNIA
		DWN H. Schmidt	
		APVD	
		APVD Geo. Hawkins	LAUNCH VEHICLE DELTA BODY-STAGE 4 1/2 MODEL LS-200-5
		ENGRG	
		CHKR	
		APVD	SIZE E; CODE IDENT 06887; DRAWING NO SKS 100022; REV LA
NEXT ASSY / USED ON APPLICATION	CONTR	APVD	SCALE 1/100; SHEET 1 OF 1
	CCA CI/FD		

FOLDOUT FRAME 2

2.5-17

REPRODUCIBILITY OF THE ORIGINAL PAGE IS POOR.

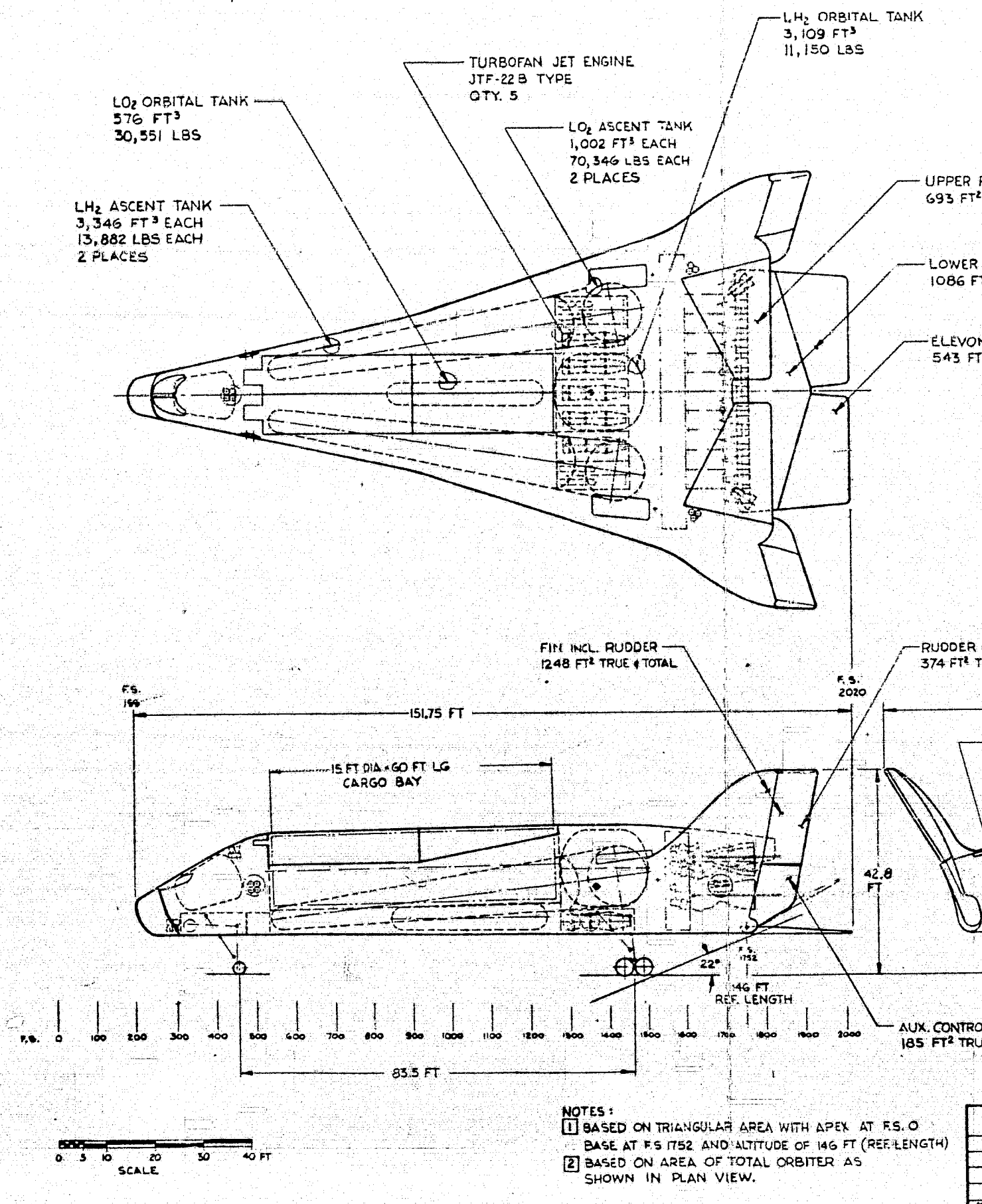

NOTES:
1. BASED ON TRIANGULAR AREA WITH APEX AT F.S. 0 BASE AT F.S 1752 AND ALTITUDE OF 146 FT (REF. LENGTH)
2. BASED ON AREA OF TOTAL ORBITER AS SHOWN IN PLAN VIEW.

FOLDOUT FRAME

REPRODUCIBILITY OF THE ORIGINAL PAGE IS POOR.

PRECEDING PAGE BLANK NOT FILMED

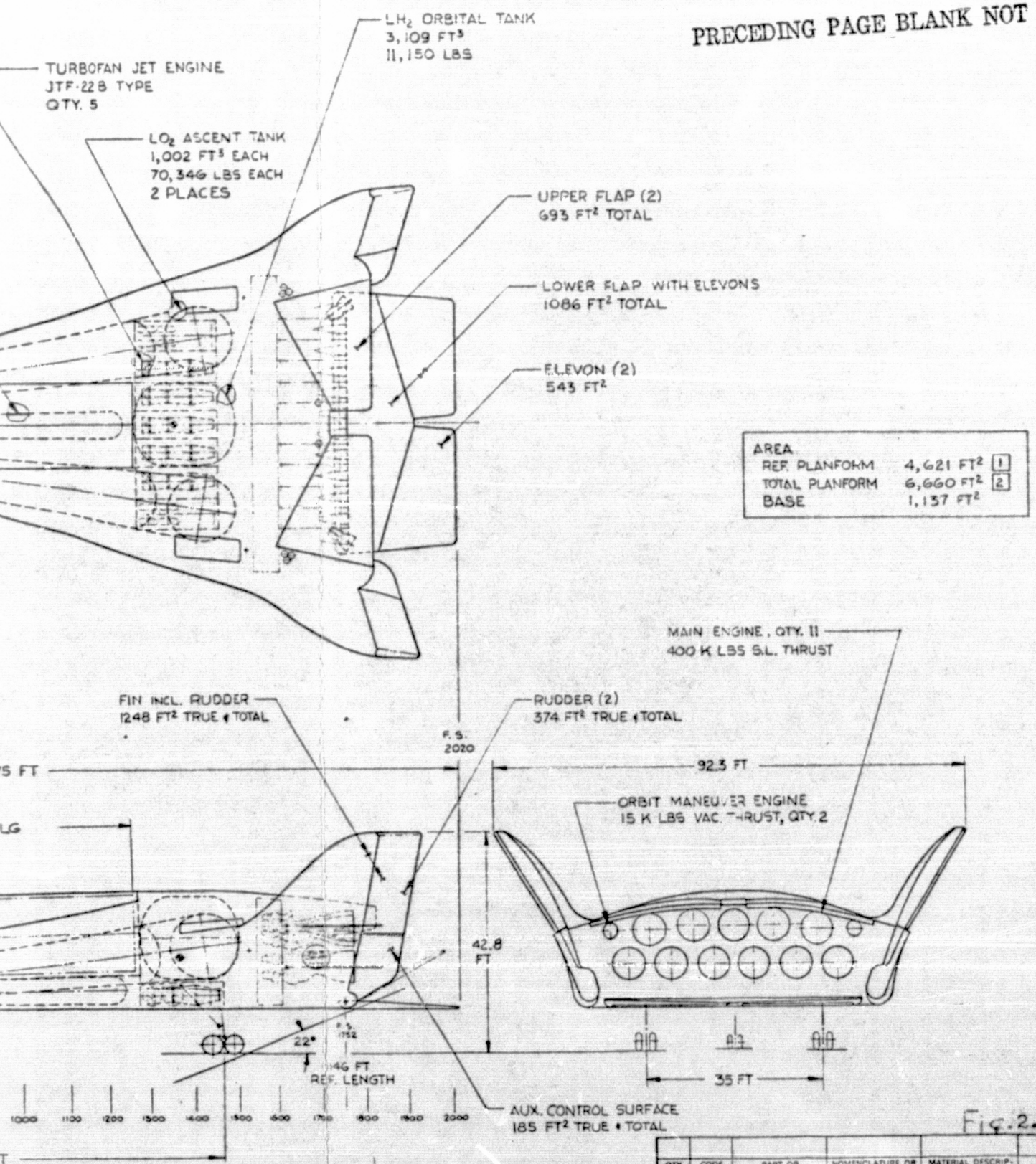

Fig. 2.5-2

NOTES:
1. BASED ON TRIANGULAR AREA WITH APEX AT F.S. 0 BASE AT F.S. 1752 AND ALTITUDE OF 146 FT (REF. LENGTH)
2. BASED ON AREA OF TOTAL ORBITER AS SHOWN IN PLAN VIEW.

QTY REQD	CODE IDENT	PART OR IDENTIFYING NO	NOMENCLATURE OR DESCRIPTION	MATERIAL DESCRIPTION OR NOTE	MATERIAL SPECIFICATION	ZONE	ITEM NO.

PARTS LIST

INTERPRET DWG PER

UNLESS OTHERWISE SPECIFIED DIM ARE IN INCHES TOLERANCES ON: FRACTIONS = ± 1/16; DECIMALS: .X = ± .1, .XX = ± .03, .XXX = ± .010; ANGLES = ± 2 DEG

DATE Nov 17, 70
DWN Hz Schmidt
APVD
APVD
ENGRG
CHKR
APVD
APVD

LOCKHEED MISSILES & SPACE COMPANY
A GROUP DIVISION OF LOCKHEED AIRCRAFT CORPORATION
SUNNYVALE, CALIFORNIA

GENERAL ARRANGEMENT
DELTA BODY - STAGE # 1/2
MODEL LS-200-5

SIZE E | CODE IDENT 06887 | DRAWING NO SKS 100021 | REV
SCALE 1/100 | SHEET 1 of 1

NEXT ASSY | USED ON
APPLICATION
CONTR
CCA CI FD

FOLDOUT FRAME 2

REPRODUCIBILITY OF THE ORIGINAL PAGE IS POOR.

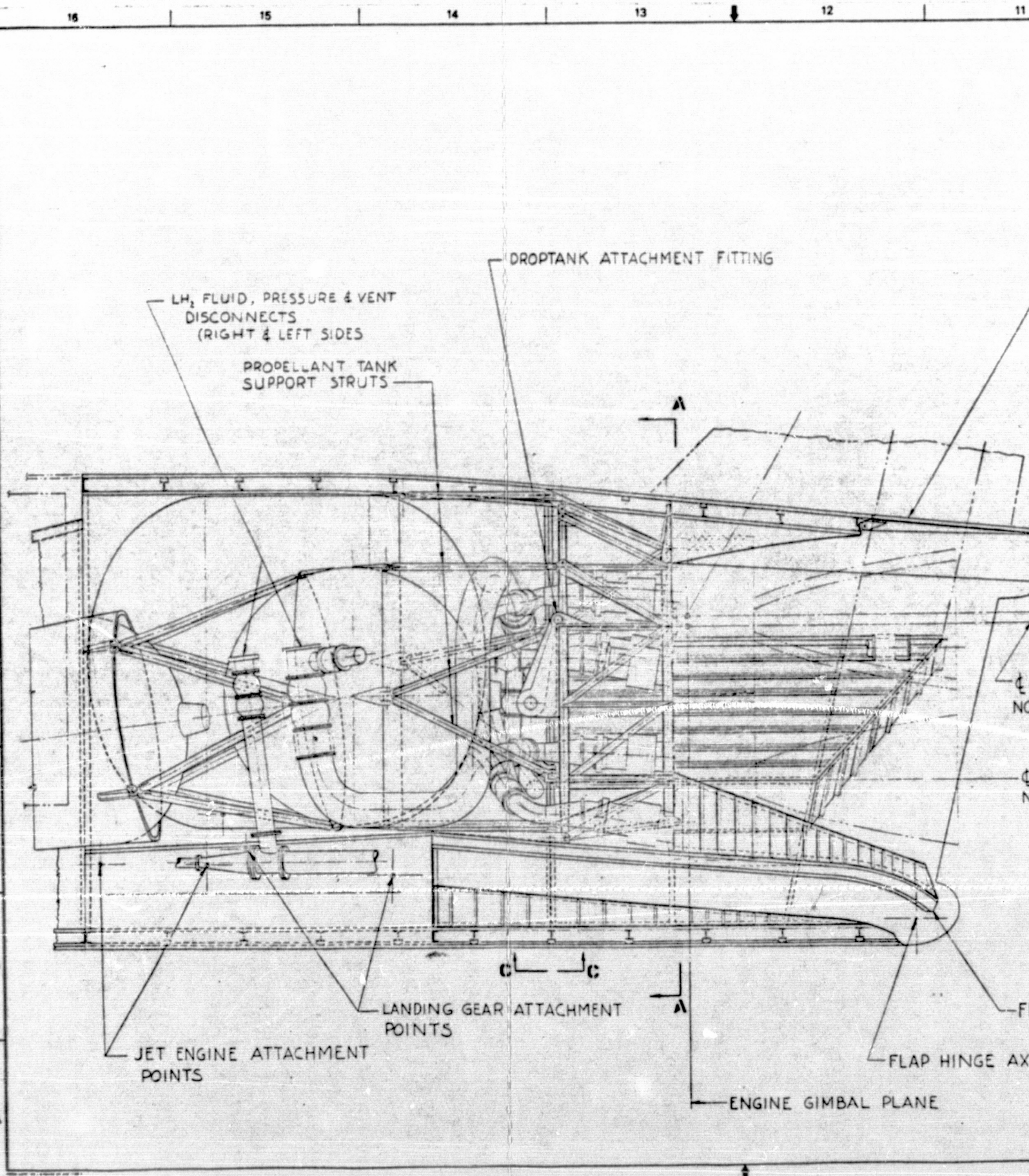

FOLDOUT FRAME

REPRODUCIBILITY OF THE ORIGINAL PAGE IS POOR

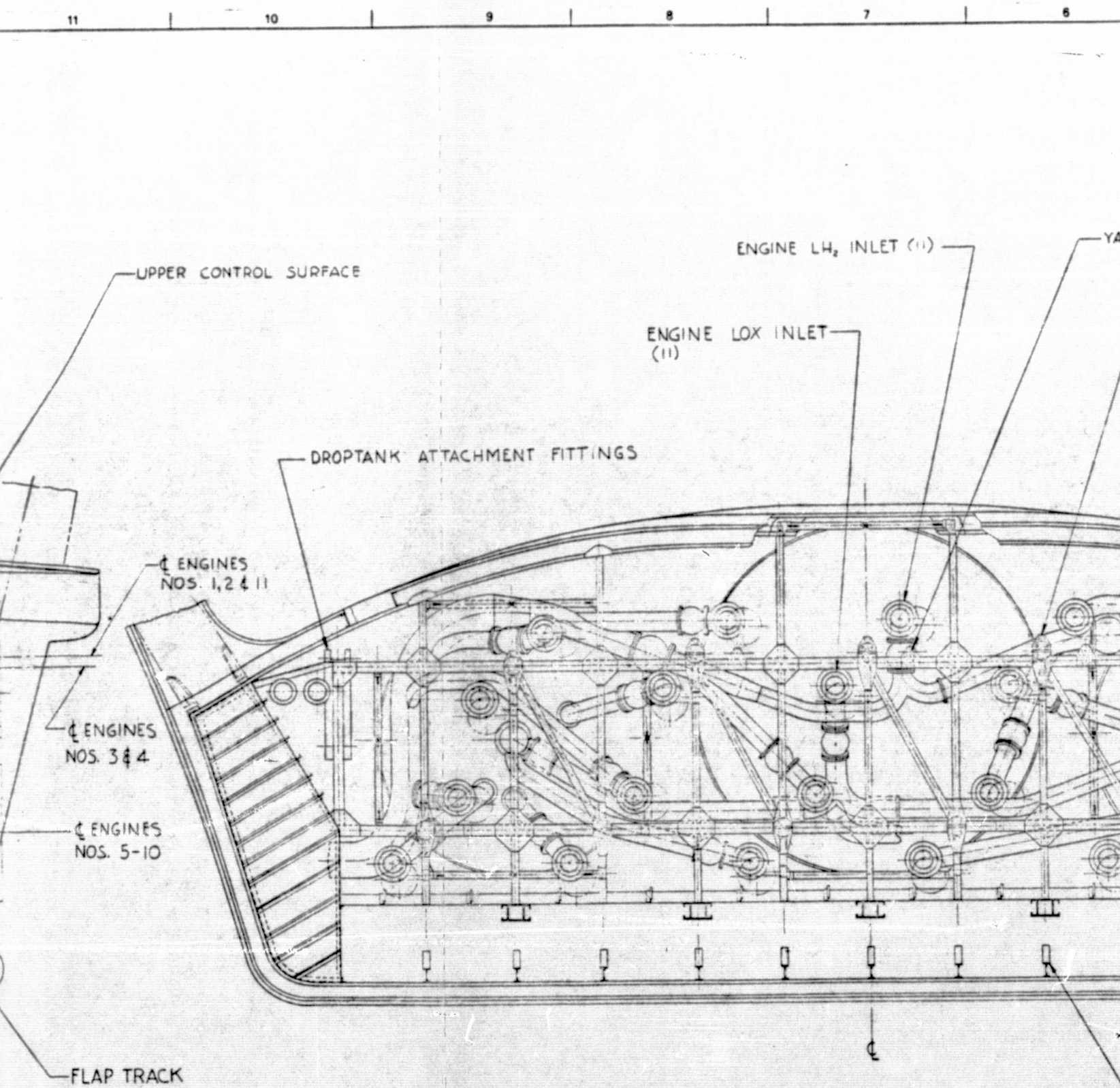

SECTION A1-A1

DRAWING NO | REV | SH

FOLDOUT FRAME 2

REPRODUCIBILITY OF THE ORIGINAL PAGE IS POOR.

PRECEDING PAGE BLANK NOT FILMED

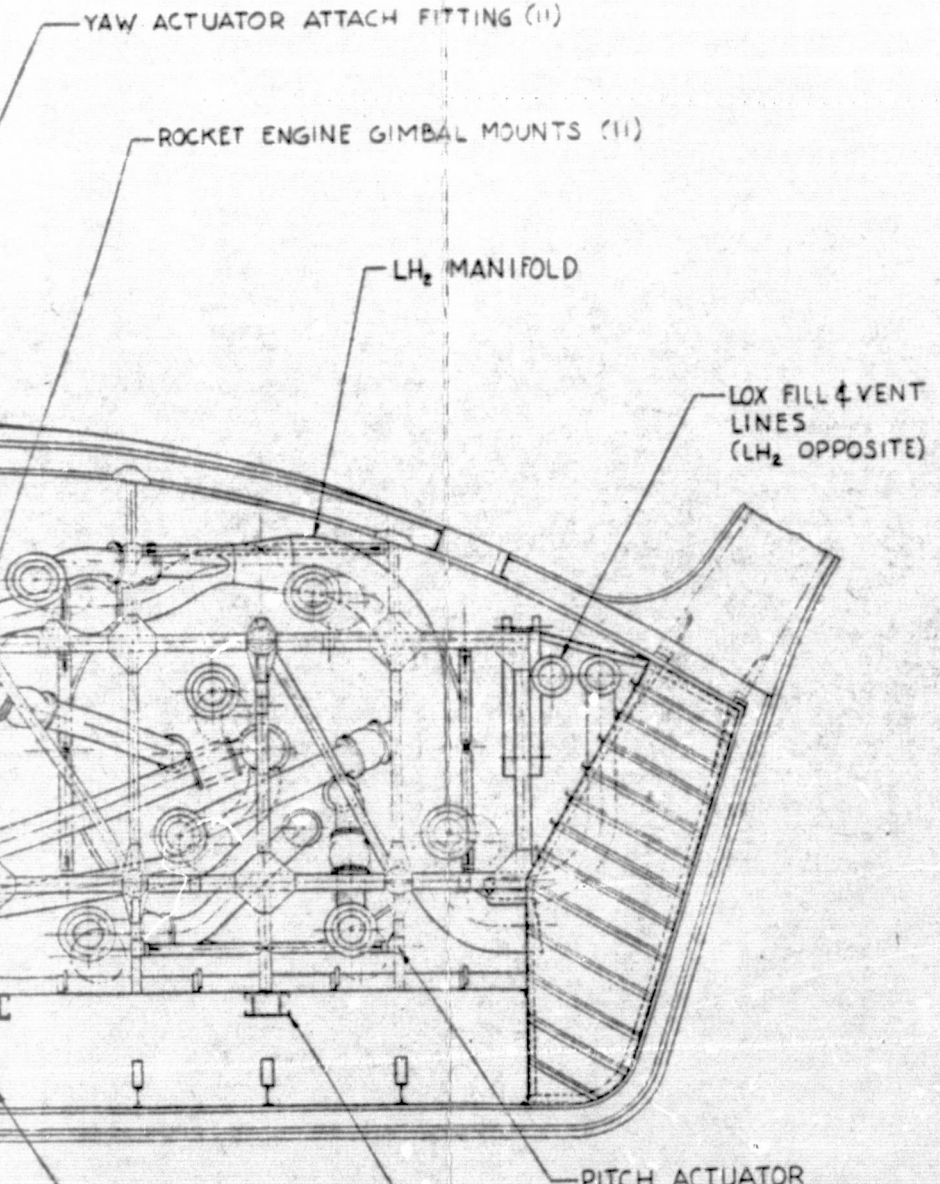

Fig. 2.5-3

FOLDOUT FRAME 3

REPRODUCIBILITY OF THE ORIGINAL PAGE IS POOR.

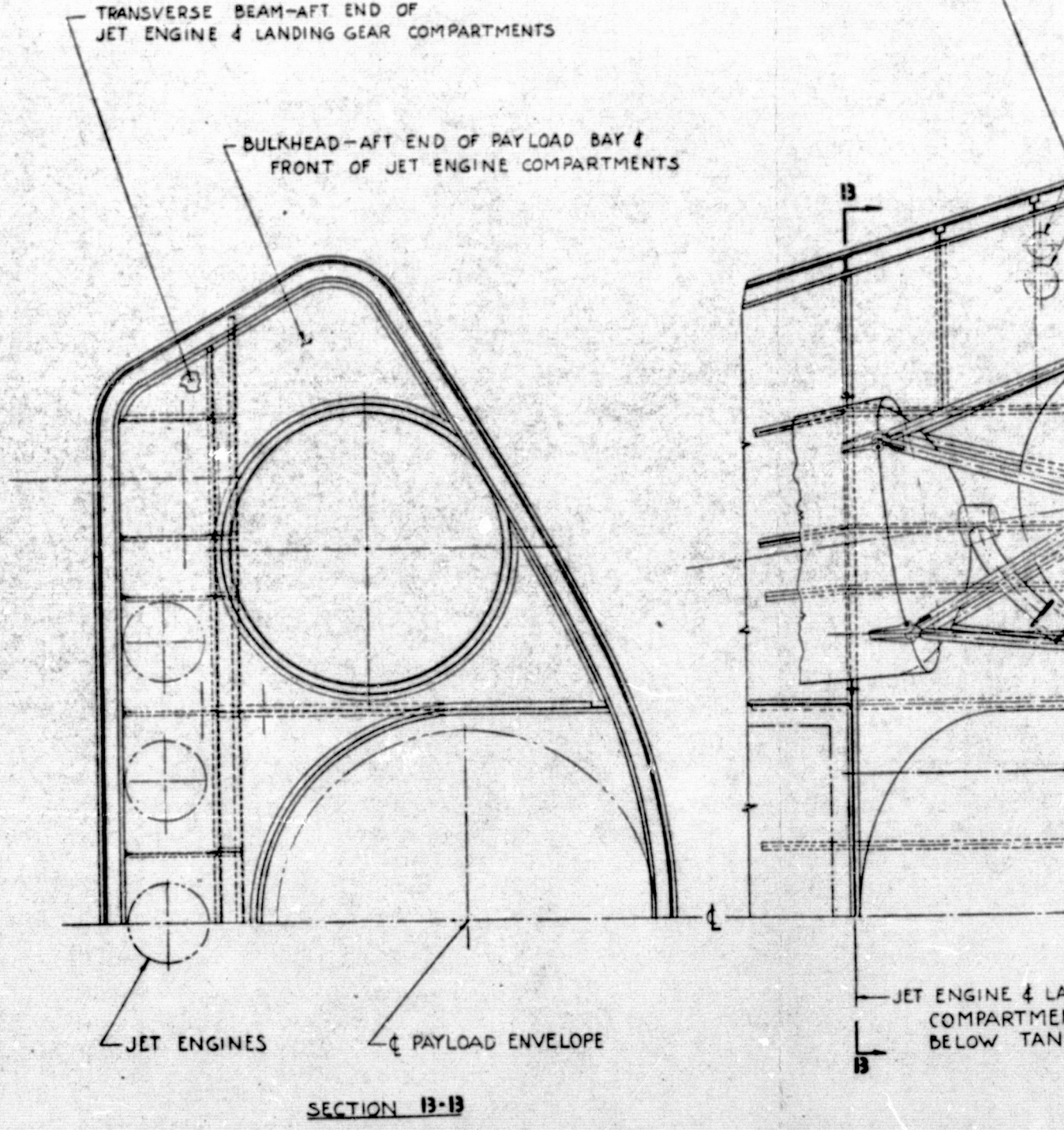

SECTION 13-13

FOLDOUT FRAME

REPRODUCIBILITY OF THE ORIGINAL PAGE IS POOR.

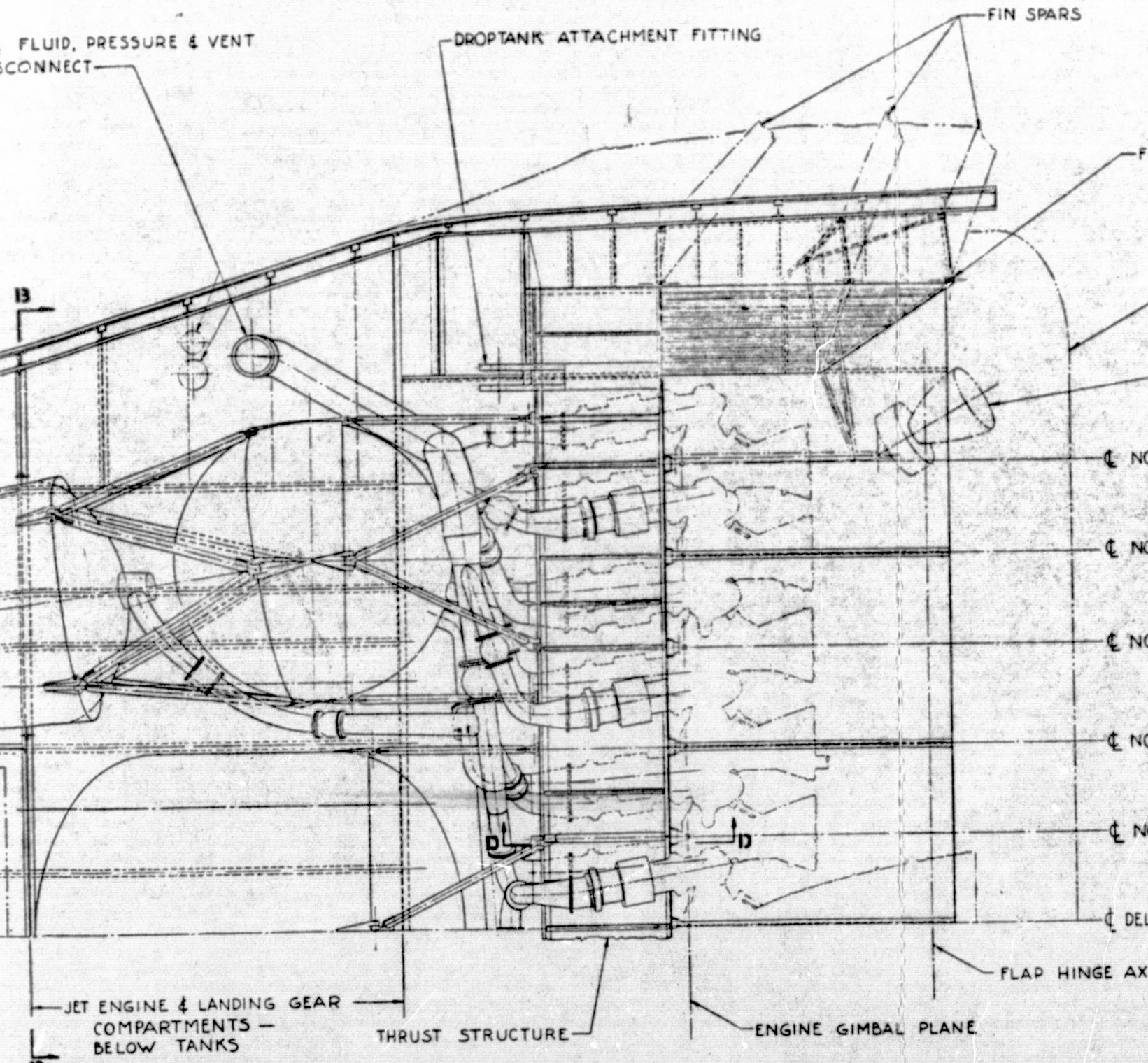

TOP VIEW
UPPER BODY SHELL STRUCTURE OMITTED

FOLDOUT FRAME 2

REPRODUCIBILITY OF THE ORIGINAL PAGE IS POOR.

PRECEDING PAGE BLANK NOT FILMED

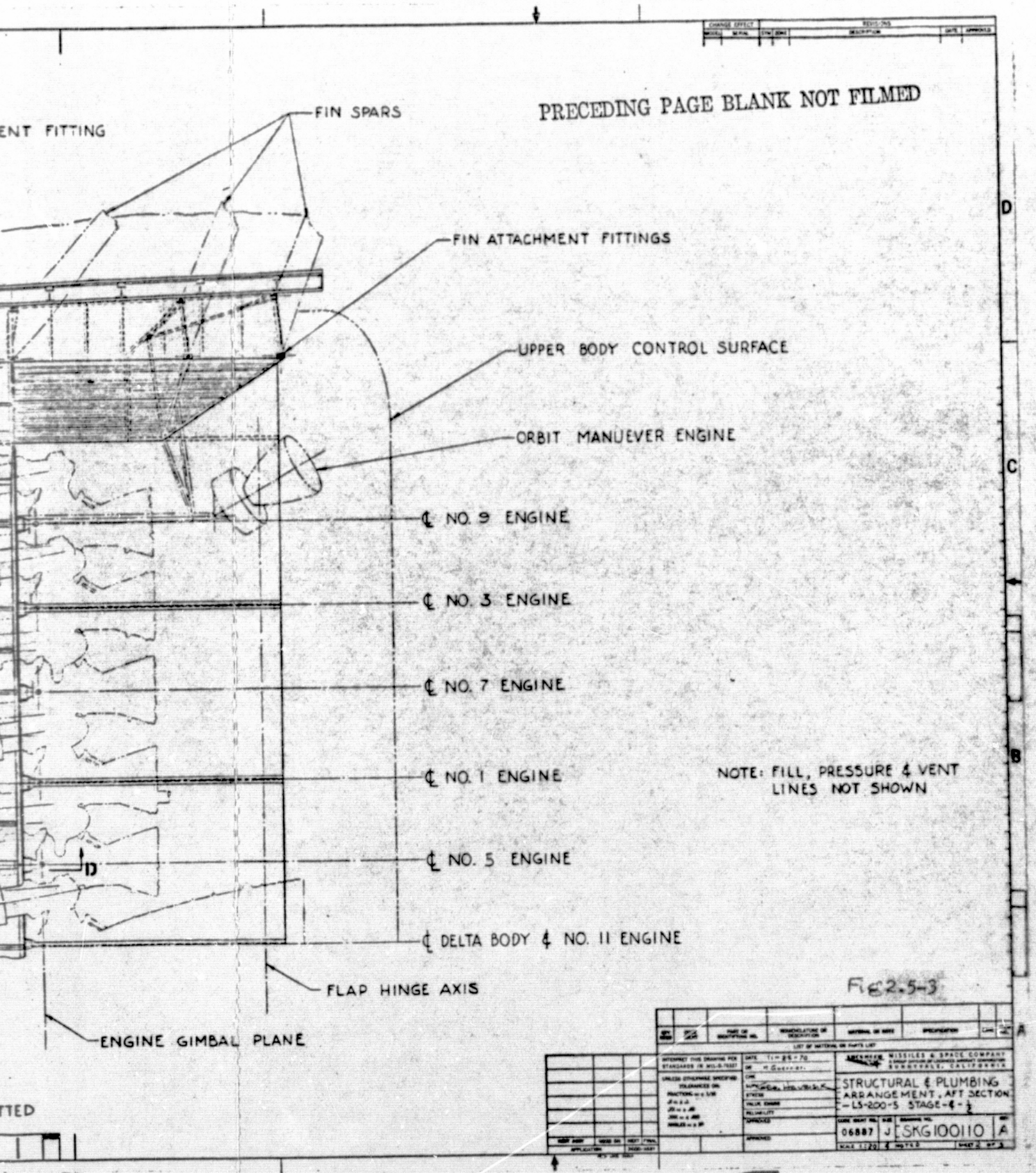

Fig 2.5-3

TTED

FOLDOUT FRAME 3

REPRODUCIBILITY OF THE ORIGINAL PAGE IS POOR.

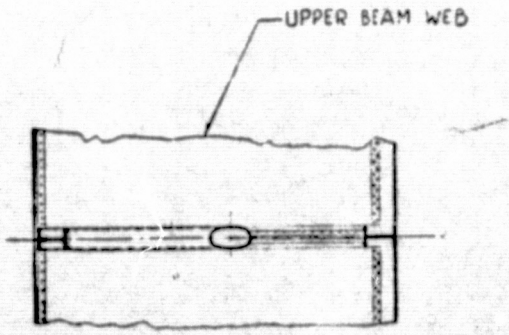

SECTION E-E
1/10 SIZE

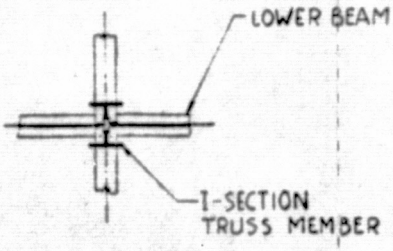

SECTION F-F
1/10 SIZE

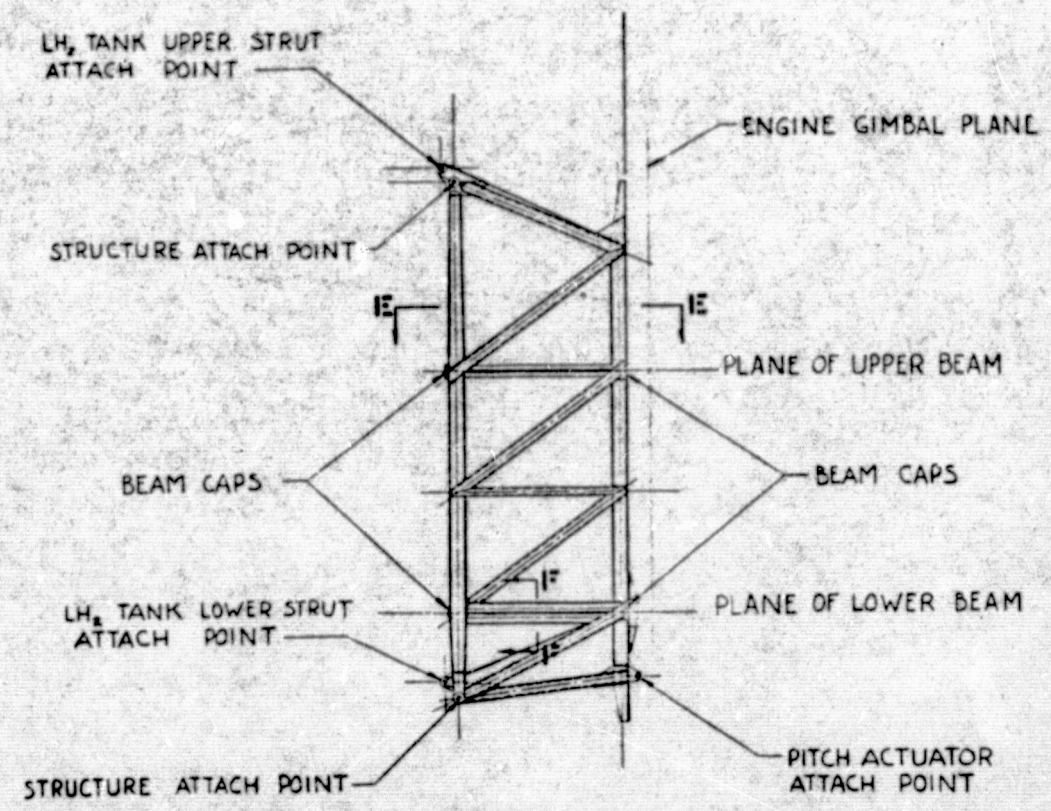

VIEW D-D
TYPICAL VERTICAL TRUSS

FOLDOUT FRAME

REPRODUCIBILITY OF THE ORIGINAL PAGE IS POOR

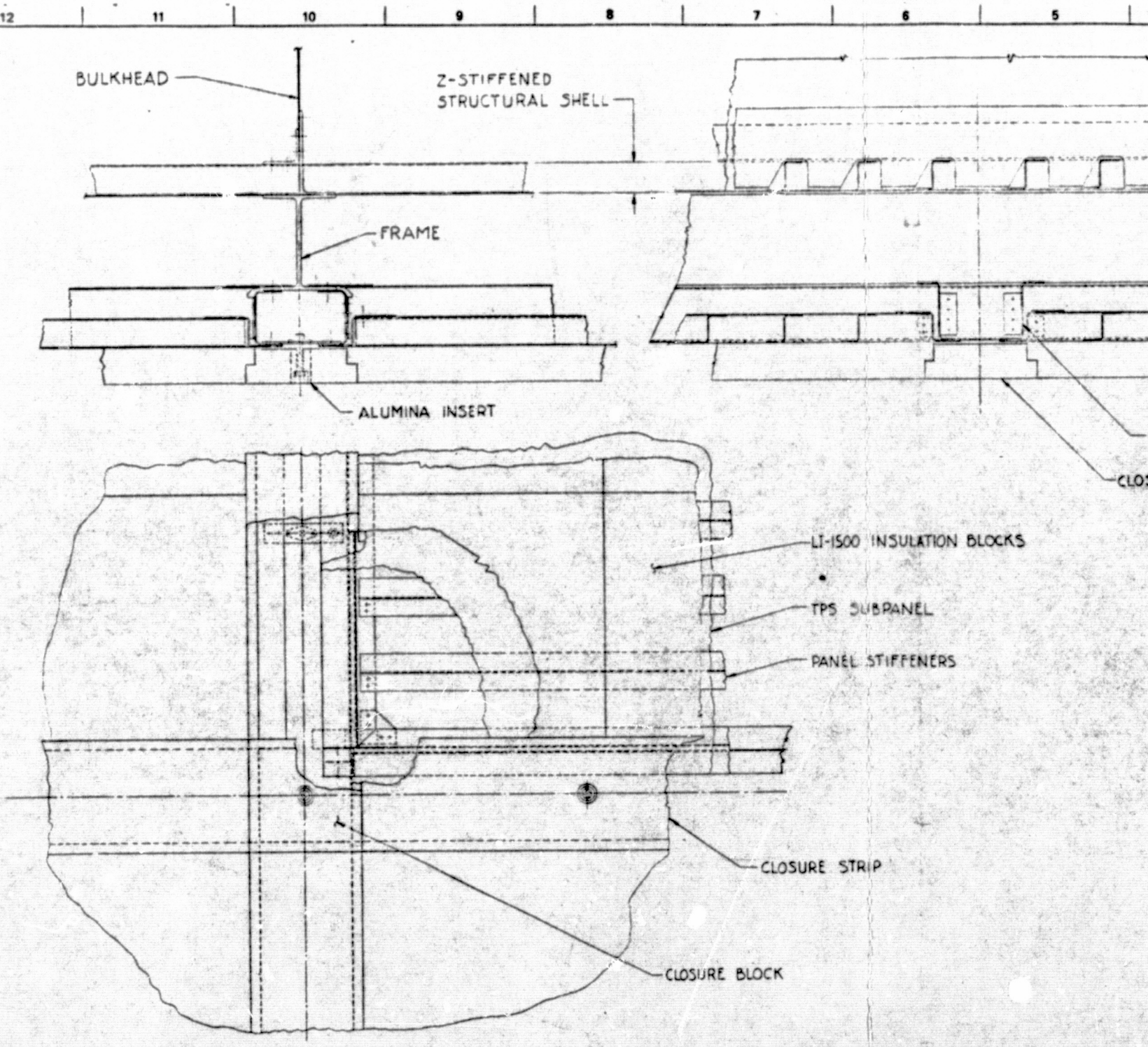

VIEW C-C
½ SIZE
TYPICAL SHELL/TPS ATTACHMENT

REPRODUCIBILITY OF THE ORIGINAL PAGE IS POOR.

PRECEDING PAGE BLANK NOT FILMED

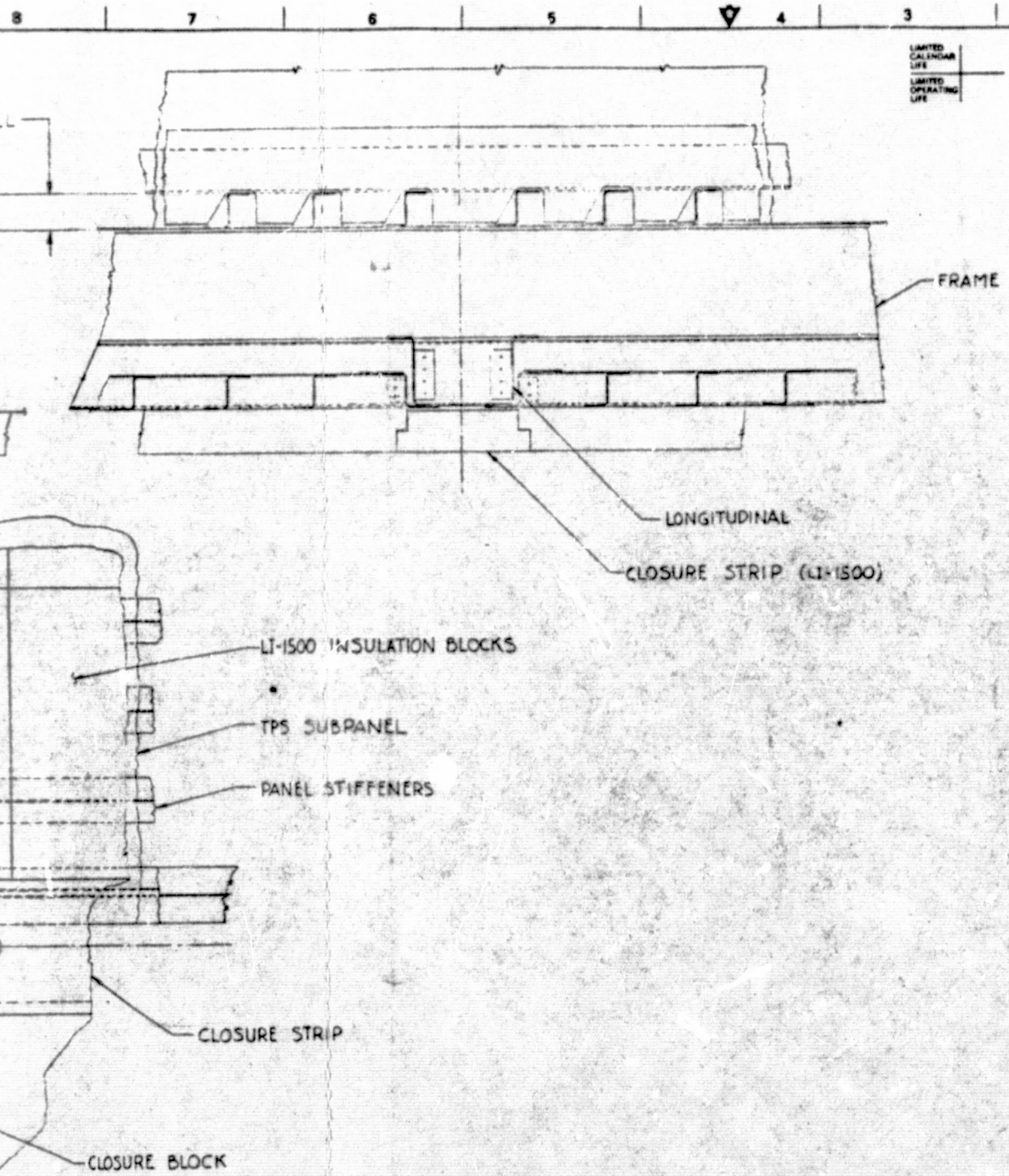

Fig 2.5-3

REPRODUCIBILITY OF THE ORIGINAL PAGE IS POOR.

FOLDOUT FRAME

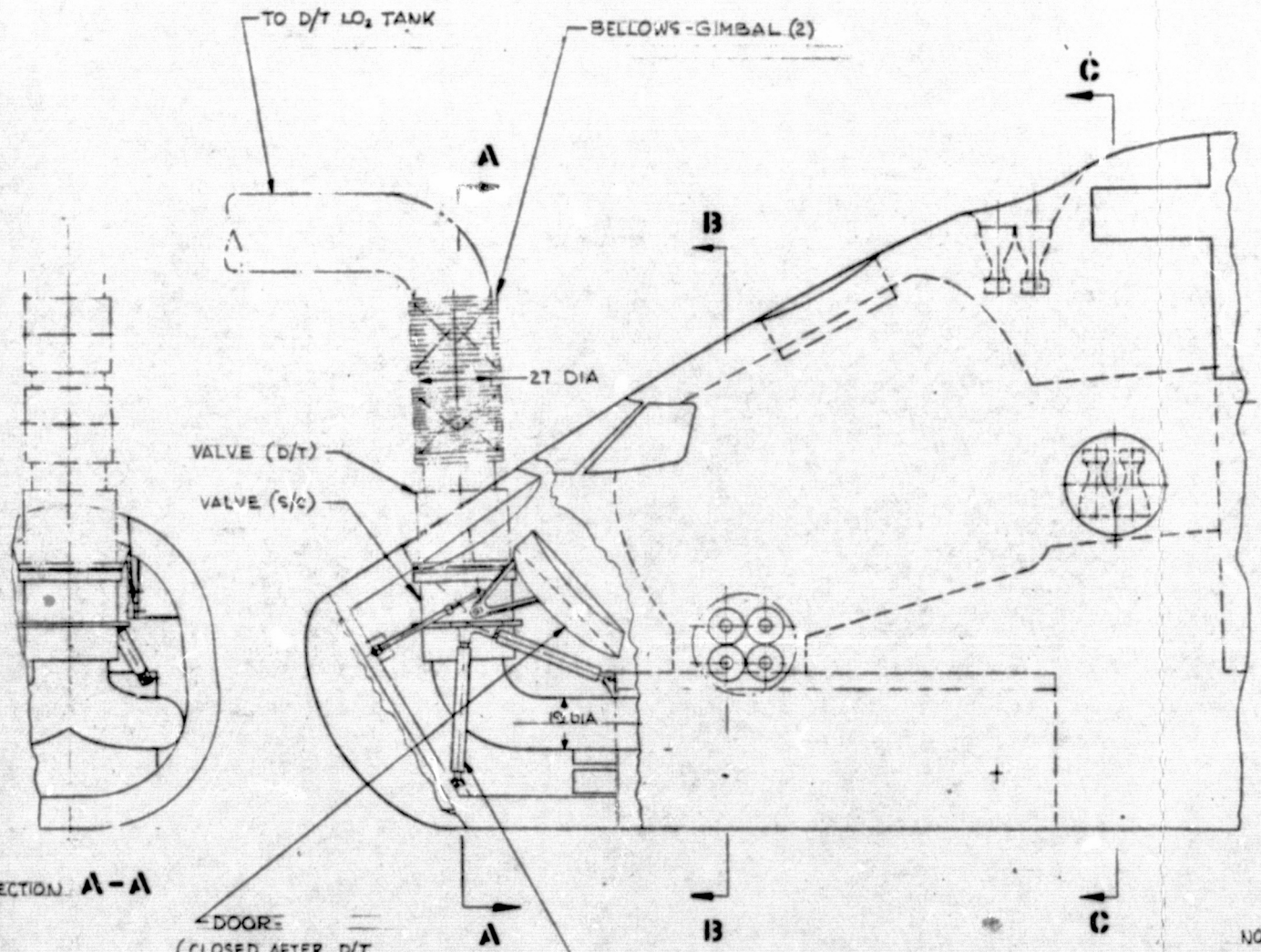

NOTE: SAME A
1. NO TR
2. NO SE
3. ONLY
4. YAW
5. PITCH

REPRODUCIBILITY OF THE ORIGINAL PAGE IS POOR.

LIMITED CALENDAR LIFE | LIMITED OPERATING LIFE

REVISIONS				
ZONE	LTR	DESCRIPTION	DATE	APVD

PRECEDING PAGE BLANK NOT FILMED

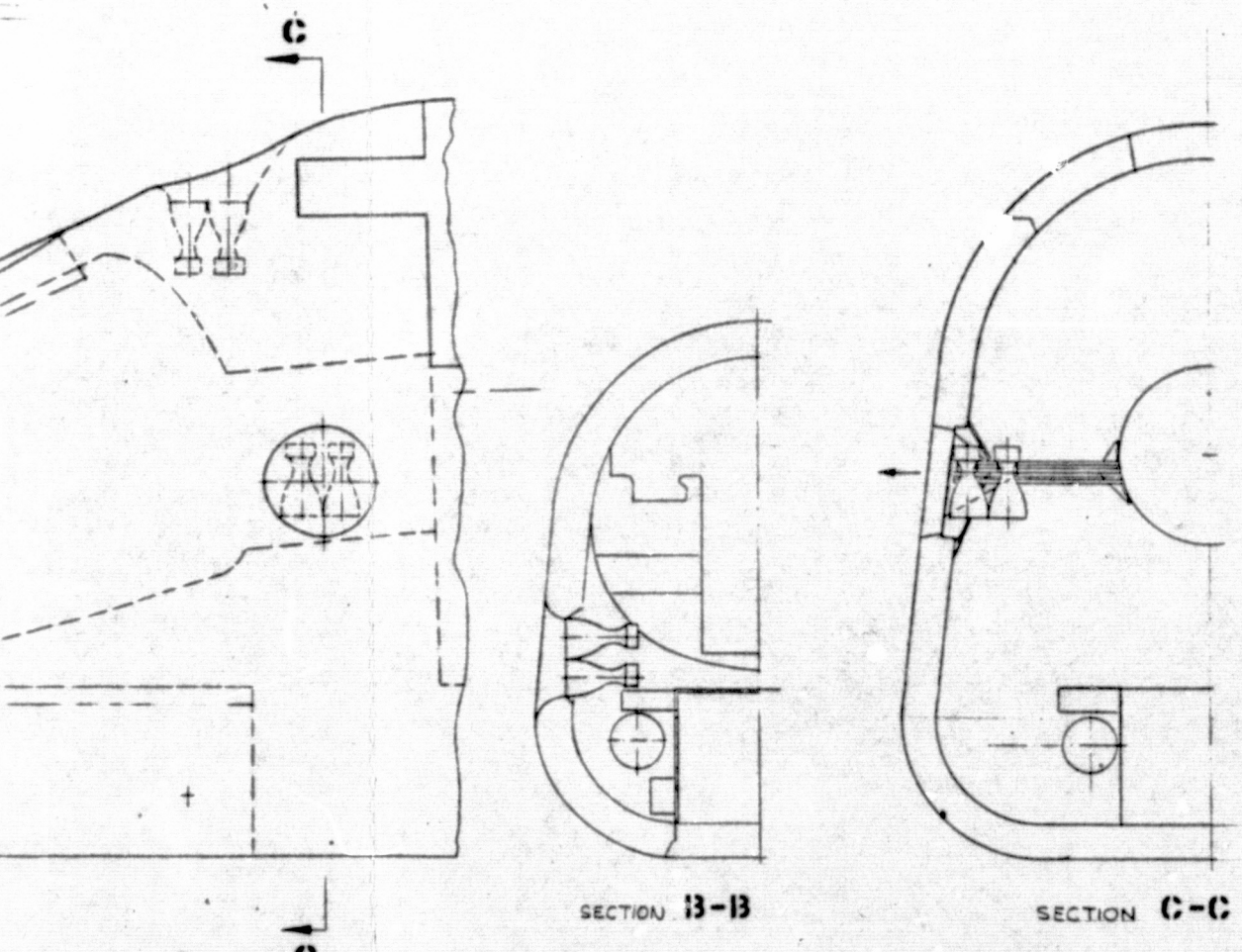

SECTION B-B

SECTION C-C

NOTE: SAME AS BASELINE (REF. DWG SKS 100023) EXCEPT:
1. NO TRANSLATED NOSE-CAP
2. NO SEPARATE D/T TO S/C TIE-IN. LO_2 LINE ACTS AS CONNECTING BAR. (SECTION A-A)
3. ONLY ONE LO_2 LINE AT DISCONNECT
4. YAW THRUSTERS RELOCATED (SECTION B-B)
5. PITCH-UP THRUSTERS RELOCATED WITH DEPLOYMENT FEATURE. (SECTION C-C)

Fig. 2.5-4

QTY REQD	CODE IDENT	PART OR IDENTIFYING NO	NOMENCLATURE OR DESCRIPTION	MATERIAL DESCRIPTION OR NOTE	MATERIAL SPECIFICATION	ZONE	ITEM NO

PARTS LIST

INTERPRET DWG PER

UNLESS OTHERWISE SPECIFIED DIM ARE IN INCHES. TOLERANCES ON:
FRACTIONS = ± 1/16
DECIMALS: .X = ± .1
.XX = ± .03
.XXX = ± .010
ANGLES = ± 2 DEG

NEXT ASSY | USED ON
APPLICATION

CONTR
CCA/L/I/FD

DATE 1-24-70
DWN
APVD
APVD
ENGRG
CHKR
APVD
APVD

LOCKHEED MISSILES & SPACE COMPANY
A GROUP DIVISION OF LOCKHEED AIRCRAFT CORPORATION
SUNNYVALE, CALIFORNIA

ALTERNATE NOSE SECTION
DELTA BODY, STAGE 1
MODEL LS-200-5

SIZE E | CODE IDENT 06887 | DRAWING NO SKS 100026 | REV -

SCALE | SHEET

REPRODUCIBILITY OF THE ORIGINAL PAGE IS POOR.

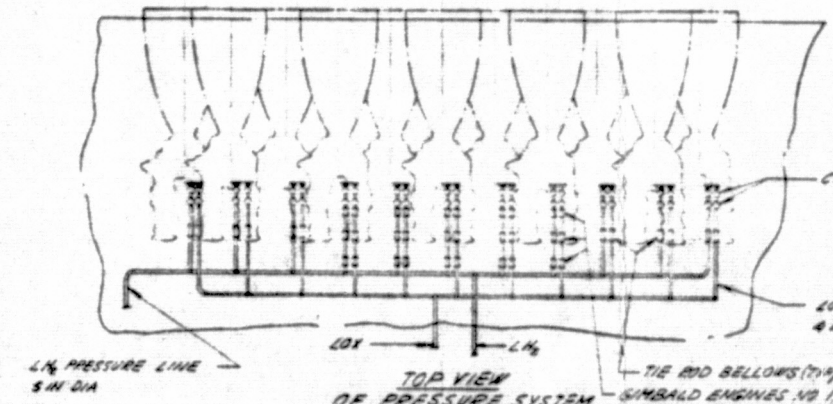

TOP VIEW OF PRESSURE SYSTEM

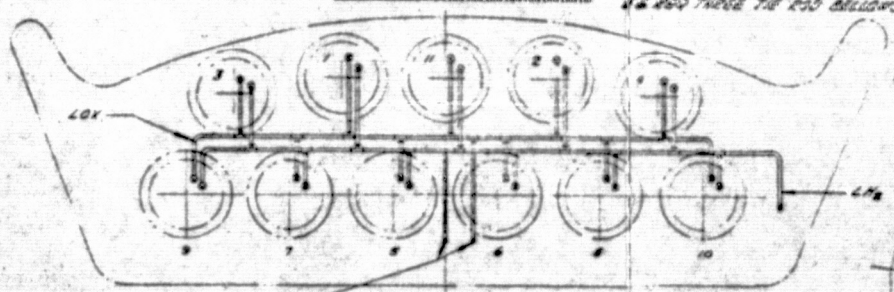

SECTION A-A
PRESSURIZATION SYSTEM SHOWN ONLY

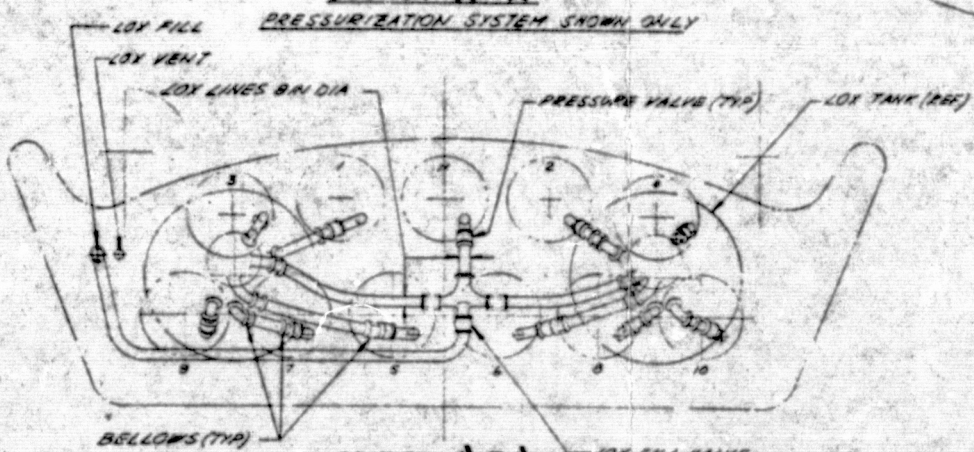

SECTION A-A
LOX SYSTEM SHOWN ONLY

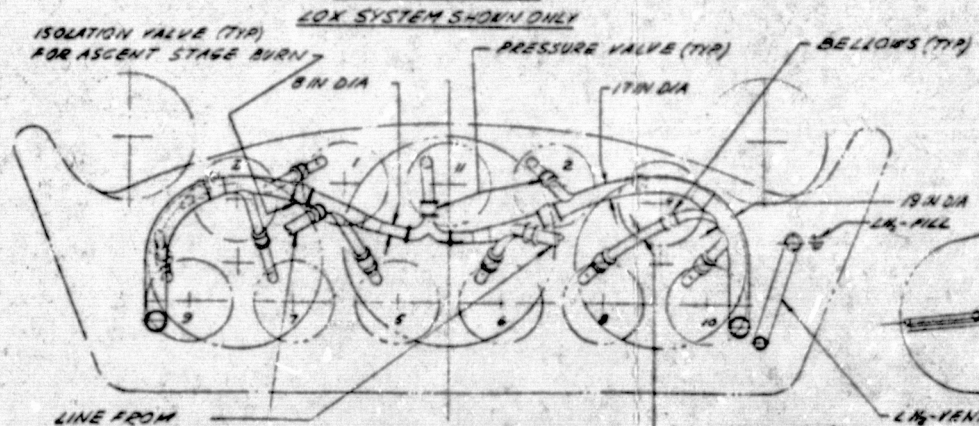

SECT A-A
LH2 SYSTEM SHOWN ONLY
(MANIFOLD)

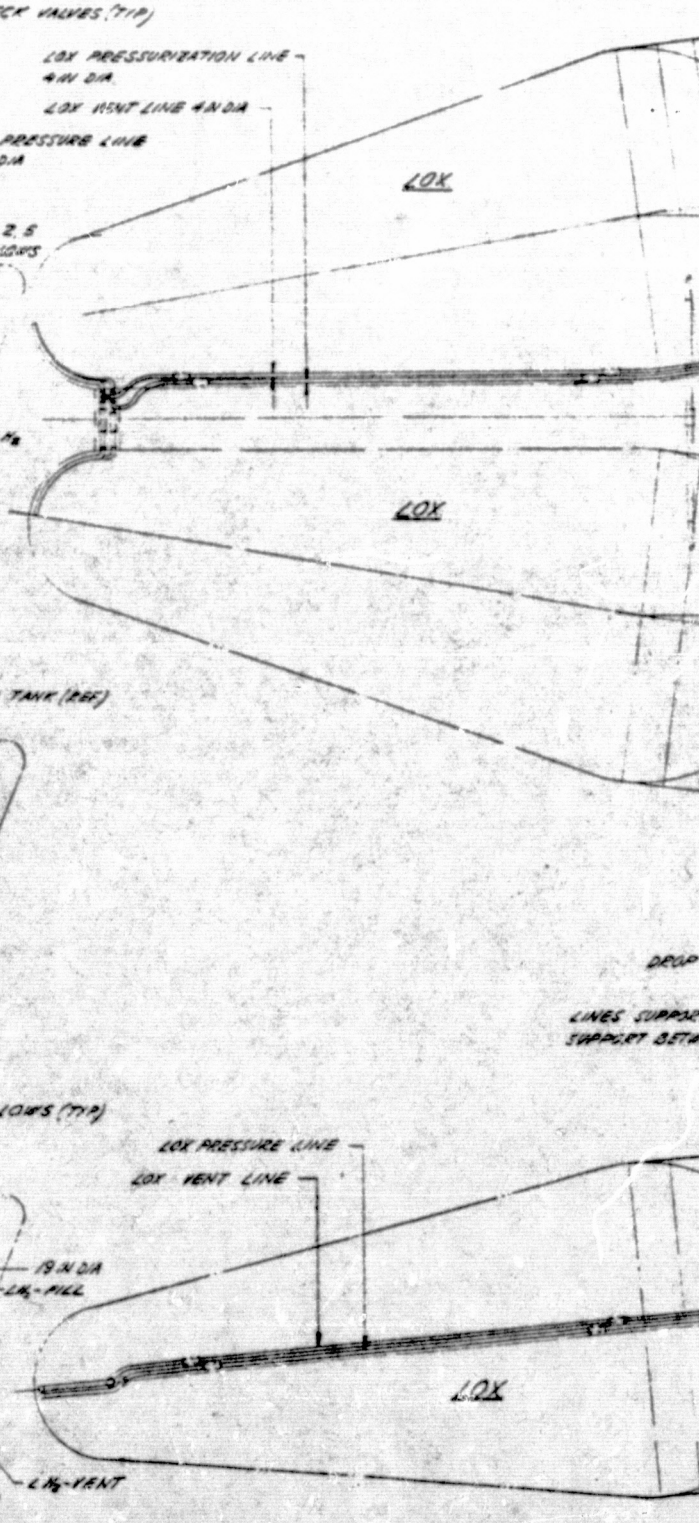

FOLDOUT FRAME

REPRODUCIBILITY OF THE ORIGINAL PAGE IS POOR.

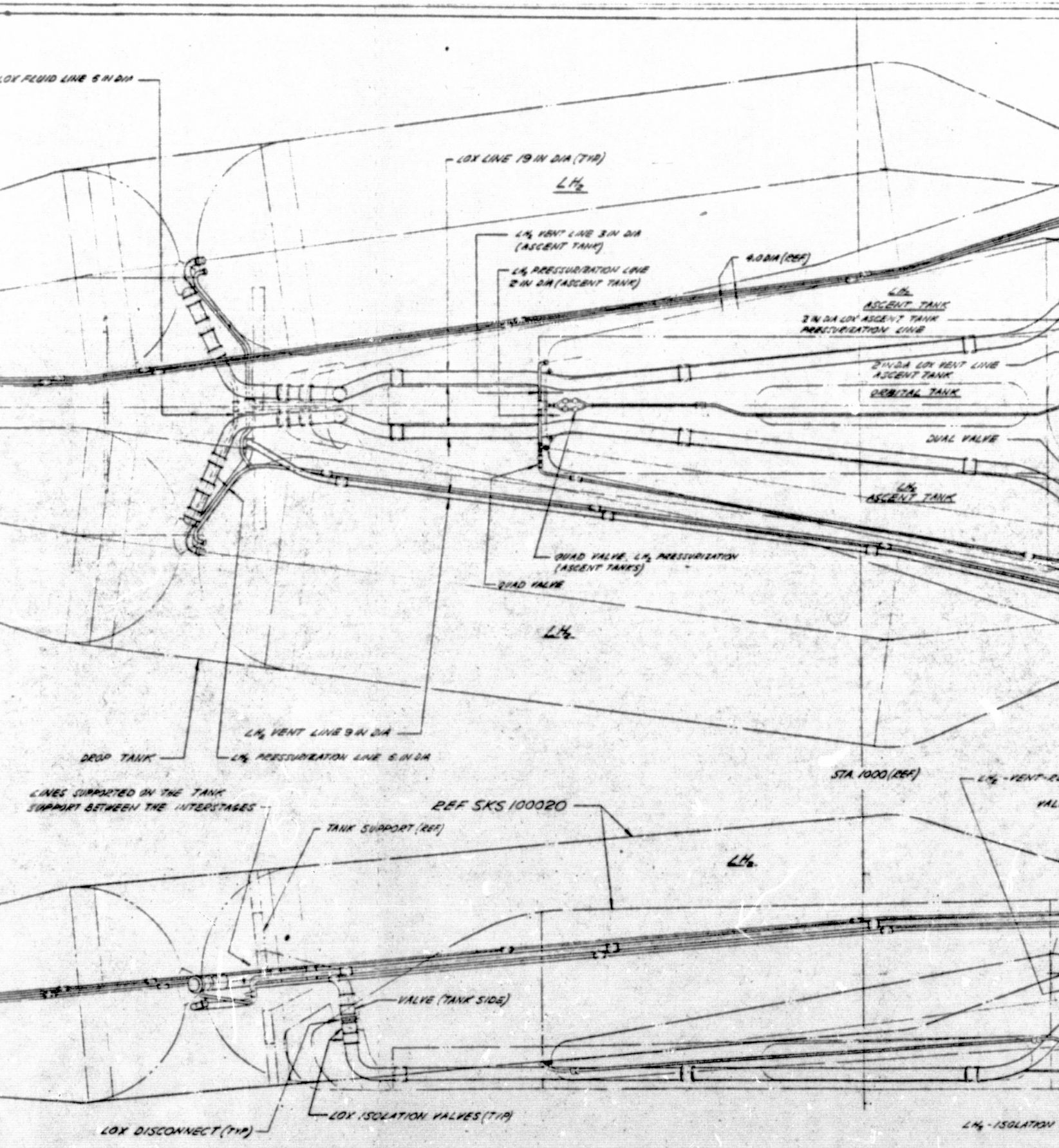

FOLDOUT FRAME 2

REPRODUCIBILITY OF THE ORIGINAL PAGE IS POOR.

PRECEDING PAGE BLANK NOT FILMED

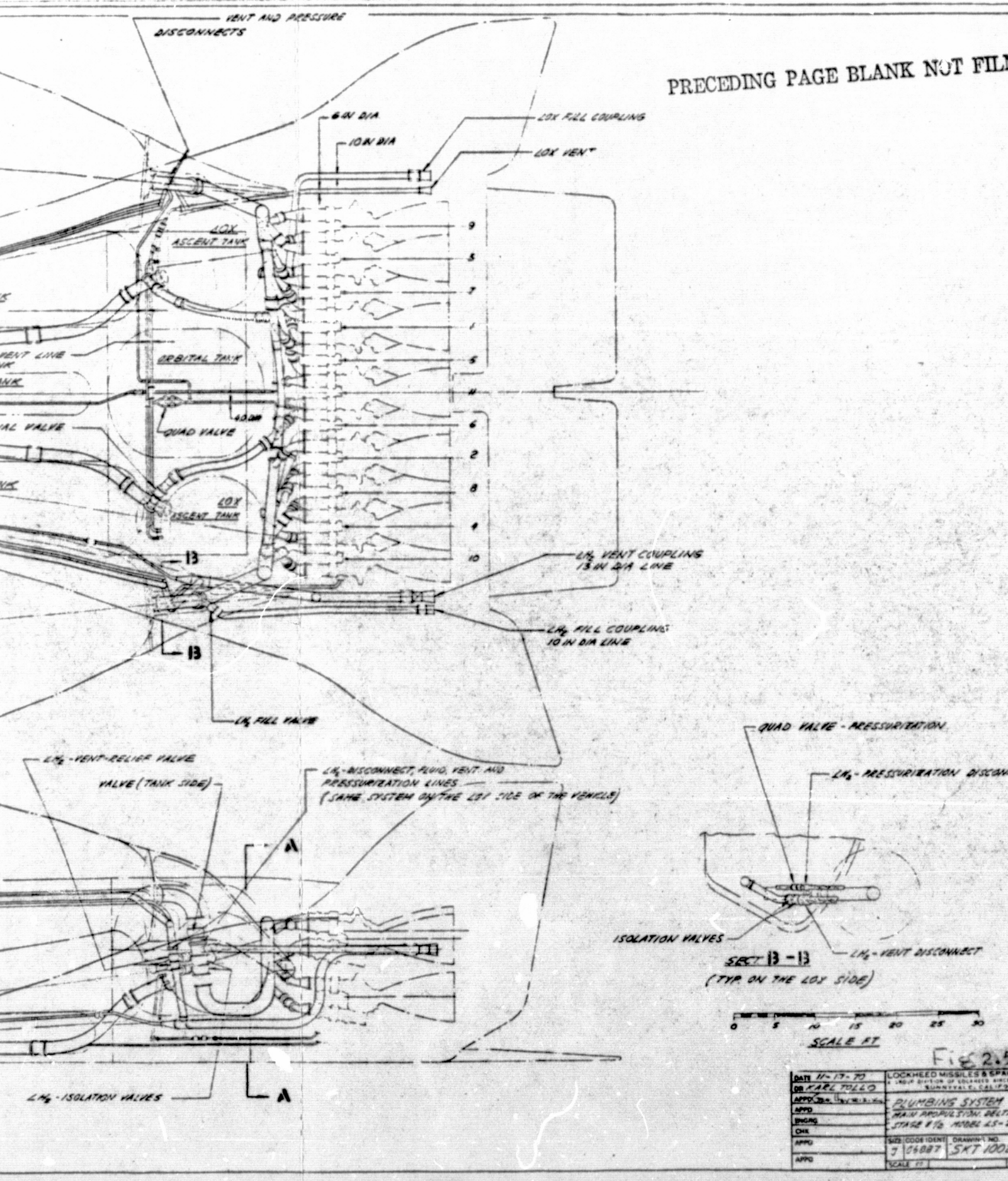

Fig 2.5-5

DATE 11-17-70	LOCKHEED MISSILES & SPACE CO.
DR EARL TOLLO	A GROUP DIVISION OF LOCKHEED AIRCRAFT CORP. SUNNYVALE, CALIFORNIA
APPD	PLUMBING SYSTEM
APPD	MAIN PROPULSION, DELTA 800
ENGRG	STAGE I & II MODEL LS-200-5
CHK	
APPD	SIZE J · CODE IDENT 24887 · DRAWING NO. SKT 100218
APPD	SCALE 1/2 · SHEET

REPRODUCIBILITY OF THE ORIGINAL PAGE IS POOR.

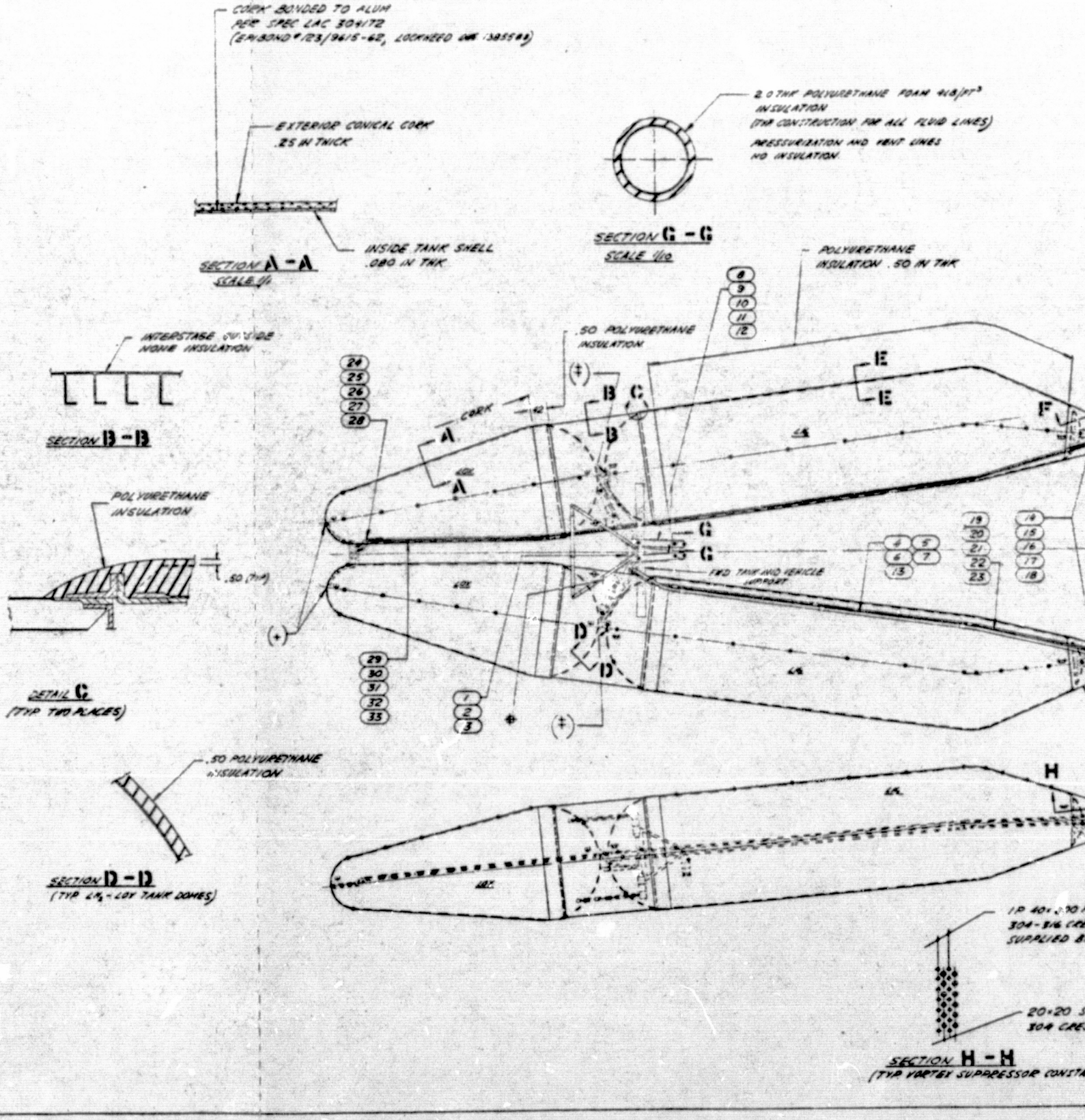

FOLDOUT FRAME

REPRODUCIBILITY OF THE ORIGINAL PAGE IS POOR.

PRECEDING PAGE BLANK NOT FILMED

URETHANE FOAM 4LB/FT³

TION FOR ALL FLUID LINES)

N AND VENT LINES

LYURETHANE
ULATION . 50 IN THK

- POLYURETHANE INSULATION . 50 IN THK

SECTION F-F

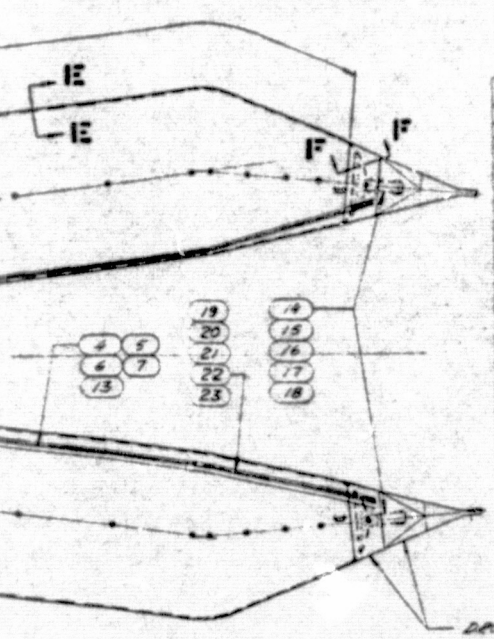

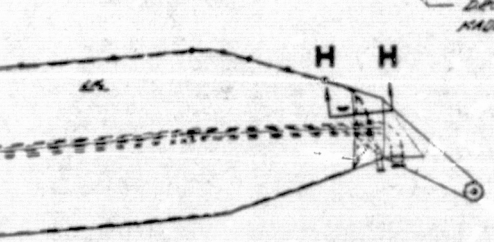

DROP TANK THRUST CONE
MADE OF .040-4V TITANIUM

INSTRUMENTATION LIST			
QTY	ITEM	SOURCE
10	HOT WIRE POINT SENSORS	
32	HOT WIRE POINT SENSORS	
4	PRESSURE TRANSDUCER	
4	PRESSURE TRANSDUCER	
2	19 PIN ELECTRICAL HEAD-TAIL CONNECTOR	
2	FEMALE MATING ELECTRICAL CONNECTOR (INSIDE TANK)	
2	MALE MATING ELECTRICAL CONNECTOR (OUTSIDE TANK)	
2	9 PIN ELECTRICAL HEAD-TAIL CONNECTOR	
2	FEMALE MATING ELECTRICAL CONNECTOR (INSIDE TANK)	
2	MALE MATING ELECTRICAL CONNECTOR (OUTSIDE TANK)	
1	MULTIPLEX UNIT	
1	PLUG QUICK DISCONNECT DBAST-27-2P	

QTY	SOURCE	DESCRIPTION	MATERIAL	ITEM
1	3	DISCONNECT 4" PRESSURIZATION LINE		33
1	COML	4" DIA x .032 WALL	2219 ALUM	32
6	2	GIMBAL JOINT 4"	ALUM WITH INCONEL BELLOWS	31
1	1	TEE 4"		30
2	1	END COUPLING 4" PRESSURIZATION LINE		29
1	3	DISCONNECT 4" VENT LINE		28
1	COML	4" DIA x .032 WALL	2219 ALUM	27
6	2	GIMBAL JOINT 4"	ALUM WITH INCONEL BELLOWS	26
1	1	TEE 4"		25
2	1	END COUPLING 4" LOX VENT LINE		24
1	1	TEE 5" PRESSURIZATION LINE		23
1	COML	5" DIA x .032 WALL 5" PRESSURIZATION LINE	2219 AL	22
1	3	DISCONNECT 5"		21
6	2	GIMBAL JOINT 5"	ALUM WITH INCONEL BELLOWS	20
2	1	END COUPLING 5" LH₂ PRESSURIZATION LINE		19
2		VALVE 19 IN DIA, 19" LH₂ FLUID LINE		18
2	COML	19" DIA x .032 WALL	2219 ALUM	17
2	3	DISCONNECT		16
4	2	GIMBAL JOINT	ALUM WITH INCONEL BELLOWS	15
2	1	END COUPLING 19" LH₂ FLUID LINE		14
1	3	DISCONNECT 9" LH₂ VENT LINE		13
2	COML	19" DIA x .070 WALL 19" LOX FLUID LINE	2219 ALUM	12
2	3	DISCONNECT		11
2		VALVE, 19" DIA		10
12	2	GIMBAL JOINT	ALUM WITH INCONEL BELLOWS	9
2	1	END COUPLING 19" LOX FLUID LINE		8
6	2	GIMBAL JOINT 9" LH₂ VENT LINE	ALUM WITH INCONEL BELLOWS	7
1	1	TEE		6
1	COML	9" DIA x .032 WALL	2219 ALUM	5
2	1	END COUPLING 9" LH₂ VENT LINE		4
3	2	GIMBAL JOINT 9" LOX FLUID LINE	ALUM WITH INCONEL BELLOWS	3
1	COML	8" DIA x .032 WALL 8" LOX FLUID LINE	2219 ALUM	2
2	1	END COUPLING 8" LOX FLUID LINE		1

PARTS LIST

QTY REQD	SOURCE IDENT	PART OR IDENTIFYING NO.	NOMENCLATURE OR DESCRIPTION	MATERIAL OR FINISH OR NOTE	MATERIAL SPECIFICATION	ZONE	ITEM NO.

INTERPRET DWG PER

UNLESS OTHERWISE SPECIFIED DIM. ARE IN INCHES TOLERANCES ON: FRACTIONS ± 1/16, DECIMALS: .X ± .1, .XX ± .03, .XXX ± .010, ANGLES ± 2 DEG.

NEXT ASSY | USED ON | APPLICATION

DATE 8-20-70
DR KARL TOLLO
APPD
APPD
ENGRG
CHK
APPD
CONTR
APPD
CCA/CEI

LOCKHEED MISSILES & SPACE COMPANY
A GR. A DIVISION OF LOCKHEED AIRCRAFT CORPORATION
SUNNYVALE, CALIFORNIA

DROP TANK ASSEMBLY
DELTA BODY - STAGE II/12
MODEL LS-200-6

SIZE J | CODE IDENT 06887 | DRAWING NO. SKT100219 | REV -

SCALE 1/24 | SHEET

Fig. 2.5-6

1.P 40 x 200 PLAIN DUTCH WEAVE
304-316 CRES WT .27 #/FT²
SUPPLIED BY MICHIGAN WIRE CLOTH

20 x 20 SQ MESH
304 CRES CLOTH

SECTION H-H
(TYP VORTEX SUPPRESSOR CONSTR)

3 DISCONNECT (TYP RIP-CORD SEPARATION SHOWN) ALTERNATE AUTOMATIC DISCONNECT WITH BACKUP OF LANYARD

12 GIMBAL SIMILAR TO SOLAR 38026 CODE 55820

SOLAR APPROVED TYPICAL AN'S FOR LINES AND FITTINGS

NOTES:

Fig. 2.5-6

REPRODUCIBILITY OF THE ORIGINAL PAGE IS POOR.

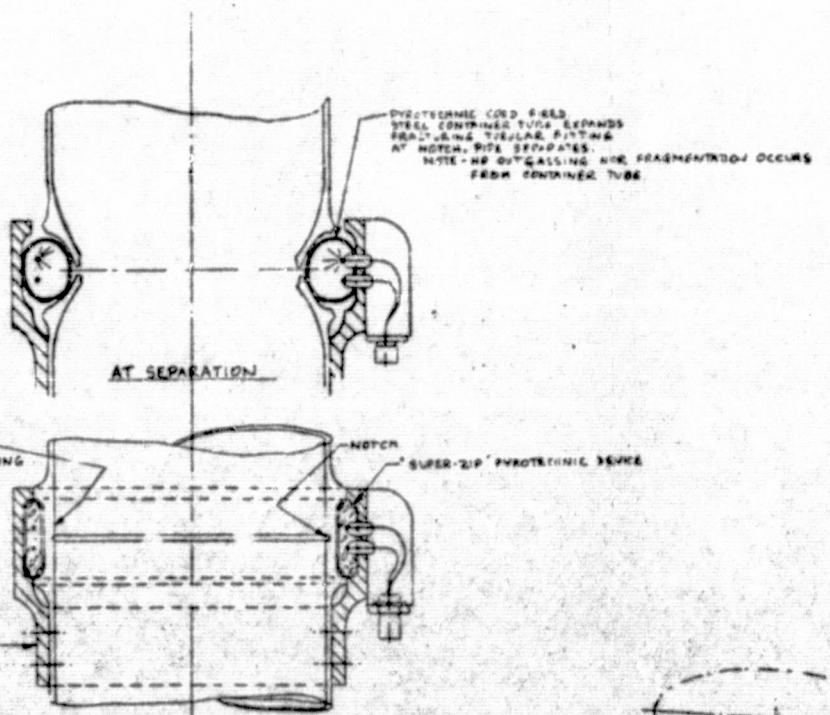

BEFORE SEPARATION

SKETCH X - ALTERNATE METHOD OF SEPARATING FLUID VENT AND PRESSURISATION LINES. TYPICAL APPLICATION OF "SUPER-ZIP" SYSTEM.

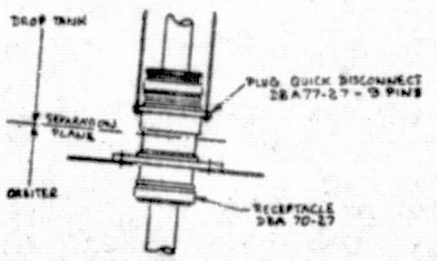

SECTION C-C
ELECTRICAL DISCONNECT

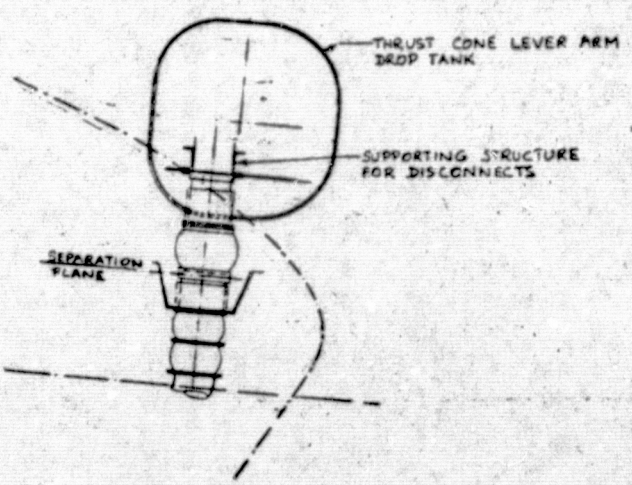

SECTION 13-13

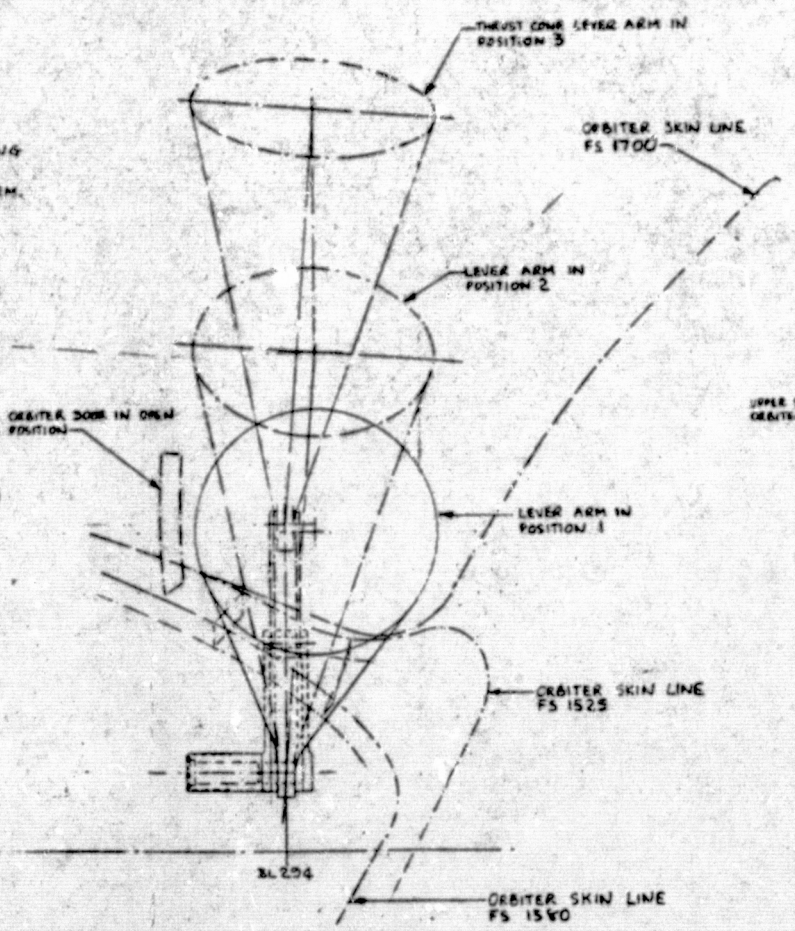

VIEW LOOKING AFT - PORT SIDE
STARBOARD SIDE SIMILAR

FOLDOUT FRAME

REPRODUCIBILITY OF THE ORIGINAL PAGE IS POOR.

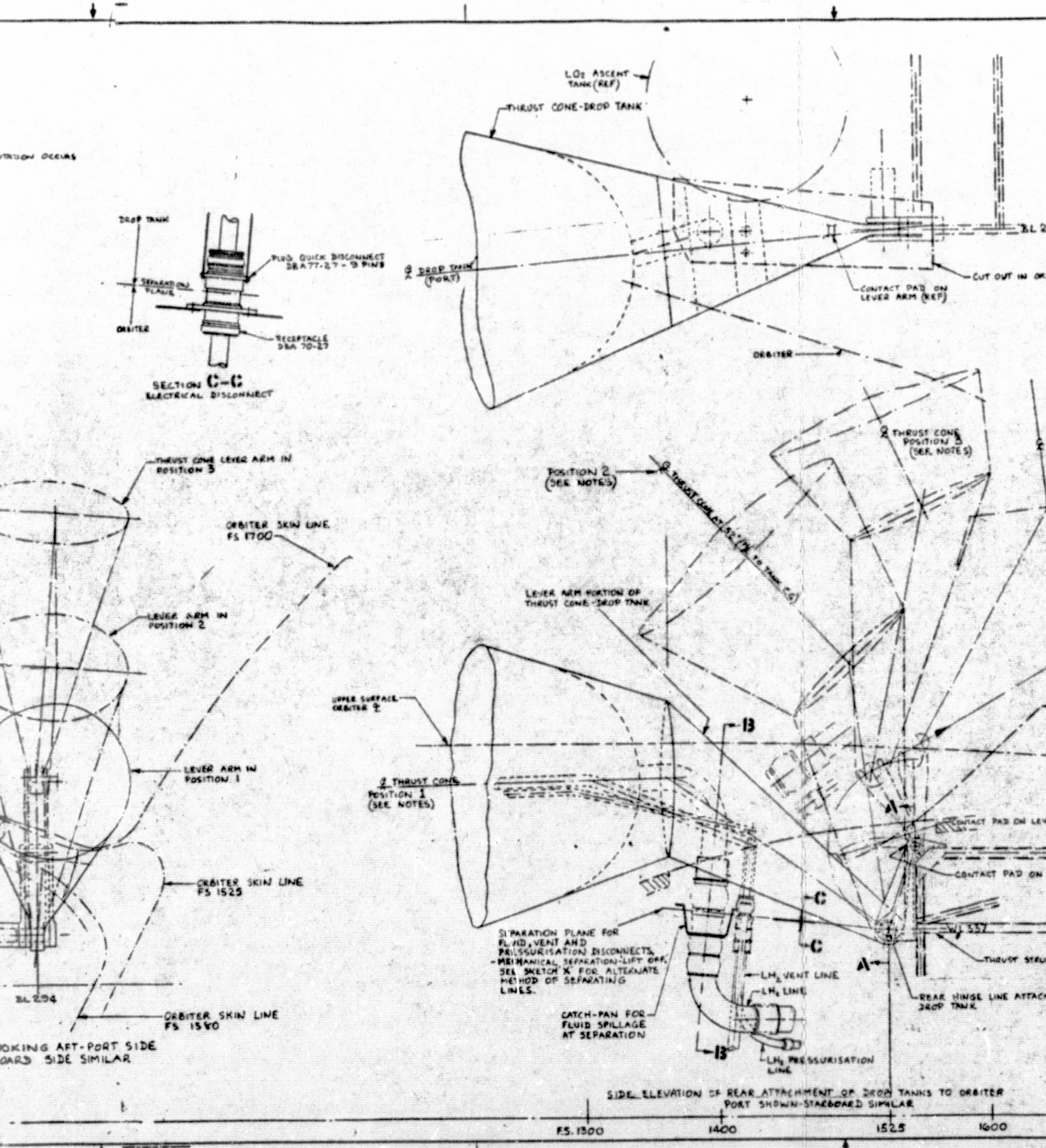

FOLDOUT FRAME 2

REPRODUCIBILITY OF THE ORIGINAL PAGE IS POOR.

PRECEDING PAGE BLANK NOT FILMED

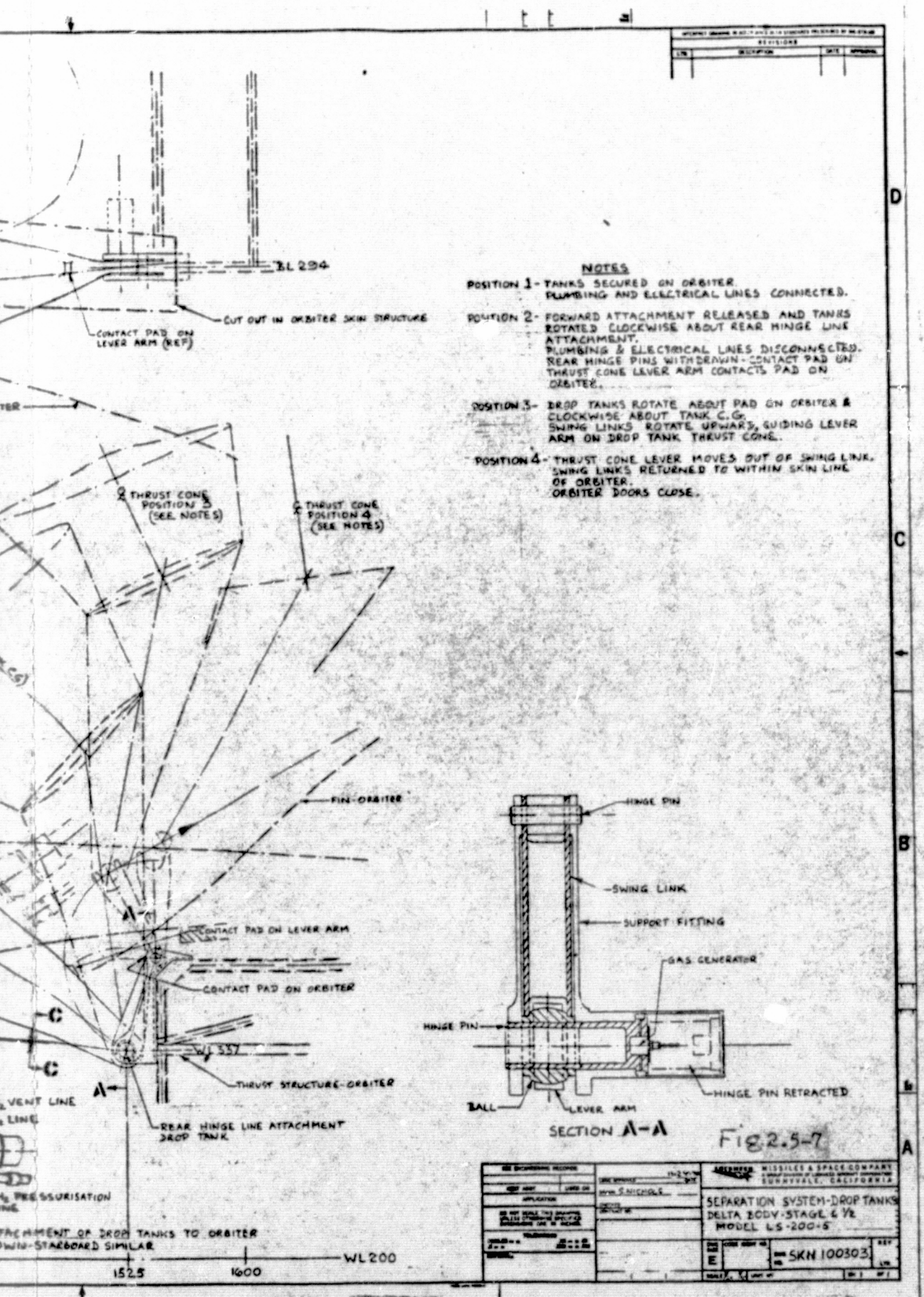

Fig 2.5-7

REPRODUCIBILITY OF THE ORIGINAL PAGE IS POOR.

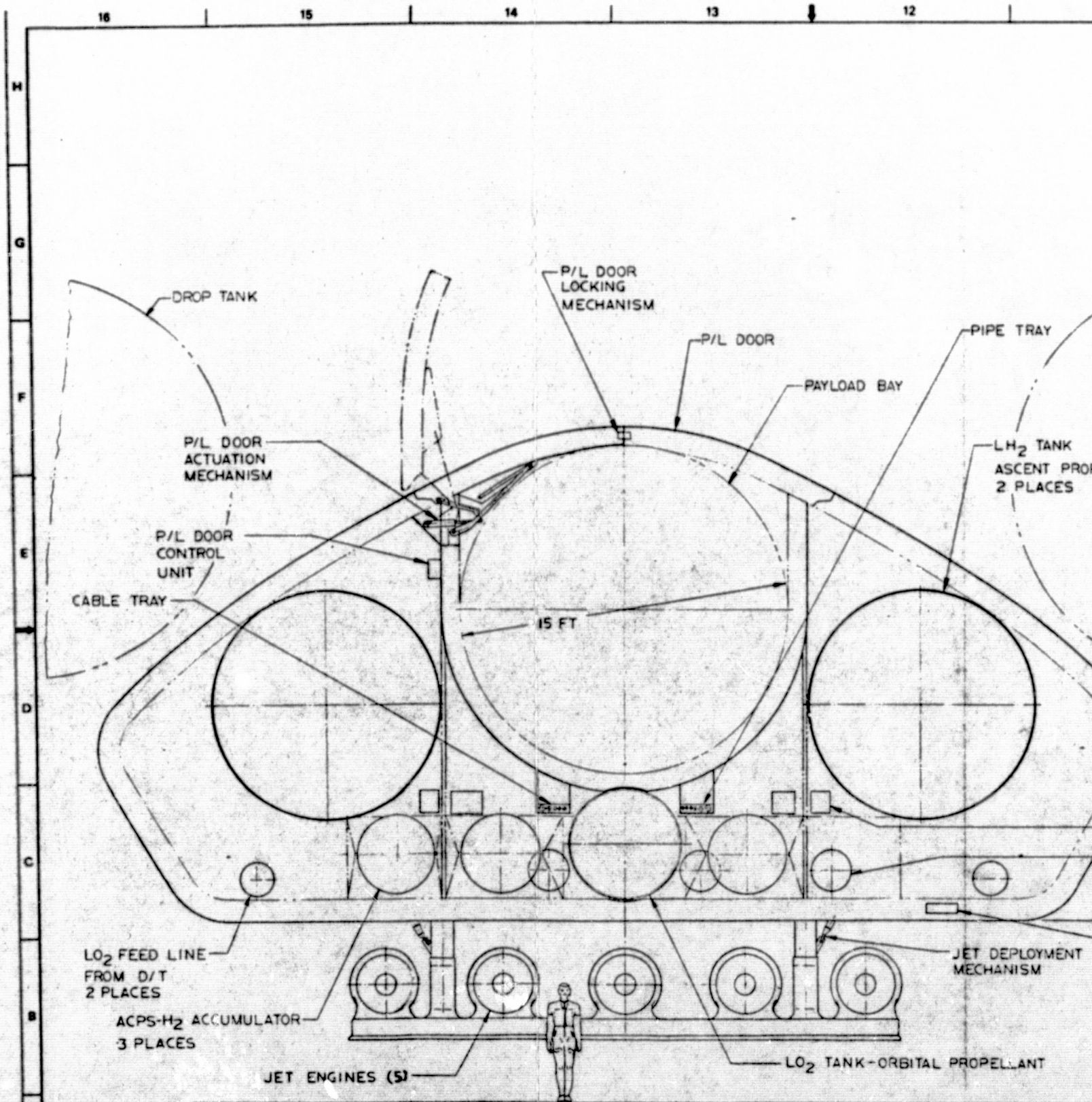

SECTION **J - J**

(FUS. STATION 1200.)

FOLDOUT FRAME

REPRODUCIBILITY OF THE ORIGINAL PAGE IS POOR.

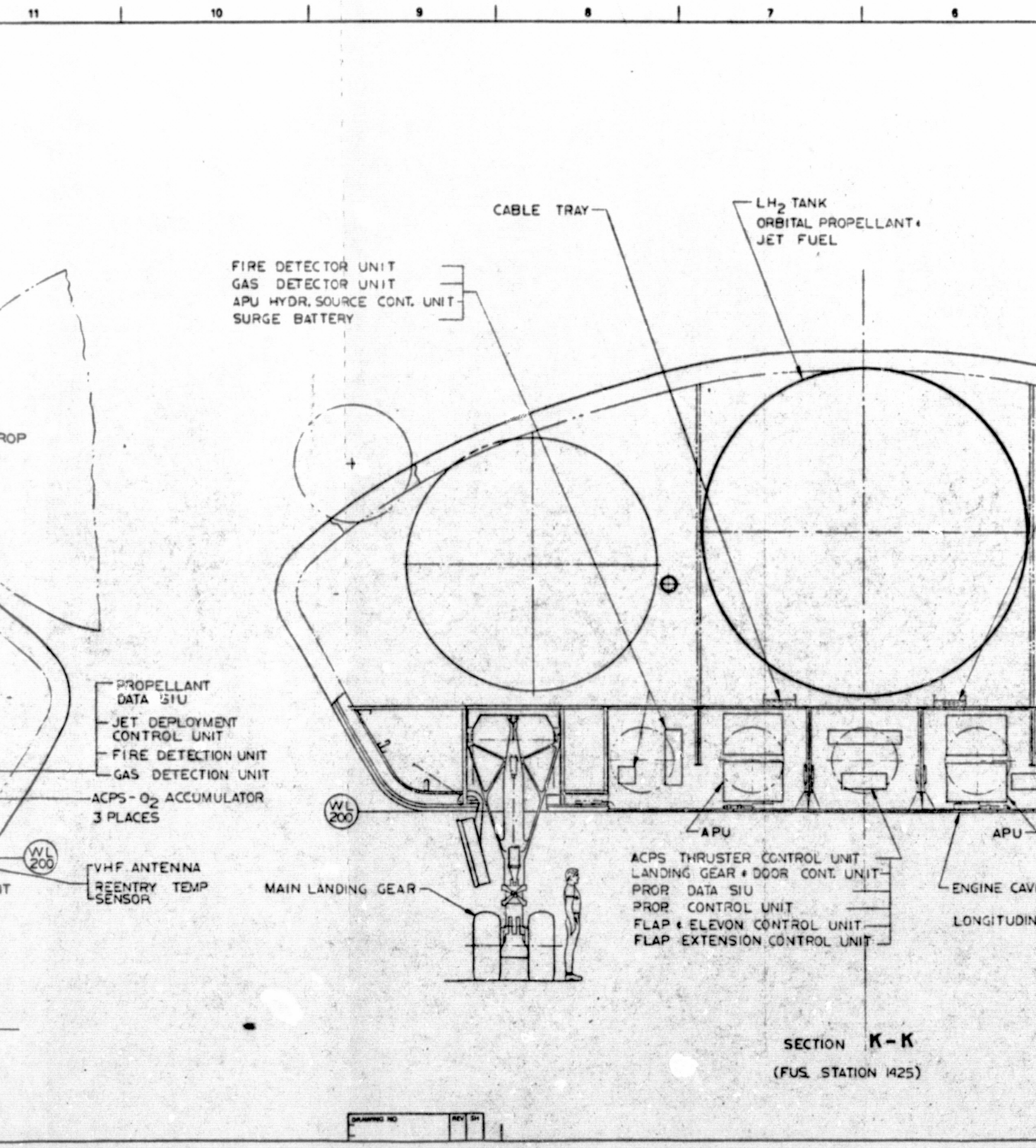

FOLDOUT FRAME 2

PRECEDING PAGE BLANK NOT FILMED

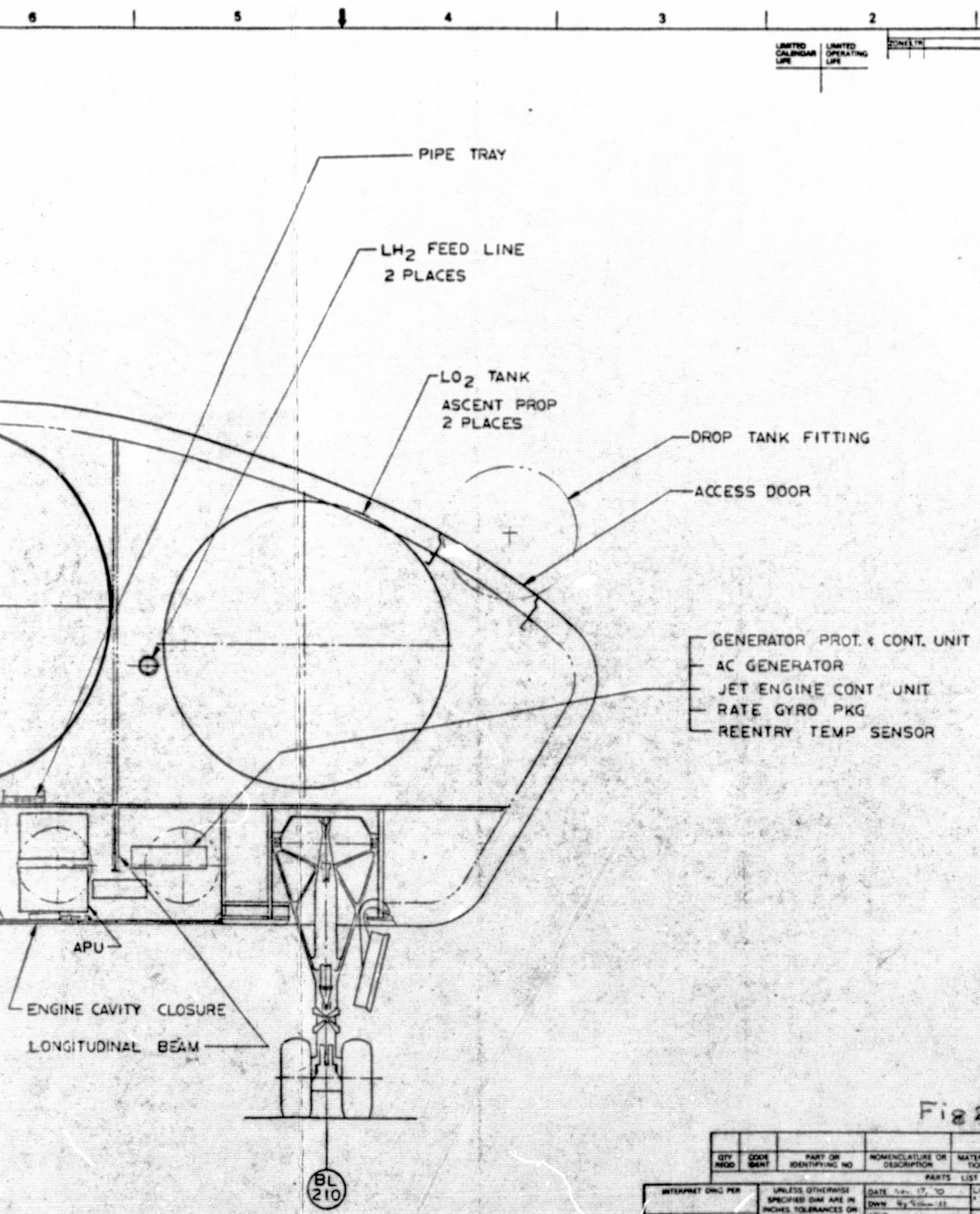

Fig 2.5-8

QTY REQD	CODE IDENT	PART OR IDENTIFYING NO	NOMENCLATURE OR DESCRIPTION	MATERIAL DESCRIPTION OR NOTE	MATERIAL SPECIFICATION	ZONE	ITEM NO

PARTS LIST

REVISIONS			
ZONE	LTR	DESCRIPTION	DATE	APVD

LIMITED CALENDAR LIFE | LIMITED OPERATING LIFE

INTERPRET DWG PER

UNLESS OTHERWISE SPECIFIED DIM ARE IN INCHES. TOLERANCES ON FRACTIONS = ± 1/16, DECIMALS .X = ± .1, .XX = ± .03, .XXX = ± .010, ANGLES = ± 2 DEG

NEXT ASSY | USED ON | APPLICATION

DATE Nov. 17, '60
DWN [illegible]
APVD
APVD E.S. Havekotte
ENGRG
CHKR
APVD
CONTR
APVD
CCA/ECI/FD

LOCKHEED MISSILES & SPACE COMPANY
A GROUP DIVISION OF LOCKHEED AIRCRAFT CORPORATION
SUNNYVALE, CALIFORNIA

INBOARD PROFILE
DELTA BODY STAGE 1½
MODEL LS-200-5

SIZE J | CODE IDENT 19687 | DRAWING NO SKS 100023 | REV

SCALE 1/2 | SHEET 1 OF 3

FOLDOUT FRAME 3 C4

REPRODUCIBILITY OF THE ORIGINAL PAGE IS POOR.

FOLDOUT FRAME

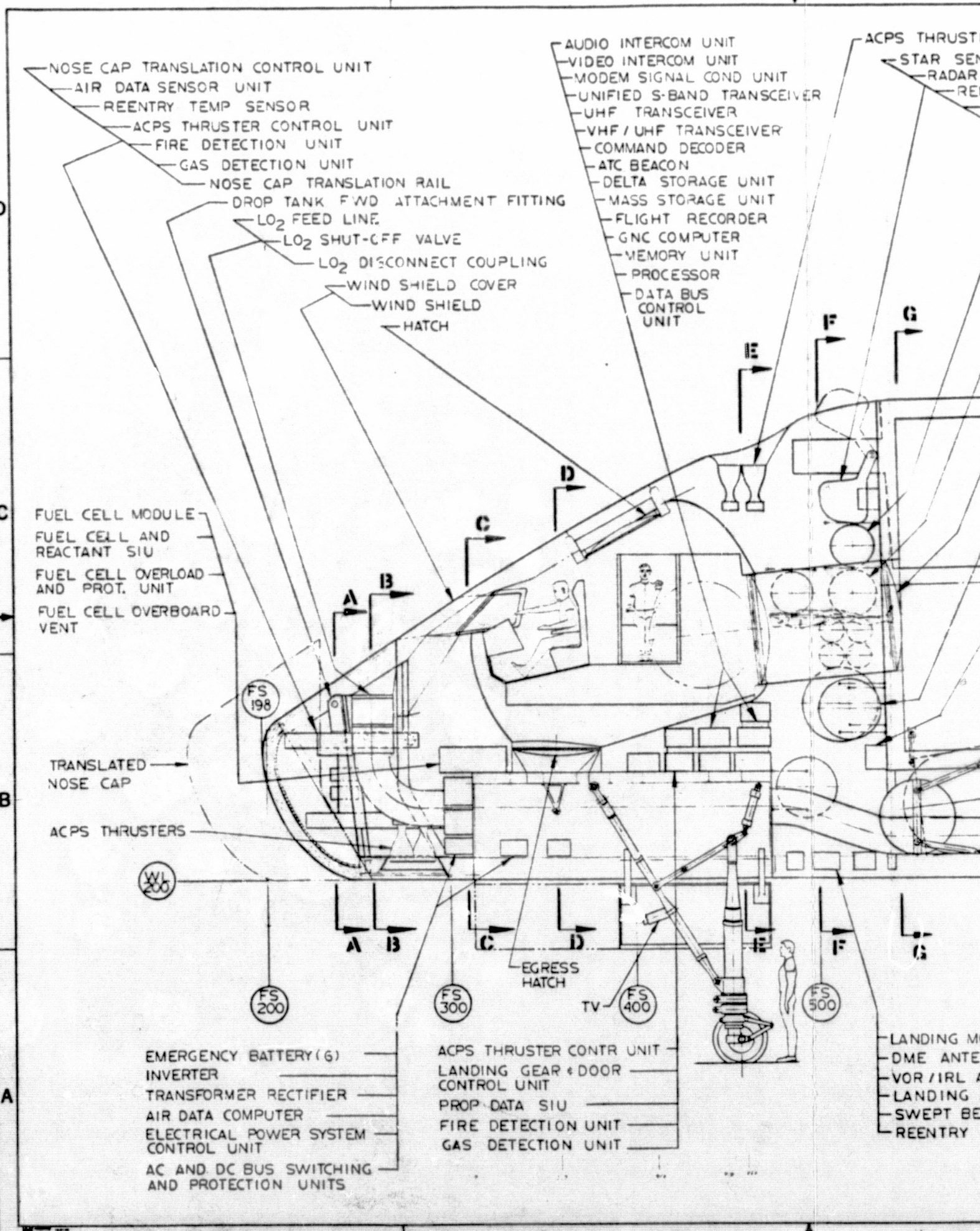

REPRODUCIBILITY OF THE ORIGINAL PAGE IS POOR.

FOLDOUT FRAME 2

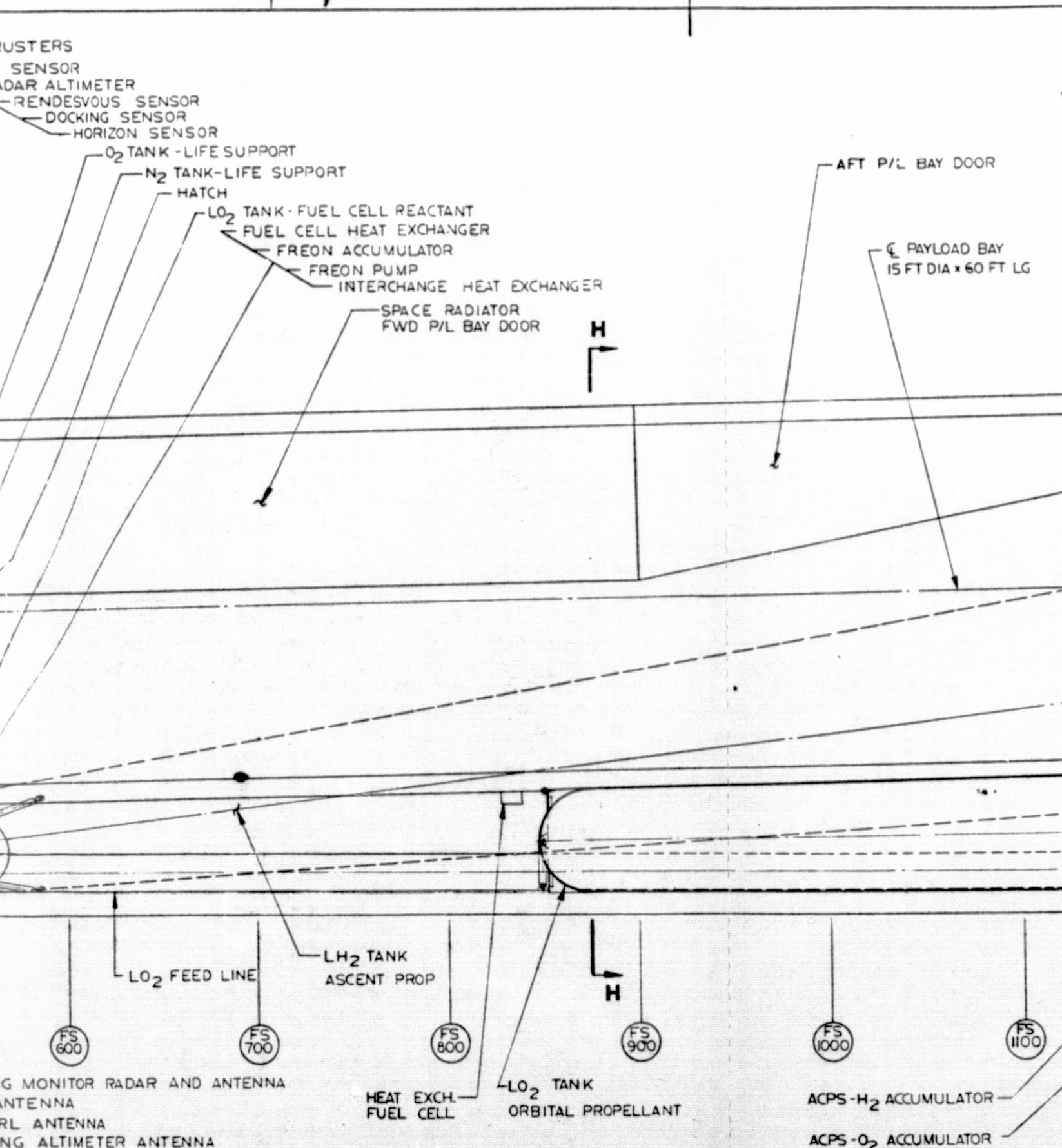

REPRODUCIBILITY OF THE ORIGINAL PAGE IS POOR.

FOLDOUT FRAME 3

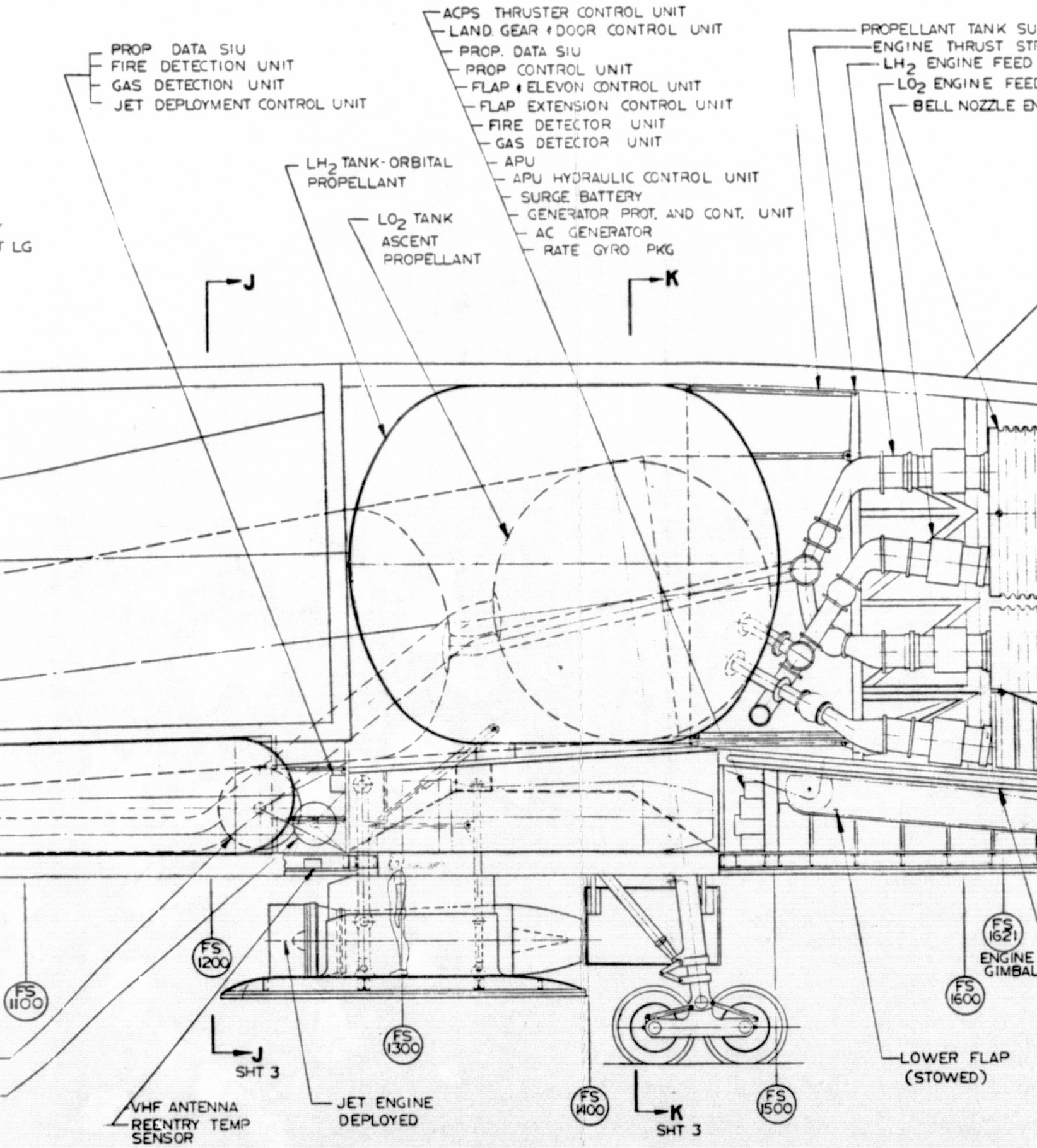

REPRODUCIBILITY OF THE ORIGINAL PAGE IS POOR.

FOLDOUT FRAME 4

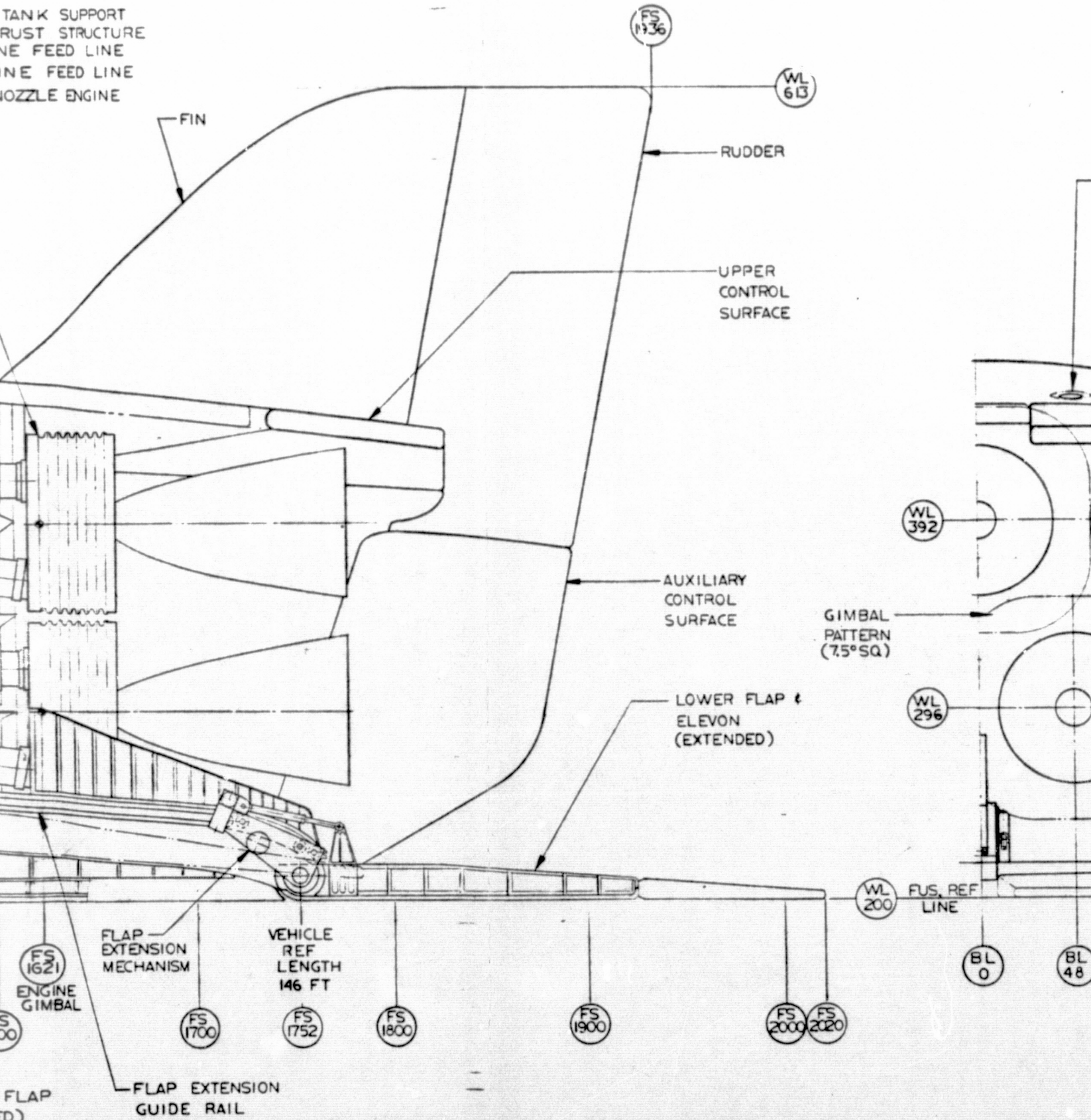

REPRODUCIBILITY OF THE ORIGINAL PAGE IS POOR.

FOLDOUT FRAME 5

PRECEDING PAGE BLANK NOT FILMED

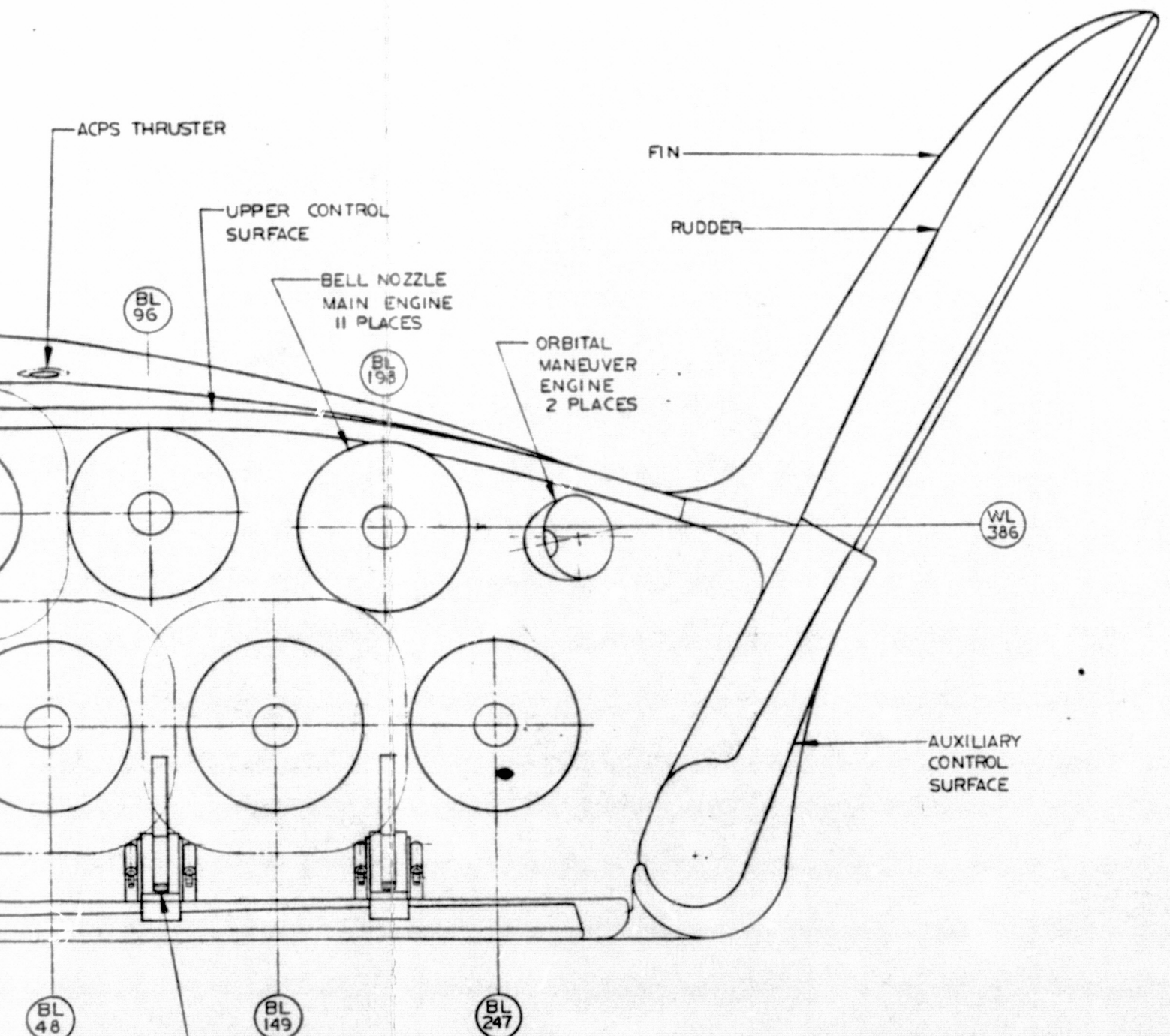

Fig. 2.5-8

LIST OF MATERIAL OR PARTS LIST

INTERPRET THIS DRAWING PER STANDARDS IN MIL-D-70327

UNLESS OTHERWISE SPECIFIED TOLERANCES ON: FRACTIONS = ± 1/16, .X = ± .1, .XX = ± .05, .XXX = ± .010, ANGLES = ± 30

DATE Nov 17, 70
DR Hg Schmidt
CHK
SUPV Sea Harris K
STRESS
VALUE ENGRG
RELIABILITY
APPROVED
APPROVED

MISSILES & SPACE COMPANY
A GROUP DIVISION OF LOCKHEED AIRCRAFT CORPORATION
SUNNYVALE, CALIFORNIA

INBOARD PROFILE
DELTA BODY STAGE & 1/2
MODEL LS-200-5

CODE IDENT NO. 06887 | SIZE J | DRAWING NO. SKS 100023

SCALE 1/20 | SHEET 1 OF 3

2.5-37

REPRODUCIBILITY OF THE ORIGINAL PAGE IS POOR.

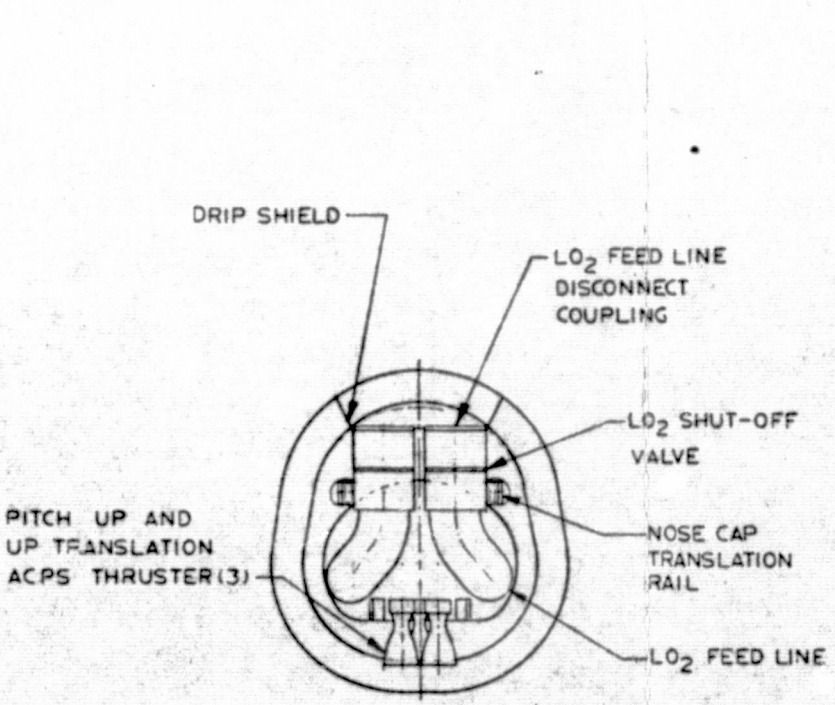

SECTION **B-B**
(FUS STATION 257)

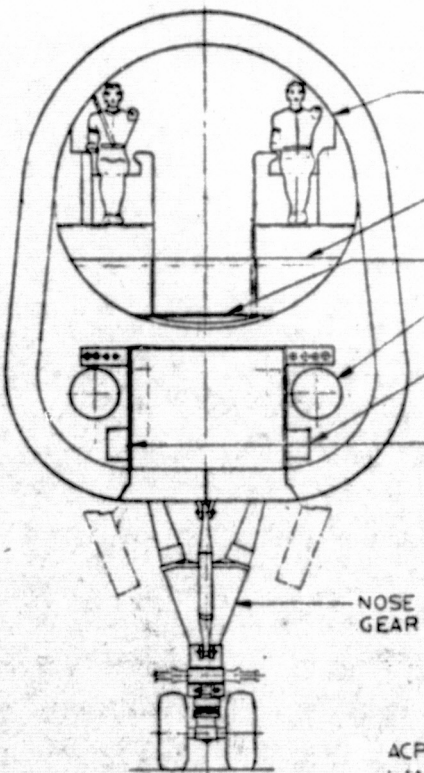

SECTION **D-D**
(FUS STATION 357)

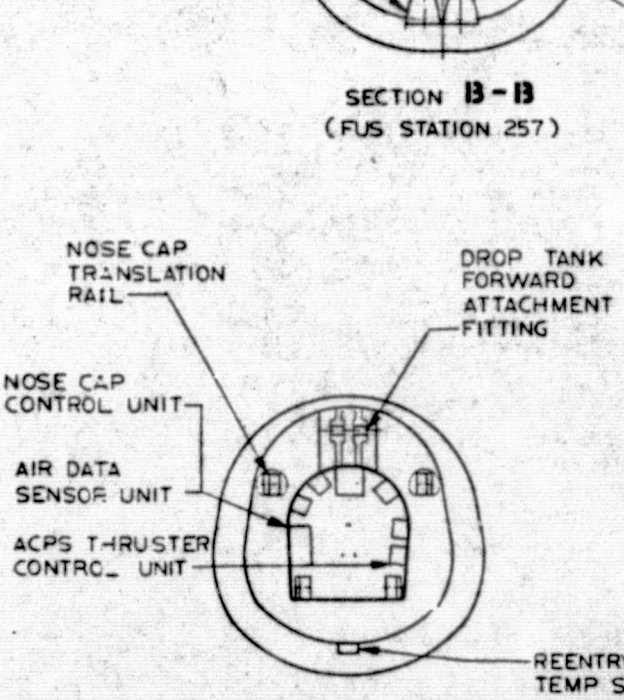

SECTION **A-A**
(FUS STATION 236)

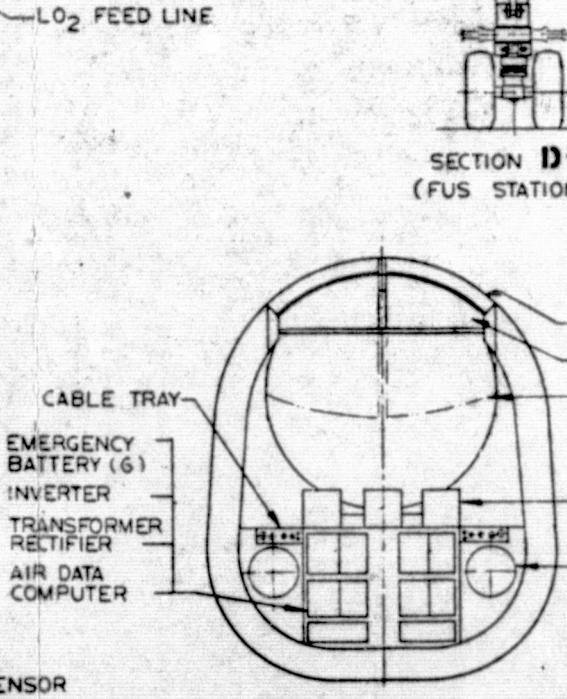

SECTION **C-C**
(FUS STATION 310)

FOLDOUT FRAME

REPRODUCIBILITY OF THE ORIGINAL PAGE IS POOR

11 | 10 | 9 | 8 | 7 | 6

—CREW STATION

—CREW SYSTEM EQUIPMENT STOWAGE

— EGRESS HATCH

—LO_2 FEED LINE 2 PLACES

—ELECTRICAL POWER SYST CONTROL UNIT

— AC AND DC BUS SWITCHING AND PROTECTION UNITS

NDING

PITCH DOWN AND DOWN TRANSLATION ACPS THRUSTER (4)

HATCH TO PASSAGE TUNNEL

THRUSTER CONTR. UNIT
NG GEAR + DOOR
OL UNIT
PROP CONTR UNIT
DATA SIU
DETECTION UNIT
DETECTION UNIT

COVER

COVER

MODULE (3)
ACTANT SIU
D AND

BLE TRAY

2 FEED LINE
PLACES

DING MONITOR RADAR ANTENNA
ANTENNA
/ IRL ANTENNA

SECTION E-E
(FUS STATION 460)

SENSORS DEPLOYED

PART OF FWD P/L DOOR

IMU

O_2 TANK - LIFE SUPPORT

N_2 TANK - LIFE SUPPORT 3 PLACES

YAW AND SIDE TRANLATION ACPS THRUSTER (4) 2 PLACES

LH_2 TANK - FUEL CELL REACTANT 2 PLACES

LO_2 TANK - FUEL CELL REACTANT 3 PLACES

CABLE TRAY

ATC ANTENNA
UHF ANTENNA
REENTRY TEMP SENSOR

STAR SENSOR
RADAR ALTIMETE
RENDEZVOUS SE
DOCKING SENSOR
HORIZON SENSO

RENDEZVOUS SE
DOCKING SENSO

PASSAGE TU N
CABIN TO P/ 3

PIPE TRAY

LO_2 FEED LINE 2 PLACES

EQUIP BAY ACCE

SECTION F-F
(FUS STATION 500)

AUDIO INTERCOM UNIT
VIDEO INTERCOM UNIT
MODEM SIGNAL COND. UNIT
UNIFIED S-BAND TRANSCEIVER
UHF TRANSCEIVER
VHF/UHF TRANSCEIVER

COMMAND DECODER
ATC BEACON
LANDING ALTIMETER
DELTA STORAGE UNIT
MASS STORAGE UNIT

FLIGHT RECORDER
DATA BUS CONTROL UNIT
PROCESSOR
MEMORY UNIT
GNC COMPUTER

LANDING ALTIMETER ANTENNA
SWEPT BEAM MICROWAVE ILS ANTENNA
REENTRY TEMP SENSOR

DROP TANK

P/L B

SPACE RADIAT

FIRE DETECTION UNIT
GAS DETECTION UNIT

CABLE TRAY

LH_2 TANK
FUEL CELL REACTANT

DRAWING NO | REV | SH

FOLDOUT FRAME 2

REPRODUCIBILITY OF THE ORIGINAL PAGE IS POOR.

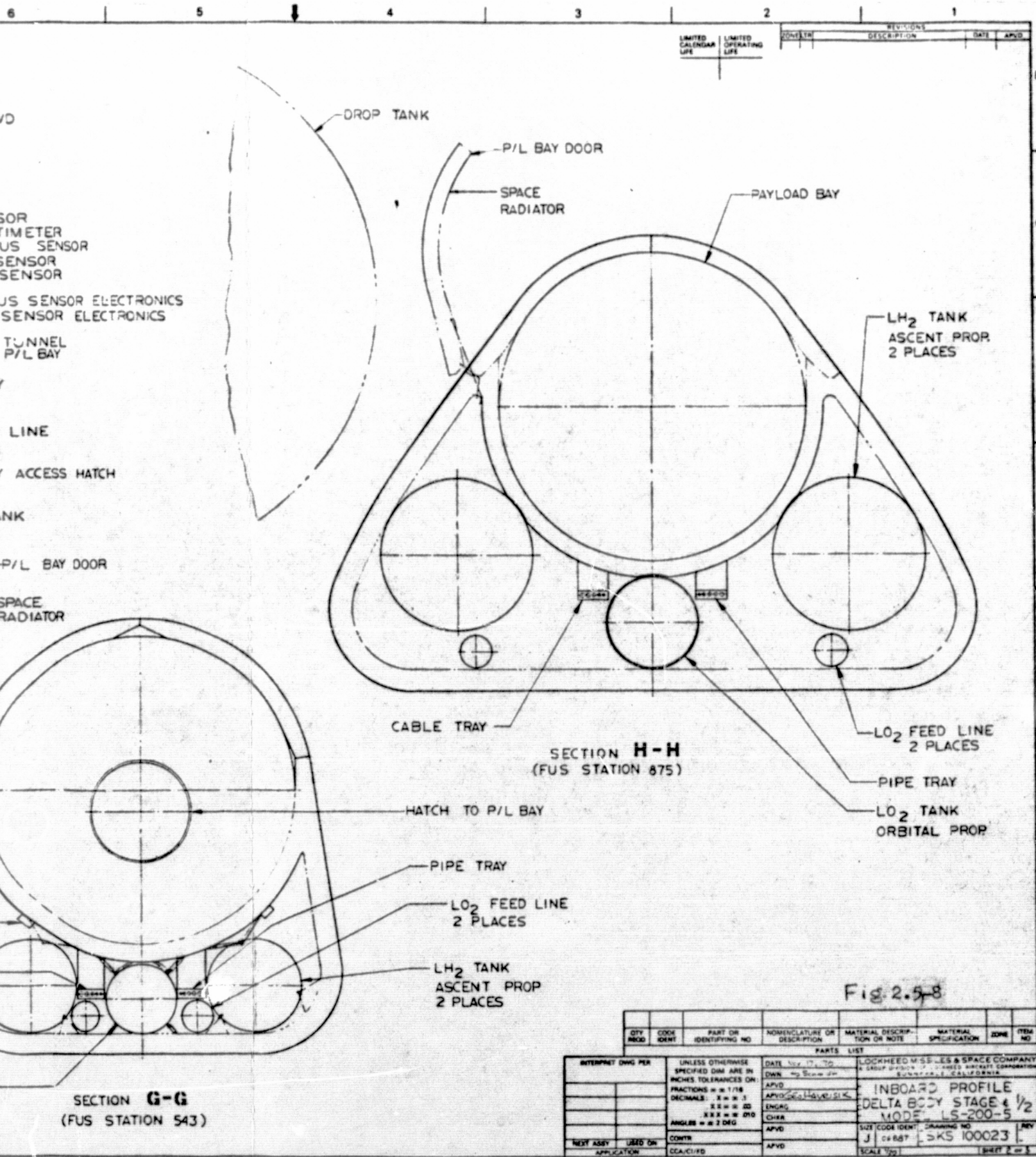

Fig. 2.5-8

FOLDOUT FRAME 3

REPRODUCIBILITY OF THE ORIGINAL PAGE IS POOR

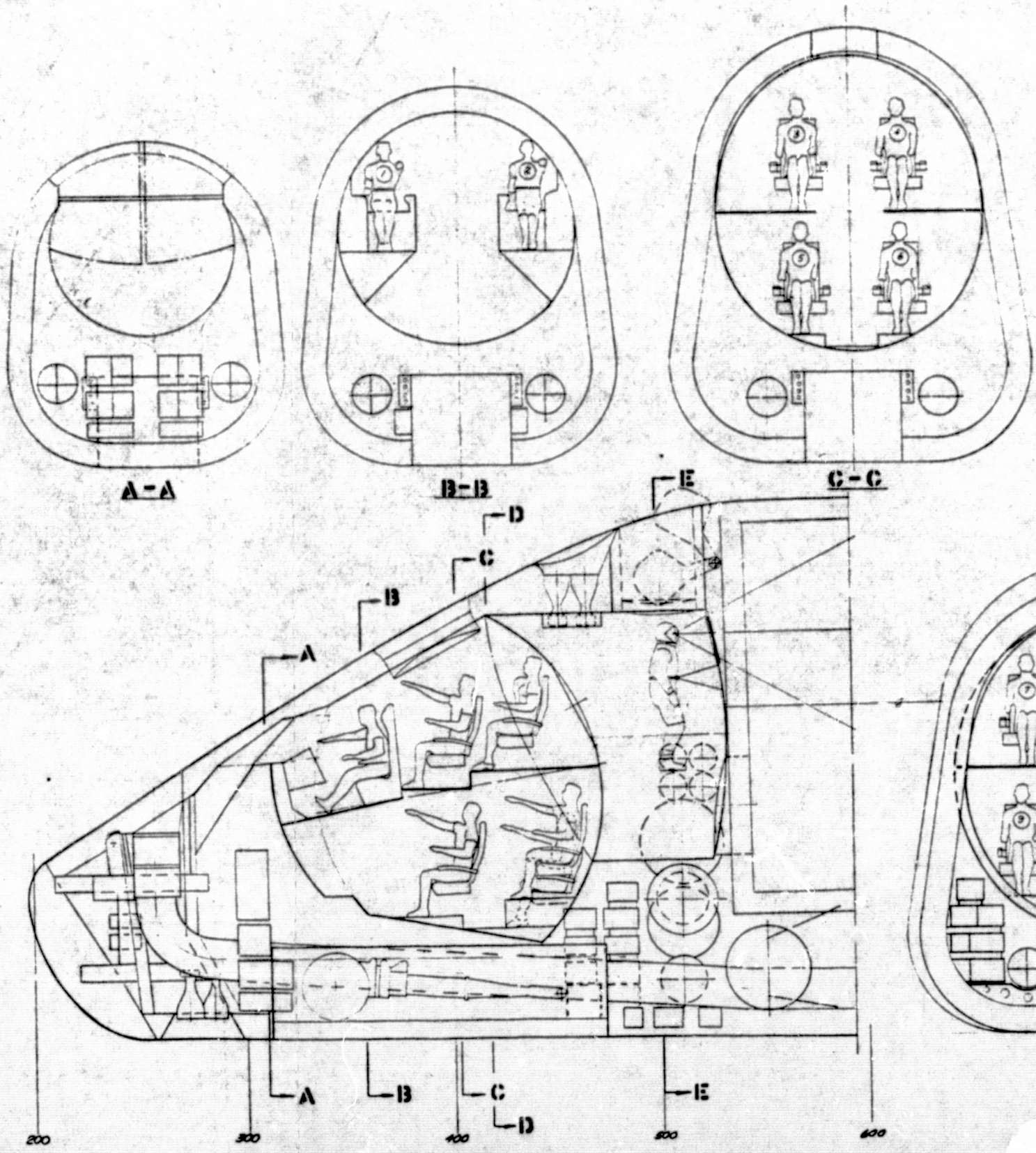

FOLDOUT FRAME

REPRODUCIBILITY OF THE ORIGINAL PAGE IS POOR.

PRECEDING PAGE BLANK NOT FILMED

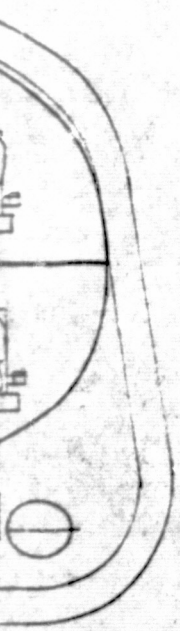

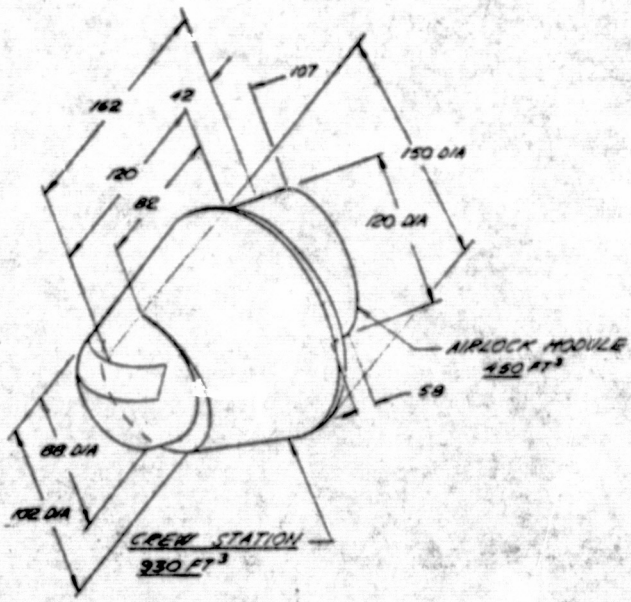

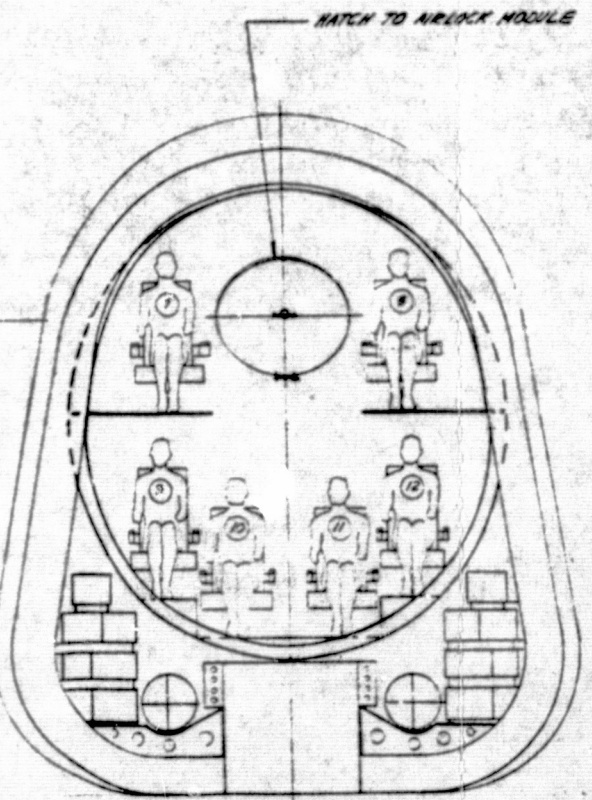

D - D

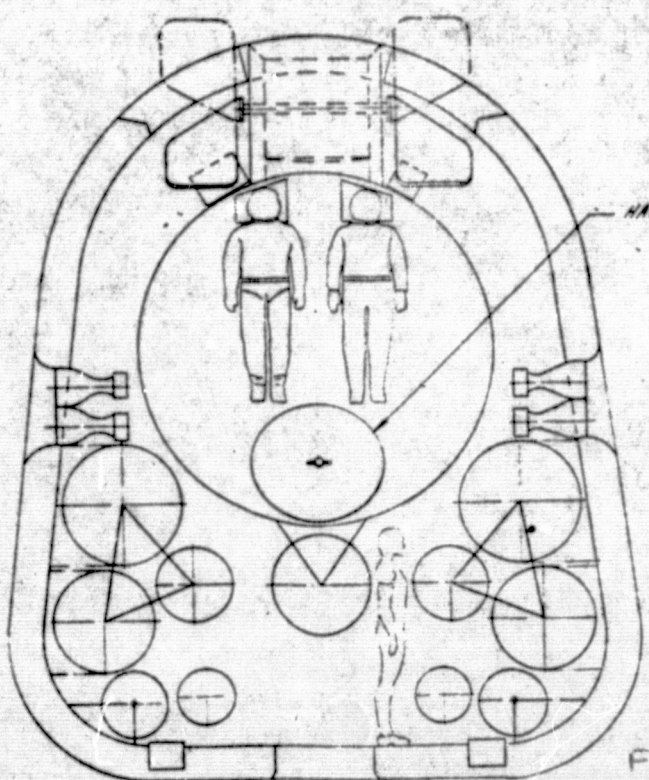

E - E

REF SKS 100023
W BOARD PROFILE

Fig 2.5-9

DATE 1-28-71	LOCKHEED MISSILES & SPACE COMPANY
BY KARL TOLLO	A GROUP DIVISION OF LOCKHEED AIRCRAFT CORPORATION
APPD Geo Hawkins	SUNNYVALE, CALIFORNIA
APPD	PASSENGER SPACE ALLOCATION
ENGRG	12-MEN ARRANGEMENT
CHK	DELTA BODY CIV. - MODEL LS 200-5
APPD	SIZE: CODE IDENT: DRAWING NO. SKT100035
APPD	SCALE 1/20

FOLDOUT FRAME 2

REPRODUCIBILITY OF THE ORIGINAL PAGE IS POOR.

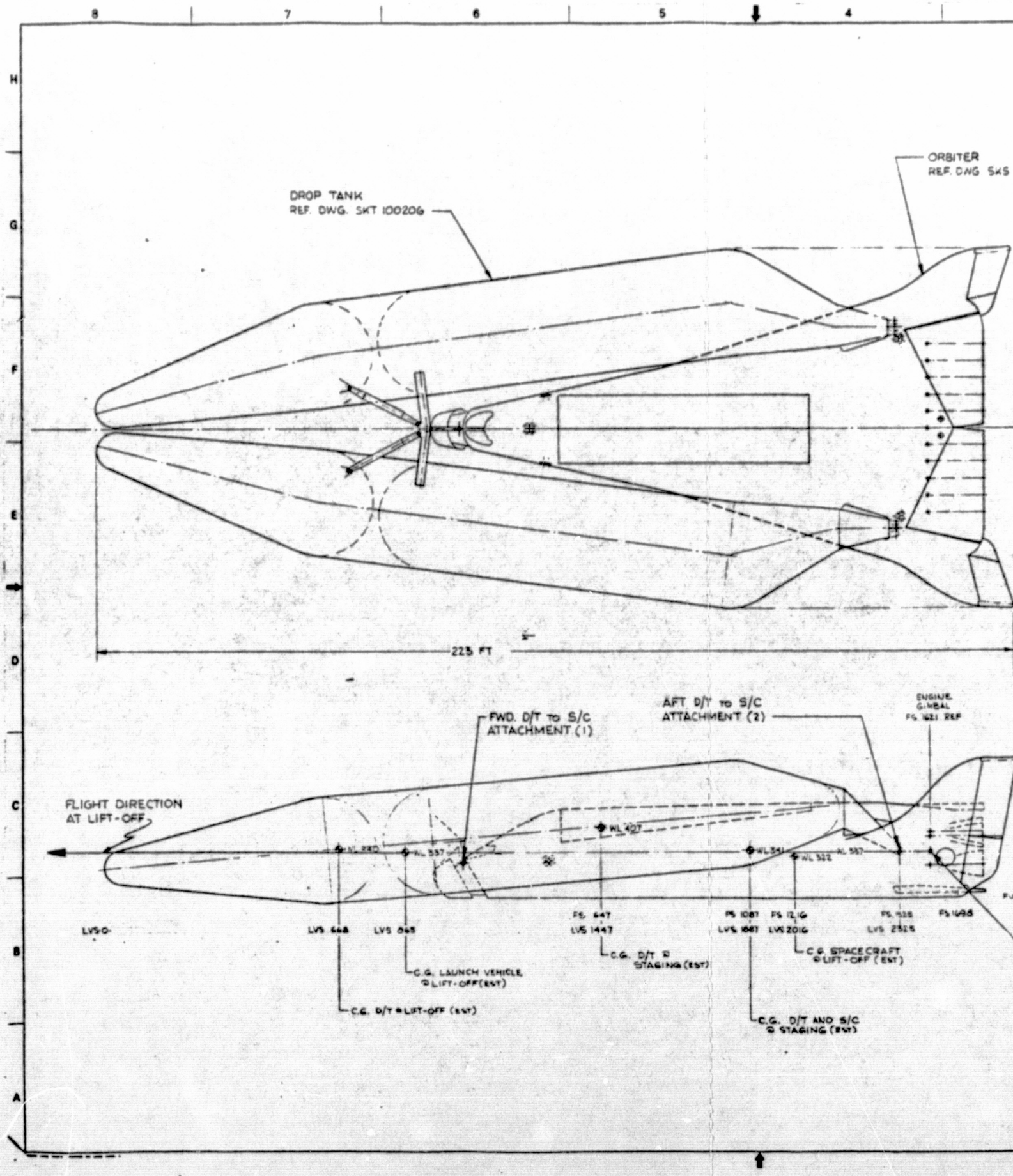

FOLDOUT FRAME

REPRODUCIBILITY OF THE ORIGINAL PAGE IS POOR.

PRECEDING PAGE BLANK NOT FILMED

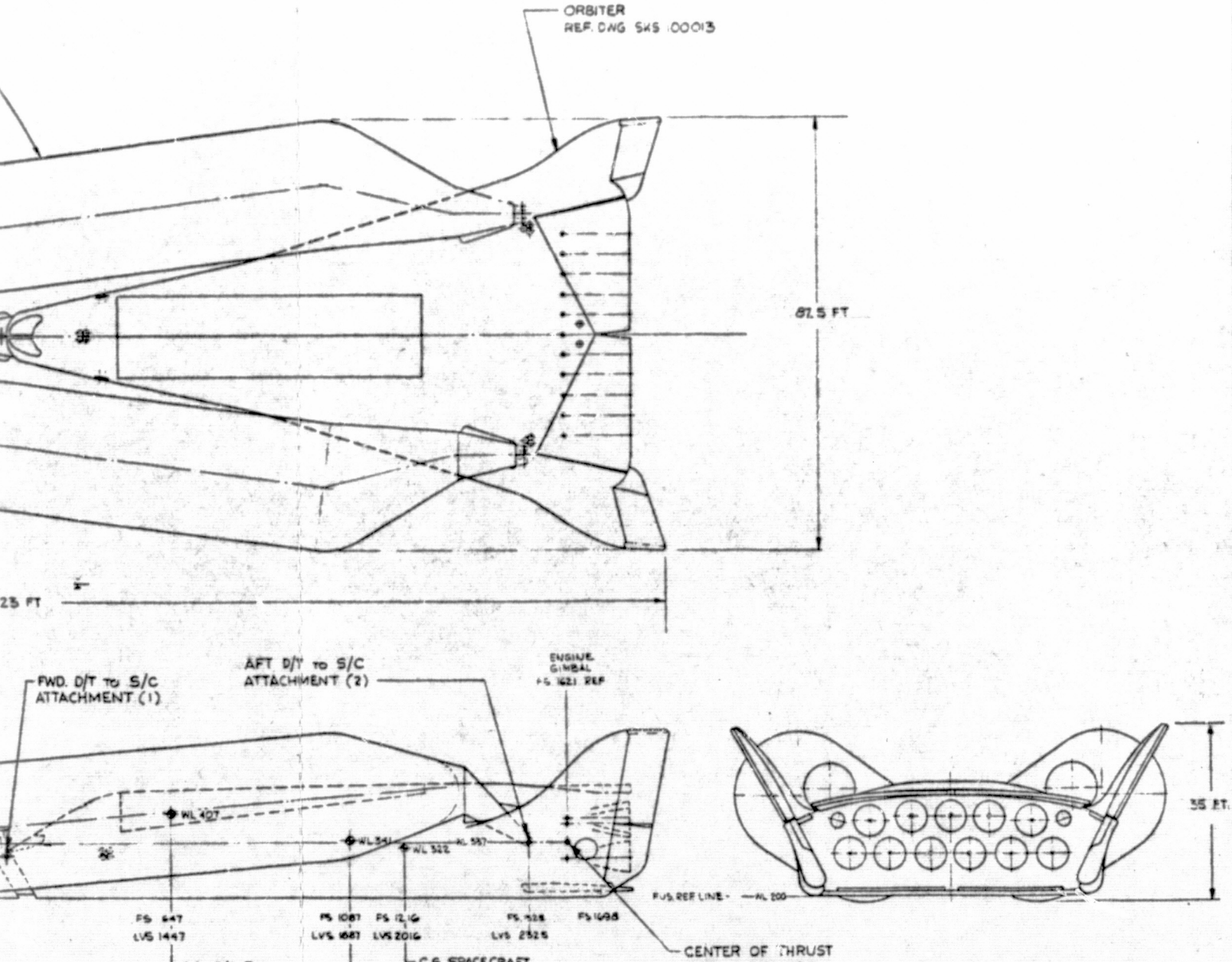

FIG 2.5-10

QTY REQD	CODE IDENT	PART OR IDENTIFYING NO	NOMENCLATURE OR DESCRIPTION	MATERIAL DESCRIPTION OR NOTE	MATERIAL SPECIFICATION	ZONE	ITEM NO

PARTS LIST

INTERPRET DWG PER	UNLESS OTHERWISE SPECIFIED DIM ARE IN INCHES. TOLERANCES ON: FRACTIONS = ± 1/16, DECIMALS: X = ± .1, .XX = ± .03, .XXX = ± .010, ANGLES = ± 2 DEG	DATE 9-25-70	LOCKHEED MISSILES & SPACE COMPANY, A GROUP DIVISION OF LOCKHEED AIRCRAFT CORPORATION, SUNNYVALE, CALIFORNIA
		DWN [illegible]	LAUNCH VEHICLE DELTA BODY - STAGE 1½ MODEL LS-200-3
		APVD [illegible]	
		APVD	
		ENGRG	
		CHKR	
		APVD	SIZE E, CODE IDENT 06887, DRAWING NO SKS 100014, REV A
NEXT ASSY	USED ON APPLICATION	CONTR	
		CCA/CI/FD	APVD
			SCALE [illegible], SHEET 1 of 1

REPRODUCIBILITY OF THE ORIGINAL PAGE IS POOR.

FOLDOUT FRAME

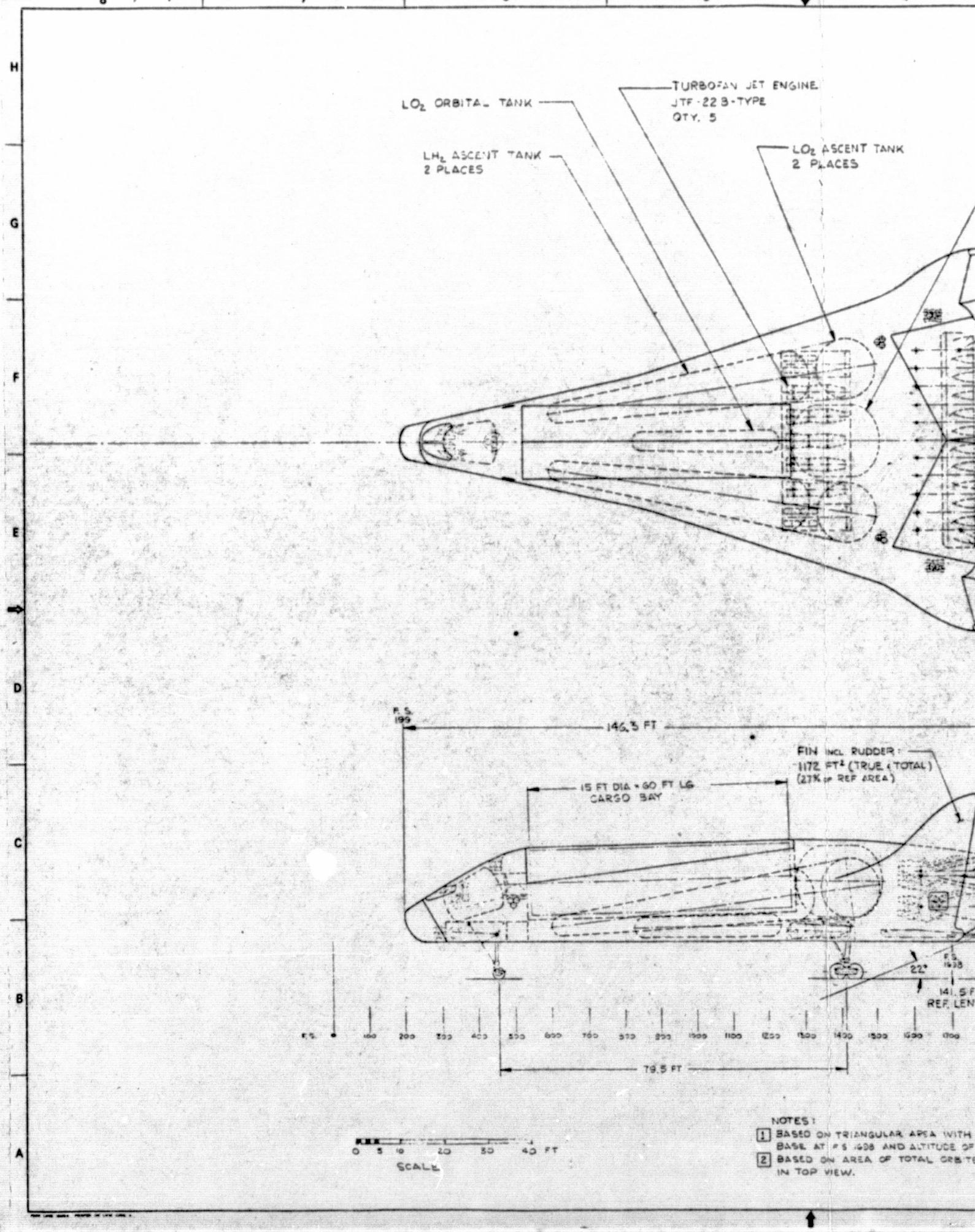

REPRODUCIBILITY OF THE ORIGINAL PAGE IS POOR.

FOLDOUT FRAME 2

PRECEDING PAGE BLANK NOT FILMED

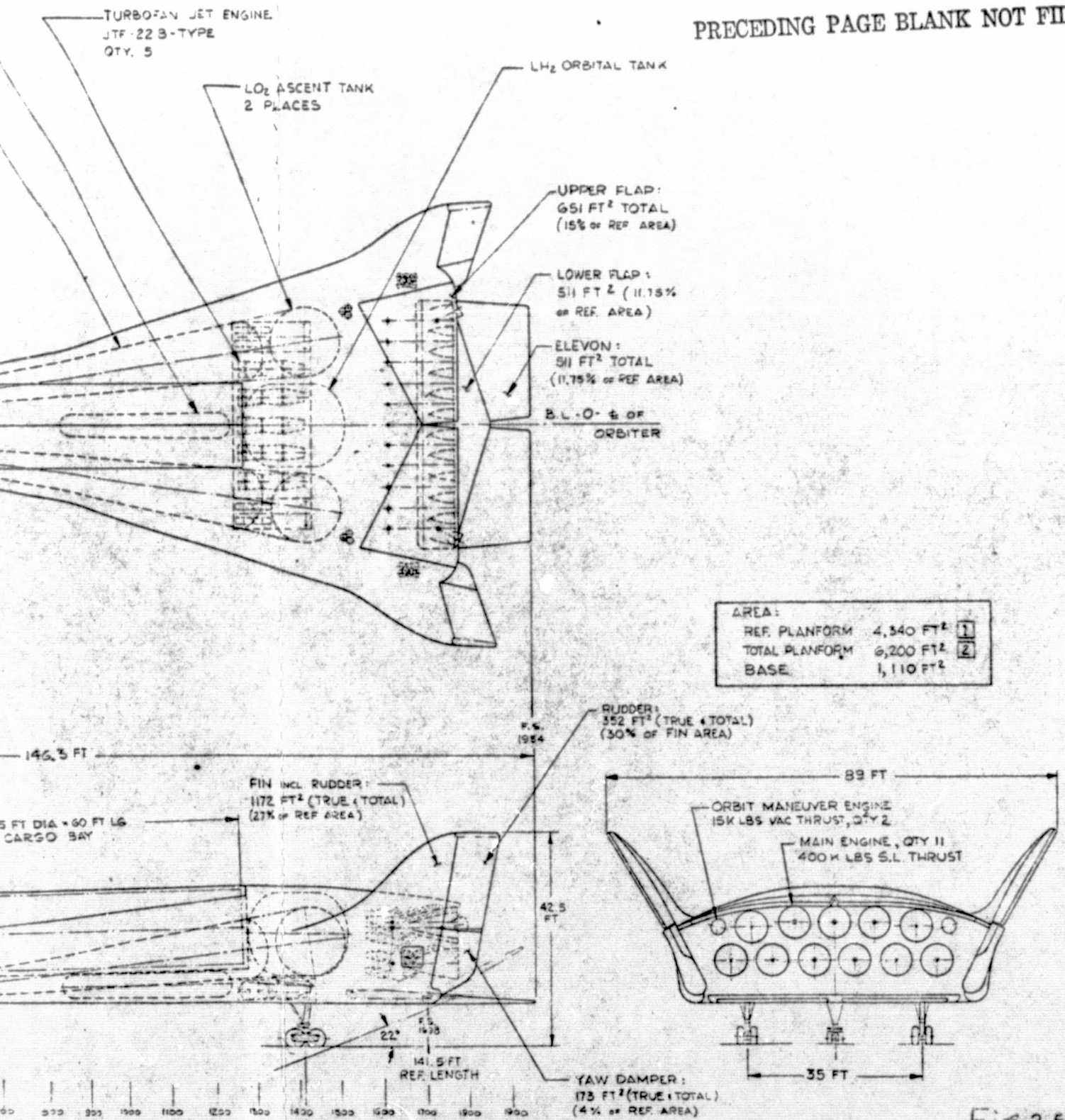

Fig. 2.5-11

NOTES:

1. BASED ON TRIANGULAR AREA WITH APEX AT F.S. 0; BASE AT F.S. 1698 AND ALTITUDE OF 141.5 FT (REF. LENGTH)
2. BASED ON AREA OF TOTAL ORBITER AS SHOWN IN TOP VIEW.

QTY REQD	CODE IDENT	PART OR IDENTIFYING NO	NOMENCLATURE OR DESCRIPTION	MATERIAL DESCRIPTION OR NOTE	MATERIAL SPECIFICATION	ZONE	ITEM NO

PARTS LIST

INTERPRET DWG PER

UNLESS OTHERWISE SPECIFIED DIM ARE IN INCHES. TOLERANCES ON: FRACTIONS = ± 1/16; DECIMALS: .X = ± .1, .XX = ± .03, .XXX = ± .010; ANGLES = ± 2 DEG

DATE / DWN / APVD / APVD / ENGRG / CHKR / APVD / APVD

LOCKHEED MISSILES & SPACE COMPANY
A GROUP DIVISION OF LOCKHEED AIRCRAFT CORPORATION
SUNNYVALE, CALIFORNIA

GENERAL ARRANGEMENT
DELTA BODY - STAGE # 1/2
MODEL LS-200-3

SIZE E | CODE IDENT | DRAWING NO LS-KS 100013 | REV

NEXT ASSY | USED ON | APPLICATION | CONTR | CCA/CI/FD | SCALE | SHEET

REPRODUCIBILITY OF THE ORIGINAL PAGE IS POOR.

FOLDOUT FRAME

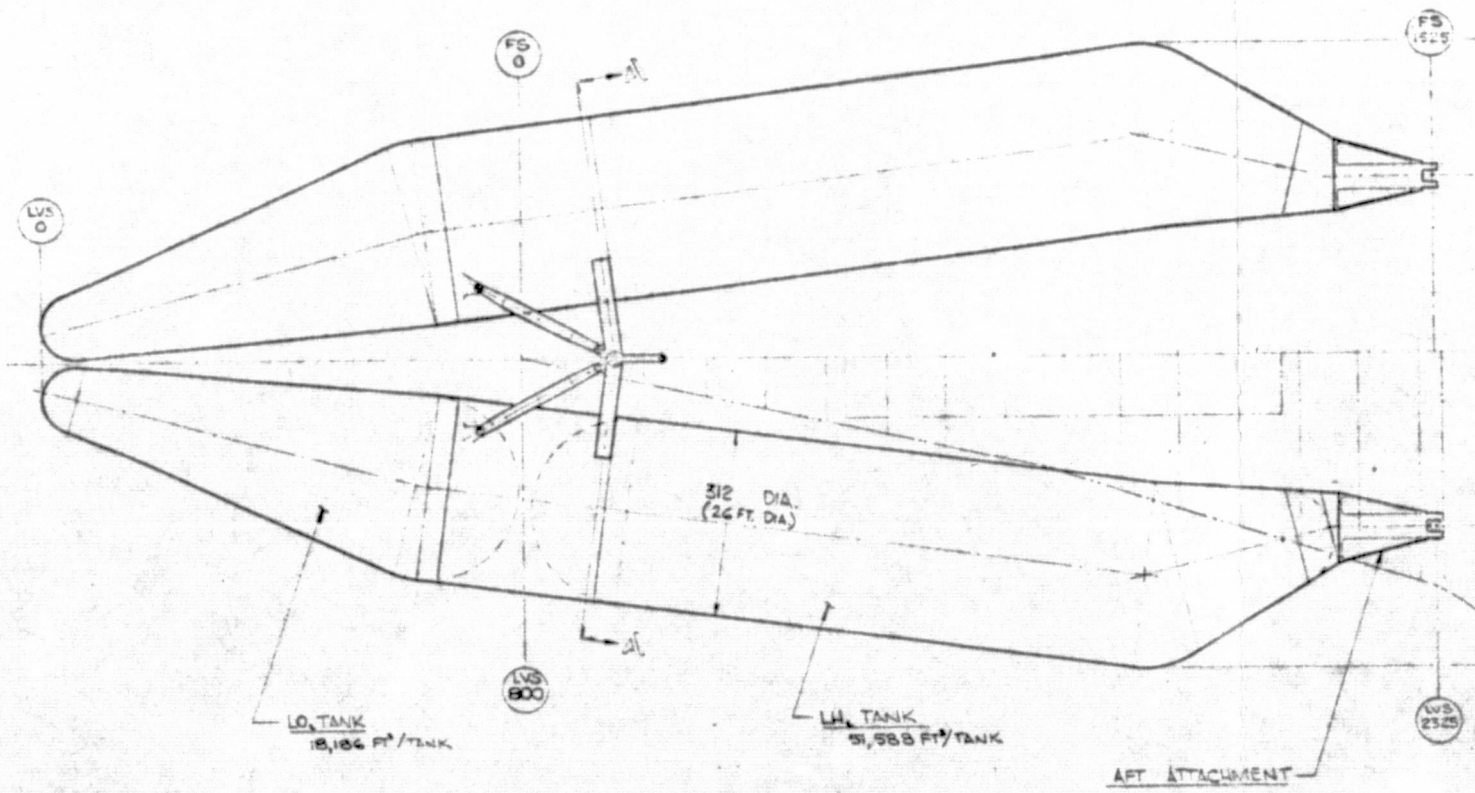

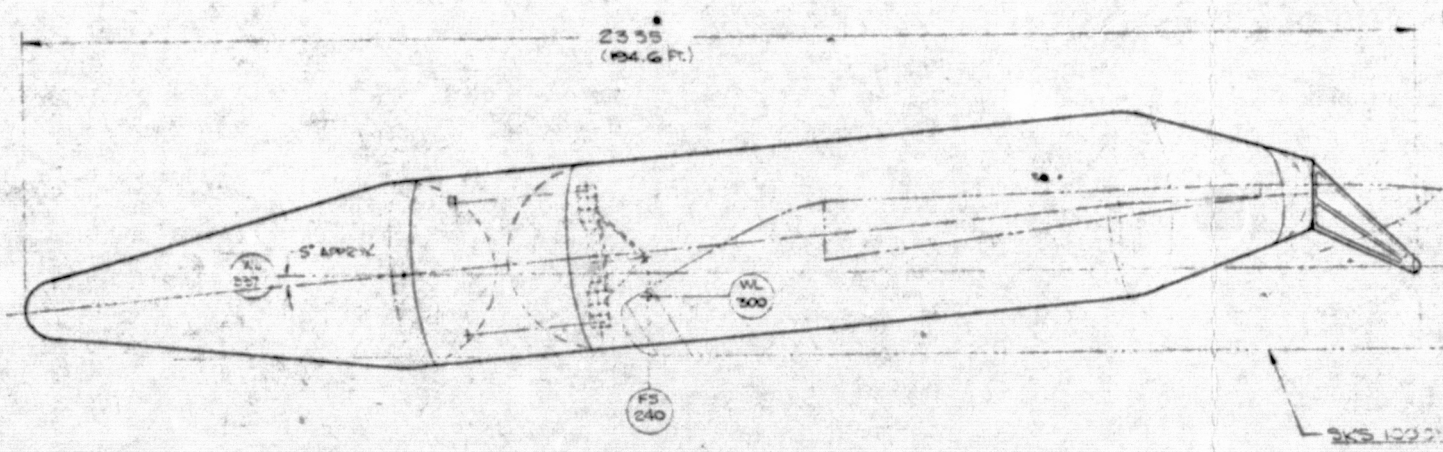

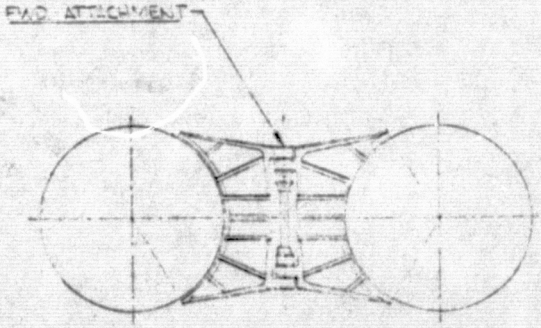

SECTION A-A

PROPELLANT DATA

Wp = 2,937,050 LBS. (GROUND
MR = 6:1
LH_2 WEIGHT = 423,130 LBS
LO_2 WEIGHT = 2,473,920 LBS.

REPRODUCIBILITY OF THE ORIGINAL PAGE IS POOR.

PRECEDING PAGE BLANK NOT FILMED

FOLDOUT FRAME 2

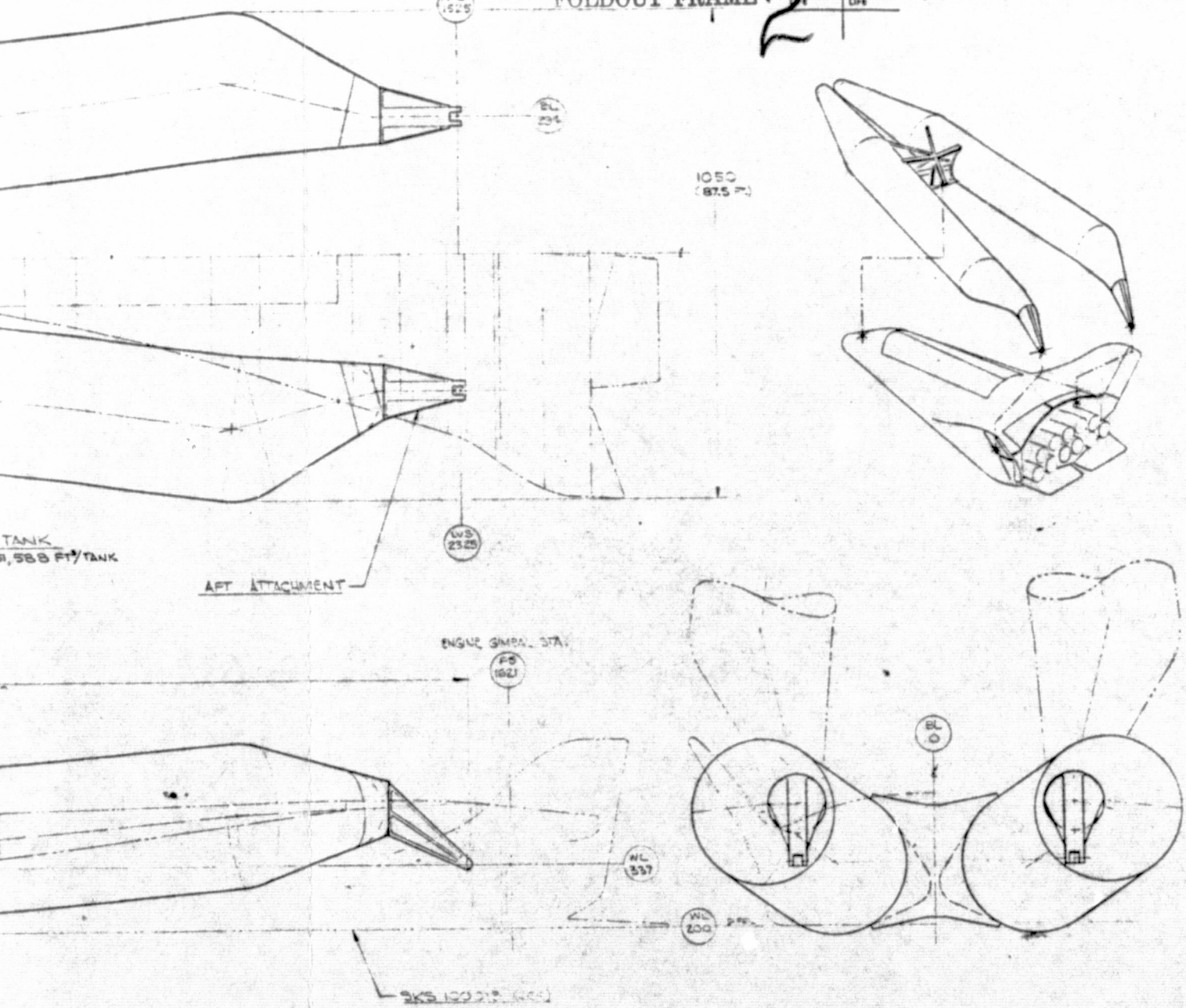

TANK
,588 FT³/TANK

PROPELLANT DATA

W_p = 2,937,050 LBS. (GROUND LOAD PROPELLANT)
VR = 6:1
W_f WEIGHT = 423,130 LBS
W_o WEIGHT = 2,473,920 LBS.

Fig 2.5-12

QTY PER	CODE IDENT	PART OR IDENTIFYING NO.	NOMENCLATURE OR DESCRIPTION	MATERIAL DESCRIPTION OR NOTE	MATERIAL SPECIFICATION	ZONE	ITEM NO.

PARTS LIST

REVISIONS				
ZONE	LTR	DESCRIPTION	DATE	APP'D

INTERPRET DWG PER

UNLESS OTHERWISE SPECIFIED DIM ARE IN INCHES TOLERANCES ON:
FRACTIONS = ± 1/16
DECIMALS: .X = ± .1
.XX = ± .03
.XXX = ± .010
ANGLES = ± 2 DEG

NEXT ASSY | USED ON APPLICATION

CONTR
CCA/CI/FD

DATE
DWN
APVD
APVD
ENGRG
CHKR
APVD
APVD

LOCKHEED MISSILES & SPACE COMPANY
A GROUP DIVISION OF LOCKHEED AIRCRAFT CORPORATION
SUNNYVALE, CALIFORNIA

DROP TANK

SIZE E | CODE IDENT 08537 | DRAWING NO SKT 100206 | REV

SCALE | SHEET

REPRODUCIBILITY OF THE ORIGINAL PAGE IS POOR.

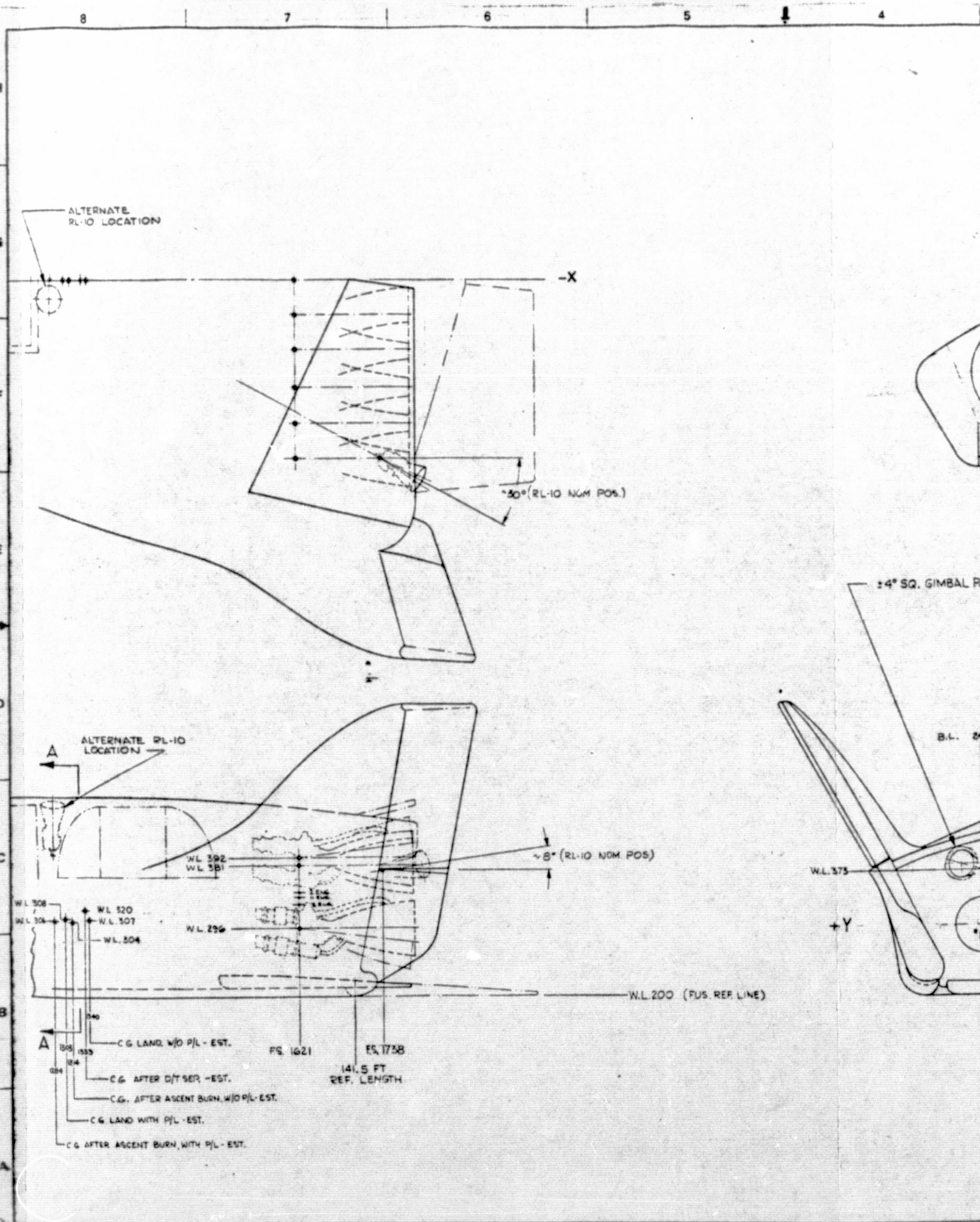

FOLDOUT FRAME

REPRODUCIBILITY OF THE ORIGINAL PAGE IS POOR.

LIMITED CALENDAR LIFE	LIMITED OPERATING LIFE

REVISIONS				
ZONE	LTR	DESCRIPTION	DATE	APVD

PRECEDING PAGE BLANK NOT FILMED

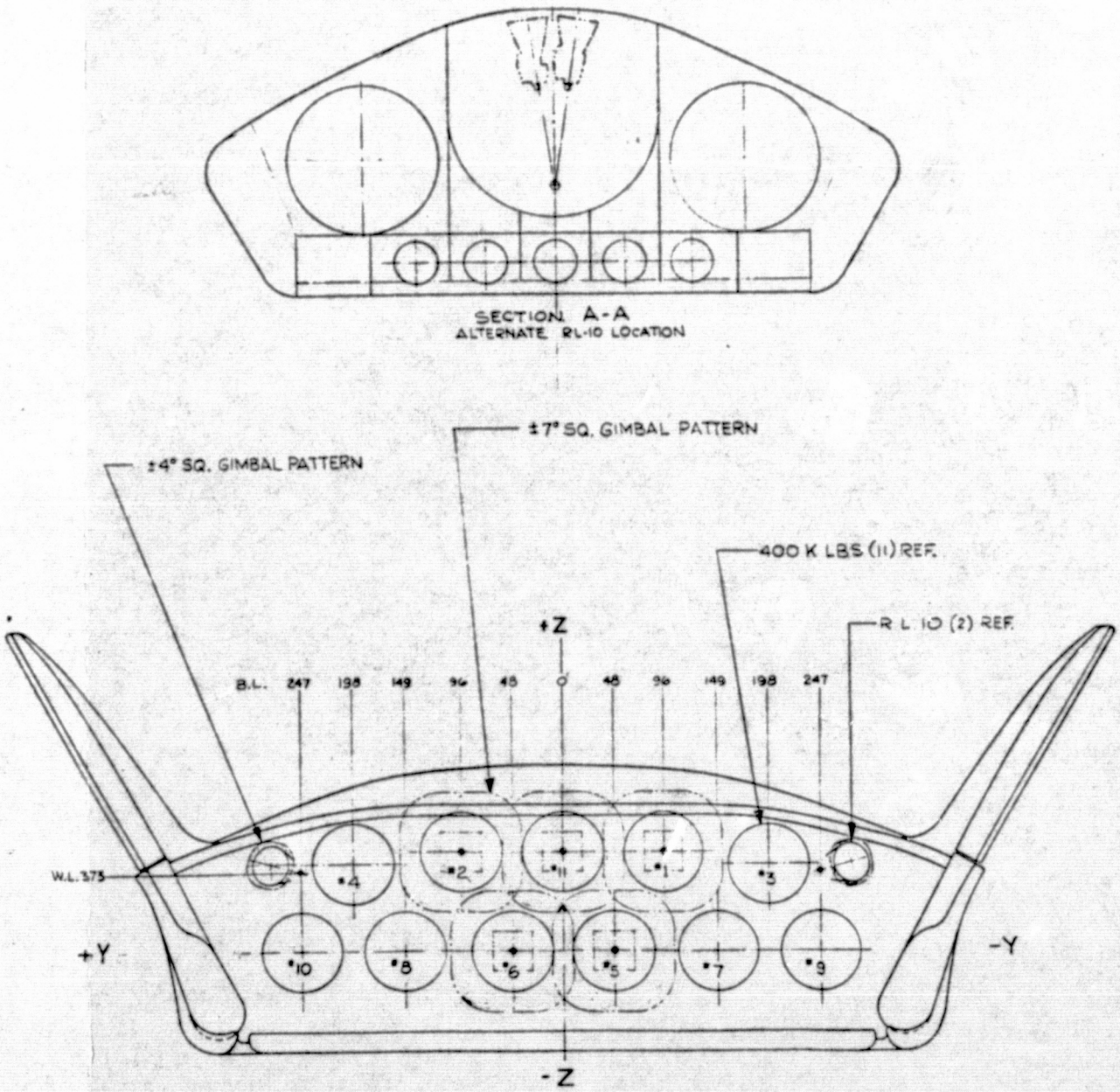

Fig. 2.5-13

QTY REQD	CODE IDENT	PART OR IDENTIFYING NO	NOMENCLATURE OR DESCRIPTION	MATERIAL DESCRIPTION OR NOTE	MATERIAL SPECIFICATION	ZONE	ITEM NO

PARTS LIST

INTERPRET DWG PER	UNLESS OTHERWISE SPECIFIED DIM ARE IN INCHES TOLERANCES ON: FRACTIONS = ± 1/16 DECIMALS: .X = ± .1 .XX = ± .03 .XXX = ± .010 ANGLES = ± 2 DEG	DATE 9-15-70 DWN H. Schmidt APVD [illegible] APVD ENGRG CHKR APVD APVD	LOCKHEED MISSILES & SPACE COMPANY A GROUP DIVISION OF LOCKHEED AIRCRAFT CORPORATION SUNNYVALE, CALIFORNIA ENGINE GIMBAL PATTERN DELTA BODY - STAGE - 1/2 MODEL LS-200-3
NEXT ASSY / USED ON	CONTR		SIZE E / CODE IDENT 06897 / DRAWING NO SKS 100205 / REV
APPLICATION	CCA/CI/FD		SCALE 1/50 / SHEET 1 OF 1

FOLDOUT FRAME 2

REPRODUCIBILITY OF THE ORIGINAL PAGE IS POOR.

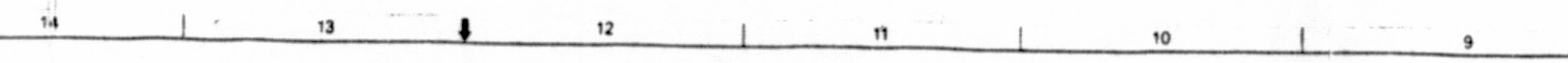

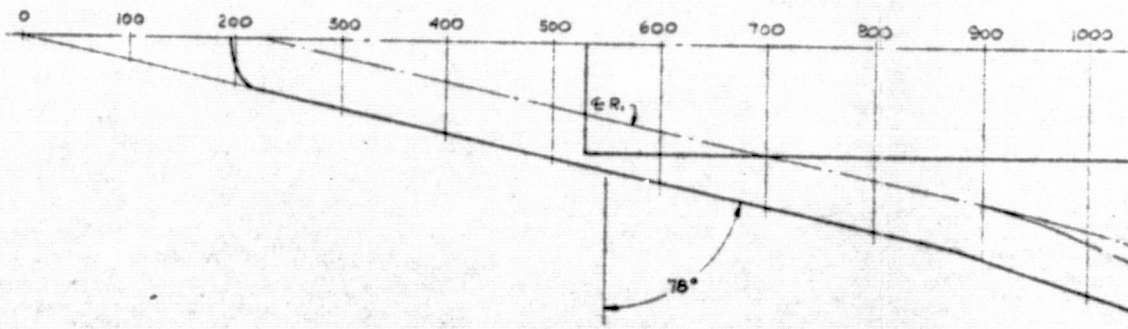

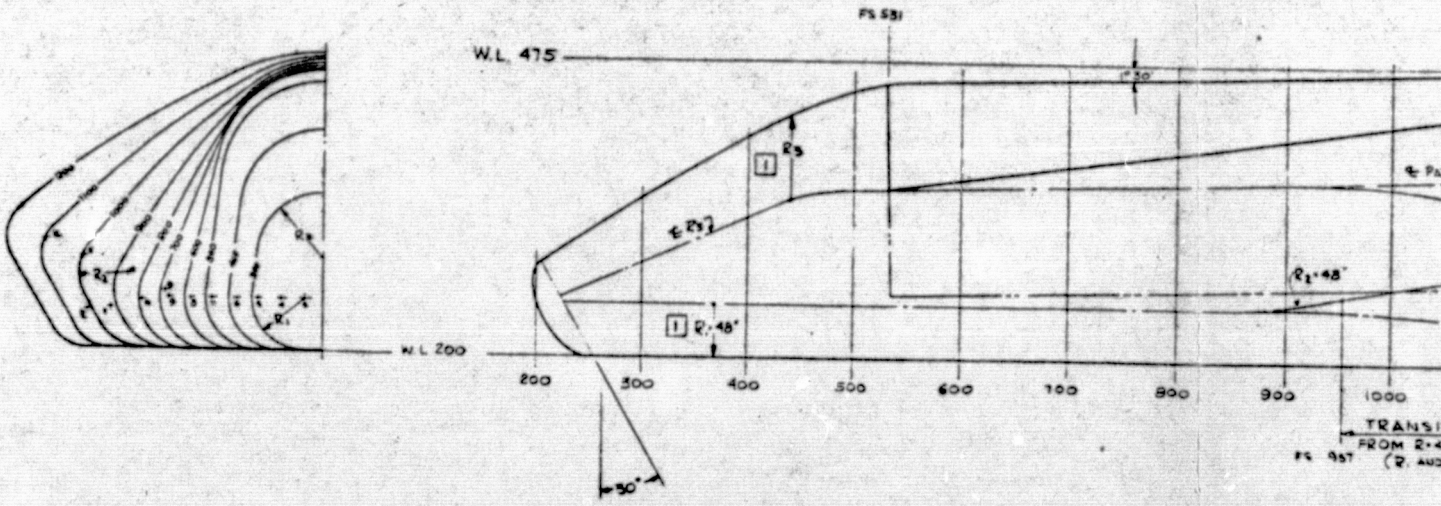

FOLDOUT FRAME

REPRODUCIBILITY OF THE ORIGINAL PAGE IS POOR.

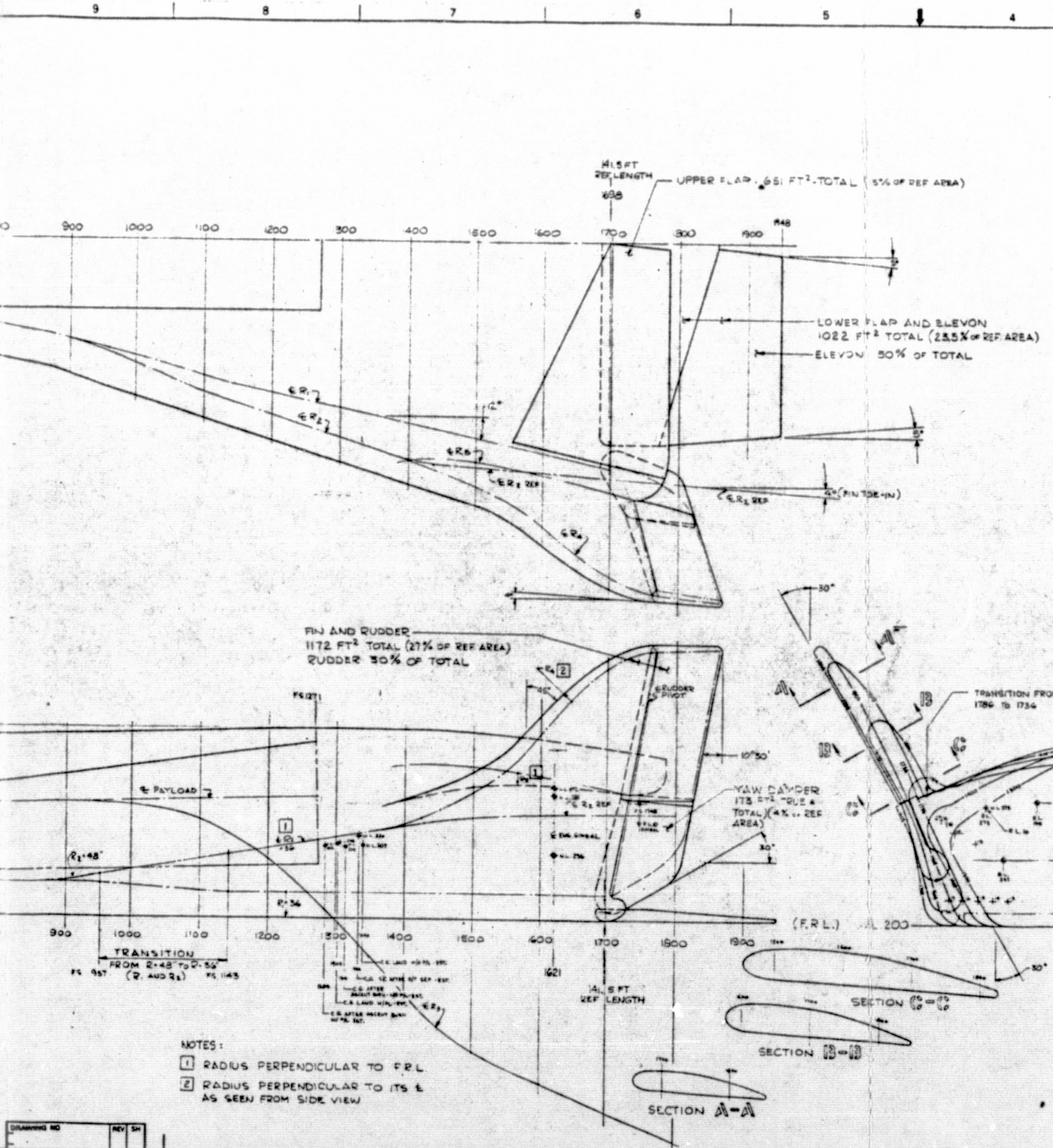

FOLDOUT FRAME 2

REPRODUCIBILITY OF THE ORIGINAL PAGE IS POOR.

PRECEDING PAGE BLANK NOT FILMED

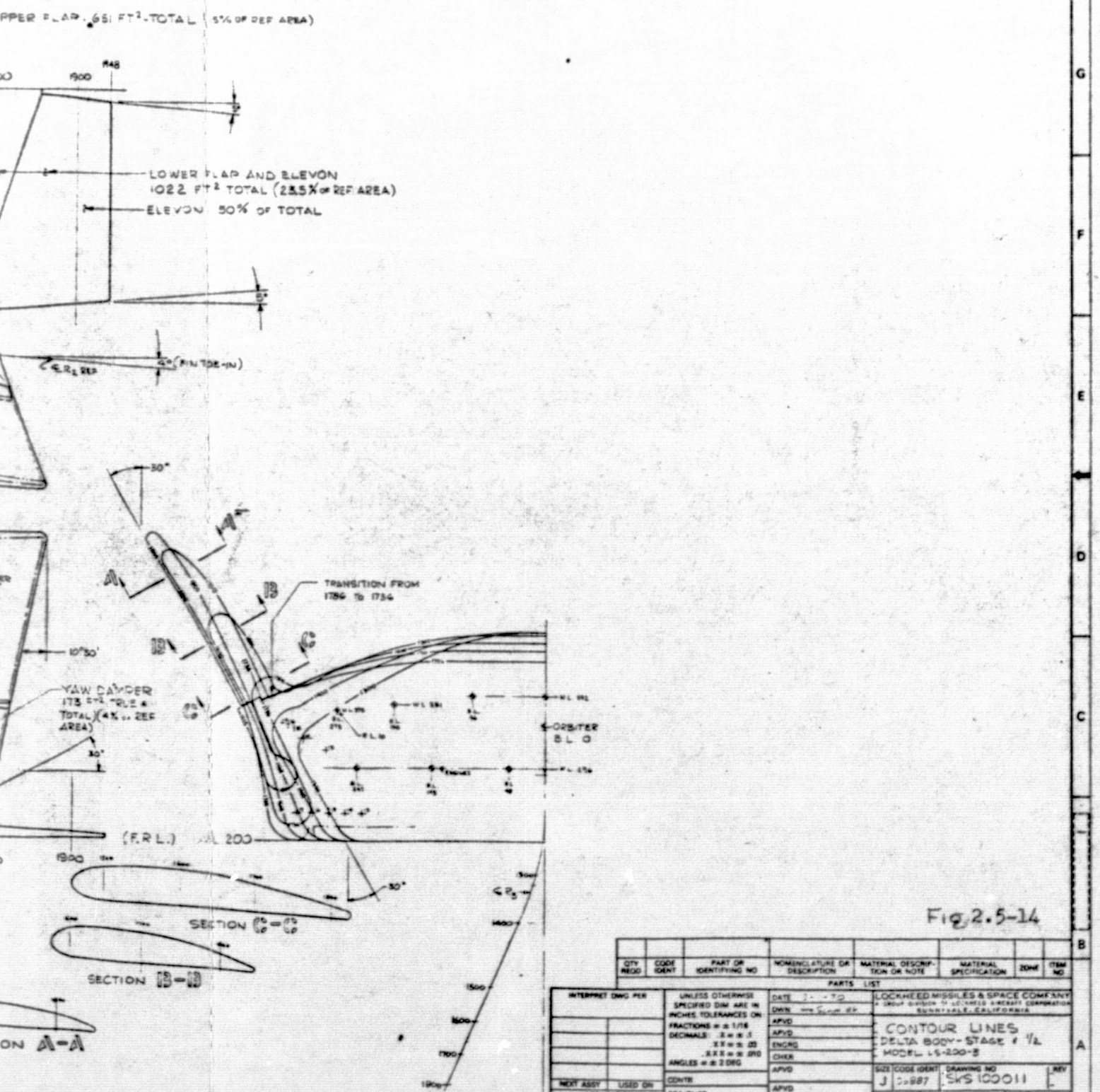

Fig. 2.5-14

QTY REQD	CODE IDENT	PART OR IDENTIFYING NO	NOMENCLATURE OR DESCRIPTION	MATERIAL DESCRIPTION OR NOTE	MATERIAL SPECIFICATION	ZONE	ITEM NO

PARTS LIST

REVISIONS				
ZONE	LTR	DESCRIPTION	DATE	APVD

LIMITED CALENDAR LIFE | LIMITED OPERATING LIFE

INTERPRET DWG PER — UNLESS OTHERWISE SPECIFIED DIM ARE IN INCHES, TOLERANCES ON: FRACTIONS ± 1/16, DECIMALS: .X ± .5, .XX ± .03, .XXX ± .010, ANGLES ± 2 DEG

DATE 1-70 | DWN [illegible] | APVD | APVD | ENGRG | CHKR | APVD | APVD | CONTR

NEXT ASSY | USED ON | APPLICATION | CGA/CI/FD

LOCKHEED MISSILES & SPACE COMPANY
A GROUP DIVISION OF LOCKHEED AIRCRAFT CORPORATION
SUNNYVALE, CALIFORNIA

CONTOUR LINES
DELTA BODY - STAGE 1 1/2
MODEL LS-200-B

SIZE J | CODE IDENT 20987 | DRAWING NO SKS 100011 | REV L

SCALE 1/50 | SHEET 1 of 1

REPRODUCIBILITY OF THE ORIGINAL PAGE IS POOR.

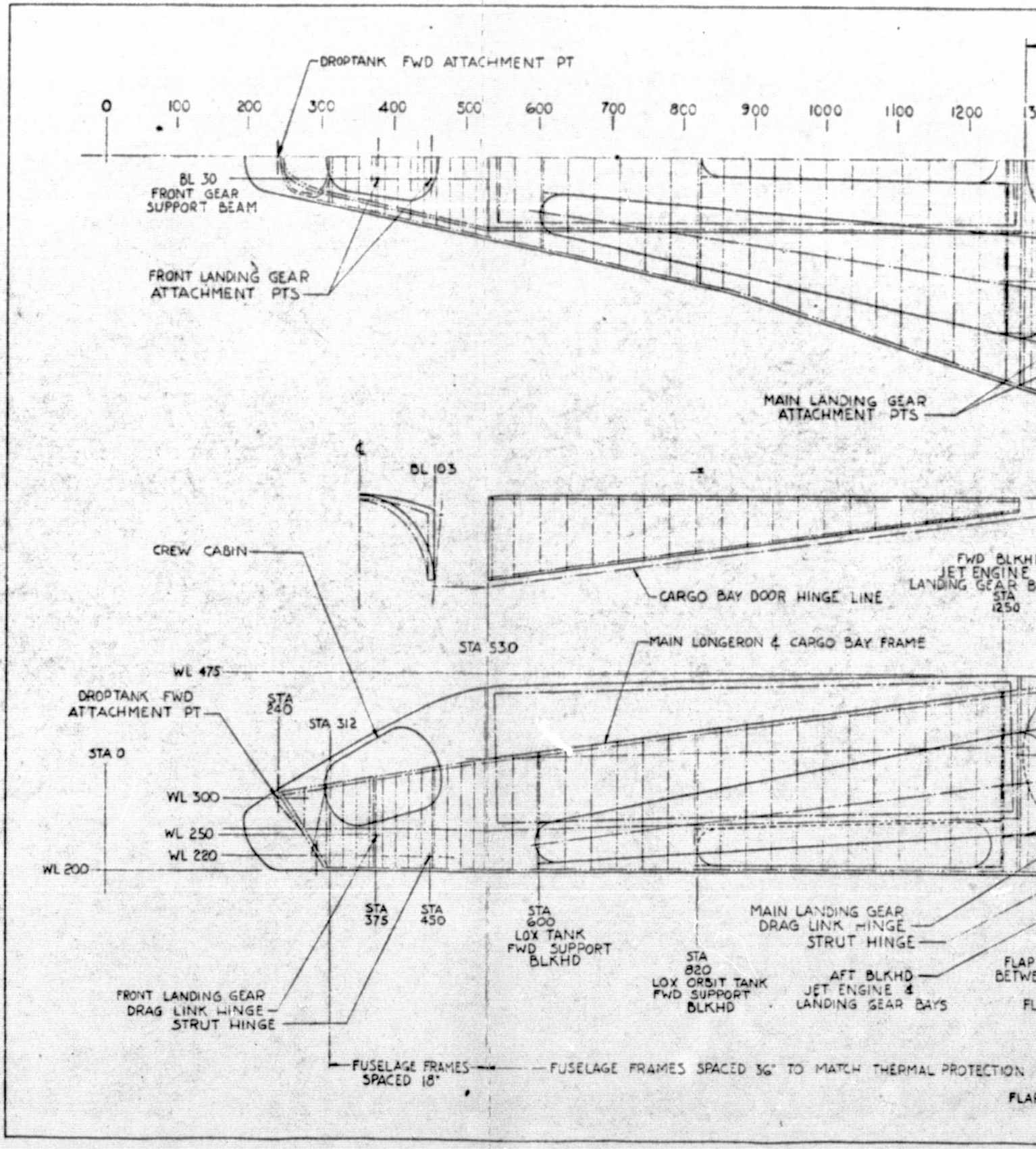

FOLDOUT FRAME

REPRODUCIBILITY OF THE ORIGINAL PAGE IS POOR.

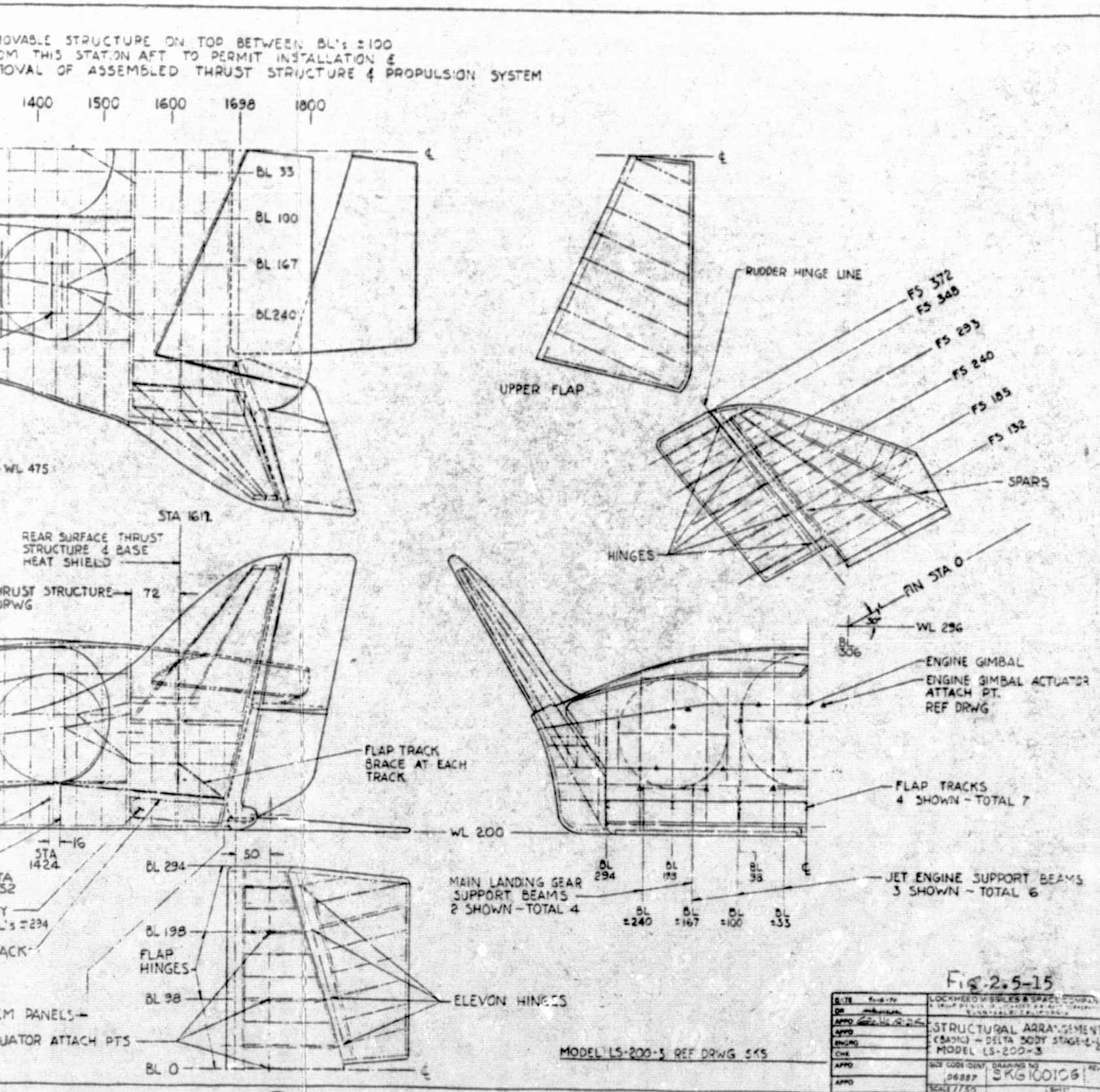

Fig. 2.5-15

DR	LOCKHEED MISSILES & SPACE COMPANY
APPD	STRUCTURAL ARRANGEMENT (BASIC) - DELTA BODY STAGE 1 & 2 MODEL LS-200-3
ENGRG	
CHK	
APPD	SIZE CODE IDENT. 06887 DRAWING NO. SKG100106 REV.
APPD	SCALE 1/50 SHEET

FOLDOUT FRAME 2

REPRODUCIBILITY OF THE ORIGINAL PAGE IS POOR.

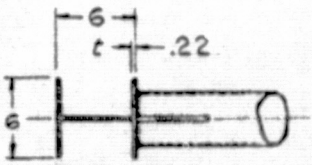

SECTION D-D
1/4 SIZE
SECTION E-E SIMILAR EXCEPT t=.44

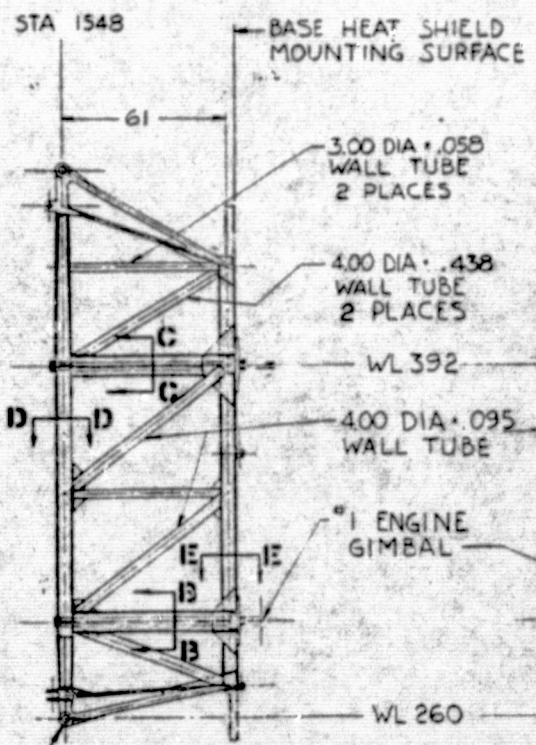

SECTION A-A

FORGED AND/OR MACHINED END MEMBERS 2 PLACES

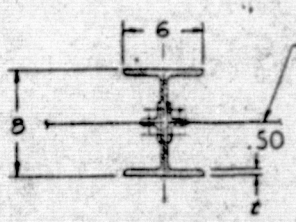

SECTION B-B
1/4 SIZE
SECTION C-C SIMILAR EXCEPT t=.25

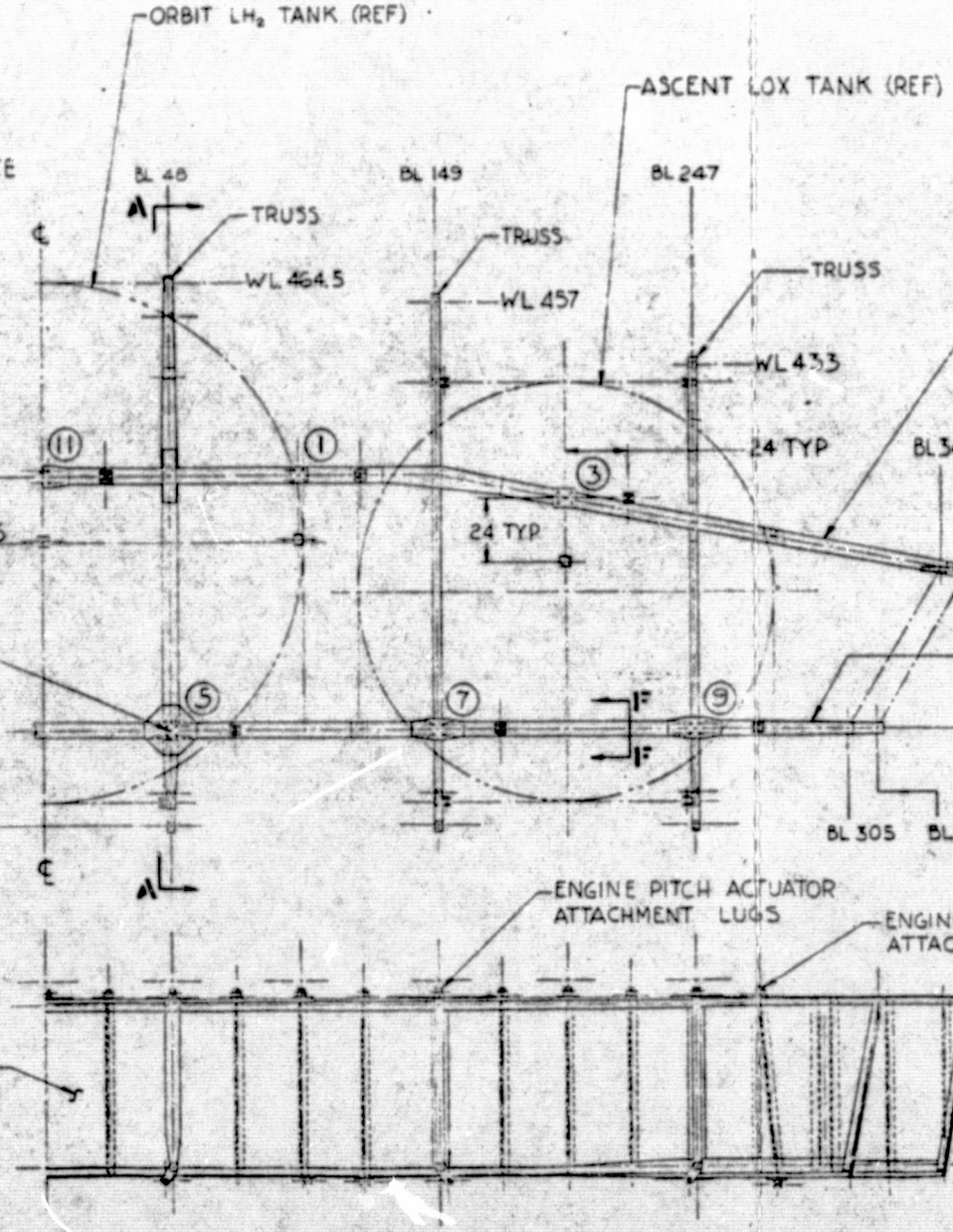

DRAWING NO | REV | SH

FOLDOUT FRAME

REPRODUCIBILITY OF THE ORIGINAL PAGE IS POOR.

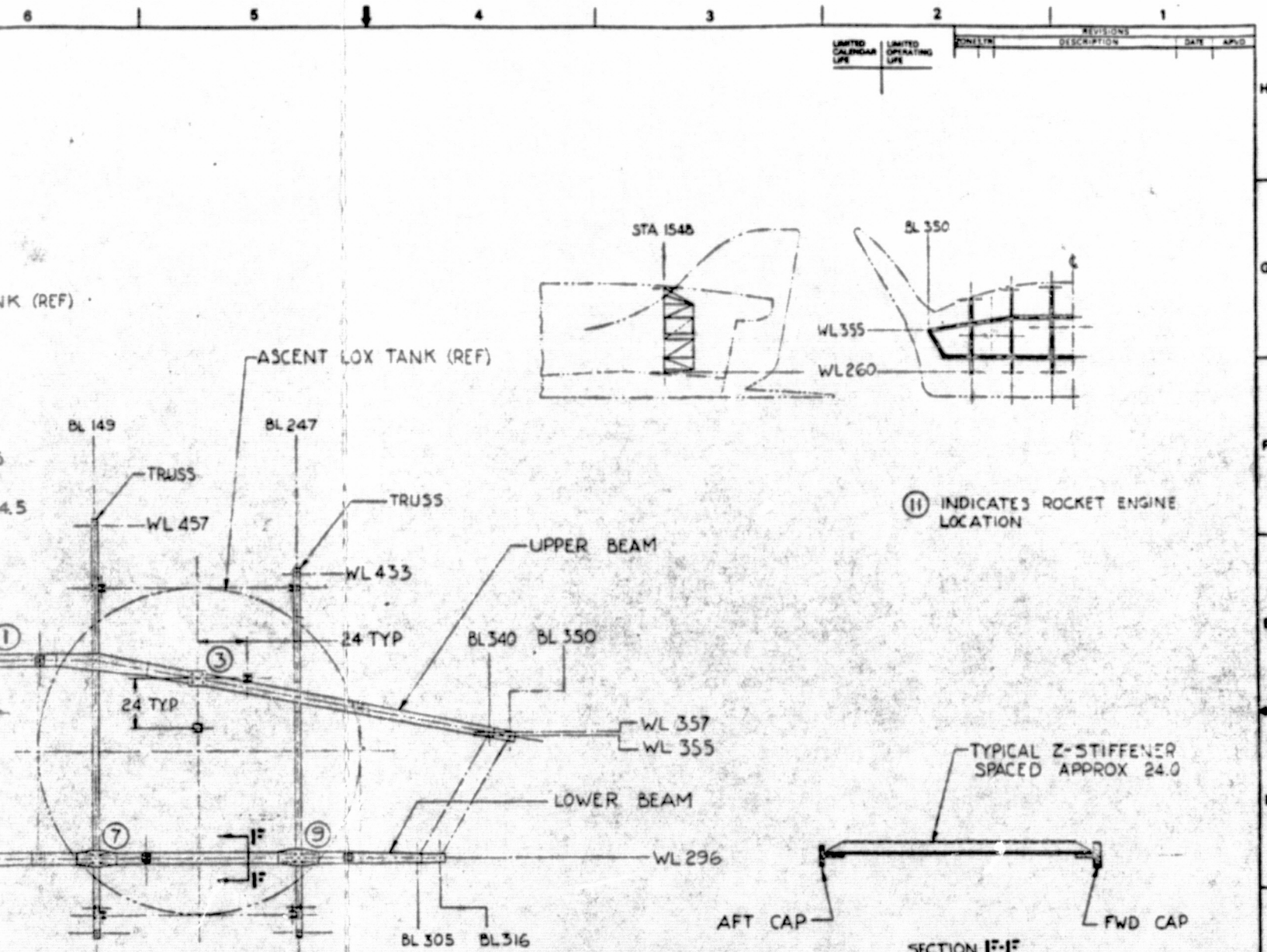

(11) INDICATES ROCKET ENGINE LOCATION

SECTION F-F

1/10 SIZE

TYPICAL SECTION THRU LOWER & UPPER BEAMS. ELEMENT DIMENSIONS VARY AS REQ'D ALONG BEAM

MATERIAL: TITANIUM (6AL-4V)

Fig. 2.5-16

QTY REQD	CODE IDENT	PART OR IDENTIFYING NO	NOMENCLATURE OR DESCRIPTION	MATERIAL DESCRIPTION OR NOTE	MATERIAL SPECIFICATION	ZONE	ITEM NO

PARTS LIST

INTERPRET DWG PER — UNLESS OTHERWISE SPECIFIED DIM ARE IN INCHES. TOLERANCES ON: FRACTIONS = ± 1/16; DECIMALS: .X = ± .1, .XX = ± .03, .XXX = ± .010; ANGLES = ± 2 DEG

DATE 3-12-70 — DWN — APVD — APVD — ENGRG — CHKR — APVD — APVD — CONTR — CCA/CI/FD

NEXT ASSY — USED ON APPLICATION

LOCKHEED MISSILES & SPACE COMPANY
A GROUP DIVISION OF LOCKHEED AIRCRAFT CORPORATION
SUNNYVALE, CALIFORNIA

THRUST STRUCTURE - DELTA BODY STAGE-E-1
MODEL L3-ECC-3

SIZE J — CODE IDENT — DRAWING NO LSG100109 — REV L

SCALE — SHEET

REPRODUCIBILITY OF THE ORIGINAL PAGE IS POOR.

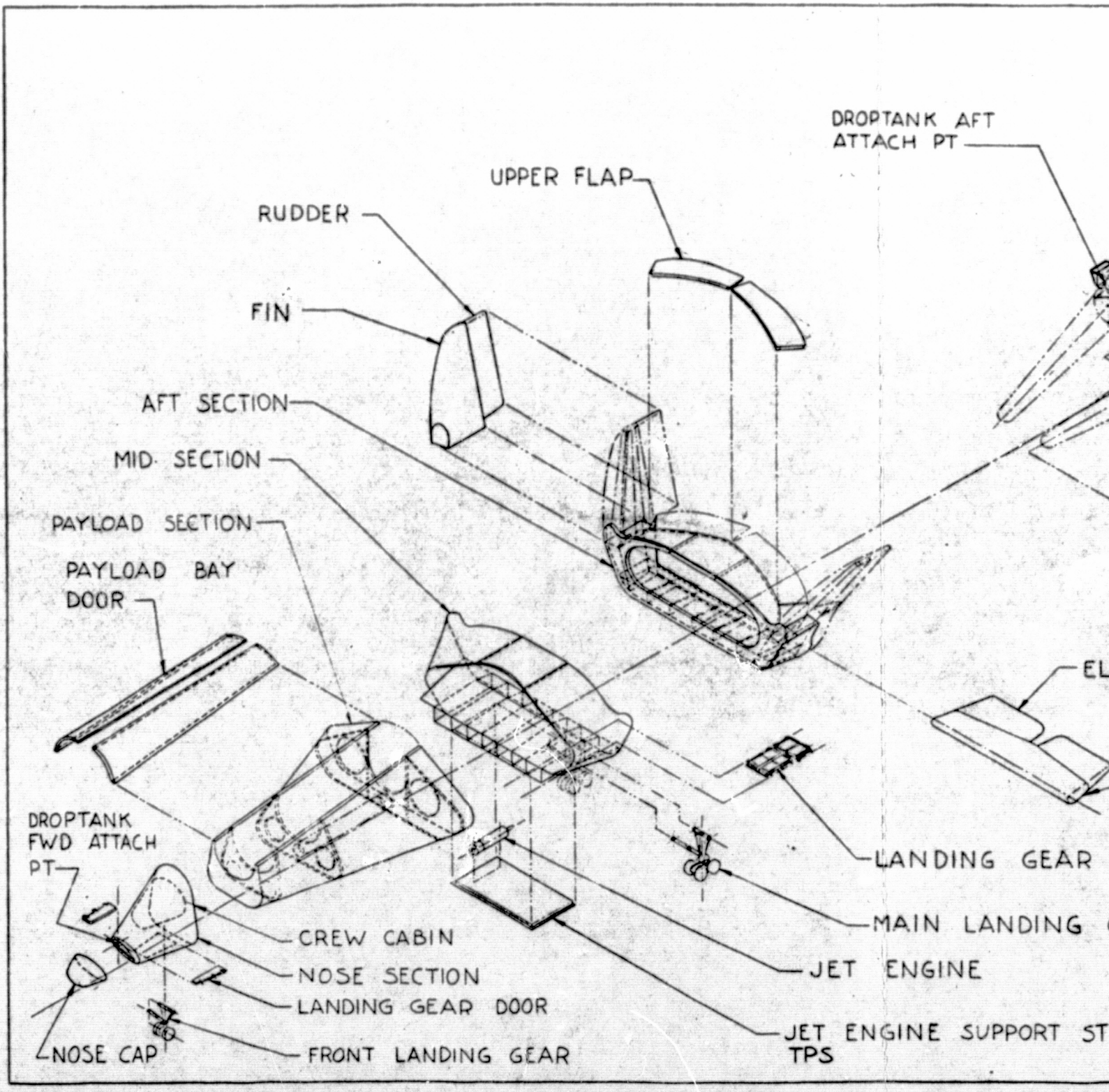

FOLDOUT FRAME 1

REPRODUCIBILITY OF THE ORIGINAL PAGE IS POOR.

PRECEDING PAGE BLANK NOT FILMED

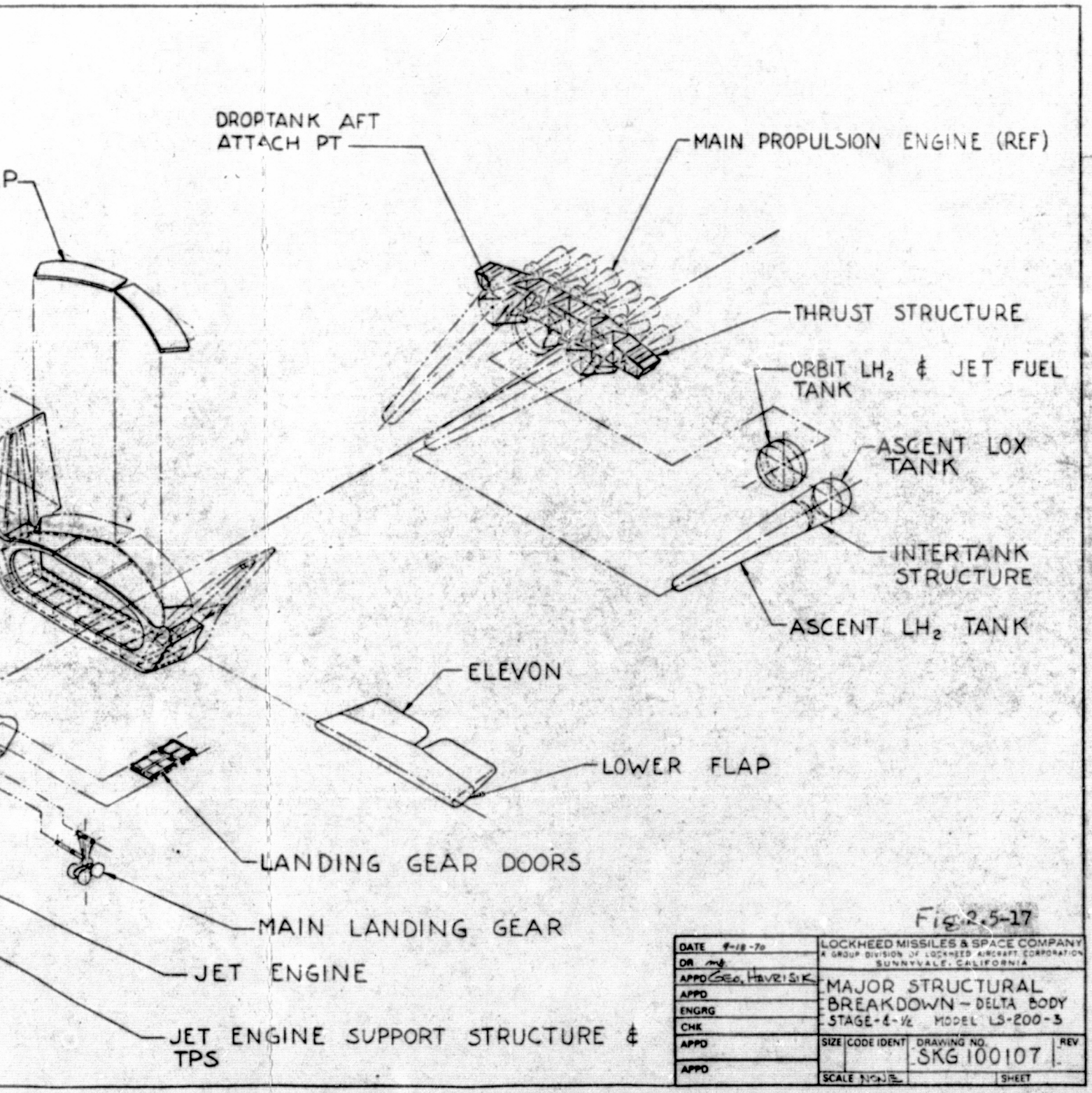

Fig. 2.5-17

DATE 9-18-70	LOCKHEED MISSILES & SPACE COMPANY A GROUP DIVISION OF LOCKHEED AIRCRAFT CORPORATION SUNNYVALE, CALIFORNIA
DR mb	
APPD Geo. Havrisik	MAJOR STRUCTURAL BREAKDOWN – DELTA BODY STAGE-1-½ MODEL LS-200-3
APPD	
ENGRG	
CHK	
APPD	SIZE: CODE IDENT: DRAWING NO. SKG 100107 REV:
APPD	SCALE NONE SHEET

FOLDOUT FRAME 2

REPRODUCIBILITY OF THE ORIGINAL PAGE IS POOR.

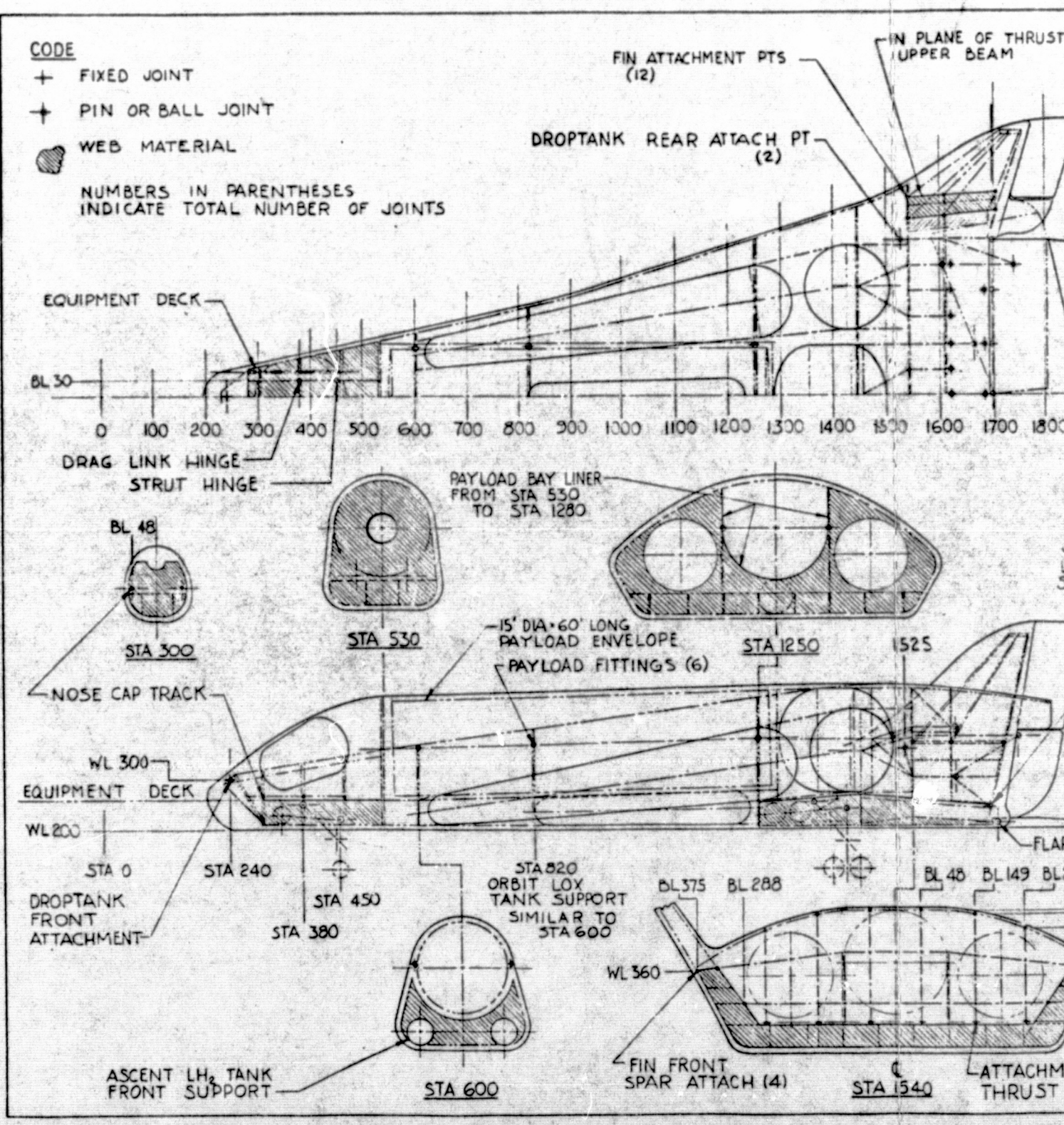

FOLDOUT FRAME 1

REPRODUCIBILITY OF THE ORIGINAL PAGE IS POOR.

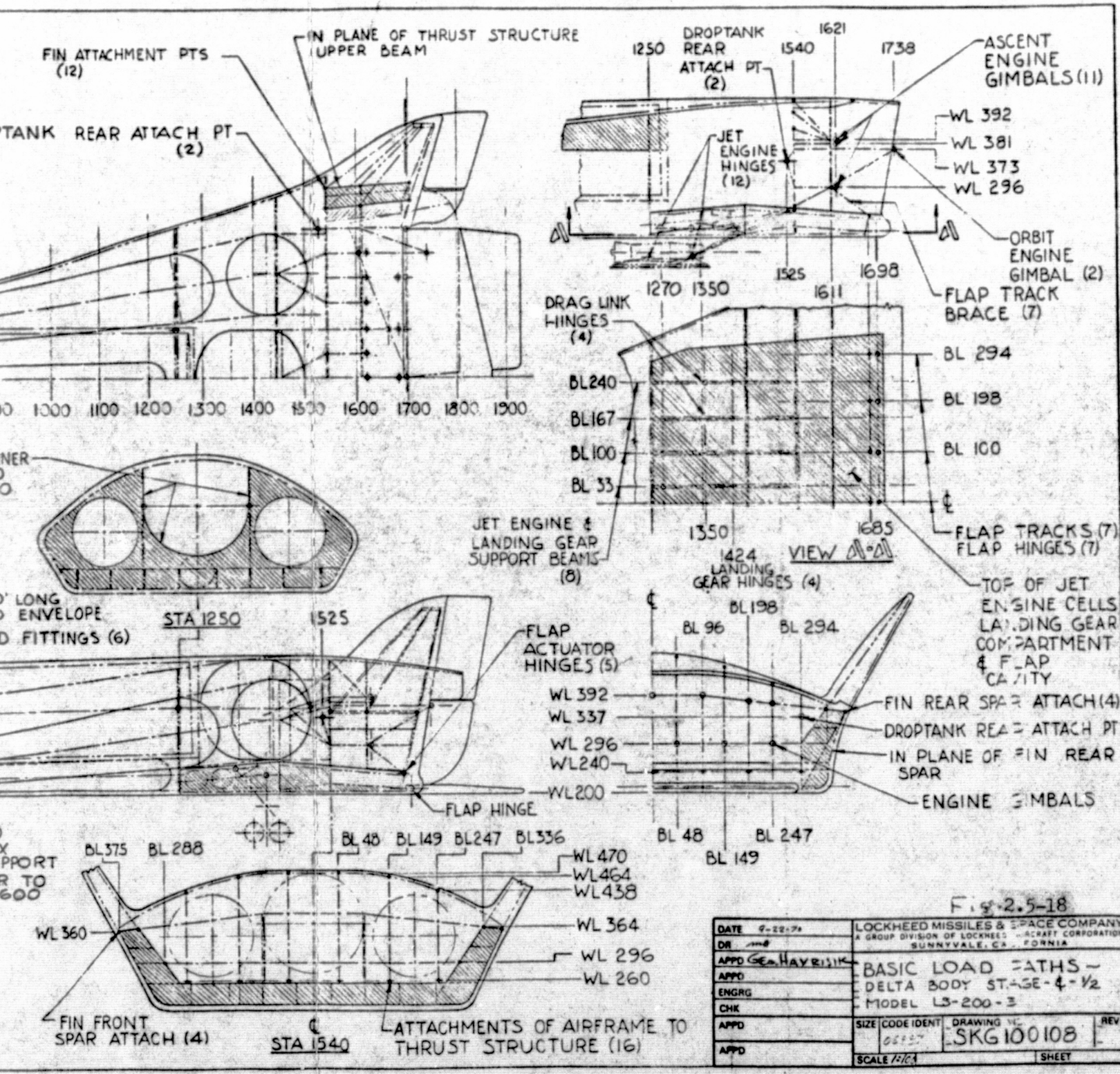

Fig. 2.5-18

2.5-59

FOLDOUT FRAME 2

REPRODUCIBILITY OF THE ORIGINAL PAGE IS POOR.

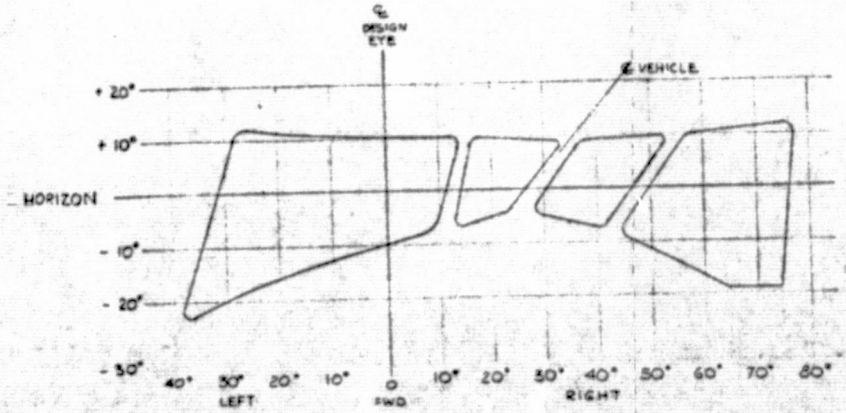

FIELD OF VIEW - LEFT PILOT

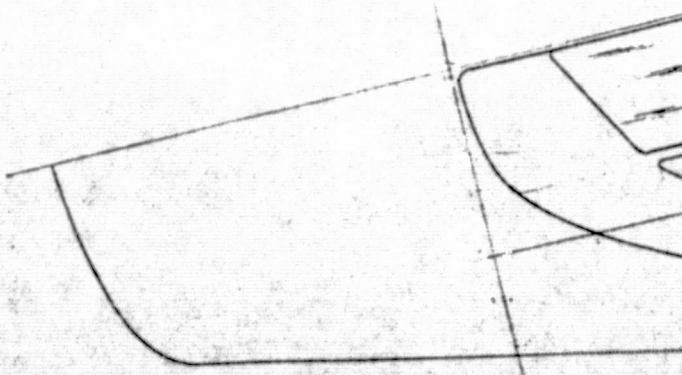

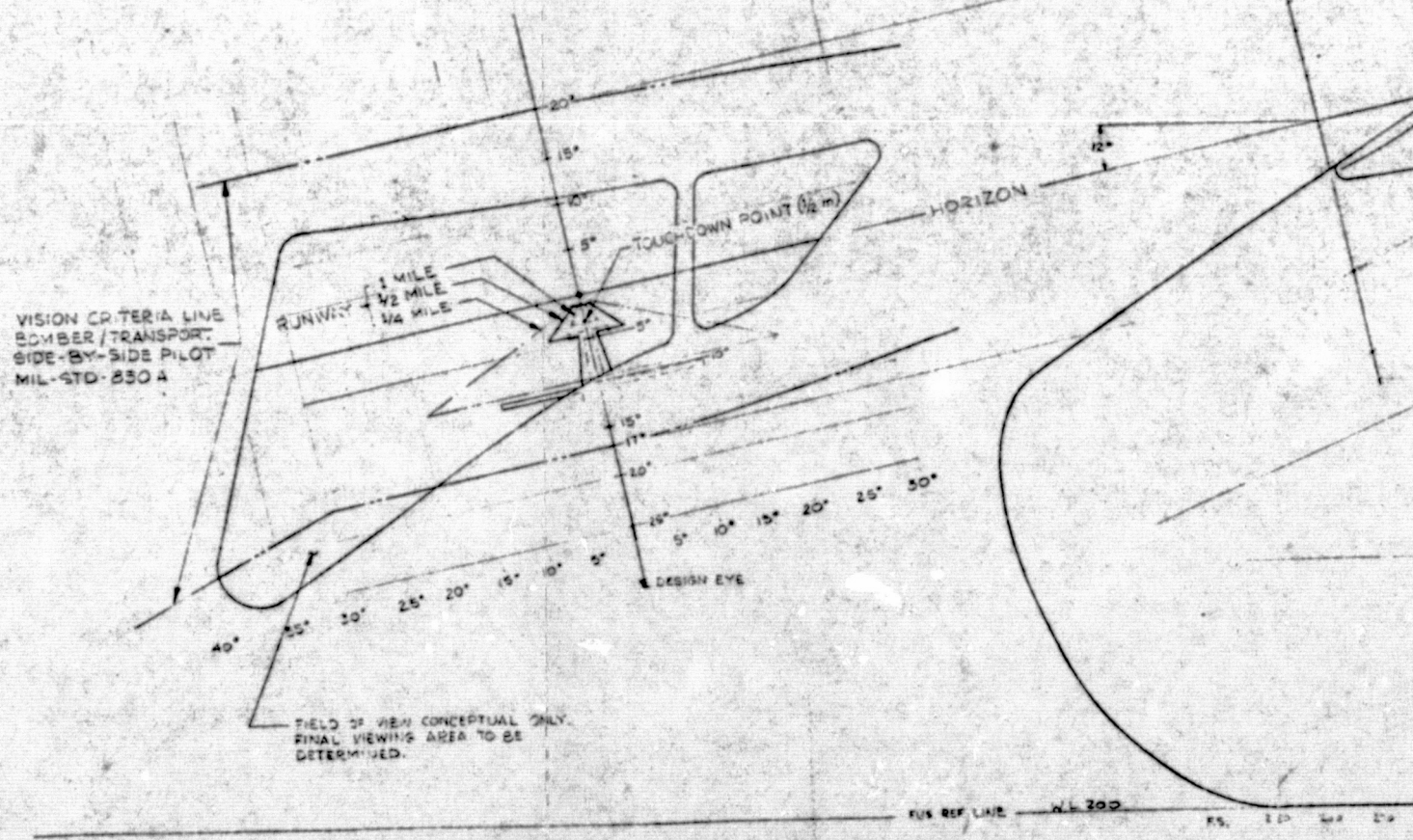

FOLDOUT FRAME

REPRODUCIBILITY OF THE ORIGINAL PAGE IS POOR.

PRECEDING PAGE BLANK NOT FILMED

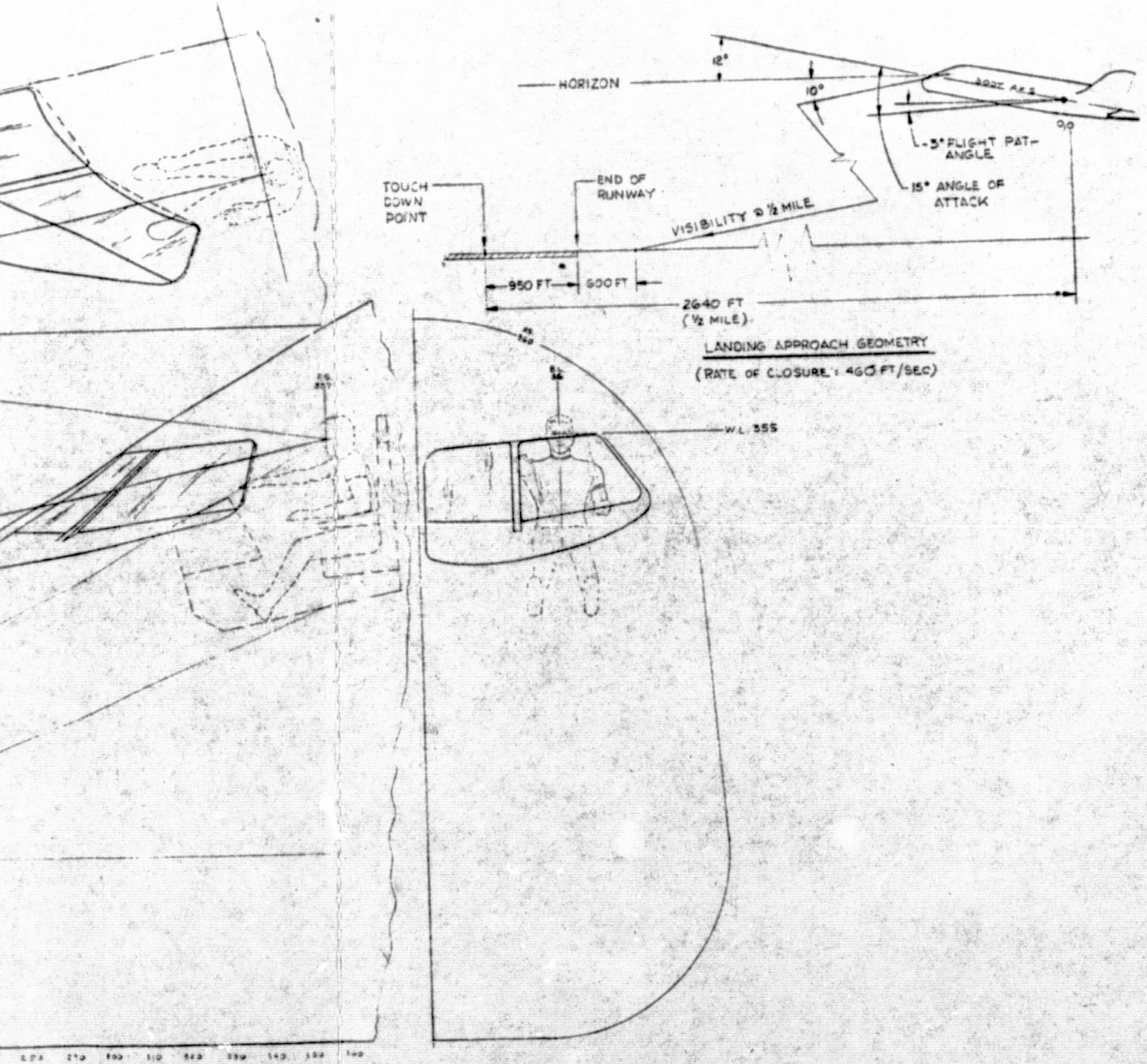

Fig 2.5-19

UNLESS OTHERWISE SPECIFIED DIM. ARE IN INCHES. TOLERANCES ON: FRACTIONS = ± 1/16 DECIMALS: .X = ± .1 .XX = ± .03 .XXX = ± .010 ANGLES = ± 2 DEG	DATE / DR / APPD / APPD / ENGRG / CHK / APPD / APPD	LOCKHEED MISSILES & SPACE COMPANY VISIBILITY STUDY DELTA BODY STAGE + ½ MODEL LS-200 B
CONTR		SIZE / CODE IDENT. 0685 / DRAWING NO. SKS 100010 / REV. E
CCA/CEI		SCALE 1/16 / SHEET

FOLDOUT FRAME 2

REPRODUCIBILITY OF THE ORIGINAL PAGE IS POOR.

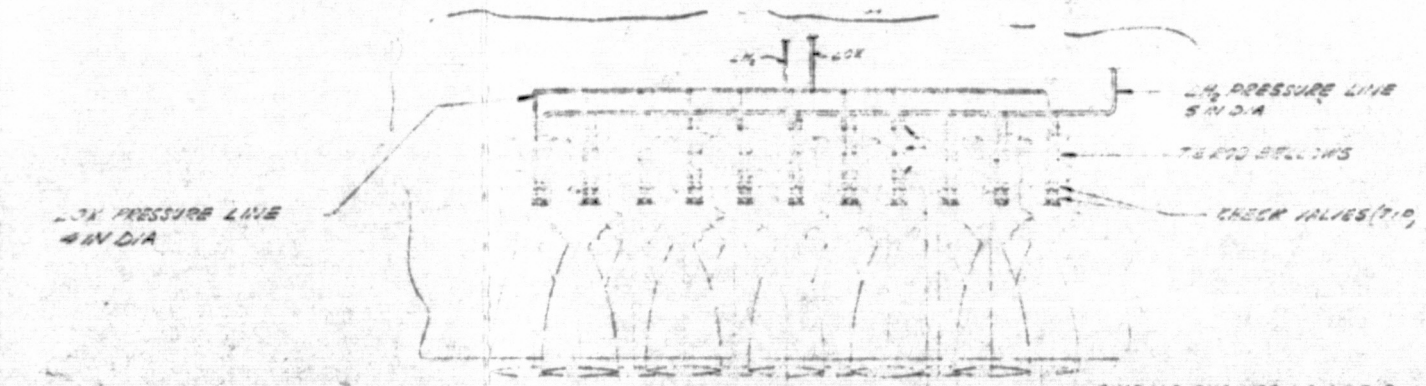

TOP VIEW OF PRESSURE SYSTEM (ROTATED 180 DEG)

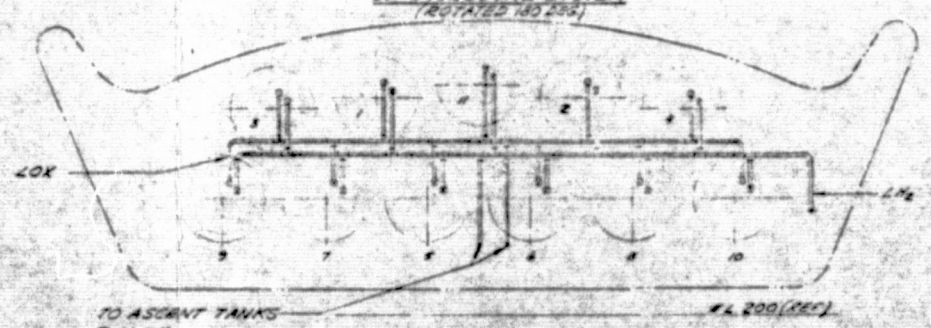

SECTION A-A
PRESSURIZATION SYSTEM SHOWN ONLY

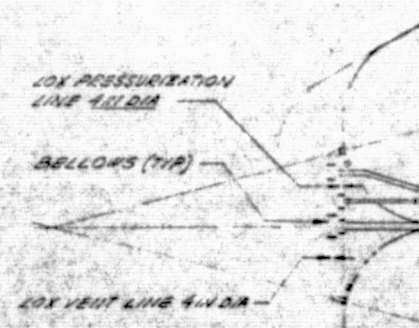

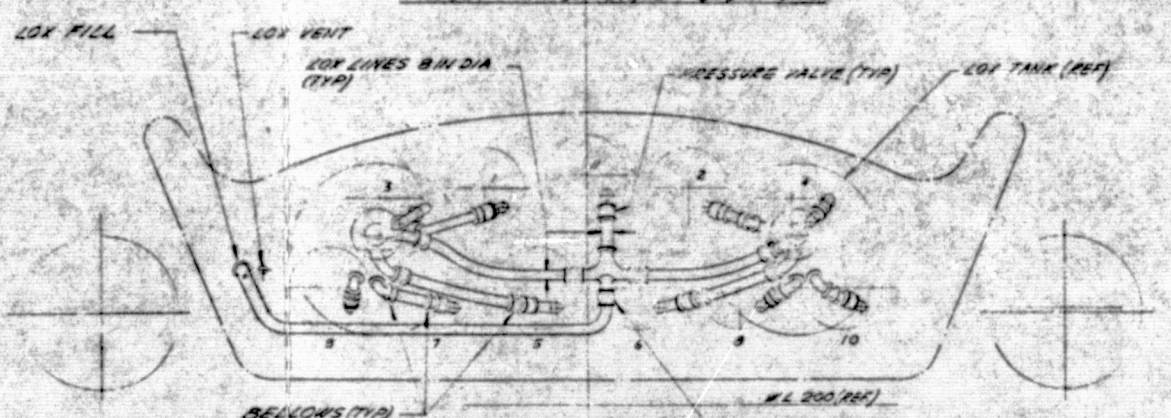

SECTION A-A
LOX SYSTEM SHOWN ONLY

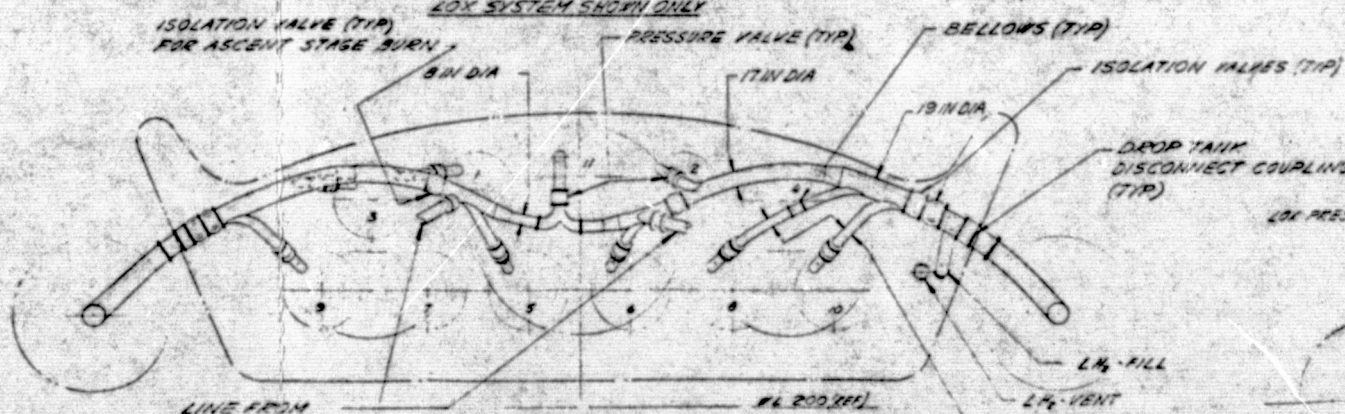

SECT A-A
LH2 SYSTEM SHOWN ONLY
(MANIFOLD)

FOLDOUT FRAME

REPRODUCIBILITY OF THE ORIGINAL PAGE IS POOR.

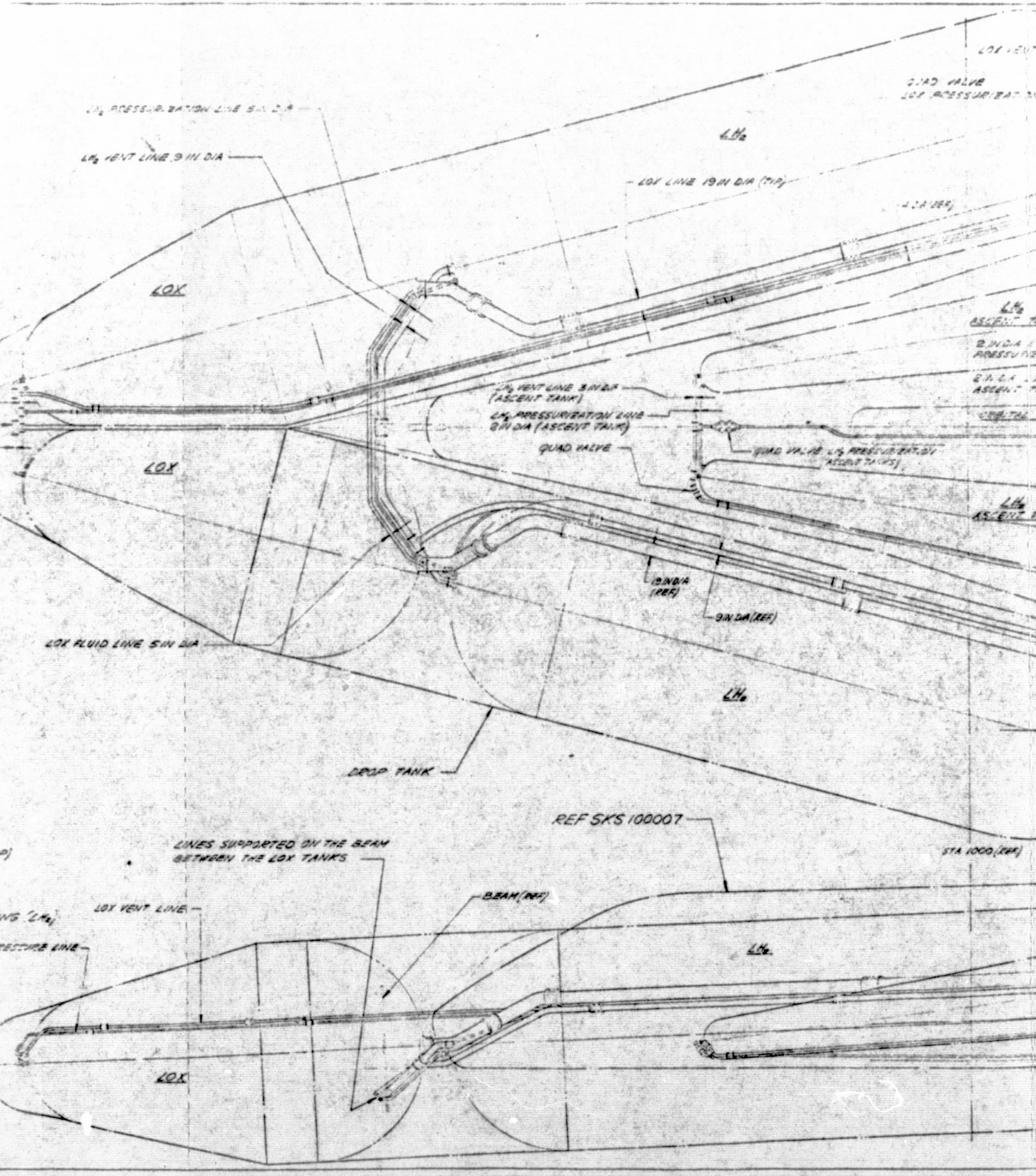

FOLDOUT FRAME 2

REPRODUCIBILITY OF THE ORIGINAL PAGE IS POOR.

PRECEDING PAGE BLANK NOT FILMED

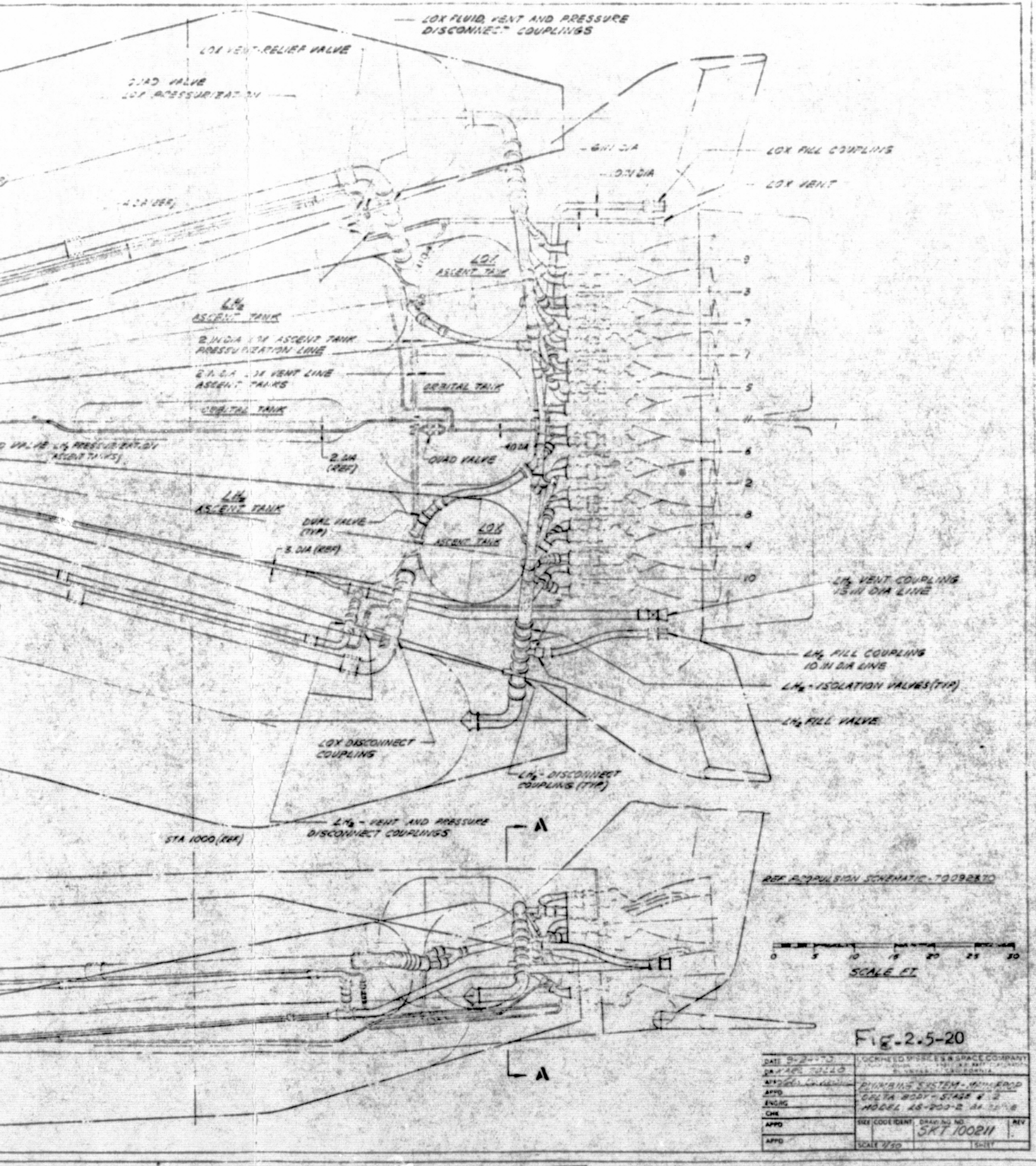

Fig-2.5-20

FOLDOUT FRAME 3

REPRODUCIBILITY OF THE ORIGINAL PAGE IS POOR.

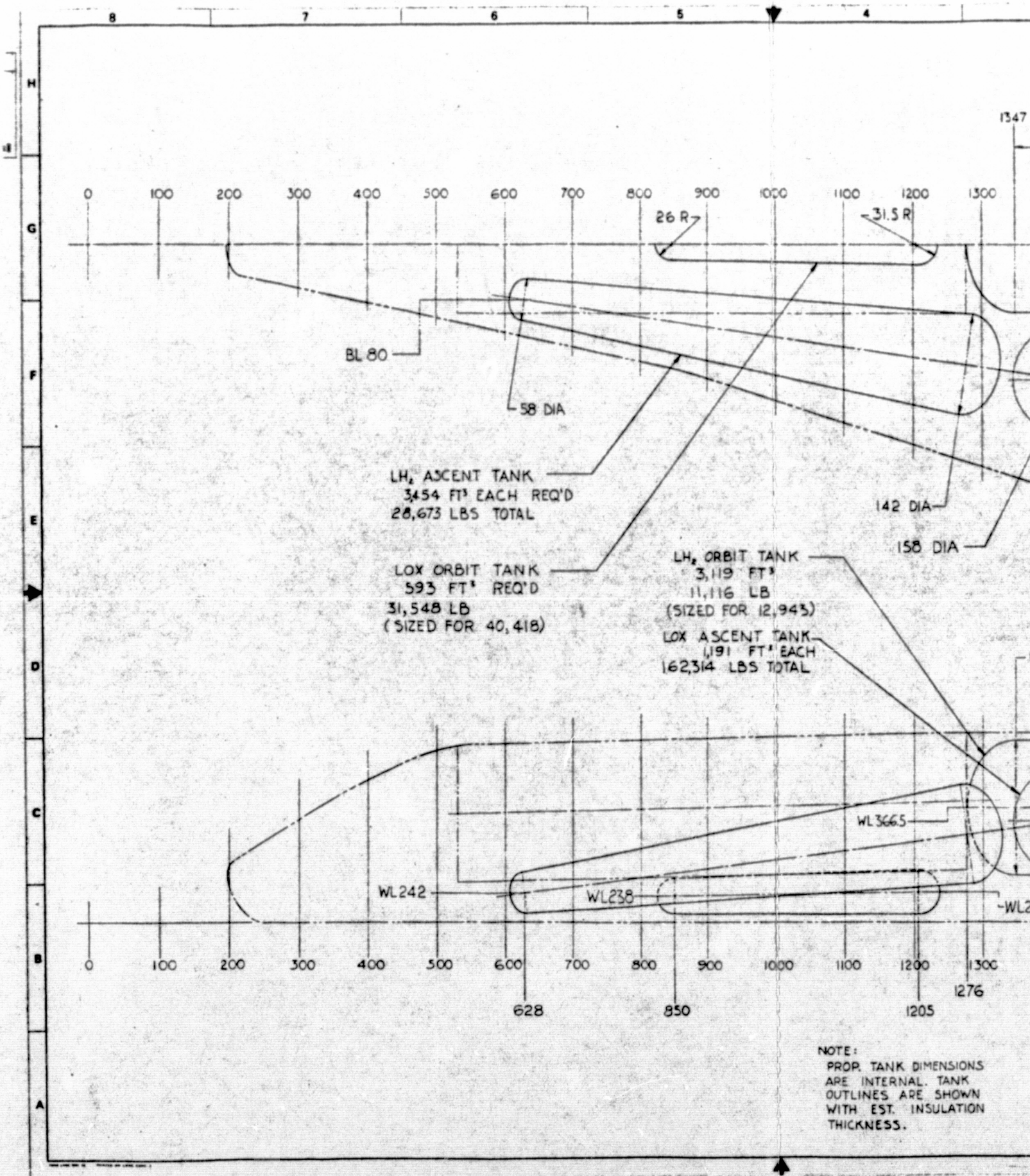

NOTE:
PROP. TANK DIMENSIONS ARE INTERNAL. TANK OUTLINES ARE SHOWN WITH EST. INSULATION THICKNESS.

FOLDOUT FRAME

REPRODUCIBILITY OF THE ORIGINAL PAGE IS POOR.

PRECEDING PAGE BLANK NOT FILMED

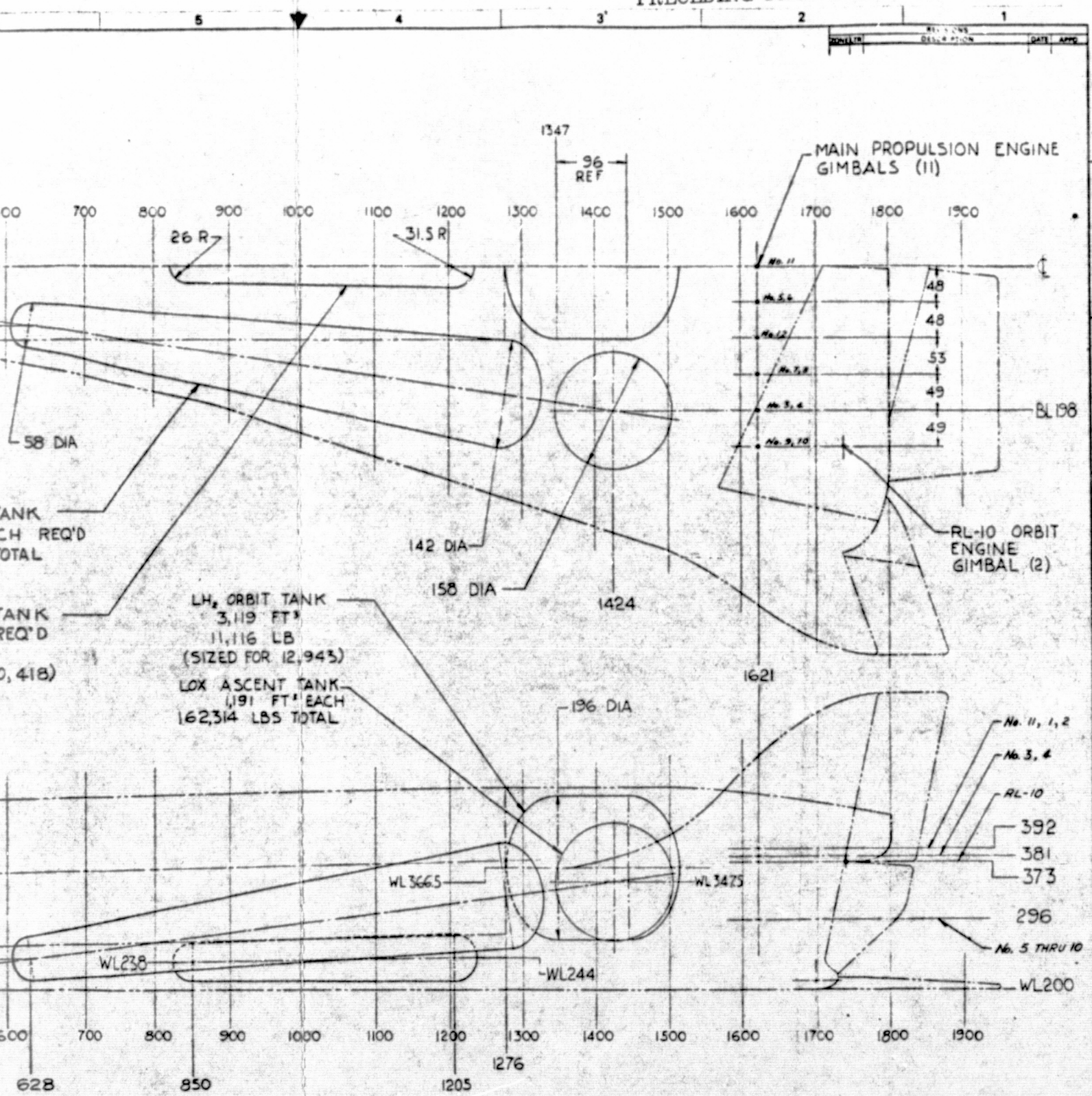

NOTE:
PROP. TANK DIMENSIONS ARE INTERNAL. TANK OUTLINES ARE SHOWN WITH EST. INSULATION THICKNESS.

FIG 2.5-21

DATE	LOCKHEED MISSILES & SPACE COMPANY, A GROUP DIVISION OF LOCKHEED AIRCRAFT CORPORATION, SUNNYVALE, CALIFORNIA
DR	
APPD	
APPD	PROP. TANK SPACE ALLOCATION
ENGRG	DELTA BODY STAGE - 4 - ½
CHK	MODEL LS-200-3
APPD	SIZE E, CODE IDENT 04807, DRAWING NO. LSKG100210, REV L
APPD	SCALE 1/60, SHEET

2.5-65

FOLDOUT FRAME 2

REPRODUCIBILITY OF THE ORIGINAL PAGE IS POOR.

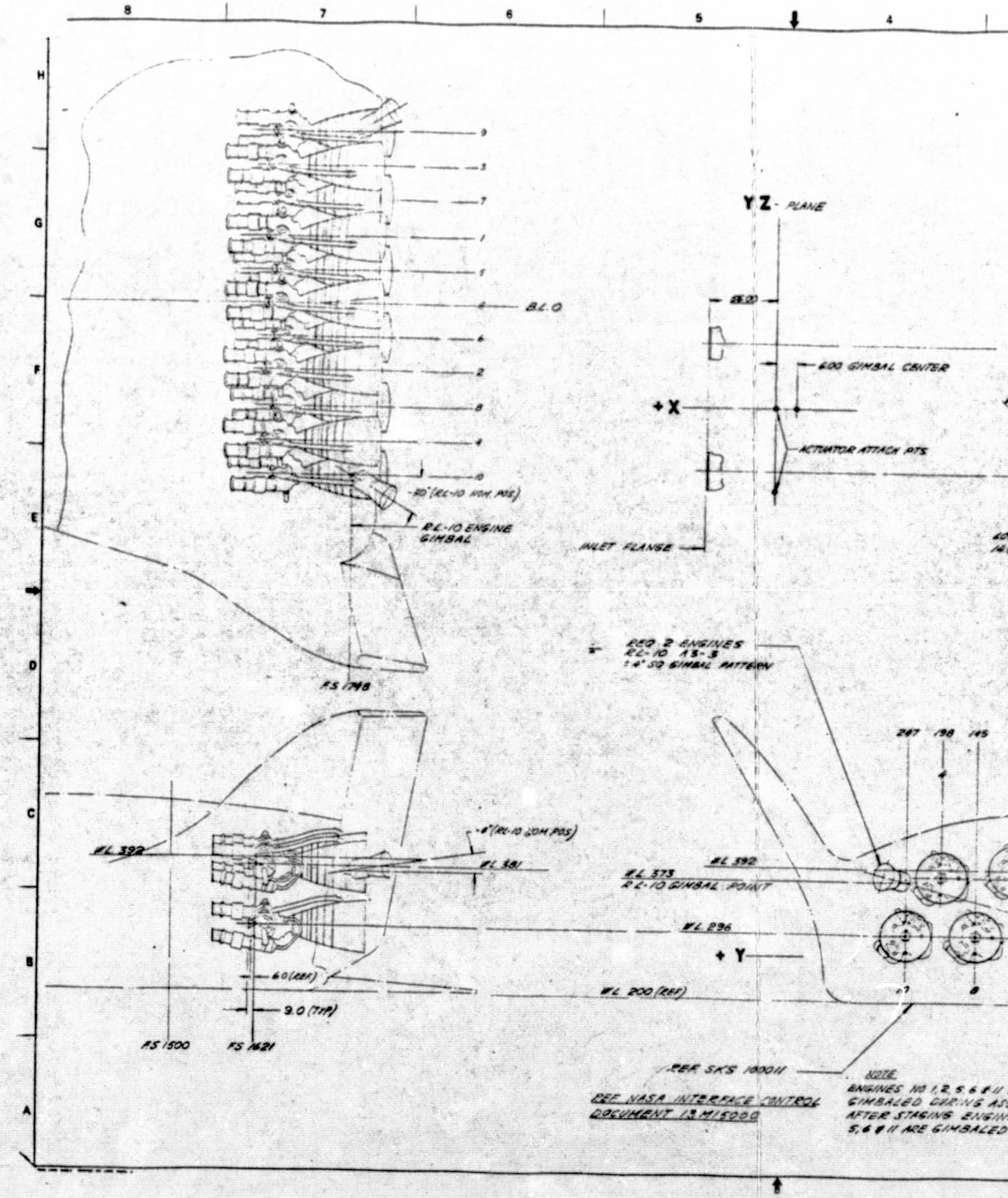

FOLDOUT FRAME

REPRODUCIBILITY OF THE ORIGINAL PAGE IS POOR.

PRECEDING PAGE BLANK NOT FILMED

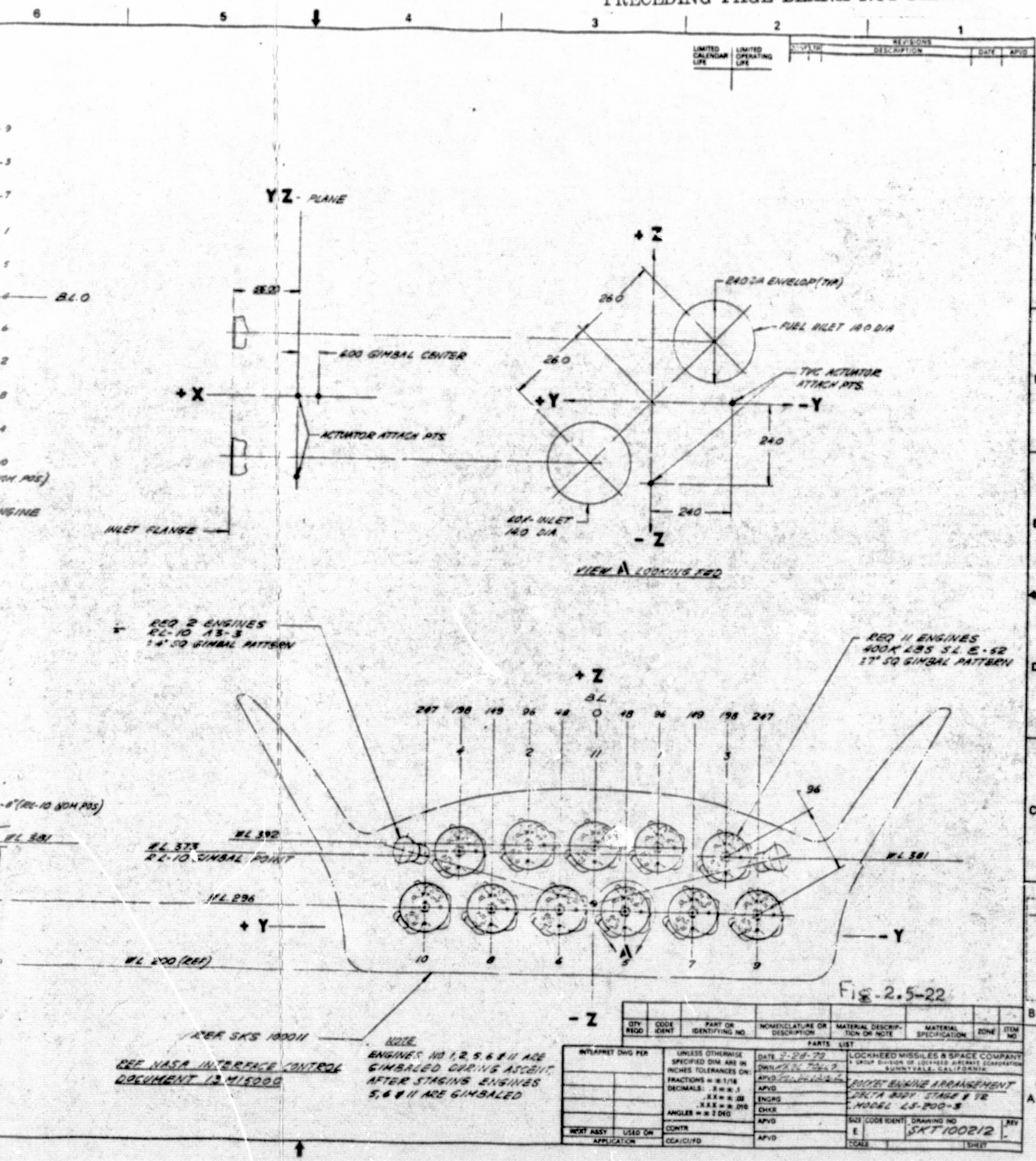

Fig. 2.5-22

FOLDOUT FRAME 2

REPRODUCIBILITY OF THE ORIGINAL PAGE IS POOR.

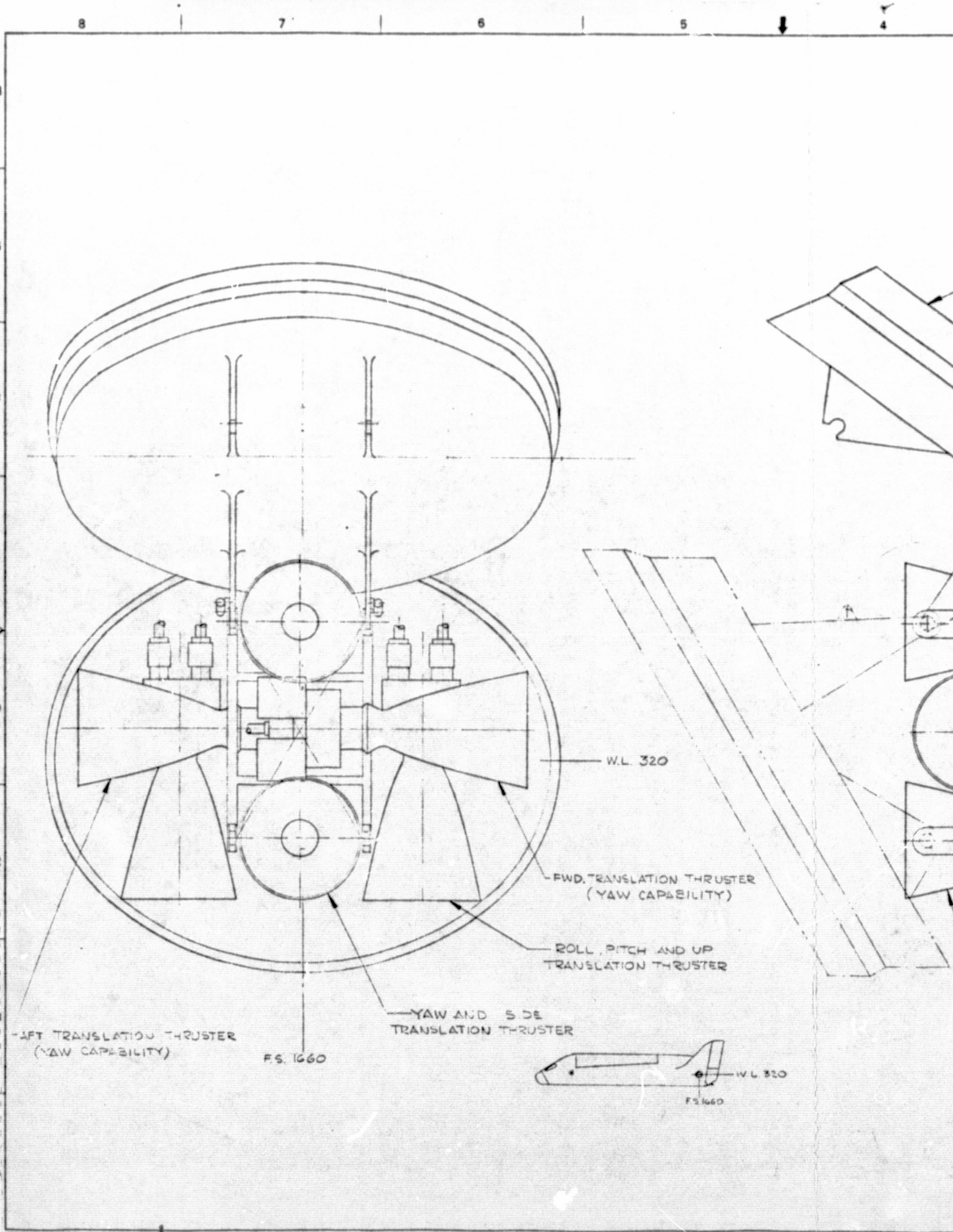

REPRODUCIBILITY OF THE ORIGINAL PAGE IS POOR.

LIMITED CALENDAR LIFE	LIMITED OPERATING LIFE

REVISIONS			
ZONE LTR	DESCRIPTION	DATE	APVD

PRECEDING PAGE BLANK NOT FILMED

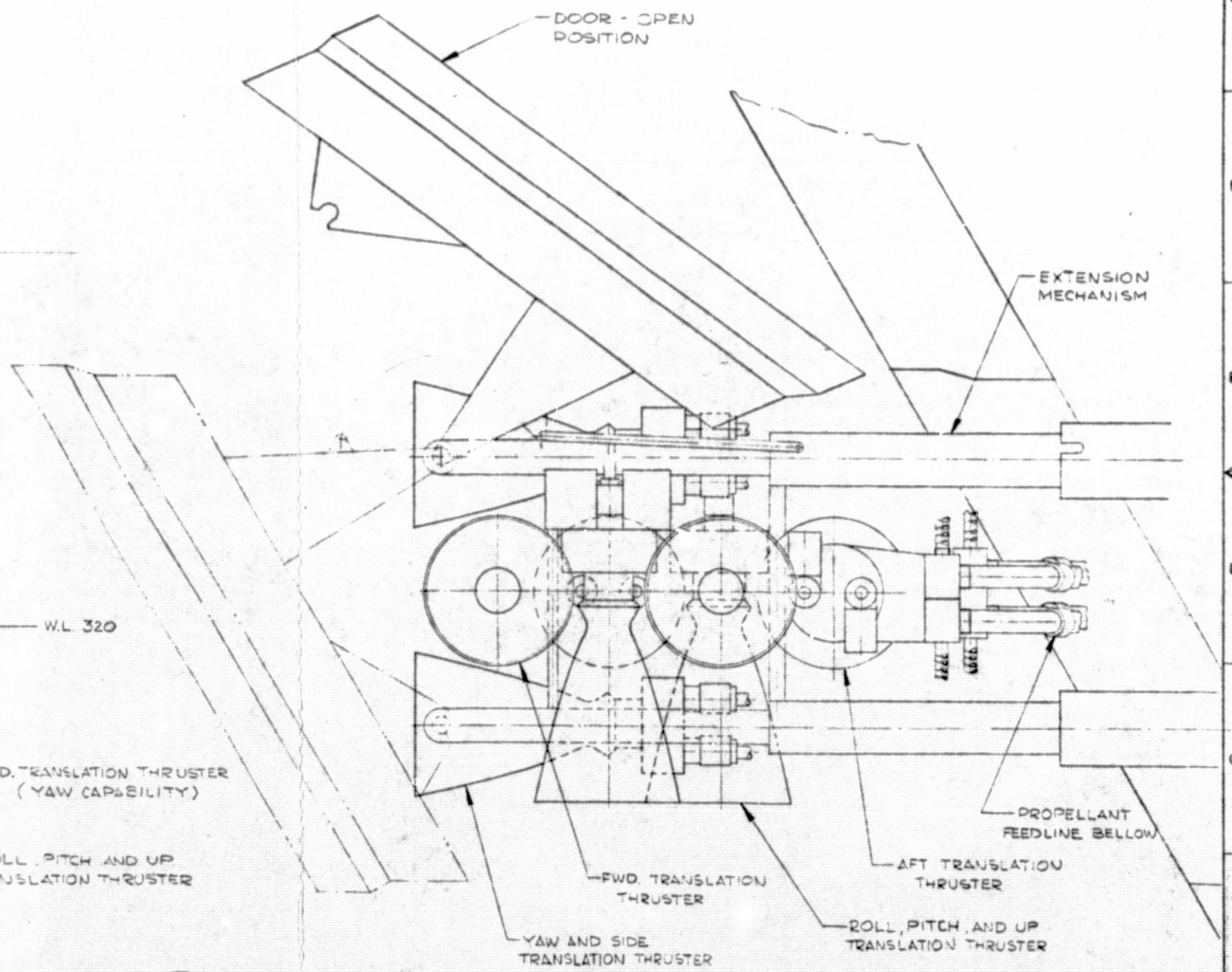

Fig. 2.5-23

QTY REQD	CODE IDENT	PART OR IDENTIFYING NO	NOMENCLATURE OR DESCRIPTION	MATERIAL DESCRIPTION OR NOTE	MATERIAL SPECIFICATION	ZONE	ITEM NO

PARTS LIST

INTERPRET DWG PER	UNLESS OTHERWISE SPECIFIED DIM ARE IN INCHES. TOLERANCES ON FRACTIONS = ± 1/16 DECIMALS: .X = ± .1, .XX = ± .03, .XXX = ± .010 ANGLES = ± 2 DEG	DATE 1-23-70 DWN APVD APVD ENGRG CHKR APVD CONTR CCA CI FD APVD	LOCKHEED MISSILES & SPACE COMPANY A GROUP DIVISION OF LOCKHEED AIRCRAFT CORPORATION SUNNYVALE, CALIFORNIA
NEXT ASSY USED ON APPLICATION			ACPS AFT THRUSTER CLUSTER DELTA BODY - STAGE 1 1/2 MODEL LS-200-3
			SIZE E CODE IDENT DRAWING NO SKS 100209 REV -
			SCALE 1/4 SHEET 1 OF 1

REPRODUCIBILITY OF THE ORIGINAL PAGE IS POOR.

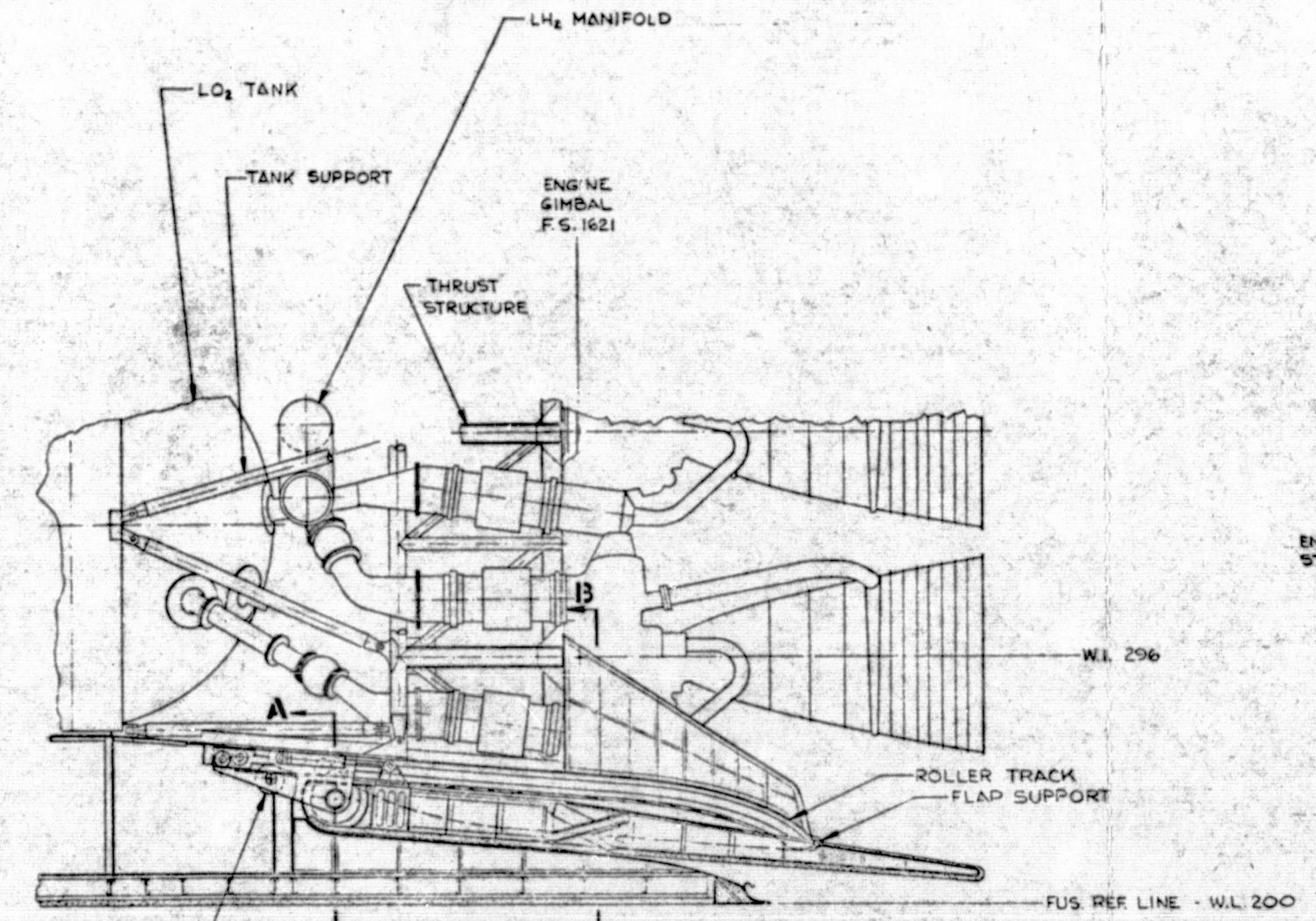

STOWED FLAP DURING ASCENT

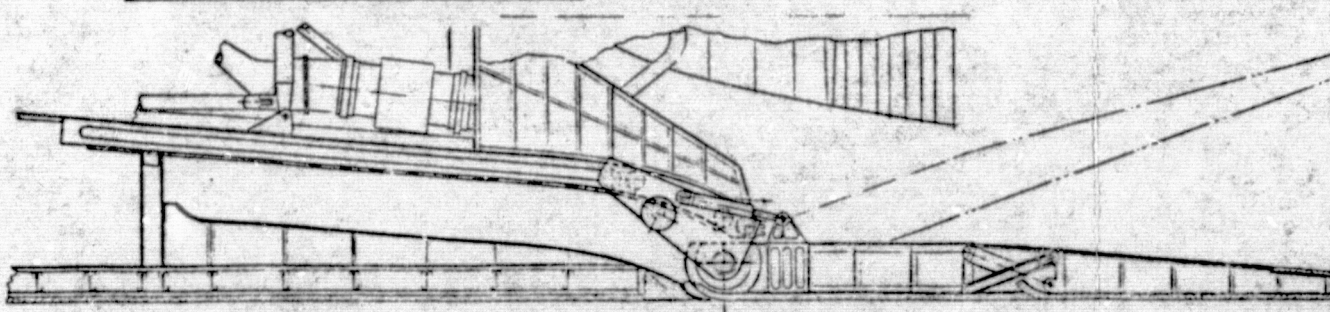

EXTENDED FLAP FOR FLIGHT OPERATIONS

F.S. 1698

FOLDOUT FRAME

REPRODUCIBILITY OF THE ORIGINAL PAGE IS POOR.

5 4 3 2 1

REVISIONS				
ZONE	LTR	DESCRIPTION	DATE	APP.

LIMITED CALENDAR LIFE | LIMITED OPERATING LIFE

PRECEDING PAGE BLANK NOT FILMED

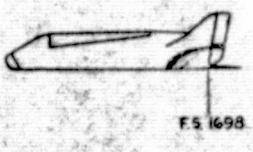

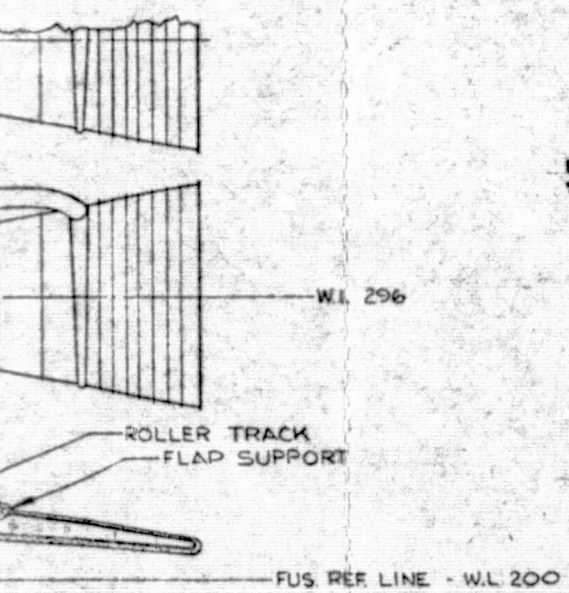

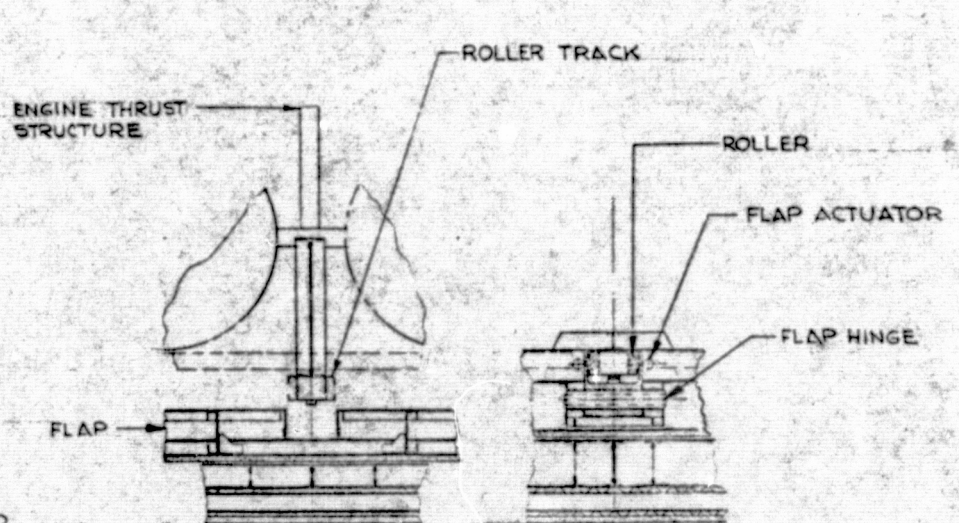

SECTION B-B SECTION A-A

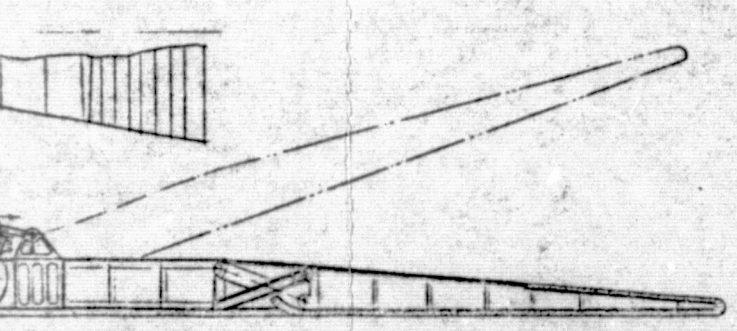

Fig 2.5-24

QTY REQD	CODE IDENT	PART OR IDENTIFYING NO	NOMENCLATURE OR DESCRIPTION	MATERIAL DESCRIPTION OR NOTE	MATERIAL SPECIFICATION	ZONE	ITEM NO

PARTS LIST

INTERPRET DWG PER	UNLESS OTHERWISE SPECIFIED DIM ARE IN INCHES. TOLERANCES ON: FRACTIONS = ± 1/16 DECIMALS: .X = ± .1, .XX = ± .03, .XXX = ± .010 ANGLES = ± 2 DEG	DATE 9-28-70 DWN [illegible] APVD [illegible] APVD ENGRG CHKR APVD APVD	LOCKHEED MISSILES & SPACE COMPANY A GROUP DIVISION OF LOCKHEED AIRCRAFT CORPORATION SUNNYVALE, CALIFORNIA
NEXT ASSY / USED ON APPLICATION	CONTR CCA/CI/FD		FLAP STOWAGE CONCEPT DELTA BODY - STAGE - ½ MODEL LS-200-3
			SIZE E CODE IDENT 02857 DRAWING NO LSKS 100015 REV L SCALE None SHEET 1 of 1

98

FOLDOUT FRAME 2

REPRODUCIBILITY OF THE ORIGINAL PAGE IS POOR.

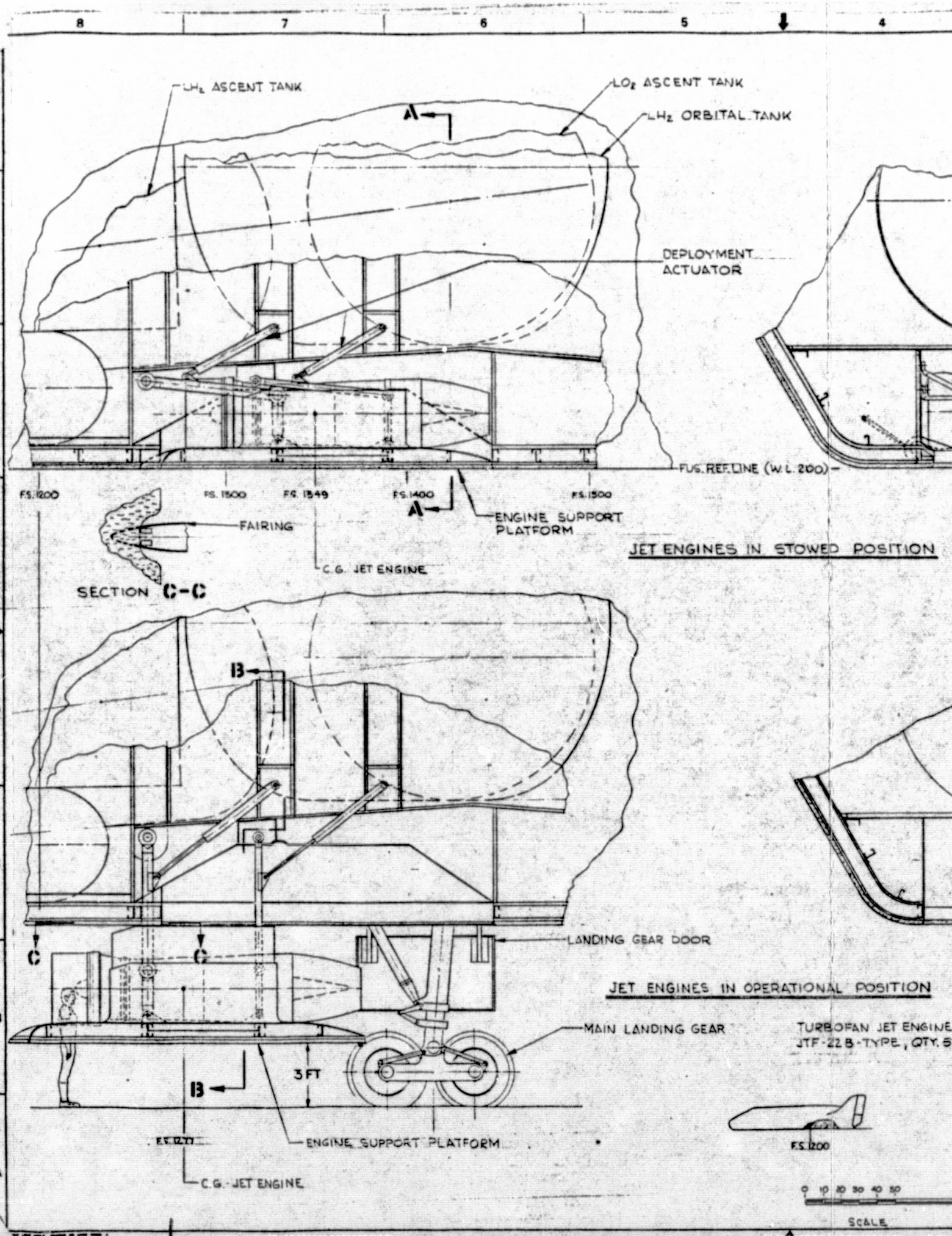

FOLDOUT FRAME

REPRODUCIBILITY OF THE ORIGINAL PAGE IS POOR.

PRECEDING PAGE BLANK NOT FILMED

LIMITED CALENDAR LIFE | LIMITED OPERATING LIFE

REVISIONS			
ZONE/LTR	DESCRIPTION	DATE	APVD

LO_2 ASCENT TANK

LH_2 ORBITAL TANK

DEPLOYMENT ACTUATOR

FUS. REF. LINE (W.L. 200)

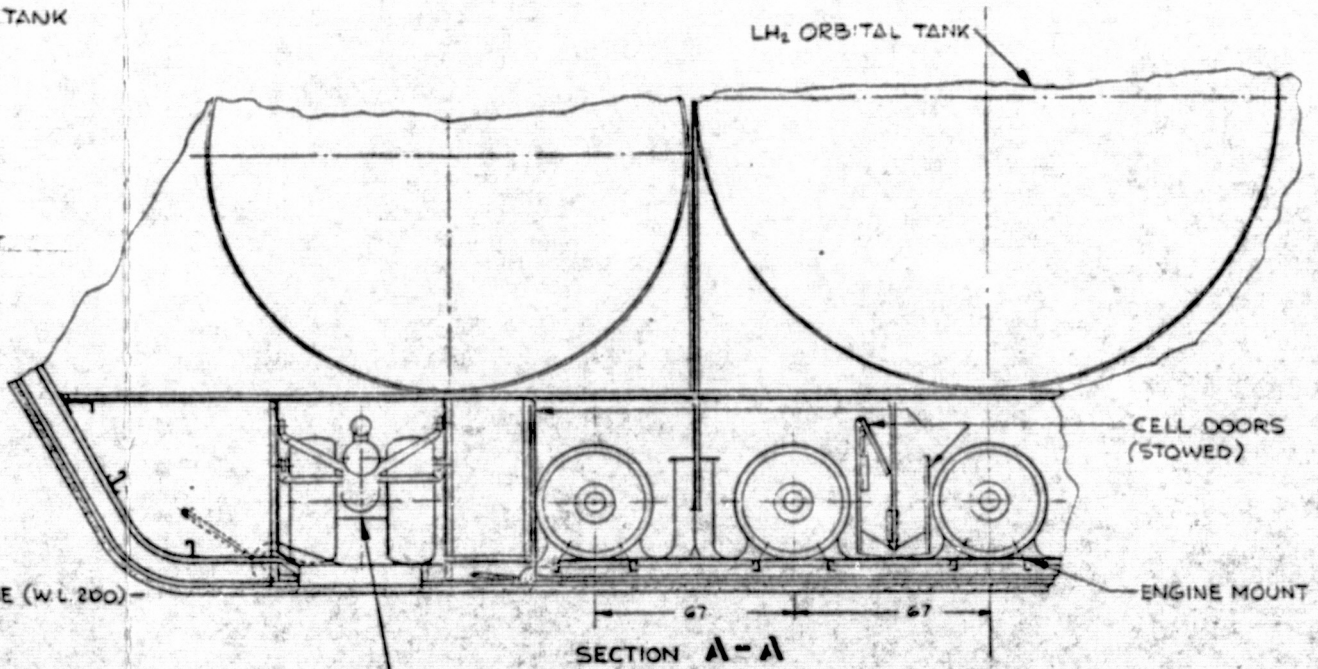

SECTION A-A

JET ENGINES IN STOWED POSITION

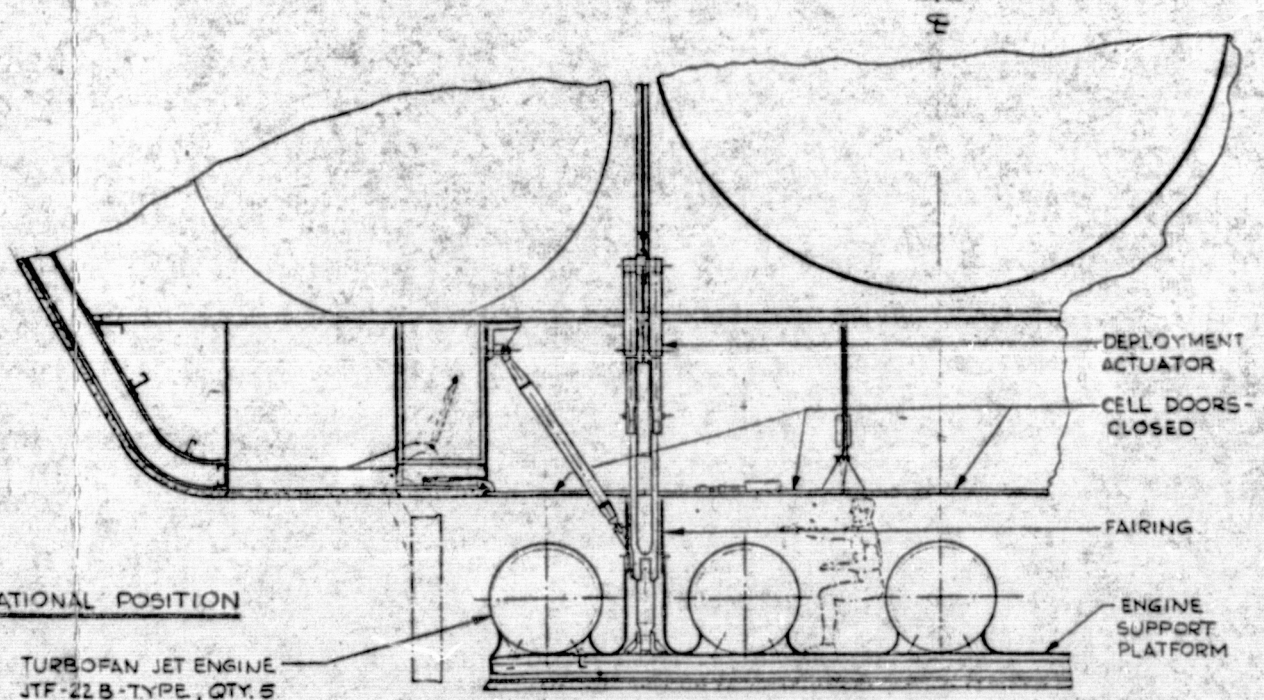

SECTION B-B

JET ENGINES IN OPERATIONAL POSITION

Fig. 215-25

QTY REQD	CODE IDENT	PART OR IDENTIFYING NO.	NOMENCLATURE OR DESCRIPTION	MATERIAL DESCRIPTION OR NOTE	MATERIAL SPECIFICATION	ZONE	ITEM NO.

PARTS LIST



0 10 20 30 40 50 100 INCH

SCALE

INTERPRET DWG PER

UNLESS OTHERWISE SPECIFIED DIM ARE IN INCHES. TOLERANCES ON: FRACTIONS = ± 1/16 DECIMALS: .X = ± .1 .XX = ± .03 .XXX = ± .010 ANGLES = ± 2 DEG

NEXT ASSY | USED ON | APPLICATION

CONTR

CCA/CI/FD

DATE Oct 6 '70

DWN

APVD

APVD

ENGRG

CHKR

APVD

APVD

LOCKHEED MISSILES & SPACE COMPANY
A GROUP DIVISION OF LOCKHEED AIRCRAFT CORPORATION
SUNNYVALE, CALIFORNIA

JET ENGINE DEPLOYMENT CONCEPT
DELTA BODY - STAGE + 1/2
MODEL LS-200-3

SIZE	CODE IDENT	DRAWING NO	REV
E	06987	LSKS 100302	L

SCALE 1/2 SHEET 1 of 1

FOLDOUT FRAME 2

2.5.73

REPRODUCIBILITY OF THE ORIGINAL PAGE IS POOR.

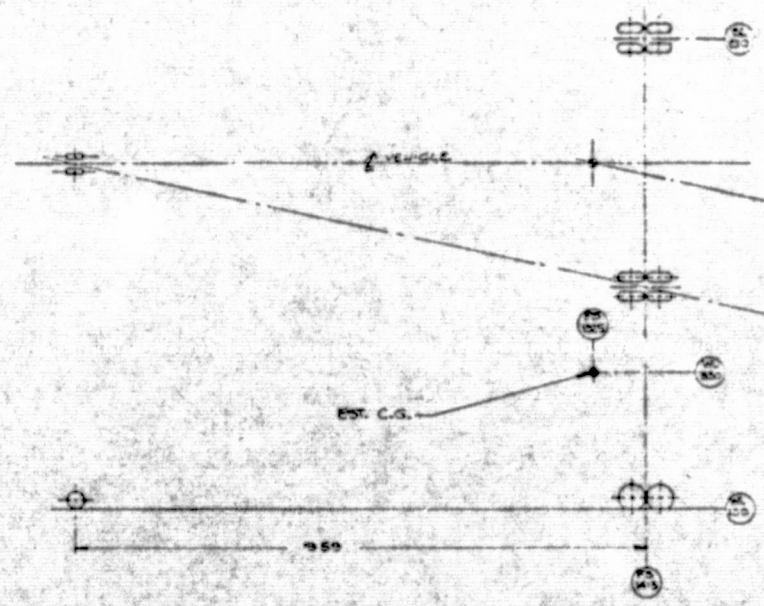

GEAR TURN-OVER DATA
SCALE: 1" = 100"

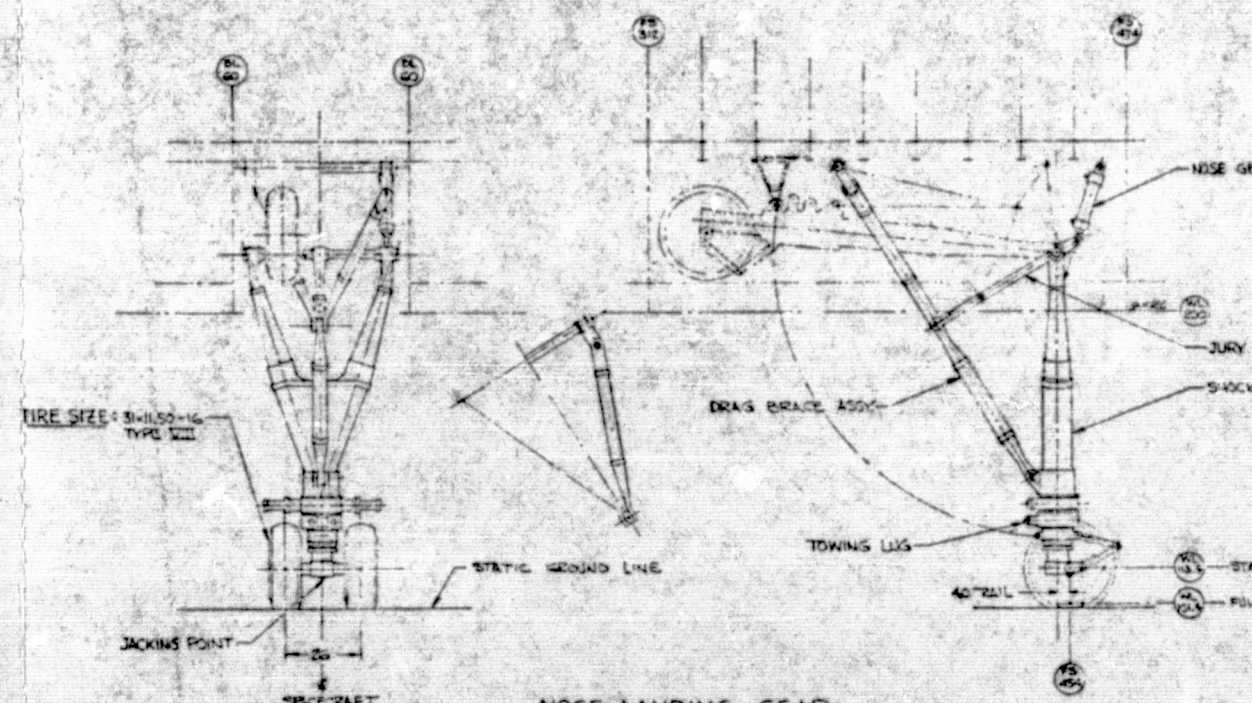

NOSE LANDING GEAR

FOLDOUT FRAME

REPRODUCIBILITY OF THE ORIGINAL PAGE IS POOR.

12 | 11 | 10 | 9 | 8 | 7 | 6

BASIC LOADS
PRELIMINARY
(LOADS ARE LIMIT & IN THE GROUND AXIS)

NOSE GEAR

CONDITION	n_z	WEIGHT	LOADS – LBS VERTICAL	DRAG	SIDE
LEVEL LANDING (LL-1)	1.5	273,000	[illegible]	[illegible]	[illegible]
SPIN-UP (LL-5)	1.5	↓	54,932	±3,184	—
SPRING-BACK (LL-6)	1.5		58,780	-19,407	—
BRAKED ROLL	1.0		37,412	—	—
UNSYMMETRICAL BRAKING	1.0		40,642	—	±[illegible]32
TURNING	1.0		29,850	—	±17,760
TAXING	2.0	↓	81,345	—	—
TOWING	1.0	278,000	42,830	255 KIPS REAR	

NOTE: TOW LOAD IS UNSPECIFIED APPLIED IN ANY OR ALL WAYS AS LISTED BELOW

LIMIT LOAD ON GEAR – LBS.	POSITION OF GEAR SWIVELED	DIRECTION OF LOAD APPLICATION
41,700	FORWARD	FORWARD
		AFT
	AFT	FORWARD
		AFT
20,850	45° FROM FWD	FORWARD OR AFT IN PLANE OF WHEELS
	45° FROM AFT	FORWARD OR AFT IN PLANE OF WHEELS

MAIN GEAR

CONDITION	n_z	WEIGHT	LOADS – LBS VERTICAL	DRAG	SIDE
LEVEL LANDING (LL-1)	1.5	273,000	[illegible]	[illegible]	[illegible]
SPIN-UP	1.5	↓	147,880	24,210	—
SPRING-BACK	1.5		215,980	-91,304	—
DRIFT LANDING	1.2		174,050	—	±[illegible] 42,550
BRAKED ROLL	1.2		166,850	133,440	—
REVERSE BRAKING					
UNSYMMETRICAL BRAKING	1.0		115,194	92,159	±10,291
TURN – OUTSIDE GEAR			212,356	—	[illegible]
TURN – INSIDE GEAR			61,129	—	25,30[illegible]
TAXING	2.0		293,482	—	—
TOWING *	1.0		130,240	255 KIPS	± 18,[illegible]
PIVOTING **	1.0		154,243	0	±[illegible]
TAIL DOWN LDG – BU	1.5	↓	98,591	85,319	—
TAIL DOWN LDG – SD	1.5	278,000	178,939	133,955	—

*TOWING LOAD = .13 F_{max} = 36,075 LBS
TOWING LOAD IS APPLIED FORWARD, AFT, OR PARALLEL TO DRAG AXIS, OR FORWARD OR AFT AT 30° TO THE DRAG AXIS.

** LOADS ARE SCRUBBING LOADS = 1,192,872 IN-LBS/[illegible]

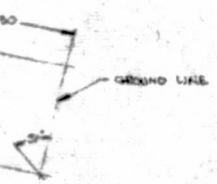

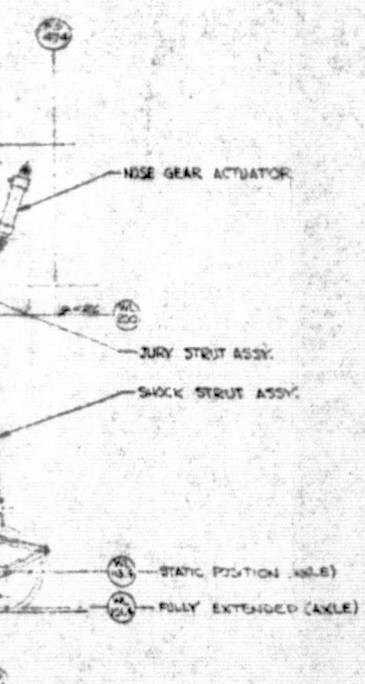

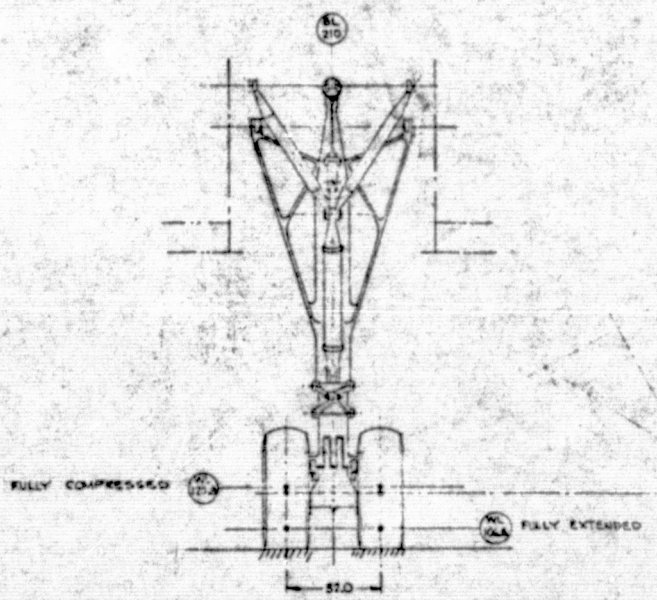

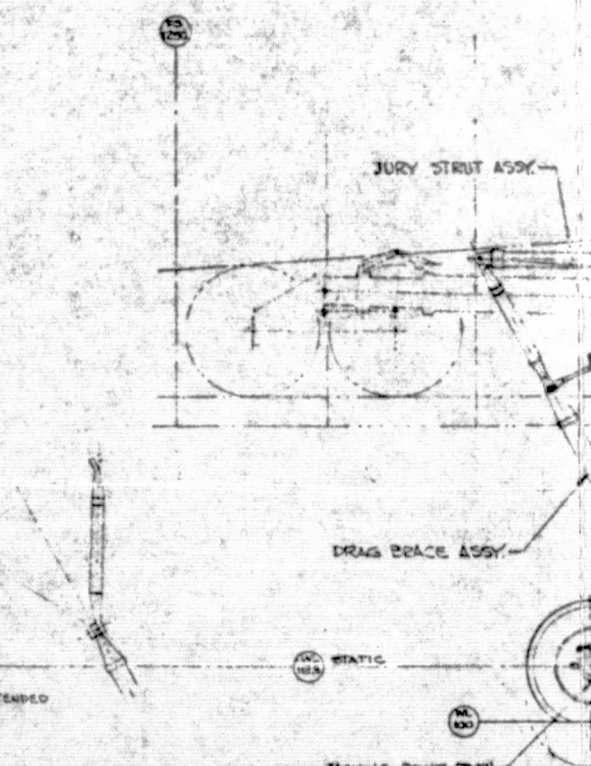

MAIN LANDING GEAR

NOTES

DRAWING NUMBER | REV | SH

FOLDOUT FRAME 2

REPRODUCIBILITY OF THE

ZONE/LTR	REVISIONS DESCRIPTION	DATE	APPD

LIMITED CALENDAR LIFE

LIMITED OPERATING LIFE

PRECEDING PAGE BLANK NOT FILMED

MAIN GEAR

DITION	No.	WEIGHT	LOADS – LBS VERTICAL	DRAG	SIDE
LANDING (UP)	1.5	273,700	238,500	24,250	—
UP	1.5		47,200	24,250	—
-BACK	1.5		215,300	90,309	—
LANDING	1.0		174,250	—	+84,000 -42,000
D 2.5LL	1.1		166,853	83,440	—
DE BRAKING					
MMETRICAL	1.0		145,194	92,159	±10,291
ICING					
SIDE GEAR			224,356	—	(-) 78
SIDE GEAR			91,128	—	±5,394
G	2.1		333,493	—	—
G	1.0		170,240	SEE NOTE	±84,000
G	1.0		126,243	SEE NOTE	±84,000
NNED G – 90	1.5		248,931	85,500	—
OWN LG – 58	1.5	278,000	178,932	88,955	—

NG LOAD = .78 F_{max} = 91,275 LBS
ING LOAD IS APPLIED FORWARD, AFT OR PARALLEL TO DRAG AXIS, OR FORWARD OR FF AT 30° TO THE DRAG AXIS.
ADS ARE SCRUBBING LOADS 4 1,150,612 IN-LBS/STRUT

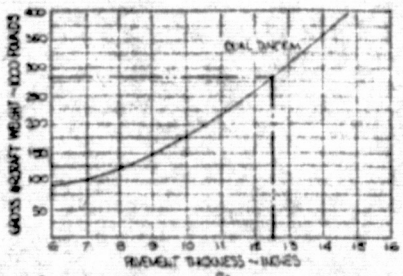

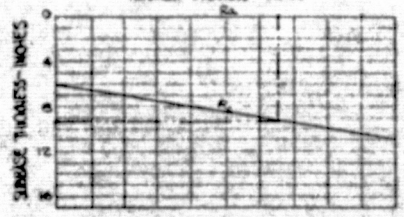

RIGID PAVEMENT DESIGN

ASSUMPTIONS:
- GEAR TYPE – DUAL TANDEM
- GROSS WEIGHT ~ 278,000 LBS
- SOIL CLASSIFICATION ~ E-7
- SUBGRADE CONDITIONS:
  - FROST ~ NONE
- SUBGRADE CLASS ~ R_4

FINAL REQUIREMENTS:

	CRITICAL AREA	NONCRITICAL AREA
PAVEMENT	12.5" USE 13"	12.5 × 0.8 = 10"
SUBBASE	31.1" – 13"	9"

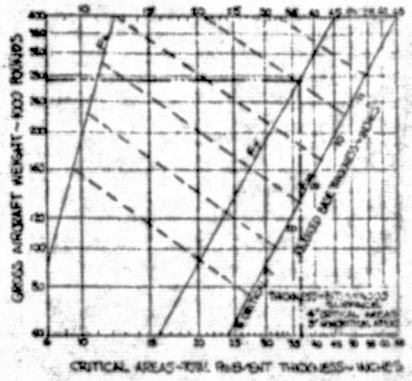

FLEXIBLE PAVEMENT DESIGN

ASSUMPTIONS:
- GEAR TYPE ~ DUAL TANDEM
- GROSS WEIGHT ~ 278,000 LBS
- SOIL CLASSIFICATION ~ E-7
- SUBGRADE CONDITIONS:
  - DRAINAGE ~ POOR
  - FROST ~ YES
- SUBGRADE CLASS ~ F-7

FINAL REQUIREMENTS: (TYP. JET AIRCRAFT FIELD)

	CRITICAL AREAS	30° NONCRITICAL AREAS	77° EDGE AREAS
SURFACE	4"	3"	2"
BASE	11"	10"	9"
SUBBASE	22"	20"	23"
FROST PROTECTION	0	4"	4"
TOTAL	37"	37"	37"

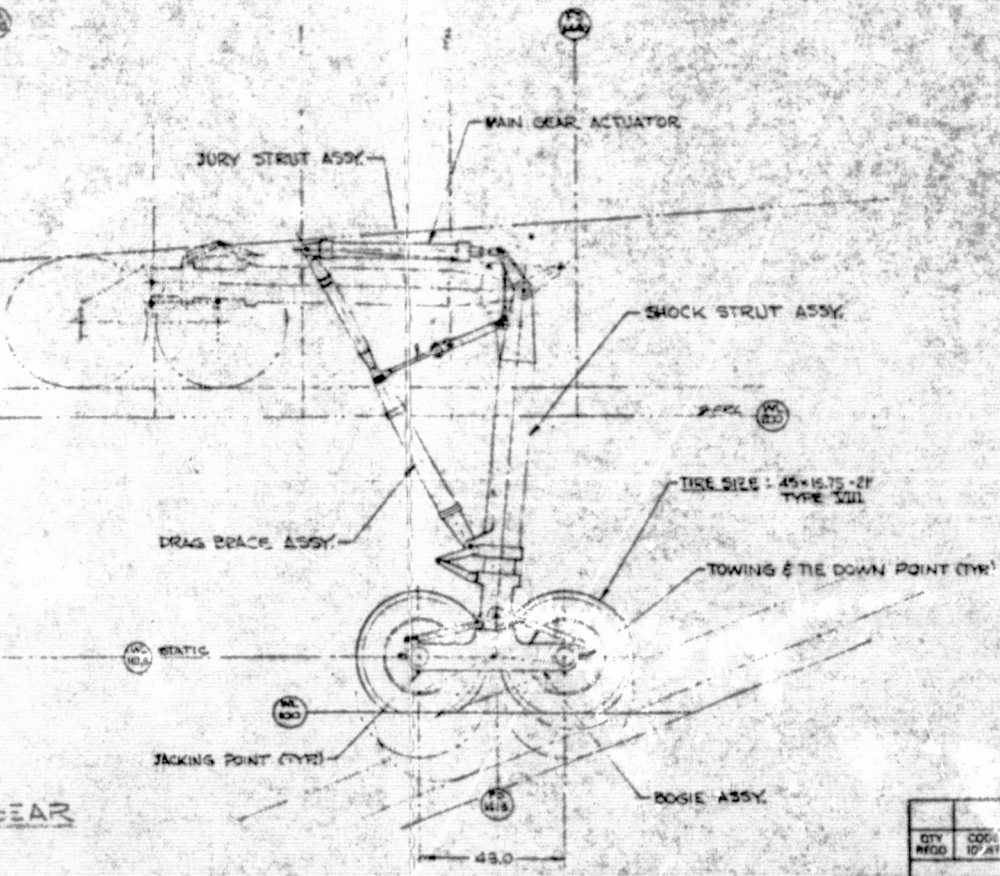

NOTES

Fig. 2.5-26

QTY PROD	CODE IDENT NO.	PART OR IDENTIFYING NO.	NOMENCLATURE OR DESCRIPTION	MATERIAL DESCRIPTION OR NOTE	MATERIAL SPECIFICATION	ZONE	ITEM NO.

PARTS LIST

INTERPRET DWG PER	UNLESS OTHERWISE SPECIFIED DIM. ARE IN INCHES. TOLERANCES ON FRACTIONS = ± 1/16 DECIMALS: .X = ± .1 .XX = ± .03 .XXX = ± .010 ANGLES = ± 2 DEG	DATE 9-15-72 DR [illegible] APPD APPD ENGRG CHK APPD APPD	LOCKHEED MISSILES & SPACE COMPANY A GROUP DIVISION OF LOCKHEED AIRCRAFT CORPORATION SUNNYVALE, CALIFORNIA LANDING GEAR CONCEPT GENERAL ARRANGEMENT – STUDY 3.1 MODEL L-1-977-3, BASELINE
NEXT ASSY USED ON APPLICATION	CONTR CCA/CEI		SIZE J CODE IDENT 06324 DRAWING NO. SKH 100301 REV SCALE SHEET

FOLDOUT FRAME 3

2.5-75

2.5.2 LS 200-10 System

The final recommended stage-and-one-half configuration system design was derived from the initial five month's design studies (LS 200-5) and the interim work on a Model LS 200-7 system. The final system was designated Model LS 200-10 and the design layout work documenting the physical definition of this arrangement is shown in the following drawings:

1. General Arrangement
   Delta-Body Stage-And-One-Half
   Model LS 200-10
   SKS 100053A - Fig. 2.5-27

2. General Arrangement ($1\frac{1}{2}$B)
   Delta-Body Stage-And-One-Half
   Model LS 200-7 and 200-9
   SKT 100038 - Fig. 2.5-28

3. Launch Vehicle
   Delta-Body Stage-And-One-Half
   Model LS 200-10
   SKS 100061 - Fig. 2.5-29

4. Volume Curve
   Delta-Body Orbiter
   Models LS 200-7 and 200-8, LS 400-5 and 400-6
   SKS 100046 - Fig. 2.5-30

The general arrangement of the final recommended stage-and-one-half orbiter is shown in Drawing SKS 100053 (Fig. 2.5-27). This arrangement is an updated version of the earlier LS 200-7 system. The major changes include the installation of the airbreather engines into the lower fuselage, the instal-

lation of the airbreather engine fuel (JP-4) in the forward end of the mid-fuselage compartment, and the space allocation for a forward-mounted payload deployment mechanism system. All these changes were adopted without a change in the vertical reference length.

Design Drawing SKT 100038 (Fig. 2.5-28) is the general arrangement of the previous stage-and-one-half concept (LS 200-7). It is an updated version of the LS 200-5 system reported on in the Fifth Monthly Progress and Status Report, and incorporates the following principal changes:

A. Aerodynamic Shape and/or Geometry

- Basic shape is the same
- Overall length was 152 ft – now 159 ft

B. Main Rocket Engine System

- Number of Engines - 9 instead of 11
- Nozzle Area Ratio was 35:1 - now 53:1
- Gimbal Pattern changed from four center engines of the bottom row and the top centerline engine, to three center engines of the bottom row and two center engines of the top row

C. Main Propellant Tankage System

- Arrangement and Operation - Same
- Number of Tanks - Same
- Capacity Required - Generally Greater
  (Ascent and Orbital oxygen tanks are larger with the orbital hydrogen tank smaller)
- Load Path - Principally the same

D. Jet Engine System

- Number of Engines - 6 instead of 5
- Location - Fuselage Base
- Operation - Fixed Engine mounts and intake ducting
- Fuel - JP4 instead of LH_2 (separate fuel tank is used and mounted forward to balance-out main engine installation)

E. Landing Gear Installation

- Arrangement - Maintained tricycle concept with main gear installed outboard of ascent tankage

F. Control Surface Arrangement

- Rudder area is a greater percent of the total Fin/Rudder area
- Upper surface flap hinge line unskewed to reduce adverse yaw forces on adjacent fin surfaces

G. Nose Cap System

Because of 1100 mile crossrange requirement and attendant reduction in anticipated temperatures, a round instead of elliptical shape has been adopted.

The LS 200-10 launch vehicle arrangement is shown in Design Drawing SKS 100061 (Fig. 2.5-29). This arrangement is an updated version of the LS 200-5 system. The major change in the system was the incorporation of a greater amount of droptank propellant by essentially increasing the tank diameter from 26 ft to 27 ft. This permitted the intertank structure, which contains the droptank-to-orbiter forward attachment and oxygen lines, to remain in its relative position to the orbiter nose.

An indication of the usable volume for a stage-and-one-half orbiter system, as well as the wetted area involved is shown in Drawing SKS 100046 (Fig. 2.5-30).

REPRODUCIBILITY OF THE ORIGINAL PAGE IS POOR.

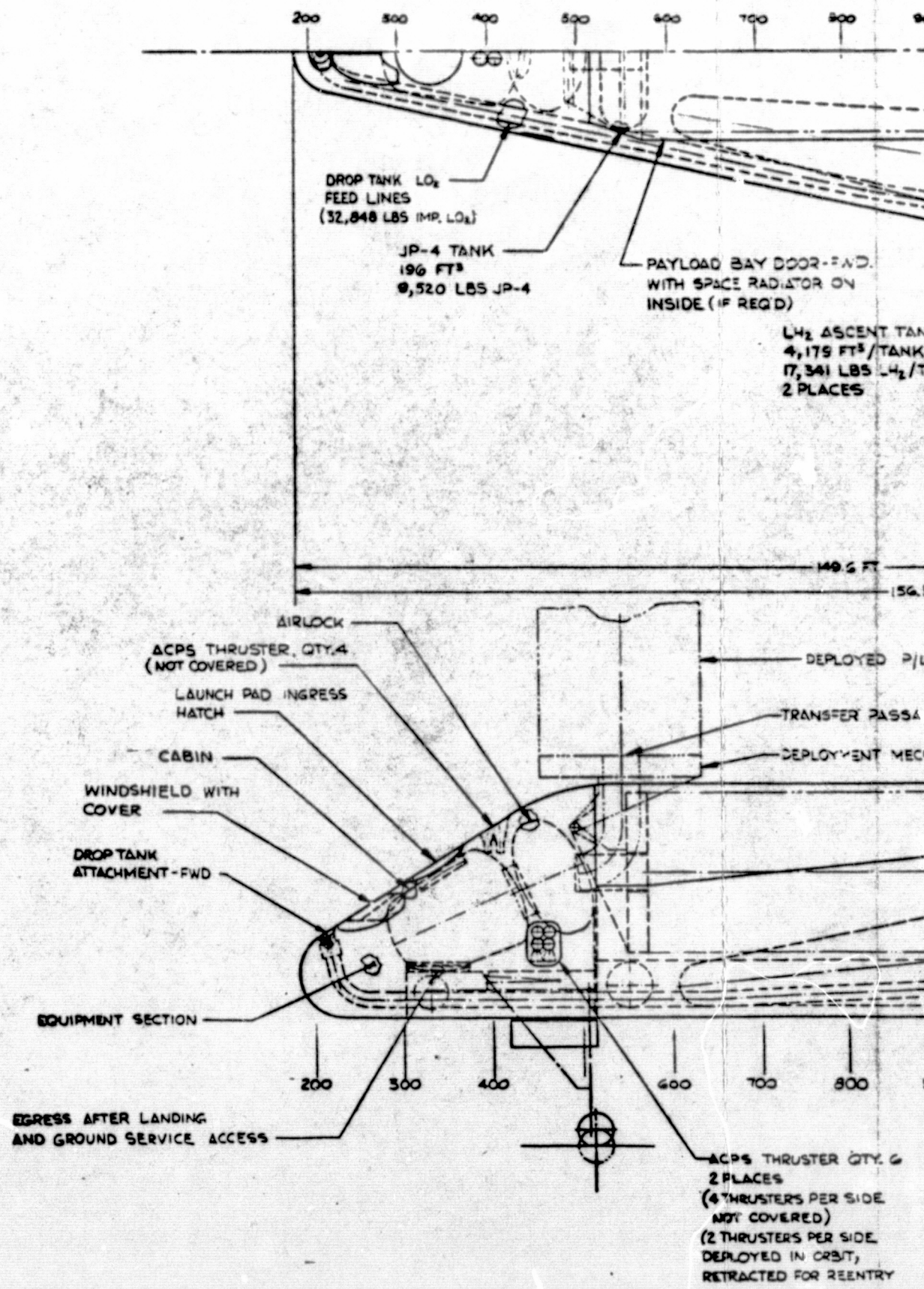

FOLDOUT FRAME

REPRODUCIBILITY OF THE ORIGINAL PAGE IS POOR.

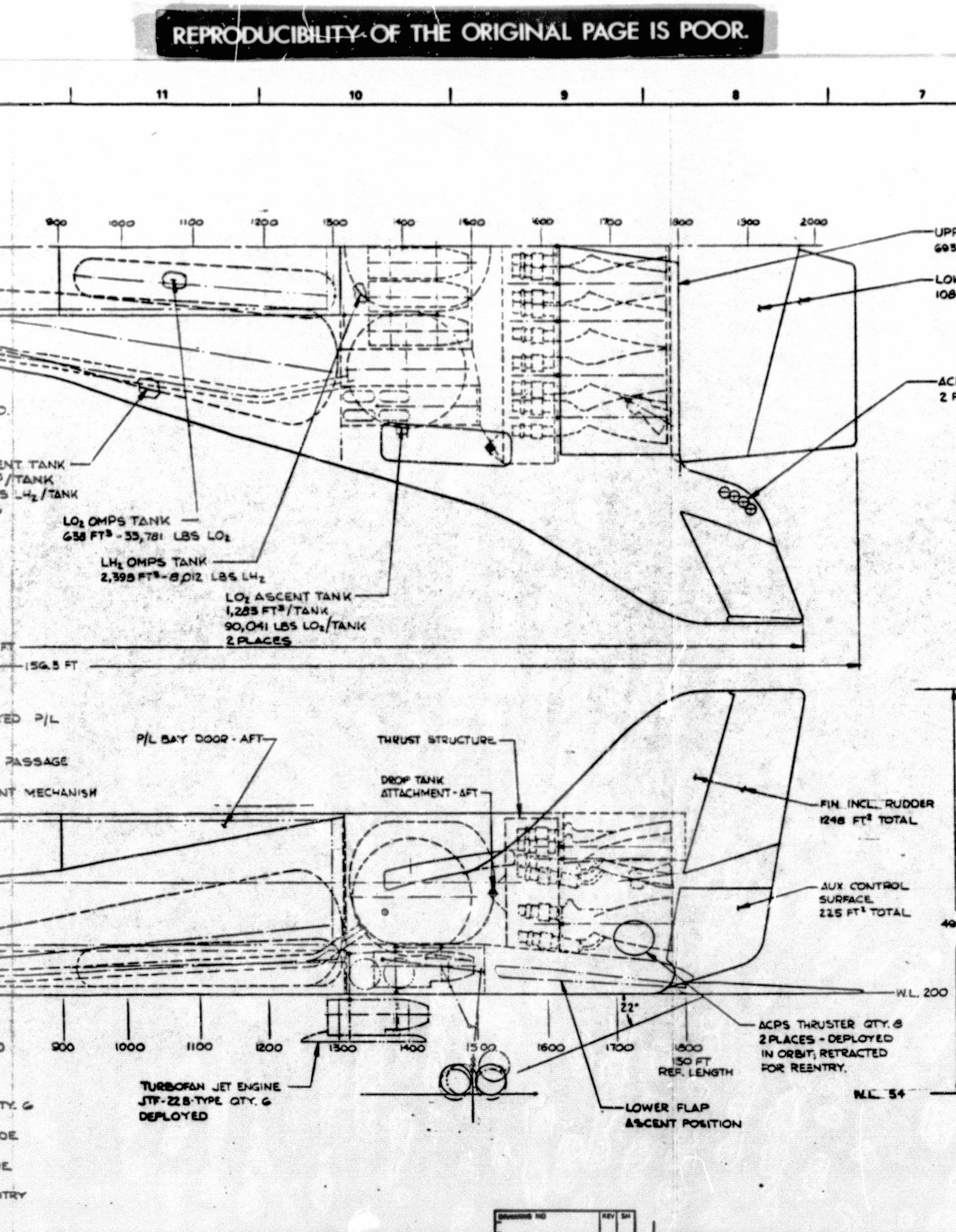

FOLDOUT FRAME 2

REPRODUCIBILITY OF THE ORIGINAL PAGE IS POOR.

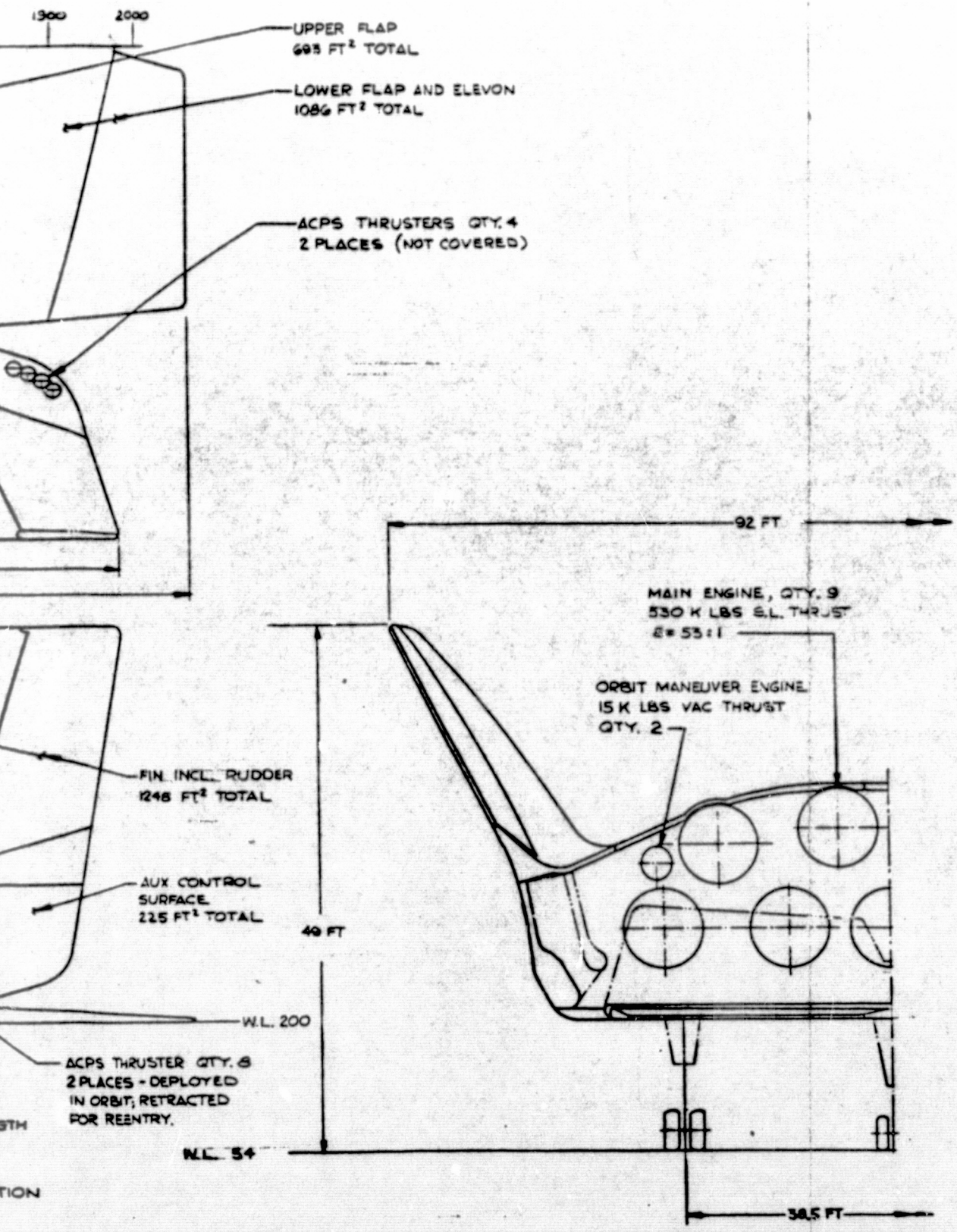

REPRODUCIBILITY OF THE ORIGINAL PAGE IS POOR.

LIMITED CALENDAR LIFE	LIMITED OPERATING LIFE

REVISIONS				
ZONE	LTR	DESCRIPTION	DATE	APVD
	A	LO_2 OMPS TANK WAS 631 FT³. 33,250 LBS, LH_2 OMPS TANK WAS 2,358 FT³ - 7,839 LBS., JP-4 TANK WAS 193 FT³ - 8,498 LBS. ADDED D/T LO_2 FEED LINE	4-29-71	[illegible]

PRECEDING PAGE BLANK NOT FILMED

FT

, QTY. 9
L. THRUST

NGINE
ST

AREA:
REF. PLANFORM : 4,878 FT²
TOTAL PLANFORM : 6,846 FT²
BASE : 1229 FT²

38.5 FT

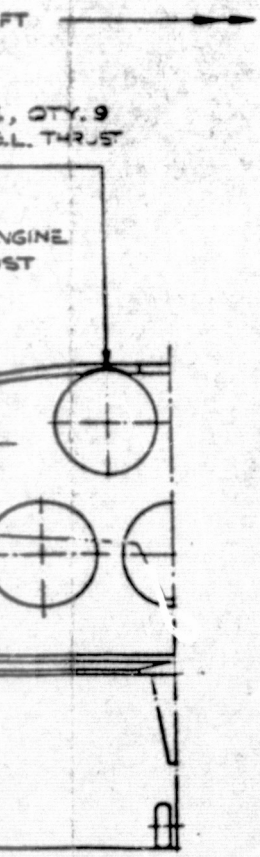

Fig. 2.5-27

QTY REQD	CODE IDENT	PART OR IDENTIFYING NO	NOMENCLATURE OR DESCRIPTION	MATERIAL DESCRIPTION OR NOTE	MATERIAL SPECIFICATION	ZONE	ITEM NO

PARTS LIST

INTERPRET DWG PER

NEXT ASSY | USED ON
APPLICATION

UNLESS OTHERWISE SPECIFIED DIM ARE IN INCHES. TOLERANCES ON:
FRACTIONS = ± 1/16
DECIMALS: .X = ± .1
.XX = ± .02
.XXX = ± .010
ANGLES = ± 2 DEG

CONTR
CCA/CI/FD

DATE 4-6-71
DWN [illegible]
APVD
APVD
ENGRG
CHKR
APVD
APVD

LOCKHEED MISSILES & SPACE COMPANY
A GROUP DIVISION OF LOCKHEED AIRCRAFT CORPORATION
SUNNYVALE, CALIFORNIA

GENERAL ARRANGEMENT
DELTA BODY - STAGE & 1/2
MODEL LS-200-10

SIZE	CODE IDENT	DRAWING NO	REV
J	06887	SKS 100053	A

SCALE 1/32 SHEET 1 OF 1

FOLDOUT FRAME 4

REPRODUCIBILITY OF THE ORIGINAL PAGE IS POOR.

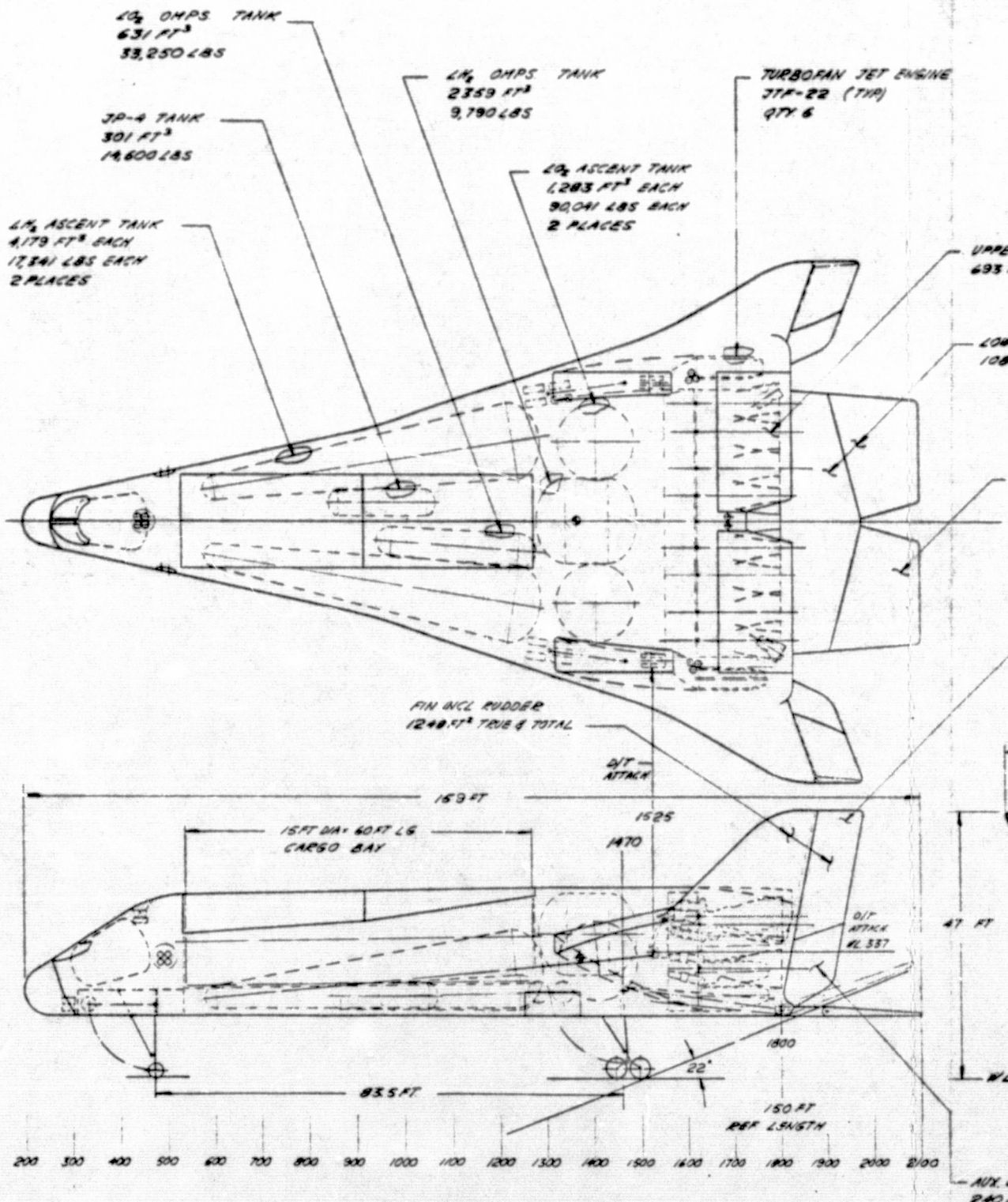

LS-200-7 (3 ENGINES)

NOTES

[1] BASED ON TRIANGULAR AREA WITH APEX AT F.S. 0
BASE AT F.S. 1800 AND ALTITUDE OF 180 FT (REF. LENGTH)

[2] BASED ON AREA OF TOTAL ORBITER AS SHOWN IN PLAN VIEW

FOLDOUT FRAME

REPRODUCIBILITY OF THE ORIGINAL PAGE IS POOR.

PRECEDING PAGE BLANK NOT FILMED

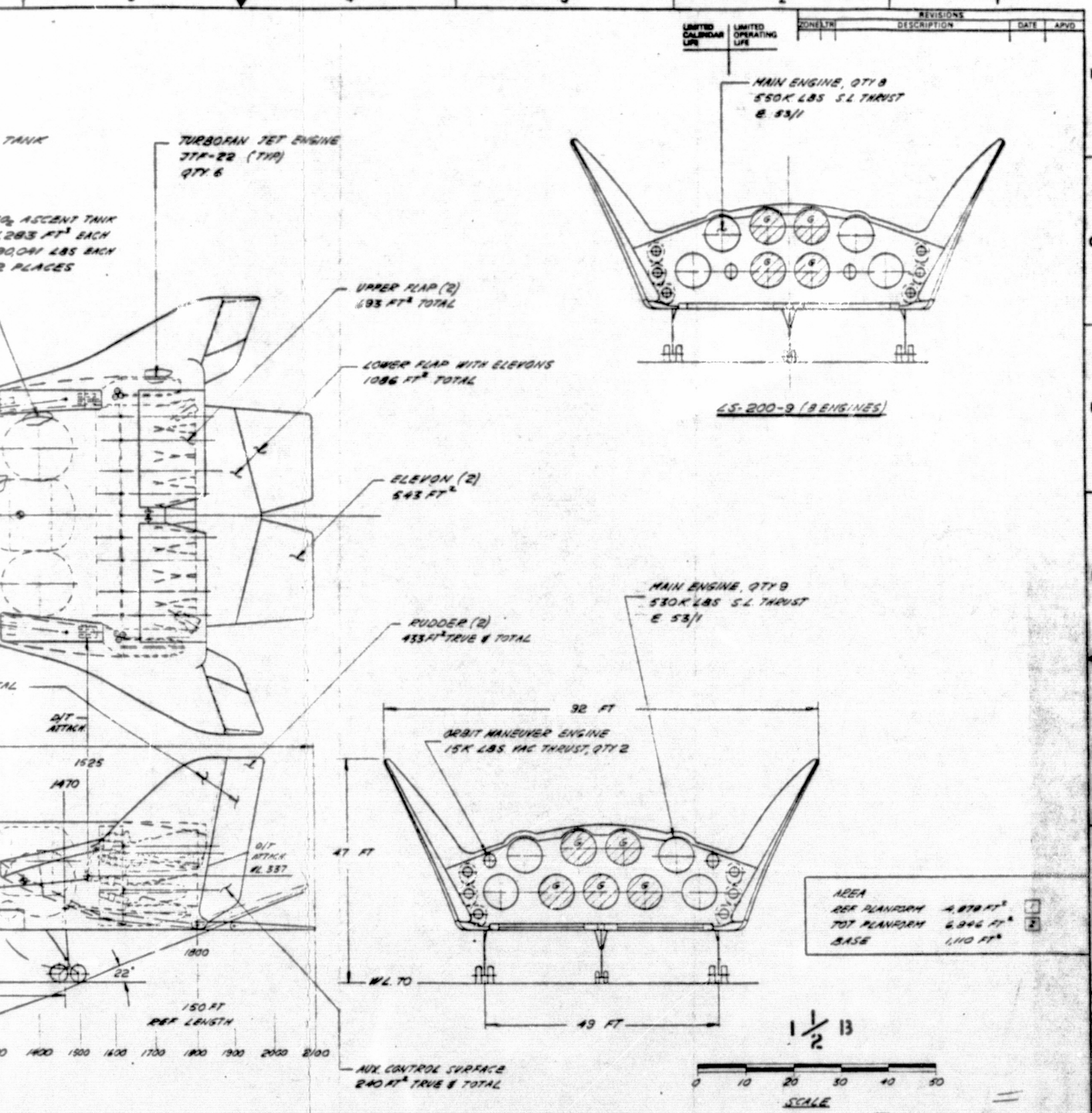

NOTES

1. BASED ON TRIANGULAR AREA WITH APEX AT F.S.0 BASE AT F.S. 1800 AND ALTITUDE OF 150 FT (REF LENGTH)
2. BASED ON AREA OF TOTAL ORBITER AS SHOWN IN PLAN VIEW

Fig 2.5-28

QTY REQD	CODE IDENT	PART OR IDENTIFYING NO	NOMENCLATURE OR DESCRIPTION	MATERIAL DESCRIPTION OR NOTE	MATERIAL SPECIFICATION	ZONE	ITEM NO

PARTS LIST

INTERPRET DWG PER

UNLESS OTHERWISE SPECIFIED DIM ARE IN INCHES. TOLERANCES ON: FRACTIONS = ± 1/16 DECIMALS: .X = ± .1 .XX = ± .03 .XXX = ± .010 ANGLES = ± 2 DEG

DATE 2-16-71
DWN KARL TOLLO
APVD Gen. Harris
APVD
ENGRG
CHKR
APVD
APVD

LOCKHEED MISSILES & SPACE COMPANY
A GROUP DIVISION OF LOCKHEED AIRCRAFT CORPORATION
SUNNYVALE, CALIFORNIA

GENERAL ARRANGEMENT (1 1/2 B)
DELTA BODY - STAGE & 1/2
MODEL LS-200-7 & 9

SIZE E | CODE IDENT 06087 | DRAWING NO SKT 100038 | REV

NEXT ASSY | USED ON | APPLICATION | CONTR | CCA/CI/FD | SCALE 1/100 | SHEET

FOLDOUT FRAME 2

REPRODUCIBILITY OF THE ORIGINAL PAGE IS POOR.

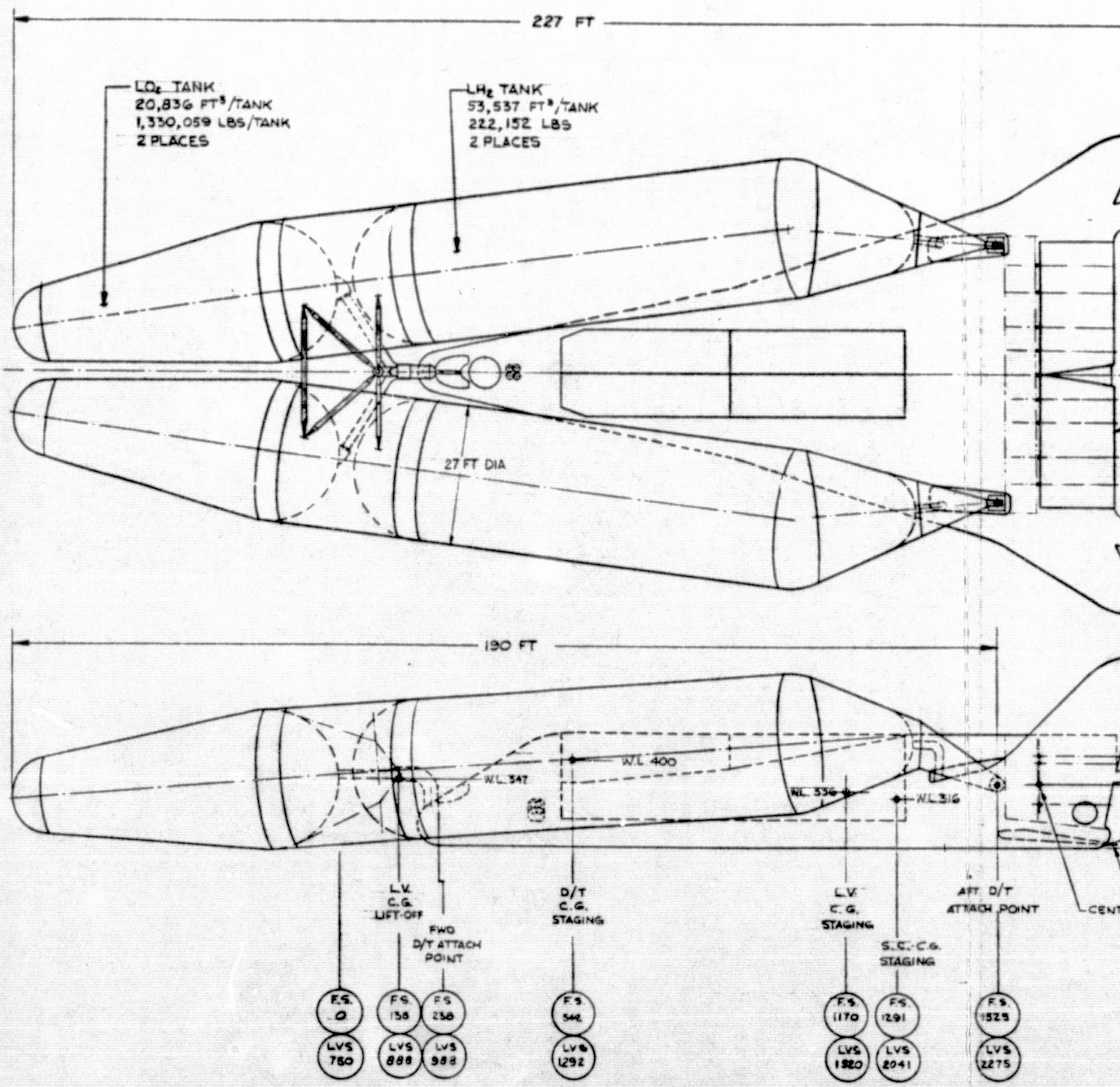

FOLDOUT FRAME

REPRODUCIBILITY OF THE ORIGINAL PAGE IS POOR.

LIMITED CALENDAR LIFE	LIMITED OPERATING LIFE

REVISIONS				
ZONE	LTR	DESCRIPTION	DATE	APVD

PRECEDING PAGE BLANK NOT FILMED

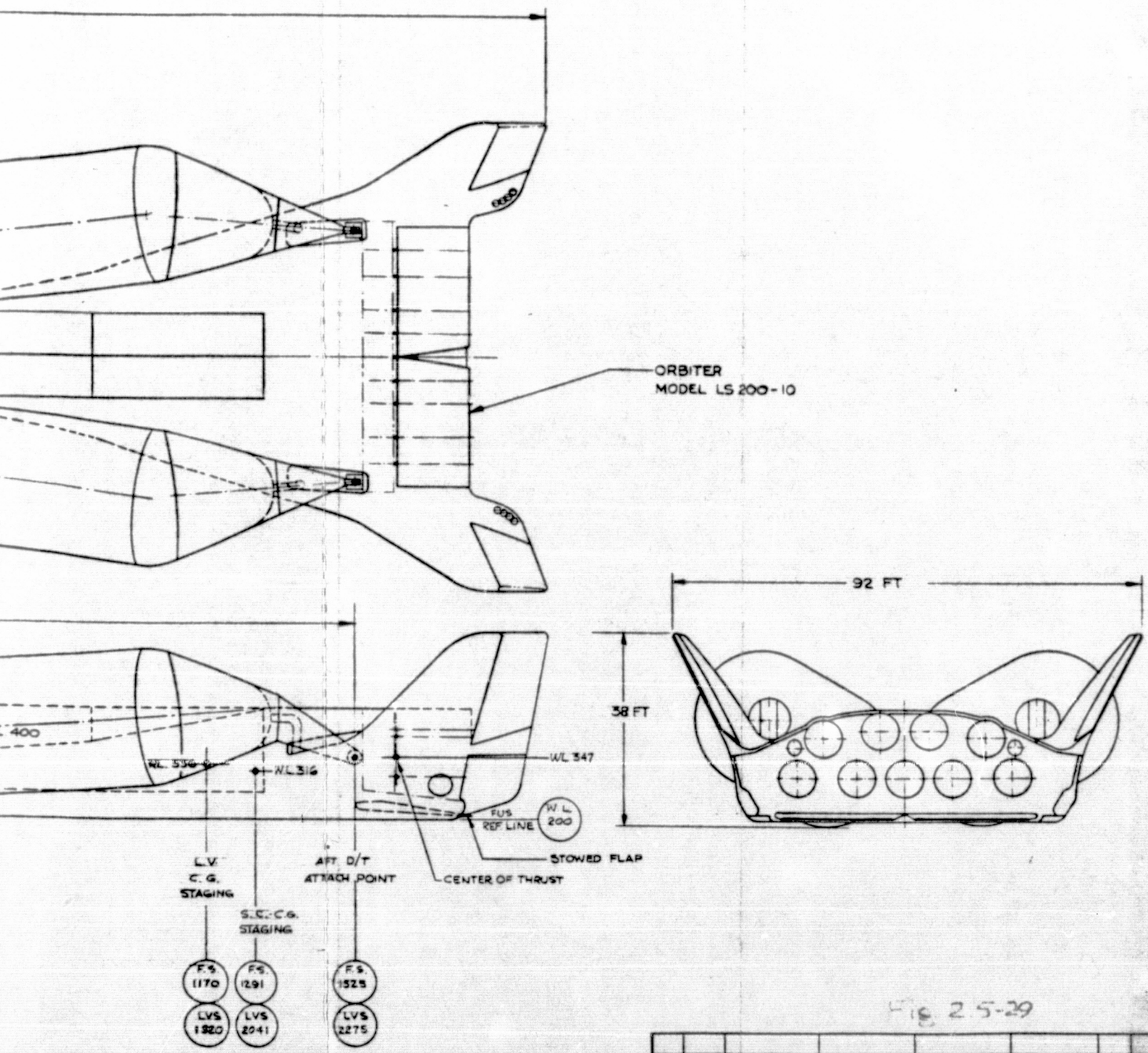

Fig. 2.5-29

QTY REQD	CODE IDENT	PART OR IDENTIFYING NO	NOMENCLATURE OR DESCRIPTION	MATERIAL DESCRIPTION OR NOTE	MATERIAL SPECIFICATION	ZONE	ITEM NO

PARTS LIST

INTERPRET DWG PER	UNLESS OTHERWISE SPECIFIED DIM ARE IN INCHES. TOLERANCES ON: FRACTIONS = ± 1/16 DECIMALS: .X = ± .1 .XX = ± .03 .XXX = ± .010 ANGLES = ± 2 DEG	DATE 5-12-71 DWN H. Schmidt APVD Geo. Havrisik APVD ENGRG CHKR APVD APVD	LOCKHEED MISSILES & SPACE COMPANY A GROUP DIVISION OF LOCKHEED AIRCRAFT CORPORATION SUNNYVALE, CALIFORNIA
NEXT ASSY / USED ON	CONTR		LAUNCH VEHICLE DELTA BODY - STAGE + 1/2 MODEL LS 200-10
APPLICATION	CCA/CI/FD		SIZE E CODE IDENT 05987 DRAWING NO SKS 100061 REV
			SCALE SHEET

REPRODUCIBILITY OF THE ORIGINAL PAGE IS POOR.

WETTED AREA

	1½C	2C
BODY	13,529	14,166
FIN	1,996	1,996
LOWER FLAP	2,190	2,190
BASE	1,110	1,045
TOTAL	18,825	19,397 FT²

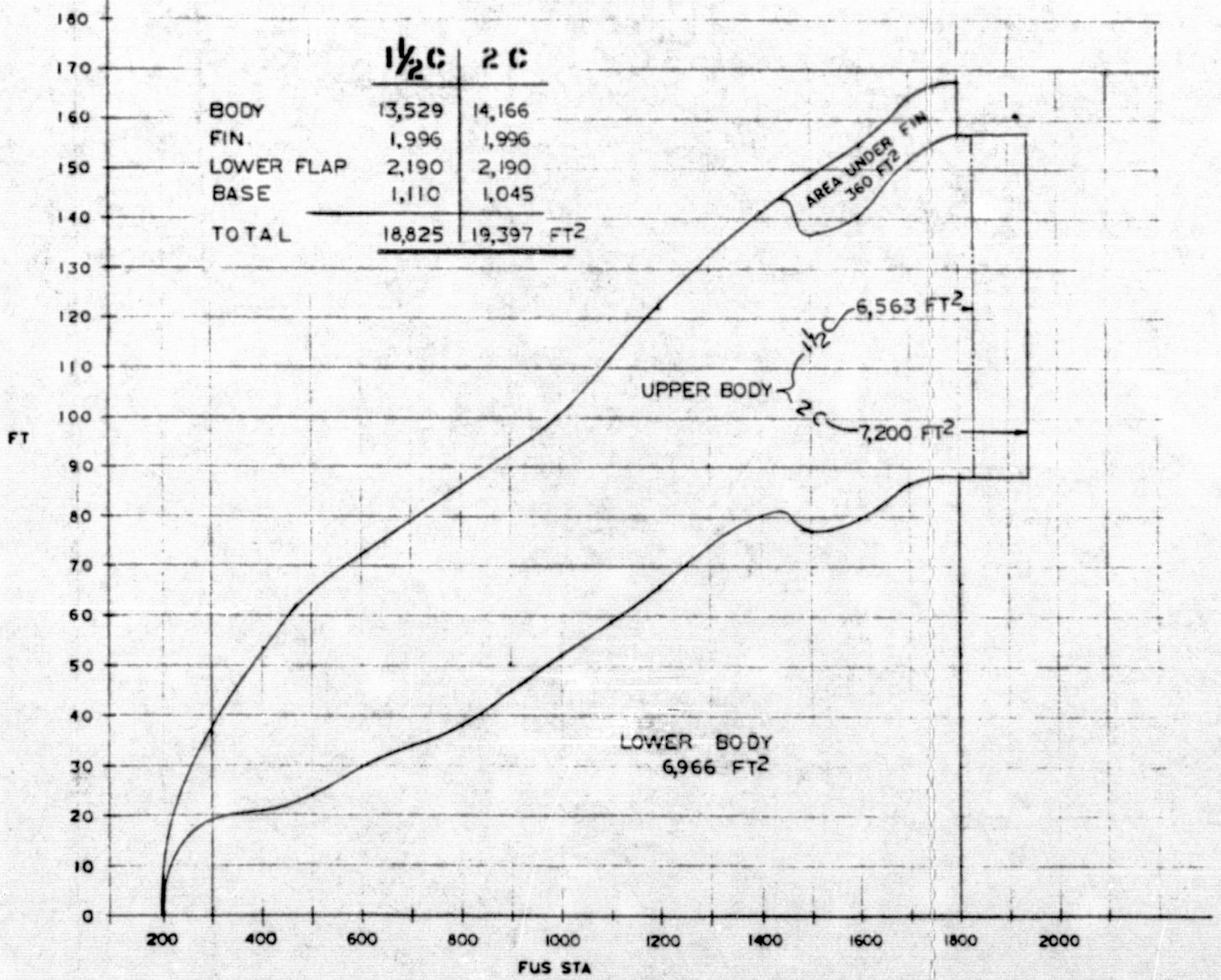

FOLDOUT FRAME

REPRODUCIBILITY OF THE ORIGINAL PAGE IS POOR.

VOLUME 1½C

AIR FRAME STRUCTURE AND TPS	9,630	FT³
CABIN	645	
WHEEL WELLS	1,820	
TUNNEL	150	
BULKHEADS END OF P/L BAY	760	
EQUIP., ECS, ACS FWD	980	
EQUIP., ACS AFT	205	
PAYLOAD BAY	10,820	
P/L BAY STRUCTURE	965	
PROP LINES, TANKS AND INSULATION	1,360	
INTERTANK STRUCT. & PROP MANIFOLD	7,630	
PROP. TANK VOLUME	14,214	
JET ENGINE AND AIR DUCT	2,806	
JET AND FIN SUPPORT STRUCTURE	4,310	
THRUST STRUCTURE	4,620	
BASE HEAT SHIELD	1,690	
BASE BETWEEN ROCKET ENGINES	4,790	
MAIN AND RL-10 ENGINES	5,900	
LOWER FLAP	1,330	
FIN, RUDDER, & AUX-SURFACE	4,330	
FLAP STOWAGE	4,270	FT³
OCCUPIED	83,225	FT³
UNOCCUPIED	14,375	FT³
TOTAL VOLUME	97,600	FT³

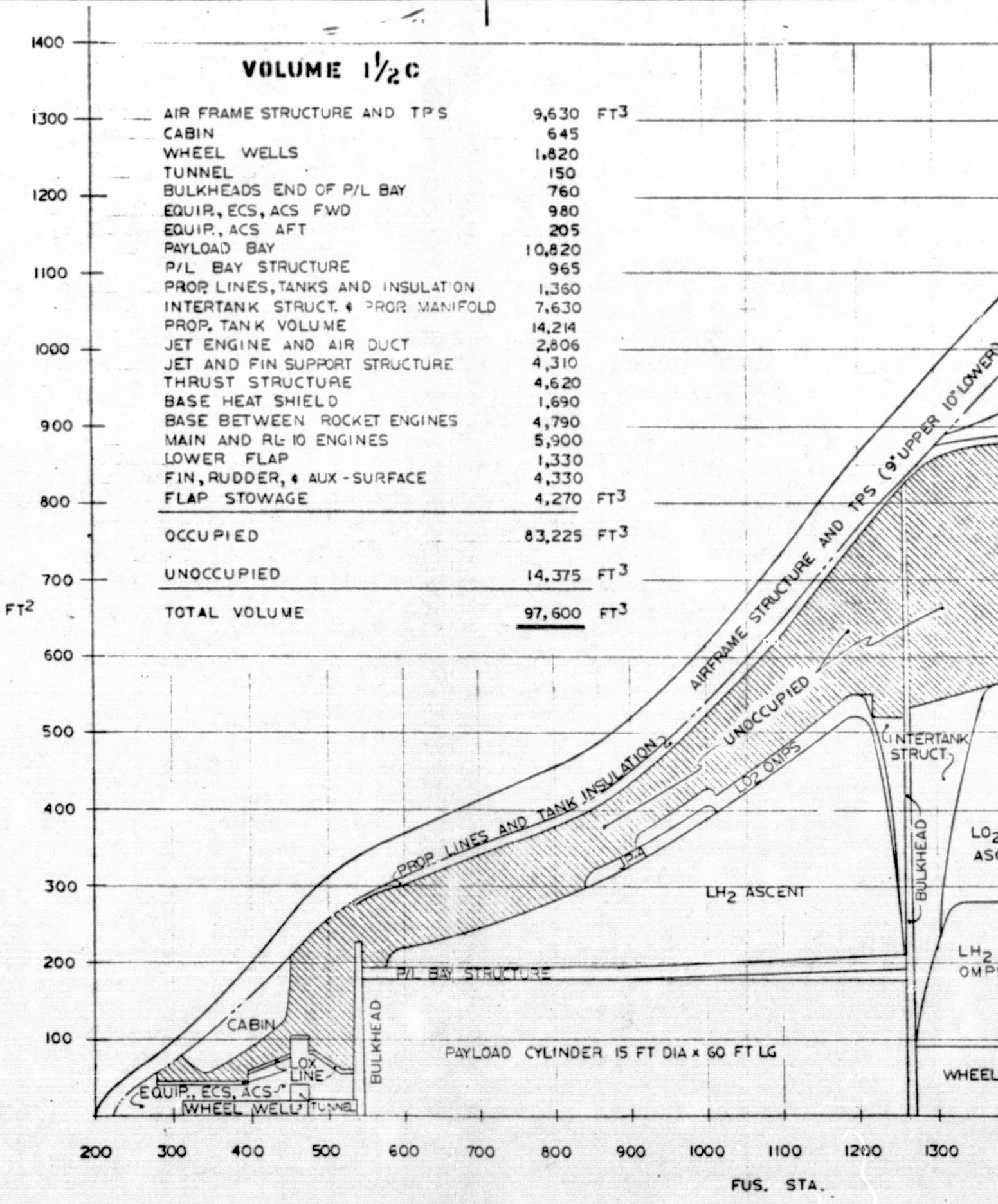

FOLDOUT FRAME 2

REPRODUCIBILITY OF THE ORIGINAL PAGE IS POOR

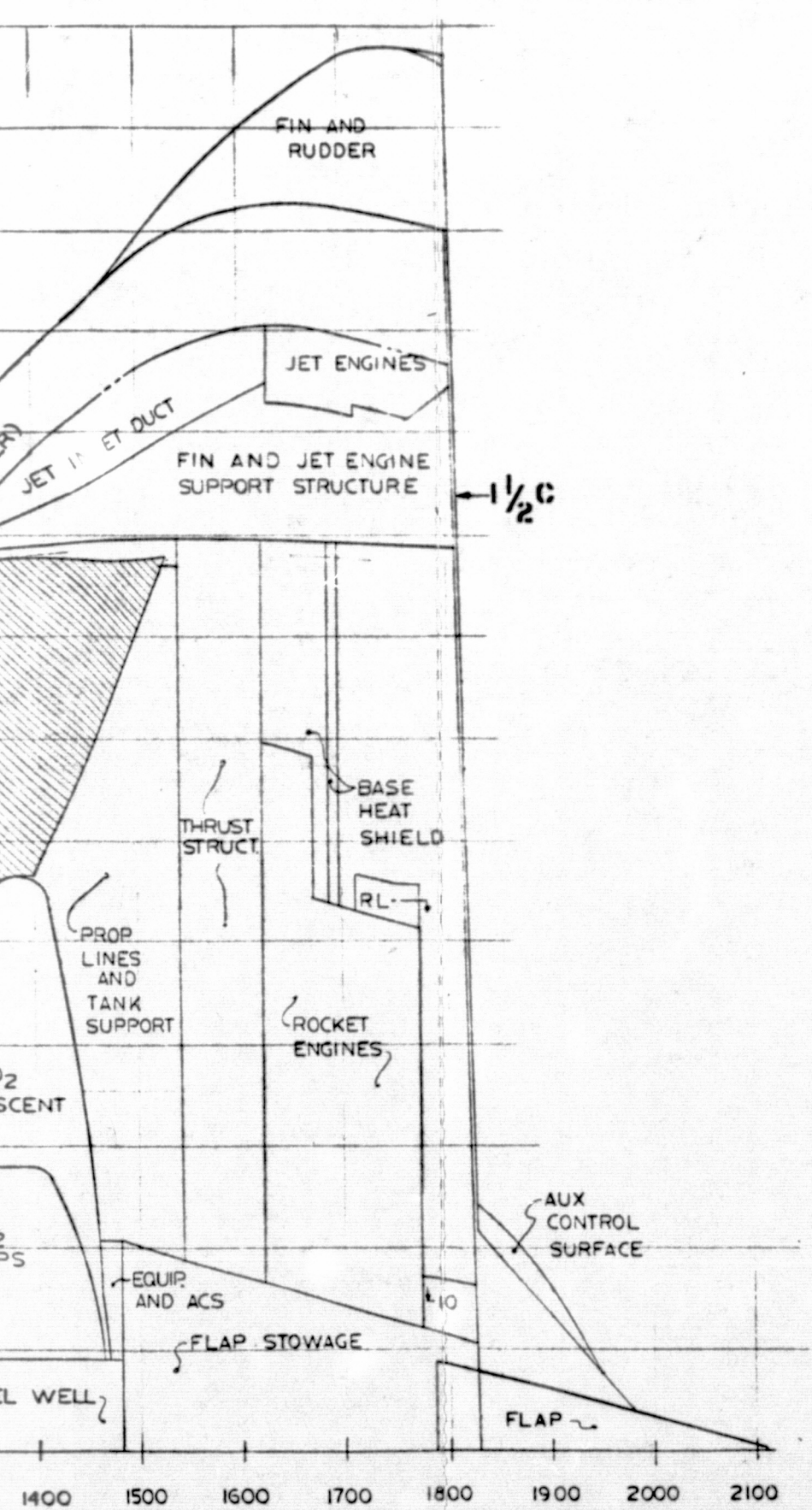

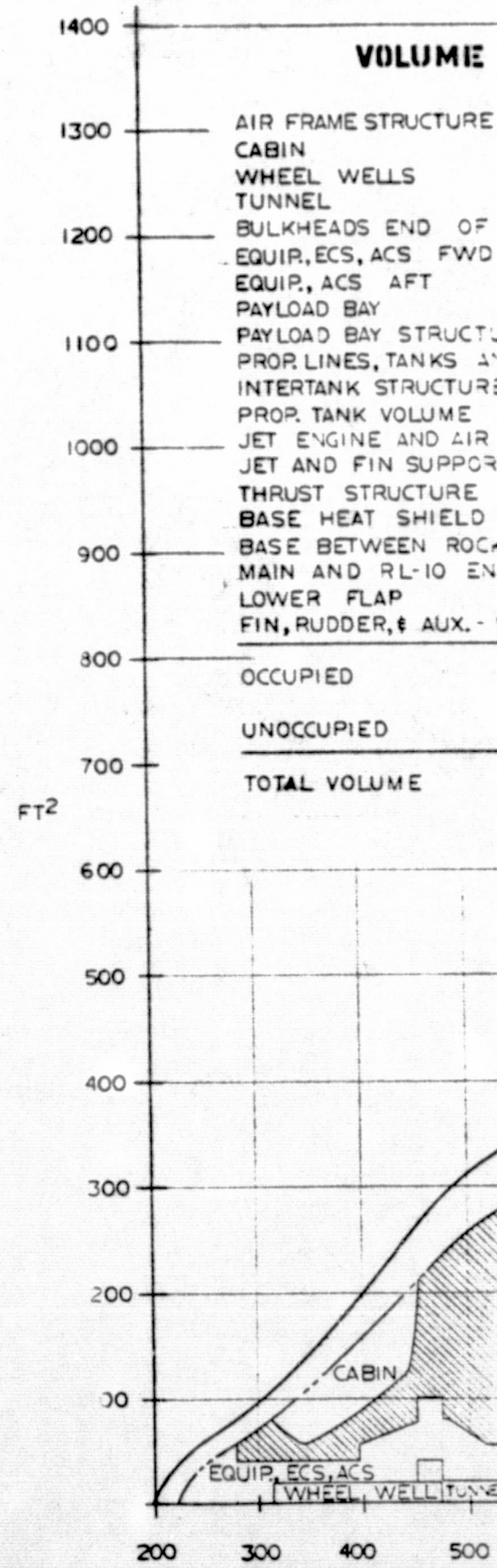

FOLDOUT FRAME 3

REPRODUCIBILITY OF THE ORIGINAL PAGE IS POOR.

OLUME 2 C

TRUCTURE AND TPS	9,980	FT^3
	645	
LLS	1,820	
	150	
END OF P/L BAY	760	
ACS FWD	970	
AFT	200	
	10,820	
Y STRUCTURE	965	
, TANKS AND INSULATION	1,920	
STRUCTURE	5,570	
VOLUME	28,753	
E AND AIR DUCT	2,807	
N SUPPORT STRUCTURE	4,310	
RUCTURE	2,940	
SHIELD	600	
VEEN ROCKET ENGINES	1,330	
RL-10 ENGINES	5,070	
AP	1,330	
R, & AUX. - SURFACE	4,330	FT^3
	85,270	FT^3
D	20,080	FT^3
UME	105,350	FT^3

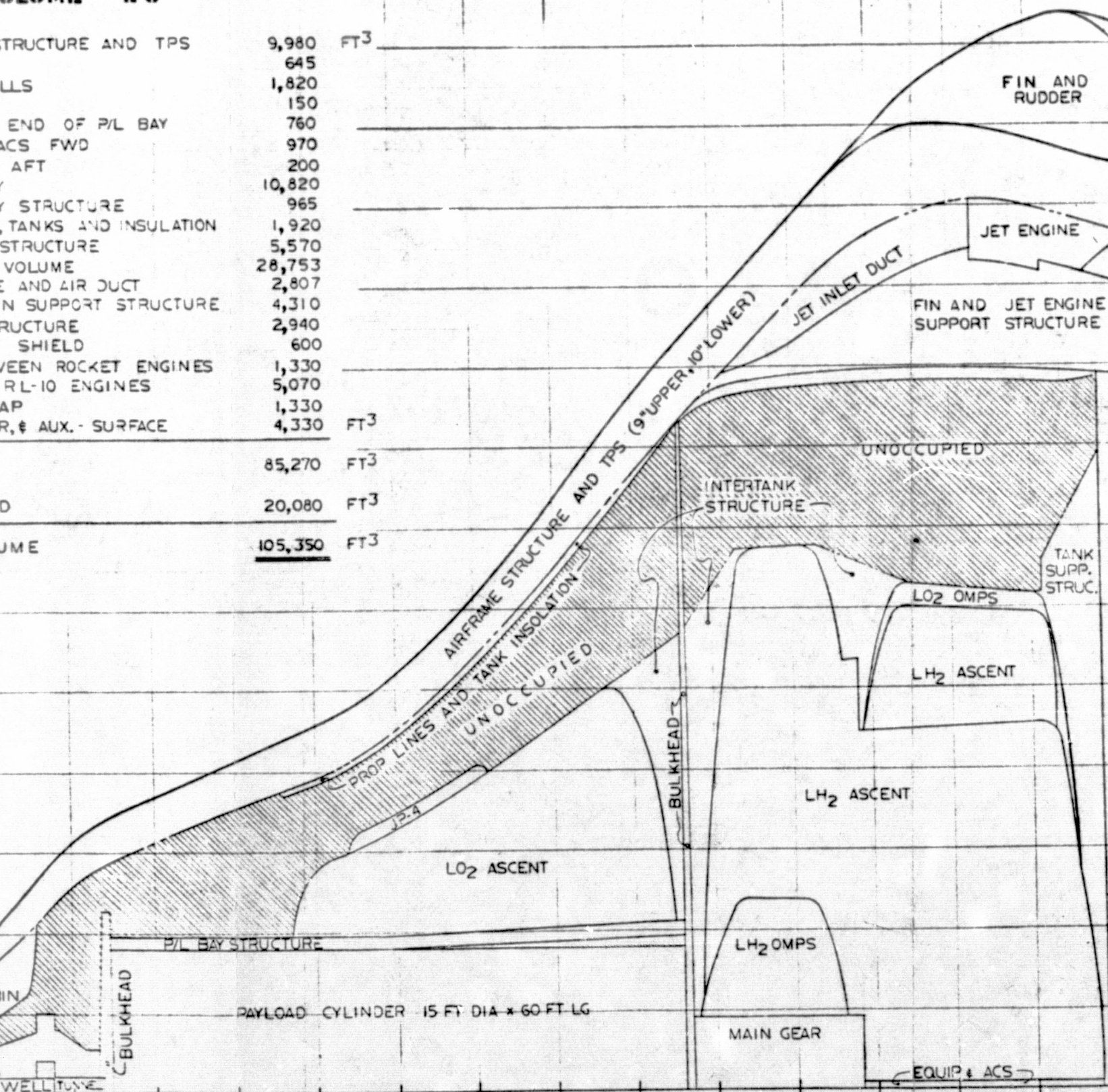

FOLDOUT FRAME 4

REPRODUCIBILITY OF THE ORIGINAL PAGE IS POOR.

PRECEDING PAGE BLANK NOT FILMED

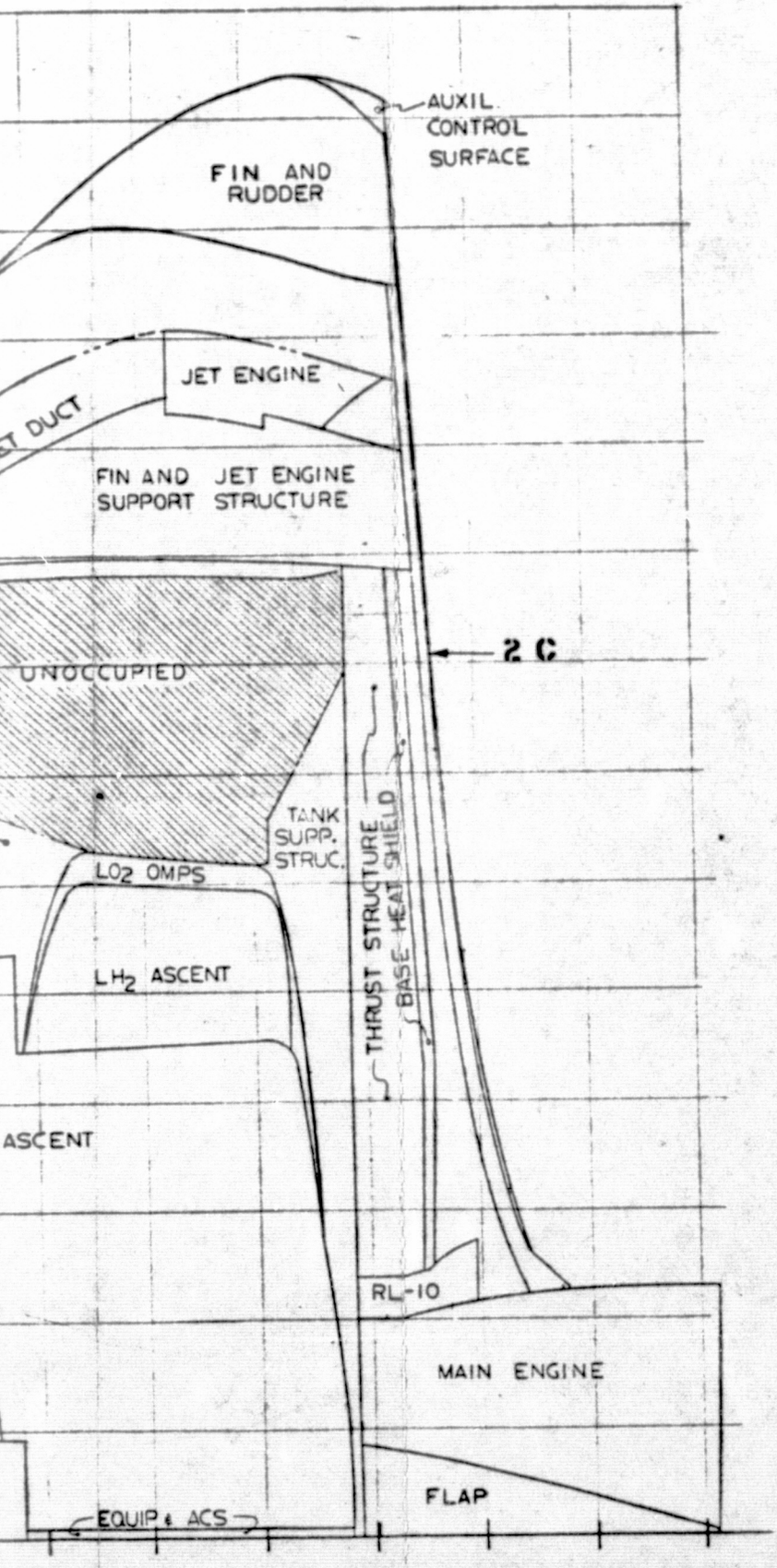

Fig. 2.5-30

QTY REQD	CODE IDENT	PART OR IDENTIFYING NO.	NOMENCLATURE OR DESCRIPTION	MATERIAL OR NOTE	SPECIFICATION	ZONE	ITEM NO.

LIST OF MATERIAL OR PARTS LIST

INTERPRET THIS DRAWING PER STANDARDS IN MIL-D-70327

UNLESS OTHERWISE SPECIFIED TOLERANCES ON: FRACTIONS = ± 1/16; .X = ± .1; .XX = ± .03; .XXX = ± .005; ANGLES = ± 1°

DATE 3-9-71
DR Hubert Schmidt
CHK
SUPV Gordon Havrisik
STRESS
VALUE ENGRG
RELIABILITY
APPROVED
APPROVED

LOCKHEED MISSILES & SPACE COMPANY
A GROUP DIVISION OF LOCKHEED AIRCRAFT CORPORATION
SUNNYVALE, CALIFORNIA

VOLUME CURVE
DELTA BODY ORBITER
MODELS LS-200-7x8, LS400-5x6

CODE IDENT NO.	SIZE	DRAWING NO.	REV
06887	J	SKS 100046	

SCALE NTS | SHEET

NEXT ASSY | USED ON | NEXT | FINAL
APPLICATION | REQD ASSY

FOLDOUT FRAME 5

2.5.3 Droptank System

The impact of droptank weights and cost on the performance and economies of the stage-and-one-half system led to a decision some time ago to perform a far more detailed design, production, and cost analysis of droptanks than is usually associated with a Phase A study.

To enhance the credibility of weight and cost estimates, it was decided to (1) generate a detailed design based on a conservative approach, utilizing only state-of-the-art materials, design concepts, and manufacturing methods, and (2) assemble a droptank bid package and invite other aerospace companies to make independent manufacturing planning and cost estimates for the procurement of the required number of tanks, based on the NASA baseline program.

A bid package was assembled, consisting of a Statement of Work for the Fabrication and Test of Stage-and-One-Half Droptanks accompanied by a Space Shuttle Droptank Data Summary. The package was released simultaneously on 20 October to NASA/MSFC (on request), CALAC**, GELAC***, AVCO, Chrysler, Rohr, and LMSC. AVCO and Rohr declined to bid.

2.5.3.1 Droptank Program Concept. For the purpose of the droptank bid package, a separate droptank program was stipulated. The estimate of the DDT&E - design, development, testing and evaluation - was performed by LMSC only; estimates of the production effort for the total operation were performed by LMSC, CALAC, GELAC, and Chrysler.

2.5.3.2 Droptank Schedule. The time spans required to develop the rather simple droptanks can be easily accommodated within the schedule of the stage-and-one-half space shuttle.

*LMSC/A980258A, 20 October 1970
**Lockheed Aircraft Corporation, California Company
***Lockheed Aircraft Corporation, Georgia Company

As shown in Fig. 2.5-31, the critical design review (CDR) of the droptanks can take place $1\frac{1}{4}$ to $1\frac{1}{2}$ years later than the CDR of the orbiter, allowing ample time to change design requirements for the droptanks if necessitated by design modifications of the orbiter. This potential for late-in-the-program changes constitutes a unique opportunity to maintain stage-and-one-half performance by relatively late changes in droptank size. The time spans shown for engineering and manufacturing are considered conservative; the system test schedule shows the utilization of six test tanks. The production schedule shows delivery of the first flight tank set by the middle of 1976 for a first manned orbital flight in late 1976. The final production schedule based on the NASA baseline program starts with five sets of tanks in 1976 and builds up to a maximum rate of 65 tanks per year by 1983.

2.5.3.3 Groundrules. For the purpose of the bid package, it was assumed that the following would be produced:

3	sets of full size test tanks
445	sets of operational flight tanks
5	sets of spare flight tanks
Total 453	sets of spare flight tanks

The following additional assumptions and groundrules were used.

- DDT&E Effort. Design will be based on proven materials, design principles (fusion welding), and manufacturing processes. An alternate design - bond spotwelding - will be defined to enable expected cost differences to be estimated. Facilities for system testing will be available at no cost to the program at MSFC and MTF. Facilities will be modified and operated by NASA. Test expendables will be supplied by NASA.

DROP TANK PROGRAM SCHEDULE

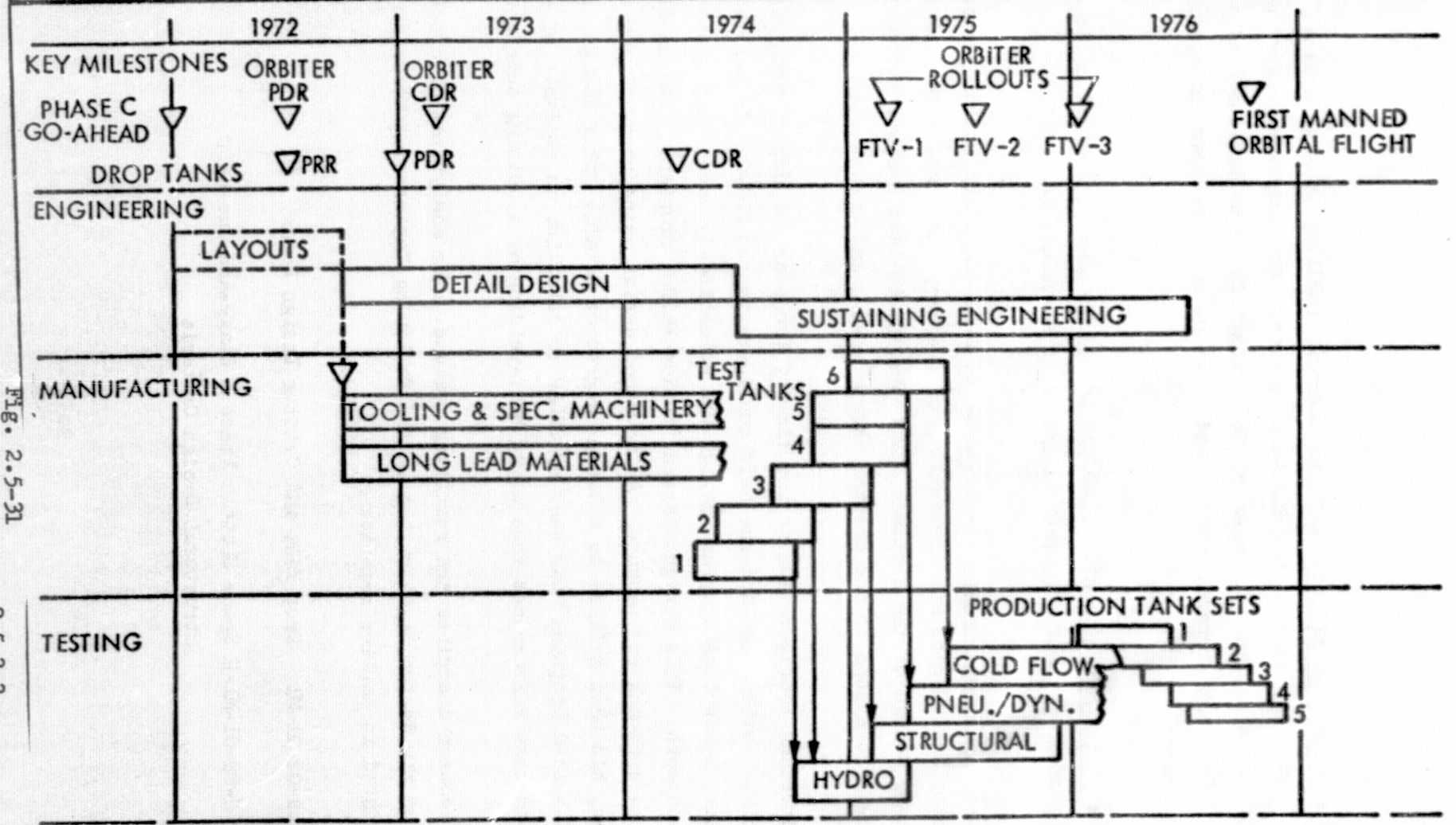

PRODUCTION DELIVERIES

	1977	1978	1979	1980	1981	1982	1983	1984	1985	1986
YEARLY PROD.	15	20	25	30	45	55	65	65	65	60
CUM. PROD.	20	40	65	95	140	195	260	325	390	450

D02266

Fig. 2.5-31

2.5.3-3

LOCKHEED MISSILES & SPACE COMPANY

IMSC-A989142
Vol. II

- Production Effort. A final assembly facility will be available at no facility cost to the droptank program. The droptank program ends with the acceptance of tanks at KSC, except for some liaison engineering. Droptank storage, mating, and erection costs are part of operations costs.

- Costing Rules. All costs are in 1970 dollars. Costs include a fee of 10 percent. No program phaseout costs are included.

2.5.3.4 Droptank Design. In order to be able to establish confidence in the droptank weights and credibility of the droptank cost, a detailed preliminary design of the droptank structure, propellant system, instrumentation, and support system to the orbiter was performed and documented.

The droptank configuration at the time of the start of design analyses was associated with stage-and-one-half configuration LS 200-2. As pointed out earlier, a baseline droptank design was established, using only state-of-the-art concepts. This design, termed "Fusion-Welded Droptank," was used throughout the droptank bid package. An advanced design using bond-welding techniques, has been defined to a lesser degree of detail. This design, called "Bond-Welded Droptank" was used by GELAC to establish an estimate of expected program cost differences when using bond-welding as a joining technique.

This section describes the resulting designs. The analytical effort in support of the design is described in the following Engineering Memorandums (EMs) documented in earlier reports:

L2-02-01-M1 Drop Tank and Orbiter Design Loads

L2-02-01-M1-2 Space Shuttle Phase A Stage-And-One-Half Structural Design Criteria

L2-02-01-M2 Structural Analyses of Delta-Body Orbiter Drop Tanks, Model LS 200-2

- General Arrangement. The droptank general arrangement shown in Dwg. SKL 100214A (Fig. 2.5-32) consists of two tank assemblies interconnected in a V-configuration, forming a single dropable expendable system. The droptank is attached to the orbiter at three places: at the orbiter nose (forward tie) and at two places at the rear to the orbiter thrust structure (aft ties). The forward tie resists only pitch loads, while the ball joint rear ties resist loads in all directions, with moments resisted by the droptanks only.

  Each tank assembly consists of a forward-located liquid oxygen tank, an aft-located liquid hydrogen tank, an intertank structure connecting both tanks, and a thrust cone assembly.

  The drawing identifies the dimensions and locations of plumbing and plumbing equipment for the pressurization, venting, fill, and drain lines for the oxygen and hydrogen tanks as well as the operational instrumentation for temperature, pressure and liquid level-sensing.

  The drawing also identifies the insulation required to protect the tanks during ascent. Cork panels 1/4-in. thick are bonded to the metallic surface of the oxygen tank forward dome and conical section. Polyurethane foam 3/8-in. thick is used for all remaining external surfaces of the oxygen and hydrogen tanks.

- Fusion-Welded Design. This section describes the baseline design used for establishing weights and drop tank costs.

Liquid Oxygen Tank (Dwg. SKT 100213, 5 Sheets - Fig. 2.5-33). The oxygen tank (18,186 cu.ft. volume) is constructed of aluminum 2219-T87. It consists

REPRODUCIBILITY OF THE ORIGINAL PAGE IS POOR.

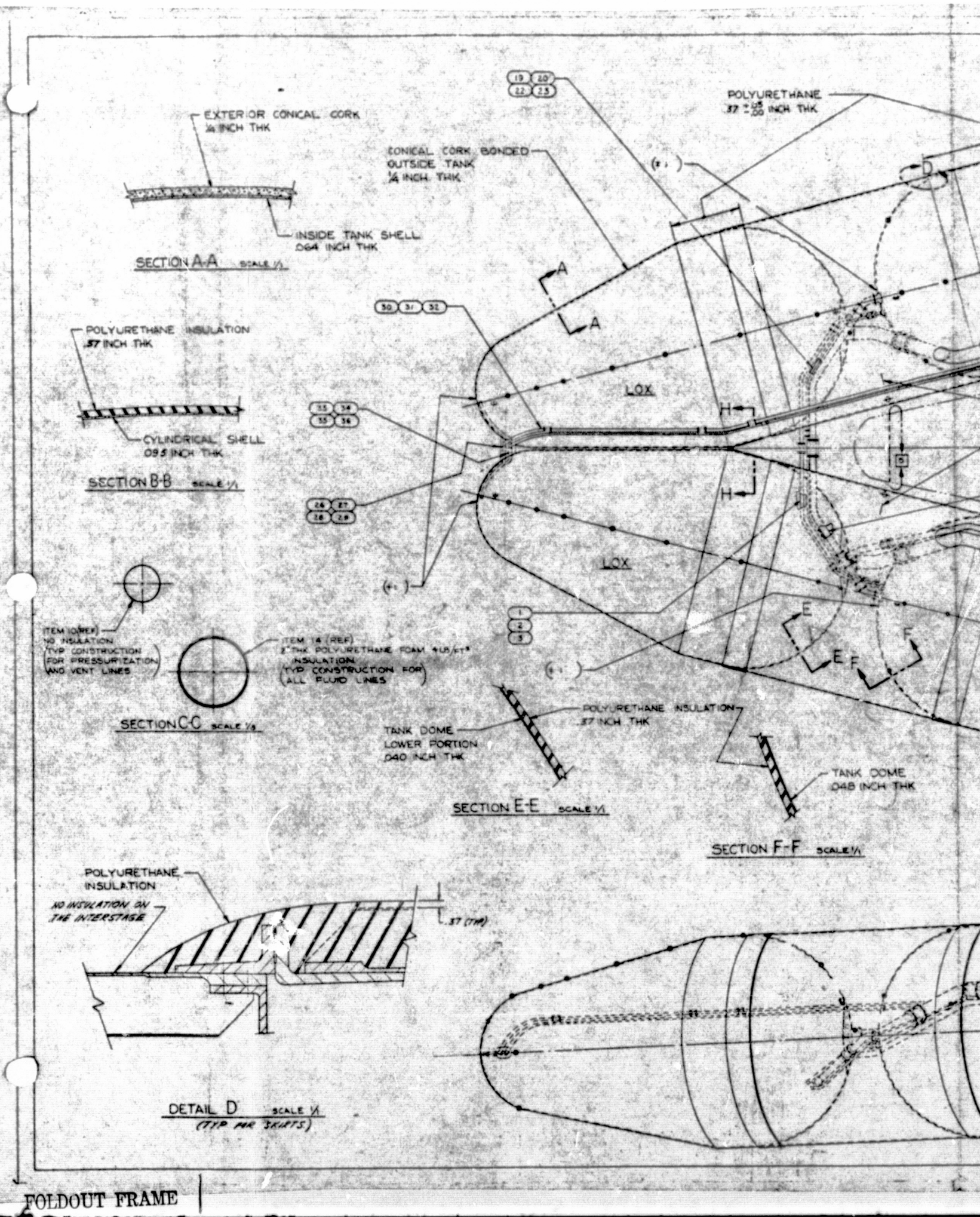

FOLDOUT FRAME

REPRODUCIBILITY OF THE ORIGINAL PAGE IS POOR.

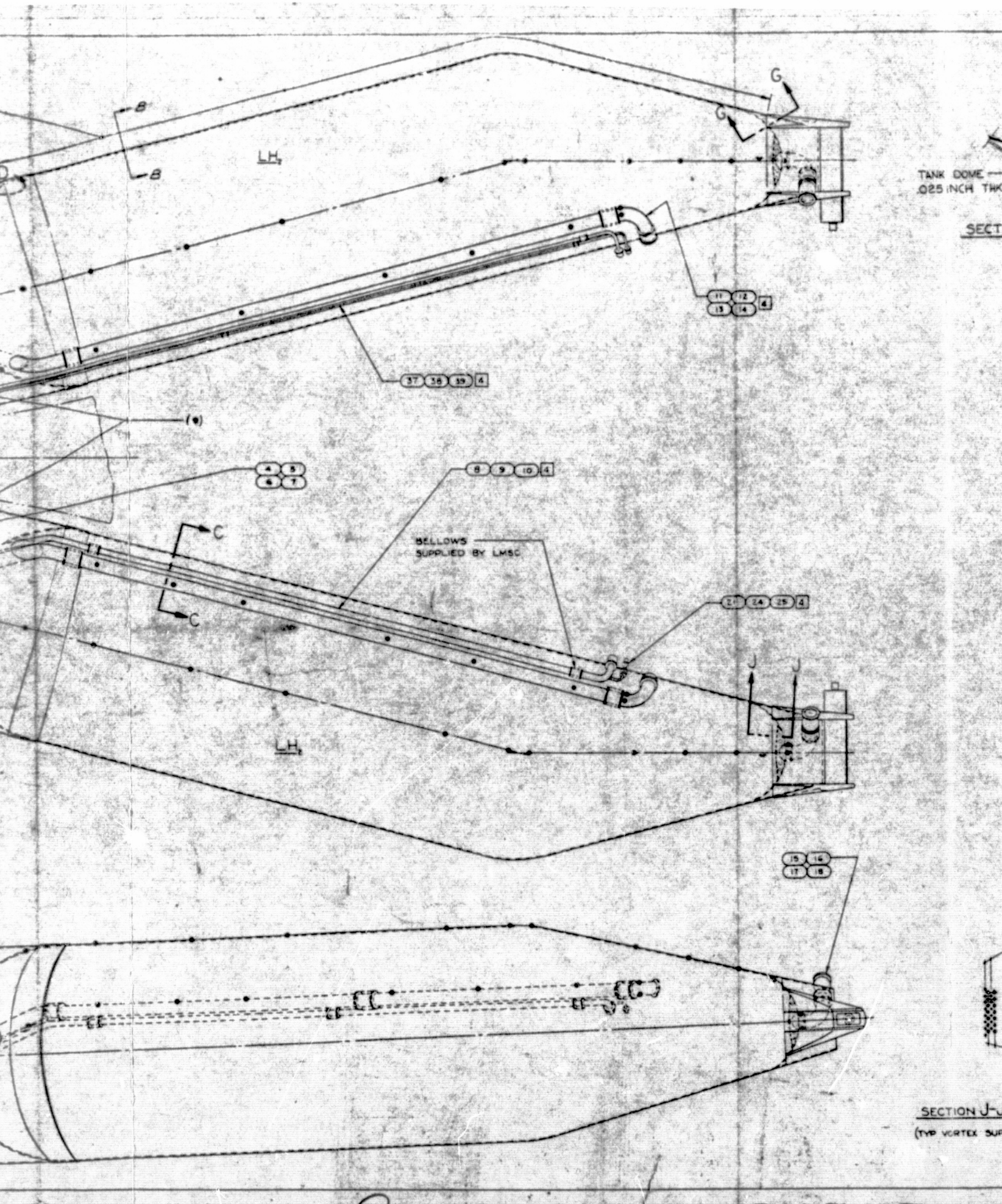

REPRODUCIBILITY OF THE ORIGINAL PAGE IS POOR.

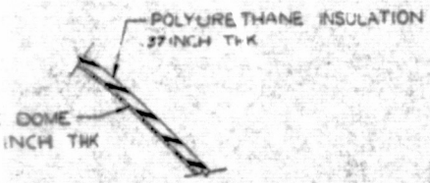

SECTION G-G SCALE 1/1

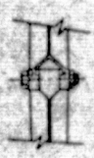

SECTION H-H SCALE 1/10

INSTRUMENTATION LIST					
QUANTITY					
LOX TANKS	LH_2 TANKS	CODE	ITEM	SOURCE	WT/LB EACH
31	---	•	HOT WIRE POINT SENSORS	LIMITED CONTROL	1.0
---	29	•	HOT WIRE POINT SENSORS	LIMITED CONTROL	1.0
4	---	•	PRESSURE TRANSDUCER	CONSOL. ENGR.	0.5
---	4	•	PRESSURE TRANSDUCER	CONSOL. ENGR.	0.5
2	---	+	1.7 PIN ELECTRICAL FEED-THRU CONNECTOR	DEUTCH	1.0
2	---		FEMALE MATING ELECTRICAL CONNECTOR (INSIDE TANK)		
2	---		MALE MATING ELECTRICAL CONNECTOR (OUTSIDE TANK)		
---	2	+	1.6 PIN ELECTRICAL FEED-THRU CONNECTOR	DEUTCH	1.0
---	2		FEMALE MATING ELECTRICAL CONNECTOR (INSIDE TANK)		
---	2		MALE MATING ELECTRICAL CONNECTOR (OUTSIDE TANK)		
1	1	•	MULTIPLEX UNIT	TO BE * CONSIDERED	4.0
1	1	•	PLUS QUICK DISCONNECT D-6477-27-2P	DEUTCH	

• REQUIREMENTS – EACH UNIT
20 WORDS MEMORY PER SIGNAL
A TO D CONVERTER
D TO A CONVERTER
BUFFER STORAGE FOR EACH SIGNAL
MULTIPLEX FOR EACH SIGNAL
ONE HAND WIRE MIX FORMAT PCB
POWER SUPPLY

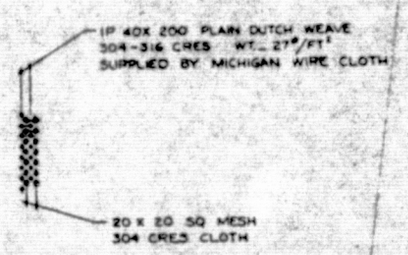

CTION J-J SCALE NONE
VORTEX SUPPRESSOR CONSTR.)

Fig. 2 5-32

[5] REFER TO DWG SKG100217, FWD SUPPORT-DROP TANK FOR SUPPORT DEFINITION.
[4] ALTERNATE CONFIGURATION: LINES AND GIMBALS INDICATED ARE DELETED FROM THE DROP TANK ASSEMBLY AND ARE RELOCATED INSIDE SPACECRAFT.
[3] DISCONNECT WITH CHECK SIMILAR TO ROYAL, HADLEY 11397 OR RMDCC185.
[2] GIMBAL SIMILAR TO SOLAR 38026, CODE 55820.
[1] SOLAR, ARROWHEAD TYPICAL MFG'S FOR LINES AND FITTINGS.

NOTES:

FOLDOUT FRAME 3

REPRODUCIBILITY OF THE ORIGINAL PAGE IS POOR.

1		SKG 100216 DROP TANK THRUST CONE				41
1		SKT 100213 DROP TANK STRUCTURE				40
1	COML	4"DIA×.032 WALL 4"LOX PRESSURIZATION LINE			75"	39
1	[3]	DISCONNECT 4"			4"	38
4	[2]	GIMBAL JOINT 4"		ALUM WITH INCONEL BELLOWS	12"	37
1	COML	5"DIA×.032 WALL 5"			5"	36
1	COML	TEE 5"-4"			2"	35
3	[2]	GIMBAL JOINT 5"		ALUM WITH INCONEL BELLOWS	6"	34
2	[1]	END COUPLING 5"LOX PRESSURIZATION LINE			4"	33
1	COML	6"DIA×.032 WALL 6"LOX VENT LINE		2219 ALUM	108"	32
1	[3]	DISCONNECT 6"			22"	31
4	[2]	GIMBAL JOINT 6"		ALUM WITH INCONEL BELLOWS	20"	30
1	COML	4"DIA×.032 WALL 4"		2219 ALUM	8"	29
1	COML	TEE 4"-6"			3"	28
3	[2]	GIMBAL JOINT 4"		ALUM WITH INCONEL BELLOWS	9"	27
2	[1]	END COUPLING 4"LOX VENT LINE			6"	26
1	COML	5"DIA×.032 WALL 5"LH_2 PRESSURIZATION LINE		2219 ALUM	60"	25
2	[2]	GIMBAL JOINT 5"		ALUM WITH INCONEL BELLOWS	8"	24
1	COML	TEE 4"-5"			4"	23
1	COML	4"DIA×.032 WALL 4"		2219 ALUM	30"	22
1	[3]	DISCONNECT 5"			7"	21
3	[2]	GIMBAL JOINT 4"		ALUM WITH INCONEL BELLOWS	2"	20
2	[1]	END COUPLING 4"LH_2 PRESSURIZATION LINE			10"	19
2	COML	19"DIA×.032 WALL 19"LH_2 FLUID LINE		2219 ALUM	28"	18
2	[3]	DISCONNECT			240"	17
4	[2]	GIMBAL JOINT		ALUM WITH INCONEL BELLOWS	280"	16
2	[1]	END COUPLING 19"LH_2 FLUID LINE			20"	15
2	COML	19"DIA×.070 WALL 19"LOX FLUID LINE		2219 ALUM	341"	14
2	[3]	DISCONNECT			240"	13
6	[2]	GIMBAL JOINT		ALUM WITH INCONEL BELLOWS	840"	12
2	[1]	END COUPLING 19"LOX FLUID LINE			20"	11
1	COML	13"DIA×.032 WALL 13"LH_2 VENT LINE		2219 ALUM	152"	10
1	[3]	DISCONNECT 13"LH_2 VENT LINE			95"	9
3	[2]	GIMBAL JOINT 13"LH_2 VENT LINE		ALUM WITH INCONEL BELLOWS	180"	8
3	[2]	GIMBAL JOINT 9"LH_2 VENT LINE		ALUM WITH INCONEL BELLOWS	75"	7
1	COML	TEE			12"	6
1	COML	9"DIA×.032 WALL		2219 ALUM	55"	5
2	[1]	END COUPLING 9"LH_2 VENT LINE			11"	4
3	[2]	GIMBAL JOINT 8"LOX FLUID LINE		ALUM WITH INCONEL BELLOWS	60"	3
1	COML	8"DIA×.032 WALL 8"LOX FLUID LINE		2219 ALUM	45"	2
2	[1]	END COUPLING 8"LOX FLUID LINE			16"	1
QTY	SOURCE	DESCRIPTION		MATERIAL	TOTAL WEIGHT	FIG NO
QTY REQD	CODE IDENT	PART OR IDENTIFYING NO.	NOMENCLATURE OR DESCRIPTION	MATERIAL DISCRIPTION OR NOTE	MATERIAL SPECIFICATION	ZONE	ITEM NO

PARTS LIST

INTERPRET DWG PER	UNLESS OTHERWISE SPECIFIED DIM ARE IN INCHES TOLERANCES ON: FRACTIONS = ± 1/16 DECIMALS: .XX = ± .1 .XX = ± .03 .XXX = ± .010 ANGLES = ± 2 DEG	DATE	LOCKHEED MISSILES & SPACE COMPANY A GROUP DIVISION OF LOCKHEED AIRCRAFT CORPORATION SUNNYVALE, CALIFORNIA	
		DR	DROP TANK ASSEMBLY DELTA BODY-STAGE & ½ MODEL LS-200-2	
		APPD		
		ENGRG APPROVAL		
		CHK		
		APPD	SIZE CODE IDENT DRAWING NO. J 06667 SKL100214	REV L-1
NEXT ASSY USED ON APPLICATION	CONTR CCA/CB	APPD	SCALE 1"=1"/10	SHEET 1 OF 1

[5] REFER TO DWG SKG100217, FWD SUPPORT-DROP TANK FOR SUPPORT DEFINITION.

[4] ALTERNATE CONFIGURATION: LINES AND GIMBALS INDICATED ARE DELETED FROM THE DROP TANK ASSEMBLY AND ARE RELOCATED INSIDE SPACECRAFT.

[3] DISCONNECT WITH CHECK SIMILAR TO ROYAL, HADLEY 11397 OR RMDCC185.

[2] GIMBAL SIMILAR TO SOLAR 38026, CODE 55820.

[1] SOLAR, ARROWHEAD TYPICAL MFG'S FOR LINES AND FITTINGS.

NOTES:

Fig. 2.5-32

Fig. 2.5-32

2.5.3-7

FOLDOUT FRAME 4

REPRODUCIBILITY OF THE ORIGINAL PAGE IS POOR.

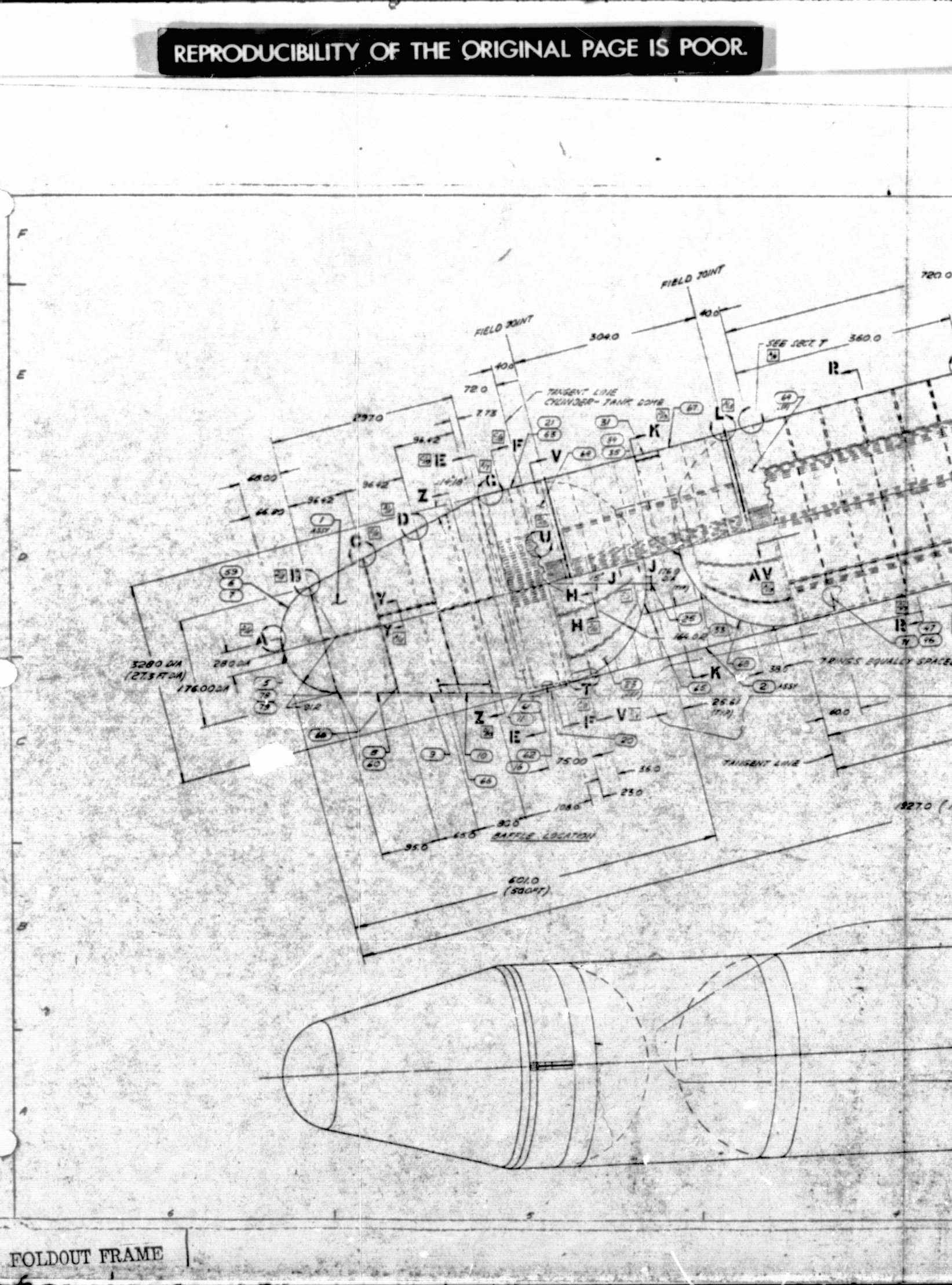

FOLDOUT FRAME

REPRODUCIBILITY OF THE ORIGINAL PAGE IS POOR.

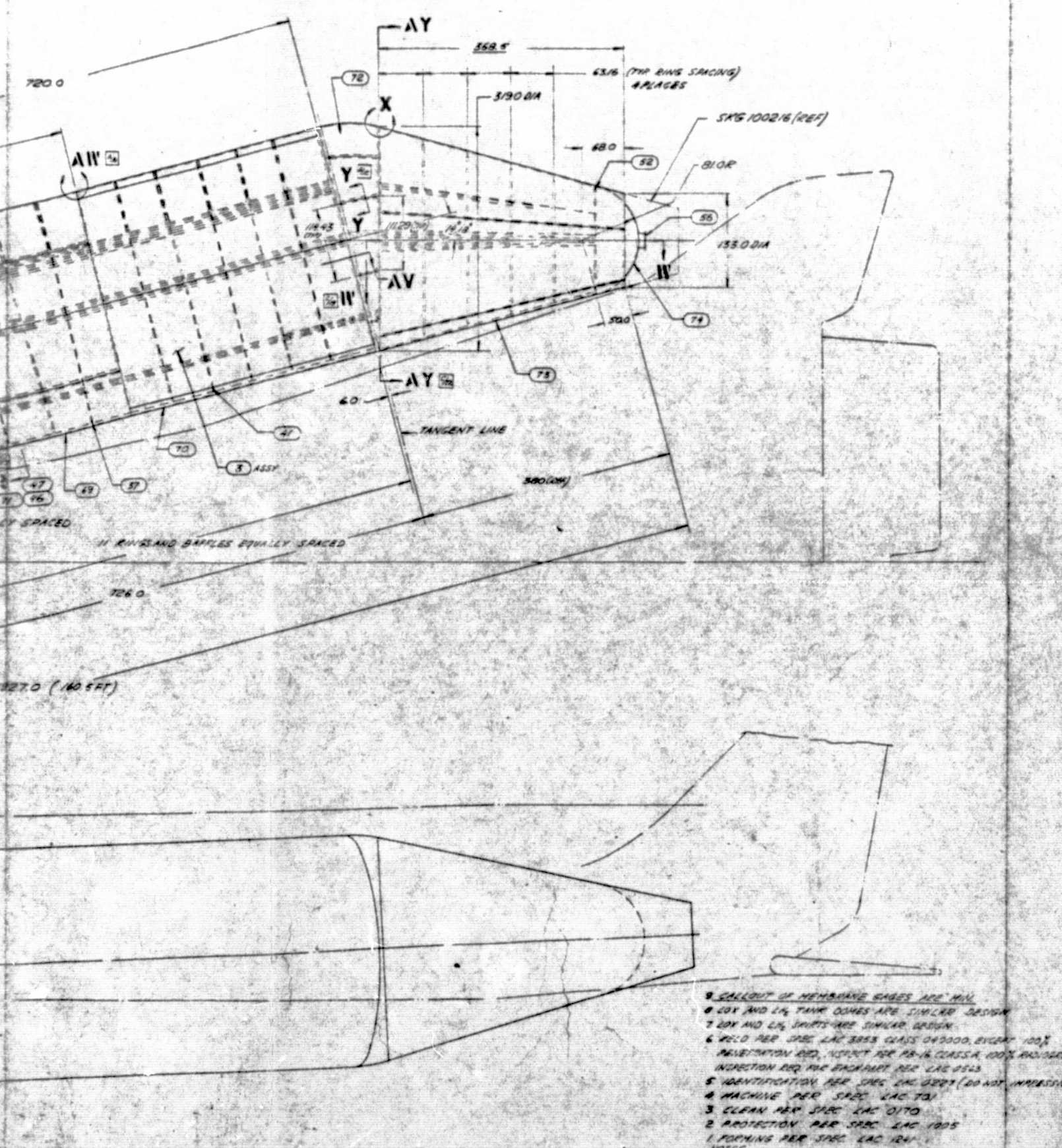

9 CALLOUT OF MEMBRANE GAGES ARE MIN.
8 LOX AND LH_2 TANK DOMES ARE SIMILAR DESIGN
7 LOX AND LH_2 SKIRTS ARE SIMILAR DESIGN
6 WELD PER SPEC LAC 3853 CLASS 040000, EXCEPT 100% PENETRATION REQ, INSPECT PER PB-16 CLASS A, 100% RADIOGRAPH INSPECTION REQ FOR EACH PART PER LAC 0563
5 IDENTIFICATION PER SPEC LAC 0227 (DO NOT IMPRESSION
4 MACHINE PER SPEC LAC 701
3 CLEAN PER SPEC LAC 0170
2 PROTECTION PER SPEC LAC 1005
1 FORMING PER SPEC LAC 1241
NOTES

FOLDOUT FRAME 2

REPRODUCIBILITY OF THE ORIGINAL PAGE IS POOR.

PRECEDING PAGE BLANK NOT FILMED

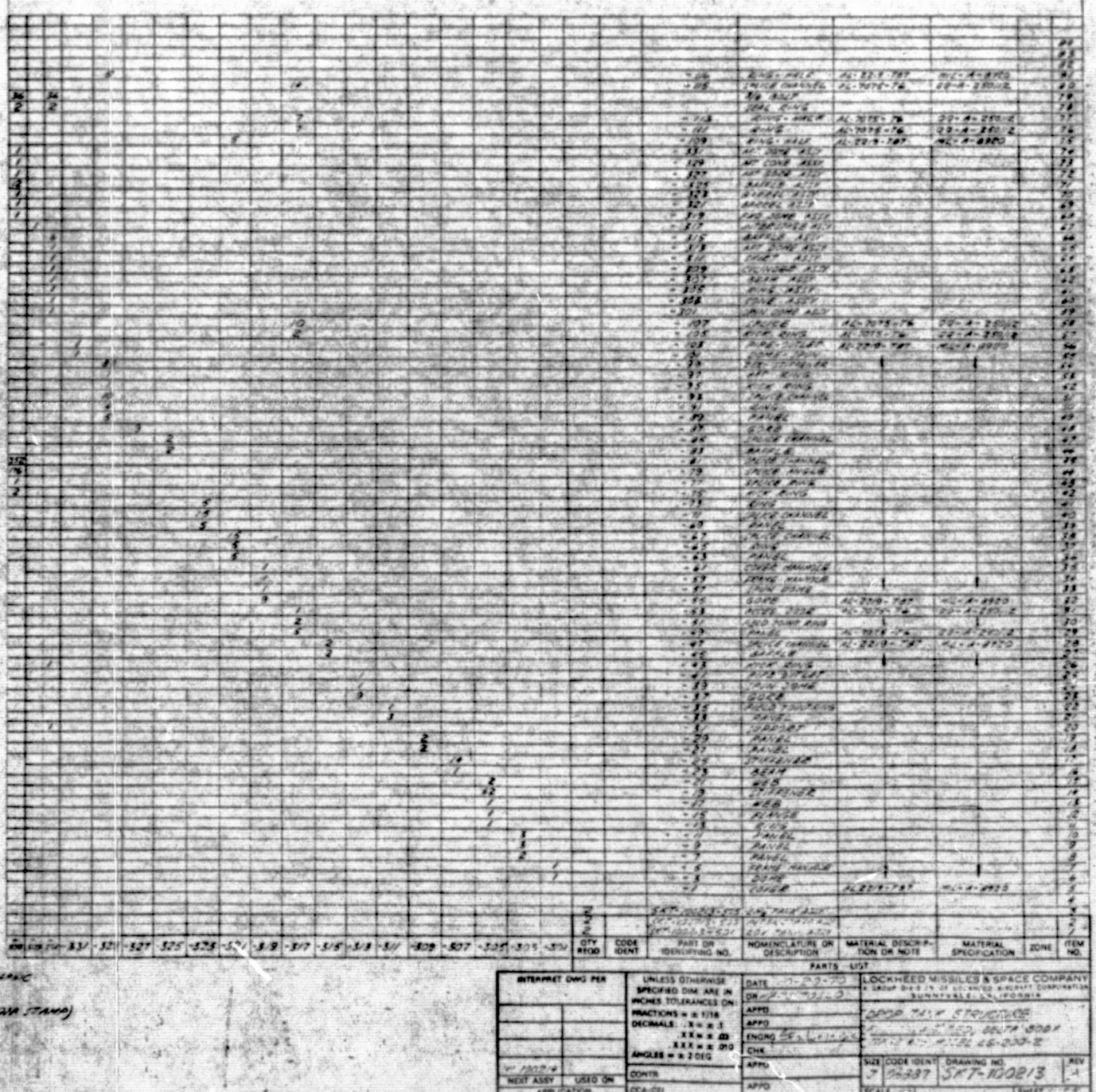

FOLDOUT FRAME 3

Fig. 2.5-33

REPRODUCIBILITY OF THE ORIGINAL PAGE IS POOR.

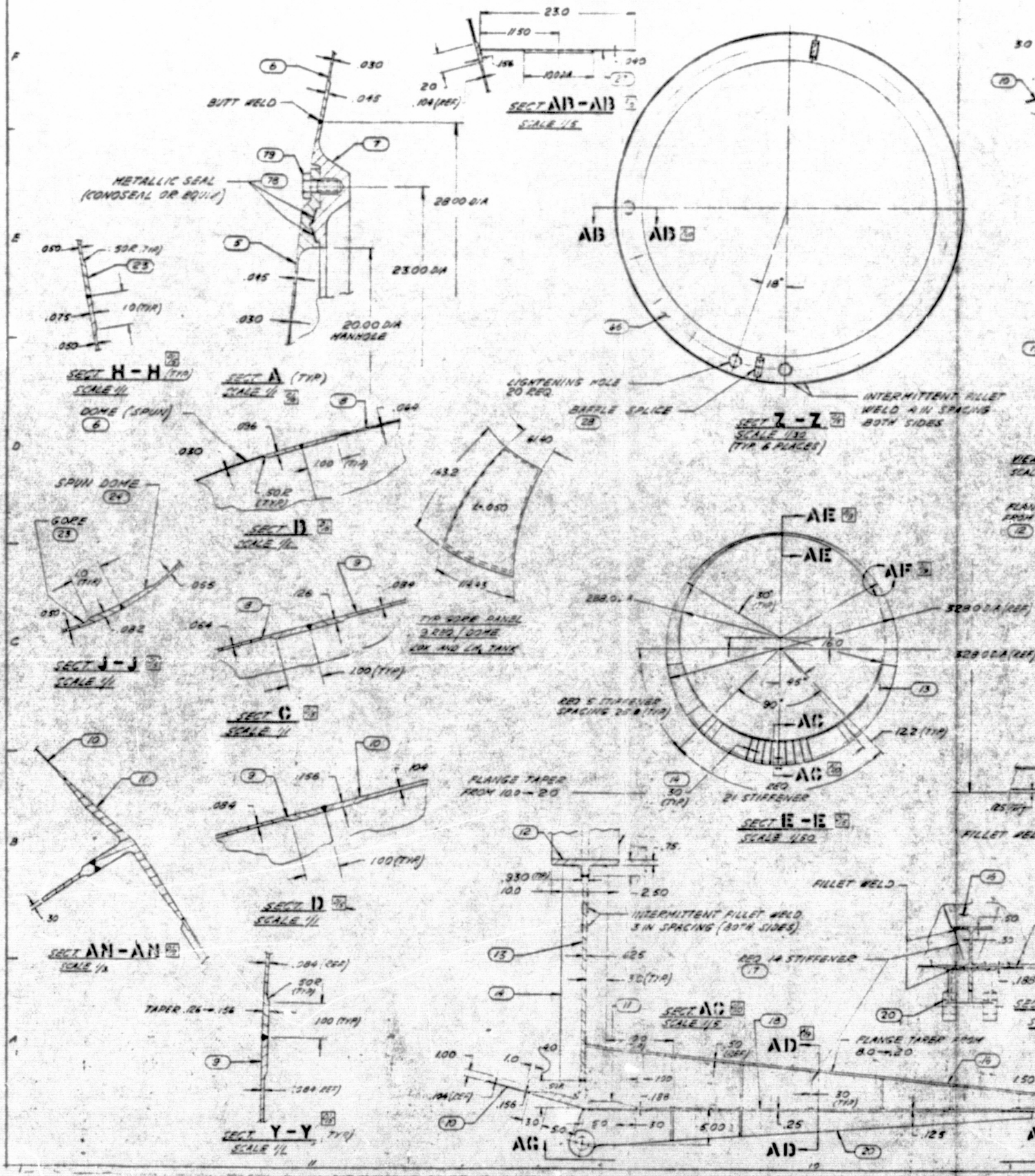

FOLDOUT FRAME

REPRODUCIBILITY OF THE ORIGINAL PAGE IS POOR.

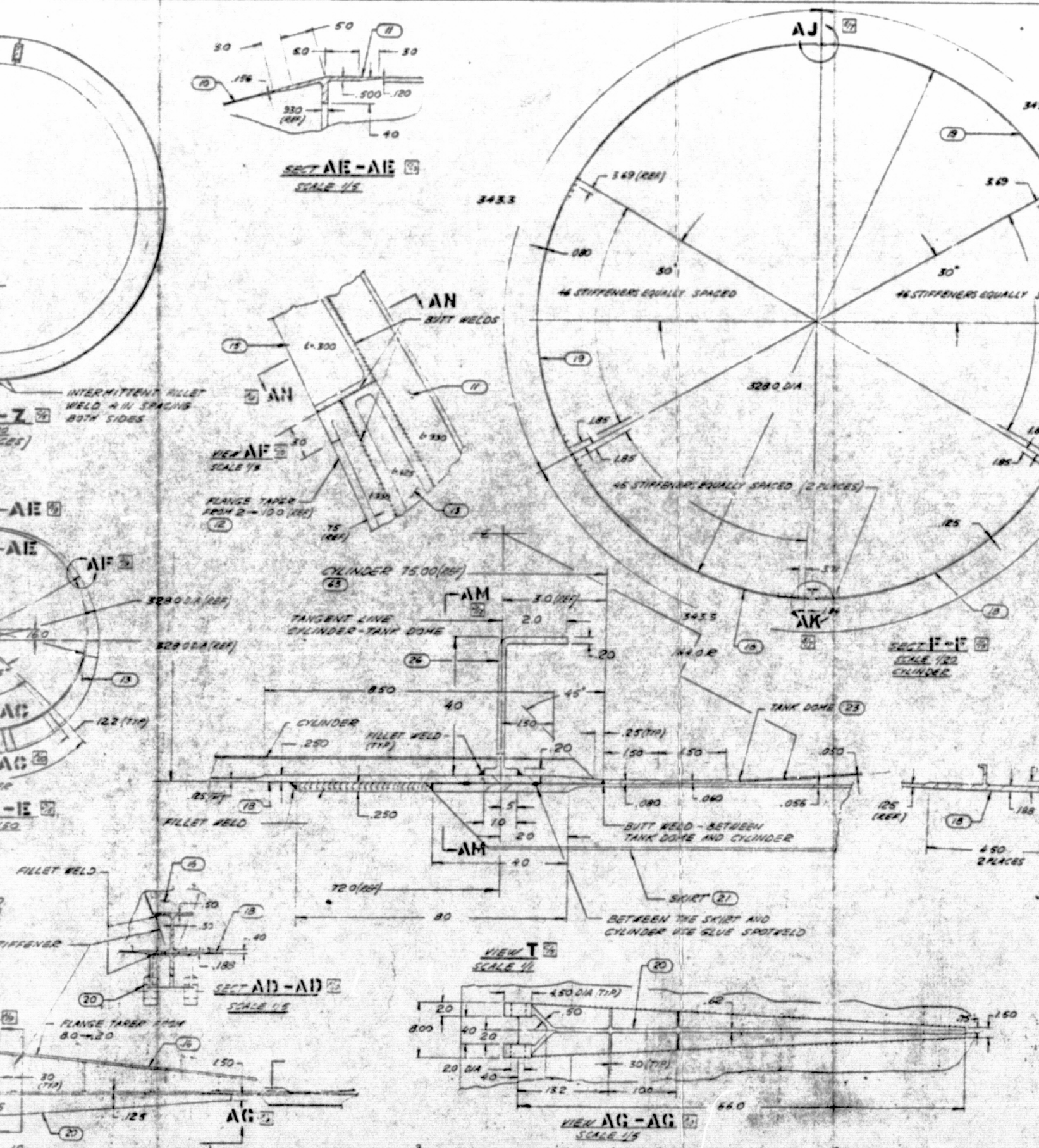

FOLDOUT FRAME 2

REPRODUCIBILITY OF THE ORIGINAL PAGE IS POOR.

PRECEDING PAGE BLANK NOT FILMED

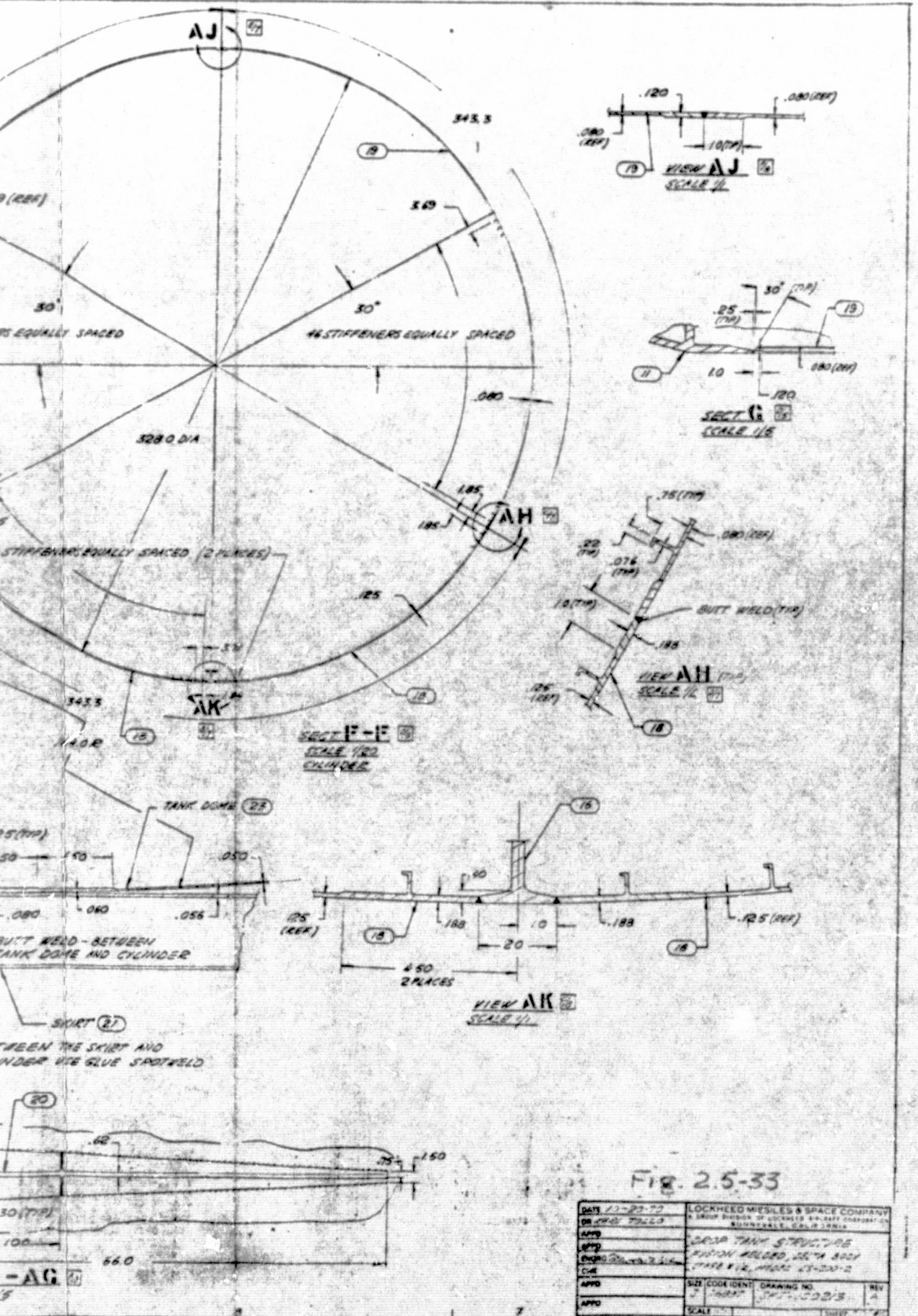

Fig. 2.5-33

2.5.3-11

FOLDOUT FRAME 3

REPRODUCIBILITY OF THE ORIGINAL PAGE IS POOR.

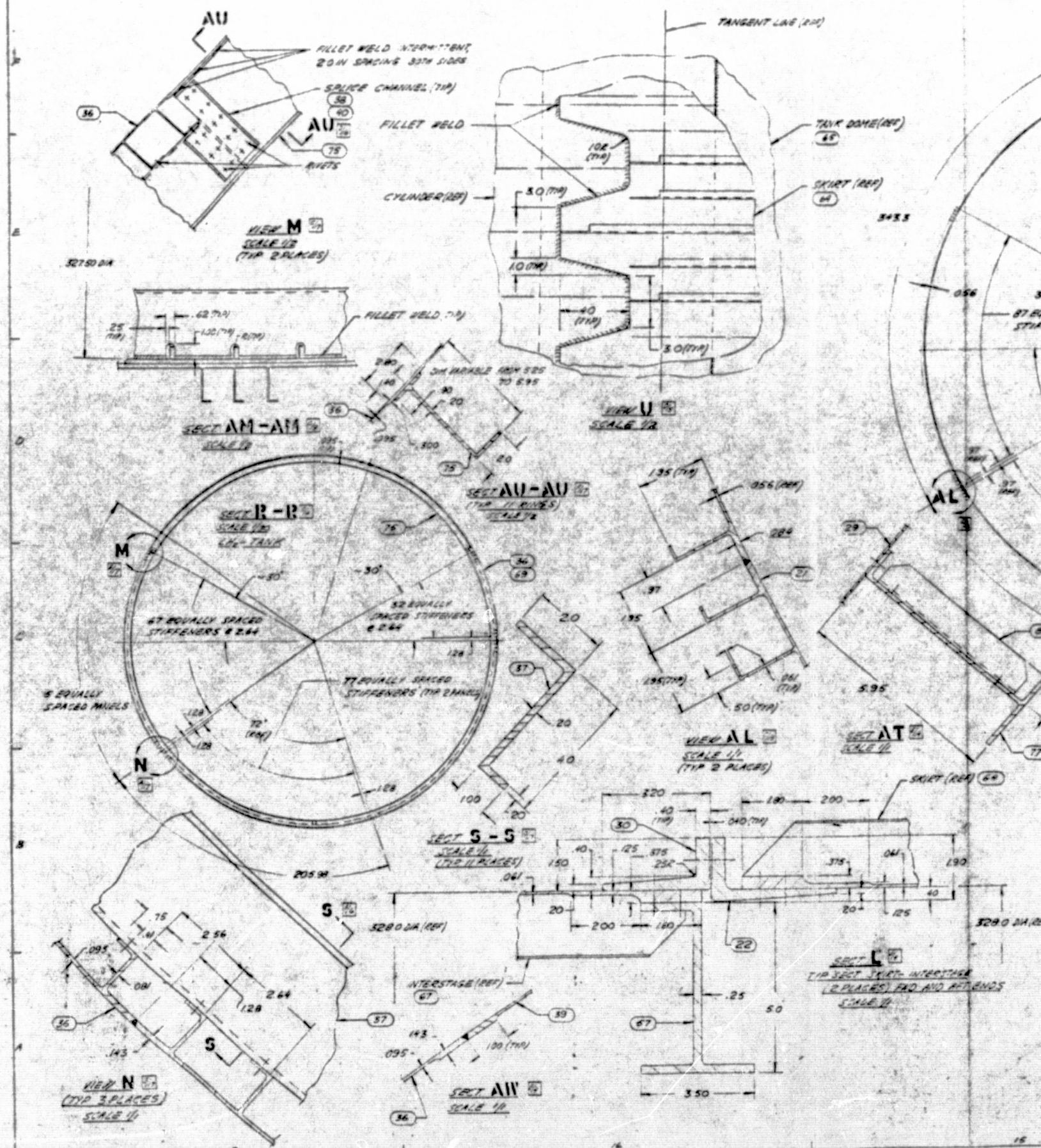

FOLDOUT FRAME

REPRODUCIBILITY OF THE ORIGINAL PAGE IS POOR.

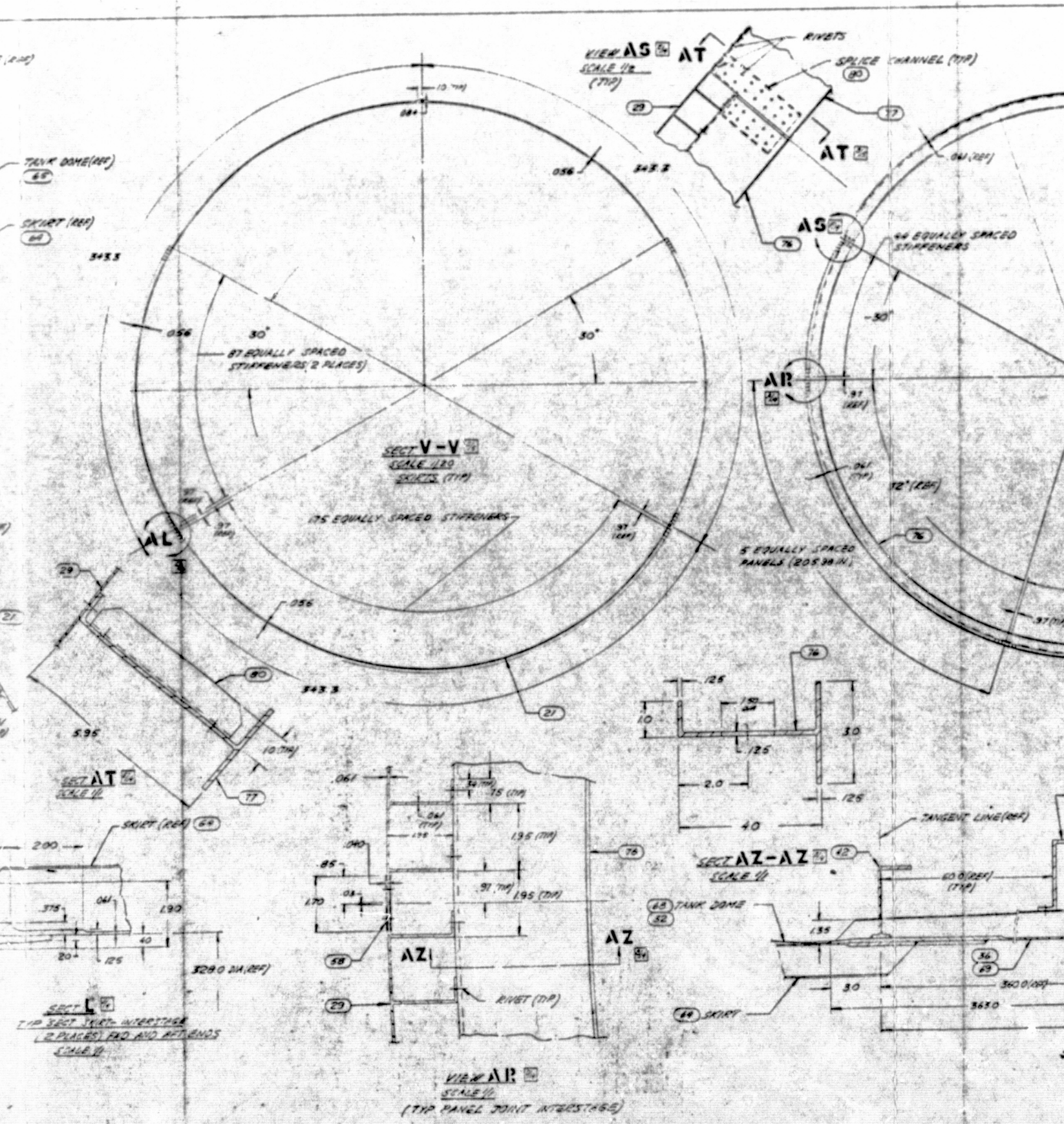

FOLDOUT FRAME 2

REPRODUCIBILITY OF THE ORIGINAL PAGE IS POOR.

PRECEDING PAGE BLANK NOT FILMED

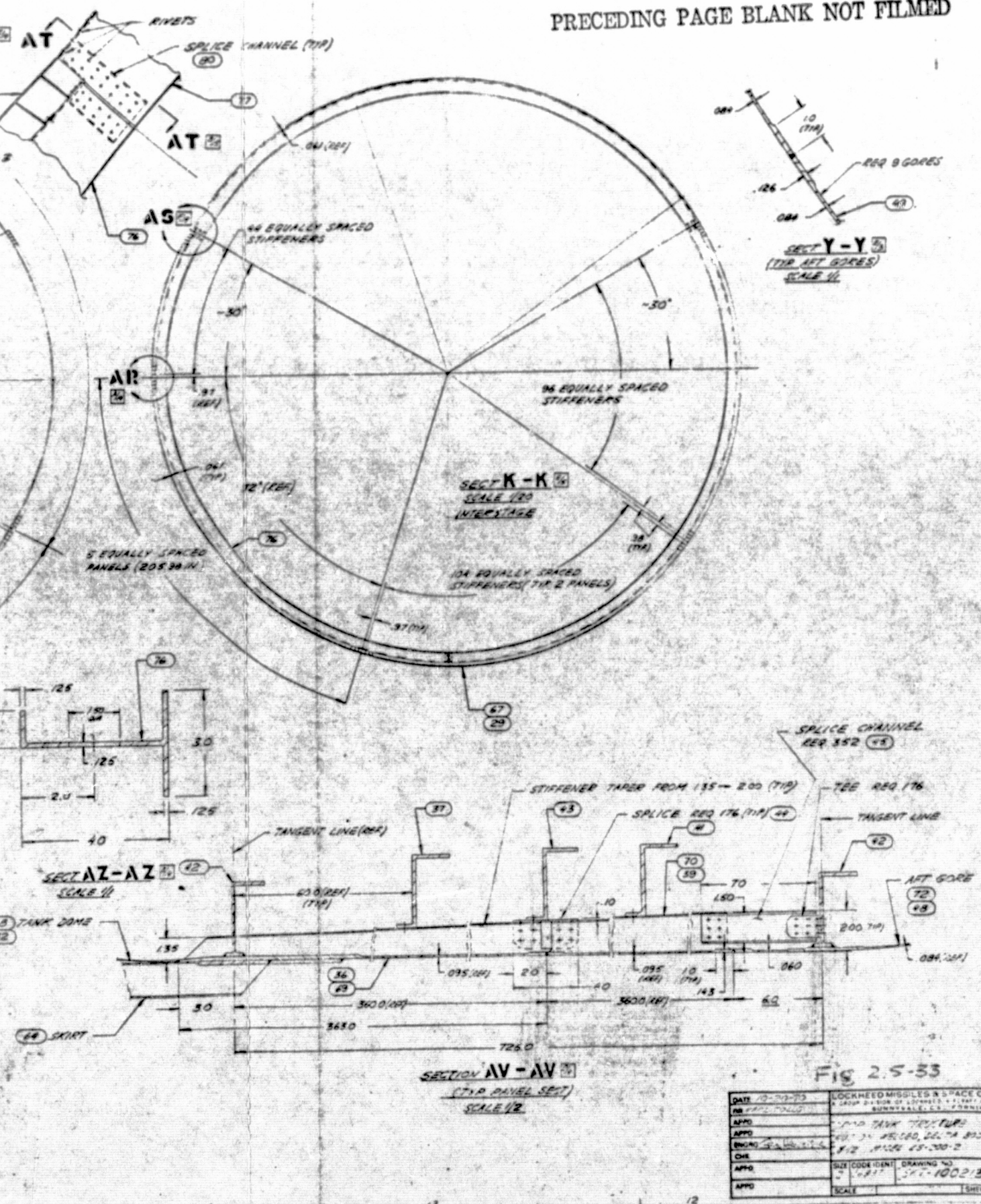

Fig 2.5-33

FOLDOUT FRAME 3

REPRODUCIBILITY OF THE ORIGINAL PAGE IS POOR.

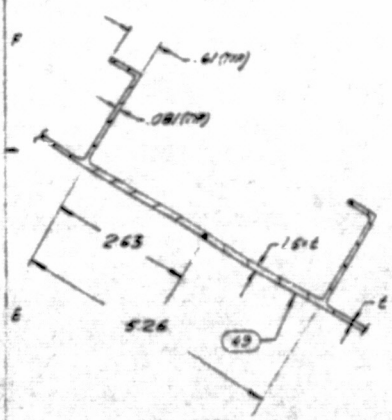

SECT BB
SCALE 1/1

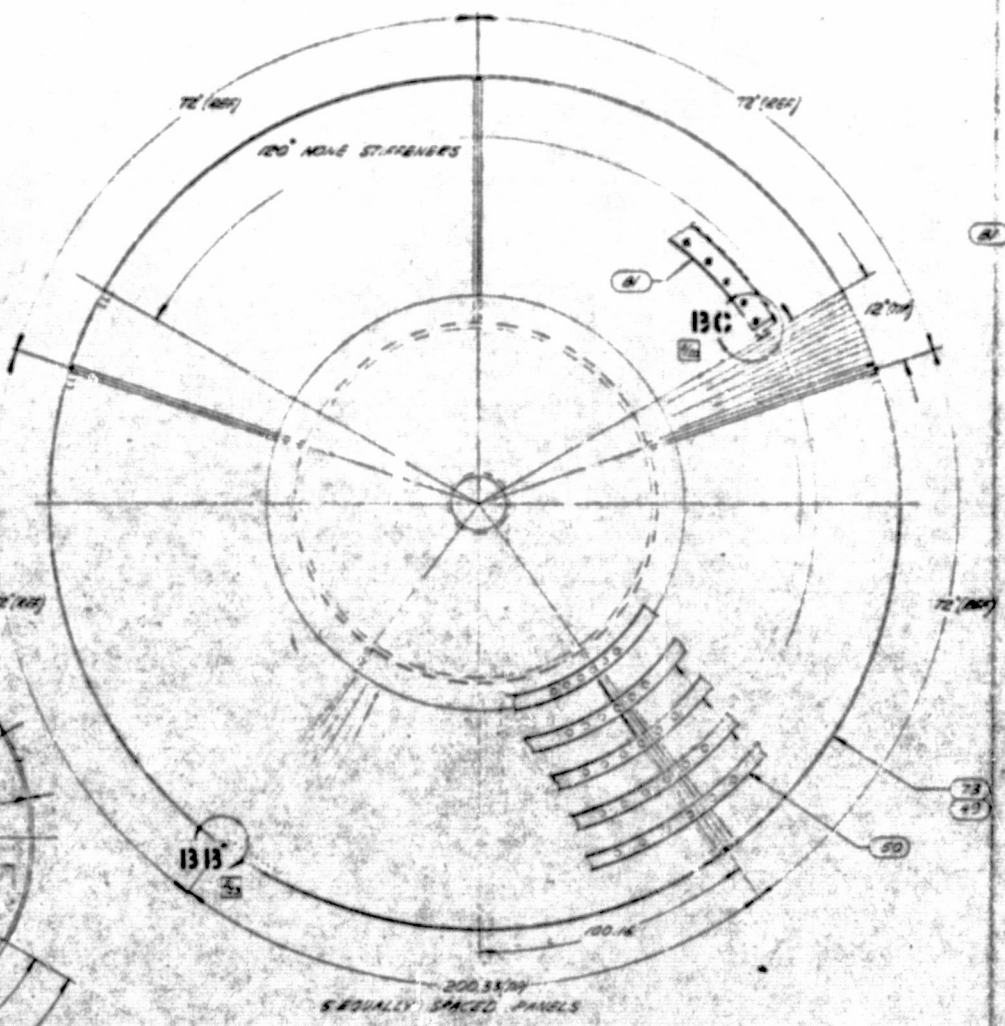

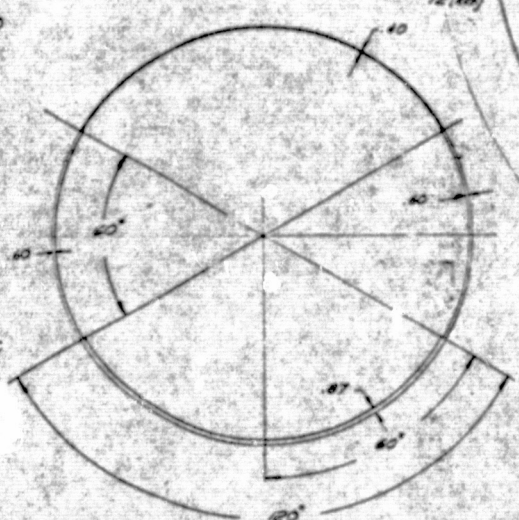

SECT BE - BE
* FOR 25 IN LENGTH OF THE PANELS, USE THE ABOVE SKIN THICKNESS
SCALE 1/20

SECT AY - AY
SCALE 1/20

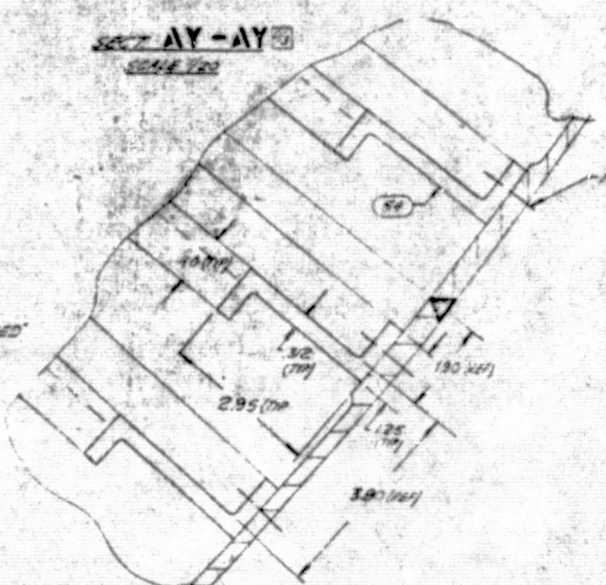

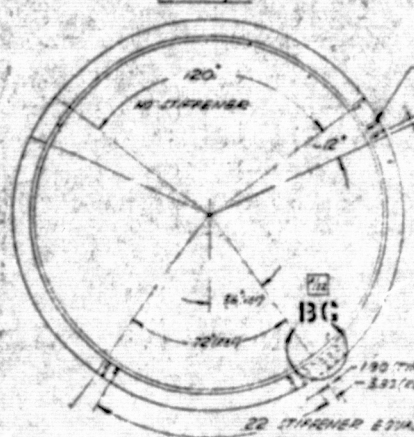

SECT BF - BF
SCALE 1/20

VIEW BG
SCALE 1/1

FOLDOUT FRAME

REPRODUCIBILITY OF THE ORIGINAL PAGE IS POOR.

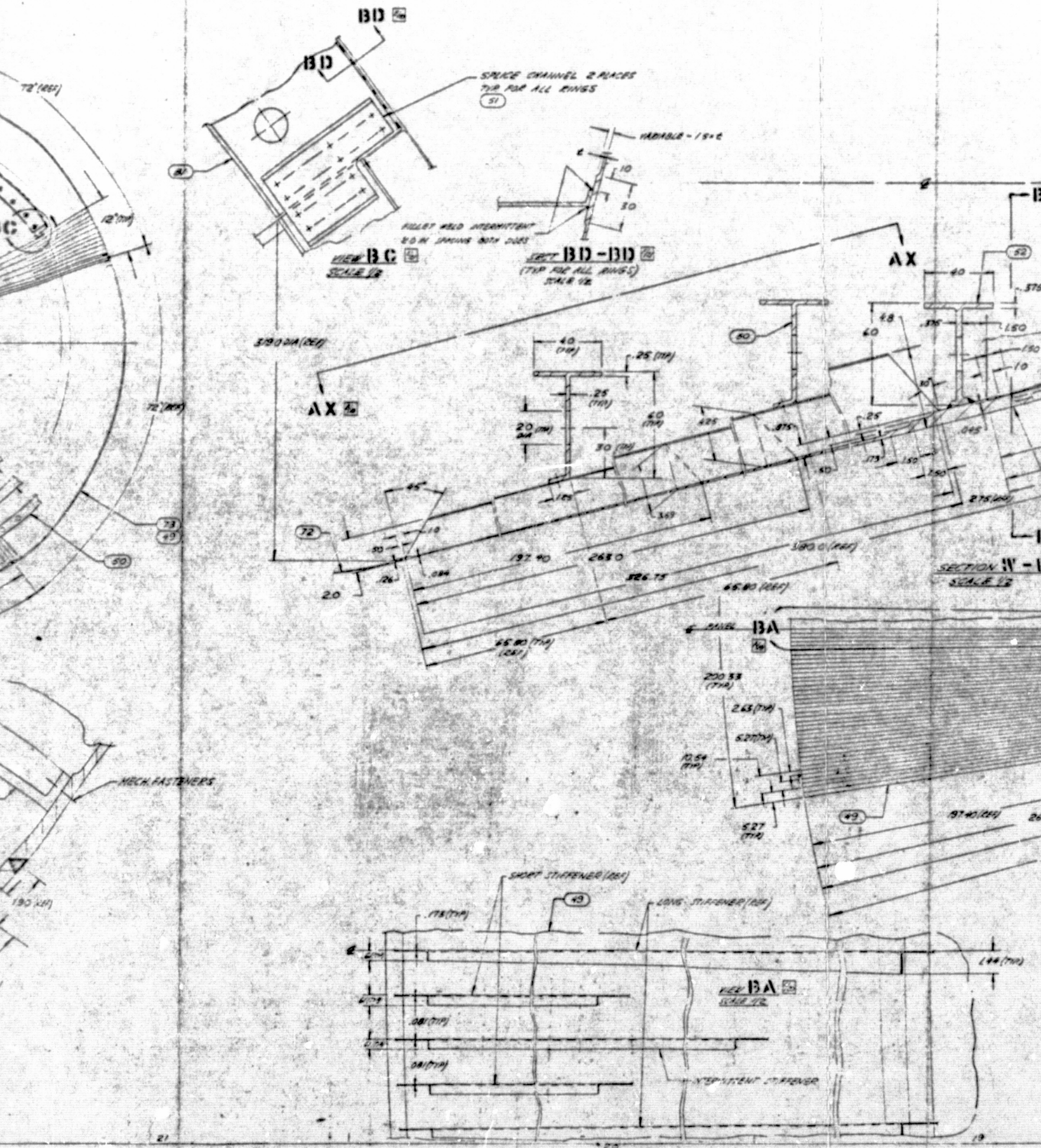

FOLDOUT FRAME 2

REPRODUCIBILITY OF THE ORIGINAL PAGE IS POOR.

PRECEDING PAGE BLANK NOT FILMED

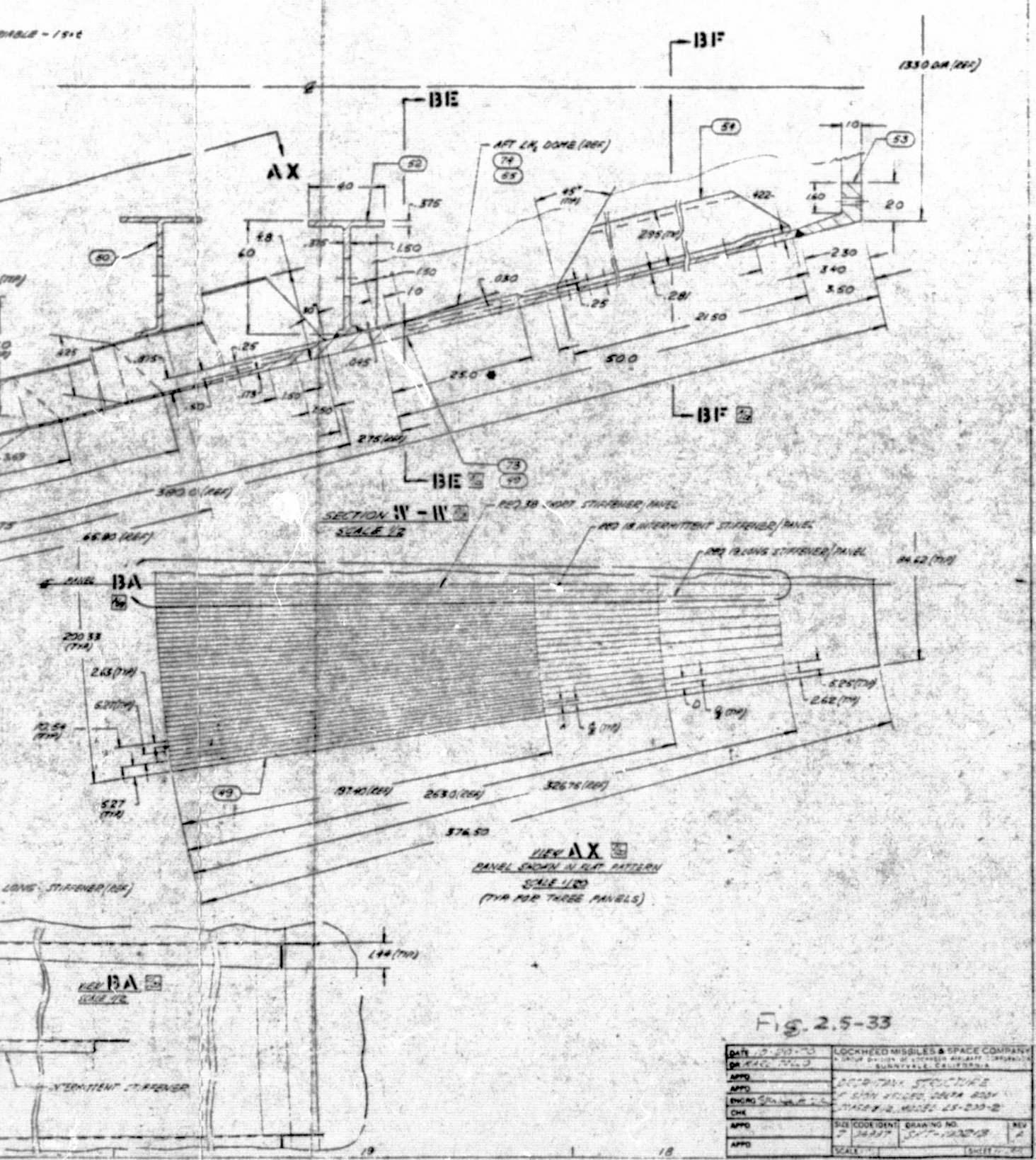

Fig. 2.5-33

FOLDOUT FRAME 3

2.5.3-15

REPRODUCIBILITY OF THE ORIGINAL PAGE IS POOR.

FOLDOUT FRAME

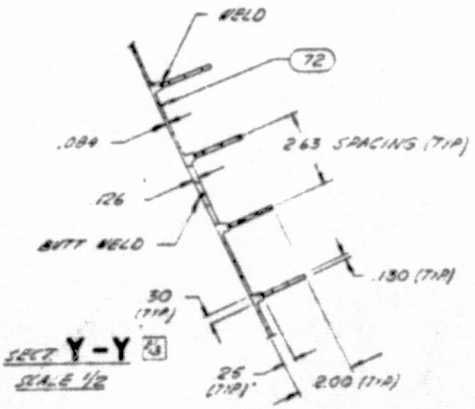

SECT Y-Y
SCALE 1/2

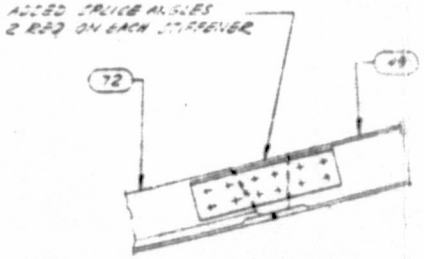

VIEW 13L
SCALE 1/2
(ADDED)

REVISION NO 3 ZONE 5/12 & 920
DROP TANK STRUCTURE
DWG SKT-100213
4/2-70 K. Tullis

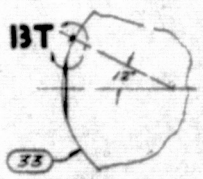

VIEW OF FWD LH2 DOME

A DIA	B DIA	C DIA	D DIA	E	t	HOLES
4	5.50	6.50	8.50	2.5	.050	2
5	6.50	7.50	9.50	2.5	.050	1
9	10.50	11.50	13.50	3.0	.050	1
19	20.50	23.00	25.00	4.0	.090	2

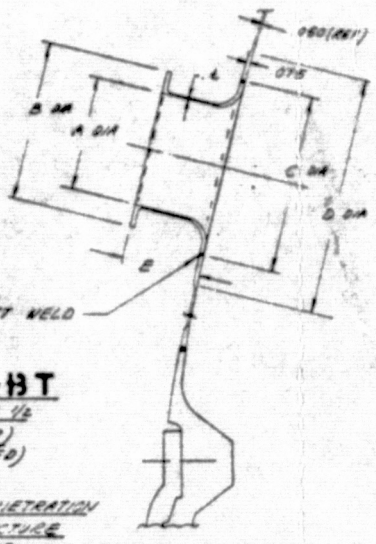

SECT 13T
SCALE 1/2
(TYP)
(ADDED)

REVISION NO 4
TYP PLUMBING PENETRATION
DROP TANK STRUCTURE
DWG SKT-100213

4/2-70 Tullis

NOTES:

1. WELD PER SPEC LAC 3853-040000 - ALL BUTT WELDS, 100% PENETRATION REQUIRED. INSPECT PER CLASS I
2. WELD PER SPEC LAC 3863-050200 ALL WELDS EXCEPT BUTT WELDS.
3. CHEMICAL MILL PER SPEC LAC 3452
4. MACHINE PER SPEC LAC 3601
5. INSTALL FASTENERS PER SPEC LAC 0581
6. FABRICATE PER SPEC LAC 1241
7. CLEAN PER SPEC LAC 0170
8. PROTECTION PER SPEC LAC 1001
9. INK MARK PER SPEC LAC 3578, METHOD
10. CALLOUT OF MEMBRANE GAGES ARE MIN.
11. LOX AND LH_2 TANK DOMES ARE SIMILAR DESIGN
12. LOX AND LH_2 SKIRTS ARE SIMILAR DESIGN

REV NO 5 ZONE 4/2 NOTES
DROP TANK STRUCTURE
DWG SKT-100213
4/2-70 Tullis

REPRODUCIBILITY OF THE ORIGINAL PAGE IS POOR.

FOLDOUT FRAME 2

PRECEDING PAGE BLANK NOT FILMED

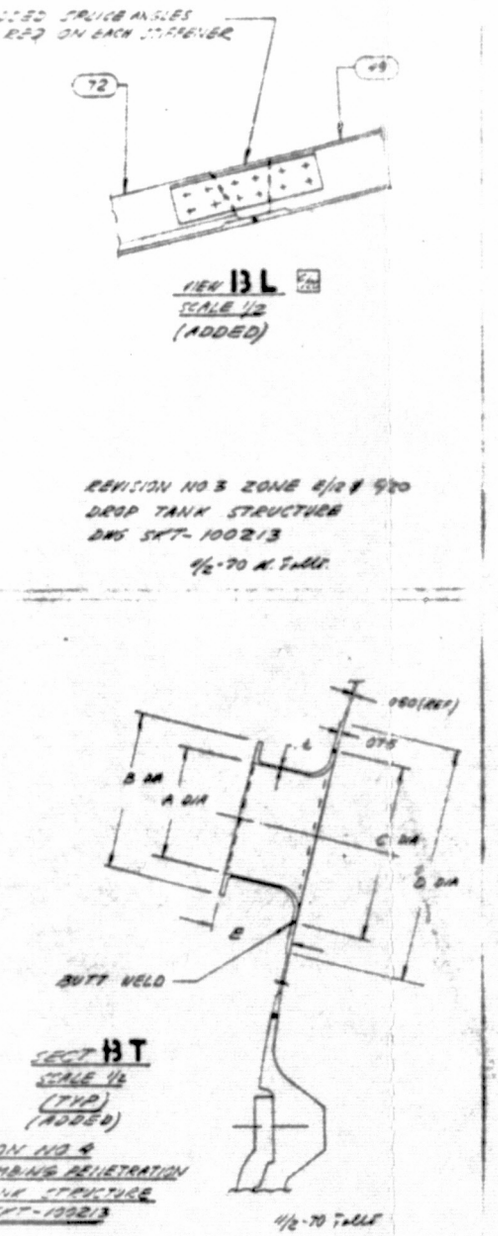

953 - 040000 - ALL BUTT WELDS,
QUIRED. INSPECT PER CLASS I
3853 - 050200 ALL WELDS
SPEC LAC 3452
LAC 3601
PER SPEC LAC 0581
LAC 1241
AC 0170
LAC 1001
PEC LAC 3575, METHOD
NE GAGES ARE MIN
ES ARE SIMILAR DESIGN
ARE SIMILAR DESIGN

REV NO 5 ZONE A/2 NOTES
DROP TANK STRUCTURE
DWG SKT-100213
11/2-70 Tollt

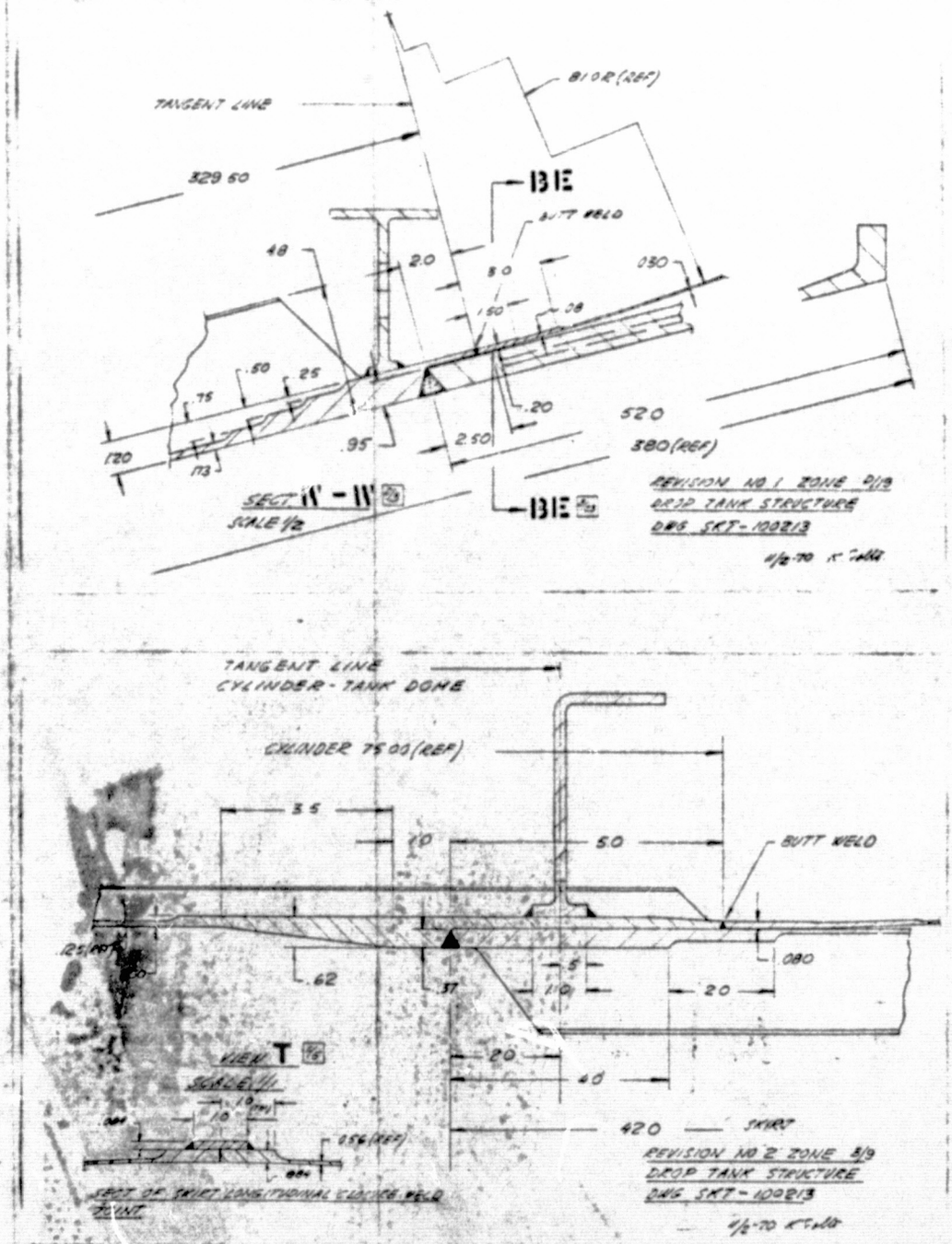

THIS SHEET SHOWS THE REVISIONS TO SHEET NO 1-4

FIG 2.5-33

QTY REQD	CODE IDENT	PART OR IDENTIFYING NO.	NOMENCLATURE OR DESCRIPTION	MATERIAL OR NOTE	SPECIFICATION	ZONE	ITEM NO.

LIST OF MATERIAL OR PARTS LIST

INTERPRET THIS DRAWING PER STANDARDS IN MIL-D-70327

UNLESS OTHERWISE SPECIFIED TOLERANCES ON: FRACTIONS ± 1/16, .X ± .1, .XX ± .03, .XXX ± .005, ANGLES ± 1°

DATE 11-2-70
DR KARL TOLLO
CHK
SUPV GEO HAVRISIK
STRESS
VALUE CHGRS
RELIABILITY
APPROVED
APPROVED

NEXT ASSY | USED ON | NEXT ASSY
APPLICATION

LOCKHEED MISSILES & SPACE COMPANY
A GROUP DIVISION OF LOCKHEED AIRCRAFT CORPORATION
SUNNYVALE, CALIFORNIA

DROP TANK STRUCTURE
FUSION WELDED, DELTA BODY
STAGE 1/2, MODEL LS-200-2

CODE IDENT NO.	SIZE	DRAWING NO.	REV
06887	E	SKT 100213	A

SCALE NOTED | SHEET 5 OF 5

PRECEDING PAGE BLANK NOT FILMED

of 4 basic elements: a hemispherical nose dome, a forward conical section, a cylindrical section, and an aft hemispherical dome. The nose dome is of monocoque design and is built up of chemically milled panels. The conical section is welded to the partially integral stiffened (L-sections) cylindrical section via a T-section ring-stiffened partial frame. This frame is the base for the lug attachment forming the intertank shear tie. The cylindrical section extends in a stub skin, partially integrally stiffened, ending in a machined ring used for bolting the oxygen tank to the intertank structure. The aft dome consists of 5 gores and a spun end cap combining the oxidizer outlet. The dome is of monocoque design with chemically milled panels butt-welded together.

Intertank Structure. The intertank structure is constructed of aluminum 7075-T6. It consists of a cylindrical shell partially stiffened with integral stiffeners stabilized by rings, with riveted connections between the longitudinal shell panels. An access door is provided in the unstiffened panel area. Both ends of the cylinder are formed by machined rings used for holding the oxygen tank and hydrogen tank to the intertank.

Liquid Hydrogen Tank. This tank (51,588 cu ft volume) is constructed of aluminum 2219-T87. It consists of 5 basic elements: a hemispherical forward dome, a cylindrical section, a transition section, an aft cone, and an aft dome. The forward dome is identical to the dome of the oxygen tank and is butt-welded to the cylindrical tank section. This section consists of two barrel sections. Each barrel section is built up of 10 longitudinal panels, partially integrally stiffened and butt-welded together. The integral stiffeners increase in depth toward the aft end of the cylinders. Z-section rings are riveted to the flanges of the integral stiffeners; kick-rings are welded to each end of the cylinders. The transition section forms part of a dome; it is integrally stiffened and butt-welded to the adjacent tank sections. The aft cone is constructed in a manner similar to the cylindrical section with internal integral tapered stiffeners and rings. A spun

monocoque dome is butt-welded to the cone to close the pressure vessel. The cone aft end carries a machined ring for attachment to the rear thrust cone assembly.

Thrust Cone Assembly. This assembly (Dwg. SKG 100216A, 3 Sheets, Fig. 2.5-34) consists of the thrust cone proper and its attachment mechanism to the orbiter. The thrust cone is built up of 6 flat titanium forgings (Ti-6Al-4V) rolled to shape and welded together. The attachment beam and mechanism transmits the tank loads to the orbiter thrust structure. A ball-bearing and piston arrangement actuated by gas pressure is used for rapid disengagement of the rear drop tank support from orbiter.

Bond-Welded Design. Even though the primary effort to establish highly assured droptank weights and cost was based on the fusion-welded design described earlier, it was found of interest to identify those areas in the droptank design to which bond-welding as a joining technique applies and to establish an estimate of the cost impact when using the bond-welding technique.

Considering the present experience with bond welding, it was decided to apply it to the design of the intertank and the forward dome and cylinder of the hydrogen tank. In these areas, line loads are not higher than 8000 lb/in, and recent tests by LMSC have indicated that the adhesive strength at liquid hydrogen temperature is at least equal to strength at room temperature. The technique is not used for the oxygen tank because compatibility of the bond material with oxygen has not yet been established. The design of the bond-welded intertank and hydrogen tank cylinders is shown in Dwg. SKS 100215, 2 Sheets, Fig. 2.5-35. The design uses a fusion-welded framelike substructure (cage) to which the preassembled skin panels and dome gores are attached. The required Z-stringers are bond-welded to the skins and the stiffening rings riveted to the stringer flanges. The bond-welded elements as described are joined with the remainder of the fusion-welded droptank elements in the same way as in the fusion-welded design.

REPRODUCIBILITY OF THE ORIGINAL PAGE IS POOR.

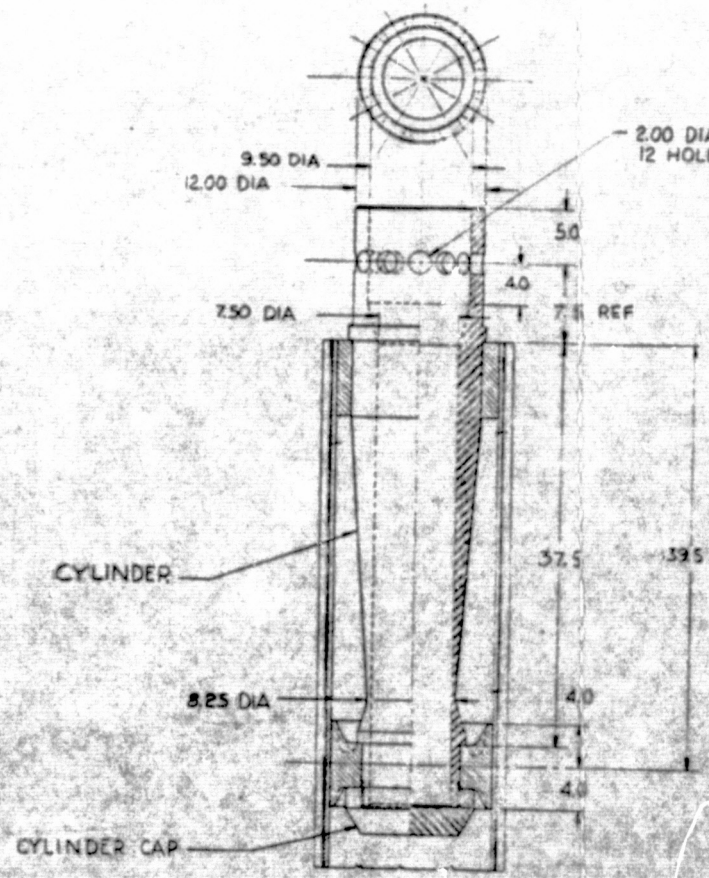

SECTION D-D
1/3 SIZE

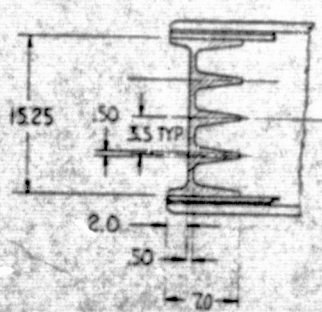

SECTION C-C
1/3 SIZE



SECTION B-
1/3 SIZE

BL 452 TANK
(RE

BEAM WE

BEAM CAP

BEAM WEB

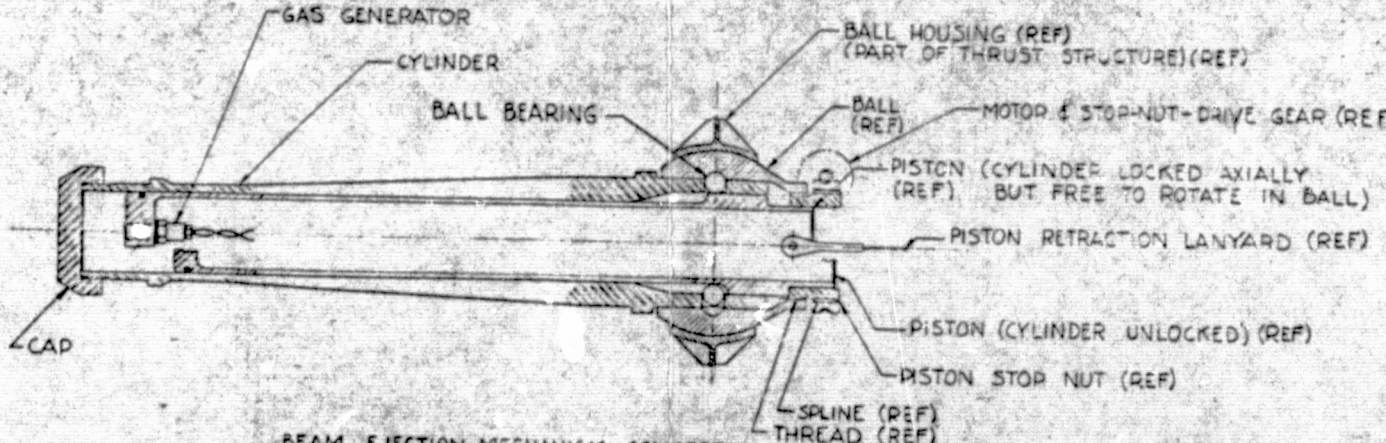

BEAM EJECTION MECHANISM CONCEPT

FOLDOUT FRAME

REPRODUCIBILITY OF THE ORIGINAL PAGE IS POOR.

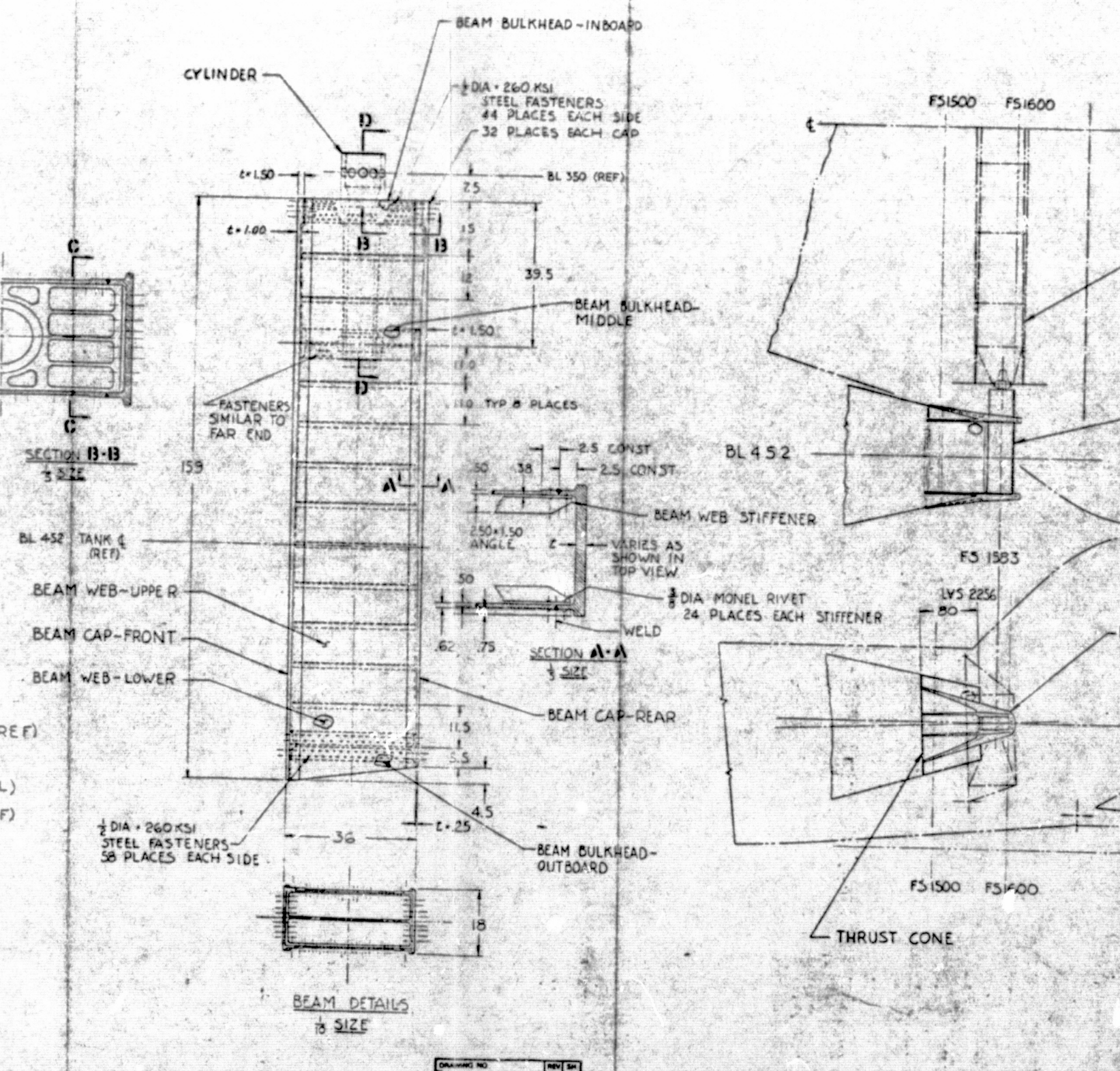

FOLDOUT FRAME 2

REPRODUCIBILITY OF THE ORIGINAL PAGE IS POOR.

PRECEDING PAGE BLANK NOT FILMED

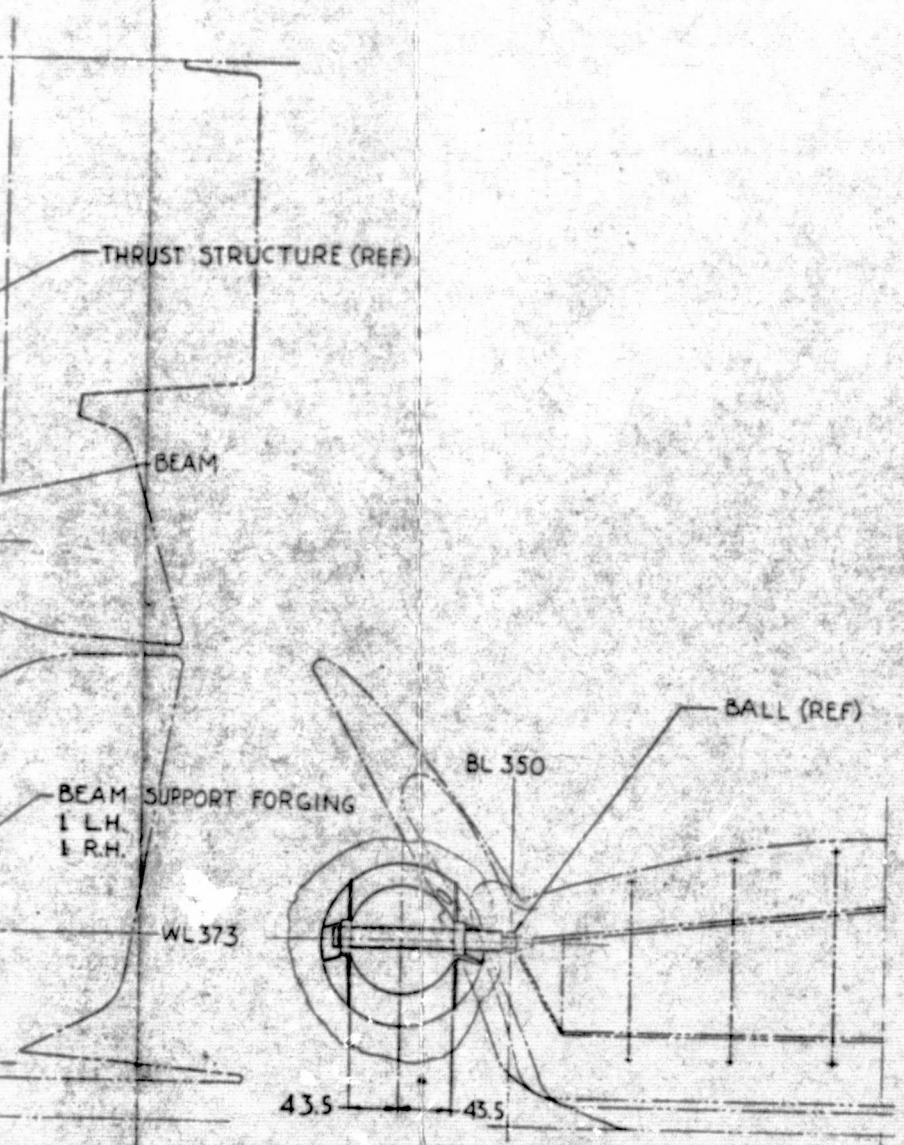

Fig. 2.5-34

FOLDOUT FRAME 3

REPRODUCIBILITY OF THE ORIGINAL PAGE IS POOR.

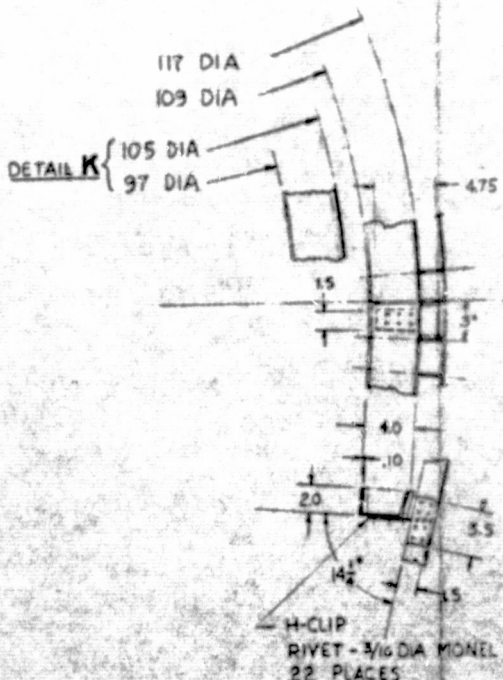

QTY REQD	CODE IDENT	PART OR IDENTIFYING NO.	NOMENCLATURE OR DESCRIPTION	MATERIAL DESCRIPTION OR NOTE	MATERIAL SPECIFICATION	ZONE	ITEM NO.
2			SKIN PANEL - SECTOR IV	SEE TABLE 2/2B	Ti-6Al-4V		2/7E
2			SKIN PANEL - SECTOR II				2/5E
1			SKIN PANEL - SECTOR III				2/6C
1			SKIN PANEL - SECTOR I		Ti-6Al-4V		2/6E
3000			RIVET - 3/16 DIA MONEL				2/11F
1000			LOCKBOLT - 3/8 DIA, TITANIUM				3/4B
1			BEAM SUPPORT FORGING - OUTBOARD	⚠			2/1E
1			BEAM SUPPORT FORGING - INBOARD	⚠			2/2D
120			H-CLIPS		Ti-6Al-4V		2/10G
1			INTERMEDIATE RING - REAR				2/3H
1			INTERMEDIATE RING - FORWARD				2/3H
1			BULKHEAD RING - INNER				2/1F
1			BULKHEAD RING - OUTER				2/2E
12			BULKHEAD STIFFENER				2/8C
1			BULKHEAD - REAR		Ti-6Al-4V		2/1D
1			GAS GENERATOR				1/15C
12			BALLS - BEARING - 2.00 DIA				1/14C
1			CYLINDER CAP	15.00 DIA x 4.00 THICK	4340 STEEL		1/15D
1			CYLINDER	15 DIA x 2.25 MIN WALL	4340 STEEL		1/15F
528			RIVET - 3/8 DIA MONEL				1/8D
376			BOLT - 1/2 DIA, 260 KSI HT STEEL				1/11B
22			BEAM WEB STIFFENER		Ti-6Al-4V		1/8D
1			BEAM BULKHEAD - OUTBOARD	⚠			1/9B
1			BEAM BULKHEAD - MIDDLE	⚠			1/9E
1			BEAM BULKHEAD - INBOARD	⚠			1/9G
1			BEAM WEB - LOWER	.500 x 38 x 160 PLATE			1/11C
1			BEAM WEB - UPPER	.564 x 38 x 160 PLATE			1/11D
1			BEAM CAP - REAR	1.5 THICK x 18 WIDE x 158 LONG PLATE			1/8C
1			BEAM CAP - FRONT	1.5 THICK x 18 WIDE x 160 LONG PLATE	Ti-6Al-4V		1/11D

PARTS LIST

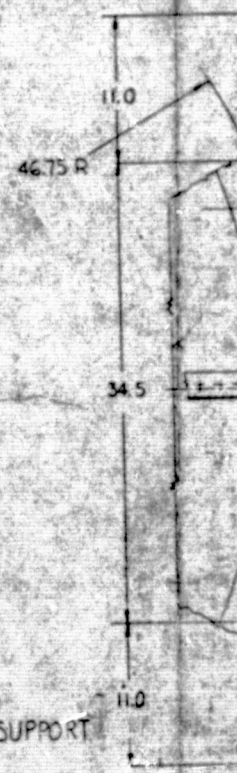

⚠ MAKE FROM SAME FORGING AS INBOARD SUPPORT
⚠ CLOSED DIE TITANIUM FORGINGS

FOLDOUT FRAME

REPRODUCIBILITY OF THE ORIGINAL PAGE IS POOR.

11 10 9 8 7 6

4.75

RING

H-CLIP 60 PLACES ON EACH RING

DETAIL F TYP
¼ SIZE

DETAIL K SIMILAR EXCEPT RING DIA

DIA MONEL

b_s STIFFENER SPACING

b_w STIFFENER WIDTH

t_s SKIN THICKNESS

t_w STIFFENER THICKNESS

SECTION G-G
NO SCALE

STIFFENER DIMENSIONS MEASURED AS SHOWN IN SECTION G-G

SECTOR	b_s	b_w	t_s	t_w
I	3.38	2.00	.11	.22
II	3.38	2.46	.115	.26
III	3.38	2.00	.11	.22
IV	3.38	1.48	.085	.17

b_w DECREASES LINEARLY ALONG THE STIFFENERS TO ZERO AT THE REAR BULKHEAD AS SHOWN IN DETAIL H

E

1.68 DIA

DETAIL D
⅛ SIZE

SECTOR I

30°

SECTOR IV

D

10 REF

8.0

.50

RIBS REQUIRED ON INBOARD FORGING ONLY

13.4

.50 R

t_s

2.0

.30

INTEGRAL STIFFENER

$1\frac{1}{2} \times 1\frac{1}{2} \times .10$ ANGLE RADIAL BULKHEAD STIFFENER 12 PLACES

92 DIA (REF)

88 DIA

DETAIL H
¼ SIZE

30°

SECTOR II

FRONT V

SECTION J-J ROTATED 90° CCW
¼ SIZE

SECTION B
¼ SIZE

DRAWING NO | REV | SH

FOLDOUT FRAME 2

REPRODUCIBILITY OF THE ORIGINAL PAGE IS POOR.

PRECEDING PAGE BLANK NOT FILMED

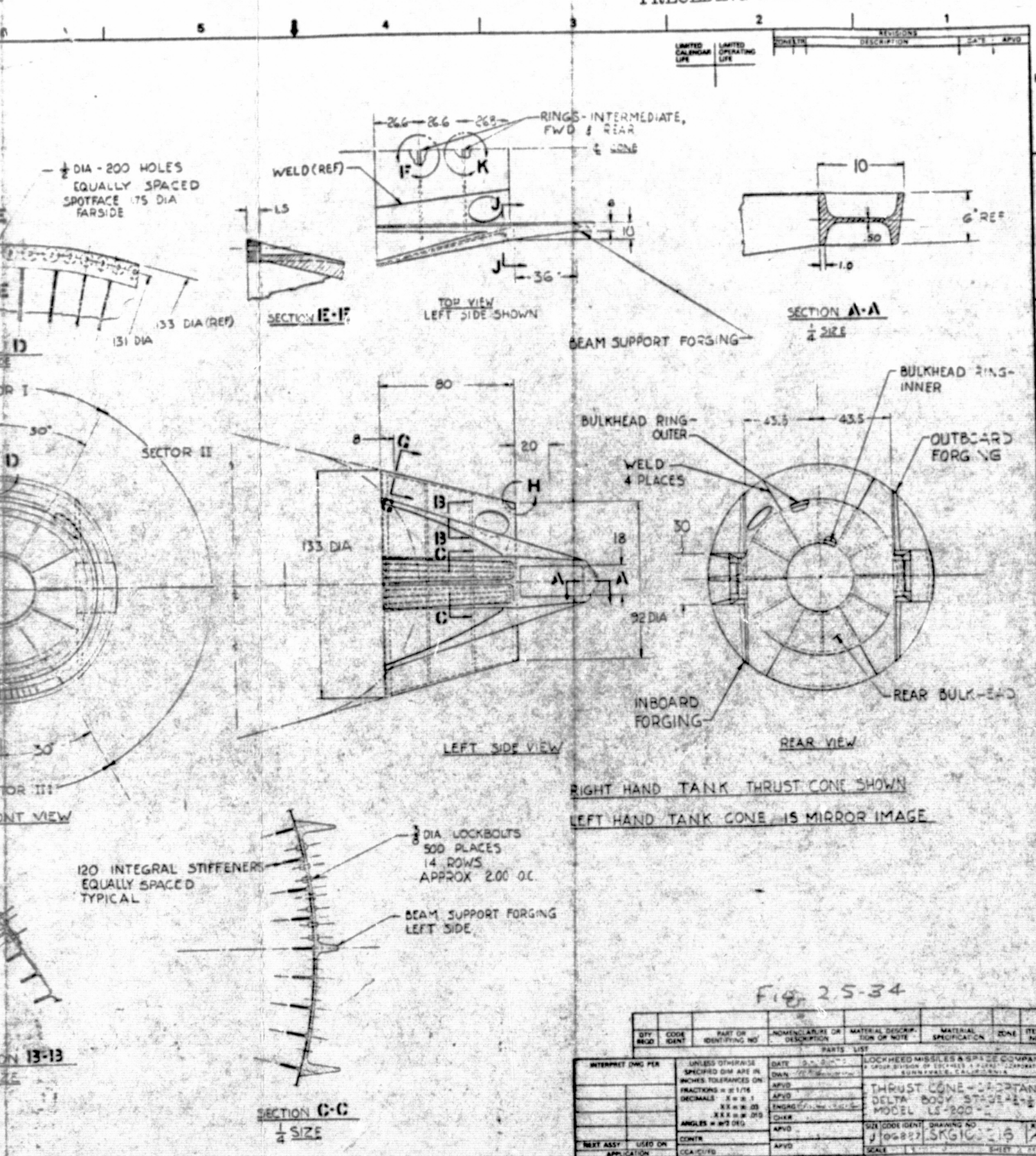

Fig. 2.5-34

FOLDOUT FRAME 3

2.5.3-23

REPRODUCIBILITY OF THE ORIGINAL PAGE IS POOR

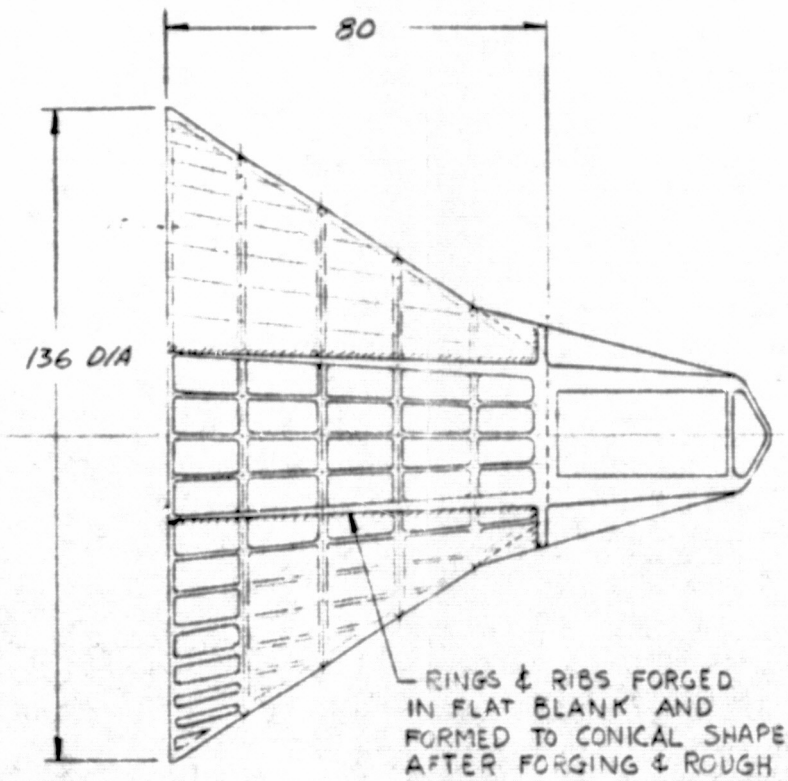

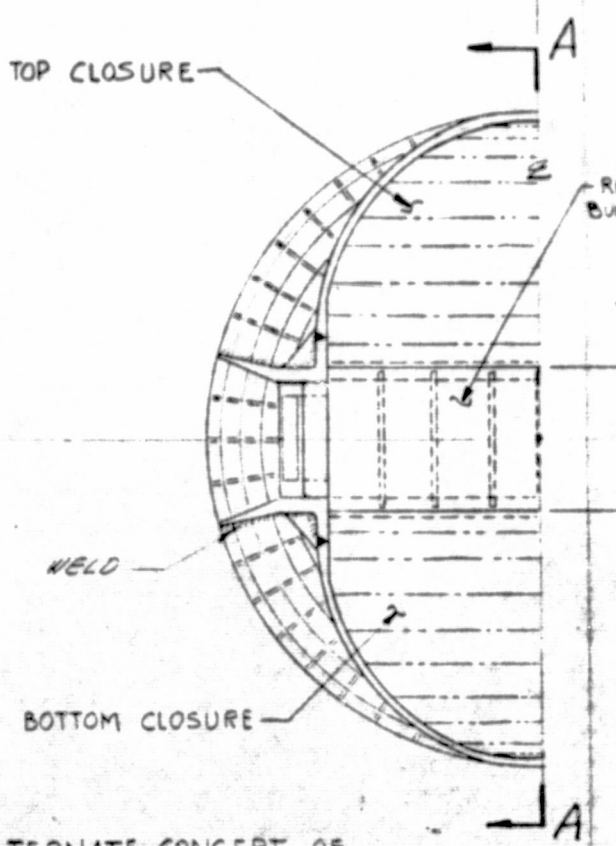

ALTERNATE CONCEPT OF SKG100216 - THRUST CONE

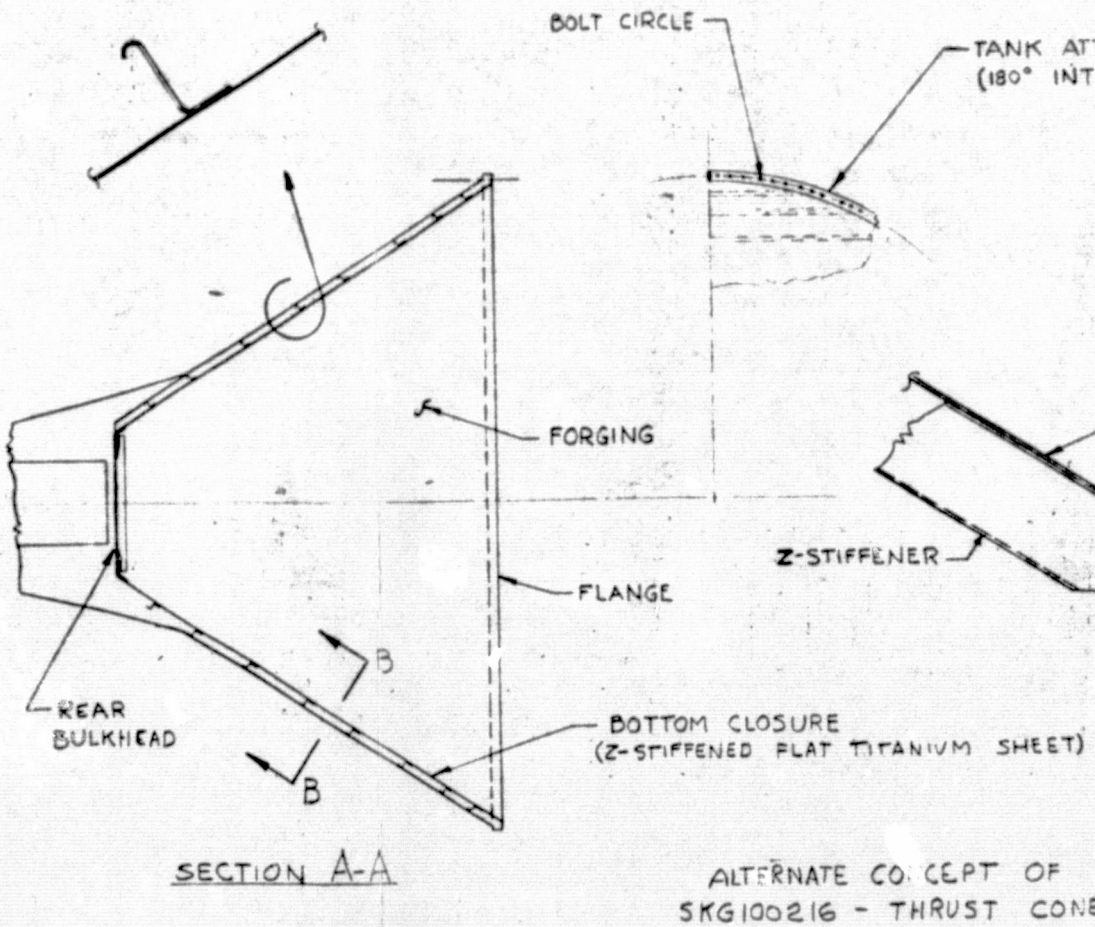

SECTION A-A

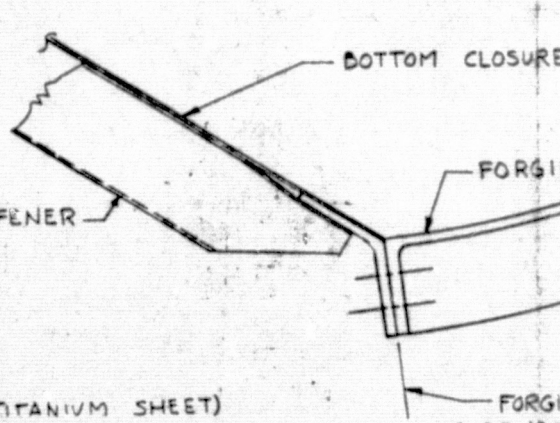

SECTION B-B

ALTERNATE CONCEPT OF SKG100216 - THRUST CONE

REPRODUCIBILITY OF THE ORIGINAL PAGE IS POOR.

LIMITED CALENDAR LIFE	LIMITED OPERATING LIFE

REVISIONS				
ZONE	LTR	DESCRIPTION	DATE	APPD

PRECEDING PAGE BLANK NOT FILMED

A

REAR BULKHEAD

30

A

SHEET 1 OF 2

RGING)

OSURE

ORGING

FORGING/
OSURE JOINT
D-B

SHEET 2 OF 2

THIS SHEET SHOWS THE REVISION OF THE THRUST CONE

Fig 2.5-34

QTY REQD	CODE IDENT	PART OR IDENTIFYING NO.	NOMENCLATURE OR DESCRIPTION	MATERIAL DESCRIPTION OR NOTE	MATERIAL SPECIFICATION	ZONE	ITEM NO.

PARTS LIST

INTERPRET DWG PER	UNLESS OTHERWISE SPECIFIED DIM. ARE IN INCHES. TOLERANCES ON: FRACTIONS = ± 1/16 DECIMALS: .X = ± .1, .XX = ± .03, .XXX = ± .010 ANGLES = ± 2 DEG	DATE 11-2-70	LOCKHEED MISSILES & SPACE COMPANY A GROUP DIVISION OF LOCKHEED AIRCRAFT CORPORATION SUNNYVALE, CALIFORNIA
		DR [illegible]	
		APPD	
		APPD	THRUST CONE - DROPTANK
		ENGRG GEO. MARUNIK	DELTA BODY STAGE - 4-1/2
		CHK	MODEL LS-200-2
	CONTR	APPD	SIZE D; CODE IDENT 06987; DRAWING NO. SKG 100216; REV A
NEXT ASSY / USED ON APPLICATION	CCA/CEI	APPD	SCALE NOTED; SHEET 3 OF 3

FOLDOUT FRAME 2

2.5.3-25

REPRODUCIBILITY OF THE ORIGINAL PAGE IS POOR.

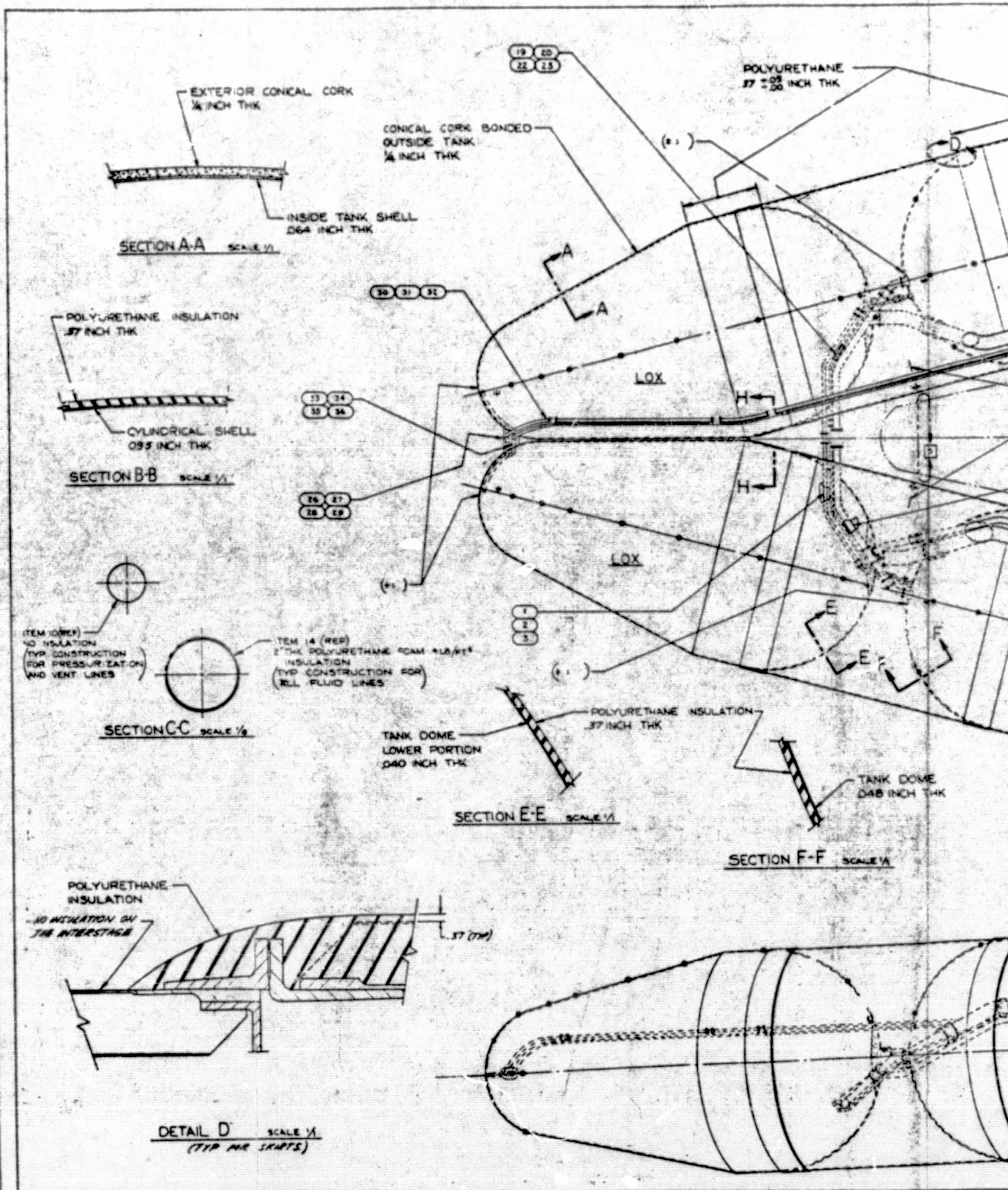

FOLDOUT FRAME 1

C5

REPRODUCIBILITY OF THE ORIGINAL PAGE IS POOR.

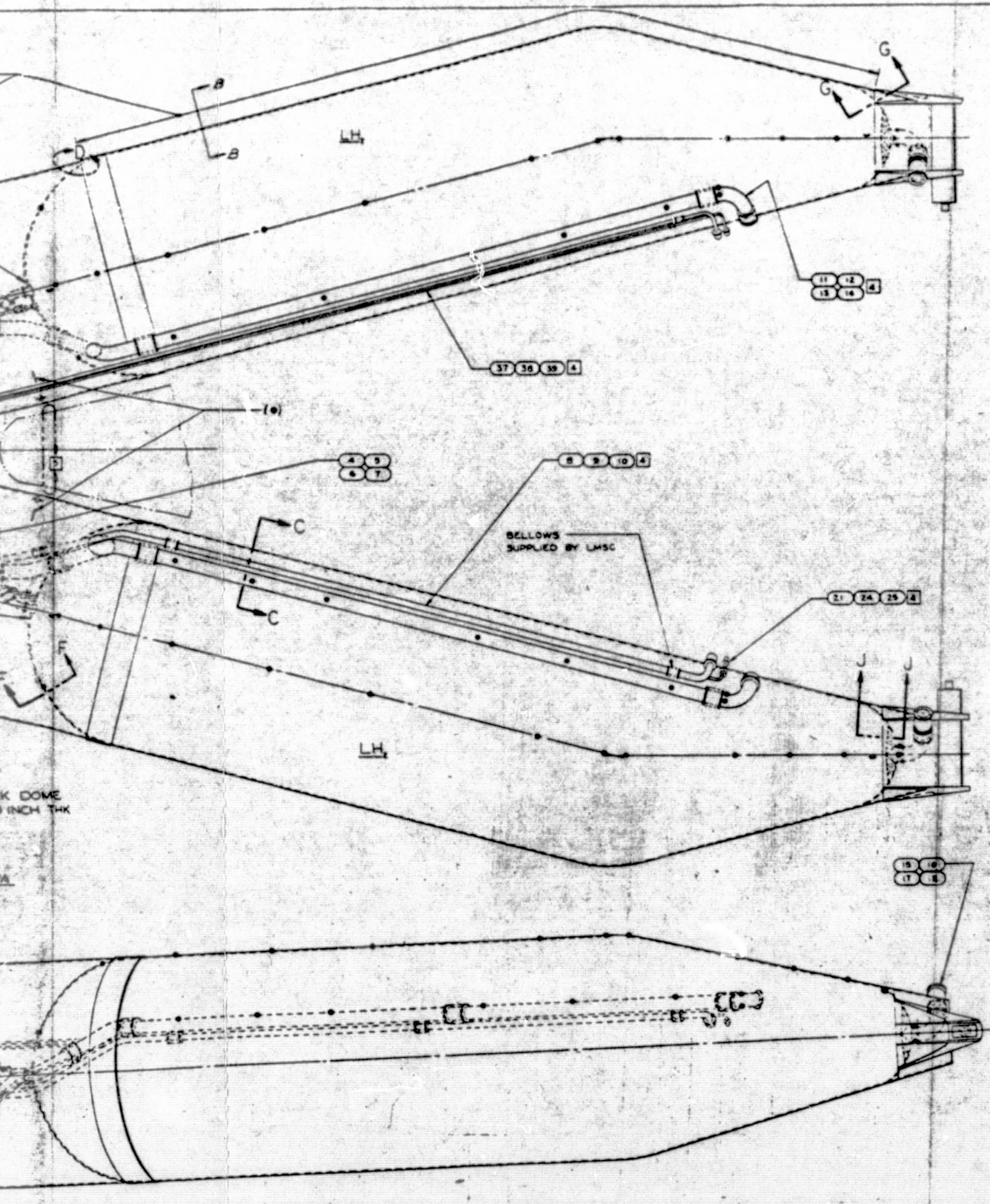

FOLDOUT FRAME 2

REPRODUCIBILITY OF THE ORIGINAL PAGE IS POOR.

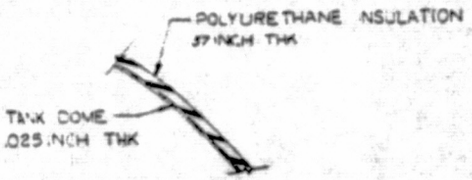

SECTION G-G SCALE 1/1



SECTION HH SCALE 1/2

INSTRUMENTATION LIST

QUANTITY LOX TANKS	QUANTITY LH2 TANKS	CODE	ITEM	SOURCE	WT. LBS EACH
31	---	●	HOT WIRE POINT SENSORS		.0
---	29	●	HOT WIRE POINT SENSORS		.0
4	---	◆	PRESSURE TRANSDUCER		.35
---	4	◆	PRESSURE TRANSDUCER		.35
2	---	▮	19 PIN ELECTRICAL FEED-THRU CONNECTOR		
2	---	▮	FEMALE MATING ELECTRICAL CONNECTOR (INSIDE TANK)	DEUTCH	1.0
2	---	▮	MALE MATING ELECTRICAL CONNECTOR (OUTSIDE TANK)		
---	2	▮	19 PIN ELECTRICAL FEED-THRU CONNECTOR		
---	2	▮	FEMALE MATING ELECTRICAL CONNECTOR (INSIDE TANK)	DEUTCH	1.0
---	2	▮	MALE MATING ELECTRICAL CONNECTOR (OUTSIDE TANK)		
1	1	◆	MULTIPLEX UNIT	[illegible]	4.0
1	1	◆	PLUS QUICK DISCONNECT D-6477-27-EP	[illegible]	

◆ REQUIREMENTS—EACH UNIT
20 WORDS MEMORY PER SIGNAL
A TO D CONVERTER
D TO A CONVERTER
BUFFER STORAGE FOR EACH SIGNAL
MULTIPLEX FOR EACH SIGNAL
ONE HAND ARE MIX FORMAT PCB
POWER SUPPLY

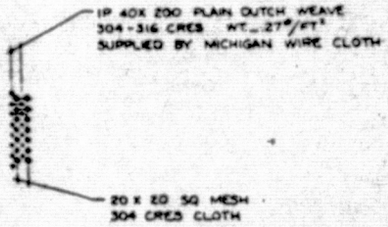

SECTION J-J SCALE NONE
(TYP VORTEX SUPPRESSOR CONSTR)

Fig. 2-5

[5] REFER TO DWG SK3-00217, FWD SUPPORT-DR
FOR SUPPORT DEFINITION.
[4] ALTERNATE CONFIGURATION: LINES AND GIMBALS
ARE DELETED FROM THE DROP TANK ASSEM
RELOCATED INSIDE SPACECRAFT.
[3] DISCONNECT WITH CHECK SIMILAR TO ROYAL,
OR RMDCC 185.
[2] GIMBAL SIMILAR TO SOLAR 38026, CODE 55820.
[1] SOLAR, ARROWHEAD TYPICAL MFG'S FOR LINES AN

NOTES:

REPRODUCIBILITY OF THE ORIGINAL PAGE IS POOR.

	LIST		
		SOURCE	
NSORS			1.0
NSORS			1.0
UGER			3.5
UGER			3.5
EED-THRU			
		DEUTCH	1.0
FEED-THRU			
		DEUTCH	1.0
	3.80		4.0

PRECEDING PAGE BLANK NOT FILMED

1		SKG 100216 DROP TANK THRUST CONE			41
1		SKT 100215 DROP TANK STRUCTURE			40
1	COML	4"DIA×.032 WALL 4"LOX PRESSURIZATION LINE		75"	39
1	[3]	DISCONNECT 4"		4"	38
4	[2]	GIMBAL JOINT 4"	ALUM WITH MONEL BELLOWS	2"	37
1	COML	5"DIA×.032 WALL 3"		5"	36
1	COML	TEE 3"-4"		2"	35
3	[2]	GIMBAL JOINT 3"	ALUM WITH MONEL BELLOWS	6"	34
2	[1]	END COUPLING 3"LOX PRESSURIZATION LINE		4"	33
1	COML	6"DIA×.032 WALL 6"LOX VENT LINE	2219 ALUM	08"	32
1	[3]	DISCONNECT 6"		22"	31
4	[2]	GIMBAL JOINT 6"	ALUM WITH MONEL BELLOWS	20"	30
1	COML	4"DIA×.032 WALL 4"	2219 ALUM	6"	29
1	COML	TEE 4"-6"		7"	28
3	[2]	GIMBAL JOINT 4"	ALUM WITH MONEL BELLOWS	3"	27
2	[1]	END COUPLING 4"LOX VENT LINE		6"	26
1	COML	5"DIA×.032 WALL 5"LH2 PRESSURIZATION LINE	2219 ALUM	60"	25
2	[2]	GIMBAL JOINT 5"	ALUM WITH MONEL BELLOWS	5"	24
1	COML	TEE 4"-5"		4"	23
1	COML	4"DIA×.032 WALL 4"	2219 ALUM	30"	22
1	[3]	DISCONNECT 5"		7"	21
3	[2]	GIMBAL JOINT 4"	ALUM WITH MONEL BELLOWS	2"	20
2	[1]	END COUPLING 4"LH2 PRESSURIZATION LINE		3"	19
2	COML	19"DIA×.032 WALL 19"LH2 FLUID LINE	2219 ALUM	28"	18
2	[3]	DISCONNECT		240"	17
4	[2]	GIMBAL JOINT	ALUM WITH MONEL BELLOWS	280"	16
2	[1]	END COUPLING 19"LH2 FLUID LINE		20"	15
2	COML	19"DIA×.072 WALL 19"LOX FLUID LINE	2219 ALUM	54"	14
2	[3]	DISCONNECT		240"	13
6	[2]	GIMBAL JOINT	ALUM WITH MONEL BELLOWS	340"	12
2	[1]	END COUPLING 19"LOX FLUID LINE		20"	11
1	COML	13"DIA×.032 WALL 13"LH2 VENT LINE	2219 ALUM	52"	10
1	[3]	DISCONNECT 13"LH2 VENT LINE		25"	9
3	[2]	GIMBAL JOINT 13"LH2 VENT LINE	ALUM WITH MONEL BELLOWS	60"	8
3	[2]	GIMBAL JOINT 9"LH2 VENT LINE	ALUM WITH MONEL BELLOWS	75"	7
1	COML	TEE		12"	6
1	COML	9"DIA×.032 WALL	2219 ALUM	55"	5
2	[1]	END COUPLING 9"LH2 VENT LINE		11"	4
3	[2]	GIMBAL JOINT 8"LOX FLUID LINE	ALUM WITH MONEL BELLOWS	60"	3
1	COML	8"DIA×.032 WALL 8"LOX FLUID LINE	2219 ALUM	45"	2
2	[1]	END COUPLING 8"LOX FLUID LINE		18"	1
QTY	SOURCE	DESCRIPTION	MATERIAL		NO
QTY REQD	CODE IDENT	PART OR IDENTIFYING NO. / NOMENCLATURE OR DESCRIPTION / MATERIAL DESCRIPTION OR NOTE	MATERIAL SPECIFICATION	ZONE	ITEM NO

PARTS LIST

[5] REFER TO DWG SKG100217, FWD SUPPORT-DROP TANK FOR SUPPORT DEFINITION.

[4] ALTERNATE CONFIGURATION: LINES AND GIMBALS INDICATED ARE DELETED FROM THE DROP TANK ASSEMBLY AND ARE RELOCATED INSIDE SPACECRAFT.

[3] DISCONNECT WITH CHECK SIMILAR TO ROYAL, HADLEY 11397 OR RMDCC185.

[2] GIMBAL SIMILAR TO SOLAR 38026, CODE 55820.

[1] SOLAR, ARROWHEAD TYPICAL MF63 FOR LINES AND FITTINGS.

NOTES:

INTERPRET DWG PER

UNLESS OTHERWISE SPECIFIED DIM ARE IN INCHES TOLERANCES ON FRACTIONS = ± 1/16 DECIMALS .X = ± .1 .XX = ± .05 .XXX = ± .010 ANGLES = ± 2 DEG

NEXT ASSY | USED ON APPLICATION

CONTR

CCA/CB

DATE

DR

APPD

APPD

ENGRG RELEASE DATE

CHK

APPD

APPD

LOCKHEED MISSILES & SPACE COMPANY

DROP TANK ASSEMBLY DELTA BODY-STAGE & 1/2

SIZE | CODE IDENT | DRAWING NO. | REV

SCALE | SHEET

Fig. 2.5-36

Fig. 2.5-36

Fig. 2.5.3-37

2.5.3-35

FUSION-WELDED DESIGN

ITEM		WEIGHT (LB)	
DROP TANK TOTAL			119,257
STRUCTURE		98,050	
LO_2 TANK	15,088		
INTERTANK	16,040		
LH_2 TANK	49,056		
THRUST CONE AND FITTINGS	16,866		
FORWARD ATTACH MECHANISM	1,000		
INSULATION		3,181	
LO_2 TANK	1,945		
INTERTANK	145		
LH_2 TANK	1,091		
PLUMBING		6,883	
LO_2	4,017		
LH_2	2,866		
INSTRUMENTATION		301	
LO_2	93		
LH_2	108		
WIRE	100		
CONTINGENCY – 10 PERCENT		10,842	

NOTE: STRUCTURAL FACTOR = .042 LB/LB: $\lambda' = 0.957$

Fig. 2.5-37 Droptank Assembly Weight Summary

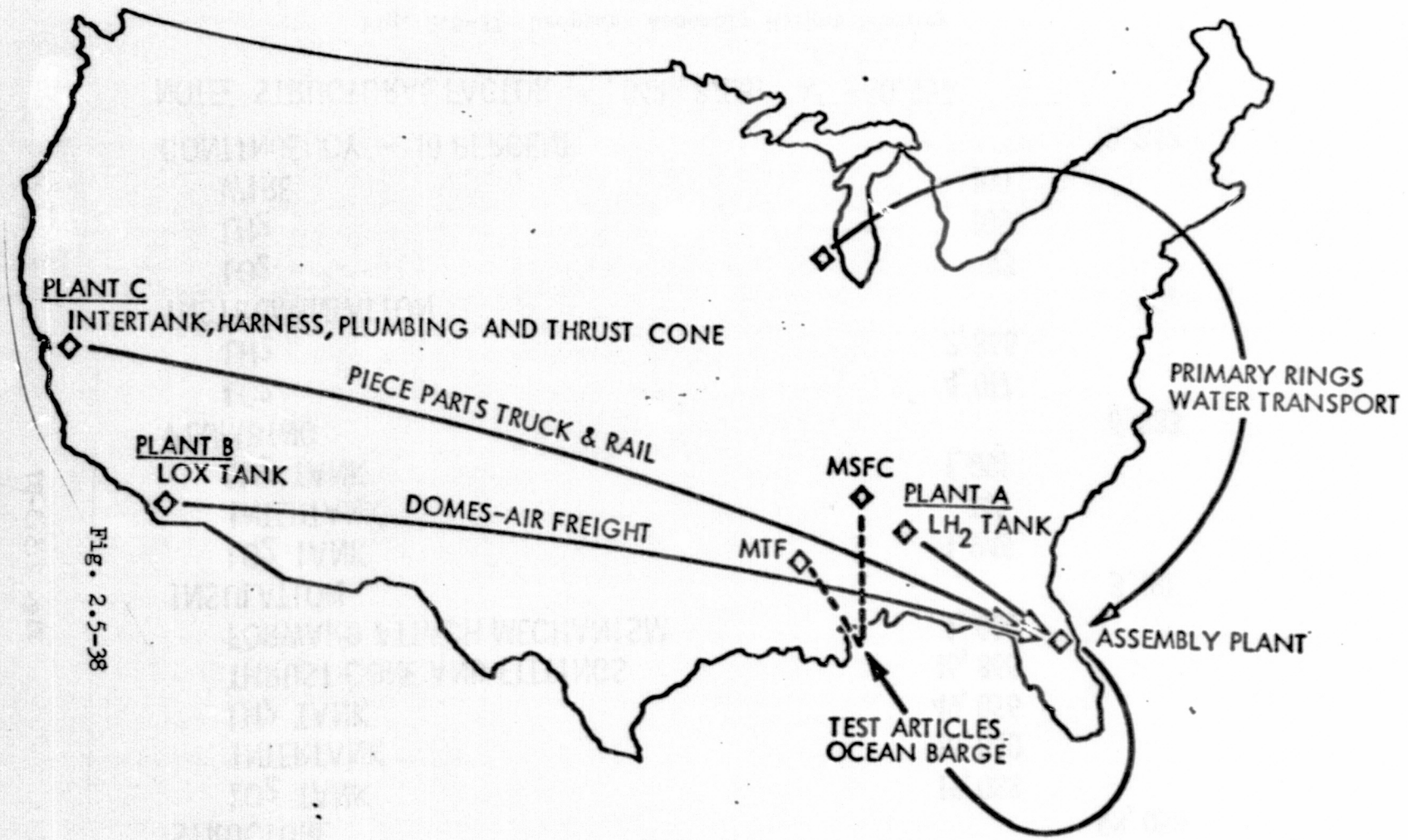

Fig. 2.5-38 Manufacturing Program Overview

as follows:

Plant A (GELAC)	Fabrication of LH_2 tank components, less hemisphere and thrust-cone forging
Plant B (CALAC)	Fabrication of LO_2 tank components plus LH_2 hemispheres
Plant C (LMSC)	Fabrication of the intertank components, wire harness, instrumentation, piping, and thrust-cone forging assembly

The selection of these plants is based primarily upon related hardware experience and their machine and facilities capabilities.

Size of raw material and fabricated parts and subassemblies is planned to be compatible with standard interstate surface transportation with the following exceptions:

Spun Domes	Procured from Spincraft of Milwaukee, Wisconsin, and air-freighted to KSC
Ring Forgings	Procured rough-machined from Ladish of Cudahy, Wisconsin, and water-transported to KSC
Test Hardware Assemblies	Water-transported from KSC to the Michoud and MSFC test sites

All fabricated parts or subassemblies are to be cleaned and protective wrapped to minimize contamination and oxidation during transportation and storage. This in turn will allow parts entry into the weld cycle without further chemical processing.

- Fabrication and Assembly. In developing the manufacturing plan for the droptank system, particular emphasis was placed on the economics of manufacture. The integrally milled skins were sized to the

maximum transportable size (10 ft x 30 ft) to reduce setup costs and optimize machine run time. Maximum utilization of full ring forgings reduced parts count and subsequent setup and run time. Specific consideration was given to tooling rate in the initial phase to optimize weld tools to reduce load and unload spans and to integrate radiographic inspection with the weld tools.

- LO_2 Tank Fabrication and Assembly. Fabrication of the primary structure (Fig. 2.5-39) consists of machining rings, forming baffles, explosive forming of dome gore segments, and milling of integrally stiffened skins.

  LOX Tank assembly (Fig. 2.5-40) consists of joining four primary subassemblies: conical section assembly, cylindrical support structure, and forward and rear dome assemblies. All longitudinal welds are jigged vertically, and internal baffles are welded horizontally.

- Intertank Fabrication and Assembly. Fabrication and assembly (Fig. 2.5-41) consists primarily of milling integrally stiffened skins, stretch forming of rings, and machining of full ring forgings for field joints. The doors are tooled for interchangeability. The assembly is joined mechanically with bolts and rivets. Assembly is accomplished in the vertical position.

- LH_2 Tank Fabrication and Assembly. Fabrication (Fig. 2.5-42) consists of stretched-formed rings and full ring forgings, milling of integrally stiffened skins, high-energy forming of dome skins, and welding of the thrust cone consisting of six forgings.

  Assembly (Fig. 2.5-43) consists of joining five primary subassemblies, the forward dome, two barrel assemblies, gore/cone/aft-dome assembly, and thrust-cone assembly. The longitudinal welds are accomplished vertically, circumferential welds horizontally, and closure welds of primary subassemblies horizontally.

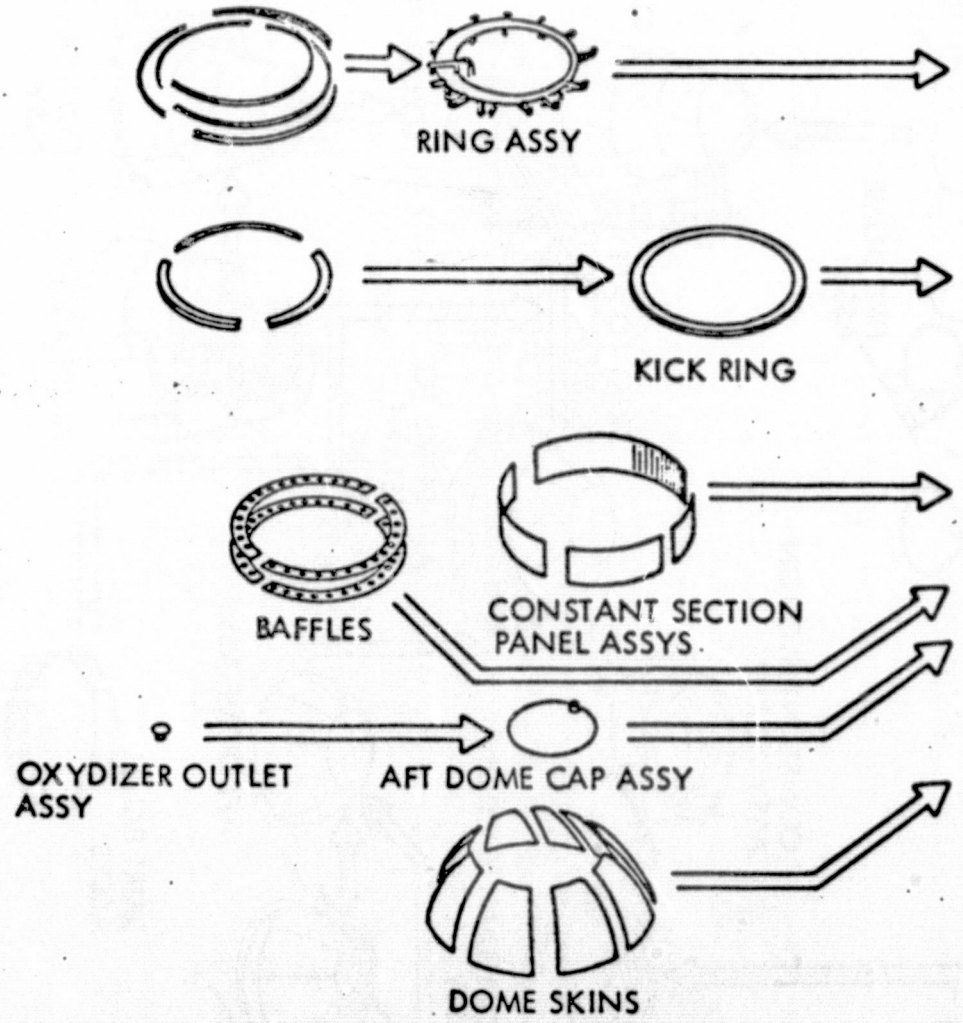

Fig. 2.5-39 LOX Tank Fabrication

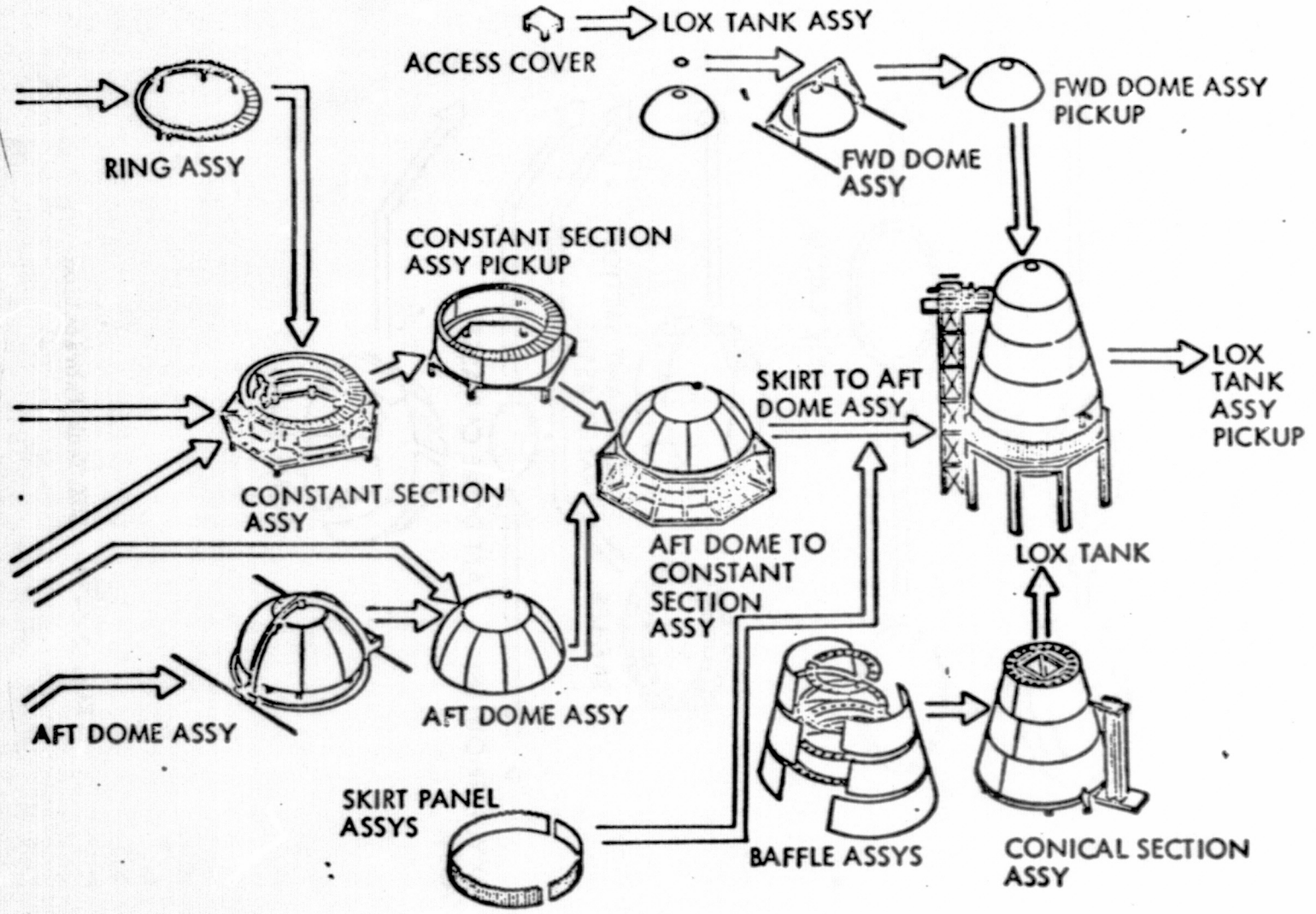

Fig. 2.5-40 LOX Tank Assembly

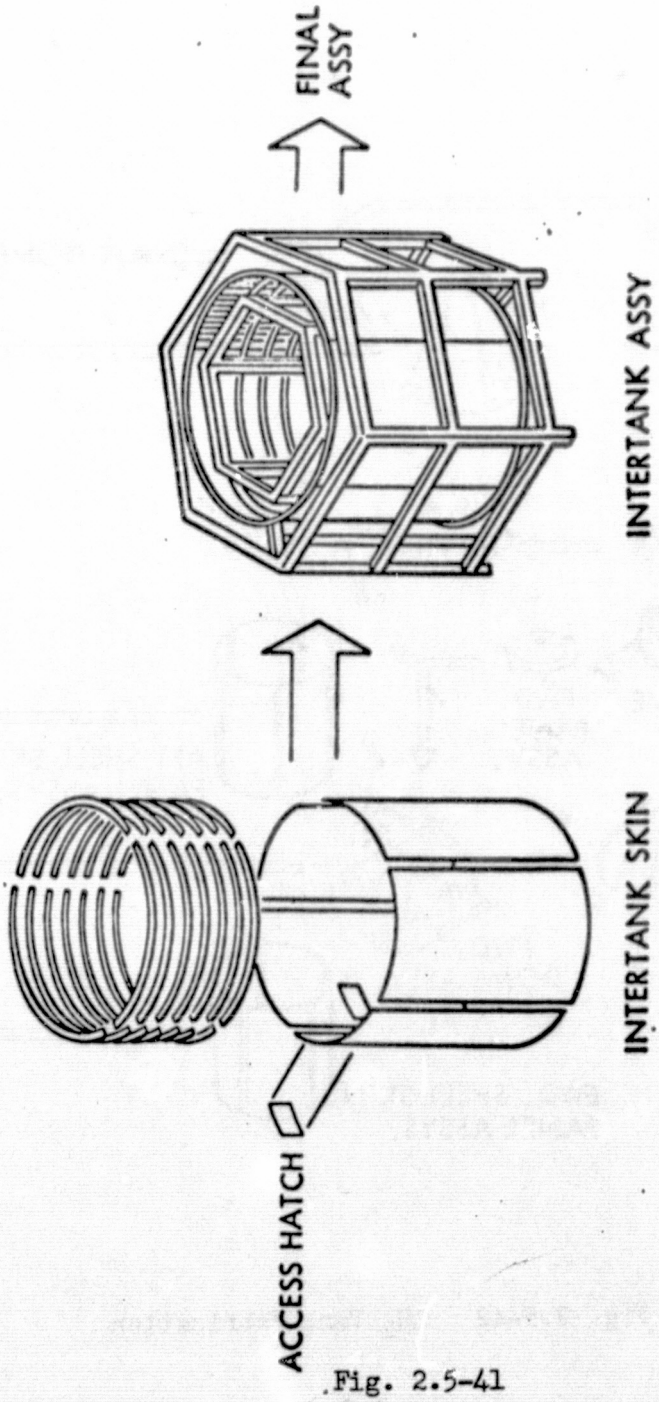

Fig. 2.5-41 Intertank Fabrication and Assembly

Fig. 2.5-41

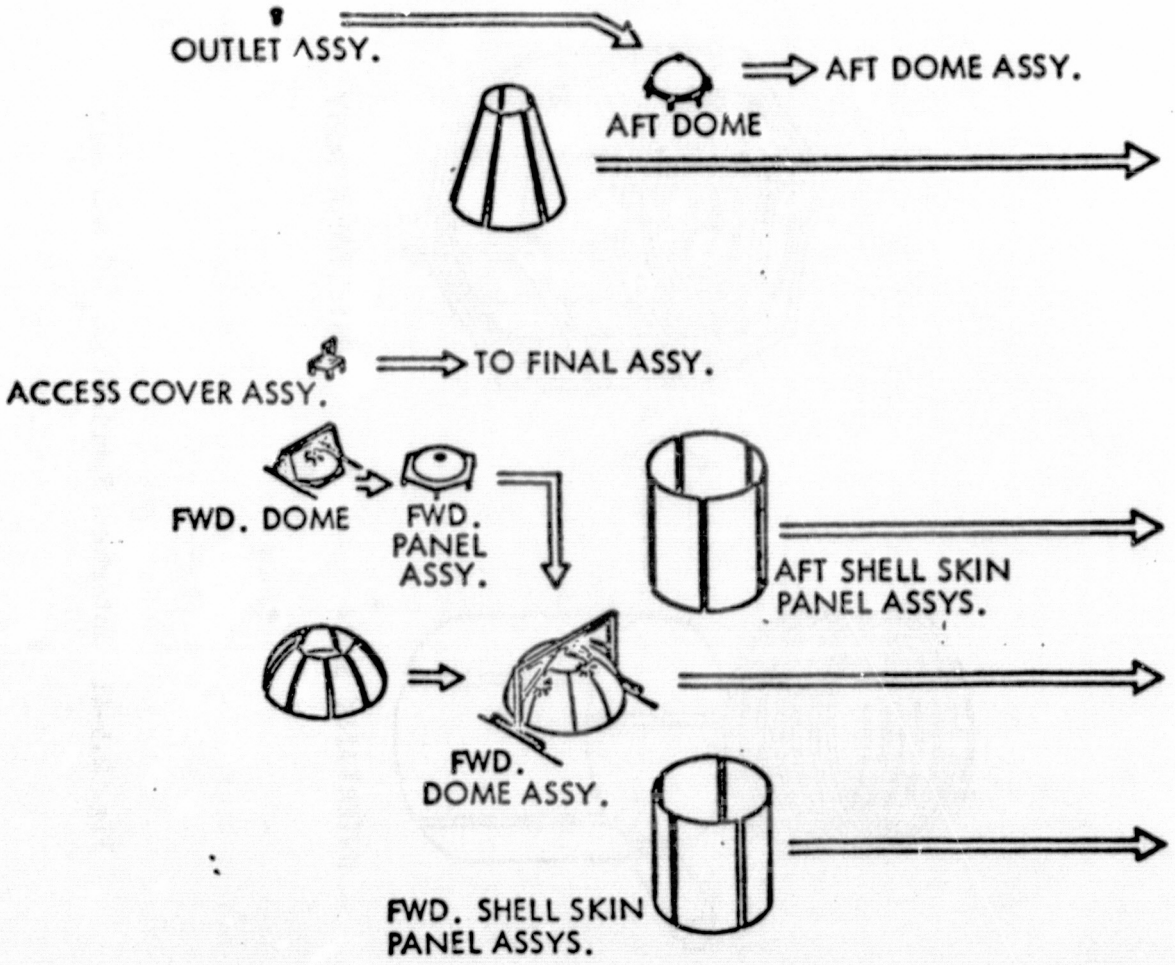

Fig. 2.5-42 LH_2 Tank Fabrication

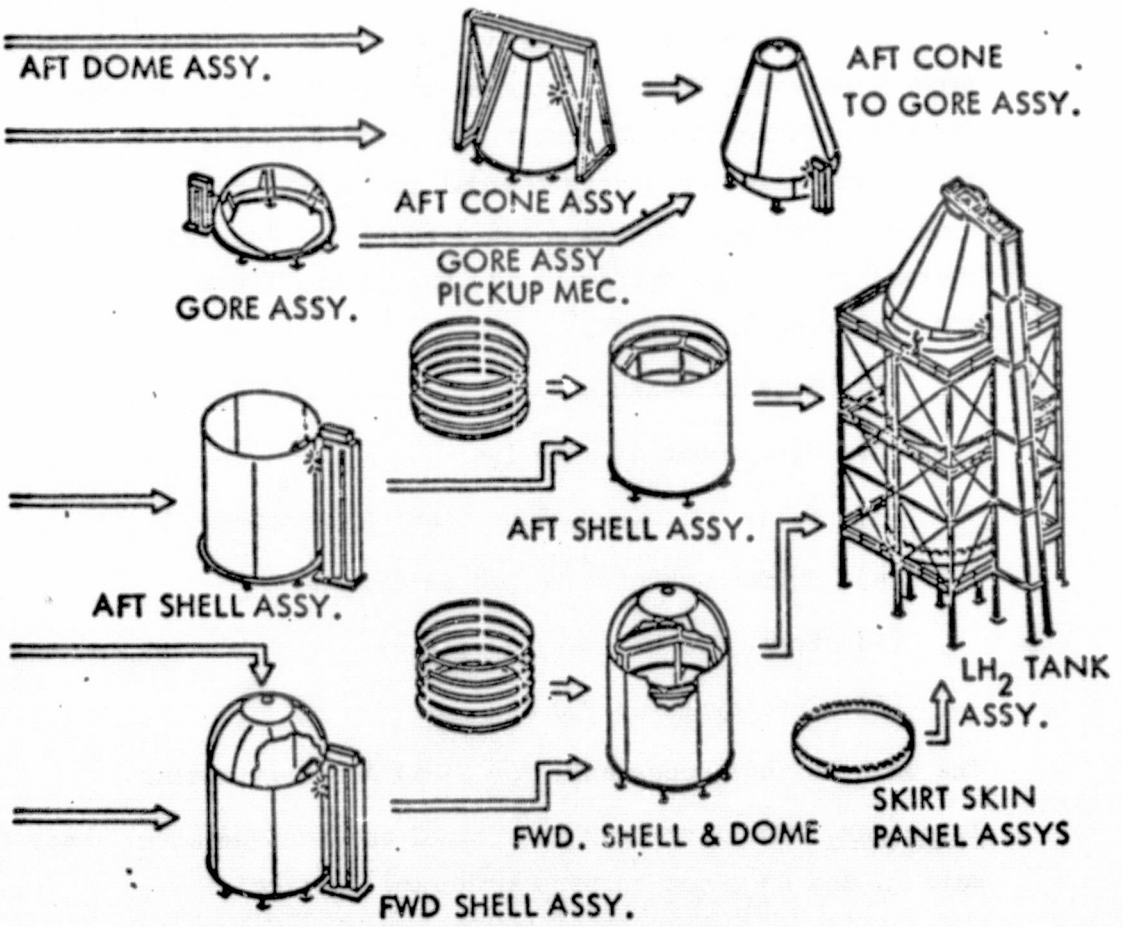

Fig. 2.5-43 LH_2 Tank Assembly

- Final Assembly Operations. The three primary assemblies, LO_2 and LH_2 tanks and intertank, are completed structurally and are then prepared for final installations, tests, acceptance, and mating (Fig. 2.5-44).

LO_2 Tank. The fuel-level sensors, pressure probes, and flat cabling are installed; the tank is then cleaned, black-light inspected, and wipe tests and milipore analysis conducted. The next operation is to proof/leak cycle check at ranges from 24.2 psig to 5 psig for 9 hours. Upon acceptance of cleanliness and proof pressure, the final operation is the installation of the thermal protective system. Cork panels are bonded to the nose dome and conic section. The application of the thermal protection system to the barrel section and aft dome involves the following operations:

(1) External wash and mask

(2) Spray coat of adhesive

(3) Spray of polyurethane foam; 2 in thick

(4) Surface machine to 3/8 in thickness

(5) Spray finish coat (cosmetic)

(6) Cure cycle at 250 deg

The unit is then acceptable for Final Assembly mating.

Intertank. The intertank is cleaned and instrumented, ready for mating, and does not require a thermal coating.

LH_2 Tank. The fuel-level sensors, pressure probes, and flat cabling are installed. Cleaning is accomplished in the same manner as for the LO_2 tank. The proof/leak cycle is accomplished at pressures ranging from 26 psig to 5 psig for 9 hours. Ultrasonic leak detectors and pressure monitoring equipment are utilized. Upon acceptance of cleanliness and pressure/leak tests, the unit is then readied for the application of the thermal protection system. This assembly is then readied for Final Assembly mating.

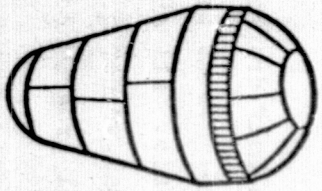

LO_2 TANK

- INSTRUMENTATION
- CLEAN
- PROOF PRESSURE & LEAK TESTS
- THERMAL INSULATION

FINAL ASSEMBLY

- MECHANICAL MATE
- FUEL & OXIDIZER LINES
- INSTRUMENTATION COMPLETE
- FINAL LEAK TEST
- FINAL INSULATION
- ACCEPTANCE

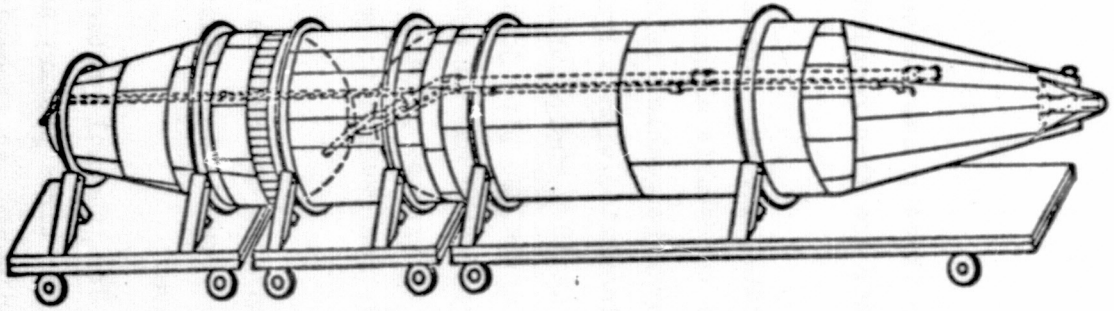

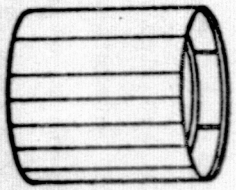

INTERTANK

- INSTRUMENTATION

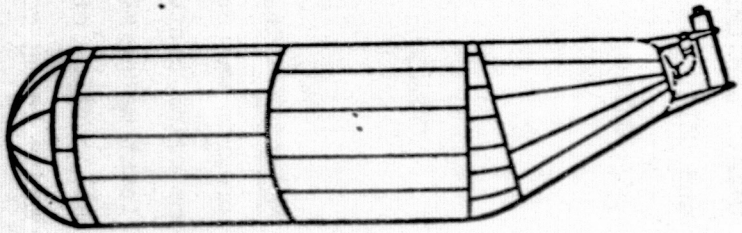

LH_2 TANK

- INSTRUMENTATION
- CLEAN
- PROOF PRESSURE & LEAK TESTS
- THERMAL INSULATION

Fig. 2.5-44 Final Assembly Operations

LOCKHEED MISSILES & SPACE COMPANY

- Final Assembly. The three primary assemblies having completed installations and acceptance are then readied for final mating, acceptance, and delivery.

  The LO_2 tank, intertank, and LH_2 tank assemblies are mated on individual dollies with a three-axis alignment capability. The segments are bolted at the interchangeable field joints. The piping which has been pretested and insulated with polyurethane foam is installed and joined. The system is then repressurized to 5 psig for final leak tests, primarily to check the pipe joints. The instrumentation harnesses are then connected and acceptance tested. The final operation is the installation of precast polyurethane foam at the field joints. The tank assembly is then readied to be positioned to the GFE transporter for delivery.

  The fabrication techniques and methods of assembly utilized by CALAC, GELAC, and LMSC were very similar. Primary differences in the GELAC and CALAC planning are:

GELAC	The thermal protection system is applied after the three primary assemblies are mated. The cleaning is accomplished vertically by a shaker method.
CALAC	Primary weldments and final mating are accomplished in the vertical position.

- Material. The bill of material for the stage-and-one-half droptank program was derived from detailed engineering drawings. Total program material costs were then determined by detailed analysis. All significant material dollar areas were priced based on verbal vendor quotes. All costing effort was based on 1970 prices with total program requirements being considered.

The following is a listing of suppliers who furnished costing data on major cost elements:

Skins and extrusions	ALCOA
Domes	Spincraft, Inc.
Ring forgings (Al)	Ladish Company
Forgings (Ti)	Arcturus Mfg Corp.
Disconnects	Royal Industries, Inc.
Fluid and vent lines	Parsons
Gimbals and bellows	Solar and Avica

2.5.3.7 Cost Estimates. The droptank cost estimate was prepared in accordance with established LMSC estimating and accounting policies and procedures. Basic ground rules and program concepts were established early in the estimating cycle and used to generate a well-defined baseline cost for the development and production of droptanks. The following assumptions were used, as discussed earlier:

- Drop Tank Program separate contract(s) from Orbiter Program
- Estimate in two phases:
  - Design, Development, Test and Evaluation (DDT&E)
  - Production
- Production Hardware

	Sets of Droptanks
- Development Test Article	Equivalent to 3 sets
- Flight Hardware	445
- Spare Hardware	5

- Schedule

- DDT&E Go-Ahead	1 January 1972
- Production Go-Ahead	4th Quarter 1972
- Final 60 sets of tanks delivered	1986

- All costs in 1970 dollars including 10 percent fee
- No Program Phaseout cost included
- Final Assembly Facility available at KSC
- Effort under Production Phase on each droptank set is complete when the tank has completed final acceptance checks. No storage, mating, or erection costs are included, since these are assumed to be part of operations costs.
- Test Facilities for Full-Scale Development/Qualification Testing at MSFC and MTF are available and are modified as necessary and operated by NASA

Work Statements were prepared for both DDT&E and Production Phases and distributed with the Droptank drawings to organizations responsible for performing tasks to develop and produce the droptanks. These responsible organizations then prepared detailed estimates of the resources (manhours, material, computer usage, etc.) necessary to perform their required effort. These resource estimates were identified by the estimators to WBS elements (Fig. 2.5-45) and spread by time as required to meet development and delivery schedules. Once the raw resource requirements were developed, the responsible Industrial Accounting personnel applied appropriate rates to arrive at the total program costs as estimated by LMSC.

The following table summarizes the results of LMSC's drop tank estimate. Additional detail is presented in the following discussion.

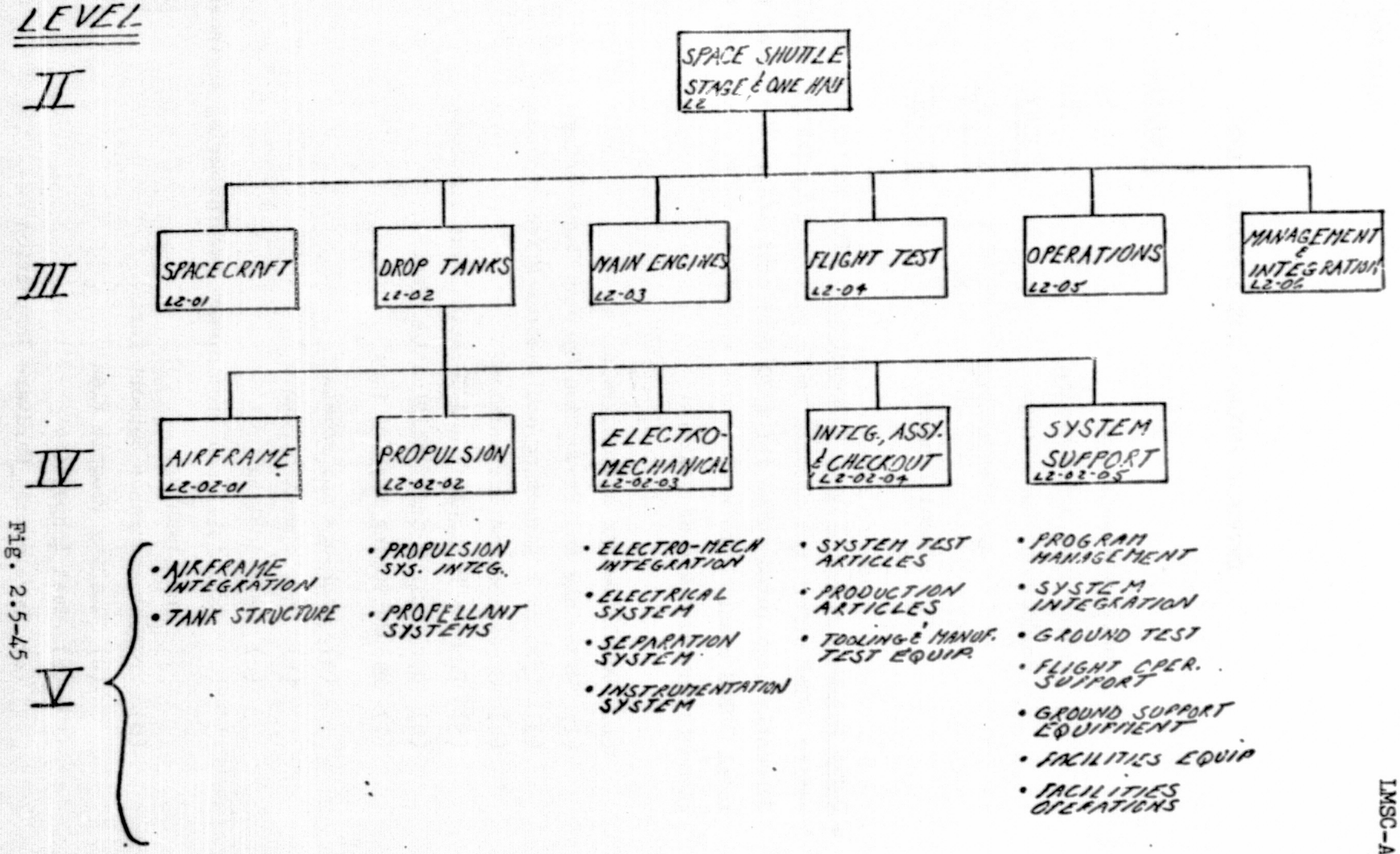

Fig. 2-5-45 Stage-and-One-Half Droptanks — DDT&E + PROD.

DROPTANK PROGRAM COST SUMMARY - LMSC

	$ Millions
DDT&E, Nonrecurring	65
Production, Nonrecurring	182
Production, Recurring	1,832
Total Production	$ 2,014
Total Program	$ 2,079

- DDT&E Estimate - $65 Million Nonrecurring. For costing purposes, the entire DDT&E effort was assumed to be performed by LMSC/Sunnyvale. Currently negotiated rates for 1970 were utilized to arrive at the total DDT&E costs. The results are summarized in Fig. 2.5-46; the cost elements included are as follows:

  (1) Detail Design and Analysis
  (2) Materials and Production Systems Engineering
  (3) Systems Engineering and Systems Effectiveness
  (4) Specification Preparation
  (5) Program Management and Technical Publications
  (6) Development and Qualification Testing
  (7) Manufacturing Support for:
    (a) Mock-ups and models
    (b) Development hardware
    (c) Soft tooling
    (d) Facilities and preliminary manufacturing engineering and planning
  (8) Product Assurance Support for:
    (a) Quality Program Plan
    (b) Test Inspection
    (c) Development Hardware Inspection

	MANHOURS (Thousands)	$ (Millions)
PROGRAM MANAGEMENT	141	2.7
ENGINEERING	1,467	27.7
TEST AND OPERATIONS SUPPORT	802	15.1
MANUFACTURING	696	12.2
PRODUCT ASSURANCE	310	5.2
MATERIAL AND COMPUTER	-	2.4
TOTAL	3,416	$65.3

Fig. 2.5-46 Non-Recurring DDT&E Cost

(9) Material:
- (a) Mock-ups
- (b) Development hardware and soft tooling
- (c) Test fixtures

- Production Estimate - $182 Million Nonrecurring; $1,832 Million Recurring. As a result of the size of the Droptank Production Program and the resources required, the LMSC manufacturing organization prepared their estimate based on fabrication labor being performed in three different subassembly plants and final assembly at one facility. For estimating and costing purposes, the subassembly plants were assumed to be three Lockheed Aircraft Corporation divisions: Lockheed Missiles & Space Company, Sunnyvale, California; Lockheed-California Company, Burbank, California; and Lockheed-Georgia Company, Marietta, Georgia. The rates used in costing effort at these three locations are currently negotiated 1970 rates and are believed to be representative of the rates that exist throughout the aerospace industry. The final assembly facility was assumed to be located at KSC and the rates used for effort at KSC are based on a labor rate representative of the southeastern U.S. and overhead rates developed by LMSC based on current manufacturing overhead rates at LMSC adjusted to reflect reductions resulting from effort being performed at a Government facility.

The nonrecurring production costs of $182 million (Fig. 2.5-47) include the following cost elements:

(1) Manufacturing
- (a) Initial planning
- (b) Tool design
- (c) Initial tool fabrication
- (d) Manufacturing Test Equipment (MTE) Design and Fabrication

	MANHOURS (Thousands)	$ (Millions)
MANUFACTURING	8,877	131.2
PRODUCT ASSURANCE	364	5.2
MATERIAL		18.3
SPECIAL MACHINERY		27.0
TRANSPORTATION		0.6
TOTAL	9,241	$182.3

Fig. 2.5-47 Non-Recurring Production Cost

(e) Manufacturing Engineering and Research
(f) Methods and Time Standards
(g) Initial Packaging and Handling
*(h) Fabrication and assembly of full-scale test hardware (equivalent to 3 sets of droptanks) and a Manufacturing Development Unit (MDU) (1 set of droptanks)

(2) Product Assurance
(a) Initial Quality Engineering
(b) Tooling Inspection
(c) Test Hardware Inspection
(d) Initial Source Product Verification

(3) Material
(a) Material for equivalent of 4 sets of droptanks
(b) Tooling and MTE

(4) Transportation costs from supplier and subassembly plants to assembly facilities for the Test Hardware and MDU and transportation of test hardware to test facilities.

(5) Special fab and assembly machinery and equipment.

The recurring production costs of $1,832 million (Fig. 2.5-48) include the following cost elements:

(1) Manufacturing
(a) Fabrication and assembly of 450 sets of droptanks
(b) Sustaining tool design and maintenance
(c) Sustaining planning and manufacturing engineering
(d) Sustaining packaging and handling

*NOTE: Development and Qualification Testing Costs of Full-Scale Test Hardware included in DDT&E estimate.

	MANHOURS (Thousands)	$ (Millions)
PROGRAM MANAGEMENT	466	7.6
SUPPORT ENGINEERING	157	2.6
MANUFACTURING	42,763	636.0
PRODUCT ASSURANCE	6,713	95.5
MATERIAL		1,074.6
TRANSPORTATION		15.7
TOTAL	50,099	$1832.0

Fig. 2.5-48 Recurring Production Cost

(2) Product Assurance
   (a) Sustaining Quality Engineering
   (b) Fab and Assembly Inspection
   (c) Continuing Source Product Verification

(3) Program Management and Support Engineering

(4) Material for 450 sets of droptanks

(5) Transportation from supplier and subassembly plants to assembly facility

- Conclusions. The distribution of costs by cost element (Fig. 2.5-49), by hardware item, and by material type (Fig. 2.5-50) resulted in the identification of areas requiring further design effort and continuing cost analysis to ensure the design and development of the lowest cost droptanks consistent with system requirements. The prime cost drivers identified are the ring forgings, the thrust-cone forgings, and the thick plates from which integrally stiffened skin panels are machined. The distribution of costs by time (Figs. 2.5-51 and 2.5-52) indicates the necessity for a commitment of substantial nonrecurring costs for planning and tooling to enable a manufacturer to attain the lowest possible recurring production costs.

2.5.3.8 Summary of Cost Estimates. In an earlier section, details of the LMSC production and cost estimating effort was described and essential differences between the approaches taken by LMSC, GELAC, and CALAC were discussed. This section shows, in summary form, the results of the three independent costing estimates (Fig. 2.5-53), and the differences in estimates for the major cost elements (Production labor, Quality Assurance labor, Material and others). The total program cost for producing the required 453 sets of droptanks ranges from $2.08 billion to $3.45 billion, representing an average cost of $4.6 million to $7.6 million for each droptank set. With a dry weight

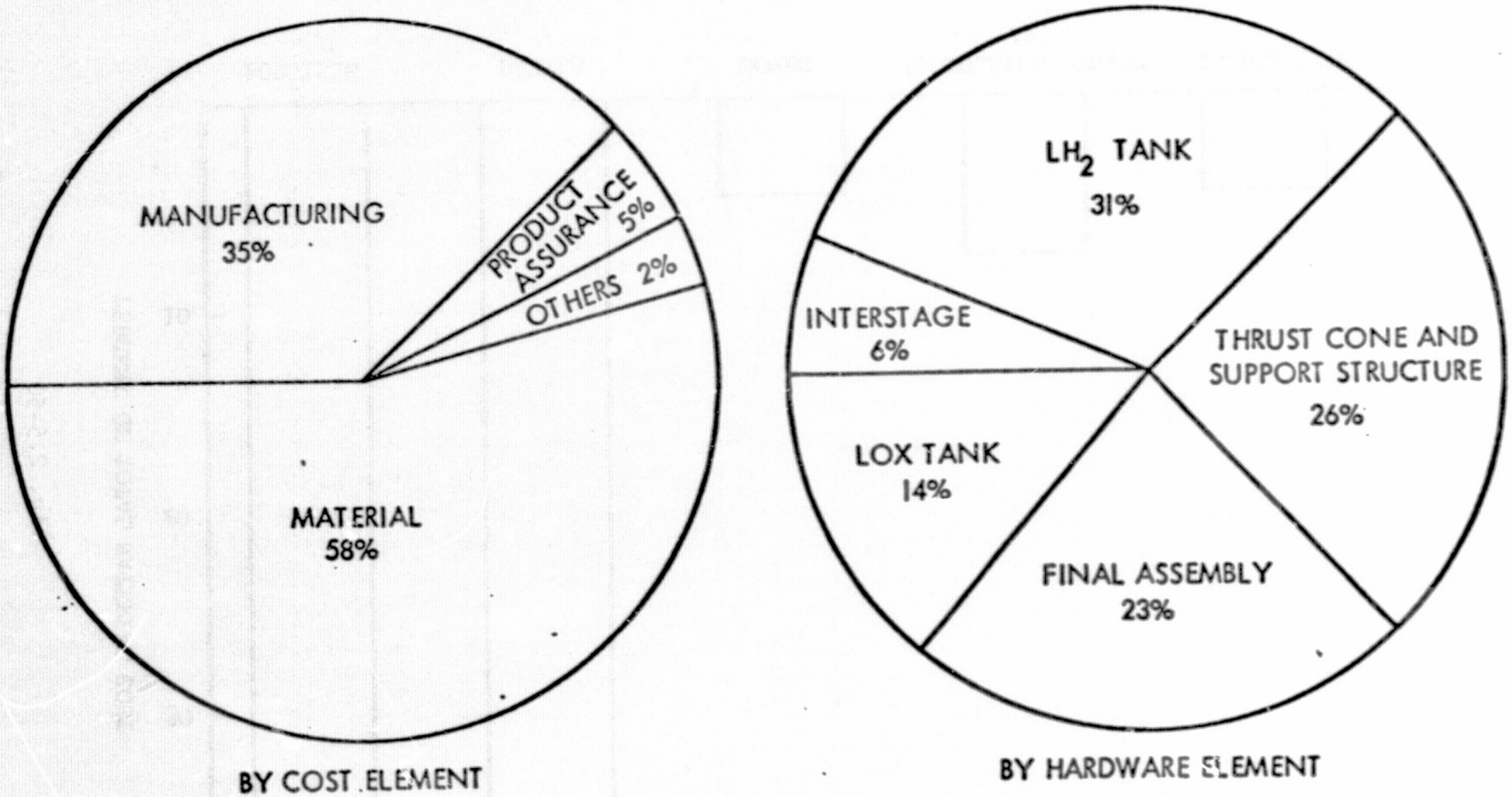

Fig. 2.5-49 Recurring Production Cost Distribution

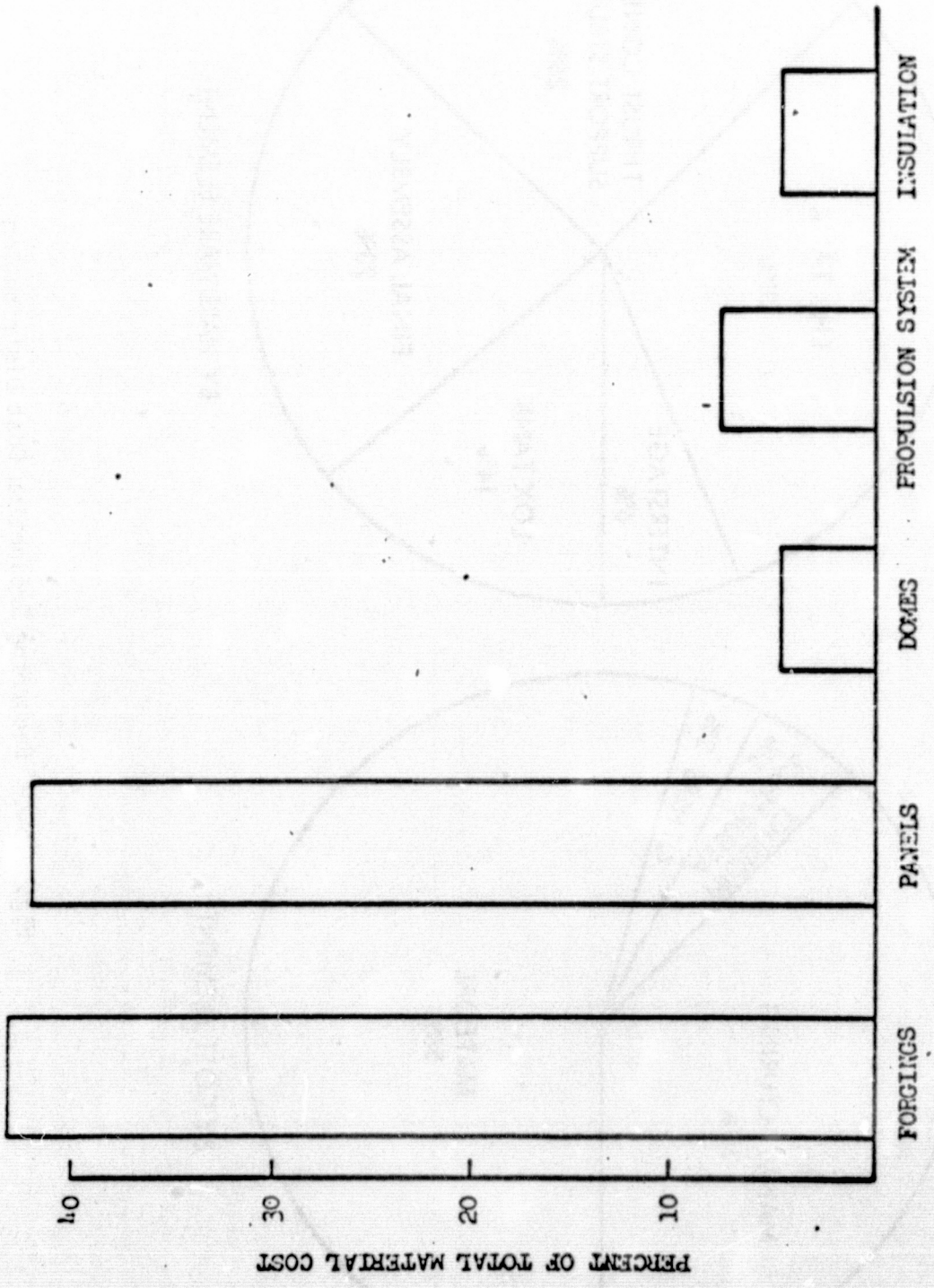

Fig. 2.5-50 Material Cost Distibution - LMSC

Fig. 2.5-50

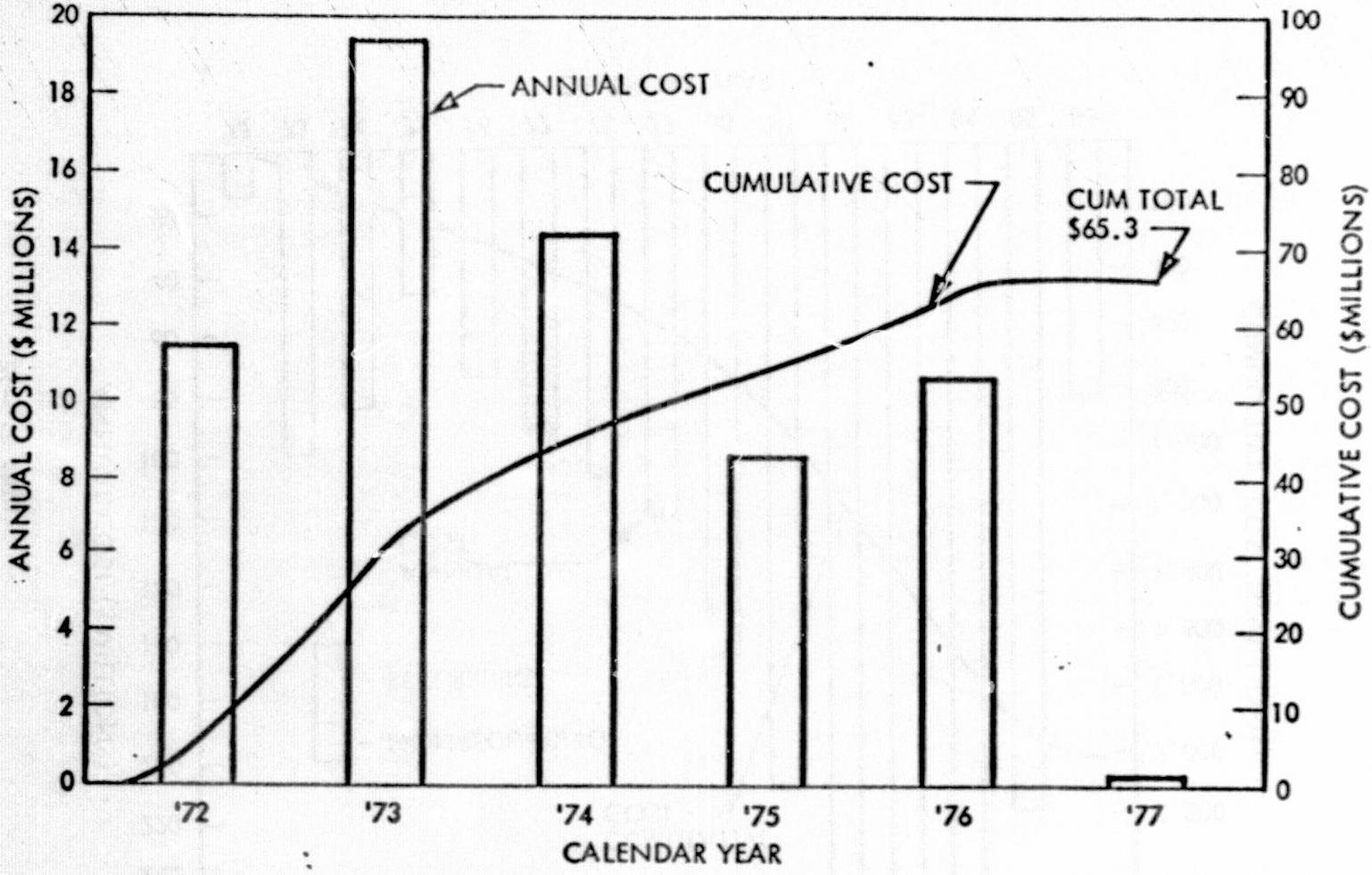

Fig. 2.5-51 DDT&E Cost Distribution - LMSC

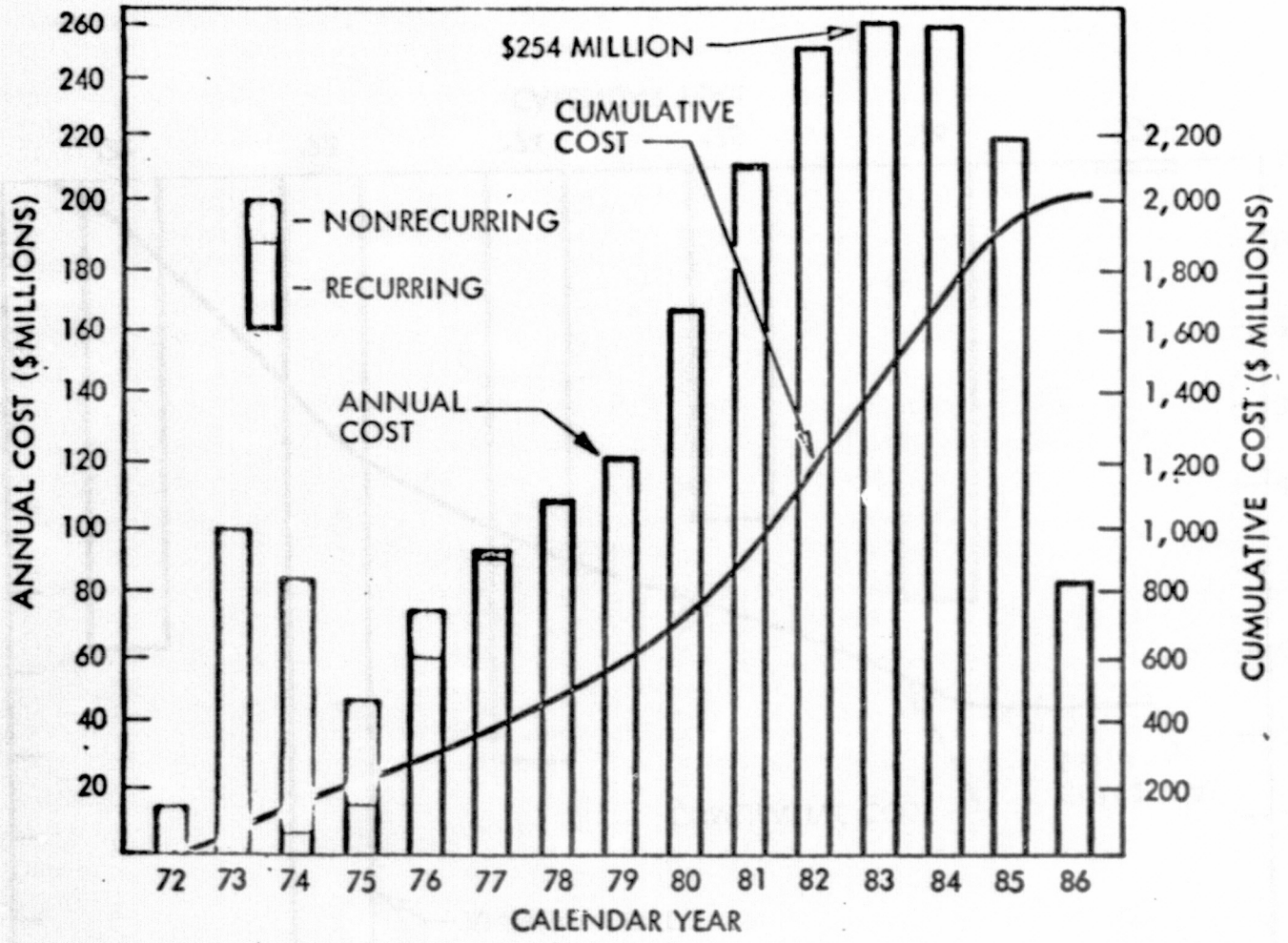

Fig. 2.5-52 Production Cost Distribution - LMSC

Fig. 2.5-52

2.5.3-(c)

2.6 AERODYNAMICS

2.6.1 Introduction

Aerodynamic characteristics are presented for the entry and launch configurations of the Lockheed version of the stage-and-one-half concept. The system consists basically of a reusable delta lifting-body orbiter on which are installed the total ascent propulsion system and expendable propellant droptanks.

2.6.2 Aerodynamic Requirements (Orbiter)

Several basic aerodynamic requirements have been imposed on the orbiter configuration – either from the NASA or from Lockheed. Since the majority of entry flight time is in the subsonic and hypersonic speed regimes, the aerodynamic design emphasis has been largely influenced by the requirements associated with these particular regimes. The basic aerodynamic performance philosophy is to attain the majority of the required 1100-nm crossrange through the use of the hypersonic lift-to-drag ratio (L/D) and to achieve adequate subsonic L/D for an acceptable landing approach; subsonic L/D also significantly impacts the orbiter ferry-range capability. Therefore, the transonic/supersonic performance has been purposely desensitized-the prime requirements in this regime being stability and control. Neutral or better longitudinal, lateral, and directional static stability have been emphasized throughout the operating attitudes and Mach numbers. Sufficient trim authority must be available to accommodate the center-of-gravity extremes afforded by the various payload combinations – both with and without airbreather engines. When aerodynamic heating is severe, an additional requirement has been imposed to limit the windward trim and control surface deflections to 5 deg or less thus assuring TPS material compatibility with anticipated thermal environment.

2.6.3 Configuration Description (Orbiter)

The orbiter is a delta planform lifting-body with appropriate aerodynamic surfaces, configured for adequate performance, stability, and control. Leading

edge sweep and radii have been parametrically studied to assure aerodynamic and aerothermodynamic compatibility. A triangular, flat-bottom body surface is required to assure a successful compromise between subsonic trim and hypersonic longitudinal stability and trim. The aft body is shaped to eliminate flow separation and to minimize the large base area associated with the stage-and-one-half concept. Aft-body compression-sharing surfaces have been utilized in an attempt to optimize the basic body shape for hypersonic yaw stability considerations. Ideally, the body sides are rolled in to prevent excessive heating, drag, and loss of directional stability at the hypersonic design angle-of-attack. To facilitate improved packaging capability — specifically where it enhances a forward cg location — the forebody side roll-in requirement has been relaxed to some extent.

To accommodate the aft cg locations inherent in the delta-body stage-and-one-half orbiter, the addition of aerodynamic surfaces is necessary to provide acceptable longitudinal and directional static stability margins. Two aft-mounted side fins have been sized and positioned (toe-in and rollout), based on directional stability requirements throughout the operating speed regime. Also, the fins contribute significantly to the low-speed lift-to-drag performance and longitudinal stability.

An aft trim flap hinged at the body-bottom base has been sized to allow acceptable hypersonic stability and subsonic trim authority. Pitch control is accomplished by deflection of two elevon surfaces which comprise the aft portion of the trim flap. These same surfaces can be differentially deflected for roll control and roll damping.

Roll coordination, dutch roll mode damping, crosswind landing and sideslip control capability, pitch trim authority, and hypersonic yaw stability are provided by two rudders (one on each fin). A speed brake-control surface is located beneath each rudder to provide glide path control and also can be used to increase hypersonic yaw stability.

Two elevons are mounted on the orbiter upper surface between the vertical fins. The functions of these surfaces are roll control and damping, takeoff rotation, landing trim and derotation, transonic/supersonic pitch stability, and trim authority.

2.6.4 Flight Characteristics (Orbiter)

An experimental wind tunnel program was funded under the Alternate Concept Study to investigate the aerodynamic characteristics of the Lockheed (LS 200-5) delta lifting-body orbiter and the stage-and-one-half launch vehicle in the NASA Ames 6 ft x 6 ft and the Langley Unitary Plan Wind Tunnels. Concurrent with this contract effort, a 0.03 scale model of the LS 200-5 orbiter with parametric variations was designed, fabricated, and tested by LMSC in the Lockheed 8 ft x 12 ft Low Speed Wind Tunnel. The objectives of both programs respectively were: (1) to provide an experimental data verification of the aerodynamic estimates, and (2) to define a credible baseline of data for future engineering studies.

The current orbiter configuration, identified as LS 200-10, utilized the findings of the LS 200-5 wind tunnel tests and, consequently, reflects minor external geometry differences. Unless noted otherwise, the LS 200-5 aerodynamic characteristics presented in the following discussion are considered to be representative of the current LS 200-10 design.
The stage-and-one-half orbiter, depending upon mission requirements, can have a cg location between 75.1 and 78 percent of the reference length (146 ft) i.e. F.S. 1316 and 1367, respectively. The following charts will present pertinent aerodynamic characteristics throughout the entry speed regime, emphasizing these two centers-of-gravity and the flexibility of the delta-body orbiter to accommodate these extremes.

These data will be discussed by speed regime - subsonic, transonic/supersonic and hypersonic - followed by summary charts of general aerodynamic characteristics and specific cases relating the reference entry trajectory. Figure 2.6-1 identifies the axis system and the nomenclature used throughout this section.

2.6.4.1 Subsonic. A low-speed wind tunnel test (Fig. 2.6-2) was conducted at the Lockheed 8 ft x 12 ft Low-Speed Wind Tunnel on a 0.03 scale model of the delta lifting-body orbiter. A wide variety of configuration combinations were run in an effort to optimize the low-speed aerodynamic configuration (see Ref. 2.6-1). Figure 2.6-3 indicates acceptable longitudinal stability and trim characteristics for the anticipated center-of-gravity extremes. The trim lift coefficients and lift-to-drag ratio are presented in Fig. 2.6-4. Maximum trimmed lift-to-drag ratios of 5.45 and 5.85 are predicted for the fore and aft cg, respectively. All L/D data include the total drag of the vehicle (including realistic base drag). Landing speeds have been computed at various angles-of-attack using the aforementioned trimmed lift coefficients. Again, the mission extremes have been presented to illustrate the range of anticipated landing speeds and attitudes (Fig. 2.6-5).

Condition	Landing Speed at $\alpha_{L/D_{Max}}$	Landing Speed at $\alpha^*_{Tailscrape}$
40K lb Cargo In/Airbreather Engines Out (Most Forward CG)	195 Kt	164 Kt
Cargo Out/Airbreather Engines In (Most Aft CG)	182 Kt	146 Kt

*Tailscrape = 22 deg

It should be emphasized that ground effects have not been included but are available and indicate reduced landing speeds and/or attitudes from those shown in the above table.

2.6.4.2 Transonic/Supersonic. A 0.01 scale steel model of the orbiter configuration was tested in the NASA/Ames 6 ft x 6 ft tunnel and the NASA/Langley Unitary Plan Wind Tunnel (see Fig. 2.6-6). The majority of effort

was concentrated on obtaining configuration combinations which would allow acceptable static stability and trim authority for the cg range. Considerable pitch and sideslip data are available between Mach 0.6 and 4.6 (see Section 3.5, Ref. 2.6-2). Figure 2.6-7 presents the longitudinal stability and trim characteristics at Mach 1.2 and is typical of this speed regime.

2.6.4.3 Hypersonic. Hypersonic characteristics are presented in Figs. 2.6-8 and 2.6-9. These are based on the Hypersonic Arbitrary Body Computer Program modified to reflect previously obtained increments between experimental and analytical results on a similar configuration.

The vehicle is longitudinally stable and trimmable over a wide range of angles-of-attack. Consistent with the anticipated thermal environment and the thermal protection system material, no windward deflections in excess of 2 deg are required for hypersonic trim. Maximum trimmed L/Ds of 1.62 to 1.65 are attained for the fore and aft cg location. The LS 200-10 configuration has a hemispherical nose cap, rather than the 2:1 ellipsoid of revolution employed by LS 200-5. Also, it has reduced fin leading edge radii. These differences should produce decreased hypersonic drag resulting in maximum trimmed L/Ds of 1.87. No significant change in stability would be predicted.

2.6.4.4 Summary. Directional stability has been expressed in terms of the dynamic yaw-stability derivative, $C_{n_{\beta_{Dynamic}}}$, where:

$$C_{n_{\beta_{Dynamic}}} = C_{n_{\beta_{Body\ Axis}}} \cos\alpha - C_{\ell_{\beta_{Body\ Axis}}} \sin\alpha \left(\frac{I_{zz}}{I_{xx}}\right)$$

Figures 2.6-10 through 2.6-12 are plots of $C_{n_{\beta_{Dynamic}}}$ versus Mach number and angle-of-attack at various rudder combinations; rudders deflected in 20 deg, 0 deg, and out 10 deg. The selected mode of rudder biasing is dependent on the Mach number. Emphasizing aerodynamic heating constraints, the rudders are nominally set at 0 deg above Mach 6.0. In the speed regime of Mach 2 to 6, the rudders

are flared 10 deg out to increase directional stability, thus effectively increasing the angle-of-attack range where stability is maintained. The rudders are biased inward 20 deg between Mach 0.6 to 2.0 to improve the trim authority as required for the far forward cg locations. In the landing approach (Mach 0.6 to touchdown), the rudders have been nominally set at 25 deg and 15 deg in for the fore and aft cg location, thus taking advantage of the positive trim pitching moment increment, increased L/D, and slightly increased longitudinal stability offered by the rudder biasing.

Maximum trimmed lift-to-drag ratio is presented versus Mach number for the cg extremes. Full-scale subsonic conditions indicate trimmed L/D_{Max} of 5.45 and 5.85 and 1.62 and 1.65 for the hypersonic conditions (see Fig. 2.6-13). The hypersonic L/Ds are representative of flight conditions at Mach 20 and 200,000 ft altitude. As previously discussed under hypersonic lift-and-drag characteristics, (Fig. 2.6-9), the maximum trimmed L/D of the LS 200-10 orbiter is estimated at 1.87 rather than 1.65.

The most descriptive summary plots illustrating the delta-body orbiter flight capability are shown in Figs. 2.6-14 and 2.6-15. These plots clearly illustrate the trimmed angle-of-attack range, where neutral or better static stability are achieved by indicating the boundaries where neutral stability occurs. The figures also indicate areas where the boundaries are determined by criteria other than stability -- e.g. pitch trim authority. As can be observed from both figures, there is a sizable operating corridor throughout the entry Mach numbers where the vehicle is statically stable and trimmable. There are "NO OPERATING AREAS OF AERODYNAMIC INSTABILITY."

Figure 2.6-16 is a typical reference entry trajectory for the high-crossrange mission -- illustrating angle-of-attack, Mach number, altitude, and crossrange. Since the majority of crossrange is attained at hypersonic speeds, considerable freedom is available to tailor the trajectories below Mach 6.0 to conform with the aforementioned aerodynamic operating corridor. Figures 2.6-17 and 2.6-18

present the pitch stability margin and the directional stability summaries of the delta-body orbiter for this particular reference entry trajectory. As is evident, the configuration is longitudinally and directionally stable and attains at least 1100-nm crossrange for all cases.

In conclusion, it can be stated that the Lockheed delta lifting-body orbiter has excellent aerodynamic characteristics and is acceptable as a candidate for the space shuttle orbiter.

2.6.5 Aerodynamic Requirement (Launch Vehicle)

Aerodynamic performance considerations have been minimal in the launch vehicle system arrangement. However, acceptable relationships between the launch system center-of-gravity locations with available aerodynamic static stability and engine gimbal-control capability – have influenced the tank placement on the orbiter. Also, the tanks forebody shape and arrangement was considered in trade studies on minimizing ascent drag losses.

2.6.6 Configuration Description (Launch Vehicle)

The launch configuration consists of the previously described orbiter with two external side-mounted propellant (LO_2 and LH_2) droptanks. These are described in considerable detail in Section 2.5. The launch vehicle axis system is referenced to the orbiter system shown in Fig. 2.6-1. All moments are referenced about the launch vehicle nose station with the reference length equal to 2472 in. and the reference area equal to 12,463 ft^2.

2.6.7 Flight Characteristics (Launch Vehicle)

The stage-and-one-half launch configuration was tested between Mach Number 0.6 and 2.0 in the NASA Ames 6 ft x 6 ft Wind Tunnel (Fig. 2.6-19) with the transonic region of maximum dynamic pressure being of most interest. Carpet

plots of the vehicle's normal force, axial force, and pitch stability characteristics with Mach number ($0.6 < M_\infty < 2.0$) and angle-of-attack ($-6 \text{ deg} < \alpha_{nom} < 10 \text{ deg}$) are presented in Figs. 2.6-20 through 2.6-22. A summary of pertinent longitudinal linear characteristics (normal force coefficient slope, pitch-plane aerodynamic center location, and zero lift-drag coefficients) is shown in Fig. 2.6-23. A similar summary of lateral-directional characteristics (side-force derivative, yaw-plane aerodynamic center location, and rolling-moment derivative) is presented in Fig. 2.6-24.

The pretest estimates have also been included on these summary plots and are indicative of reasonable correllation. Comparing with the estimated aerodynamic characteristics, the data show less drag, more C_{N_α}, approximately the same pitch plane aerodynamic center location, further aft yaw plane aerodynamic center locations, and more negative C_{ℓ_β}

REFERENCES

2.6-1 H. Drosdat: Low Speed Testing of a Lockheed Delta Body Space Shuttle Reentry Vehicle, LMSC-A990514

2.6-2 F. Velligan and H. Svendsen: Aerodynamic Characteristics of the Lockheed Delta-Body Orbiter and Stage-and-One-Half Launch Vehicle, LMSC-A989204

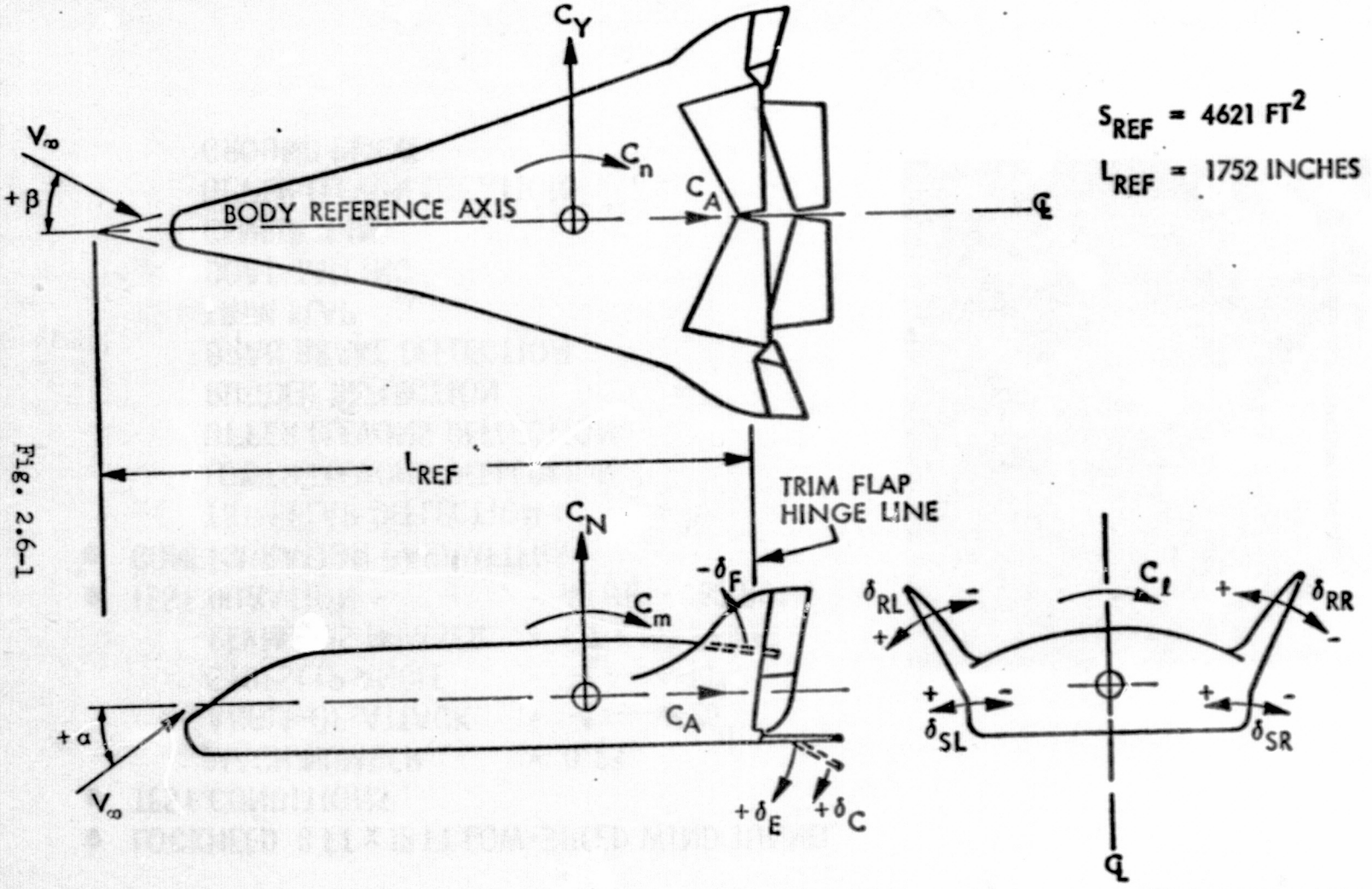

Fig. 2.6-1 Orbiter Body Axis System

LOW-SPEED WIND TUNNEL TEST

- LOCKHEED 8 FT x 12 FT LOW-SPEED WIND TUNNEL
- TEST CONDITIONS
  - MACH NUMBER = 0.23
  - ANGLE-OF-ATTACK = $-4 \longrightarrow 26^{0}$
  - SIDESLIP ANGLE = $-4 \longrightarrow 10^{0}$
  - REYNOLDS NUMBER = 1.7×10^{6} PER FT
- TEST DURATION = 40 HR – 60 RUNS
- CONFIGURATION PARAMETERS
  - TRIM FLAP DEFLECTION
  - LOWER ELEVONS DEFLECTION
  - UPPER ELEVONS DEFLECTION
  - RUDDER DEFLECTION
  - DRAG BRAKE DEFLECTION
  - TRIM FLAP
  - BOAT-TAILING
  - CENTER FIN
  - UPPER ELEVON LOCATION
  - GROUND PLANE



Fig. 2.6-2 Low-Speed Wind Tunnel Test

Fig. 2.6-2

fav
3-2-71
D02552(1)

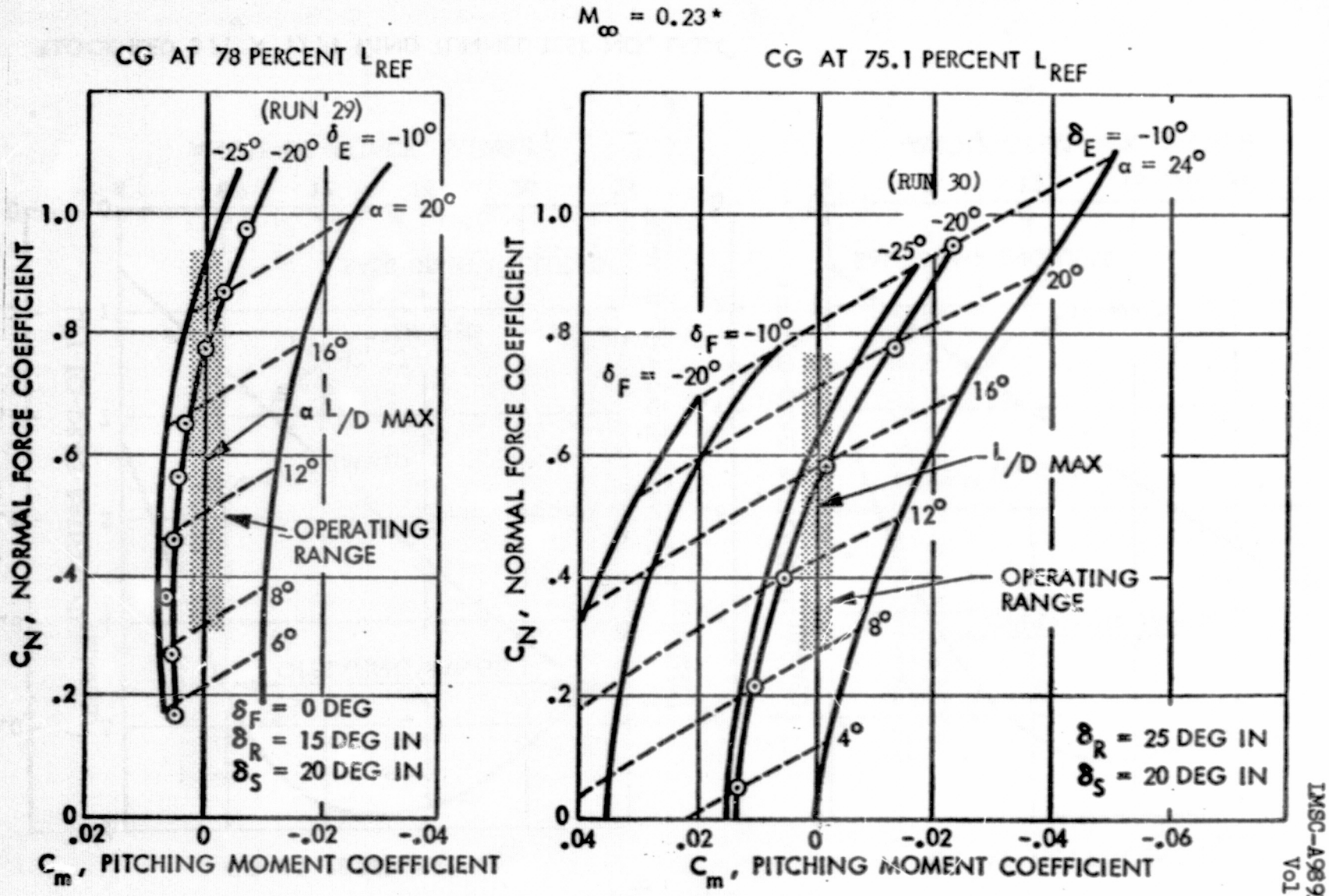

*LOCKHEED 8 FT X 12 FT WIND TUNNEL TEST L-324

Fig. 2.6-3 Longitudinal Stability and Trim

LOCKHEED MISSILES & SPACE COMPANY

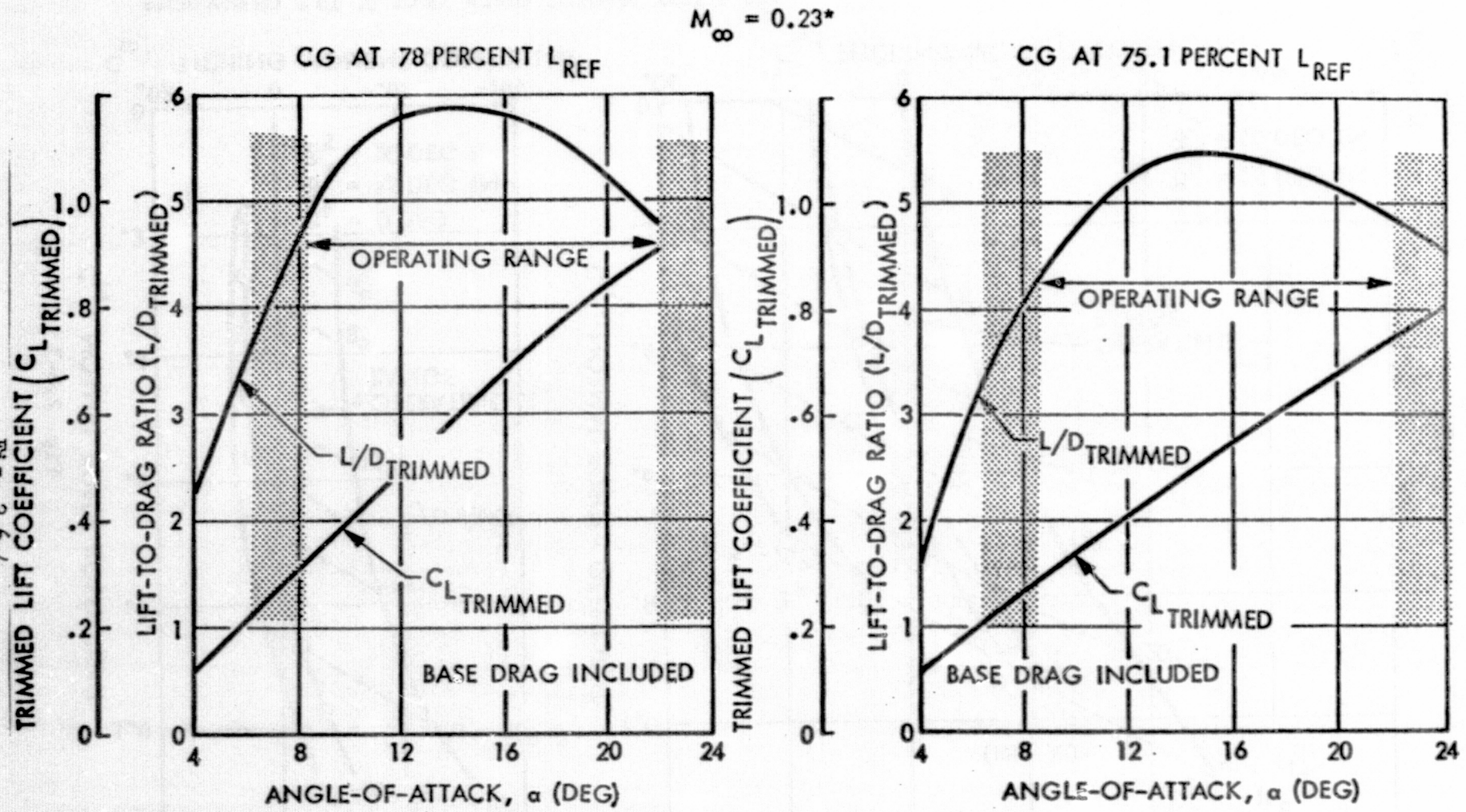

*LOCKHEED 8 FT X 12 FT WIND TUNNEL TEST NO. L-324

Fig. 2.6-4 Lift and Drag Characteristics

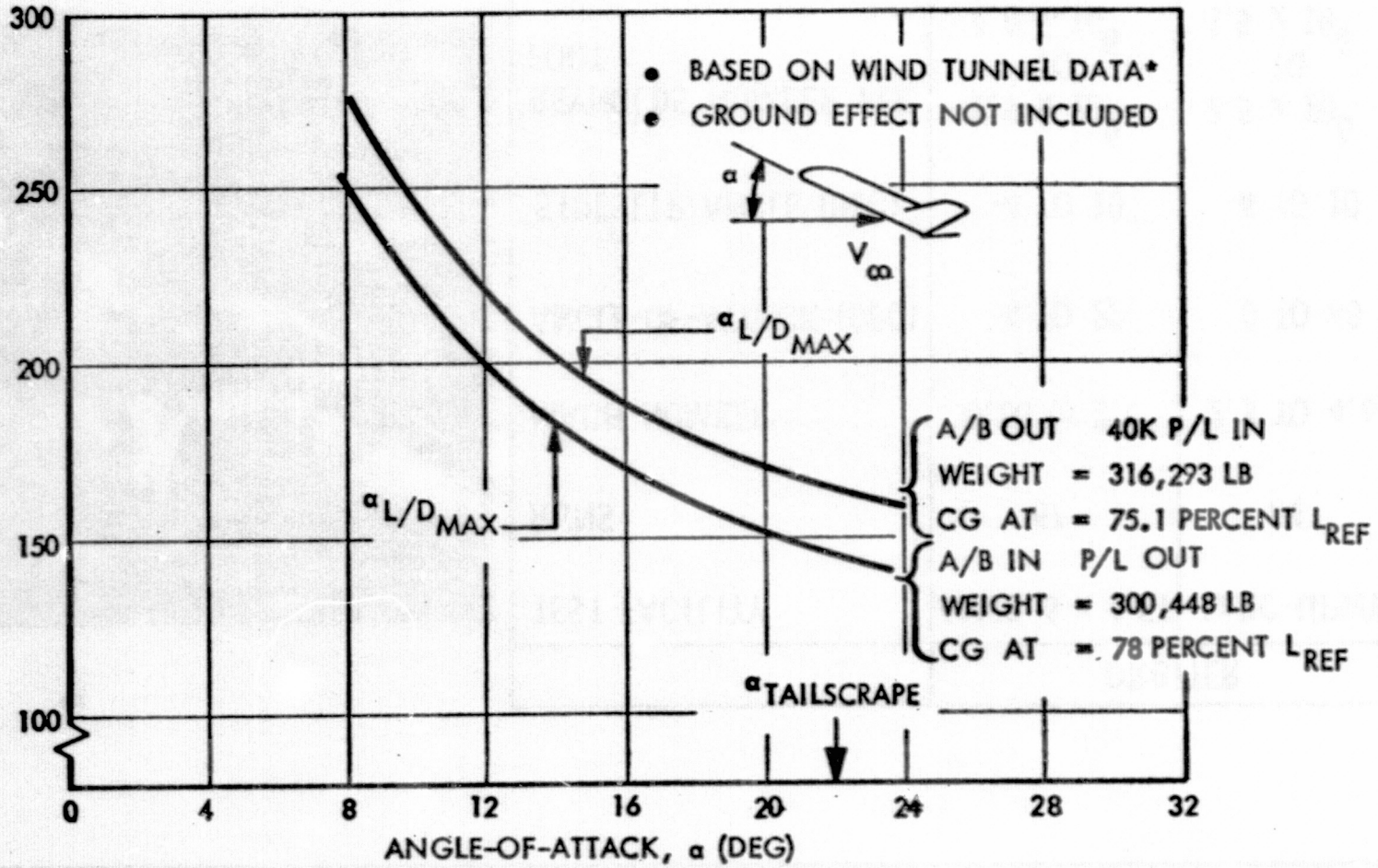

*LOCKHEED 8 FT X 12 FT WIND TUNNEL TEST NO. L-324

Fig 2.6-5 Landing Speed and Attitude

ORBITER CONFIGURATION

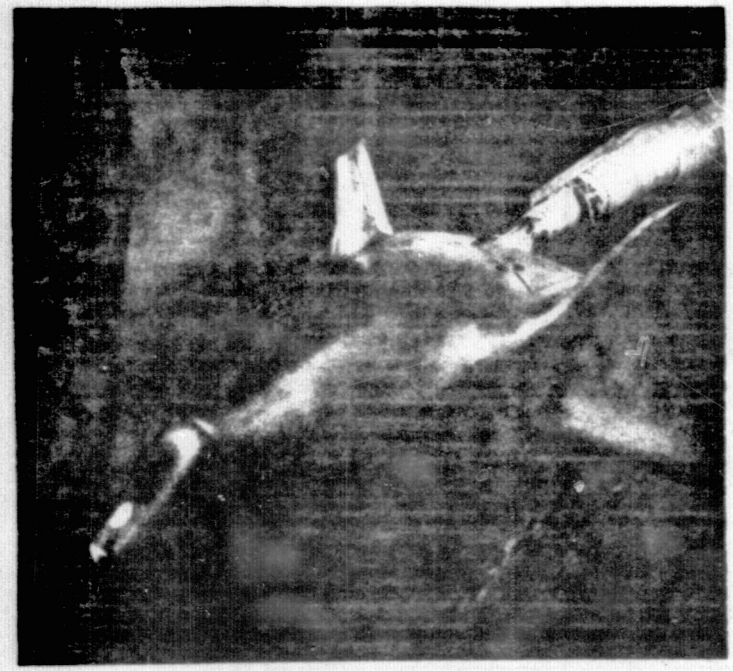

	ORBITER	
TEST FACILITY	AMES 6 x 6 FT	LaRC-UPWT
RUNS	67	84
MACH NUMBER	0.60 to 2.0	2.3 TO 4.6
ANGLE-OF-ATTACK (DEG)	-4 TO 22	0 TO 60
SIDESLIP ANGLE (DEG)	-4 TO 10	-4 TO 10
REYNOLDS NUMBER PER FOOT	2.5×10^6 TO 4.0×10^6	2.5×10^6 TO 4.5×10^6

Fig. 2.6-6 Orbiter Configuration

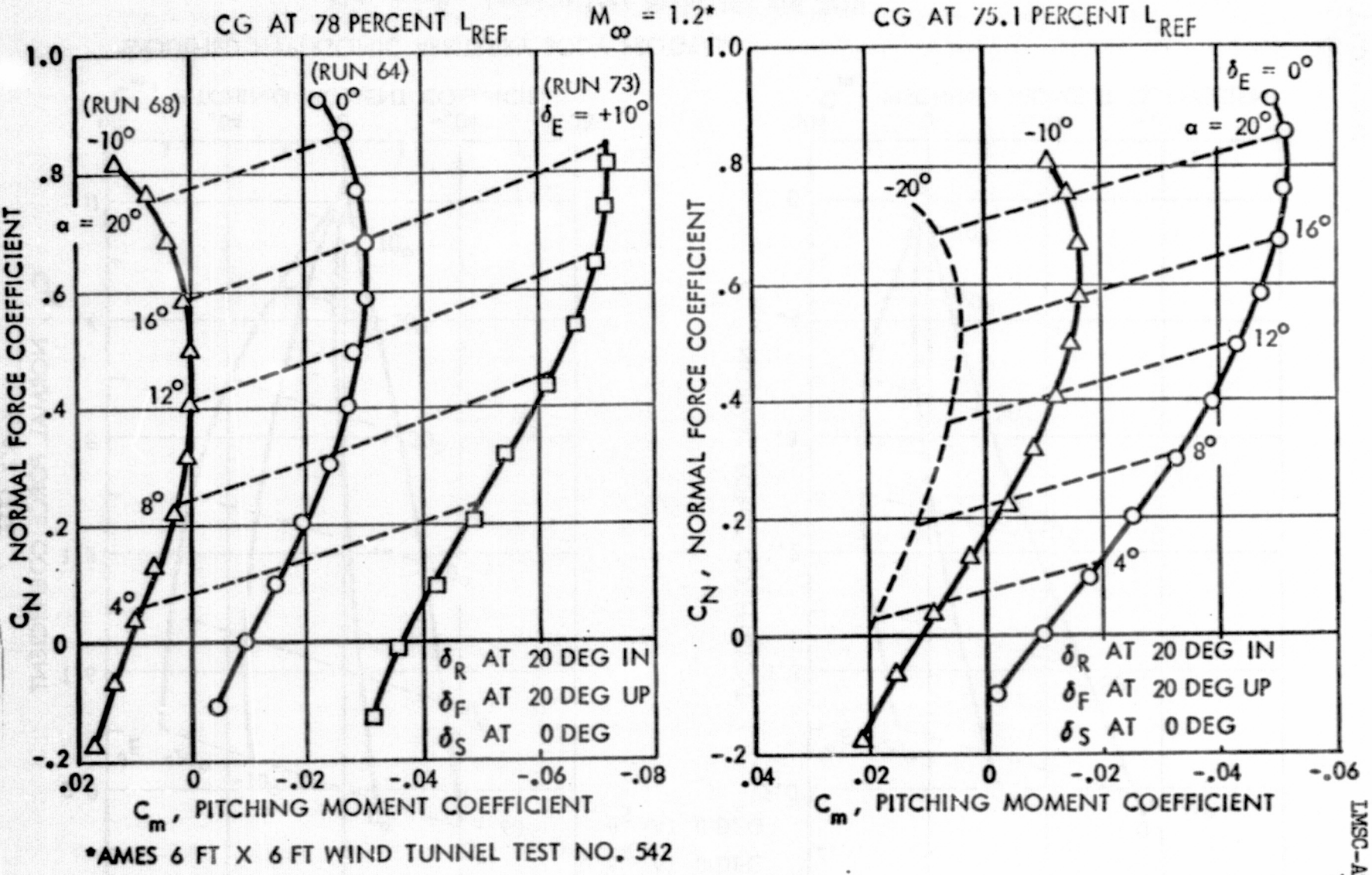

*AMES 6 FT X 6 FT WIND TUNNEL TEST NO. 542

Fig. 2.6-7 Longitudinal Stability and Trim

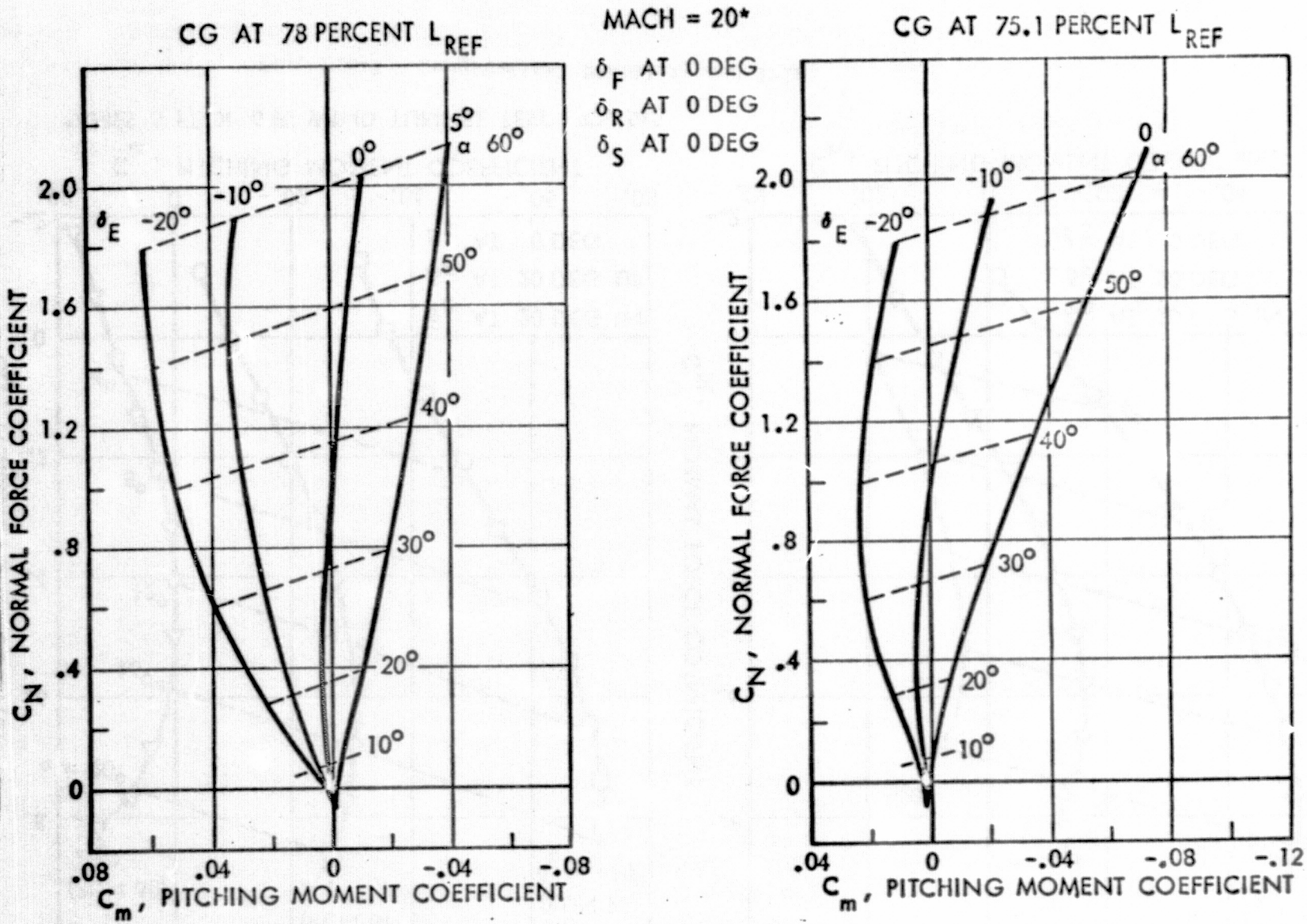

*MODIFIED HYPERSONIC ARBITRARY BODY PROGRAM

Fig. 2.6-8 Longitudinal Stability and Trim

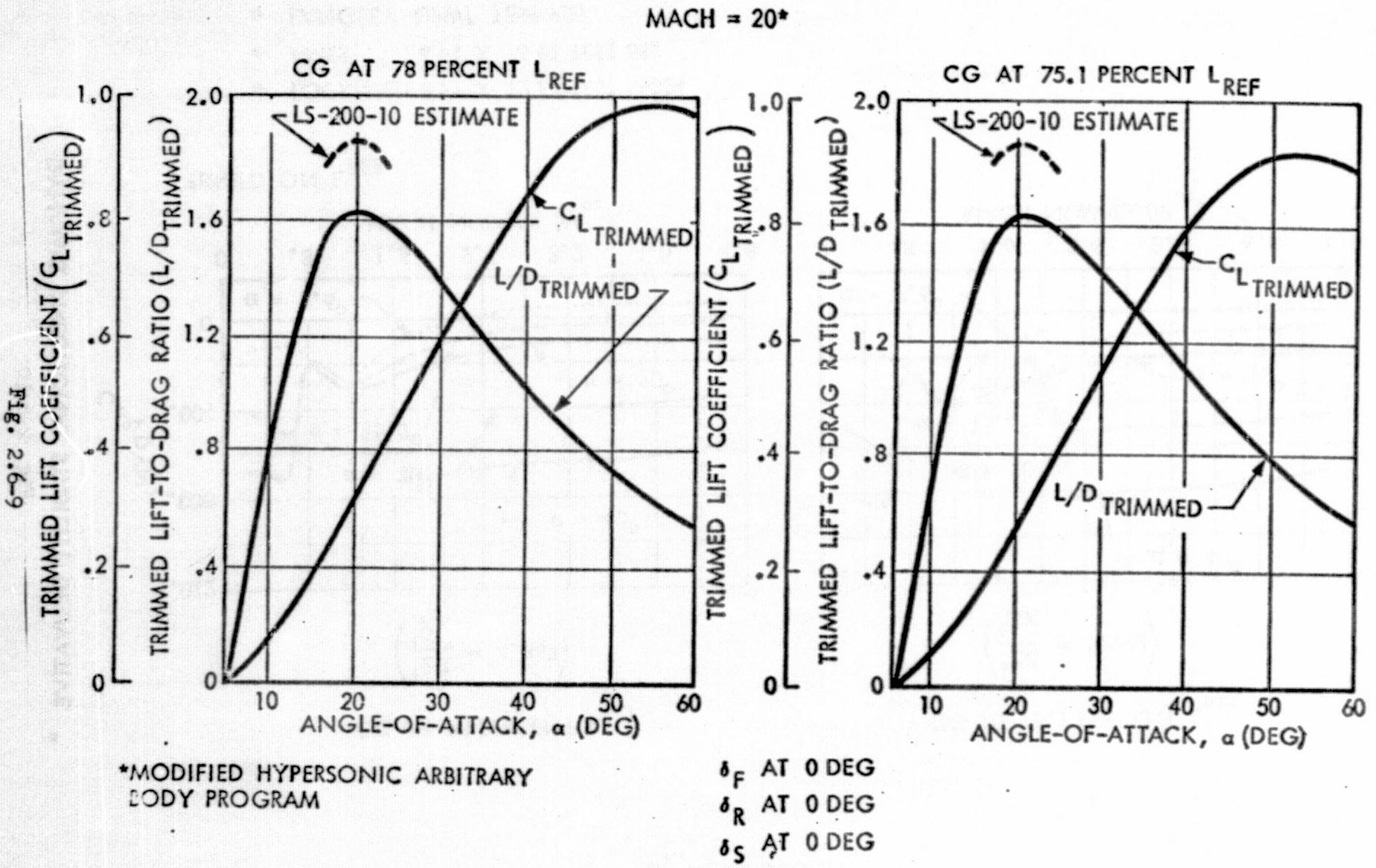

*MODIFIED HYPERSONIC ARBITRARY BODY PROGRAM

δ_F AT 0 DEG
δ_R AT 0 DEG
δ_S AT 0 DEG

Fig. 2.6-9 Lift and Drag Characteristics

δ_R AT 20 DEG IN

CG AT 78 PERCENT L_{REF}

$\left(\frac{I_{ZZ}}{I_{XX}} = 4.367\right)$

CG AT 75.1 PERCENT L_{REF}

$\left(\frac{I_{ZZ}}{I_{XX}} = 5.022\right)$

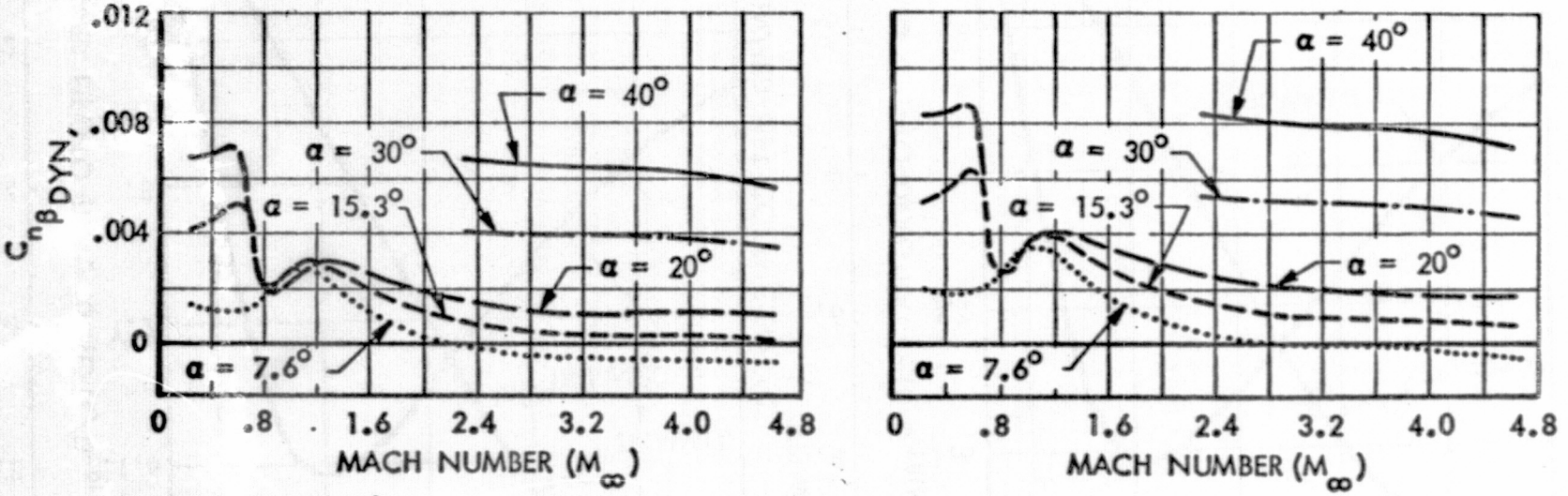

*BASED ON L_{REF}

- LOCKHEED 8 FT X 12 FT TEST L-324
- AMES 6 FT X 6 FT TEST 542
- LANGLEY UPWT TEST 955

Fig. 2.6-10 Directional Stability Summary

DYNAMIC DIRECTIONAL STABILITY DERIVATIVE *

Fig. 2.6-10

δ_R AT 0 DEG

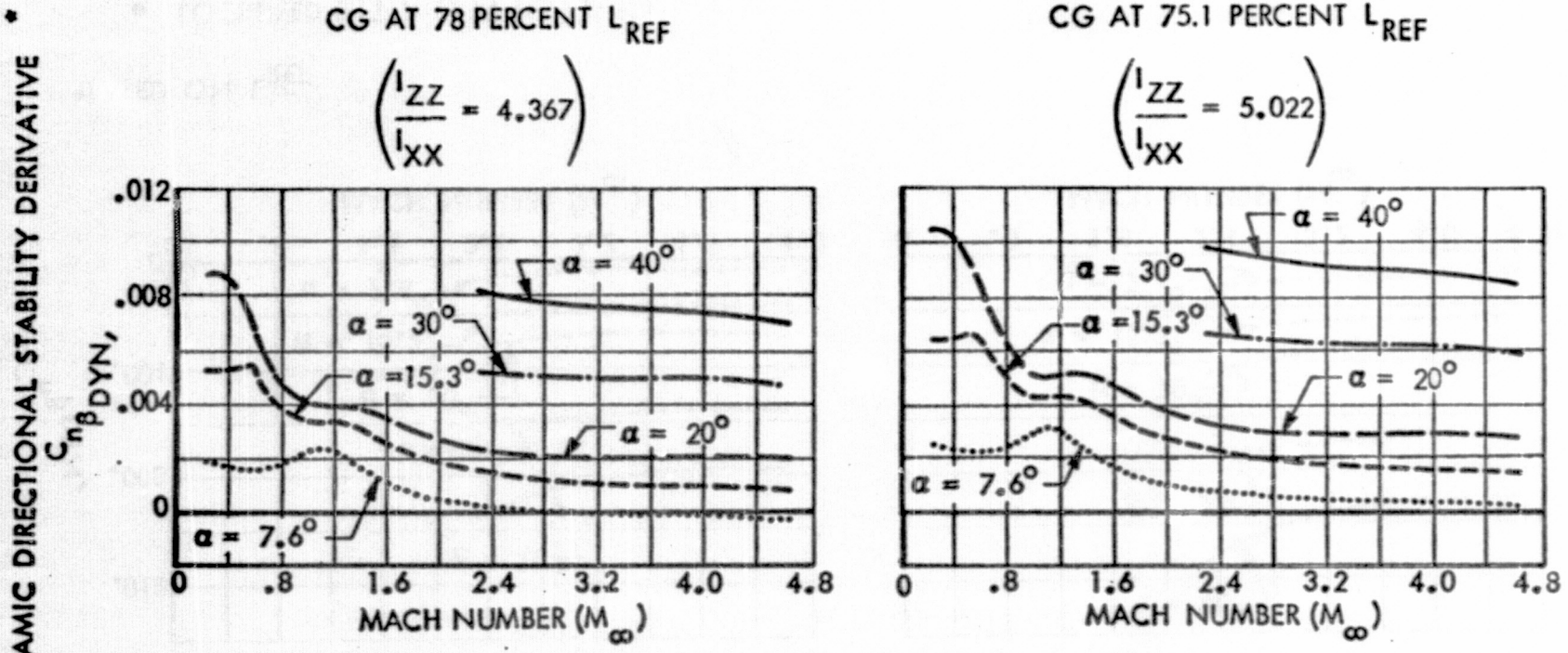

*BASED ON L_{REF}

- LOCKHEED 8 FT X 12 FT TEST L-324
- AMES 6 FT X 6 FT TEST 542
- LANGLEY UPWT TEST 955

Fig. 2.6-11 Directional Stability Summary

δ_R AT 10 DEG OUT

CG AT 78 PERCENT L_{REF}

$\left(\frac{I_{ZZ}}{I_{XX}} = 4.367\right)$

CG AT 75.1 PERCENT L_{REF}

$\left(\frac{I_{ZZ}}{I_{XX}} = 5.022\right)$

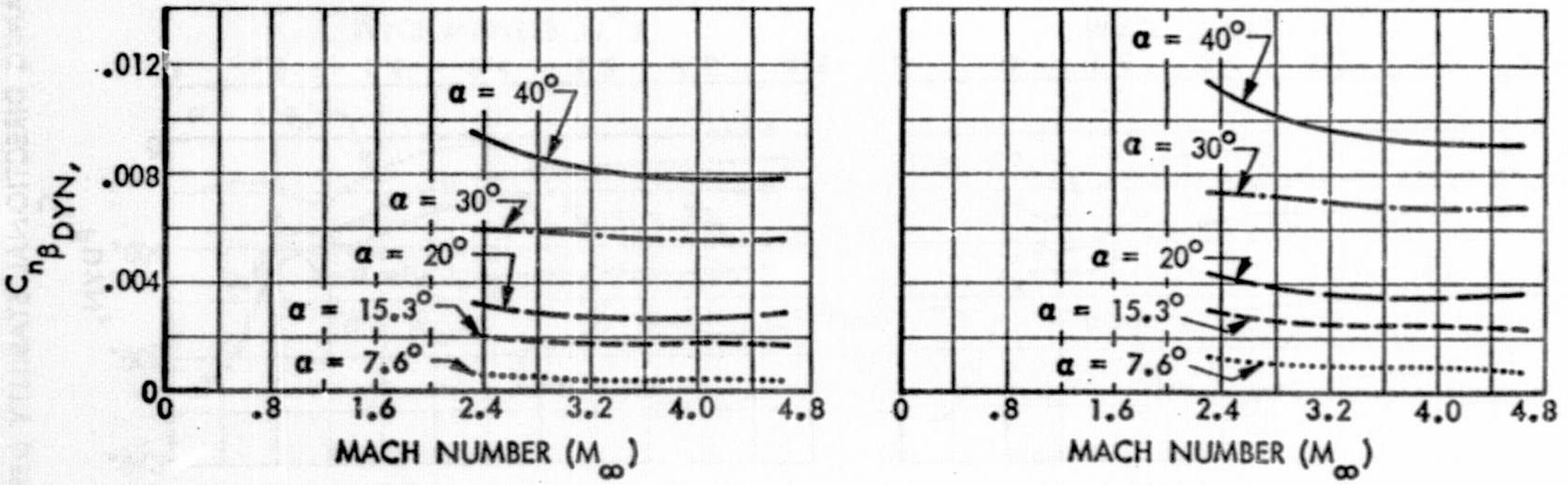

*BASED ON L_{REF}

- LOCKHEED 8 FT X 12 FT TEST L-324
- AMES 6 FT X 6 FT TEST 542
- LANGLEY UPWT TEST 955

Fig. 2.6-12 Directional Stability Summary

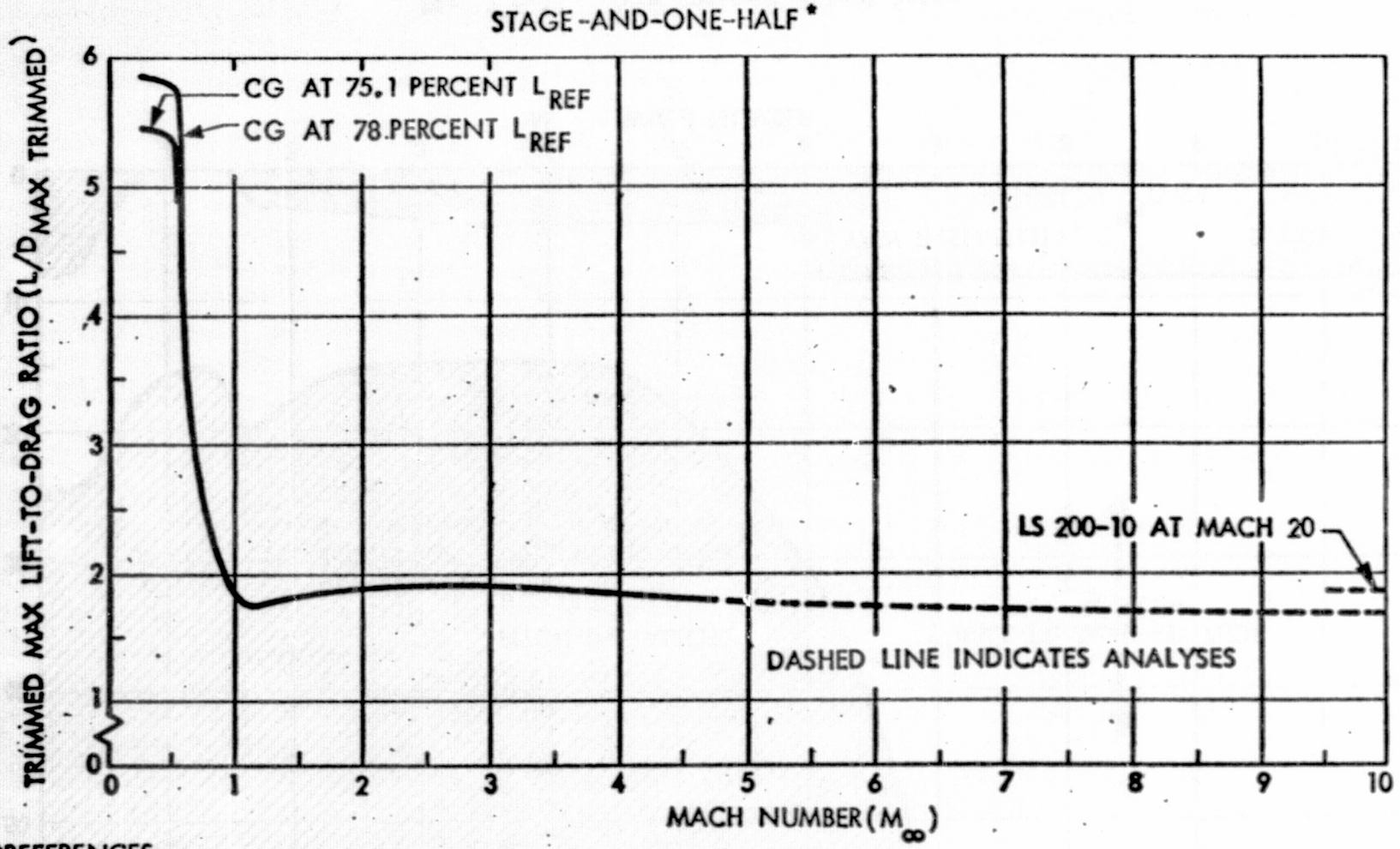

*REFERENCES:

- LOCKHEED 8 FT X 12 FT TEST NO. L-324
- AMES 6 FT X 6 FT TEST NO. 542
- LANGLEY UPWT TEST NO. 955

Fig. 2.6-13 Aerodynamic Lift-to-Drag Summary

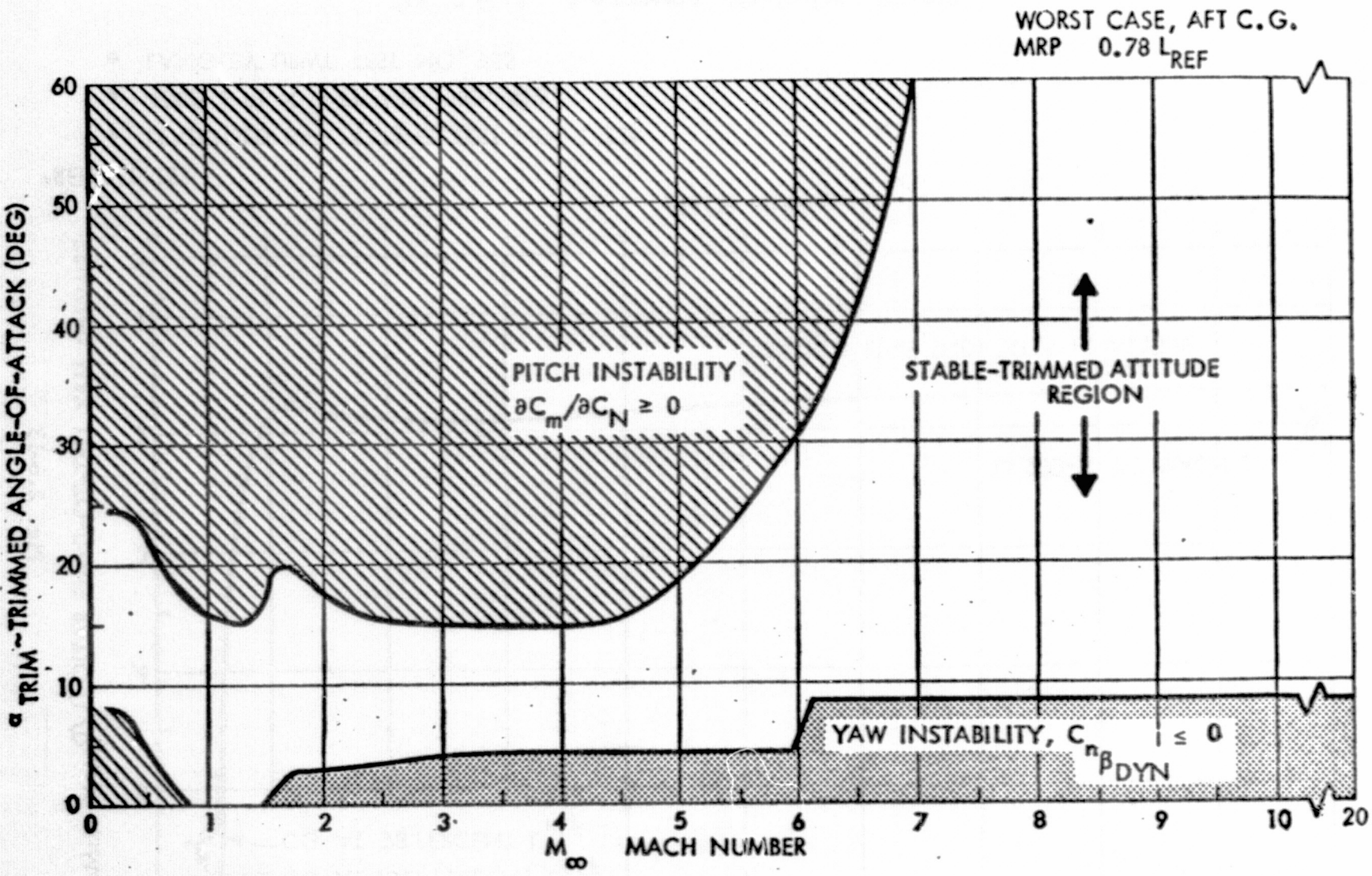

Fig. 2.6-14 Trim Angle-Of-Attack Range

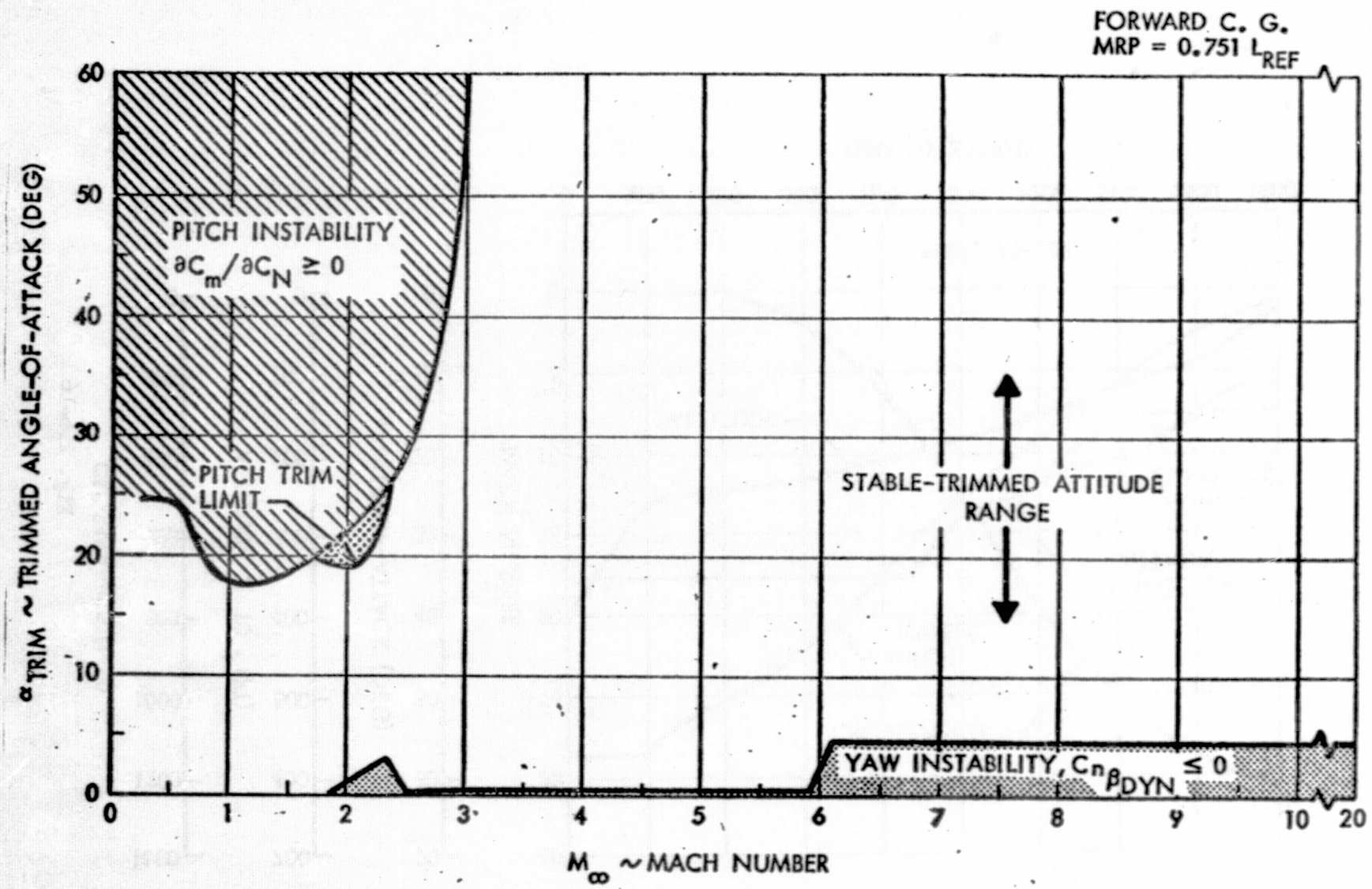

Fig. 2.6-15 Trim Angle-Of-Attack Range

Fig. 2.6-16 Reference Entry Trajectory

(RE 222 TRAJECTORY)

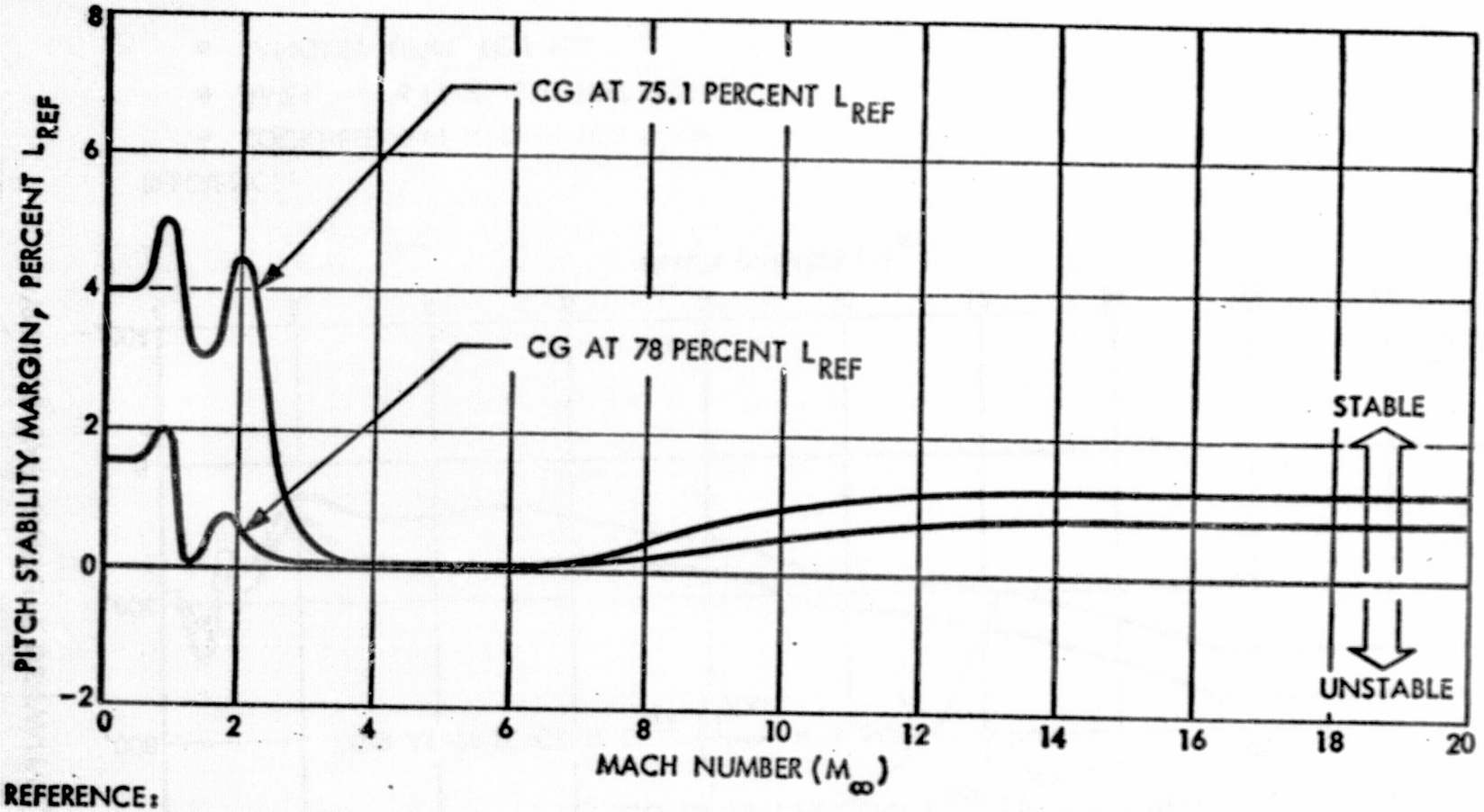

REFERENCE:

- LOCKHEED 6 FT X 12 FT TEST L-324
- AMES 6 FT X 6 FT TEST 542
- LANGLEY UPWT TEST 955

Fig. 2.6-17 Longitudinal Stability Summary

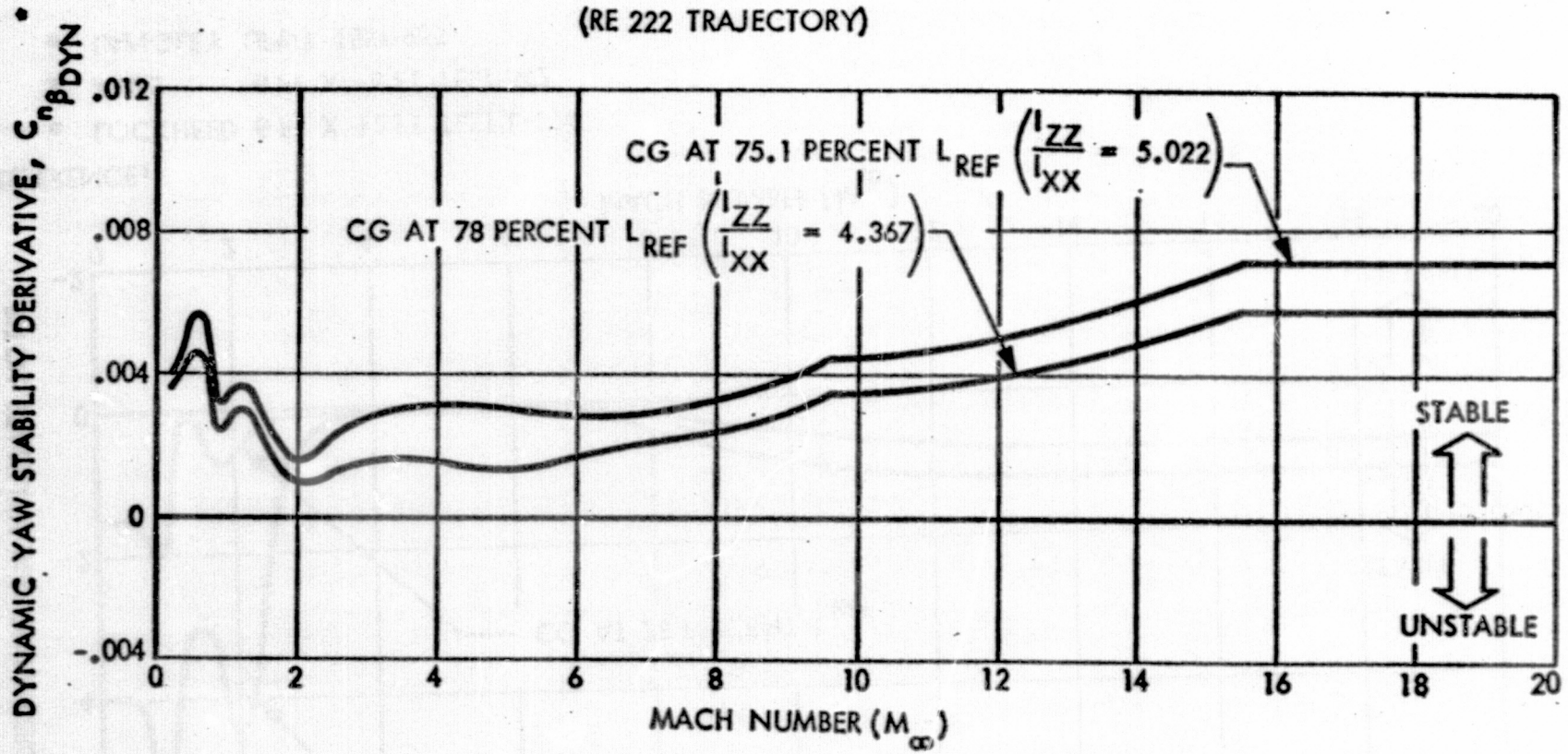

REFERENCE:

- LOCKHEED 8 FT X 12 FT TEST L-324
- AMES 6 FT X 6 FT TEST 542
- LANGLEY UPWT TEST 955

*BASED ON L_{REF}

Fig. 2.6-18 Directional Stability Summary

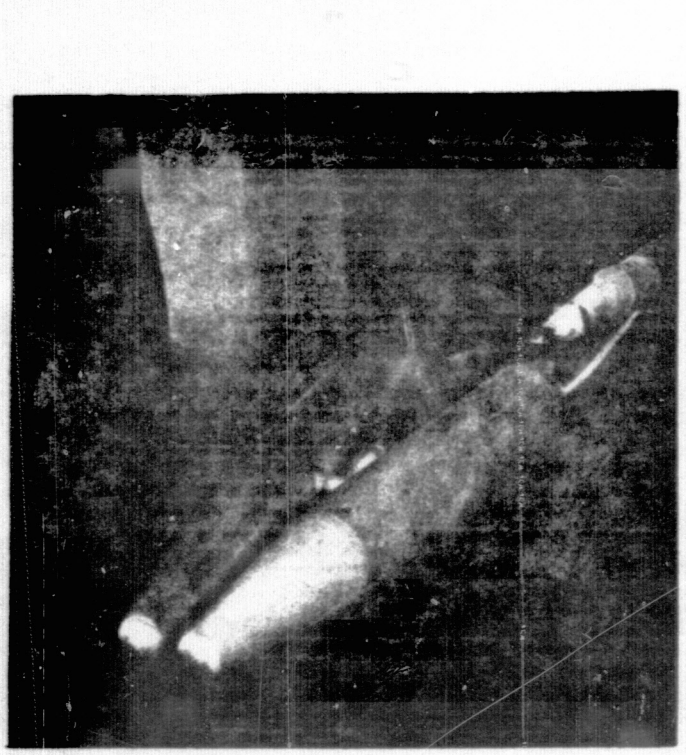

	LAUNCH VEHICLE
TEST FACILITY	AMES 6 x 6 FT
RUNS	28
MACH NUMBER	0.60 TO 2.0
ANGLE-OF-ATTACK (DEG)	-10 TO 10
SIDESLIP ANGLE (DEG)	-4 TO 10
REYNOLDS NUMBER PER FOOT	2.5×10^6 TO 4.5×10^6

Fig. 2.6-19 Launch Configuration

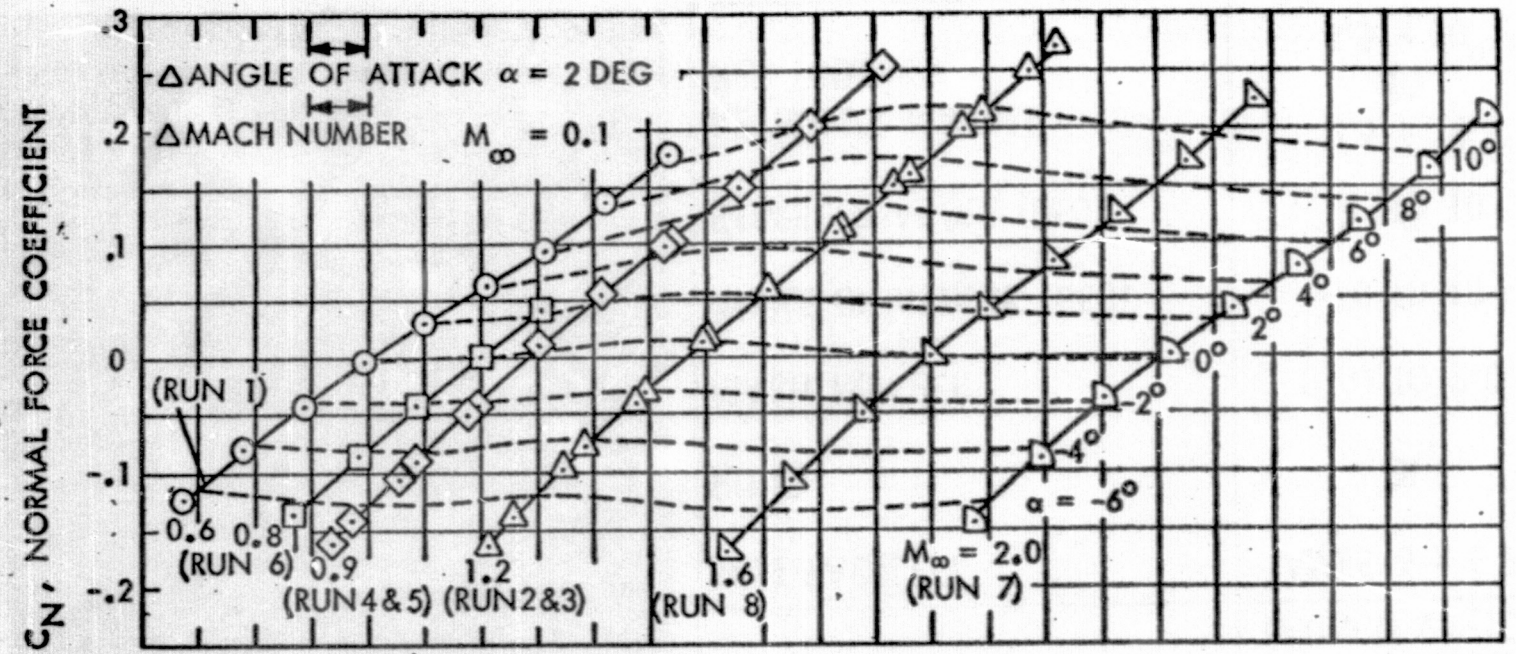

AMES 6 X 6 FT WIND TUNNEL TEST NO. 542

Fig. 2.6-20 Normal Force Characteristics

LAUNCH VEHICLE – 1-1/2 STAGE (LS 200-5)

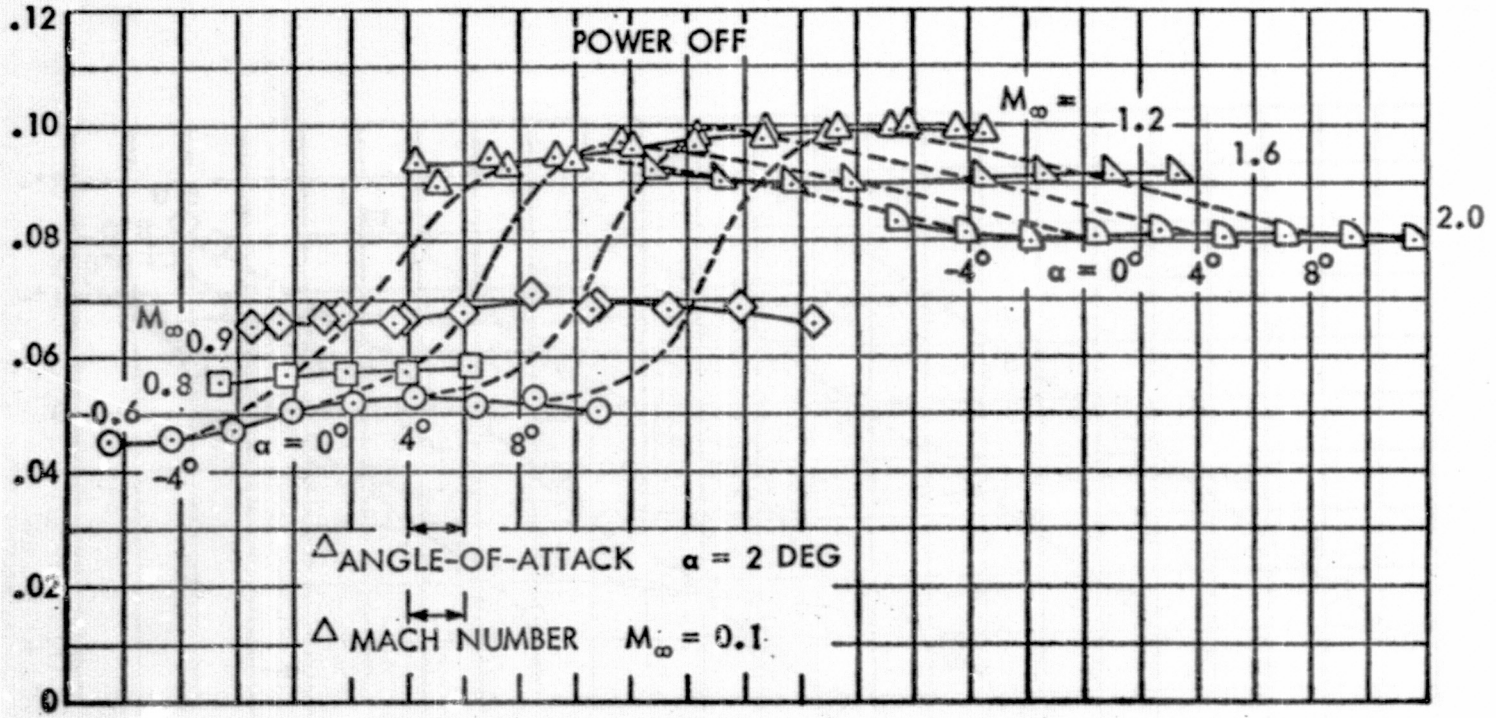

AMES 6 X 6 FT WIND TUNNEL TEST NO. 542

Fig. 2.6-21 Axial Force Characteristics

LOCKHEED MISSILES & SPACE COMPANY

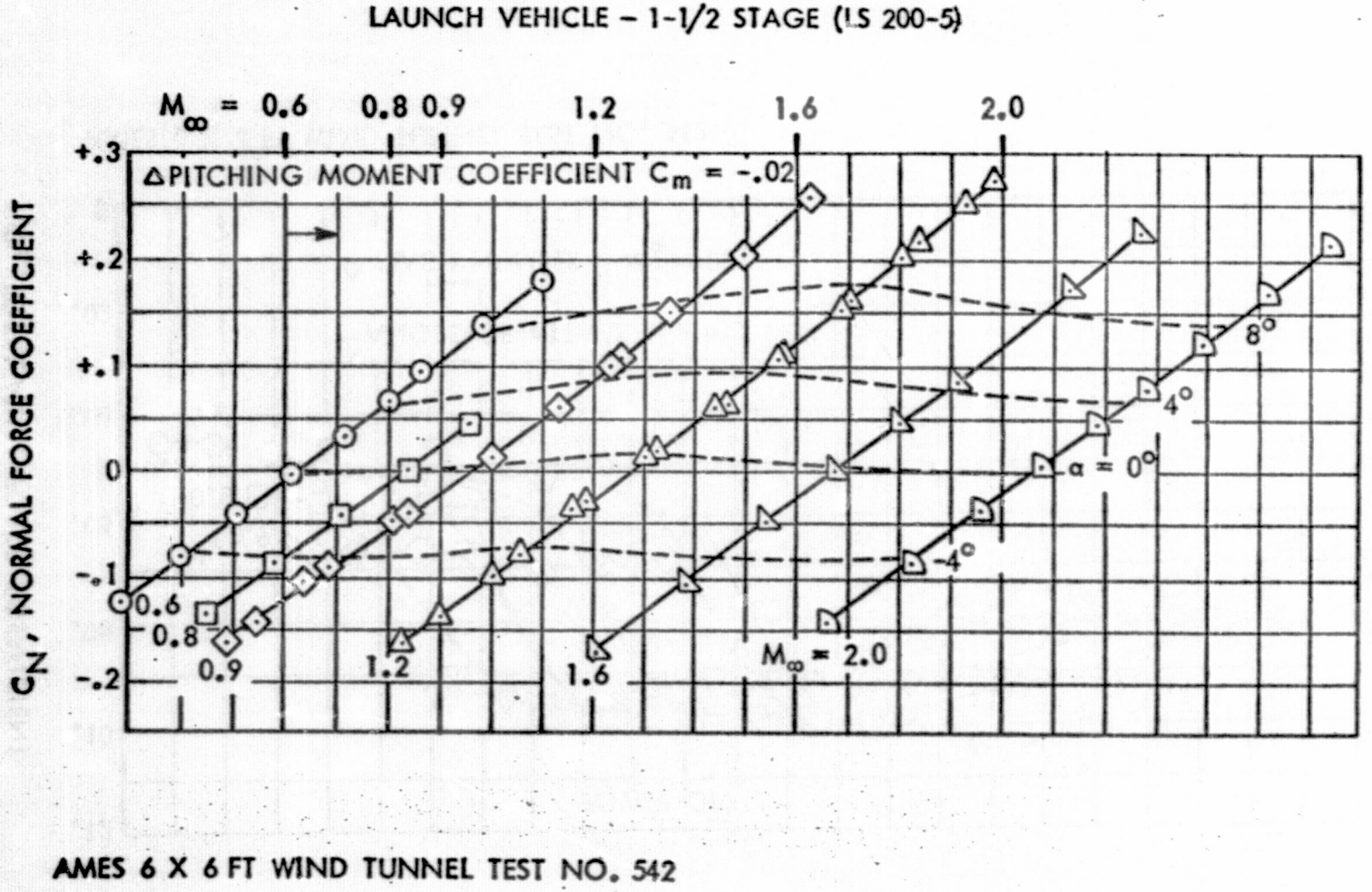

Fig. 2.6-22

Fig. 2.6-22 Longitudinal Stability Characteristics

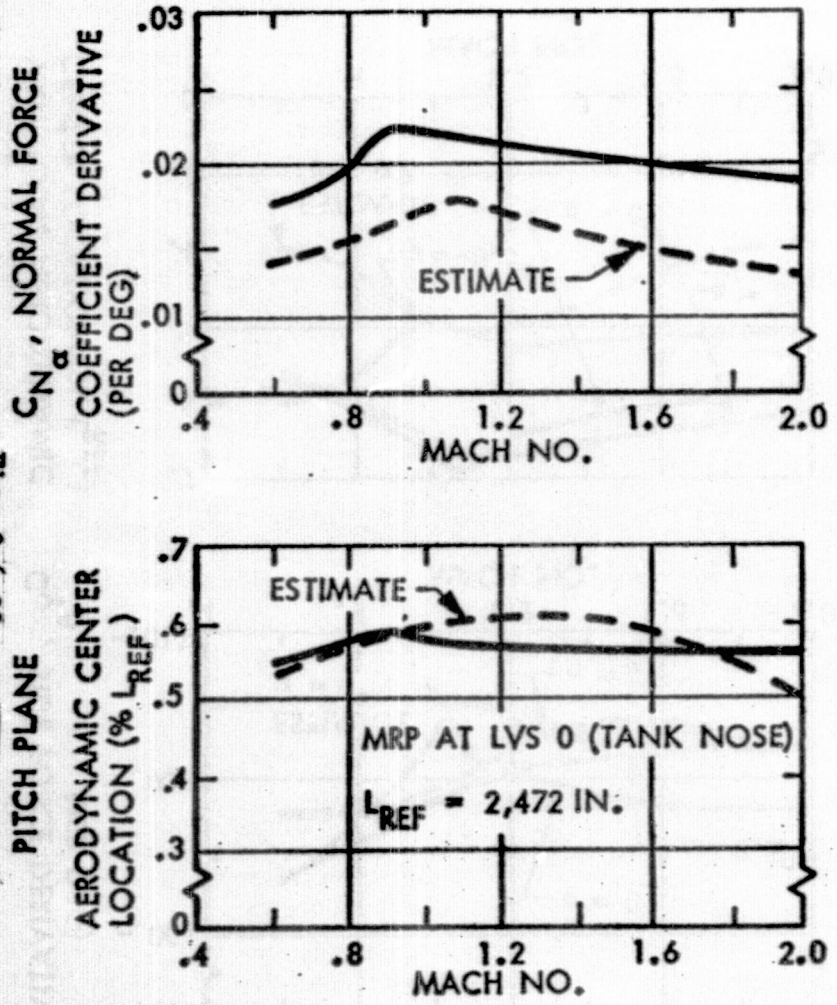

$S_{REF} = 12463\ FT^2$

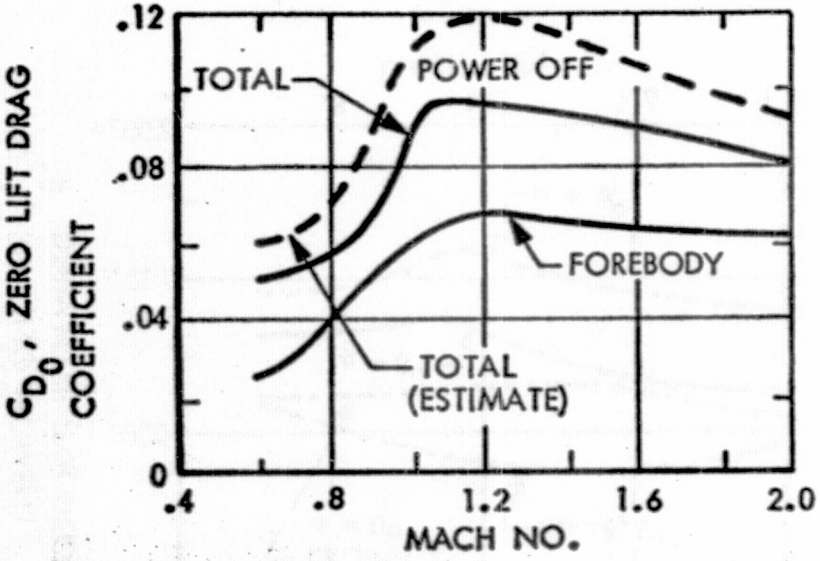

Fig. 2.6-23 Longitudinal Characteristics

LAUNCH VEHICLE – 1-1/2 STAGE (LS 200-5)

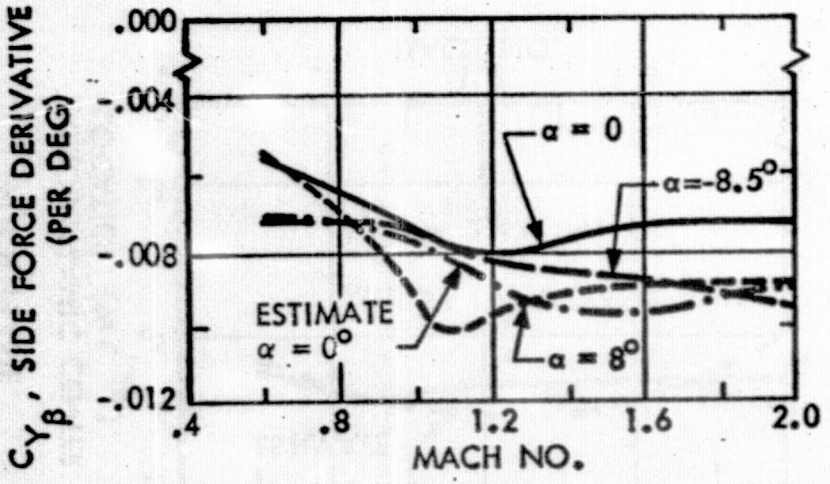

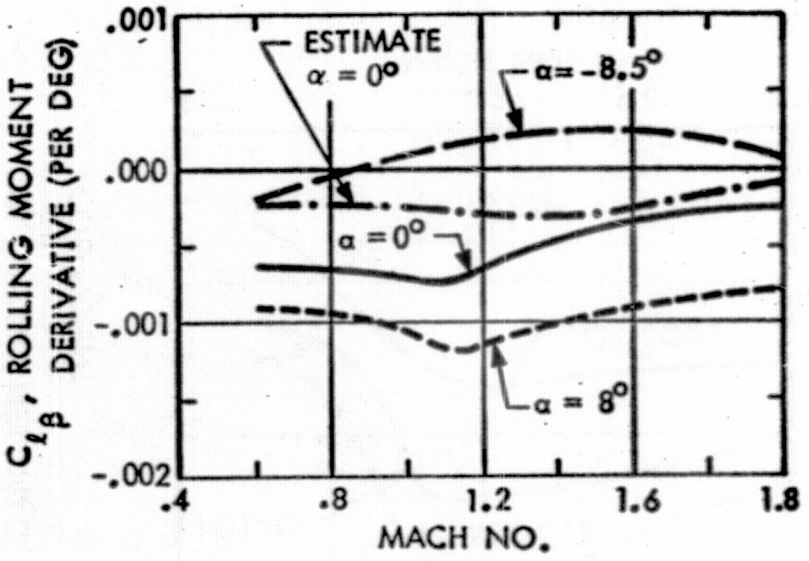

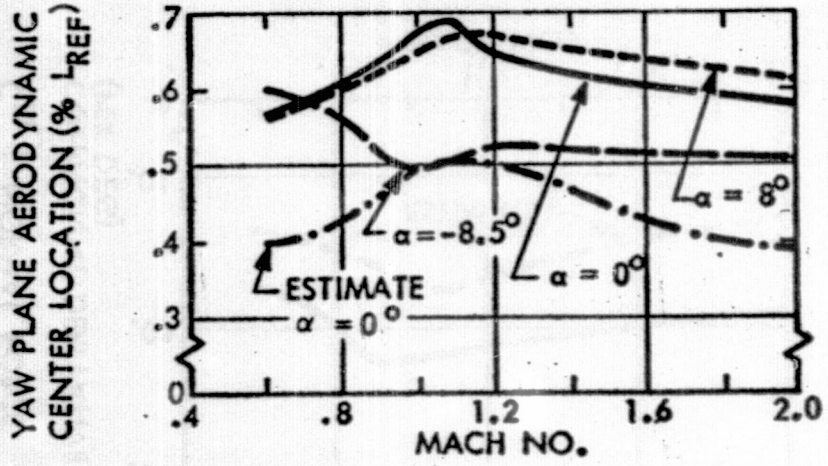

AMES 6 X 6 FT WIND TUNNEL TEST NO. 542

Fig. 2.6-24 Lateral-Directional Characteristics

Fig. 2.6-24

2.7 AEROTHERMODYNAMICS AND TPS

Thermodynamic analyses were performed to establish orbiter entry heating boundaries, to define the entry thermal environment, and to determine thermal protection system (TPS) material and insulation requirements. Primary results of these studies are presented below, following a discussion of orbiter heating prediction methods. Predictions of the droptank thermal environment and TPS requirements are contained in Appendix A.

2.7.1 Aerothermodynamic Prediction Methods

During the past several years, approximately 1000 wind-tunnel occupancy hours have been expended by Lockheed in obtaining heat transfer and flow field data on delta-body configurations. In addition, extensive wind tunnel testing of lifting-body configurations has been accomplished by NASA and the Air Force. Analysis and correlation of these data have resulted in aerodynamic heating prediction methods suitable for orbiter preliminary design calculations.

Table 2.7-1 summarizes the methods used to generate the aerothermodynamic data presented in this report. In all cases, heating rates are based on 1962 Standard Atmosphere data (Ref. 2.7-1) and Hansen's equilibrium air properties (Ref. 2.7-2). Heating rates to the body- and fin-leading edges are based on isolated swept-cylinder theory , with empirical corrections applied to fin-leading edge predictions to account for flow-interference effects. No evidence of shock impingement has been observed on the fins and the slight heating increases, relative to isolated cylinder theory, are assumed to result from flow disturbances created by the body shockwave. The leading-edge boundary-layer-transition criteria are (1) $Re_{\infty D}$ = 800,000 for undisturbed-leading edges, such as the body-leading edge, and (2) $Re_{\infty D}$ = 200,000 for the fin. These criteria are based on recommendations of Bushnell (Ref. 2.7-3).

Table 2.7-1

HEATING PREDICTION SUMMARY

Location	Theory	Comments
Stagnation Point	Fay and Riddell	
Leading Edge	Fay and Riddell (Laminar) Beckwith and Gallagher (Turbulent)	Sweep Independence Principle Empirical Correction Factors
Lower Surface	Reference Enthalpy (Laminar) Spalding-Chi (Turbulent)	Sharp Wedge or Swept Cylinder Flow Properties Empirical Outflow Correction Experimental Spanwise Distribution
Body Side	Reference Enthalpy (Laminar) Spalding-Chi (Turbulent)	Experimental Pressure Coefficient Empirical Boundary Layer Origin
Upper Surface and Fins	--	Experimental Distributions
Base	--	Space Shuttle ICD 13M15000A

Lower-surface heating rates are computed by the reference enthalpy (Ref. 2.7-4) and Spalding-Chi (Ref. 2.7-5) methods for laminar and turbulent flow, respectively. Empirical outflow corrections (Ref. 2.7-6) are applied to account for streamline divergence at high angles-of-attack. Local flow properties are based on real gas oblique shock theory whenever the shockwave is attached ($\alpha \lesssim 45$ deg) and by swept-cylinder theory when the shock is detached. Except for leading edge regions, the onset of boundary layer transition is based on the following criteria, as recommended by the Space Shuttle Heating Panel (Ref. 2.7-7):

$$\frac{Re_\theta}{M_e\,(Re_e/ft)^{0.2}} = f(\alpha_L)$$

where the local angle-of-attack function, $f(\alpha_L)$, is 10 for $\alpha_L \leq 20$ deg and increases to 20 for $\alpha_L = 60$ deg. Progressive transition is assumed with the end-of-transition Reynolds number twice the onset value.

Base heating rates for both ascent and entry were computed using NASA-generated data (Ref. 2.7-8). Although the base heating levels during engine operation (ascent) establish the peak heat shield temperature, the base TPS is sized from entry considerations.

References 2.7-6, 2.7-7, and 2.7-9 contain more detailed descriptions of the heating prediction methods, including the equations solved and the mechanics of the computational procedures.

2.7.2 Entry Heating Boundaries

Heating boundaries have been generated for the delta-body orbiter to serve as a constraint in entry-trajectory analyses. As shown in Fig. 2.7-1, the heating boundaries are based on temperature limits of 2300°F for the lower surface and fin-leading edge, and 2800°F for the nose cap. These temperatures are the assumed design limits, with 200°F margin, for the proposed heat shield materials

REPRODUCIBILITY OF THE ORIGINAL PAGE IS POOR

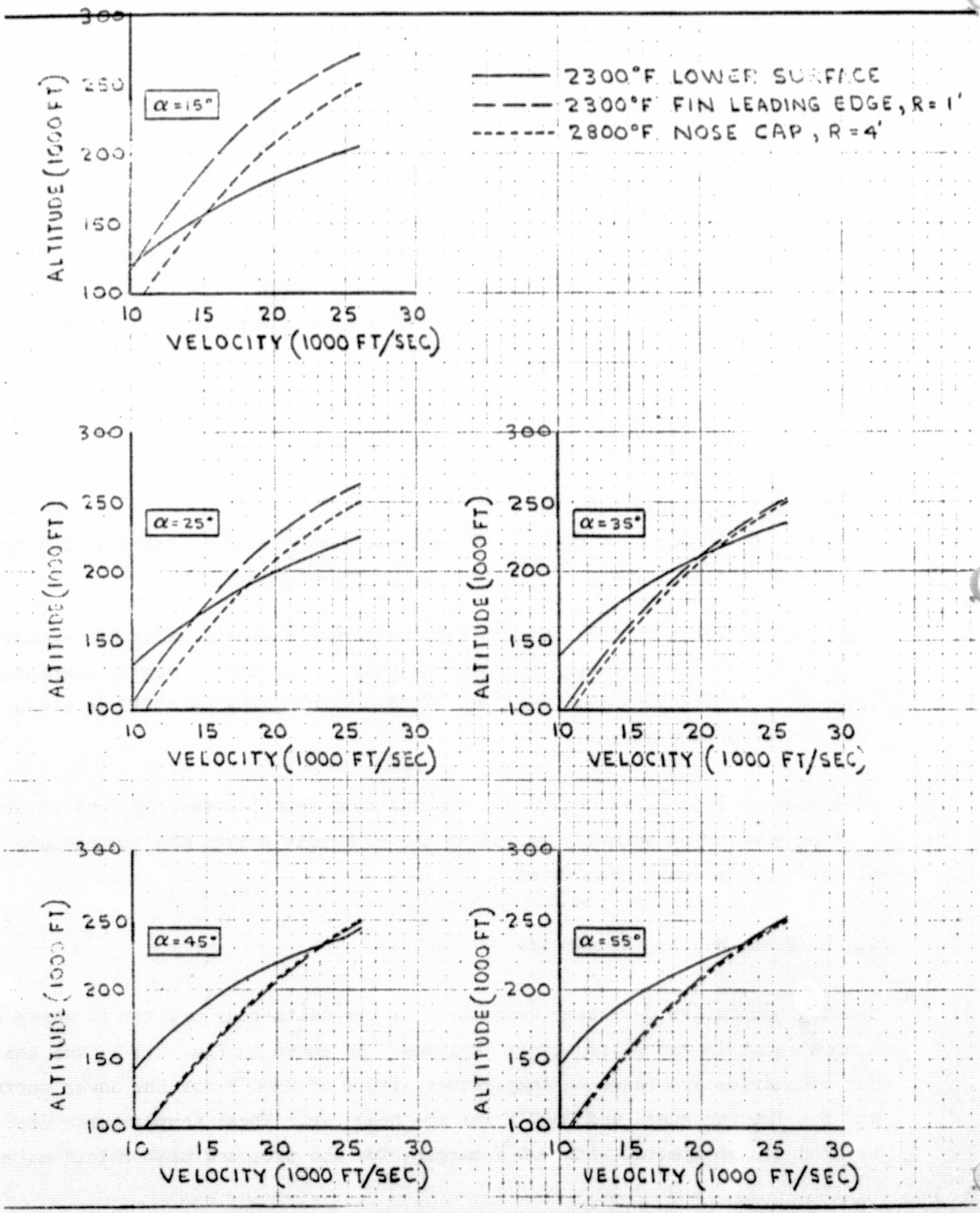

Fig. 2.7-1 Delta-Body Orbiter Heating Boundaries For Lower-Surface, Fin Leading Edge, and Nose Cap

(LI-1500 up to 2300°F; coated tantalum up to 2800°F). The governing constraint at high velocities and low angles-of-attack is laminar heating to stagnation regions, whereas the constraint at lower velocities is turbulent heating on the lower surface. Figure 2.7-2 shows the individual heating boundaries from Fig. 2.7-1 in composite form.

To satisfy fin heating constraints, a minimum angle-of-attack of about 32 deg is employed at pullup. The angle-of-attack is subsequently reduced, for large crossrange missions, to increase the lift-to-drag ratio. The bank angle is also modulated during entry to follow the heating boundaries and, thereby, minimize entry duration and TPS insulation weight.

2.7.3 Entry Thermal Environment

Figure 2.7-3 shows the stage-and-one-half design entry trajectory. This trajectory, designated RE-214, generates 1,126-nm crossrange from a 270-nm, 55-deg inclination orbit. Entry time from 400,000 ft to touchdown is 2,600 sec, including approximately 500 sec for go-around. The heating duration, however, is less than 1,700 sec.

Figure 2.7-4 shows surface-temperature histories at representative stagnation region and lower centerline locations for trajectory RE-214. Figure 2.7-5 shows the LS 200-10 orbiter peak surface temperatures in the form of isotherms; these are radiation equilibrium temperatures based on a surface-emittance of 0.8. Peak temperatures are 2810°F on the nose cap, 2110°F on the body leading edge, 2280°F on the fin leading edge, 2210°F on the lower surface, and generally less than 800°F on the upper surface. Turbulent heating determines peak temperatures on virtually the entire lower surface but is relatively insignificant for leading edge regions.

Surface temperatures for the design entry trajectory are relatively high, because the trajectory is based on minimum TPS weight. Figures 2.7-6 and 2.7-7

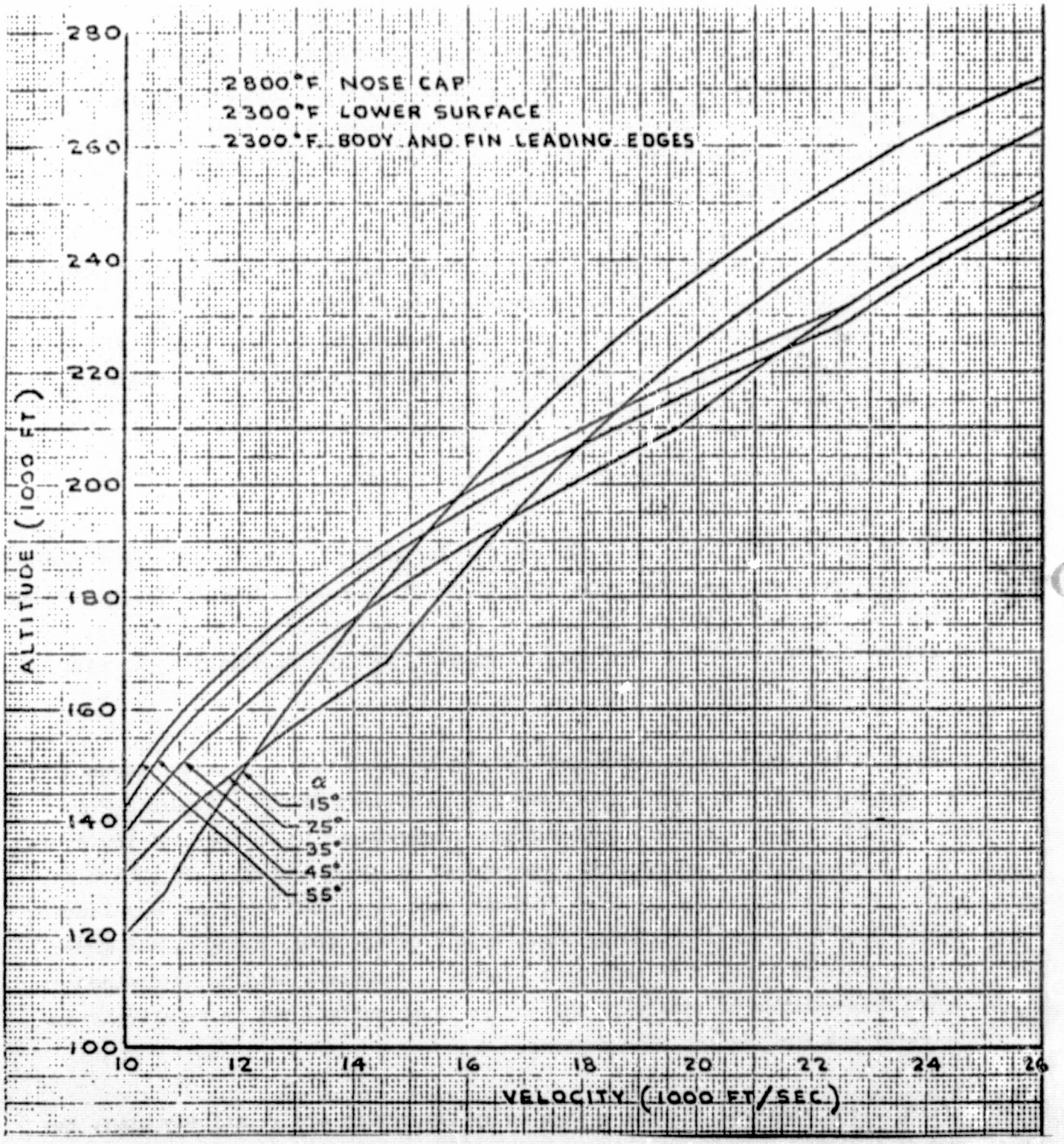

Fig. 2.7-2 Delta-Body Orbiter Composite Heating Boundaries

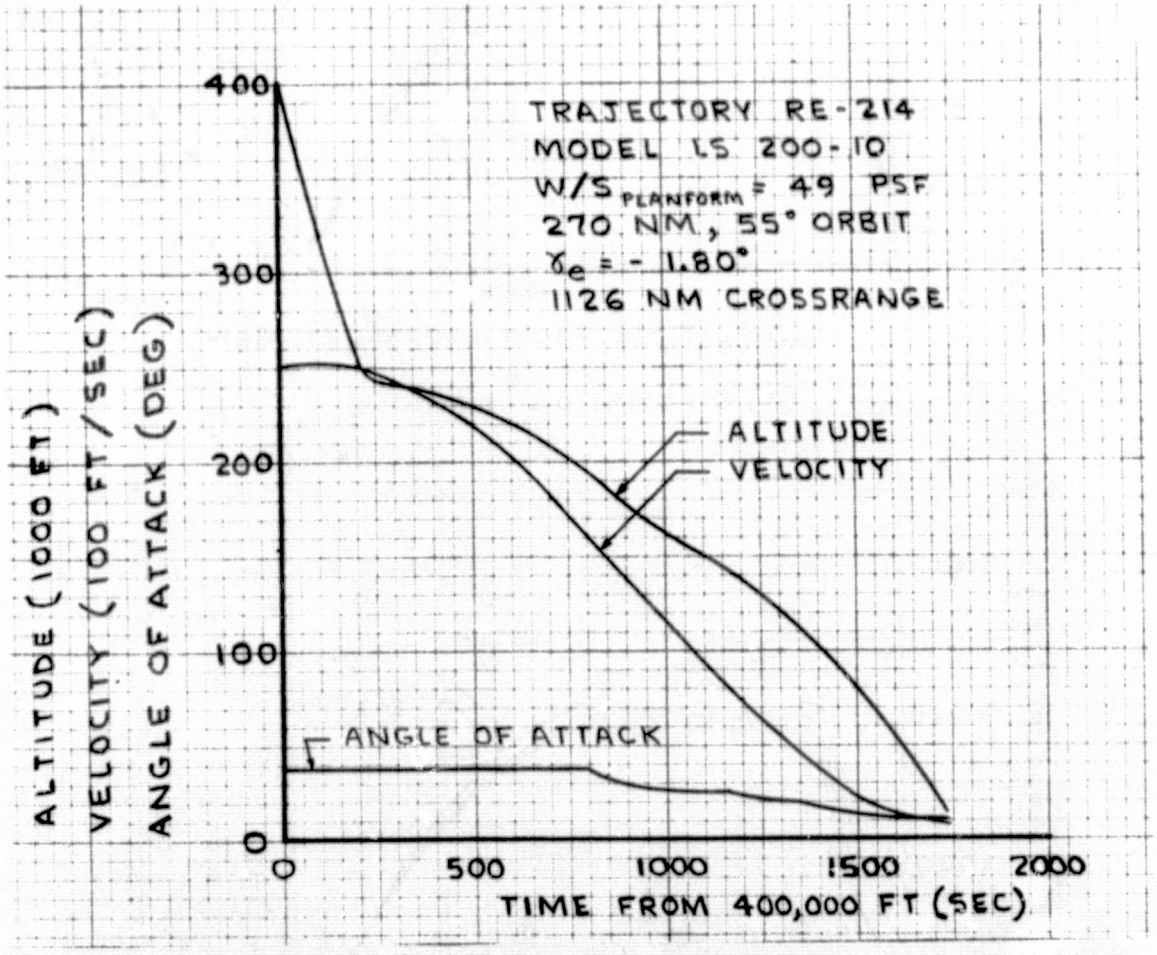

Fig. 2.7-3 Stage-And-One-Half Orbiter 1100-nm Crossrange Design Entry Trajectory (RE-214)

REPRODUCIBILITY OF THE ORIGINAL PAGE IS POOR.

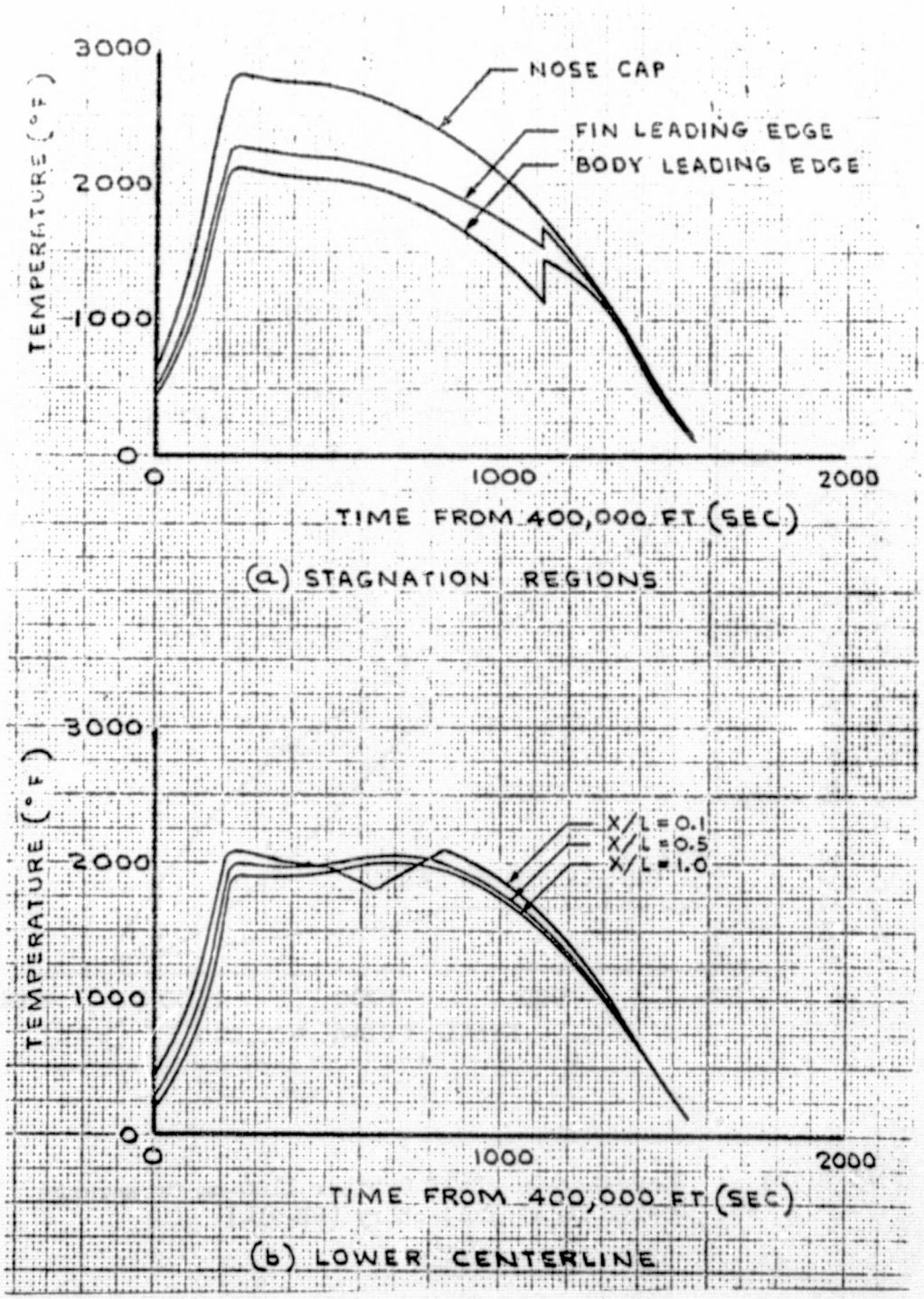

Fig. 2.7-4 Stage-And-One-Half Orbiter Surface-Temperature Histories For Design Entry Trajectory (RE-214)

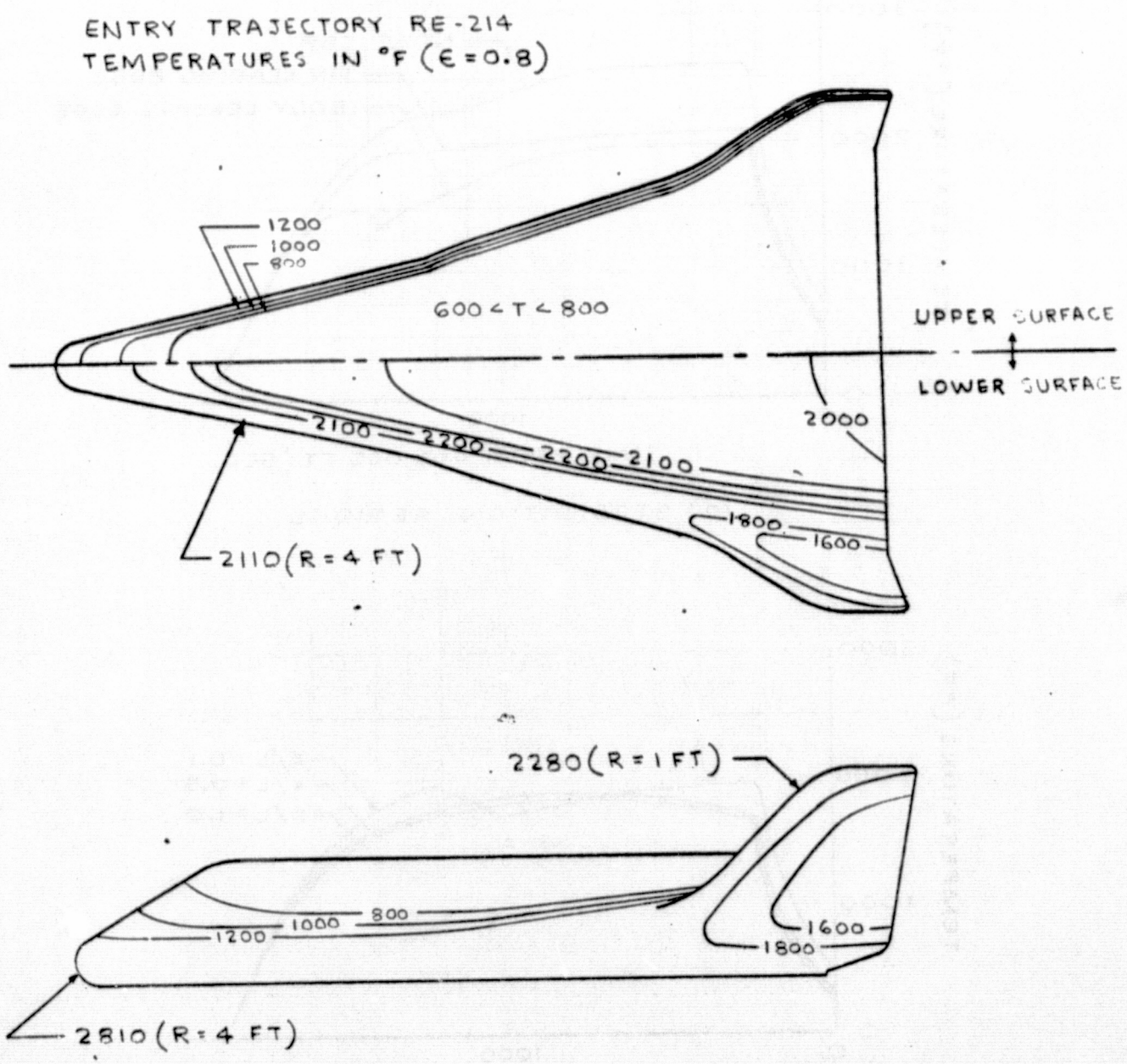

Fig. 2.7-5 Stage-And-One-Half Orbiter Peak-Temperature Isotherms For Design Entry Trajectory (RE-214)

REPRODUCIBILITY OF THE ORIGINAL PAGE IS POOR.

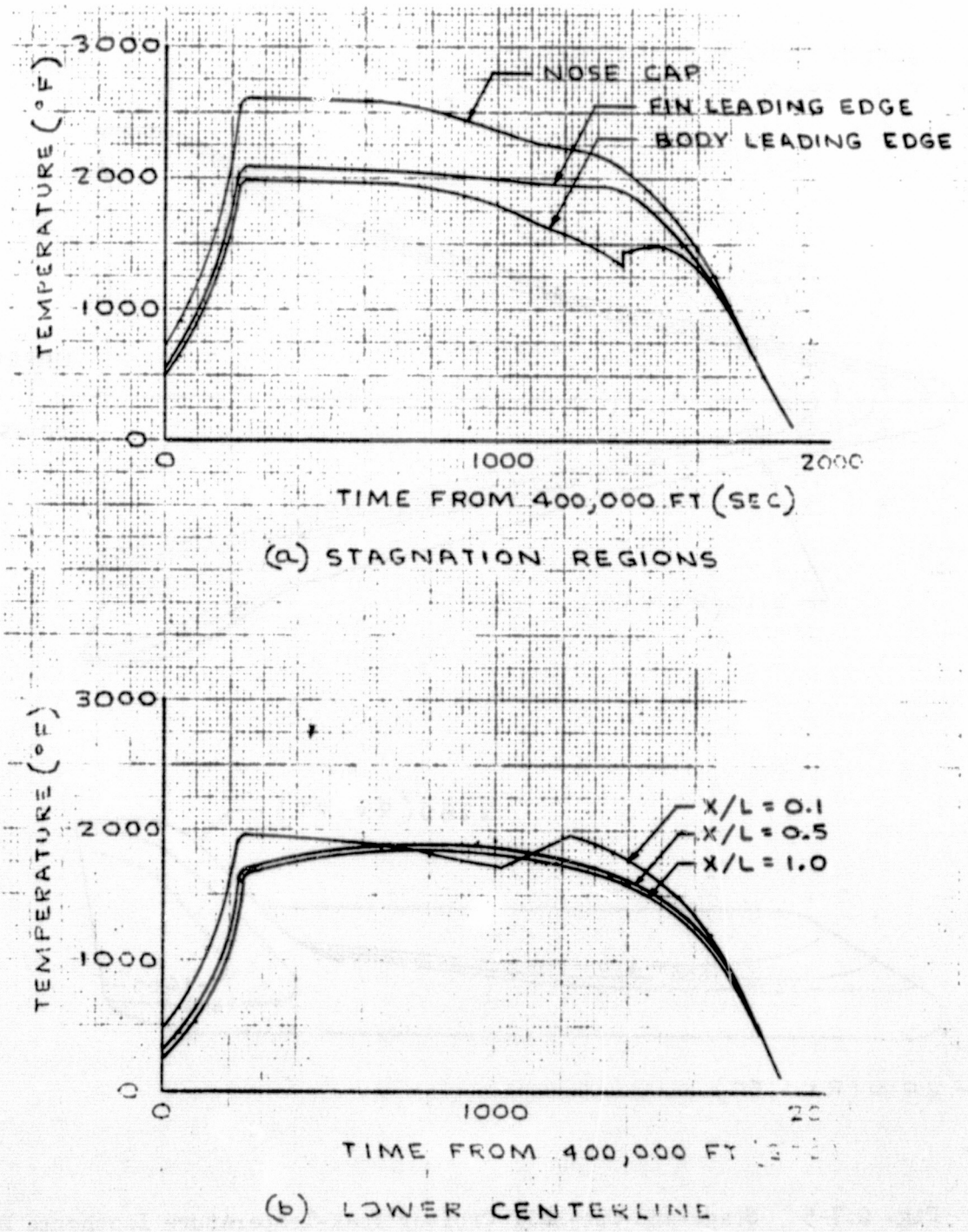

Fig. 2.7-6 Stage-And-One-Half Orbiter Surface-Temperature Histories For Low-Temperature Trajectory (RE-216)

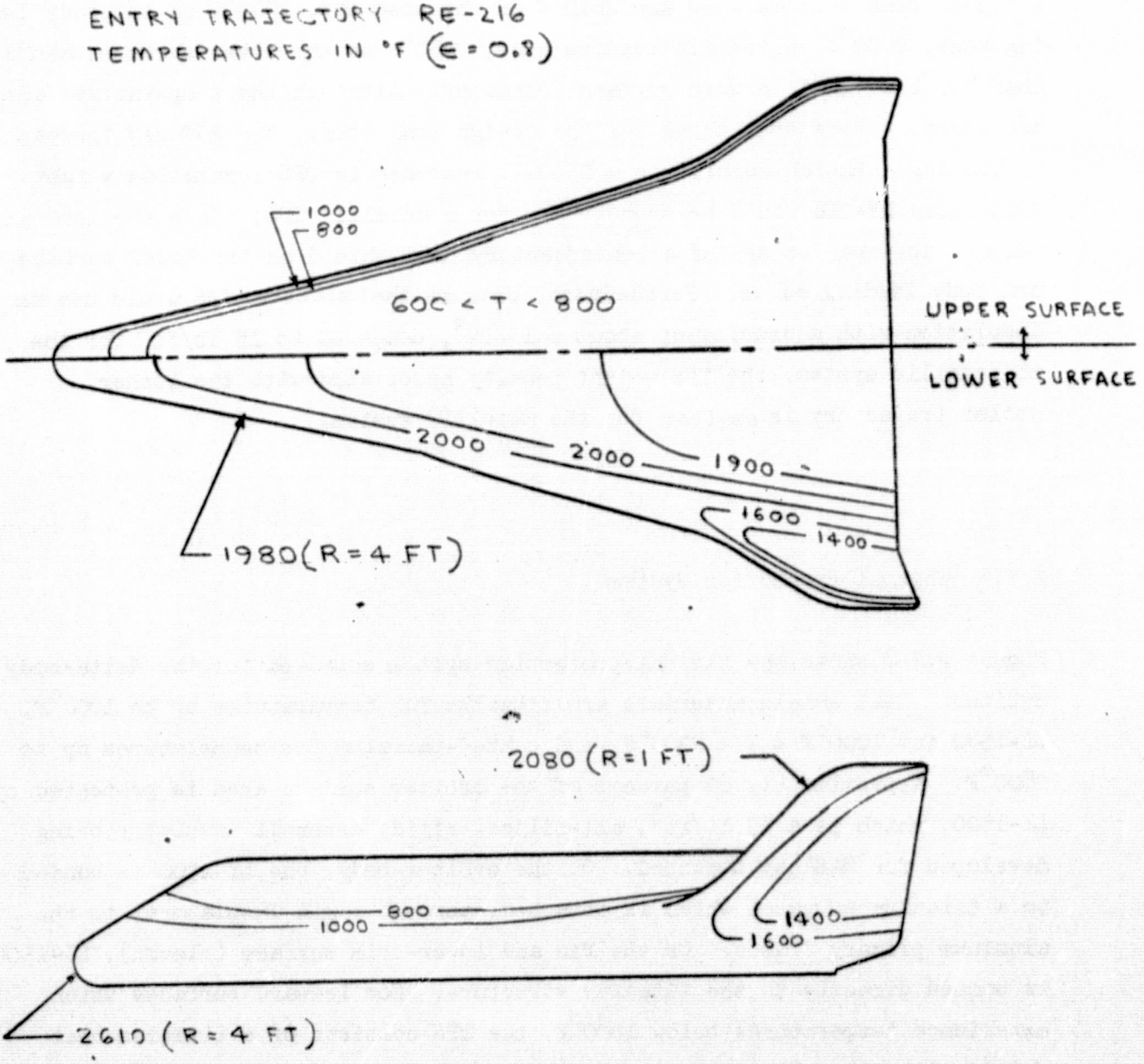

Fig. 2.7-7 Stage-And-One-Half Orbiter Peak-Temperature Isotherms For Low-Temperature Trajectory (RE-216)

show surface-temperature histories and peak-temperature isotherms for an alternate, cooler 1,100-nm crossrange trajectory designated RE-216 (see paragraph 2.4.5). Peak temperatures are 2610°F on the nose cap, 1980°F on the body leading edge, 2080°F on the fin leading edge, 2050°F on the lower surface, and less than 800°F at most leeward surface locations. Although the temperatures are considerably less than those for the design trajectory, the 350-sec increase in heating duration results in a 2500-lb increase in TPS insulation weight. Trajectory RE-216 would be appropriate for a metallic TPS, since the moderate temperatures permit use of a nonrefractory heat shield on the lower surface and body leading edges. Furthermore, because the metallic TPS would use an insulation with a density of about 6 lb/ft^3, compared to 15 lb/ft^3 for the nonmetallic system, the TPS weight penalty associated with the longer, cooler trajectory is smaller for the metallic system.

2.7.4 Thermal Protection System

Figure 2.7-8 shows the thermal protection system selected for the delta-body orbiter. Heat shield materials are titanium for temperatures up to 1000°F, LI-1500 for $1000°F \leq T < 2300°F$, and coated-tantalum for temperatures up to 2800°F. Approximately 60 percent of the orbiter surface area is protected by LI-1500, which is a 15 lb/ft^3, all-silica, rigid, external insulator being developed for NASA by Lockheed. On the orbiter-body, the LI-1500 is bonded to a titanium subpanel which is attached, through rigid insulators, to the aluminum primary frames. On the fin and lower-trim surface (elevon), LI-1500 is bonded directly to the titanium structure. For leeward surfaces which experience temperatures below 1000°F, the TPS consists of a titanium heat shield with fibrous insulation attached to the interior surface. Coated tantalum is used only on the nose cap, since this is the only region which experiences temperatures above 2300°F.

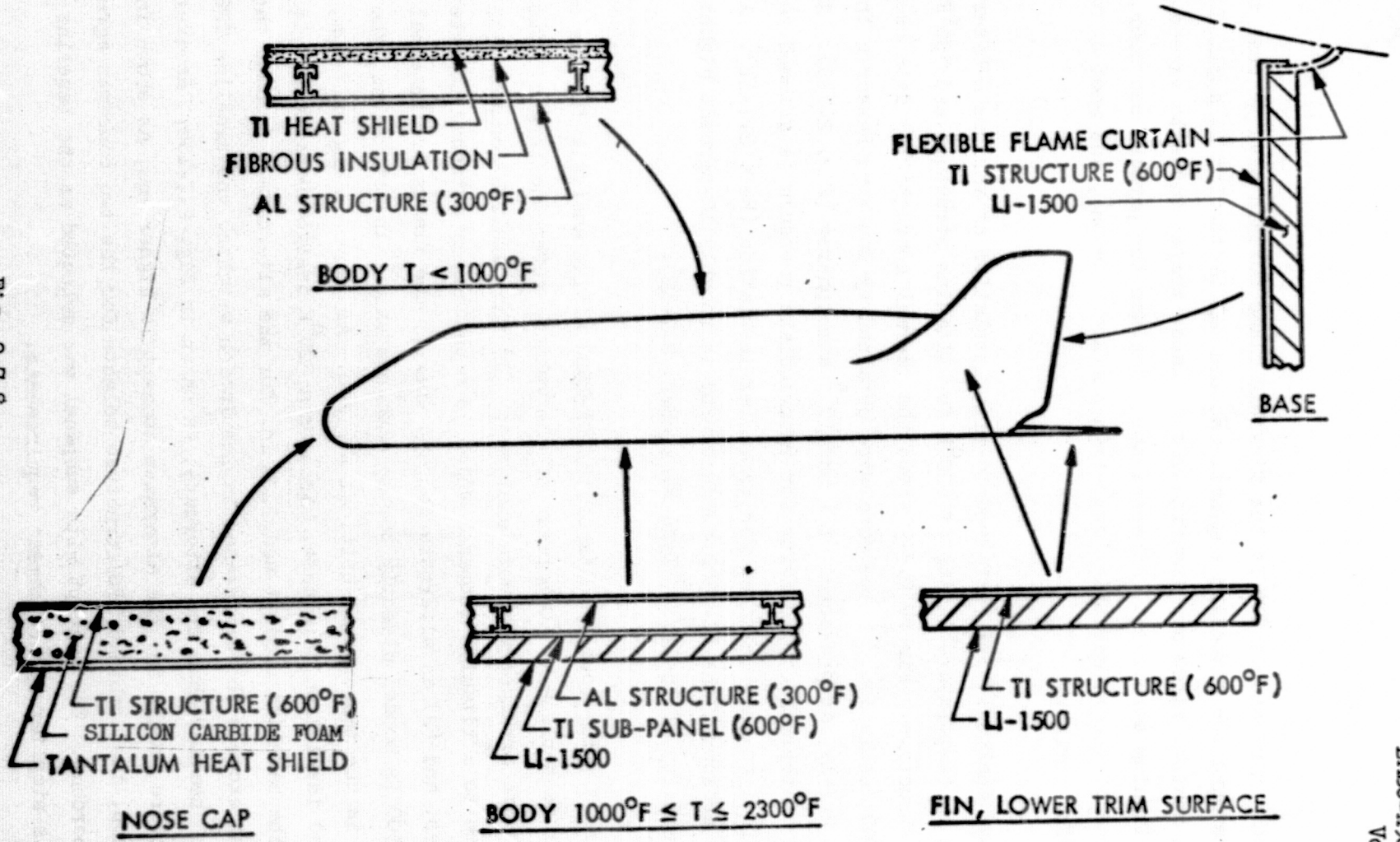

Fig. 2.7-8 Orbiter Thermal Protection System

The only nonreusable TPS is the flexible flame curtain used to seal the base area around the gimballed engines. No thermal protection is applied to areas where heating rates are insufficient to cause temperatures to exceed 600°F on the titanium structure. Affected areas include the payload bay door, upper surface of the retractable lower-trim surface (elevon), and most of the fin-interior surface.

Thermal analyses were performed to size insulation at various orbiter locations, based on temperature limits of 600°F for titanium structure and 300°F for aluminum structure. Figure 2.7-9 shows the thermal conductivity data used to size LI-1500 insulation. These data were obtained by Southern Research Institute (Ref. 2.7-10) at pressures of 1 and 10^{-5} atmospheres (Fig. 2.7-9). The variation of thermal conductivity for intermediate pressure is assumed to be identical to that obtained for Dyna-Flex insulation (Ref. 2.7-11). At 1 atmosphere pressure, the LI-1500 conductivity is roughly 10-percent higher than the conductivity of 15 lb/ft^3 Dyna-Flex (Ref. 2.7-12).

Figure 2.7-10 shows results of the LI-1500 sizing analysis for the orbiter lower centerline at 50 percent of the vehicle reference length. Two TPS/structure arrangements were analyzed: (1) the baseline concept with LI-1500 bonded to a titanium subpanel which is mechanically attached to external frames, and (2) an alternate concept whereby the frames are internal and the LI-1500 is bonded directly to the aluminum skin. In both cases, the aluminum skin is the temperature-critical surface. As shown in Fig. 2.7-10a, the required insulation thickness, based on a 300°F design temperature, is 1.82 in. for the baseline concept and 2.28 in. for the alternate. Because the subpanel weight exceeds the difference in insulation weights, the baseline TPS is 0.27 lb/ft^2 heavier than the alternate, as shown in Fig. 2.7-10b. However, the structure weight for the alternate concept is higher and, as shown in Fig. 2.7-10b, the combined TPS/structure weights for the two concepts agree within two percent. The concept with subpanel was selected as the baseline because of its simplier refurbishment requirements.

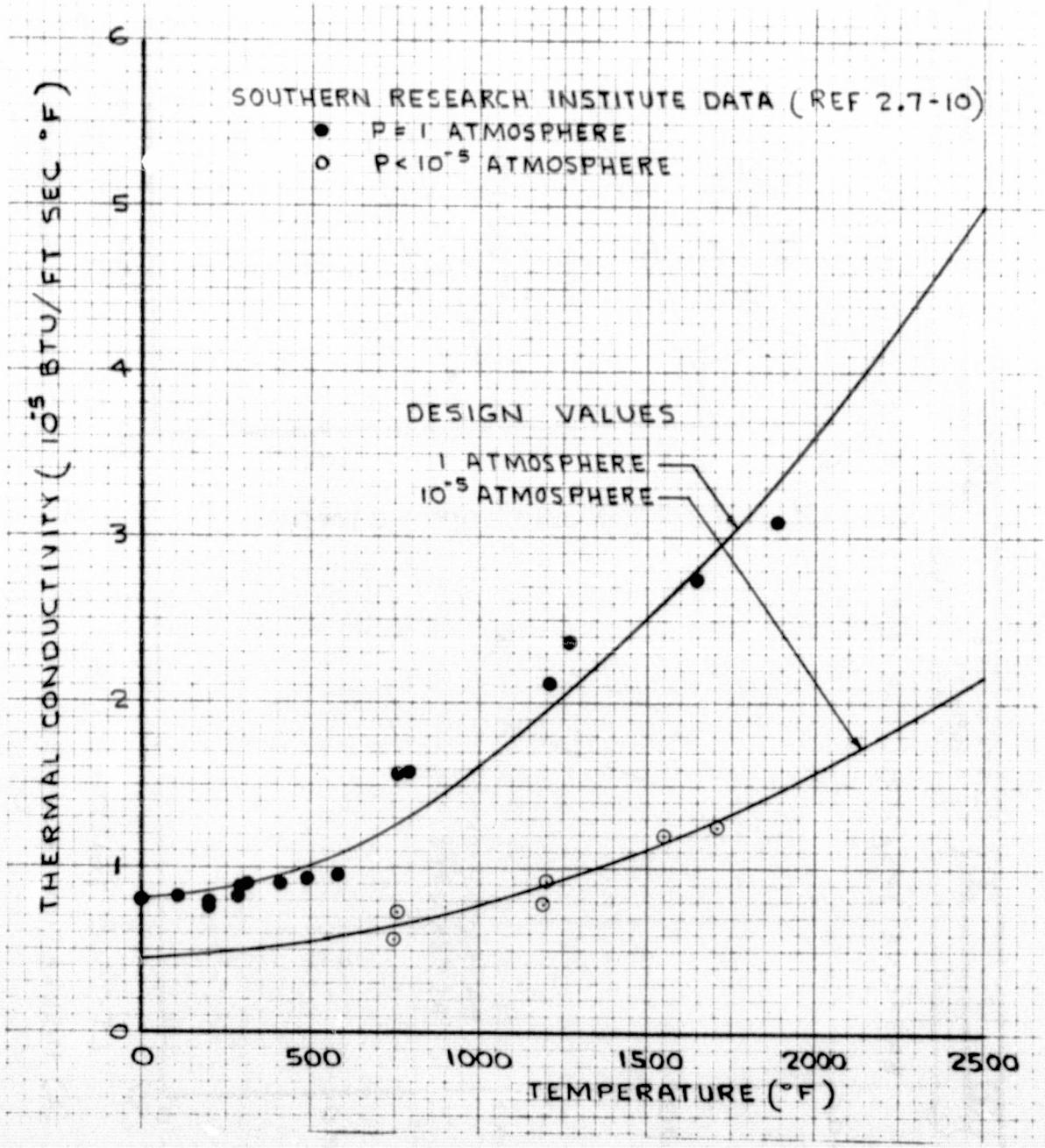

Fig. 2.7-9 LI-1500 Thermal Conductivity

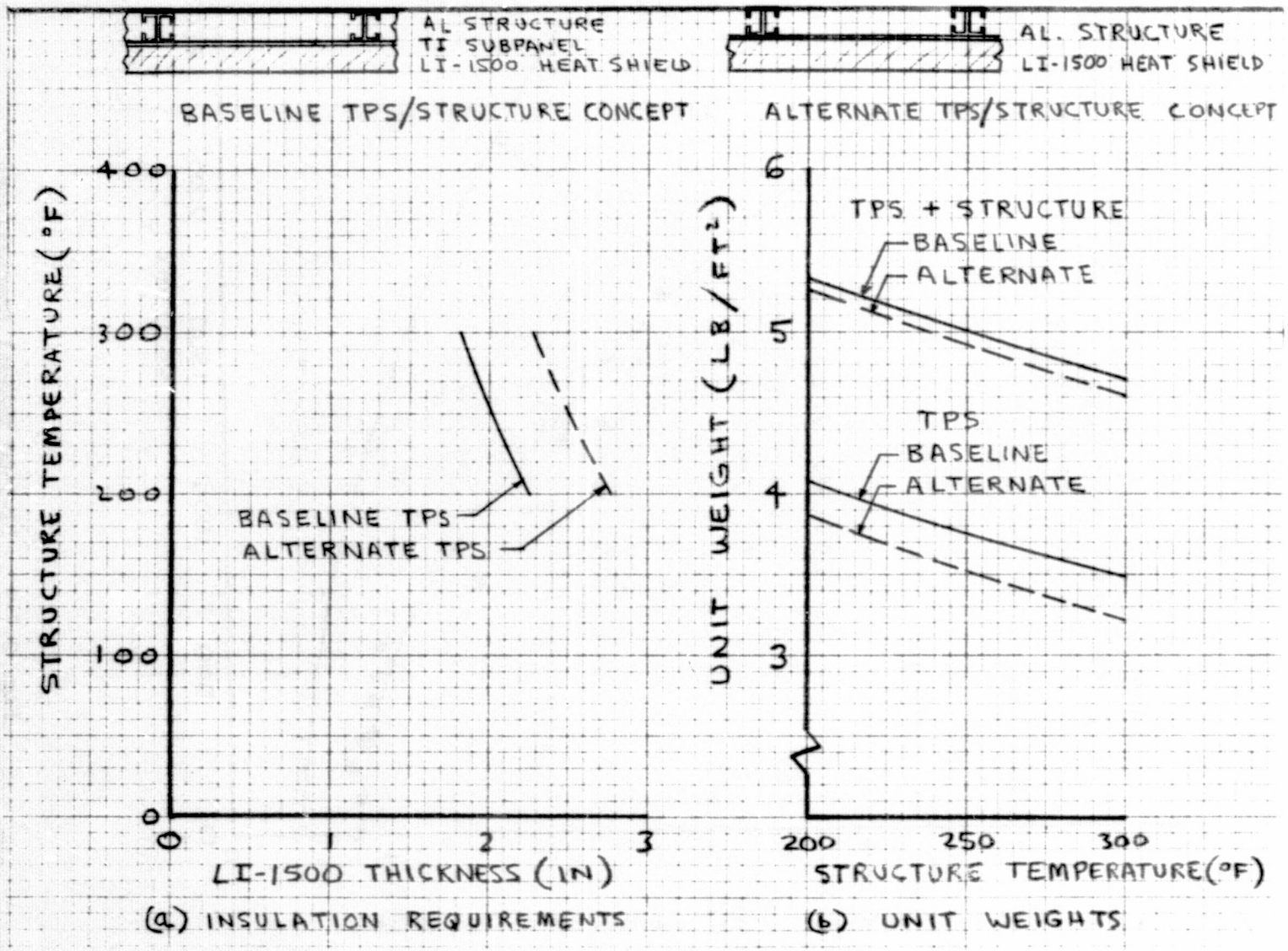

Fig. 2.7-10 Stage-And-One-Half Lower Surface TPS Comparison

LOCKHEED MISSILES & SPACE COMPANY

Table 2.7-2 summarizes insulation thicknesses and TPS weights for the baseline LS-200-10 stage-and-one-half orbiter. These weights are based on the 1100-nm design entry trajectory with an assumed 500-sec go-around. To minimize insulation weight, the aluminum structure is assumed to be cooled with air supplied by ground support equipment, starting five minutes after touchdown. This is accomplished by passing low-velocity, ambient-temperature air through the fuselage; therefore, a minimum of ducting is required.

Due to the small spatial variation in total heat input, a constant LI-1500 thickness of 1.82 in. is used on the lower surface. Insulation thickness shown in Table 2.7-2 for other locations are averages for the particular surface areas. For example, the body leading-edge insulation thickness varies from 1.82 in. at the lower-surface tangent point to 1.25 in. at the upper-surface tangent point, for an area-averaged thickness of 1.40 in.

Table 2.7-2
STAGE-AND-ONE-HALF ORBITER TPS WEIGHTS*

LOCATION	Area (ft^2)	t (in)	W (lb)
Body Lower Surface	3,952	1.82	13,811
Body Leading Edge	2,753	1.40	8,104
Body Upper Surface ($T \geq 1000^{\circ}F$)	937	1.20	2,512
Body Upper Surface ($T < 1000^{\circ}F$)	3,734	0.50**	3,340
Fin Leading Edge	284	0.90	403
Fin Side	1,482	0.70	1,715
Lower Trim Surface (Bottom)	1,086	1.55	2,468
Nose Cap and Skirt	203	---	1,147
Base	1,229	0.75	1,439
Base Flame Curtain	---	---	777
TOTAL	15,660		35,716

*LS-200-10 Configuration (Drawing SKS 100053)
**6 PCF Dyna-Flex; Remainder is 15 PCF LI-1500

As shown in Table 2.7-2, total TPS weight for the stage-and-one-half orbiter is 35,716 lb, based on application of thermal protection to 15,660 ft^2 of surface area.

In addition to the results described above for the baseline TPS, an analysis was performed to compare active and passive TPS weights for the LS 200-5 delta-body orbiter lower surface as a function of entry crossrange (Refs. 2.7-13 and 2.7-14). As shown schematically in Fig. 2.7-11, the active TPS is a redundant, indirect cooling system which uses water-glycol as the transport fluid, and water and ammonia as expendable coolants. For this study, LI-1500 insulation was assumed to be bonded directly to the aluminum skin, which is cooled by flowing water-glycol through aluminum tubes attached to the backface. TPS insulation thickness and hardware are optimized for minimum weight at 1,500-nm crossrange, and the reduction is expendable coolant and APU fuel weights was computed for shorter crossrange. For the passive system, TPS insulation was sized as a function of crossrange.

Figure 2.7-12 compares active and passive TPS weights versus crossrange. The active system weighs about 2,900 lb less than the passive at minimum crossrange, 4,500 lb less at 1,100 nm, and 5,500 lb less at 1,500 nm, based on a lower-surface area of 4,455 ft^2. In addition to TPS weight advantages, the active system allows for TPS integration with other thermal conditioning/life-support systems, provides the ability to reduce TPS weight for missions requiring less than the design crossrange, reduces TPS weight sensitivity to crossrange, and eliminates the requirement for ground cooling. Primary disadvantages of an active TPS are increased costs and decreased reliability, relative to a passive TPS. Consequently, until more detailed studies are performed to substantiate the predicted weight savings and to assess cost and reliability aspects of an active cooling system, it is recommended that the passive system be retained as the baseline TPS.

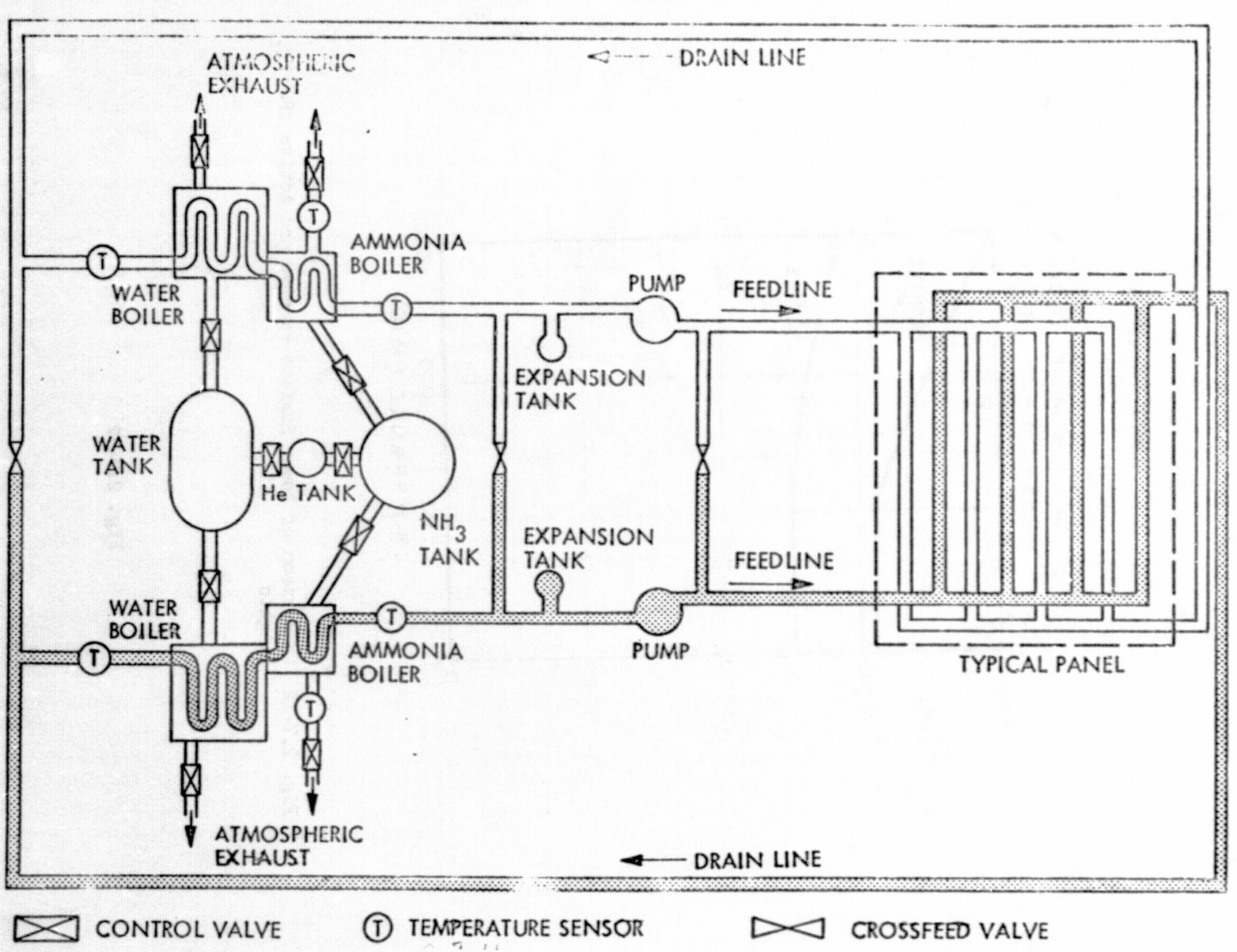

Fig. 2.7-11 Active Cooling Schematic

LOCKHEED MISSILES & SPACE COMPANY

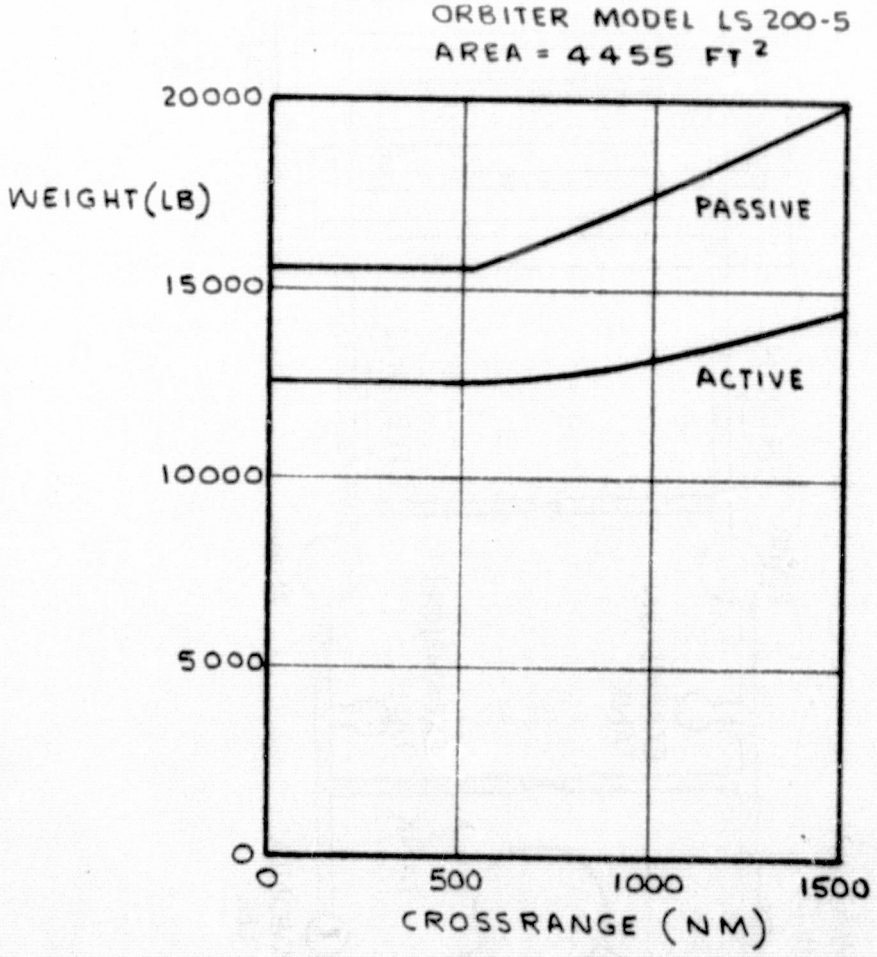

Fig. 2.7-12 Comparison of Lower Surface Passive and Active TPS Weights

Fig. 2.7-12

REFERENCES

2.7-1 U. S. Standard Atmosphere for 1962, U.S. Government Printing Office, December 1962.

2.7-2 Hansen, C.F., "Approximations for the Thermodynamic and Transport Properties of High Temperature Air," NASA TR R-50, 1959.

2.7-3 Bushnell, D., "Effects of Shock Impingement and Other Factors on Leading Edge Heat Transfer," NASA TN D-4543, April 1968.

2.7-4 Eckert, E.R.G., "Survey on Heat Transfer at High Speeds," WADC TR 54-70, April 1954.

2.7-5 Neal, L. and Bertram, M., "Turbulent Skin Friction and Heat Transfer Charts Adapted from the Spalding-Chi Method," NASA TN D-3969, May 1967.

2.7-6 Schultz, H. D., "Computer Program for Flow Field, Aerodynamic Heating and Radiation Equilibrium Surface Temperature Calculations," LMSC-A983836, January 1971.

2.7-7 Aerothermodynamics/Configuration Working Group Meeting Held at NASA-MSFC, 25 January 1971.

2.7-8 "Space Shuttle Vehicle/Engine 550K (SL) Interface Control Document," 13M15000B, 1 March 1971.

2.7-9 McGee, K. W., "Base Thermal Environment and Thermal Protection System Design," LMSC EM L2-01-01-M3-8, Fifth Letter Progress and Status Report, Study of Alternate Space Shuttle Concepts," LMSC-A981489, December 1970.

2.7-9 Guard, F. L., "Delta-Body Aerodynamic Heating Prediction Methods," LMSC EM L2-01-01-M4-3, Fourth Letter Progress and Status Report, Study of Alternate Space Shuttle Concepts, LMSC-A980360, 15 November 1970.

2.7-10 Smyly, E. D. and Pears, C. D., "Properties of Ablation and Insulation Materials; Vol III, Thermal Properties of Three Rigidized Fibrous Insulators," Southern Research Institute Report, prepared under contract NAS 1-7732-1 (to be published).

2.7-11 Cross, R. I. and Black, W. E., "Optimization of Insulation and Mechanical Supports for Hypersonic and Entry Vehicles," AFML-TR-66-414, April 1967.

2.7-12 Dyna-Flex Thermophysical Data, Johns-Manville Aerospace Products, January 1967.

2.7-13 Schultz, H. D., "Comparison of Passive and Active Thermal Protection System Weights for the Delta-Body Orbiter," LMSC EM L2-01-01-M3-6, Fifth Letter Progress and Status Report, Study of Alternate Space Shuttle Concepts, LMSC-A981489, December 1970.

2.7-14 Schultz, H. D., "Comparison of Passive and Active Thermal Protection System Weights for LI-1500 and Metallic Heat Shields," LMSC EM-L2-01-01-M3-9, Fifth Letter Progress and Status Report, Study of Alternate Space Shuttle Concepts, LMSC-A981489, December 1970.

2.8 STRUCTURES

2.8.1 Introduction

The stage-and-one-half structural system employs the delta-body orbiter in combination with two nonrecoverable propellant tank systems interconnected and arranged to form a single V-type droptank module. The droptank assembly is attached to the spacecraft at three locations: one forward in the nose section and two aft at the spacecraft rocket-engine thrust structure. During the sequence of events from prior to launch release to separation, the droptank module is self-supporting to resist axial and bending loads.

The droptank module structural concept makes use of the elementary three-hinged arch concept. Droptanks are comprised of aluminum shell elements, stiffened with longitudinal stringers and circumferential rings, placed internally to facilitate external insulation and minimize aerodynamic heating.

The delta-body orbiter airframe and aerodynamic surfaces comprise the assemblage of shell elements and structural shapes common to the aerospace industry. As will be discussed subsequently, the airframe structure consists of aluminum zee-stiffened panels supported by aluminum frames and longerons. Aluminum bulkheads are located where heavy concentrated loads are introduced. Trade studies revealed that use of titanium in the airframe does not result in weight savings. Studies further revealed (EM-L2-01-01-M1-3, Sixth Letter Progress Report) that the lightest weight thermal protection system (TPS) makes use of titanium subpanels to which LI-1500 is bonded. These subpanels, which are designed for airload and differential pressures, are supported from the fuselage frames. A titanium payload-compartment door was selected over aluminum, however, because the maximum temperature of that area of the fuselage is less than 1000°F.

Aerodynamic surfaces are conventional aircraft structure design except for the provisions for supporting the TPS. Trade studies revealed that use of titanium in lieu of aluminum results in weight savings. Where surface temperatures exceed 1000°F, LI-1500 is bonded to the titanium skin and limited to a bondline temperature of 600°F.

The stage-and-one-half thrust structure represents about one-third of the orbiter weight and acts essentially as the "strongback" of the vehicle; supporting the internal tanks, droptanks, and fins. Trade studies resulted in the selection of titanium to yield the least weight for a thrust structure.

Conventional materials are employed throughout the vehicle system except for the TPS. Studies show that considerable weight savings could be achieved with the employment of beryllium to such areas as the payload-compartment door, TPS subpanels, and aerodynamic surfaces, but program direction required such considerations only for trade information.

Aluminum 7075-T6 is employed on the airframe skin where conventional mechanical fasteners are used and surface temperatures are limited to 300°F. Aluminum 2219-T87 is selected for all propellant tankage, on the basis of excellent fracture toughness, good weldability, and excellent compatibility with cryogenics. Titanium 6Al-4V is used for areas where added strength and/or where temperature extremes prohibit the use of aluminum without protection. Titanium 6Al-4V is limited to 600°F. Titanium 6Al-2Sn-4Zr-2Mo is selected for special areas such as aerodynamic surfaces and the payload-compartment doors where the surface temperatures are permitted to reach 1000°F without thermal protection. Also, this material is used for TPS panels for the fuselage, where it is employed in combination with dynaflex for surface temperatures below 1000°F, and with LI-1500 for surface temperatures above 1000°F.

Subsequent pages of this section discuss in detail the conditions affecting design, various structural aspects contributing to the major weights, and structural concepts peculiar to the stage-and-one-half system.

2.8.2 Materials

2.8.2.1 Survey of Materials and Selection Criteria. Selection of a material or material system is determined by the strength, mechanical and metallurgical stability, and oxidation resistance. Table 2.8-1 is a compilation of selected

Table 2.8-1

CANDIDATE METALLIC SUMMARY

	Melting Point (°F)	Alloy Designation	Max. Structural Utilization Temperature (°F)	Area of Proposed Application
Light Metals				
Aluminum	1,200	2219-T81	300	Internal load-carrying structures, and tanks
		6061-T6		
		7075-T6	250	
Titanium	3,100	8A-1 Mo-1V		Internal load-carrying structures, and heat shields
		6Al-4V	600	
		5Al-2.5Sn		
		6Al-2Sn-4Zr-2Mo	1,000	
Beryllium	2,345	Cross-rolled	1,000	Aerodynamic surfaces, payload-compartment door, TPS subpanels
Superalloys				
Nickel Base	2,650	Inconel 718	1,400	External load-carrying structure and heat shields (1,800°F)
		Inco 625	1,400	
		Rene 41	1,600	
Dispersion-Strengthened	2,650	TD NiCr	2,200	External load-carrying structure and heat shields
		TD Ni		
Cobalt Base	2,700	Haynes 188	1,800	External load-carrying structure and heat shields
Refractory Alloy				
Tantalum	5,425	90Ta-10W	3,000	Nose cap
Columbium	4,380	Cb752	2,500	Heat Shields
Tungsten	6,100	W-2% ThO_2	3,200	Nose cap

candidate alloys, based on an analysis of availability, fabricability, mechanical and physical properties, and their maximum structural utilization temperature. Illustrated in Table 2.8-2 are merit indexes, devised to relate representative materials to various design characteristics and to provide an efficient index for materials comparison. Data included in preparation of these indexes include the following factors:

a. Structural stability during cyclic exposure ($\rho/E_c^{\frac{1}{2}}$)

b. Fabricability

c. Physical properties (α, K, C_p, and emissivity)

d. Mechanical properties (F_{tu}/ρ, F_{cy}/ρ, and creep)

e. t_m: material practical minimum gage thickness

f. Oxidation characteristics

g. Metallurgical stability during cycling environment

2.8.2.2 Light Metals. Use of low-density metals and their alloys, within the operating limits of the materials, usually results in an optimum weight structure. The most important considerations in comparison and selection are that candidate materials be capable of surviving cyclic thermal exposures of service, have adequate strength, and are easily fabricated. Material comparisons in terms of the stability index are shown in Fig. 2.8-1.

2.8.2.2.1 Aluminum Alloy. Aluminum alloy 2219-T81 is a leading candidate for unpressurized structural applications requiring welding because of its superior strength and thermal stability at high temperatures in the heat-treated condition. This alloy offers excellent formability and weldability and is available in all mill forms. Maximum service temperature should not exceed 300°F. Aluminum alloy 2219-T87 was selected for tankage because of increased tensile strength.

Aluminum alloy 7075-T6 was selected for skin panel applications not requiring welding on the basis of its high strength, stability, and good fabricability. Long service temperatures should not exceed 300°F maximum.

Table 2.8-2

MERIT INDEXES FOR CANDIDATE MATERIALS

TEMPERATURE RANGE (°F)	VEHICLE STRUCTURAL APPLICATION	CANDIDATE MATERIAL(1)	PHYSICAL PROPERTIES(2) P S G E	TENSILE PROPERTIES(2) P S G E	CREEP RESISTANCE(2,3) P S G E	FORMABILITY(2) P S G E	WELDABILITY(2) P S G E	OXIDATION RESISTANCE(2) P S G E	LEADING CANDIDATE MATERIALS	REMARKS
1,800 - 421	WING, TANKS, BODY STRUCTURE	2219-T81							*2219-T81	GOOD FABRICABILITY AND STRENGTH
		6061-T6								GOOD WELDABILITY, MODERATE STRENGTH
		7075-T6							*7075-T6	HIGH STRENGTH, WELDING NOT PRACTICAL
		Be 38A1					(4)			NOT WELDABLE
		AVE 7902					(4)			
		8A1-1Mo-1V								GOOD STRENGTH AND FABRICABILITY
		6A1-4V							6A1-4V	GOOD STRENGTH AND FABRICABILITY
		8A1-2,5Sn								LOW STRENGTH, GOOD FABRICABILITY
1,800 - 2,800	UPPER SURFACE PRIMARY AND SECONDARY STRUCTURE HEAT SHIELD	COBALT BASE ALLOY: HAYNES 25							*HAYNES 25	ANNEALED MATERIAL WITH MODERATE TENSILE PROPERTIES, GOOD OXIDATION RESISTANCE TO 1,400°F
		NICKEL BASE ALLOY: INCO 625 (1,400°F)							*INCO 625	MATRIX STRENGTHENED ALLOY WITH MODERATE TENSILE PROPERTIES, METALLURGICALLY UNSTABLE ABOVE 1,400°F
		INCO 718 (1,400°F)								AGE-HARDENABLE ALLOY WITH HIGH-TENSILE PROPERTIES, MODERATE CREEP RESISTANCE
		HASTALLOY I								SUPERIOR OXIDATION RESISTANCE TO 2,000°F
		RENE 41(ACC.)							*RENE 41	AVERAGE WELDABILITY, SUBJECT TO EMBRITTLEMENT AND ALLOY DEPLETION ABOVE 1,400°F
		TD NICKEL								NOT COMPETITIVE WITH MECHANICAL PROPERTIES OF OTHER SUPERALLOYS
		TD NiCr							*TD NiCr	CANDIDATE UNCOATED MATERIAL FOR APPLICATION TO 2,200°F

(1) MAXIMUM STRUCTURAL TEMPERATURE LIMIT

(2) RATING LEGEND: P-POOR, S-SATISFACTORY, G-GOOD, E-EXCELLENT

(3) BASED ON 0.5 PERCENT CREEP AT SPECIFIED TEMPERATURE

(4) NOT APPLICABLE

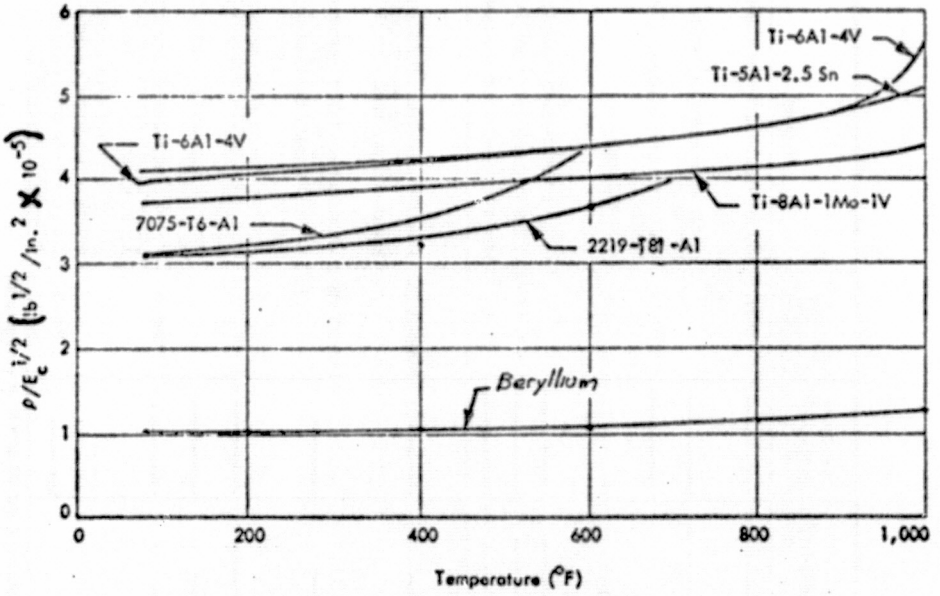

Fig. 2.8-1 Structural Stability Comparison of Aluminum, Titanium Alloys and Beryllium

2.8.2.2.2 Titanium Alloy. Titanium alloy 6AL-4V has been examined for applications up to 600°F because of its excellent response to fabricability, high strength, and extensive history of use in manufacturing. Titanium alloy 6Al-2Sn-4Zr-2Mo, according to preliminary investigations, will survive continuous service at 1,000°F with good hot-salt stress corrosion characteristics and is a leading candidate for heat shields at temperatures less than 1,000°F.

2.8.2.2.3 Beryllium. Beryllium cross-rolled sheet has been examined for applications up to 1,000°F because of its unique combination of properties. Its high modulus of elasticity is beneficial to stability-critical structure (e.g., aerodynamic surfaces) and structure subjected to flutter, acoustic, and dynamic environments. Its elevated temperature capability in combination with its high specific heat coefficient reduces TPS and insulation requirements. The material's high thermal conductivity and dimensional stability leads to low thermal gradients, stresses, and warpage. Although beryllium's fatigue resistance is excellent, it has other characteristics which must be evaluated in terms of material characterization, design technique, and fabrication methods. Beryllium can be subjected to temperatures up to 1,400°F without material degradation, but it is

recommended that the temperature should not exceed 1,000°F for structural utilization.

2.8.3.3 Superalloys. The term superalloy usually defines the nickel-, cobalt-, and iron-base alloys that are intended for structural use in the temperature range of 1,000° to 2,000°F. They have more oxidation-resistance than stainless steels and display considerably more strength above 1,000°F. Generally, the cobalt-base alloys are more chemically and metallurgically stable at higher temperatures than the nickel-base alloys. Most superalloys display good weldability with the exception of the thoria-dispersed strengthened alloys. Therefore, the metallurgical and chemical stability must be considered in determining the relative merits of the candidate alloys for this program. Figure 2.8-2 shows temperature-property data in terms of the structural stability index.

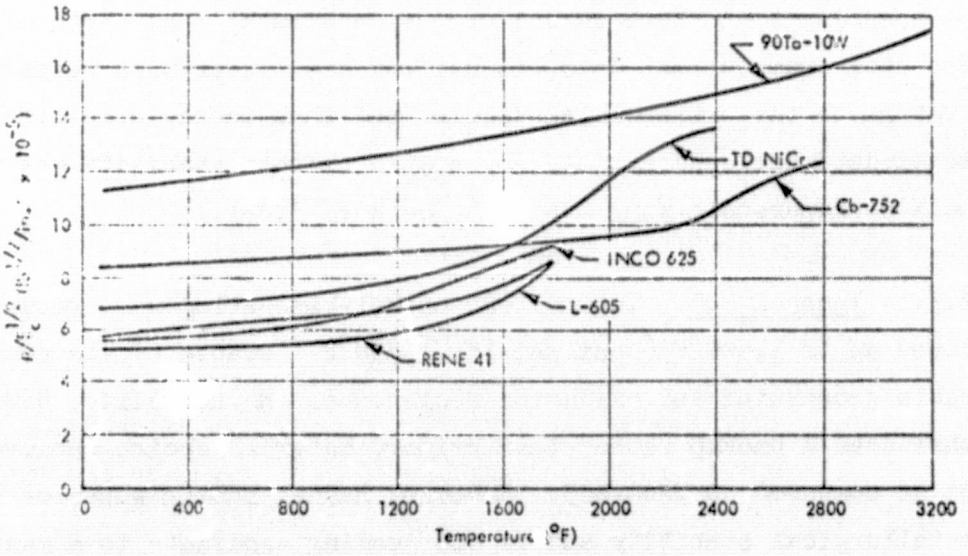

Fig. 2.8-2 Structural Stability Comparison of Candidate High-Temperature Materials

Superalloys are oxidation-resistant but will oxidize at high temperatures. Oxidation behavior of a metal or alloy is dependent upon not only the composition of the reactants and the environment, but also can be affected by the internal and surface structure, state of stress, and geometry of the part.

Additionally the process of oxidation is sensitive to velocity, density, composition, and the flow pattern of the oxidizing environment. Alloys designed for strength may not have maximum oxidation resistance; when maximum strength is desired, protective coatings should be considered. Usually a light surface-oxide is desirable for high emittance; however, intergranular oxidation in small amounts can be a serious problem on thin sections. It not only reduces the cross section but can act as a notch in notch-sensitive materials. Of the super-alloys, the precipitation hardenable nickel-base alloys, such as Rene 41, are the most susceptible to intergranular oxide penetration. As previously mentioned, stress also affects the oxidation rate. It appears that oxidation proceeds at a constant rate with increasing stress until a threshold level is reached, where oxidation then proceeds more rapidly. Static-oxidation behavior at one atmosphere is used for initial alloy comparison as illustrated in Fig. 2.8-3. Depth of penetration per side for the candidate superalloys is presented -- assuming that there is uniform oxide attack; that depth of penetration, extrapolated from current data, is uniform and linear with respect to time and temperature to the extrapolated points; and that there is no stress. These published data are substantiated by static thermal stability tests conducted in the NASA Hypersonic Wing Study. (See Ref. 3.8-1.)

2.8.2.3.1 Inconel 625. Inconel 625 nickel-base alloy was evaluated for temperatures up to 1,400°F (heat shield, 1,800°F) because of its combination of desirable properties and oxidation resistance. Haynes alloy, H.S. 25 (L605), is considered a backup rather than primary material choice because of higher weight as compared to Inco-625. However, Haynes 188 is superior in thermal and metallurgical stability and is the leading candidate to a maximum service temperature of 1,800°F for heat shields.

2.8.2.3.2 TD-NiCr. Thoria-dispersed strengthened alloy, TD-NiCr, was evaluated for application to heat shields and leading-edge designs up to 2,200°F. TD-NiCr is a nickel/chromium-base alloy strengthened by an ultrafine and a highly uniform dispersion of thoria (ThO_2) that has outstanding oxidation resistance, structural stability, and moderate strength up to 2,400°F. This alloy was primarily developed for long-time service in severe applications at

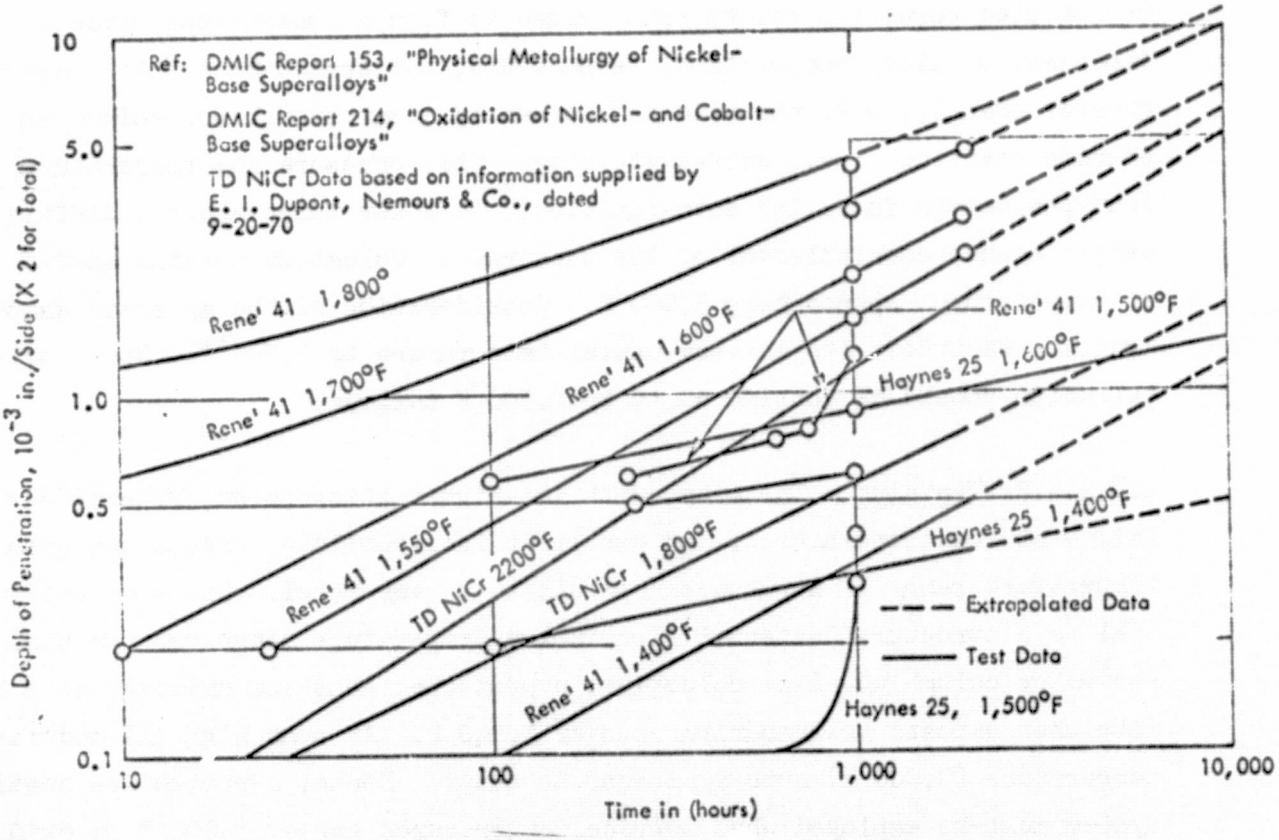

Fig. 2.8-3 Depth of Oxidation Versus Temperature for Rene 41, TD-NiCR, and H.S. 25

temperature ranges bridging that served by superalloys and coated refractory metals. However, the limited area for application of this material led to dropping it from consideration for this study.

2.8.2.4 Refractory Metals. Increasing demand for structural materials capable of operating at temperatures higher than superalloys requires consideration of refractory-base materials.

2.8.2.4.1 Columbium. Columbium possesses several outstanding properties that make it attractive for high-temperature structural applications. The metal and most of its alloys possess excellent fabricability and its density is less than most of the refractory materials. However, use of columbium at temperatures greater than 1,000°F requires an oxidation-protective system, because the oxide of columbium is nonprotective.

Unprotected columbium reacts with oxygen to form a nonadherent oxide at a rate dependent on alloy composition, temperature, and environment. At temperatures greater than 2,700°F, the rate is apparently great enough to produce an exothermic reaction; i.e., self-sustaining. This pressure and temperature dependent phenomenon is called auto-ignition. At lower temperatures, diffusion of oxygen causes embrittlement of the substrate. Columbium retains useful strength to temperatures approaching 3,000°F. Consideration of the apparent auto-ignition restricts its maximum useful temperature to 2,700°F. Reuse of coated columbium should be considered to be 2,500°F maximum.

2.8.2.4.2 Tantalum. Tantalum, with its high-melting point, retention of ductility at low temperatures, and excellent fabricability, offers the greatest temperature range of structural usefulness of any metal. Its greatest potential as a structural material lies in the temperature range greater than that served by columbium. Like columbium, unprotected tantalum oxidizes at a high rate when exposed to temperatures over 1,000°F. At some high and undefined temperature (3,000°F) auto-ignition can occur. Hence, a protective coating system must be employed when service temperatures exceed 1,000°F in oxidizing environments.

2.8.2.4.3 Tungsten. Tungsten is a candidate material for ultrahigh temperature application. If used in a materials system employing a silicide protective coating, maximum service temperatures under oxidizing environments are limited to 3,200°F because of coating limitations. Possible use of this material as an uncoated nose cap is practical because of the oxidation mode at ultrahigh temperatures. However, the optimum potential of this candidate system has not been investigated fully nor considered in this survey.

2.8.3 Structural Criteria

Basic criteria and interpretive information governing structural design for all service conditions to be analyzed during Phase A studies are discussed. Included herein are design objectives pertinent to structural design and basic design characteristics which the vehicle must exhibit.

2.8.3.1 Design Objectives. The basic philosophy of these studies is that structural, mechanical, and propulsion elements shall be designed for minimum weight, while retaining structural capability for 100-mission cycles.

2.8.3.1.1 Fail-Safe/Safe-Life. Generally, both fail-safe and safe-life philosophies shall be applied to the structural design. In certain structural cases, such as pressurized vessels and landing gear where this is impractical, safe-life philosophy shall be applied.

2.8.3.1.2 Performance. Structural design shall be based only upon critical flight conditions and no additional flight weight shall result from nonflight loadings and environments associated with handling, transportation, testing, erection, static firing, explosions of support equipment or other space vehicles, or sonic booms. Overall vehicle loads associated with ferry conditions shall not exceed design levels associated with other operational modes by restrictions on the aircraft performance envelope.

2.8.3.1.3 Safety. Structural design shall be consistent with strict safety requirements and consideration shall be given to crew and passenger safety in the selection of concepts and materials -- including flammability, toxicity, escape times, radiation and meteoroid shielding, and thermal and dynamic environments.

2.8.3.1.4 Miscellaneous. Structural design shall (1) emphasize simplicity and minimum weight concepts; (2) enable application of proven producibility techniques; (3) provide for ease of maintainability and accessibility with minimal cost and flight weight penalties; (4) provide for interchangeability of parts without degradation of structural characteristics; and (5) incorporate materials compatible with parts, components, systems fluids, and gases.

2.8.3.2 Design Characteristics. The structure shall be designed to withstand simultaneously limit loads, pressures, temperatures, and accompanying environments without detrimental deformation or detrimental degradation of strength throughout its service life.

2.8.3.2.1 Limit Loads. Vehicle design limit loads shall be determined from steady-state and/or dynamic analyses which, as appropriate, shall account for the following:

a. Vehicle inertia, flexibility, and structural damping
b. Engine thrust and thrust perturbations
c. Aerodynamic characteristics
d. Fluid dynamics
e. Control-system interactions

In lieu of dynamic analyses, appropriate factors shall be used. Limit loads shall be based upon combinations of loads from various sources occurring at a particular instant, rather than "worst-on-worst" approaches.

2.8.3.2.2 Limit Pressure Loads.

Regulated. Design limit values for regulated pressure (e.g., propellant tanks, crew and cargo compartments) shall be based upon the upper limit of the relief-valve setting when pressure is detrimental to the load-carrying capability of the structure. When pressure increases the load-carrying capability, the lower limit of the operating pressure shall be used to determine design limit load.

Nonregulated. Nonregulated pressures (e.g., vented compartments, external aerodynamics and buffet excitations) shall be determined on the basis of a rational statistical analysis of parameters affecting these load sources (e.g., trajectories). When the pressure is detrimental to structure load-carrying capability, the 99.9-percent nonexceedance level shall be used to determine limit design load. When the pressure increases load-carrying capability of the structure, the 0.1-percent nonexceedance value shall be used to determine limit design load.

2.8.3.2.3 Design Factors.

Factors of Safety. Factors of safety shall be applied only to mechanically induced limit loads and pressures; thermally induced limit loads shall not be multiplied by a factor of safety. The factors of safety shown in Table 2.8-3 shall be used.

Table 2.8-3

ORBITER VEHICLE FACTORS OF SAFETY

Component	Yield	Proof	Ultimate	
			Liftoff Through Orbit	Deorbit Through Landing
General structure (vented)	1.0	(1)	1.4	1.5
Pressurized Compartment	1.5	(2)	2.0 (3)(4)	2.0 (3)(4)
Cryogenic Pressure Vessels (applied to ullage plus hydrostatic pressure)	LH_2	(2)(5)	2.0 (3)(4)(5)	2.0 (3)(4)(5)
	LO_2	(2)(5)	1.78 (3)(4)(5)	1.78 (3)(4)(5)
Hydraulic-System Complete	(2)	1.5	2.5	2.5
Pneumatic System Complete	(2)	2.0	4.0	4.0
Droptanks Structure, General	1.0	(2)	1.4	(1)

(1) Not applicable

(2) To be determined

(3) In compression-critical cases for load-carrying tanks, a factor of 1.5 is applied to flight-maneuver loads where the pressure is stabilizing, in which case no factor is applied to the pressure. In noncompression-critical cases (where pressure is nonstabilizing), a factor of 2.0 or 1.78 (as applicable) shall be applied to the line loading (determined from combining the pressure load and the maneuver load).

(4) Applied to limit pressure when flight-maneuver loads are insignificant

(5) Based on fracture-mechanics analysis

Table 2.8-3

Miscellaneous Factors. Appropriate hazard, fitting, casting, bearing, weld, and stress concentration factors, as well as other special factors that may be relevant to personnel safety, strength, compatibility of materials, or type of construction, shall be defined and accounted for in addition to factors of safety.

2.8.3.2.4 Material Allowables. Material strength and stiffness properties shall be based on sufficient authoritative test data to establish design values on a statistical basis. In establishing allowable strength properties, the effects of temperature, thermal cycling, environments, and corrosive agents shall be accounted for.

Documents cited in MIL-HDBK-5A, MIL-HDBK-17, and MIL-HDBK-23 are acceptable sources of data for allowable strength properties of materials and joints and fasteners.

Material A (99-percent exceedance) allowables shall be used in all applications where failure of a single load path would result in catastrophic loss of vehicle structural integrity. Material B (90-percent exceedance) allowables may be used in redundant structures in which the failure of an element would not result in catastrophic vehicle failure.

2.8.3.2.5 Stiffness. In addition to fulfilling strength requirements of the preceding paragraph, structural design must satisfy the following stiffness requirements. The effect of temperature environments on stiffness properties shall be accounted for.

Deformation at Limit Load and Pressure. The structure shall not experience excessive deformation when subjected to limit loads and pressures in the coexisting thermal environments. Structural deformations shall be considered excessive if they: (1) cause unintentional contact, or (2) cause components to exceed specified dynamic envelopes. There shall be no permanent detrimental deformation at limit load.

Deformation at Ultimate Loads and Pressures. Structural deformation shall not precipitate a strength failure when subjected to ultimate loads and pressures in the expected coexisting thermal environment.

Buckling. Structural components consisting of thin, curved, isotropic, or composite sheet shall be designed so that (1) buckling resulting in collapse of the component will not occur from application of ultimate loads and (2) buckling deformation resulting from limit loads shall not impair functions of nearby equipment or produce undesirable changes in loading distribution.

Dynamics and Aeroelasticity. The structure shall be designed to (1) minimize all detrimental instabilities associated with coupling mechanisms of structural vibration modes; (2) minimize detrimental effects on loads and dynamic response which are associated with structural flexibility; (3) minimize detrimental interaction between the structure and other vehicle systems; (4) preclude impairment of safety, performance, and comfort of crews; and (5) avoid detrimental effect on vehicle stability and control.

Provisions shall be made in propellant-tank design for possible incorporation of fuel-slosh supporting devices. Necessity for such devices shall be determined on the basis of the impact of slosh damping on overall vehicle loads, control-system effectiveness, and overall vehicle stability.

Vehicle design shall prevent structure-propulsion system coupling (POGO) to the extent that (1) loads in excess of design values, established by other conditions, are not developed and (2) accelerations in excess of those specified for man-rating are not exceeded. If instability is evidenced, suitable modification to the coupled system shall be incorporated.

Dynamic-Induced Environments. The vehicle shall be designed to limit the structural response due to acoustic and aerodynamic noise, and vibration and shock environments in such a maneuver as to preclude (a) structural failure, (b) reduction in service life to an unacceptable level, (c) system or component

malfunction or performance degradation beyond specified limits, and (d) impairment to safety, performance, and comfort of the crew.

Vehicle load structures (such as brackets and trusses) shall provide required structural stiffness and transmissibility characteristics to limit response due to vibration and shock environments to those compatible with component or system environmental specifications.

2.8.3.2.6 Thermal Characteristics. The structure shall be designed to withstand effects of natural and induced thermal environments throughout its service life. Thermal environments shall not (1) precipitate failure or detrimental deformation; (2) exceed limiting temperatures set for crew, payload, and components of other systems specifications; nor (3) cause failure to meet mission objectives.

2.8.3.2.7 Thermal Protection Systems.

Elevated Temperatures. The thermal protection system (TPS) for elevated temperatures shall be designed to maintain the structure and other affected components in the vehicle at temperatures within design constraints for all ground- and flight-operating conditions resulting from mission requirements. Thermal protection shall be compatible with the cryogenic TPS and adjacent structure in terms of temperature limitations, deflections, and loads.

Cryogenic Temperatures. The cryogenic TPS shall be designed to maintain structures and other related components at temperatures within design constraints for all ground- and flight-operating conditions resulting from mission requirements. Also, it must be compatible with the elevated TPS and adjacent structure in terms of temperature limitations, deflections, and loads.

2.8.4 Structural Loads

2.8.4.1 Loads Criteria and Assumptions. The loads criteria are contained in EM L-1-02-10-M1. Excerpts and deviations are included in the following paragraphs.

2.8.4.1.1 Maximum αq Condition. The design maximum product of pitch angle-of-attack and dynamic pressure during ascent is assumed to be $\pm$2000 deg psf. This value is substantiated by guidance-trajectory computer analysis which includes the effects of a 95 percentile quasi-steady-state wind-speed envelope for ETR combined with 85 percent of the 99 percentile quasi-square wave gust. Also, the trajectory analysis shows that for the sidewind condition (βq), a roll maneuver is possible which reduces the βq condition to non-critical values.

2.8.4.1.2 Orbiter Landing. The orbiter landing condition was investigated and found to be a critical condition. The criteria sink rate of 10 ft/sec combined with a 1g airload has been used for orbiter landing loads analysis. The main gear reaction was found to be 1.7 times the landing weight of the orbiter.

2.8.4.1.3 Launch Release. The launch release condition was found to be a critical droptank loading condition. A thrust-to-weight ratio of 1.25 was assumed. A load factor of $\pm$ 0.25 g axial was combined with the rigid-body axial load factor to account for elastic response during liftoff.

2.8.4.1.4 Noncritical Conditions. Loading conditions investigated and found to be noncritical for either the droptanks or orbiter fuselage are as follows:

a. Post release with one engine out. Axial load factor of 1.25g and +0.1g dynamic axial factor.

b. Maximum axial load factor of 3g (including dynamic effects).

2.8.4.2 Results. The analysis consisted of determining design loads for the droptanks and orbiter for the critical flight conditions of a vehicle designated as LS 200-5. Loads found to be critical to the design of major structural components are presented on the following Table and Figures:

a. Tanks to Orbiter Attachment Reactions and Ascent Load Factors (Table 2.8-4)
b. Launch Release Droptank Loads in the Pitch Plane (Fig. 2.8-4)
c. Launch Release Droptank Loads in the Yaw Plane (Fig. 2.8-5)
d. Maximum αq Droptank Loads in the Pitch Plane (Fig. 2.8-6)
e. Maximum αq Droptank Loads in the Yaw Plane (Fig. 2.8-7)
f. Delta Body Orbiter Fuselage Design Loads (Fig. 2-8-8)
g. Delta Body Orbiter Reentry Pressures on Fuselage Lower Surface; 378 nm Crossrange (Fig. 2.8-9)
h. Delta Body Orbiter Reentry Pressures on Fuselage Lower Surface; 1500 nm Crossrange (Fig. 2.8-10)

2.8.4.3 Droptank Design Loads. The determination of preliminary design loads for the droptank was based on an evaluation of three distinct loading conditions; those considered were the most severe for the prelaunch, launch, and ascent phases. The three conditions analyzed were (1) launch release (all-engines operating), (2) postrelease (one outboard-engine out), and (3) maximum αq (95-percent headwind plus gust). It was found that the tank loads during the launch release condition were more severe than in either tank for the postrelease case; therefore, the load distributions for the postrelease condition have not been presented.

Limit loads on the droptank structure during the launch-release condition are shown in Figs. 2.8-4 and 2.8-5 for the pitch and yaw planes, respectively. Distributions of bending moment and axial load are given over the tank length and apply to either tank. These loads are entirely inertia- and -geometry-produced. It is considered that ground winds would have a relatively insignificant effect on loads of this magnitude, and accordingly they have been ignored in this analysis.

Table 2.8-4

TANKS TO ORBITER ATTACHMENT REACTIONS AND ASCENT LOAD FACTORS

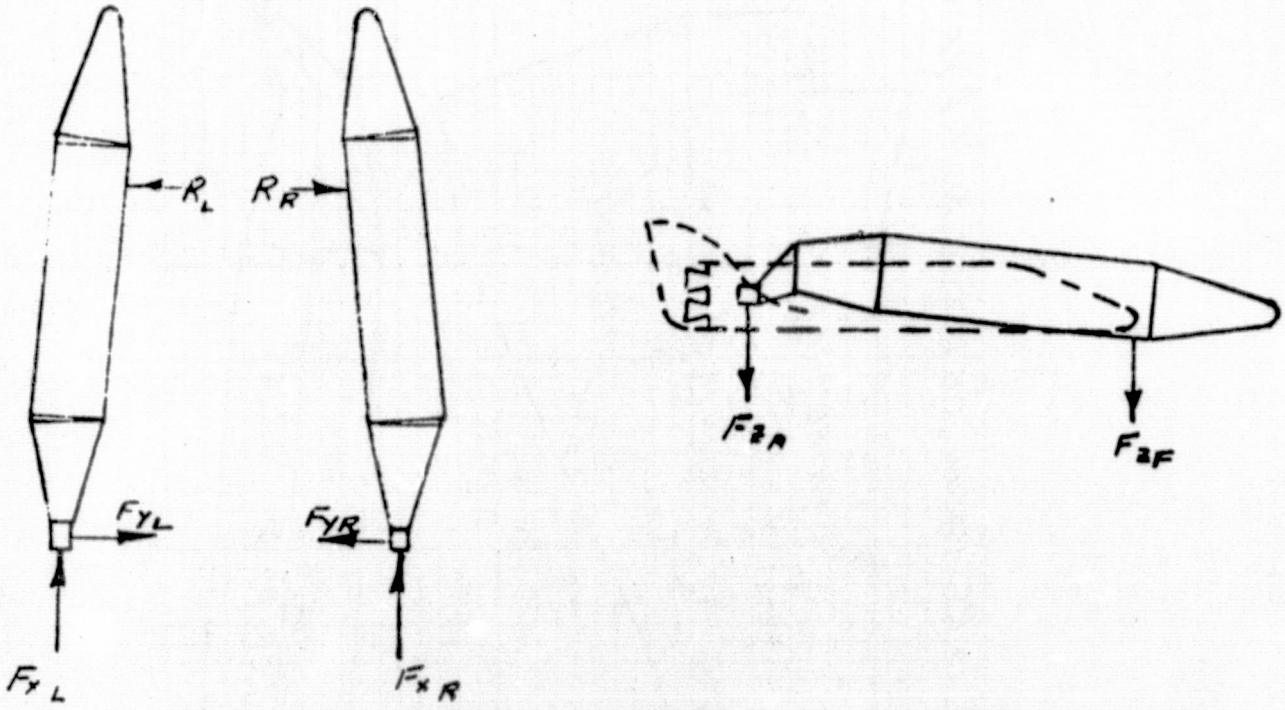

REACTIONS IN EACH TANK ~ KIPS (+ AS SHOWN)

CONDITION	R_R & R_L	F_{XR} & F_{XL}	F_{YR} & F_{YL}	F_{ZA}	F_{ZF}
LAUNCH RELEASE	176.0	2,280.0	176.0	0.0	0.0
MAX α Q	648.0	2.040.0	223.0	24.55	45.95

LOAD FACTORS

CONDITION	n_x	n_y	n_z
LAUNCH RELEASE	1.5	0.0	0.0
MAX α Q	1.7	0.0	0.212

Table 2.8-4

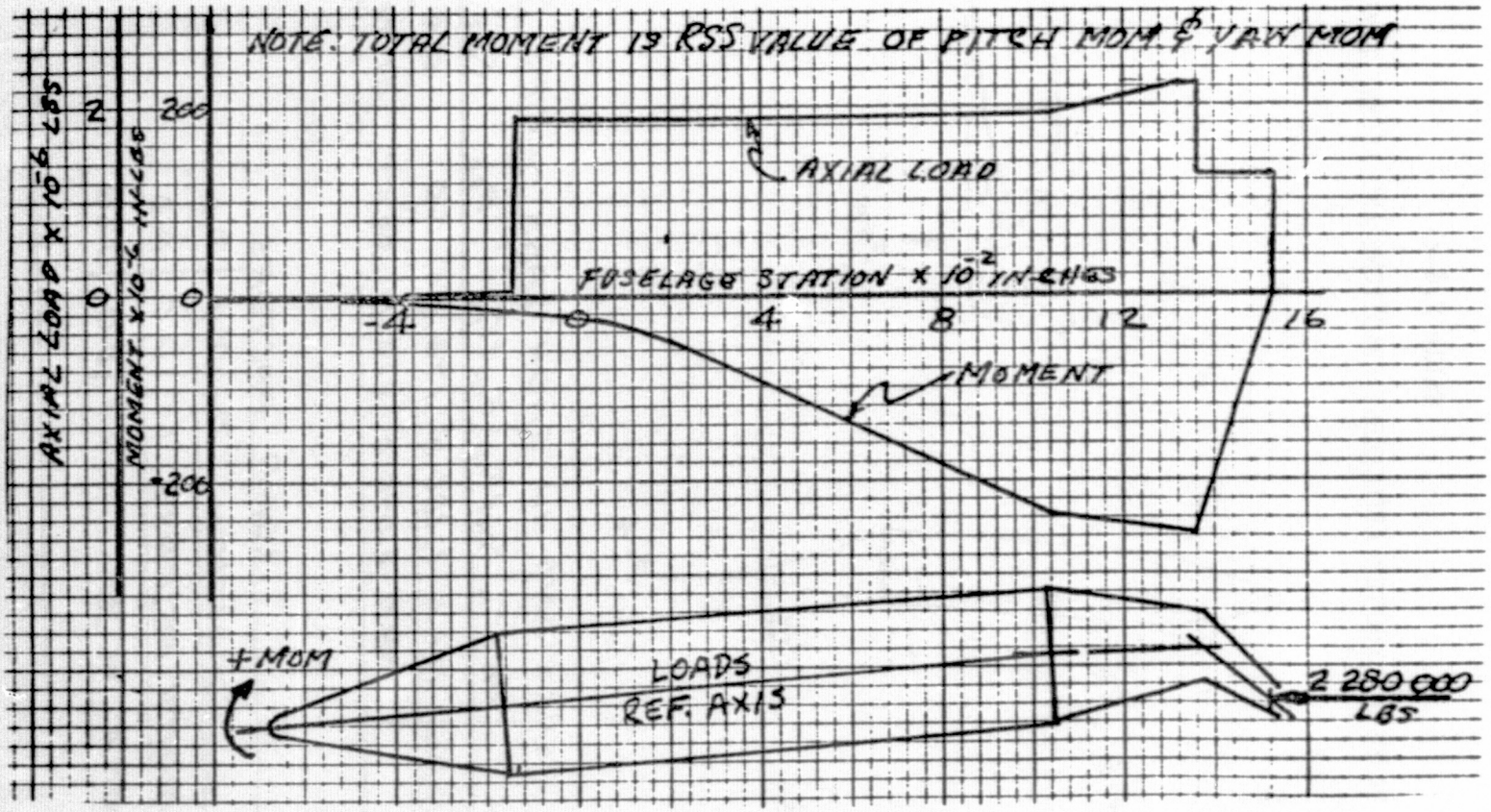

Fig. 2.8-4

Fig. 2.8-4 Droptank Loads Launch Release Condition - Loads in Pitch Plane

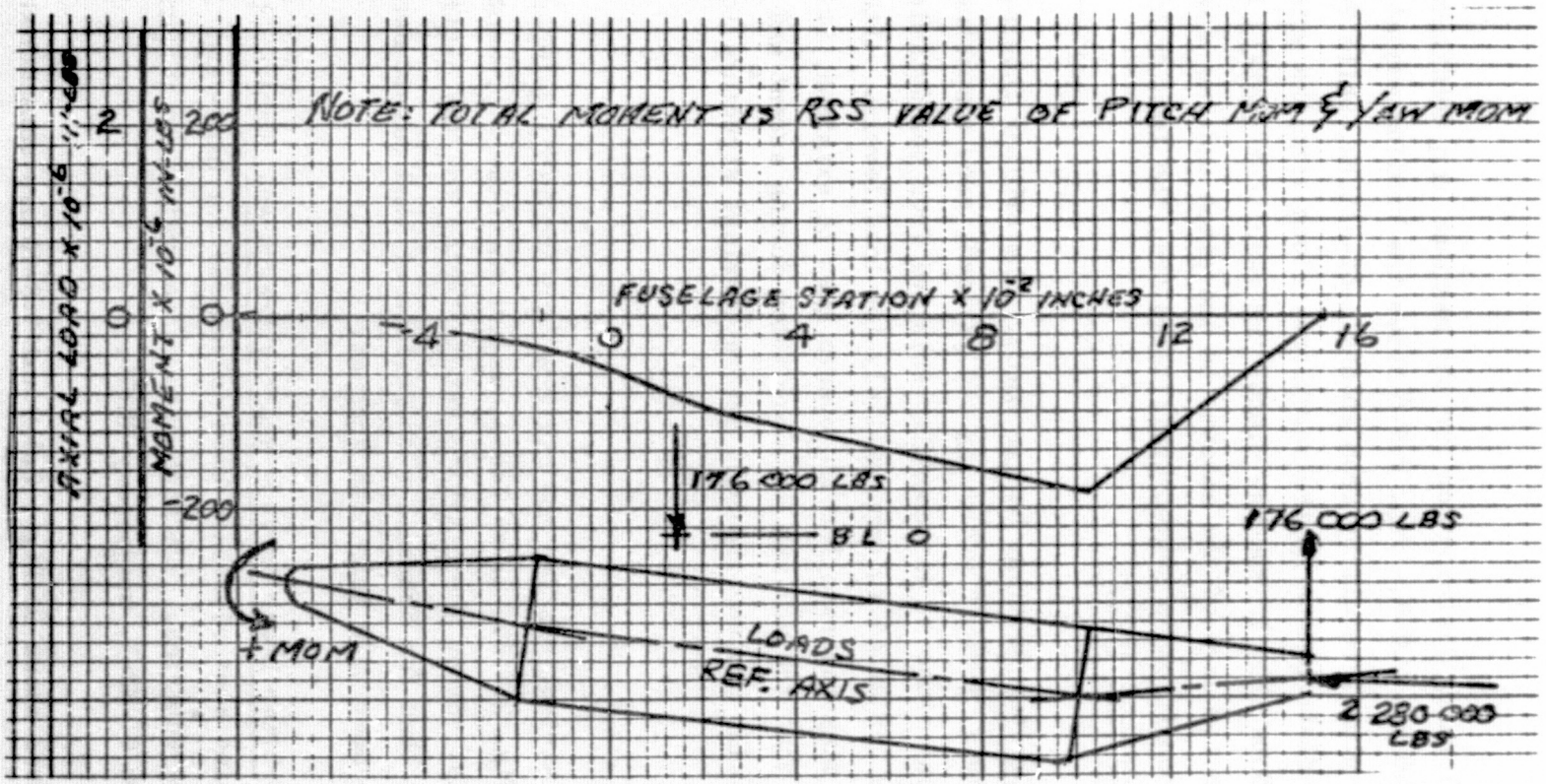

Fig. 2.8-5 Droptank Loads Launch Release Condition - Loads in Yaw Plane

Droptank loading distribution for the maximum αq condition are presented in Figs. 2.8-6 and 2.8-7. Fig. 2.8-6 shows the bending moment distribution in the pitch plane, resulting from an angle-of-attack, while Fig. 2.8-7 shows the momen distribution in the yaw plane, along with the axial load distribution. Note that in the yaw plane; the resultant (total) bending moment is the root-sum-square of the moments in the pitch and yaw planes. The loading for this condition is symmetrical; therefore, the loading distributions are the same in each tank.

2.8.4.4 Orbiter Fuselage Design Loads. The orbiter fuselage, since it is essentially a "shroud" enclosing the payload, crew compartment, and internal tankage, and since it is generally shielded from aerodynamic loading during ascent, is subjected to comparatively low load levels. Although, in the final analysis, many separate loading events must be examined, it is considered at this time that the maximum αq condition during ascent and the landing-impact condition will produce the most severe fuselage structure loading.

Loading distributions for the maximum αq and landing-impact conditions are shown in Fig. 2.8-8. These loads, as are the others presented herein are limit loads. Since the ultimate safety factor for the orbiter is different for ascent than for descent, a comparison of load magnitudes for the two conditions must take this into account.

2.8.4.5 Orbiter Lower Surface Reentry Pressures. Orbiter lower-surface pressure time histories have been determined for high- and low-crossrange reentry trajectories. The high-crossrange trajectory information is contained in EM L2-06-01-M2-3, trajectory RE171.

The pressures shown in Figs. 2.8-9 and 3.8-10 are considered to be uniformly distributed over the orbiter surface, in accordance with hypersonic flow theory, and are the dynamic component of total pressure - orbiter internal

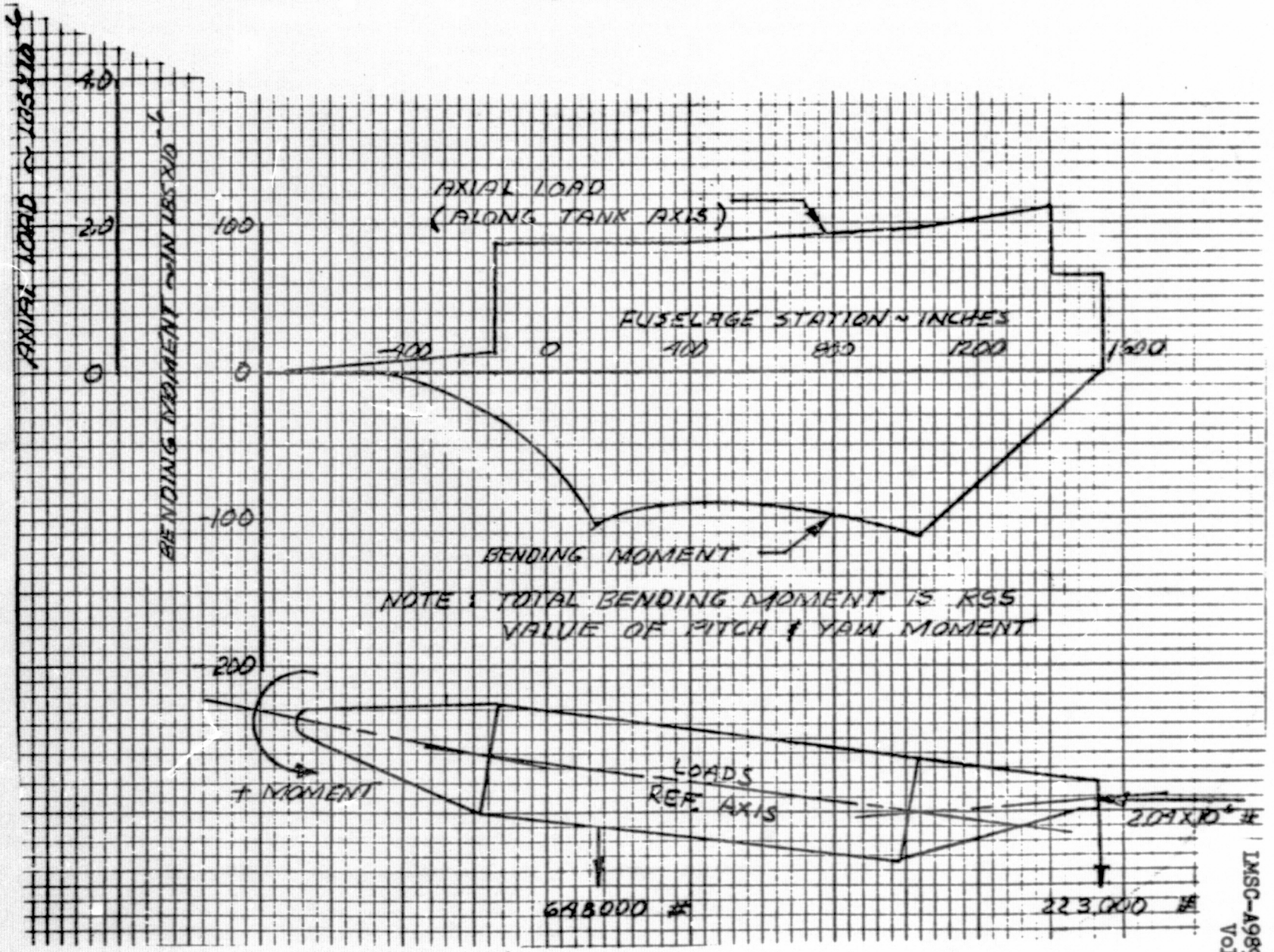

Fig. 2.8-7

Fig. 2.8-7 Droptank Loads Max **α** q Condition Tank Loads in the Yaw Plane

PRECEDING PAGE BLANK NOT FILMED

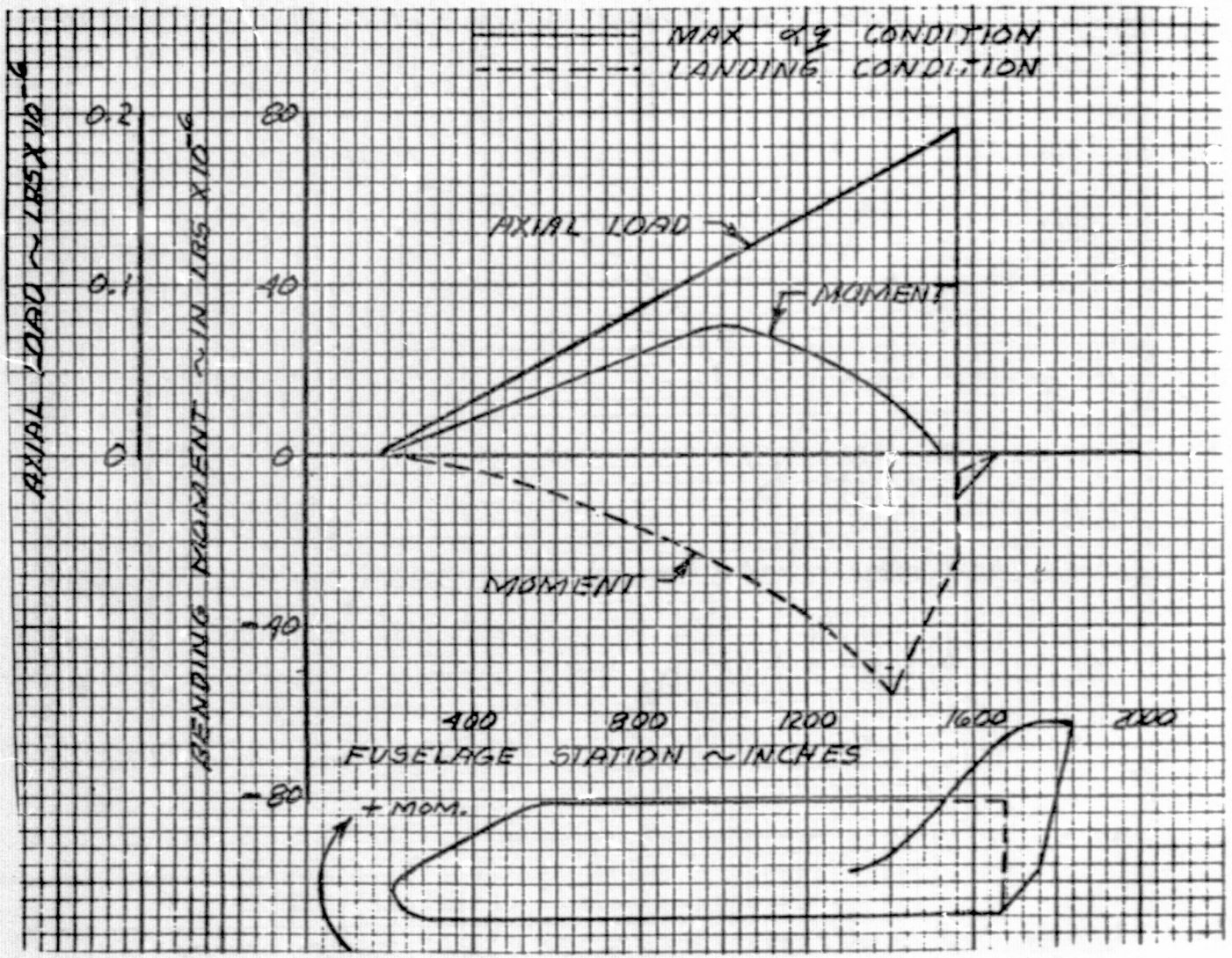

Fig. 2.8-8 Fuselage Loads Max α q and Landing Conditions

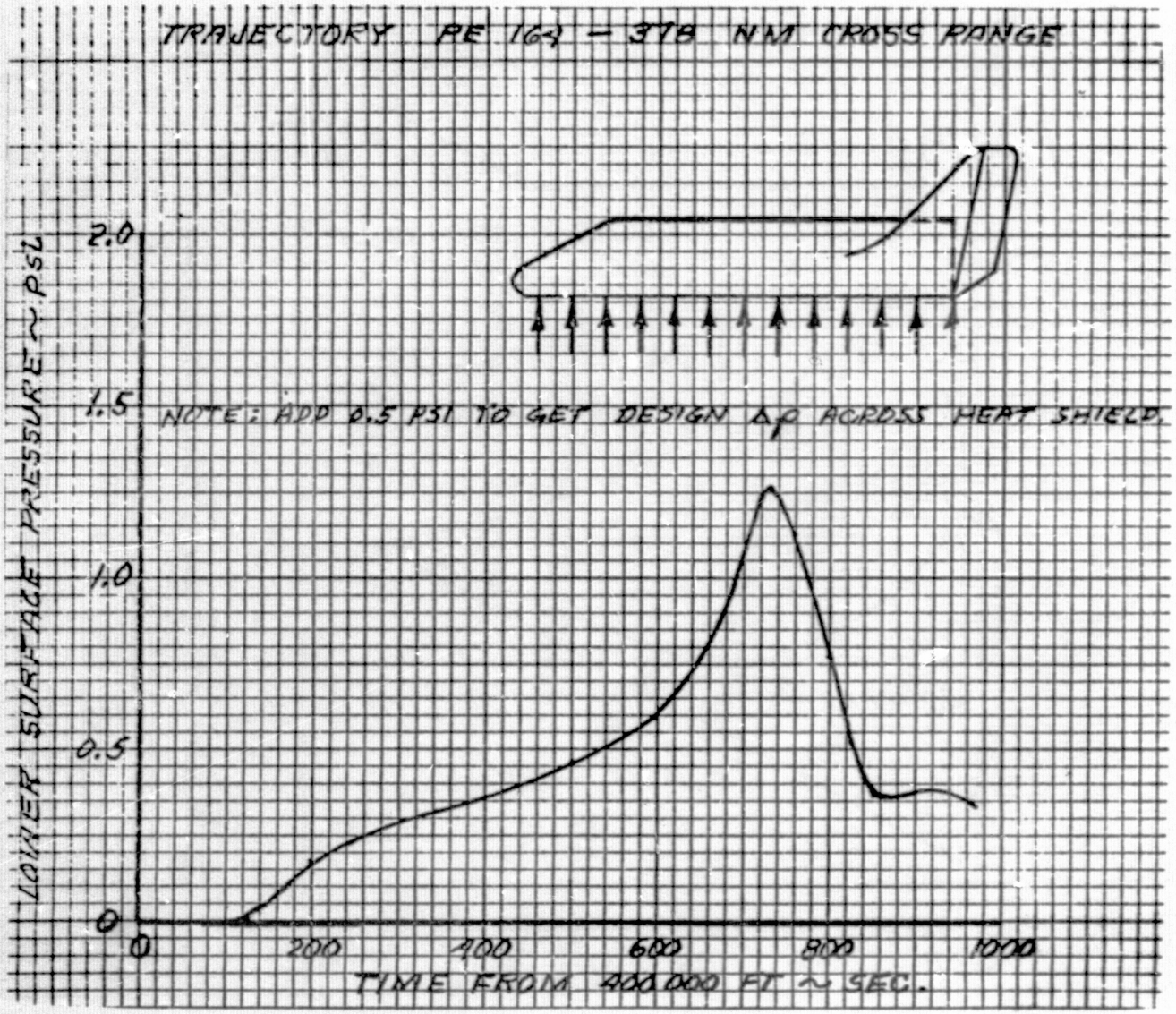

Fig. 2.8-9 Delta-Body Orbiter Lower Surface Pressure During Hypersonic - Supersonic Entry

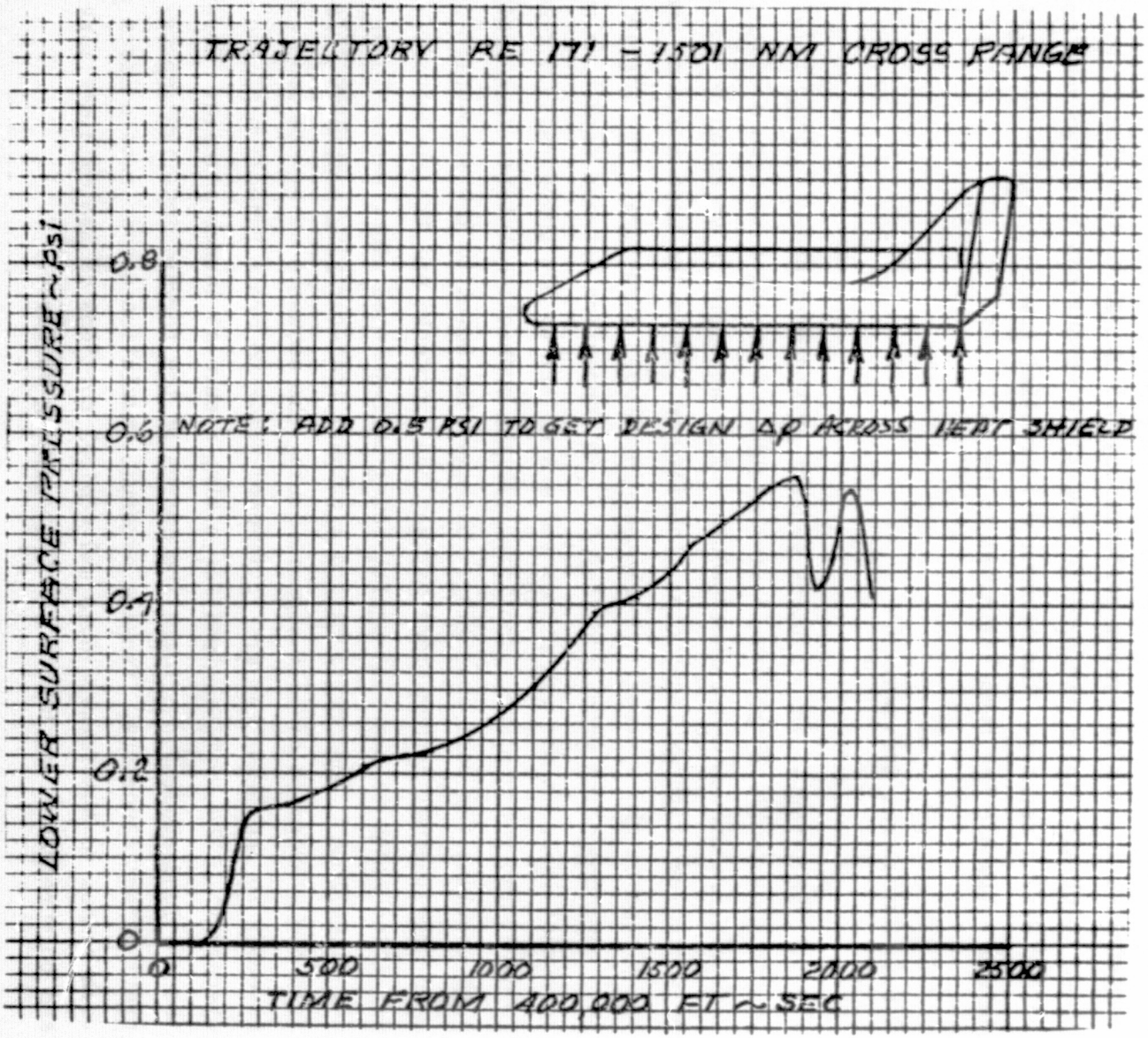

Fig. 2.8-10 Delta-Body Orbiter Lower Surface Pressure During Hypersonic-Supersonic Entry

pressure assumed to be free-stream ambient pressure. However, because of uncertainties in venting system performance, 0.5 psi is to be added to the values shown to obtain design differential pressures across the lower-surface heat shield during reentry. The maximum differential pressure across the heat shield subpanels has been estimated to be $\pm$0.25 psi.

2.8.5 Structural Arrangement

2.8.5.1 Droptanks. The droptank general arrangement shown in Fig. 1.2-3 consists of two tank systems interconnected and arranged to form a single V-type nonrecoverable droptank module. This assembly is attached to the delta-body orbiter at three locations: the forward tie in the nose section, and at two places on the spacecraft rocket-engine thrust structure. The forward tie is a compound joint which provides for pin connection between each tank system to resist loads in the yaw plane, and a link tie to the spacecraft to react loads in the pitch plane. The intertank pin connection between tank systems also provides for roll stability. Linkage attachment to the spacecraft permits free thermal deformations between the droptanks and the spacecraft. Aft attachments to the spacecraft, being ball-jointed pins, resist loads in all directions. The droptanks are a primary load-carrying structure only from the standpoint of self-support during the sequence of events from ground assembly to the time they are jettisoned prior to orbit injection of the spacecraft. The critical load for sizing occurs at launch release. However, the α q load condition affects the design of the forward intertank/spacecraft attach structure. Tankage external insulation consists of a layer of cork bonded to the forward dome and conical portions of the oxidizer tank, and polyurethane foam bonded to the remaining surfaces.

Each tank system consists of the following major components: LO_2 tank, intertank structure, LH_2 tank, and forward and aft support structures. The propellant tank material is aluminum alloy 2219-T87, selected on the basis of excellent fracture toughness, good weldability, and excellent compatibility with cyrogenic fluids. Aluminum alloy 7075-T6 is selected for the intertank

and forward support structure on the basis of excellent strength-to-density and modulus ratios and because conventional mechanical fasteners can be used. The aft support structure is made from the titanium alloy 6Al-4V-STA, because of the added strength required to resist the highly concentrated load in that area.

Tank pressure and temperature criteria are presented in Tables 2.8-5 and 2.8-6; the loads are presented in Section 2.8.4. Internal pressure during the ascent intervals establishes minimum tank membrane requirements. Two critical conditions are investigated: launch-release (liftoff) condition and droptank burnout condition. At liftoff, the load factor (including dynamic response) is 1.50. Thus, the combination of ullage presssure at liftoff and hydrostatic pressure of the fluid head establishes a linear pressure variation along the tank length, but the tank, in contact with the cryogenic fluid, is at constant temperature. In the ullage area, hot gas causes the wall temperature to be hotter, as noted in Table 2.8-6. At the conclusion of burn when the tank is void of fuel, internal pressure is constant throughout the tank (due to ullage), but wall temperature varies (linearly) along the length of the tank within the temperature range shown in Table 2.8-6. In addition to internal-pressure conditions, the overall droptank system is sized to resist axial and bending loads occurring during ascent while attached to the orbiter. These load conditions are shown and discussed in Section 2.8.4. The critical load for design occurs just after launch release.

Table 2.8-5

Ullage Pressure
(Excluding Hydrostatic)

Flight Interval	Ullage Pressure * (psia)	
	LO_2	LH_2
Start transient to 1 sec at full thrust	18.2	26.2
1 to 280 sec	18.2 slow 21.2	23.5
280 to 300 sec	21.2	27.6

*All pressures include +3 psia to account for valve tolerance.

Table 2.8-6

Tank Wall Temperatures

Flight Interval	Tank Wall Temperature * (^{o}R)	
	LO_2	LH_2
Boost Burn	600 Top (ullage) 162 Wetted Tank	360 Top (ullage) 40 Wetted Tank

*Assume linear temperature profile as a function of station from forward ullage level to aft end of tank.

To facilitate the tank wall structure design, the interaction of the external loads with internal ullage pressure is transposed into ultimate shell stress resultants in the following manner:

$$\text{Maximum compression} \quad N_{x_{ULT}} = F.S. \times \left[\frac{A}{2\pi R} + \frac{M}{\pi R^2} \right] - \frac{p_r R}{2}$$

$$\text{Maximum tension} \quad N_{x_{ULT}} = F.S. \times \left[\frac{p_t R}{2} + \frac{M}{\pi R^2} - \frac{A}{2\pi R} \right]$$

where:

A = axial force, lb

M = bending moment, lb-in

p_r = minimum relieving internal gage pressure (ullage gage pressure less valve tolerance)

p_t = maximum internal gage pressure (ullage gage pressure with valve tolerance included)

R = shell mean radius

F.S. = droptank factor-of-safety = 1.40 for this study

The droptank stress resultant envelope for the maximum ultimate tension and compression loads is shown in Fig. 2.8-11 for the LS 200-5 droptank configuration. Should a tank leak develop during ascent, compression loads will not increase significantly, because bulk vapor pressures of 15.2 and 16.7 psia

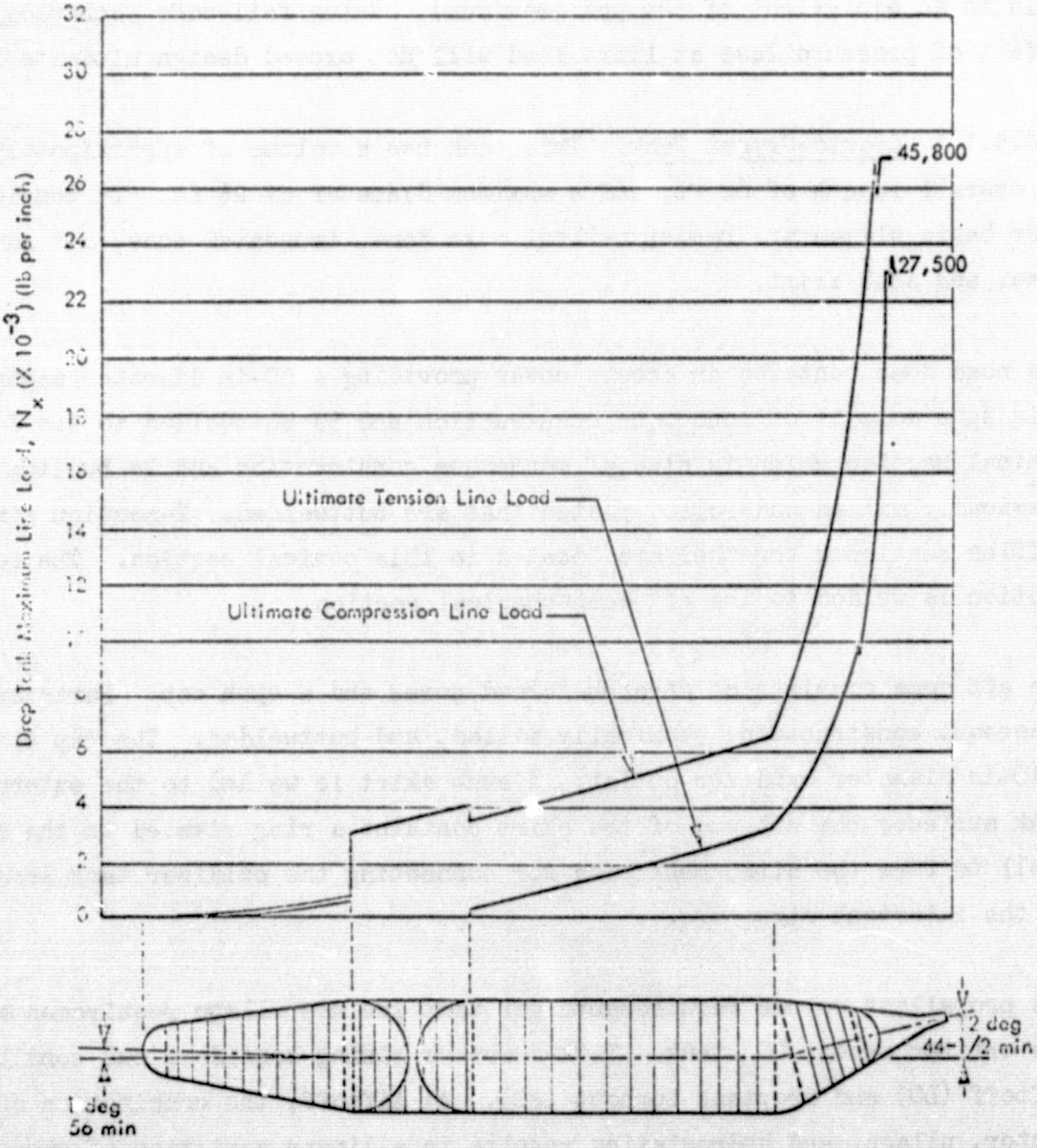

Fig. 2.8-11 LS 200-5 Droptank Design Stress Resultants

will be maintained in the LO_2 and LH_2 tanks, respectively, as long as fluid is present. The LO_2 value of 15.2 psia is the relieving value used to establish launch-release loads, and the value of 16.7 psia is 6.5 psia less than relief pressure used to establish design-stress resultants for the LH_2 tank. This is an equivalent of 526 ppi (maximum). Using fail-safe technology, the effect of pressure loss at limit load will not exceed design ultimate loads.

2.8.5.1.1 Liquid-Oxygen Tank. This tank has a volume of approximately 18,200 ft^3, an overall length of 62 ft, and a maximum diameter of 26 ft. It consists of four basic elements: hemispherical nose dome, truncated cone, aft hemispherical dome, and stub skirt.

The nose dome contains an access cover providing a 20-in diameter manhole. This spun dome is of monocoque construction and is buttwelded to the forward conical section which is also of monocoque construction and is builtup of chemically milled and rolled plates that are buttwelded. T-section ring-baffles sectioned together are located in this conical section. The conical section is welded to the aft hemispherical section.

The aft dome consists of stretch-formed gores and a spun cap. Parts are of monocoque construction, chemically milled, and buttwelded. The cap contains a 19-in diamater oxidizer outlet. A stub skirt is welded to the external tank surface; the aft end of the skirt contains a ring riveted to the skirt shell to form the attachment base for connecting the oxidizer tank assembly to the intertank structure.

The propellant volume requirements per tank include ullage requirements for the orbiter ascent LO_2 tank. Tank-membrane sizing considers two conditions: liftoff (LO) and droptank burnout (BO). At liftoff, the combination of load factor, ullage, and hydrostatics results in a linear variation of gage pressure from top-to-bottom of the tank. In the ullage area (top), hot gas causes the wall temperature to be hotter than the area in contact with the cryogenic fluid; this temperature variation affects material strength significantly

(Ref: MIL-HDBK-5A, Fig. 3.2.25.5.1(a)). Material strength, gage pressure, and shell radius determine membrane-thickness requirements at liftoff.

At conclusion of burn, when the tank is void of oxidizer, internal pressure becomes constant through the tank, but as the tank empties, the hot gas expands and warms the tank wall. For purposes of preliminary design, it is assumed that the temperature variation is linear from top to bottom. Linear-temperature variation causes a nonlinear material strength variation. A second set of membrane-thickness requirements are then determined from this condition of constant pressure at BO in combination with a nonlinear wall-strength variation. The envelope of these two design requirements establishes gage requirements. A combined plot quickly shows where each condition is critical. All designs show that approximately the upper two-thirds of the tank is designed by the BO condition while the lower third is designed by LO. Another consideration that quite often dictates membrane-thickness requirements is minimum gage limits. Usually, the upper dome of the LO_2 tank is dictated by this limitation which is set for this design at 0.025 in.

Investigation and design for external loading follows the design for membrane requirements; two types of design may be considered. The first design is a monocoque shell with intermediate rings and the second design includes longitudinal stiffeners. All designs of this class of vehicles show that membrane shell-thickness must be increased beyond that required for maximum internal pressure to resist external bending and axial loading if it is to be designed as a monocoque shell. To avoid thickening the shell, the alternate procedure of adding longitudinal stiffeners, in general, will be the more structurally efficient (lighter design) way to resist added loading. This investigation requires examination of three important modes of buckling: local buckling of stiffeners, panel buckling (between stiffeners and rings), and general buckling (across rings and stiffeners).

From a comparison of the two concept designs, it is revealed that small weight savings can be achieved by consideration of the longitudinal stiffeners for

the LO_2 tank. Omitting stiffeners reduces the complexity factor for fabrication, decreases proof-test complexities, and/or decreases operating-pressure limitations. It was therefore decided to use the monocoque-ring stiffened configuration. Details of this analysis are presented in EM L2-01-02-M5-2

2.8.5.1.2 Liquid-Hydrogen Tank. The tank having a volume of 49,900 ft^3, consists geometrically of six basic elements: hemispherical forward dome, forward stub skirt, cylindrical section, transition section, aft cone, aft dome, and the forward dome.

The forward dome, containing a 20-in diameter manhole system is similar in construction to that described for the oxidizer tank domes and is buttwelded to the integrally stiffened cylindrical section. This section is arranged to use five rolled-panels equally spaced and buttwelded to form a 26-ft diameter barrel section. Two barrel sections buttwelded together are required to form the total cylindrical section. The integral stiffeners are L-shaped, increasing in section depth toward the aft end of the cylinder. Appropriate Z-section rings spaced approximately 60 in. apart are riveted to the stiffener flanges. Kick rings are welded at each end of the cylinder at tangent points with the dome, buttwelded to the aft end of the tank cylinder, and then scarfed to form butt joint for welding this section to the aft cone. The aft cone is constructed in a manner similar to the cylindrical section with internal integral tapered stiffeners and rings riveted to the stiffener flanges. The cone is extended past the appropriate station at which the aft spun dome is buttwelded and forms the aft stub skirt shell. Z-section stiffeners are riveted to the internal surface of this stub skirt between the aft dome attachment weld and a buttwelded end ring used for attachment of the thrust cone assembly.

Volumetric sizing included 3-percent ullage volume. Tank membrane sizing (similar to the LO_2 tank sizing) considers the two conditions: liftoff and burnout. The procedure for determining thickness requirements for each condition is the same as previously discussed for the LO_2 tank. Results show that the liftoff condition is not critical for the LH_2 tank. The aft-dome thickness is based on minimum gage requirements. The aft-cone section

membrane thickness is sized for external load requirements. Internal pressure is not a design consideration. As in the case of the LO_2 tank, the membrane thickness required for pressure is not adequate for the ascent axial and bending loads. Internal integral stiffeners and rings are required, even though internal-pressure stabilization is considered in the analysis. Stiffening requirements are determined using minimized weight wide-column equations, equating wide-column buckling to local buckling, for the L-stiffened shell. For optimum efficiency (minimum weight), the equation reduces to

$$\bar{t} = 1.72\, R\left(\frac{N_x}{RE\,\eta^*}\right)^{0.6}$$

where:

$\bar{t}$ = effective shell thickness, stiffeners combined with skin

R = cylinder radius

E = material modulus of elasticity in compression

η^* = plasticity factor = $(E_T/E)^{1/2}$

Fig.2.8-12 is a plot of the above equation as a function of (b_w/b_s), letting $t_w/t_s = 1.0$. Note that as b_w/b_s is reduced from 1.0, $\bar{t}$ becomes less efficient (weight goes up). Although desirable, optimum efficiency is not always possible because of the driving parameter, shell thickness, t_s. Internal-pressure requirements establish the minimum membrane thickness that the tank must have.

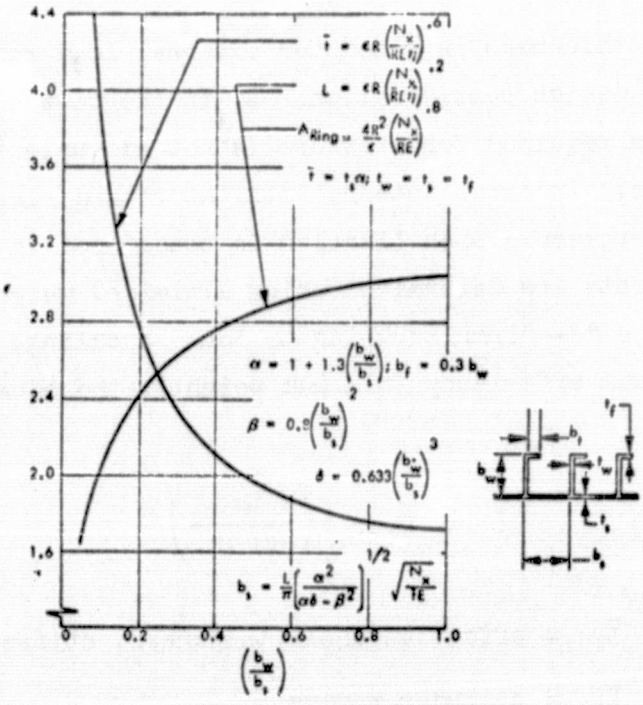

Fig. 2.8-12 Design Parameters for L-Stiffened Cylindrical Shells

Using the above equation at discrete locations along the tank will yield sets of geometric parameters which are not compatible, i.e., the stiffener geometry varies. Compromise is required to establish a uniform stiffener-spacing along the length of the tank, while providing the discrete cross-sectional area requirements at each location and preserving membrane-thickness requirements. Since bending moment is a predominant loading and because the droptank has a permanent fixed-position with reference to loading axes, effective thickness requirements can be reduced circumferentially in proportion to reduced line load. A practical way to design for reduced loading is to vary the spacing of stiffeners around the circumference. Therefore, the tank is subdivided into four quadrants with one quadrant having the maximum number of stiffeners, one quadrant having no stiffeners where tension exists, and two quadrants having half the number of stiffeners. This procedure was used to determine the tank cylinder and cone weight. Similarly to design of the LO_2 aft stub skirt, a forward monocoque stub skirt is provided to facilitate mechanical attachment to the intertank shell. Also, an aft stub skirt is provided to

which the thrust-cone aft structure is attached mechanically. The analytical detail for this tank are presented in EM L2-01-02-M5-2, of the Fifth Letter Progress Report.

2.8.5.1.3 Intertank Structure. The cylindrical intertank structure is 21.5-ft long, uses two field joints to connect the LO_2 tank with the LH_2 tank, and incorporates an access door. Since the shell is not required to operate at specified internal pressures, the shell geometry is designed for optimum integrally stiffened proportions of longitudinal L-stiffeners and circumferential rings. To take advantage of higher strength properties, aluminum alloy 7075-T6 with conventional mechanical fasteners is selected in lieu of fusion-welded 2219 aluminum. No advantage can be achieved by using titanium in this area, since the line load level is relatively low (and cool).

An alternate shell geometry using open-faced trapezoidal shell is investigated for weight comparison only. Even though there is a theoretical weight advantage to open-faced corrugated shell, it becomes a poor choice for this design for the following reasons:

- Besides providing continuity between LO_2 and LH_2 tanks, this structure also is used to connect the two droptank systems together to form a Vee-droptank system and to provide interstage attachment to the spacecraft (delta-body orbiter). Localized load reactions occur in the intertank shell caused by the struts and frames performing these functions.
- Secondly, a slight overpressure occurs around the shell due to ascent angle-of-attack. For purposes of design, it is assumed that the shell must be capable of sustaining a crushing pressure of 0.7 psig (ultimate) during maximum αq. However, maximum axial loads do not occur when this pressure is present.
- Finally, aerodynamic heating during ascent in the area of the intertank shell does not require insulation if a smooth-faced shell is used, whereas, open-faced corrugation causes higher temperatures which require insulation.

2.8.5.1.4 Droptank Support Structure. The droptank-to-spacecraft forward tie consists of a set of struts arranged to permit contraction of the tanks while serving as the base for supporting a two-force member attached between the strut and the spacecraft nose section. This tie permits contraction of the tanks when filled with the cryogenic propellant. The two-force member is connected to the structures via a ball-joint so as to allow relative motion between the spacecraft and droptank system except in the pitch plane.

The aft support structure is made from titanium alloy 6AL-4V-STA because of the added strength required to resist the highly concentrated load in this area. This structure ties the aft section of the droptank to the orbiter. The circular forward section is a ring-stringer stiffened conical shell which attaches to the aft-stub skirt of the droptank at its forward end. The aft end is a field joint which attaches to the aft section of the aft support structure.

The aft section includes a transition from the circular field-joint section to a rectangular boxbeam at the aft end, having a lug-type fitting at its end to which a cylindrical eject pin attaches. This section performs a dual role in also providing the primary launch support pads which are integrated into this structure.

2.8.5.2 Delta-Body Airframe. The basic airframe material is aluminum alloy with construction similar to conventional-aircraft airframes, consisting of stressed-skin stiffened by frames, longerons, and stringers. Bulkheads are located at stations where heavy concentrated loads are introduced into the basic shell. To provide a convenient structural attachment for the thermal-protection panels that form the external aerodynamic shape of the spacecraft the fuselage frames are arranged external to the skin rather than inside as in conventional aircraft design.

Designs of the cover panel and supporting frame structure to carry the critical compression line loads were based upon the following groundrule constraints: (1) heat-shield design constrains the primary load-carrying structure to a maximum temperature of 300°F, (2) the maximum differential pressure across the primary structure carried by aerodynamic venting loads is constrained to 0.25-psi limit at the critical flight-loading conditions. To achieve the lightest weight structural panel, initial screening of several cover-panel configurations, based upon wide-column analysis, showed that the corrugated-panel concept, shown in Fig. 2.8-13, is the most efficient construction. A comparison of the weight penalty associated with the other configurations compared to the corrugated-panel design is also presented in the figure. Values shown in Fig. 2.8-13 are based upon the generalized instability equation:

$$\frac{N}{LE} = \epsilon \left(\frac{\bar{t}}{L}\right)^2$$

where

N = line load, lb/in.
ϵ = efficiency factor
$\bar{t}$ = average thickness per unit width, in.
L = panel length, in.
E = modulus of elasticity, lb/in^2

Although open-faced corrugation is theoretically the most efficient structural concept, it is not the most ideal for application to this vehicle which is conically shaped, and in many areas, has double curvature. Running corrugations having variable pitch, and accommodating changes in load magnitude make the corrugation concept very difficult to handle both for design and manufacturing. Structurally, it also requires difficult splicing and attachment procedures for doors, frames, and bulkheads, which will detract from its efficiency. For these reasons, the Z-stiffened panel concept was selected as the primary structural concept for the delta-body orbiter airframe.

Configuration	ϵ	Percent Weight Penalty
	1.60	Base
	1.23	14
	1.15	18
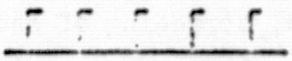	1.03	25
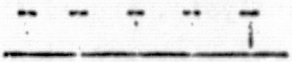	1.00	27
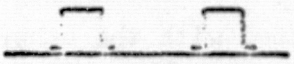	0.93	31
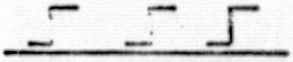	0.91	33
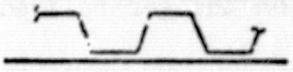	0.69	52
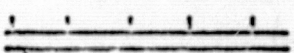	0.66	56
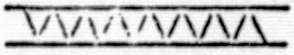	0.605	62

Fig. 2.8-13 Ideal Structural Efficiency of Panel Concepts

The orbiter fuselage panel and frames are sized in the following manner. Panel cross sections are sized such that local and general instability failure modes occur simultaneously. (See equation, page 2.8.1-39). Frames are designed to provide the stiffness required. The required frame flexural rigidity is given by Reference 2.8-1.

$$E_F I_F = 4\left(\frac{b}{\pi}\right)^4 \left(\frac{N_x}{L}\right),$$

where

b = longeron spacing, in.
L = frame spacing, in.
N_x = panel line load, in.

and the frame cross-section area is

$$A_F = \left(\frac{I_F}{5.24}\right)^{1/2}$$

A conventional aircraft fuselage is cylindrical and the frame size and spacing is dependent on shell radius. The shape of the delta-body orbiter class vehicles is composed essentially of three flat-sided elements, however, so that other techniques are required for selecting frame spacing and size. A severe weight penalty occurs if the frame length remains unsupported over the entire flat-sided surface. To minimize this penalty, longerons and posts are employed to add stiffness to the frames. Longeron spacings of 100 in. are recommended (Reference 2.8-2). Post supports can be used efficiently in the payload compartment region as shown in Fig. 2.8-14.

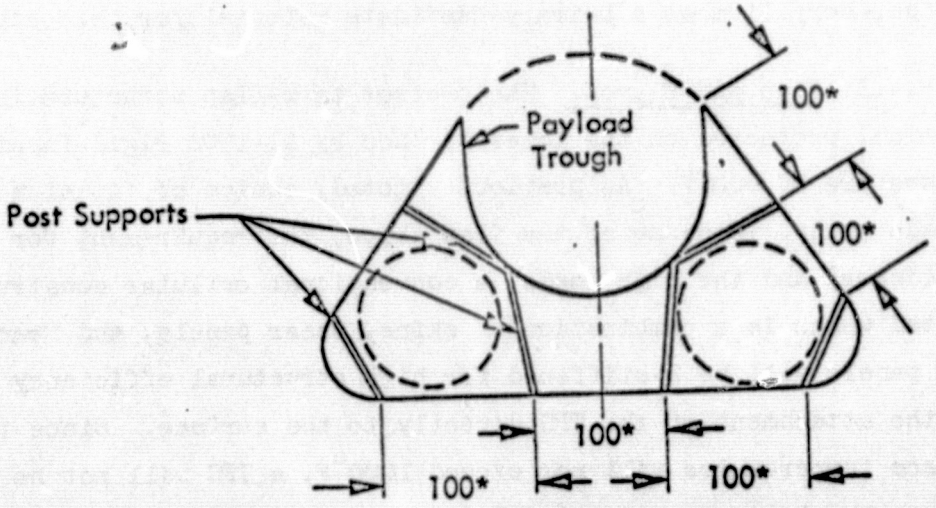

*b Panel Width in Inches

Fig. 2.8-14 Typical Intermediate Frame Support

Panel and frame equivalent thicknesses (where the thickness is the panel area divided by its width, b, and the frame thickness is the frame area divided by the frame spacing, L) are presented in Figs. 2.8-15 and 2.8-16, respectively, as a function of fuselage line load. The two materials investigated, 7075-T6 and 6A1-4V titanium, are considered to act at two discrete temperatures: room temperature for both, 200°F for aluminum, and 600°F for titanium. Titanium at 600°F assumes that TPS reduces the backface skin temperature to 600°F, and aluminum at 200°F assumes that the TPS is capable of reducing the backface skin temperature to 200°F. The allowable compressive line load for a skin minimum gage of 0.015 in. is also shown in Fig. 2.8-15.

The orbiter fuselage loads, presented in Section 2.8.4, are transposed to line load intensities using an LMSC-developed computer program. Details of this analysis are presented in EM L2-01-01-M1-3, of the Sixth Letter Progress Report. The maximum upper- and lower-surface line loads are shown here in Figs. 2.8-17 and 2.8-18, respectively. The critical loading conditions for the upper surface is + α q, while the lower surface is critical at -αq and landing impact. It is noted that most of the orbiter fuselage shell structure is sized by ascent-loading conditions. The landing-impact condition is critical over a relatively small area of the lower surface.

Based on optimum material/structure concept and frame spacing, Z-stiffened aluminum panel and frame average unit-weight distributions versus fuselage station are shown in Fig. 2.8-19 for the LS 200-5 orbiter. For a given fuselage cross-section (station), the average unit weight is obtained from the ratio of total cross-section weight per inch divided by the cross-section perimeter. The maximum unit fuselage weight of 1.4 lb/ft^2 includes the weight of the payload-compartment trough and a nonoptimum factor of 1.25 to account for fasteners, panel-edge closeouts, and frame stiffeners.

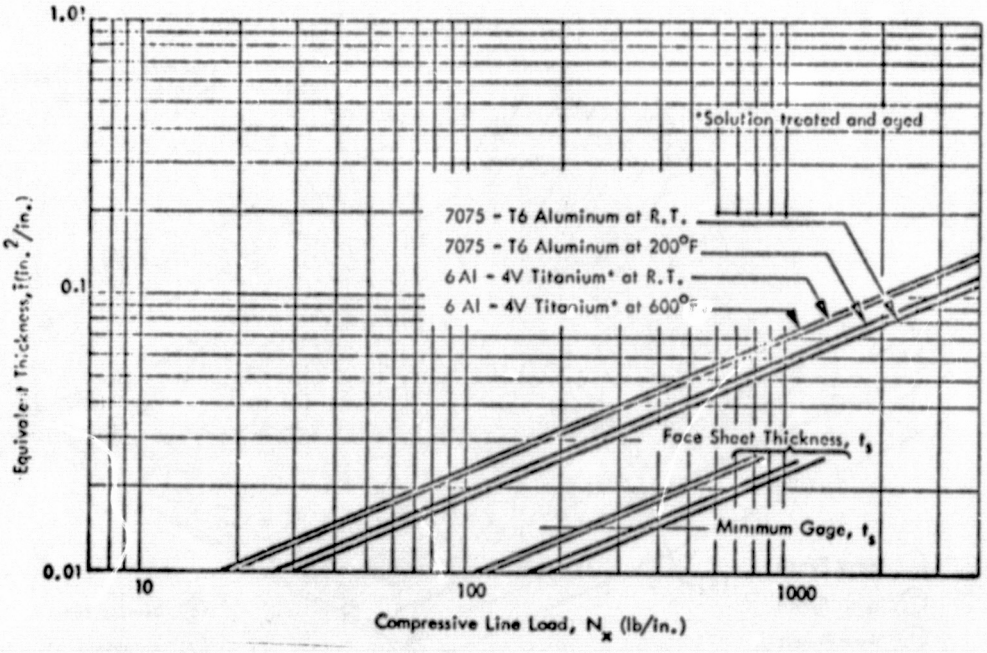

Fig. 2.8-15 Z-Stiffened Panel Equivalent Thickness Versus Compressive Line Load for Frame Spacing of 50-in and Longeron Spacing of 100-in

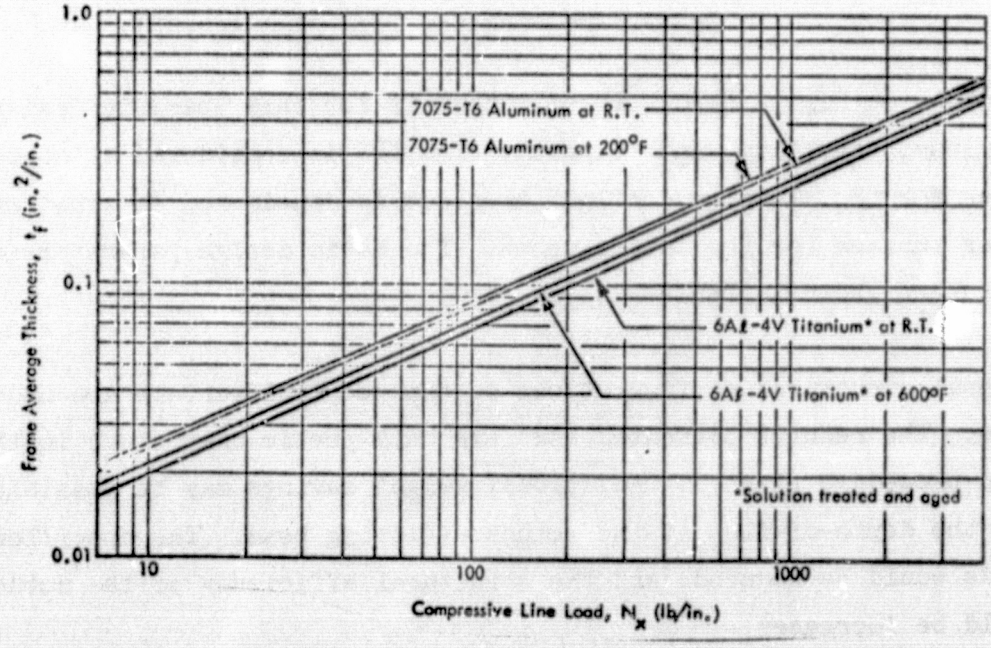

Fig. 2.8-16 Effect of Compressive Line Load on Frame Equipment Thickness for Frame Spacing of 50-in and Longeron Spacing of 100-in

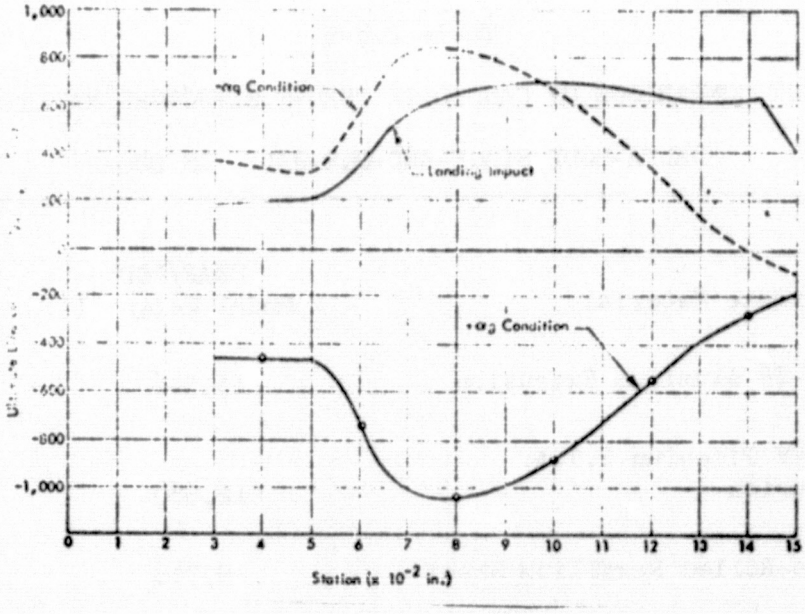

Fig. 2.8-17 Typical Maximum Upper-Surface Design Loads of Delta-Body Stage-and-One-Half

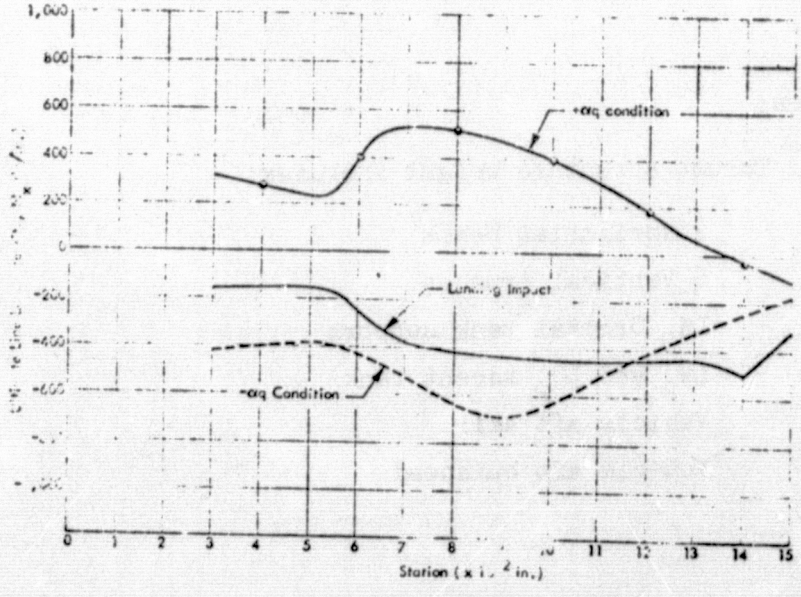

Fig. 2.8-18 Typical Maximum Lower-Surface Design Loads of Delta-Body Stage-and-One-Half

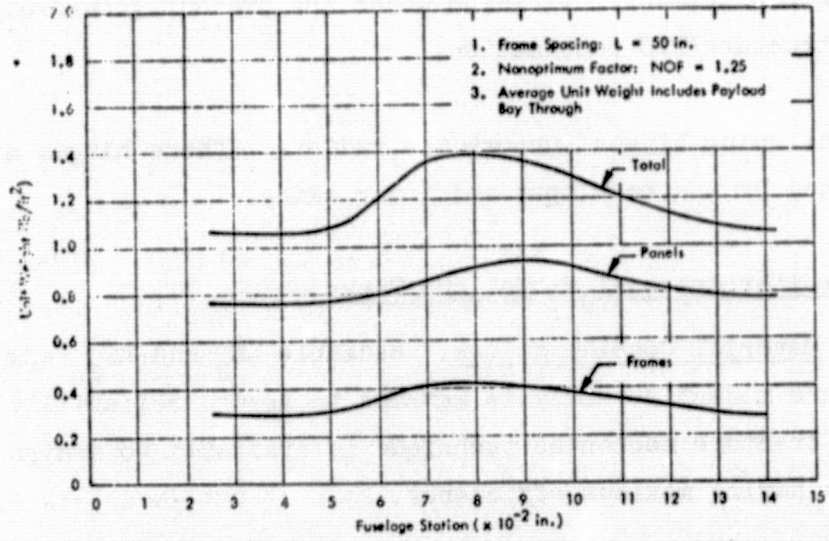

Fig. 2.8-19 Z-Stiffened Aluminum Panel and Frame Average Unit Weight

The value of 1.4 lb/ft^2 may seem low in comparison to aircraft fuselages, but essentially, the orbiter fuselage is a "shroud" enclosing a payload, crew compartment, and internal tankage, since it is generally shielded from aero-dynamic loading by the droptanks during ascent, and is subjected to comparatively low load levels.

Typical low-surface panel and frame dimensions and detail design data for the fuselage are presented in Figs. 2.8-20 and 2.8-21.

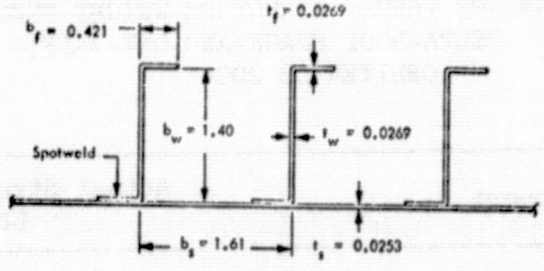

Panel Data

Material: 7075-T6 Aluminum at Room Temperature
Allowable Compressive Stress σ = 12,000 psi
Allowable Compressive Line Load N_x = 753 lb/in.
Frame Spacing L = 50 in.
Panel $\bar{t}$ = 0.0627 in.
Panel Unit Weight W = 0.912 lb/ft^2

Fig. 2.8-20 Typical Lower-Surface Panel Dimensions of Orbiter Fuselage Structure

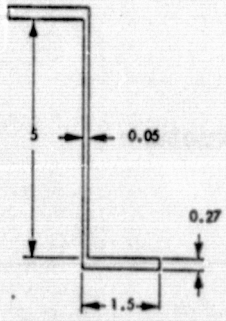

Frame Data

Material: 7075-T6 Aluminum at Room Temperature
Allowable Compressive Panel Stress: σ = 12,000 psi
Allowable Compressive Panel Line Load: N_x = 753 lb/in.
Frame Spacing: L = 50 in.
Longeron Spacing: b = 100 in.
Frame $\bar{t}$ = 0.0212 in.
Frame Unit Weight: W = 0.308 lb/ft^2

Fig. 2.8-21 Typical Lower-Surface Frame Dimensions of Orbiter Fuselage Structure

2.8.5.3 Thrust Structure. The delta-body stage-and-one-half thrust structure consists of six vertical trusses, two horizontal beams, supports for ascent and orbital propellant tanks, vehicle aft skirt, and vehicle aft bulkhead. The structural function of each thrust structure component is as follows. Vertical trusses distribute thrust loads to the aft vehicle, provide lateral stability and intermediate support to the horizontal beams, and act as a base for the tank supports and engine pitch actuators. Horizontal beams distribute thrust loads to the droptanks by bridging the vehicle base; they provide a tension tie for droptank kick loads and attach points for engine yaw actuators. Ascent and orbital propellant tank supports provide a smooth transition of longitudinal and shear loads from the tank skirt to the forward edge of the truss/beam grid work. Tank shear loads are transmitted by vee diagonal trusses on each quadrant of the tank supports. The vehicle aft skirt transmits thrust loads to the drop tank by shear flow and provides a smooth transition of peak stresses due to large thrust and droptank point loads into relatively light vehicle structure. The vehicle aft bulkhead is formed by the aft edge of the vehicle skirt and the forward edge of the truss/beam grid work. Diagonal members provide shear stiffness to the vehicle base.

Support attachment lugs are provided for engines, gimbal actuators, and spacecraft propellant-tankage-support struts on the appropriate beam or truss. For the upper bank of engines, the pitch-gimbal actuators are attached to the base heat-shield-mounted lug system, which is stiffened and reinforced locally with diagonal braces to the beams. The base heat shield is mounted essentially to the smooth backfaces provided by the T-section aft caps on the spanwise beams and the I-beams aft chorts of the vertical trusses. The base heat shield also serves as the shear material, preventing any translation of the beam system in a sideways direction. Deflection of the thrust structure under ascent loading and resulting effects on vehicle systems was also investigated. The thrust structure has been examined in a materials trade study, and 6Al-4V titanium was chosen as the baseline material.

The LS 200-5 orbiter thrust structure was sized using the SNAP/FSD finite element code, which automatically generates fully stressed designs of large

bar/shear panel structures. The SNAP/FSD computer output includes optimum structural weights, internal loads, stresses, deflections, and member sizes. Because of structural and assumed loading symmetry only half of the thrust structure was represented in the structural model. The finite element model included 283 bars, 37 shear panels, and 122 joints. Minimum bar area and shear panel thickness was 0.5 $in.^2$ and 0.02 in., respectively. The thrust structure factor-of-safety for ascent loading conditions was F.S. = 1.4.

Details for the LS-200-5 thrust structure analysis are presented in EM L2-01-02-M6-1, of the Fifth Letter Progress Report. Four materials were originally considered: (1) 7075-T6 Aluminum, (2) 6Al-4V Titanium, (3) Beryllium cross-rolled sheet, and (4) 260 ksi H.T. Alloy Steel. The results, shown here as Table 2.8-5, were reported in EM L2-01-04-M6 of the Third Letter Progress Report. Note that beryllium offers considerable weight savings over the conventional materials. The titanium thrust structure, being the lightest among the conventional materials, was selected as the baseline.

A diagram of the model used for analysis, indicating the load conditions considered, is shown in Fig. 2.8-22. The baseline thrust structure weight summary for the LS 200-5 orbiter vehicle is shown in Table 2.8-6. To establish actual thrust structure weights for the LS-200-5 orbiter, a conservative non-optimum factor of 1.5 was applied to the SNAP/FSD model weight bars and 1.25 was applied to shear panels. The nonoptimum factor conservatively accounts for practical design constraints such as gussets, end fittings, local stiffeners, standard sheet gages, and standard structural shapes. Thrust structure weight for the LS 200-5 orbiter is 20,757 lb.

In addition to preliminary weight assessment of the thrust structure, deflections were examined. Longitudinal and angular deflections of the horizontal engine thrust beams for the LS 200-5 orbiter are shown in Fig. 2.8-23 and 2.8-24 respectively. Maximum longitudinal engine deflection on the upper- and lower-thrust beams was 1.6 deg for engine numbers 3 and 4 and 2.15 deg for engine numbers 9 and 10, respectively. Engine thrust-beam deflections will be considered in the design of the thrust vector control system.

Table 2.8-5

WEIGHT COMPARISON OF CANDIDATE THRUST STRUCTURE MATERIALS[1]

DELTA-BODY STAGE-AND-ONE-HALF, LS 200-2

Candidate Material	SNAP/FSD Model Weight (lb)
7075-T6 Aluminum Extrusion	15,546
6Al-4V Titanium S.T.A. Extrusion	12,680
Cross-Rolled Beryllium Sheet	9,746
260 ksi H.T. Alloy Steel (AlSl 4340 and D6A)	14,202

Notes:

1 Thrust structure weight includes:

- 2 Horizontal beams
- 6 Vertical trusses
- LH_2 Orbital tank support
- LH_2 and LO_2 ascent tank
- Vehicle aft skirt
- Vehicle aft bulkhead

Table 2.8-5

PRECEDING PAGE BLANK NOT FILMED

Table 2.8-6

BASELINE THRUST STRUCTURE WEIGHT SUMMARY,
DELTA-BODY STAGE-AND-ONE-HALF,
ORBITER LS 200-5

Thrust Structure Component	Actual Structure Weight (lb) LS-200-5*
Vertical Trusses at BL ± 48	2,004
Vertical Trusses at BL ± 144	1,272
Vertical Trusses at BL ± 240	1,000
Upper Horizontal Beam	3,962
Lower Horizontal Beam	3,940
Orbital Tank Support	221
Ascent Tank Supports	492
Vehicle Skirt	3,382
Vehicle Aft Bulkhead	1,772
Droptank Attach Structure	2,712
Total Thrust Structure	20,757

Notes:

* Nonoptimum Factor, NOF = 1.5 for bars and
NOF = 1.25 for shear panels

Table 2.8-6

REPRODUCIBILITY OF THE ORIGINAL PAGE IS POOR.

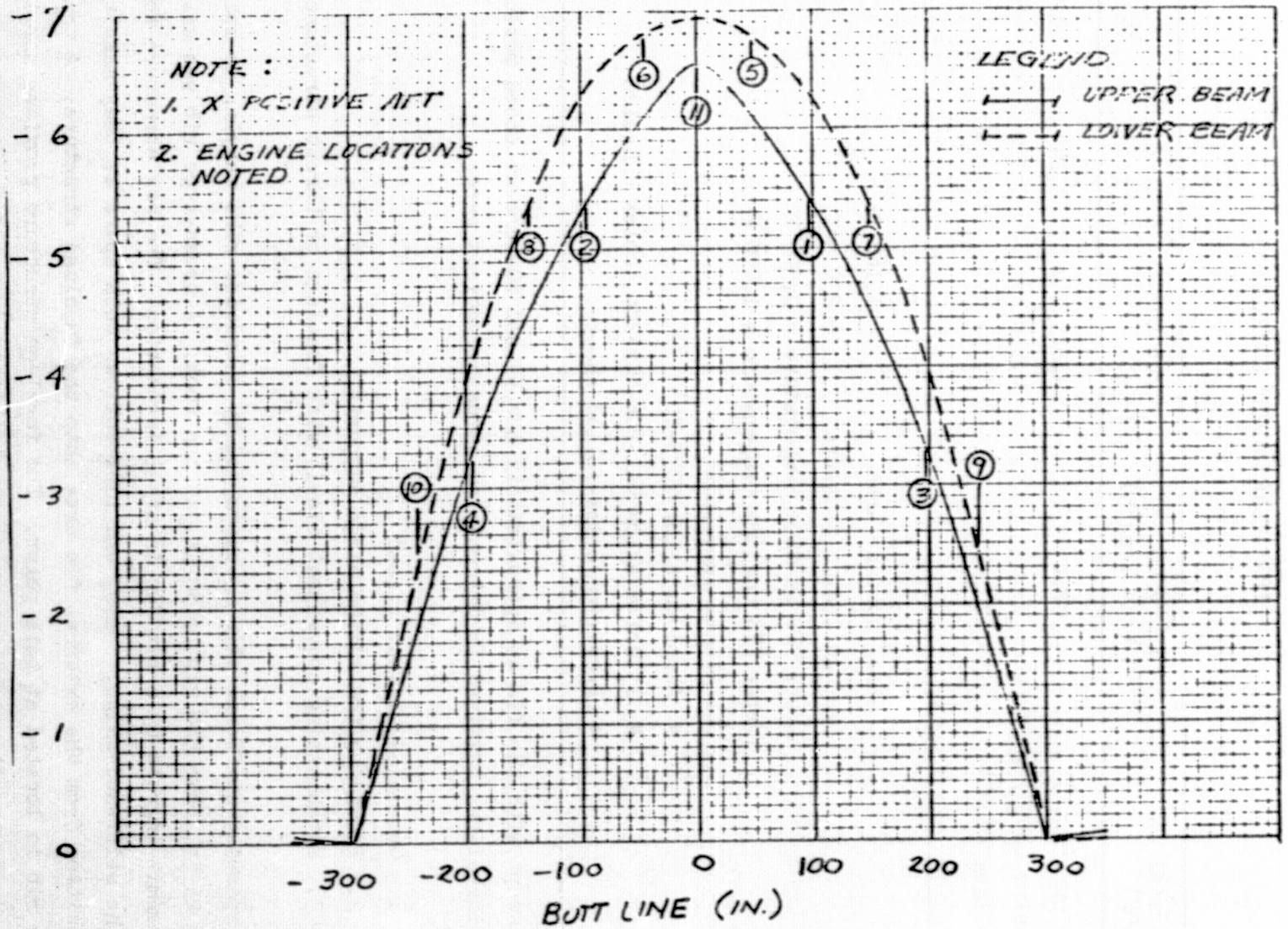

Fig. 2.8-23 Longitudinal Deflection of Engine Thrust Beams at Maximum αq

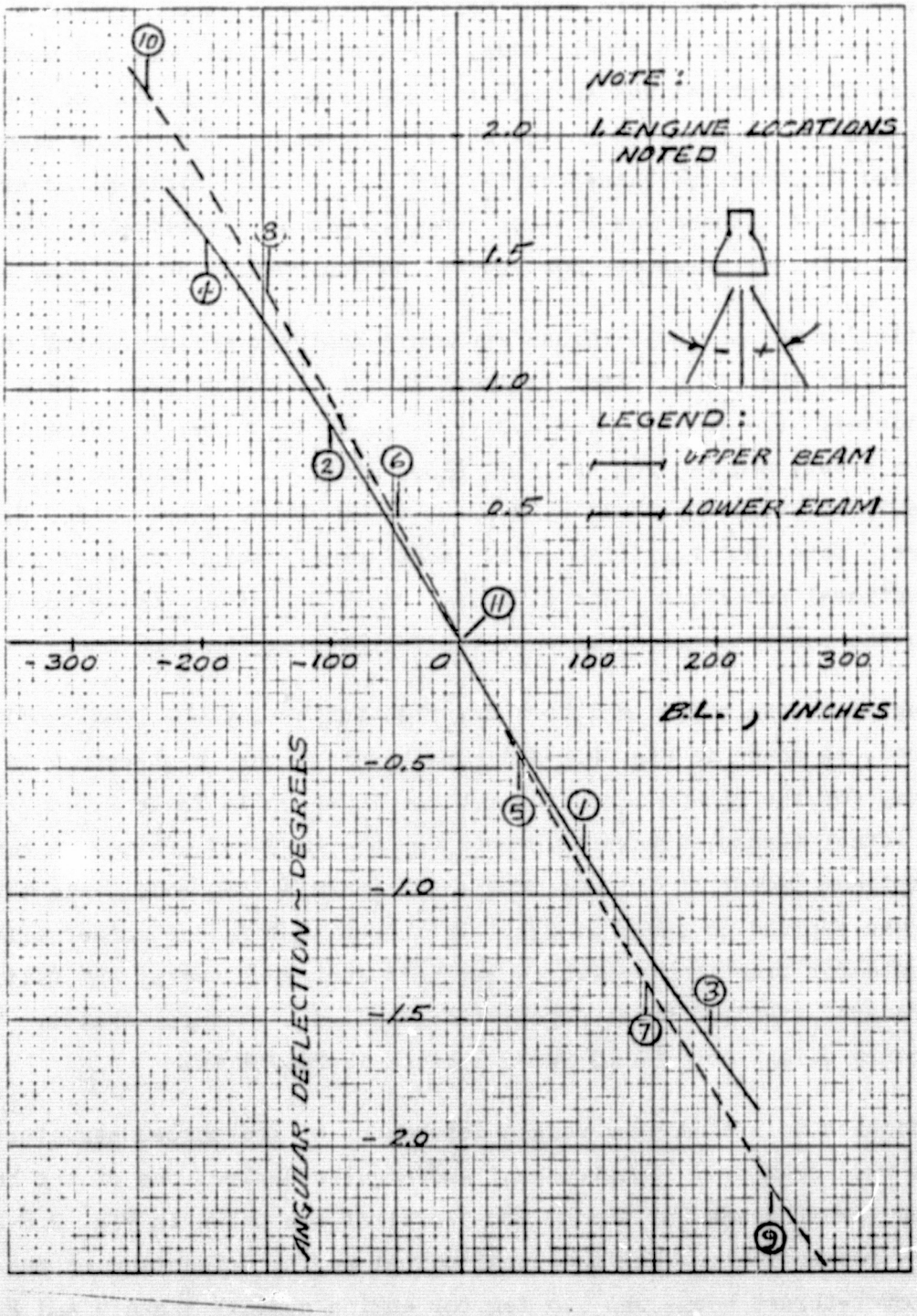

Fig. 2.8-24 Angular Deflection of Engine Thrust Beams at Maximum αq

The results of this study further revealed that a deflection constraint on thrust structure incurs a severe weight penalty. This is shown in Fig. 2.8-25. Reducing deflections 50% will double the thrust structure weight.

2.8.5.4 Aerodynamic Surfaces. Aerodynamic surfaces are most weight-sensitive on delta-body orbiters because of their aft position on the vehicle. Fins, elevons, rudders, and flaps should be as light as possible from both weight and forward cg standpoints. Trade studies involving both structural materials and TPS revealed that, although titanium structure is heavier than aluminum, the TPS weight saved by the higher operating temperature more than compensated for the use and provided a total weight advantage of about 30 percent.

Beryllium has a further advantage over either titanium or aluminum because of beryllium's excellent stiffness, lower density, and greater specific-heat coefficient. These three properties not only yield a light structural weight but also less TPS requirements. Although beryllium has potential prospects of being cost-effective in this area, titanium is selected as the baseline material for all aerodynamic surfaces because of the program directive not to consider beryllium as a primary candidate material for this study.

2.8.5.4.1 Flap and Elevon. The orbiter trim-flap structure is basically titanium, protected on the lower surface by LI-1500 rigid-insulation to a temperature of 600°F. As previously noted, choice of titanium was based on a trade study. Because of the flat shape, the requirement for elevon hinges at midchord and the high loads, a conventional cellular construction was adopted which is a combination of skins, shear panels, and transverse panels. Skin panels will be Z-stiffened for high structural efficiency and for allowing the attachment of the TPS directly to the surface. Since the upper-surface temperatures will not exceed 1000°F, a TPS will not be necessary because the basic material 6-2-4-2 titanium can withstand short-time exposure to these levels with little or no degradation.

The material trade study, performed and documented in EM L1-02-14-M5, considered a flap planform area of 1,148 ft.^{2}. The configuration used for study

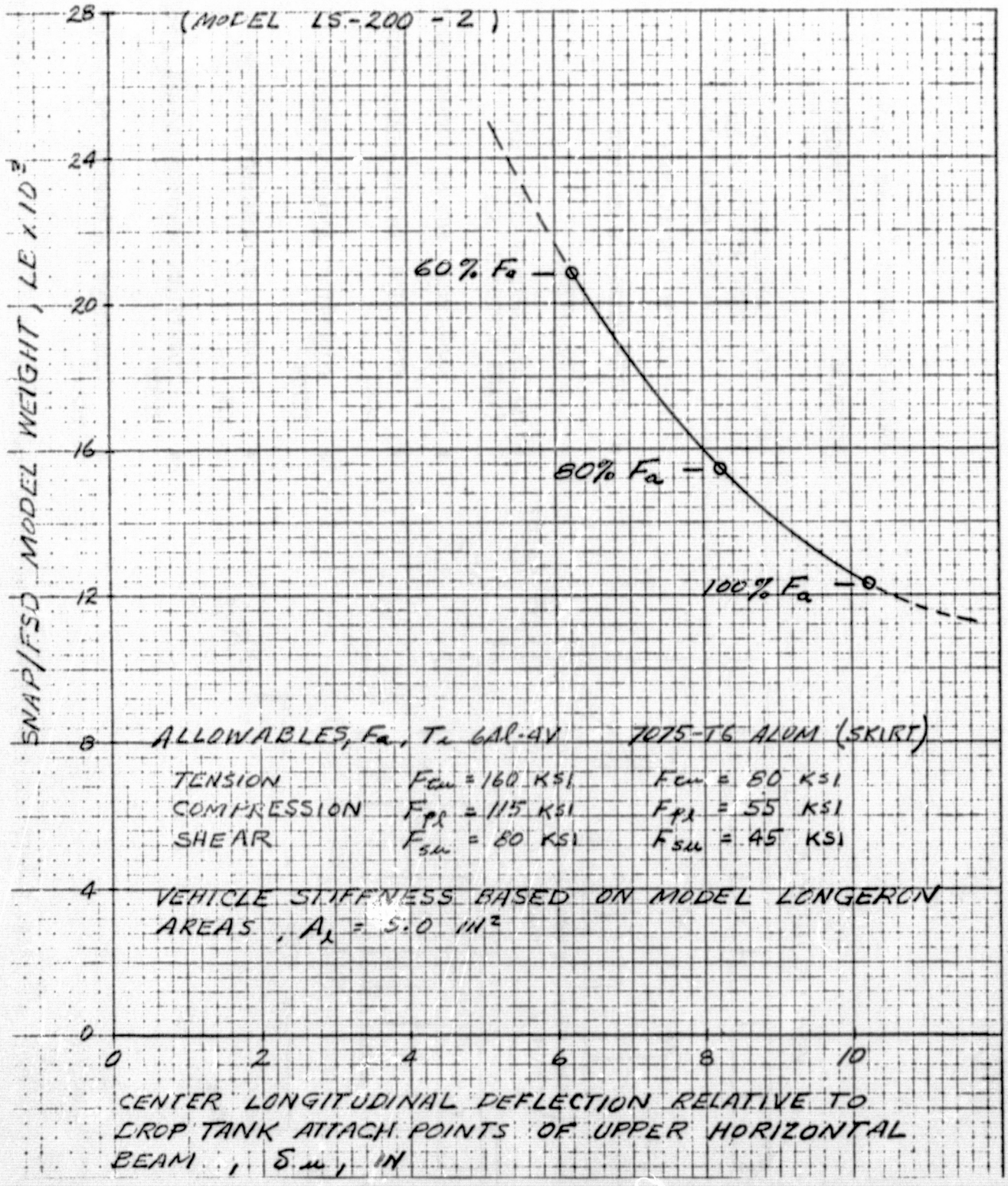

Fig. 2.8-25 Effect of Allowable Stresses on SNAP/FSD Thrust Structure Model Weight and Upper Horizontal Beam Deflection (Model LS-200-2)

REPRODUCIBILITY OF THE ORIGINAL PAGE IS POOR.

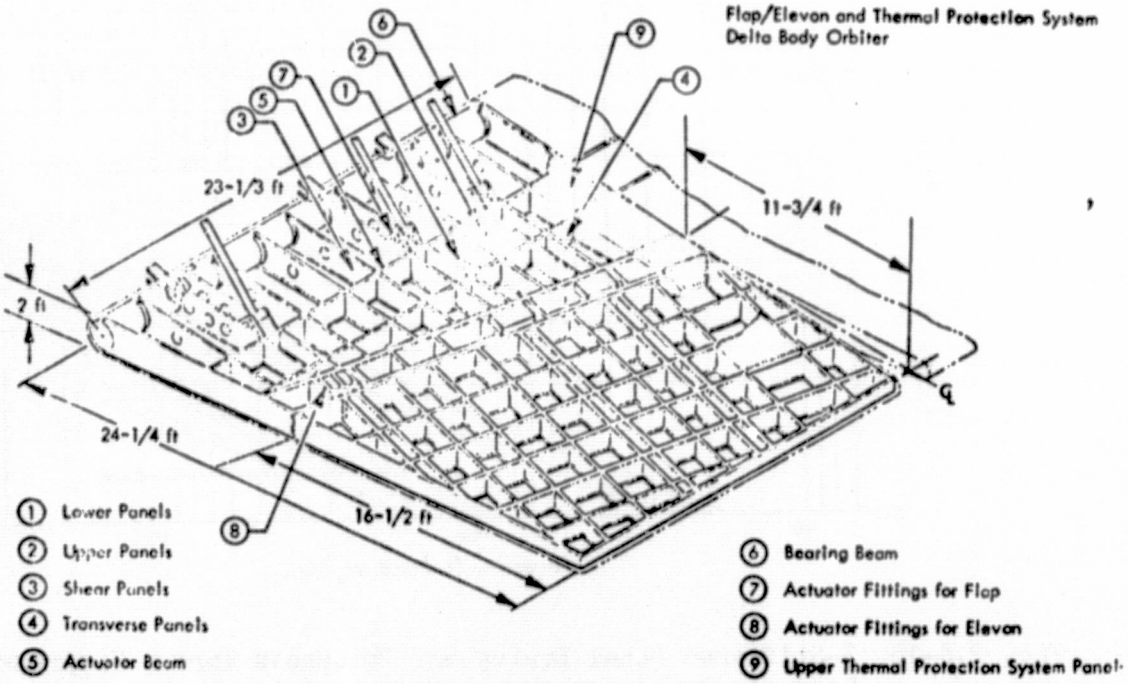

Fig. 2.8-26 Orbiter Trim-Flap Assembly

is shown in Fig. 2.8-26. Three materials for this specific design were studied; aluminum, beryllium, and titanium. The TPS is considered attached to both surfaces for the aluminum configuration but is considered attached only to the lower surface for the latter cases. The basic design parameters and study results are shown in Table 2.8-7.

Several structural configurations of this control surface are under consideration. The results presented here are only preliminary steps in the optimization procedure planned. Additional weight savings may be possible by increasing the depth-of-flap at the actuator-fitting beam. The upper/lower skin line loads would be reduced, and the structural efficiency of the actuator crossbeam would be increased.

2.8.5.4.2 Fin Structure. Evolved during this study was a fin concept consisting of a conventional two-spar, stiffened-skin, multiribbed box. The two spars

Table 2.8-7

TRIM-FLAP WEIGHT COMPARISON

Material (°F)	Entry CG (% body length)	Structure Weight (lb)	TPS Weight (lb)	Total Weight (lb)
Aluminum (200°)	77.1	3,615	9,244	12,859
Titanium (800°)	76.6	4,510	3,910	8,420
Beryllium (600°)	76.5	3,073	3,242	6,315

Control surface area = 1,148 ft^2
Average design pressure = 200 psf
Lower TPS surface temperature = 2,500°F
Upper TPS surface temperature = 1,000°F
Structural materials:

- Aluminum alloy 7075-T6
- Titanium alloy 6Al-2Sn-4Zr-2Mo duplex annealed
- Beryllium cross-rolled sheet

are swept with the fin at approximately the 5- and 60-percent chord positions. Considerations involved in determining actual locations were:

1. Obtaining maximum spread
2. Providing for rudder hinge supports
3. Establishing convenient tie-in with fuselage or thrust structure

The spanwise-stiffened skin is supported by chordwise ribs varying in spacing from 25 in. near the tip to 50 in. at the root. A truss-type rib was selected to permit ingress by a man for internal inspection. The box structure formed by the stiffened-skins, spars, and ribs follows both spars as they make the transition from the external fin area into the fuselage structure. A transition rib is located at this point. The fuselage structure provides normal reactions to the fin structure where the transition rib and terminal rib intersect the two spars.

The material choice was made in the same manner as for the flap. With the decreased TPS requirements, titanium under the present groundrules provides the lightest structure/TPS combination.

Four self-aligning hinges support the rudders. These hinges are held in brackets supported by the rear spar and cover skins.

2.8.5.5 Orbiter Internal Propellant Tanks.

2.8.5.5.1 Material Considerations. Reusable LH_2 and LO_2 tank designs depend upon fracture mechanics analysis methods to assure reliability and minimum weight. A fracture mechanics technique is available to design a reliable pressure vessel having maximum efficiency.

Extensive material testing and characterization of 2219 alloys for Saturn booster tanks and the Apollo vehicle tanks makes this alloy the leading contender for space shuttle tanks. High fracture toughness, good producibility, and excellent structural characteristics make this the most cost-effective choice. A leading alternate alloy is 2021 which has enjoyed Air Force acceptance in some recent Lockheed contracts. The alloy 2014 deserves consideration in detail analyses.

2.8.5.5.2 Fracture Mechanics Technology for Optimum Pressure Vessel Design. A technique has been developed to design a maximum efficiency reliable pressure vessel of given geometry and service life. The technique for ensuring minimum weight vessel reliability relies on the application of linear elastic fracture mechanics.

Analyses of many pressure-vessel service failures have shown that a critical size flaw (surface or imbedded) is the origin of fracture. For reliability, a pressure vessel design should incorporate consideration of these pre-existing defects. The design must account for the possibilities of fracture upon the first pressurization, growth to critical size from repetitive pressure cycles, and growth to critical size from environmentally induced crack growth.

Linear elastic-fracture mechanics provides a single valued parameter, which relates flaw size and applied stress. The parameter, K_I, is called the stress-intensity factor. Fracture results when K_I reaches a critical value, K_{Ic}, which relates the combination of stress and flaw size necessary to cause fracture. K_{Ic} is a material property. For surface flaw

$$K_I = 1.1\ \sigma\ (\pi\ a/Q)^{\frac{1}{2}}$$

where σ = applied stress level
a = semi-elliptical crack depth
Q = surface flaw-shape factor

Thus, for a given stress level in a pressure vessel, the maximum permissible size defect is known. Any defects, then, must be smaller than the known critical size.

Defects which are not of a critical size may grow during the lifetime of the vessel. This growth may be due to either, or both, of two causes: (1) fatigue-crack extension, and (2) environmental crack extension. Experimentation has shown that crack extension, due to a combination of stress and chemical environment, is governed by the stress-intensity factor. Apparently, there is a threshold value, K_{TH}, below which no crack growth will take place in a given environment. Thus, if a pressure vessel operates below K_{TH}, no environmental crack extension can occur; therefore, no failure can occur.

Also, subcritical defects may grow from fatigue. Experimentation has conclusively shown that fatigue-crack growth is primarily depending on the change in stress-intensity, ΔK. The rate dependence is usually of the form

$$da/dN = C\ (\Delta K)^n$$

where da/dN = crack extension per cycle
C & n = constants

Thus, knowing the operating conditions in a given pressure vessel and the lifetime (pressure cycles), potential fatigue-crack growth can be accurately predicted.

Fracture mechanics have provided proven concepts that may be applied to the design of pressure vessels. In aerospace applications, especially, weight is a prime consideration. Therefore, a procedure has been developed by which a reliable vessel of minimum weight for a given configuration can be designed. The procedure assumes a linear relationship between pressure and stress.

The procedure for applying fracture mechanics to pressure vessel design consists of three steps, as follows, for the general case where vessel pressure and temperature vary with time:

a. Determine the necessary data

   1. Pressure-temperature-time requirements for the given configuration
   2. Mechanical properties of the candidate materials
   3. Fracture-toughness properties (K_{Ic}, K_{TH}, da/dN) of the candidate materials

b. Determine the maximum permissible K_{Ii} for each vessel region (i.e., welds, base metal, etc.)

   1. Operating temperature at which (K_{TH}/P_{op}) is a minimum, where P_{op} is the operating pressure (determines the pacing conditions for environmental cracking).

   2. Maximum permissible K_{Ii} (calculated using the pressure-temperature-time profile, done by determining the lifetime fatigue-crack growth, such that K_{TH}, at the temperature found in step b.1, is just reached on the last pressure cycle of the vessel's service life; if the actual K_{Ii} is equal to, or less than, this calculated K_{Ii} value, then the planned vessel lifetime is assured).

c. Maximize the operating stress levels in the vessel, such that the calculated maximum permissible K_{Ii} is met in each region. This minimizes wall thickness and, therefore, weight for a given vessel configuration. The maximum operating stress is dependent on the maximum possible flaw size in a region. Usually, this worst case of flaw size is determined by a proof test. As a result, the minimum wall thickness at proof pressure is specified, since

$$t_{min} \sim (P_{pr}/\sigma_{pr})\ \text{min.}$$

where

t_{min} = minimum permissible wall thickness
σ_{pr} = material yield strength at proof test temperature (in most cases)
P_{pr} = required proof test pressure

The value of the required proof test pressure is determined by

$$P_{pr} = K_{Ic}/(K_{Ii}/P_{op})_{min.}$$

where

(K_{Ii}/P_{op}) is obtained from Step b.

Applications of this procedure will result in a reliable minimum-weight pressure vessel for a given configuration.

2.8.5.5.3 Fracture Mechanics Study of Tank Factory-of-Safety for Preliminary Designs. Fracture mechanics procedures were developed for tank design, because tank safety and reliability are not guaranteed by specifying a factor-of-safety, no matter how large. This procedure results in the specification of a proof pressure test to guarantee safe operation during the tank lifetime. This specification considers: (1) the "worst case" initial flaw size, (2) cyclic flaw growth, and (3) environmental extension of flaw at constant pressure.

Figure 2.8-27 presents a summary plot of a preliminary study showing the procedure followed to establish design proof and ultimate factors. This figure shows the basis for a proof factor, α, of 1.43 in main tankage. $K_{Ii} = 0.70\ K_{Ic}$ will result in operation below K_{TH} during the 200-cycle lifetime: $\alpha = K_{Ic}/K_{Ii} = 1/0.70 = 1.43$. Since tankage will have very thin walls of 0.020-in. to 0.150-in. thick 2219-T87, the crack-growth-rate data, d (a/Q)/dN, for 0.063-in. thick 2219-T87 (NAS Cr 72606) were used to construct the figure. $K_{TH} = 0.86$ (NAS Cr 54837) was determined for 1.0-in. thick 2219-T87 and is the only estimate available for 0.020-in. to 0.150-in. thick 2219-T87. Leakage in the metal that is thinner than 0.080 in. is possible in less than the planned 200-cycle lifetime, if the "worst case" initial defect from proof test information is present. However, if nondestructive inspection or other means can guarantee a smaller "worst case" initial defect, leakage may not be a problem.

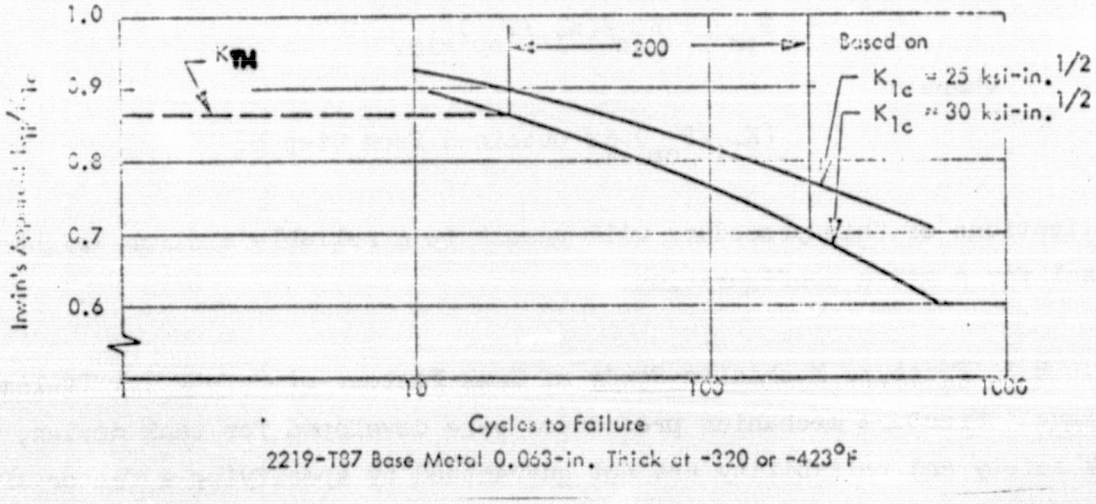

Fig. 2.8-27 Orbiter-Pressure-Vessel Factors-of-Safety

A proof factor of 1.43 is assumed to be adequate for welds as well as base metal. The ultimate factor-of-safety derivation is shown below:

Cryogen	Temperature (°F)	$F_{proof} = F_{ty}$ (ksi)	F_{tu} (ksi)	$f_{Operating} = f_{proof}/1.43$ (ksi)	Ultimate Factor-of Safety (F_{tu}/f_{op})
LH_2	-423	67.6	94.5	47.3	2.0
LO_2	-298	60.5	75.0	42.3	1.78

2.8.5.5.4 Tank Preliminary Design Analysis. The orbiter internal propellant tanks are nonprimary load-carrying tanks, fabricated of 2219-T87 aluminum with monocoque construction. The ascent LO_2 tanks and the on-orbit LH_2 tank are supported from the rocket-engine thrust structure. The ascent LH_2 tanks are supported longitudinally by the ascent LO_2 tanks, while the on-orbit LO_2 tank is supported from the airbreathing engine support structure. The on-orbit LH_2 tank, dependent on the load path selected in fuselage studies, can support the longitudinal reactions from the payload bay, without added shell stiffening to the tank.

Except for the LO_2 ascent tanks, the internal orbiter tanks are separately pressured for optimum engine/plumbing pressures. The LO_2 ascent tank design pressure occurs from the combination of droptank ullage pressure and hydrostatic head from the fluid level in the droptank. Maximum total pressure occurs when the vehicle first reaches 3g acceleration, which occurs at 160 sec of booster burn. At this time, the LO_2 head in the droptank is ~ 200-in. high. The pressure-acceleration condition designs these tanks. A propulsion trade study (Ref: Second Letter Progress Report, LMSC-A976286, Study of Alternate Space Shuttle Concepts) revealed this approach to be a minimum-weight solution when considering residuals and manifold requirements.

The critical design condition for the LO_2 on-orbit tank is a combination of two conditions: the forward 75 percent is caused by maximum ullage pressure in the warmed-up empty condition, and the aft 25 percent is caused by the maximum 3g acceleration-full condition.

For the LH_2 ascent tank, the critical design condition occurs when the propellant is just expired and maximum ullage pressure is reached. This combination, combined with rising wall temperature, establishes the tank membrane gages except for the upper dome, which is established on the basis of minimum gage.

The critical design condition for the LH_2 on-orbit tank is the same as for the LH_2 ascent tank.

Design criteria used for sizing the tankage are presented in Tables 2.8-8 through 2.8-11, inclusive. Based on the preliminary fracture-mechanics study, discussed above, the ultimate factors-of-safety for LO_2 and LH_2 tanks are 1.78 and 2.0, respectively. Local thickening will be required because of the loss in parent-metal strength in the welded and heat-affected zones (40-percent membrane thickness). Also, at the dome junctures, lug, and/or stub skirt, provisions are added for tank support.

The most recent detailed analysis for LS 200-5 stage-and-one-half internal tankage is presented in EM L2-01-04-M5-2 in the Fifth Letter Progress Report. Table 2.8-12 presents a summary of the tank design parameters that lead to the system weights.

Table 2.8-8
ULLAGE PRESSURE (EXCLUDING HYDROSTATIC PRESSURE)

Flight Event	Ascent Tanks		On-Orbit Tanks	
	LO_2 (psia)	LH_2 (psia)	LO_2 (psia)	LH_2 (psia)
Boost	f(drop tank)*	21	19	21
Staging to Injection	28	26	19	21
Orbit Maneuvers	18	18	50	27

*LO_2 ascent tank is cascaded from LO_2 droptank, receiving ullage pressure of 21.2 psia, plus a static head from the droptank.

Table 2.8-9

ACCELERATION (INCLUDING ELASTIC RESPONSE)

Flight Event	Acceleration (g)
Liftoff	1.50
Maximum αq (~ 80 sec)	1.70
Booster Maximum Acceleration (~ 160 sec)	3.0
Orbiter Burn	3.0
Orbiter Burnout	3.0
Reentry	2.5 transverse

Table 2.8-10

TANK-WALL TEMPERATURES

	Ascent Tanks		On-Orbit Tanks	
Flight Interval	LO_2 (^oR)	LH_2 (^oR)	LO_2 (^oR)	LH_2 (^oR)
Booster Burn	162	40	162	40
Orbiter Burn*	500 top 162 (wetted tank)	360 top 40 (wetted tank)	600 top 162 (wetted tank)	360 top 40 (wetted tank)
Reentry	500	400	500	400

Table 2.8-11

MATERIAL PROPERTIES - 2219-T87 ALUMINUM**

Temperature	F_{tu} (psi)	F_{ty} (psi)	E x 10^{-6} (psi)
Room	63,000	52,000	10.5
162^oR (LO_2)	75,000	60,000	11.8
40^oF (LH_2)	94,500	67,500	12.5

* Assume linear temperature profile as a function of station from forward ullage to aft end of tank.

** Ref: MIL-HDBK-5A

Table 2.8-12

ORBITER TANK DESIGN DETAILS

Design Parameter	Ascent Tanks		On-Orbit Tanks	
	LO_2	LH_2	LO_2	LH_2
Factor-of-Safety	1.78	2.0	1.78	2.0
Tank Minimum Gage Thickness (in.)	0.025	0.025	0.025	0.025
Material Density, 2219-T87	0.102	0.102	0.102	0.102
Dome Shape	Spherical	Spherical/ $\sqrt{2}$ Ellipse	Spherical	$\sqrt{2}$ Ellipse
Ullage Pressure (psia)	207*	21	19	21
Burnout Pressure (psia)	28	26	50	27
Ullage Volume (%)	0	3	3	3
Propellant Density (pcf)	70.2	4.274	70.2	4.274
Cryogenic Material Strength (psi)	75,000	94,500	75,000	94,500
Average Burnout Material Strength (psi)	67,300	75,000	67,300	75,000
Forward Radius (in)	74.5	27	27	96
Aft Radius (in)	74.5	67	31	96
Total Length (in)	149	795	396	231
Volume (cu ft)	1,002	3,346	576	3,109
Surface Area (ft^2)	484.4	1,681.1	501.5	1,051.7
Propellant Weight (lb)	70,340	13,884	39,258	12,900
Tank Weight (lb)	1,359	872	270	830
Tank NOF (lb)	341**	308	95	290
Number of Tanks	2	2	1	1
Total Weight (lb)	3,400	2,360	365	1,120

*Ullage pressure results from the combination of ullage in droptank plus hydrostatic head when 3g is reached (head to inlet = 1,536 in.)

**NOF for spherical tanks statistically show less weight penalty. For this reason, a value of 0.25 is used; whereas, for other type, the NOF is assumed to be 0.35

2.8.5.6 Payload Compartment and Door. The payload compartment extends from the nose-section rear bulkhead (Sta. 530) to a bulkhead located at Sta. 1270. The payload compartment trough (See Fig. 2.8-14, Section 2.8.5.2) is an open-faced, corrugated, stiffened-shell structure, supported by fuselage frames. This U-shaped shell provides continuity of the airframe shell structure around the opening for the payload compartment door. Hard points for supporting various payloads are located on several intermediate fuselage frames. The forward (nose section) and aft bulkheads provide primary transverse support for the ascent propellant tanks.

The payload-compartment door is designed not to react vehicle primary loads but is sized for its own inertial loading conditions and induced aerodynamic pressure loads during ascent- and entry-flight phases. The present design is a clamshell barrel (three-hinged arch) door of 6Al-2Sn-4Zr-2Mo Titanium alloy. This door is uninsulated and designed to sustain a load at 800°F. The design-limit pressures for the door are tentatively:

Booster ascent

P (burst) = 0.25 psi

P (collapse) = 2.0 psi

Reentry subsonic

P (burst) = 1.60 psi

P (collapse) = 0.65 psi

2.8.5.7 Pressurized Structure. The crew cabin, tunnel, and airlock constitutes the major pressurized structure, other than the propellant tanks. Preliminary sizing has been performed in terms of volumetric requirements, pilot visibility and location, etc., but airframe-type and sizing remain to be determined. The pressurized structures are designed as typical airframe pressure vessels, preliminarily sized for a safety factor of 2.0. Detailed study will consider fracture mechanics to assess fatigue and fail-safe criteria.

The forward payload-compartment (nose section) bulkhead supports the loads from the crew cabin, forward equipment, and RCS components in addition to the nose-gear transverse and drag loads.

2.8.5.8 Landing Gear and Airbreathing Engine Support Structure. Intercostal beams running from the aft payload-compartment bulkhead to thrust structure (bulkhead) react the main-landing-gear transverse loads. Axial loads associated with the drag loads from the main landing gear and thrust from the airbreathing engines are transferred to the intercostals, hence to the thrust structure. Figure 2.8-28 illustrates this design concept.

Also, the intercostal beams provide the sidewalls for the flap-track stowage assembly. This recessed area is required to stow the lower flap during ascent. The upper-shelf of the flap-track stowage assembly provides the additional intermediate support of the airbreathing engine support structure as well as the continuity of the lower-fuselage surface forward of the thrust structure. Figure 2.8-29 illustrates this design concept.

The airbreathing engines, located in a recessed area forward of the flap-track stowage assembly, are stowed within the fuselage except when in use. When lowered for use, the upper-shelf of the engine support structure closes the opening created by the engines being distended.

References

2.8-1 D. N. Emro and L. Spunt, "Wing Box Optimization Under Combined Shear and Bending," AIAA Journal of Aircraft, Mar-Apr 1966

2.8-2 A. B. Burns, "Exploratory Structural Optimization Studies for Manned Lifting Entry Vehicles Suitable for Space Shuttle Operation," LMSC-A966022, Jan 1970

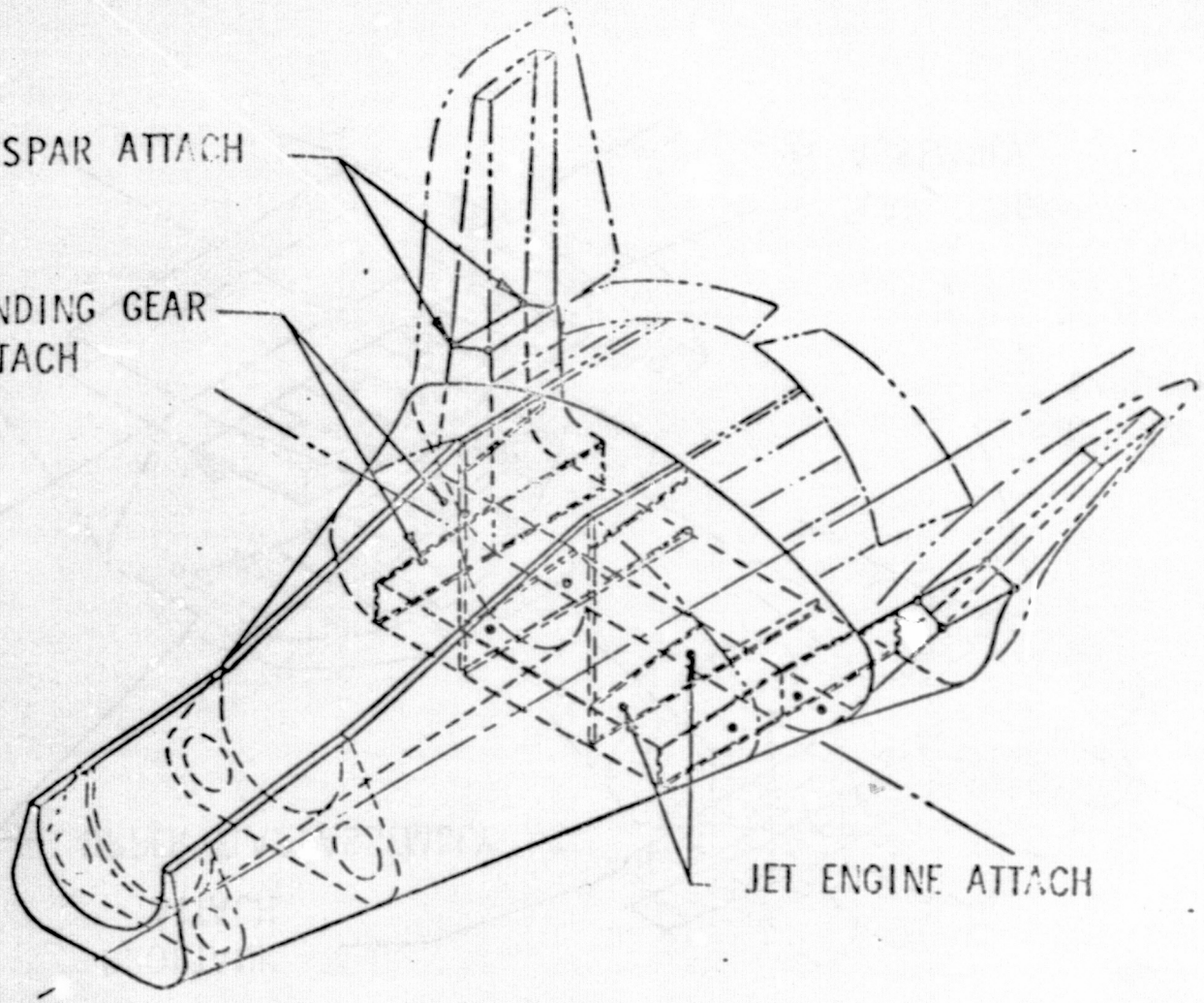

Fig. 2.8-28 Delta-Body Orbiter Stage-and-One-Half/Two-Stage Common Structure

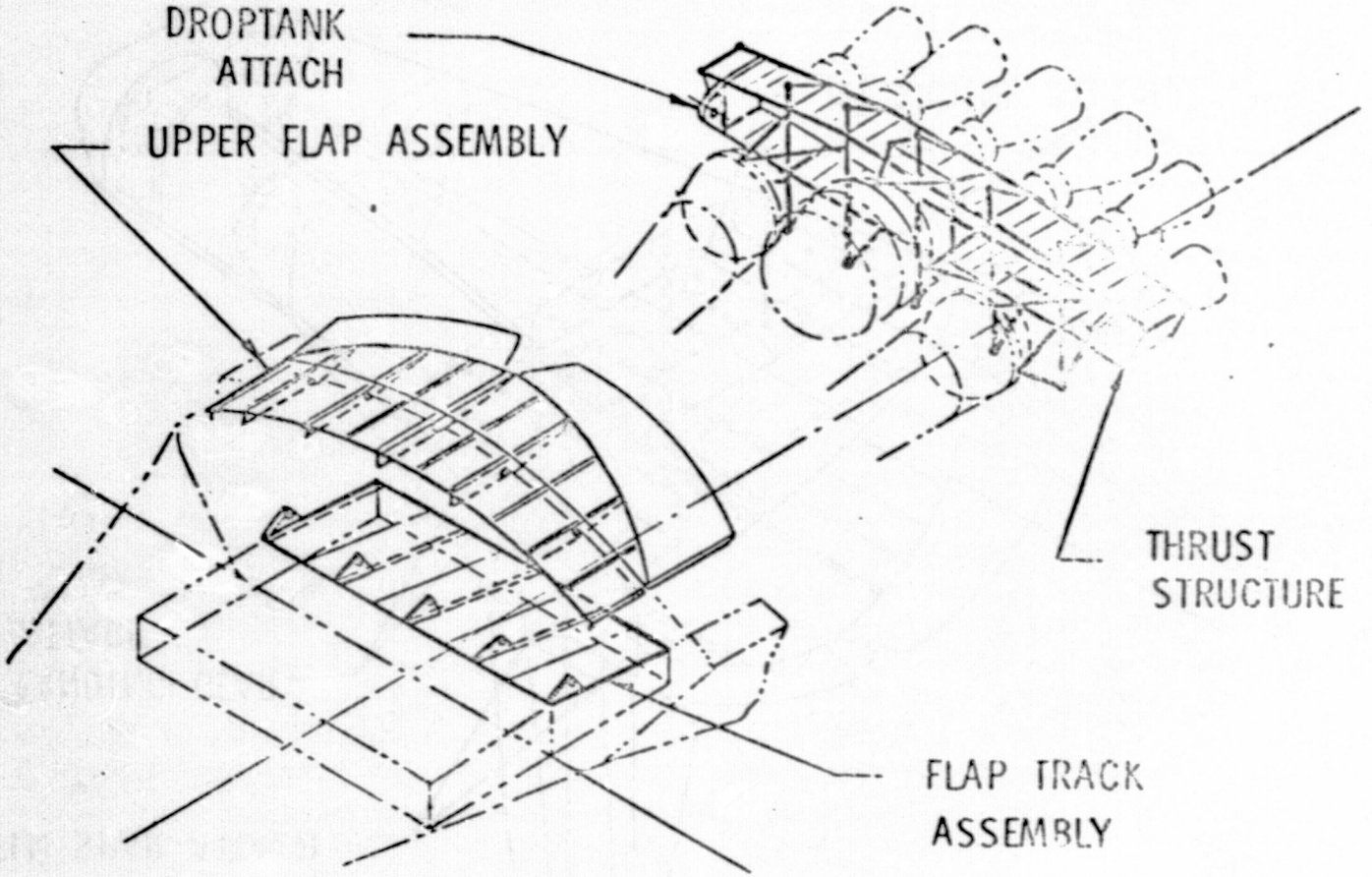

Fig. 2.8-29 Delta-Body Orbiter Stage-and-One-Half Structure

2.9 PROPULSION SYSTEMS

Propulsion requirements for launch and ascent, orbit transfer, orbital maneuvers, reentry retro, vehicle attitude control, and subsonic landing assistance are satisfied by the operational capabilities of four propulsion systems. These four systems and their major functions are listed as follows:

a. Main propulsion system for vehicle launch and ascent into injection orbit.

b. Orbit maneuver propulsion system for orbit-to-orbit transfer, on-orbit maneuvers, and reentry retro.

c. Attitude control propulsion system for vehicle orientation and minor translations on-orbit and vehicle orientation during the initial portion of reentry after retro.

d. Airbreathing propulsion system for landing field approach and landing go-around. Supplemental propulsion subsystems may be required for subsonic ferry flights between the landing field and the launch site. These supplemental subsystems are separate from the basic airbreathing propulsion system and are provided in kit form.

The propulsion systems for the stage-and-one-half vehicle have been designed to overcome the vehicle-peculiar problems and to produce maximum performance with logical conservatism. A list of symbols used in propulsion system schematics is presented as Fig. 2.9-1.

2.9.1 Main Propulsion System

The main propulsion system provides thrust to inject the space shuttle vehicle into a 50-nm by 100-nm elliptical orbit. A summary of system characteristics is presented in Table 2.9-1.

Fig. 2.9-1
LIST OF SYMBOLS


Isolation Valve


3-Way Valve


Check Valve


Pressure Regulator


High Pressure Pump


Compressor


Turbine


Control Orifice


Heat Exchanger


Thruster (Without Valves)

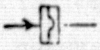
Burst Disc


Relief Valve


Disconnect


Capped Port

Uncapped Port


Line Connected to Common Manifold


Flow Meter


Circulation Fan With Motor


Pressure Switch


Boost Pump


Electrical Heater


Gas Generator


Control Unit


Proportional Valve

LO_2	Liquid Oxygen
GO_2	Gaseous Oxygen
LH_2	Liquid Hydrogen
GH_2	Gaseous Hydrogen
He	Helium

Fig. 2.9-1

Table 2.9-1

Main Propulsion System Characteristics Summary

A. Engine System	
Engine Type	As defined by Space Shuttle Vehicle/ Engine 550K(SL) Interface Control Document 13M15000B, and modified to 53:1 Expansion Ratio
Propellant Type	LO_2 and LH_2
Nozzle Expansion Ratio	53:1
Throttle Range, Percent NPL	50 to 109
Number of Engines:	
Total	9
Operating at Liftoff	9
Prior Separation	
At Separation	
After Separation	
Thrust Vector Control:	
Engine Gimbal Capability, deg	±7, Square Pattern
Overshoot, deg	0.5
Number of Gimballed Engines	5
Arrangement of Gimballed Engines	Two center engines in upper row and Three center engines in lower row
Performance, NPL:	
Thrust (9 engines), nominal, lb	
Sea Level	4,770,000
Vacuum	5,508,00
Specific Impulse,	
Sea Level	386 ±3
Vacuum	445 ±3
Specific Impulse, Min-guaranteed, sec	
Single Engine	
Sea Level	383
Vacuum	442
Clustered Engines	Single engine deviations are divided by $\sqrt{}$ of number of engines in cluster
Mixture Ratio O/F	
Nominal	6.0
Operating Time	
Liftoff to Droptank Staging, sec	295
Droptank Staging to Orbit Injection, sec	90

Table 2.9-1 (Cont'd)

B. Propellant System

Tank/Feed Configuration:

Two LO_2 droptanks cascade-coupled to LO_2 orbiter ascent tanks

Two LH_2 droptanks parallel-coupled to LH_2 ascent tanks

Orbiter ascent-tank/feed system independent from orbiter orbital-tank/feed systems

Individual feedlines from LO_2 tanks to engines

LH_2 fed to engines by manifold

Propelled Weight, lb:	Droptanks	Orbiter Tanks
Loaded	3,105,000	255,200 (1)
Reserve (FPR)	0	8,079
Ground Hold	31,122	N/A
Impulse	3,063,000	239,200

Tank Ullage Pressures, psia:	
O_2 Droptank	28
O_2 Ascent Tank	28
H_2 Droptank	27
H_2 Ascent Tank	27

(1) Includes 29,400 lbm LOX propellant in feedlines from droptanks

Table 2.9-1

The main propulsion system consists of 9 high-pressure oxygen-hydrogen rocket engines supported by a propellant storage and feed system incorporating flow controls including propellant-utilization control, pressurization, venting, and thermal protection subsystems. The 9 candidate rocket engines installed in the base of the vehicle are identical with the engine used for the Phase B studies (defined in NASA Interface Control Document 13M15000B, dated 1 March 1971), with the exception that the nozzle expansion ratio is increased to a value of 53:1. Selection of the 53:1 nozzle expansion ratio is the result of an analysis of vehicle performance (see Ref. 2.9-1). Further consideration leading to a final selection should include rocket engine thrust level, engine development program costs and vehicle size/payload constraints. Five of the 9 rocket engines are gimballed $\pm$ 7 deg (square pattern) to provide thrust vector control (TVC) in roll, pitch, and yaw modes during the ascent-to-orbit injection. The remaining 4 nongimballed engines are spaced on either side of the gimballed engines with 109 in. (minimum) between engine centerlines.

The selection of the 5 center engines for gimballing to meet flight control criteria has been based on an analysis (see Section 2.13) which allowed for encountering worst winds at maximum q conditions when encumbered with an any one-engine-out (fixed/gimballed) operational condition. While the analysis was performed using 5 gimballed engines out of 11 installed (400K thrust level), the present baseline configuration of 5 gimballed engines out of 9 installed (530K thrust level) meets/exceeds all criteria for flight control established in the prior analysis. All engines are ignited at liftoff. During the pre-staging ascent phase, the acceleration is maintained at a 3g level by throttling and shutting down the engines in a sequence minimizing specific impulse losses. Just prior to separation, the number of operative engines is reduced to 3 with 2 of these used for normal operation while the remaining engine is on standby status. During separation, the 2 operating engines are throttled close to the minimum power level to reduce the vehicle acceleration during the separation maneuver to approximately a 1g level.

Propellant tankage for the main propulsion system includes both the droptanks and the ascent tanks in the spacecraft. During liftoff and ascent, the rocket engines are fed propellants from the droptanks with the oxygen cascaded through

the spacecraft ascent tanks and the hydrogen direct-coupled to the engines via a manifold. After droptank separation, the two operating engines draw propellants from the spacecraft ascent propellant tanks. Cascading the oxygen from the droptanks through the spacecraft ascent oxygen tanks provides for minimal residual propellant weight in the droptanks at separation, since the oxygen droptanks drain essentially dry into the spacecraft tanks without interrupting flow to the operating rocket engines. These LOX propellant transfer lines contain approximately 30,000 lbm within the orbiter vehicle and thus are treated as an extended part of the spacecraft spherical storage tanks. Location of the LOX propellant transfer line within the orbiter provides a payload advantage of 780 lbm/mission (see Ref. 2.9-2) when effects on droptank/orbiter plumbing and insulation weights are considered.

A smooth transition of terminating propellant flow from the droptanks while initiating flow from the orbiter ascent tanks during separation is provided by reducing the flow rates to approximately 14 percent of the full-flow rates. This is accomplished by reducing the number of operating engines to those maintained operational after staging and by throttling these engines to the 50-percent power level. During this period, flow from the ascent tanks is initiated and the droptank isolation valves are slowly closed.

A unique capability of the stage-and-one-half concept is the opportunity to accomplish recovery of propellants trapped in feedlines of shutdown engines and subsequently convert this propellant to useful impulse. The propellant recovery system described in the following section has been estimated to provide 4200 lb of propellant for subsequent conversion to delivered impulse.

2.9.1.1 Propellant Fill and Feed System. A schematic diagram of the propellant fill and feed system is presented in Fig. 2.9-2.

Propellant tank size for ascent and droptanks is determined from a performance analysis of staging and an operational analysis which takes into account the average density of propellant in the tanks at liftoff with volume allowances for impulse propellant (based on minimum performance of the rocket engines),

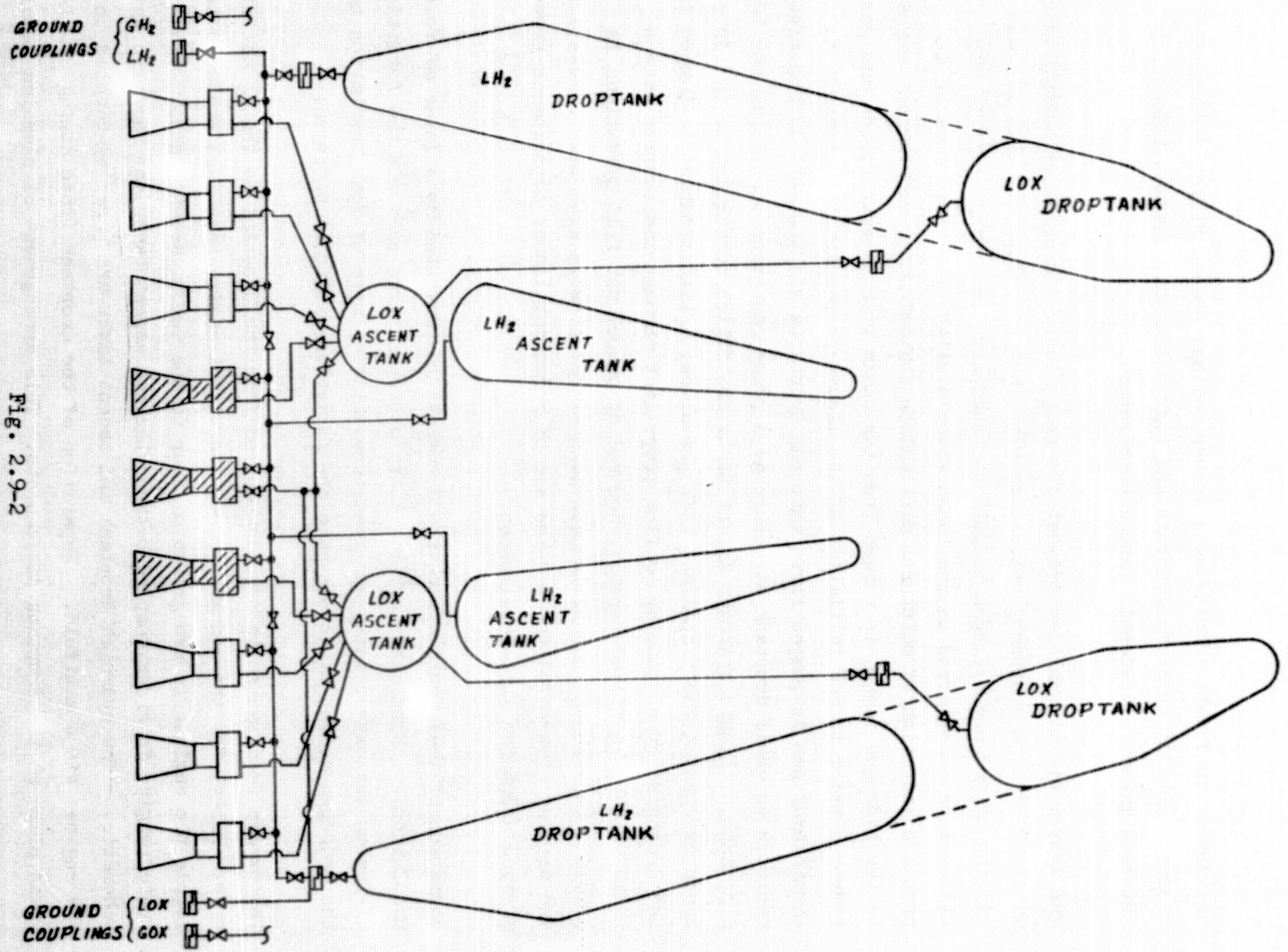

Fig. 2.9-2 1 1/2-Stage Orbiter Propellant Fill and Feed System

residuals, in-flight liquid/vapor losses, ullage space, flight performance reserve, loading tolerances/errors and tank volumetric changes induced by internal pressure/cryogenic liquid temperature.

The system operational requirement for propellant loading to be accomplished within 2 hr from a standby status, results in a procedure for chilling and filling oxygen and hydrogen propellant tanks simultaneously. Inert, dry nitrogen gas, contained in the tanks under a slight positive pressure to preclude induction of moisture, particulate contaminants, and ambient oxygen in the hydrogen tanks, is purged from the tanks with gaseous oxygen and gaseous hydrogen prior to the initiation of the liquid propellant fill operation. Liquid hydrogen is pumped first into the droptanks via the vehicle crossfeed manifold to chill droptank structure as a prior condition to filling the LOX droptanks. Liquid hydrogen ascent tanks are filled subsequent to the droptanks by opening the propellant tank prevalves. Liquid oxygen is pumped into the droptanks by continuing to flow propellant through the orbiter ascent tanks which were filled first. Control of propellant fill operations is provided through the use of in-tank point-level sensors with fill completion and topping controlled through the use of redundant linear capacitance probes arrayed about the full-level point.

Formation of ice/liquid air on the droptanks is prevented by a layer of foam insulation. Within the orbiter a dry nitrogen purge prevents the formation of ice on the oxygen tanks and feedlines while a layer of foam insulation on the hydrogen ascent tanks prevents the formation of liquid nitrogen.

The oxygen feed system is cascade-coupled from the droptank to the O_2 ascent tank. Except for the center engine, individual engine feedlines are used to couple the engines in two groups of four to the two O_2 ascent tanks. The center engine is cross-coupled between the two ascent tanks, as shown in the schematic. The hydrogen droptank and ascent tanks are parallel-coupled to the engines via a manifold. Separation of the droptank lines during staging takes place at the droptank disconnects. This arrangement of plumbing resulted

from an analysis (reported in Ref. 2.9-3) of 4 feedline configurations in which the relative merits of cascade flow and manifolded flow schemes were determined by their impact upon payload weight capability. Factors considered in the analysis included dry weight of tanks, valves, lines, trapped or unusable liquid propellants and residuals.

Prior to droptank staging, all engines except the center three are shutdown. Series dual-redundant O_2 valves just downstream of the droptank disconnects are closed immediately after oxygen droptank depletion. These valves are powered by helium actuators. Shutoff sequencing of these valves is not critical with respect to maintaining suitable pump inlet conditions during the process of isolating the droptanks, especially since the O_2 droptanks normally are depleted of liquid before the valves are closed. With the ascent O_2 tanks already feeding the engines, the transfer process becomes a matter of deactivation of the droptank pressurization circuit and simultaneous activation of the ascent tank pressurization circuit. Shutdown of the dual valves downstream of the O_2 droptank disconnect immediately follows pressurization switchover.

Dual valves also are used between the H_2 droptank disconnects and hydrogen manifold. It is considered desirable to have a slow-acting check valve downstream of these shutoff valves (possibly replacing one valve) to prevent reverse flow of hydrogen into the droptanks when the ascent tank valves are opened prior to staging.

Pressure rise in the manifold, due to the deceleration of hydrogen in the droptank lines, is less than 0.5 psi based upon reaching zero droptank line flow in 0.5 sec from the initiation of the flow shutoff sequence.

The initiation of H_2 tank switching is based on liquid level-sensing in the LOX propellant transfer line and is timed to allow sufficient liquid hydrogen reserve to cover system variability and instrumentation error. This minimizes the risk of pressurant flow into the H_2 manifold.

Feedlines and engine pumps are kept chilled prior to launch within the operating temperature range by means of a pumped-propellant circulation system. Electrically powered centrifugal pumps submerged in the ascent oxidizer and fuel tanks circulate propellant to the respective oxidizer and fuel circulation manifolds. Propellant from each manifold flows into the engines downstream of the pumps via series-redundant check valves. From the engine, the propellants flow counter-current into the respective feedlines and back to the respective ascent tanks. Initial chilldown of engines and lines takes place during the propellant-tank filling operation. Part of the fill propellant is bypassed into the respective circulation manifolds, resulting in some propellant flowing into the tanks directly through the check valves and then to the tanks via the feedlines. This approach eliminates the type of geysering that would take place if an attempt were made to fill a tank without prior chilling of lines.

The residuals in Space Shuttle vehicles represent significant penalties, and means are provided in this design for recovery and use of a major portion of the residuals. The greatest propellant salvage interest is in the oxygen system, because the penalties with the dense oxygen are very significant, while those in the hydrogen system may not warrant the design and operational effort to salvage hydrogen. The oxygen propellant salvage system design makes ancillary use of the main pressurization system and the ascent tank prelaunch propellant circulation system to save weight and to reduce complexity. As thrust is progressively reduced to stay within 3g acceleration, engines are shutdown in pairs, one on each side. With shutdown of the engines and closure of the prevalves in the respective engine feedlines, propellant salvage can be immediately initiated.

For each pair of lines, this is accomplished by opening a valve coupling the pressurization system to this pair of feedlines. Pressurant flow, controlled by an orifice and introduced at the tank end of the feedline, displaces the liquid which flows into the oxygen propellant circulation manifold via the series-redundant check valves at the engine end of the feedline. Oxygen entering

the manifold flows into the ascent tank counter-current through the centrifugal circulation pump inside the tank. The valve is timed to close when the propellant is expelled from each pair of feedlines. This timing is not critical because any pressurant entering the propellant tank via the salvage system due to late closing of the valve will have little effect on the pressurization of the tank, since the flow volume is very small compared with the pressurization gas flow volume required to satisfy the requirements of the engines still in operation. Gas flow entering the tank via the salvage system is prevented from entrainment with propellant flowing downward into the feedlines of the still-operating engines by a screen baffle adjacent to the circulation pump. The system also is not sensitive to failure of the quad valve closure since pressurant flow, derived from the engines, will stop as soon as all engines are shutdown.

2.9.1.2 Pressurization and Venting System. The baseline-vehicle main propulsion pressurization system design utilizes propellant gases supplied by the engine and regulated by orifices and on-off operation of flow-control valves.

Separate valve clusters and orifices are used on droptank and ascent tanks, each optimized to its respective flow demands. The pressurization/vent system is shown schematically in Fig. 2.9-3. In the event that integration of the rocket engine pressurant supply with the orbiter stage requires use of a noninterrupted, constant mass-rate bleed from the rocket engine, reanalysis and some minor modifications of the system described in the following paragraphs will be necessary to accommodate these criteria.

The valve cluster system is designed to regulate pressurant flow through the use of fixed orifices in parallel with flow through each orifice controlled by redundant shutoff valves. The orifices are sized so that continuous flow-through the principal orifice will not be sufficient to maintain a constant tank pressure while continuous flow through both orifices will exceed pressurant mass flow requirements and cause the tank pressure to rise. Pressure sensors

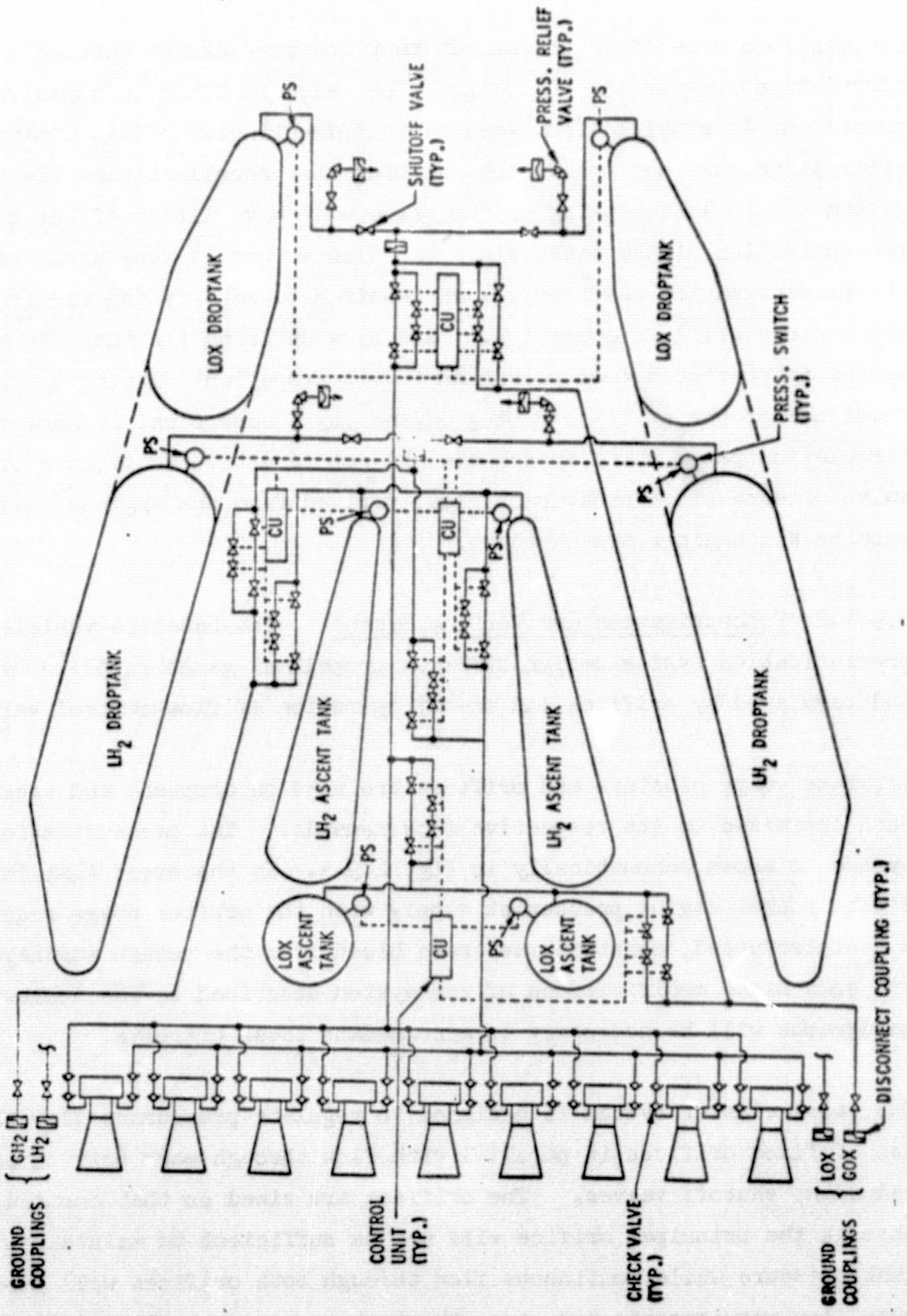

Fig. 2.9-3 1 1/2-Stage Orbiter Pressurization and Vent Syster

in the respective tank systems coupled to the control system initiate valve action to maintain ullage pressure within specified limits. Response lags, due to pressure drops from the valve cluster to the tanks, are biased out by the control system.

Vent and pressurization lines are independent of each other. The vent system, however, is used for tank prepressurization through the ground couplings before liftoff. Again, separate valve clusters are used for the respective droptank and ascent tank systems. The individual valves are combined vent/relief valves.

Sensors for the ascent tank relief valves are attached directly to the tanks, eliminating the possibility of chatter caused by feedback of the pressure drop upstream in the primary flow lines. In the case of the droptanks, a combination of (1) direct-sensing, to initiate the vent cycle, and (2) an electrical loop, to shutoff venting when sensors located on the tank indicate that safe pressure is restored, appears to be a reasonable solution. In this manner, direct-sensing initiates the action to prevent catastrophic failure by overpressurization of tanks.

Series-redundant check valves are particularly well suited to the job of controlling pressurant at high pressure between the engine and manifold. The function of these valves is to prevent backflow of pressurant into engines as they are shutdown during ascent. Check valves operate particularly well in this application where self-actuation and high check pressure are available to hold the poppet tightly against its seat.

2.9.1.2.1 Liquid Oxygen Pressure Profiles. Fig. 2.9-4a shows that the pressure at the engine oxidizer-pump inlet is dominated by the high hydrostatic pressure (labeled static pressure on the figure) up to the time of droptank staging at 300 sec. In the design of feedline plumbing, the lines are sized to take advantage of this pressure to overcome friction and inertial pressure to overcome friction and inertial pressure dip at starting. The curves shown in this figure are based on the thrust-acceleration-time profile of the baseline ascent trajectory.

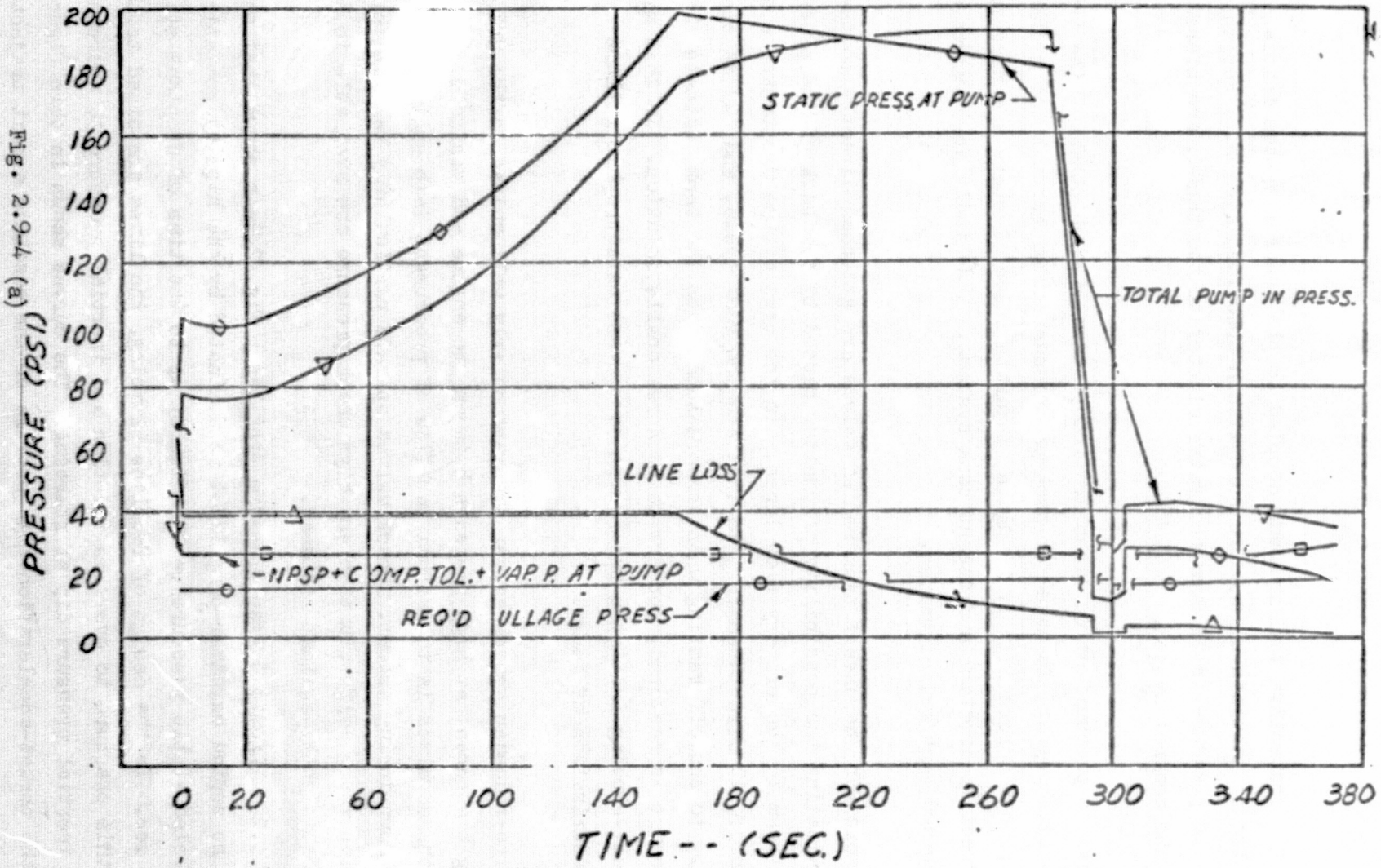

Fig. 2.9-4 (a) Pressure Profiles — Oxygen

LOCKHEED MISSILES & SPACE COMPANY

The vapor pressure at the droptank liquid-vapor interface was based on the assumption of a 3-deg temperature rise (equivalent to approximately 3 psi) due to stratification. Because of the cascade tank arrangement with the oxidizer droptanks draining into the top of the oxidizer ascent tanks, this stratified layer would be transferred into the top of the ascent tanks as the droptanks deplete, especially if efficient baffling were to be used at the ascent tank inlets. The approach used is to design the ascent tank inlet to cause deliberate mixing in order to reduce the liquid temperature at the liquid-vapor interface of the oxidizer ascent tank. Stratified propellant in the ascent tanks was considered in determining the effect on ascent tank ullage-pressure requirements. In the pressure relationships shown in Fig. 2.9-4a, there is sufficient static pressure remaining at the end of burning to satisfy NPSP and line pressure drop requirements with a $3^{\circ}R$ temperature rise at the liquid-vapor interface at shutdown. The foregoing assumption of a $3^{\circ}R$ rise in propellant temperature has been confirmed in a computer analysis assuming propellant stratification as described in Ref. 2.9-4. This analysis further established that increasing insulation thickness induced a minor increase in ullage vapor mass due to the lower average ullage gas temperature in the tanks at propellant depletion (see Fig. 2.9-4b). However, the effect of rocket engine bleed gas temperature (used for pressurant) is more significant and indicates that a $700^{\circ}R$ bleed gas temperature will result in a lower residual gas weight penalty than any lower pressurant temperature. In the final vehicle design analysis, a balance between ullage gas residual weights and tank structural weights, which are affected by ullage gas temperatures and pressures, will be sought to reduce vehicle system weights to a minimum.

2.9.1.2.2 Liquid Hydrogen Pressure Profiles. In contrast with the oxygen pressure profiles, the hydrostatic pressure in the hydrogen system (Fig. 2.9-5a) falls short of meeting NPSP line loss and component tolerance requirements. This shortage is made up by pressurizing the ullage to 11 psi above bulk vapor pressure (16.7 psia). Unlike the oxidizer system, the droptanks are not cascaded into the ascent tanks. Therefore, the warm layer at the tank top reaches the pump inlet just before staging rather than near the end of

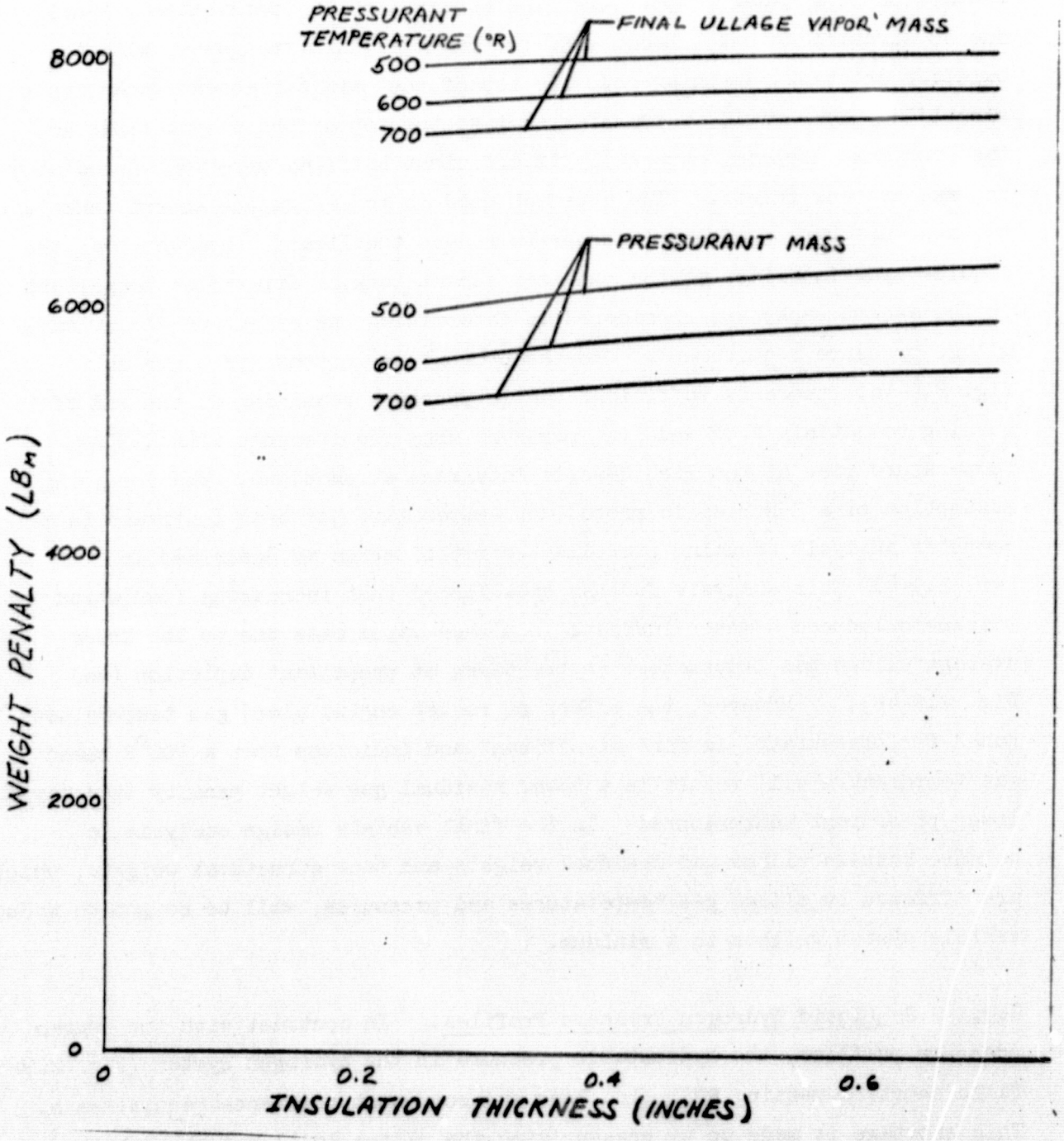

Fig. 2.9-4b Lox Droptank Pressurant and Residual Vapor Weights

Fig. 2.9-4b

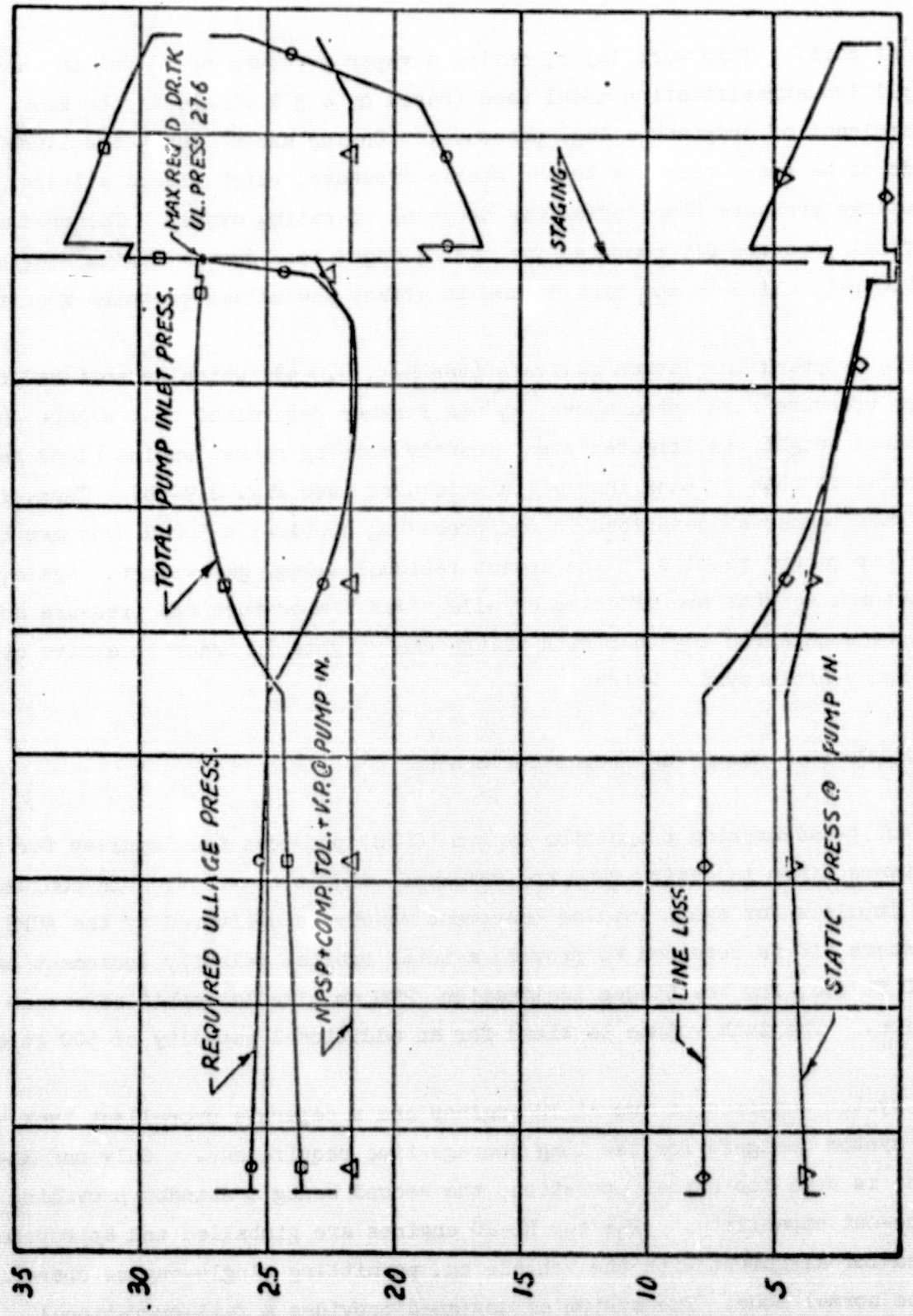

Fig. 2.9-5a Pressure Profiles — Hydrogen

Fig. 2.9-5a

ascent burn. This warm layer, having a vapor pressure of 23 psi in the simplified stratification model used (based on a $3^{\circ}R$ rise), is the key determinant of droptank ullage pressure. During ascent burn, the line loss tends to be small relative to the static pressure, which places a lesser demand on ullage pressure than during the droptank operating cycle. The maximum inertial pressure dip computed for the hydrogen feed system during startup is 0.8 psi, which is not high enough to affect the ullage pressure requirement.

In the droptank insulation analysis (see Ref. 2.9-4), which established the $3^{\circ}R$ vapor pressure rise noted above, it was further determined that ullage gas residual weight was affected significantly more by rocket engine bleed gas temperature than by tank insulation thickness (see Fig. 2.9-5b). Thus, in the same manner as described in the preceding section, a $500^{\circ}R$ hydrogen bleed gas temperature results in the lowest residual ullage gas weight. Again, tank structural weights are affected by ullage gas temperature and pressure and must be considered together with ullage gas weights in order to arrive at a minimum vehicle system weight.

2.9.2 Orbit Maneuvering Propulsion System

The orbit-maneuvering propulsion system (OMPS) provides the impulses for orbit maneuvers after injection into the reference injection orbit. In conjunction with impulses for small impulse increment maneuvers delivered by the ACPS thrusters, it is required to provide a total orbital velocity increment of 1,500 ft/sec, for the 55 deg inclination, 270 nm circular orbit reference mission. The tank volume is sized for an additional capacity of 500 ft/sec.

This system consists of two RL-10 engines and a separate propellant tank and feed system designed for the long storage-time requirement. Only one RL-10 engine is used for normal operation, the second being a standby providing engine-out capability. The two RL-10 engines are gimballed and appropriately canted for alignment with the vehicle cg, permitting single-engine operation as the normal mode. The system as designed provides a fail-operational capability in the event of an RL-10 engine failure. If the second RL-10

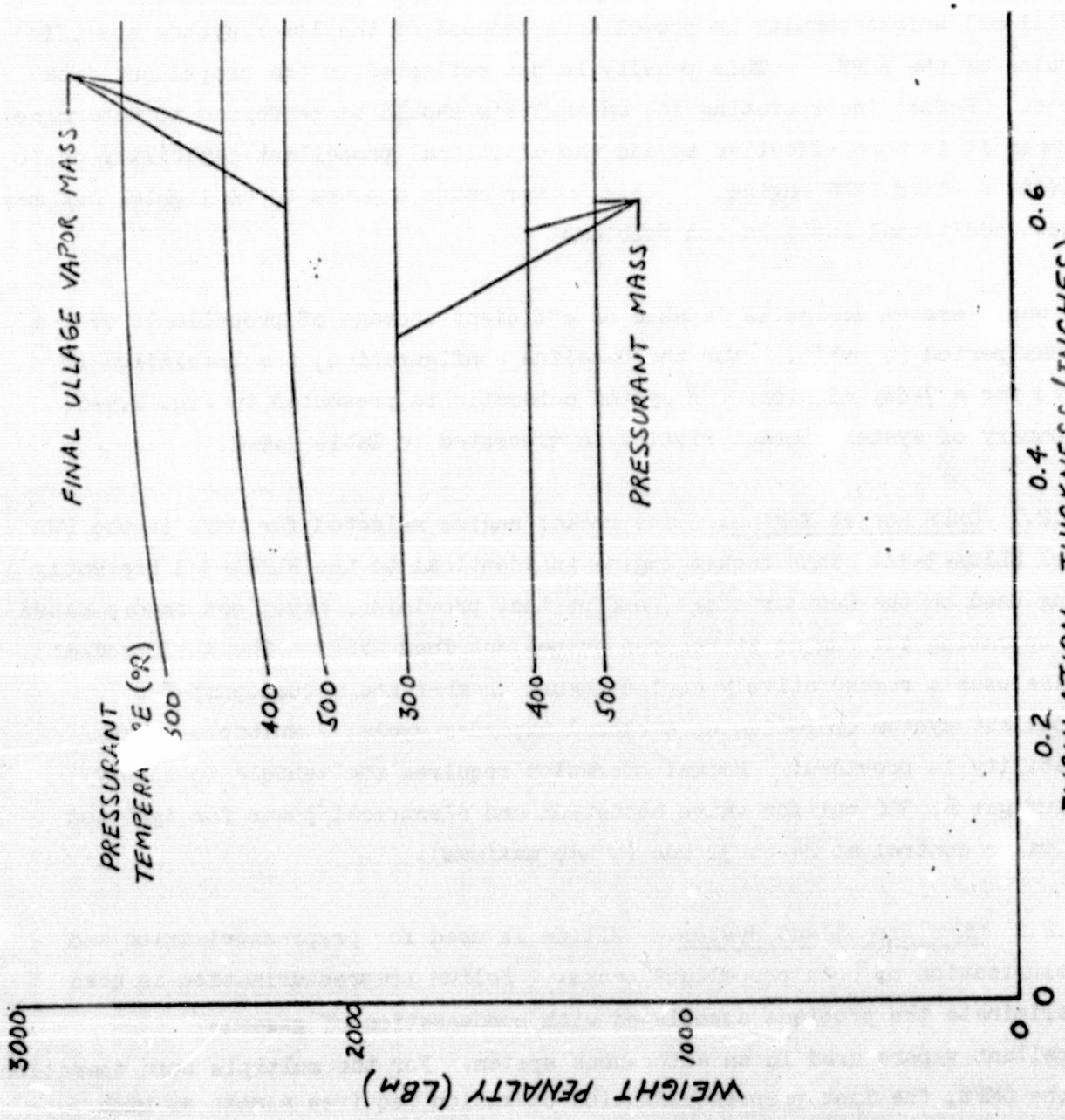

Fig. 2.9-5b LH_2 Droptank Pressurant and Residual Vapor Weights

Fig. 2.9-5b

fails, the retro maneuver would have to be accomplished with the ACPS, at an additional weight penalty in propellants because of the lower system specific impulse of the ACPS. This penalty is not reflected in the propellant data given. Before incorporating it, an analysis should be performed to determine whether it is more effective to add the additional propellant capability or to provide a third OMPS engine. This latter cause appears to be lighter but may impose additional installation problems.

The basic system design is capable of efficient storage of propellants over a 30-day period in orbit. For the baseline configuration, the insulation is sized for a 7-day mission. A system schematic is presented in Fig. 2.9-6. A summary of system characteristics is presented in Table 2.9-2.

2.9.2.1 OMPS Rocket Engine. The rocket engine selected for OMPS is the PWA Model RL10A-3-3A. This rocket engine is identical to the RL10A-3-3 presently being used on the Centaur stage, except that provisions have been incorporated for operating the engine at reduced propellant feed NPSP. The RL-10 rocket engine uses a regeneratively cooled thrust chamber and a turbopump-fed propellant system operating on a closed expander cycle. Multiple-start capability is provided. Normal operation requires the vehicle to supply helium gas at 500 psi for valve actuation and electrical power for ignition and valve control at 24 to 32 vdc (9 amp maximum).

2.9.2.2 OMPS Propellant System. Helium is used for prepressurization and pressurization of both propellant tanks. Helium prepressurization is used to eliminate the problems associated with condensation of gaseous propellant vapors used in an autogenous system. For the multiple burn operation of the OMPS, the last prepressurization operation requires almost as much helium as is required for the burn itself. Thus, the simplest system is helium pressurization. The helium is stored in two tanks, one for each propellant. These tanks are located outside the propellant tank but under its insulation so that the helium is at the same temperature as the propellant

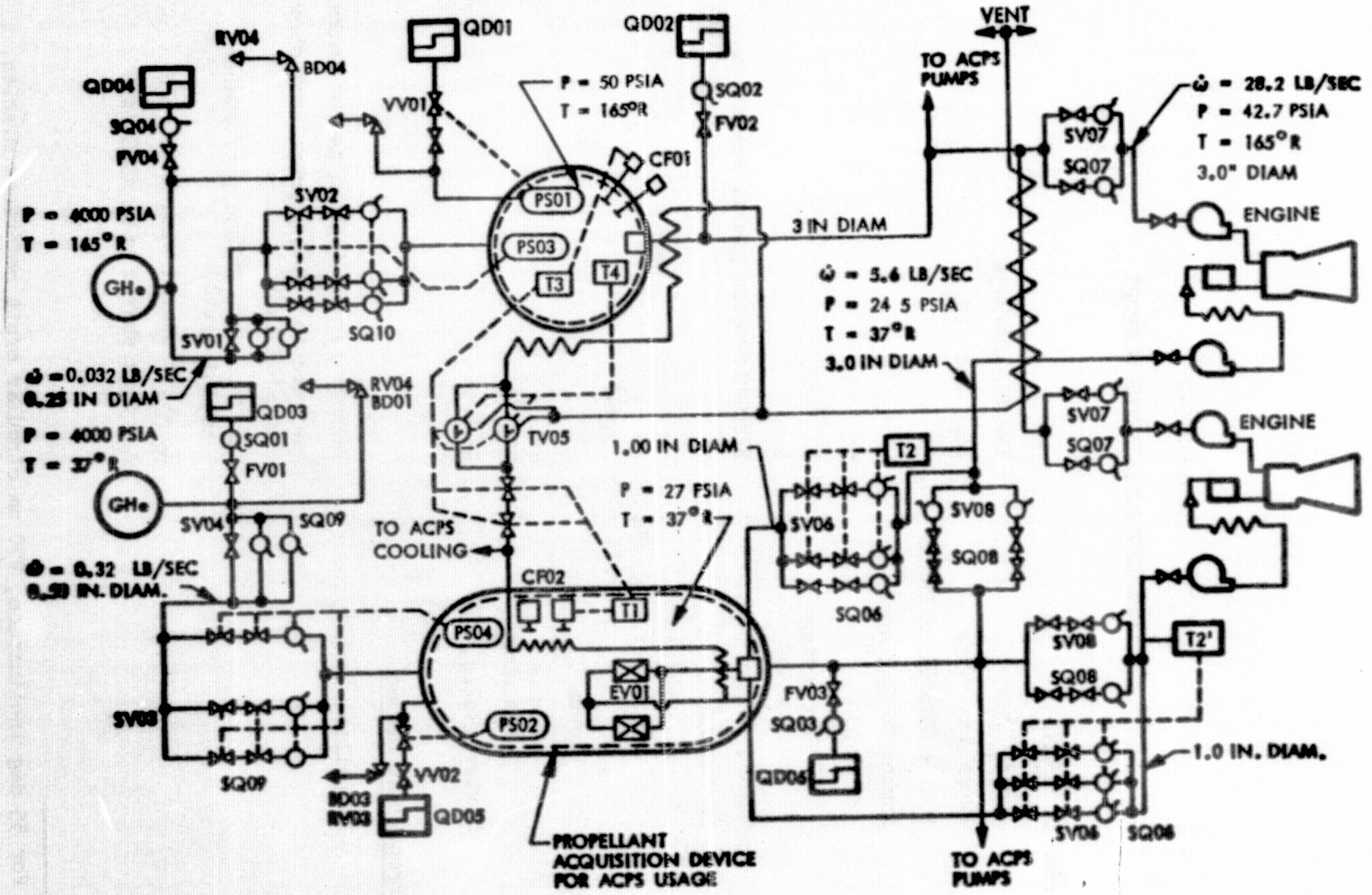

Fig. 2.9-6 Orbit Maneuvering Propulsion System

Fig. 2.9-6

Table 2.9-2

OMPS CHARACTERISTICS SUMMARY

A. Engine System

Engine Type	PWA RL-10A-3-3A
Propellant Type	LO_2 and LH_2
Nozzle Expansion Ratio	57
Number of Engines:	
Total	2
Operating	1
Standby	1
Thrust Vector Control	Electric-motor gimbal actuation
Performance:	
Thrust (nom vacuum per engine), lb	15,000
Vacuum I_{sp}, sec	
Nominal	444
Minimum	439
Mixture Ratio, O/F	5

B. Propellant System

Propellant Feed System:	Tankage separated from ascent tankage
	Designed for 30-day propellant storage capability
	Sized to 2000-ft/sec performance capability(1)
	H_2 tank shared with ACPS, APS
	O_2 tank shared with ACPS, APS

(1) For 55 deg inclination, 270 nm circular orbit reference mission.

Table 2.9-2 (Cont'd)

Propellant Weight, lbm(1)	
Loaded	41,869(2)
Impulse	34,207(3)
Flight Performance Reserve	0(4)
In-Flight Losses	463
Residuals	183
Tank Ullage Pressure, psi:	
H_2 Tank	27
O_2 Tank	50
Other Requirements:	
Insulation	Purged Multilayer – Tanks Vacuum Jacketed – Lines
Line and Tank Temp Control	By TCU System
Propellant Gauging and Instrumentation	TBD
System Electric Power (Maximum), KWDC	0.25
System Helium, Total, lb	178

(1) For 270 nm, 55 deg inclination Reference Mission.
(2) Includes ACPS and APU propellant.
(3) The 2,000 ft/sec Orbital-Vehicle ΔV capability (reduced by 142 ft/sec provided by ACPS).
(4) Flight reserve allowance included in ΔV capability requirement.

to be pressurized. This eliminates collapse problems during operation, and does not increase the tank temperature since a hot gas is not introduced. Thus the tank design can fully utilize the higher material properties at cryogenic temperatures.

The propellant transfer system is designed to feed either of the two RL-10 engines. A different technique is used for each propellant. For the hydrogen, selector valves located near the tank are used to isolate the lines to each engine, so that only one need be chilled for each operation. The line is dumped at engine shutdown. Line chilling up to the engine is accomplished by a secondary flow line which takes propellant from the propellant acquisition device in the tank. The propellant acquisition and retention system is configured to satisfy ACPS operational requirements for on-orbit, low-g conditions. The oxygen feed system uses selector valves located near the engine and between engine firings, the feedline is chilled up to that point, using hydrogen vapor from the thermal control unit (TCU) in the hydrogen tank.

The TCU operates in an open expansion refrigeration cycle to maintain a constant LH_2 temperature ($37^{\circ}R$) in orbit. Hydrogen is expanded through a Joule-Thompson valve and is passed through an in-tank heat exchanger to remove excess heat from the tank contents. Small circulation fans stir the hydrogen tank contents to ensure uniform conditions. The hydrogen vent gas is then used to chill the LO_2 tank and its acquisition and retention device and the LO_2 feedline. Circulation fans in the LO_2 tank are driven by a motor located outside the tank and magnetically coupled to the fans. Tank temperature sensors are used to open the hydrogen vent system and select whether the tank is chilled or not. A separate H_2 vent line, separately controlled, is used to provide hydrogen for cooling the ACPS pumps.

The integrated storage tanks hold the hydrogen and oxygen required for the OMPS, the ACPS, and the APU. The tanks and the OMPS hydrogen feedlines are insulated with high-performance multilayer insulation, which is optimized for a 7-day

period in orbit, and purged during atmospheric operations. The OMPS LO_2 feedlines are filled during ground operations, and are insulated with vacuum-jacketed multilayer insulation. It is noted that this insulation system may prove unsatisfactory during the entry and landing phases when some APU reactants are required. If so, a small vacuum-jacketed tank, filled from the main tank, may be required.

2.9.3 Attitude Control Propulsion System

The attitude control propulsion system provides roll control during operation of the OMPS. During orbit and reentry operations, it provides attitude control and three-axis rotational and three-axis translational maneuver capability.

The thrusters use high-pressure GO_2 - GH_2 propellant stored in liquid form in the orbital propellant tanks. The liquids, pumped through heat exchangers, are converted to propellant vapors and stored in accumulators from which they flow at regulated pressure to the thrusters.

Forty identical 1,500-lb thrust thrusters are used, with 16 located in the forward section and 24 in the aft section. The number of thrusters results from the selection of single thrust-level thrusters and from the necessity to meet fail-operational/fail-safe capability under all conditions including reentry when the down-firing thrusters must be retracted. Pure rotational couples about all three axes is achieved during orbital flight. During the reentry flight phase, however, pure couples are not possible about all axes, because all down-firing thrusters are retracted into the vehicle. Forward and aft and up and down translation in orbit is accomplished without cross-coupling. Lateral translations in orbit, however, produce cross-coupling.

A summary of system characteristics is presented in Table 2.9-3. The design data assumptions, which have been the basis for sizing analyses, are listed in Table 2.9-4.

Table 2.9-3

ACPS Design/Performance Characteristics

Propellant:	
Type	GO_2 and GH_2
Weight, lb	
Loaded	6,273
Impulse	5,617
Reserve (10% of impulse)	562
Thrusters:	
Type	TBD Single Design
Number	40
Thrust, per Thruster, lb	1,500
Min. Impulse Bit, lb-sec	
Thruster	50
Igniter Pulsing	5
Chamber Pressure, psia	250
Specific Impulse, Steady-State, sec	425
Propellant Supply System:	
Propellant Storage	In OMPS Tanks
Propellant Conditioning	Gas Generator - Heat Exchanger Assemblies
Number of Units, O_2/H_2	3/3
Outlet Temperature, ^oR	380
Outlet Pressure, Range psia	2,000/500
Gas Accumulators	
Number O_2/H_2	1/1
Operating Pressure Range, psia	2,000/500
Storage Capacity (usable total) O_2/H_2, lb	208.5
System Power Requirements:	
Maximum, KWDC	3.5
System Performance:	
Specific Impulse, sec	
Sustained Burn	362
Pulsed Burn	352
O/F Ratio	3.3
System Orbital Control Capability	
Rotational Acceleration, deg/sec^2	1.0 (all axes)
Translation Acceleration, ft/sec^2	0.5 (all axes)
Total Vehicle Translation Capability, ft/sec	142
Sustained Operation Capability	4 Thrusters at 1.5K thrust
Total Impulse Capability Without Reloading of Gas Accumulators, lb-sec	88,600

Table 2.9-3

Table 2.9-4

ACPS Design Data Assumptions

Vehicle Weight On-Orbit, lb	373,000 to 335,000
Moments Inertia, slug/ft^2:	Reentry
Pitch	10.4×10^6
Yaw	13.6×10^6
Roll	2.7×10^6
Orbital Rotational Acceleration, deg/sec^2	1. (all axes)
Orbital Translational Acceleration, ft/sec^2	0.5 (all axes)
Reentry Rotational Acceleration, deg/sec^2	
Pitch	0.8
Yaw	1.0
Roll	0.67

Table 2.9-4

2.9.3.1 Thruster Characteristics. The minimum impulse value per thruster in its regular operation mode is 50 lb-sec. In order to minimize propellant consumption for attitude hold, when the use rate is determined chiefly by the minimum impulse of the thrusters in a limit cycle mode of operation, the desired low thrust can be achieved by pulsing the igniters only. The minimum impulse value per thruster obtained by this mode of operation is assumed to be 5 lb-sec.

Other performance characteristics are listed in Table 2.9-5.

Table 2.9-5

ACPS THRUSTER CHARACTERISTICS

Thrust, lb	1,500
Min Impulse Bit, lb-sec:	
Thruster	50
Pulsing Igniter	5
Chamber Pressure, psia	250
O/F Ratio:	
Thruster	4.0
Pulsing Igniter	1.0
Specific Impulse, sec	
Full Thrust	425
Minimum Impulse Bit (Thruster)	TBD
Minimum Impulse Bit (Igniter Pulsing)	TBD

2.9.3.2 Thruster Installation Arrangement. Forty 1,500-lb thrust thrusters on the orbiter, with 16 located in the forward section and 24 in the aft section as indicated in Fig. 2.9-7. With this thruster configuration and thrust level limited to 1,500 lb per thruster, it is possible to achieve rotation and translation in all axes (except lateral translation) without cross-coupling

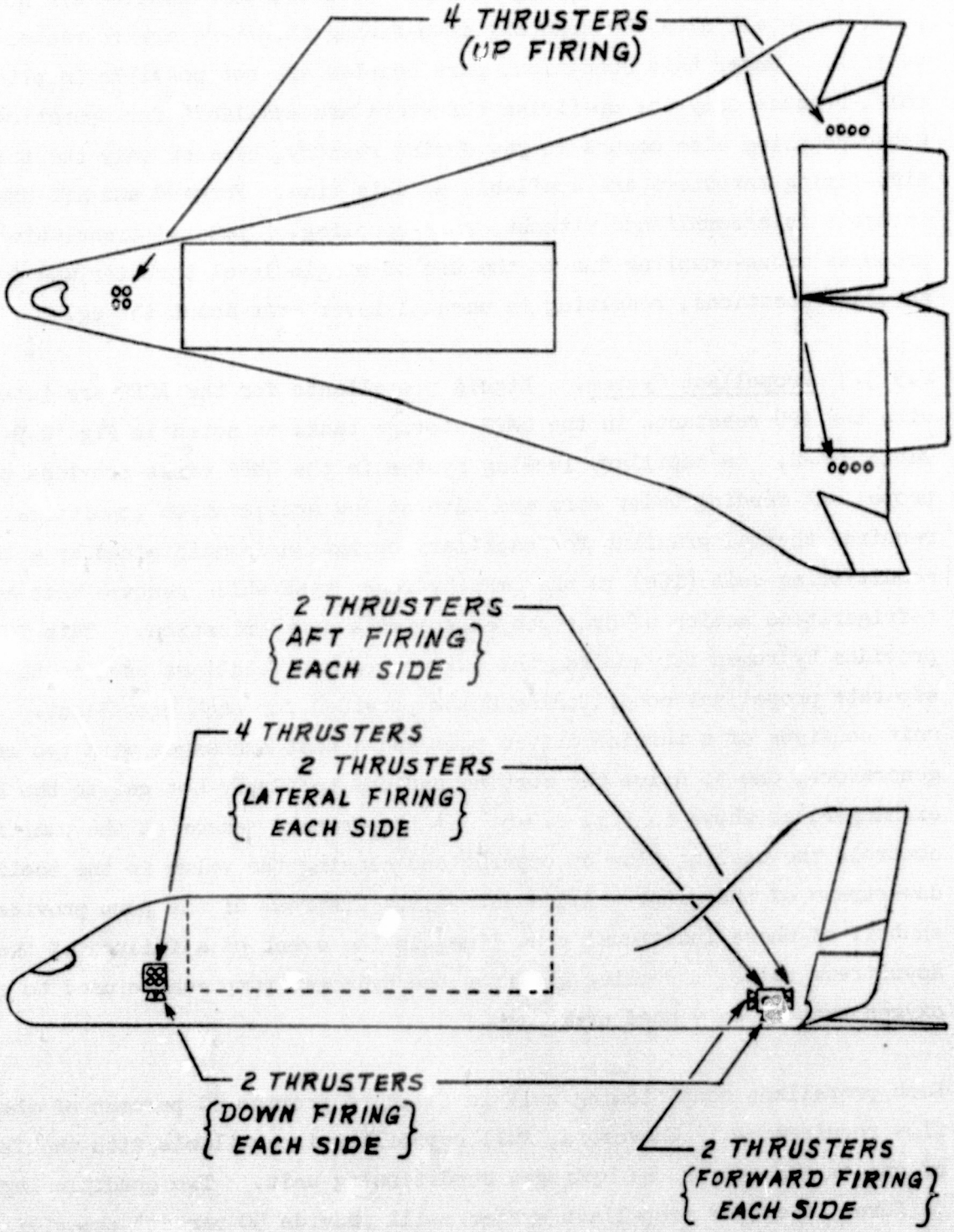

Fig. 2.9-7 ACPS Thruster Locations

during orbital flight. During reentry, however, pure couples are not possible in all axes, because all down-firing thrusters are retracted into the vehicle. Under this condition, pure couples are not possible in pitch and roll, because only the up-firing thrusters are available for operation. Cross-coupling also occurs in yaw during reentry, because only the forward side-firing thrusters are available at this time. Forward and aft translation in orbit is accomplished without cross-coupling. Lateral translation, however, produces cross-coupling due to the use of single level thruster and available thruster locations, resulting in unequal lever arms about the cg.

2.9.3.3 Propellant System. Liquid propellants for the ACPS are integrated with the APU reactants in the OMPS storage tanks as noted in Fig. 2.9-6 and Table 2.9-2. A capillary feeding system in the OMPS tanks provides positive propellant feeding under zero and adverse low acceleration conditions. The required thermal gradient for capillary operation is maintained by a thermal conditioning unit (TCU) in the OMPS hydrogen tank which removes heat by the refrigeration action of hydrogen expansion and vaporization. This TCU also provides hydrogen for cooling the ACPS pumps and feedlines used in the three separate propellant conditioning units provided for each propellant. Each unit consists of a turbine driven pump and a heat exchanger with two gas generators, one to drive the turbine and one to supply hot gas to the heat exchanger, as shown in Fig. 2.9-8. A temperature sensor at the pump inlet controls the cooling flow by opening and closing the valve in the cooling line downstream of the pump. Redundant valves upstream of the pump provide a shutoff of these individual vent lines in the event of a failure of the downstream valve. Cooling gas from the hydrogen pump can be used to cool the oxygen pump or be vented overboard.

Each propellant conditioning unit is sized to provide 50 percent of the full-flow requirement. Therefore, full capability is available with the failure of one oxygen and/or one hydrogen conditioning unit. Two conditioning unit failures in either propellant system still provide 50 percent capability which will provide safe operating characteristics.

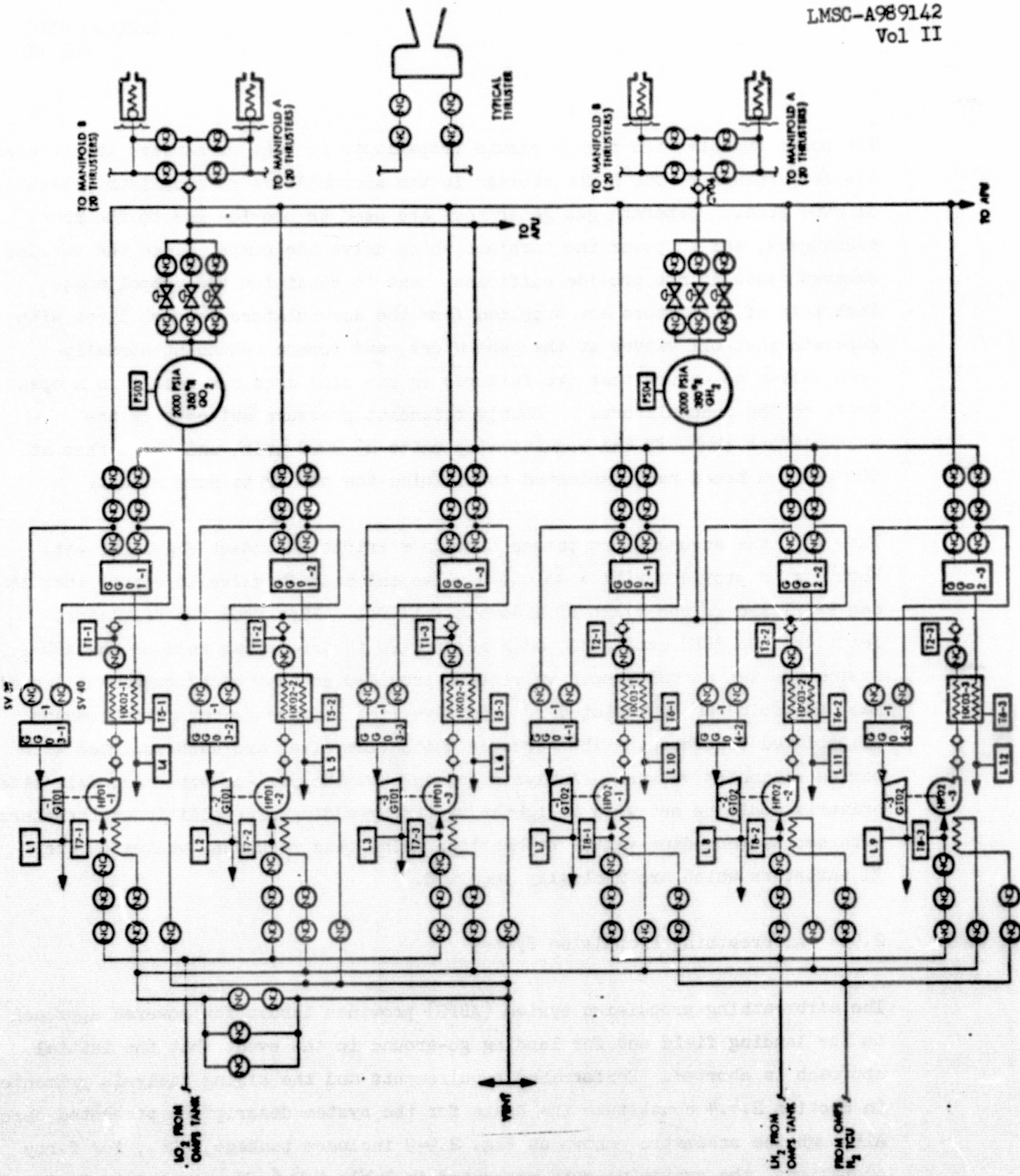

Figure 2.9-8 ACPS Propellant Conditioning System

The pumps transfer the high pressure propellants to heat exchangers which raise its temperature to 380°R for storage in the accumulators at a maximum pressure of 2000 psia. Separate gas generators are used to provide gas to the heat exchangers, and to power the turbines which drive the pumps, since the turbine exhaust gases do not provide sufficient heat to condition the propellants. Each pair of generators are supplied from the accumulators through lines with separate shut-off valves at the generators, and common redundant normally-open valves to ensure that two failures in one line does not result in a open drain on the accumulators. Doubly redundant pressure switches in the accumulators shut-off the conditioning units at 2000 psia, and start them at 900 psia, a broad range selected to minimize the number of pump cycles.

Flow from the accumulators passes through a triple redundant regulator set. Each leg is provided with a solenoid valve and a squib valve to ensure that it can be closed in the event of a double failure. Flow from the regulators feeds the two ACPS manifolds, each serving 20 thrusters, as well as the APU system. Two normally-open valves are provided so that each propellant leg of each manifold can be isolated if excessive line leakages occurs which cannot be isolated elsewhere. The thruster units themselves are each equipped with series redundant valves. Analysis showed that the fail-operational, fail-safe criteria could be met with a lighter system by adding nine additional thrusters with series redundant valves rather than using quad redundant valves on the 31 thrusters which are minimally required.

2.9.4 Airbreathing Propulsion System

The airbreathing propulsion system (ABPS) provides thrust for powered approach to the landing field and for landing go-around in the event that the initial approach is aborted. Performance requirements and the sizing analysis presented in Section 2.4.4 constitute the basis for the system description presented here. Although the schematic shown as Fig. 2.9-9 includes tankage, etc., for ferry operations, the system weights presented in Table 2.9-6 are limited to fuel and components required for return from an orbital mission.

Fig. 2.9-9 Airbreathing Propulsion System (JP-Fuel)

Table 2.9-6

ABPS Characteristics Summary

Requirements:	
Gross Net Thrust, lb	90,500
Altitude, ft	2,000
Flight Mach Number	0.3
Engine Start Altitude, ft	35,000
Engine Start Mach Number	0.55
Maximum Operating Time, min	17.5
Design Characteristics:	
Number of Airbreathing Engines	6
Engine Thrust Rating (Sea Level), lb	(Classified Data)
Engine SFC Rating (Sea Level), lb/lb-hr	(See PWA PDS-4251)
Engine Type	JTF 22 A-4
Ducting Thrust Losses	3%
Fuel Type	JP-4
Fuel Weight - Loaded	9,635 lb
Fuel Weight - Impulse	8,430 lb
Fuel Weight - Reserve (15%)	1,205 lb
Engine Installation	Stowed-Deployable
Engine Weight, each, lb	2,415
Installation Weight, lb	20,603

Table 2.9-6

This system is composed of 6 low bypass-ratio turbofan engines supported by a fuel storage and feed system. Sizing analyses that have been conducted have established the landing go-around conditions as the limiting condition. The design condition assumed for the baseline configuration includes a spacecraft weight of 333,000 lb and L/D = 5.5 at a flight Mach number of 0.32 in the go-around configuration. Jet engine selection to meet the thrust requirements involved considerations of engine thrust/weight ratio, installation volume, engine specific fuel consumption, and system weight. The selection of the PWA Model JTF 22A-4 turbofan engine is based on operational requirements, system design considerations, and the engine performance as presented in PWA PDS-4251 (Confidential Document) "Performance Estimates for JTF 22A-4 Turbofan Engine (Nonaugmented Derivative of F401-PW-400), (Title Unclassified), dated 15 March 1971.

The engines are installed on a deployable tray which is extended through the lower surface of the vehicle by a set of hydraulic actuators after the vehicle flight speed has become subsonic (see Fig. 2.9-27). In the stowed position, the engines occupy space aft of the payload bay, under the OMPS propellant tanks and between the main landing gear. This position close to the vehicle cg was selected to provide maximum performance and ease of maintenance and to facilitate compliance with the requirement for jet engine removal with minimum scar weight. The JP fuel storage tank is installed under the payload bay between the conical hydrogen tanks. A thermal protection system consisting of insulation and electric heating units is employed to prevent fuel freezing while in orbit.

Dual boost pumps mounted in the fuel tank (see Fig. 2.9-9), feed the manifold which is connected to each engine. Flexible hose is provided in the feedline to accommodate deployment of the engine through the lower surface of the spacecraft. To satisfy fail operational/fail-safe criteria, the inert gas pressurant supply is designed to satisfy pressure and flow requirements for JP fuel fed to the jet engines in the event that both boost pumps fail. Engine

starting is accomplished by windmilling the engine rotor in the airstream with supplemental starting torque supplied by a hydraulic motor driving through the engine gear box. Hydraulic power for this motor is furnished by the vehicle APU system.

While the use of JP fuel for turbojet engine operation has been established by a NASA Level I decision, it was considered important to assess the impact of this decision on cost, weight, and abort capability. To maintain the payload capability of a stage-and-one-half vehicle when JP fuel is used in lieu of LH_2, an increase in GLOW of 157,000 lbm is estimated. This would result in a $11M increase in program costs. Mission abort analyses have been prepared which utilize the ABPS for subsonic cruiseback from an overwater launch trajectory. The use of JP fuel limits the cruiseback range to 50 nm, while the use of LH_2 extends this range to 350 nm due to the availability of unused propellant in the OMPS tanks at the time of abort. The program cost advantage attributable to this mode of abort recovery is dependent on estimates of abort probability but have been estimated to be $171M (Ref. 2.9-5).

REFERENCES

2.9-1 Alternate Concepts Study, Third Letter Progress and Status Report, LMSC-A977725, pp. 2.2-13 and 2.7-1

2.9-2 -----, Fourth Letter Progress and Status Report, LMSC-A980360, pp. 2.5-2

2.9-3 ....., Second Letter Progress and Status Report, LMSC-A976286, pp. 2.7-7

2.9-4 ....., Fifth Letter Progress and Status Report, LMSC-A981489, pp. 2.6-6

2.9-5 ....., Seventh Letter Progress and Status Report, LMSC-A984210, pp. 2.1.2-2

2.10 POWER SYSTEMS

2.10.1 Electrical Power System

The basic electrical power system (EPS) design concepts established during the initial Phase A stage-and-one-half study segment are unchanged from the baseline reported in the A revision of EM L2-01-06-M1-1A, dated 2 November 1970 for Model LS 200-5 and included in the fifth monthly ACS progress report. Detailed design data estimates for the Model LS 200-7 stage-and-one-half employing nine (9) main rocket engines (to Interface Control Document 13M15000B dated 1 March 1971) are provided in EM L2-01-06-M1-1B dated 23 March 1971 (see Appendix B of this report).

The EPS employs three types of electrical energy sources (see Fig. 2.10.1-1).

Emergency silver-zinc batteries are provided to supply 12,000 watt-hours of energy on demand.

Primary mission electrical demands are supplied by three five (5) kilowatt capillary matrix fuel-cell modules. A single module supplies all power required except for short periods during ascent, rendezvous/docking, and separation (see Fig. 2.10.1-2).

Electrical energy for the peak demands of prelaunch, ascent and atmospheric flight (reference Figs. 2.10.1-2 and -3) are supplied by three (40) KVA AC generators (triply redundant) driven independently by the chemically fueled turbines used to supply hydraulic power. The distribution system is based on use of remotely located circuit breaker/control units under the control of a multiplexed data management subsystem, except for survival-critical circuits whose breakers are accessible to the crew.

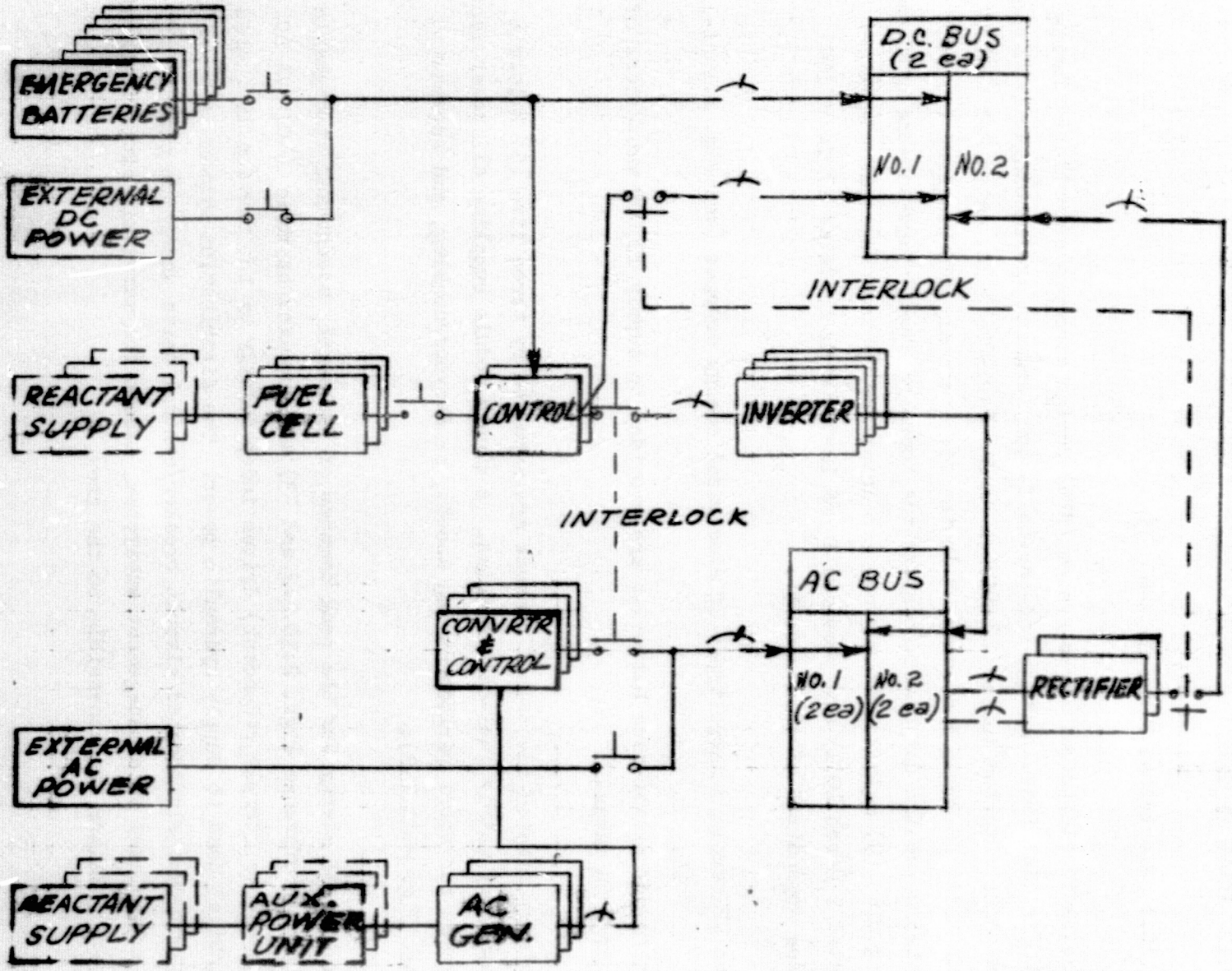

Fig. 2.10.1-1 Electrical Power Subsystem Block Diagram

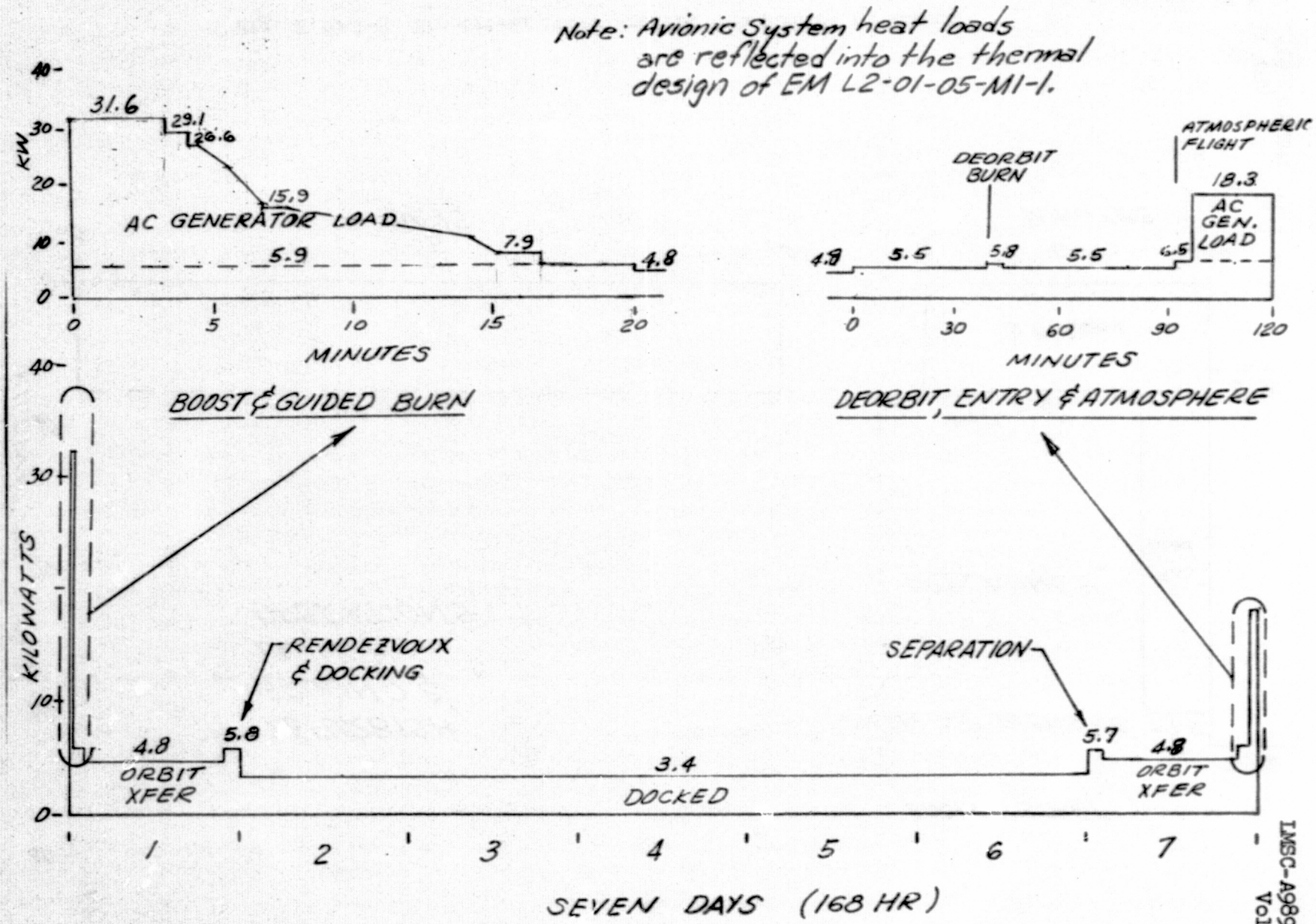

Fig. 2.10.1-2 Electrical Power Profile – Launch to Rollout

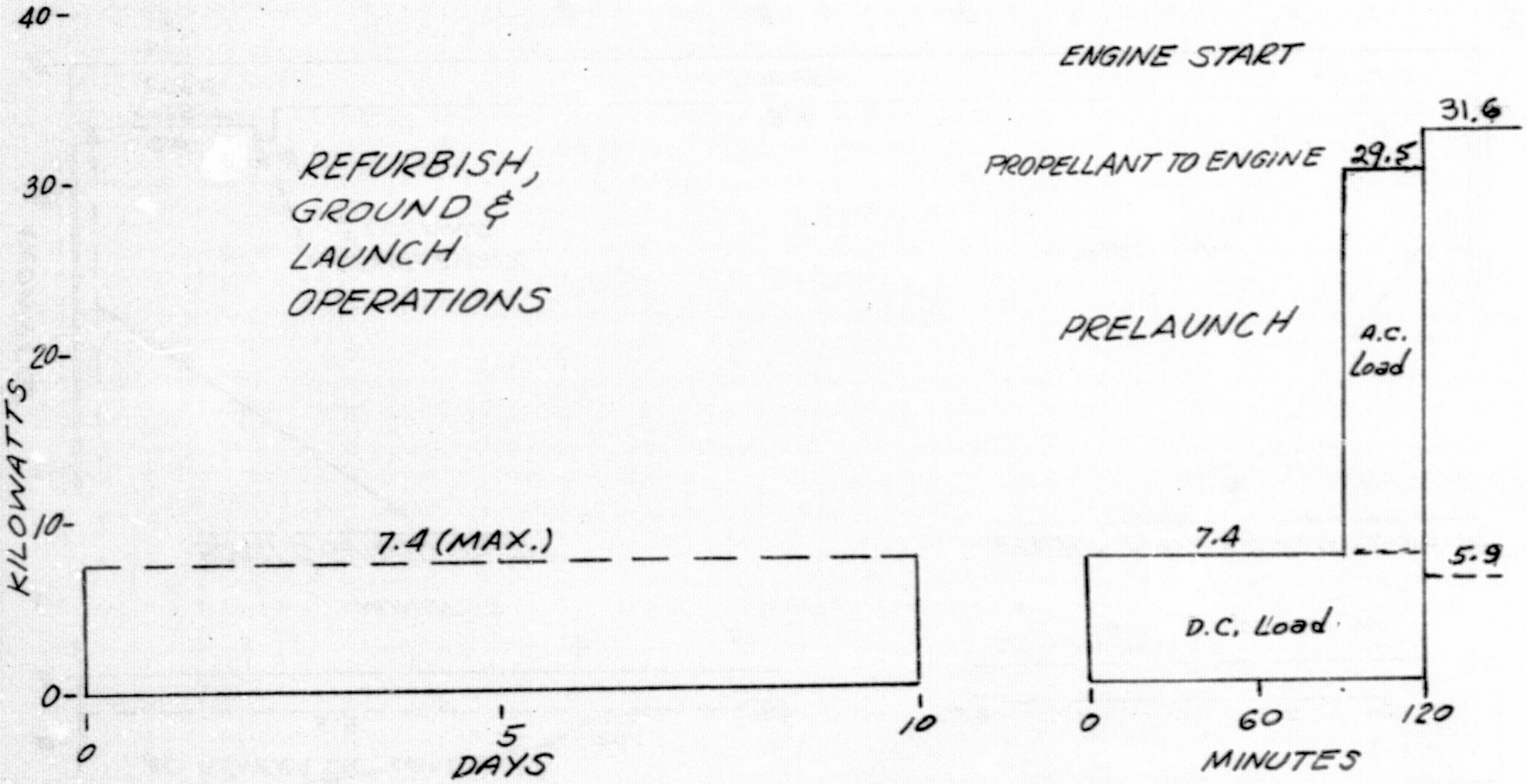

Fig. 2.10.1-3 Electrical Power Profile – Refurbish to Launch

A quad-redundant power bus is provided for critical loads, with dual-redundant for the remainder.

Electrical power system weight, (exclusive of tankage, reactants, thermal control radiator system) including signal cables and installation requirements is 4569 lb. Itemized weights are provided in EM L2-01-06-M1-1B and the weights for tankage, reactants, and thermal control are included in this report in Section 2.14, Mass Properties.

2.10.2 Hydraulic Power System

The hydraulic power system provides power and adequate response characteristics for main propulsion and orbit maneuvering rocket engine thrust vector actuation, for aerocontrol surface actuation, for airbreathing engine platform and landing gear extension, for ACPS thruster deployment and retraction, for cargo door operation, and for other functions.

The principal hydraulic power requirements are generated by rocket engine TVC during ascent (5 gimballed engines) and by aerocontrol surface operation during reentry. The peak hydraulic power load during ascent is estimated to be 370 HP with the average power level amounting to 195 HP. These conditions include the use of hydraulic-actuated engine controls and are in compliance with criteria specific in the NASA document 13M15000B, which establishes the vehicle/rocket engine interface. The hydrualic power requirements during reentry have been estimated on the basis of the results of a computer-aided reentry simulation study conducted under NASA Contract NAS 9-11459. These study results expressed as control surface deflections are presented in Fig. 2.10.2-1. Duty cycle and response rate effects are summarized in Fig. 2.10.2-2 in that maximum hinge moments have been identified for each control surface to enable actuator size/power levels to be established. The maximum power required during reentry has thus been identified as occurring during subsonic flight and is estimated to be 455 HP. Using electric power and hydraulic power data generated in these analyses, a duty cycle for APU operation has been assembled, see Fig. 2.10.2-3, to assist in the establishment of the overall APU power level. The maximum power level is estimated to be 485 HP.

The system (see Fig. 2.10.2-4) consists of multiple hydraulic pumps driven by APUs and arranged with interconnecting plumbing in parallel systems to satisfy redundancy criteria which specify a fail operational, fail operational, fail safe functional mode. The 3 parallel hydraulic supply systems are pressurized by 12 hydraulic pumps driven by 4 APUs (3 hydraulic pumps per APU). With this arrangement, vehicle power requirements can be satisfied by the complete output

from any 2 APUs or any 6 hydraulic pumps. Propellants for APU operation (gaseous hydrogen and gaseous oxygen) are drawn from the ACPS propellant gas generation supply system. Hydraulic actuators for rocket engine TVC, aerocontrol surfaces, etc., are connected to these parallel hydraulic power supply systems. Actuator redundancy is achieved through the use of a quadraplex design which utilizes the 3 hydraulic supply services and 4 electrical signal inputs. This electrical input design arrangement, which consists of 3 real channels and one electronic model, eliminates the need for a fourth hydraulic system

Estimates of component weights for the hydraulic system and APU have been made and are presented in Fig. 2.10.2-5.

DELTA BODY 1-1/2-STAGE SPACECRAFT
C.G. @ 72.5% L_{REF} WORST CASE FORWARD

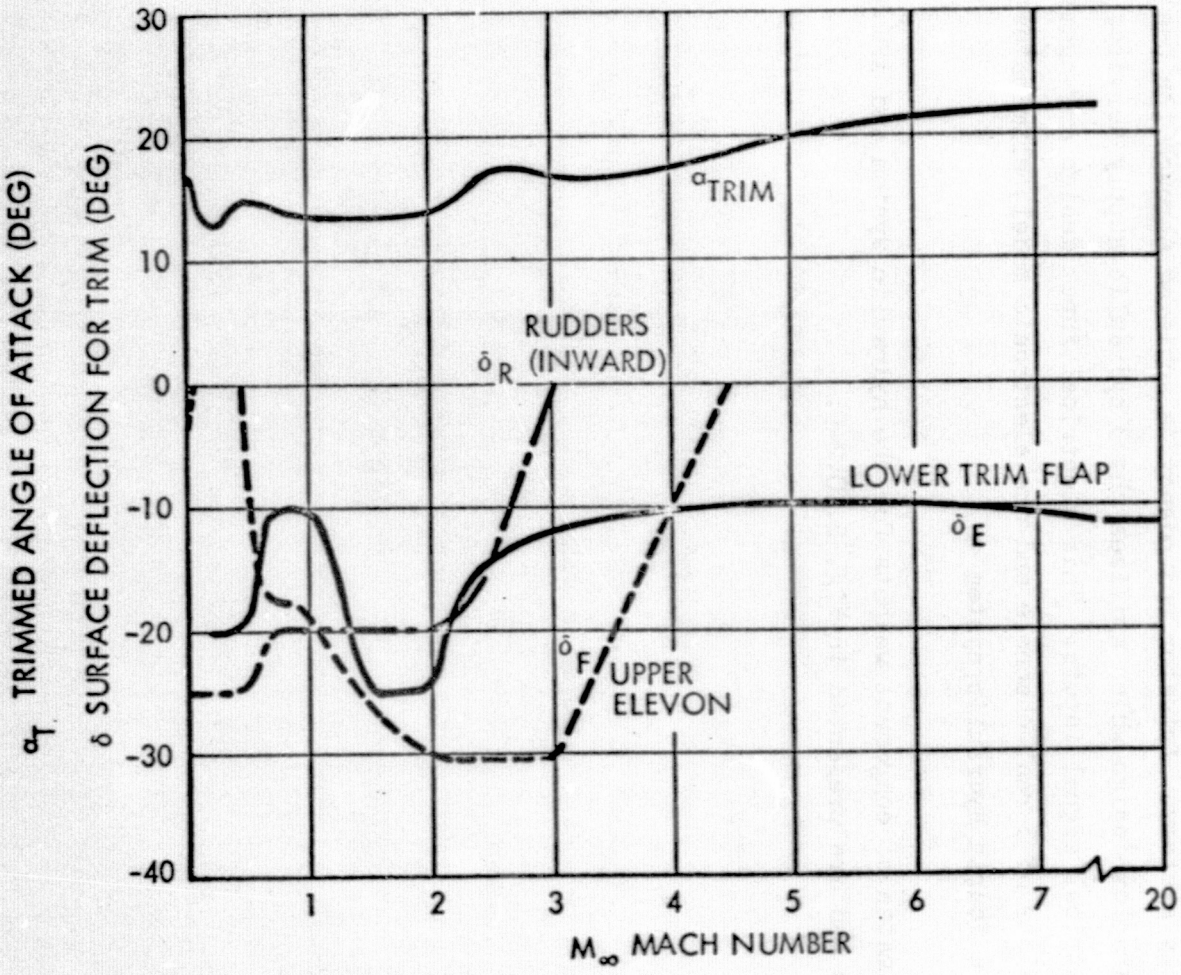

Fig. 2.10.2-1 Reentry Control - Worst Trim Profiles

CONTROL SURFACE	MAX. HINGE MOMENTS (FT-LBS)	FLIGHT CONDITIONS
TRIM FLAP (LOWER)	966,000	SUBSONIC
ELEVONS	201,000	SUBSONIC
RUDDERS	364,000	SUBSONIC
UPPER FLAPS	788,000	TRANSONIC
AUX. SURFACES	367,000	SUBSONIC

MAX. POWER REQUIRED (SUBSONIC - W/O TRIM TABS) 455 HP

Fig. 2.10.2-2 Reentry Control Hydraulic Power Requirements (Stage and One-Half)

MISSION PHASE	DURATION (MIN)	ELEC. PWR. PEAK KW	ELEC. PWR. AVE. KW	HYD. PWR. PEAK HP	HYD. PWR. AVE. HP	TOTAL POWER PEAK HP	TOTAL POWER AVE. HP
PRELAUNCH TO LIFTOFF	30	22	6	150	50	190	61
LIFTOFF TO 20,000 FT	1	25	25	370	195	415	240
20,000 FT TO STAGING	4	25	20	370	180	415	216
STAGING TO ENGINE C.O.	2	17	15	260	65	290	92
ENGINE C.O. TO APU SHUTDOWN	10	13	7	30	30	53	42
ORBIT CHECKOUT	2	18	18	150	150	182	182
IDLE MODE RETRO TO 270K'	42	4	4	30	30	37	37
270,000 FT TO 20,000 FT	48	18	5	455	85	485	94
20,000 FT TO GO-AROUND	8	18	18	455	455	485	485
GO-AROUND TO TOUCHDOWN	6	18	18	455	455	485	485
TOUCHDOWN TO ROLLOUT	2	18	18	150	50	190	61

Fig. 2.10.2-3 APU Duty Cycle - Stage-and-One-Half Orbiter

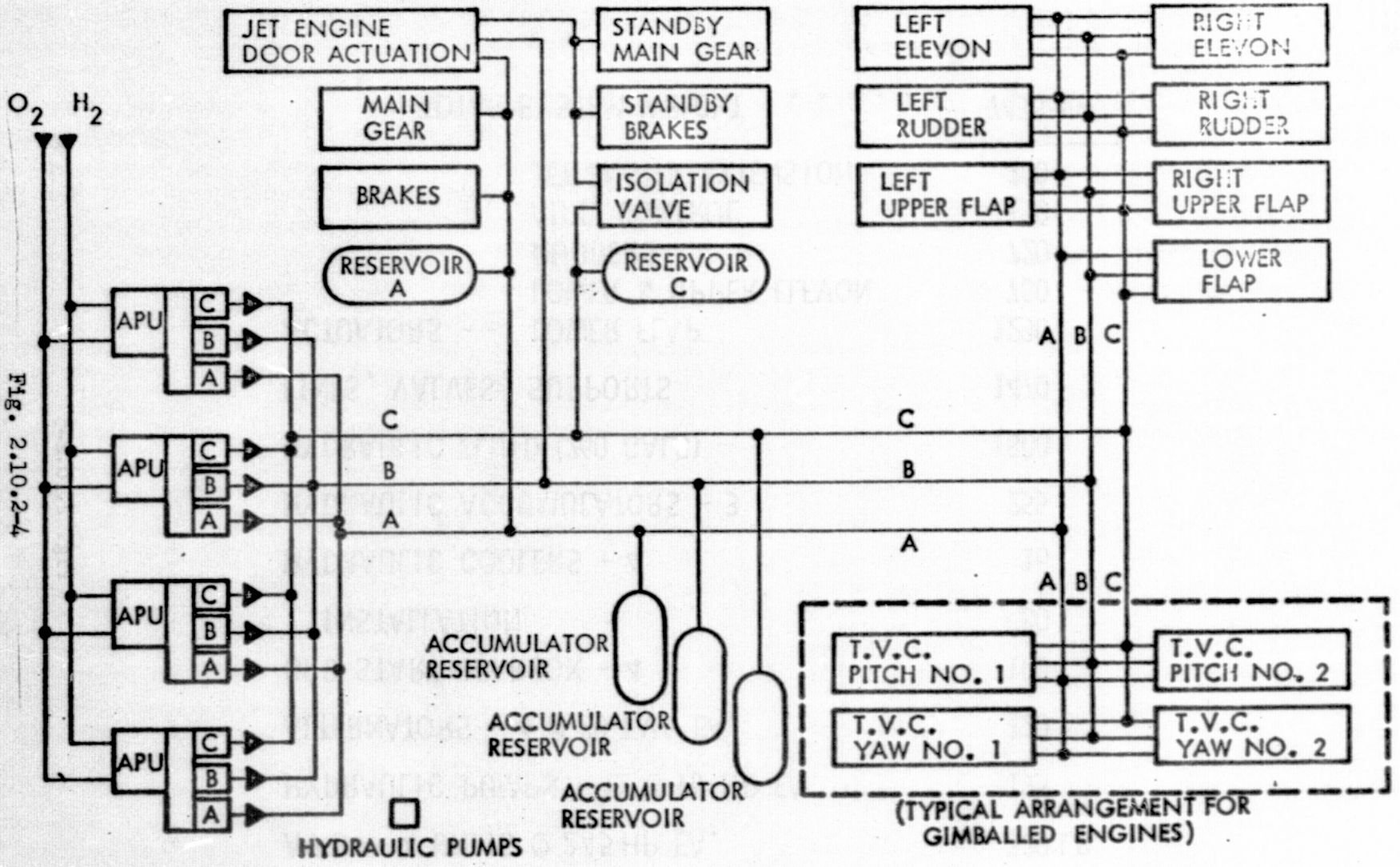

FIG. 2.10.2-4 APU - HYDRAULIC POWER SCHEMATIC

APU - 4 UNITS @ 245 HP EA.		320 LB
HYDRAULIC PUMPS - 12 @ 76 HP EA.		195
ALTERNATORS - 4 @ 20 KVA EA.		120
GRD START GEARBOX - 4		100
INSTALLATION		80
HYDRAULIC COOLERS - 4		16
HYDRAULIC ACCUMULATORS - 3		255
HYDRAULIC FLUID (260 GALS)		1800
LINES, VALVES, SUPPORTS		1470
ACTUATORS --	LOWER FLAP	1230
	LOWER & UPPER ELEVON	780
	RUDDERS	720
	AUX. CONTROL	150
	JET ENGINE EXTENSION	200
TOTAL SYSTEM WEIGHT		7436 LB

Fig. 2.10.2-5 Hydraulic System APU Weights

2.11 ENVIRONMENTAL CONTROL/LIFE SUPPORT SYSTEM

The environmental control and life support system (EC/LSS) provides the crew with an environment that ensures their safety and functional capability throughout the mission. The system also provides total internal thermal control (passive and active) for vehicle systems, compartments, and components. The concepts presented herein are compatible with the 14.7 psia Space Station atmosphere. The system is designed to sustain two crew members for 7 days. Sufficient space (645 ft^3) has been provided in the crew compartment to include two cargo handlers. Their life support provisions, however, will be charged to the payload.

Figs. 2.11-1 through 2.11-5 are simplified schematics for EC/LSS subsystems and provide the following functions:

- Atmosphere Supply
- Atmosphere Control
- Humidity Control
- Carbon Dioxide Removal
- Trace Contaminant Control
- Cabin and Equipment Thermal Control
- Food and Water Supply
- Waste Management, Personal Hygiene, and First Aid

Tables 2.11-1 through 2.11-4 show vehicle design parameters, metabolic and cabin data, estimated power requirements, and thermal loads. System weights are tabulated in Section 2.14.

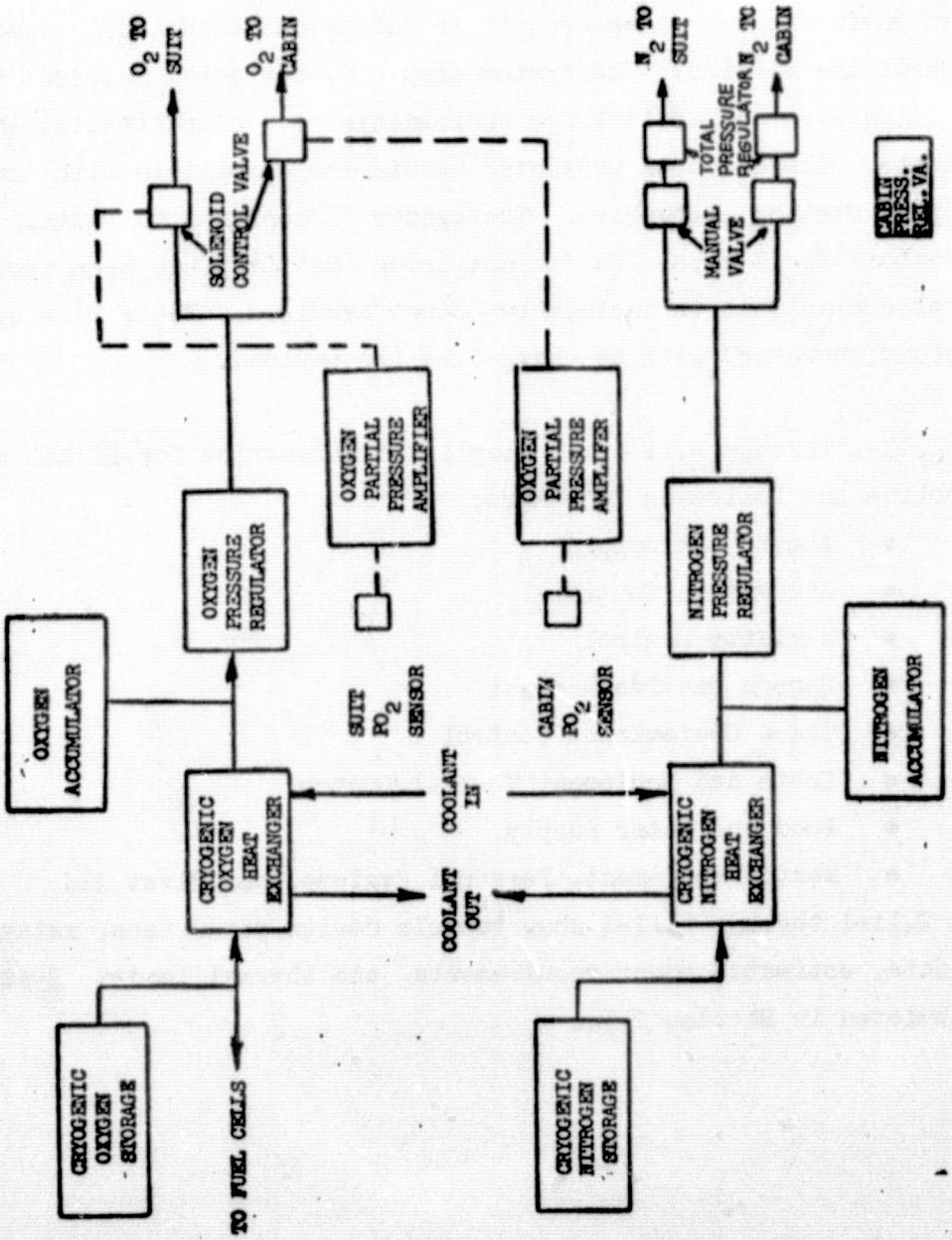

Fig. 2.11-1 Gas Supply and Control

Fig. 2.11-1

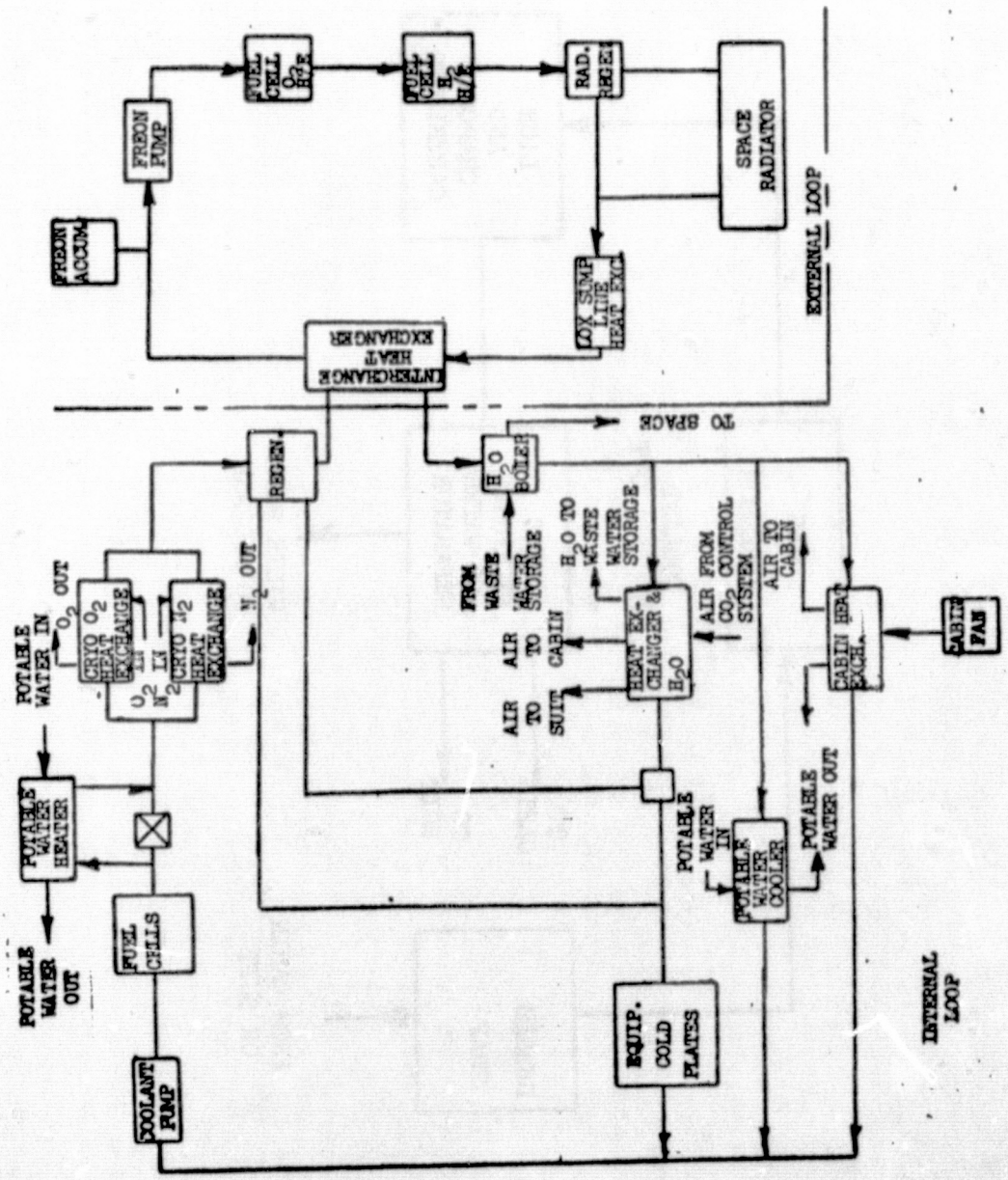

Fig. 2.11-2 Thermal and Humidity Control

Fig. 2.11-2

Fig. 2.11-3 Carbon Dioxide and Contaminant Removal

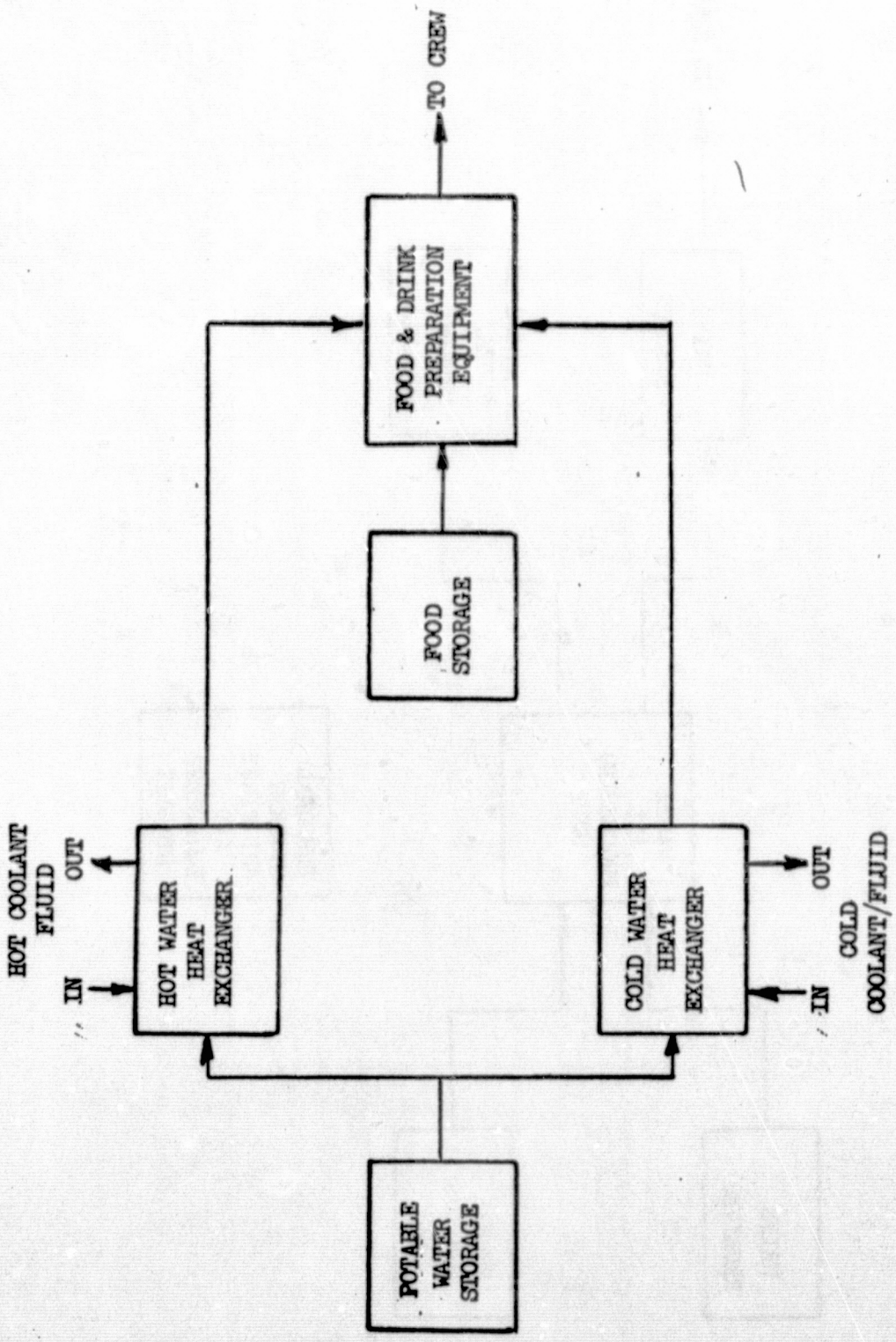

Fig. 2.11-4 Food and Water Supply

Fig. 2.11-4

Fig. 2.11-5 Waste Management and Personal Hygiene

LOCKHEED MISSILES & SPACE COMPANY

Table 2.11-1

ORBITER DESIGN PARAMETERS

Mission Duration	7 days
Crew Size	2
Cabin Volume	645 ft^3
EVA Required	None
Number of Repressurizations	1
Operational Modes	Suited and Shirtsleeve

Table 2.11-2

ORBITER METABOLIC AND CABIN DATA

Cabin Atmosphere Constituents	O_2, N_2
Cabin Total Pressure	14.7 psia
O_2 Partial Pressure	3.1 psia
N_2 Partial Pressure	11.6 psia
Carbon Dioxide Partial Pressure Limit	
Normal	5 MM Hg
Normal Peak	8 MM Hg
Emergency	15 MM hg for 30 Min.
Cabin Temperature	65-75°F.
Cabin Relative Humidity	35-65%
Cabin Leakage Rate	6 lb/day
Oxygen Consumption (Metabolic)	1.84 lb/man-day
Carbon Dioxide Generation	2.12 lb/man-day
Latent Heat (Metabolic)	4300 BTU/man-day
Sensible Heat (Metabolic)	6900 BTU/man-day
Food (Including Packaging)	
Frozen	3.30 lb/man-day
Freeze Dried	1.78 lb/man-day
Water of Oxidation	0.78 lb/man-day
Water Consumption Rates	
Drinking and Food Preparation	6.99 lbs/man-day
Washing and Personal Hygiene	3.90 lbs/man-day
Urine Receiver Rinse	2.00 lbs/man-day
Water Production Rates	
Urine	3.08 lb/man-day
Including Solids	3.24 lb/man-day
Fecal Water	.25 lb/man-day
Including Solids	.34 lb/man-day
Water in Food Waste	.14 lb/man-day
Evaporative Water	4.30 lb/man-day

Table 2.11-3

THERMAL LOADS (BTU/HR)

	FERRY	PRELANDING	ASCENT	ORBIT (MAX)	ORBIT (MIN)	ENTRY ***	LANDING ***
External Cabin Heat Load	- 1,000	+ 700	+ 1,200	+ 400	- 1,300	+ 2,400	- 1,000
Metabolic Heat Load (2-Man Totals)							
• Sensible	500	500	500	500	440	*	*
• Latent	600	600	600	900	220	*	*
Cabin Electronic Heat Loads							
• Air Cooled	4,020	3,320	2,020	3,570	1,250	3,120	4,150
• Cold Plate	9,400	9,200	4,770	10,400	3,640	8,790	8,750
Fuel Cell Heat Loads	--	10,300**	8,230**	11,300**	3,600**	9,800**	7,500**

*Transient Analysis

**Fuel cell loads are based on a vapor condenser load of 4200 btu/hr and stack cooling loop load of 6100 btu/hr = 10,300 btu/hr during prelaunch. Ascent, orbit max, entry and landing loads are ratioed to the total electronic heat loads $\left[\text{i.e., entry, } \frac{\text{Fuel Cell Heat Load}}{11{,}910 \text{ btu/hr}} = \frac{10{,}300 \text{ btu/hr}}{12{,}520 \text{ btu/hr}}\right]$

orbit miniminum is 35% of maximum

***The entry and landing baseline profile considered for transient entry analysis is as follows:

- Time zero at 400,000 ft
- Ram air-cooling at 45,000 ft (1880 sec)
- Start landing phase at 40,000 ft (2000 sec)
- Touchdown (2300 sec)
- Ground cart hookup (3000 sec) 2.11-9

Table 2.11-4

ORBITER ECS/LSS POWER REQUIREMENTS (WATTS)

	PRELAUNCH	LAUNCH ASCENT	ORBIT	RENDEZVOUS & DOCKING	DEORBIT	REENTRY	LANDING
Suit compressors	100/200	100/200	100/200	100/200	100/200		100/200
Cabin blower	80	80	80	80	80	80	80
Cabin vent fans	80	80	80	80	80		80
Coolant pumps	125/250	125/250	125/250	125/250	125/250	125/250	125/250
Water and waste management	①	-	①	-	①	-	①
PO_2 monitor and control	50	50	50	50	50	50	-
Heaters	-	-	②	②	②	-	-
TOTAL AVG/PEAK	435/860	435/660	435/1360	435/1160	435/1360	255/380	385/810

① Intermittent operation (50% duty cycle at 200 watts)

② Intermittent operation (50% duty cycle at 500 watts)

2.11.1 Atmosphere Supply and Control

The system for the orbiter supplies a 14.7 psia nitrogen-oxygen atmosphere with an oxygen partial pressure of 3.1 psia. Each gas is stored in supercritical cryogenic tanks, and oxygen is shared with the electrical power subsystem. The gases are heated by the cryogenic heat exchangers prior to admittance to the cabin. The gaseous supply, stored in accumulators from tank venting, is maintained for emergency or high usage rates. Tank pressures are reduced by regulators.

Two modes of operation are provided. The primary mode occurs with the crew in shirtsleeves with the gas circulating loop open to the cabin. An alternate, closed-loop suited mode is available for emergency operation. Oxygen partial pressure control is identical for either suited or shirtsleeve operation. Oxygen partial pressure is sensed by a polargraphic sensor. The sensor signal is interpreted by an amplifier, which actuates a solenoid valve to admit oxygen as needed. Total pressure is maintained with nitrogen by an absolute pressure regulator. For the suited mode, the total pressure is maintained slightly positive with respect to cabin pressure.

The oxygen accumulator is sized to provide a quantity sufficient for one cabin repressurization to 3.1 psia. The nitrogen accumulator is sized for 1 day's leakage. Repressurization is performed with oxygen over a short time period, and nitrogen is added at a slow rate to build the total pressure to 14.7 psia.

Gas quantities indicated in Section 2.14 are basic requirements and do not reflect additional needs for fail-operational, fail-safe reliability. They do, however, reflect one additional day's quantity for contingency. To provide the additional reliability, it is likely that the cryogenic tanks will be doubled, thereby doubling the listed weight and volumes for tankage and gases.

2.11.2 Thermal and Humidity Control

Heat generated by onboard systems, power sources, and crew members is rejected to space by a space radiator. The radiator is estimated to be 420 ft^2 for an assumed upper surface location and an $\alpha/\epsilon = 0.05/0.8$ and an average load of 23,000 Btu/hr. However, maximum orbital loads are 27,120 Btu/hr and growth to 35,000 Btu/hr should be anticipated. In this event, the radiator area could exceed 640 ft^2 for the same location and surface characteristics.

The system consists of two coolant loops: an internal loop within the crew compartment and an external loop throughout the remaining unpressurized areas of the vehicle. The internal loop uses water as the coolant medium and the external loop uses Freon FC-21.

In the crew compartment, heat is transferred to the water loop either passively to the atmosphere and then through the gas/liquid cabin or suit loop heat exchanger or actively through cold plates. The heat added to the water loop is transferred to the external freon loop through a liquid/liquid interchange heat exchanger. Part of the heat is used for fuel cell cryogenic heating, and the excess is radiated to space by the radiator.

Supplementary cooling is achieved by utilizing water boilers which boil excess fuel cell water. Use of venting cryogenics as heat sinks during post-launch and reentry is achieved through additional heat exchangers. The LOX sump line heat exchanger as shown in Fig. 2.11-2 is typical of this application.

To maintain a 50-percent relative humidity within the crew compartment, the coolant inlet temperature at the suit heat exchanger is 45-50°F. This temperature condenses the latent load generated by the crew and the lithium hydroxide reaction. The condensed water is separated from the heat exchanger and stored either in the potable water tank or in the waste water tank. It is then either consumed by the crew or evaporated in the water boiler for auxiliary cooling.

2.11.3 Carbon Dioxide and Trace Contaminant Removal

Because of the short mission duration of the vehicle, lithium hydroxide and charcoal were selected for removing carbon dioxide and odors. Since cabin leakage is assumed at 6 lb/day, this rate will limit concentration of contaminants not removed by the lithium hydroxide/charcoal cartridges. If leakage rates are small, a catalytic oxidizer could be added to eliminate the major contaminants, such as methane, carbon monoxide, hydrogen, and other minor contaminants.

The atmosphere is circulated by compressors through the debris trap, lithium hydroxide and charcoal beds, and suit heat exchanger. The same beds are used regardless of whether the operational mode is suited or shirtsleeve.

2.11.4 Food and Water

A combination of freeze-dried and frozen food will be carried in individual servings. Reconstitution of the dried food will be performed at the preparation station. A freezer is provided for the frozen food and an oven for cooking.

Water is supplied from the fuel cell output which produces a quantity in excess of metabolic requirements. The potable water tank is sized to carry 1 day's requirement (26 lb). Bladder tanks, pressurized from the nitrogen system, are used for both the potable and waste tanks. The waste tank, which stores water for boiling, is sized to carry 75 lb of water.

Heating of the potable water for food reconstitution or chilling for direct consumption is accomplished by the coolant fluid. An electrical heater supplements the hot coolant for water heating.

Additional supplies, such as trays, utensils, towels, etc., are stored at the preparation station.

2.11.5 Waste Mangement, Personal Hygiene, First Aid

Urine and fecal material are collected at a waste management station in the crew compartment. The waste materials are collected by an air transport system contained within the collection unit. Urine is phase-separated from the transport air and either heated and vented to space as a gas or dumped directly through a heated dump valve. While docked to the Space Station or when in the vicinity of experiments, the urine is temporarily stored.

Feces is vacuum-dried and stored in a waste container along with debris and other miscellaneous trash. The container is later emptied as a ground servicing operation.

Personal hygiene items for bathing and grooming are stored at the management station, along with medical supplies.

2.12 AVIONICS SYSTEMS

The avionics systems of the stage-and-one-half space shuttle vehicle (SSV) have been detailed in engineering memorandums (EMs) and as follows: (1) Data Management, EM L2-01-03-M1-1B, Appendix B of this report; (2) Guidance Navigation, EM L2-01-03-M1-2A, ACS Fifth Monthly Report; (3) Communications, EM L2-01-03-M1-3A, ACS Fifth Monthly Report; and (4) Control Display, EM L2-01-03-M1-4, ACS Fifth Monthly Report.

Review of the basic avionics systems concepts established for the Model LS 200-5 against the requirements of Model LS 200-7 resulted in changes to the data management system only. These changes were required to accommodate the changes in number of engines from 11 to 9 for main rocket engines and from 4 to 6 for turbojet landing engines. The changes in avionics since the ACS Fifth Monthly Report are seen to be limited to revisions to details which primarily impact weight and power rather than concept.

The baseline avionics system is predicated on significant levels of development and innovation in the integrated data management concepts employed; however, the system can be implemented with currently available general-purpose computers.

A brute force concept for satisfying redundancy is employed, utilizing triple and quadruple redundancy at equipment levels. It is anticipated that design refinements can reduce the weight fractions estimated; however, the selected approach provides a conservative design estimate.

An executive level review of each avionics system is provided in the following sections; details are included in the EMs listed earlier

2.12.1 Data Management System

The data management system (DMS) includes the mechanization of data collection, translation, analysis, and distribution functions. This is accomplished by means of a data distribution system, a computer system, and their interfaces. These are shown in block diagram form in Fig. 2.12-1.

The computer system is distributed into three functional areas: the executive command and control, guidance and navigation, and vehicle control, each having its own computer, as shown. The individual computers perform those tasks associated with their functional areas in addition to controlling the local flow of data. The command and control computer serves in an executive role, assigning and directing the tasks to be performed in the other computer areas. The transfer of data in each of the functional areas is broken into several logical subgroupings, each connected to its associated computer.

A dedicated substation controller (SSC) is assigned to each geographically contiguous subgroup to manage the data transfer within the elements served by the SSC. The SSC allows local data transfer and buffer updates to occur at their natural frequency without disturbing other vehicle substations. Individual substation areas may have changes incorporated with no impact on adjacent areas. This applies to the dedicated functional computers as well.

The mutual exchange of data between the functional computers, as well as SSC is accomplished by means of a data bus. The basic means of combining various data in an orderly manner is via a multiplex data distribution system which consists of a data bus network and the necessary electronics for getting data on or off the data bus.

The functional computers perform all computational algorithms including checkout of those elements they serve and interface the individual subsystems with the command and control computer for status and abort decisions. This permits an orderly allocation of responsibility. Self-test and warning is

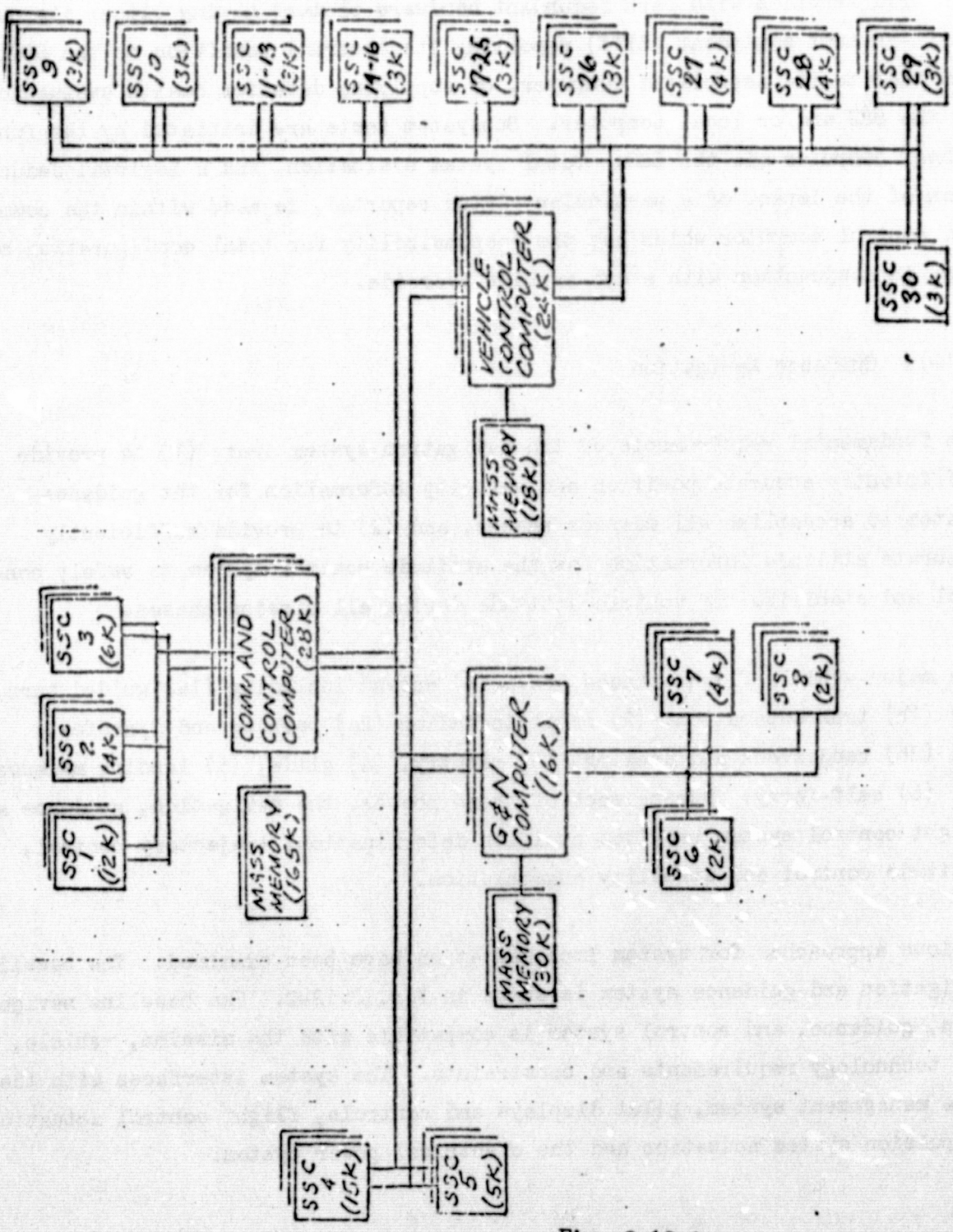

Fig. 2.12-1 Data Management - System Block Diagram

Fig. 2.12-1

a hybrid function with each redundant hardware element having either its own built-in test equipment (BITE) reporting its internal condition to the SSC, and then to its associated computer, or supplying data for health evaluation by the SSC and/or local computer. Subsystem tests are initiated by the functional computer via the SSC. Total system evaluation, and a logicial deduction of the impact of a particular status reported, is made within the command and control computer which has the responsibility for total configuration control in conjunction with a man-machine override.

2.12.2 Guidance Navigation

The fundamental requirements of the navigation system are: (1) to provide sufficiently accurate position and velocity information for the guidance system to accomplish all mission phases, and (2) to provide sufficiently accurate attitude information for the attitude control system to safely control and stabilize the vehicle attitude during all mission phases.

The major vehicle flight phases are: (1) ascent including (1a) guided burn, and (1b) tank separation, (2) orbit including (2a) parking and transfer, and (2b) rendezvous and docking, (3) reentry, (4) glide, (5) landing maneuvers, and (6) self-ferry. During each of these phases, the navigation, guidance and flight control system provides position determination, trajectory control, attitude control and stability augmentation.

Various approaches for system implementation have been examined. The baseline navigation and guidance system is shown in Fig. 2.12-2. The baseline navigation, guidance, and control system is compatible with the mission, vehicle, and technology requirements and constraints. The system interfaces with the data management system, pilot displays and controls, flight control actuation, propulsion system actuation and the electrical power system.

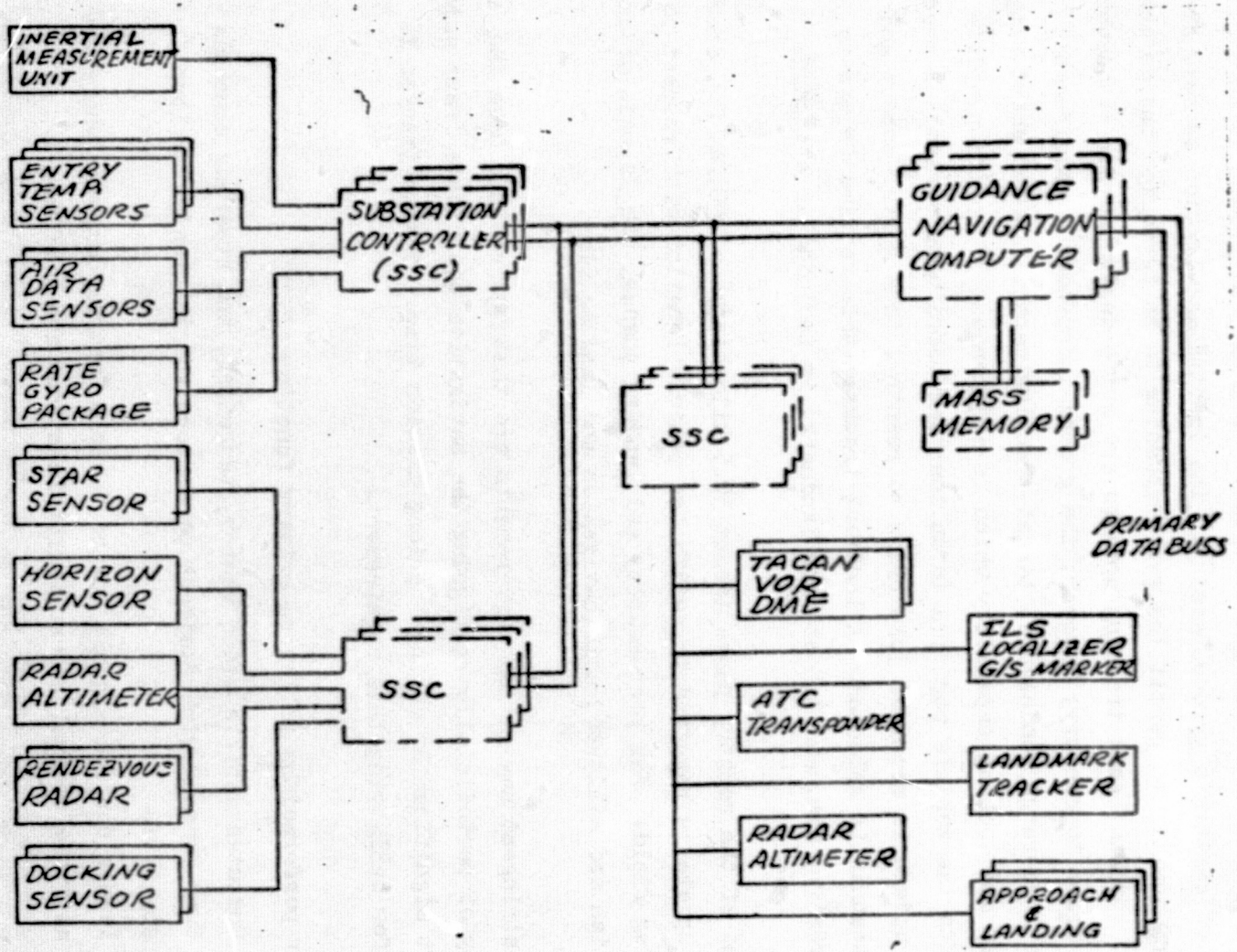

Fig. 2.12-2 Navigation and Guidance System – Block Diagram

LOCKHEED MISSILES & SPACE COMPANY

A requirement for minimum dependence on ground equipment imposes further constraints on a number of navigation areas. Prelaunch alignment is accomplished by means of earthrate gyrocompassing. The inertial navigation sensors are of sufficient quality to permit the gyrocompassing to be performed inside the computer. Ground-based tracking updates are quite desirable for rendezvous and just prior to reentry; however, the ground independence requirement demands a long-range rendezvous, target-tracking capability and short-range rendezvous and docking capability which is independent of position update in addition to the vehicle position in an inertial coordinate system. A precise position update is required just prior to reentry, thus a star sensor and horizon scanner is selected. A landmark tracker (this requires a man to select, verify, aim, and "shoot" the landmark) is included as a backup.

At the end of the reentry phase (about 30.5 kilometers or 100,000 ft), another position update is required to verify the vehicle location with respect to the landing field. For post-reentry and landing phases, use is made of existing civilian and military radio navigation and landing aids.

The most stringent navigation requirements are that the vehicle have the capability of periodicially realigning the navigation coordinate frame which will drift significantly during the long mission time. A star tracker is included for satisfying this requirement.

A computer performs the following primary functions:

(1) Computes vehicle state vector, targeting, and steering commands
(2) Sums command with feedback parameters and insures outer loop stability
(3) Issues control signals to the Vehicle Control Computer where the attitude control and autopilot functions are performed.

2.12.3 Communications

The communication subsystem is the link between the spacecraft and the ground; spacecraft and the Space Station; and spacecraft and other external space vehicle or personnel. As a voice link, it gives the crew, the ground, the Space Station and the EVA and other spacecraft the capability of direct communication. As a data link, it provides critical data through the Data Management System to the ground and Space Station as a backup to the information furnished to the crew onboard the spacecraft. As a command link from the ground or Space Station, it transfers command information into the spacecraft automatically as a backup to the crew. The Communication Subsystem also provides for communication between the crew members onboard the spacecraft, between crew members onboard the spacecraft and EVA and other spacecraft.

Alternatives considered in defining the communication subsystem for the stage-and-one-half include the link method of communicating between the ground and the spacecraft (direct or via satellite), selection of frequency bands; multiple or single frequency within the band, critical data and its rate; omnidirectional or directive antennas, modulation techniques, signal error correcting techniques, and spacecraft communication capability during reentry.

The communication link for long range will use a low-power transmitter (may be solid-state) directly to the ground when feasible, with additional power amplifier stages to go to the communication satellite when necessary. The receiving function will have regular front ends for the ground communication with the addition of a cryogenic front end for satellite links. Also, the antennas will be flush-mounted on both top and bottom of the vehicle with omndirectional capability to the ground, and electronically controlled directivity for communication with the satellite. This will allow the use of minimum power when possible.

For short-range communication during ascent, orbit (to EVA and other spacecraft), rendezvous and docking, and landing, a UHF frequency link will be used. This will minimize the number of configurations and still meet the FAA control requirements during the landing phase. The UHF antenna configuration must be worked into the vehicle configuration but should not present a major technological problem.

The UHF link is used primarily for short-range communication with the ground during launch and landing; with the Space Station during rendezvous and docking; and with EVA and other spacecraft in orbit. This link can also be used as an emergency backup in the case of troubles in the other links, but with loss in quality of information.

The S-band link's primary use is for long-range communication with the ground during orbit, when contact with the ground is available. This communication link is not to require a large ground network system implementation. It will be used only when a ground station is available.

The satellite communication link requires the addition of power for transmission and the addition of low-noise "front end" preamplifiers for receving signals from the satellite. The exact frequency to be used, the exact power, and the exact noise temperature of the preamp will be determined when a definite satellite is selected. These units may have separate modulator driver/receiver demodulator units or may use the standard ground transmitter/receiver with proper interfacing. The block diagram (Fig. 2.12-3) shows a separate system configuration.

The antennas may be grouped into three separate antenna systems because of the three separate communication links. The UHF antenna will present problems of size and placement. The frequency of the UHF band requires large openings (slots) in order to be effective. This causes problems in the skin/structure configuration of the vehicle. Also, the need for UHF during docking and landing means that a forward and down beam is needed. With launch and ascent, a back-

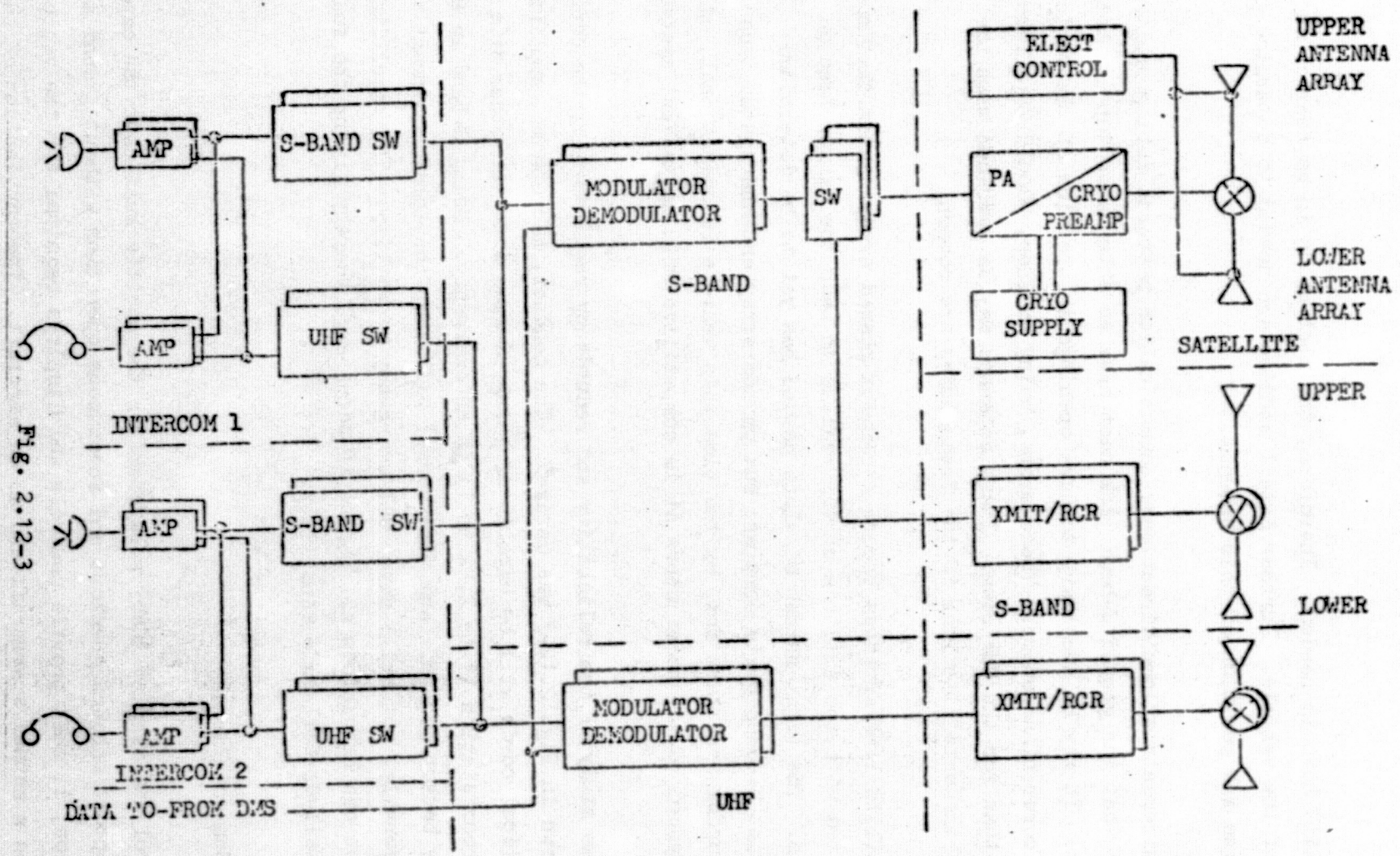

Fig. 2.12-3 Communication System

LOCKHEED MISSILES & SPACE COMPANY

ward (tail) beam is needed. Therefore, the slot needs to be near or on the bottom of the vehicle. Further detail studies are needed to determine the exact size and position of this antenna.

The requirements of omnidirectional communication patterns during orbit dictates that the ground S-band link must have an antenna on top and bottom, at least. It may be necessary to have openings in the side of the vehicle also to cover blind spots. These slots, being smaller, should be a lesser problem than for the UHF case. These antennas may be combined with the array of the satellite link if the frequencies are common.

The satellite link antennas become a complex phased array system that must be coordinated with the attitude of the vehicle to keep the narrow beam on the satellite. The total number of slots needed has yet to be determined. The arrangement becomes quite complex; but phased array antenna system technology is developing very fast and, by the time this vehicle is operational, will have advanced to the point where it is competitive with mechanical systems.

After some study of the reliability and redundancy requirements, the configuration shown in Fig. 2.12-3 was derived. The headset, microphone, amplifier, and umbilical cords will be capable of being plugged into the other side of the intercom station (1 to 2, 2 to 1) in an emergency. Using S-band as an emergency backup for UHF (and vice-versa) will keep the total equipment requirement reasonable, but still give full emergency capability. The satellite communication can be used in all phases if necessary, thereby giving the full fail-op-fail-op-fail-safe capability.

2.12.4 Control Display

The control and display (C&D) subsystem for the shuttle must have the capability to support onboard checkout and autonomous operation without ground support. In addition, it must provide controls and displays required for the vehicle to operate as a manned spacecraft and as an aircraft. The combination of these

requirements into one system represents a significant development task.

The basic flight program for the spacecraft is planned for automatic control, with the crew providing dynamic monitoring of the flight display management system with takeover capability provided at any point in the mission profile. This concept strongly suggests an integrated display management and control system in addition to minimal basic flight instruments.

The data management system computer system in cooperation with the programmable control display system would automatically configure each display element for the next sequence, thus reducing crew task time considerably. Inherent in this management display system is a built-in computer program, which commands the display system to return to the automatically programmed configuration as the flight progresses. This is necessary since the pilot can call up desired information, thereby changing his displays to a highly nonroutine configuration. Thus, the pilot cannot become "lost" in the display network and configuration. A simplified control command is provided to permit him to reset the display system to the automatic mode, thus reestablishing the display configuration to that particular mission mode and phase.

Basic control and display requirements or goals for the shuttle are:

(1) Operation by a two-man crew; operable by one from either seat.
(2) Minimization of number of displays and controls.
(3) Elimination of circuit breakers.
(4) All-electronic display.
(5) Optimization of display area; clarity and comprehension of displayed data.
(6) Interface with a data bus and maximum utilization of digital information.
(7) Complete display flexibility and adaptation to vehicular system changes.
(8) Integration of the display tasks.

The proposed functional control and display system chosen for this conceptual design is depicted in Fig. 2.12-4. It consists of two electronic attitude directors (EADIs), two horizontal situation displays (HSDs); a multifunction display (MFD), two groups of vertical scale indicators, and a group of dedicated instruments. One heads-up display (HUD) is used to improve efficiency in rendezvous both for space station and uncooperative satellites. This selection is based on the display requirements known at this time. The two crew stations are identical to satisfy the requirements for operation by one man plus making it possible to display to the second crewman the same information as the pilot sees during periods of critical activity. During other mission phases, the second crew station displays are utilized to perform subsystem checkout, malfunction isolation, configuration monitoring, and other housekeeping activities. A single MFD is available for observation by both crew members with mission status, configuration and action required cues displayed.

The entire repetoire of displays can be programmed to display different information during various modes of shuttle flight. Critical events or status can be programmed to take precedence over a noncritical display. Other modes may be controlled manually by the crew, or the formats can be changed automatically by the computer.

Programmable redundancy is incorporated to improve reliability and conform to the reliability requirements of the shuttle.

The block diagram of the control/display system shown in Fig. 2.12-4 is presented to show the flow of data between data bus and display. The computer-managed system eliminates the requirement for separate electronics memory, formatter, and controls for each display system by combining all these functions in a computer-managed unit with internal redundancy.

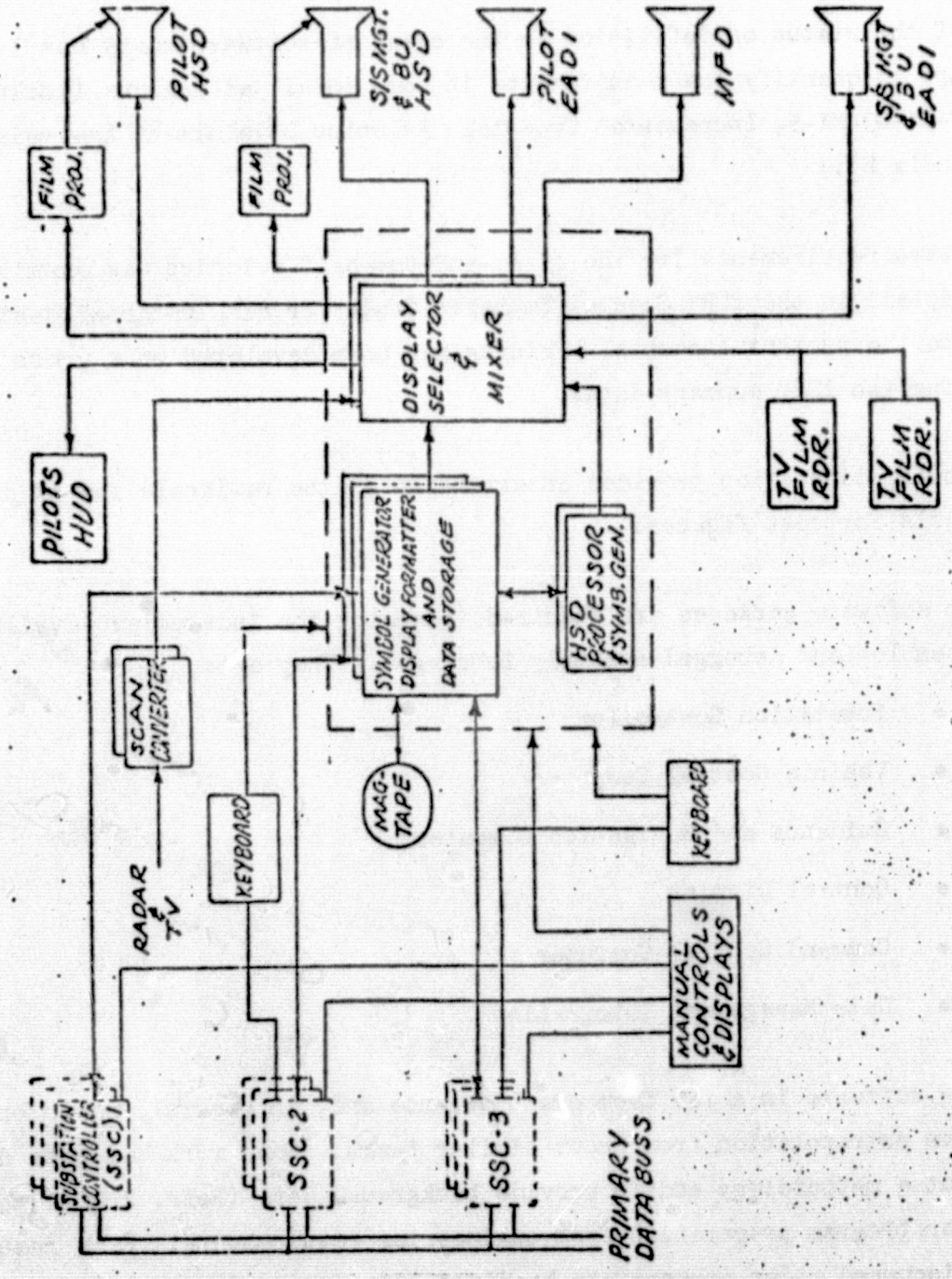

Fig. 2.12-4 Programmable Control and Display System - Block Diagram

Fig. 2.12-4

2.12.5 Software

Review of the status of definition in the areas of software costs has led to an attempt to quantify the requirements in some detail as follows (included in EM L2-01-03-M1-5, Incremental Two-Stage Avionics Development Analysis, see Appendix B).

The software requirements for the stage-and-one-half avionics was examined in some detail in the ILRV Special Emphasis Study for single-thread design similar to the present concepts. Pricing has been developed on a gross basis using the ILRV summary data.

The following discussion provides an extension of the rationale and an improved basis for cost figures.

Six basic software packages are required (assuming the independent availability of an assembler and debugged assembly language). They are:

- Substation Controller
- Vehicle Control Computer
- Guidance and Navigation Computer
- Control Display
- Command Control Computer
- Data Management Integration

Estimating software is a far from exact science and, in general, rests on imaginative extrapolation from known similar tasks. Some work has been done to document a methodology and to provide background data (Refs. 2.12-1 through 2.12-4) for program preparation from engineering requirements. Each requirement is discussed under appropriate headings using the referenced data as indicated (See Appendix 2.12 for estimating curves).

Substation Controller - A program averaging 20 words per signal is assumed within the SSCs which in aggregate totals 120K words. The program is relatively simple in that each SSC performs as an independent special-purpose computer with an average 4K word memory. It is assumed that the basic task for each SSC is functionally identical; therefore, a single development program should suffice with thirty application adaptations involving an estimated 60% uniqueness factor. At this level, a 1.5:1 ratio is assumed between instructions and memory words.

Development based on operational program costs (Refs. 2.12-1 and -2) is 27.8 manmonths which at an assumed cost of $2,500.00 per mm amounts to $69.3K. Adaptations based on utility program costs is $27K each for thirty SSCs or $810K for design, production and test less documentation.

Documentation costs (Refs. 2.12-1 and -2) are based on an assumed 1000 pages for the development @ $40.00 per page and 6000 pages (200 per SSC) for the adaptation at $40.00 per page or $280K.

Total cost is estimated to be $1.16M.

Vehicle Control Computer - A total of 42K words (18K off line) of memory are involved. Assuming two instructions per word equates to 84K instructions.

Based on operational program factors, 389 manmonths of effort are required at a cost of $972.5K. Documentation is 1800 pages for a cost (@ $40.00 per page) of $72K.

Total cost is estimated to be $1.045M.

Guidance and Navigation Computer - An estimated 46K words (30K off line) applying the rationale of VCC pricing, equates to $1.07M for design, production, and test (DP & T) and $76K for documentation.

Total cost is $1.146M.

Control Display - The programmable formats of the multifunction displays are assumed to be supplied from the command control computer (CCC) and are covered under that heading. Software for the film pack and tape-stored technical-order data for crew support, arrived by applying a 1.3 factor to C-5 MADAR on-board support data costs, estimated to require $1.95M.

Command Control Computer - A total memory of 193K words (165K off line), are involved. The 28K computer memory requires $650K for DP & T and $60K for documentation.

Since curves do not exist in the examined literature for the massive 165K word off line program, the value of 3,500 manmonths per 300K instructions is used, employing a very modest extrapolation of the data (Refs. 2.12-1 and -2). This gives an estimated $48.125M for DP & T and $858K for documentation or $49.69M total.

Assuming one half of the software development is accomplished on ground-based computers at a ratio of 5.5 computer hours per manmonths (Ref. 2.12-2) equates to 11K hours of computer support required and at $400.00 an hour equates to $4.4M.

Data Management Integration - No explicit rationale has been identified suitable for defining this task. The tasks to be addressed is designing the previously identified programming elements into a unified system. Additionally, the unified system must be implemented in triplicate (quad redundant CCC). One may also speculate that the integration group should be responsible for coordinating the efforts of the programming centers developing the programs discussed earlier. Logically the basic controlling specification should originate and be maintained in this effort.

Assuming this effort is one half the magnitude of the sum of the other tasks (which take 21,780 manmonths) suggests this effort may cost $54.45M plus documentation costs of $500K (assuming roughly half the cost of the CCC documentation) for a total of $54.95M.

The above costs are for the conversion of basic engineering requirements into machine language including validity testing and documentation. The engineering effort required to define the programmer's task is a significant effort.

Pending a more definite measure of the engineering effort required to define the detailed system requirements to be implemented in the software package (e.g., signal source, characteristics, destination, enroute operations, priorities, etc.), a ratio of 1:4 is assumed. That is, it is assumed one engineering manhour is required to generate the requirement and four programmer hours are required for DP & T in implementing the engineers request. This rationale establishes 5,445 manmonths of engineering at $13.61M for the engineering definition on which the software is based. A flat $500K documentation cost is assumed.

The total cost of software is thus $128.451M.

The development span of software is seen to be critical from sheer magnitude and merits particular attention as a possible driving influence in the development cycle (Ref. 2.12-4). Funds and time do not permit exploring this factor at the present, however, five to seven years are required with a high potential for delays in attaining full operational capability.

REFERENCES

2.12-1 Farr, L. and Names, B.: Cost Aspects of Computer Programming for Command and Control, System Development Corporation, Santa Monica, California, Conference Proceedings, 1964 National Winter Convention on Military Electronics Vol III.

2.12-2 Farr, L. and Zagorski, H.J.: Factors that Affect the Cost of Computer Programming, prepared under AF 29(628)-3418.

2.12-3 Boehm, B. W.: Some Information Processing Implication of Air Force Space Missions in the 1970s, The Rand Corporation; Astronautics & Aeronautics, January 1971.

2.12-4 Carey, L. J. and Sturm, W. A.: Space Software at the Crossroads, System Development Corporation and Aerospace Corp., Space/Aeronautics, December 1968.

APPENDIX 2.12

AN EXCERPT FROM

FACTORS THAT AFFECT THE COST OF COMPUTER PROGRAMMING

TECHNICAL DOCUMENTARY REPORT NO. ESD-TDR-64-448

JULY 1964

L. Farr
B. Nanus

DIRECTORATE OF COMPUTERS
ELECTRONIC SYSTEMS DIVISION
AIR FORCE SYSTEMS COMMAND
UNITED STATES AIR FORCE
L. G. Hanscom Field, Bedford, Massachusetts

(Prepared under Contract No. AF 19 (628)-1648 by the System Development Corp., Santa Monica, California, 90406.)

Program Design and Production

Program Design and Production includes cost factors associated with support programs, and the operational programs as determined by the constraints of personnel, hardware, and operational requirements.

In the program design activity, the operating system description and the operational specifications are used to create the detailed programming specifications. Design of the program system involves the determination of its broad logical subdivisions, the design of an executive program that controls the sequencing of subprograms, the design of the data base structure, the allocation of computer storage, and the specifications for any utility and support programs required.

The utility programs are the tools with which other programs are built. Some of them may be already designed and available, but usually some special tools will have to be designed and produced. Since preparation of utility programs may take many months, both this time and the associated cost must be considered in the costing of the operational program.

The factors in this category, as in Operational Design, center around the question, "How clearly understood are the (program) requirements?" Again, completeness, clarity, and detail combine to act as a damping factor on cost. Additionally, the program design factors include size and complexity.

(1) Number of computer program instructions and the types of programs that must be produced.

Sheer magnitude is a critical factor in allocating both resources: men and computer time. As a numerical entity, it is the basis for many of the rules of thumb currently in use by managers. Despite its importance, little research has been done to develop reliable methods for estimating the number of instructions. Very often, these estimates turn out to be grossly inaccurate. One humorous observation on this situation was made by J. W. Garwick: "Programs do always get K times larger than a first thorough calculation indicates. I use $K = \pi$."*

In the design of business data-processing systems, the number of instructions has been poorly estimated. The Controller's Institute says: "From the detailed flow chart, the number of instructions required to carry out the operation must then be determined. This is possibly one of the phases which has caused the greatest trouble to most companies, since most EDP groups have at one time or another seriously underestimated the number of instructions required. Most companies report that their estimates become more accurate as they gain more experience in programming work, but they still are forced to do a great deal of educated guessing, based on a subjective evaluation of the complexity of the current operation as compared to one previously programmed....Every company we visited added a substantial safety factor varying from 20 per cent for a company which claimed, due to experience, a reasonable accuracy in its estimating procedures, to 400 per cent for a company which had found itself that far out on a previous estimate."**

An experienced estimator examining a proposed system that will have many similarities to previous systems may predict the number of instructions with some accuracy. This is the case with some command and control system programs that are designed in an evolutionary manner--that is, by a series of models or phases. For example, some cost guides for the 425L program for the NORAD Combat Operations Center have been developed based upon earlier versions of the program system. The instruction estimates are based upon number of registers for status and summary type messages, for display manipulation functions, for input/output tables, and so forth. Unfortunately, program histories and costs are not often documented in sufficient detail (such as this) to be useful in preparing such guidelines.

When no experience with a similar system is available, the number of instructions is much more difficult to predict, since it can be done, under the current state-of-the-art, only by weighing

---

*Leth-Espensen, J., On the General Problem of Compatibility of Computer Programs and the Particular Difficulties Embodied in Programming for Large-Scale Defense Systems, NATO, unclassified, ASTIA Document 273 710, p.51.

**Business Experience with Electronic Computers, New York, Controller's Institute Research Foundation, 1959, p.111.

subjectively many of the factors listed in this paper such as the performance of the compiler, the nature of the hardware, etc. One promising quantitative approach has been suggested by one of our associates.* For a limited sample of program systems, he has demonstrated certain consistencies in the relationship between the frequency of occurrence of the decision class of instructions and the total number of instructions in the program. This may be an important step toward estimating instructions directly from operational requirements.

With an estimate of the number of instructions, managers have estimated cost in terms of the number of man months and computer hours. (Number of instructions refers to machine language instructions.) In some prior work at SDC, it appeared from a small sample that the total number of man months is an exponential function of program size. Figure 2 is based upon the results of implementing eleven program systems. The dashed line is 200 instructions per man month, a frequently used rule of thumb for large programs. Attempts to explain this nonlinearity (the deviation from the rule of thumb) include recognition of such factors as increases in communication and coordination and increased complexity in the larger programs that may require an increased amount of labor.

In work on smaller programs or program systems (of, for example, less than 10,000 instructions), data showed rates ranging from 400 to 1000 instructions per man month for individual programs. A further analysis of the data shown in Figure 2 revealed that an average of 225 instructions per man month are produced for operational programs, and 311 per man month for utility programs (see figures 2a and 2b). One possible explanation for the lower cost of utility programs is that the program developer is the user and therefore can write his own requirements with little external coordination.

A similar investigation of the relationship between number of instructions and number of computer hours has resulted in the hypothesis that the number of computer hours used to develop a large-scale program is directly proportional to the program size. Figure 3 is based on experience with seven large program development efforts.** A statistical analysis of these data is given in

* Bleier, R. E., Frequency Analysis of Machine Instructions in Computer Program Systems, TM-1603, 19 November 1963.

**Management of Computer Programming for Command and Control Systems, Heinze, K., N. Claussen, and V. LaBolle. System Development Corp., TM-903, 8 May 1963.

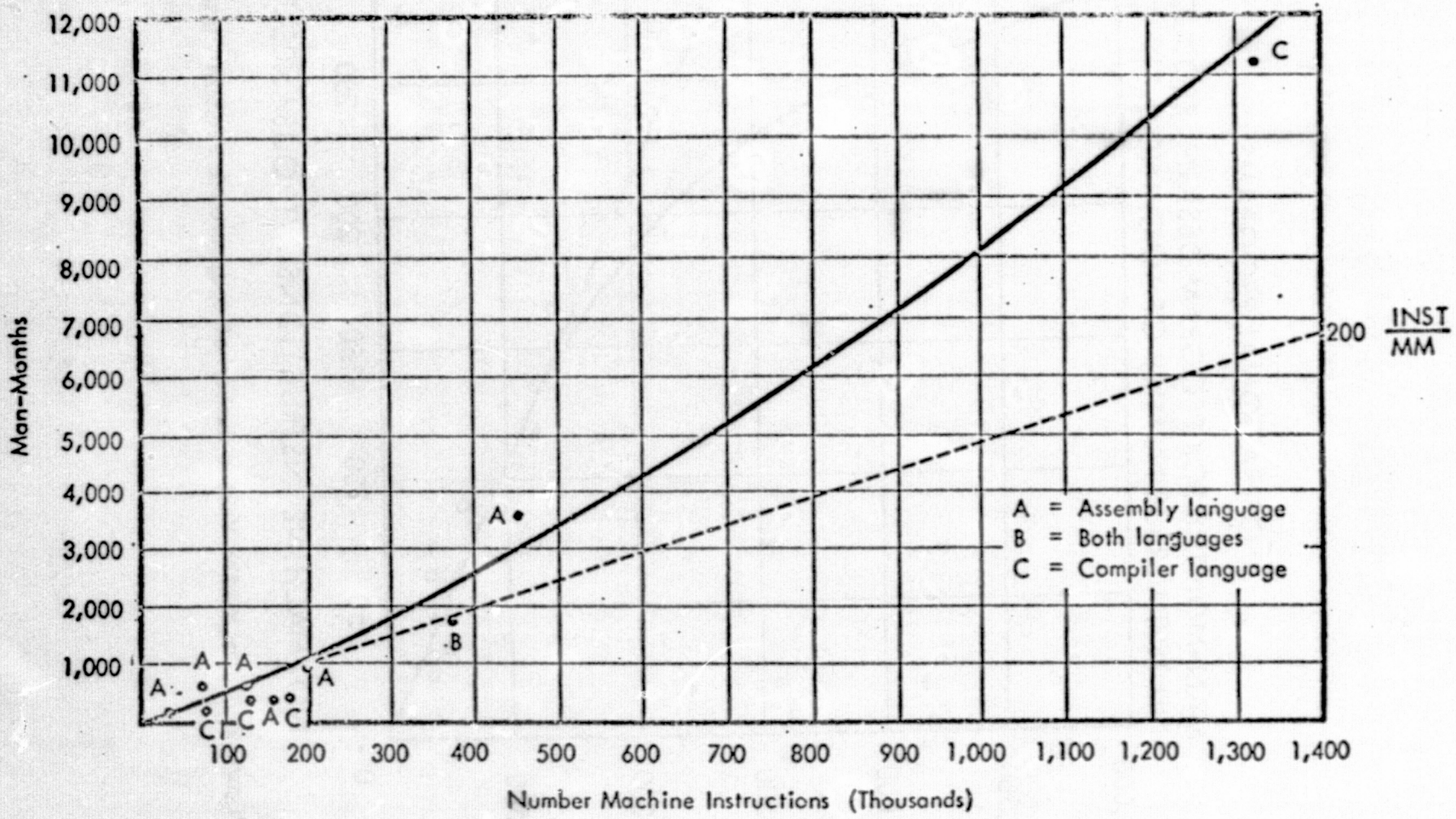

Figure 2. Man Months for Program Design, Production and Test Versus Program Size

This figure shows the costs of programming in man months as a function of the total number of instructions written (for both operational and utility programs). Because the data are so gross, no attempt was made to calculate an estimating function. The curve is an "eye-fit." For comparison, a dashed line representing a rate of 200 instructions per man month, a popular rule of thumb, has been inserted. In this range of program size, it appears that the cost of programming is an exponential function of program size. This may be due to such factors as increases in communication and coordination and increased complexity in the larger, interrelated programs.

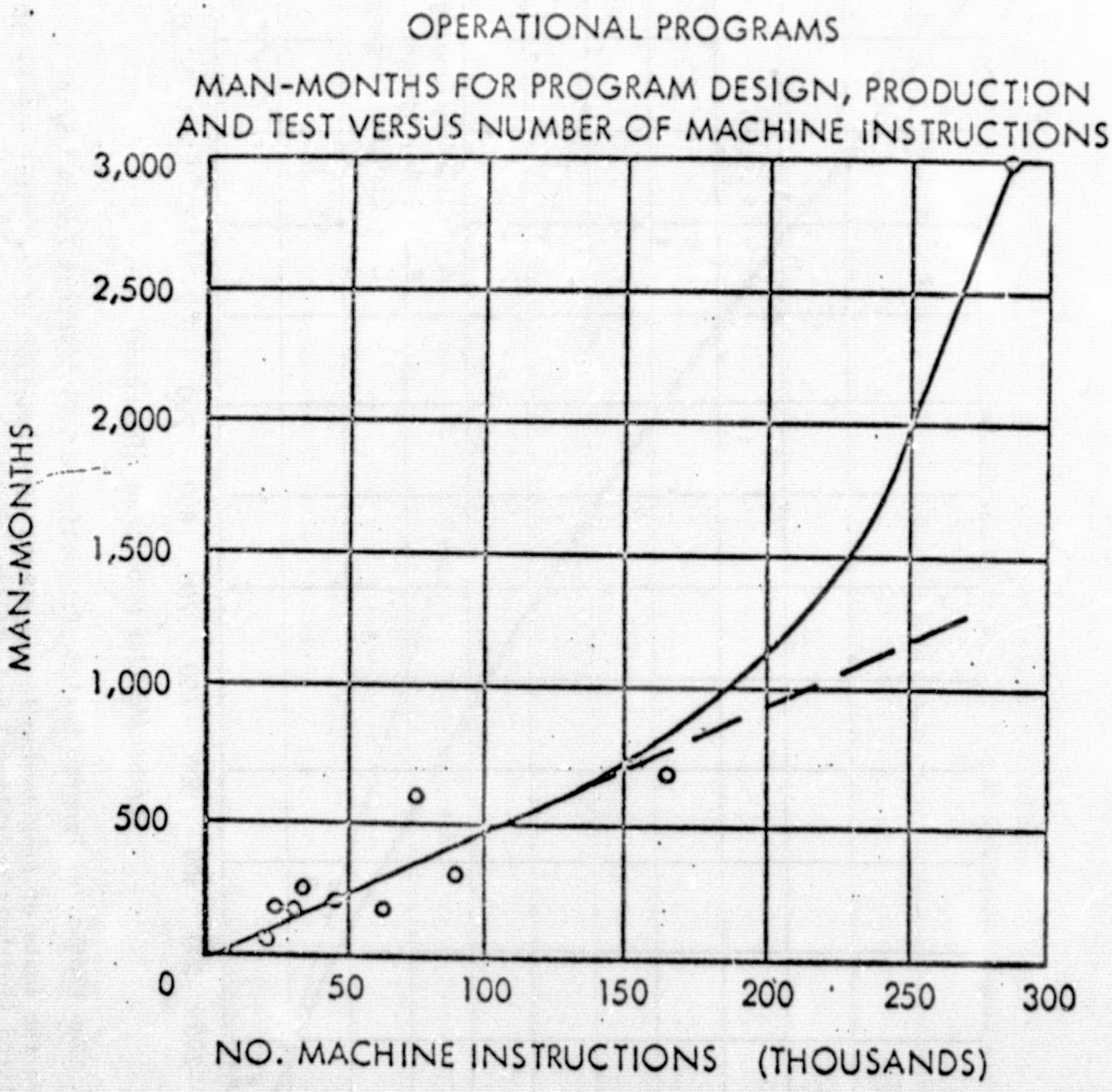

Figure 2a. Man Months Versus Number of Operational Program Instructions

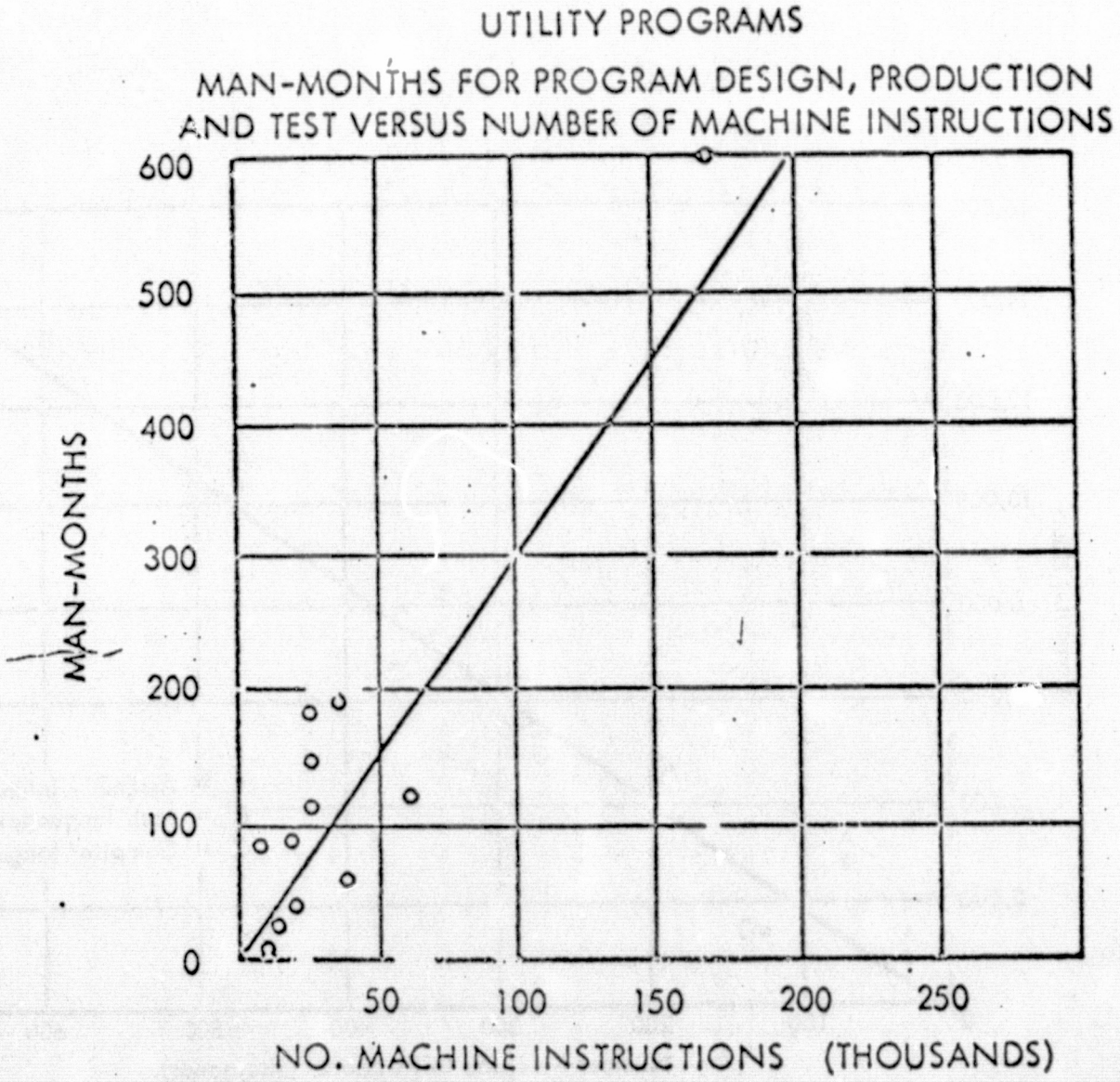

Figure 2b. Man Months Versus Number of Utility Program Instructions

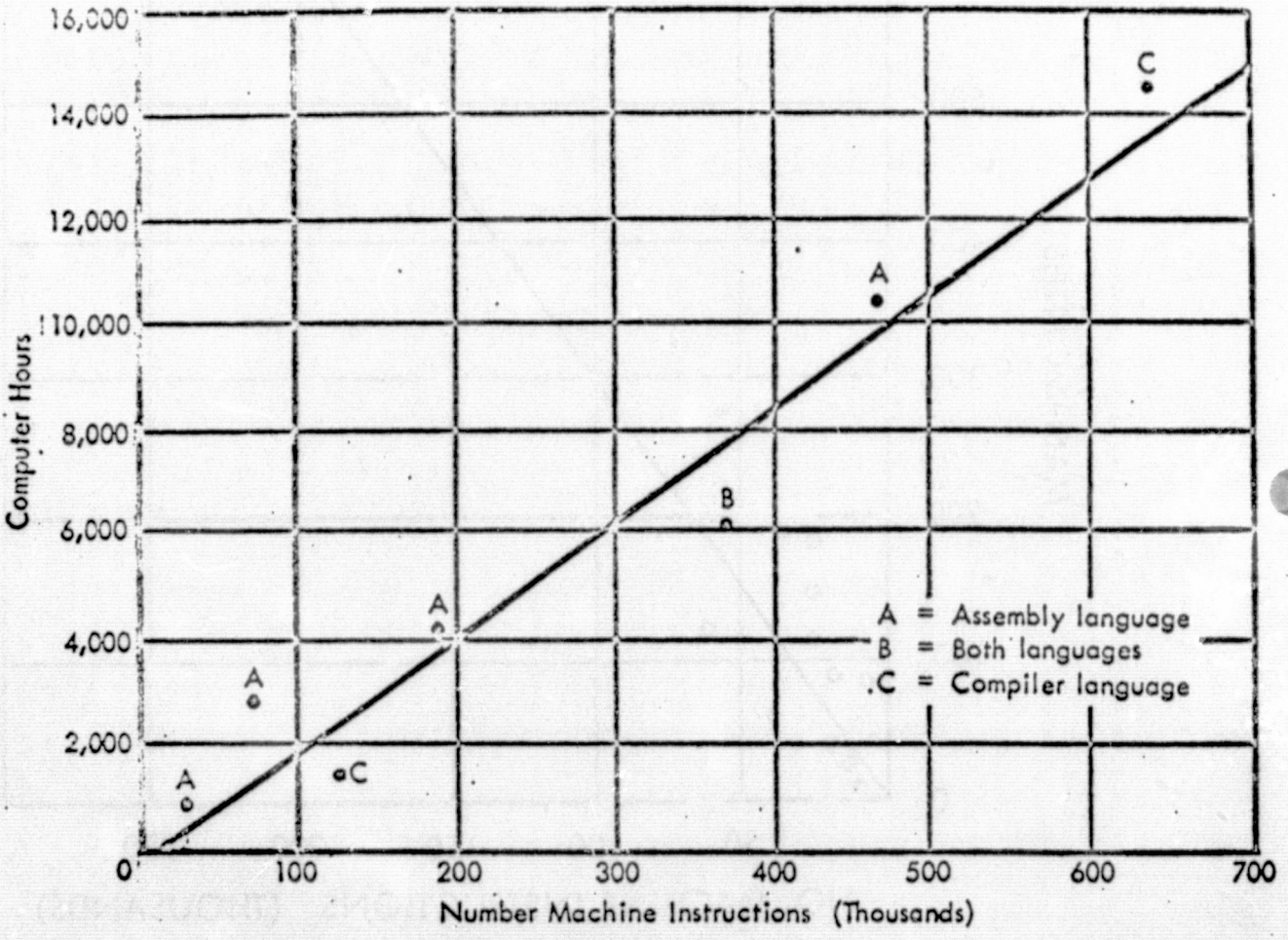

Figure 3. Computer Hours Used as a Function of Program Size

Appendix II shows the calculations to arrive at a least-squares fit to these data points. The resulting equation is $y = -174.3 + 21.7x$ where y = computer hours and x = machine instructions in thousands.

Appendix II to illustrate what could be done with a greater quantity of more reliable data. In this case, the resulting equation suffers from insufficient and unreliable data, and would be useful for estimating computer time only if an accurate means were available of estimating number of instructions.

In the case of the relationship of number of instructions to man months, the curves in Figures 2a and 2b are eye-fits and should be interpreted only as a first approximation, particularly since the data depicted were not entirely consistent. To be valid, these plots comparing data require clear definitions of program products, performance characteristics and quality measures. For example, in measures of number of machine language instructions, program systems should be classified as to the percentage of instructions derived from subroutines and from previous versions of the same program system.

(2) Number, types, and frequency of inputs and outputs to the computer(s).

In addition to influencing the cost of the program, the number and variety of inputs and outputs to and from the computer may be a clue to the size of the program needed. In any event, the greater the number of inputs and outputs, the greater the expense of both the operational and the program design. Increased input-output capability implies increased capability of both equipment and programs, and correspondingly, the increased analysis to insur compatibility with the input-output terminals.

Other input-output factors that influence cost are the rate of arrival (or departure) for messages and the amount of format conversion, i.e., pre- or postprocessing, needed. Higher rate of input-output is more costly, and obviously the more processing required for input or output data, the greater the cost.

(3) Extent of innovation required in the program system; that is, the degree to which programs are similar in nature to those previously written.

If programs to be developed will be similar to previously developed programs, such as in the mathematical, clerical, or logical areas, and this similarity is recognized, the cost of programming the new system will clearly be less. For example, the availability of reliable, well documented utility and support programs will help reduce costs. The primary point is that the development of new program applications will result in increased costs.

One approach to the development of new and unique programs is to test feasibility with experimental or prototype programs. Although it is costly to design and test a prototype or experimental program, this reduces the impact of innovation and so provides savings in over-all program design. It also clarifies requirements and operating procedures, and program development techniques, enabling the operational program to be developed with more confidence and fewer errors. The quantitative trade-off relationship between the cost of a prototype and the savings that result from it is not known.

(4) Number, types, and quality of publications and documentation for both customer and internal use.

Documentation is an inherent part of programming, though its cost and extent are often underestimated. The experience data shown in Figure 4 suggest that the number of pages of formal documentation is linearly proportional to the total number of instructions in the program.

Some rules of thumb used to estimate the amount and cost of documentation are as follows:

(a) Approximately 10.5 pages of documentation are needed per thousand lines of program code.

(b) A drafting rate is 3 to 5 pages (750 to 1250 words) per man day.

(c) Technical review rates of 20 pages per man day are average and may range to 50 or 100 pages per day.

(d) Typing rates average 15 to 20 pages per man day.

(e) Illustrations in line drawing (e.g., flow charts) average approximately 40 pages per man day, and revision of these, up to 80 pages per man day.

(f) Duplication of a large document is at a rate of about 25,000 pages per man day; this rate varies considerably with the process.

From these rules of thumb, a reliable prediction of documentation costs is feasible, given reliable knowledge of the over-all size and scope of the project in terms of documentation requirements.

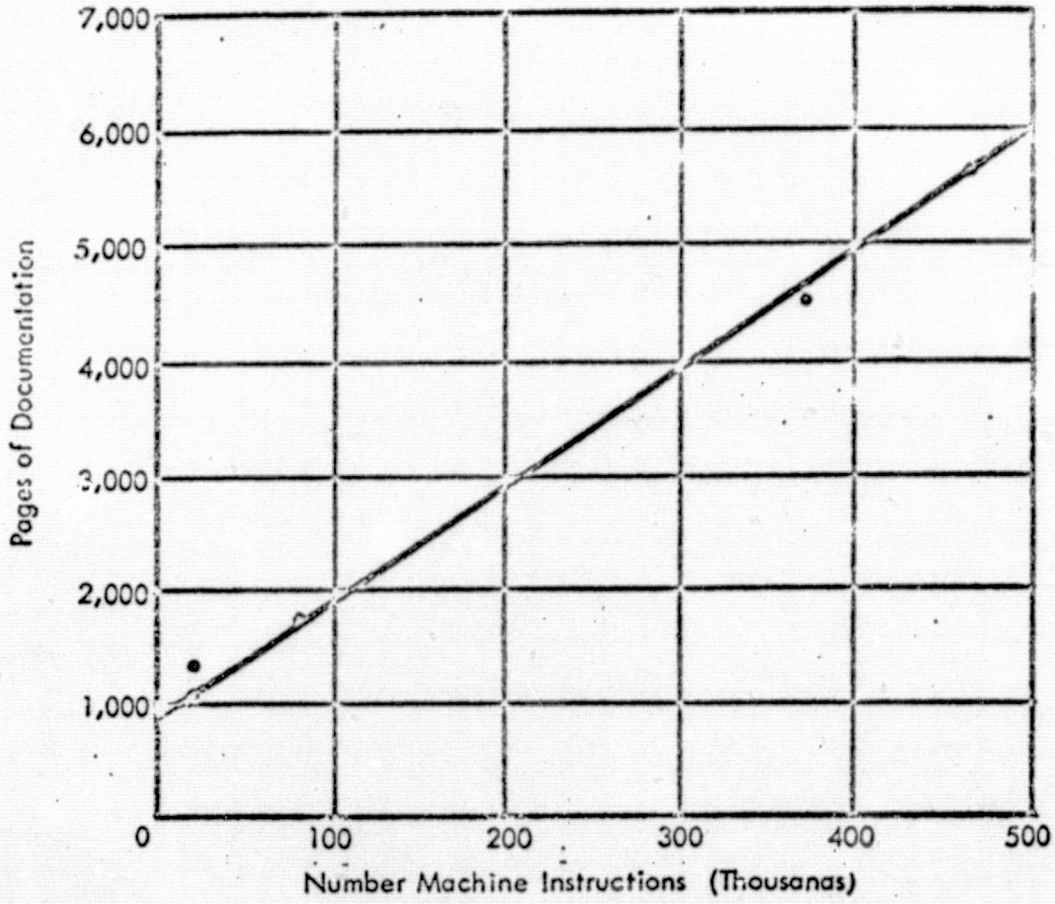

Figure 4. Number of Pages of Contract Required Documentation Versus Program Size

Data here are for five program systems. Pages of documentation refer to the number of contract pages of documentation actually produced. The graph suggests that program size in this range and number of pages of contract-required documentation are linearly proportional; it also illustrates the recognition of documentation as a major integral part of programming for command and control systems.

2.13 FLIGHT CONTROL SYSTEM

Flight control system activity was primarily directed at establishing requirements that the flight control system imposes on the other subsystem such as propulsion, electric power, loads and dynamics, and vehicle design. To achieve these objectives, preliminary control concepts for the ascent and approach-landing phases were developed and demonstrated in computer simulation. However, the scope of the study did not permit any appreciable level of control system optimization.

2.13.1 Vehicle Control During Ascent

During ascent, the critical control phase occurs after liftoff and through the region of high dynamic pressure ($\bar{q}$) . In this flight phase, control requirements were evaluated using the stage-and-one-half configuration. All computer evaluation of vehicle control concepts were based on the wind profile shown in Fig. 2.13-1. A 6-D computer simulation was used with the disturbance applied as a head, tail, and side wind.

This study has shown that the pacing control problem for vehicles of the shuttle class occurs in the roll axis. The reason is that a relatively high rolling-moment proportional to C_{ℓ_β} is induced on the vehicle in a sidewind condition. Since the rolling moment is proportional to the sideslip angle (β), limiting the angle (β) to small values at any flight condition is an important design consideration.

The sideslip angle (β) can be controlled using lateral acceleration or (β) feedback to the yaw axis. This alone does not maintain β at the low values required for limiting the induced aerodynamic rolling moments to the levels desired. With all engines deflected for roll control, the available control torques are generally not sufficient to maintain a fixed roll attitude with the design distrubances considered.

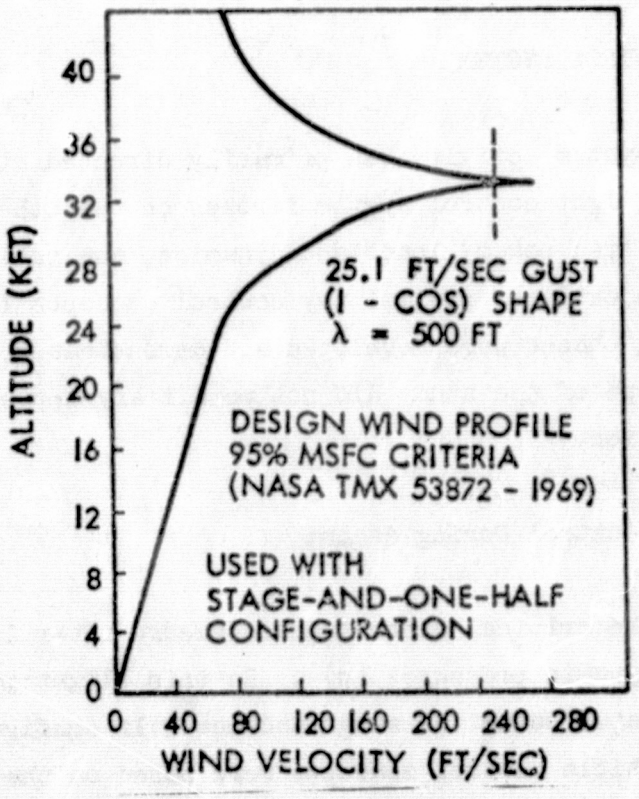

Fig. 2.13-1 Ascent Phase Wind Profile

The question that arise is "What exactly are the roll-attitude constraints for shuttle vehicles during the ascent phase?" An evaluation of the required roll-attitude constraints has shown that a fixed attitude has to be maintained during liftoff to clear all structural support fixtures. Also, fixed roll attitude is desired at separation/staging to start the return maneuver for the booster or to jettison the tanks of the stage-and-one-half configuration in a preferred vehicle attitude. Between the initial and final points of the first-stage ascent trajectory no fixed roll-attitude constraints are generally indicated. The following additional observations on the roll-attitude constraints can be made:

a. For vehicles flown without any intentional lift bias, guidance accuracy and path control are essentially independent of the roll orientation.

b. Limited roll excursions should not induce any pilot disorientation.

c. From the standpoint of vehicle design, the primary criteria for the roll axis should be limiting of roll rate and roll acceleration.

With the roll-attitude constraint relaxed, 6-D computer simulations have shown that, by allowing the vehicle to seek its preferred roll attitude when it encounters severe winds, loads and the required gimbal deflections can be reduced considerably. Various arrangements of gimballed engines were evaluated; three systems examined in detail are shown in Fig. 2.13-2 (also, Ref. 2.13-1).

Control during ascent was simulated for all systems using the wind conditions discussed. Normal and single engine-out operations were considered. Configuration 1 has the lowest torque capability in roll. Figure 2.13-3 shows the roll-channel time histories for this system with all engines operating and with engine 1 shut down. The maximum allowable gimbal deflection used in all runs was set at $\pm$ 7 deg in either pitch or yaw. Table 2.13-1 summarizes pertinent data for all three configurations shown in Fig. 2.13-2 and with all engines gimballed. The flight condition selected is at the time of maximum dynamic pressure (t = 75 sec). Note the small difference in the maximum roll rate with all engines gimballed (1.70 deg/sec) and configuration 1 (1.76 deg/sec). With engine 1 out, configuration 1 reached a maximum roll excursion of 31.5 deg. All simulation runs were performed using the ascent trajectory defined in Ref. 2.13-2.

Figures 2.13-4 and 2.13-5 show the control system configuration used for roll and yaw. For the runs summarized in Table 2.13-1, the roll-attitude gain (W), the yaw-attitude gain (H), and the lateral acceleration gain (G) were time-scheduled as shown in Table 2.13-2.

The simulated stage-and-one-half configuration is sufficiently stable (statically) in pitch so that satisfactory control can be provided using just attitude and attitude-rate feedback. Load relief with acceleration feedback was not deemed required. The constant control system gains used for the stage-and-one-half simulation are summarized in Table 2.13-3.

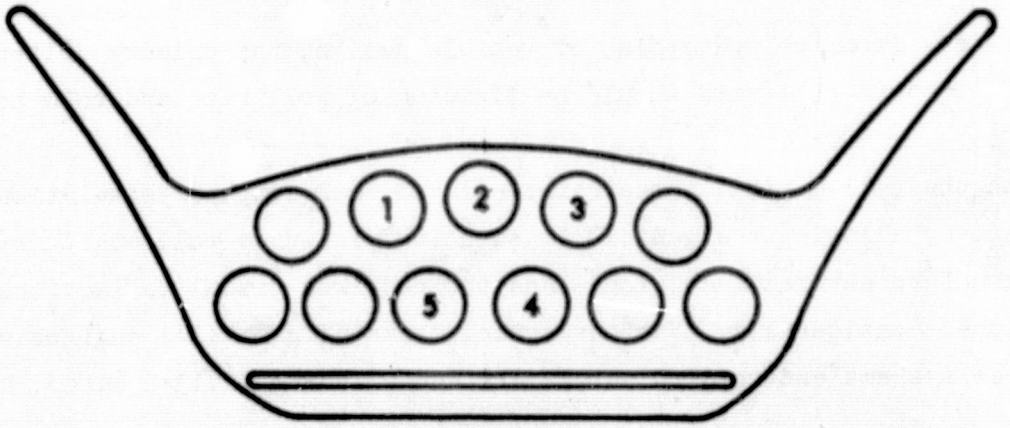

CONFIGURATION 1

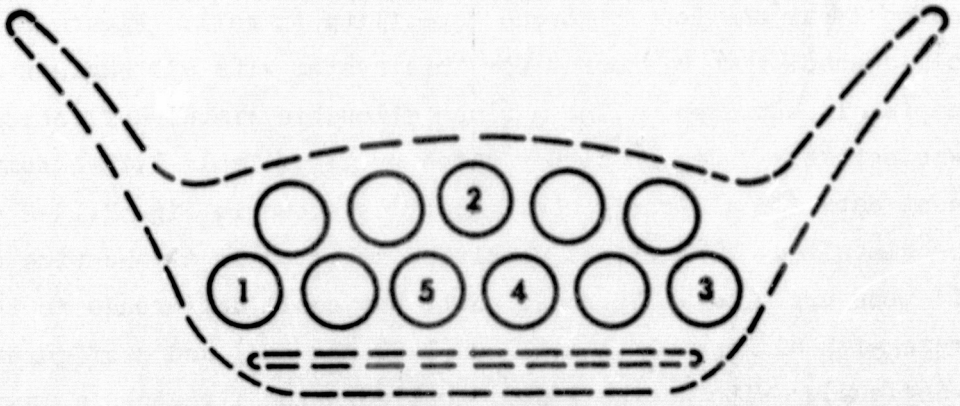

CONFIGURATION 2

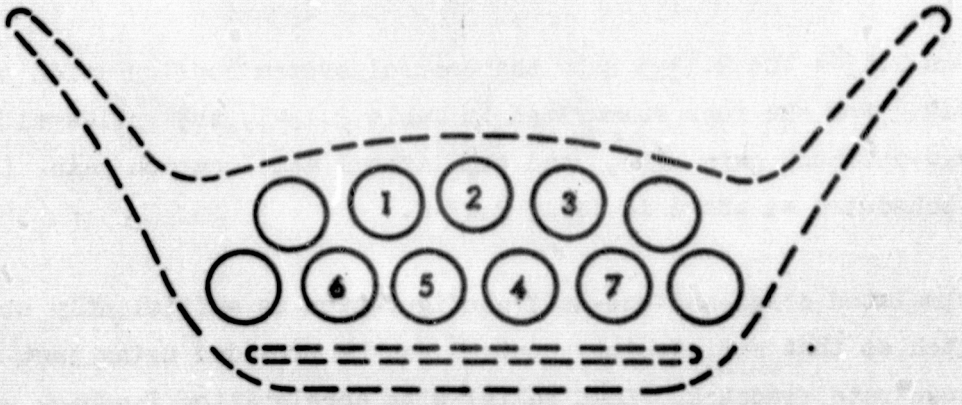

CONFIGURATION 3

Fig. 2.13-2 Three Systems Evaluated By 6-D Computer Simulations

ALL ENGINES OPERATING

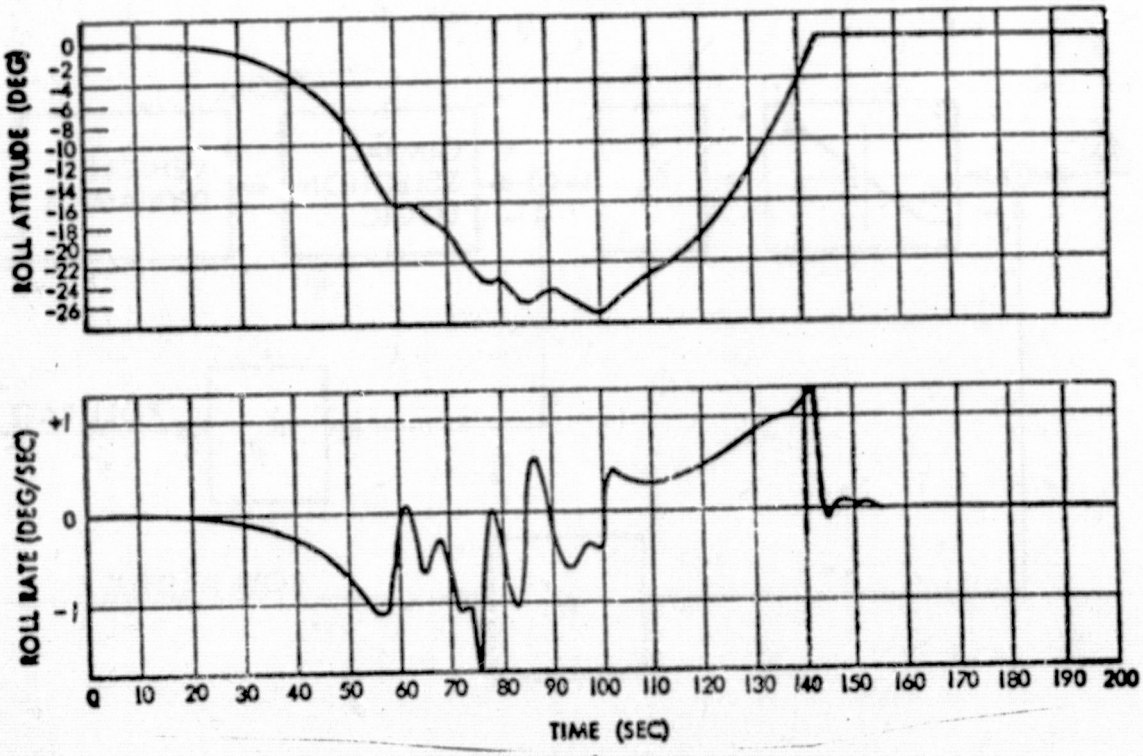

ENGINE NO. 1 SHUTDOWN

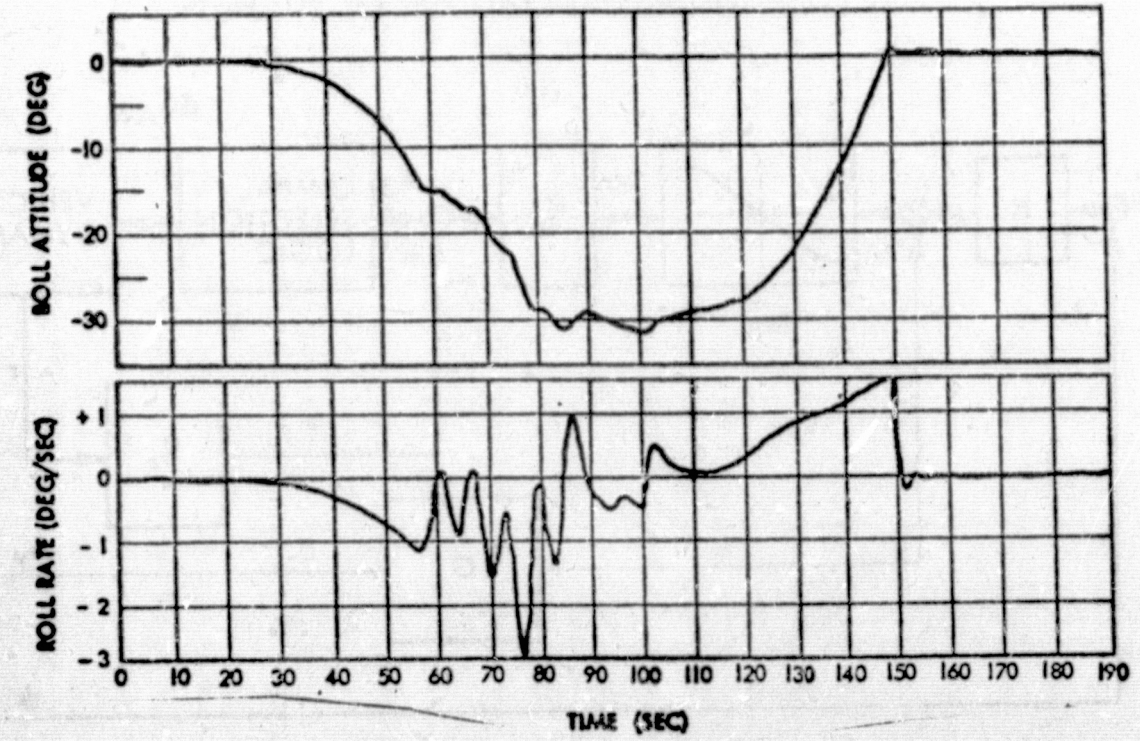

Fig. 2.13-3 ACS Stage-and-One-Half Five-Gimballed-Engine Configuration No. 1: Roll Attitude and Rates With Sidewind

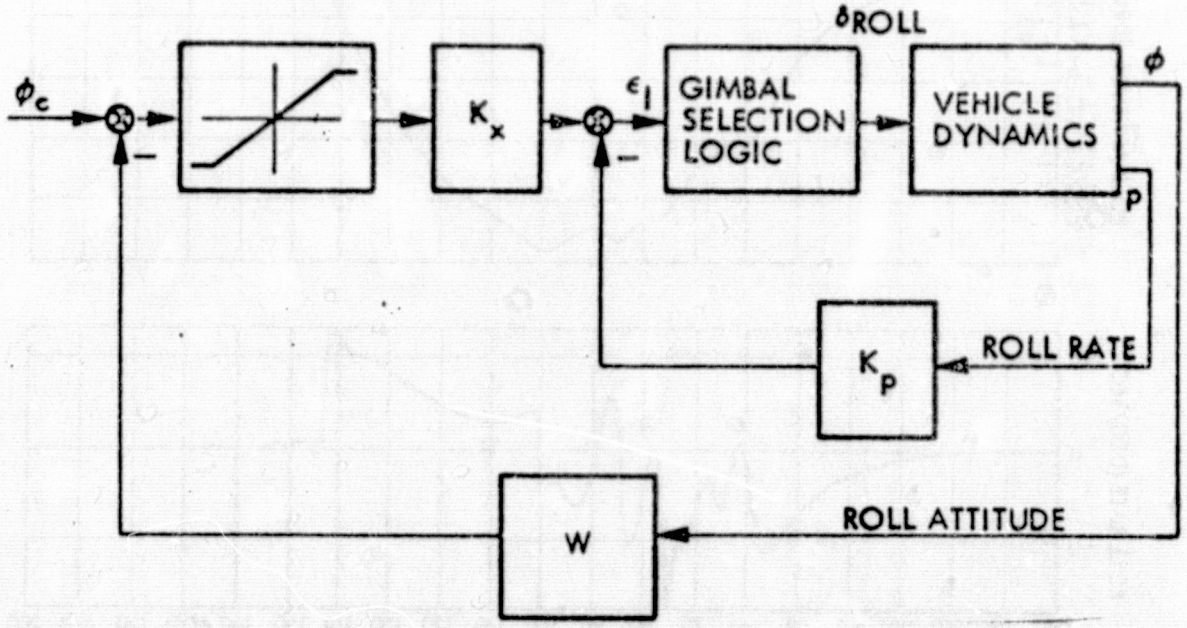

Fig. 2.13-4 Boost Phase Roll Control TVC Logic

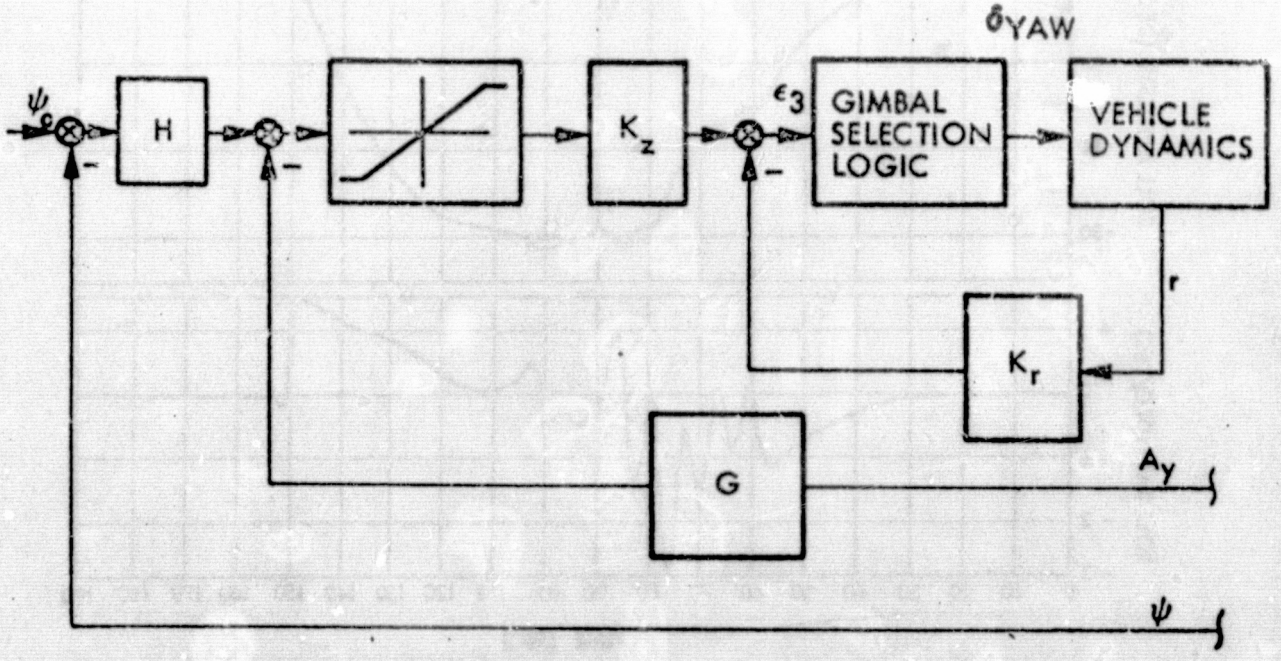

Fig. 2.13-5 Boost Phase Yaw Control TVC Logic

Table 2.13-1

SUMMARY OF DATA FOR THREE CONFIGURATIONS

Configuration	Engine Out	Maximum Roll Rate (t = 75) (deg/sec)	Maximum Gimbal Deflection (t = 75) (deg)	Average Gimbal Deflection (t = 75) (deg)
1	None	1.76	7.00	3.74
1	1	2.84	7.00	4.77
2	None	1.70	6.49	1.91
2	1	2.47	7.00	2.09
3	None	1.70	5.78	2.05
3	6	2.38	6.55	2.20
All	None	1.70	3.25	0.95

Table 2.13-2

SWITCHED GAIN SCHEDULES

	Time From Liftoff (sec)		
Gain	0-56	50-100	<56
W	0	0	1
G	0	1	0
H	1	0.2	1

Table 2.13-3

CONSTANT CONTROL SYSTEM GAINS

I_x/K_p = 0.67 sec;		K_p/K_x = 0.67 sec	
I_y/K_q = 1.41 sec		K_q/K_y = 1.41 sec	
I_z/K_r = 1.41 sec		K_r/K_z = 1.41 sec	

To realize the required control torques with the minimum gimbal deflections, the simulations incorporated a gimbal-selection logic that minimizes the sum of the squares of gimbal deflections. Reference 2.13-1 presents the underlying mathematical development of this gimbal selection logic. Is is feasible to assign such an additional constraint on the control logic, because a freedom exists in selecting gimbals for differential deflection for roll control. This approach not only minimizes the maximum gimbal deflection requirements but, in effect, will reduce the bending moments on the vehicle – i.e., $M_{B\delta_i}\ \delta_i$ is minimized as the sum of the squares.

Based upon simulation studies of alternate gimballing arrangements for the stage-and-one-half configuration described above, it was established that the vehicle can be controlled adequately using five gimballed engines only. The

maximum loads with an engine out, at the time of maximum dynamic pressure, were limited to the values given below

$$\bar{q}\beta \quad \text{at} \quad \bar{q}_{max} < 1{,}800 \ \frac{\text{lb-deg}}{\text{ft}^2}$$

$$\bar{q}\alpha \quad \text{at} \quad \bar{q}_{max} < 1{,}200 \ \frac{\text{lb-deg}}{\text{ft}^2}$$

The final configuration is shown in Fig. 2.13-6. This configuration was preferred over configuration 1 shown in Fig. 2.13-2, primarily because it provides increased roll-torque capability.

No control studies were performed for the 9 engine configuration. This configuration has 5 out of the total of 9 engines gimballed. Since each engine produces a higher thrust, the nine engine configuration with the inverted W gimballing arrangement provides even higher roll torque capability than the configuration shown in Fig. 2.13-6

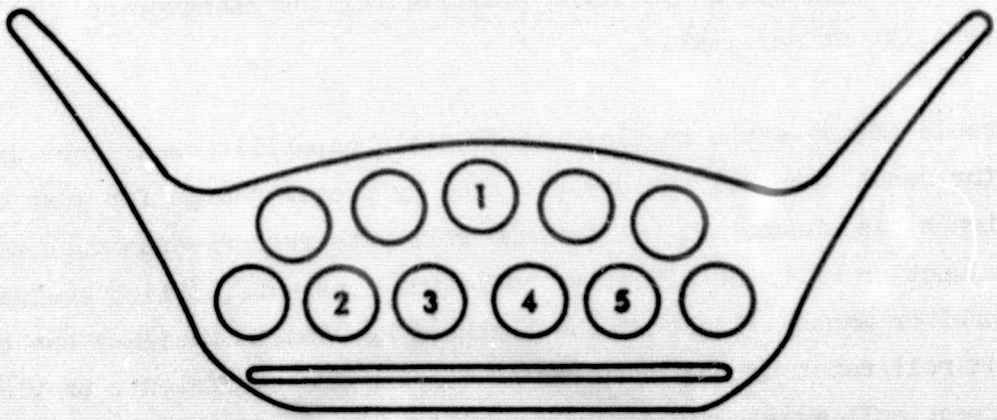

Fig. 2.13-6 Preferred Five-Gimballed Engine Arrangement

2.13.2 Vehicle Control During Approach and Landing

Analysis and simulation studies performed for the approach and landing phases have emphasized manual flying capabilities. Manual flying quality requirements place the more severe response requirements on the flight control system when compared to automatic systems.

Computer simulation studies and manual flight simulations have shown that good flying qualities can be achieved during the approach and landing phase of the delta-body through the use of proper stability augmentation.

Flight control system design for the aerodynamic flight phase requires that the sideslip angle (β) is held to very low values during rolling maneuvers. This is primarily dictated by the large negative values of C_{ℓ_β}, a characteristic of all shuttle vehicles. This requirement becomes even more significant with increasing values of α, since C_{ℓ_β} increases with angle-of-attack, particulary at subsonic Mach numbers. Also, with manual control capabilities, it is desirable that the induced yaw is all adverse. Proverse yaw (i.e., negative β during a positive rolling maneuver-roll to the right) is generally not acceptable.

Acceptable steady-state angular rate vehicle capabilities are not only a requirement for manual control but are dictated by proper design for gust conditions. Experience has shown that the maximum roll-rate requirements must be evaluated in conjunction with the effective roll-time constants. Pilot evaluation of delta-body orbiter manual flight at the Lockheed Rye Canyon facility has shown that maximum roll rates of the order of 10 deg/sec are sufficient, provided a sufficient roll acceleration, as measured by the roll-time constant (τ_R), exists. The latter requirement is dictated by roll recovery during gust upset near landing.

The pacing consideration for the design of the pitch axis control system with manual capabilities is sufficient pitch rate of the vehicle. Limiting the maximum pitch rate, as through excessive rate feedback, will cause saturation of the control system in severe gust and will make the vehicle sluggish for manual control.

A candidate system for manual control is shown in Fig. 2.13-7. This system has evolved from delta-body simulation studies performed at Lockheed/Sunnyvale and has performed well in the simulator evaluation. Key system elements include a roll-yaw crossfeed, lateral acceleration feedback through a low-pass filter to the yaw channel, and rate feedbacks in yaw and roll. Also, roll coordination assist is provided by $(g/V)\ \sin\phi$ feedback. The roll-yaw crossfeed is necessitated by the high values of C_{ℓ_β} to counteract the vehicle's tendency to roll out. Lateral acceleration feedback helps to limit steady-state sideslip.

With moderate gain scheduling, this system provides acceptable response in all axes. The key element for the roll axis is the proper adjustment of the cross-feed gain (see Fig. 2.13-8). Experience has shown that in addition to C_{ℓ_β}, a limiting factor in achieving good roll-rate capabilities is $C_{\ell_{\delta_R}}$. The reason is because as the rudder is deflected during a rolling maneuver to coordinate the turn, a large positive value of $C_{\ell_{\delta_R}}$ will further inhibit the roll for a vehicle with adverse yaw; this is a characteristic of all delta configurations. To extend the roll-rate capabilities generally requires some form of destabilization, such as using a roll-rate signal input to the rudder for the system shown in Fig. 2.13-7.

Pitch-axis control concepts evaluated for the aerodynamic return phase of the delta-body emphasized various forms of pitch-rate command systems. Generally, these systems have been especially successful in modern aircraft in which manual-control capability is emphasized. In such systems, a pitch-attitude loop in the form of an attitude-hold autopilot mode is provided. Forms of rate command systems evaluated include:

a. Pure pitch rate command
b. Blended feedback control (C*)
c. Pitch damping

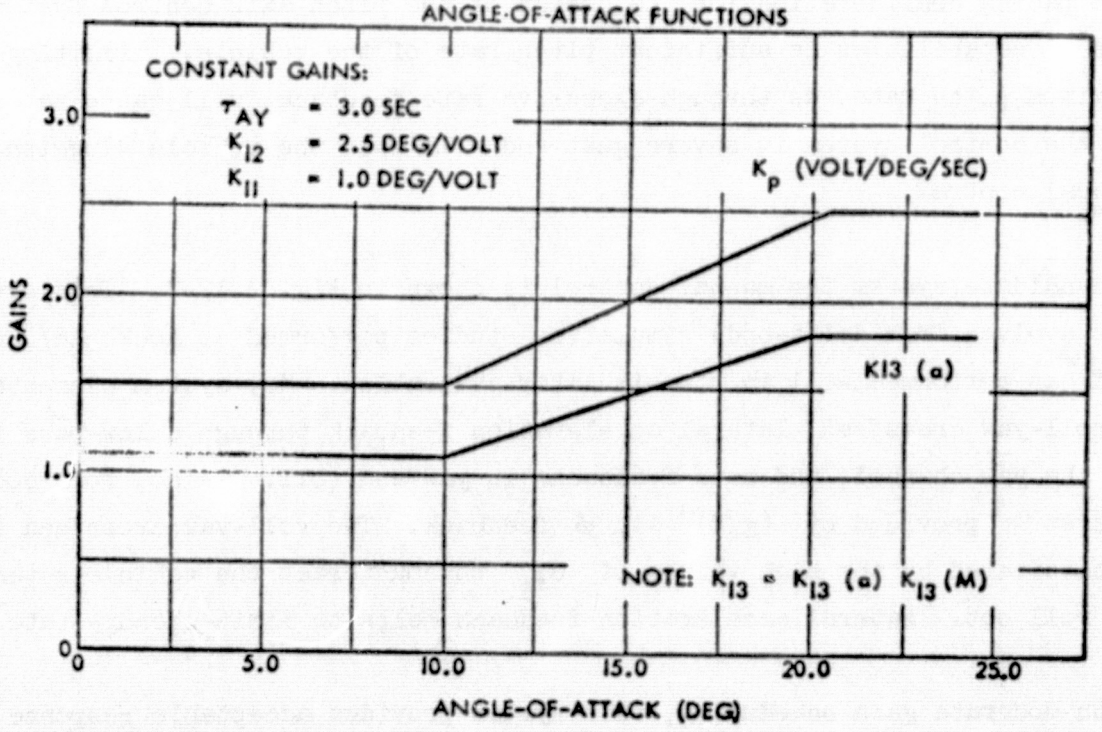

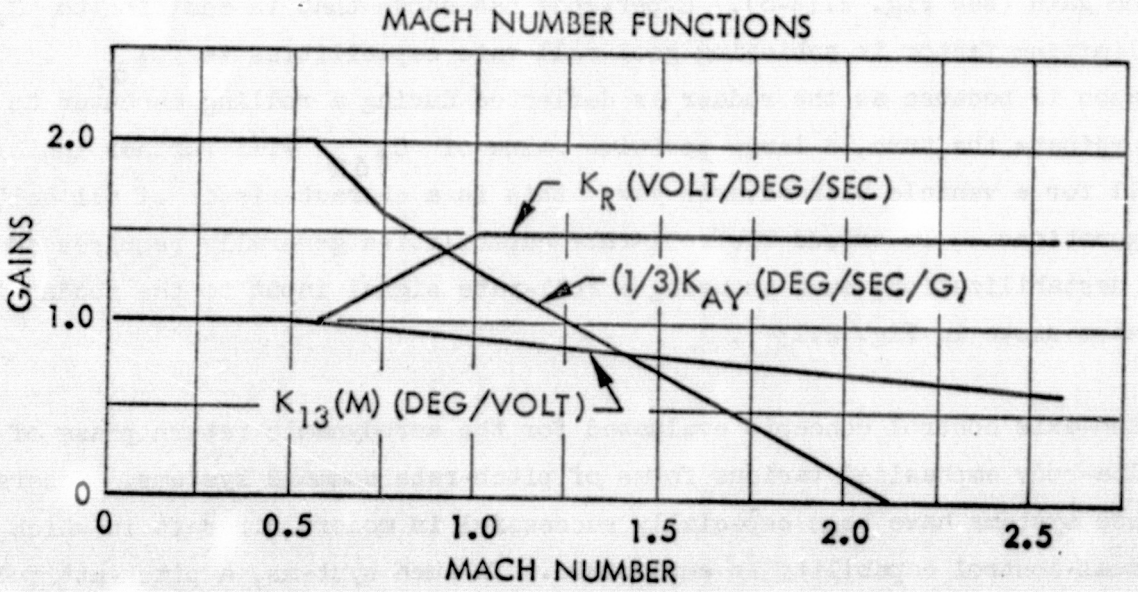

Fig. 2.13-7 Three-Axis Rate-Command System Schematic for Delta-Body Orbiter

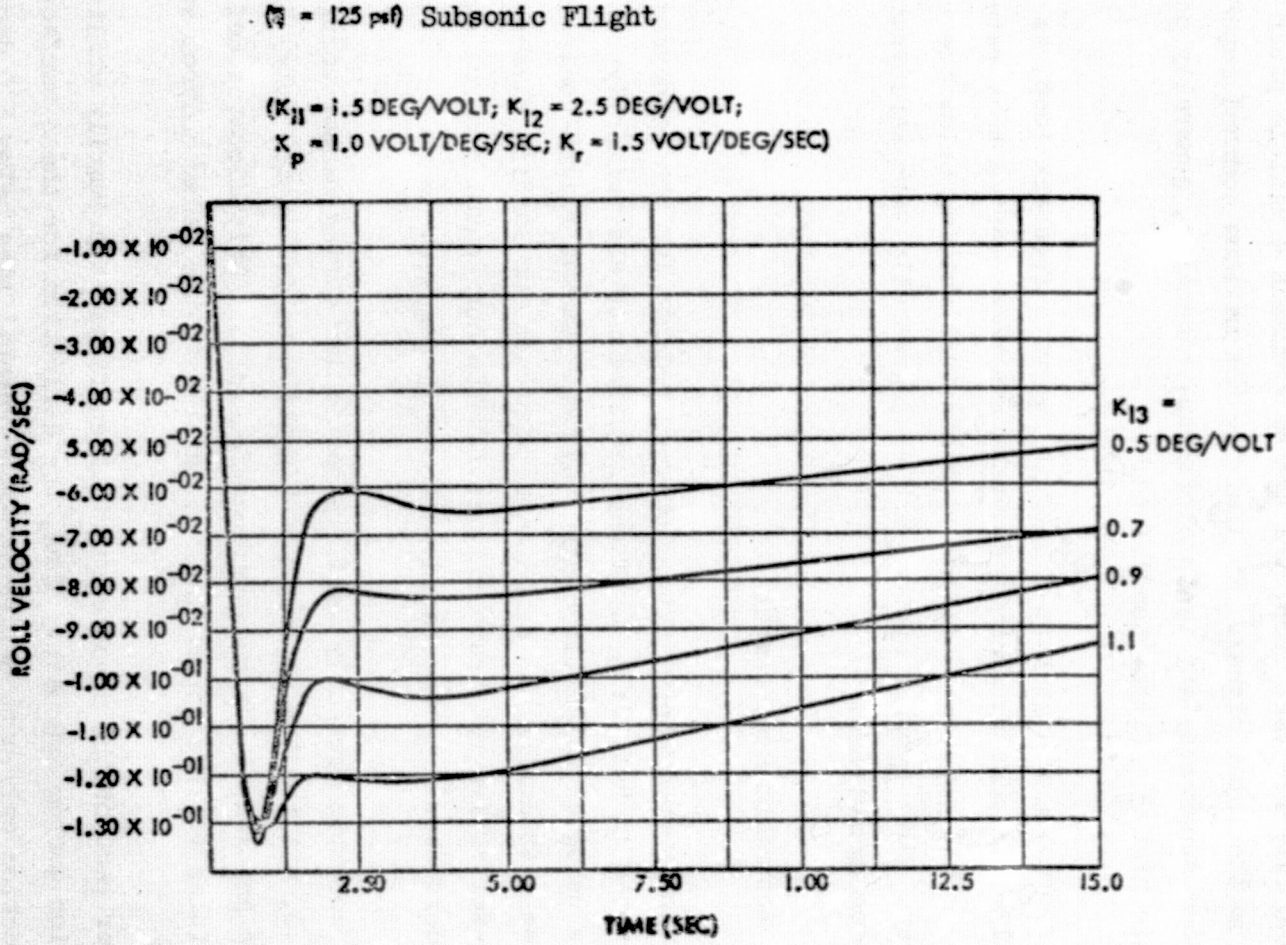

Fig. 2.13-8 Lockheed Two-Stage Delta-Body Orbiter: Rate Command System Linear Step Response to Roll-Axis Control Handle Input At Subsonic Flight - Effect of Crossfeed Gain K_{13}

A pitch-axis rate command system represents the simplest form of augmentation for statically stable and unstable vehicle configurations. Using a fairly high-gain rate feedback loop, the system commands a vehicle pitch rate proportional to the input signal. By limiting the maximum command input signal, the system suppresses any vehicle pitchup tendencies, generally occurring at transonic high α flight conditions.

By incorporating a high-pass filter in the rate feedback loop, as shown in Fig. 2.13-7, a pure rate command system can be converted to a rate damping system. This requires a filter time-constant setting below the control frequency. Rate damping systems are used generally with aerodynamically stable configurations.

2.13.3 Actuation Requirements

A preliminary analysis of actuation requirements for the aerodynamic surfaces is presented in Ref. 2.13-3. These requirements are primarily based on control concepts using an automatic control system. Manual flight-control simulation indicates that during the aerodynamic approach and landing phases the control-surface-deflection rate capabilities for the horizontal control surfaces and the rudders should be increased to above 15 deg/sec.

Control concepts presently used, in particular during manual control below $M = 2.0$, utilize the upper flaps (negative-up deflection only) in conjunction with the horizontal control surfaces for roll. This dictates deflection-rate capabilities for the upper flaps comparable to the other control surfaces.

The lower part of the movable vertical surfaces is primarily utilized for drag modulation during approach. Thus, the deflection for these surfaces is in one direction only with deflection-rate capabilities below 5.0 deg/sec.

REFERENCES

2.13-1 S. W. Beach, "Flight Control – Investigation of the Thrust Vector Control System Requirements," LMSC Space Shuttle Project EM L2-01-03-M2-3, 23 October 1970

2.13-2 J. Machnick, "Nominal Ascent Trajectory for Stage-and-One-Half (1-1/2) Vehicle," LMSC Space Shuttle Project EM L2-06-02-M13-2, 18 August 1970

2.13-3 A. J. Besonis, "Flight Control – Actuation Requirements for the Aerodynamic Control Surfaces," LMSC Space Shuttle Project EM L2-01-03-M2-12, 6 November 1970